VOLUME 28 / NUMBER 4
FEBRUARY 23, 1990
ACC. NOS. N90-12495 TO N90-13322

STAR
AN ABSTRACT JOURNAL

Scientific and Technical Aerospace Reports

PRODUCED BY THE
SCIENTIFIC AND TECHNICAL
INFORMATION
DIVISION

NASA

NATIONAL AERONAUTICS AND SPACE ADMINISTRATION

WHAT YOU CAN DO FOR *STAR*

All users of this abstract service are urged to forward reports to be considered for announcement in *STAR*. This will aid NASA in its efforts to provide the fullest possible coverage of all scientific and technical publications that might support aeronautics and space research and development. If you have prepared relevant reports (other than those that you will transmit to NASA, DOD, or DOE through the usual contract- or grant-reporting channels), please send them for consideration to the NASA Scientific and Technical Information Facility, P.O. Box 8757, BWI Airport, MD 21240.

Reprints of journal articles, book chapters, and conference papers are also welcome. These will be considered for announcement in *STAR's* companion journal, *International Aerospace Abstracts*.

You may specify a particular source to be included in a report announcement if you wish; otherwise the report will be placed on public sale at the National Technical Information Service. Copyrighted publications will be announced but not distributed or sold.

PURCHASE OF *STAR*

The semimonthly issues are available to registered users on annual subscription from the NASA Scientific and Technical Information Facility, ATTN: Registration Services, P.O. Box 8757, BWI Airport, MD 21240. *STAR* is publicly available on annual subscription from the Superintendent of Documents, U.S. Government Printing Office, Washington, DC 20402.

PUBLISHED BY:

UNITED STATES GOVERNMENT
NATIONAL AERONAUTICS AND SPACE ADMINISTRATION
SCIENTIFIC AND TECHNICAL INFORMATION DIVISION
Scientific and Technical Aerospace Reports, Volume 28, is prepared by the NASA Scientific and Technical Information Facility operated for the National Aeronautics and Space Administration by RMS Associates.

The Administrator of the National Aeronautics and Space Administration has determined that the publication of this periodical is necessary in the transaction of the public business required by law of this agency. Use of funds for printing this periodical has been approved by the Director of the Office of Management and Budget through March 22, 1991.

US ISSN 0036-8741

Scientific and Technical Aerospace Reports (STAR) is issued twice a month and contains abstracts and indexes of meeting papers, conference proceedings, and unlimited distribution reports that have been added to the NASA Scientific and Technical Information Database during the preceding period. These citations may also be accessed online via NASA/RECON or via AIAA's Aerospace Database (File 108) through Dialog Information Services, Inc.

STAR subject coverage includes all aerospace-related areas that will help NASA achieve its mission. Material is gathered from all over the world and includes significant input from many countries under exchange and access agreements.

Consult the indexes at the back of this volume to help zero in on what you are looking for. These include:

Subject Index
Personal Author Index
Corporate Source Index
Contract Number Index
Report/Accession Number Index

STAR's companion abstract journal *International Aerospace Abstracts* should be used if you are looking for references to periodicals, books, and published meeting papers or conference proceedings.

Questions and comments should be addressed to:

NASA Scientific and Technical Information Facility
User Services
P.O. Box 8757
BWI Airport, MD 21240
301-621-0150

VOLUME 28 NUMBER 4 / FEBRUARY 23, 1990

TABLE OF CONTENTS

AERONAUTICS

Includes aeronautics (general); aerodynamics; air transportation and safety; aircraft communications and navigation; aircraft design, testing and performance; aircraft instrumentation; aircraft propulsion and power; aircraft stability and control; and research and support facilities (air).

For related information see also *Astronautics.*

01 AERONAUTICS (GENERAL) 437

02 AERODYNAMICS 437

Includes aerodynamics of bodies, combinations, wings, rotors, and control surfaces; and internal flow in ducts and turbomachinery.

For related information see also *34 Fluid Mechanics and Heat Transfer.*

03 AIR TRANSPORTATION AND SAFETY N.A.

Includes passenger and cargo air transport operations; and aircraft accidents.

For related information see also *16 Space Transportation* and *85 Urban Technology and Transportation.*

04 AIRCRAFT COMMUNICATIONS AND NAVIGATION 449

Includes digital and voice communication with aircraft; air navigation systems (satellite and ground based); and air traffic control.

For related information see also *17 Space Communications, Spacecraft Communications, Command and Tracking* and *32 Communications and Radar.*

05 AIRCRAFT DESIGN, TESTING AND PERFORMANCE 450

Includes aircraft simulation technology.

For related information see also *18 Spacecraft Design, Testing and Performance* and *39 Structural Mechanics.* For land transportation vehicles see *85 Urban Technology and Transportation.*

06 AIRCRAFT INSTRUMENTATION 454

Includes cockpit and cabin display devices; and flight instruments.

For related information see also *19 Spacecraft Instrumentation* and *35 Instrumentation and Photography.*

07 AIRCRAFT PROPULSION AND POWER 454

Includes prime propulsion systems and systems components, e.g., gas turbine engines and compressors; and onboard auxiliary power plants for aircraft.

For related information see also *20 Spacecraft Propulsion and Power, 28 Propellants and Fuels,* and *44 Energy Production and Conversion.*

08 AIRCRAFT STABILITY AND CONTROL 457

Includes aircraft handling qualities; piloting; flight controls; and autopilots.

For related information see also *05 Aircraft Design, Testing and Performance.*

09 RESEARCH AND SUPPORT FACILITIES (AIR) 458

Includes airports, hangars and runways; aircraft repair and overhaul facilities; wind tunnels; shock tubes; and aircraft engine test stands.

For related information see also *14 Ground Support Systems and Facilities (Space).*

ASTRONAUTICS

Includes astronautics (general); astrodynamics; ground support systems and facilities (space); launch vehicles and space vehicles; space transportation; space communications, spacecraft communications, command and tracking; spacecraft design, testing and performance; spacecraft instrumentation; and spacecraft propulsion and power.

For related information see also *Aeronautics.*

12 ASTRONAUTICS (GENERAL) 460

For extraterrestrial exploration see *91 Lunar and Planetary Exploration.*

13 ASTRODYNAMICS 460

Includes powered and free-flight trajectories; and orbital and launching dynamics.

14 GROUND SUPPORT SYSTEMS AND FACILITIES (SPACE) N.A.

Includes launch complexes, research and production facilities; ground support equipment, e.g., mobile transporters; and simulators.

For related information see also *09 Research and Support Facilities (Air).*

15 LAUNCH VEHICLES AND SPACE VEHICLES 461

Includes boosters; operating problems of launch/space vehicle systems; and reusable vehicles.

For related information see also *20 Spacecraft Propulsion and Power.*

16 SPACE TRANSPORTATION N.A.

Includes passenger and cargo space transportation, e.g., shuttle operations; and space rescue techniques.

For related information see also *03 Air Transportation and Safety* and *18 Spacecraft Design, Testing and Performance.* For space suits see *54 Man/System Technology and Life Support.*

17 SPACE COMMUNICATIONS, SPACECRAFT COMMUNICATIONS, COMMAND AND TRACKING N.A.

Includes telemetry; space communications networks; astronavigation and guidance; and radio blackout.

For related information see also *04 Aircraft Communications and Navigation* and *32 Communications and Radar.*

18 SPACECRAFT DESIGN, TESTING AND PERFORMANCE 462

Includes satellites; space platforms; space stations; spacecraft systems and components such as thermal and environmental controls; and attitude controls.

For life support systems see *54 Man/System Technology and Life Support.* For related information see also *05 Aircraft Design, Testing and Performance, 39 Structural Mechanics,* and *16 Space Transportation.*

19 SPACECRAFT INSTRUMENTATION N.A.

For related information see also *06 Aircraft Instrumentation* and *35 Instrumentation and Photography.*

20 SPACECRAFT PROPULSION AND POWER 463

Includes main propulsion systems and components, e.g. rocket engines; and spacecraft auxiliary power sources.

For related information see also *07 Aircraft Propulsion and Power, 28 Propellants and Fuels, 44 Energy Production and Conversion,* and *15 Launch Vehicles and Space Vehicles.*

CHEMISTRY AND MATERIALS

Includes chemistry and materials (general); composite materials; inorganic and physical chemistry; metallic materials; nonmetallic materials; propellants and fuels; and materials processing.

23 CHEMISTRY AND MATERIALS (GENERAL) 464

24 COMPOSITE MATERIALS 465

Includes physical, chemical, and mechanical properties of laminates and other composite materials.

For ceramic materials see *27 Nonmetallic Materials.*

25 INORGANIC AND PHYSICAL CHEMISTRY 468

Includes chemical analysis, e.g., chromatography; combustion theory; electrochemistry; and photochemistry.

For related information see also *77 Thermodynamics and Statistical Physics.*

26 METALLIC MATERIALS 474

Includes physical, chemical, and mechanical properties of metals, e.g., corrosion; and metallurgy.

27 NONMETALLIC MATERIALS 477

Includes physical, chemical, and mechanical properties of plastics, elastomers, lubricants, polymers, textiles, adhesives, and ceramic materials.

For composite materials see *24 Composite Materials.*

28 PROPELLANTS AND FUELS 482

Includes rocket propellants, igniters and oxidizers; their storage and handling procedures; and aircraft fuels.

For related information see also *07 Aircraft Propulsion and Power, 20 Spacecraft Propulsion and Power,* and *44 Energy Production and Conversion.*

29 MATERIALS PROCESSING 482

Includes space-based development of products and processes for commercial application.

For biological materials see *55 Space Biology.*

ENGINEERING

Includes engineering (general); communications and radar; electronics and electrical engineering; fluid mechanics and heat transfer; instrumentation and photography; lasers and masers; mechanical engineering; quality assurance and reliability; and structural mechanics.

For related information see also *Physics.*

31 ENGINEERING (GENERAL) 483

Includes vacuum technology; control engineering; display engineering; cryogenics; and fire prevention.

32 COMMUNICATIONS AND RADAR 484

Includes radar; land and global communications; communications theory; and optical communications.

For related information see also *04 Aircraft Communications and Navigation* and *17 Space Communications, Spacecraft Communications, Command and Tracking.* For search and rescue see *03 Air Transportation and Safety,* and *16 Space Transportation.*

33 ELECTRONICS AND ELECTRICAL ENGINEERING 494

Includes test equipment and maintainability; components, e.g., tunnel diodes and transistors; microminiaturization; and integrated circuitry.

For related information see also *60 Computer Operations and Hardware* and *76 Solid-State Physics.*

34 FLUID MECHANICS AND HEAT TRANSFER 499

Includes boundary layers; hydrodynamics; fluidics; mass transfer and ablation cooling.

For related information see also *02 Aerodynamics* and *77 Thermodynamics and Statistical Physics.*

35 INSTRUMENTATION AND PHOTOGRAPHY 504

Includes remote sensors; measuring instruments and gauges; detectors; cameras and photographic supplies; and holography.

For aerial photography see *43 Earth Resources and Remote Sensing.* For related information see also *06 Aircraft Instrumentation* and *19 Spacecraft Instrumentation.*

36 LASERS AND MASERS 505

Includes parametric amplifiers.

For related information see also *76 Solid-State Physics.*

37 MECHANICAL ENGINEERING 507

Includes auxiliary systems (nonpower); machine elements and processes; and mechanical equipment.

38 QUALITY ASSURANCE AND RELIABILITY 511

Includes product sampling procedures and techniques; and quality control.

39 STRUCTURAL MECHANICS 511

Includes structural element design and weight analysis; fatigue; and thermal stress.

For applications see *05 Aircraft Design, Testing and Performance* and *18 Spacecraft Design, Testing and Performance.*

GEOSCIENCES

Includes geosciences (general); earth resources and remote sensing; energy production and conversion; environment pollution; geophysics; meteorology and climatology; and oceanography.

For related information see also *Space Sciences.*

42 GEOSCIENCES (GENERAL) 514

43 EARTH RESOURCES AND REMOTE SENSING 514

Includes remote sensing of earth resources by aircraft and spacecraft; photogrammetry; and aerial photography.

For instrumentation see *35 Instrumentation and Photography.*

44 ENERGY PRODUCTION AND CONVERSION 515

Includes specific energy conversion systems, e.g., fuel cells; global sources of energy; geophysical conversion; and windpower.

For related information see also *07 Aircraft Propulsion and Power, 20 Spacecraft Propulsion and Power,* and *28 Propellants and Fuels.*

45 ENVIRONMENT POLLUTION 516

Includes atmospheric, noise, thermal, and water pollution.

46 GEOPHYSICS 517

Includes aeronomy; upper and lower atmosphere studies; ionospheric and magnetospheric physics; and geomagnetism.

For space radiation see *93 Space Radiation.*

47 METEOROLOGY AND CLIMATOLOGY 519

Includes weather forecasting and modification.

48 OCEANOGRAPHY 521

Includes biological, dynamic, and physical oceanography; and marine resources.

For related information see also *43 Earth Resources and Remote Sensing.*

LIFE SCIENCES

Includes life sciences (general); aerospace medicine; behavioral sciences; man/system technology and life support; and space biology.

51 LIFE SCIENCES (GENERAL) N.A.

52 AEROSPACE MEDICINE 522

Includes physiological factors; biological effects of radiation; and effects of weightlessness on man and animals.

53 BEHAVIORAL SCIENCES 525

Includes psychological factors; individual and group behavior; crew training and evaluation; and psychiatric research.

54 MAN/SYSTEM TECHNOLOGY AND LIFE SUPPORT 526

Includes human engineering; biotechnology; and space suits and protective clothing.

For related information see also *16 Space Transportation.*

55 SPACE BIOLOGY N.A.

Includes exobiology; planetary biology; and extraterrestrial life.

MATHEMATICAL AND COMPUTER SCIENCES

Includes mathematical and computer sciences (general); computer operations and hardware; computer programming and software; computer systems; cybernetics; numerical analysis; statistics and probability; systems analysis; and theoretical mathematics.

59 MATHEMATICAL AND COMPUTER SCIENCES (GENERAL) N.A.

60 COMPUTER OPERATIONS AND HARDWARE 528

Includes hardware for computer graphics, firmware, and data processing.

For components see *33 Electronics and Electrical Engineering.*

61 COMPUTER PROGRAMMING AND SOFTWARE 528

Includes computer programs, routines, algorithms, and specific applications, e.g., CAD/CAM.

62 COMPUTER SYSTEMS 535

Includes computer networks and special application computer systems.

63 CYBERNETICS 536

Includes feedback and control theory, artificial intelligence, robotics and expert systems.

For related information see also *54 Man/System Technology and Life Support.*

64 NUMERICAL ANALYSIS 538

Includes iteration, difference equations, and numerical approximation.

65 STATISTICS AND PROBABILITY 546

Includes data sampling and smoothing; Monte Carlo method; and stochastic processes.

66 SYSTEMS ANALYSIS N.A.

Includes mathematical modeling; network analysis; and operations research.

67 THEORETICAL MATHEMATICS 548

Includes topology and number theory.

PHYSICS

Includes physics (general); acoustics; atomic and molecular physics; nuclear and high-energy physics; optics; plasma physics; solid-state physics; and thermodynamics and statistical physics.

For related information see also *Engineering.*

70 PHYSICS (GENERAL) 548

For precision time and time interval (PTTI) see *35 Instrumentation and Photography;* for geophysics, astrophysics or solar physics see *46 Geophysics, 90 Astrophysics,* or *92 Solar Physics.*

71 ACOUSTICS 549
Includes sound generation, transmission, and attenuation.
For noise pollution see *45 Environment Pollution.*

72 ATOMIC AND MOLECULAR PHYSICS 552
Includes atomic structure, electron properties, and molecular spectra.

73 NUCLEAR AND HIGH-ENERGY PHYSICS 554
Includes elementary and nuclear particles; and reactor theory.
For space radiation see *93 Space Radiation.*

74 OPTICS 554
Includes light phenomena and optical devices.
For lasers see *36 Lasers and Masers.*

75 PLASMA PHYSICS 556
Includes magnetohydrodynamics and plasma fusion.
For ionospheric plasmas see *46 Geophysics.* For space plasmas see *90 Astrophysics.*

76 SOLID-STATE PHYSICS 557
Includes superconductivity.
For related information see also *33 Electronics and Electrical Engineering* and *36 Lasers and Masers.*

77 THERMODYNAMICS AND STATISTICAL PHYSICS 561
Includes quantum mechanics; theoretical physics; and Bose and Fermi statistics.
For related information see also *25 Inorganic and Physical Chemistry* and *34 Fluid Mechanics and Heat Transfer.*

SOCIAL SCIENCES

Includes social sciences (general); administration and management; documentation and information science; economics and cost analysis; law, political science, and space policy; and urban technology and transportation.

80 SOCIAL SCIENCES (GENERAL) 562
Includes educational matters.

81 ADMINISTRATION AND MANAGEMENT 562
Includes management planning and research.

82 DOCUMENTATION AND INFORMATION SCIENCE 563
Includes information management; information storage and retrieval technology; technical writing; graphic arts; and micrography.
For computer documentation see *61 Computer Programming and Software.*

83 ECONOMICS AND COST ANALYSIS N.A.
Includes cost effectiveness studies.

84 LAW, POLITICAL SCIENCE AND SPACE POLICY 563
Includes NASA appropriation hearings; aviation law; space law and policy; international law; international cooperation; and patent policy.

85 URBAN TECHNOLOGY AND TRANSPORTATION 564
Includes applications of space technology to urban problems; technology transfer; technology assessment; and surface and mass transportation.
For related information see *03 Air Transportation and Safety, 16 Space Transportation,* and *44 Energy Production and Conversion.*

SPACE SCIENCES

Includes space sciences (general); astronomy; astrophysics; lunar and planetary exploration; solar physics; and space radiation.
For related information see also *Geosciences.*

88 SPACE SCIENCES (GENERAL) N.A.

89 ASTRONOMY 564
Includes radio, gamma-ray, and infrared astronomy; and astrometry.

90 ASTROPHYSICS 565
Includes cosmology; celestial mechanics; space plasmas; and interstellar and interplanetary gases and dust.
For related information see also *75 Plasma Physics.*

91 LUNAR AND PLANETARY EXPLORATION N.A.
Includes planetology; and manned and unmanned flights.
For spacecraft design or space stations see *18 Spacecraft Design, Testing and Performance.*

92 SOLAR PHYSICS 566
Includes solar activity, solar flares, solar radiation and sunspots.
For related information see *93 Space Radiation.*

93 SPACE RADIATION 569
Includes cosmic radiation; and inner and outer earth's radiation belts.
For biological effects of radiation see *52 Aerospace Medicine.* For theory see *73 Nuclear and High-Energy Physics.*

GENERAL

Includes aeronautical, astronautical, and space science related histories, biographies, and pertinent reports too broad for categorization; histories or broad overviews of NASA programs.

99 GENERAL 569

Note: N.A. means that no abstracts were assigned to this category for this issue.

SUBJECT INDEX I-1
PERSONAL AUTHOR INDEX I-57
CORPORATE SOURCE INDEX I-65
CONTRACT NUMBER INDEX I-77
REPORT/ACCESSION NUMBER INDEX I-79
APPENDIX—ABOUT STAR A-1

TYPICAL CITATION AND ABSTRACT

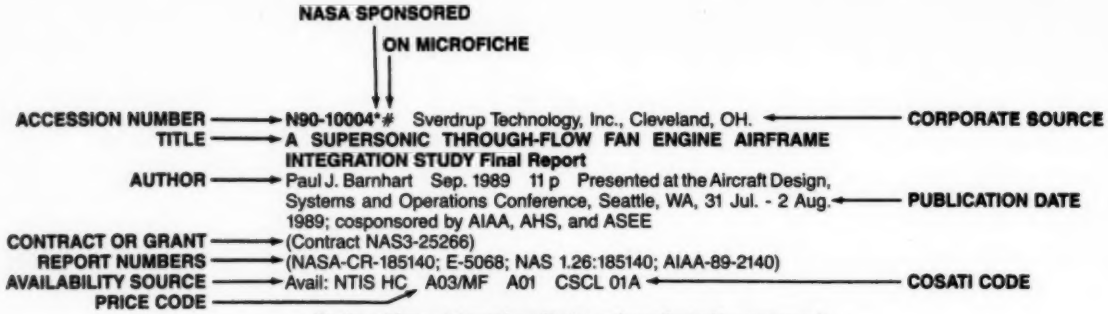
NASA SPONSORED
ON MICROFICHE
ACCESSION NUMBER
N90-10004*# Sverdrup Technology, Inc., Cleveland, OH.
CORPORATE SOURCE
TITLE
A SUPERSONIC THROUGH-FLOW FAN ENGINE AIRFRAME INTEGRATION STUDY Final Report
AUTHOR
Paul J. Barnhart Sep. 1989 11 p Presented at the Aircraft Design, Systems and Operations Conference, Seattle, WA, 31 Jul. - 2 Aug. 1989; cosponsored by AIAA, AHS, and ASEE
PUBLICATION DATE
CONTRACT OR GRANT
(Contract NAS3-25266)
REPORT NUMBERS
(NASA-CR-185140; E-5068; NAS 1.26:185140; AIAA-89-2140)
AVAILABILITY SOURCE
Avail: NTIS HC A03/MF A01 CSCL 01A
COSATI CODE
PRICE CODE

Engine airframe integration effects are investigated for superonsic through-flow fan engines installed on a Mach 3.20 supersonic cruise vehicle. Six different supersonic through-flow fan engine installations covering the effects of engine size, nacelle contour, nacelle placement, and approximate bypass plume effects are presented. The different supersonic through-flow fan installations are compared with a conventional turbine bypass engine configuration on the same basic airframe. The supersonic through-flow fan engine integrations are shown to be comparable to the turbine bypass engine configuration on the basis of installed nacelle wave drag. The supersonic through-flow fan engine airframe integrated vehicles have superior aerodynamic performance on the basis of maximum lift-to-drag ratio than the turbine bypass engine installation over the entire operating Mach number range from 1.10 to 3.20. When approximate bypass plume modeling is included, the supersonic through-flow fan engine configuration shows even larger improvements over the turbine bypass engine configuration. Author

VOLUME 28 NUMBER 4 / FEBRUARY 23, 1990

Scientific and Technical Aerospace Reports

A Semimonthly Publication of the National Aeronautics and Space Administration

01 AERONAUTICS (GENERAL)

N90-12495# Naval Postgraduate School, Monterey, CA.
ESTIMATING THE RELATIONSHIPS BETWEEN THE STATE OF THE ART OF TECHNOLOGY AND PRODUCTION COST FOR THE US AIRCRAFT M.S. Thesis
Robert E. Lowe Jun. 1989 80 p
(AD-A212127) Avail: NTIS HC A05/MF A01 CSCL 01/3

The primary objective is to determine relationships that exist between production cost and the state of the art of technology and extensions in technology for high-technology systems. The data sample selected for study was U.S. military tactical aircraft. The central methodology used in the analysis of the aircraft data base includes: the development of measures for the state of the art of technology and the level of technology advance that exists within U.S. fighter and attack aircraft programs; the development of measures for each aircraft program's production cost; and the application of various statistical procedures (regression analysis) to test specific hypotheses and build models to explain the relationships between technology and cost. General conclusion from this study are that significant relationships do in fact exist between aircraft production cost and specific technology measures. GRA

N90-12496# Institute for Defense Analyses, Alexandria, VA.
THE NASA EXPERIENCE IN AERONAUTICAL R AND D: THREE CASE STUDIES WITH ANALYSIS Final Report, Jan. 1985 - May 1987
John S. Langford, III Mar. 1989 227 p
(AD-A211486; AD-E501144; IDA-R-319; IDA/HQ-87-32596)
Avail: NTIS HC A11/MF A01 CSCL 01/1

Recent policy studies have failed to provide adequate guidance for planning and evaluating the nation's program of aeronautical research and development. In particular, the government's use of experimental systems to bridge the gap between laboratory research and operational systems remains controversial. This thesis used retrospective examinations of NASA's work in aircraft noise reduction, powered-lift technology, and hypersonic flight technology to analyze the impact and effectiveness of such programs under four general circumstances that may justify government involvement in a market-driven economy. It concludes that the NASA proof-of-concept program has had mixed results, with technical goals more successfully accomplished than policy goals. The public benefits of the successes, however, far outweigh the costs of the disappointments. The thesis concludes that such demonstration programs in aeronautical research and development should continue, with a series of analytical and institutional changes to couple them more closely with policy goals. GRA

N90-12497* National Aeronautics and Space Administration, Washington, DC.
AERONAUTICAL ENGINEERING: A CONTINUING BIBLIOGRAPHY WITH INDEXES (SUPPLEMENT 245)
Nov. 1989 148 p
(NASA-SP-7037(245); NAS 1.21:7037(245)) Avail: NTIS HC A07; NTIS standing order as PB89-914100, $10.50 domestic, $21.00 foreign CSCL 01B

This bibliography lists 537 reports, articles, and other documents introduced into the NASA scientific and technical information system in October, 1989. Subject coverage includes: design, construction and testing of aircraft and aircraft engines; aircraft components, equipment and systems; ground support systems; and theoretical and applied aspects of aerodynamics and general fluid dynamics. Author

02 AERODYNAMICS

Includes aerodynamics of bodies, combinations, wings, rotors, and control surfaces; and internal flow in ducts and turbomachinery.

For related information see also *34 Fluid Mechanics and Heat Transfer.*

N90-12498*# Eloret Corp., Sunnyvale, CA.
ROTATIONAL AND VIBRATIONAL NONEQUILIBRIUM EFFECTS IN RAREFIED, HYPERSONIC FLOW
Iain D. Boyd 1989 11 p
(Contract NCC2-582)
(NASA-CR-182559; NAS 1.26:182559) Avail: NTIS HC A03/MF A01 CSCL 01A

Results are reported for an investigation into the methods by which energy transfer is calculated in the Direct Simulation Monte Carlo method. Description is made of a recently developed energy exchange model that deals with the translational and rotational modes. A new model for simulating the transfer of energy between the translational and vibrational modes is also explained. This model allows the vibrational relaxation time to follow the temperature dependence predicted by the Landau-Teller theory at moderate temperatures. For temperatures in excess of about 8000K the vibrational model is extended to include an empirical result for the relaxation time. The effect of introducing these temperature dependent collision numbers into the DSMC technique is assessed by making calculations representative of the stagnation streamline of a hypersonic space vehicle. Both thermal and chemical nonequilibrium effects are included while the flow conditions have been chosen such that ionization and radiation may be neglected. The introduction of these new models is found to significantly affect the degree of thermal nonequilibrium observed in the flowfield. Larger, and more widely ranging, differences in the results obtained with the different energy exchange probabilities are found when a significant amount of internal energy is included in the calculation of chemical nonequilibrium. Author

N90-12499*# California Univ., Davis. Dept. of Mechanical Engineering.
NUMERICAL ALGORITHMS FOR STEADY AND UNSTEADY INCOMPRESSIBLE NAVIER-STOKES EQUATIONS Semiannual Status Report, 1 May 1987 - 30 Apr. 1989
Mohammed Hafez and Jennifer Dacles 3 Aug. 1989 28 p
(Contract NCA2-210)
(NASA-CR-186039; NAS 1.26:186039) Avail: NTIS HC A03/MF A01 CSCL 01A

The numerical analysis of the incompressible Navier-Stokes equations are becoming important tools in the understanding of some fluid flow problems which are encountered in research as well as in industry. With the advent of the supercomputers, more realistic problems can be studied with a wider choice of numerical

algorithms. An alternative formulation is presented for viscous incompressible flows. The incompressible Navier-Stokes equations are cast in a velocity/vorticity formulation. This formulation consists of solving the Poisson equations for the velocity components and the vorticity transport equation. Two numerical algorithms for the steady two-dimensional laminar flows are presented. The first method is based on the actual partial differential equations. This uses a finite-difference approximation of the governing equations on a staggered grid. The second method uses a finite element discretization with the vorticity transport equation approximated using a Galerkin approximation and the Poisson equations are obtained using a least squares method. The equations are solved efficiently using Newton's method and a banded direct matrix solver (LINPACK). The method is extended to steady three-dimensional laminar flows and applied to a cubic driven cavity using finite difference schemes and a staggered grid arrangement on a Cartesian mesh. The equations are solved iteratively using a plane zebra relaxation scheme. Currently, a two-dimensional, unsteady algorithm is being developed using a generalized coordinate system. The equations are discretized using a finite-volume approach. This work will then be extended to three-dimensional flows. Author

N90-12500*# Georgia Inst. of Tech., Atlanta. School of Aerospace Engineering.
NUMERICAL SIMULATION OF UNSTEADY ROTATIONAL FLOW OVER PROPFAN CONFIGURATIONS Semiannual Status Report, 1 May - 30 Nov. 1989
R. Srivastava and L. N. Sankar Nov. 1989 33 p Presented at the AIAA 28th Aerospace Sciences Meeting and Exhibit, Reno, NV, 8-11 Jan. 1990
(Grant NAG3-730)
(NASA-CR-186037; NAS 1.26:186037) Avail: NTIS HC A03/MF A01 CSCL 01A

The objective is to develop efficient numerical techniques for the study of aeroelastic response of a propfan in an unsteady transonic flow. A three dimensional unsteady Euler solver is being modified to address this problem. Author

N90-12501# Aeronautical Research Labs., Melbourne (Australia).
ADDITIONS AND CORRECTIONS TO SUPER: A PROGRAM FOR CALCULATING STEADY AND OSCILLATORY SUPERSONIC FLOW OVER A THIN WING, TAIL PLANE AND FIN
I. H. Grundy Apr. 1989 26 p
(AD-A211771; ARL-STRUC-TM-504; DODA-AR-005-591) Avail: NTIS HC A03/MF A01 CSCL 01/1

Changes are described for the computer program SUPER, which correct errors identified in the previous version of the program, and enable the calculation of generalized forces. Tables of generalized forces, calculated using SUPER and other programs, are presented for a standard AGARD configuration. GRA

N90-12502# Centre d'Etudes et de Recherches, Toulouse (France). Dept. d'Etudes et de Recherches en Aerothermodynamique.
HYPERSONIC BOUNDARY LAYERS. VISCOUS EFFECTS WITHIN THE SHOCK LAYER Final Report [COUCHES LIMITES HYPERSONIQUES. EFFETS VISQUEUX DANS LA COUCHE DE CHOC]
B. Aupoix and A. Lafon Dec. 1988 41 p In FRENCH
(Contract DRET-88-002-19)
(CERT-RSF-OA-25/5005-AYD; DERAT-25/5005.13; ETN-89-95277) Avail: NTIS HC A03/MF A01

Experiments on gaseous phenomena in hypersonic boundary layers are described. A calculation method based on an arbitrary gas mixture able to take degassing phenomena into account, and allowing modifications to be made on the thermodynamic properties or transportation properties of the gas mixture, is developed. A method of solving Navier-Stokes problems for two dimensional asymmetric flow is developed. Emphasis is given to the improvement of the numeric scheme to obtain second order precision and to take into account real gas behavior according to a chemical equilibrium hypothesis. ESA

N90-12503*# National Aeronautics and Space Administration. Langley Research Center, Hampton, VA.
RESEARCH IN NATURAL LAMINAR FLOW AND LAMINAR-FLOW CONTROL, PART 1
Jerry N. Hefner, comp. and Frances E. Sabo, comp. Dec. 1987 322 p Symposium held in Hampton, VA, 16-19 Mar. 1987
(NASA-CP-2487-Pt-1; L-16350-Pt-1; NAS 1.55:2487-Pt-1) Avail: NTIS HC A14/MF A02 CSCL 01A

Since the mid 1970's, NASA, industry, and universities have worked together to conduct important research focused at developing laminar flow technology that could reduce fuel consumption for general aviation, commuter, and transport aircraft by as much as 40 to 50 percent. The symposium was planned in view of the recent accomplishments within the areas of laminar flow control and natural laminar flow, and the potential benefits of laminar flow technology to the civil and military aircraft communities in the United States. Included were technical sessions on advanced theory and design tool development; wind tunnel and flight research; transition measurement and detection techniques; low and high Reynolds number research; and subsonic and supersonic research. For individual titles, see N90-12504 through N90-12518.

N90-12504*# Boeing Commercial Airplane Co., Seattle, WA.
LAMINAR FLOW: CHALLENGE AND POTENTIAL
Mark E. Kirchner *In* NASA, Langley Research Center, Research in Natural Laminar Flow and Laminar-Flow Control, Part 1 Dec. 1987 p 25-44 (For primary document see N90-12503 04-02)
Avail: NTIS HC A14/MF A02 CSCL 01A

Commercial air transportation has experienced revolutionary technology advances since WWII. These technology advances have resulted in an explosive growth in passenger traffic. Today, however, many technologies have matured, and maintaining a similar growth rate will be a challenge. A brief history of laminar flow technology and its application to subsonic and supersonic air transportation is presented. Author

N90-12505*# Douglas Aircraft Co., Inc., Long Beach, CA.
LFC: A MATURING CONCEPT
John Morris *In* NASA, Langley Research Center, Research in Natural Laminar Flow and Laminar-Flow Control, Part 1 Dec. 1987 p 45-51 (For primary document see N90-12503 04-02)
(Douglas-Paper-7878) Avail: NTIS HC A14/MF A02 CSCL 01A

The existence of both turbulent and laminar flow was known for a long time, but it was not until the middle of the last century that the first systematic tests with fluids were conducted to establish the physical relationships and governing laws. The importance of turbulent and laminar airflows in aeronautics was recognized as early as the 1930's, but actual laminar flow control (LFC) investigations were not undertaken until the 1940's. This overview briefly touches on some of the historical development of LFC leading up to current activities. It then examines the technical problems being addressed and potential long-term LFC applications. Past and current Douglas activities are examined and the required future testing involving hybrid laminar flow control (HLFC) is discussed. Author

N90-12506*# Lockheed-Georgia Co., Marietta.
LOCKHEED LAMINAR-FLOW CONTROL SYSTEMS DEVELOPMENT AND APPLICATIONS
Roy H. Lange *In* NASA, Langley Research Center, Research in Natural Laminar Flow and Laminar-Flow Control, Part 1 Dec. 1987 p 53-77 (For primary document see N90-12503 04-02)
Avail: NTIS HC A14/MF A02 CSCL 01A

Progress is summarized from 1974 to the present in the practical application of laminar-flow control (LFC) to subsonic transport aircraft. Those efforts included preliminary design system studies of commercial and military transports and experimental investigations leading to the development of the leading-edge flight

test article installed on the NASA JetStar flight test aircraft. The benefits of LFC on drag, fuel efficiency, lift-to-drag ratio, and operating costs are compared with those for turbulent flow aircraft. The current activities in the NASA Industry Laminar-Flow Enabling Technologies Development contract include summaries of activities in the Task 1 development of a slotted-surface structural concept using advanced aluminum materials and the Task 2 preliminary conceptual design study of global-range military hybrid laminar flow control (HLFC) to obtain data at high Reynolds numbers and at Mach numbers representative of long-range subsonic transport aircraft operation. Author

N90-12507*# Cessna Aircraft Co., Wichita, KS.
LAMINAR FLOW: THE CESSNA PERSPECTIVE
Bruce E. Peterman *In* NASA, Langley Research Center, Research in Natural Laminar Flow and Laminar-Flow Control, Part 1 Dec. 1987 p 79-88 (For primary document see N90-12503 04-02)
Avail: NTIS HC A14/MF A02 CSCL 01A

A review of Natural Laminar Flow (NLF) and Laminar-Flow Control activities over the last twenty years at the Cessna Aircraft Company is presented. Expected NLF benefits and remaining challenges are then described. Author

N90-12508*# Analytical Services and Materials, Inc., Hampton, VA.
LONG-RANGE LFC TRANSPORT **c05**
Werner Pfenninger *In* NASA, Langley Research Center, Research in Natural Laminar Flow and Laminar-Flow Control, Part 1 Dec. 1987 p 89-115 (For primary document see N90-12503 04-02)
Avail: NTIS HC A14/MF A02 CSCL 01C

M = 0.83 Laminar Flow Control (LFC) transports, carrying large percentage payloads over a range of 20000 kilometers at cruise L/D's of 39 appear feasible with large space externally braced wings, external fuel pods, active controls, and 70 percent laminar flow on wing and tail surfaces, engine nacelles and struts, and a turbulent fuselage. A combination of a swept-forward inboard and a swept-back outer wing appears superior overall, especially for laminar flow and eliminating leading edge contamination probably caused by flyspecks and ice crystals. Wing divergence appears controllable by a combination of various methods. Wind-mounted superfans with extensive laminar flow on their nacelles appear practical. Their dominant tone noise is below the frequency range of the most strongly amplified TS-waves. Author

N90-12509*# National Aeronautics and Space Administration. Hugh L. Dryden Flight Research Facility, Edwards, CA.
DEVELOPMENT FLIGHT TESTS OF JETSTAR LFC LEADING-EDGE FLIGHT TEST EXPERIMENT **c05**
David F. Fisher and Michael C. Fischer (National Aeronautics and Space Administration. Langley Research Center, Hampton, VA.) *In* NASA, Langley Research Center, Research in Natural Laminar Flow and Laminar-Flow Control, Part 1 Dec. 1987 p 117-140 (For primary document see N90-12503 04-02)
Avail: NTIS HC A14/MF A02 CSCL 01C

The overall objective of the flight tests on the JetStar aircraft was to demonstrate the effectiveness and reliability of laminar flow control under representative flight conditions. One specific objective was to obtain laminar flow on the JetStar leading-edge test articles for the design and off-design conditions. Another specific objective was to obtain operational experience on a Laminar Flow Control (LFC) leading-edge system in a simulated airline service. This included operational experience with cleaning requirements, the effect of clogging, possible foreign object damage, erosion, and the effects of ice particle and cloud encounters. Results are summarized. B.G.

N90-12510*# Douglas Aircraft Co., Inc., Long Beach, CA.
THE RIGHT WING OF THE LEFT AIRPLANE
Arthur G. Powell *In* NASA, Langley Research Center, Research in Natural Laminar Flow and Laminar-Flow Control, Part 1 Dec. 1987 p 141-161 (For primary document see N90-12503 04-02)
Avail: NTIS HC A14/MF A02 CSCL 01A

The NASA Leading-Edge Flight Test (LEFT) program addressed the environmental issues which were potential problems in the application of Laminar Flow Control (LFC) to transport aircraft. These included contamination of the LFC surface due to dirt, rain, insect remains, snow, and ice, in the critical leading-edge region. Douglas Aircraft Company designed and built a test article which was mounted on the right wing of the C-140 JetStar aircraft. The test article featured a retractable leading-edge high-lift shield for contamination protection and suction through perforations on the upper surface for LFC. Following a period of developmental flight testing, the aircraft entered simulated airline service, which included exposure to airborne insects, heavy rain, snow, and icing conditions both in the air and on the ground. During the roughly 3 years of flight testing, the test article has consistently demonstrated laminar flow in cruising flight. The experience with the LEFT experiment was summarized with emphasis on significant test findings. The following items were discussed: test article design and features; suction distribution; instrumentation and transition point reckoning; problems and fixes; system performance and maintenance requirements. Author

N90-12511*# National Aeronautics and Space Administration. Langley Research Center, Hampton, VA.
PERFORMANCE OF LAMINAR-FLOW LEADING-EDGE TEST ARTICLES IN CLOUD ENCOUNTERS **c05**
Richard E. Davis, Dal V. Maddalon, and Richard D. Wagner *In its* Research in Natural Laminar Flow and Laminar-Flow Control, Part 1 Dec. 1987 p 163-193 (For primary document see N90-12503 04-02)
Avail: NTIS HC A14/MF A02 CSCL 01C

An extensive data bank of concurrent measurements of laminar flow (LF), particle concentration, and aircraft charging state was gathered for the first time. From this data bank, 13 flights in the simulated airline service (SAS) portion were analyzed to date. A total of 6.86 hours of data at one-second resolution were analyzed. An extensive statistical analysis, for both leading-edge test articles, shows that there is a significant effect of cloud and haze particles on the extent of laminar flow obtained. Approximately 93 percent of data points simulating LFC flight were obtained in clear air conditions; approximately 7 percent were obtained in cloud and haze. These percentages are consistent with earlier USAF and NASA estimates and results. The Hall laminar flow loss criteria was verified qualitatively. Larger particles and higher particle concentrations have a more marked effect on LF than do small particles. A particle spectrometer of a charging patch are both acceptable as diagnostic indicators of the presence of particles detrimental to laminar flow. Author

N90-12512*# National Aeronautics and Space Administration. Langley Research Center, Hampton, VA.
SIMULATED AIRLINE SERVICE EXPERIENCE WITH LAMINAR-FLOW CONTROL LEADING-EDGE SYSTEMS **c05**
Dal V. Maddalon, David F. Fisher, Lisa A. Jennett (National Aeronautics and Space Administration. Hugh L. Dryden Flight Research Facility, Edwards, CA.), and Michael C. Fischer *In its* Research in Natural Laminar Flow and Laminar-Flow Control, Part 1 Dec. 1987 p 195-218 (For primary document see N90-12503 04-02)
Avail: NTIS HC A14/MF A02 CSCL 01C

The first JetStar leading edge flight test was made November 30, 1983. The JetStar was flown for more than 3 years. The titanium leading edge test articles today remain in virtually the same condition as they were in on that first flight. No degradation of laminar flow performance has occurred as a result of service. The JetStar simulated airline service flights have demonstrated that effective, practical leading edge systems are available for future commercial transports. Specific conclusions based on the results of the simulated airline service test program are summarized. Author

N90-12513*# High Technology Corp., Hampton, VA.
STABILITY THEORY APPLICATIONS TO LAMINAR-FLOW CONTROL

Mujeeb R. Malik *In* NASA, Langley Research Center, Research in Natural Laminar Flow and Laminar-Flow Control, Part 1 Dec. 1987 p 219-244 (For primary document see N90-12503 04-02)
Avail: NTIS HC A14/MF A02 CSCL 01A

In order to design Laminar Flow Control (LFC) configurations, reliable methods are needed for boundary-layer transition predictions. Among the available methods, there are correlations based upon R sub e, shape factors, Goertler number and crossflow Reynolds number. The most advanced transition prediction method is based upon linear stability theory in the form of the e sup N method which has proven to be successful in predicting transition in two- and three-dimensional boundary layers. When transition occurs in a low disturbance environment, the e sup N method provides a viable design tool for transition prediction and LFC in both 2-D and 3-D subsonic/supersonic flows. This is true for transition dominated by either TS, crossflow, or Goertler instability. If Goertler/TS or crossflow/TS interaction is present, the e sup N will fail to predict transition. However, there is no evidence of such interaction at low amplitudes of Goertler and crossflow vortices. B.G.

N90-12514*# Virginia Univ., Charlottesville. Dept. of Engineering Science and Mechanics.
NONPARALLEL STABILITY OF BOUNDARY LAYERS
Ali H. Nayfeh *In* NASA, Langley Research Center, Research in Natural Laminar Flow and Laminar-Flow Control, Part 1 Dec. 1987 p 245-259 (For primary document see N90-12503 04-02)
Avail: NTIS HC A14/MF A02 CSCL 01A

The asymptotic formulations of the nonparallel linear stability of incompressible growing boundary layers are critically reviewed. These formulations can be divided into two approaches. The first approach combines a numerical method with either the method of multiple scales, or the method of averaging, of the Wentzel-Kramers-Brillouin (WKB) approximation; all these methods yield the same result. The second approach combined a multi-structure theory with the method of multiple scales. The first approach yields results that are in excellent agreement with all available experimental data, including the growth rates as well as the neutral stability curve. The derivation of the linear stability of the incompressible growing boundary layers is explained. B.G.

N90-12515*# National Aeronautics and Space Administration. Langley Research Center, Hampton, VA.
INTERACTION OF TOLLMIEN-SCHLICHTING WAVES AND GOERTLER VORTICES
Phil Hall *In its* Research in Natural Laminar Flow and Laminar-Flow Control, Part 1 Dec. 1987 p 261-271 Prepared in cooperation with Exeter Univ., England (For primary document see N90-12503 04-02)
Avail: NTIS HC A14/MF A02 CSCL 01A

There are many fluid flows of practical interest where transition can be caused by competing hydrodynamic instabilities. Thus in three-dimensional boundary-layer flows over curved walls, instability might be caused by Tollmien-Schlichting waves, Goertler vortices or crossflow vortices. If a particular type of instability is suppressed by some means, there is the possibility that another one might be stimulated. Hence it is important to understand the mechanisms by which these different instabilities interact. Some properties of the interaction which can take place between Goertler vortices and Tollmien-Schlichting waves are discussed. Author

N90-12516*# Arizona Univ., Tucson.
BOUNDARY-LAYER RECEPTIVITY AND LAMINAR-FLOW AIRFOIL DESIGN
Edward J. Kerschen *In* NASA, Langley Research Center, Research in Natural Laminar Flow and Laminar-Flow Control, Part 1 Dec. 1987 p 273-287 (For primary document see N90-12503 04-02)
Avail: NTIS HC A14/MF A02 CSCL 01A

Boundary-layer receptivity examines the way in which external disturbances generate instability waves in boundary layers. Receptivity theory is complementary to stability theory, which studies the evolution of disturbances that are already present in the boundary layer. A transition prediction method which combines receptivity with linear stability theory would directly account for the influence of free-stream disturbances and also consider the characteristics of the boundary layer upstream of the neutral stability point. The current e sup N transition prediction methods require empirical correlations for the influence of environmental disturbances, and totally ignore the boundary layer characteristics upstream of the neutral stability point. The regions where boundary-layer receptivity occurs can be separated into two classes, one near the leading edges and the other at the downstream points where the boundary layer undergoes rapid streamwise adjustments. Analyses were developed for both types of regions, and parametric studies which examine the relative importance of different mechanisms were carried out. The work presented here has focused on the low Mach number case. Extensions to high subsonic and supersonic conditions are presently underway. Author

N90-12517*# National Aeronautics and Space Administration. Langley Research Center, Hampton, VA.
GOERTLER INSTABILITY ON AN AIRFOIL
Vijay Kalburgi, Siva M. Mangalam, J. Ray Dagenhart, and S. N. Tiwari (Old Dominion Univ., Norfolk, VA.) *In its* Research in Natural Laminar Flow and Laminar-Flow Control, Part 1 Dec. 1987 p 289-300 (For primary document see N90-12503 04-02)
Avail: NTIS HC A14/MF A02 CSCL 01A

An effective computational scheme was developed to study the growth/damping of Goertler vortices along walls of variable curvature. Computational experiments indicate that when the amplification rates for the u-, v-, and w-perturbations are the same, the finite difference approach to solve the initial value problem and the normal mode approach give identical results for the Blasius boundary layer on constant curvature concave walls. The growth of Goertler vortices was rapid in the concave regions and was followed by sharp damping in the convex region. However, multiple sets of counter-rotating vortices were formed and remained far downstream in the convex region. The current computational scheme can be easily extended to more realistic problems including variable pressure gradients and suction effects. Author

N90-12518*# Virginia Univ., Charlottesville. Dept. of Engineering Science and Mechanics.
EFFECT OF ROUGHNESS ON THE STABILITY OF BOUNDARY LAYERS
Ali H. Nayfeh, Saad A. Ragab, and Ayman Al-Maaitah *In* NASA, Langley Research Center, Research in Natural Laminar Flow and Laminar-Flow Control, Part 1 Dec. 1987 p 301-315 (For primary document see N90-12503 04-02)
Avail: NTIS HC A14/MF A02 CSCL 01A

An analysis is conducted on the effect of imperfections consisting of humps and dips on the stability of incompressible flows over flat plates. The mean flow is calculated using interacting boundary layers. Linear quasiparallel spatial stability is used to calculate the growth rates and mode shapes of two-dimensional disturbances. Then, the amplification factor is computed. A search for the most dangerous frequency is conducted based on an amplification factor of 9 in the shortest distance. Correlations are made with the transition experiment of Walker and Greening using the e sup 9 method. Author

N90-12519*# National Aeronautics and Space Administration. Langley Research Center, Hampton, VA.
RESEARCH IN NATURAL LAMINAR FLOW AND LAMINAR-FLOW CONTROL, PART 2
Jerry N. Hefner, comp. and Frances E. Sabo, comp. Dec. 1987 328 p Symposium held in Hampton, VA, 16-19 Mar. 1987 (NASA-CP-2487-Pt-2; L-16350-Pt-2; NAS 1.55:2487-Pt-2) Avail: NTIS HC A15/MF A02 CSCL 01A

Part 2 of the Symposium proceedings includes papers addressing various topics in basic wind tunnel research/techniques

and computational transitional research. Specific topics include: advanced measurement techniques; laminar flow control; Tollmien-Schlichting wave characteristics; boundary layer transition; flow visualization; wind tunnel tests; flight tests; boundary layer equations; swept wings; and skin friction. For individual titles, see N90-12520 through N90-12538.

N90-12520*# National Aeronautics and Space Administration. Langley Research Center, Hampton, VA.
ADVANCED MEASUREMENT TECHNIQUES, PART 1
Bruce J. Holmes, Debra L. Carraway, Gregory S. Manuel, and Cynthia C. Croom *In its* Research in Natural Laminar Flow and Laminar-Flow Control, Part 2 Dec. 1987 p 317-340 (For primary document see N90-12519 04-02)
Avail: NTIS HC A15/MF A02 CSCL 01A

In modern laminar flow flight and wind tunnel research, it is important to understand the specific cause(s) of laminar to turbulent boundary layer transition. Such information is crucial to the exploration of the limits of practical application of laminar flow for drag reduction on aircraft. The process of transition involves both the possible modes of disturbance growth, and the environmental conditioning of the instabilities by freestream or surface conditions. The possible modes of disturbance growth include viscous, inviscid, and modes which may bypass these natural ones. Theory provides information on the possible modes of disturbance amplification, but experimentation must be relied upon to determine which of those modes actually dominates the transition process in a given environment. The results to date of research on advanced devices and methods used for the study of transition phenomena in the subsonic and transonic flight and wind tunnel environments are presented. Author

N90-12521*# National Aeronautics and Space Administration. Langley Research Center, Hampton, VA.
FLOW QUALITY MEASUREMENTS IN COMPRESSIBLE SUBSONIC FLOWS
P. Calvin Stainback and Charles B. Johnson *In its* Research in Natural Laminar Flow and Laminar-Flow Control, Part 2 Dec. 1987 p 345-357 (For primary document see N90-12519 04-02)
Avail: NTIS HC A15/MF A02 CSCL 01A

The purpose is to re-examine the heat transfer from a hot-wire probe in the compressible subsonic flow regime; describe the three-wire hot-wire probe calibration and data reduction techniques used to measure the velocity, density, and total temperature fluctuation; and present flow quality results obtained in the Langley 0.3 meter Transonic Cryogenic Wind Tunnel and in flight with the NASA JetStar from the same three-wire hot-wire probe. Author

N90-12522*# National Aeronautics and Space Administration. Langley Research Center, Hampton, VA.
HOT-FILM SYSTEM FOR TRANSITION DETECTION IN CRYOGENIC WIND TUNNELS **c09**
Charles B. Johnson, Debra L. Carraway, P. Calvin Stainback, and M. F. Fancher (Douglas Aircraft Co., Inc., Long Beach, CA.) *In its* Research in Natural Laminar Flow and Laminar-Flow Control, Part 2 Dec. 1987 p 358-376 (For primary document see N90-12519 04-02)
Avail: NTIS HC A15/MF A02 CSCL 14B

It is well known that the determination of the location of boundary-layer transition is necessary for the correct interpretation of aerodynamic data in transonic wind tunnels. In the late 1970s the Douglas Aircraft Company developed a vapor deposition hot-film system for transition detection in cryogenic wind tunnels. Tests of the hot-films in a low-speed tunnel demonstrated the ability to obtain on-line transition data with an enhanced simultaneous hot-film data acquisition system. The equipment design and specifications are described. B.G.

N90-12523*# National Aeronautics and Space Administration. Langley Research Center, Hampton, VA.
PREDICTED AND HOT-FILM MEASURED TOLLMIEN-SCHLICHTING WAVE CHARACTERISTICS
John P. Stack, Robert B. Yeaton, and J. Ray Dagenhart *In its* Research in Natural Laminar Flow and Laminar-Flow Control, Part 2 Dec. 1987 p 377-380 (For primary document see N90-12519 04-02)
Avail: NTIS HC A15/MF A02 CSCL 01A

The Tollmien-Schlichting (TS) instability is a time-dependence instability which can lead to transition of laminar boundary layers on airfoils. A comparison of theoretical predictions and experimental observations of the TS instability on the NLF(1)-0414F airfoil designed by Viken and Pfenninger. The theoretical predictions were obtained using the SALLY stability code. Test results, from the same hot films that were used to detect transition, revealed that TS waves could be detected by the hot films if the hot-film signal was adequately modified. Author

N90-12524*# National Aeronautics and Space Administration. Langley Research Center, Hampton, VA.
REMOTE DETECTION OF BOUNDARY-LAYER TRANSITION BY AN OPTICAL SYSTEM **c74**
Robert M. Hall, Medhat Azzazy, and Dariush Modarress (Spectron Development Labs., Inc., Costa Mesa, CA.) *In its* Research in Natural Laminar Flow and Laminar-Flow Control, Part 2 Dec. 1987 p 381-388 (For primary document see N90-12519 04-02)
Avail: NTIS HC A15/MF A02 CSCL 20F

This instrument development program was funded because of the urgent need to measure boundary-layer transition in wind tunnels. In the course of this development program, a prototype was designed, built, and tested. Recent transonic experiments in the Boeing Model Transonic Wind Tunnel show that the interferometer results correlate very well with sublimating chemical tests. Author

N90-12525*# National Aeronautics and Space Administration. Langley Research Center, Hampton, VA.
THREE-COMPONENT LASER DOPPLER VELOCIMETER MEASUREMENTS IN A JUNCTURE FLOW **c36**
L. R. Kubendran and Jim F. Meyers *In its* Research in Natural Laminar Flow and Laminar-Flow Control, Part 2 Dec. 1987 p 389-400 (For primary document see N90-12519 04-02)
Avail: NTIS HC A15/MF A02 CSCL 20E

A single-axis, five-beam, three-component laser velocimeter (LV) system was used in a major experiment. Satisfactory results were obtained with the LV system in the juncture flow. Limited optical access to the tunnel proved to be a problem for the three component LV system in determining the third component. Author

N90-12526*# National Aeronautics and Space Administration. Langley Research Center, Hampton, VA.
BASIC AERODYNAMIC RESEARCH FACILITY FOR COMPARATIVE STUDIES OF FLOW DIAGNOSTIC TECHNIQUES **c09**
Gregory S. Jones, Luther R. Gartrell, and P. Calvin Stainback *In its* Research in Natural Laminar Flow and Laminar-Flow Control, Part 2 Dec. 1987 p 401-406 (For primary document see N90-12519 04-02)
Avail: NTIS HC A15/MF A02 CSCL 14B

Current flow diagnostic research efforts are focusing on higher order flow field data bases, such as those generated by laser velocimetry (LV), hot-wire anemometry, and multi-hole pressure probes. Recent low-speed comparisons of results obtained with LV and hot wires have revealed strengths and weaknesses of each instrument. A seeding study will be initiated to determine particulate tracking ability. B.G.

N90-12527*# National Aeronautics and Space Administration. Langley Research Center, Hampton, VA.
RECENT TESTS AT LANGLEY WITH A UNIVERSITY OF TENNESSEE SPACE INSTITUTE (UTSI) SKIN FRICTION BALANCE **c35**
Pierce L. Lawing, A. D. Vakili, and J. M. Wu (Tennessee Univ. Space Inst., Tullahoma.) *In its* Research in Natural Laminar

Flow and Laminar-Flow Control, Part 2 Dec. 1987 p 407-411 (For primary document see N90-12519 04-02)
Avail: NTIS HC A15/MF A02 CSCL 14B

The experience at LaRC with the University of Tennessee Space Institute skin friction balances is summarized. The Karman-Schoenherr flat plate skin friction formulation is included for comparison. It is concluded that the balance is capable of operation in environments as diverse as cryogenic, transonic, high-shear rate of the 0.3 meter Transonic Cryogenic Tunnel, and high-temperature supersonic environment of the Unitary Plan Wind Tunnel. Proposed new research is outlined. B.G.

N90-12528*# National Aeronautics and Space Administration. Langley Research Center, Hampton, VA.
RECENT FLOW VISUALIZATION STUDIES IN THE 0.3-m TCT
c09
Walter L. Snow, Alpheus W. Burner, and William K. Goad *In its* Research in Natural Laminar Flow and Laminar-Flow Control, Part 2 Dec. 1987 p 412-419 (For primary document see N90-12519 04-02)
Avail: NTIS HC A15/MF A02 CSCL 14B

Light beams are altered by refractive index changes; flow induced refractive index changes provide the impetus for conventional visualization techniques such as schlieren and shadowgraph. Unfortunately effects related to the flow can be masked by refractive index inhomogeneities external to the test section. A simple shadowgraph scheme was used to assess the flow quality of the Langley 0.3 meter Transonic Cryogenic Tunnel. When the penetration tubes were evacuated the quality of the shadowgraph improved dramatically. B.G.

N90-12529*# National Aeronautics and Space Administration. Langley Research Center, Hampton, VA.
EXPERIMENTAL STUDIES ON GOERTLER VORTICES
Siva M. Mangalam (Analytical Services and Materials, Inc., Hampton, VA.), J. Ray Dagenhart, and Jim F. Meyers *In its* Research in Natural Laminar Flow and Laminar-Flow Control, Part 2 Dec. 1987 p 421-433 (For primary document see N90-12519 04-02)
Avail: NTIS HC A15/MF A02 CSCL 01A

Goertler vortices arise in laminar boundary layers along concave walls due to an imbalance between pressure and centrifugal forces. In advanced laminar-flow control (LFC) supercritical airfoil designs, boundary-layer suction is primarily used to control Tollmien-Schlichting instability and c ccross-flow vortices in the concave region near the leading edge of the airfoil lower surface. The concave region itself is comprised of a number of linear segments positioned to limit the total growth of Goertler vortices. Such an approach is based on physical reasonings but rigorous theoretical justification or experimental evidence to support such an approach does not exist. An experimental project was initiated at NASA Langley to verify this concept. In the first phase of the project an experiment was conducted on an airfoil whose concave region has a continuous curvature distribution. Some results of this experiment were previously reported and significant features are summarized. Author

N90-12530*# Lockheed-Georgia Co., Marietta.
AN EXPERIMENTAL EVALUATION OF SLOTS VERSUS POROUS STRIPS FOR LAMINAR-FLOW APPLICATIONS
Kenneth C. Cornelius *In* NASA, Langley Research Center, Research in Natural Laminar Flow and Laminar-Flow Control, Part 2 Dec. 1987 p 435-451 (For primary document see N90-12519 04-02)
Avail: NTIS HC A15/MF A02 CSCL 01A

Detailed mean velocity and disturbance amplitude measurements were conducted in a Blasius boundary-layer flow with wall suction applied at three downstream locations. The main emphasis was a direct comparison of the growth rate of the instability wave with discrete spanwise slots versus wide porous strips. The results demonstrate that the local effects of suction through slots or very narrow porous strips have a greater beneficial effect on the stability of the boundary-layer flow relative to the suction influence of a wide porous strip. Codes which use continuous suction for the growth rates of the instability waves to determine the suction quantities for a multiple series of slots will be quite conservative in the estimation of the suction quantity. Guidelines were provided for suction-chamber design and flow rates to minimize internal oscillations which propagate into the boundary-layer flow. Author

N90-12531*# National Aeronautics and Space Administration. Langley Research Center, Hampton, VA.
RESULTS OF LFC EXPERIMENT ON SLOTTED SWEPT SUPERCRITICAL AIRFOIL IN LANGLEY'S 8-FOOT TRANSONIC PRESSURE TUNNEL
Cuyler W. Brooks, Jr. and Charles D. Harris *In its* Research in Natural Laminar Flow and Laminar-Flow Control, Part 2 Dec. 1987 p 453-469 (For primary document see N90-12519 04-02)
Avail: NTIS HC A15/MF A02 CSCL 01A

A large chord swept supercritical laminar-flow control (LFC) airfoil was designed, constructed, and tested in the Langley 8-foot Transonic Pressure Tunnel (TPT). The LFC airfoil experiment was established to provide basic information concerning the design and compatibility of high performance supercritical airfoils with suction boundary-layer control achieved through fine slots or porous surface concepts. Shockless pressure distribution was achieved. Full chord laminar flow was achieved on upper and lower surfaces. Full chord laminar flow was maintained at subcritical speeds and over large supercritical zones. Feasibility of combined suction laminarization and supercritical airfoil techology was demonstrated. B.G.

N90-12532*# National Aeronautics and Space Administration. Langley Research Center, Hampton, VA.
BOUNDARY-LAYER STABILITY ANALYSIS OF LANGLEY RESEARCH CENTER 8-FOOT LFC EXPERIMENTAL DATA
Scott Berry (Analytical Services and Materials, Inc., Hampton, VA.), J. Ray Dagenhart, Cuyler W. Brooks, Jr., and Charles D. Harris *In its* Research in Natural Laminar Flow and Laminar-Flow Control, Part 2 Dec. 1987 p 471-489 (For primary document see N90-12519 04-02)
Avail: NTIS HC A15/MF A02 CSCL 01A

An analytical study of linear-amplifying instabilities of a laminar boundary layer as found in the experimental data of the LaRC/8-foot laminar-flow control (LFC) experiment was completed and the results are presented. The LFC airfoil used for this experiment was a swept, supercritical design which removed suction air through spanwise slots. The amplification of small disturbances by linear processes on a swept surface such as this can be due to either Tollmien-Schlichting (TS) and/or crossflow (CF) mechanisms. This study consists of the examination of these two instabilities by both the commonly used incompressible (SALLY and MARIA) analysis and the more involved compressible (COSAL) analysis. A wide range of experimental test conditions with variations in Mach number, Reynolds number, and suction distributions were available for this study. Experimentally determined transition locations were found from thin-film techniques and were used to correlate the n-factors at transition for the range of test cases. Author

N90-12533*# National Aeronautics and Space Administration. Langley Research Center, Hampton, VA.
SENSITIVITY OF LFC TECHNIQUES IN THE NON-LINEAR REGIME
Dennis M. Bushnell, M. Y. Hussaini (Institute for Computer Applications in Science and Engineering, Hampton, VA.), and Tom A. Zang *In its* Research in Natural Laminar Flow and Laminar-Flow Control, Part 2 Dec. 1987 p 491-516 (For primary document see N90-12519 04-02)
Avail: NTIS HC A15/MF A02 CSCL 01A

For all the Laminar Flow Control (LFC) techniques examined, finite-amplitude effects are destabilizing, i.e., finite-amplitude 2-D Tollmien-Schlichting (TS) waves grow faster than predicted by linear theory. It was also found, in direct contrast to the results from

linear theory for low-amplitude waves, that temperature fluctuations exert a further destabilizing influence on finite amplitude 2-D TS waves. The controlled boundary layers are, of course, subject to intense 3-D secondary instabilities. The instantaneous growth rates of both the fundamental and subharmonic instabilities are strongly tied to the amplitude of the primary 2-D wave. The principal finite-amplitude effects upon the 3-D secondary instabilities occur through the faster growth of the 2-D waves. Author

N90-12534*# National Aeronautics and Space Administration. Langley Research Center, Hampton, VA.

NUMERICAL SOLUTIONS OF THE COMPRESSIBLE 3-D BOUNDARY-LAYER EQUATIONS FOR AEROSPACE CONFIGURATIONS WITH EMPHASIS ON LFC

Julius E. Harris, Venkit Iyer, and Samir Radwan (High Technology Corp., Hampton, VA.) *In its* Research in Natural Laminar Flow and Laminar-Flow Control, Part 2 Dec. 1987 p 517-545 (For primary document see N90-12519 04-02)

Avail: NTIS HC A15/MF A02 CSCL 01A

The application of stability theory in Laminar Flow Control (LFC) research requires that density and velocity profiles be specified throughout the viscous flow field of interest. These profile values must be as numerically accurate as possible and free of any numerically induced oscillations. Guidelines for the present research project are presented: develop an efficient and accurate procedure for solving the 3-D boundary layer equation for aerospace configurations; develop an interface program to couple selected 3-D inviscid programs that span the subsonic to hypersonic Mach number range; and document and release software to the LFC community. The interface program was found to be a dependable approach for developing a user friendly procedure for generating the boundary-layer grid and transforming an inviscid solution from a relatively coarse grid to a sufficiently fine boundary-layer grid. The boundary-layer program was shown to be fourth-order accurate in the direction normal to the wall boundary and second-order accurate in planes parallel to the boundary. The fourth-order accuracy allows accurate calculations with as few as one-fifth the number of grid points required for conventional second-order schemes. B.G.

N90-12535*# National Aeronautics and Space Administration. Langley Research Center, Hampton, VA.

THEORETICAL METHODS AND DESIGN STUDIES FOR NLF AND HLFC SWEPT WINGS AT SUBSONIC AND SUPERSONIC SPEEDS

Suresh H. Goradia (Vigyan Research Associates, Inc., Hampton, VA.) and Harry L. Morgan, Jr. *In its* Research in Natural Laminar Flow and Laminar-Flow Control, Part 2 Dec. 1987 p 547-575 (For primary document see N90-12519 04-02)

Avail: NTIS HC A15/MF A02 CSCL 01A

Laminarization of the boundary layer on the surface of aircraft wings can be accomplished by the use of concepts such as Natural Laminar Flow (NLF), Laminar-Flow Control (LFC), and Hybrid Laminar-Flow Control (HLFC). Several integral boundary-layer methods were developed for the prediction of laminar, transition, and separating turbulent boundary layers. These methods were developed for use at either subsonic or supersonic speeds, have small computer execution times, and are simple to use. The theoretical equations and assumptions which form the basis of the boundary-layer method, are briefly outlined and the results of several correlation cases with exciting experimental data are presented. B.G.

N90-12536*# Colorado Univ., Boulder. Dept. of Aerospace Engineering Sciences.

NUMERICAL EXPERIMENTS ON TRANSITION CONTROL IN WALL-BOUNDED SHEAR FLOWS

S. Biringen and M. J. Caruso *In* NASA, Langley Research Center, Research in Natural Laminar Flow and Laminar-Flow Control, Part 2 Dec. 1987 p 577-592 (For primary document see N90-12519 04-02)

Avail: NTIS HC A15/MF A02 CSCL 01A

Results are presented from a numerical simulation of transition control in plane channel and boundary layer flows. The analysis is based on a pseudo-spectral/finite difference semi-implicit solution procedure employed to numerically integrate the time-dependent, three-dimensional, incompressible Navier-Stokes equations in a doubly periodic domain. In the channel flow, it was found that the active periodic suction/blowing method was effective in controlling strongly three-dimensional disturbances. In the boundary layer, the preliminary analysis indicated that in the early stages, passive control by suction is as effective as active control to suppress instabilities. The current work is focused on a detailed comparison of active and passive control by suction/blowing in the boundary layer. Author

N90-12537*# National Aeronautics and Space Administration. Langley Research Center, Hampton, VA.

APPLICATION OF SOUND AND TEMPERATURE TO CONTROL BOUNDARY-LAYER TRANSITION

Lucio Maestrello, Paresh Parikh, A. Bayliss (Northwestern Univ., Evanston, IL.), L. S. Huang, and T. D. Bryant *In its* Research in Natural Laminar Flow and Laminar-Flow Control, Part 2 Dec. 1987 p 593-616 (For primary document see N90-12519 04-02)

Avail: NTIS HC A15/MF A02 CSCL 01A

The growth and decay of a wave packet convecting in a boundary layer over a concave-convex surface and its active control by localized surface heating are studied numerically using direct computations of the Navier-Stokes equations. The resulting sound radiations are computed using linearized Euler equations with the pressure from the Navier-Stokes solution as a time-dependent boundary condition. It is shown that on the concave portion the amplitude of the wave packet increases and its bandwidth broadens while on the convex portion some of the components in the packet are stabilized. The pressure field decays exponentially away from the surface and then algebraically, exhibiting a decay characteristic of acoustic waves in two dimensions. The far-field acoustic behavior exhibits a super-directivity type of behavior with a beaming downstream. Active control by surface heating is shown to reduce the growth of the wave packet but have little effect on acoustic far field behavior for the cases considered. Active control by sound emanating from the surface of an airfoil in the vicinity of the leading edge is experimentally investigated. The purpose is to control the separated region at high angles of attack. The results show that injection of sound at shedding frequency of the flow is effective in an increase of lift and reduction of drag. Author

N90-12538*# PRC Kentron, Inc., Hampton, VA.

NEAR-FIELD NOISE PREDICTIONS OF AN AIRCRAFT IN CRUISE **c71**

John W. Rawls, Jr. *In* NASA, Langley Research Center, Research in Natural Laminar Flow and Laminar-Flow Control, Part 2 Dec. 1987 p 617-636 (For primary document see N90-12519 04-02)

Avail: NTIS HC A15/MF A02 CSCL 20A

The physics of the coupling of sound waves with the boundary layer is not yet well understood. It is believed, however, that for effective coupling of the sound waves and instability waves in the boundary layer, a matching of both frequency and wave number must occur. This requires that the sound field be accurately defined in both space and time. Currently analytical prediction methods lack sufficient accuracy to predict the noise levels from components of a turbofan engine. Although empirical methods do not yield the detail required for an analysis of the receptivity of sound by a boundary layer, valuable insight can be gained as to the changes in noise levels that might be expected under various operating conditions and aircraft configurations. Author

N90-12539*# National Aeronautics and Space Administration. Langley Research Center, Hampton, VA.

RESEARCH IN NATURAL LAMINAR FLOW AND LAMINAR-FLOW CONTROL, PART 3

Jerry N. Hefner, comp. and Frances E. Sabo, comp. Dec. 1987 399 p Symposium held in Hampton, VA, 16-19 Mar. 1987

(NASA-CP-2487-Pt-3; L-16350-Pt-3; NAS 1.55:2487-Pt-3) Avail: NTIS HC A17/MF A03 CSCL 01A

Part 3 of the Symposium proceedings contains papers addressing advanced airfoil development, flight research experiments, and supersonic transition/laminar flow control research. Specific topics include the design and testing of natural laminar flow (NLF) airfoils, NLF wing gloves, and NLF nacelles; laminar boundary-layer stability over fuselage forebodies; the design of low noise supersonic/hypersonic wind tunnels; and boundary layer instability mechanisms on swept leading edges at supersonic speeds. For individual titles, see N90-12540 through N90-12559.

N90-12540*# National Aeronautics and Space Administration. Langley Research Center, Hampton, VA.

DESIGN OF THE LOW-SPEED NLF(1)-0414F AND THE HIGH-SPEED HSNLF(1)-0213 AIRFOILS WITH HIGH-LIFT SYSTEMS

Jeffrey K. Viken, Sally A. Watson-Viken, Werner Pfenninger (Analytical Services and Materials, Inc., Hampton, VA.), Harry L. Morgan, Jr., and Richard L. Campbell *In its* Research in Natural Laminar Flow and Laminar-Flow Control, Part 3 Dec. 1987 p 637-671 (For primary document see N90-12539 04-02)

Avail: NTIS HC A17/MF A03 CSCL 01A

The design and testing of Natural Laminar Flow (NLF) airfoils is examined. The NLF airfoil was designed for low speed, having a low profile drag at high chord Reynolds numbers. The success of the low speed NLF airfoil sparked interest in a high speed NLF airfoil applied to a single engine business jet with an unswept wing. Work was also conducted on the two dimensional flap design. The airfoil was decambered by removing the aft loading, however, high design Mach numbers are possible by increasing the aft loading and reducing the camber overall on the airfoil. This approach would also allow for flatter acceleration regions which are more stabilizing for cross flow disturbances. Sweep could then be used to increase the design Mach number to a higher value also. There would be some degradation of high lift by decambering the airfoil overall, and this aspect would have to be considered in a final design. E.R.

N90-12541*# National Aeronautics and Space Administration. Langley Research Center, Hampton, VA.

WIND TUNNEL RESULTS OF THE LOW-SPEED NLF(1)-0414F AIRFOIL

Daniel G. Murri, Robert J. McGhee, Frank L. Jordan, Jr., Patrick J. Davis, and Jeffrey K. Viken (Mandex, Inc., Falls Church, VA.) *In its* Research in Natural Laminar Flow and Laminar-Flow Control, Part 3 Dec. 1987 p 673-696 (For primary document see N90-12539 04-02)

Avail: NTIS HC A17/MF A03 CSCL 01A

The large performance gains predicted for the Natural Laminar Flow (NLF)(1)-0414F airfoil were demonstrated in two-dimensional airfoil tests and in wind tunnel tests conducted with a full scale modified Cessna 210. The performance gains result from maintaining extensive areas of natural laminar flow, and were verified by flight tests conducted with the modified Cessna. The lift, stability, and control characteristics of the Cessna were found to be essentially unchanged when boundary layer transition was fixed near the wing leading edge. These characteristics are very desirable from a safety and certification view where premature boundary layer transition (due to insect contamination, etc.) must be considered. The leading edge modifications were found to enhance the roll damping of the Cessna at the stall, and were therefore considered effective in improving the stall/departure resistance. Also, the modifications were found to be responsible for only minor performance penalties. Author

N90-12542*# National Aeronautics and Space Administration. Langley Research Center, Hampton, VA.

WIND TUNNEL RESULTS OF THE HIGH-SPEED NLF(1)-0213 AIRFOIL

William G. Sewall, Robert J. McGhee, David E. Hahne, and Frank L. Jordan, Jr. *In its* Research in Natural Laminar Flow and Laminar-Flow Control, Part 3 Dec. 1987 p 697-726 (For primary document see N90-12539 04-02)

Avail: NTIS HC A17/MF A03 CSCL 01A

Wind tunnel tests were conducted to evaluate a natural laminar flow airfoil designed for the high speed jet aircraft in general aviation. The airfoil, designated as the High Speed Natural Laminar Flow (HSNLF)(1)-0213, was tested in two dimensional wind tunnels to investigate the performance of the basic airfoil shape. A three dimensional wing designed with this airfoil and a high lift flap system is also being evaluated with a full size, half span model. Author

N90-12543*# Boeing Military Airplane Development, Seattle, WA.

DESIGN AND TEST OF A NATURAL LAMINAR FLOW/LARGE REYNOLDS NUMBER AIRFOIL WITH A HIGH DESIGN CRUISE LIFT COEFFICIENT

C. E. Kolesar *In* NASA, Langley Research Center, Research in Natural Laminar Flow and Laminar-Flow Control, Part 3 Dec. 1987 p 727-751 (For primary document see N90-12539 04-02)

Avail: NTIS HC A17/MF A03 CSCL 01A

Research activity on an airfoil designed for a large airplane capable of very long endurance times at a low Mach number of 0.22 is examined. Airplane mission objectives and design optimization resulted in requirements for a very high design lift coefficient and a large amount of laminar flow at high Reynolds number to increase the lift/drag ratio and reduce the loiter lift coefficient. Natural laminar flow was selected instead of distributed mechanical suction for the measurement technique. A design lift coefficient of 1.5 was identified as the highest which could be achieved with a large extent of laminar flow. A single element airfoil was designed using an inverse boundary layer solution and inverse airfoil design computer codes to create an airfoil section that would achieve performance goals. The design process and results, including airfoil shape, pressure distributions, and aerodynamic characteristics are presented. A two dimensional wind tunnel model was constructed and tested in a NASA Low Turbulence Pressure Tunnel which enabled testing at full scale design Reynolds number. A comparison is made between theoretical and measured results to establish accuracy and quality of the airfoil design technique. Author

N90-12544*# National Aeronautics and Space Administration. Langley Research Center, Hampton, VA.

DESIGN AND TEST OF AN NLF WING GLOVE FOR THE VARIABLE-SWEEP TRANSITION FLIGHT EXPERIMENT c05

Ed G. Waggoner, Richard L. Campbell, Pam S. Phillips, and James B. Hallissy *In its* Research in Natural Laminar Flow and Laminar-Flow Control, Part 3 Dec. 1987 p 753-776 (For primary document see N90-12539 04-02)

Avail: NTIS HC A17/MF A03 CSCL 01C

Gloves for M = 0.7 and 0.8 design points were computationally designed and analyzed at conditions over the proposed flight test envelope. The resulting computational pressure distributions were analyzed in a boundary layer stability code. These results indicate that the available pressure distributions offer a wide range of combinations of cross flow and Tollmien-Schlichting N-factors. The glove designs along with the baseline configuration were tested in an entry into the National Transonic Facility. Analysis of the force and moment data showed no significant differences in the performance and stability and control characteristics between the baseline and gloved configurations. The rolling moment constraint was met over the entire flight test envelope for the gloved configuration. Pressure distributions for the NTF test confirmed the design pressure distributions were achieved. However, it was decided that with minor modifications to the inboard region of the glove, useful available data could be significantly increased by adding another row of pressure orifices at span station 167. Author

N90-12545*# National Aeronautics and Space Administration. Langley Research Center, Hampton, VA.
THE DESIGN OF AN AIRFOIL FOR A HIGH-ALTITUDE, LONG-ENDURANCE REMOTELY PILOTED VEHICLE c05
Mark D. Maughmer (Pennsylvania State Univ., University Park.) and Dan M. Somers *In its* Research in Natural Laminar Flow and Laminar-Flow Control, Part 3 Dec. 1987 p 777-794 (For primary document see N90-12539 04-02)
Avail: NTIS HC A17/MF A03 CSCL 01C

Airfoil design efforts are studied. The importance of integrating airfoil and aircraft designs was demonstrated. Realistic airfoil data was provided to aid future high altitude, long endurance aircraft preliminary design. Test cases were developed for further validation of the Eppler program. Boundary layer, not pressure distribution or shape, was designed. Substantial improvement was achieved in vehicle performance through mission specific airfoil designed utilizing the multipoint capability of the Eppler program. Author

N90-12546*# Boeing Commercial Airplane Co., Seattle, WA.
THE 757 NLF GLOVE FLIGHT TEST RESULTS c05
L. Jim Runyan, G. W. Bielak, R. A. Behbehani, A. W. Chen, and Roger A. Rozendaal *In* NASA, Langley Research Center, Research in Natural Laminar Flow and Laminar-Flow Control, Part 3 Dec. 1987 p 795-818 (For primary document see N90-12539 04-02)
Avail: NTIS HC A17/MF A03 CSCL 01C

A major concern in the application of a laminar flow wing design to commercial transports is whether laminar flow can be sustained in the presence of the noise environment due to wing mounted turbofan engines. To investigate this issue, a flight test program was conducted using the Boeing 757 flight research airplane with a portion of the wing modified to obtain natural laminar flow. The flight test had two primary objectives. The first was to measure the noise levels on the upper and lower surface of the wing for a range of flight conditions. The second was to investigate the effect of engine noise on laminar boundary layer transition. The noise field on the wing and transition location on the glove were then measured as a function of the engine power setting at a given flight condition. The transition and noise measurement on the glove show that there is no apparent effect of engine noise on the upper surface transition location. On the lower surface, the transition location moved forward 2 to 3 percent chord. A boundary layer stability analysis to the flight data showed that cross flow disturbances were the dominant cause of transition at most flight conditions. Author

N90-12547*# National Aeronautics and Space Administration. Hugh L. Dryden Flight Research Facility, Edwards, CA.
F-14 VSTFE AND RESULTS OF THE CLEANUP FLIGHT TEST PROGRAM c05
Robert R. Meyer, Bianca M. Trujillo, and Dennis W. Bartlett (National Aeronautics and Space Administration. Langley Research Center, Hampton, VA.) *In* NASA, Langley Research Center, Research in Natural Laminar Flow and Laminar-Flow Control, Part 3 Dec. 1987 p 819-844 (For primary document see N90-12539 04-02)
Avail: NTIS HC A17/MF A03 CSCL 01C

Flight transition data applicable to swept wings at high subsonic speeds are needed to make valid assessments of the potential for natural laminar flow or laminar flow control for transports of various sizes at various cruise speeds. NASA initiated the variable sweep transition flight experiment (VSTFE) to help establish a boundary layer transition data base for use in laminar flow wing design. The carrier vehicle for this experiment is an F-14, which has variable sweep capability. The variable sweep outer panels of the F-14 were modified with natural laminar flow gloves to provide not only smooth surfaces but also airfoils that can produce a wide range of pressure distributions for which transition location can be determined. The VSTFE program is briefly described and some preliminary glove I flight results are presented. Author

N90-12548*# Boeing Commercial Airplane Co., Seattle, WA.
VARIABLE-SWEEP TRANSITION FLIGHT EXPERIMENT (VSTFE): STABILITY CODE DEVELOPMENT AND CLEAN-UP GLOVE DATA ANALYSIS c05
Roger A. Rozendaal *In* NASA, Langley Research Center, Research in Natural Laminar Flow and Laminar-Flow Control, Part 3 Dec. 1987 p 845-859 (For primary document see N90-12539 04-02)
Avail: NTIS HC A17/MF A03 CSCL 01C

The primary objective of the Variable Sweep Transition Flight Experiment (VSTFE) was to establish an improved swept wing transition criterion. The development of the Unified Stability System gave a way of quickly examining disturbance growth for a wide variety of laminar boundary layers. The disturbance growth traces shown are too scattered to define a transition criteria to replace the F-111 data band, which has been used successfully to design NLF gloves. Still, a careful review of the clean-up glove data may yield cases for which the transition location is known more accurately. Liquid crystal photographs of the clean-up glove show much spanwise variation in the transition front for some conditions, and this further complicates the analyses. Several high quality cases are needed in which the transition front is well defined and at a relatively constant chordwise station. Author

N90-12549*# National Aeronautics and Space Administration. Langley Research Center, Hampton, VA.
EXPERIMENTAL AND NUMERICAL ANALYSES OF LAMINAR BOUNDARY-LAYER FLOW STABILITY OVER AN AIRCRAFT FUSELAGE FOREBODY
Paul M. H. W. Vijgen (Kansas Univ., Lawrence.) and Bruce J. Holmes *In its* Research in Natural Laminar Flow and Laminar-Flow Control, Part 3 Dec. 1987 p 861-886 (For primary document see N90-12539 04-02)
Avail: NTIS HC A17/MF A03 CSCL 01A

Fuelled by a need to reduce viscous drag of airframes, significant advances have been made in the last decade to design lifting surface geometries with considerable amounts of laminar flow. In contrast to the present understanding of practical limits for natural laminar flow over lifting surfaces, limited experimental results are available examining applicability of natural laminar flow over axisymmetric and nonaxisymmetric fuselage shapes at relevantly high length Reynolds numbers. The drag benefits attainable by realizing laminar flow over nonlifting aircraft components such as fuselages and nacelles are shown. A flight experiment to investigate transition location and transition mode over the forward fuselage of a light twin engine propeller driven airplane is examined. Author

N90-12550*# National Aeronautics and Space Administration. Langley Research Center, Hampton, VA.
STATUS REPORT ON A NATURAL LAMINAR-FLOW NACELLE FLIGHT EXPERIMENT Abstract Only c05
Earl C. Hastings, Jr., G. K. Faust, Parma Mungur, Clifford J. Obara, S. S. Dodbele, James A. Schoenster, and Michael G. Jones (PRC Kentron, Inc., Hampton, VA.) *In its* Research in Natural Laminar Flow and Laminar-Flow Control, Part 3 Dec. 1987 p 887-890 (For primary document see N90-12539 04-02)
Avail: NTIS HC A17/MF A03 CSCL 01C

The natural laminar flow (NLF) nacelle experiment is part of a drag reduction production program, and has the dual objectives of studying the extent of NLF on full scale nacelles in a flight environment and the effect of acoustic disturbance on the location of transition on the nacelle surface. The experiment is being conducted in two phases: (1) an NLF fairing was flown on a full scale Citation nacelle to develop the experiment technique and establish feasibility; (2) full scale, flow through, NLF nacelles located below the right wing of an experimental NASA OV-1 aircraft are evaluated. The measurements of most interest are the static pressure distribution and transition location on the nacelle surface, and the fluctuating pressure levels associated with the noise sources. Data are collected in combinations of acoustic frequencies and sound pressure levels. The results of phase 2 tests to date indicate that on shape GE2, natural laminar flow was maintained

as far aft as the afterbody joint at 50 percent of the nacelle length. An aft facing step at this joint caused premature transition at this station. No change was observed in the transition pattern when the noise sources were operated. Author

N90-12551*# General Electric Co., Cincinnati, OH.
NACELLE DESIGN **c05**
G. K. Faust and Parma Mungur *In* NASA, Langley Research Center, Research in Natural Laminar Flow and Laminar-Flow Control, Part 3 Dec. 1987 p 891-907 (For primary document see N90-12539 04-02)
Avail: NTIS HC A17/MF A03 CSCL 01C

The external cowlings of engine nacelles on large turbofan powered aircraft are good candidates for application of natural laminar flow. These nacelles usually have shorter characteristic lengths than other candidate surfaces such as wings and fuselages and therefore have lower characteristic Reynolds numbers. A conceptive figure of the natural flow nacelle (NLF) is shown. On the typical nacelle the flow accelerates to a curvature induced velocity peak near the lip and then decelerates over the remainder of the nacelle length. Transition occurs near the start of the deceleration, so turbulent flow with high friction coefficient exists over most of the nacelle length. On the other hand, the NLF nacelle is contoured to have an accelerating flow over most of its length, so transition is delayed, and a relatively lower friction drag exists over most of the nacelle. The motivation for development of the LFN is a potential 40 to 50 percent reduction in nacelle friction drag. Author

N90-12552*# PRC Kentron, Inc., Hampton, VA.
NACELLE AERODYNAMIC PERFORMANCE **c05**
Clifford J. Obara and S. S. Dodbele (Vigyan Research Associates, Inc., Hampton, VA.) *In* NASA, Langley Research Center, Research in Natural Laminar Flow and Laminar-Flow Control, Part 3 Dec. 1987 p 908-913 (For primary document see N90-12539 04-02)
Avail: NTIS HC A17/MF A03 CSCL 01C

The boundary layer transition location was measured on a nacelle shape using the sublimating chemical flow visualization technique. This technique involves coating the surface with a thin film of volatile chemical solid, which, during exposure to a free stream airflow, rapidly sublimates in the turbulent boundary layer as a result of high shear stress and high mass transfer near the surface. Transition is indicated because the chemical coating remains relatively unaffected in the laminar region due to lower shear and low mass transfer. The slow response time of the chemical in a laminar boundary allowed for two test conditions during the same flight. The aircraft was first flown at the desired airspeed and altitude with the noise source off. Once a pattern had developed, the noise source was turned on to the desired setting and a new chemical pattern was sought. In this fashion a direct comparison of the effect of the noise could be determined. Author

N90-12553*# National Aeronautics and Space Administration. Langley Research Center, Hampton, VA.
EFFECTS OF ACOUSTIC SOURCES **c71**
James A. Schoenster and Michael G. Jones (PRC Kentron, Inc., Hampton, VA.) *In its* Research in Natural Laminar Flow and Laminar-Flow Control, Part 3 Dec. 1987 p 914-921 (For primary document see N90-12539 04-02)
Avail: NTIS HC A17/MF A03 CSCL 20A

An experiment was conducted to determine the effect of acoustics on the laminar flow on the side of a nacelle. A flight test was designed to meet this goal and a brief review of the purpose is given. A nacelle with a significant length of laminar flow was mounted on the wing of NASA OV-1. Two noise sources are also mounted on the wing: one in the center body of the nacelle; the second in a wing mounted pod outboard of the nacelle. These two noise sources allow for a limited study of the effect of source direction in addition to control of the acoustic level and frequency. To determine the range of Tollmien-Schlichting frequencies, a stability analysis using the pressure coefficient distribution along the side of the nacelle was performed. Then by applying these frequencies and varying the acoustic level, a study of the receptivity of the boundary layer to the acoustic signal, as determined by the shortening of the length of laminar flow, was conducted. Results are briefly discussed. Author

N90-12554*# National Aeronautics and Space Administration. Langley Research Center, Hampton, VA.
SUPERSONIC LAMINAR-FLOW CONTROL
Dennis M. Bushnell and Mujeeb R. Malik (High Technology Corp., Hampton, VA.) *In its* Research in Natural Laminar Flow and Laminar-Flow Control, Part 3 Dec. 1987 p 923-946 (For primary document see N90-12539 04-02)
Avail: NTIS HC A17/MF A03 CSCL 01A

Detailed, up to date systems studies of the application of laminar flow control (LFC) to various supersonic missions and/or vehicles, both civilian and military, are not yet available. However, various first order looks at the benefits are summarized. The bottom line is that laminar flow control may allow development of a viable second generation SST. This follows from a combination of reduced fuel, structure, and insulation weight permitting operation at higher altitudes, thereby lowering sonic boom along with improving performance. The long stage lengths associated with the emerging economic importance of the Pacific Basin are creating a serious and renewed requirement for such a vehicle. Supersonic LFC techniques are discussed. Author

N90-12555*# National Aeronautics and Space Administration. Langley Research Center, Hampton, VA.
DESIGN AND FABRICATION REQUIREMENTS FOR LOW NOISE SUPERSONIC/HYPERSONIC WIND TUNNELS **c09**
Ivan E. Beckwith, Fang-Jeng Chen, and Mujeeb R. Malik (High Technology Corp., Hampton, VA.) *In its* Research in Natural Laminar Flow and Laminar-Flow Control, Part 3 Dec. 1987 p 947-964 (For primary document see N90-12539 04-02)
Avail: NTIS HC A17/MF A03 CSCL 14B

A schematic diagram of the new proposed Supersonic Low Disturbance Tunnel (SLDT) is shown. Large width two dimensional rapid expansion nozzles guarantee wide quiet test cores that are well suited for testing models at large angle of attack and for swept wings. Hence, this type of nozzle will be operated first in the new proposed large scale SLDT. Test results indicate that the surface finish of pilot nozzles is critical. The local roughness Reynolds number criteria R sub k is approx. = 10 will be used to specify allowable roughness on new pilot nozzles and the new proposed tunnel. Experimental data and calculations for M = 3.0, 3.5, and 5.0 nozzles give N-factors from 6 to 10 for transition caused by Goertler vortices. The use of N is approx. = 9.0 for the Goertler instability predicts quiet test cores in the new M = 3.5 and M = 6.0 axisymmetric long pilot nozzles that are 3 to 4 times longer than observed in the test nozzles to date. The new nozzles utilize a region of radial flow which moves the inflection point far downstream and delays the onset and amplification of the Goertler vortices. Author

N90-12556*# National Aeronautics and Space Administration. Langley Research Center, Hampton, VA.
THE EFFECTS OF WALL SURFACE DEFECTS ON BOUNDARY-LAYER TRANSITION IN QUIET AND NOISY SUPERSONIC FLOW
E. Leon Morrisette and Theodore R. Creel, Jr. *In its* Research in Natural Laminar Flow and Laminar-Flow Control, Part 3 Dec. 1987 p 965-980 (For primary document see N90-12539 04-02)
Avail: NTIS HC A17/MF A03 CSCL 01A

The design of supersonic vehicles with laminar flow control and vehicles such as the Space Shuttle requires information on allowable transition tolerances to fabrication defects such as discrete surface roughness and waviness. A relatively large data base on the effects of discrete roughness on transition exists for subsonic and supersonic speeds. The existing supersonic wind tunnel transition data are contaminated by wind tunnel noise emanating from the turbulent boundary layers on the nozzle walls.

Roughness and waviness transition data obtained in a quiet Mach 3.5 supersonic wind tunnel are compared with those obtained in conventional noisy flows. Author

N90-12557*# National Aeronautics and Space Administration. Langley Research Center, Hampton, VA.
EXPERIMENTAL AND THEORETICAL INVESTIGATION OF BOUNDARY-LAYER INSTABILITY MECHANISMS ON A SWEPT LEADING EDGE AT MACH 3.5
Theodore R. Creel, Jr., Mujeeb R. Malik (High Technology Corp., Hampton, VA.), and Ivan E. Beckwith *In its* Research in Natural Laminar Flow and Laminar-Flow Control, Part 3 Dec. 1987 p 981-995 (For primary document see N90-12539 04-02)
Avail: NTIS HC A17/MF A03 CSCL 01A

A brief outline of the experimental and theoretical investigation of boundary layer instability mechanisms on a swept leading edge at Mach 3.5 is presented. Transition is affected by wind tunnel noise only when roughness is present. Local bar-R sub * Reynolds number and k/eta sub * are useful correlation parameters for a wide range of free stream Mach numbers. Stability theory is in good agreement with the experimental cross flow vortex wavelength. These conclusions are briefly discussed. Author

N90-12558*# National Aeronautics and Space Administration. Langley Research Center, Hampton, VA.
SUPERSONIC BOUNDARY-LAYER TRANSITION ON THE LARC F-106 AND THE DFRF F-15 AIRCRAFT. PART 1: TRANSITION MEASUREMENTS AND STABILITY ANALYSIS
Fayette S. Collier, Jr., Joseph B. Johnson, Ollie J. Rose (PRC Kentron, Inc., Hampton, VA.), and D. S. Miller *In its* Research in Natural Laminar Flow and Laminar-Flow Control, Part 3 Dec. 1987 p 997-1014 (For primary document see N90-12539 04-02)
Avail: NTIS HC A17/MF A03 CSCL 01A

For the case of the F-15 flight tests, boundary layer transition was observed up to Mach numbers of 1.2. For very limited and specific flight conditions, laminar flow existed back to about 20 percent chord on the surface clean up glove. Hot film instrumentation was effective for locating the region of transition. For the F-106 flight tests, transition on the wing or vertical tail generally occurred very near the attachment line. Transition was believed to be caused by either attachment line contamination or strong cross flow development due to the high sweep angles of the test articles. The compressibility analysis showed that cross flow N-factors were in the range of 5 to 12 at transition. Author

N90-12559*# National Aeronautics and Space Administration. Langley Research Center, Hampton, VA.
SUPERSONIC BOUNDARY-LAYER TRANSITION ON THE LARC F-106 AND THE DFRF F-15 AIRCRAFT. PART 2: AERODYNAMIC PREDICTIONS
Ollie J. Rose (PRC Kentron, Inc., Hampton, VA.) and D. S. Miller *In its* Research in Natural Laminar Flow and Laminar-Flow Control, Part 3 Dec. 1987 p 1015-1024 (For primary document see N90-12539 04-02)
Avail: NTIS HC A17/MF A03 CSCL 01A

In the leading edge region, the measured pressure distributions exhibit extreme variations from strong suction peaks to a pressure maximum at the attachment line. These variations occur over short distances on the wing surface, and their character changes with changes in Mach number and angle of attack. The data/theory comparisons show that the character of the measured pressure distributions is well predicted for every Mach number and/or angle of attack condition considered. There is good agreement between theory and experiment for the location of the attachment line and suction peaks. The pressure magnitudes are well represented in the critical leading edge region, including the pressure maximum on the attachment line. The wing/body/inlet results agree well with the wing alone back to about 20 percent of chord where the upper surface suction peak typically occurs. The largest differences between theory and measurement always occur in the vicinity of suction peaks, with the difference being approximately 15 percent or less. In regions of largest error, the predicted pressures underestimate the suction peak strength for each case considered. The ability of the NCOREL code to reproduce wing pressure characteristics is shown. Author

N90-12560*# National Aeronautics and Space Administration. Lewis Research Center, Cleveland, OH.
PREDICTION OF UNSTEADY BLADE SURFACE PRESSURES ON AN ADVANCED PROPELLER AT AN ANGLE OF ATTACK
M. Nallasamy (Sverdrup Technology, Inc., Cleveland, OH.) and J. F. Groeneweg Nov. 1989 28 p Presented at the 12th Aeroacoustics Conference, San Antonio, TX, 10-12 Apr. 1989; sponsored by AIAA Previously announced in IAA as A89-40473
(Contract NAS3-25266)
(NASA-TM-102374; E-5108; NAS 1.15:102374; AIAA-89-1060)
Avail: NTIS HC A03/MF A01 CSCL 01A

The numerical solution of the unsteady, three-dimensional, Euler equations is considered in order to obtain the blade surface pressures of an advanced propeller at an angle of attack. The specific configuration considered is the SR7L propeller at cruise conditions with a 4.6 deg inflow angle corresponding to the plus 2 deg nacelle tilt of the Propeller Test Assessment (PTA) flight test condition. The results indicate nearly sinusoidal response of the blade loading, with angle of attack. For the first time, detailed variations of the chordwise loading as a function of azimuthal angle are presented. It is observed that the blade is lightly loaded for part of the revolution and shocks appear from hub to about 80 percent radial station for the highly loaded portion of the revolution. Author

N90-12561*# National Aeronautics and Space Administration. Lewis Research Center, Cleveland, OH.
SOME OBSERVATIONS ON TRANSITORY STALL IN CONICAL DIFFUSERS
K. B. M. Q. Zaman and M. D. Dahl 1989 13 p Presented at the 28th Aerospace Sciences Meeting, Reno, NV, 8-11 Jan. 1990; sponsored by AIAA
(NASA-TM-102387; E-5128; NAS 1.15:102387; AIAA-90-0048)
Avail: NTIS HC A03/MF A01 CSCL 01A

Results from an experimental investigation on the flow through conical diffusers are presented. The mean and fluctuating velocity fields are compared for three diffusers with total diffusion angles of 16, 20 and 24 degrees, in the throat Mach number (M sub t) range of 0.05 to 0.95. Each of the diffusers were 14 cm long and had a 5.08 cm inlet diameter, and the flow exited into the ambient. The boundary layer at the throat was thin with the throat diameter (D sub t) to momentum thickness (O) ratio being as high as 800 at M(sub t) = 0.4. While the 16 deg diffuser flow exited with a top-hat mean velocity profile, increasing losses due to increasing separation resulted in fuller profiles for the 20 and 24 degree cases. A detailed flow field study was conducted for the 16 deg. diffuser. The u'-spectrum, measured at the exit plane, exhibited a peak apparently due to the ensuing jet column instability throughout the M(sub t) range covered. In addition, a much lower frequency spectral peak also occurred in the M(sub t) range of 0.3 to 0.7. Both of the spectral peaks were due to axisymmetric flow fluctuations. A self-sustaining flow oscillation occurred in the M(sub t) range of 0.6 to 0.85, emitting a loud tone, when the jet column instability frequency matched the resonance frequency of the diffuser. Limited data showed that artificial acoustic excitation was effective in reducing the flow fluctuations, with a resultant increase in the pressure recovery, at low M(sub t). Author

N90-12562# Royal Aerospace Establishment, Farnborough (England).
IMPROVEMENTS IN THE FORMULATIONS AND NUMERICAL SOLUTION OF THE EULER PROBLEM FOR SWEPT WINGS
M. F. Paisley and M. G. Hall 17 Aug. 1988 14 p Presented at the IUTAM Symposium Transsonicum 3, Goettingen, Fed. Republic of Germany, 24-27 May 1988
(RAE-TM-AERO-2139; BR108362; ETN-89-94829) Copyright
Avail: NTIS HC A03/MF A01

A method to calculate steady inviscid transonic flow for swept wings is described. It is based on a multigrid cell vertex finite

volume Euler method. The effect of velocity perturbations generated from Klunker's analytic asymptotic solution to the transonic small disturbance equation, is applied. The geometry of the wing tip is modeled with three successively finer C-O grids. The results show marked differences in comparison with those obtained on C-H grids. The results indicate that a shock wave mechanism can contribute to the generation of tip vortices in compressible inviscid flow. For reliable prediction of wing performance the importance in good modeling of both the wing tip geometry and the flow around the tip is shown. ESA

N90-12563# Royal Aerospace Establishment, Farnborough (England).
CFD METHODS FOR DRAG PREDICTION AND ANALYSIS CURRENTLY IN USE IN UK
P. R. Ashill 14 Oct. 1988 22 p
(RAE-TM-AERO-2146; BR109770; ETN-89-95001) Copyright
Avail: NTIS HC A03/MF A01

The computational method developed in UK for the prediction of the drag of aircraft components at subsonic and supersonic speeds in the field of Computational Fluid Dynamics (CFD), are reviewed. The flow modeling is analyzed. The methods have a useful function both in the early stages of aircraft design, and later in support of windtunnel test as a diagnostic tool, and also to extrapolate the data to full scale. ESA

N90-12564# Institut Franco-Allemand de Recherches, Saint-Louis (France).
VOLUMETRIC ANALYSIS BY SPONTANEOUS RAMAN DIFFUSION IN A SUPERSONIC WIND TUNNEL [MESURE DE LA MASSE VOLUMIQUE MOYENNE LOCALE PAR DIFFUSION RAMAN SPONTANEE DANS UNE SOUFFLERIE SUPERSONIQUE]
L. Bobin and G. Brom 27 Apr. 1988 17 p In FRENCH
Original contains color illustrations
(Contract DRET-87-068)
(ISL-R-109/88; ETN-89-95028) Avail: NTIS HC A03/MF A01

Measurements of average local volumetric mass using laser Raman techniques in a supersonic wind tunnel are described. Although the set-up needs improvement, the technique is concluded to be useable. Impact of the laser beam on any object in motion should be avoided. The measuring point should be far from the impact area of the beam. The precision of measurement can be improved by significantly increasing the integration period. Photographs of the experimental apparatus and preliminary results are provided. ESA

N90-12565# Office National d'Etudes et de Recherches Aerospatiales, Paris (France). Direction de l'Aerodynamique.
BASIC RESEARCH ON METHODS OF CALCULATING SUPERSONIC AND HYPERSONIC FLOW Final Report [RECHERCHES FONDAMENTALES SUR DES METHODES DE CALCULS D'ECOULEMENTS SUPERSONIQUES ET HYPERSONIQUES]
R. Abgrall Sep. 1988 57 p In FRENCH
(Contract DRET-88-34-001)
(ONERA-RSF-19/1123-AY-234A; ETN-89-95285) Avail: NTIS HC A04/MF A01

The adaptation or creation of calculation methods for analysis of gas mixtures at supersonic and hypersonic velocities is described. Riemann solvers are developed in order to calculate the outflow of perfect gases of varying concentrations which do not react. The solvers are tested on a number of single and two dimensional cases. A study of outflow of reactive gases is undertaken, with the introduction of real gas phenomena using an Osher solver. ESA

N90-12566# Aeronautical Research Labs., Melbourne (Australia).
DEVELOPMENT OF A VSAERO (VORTEX SEPARATION AERODYNAMICS) MODEL OF THE F/A-18
R. Toffoletto Mar. 1989 29 p
(AD-A212442; ARL-FLIGHT-MECH-TM-404; DODA-AR-005-543)
Avail: NTIS HC A03/MF A01 CSCL 01/1

Vortex Separation AERODynamics (VSAERO) was used to produce an aerodynamic model of the aircraft. When fully developed, results from the model will be compared with results obtained from experiments planned to be carried out in the ARL wind tunnel. The velocity field and wake geometry in the vicinity of the aircraft, and the pressure distribution on the aircraft were calculated for various flight conditions. Calculated lift coefficients for the whole aircraft were compared with wind tunnel results obtained from McDonnell Aircraft company. The model was also used to study the effect of engine intake velocity on the aerodynamics of the aircraft. The major problem encountered during the development of the model was a numerical instability caused by the complicated vortex/vortex and vortex/body interactions in the vicinity of the tail of the aircraft. During this time, a new version of VSAERO was installed at ARL which promised greater stability in this area. It also allowed for a denser grid in the wake structure. Comparisons were made between the old and new versions to determine the extent of the improvements. GRA

N90-12567# Air Force Armament Lab., Eglin AFB, FL. Aeromechanics Div.
AERODYNAMIC TEST AND ANALYSIS OF A SLENDER GENERIC MISSILE CONFIGURATION Interim Report, Nov. 1987 - Aug. 1989
Roger S. Gates, G. L. Winchenbach, John R. Cipolla, and Mark A. Fischer (General Electric Co., Burlington, VT.) Sep. 1989 10 p Presented at the AIAA Atmospheric Flight Mechanics Symposium, Boston, MA, Aug. 1989
(AF Proj. 2567)
(AD-A212522; AFATL-TP-89-17) Avail: NTIS HC A02/MF A01 CSCL 16/2

This paper discusses the aerodynamic predictions, tests, and analyses of a slender fin stabilized missile configuration at Mach numbers from 1.0 to 5.0. Prediction techniques consisted of both empirical and analytical methods, including state-of-the-art computational fluid dynamic codes. Free flight tests were also conducted on subscale models to obtain an aerodynamic baseline to which the various predictions could be compared. This paper summarizes these results, attempts to identify the physics governing the flight trajectories, and proposes new ideas for further research in this technology area. GRA

N90-12568# Defence Research Establishment Atlantic, Dartmouth (Nova Scotia).
CHORDWISE LOADING AND CAMBER FOR TWO-DIMENSIONAL THIN SECTIONS
Michael Mackay Aug. 1989 20 p
(AD-A213318; DREA-TM-89/219) Avail: NTIS HC A03/MF A01 CSCL 01/1

Derivations are given for the calculation of section camberline from a given segmented chordwise load distribution, and for the inverse problem. In both cases, the algorithms are exact within the limits of thin wing theory. Two dimensional, thin, lifting sections were studied and the derivation is given of the camberline from a segmented chordwise loading (the design problem) and the calculation of loading from a discretely-defined camberline (the analysis problem). To the author's knowledge, these derivations have not been published for the general case, although the results for some specific cases are well known, good examples are the NACA a-series camberlines, obtained from simple two-segment load distributions, which have been widely used for many years. GRA

03 AIR TRANSPORTATION AND SAFETY

Includes passenger and cargo air transport operations; and aircraft accidents.

For related information see also *16 Space Transportation* and *85 Urban Technology and Transportation.*

No abstracts in this category.

04 AIRCRAFT COMMUNICATIONS AND NAVIGATION

Includes digital and voice communication with aircraft; air navigation systems (satellite and ground based); and air traffic control.

For related information see also *17 Space Communications, Spacecraft Communications, Command and Tracking* and *Communications and Radar.*

N90-12569 Rhode Island Univ., Kingston.
OPTIMAL OBSERVER MOTION FOR BEARINGS-ONLY LOCALIZATION AND TRACKING Ph.D. Thesis
Sherry Elizabeth Hammel 1988 159 p
Avail: Univ. Microfilms Order No. DA8901705

The nonlinear tracking problem is examined where a single moving observer passively monitors noise bearings emitted from a source and processes the data to obtain estimates of source position and velocity. Specific optimal paths are derived for general scenarios characterized by the effective range-to-baseline ratio. Observability requirements are the first consideration with regard to observer motion. A simplified criterion for establishing such requirements is presented. This criterion is then utilized to determine necessary and sufficient conditions for a tracking solution in a class of nonlinear problems involving both bearing and other angle-of-arrival measurements. Emphasis is then directed toward establishing a theoretical relationship between system observability, observer motion, and estimation accuracy. This is accomplished by analyzing properties of the error covariance matrix and Fisher Information Matrix. As is common with nonlinear optimization problems, an explicit analytical solution for optimal observer motion is difficult to obtain. The formation of the estimation problems considered leads to a cost function that is not amenable to conventional study. However, it is shown how decomposition of the Fisher Information matrix leads to a numerical procedure that generates optimal observer motion comprised of a series of constant course trajectories. Observer trajectories are also derived analytically for bearings-only estimation by utilizing an alternative criterion. The problem is solved within the context of classical control theory by invoking necessary conditions involving the Hamiltonian. The error ellipses associated with the trajectories are compared and analyzed. Dissert. Abstr.

N90-12570# Federal Aviation Administration, Washington, DC. Office of Management Systems.
FAA AIR TRAFFIC ACTIVITY: FISCAL YEAR 1988
1988 200 p
(AD-A211338) Avail: NTIS HC A09/MF A01 CSCL 01/5

Terminal and en route air traffic activity information of the National Airspace System are furnished. The data were reported by the FAA-operated Airport Traffic Control Towers (ATCTs), Air Route Traffic Control Centers (ARTCCs), Flight Service Stations (FSSs), Approach Control Facilities, and FAA contract-operated towers. These reports are used as a guide in determining the need for larger or additional facilities, and possible increases in personnel at existing facilities. GRA

N90-12571# Technische Univ., Delft (Netherlands). Faculty of Geodesy.
ON THE PRECISION AND RELIABILITY OF GPS NETWORKS COMPUTED USING THE DOUBLE DIFFERENCE OBSERVABLE Thesis
Peter Joosten 1988 137 p
(ETN-89-95719) Avail: NTIS HC A07/MF A01

The project concerning the use of Global Positioning System (GPS) double difference observations, for a terrestrial survey network, is reported. The precision and reliability of the final network are investigated. The description of the GPS is given. The generation of satellite and station coordinates is described. To perform the GPS network design, the procedure involving the method of planning a survey design known as the Delft Approach, together with the SCAN-2 software, is investigated. The results obtained from test computations allow the setting of basic rules for designing a GPS network. ESA

N90-12572 Civil Aviation Authority, London (England). Air Traffic Control Evaluation Unit.
DEVELOPMENT AND EVALUATION AT ATCEU OF EXECUTIVE AND SUPPORT OPERATIONS, PHASE 4A/3D
M. J. Dowsett, A. E. Johnson, and C. S. Narborough-Hall (Royal Air Force, London, England) Dec. 1988 95 p
(CAA-Paper-88017; EU404; Rept-508; ETN-89-95246) Copyright Avail: Civil Aviation Authority, Greville House, 37 Gratton Road, Cheltenham, United Kingdom

The phase 3c and phase 4a and 3d simulations, concerned with developing and evaluating the executive and support mode (ES) of controller operation proposed in the London air traffic control center development plan are described. Phase 3c examines civil aspects of the ES operation. It concentrates on display and message formats and on automatic coordination procedures. Phase 4a and 3d study problems associated with joint civil/military use of the concepts. Recommendations about areas requiring further development and study are made. ESA

N90-12573 Civil Aviation Authority, London (England). Air Traffic Control Evaluation Unit.
OPERATIONAL TRIAL OF EFFECT OF RAISING MINIMUM STACK LEVEL IN HEATHROW STACKS
A. E. Johnson Feb. 1989 25 p
(CAA-Paper-89003; EU656; Rept-549; ETN-89-95247) Copyright Avail: Civil Aviation Authority, Greville House, 37 Gratton Road, Cheltenham, United Kingdom

The results of a field trial to measure the effects upon Heathrow, London, of raising the transition altitude above 6000 ft. are described. The effects were simulated by sterilizing the minimum stack level in the Heathrow stacks for a period from 27 Jun. until 22 Jul. 1988. Subjective opinion was divided as to how much the inbound traffic was penalized. Measurements showed there was very little effect. The questionnaires used for the subjective opinion data are included, as are numerical results recorded during the trial period. The trial period was interrupted for 40 period of the time due to heavy impending traffic. ESA

N90-12574# Federal Aviation Administration, Atlantic City, NJ.
PARALLEL APPROACH SEPARATION AND CONTROLLER PERFORMANCE: A STUDY OF THE IMPACT OF TWO SEPARATION STANDARDS
Earl S. Stein Nov. 1989 99 p
(Contract F2006D)
(DOT/FAA/CT-TN89/50) Avail: NTIS HC A05/MF A01

A small sample study of the possible impact of altering the separation minimum between aircraft approaches to dependent parallel runways is described. The current standard is 2 nautical miles (nmi) and the proposed new standard is 1.5 nmi. Four full performance level air traffic controllers participated in 12 hours of simulated air traffic control activity in which separation standards were altered in a balanced fashioned after each 1 hour block of simulation. Data were collected on multiple airspace and operator performance variables. Also collected were workload and observer estimates. The goal was to determine if system performance could

be improved without compromising safety. Results indicated an increased frequency of landings using the 1.5 nmi standard indicating a finite increase in airport capacity. There were no indications of reduced safety or increased operator workload. Since the data were generated based on a small sample, results should be considered indicative rather than conclusive. Author

N90-12575# Royal Signals and Radar Establishment, Malvern (England).
SOFTWARE FAULT TOLERANCE
L. N. Simcox Jun. 1988 33 p Sponsored by the Civil Aviation Authority, London, England
(RSRE-Memo-4237; BR108878; ETN-89-94842) Copyright
Avail: NTIS HC A03/MF A01

The principles of software fault tolerance are presented. Various schemes for achieving it are described. Emphasis is placed on the N-version programming and the recovery blocks schemes. The areas of research include reliability modeling, version independence, and system simulation. A description of the use of software fault tolerance in aerospace applications is given. The cost effectiveness is addressed. The potential benefits to air traffic control systems are identified. Areas where further study and research are desirable, are indicated. ESA

N90-12576# Royal Signals and Radar Establishment, Malvern (England).
ROUTE DATA REPRESENTATION FOR ATC SIMULATION EXPERIMENTS
W. Finch 25 Oct. 1988 30 p Sponsored by the United Kingdom National Air Traffic Services
(RSRE-Memo-4133; BR109148; ETN-89-95004) Copyright
Avail: NTIS HC A03/MF A01

The research performed by Terminal Control Systems Development Group (UK), on the air route data structure is described. The route structure representation is designed to model an area around southeast England. A real time simulation of an air traffic control system, an ATC (air traffic simulator), using computer assistance for arrivals management, is effectuated. It is shown that the route segment feature removes a little of the transparency of the input file, and constraints such as allowed heights and speeds which are often imposed. ESA

N90-12577# Deutsche Forschungs- und Versuchsanstalt fuer Luft- und Raumfahrt, Brunswick (Germany, F.R.). Abteilung Systemtechnik und Navigation.
HYBRID ANGULAR VELOCITY REFERENCE SYSTEM FOR THE INVESTIGATION OF DYNAMIC PROPERTIES OF STRAPDOWN GRYOS
Helmut Niederstrasser Dec. 1988 76 p In GERMAN; ENGLISH summary Report will also be announced as translation (ESA-TT-1181)
(DFVLR-FB-89-25; ISSN-0171-1342; ETN-89-95834) Avail: NTIS HC A05/MF A01; DFVLR, VB-PL-DO, Postfach 90 60 58, 5000 Cologne, Fed. Republic of Germany, 28 Deutsche marks

A hybrid angular velocity reference for the investigation of the dynamic behavior of strapdown gyros using a conventional single-axis test table is described. The reference system consists of an inductosyn, a tachometer and a linear accelerometer. Investigation of the laser gyro dynamics is calculated by the power spectral densities of the gyro measurement error and the gyro transfer function. The dynamics of the test table, the properties of the reference system and its improvement are discussed. ESA

N90-12578# Naval Postgraduate School, Monterey, CA.
CASE STUDY ON RAPID SOFTWARE PROTOTYPING AND AUTOMATED SOFTWARE GENERATION: AN INERTIAL NAVIGATION SYSTEM M.S. Thesis
Herbert Guenterberg Jun. 1989 98 p
(AD-A212272) Avail: NTIS HC A05/MF A01 CSCL 17/7

The discipline of software engineering is on the move from an art to an engineering science based on mathematical rules. Along this way methods of rapid prototyping and tools for automatic program generation are being developed to aid the process of software development. This thesis takes a real life example of an Inertial Navigation System and develops it according to the automation principles for computer aided software development. The techniques of rapid software prototyping are also applied to the same problem. The software prototype of the Inertial Navigation System can further be run through The Computer Aided Prototyping System (CAPS) to mechanically generate Ada software. All implementation work is done in Ada as required by DOD for all embedded weapons systems. The two approaches will be integrated for analysis. GRA

N90-12579# Aeronautical Research Labs., Melbourne (Australia).
RTSIN1: A MODEL OF A STRAPDOWN INS ON A TWO-AXIS RATE TABLE
R. B. Miller Jul. 1989 26 p
(AD-A212406; ARL-SYS-TM-102; DODA-AR-004-598) Avail: NTIS HC A03/MF A01 CSCL 17/7

A two axis rate table is very useful laboratory equipment for testing of strapdown inertial navigation systems (INS). In practice, tables are used both for angular positioning of the INS and for application of angular velocities about one or two axes. In the former, the INS may be aligned at some required attitude, and then rotated to some other attitude, and left there navigating under the influences of gravity and earth rotation only, while its outputs are observed. A series of different such alignments and rotations can be used to deduce information about the system's sensor errors and characteristics. This computer program simulates the outputs of a strapdown INS and the errors in those outputs, when the system is mounted on a two axis rate table, undergoing a user specified motion sequence, and when user specified sensor and system errors are present. The strapdown INS is simulated by SINS1. The program contains a simulation of the rate table, which provides angular velocity and specific force at the reference point of the INS, which may be located at any user specified position relative to the intersection of the table axes, and attitude relative to the table disc. GRA

05 AIRCRAFT DESIGN, TESTING AND PERFORMANCE

Includes aircraft simulation technology.

For related information see also *18 Spacecraft Design, Testing and Performance* and *39 Structural Mechanics*.For land transportation vehicles see *85 Urban Technology and Transportation.*

N90-12580*# National Aeronautics and Space Administration. Langley Research Center, Hampton, VA.
INTEGRATED MULTIDISCIPLINARY OPTIMIZATION OF ROTORCRAFT: A PLAN FOR DEVELOPMENT
Howard M. Adelman, ed. and Wayne R. Mantay, ed. May 1989 83 p
(NASA-TM-101617; NAS 1.15:101617; AVSCOM-TM-89-B-004)
Avail: NTIS HC A05/MF A01 CSCL 01C

This paper describes a joint NASA/Army initiative at the Langley Research Center to develop optimization procedures aimed at improving the rotor blade design process by integrating appropriate disciplines and accounting for important interactions among the disciplines. The paper describes the optimization formulation in terms of the objective function, design variables, and constraints. Additionally, some of the analysis aspects are discussed, validation strategies are described, and an initial attempt at defining the interdisciplinary couplings is summarized. At this writing, significant progress has been made, principally in the areas of single discipline optimization. Accomplishments are described in areas of rotor aerodynamic performance optimization for minimum hover horsepower, rotor dynamic optimization for vibration reduction, and rotor structural optimization for minimum weight. For individual titles, see N90-12581 through N90-12588.

N90-12581*# National Aeronautics and Space Administration. Langley Research Center, Hampton, VA.
GENERAL APPROACH AND SCOPE
Howard M. Adelman and Wayne R. Mantay (Army Aviation Systems Command, Hampton, VA.) *In its* Integrated Multidisciplinary Optimization of Rotorcraft: A Plan for Development May 1989 p 3-10 (For primary document see N90-12580 04-05)
Avail: NTIS HC A05/MF A01 CSCL 01C

This paper describes a joint activity involving NASA and Army researchers at the NASA Langley Research Center to develop optimization procedures aimed at improving the rotor blade design process by integrating appropriate disciplines and accounting for all of the important interactions among the disciplines. The disciplines involved include rotor aerodynamics, rotor dynamics, rotor structures, airframe dynamics, and acoustics. The work is focused on combining these five key disciplines in an optimization procedure capable of designing a rotor system to satisfy multidisciplinary design requirements. Fundamental to the plan is a three-phased approach. In phase 1, the disciplines of blade dynamics, blade aerodynamics, and blade structure will be closely coupled, while acoustics and airframe dynamics will be decoupled and be accounted for as effective constraints on the design for the first three disciplines. In phase 2, acoustics is to be integrated with the first three disciplines. Finally, in phase 3, airframe dynamics will be fully integrated with the other four disciplines. This paper deals with details of the phase 1 approach and includes details of the optimization formulation, design variables, constraints, and objective function, as well as details of discipline interactions, analysis methods, and methods for validating the procedure.
K.C.D.

N90-12582*# National Aeronautics and Space Administration. Langley Research Center, Hampton, VA.
ROTOR BLADE AERODYNAMIC DESIGN
Joanne L. Walsh and Kevin W. Noonan (Army Aviation Systems Command, Hampton, VA.) *In its* Integrated Multidisciplinary Optimization of Rotorcraft: A Plan for Development May 1989 p 10-13 (For primary document see N90-12580 04-05)
Avail: NTIS HC A05/MF A01 CSCL 01C

Aerodynamic performance aspects of rotor blade design are presented. Design considerations, aerodynamic constraints and design variables are described. K.C.D.

N90-12583*# National Aeronautics and Space Administration. Langley Research Center, Hampton, VA.
ROTOR BLADE DYNAMIC DESIGN
Jocelyn I. Pritchard, Howard M. Adelman, and Wayne R. Mantay (Army Aviation Systems Command, Hampton, VA.) *In its* Integrated Multidisciplinary Optimization of Rotorcraft: A Plan for Development May 1989 p 13-17 (For primary document see N90-12580 04-05)
Avail: NTIS HC A05/MF A01 CSCL 01C

The rotor dynamic design considerations are essentially limitations on the vibratory response of the blades which in turn limit the dynamic excitation of the fuselage by forces and moments transmitted to the hub. Quantities which are associated with the blade response and which are subject to design constraints are discussed. These include blade frequencies, vertical and inplane hub shear, rolling and pitching moments, and aeroelastic stability margin. K.C.D.

N90-12584*# Army Aviation Systems Command, Hampton, VA. Structural Dynamics Div.
ROTOR BLADE STRUCTURAL DESIGN
Mark W. Nixon *In* NASA, Langley Research Center, Integrated Multidisciplinary Optimization of Rotorcraft: A Plan for Development May 1989 p 17-22 (For primary document see N90-12580 04-05)
Avail: NTIS HC A05/MF A01 CSCL 01C

The structural design of rotor blades is discussed. The various topics associated with the structural design include constraints, load cases, and analyses. K.C.D.

N90-12585*# National Aeronautics and Space Administration. Langley Research Center, Hampton, VA.
ACOUSTIC DESIGN CONSIDERATIONS: REVIEW OF ROTOR ACOUSTIC SOURCES
Ruth M. Martin *In its* Integrated Multidisciplinary Optimization of Rotorcraft: A Plan for Development May 1989 p 22-27 (For primary document see N90-12580 04-05)
Avail: NTIS HC A05/MF A01 CSCL 01C

It is not sufficient to optimize a rotor design in terms of a single noise level calculated for a single flight condition and a single measurement location. The various noise sources, their frequency content, amplitude, and directivity as a function of operating condition must be considered. A summary of the frequency ranges, directivity patterns and the most important operational and design parameters for major rotor noise sources is presented. It is difficult to generalize design requirements for rotor noise because the acoustic output varies so widely depending on the noise source, flight condition, measurement location, and frequency range. However, assuming the rotor must lift a fixed nominal payload and operate over a wide range of flight conditions, three general design guidelines can be stated: (1) minimize tip Mach number; (2) minimize blade thickness in the tip region; and (3) minimize gradients in the spanwise lift distribution in the tip region. Constraints on blade thickness, maximum values for hover tip Mach number, advancing tip Mach number and spanwise lift coefficient gradient will be specified during the aerodynamic, dynamic and structural optimization process. The rotor noise sources to be considered include the low frequency loading and thickness noise, and the higher frequency noise due to blade-vortex interactions (BVI). The analyses to be employed will include the comprehensive rotor analysis and design program CAMRAD and the rotor noise prediction program WOPWOP. K.C.D.

N90-12586*# National Aeronautics and Space Administration. Langley Research Center, Hampton, VA.
AIRFRAME DESIGN CONSIDERATIONS: OVERVIEW
Raymond G. Kvaternik and T. Sreekanta Murthy (Planning Research Corp., Hampton, VA.) *In its* Integrated Multidisciplinary Optimization of Rotorcraft: A Plan for Development May 1989 p 27-30 (For primary document see N90-12580 04-05)
Avail: NTIS HC A05/MF A01 CSCL 01C

Aspects of airframe structural dynamics that have a strong influence on rotor design optimization are presented . Primary emphasis is on vibration requirements. The constraints imposed on rotor design by airframe dynamics are discussed. Rotor/airframe modeling enhancements are also described. K.C.D.

N90-12587*# Army Aviation Systems Command, Hampton, VA. Aerostructures Directorate.
VALIDATION OF THE PROCEDURES
Wayne R. Mantay *In* NASA, Langley Research Center, Integrated Multidisciplinary Optimization of Rotorcraft: A Plan for Development May 1989 p 31-37 (For primary document see N90-12580 04-05)
Avail: NTIS HC A05/MF A01 CSCL 01C

Validation strategies are described for procedures aimed at improving the rotor blade design process through a multidisciplinary optimization approach. Validation of the basic rotor environment prediction tools and the overall rotor design are discussed.
K.C.D.

N90-12588*# National Aeronautics and Space Administration. Langley Research Center, Hampton, VA.
APPENDIX: RESULTS OBTAINED TO DATE
Joanne L. Walsh, Aditi Chattopadhyay, Jocelyn I. Pritchard, and Mark W. Nixon (Army Aviation Systems Command, Hampton, VA.) *In its* Integrated Multidisciplinary Optimization of Rotorcraft: A Plan for Development May 1989 p 38-78 (For primary document see N90-12580 04-05)
Avail: NTIS HC A05/MF A01 CSCL 01C

Optimization procedures are described for the rotor blade design process by integrating appropriate disciplines and accounting for important interactions among the disciplines. Progress is reported

in the areas of aerodynamic performance optimization, dynamic optimization, optimum placement of tuning masses for vibration reduction, and structural optimization. Selected results from these activities are highlighted in this appendix. K.C.D.

N90-12589*# National Aeronautics and Space Administration. Ames Research Center, Moffett Field, CA.
POWERED-LIFT AIRCRAFT TECHNOLOGY
W. H. Deckert and J. A. Franklin 1989 36 p Original contains color illustrations
(NASA-SP-501; NAS 1.21:501; LC-89-39482) Avail: SOD HC $4.25 as 033-000-01062-1; NTIS HC A03/MF A01 CSCL 01C

Powered lift aircraft have the ability to vary the magnitude and direction of the force produced by the propulsion system so as to control the overall lift and streamwise force components of the aircraft, with the objective of enabling the aircraft to operate from minimum sized terminal sites. Power lift technology has contributed to the development of the jet lift Harrier and to the forth coming operational V-22 Tilt Rotor and the C-17 military transport. This technology will soon be expanded to include supersonic fighters with short takeoff and vertical landing capability, and will continue to be used for the development of short- and vertical-takeoff and landing transport. An overview of this field of aeronautical technology is provided for several types of powered lift aircraft. It focuses on the description of various powered lift concepts and their operational capability. Aspects of aerodynamics and flight controls pertinent to powered lift are also discussed. Author

N90-12590*# Auburn Univ., AL.
LOW EARTH ORBIT RAIDER (LER) WINGED AIR LAUNCH VEHICLE CONCEPT Final Report
Karl Feaux, William Jordan, Graham Killough, Robert Miller, and Vonn Plunk Jun. 1989 100 p
(Contract NASw-4435)
(NASA-CR-186057; NAS 1.26:186057) Avail: NTIS HC A05/MF A01 CSCL 01C

The need to launch small payloads into low earth orbit has increased dramatically during the past several years. The Low Earth orbit Raider (LER) is an answer to this need. The LER is an air-launched, winged vehicle designed to carry a 1500 pound payload into a 250 nautical mile orbit. The LER is launched from the back of a 747-100B at 35,000 feet and a Mach number of 0.8. Three staged solid propellant motors offer safe ground and flight handling, reliable operation, and decreased fabrication cost. The wing provides lift for 747 separation and during the first stage burn. Also, aerodynamic controls are provided to simplify first stage maneuvers. The air-launch concept offers many advantages to the consumer compared to conventional methods. Launching at 35,000 feet lowers atmospheric drag and other loads on the vehicle considerably. Since the 747 is a mobile launch pad, flexibility in orbit selection and launch time is unparalleled. Even polar orbits are accessible with a decreased payload. Most importantly, the LER launch service can come to the customer, satellites and experiments need not be transported to ground based launch facilities. The LER is designed to offer increased consumer freedom at a lower cost over existing launch systems. Simplistic design emphasizing reliability at low cost allows for the light payloads of the LER. Author

N90-12591# Aeritalia S.p.A., Turin (Italy). Gruppo Velivoli da Combattimento.
DEVELOPMENT AND APPLICATIONS OF RELIABILITY AND MAINTAINABILITY DESIGN CRITERIA IN MILITARY AIRCRAFT [SVILUPPO E APPLICAZIONE DI UN PIANO DI AFFIDABILITA' E MANUTENIBILITA' PER UN VELIVOLO MILITARE]
D. Ala, R. Buffardi, and B. Inglese 1989 14 p In ITALIAN; ENGLISH summary
(ETN-89-95208) Avail: NTIS HC A03/MF A01

The reliability and maintainability programs applied to the AM-X aircraft development are described. The requirements, the design criteria, the allocation of requirements at subsystem and equipment level and the relevant analysis and demonstration methods are discussed. The demonstration program is limited to some activities that are estimated sufficient to assess the effectiveness of the system. ESA

N90-12592# Office National d'Etudes et de Recherches Aerospatiales, Paris (France). Direction de l'Aerodynamique.
EULER EQUATION SOLUTIONS APPLIED TO A HELICOPTER ROTOR IN FORWARD MOVING FLIGHT Final Report [RESOLUTION DES EQUATIONS D'EULER APPLIQUEE A UN ROTOR D'HELICOPTERE EN VOL D'AVANCEMENT]
J. Sides Feb. 1989 63 p In FRENCH
(Contract DRET-88-34-001)
(ONERA-RSF-32/1285-AY-346A; ETN-89-95286) Avail: NTIS HC A04/MF A01

A numeric approach to helicopter rotor design based on Euler equations for nonstationary three dimensional compressible phenomena is presented. This approach is applied to a modeling problem for a thin wing submitted to shocks at transonic speeds. Precise solutions are found for both a fixed wing situation and an oscillating wing in transition, using the approach. Addition of artificial viscosity is not needed thanks to the implicit nature of the approach. ESA

N90-12593# Rolls-Royce Ltd., Derby (England).
WHAT SHOULD BE DONE WITH THOSE NOISY OLD AIRCRAFT
M. J. T. Smith and V. M. Szewczyk 2 Sep. 1988 10 p Presented at the AVMARK International Ltd. Conference of European Aircraft Noise Legislation: Consequences for the Aviation Industry, London, England, 2 Sep. 1988
(PNR90562; ETN-89-95549) Copyright Avail: NTIS HC A02/MF A01

The problem of adapting older noisy aircraft to more stringent noise legislation is discussed. The use of bolt-on hushkits as a means of quieting older aircraft is criticized. Further noise restrictions demand a truly re-engined aircraft. It is predicted that hushkit equipped planes will experience increasing difficulty when operating in noise sensitive airports. The author admits that Rolls Royce has a commercial interest in recommending that older planes be re-engined with stage three turbo fan engines. ESA

N90-12594 Department of the Navy, Washington, DC.
PIVOTAL MONO WING CRUISE MISSILE WITH WING DEPLOYMENT AND FASTENER MECHANISM Patent
Frederick D. Groutage, inventor (to Navy), Samuel N. Conjerti, inventor (to Navy), and Lockburn S. Shaw, inventor (to Navy) 27 Jun. 1989 10 p Filed 8 Feb. 1988
(AD-D014191; US-Patent-4,842,218; US-Patent-Appl-SN-159423; US-Patent-Class-244-328) Avail: U.S. Patent and Trademark Office CSCL 11/2

This patent discloses moveable wing aircraft including a quick release, attachment mechanism for carrying the aircraft on a bomb rack or other carrier and a mechanism for deploying the moveable wing from its captive carry position to its extended free flight position. The aircraft includes an elongate fuselage, a portion of the top surface of which is substantially flat in order to accommodate the moveable wing. The moveable wing is positionable between a captive carry position in which it is aligned with the longitudinal axis of the fuselage and an extended free flight position. The single, moveable wing is pivoted around a central point from its captive carry position to its extended free flight position such that it is substantially perpendicular to the aircraft fuselage. The quick release mechanism extends through apertures in the wing in its captive carry position and is spring biased to retract through the wing and into the aircraft fuselage when released from the bomb rack or other carrier. The deployment mechanism includes a spring loaded cable and pulley arrangement and serves to connect the moveable wing to the fuselage and to bias it from its captive carry position to its extended free flight position when activated upon release of the quick release mechanism. GRA

N90-12595# Aeronautical Research Labs., Melbourne (Australia).
FPG2: A FLIGHT PROFILE GENERATOR PROGRAM
R. B. Miller Jul. 1989 48 p
(AD-A212408; ARL-SYS-TM-98; DODA-AR-004-574) Avail: NTIS HC A03/MF A01 CSCL 17/7

This computer program simulates the environment of a strapdown inertial measurement unit in an aircraft executing a user-specified series of idealized maneuvers. The program generates a file containing a sequence of specific forces and angular velocities in body axes coordinates, or a file containing a sequence of integrated (in body axes) specific forces and angular velocities, or both. The sequences are time-tagged, and also include aircraft height. For reference purposes, it generates a file containing a sequence of nominally true position, velocity, and attitude of the aircraft. GRA

N90-12596# Aeronautical Research Labs., Melbourne (Australia).
RAN (ROYAL AUSTRALIAN NAVY) VIBRATION ANALYSIS SYSTEM OPERATOR'S GUIDE
B. D. Forrester Apr. 1989 33 p
(AD-A212441; ARL-PROP-TM-441; DODA-AR-004-525) Avail: NTIS HC A03/MF A01 CSCL 01/3

A computerized vibration analysis system consisting of hardware purchased by the Royal Australian Navy and software developed by Aeronautical Research Laboratory has been installed at NAS Nowra. The primary purpose of the system is to detect incipient failure of Wessex helicopter main rotor gear box input pinions. GRA

N90-12597# Aeronautical Research Labs., Melbourne (Australia).
EVALUATION OF A DAMAGED F/A-18 HORIZONTAL STABILATOR Aircraft Structures Technical Memorandum
J. Paul Feb. 1989 31 p Original contains color illustrations
(AD-A212573; ARL-STRUC-TM-503; DODA-AR-005590) Avail: NTIS HC A03/MF A01 CSCL 01/3

This paper describes the results of a static and dynamic structural test on a damaged F/A-18 Horizontal Stabilator. The structure was subjected to incremental static loading and the strains were recorded at each load increment. The structure was then vibrated at its fundamental bending frequency and the thermal emission profile of the critical area was measured using SPATE. GRA

N90-12508*# Analytical Services and Materials, Inc., Hampton, VA.
LONG-RANGE LFC TRANSPORT
Werner Pfenninger *In* NASA, Langley Research Center, Research in Natural Laminar Flow and Laminar-Flow Control, Part 1 Dec. 1987 p 89-115 (For primary document see N90-12503 04-02)
Avail: NTIS HC A14/MF A02 CSCL 01C

N90-12509*# National Aeronautics and Space Administration. Hugh L. Dryden Flight Research Facility, Edwards, CA.
DEVELOPMENT FLIGHT TESTS OF JETSTAR LFC LEADING-EDGE FLIGHT TEST EXPERIMENT
David F. Fisher and Michael C. Fischer (National Aeronautics and Space Administration. Langley Research Center, Hampton, VA.) *In* NASA, Langley Research Center, Research in Natural Laminar Flow and Laminar-Flow Control, Part 1 Dec. 1987 p 117-140 (For primary document see N90-12503 04-02)
Avail: NTIS HC A14/MF A02 CSCL 01C

N90-12511*# National Aeronautics and Space Administration. Langley Research Center, Hampton, VA.
PERFORMANCE OF LAMINAR-FLOW LEADING-EDGE TEST ARTICLES IN CLOUD ENCOUNTERS
Richard E. Davis, Dal V. Maddalon, and Richard D. Wagner *In its* Research in Natural Laminar Flow and Laminar-Flow Control, Part 1 Dec. 1987 p 163-193 (For primary document see N90-12503 04-02)
Avail: NTIS HC A14/MF A02 CSCL 01C

N90-12512*# National Aeronautics and Space Administration. Langley Research Center, Hampton, VA.
SIMULATED AIRLINE SERVICE EXPERIENCE WITH LAMINAR-FLOW CONTROL LEADING-EDGE SYSTEMS
Dal V. Maddalon, David F. Fisher, Lisa A. Jennett (National Aeronautics and Space Administration. Hugh L. Dryden Flight Research Facility, Edwards, CA.), and Michael C. Fischer *In its* Research in Natural Laminar Flow and Laminar-Flow Control, Part 1 Dec. 1987 p 195-218 (For primary document see N90-12503 04-02)
Avail: NTIS HC A14/MF A02 CSCL 01C

N90-12544*# National Aeronautics and Space Administration. Langley Research Center, Hampton, VA.
DESIGN AND TEST OF AN NLF WING GLOVE FOR THE VARIABLE-SWEEP TRANSITION FLIGHT EXPERIMENT
Ed G. Waggoner, Richard L. Campbell, Pam S. Phillips, and James B. Hallissy *In its* Research in Natural Laminar Flow and Laminar-Flow Control, Part 3 Dec. 1987 p 753-776 (For primary document see N90-12539 04-02)
Avail: NTIS HC A17/MF A03 CSCL 01C

N90-12545*# National Aeronautics and Space Administration. Langley Research Center, Hampton, VA.
THE DESIGN OF AN AIRFOIL FOR A HIGH-ALTITUDE, LONG-ENDURANCE REMOTELY PILOTED VEHICLE
Mark D. Maughmer (Pennsylvania State Univ., University Park.) and Dan M. Somers *In its* Research in Natural Laminar Flow and Laminar-Flow Control, Part 3 Dec. 1987 p 777-794 (For primary document see N90-12539 04-02)
Avail: NTIS HC A17/MF A03 CSCL 01C

N90-12546*# Boeing Commercial Airplane Co., Seattle, WA.
THE 757 NLF GLOVE FLIGHT TEST RESULTS
L. Jim Runyan, G. W. Bielak, R. A. Behbehani, A. W. Chen, and Roger A. Rozendaal *In* NASA, Langley Research Center, Research in Natural Laminar Flow and Laminar-Flow Control, Part 3 Dec. 1987 p 795-818 (For primary document see N90-12539 04-02)
Avail: NTIS HC A17/MF A03 CSCL 01C

N90-12547*# National Aeronautics and Space Administration. Hugh L. Dryden Flight Research Facility, Edwards, CA.
F-14 VSTFE AND RESULTS OF THE CLEANUP FLIGHT TEST PROGRAM
Robert R. Meyer, Bianca M. Trujillo, and Dennis W. Bartlett (National Aeronautics and Space Administration. Langley Research Center, Hampton, VA.) *In* NASA, Langley Research Center, Research in Natural Laminar Flow and Laminar-Flow Control, Part 3 Dec. 1987 p 819-844 (For primary document see N90-12539 04-02)
Avail: NTIS HC A17/MF A03 CSCL 01C

N90-12548*# Boeing Commercial Airplane Co., Seattle, WA.
VARIABLE-SWEEP TRANSITION FLIGHT EXPERIMENT (VSTFE): STABILITY CODE DEVELOPMENT AND CLEAN-UP GLOVE DATA ANALYSIS
Roger A. Rozendaal *In* NASA, Langley Research Center, Research in Natural Laminar Flow and Laminar-Flow Control, Part 3 Dec. 1987 p 845-859 (For primary document see N90-12539 04-02)
Avail: NTIS HC A17/MF A03 CSCL 01C

N90-12550*# National Aeronautics and Space Administration. Langley Research Center, Hampton, VA.
STATUS REPORT ON A NATURAL LAMINAR-FLOW NACELLE FLIGHT EXPERIMENT Abstract Only
Earl C. Hastings, Jr., G. K. Faust, Parma Mungur, Clifford J. Obara, S. S. Dodbele, James A. Schoenster, and Michael G. Jones (PRC Kentron, Inc., Hampton, VA.) *In its* Research in Natural Laminar

Flow and Laminar-Flow Control, Part 3 Dec. 1987 p 887-890 (For primary document see N90-12539 04-02)
Avail: NTIS HC A17/MF A03 CSCL 01C

N90-12551*# General Electric Co., Cincinnati, OH.
NACELLE DESIGN
G. K. Faust and Parma Mungur *In* NASA, Langley Research Center, Research in Natural Laminar Flow and Laminar-Flow Control, Part 3 Dec. 1987 p 891-907 (For primary document see N90-12539 04-02)
Avail: NTIS HC A17/MF A03 CSCL 01C

N90-12552*# PRC Kentron, Inc., Hampton, VA.
NACELLE AERODYNAMIC PERFORMANCE
Clifford J. Obara and S. S. Dodbele (Vigyan Research Associates, Inc., Hampton, VA.) *In* NASA, Langley Research Center, Research in Natural Laminar Flow and Laminar-Flow Control, Part 3 Dec. 1987 p 908-913 (For primary document see N90-12539 04-02)
Avail: NTIS HC A17/MF A03 CSCL 01C

06 AIRCRAFT INSTRUMENTATION

Includes cockpit and cabin display devices; and flight instruments.

For related information see also *19 Spacecraft Instrumentation* and *35 Instrumentation and Photography.*

N90-12598# Aeritalia S.p.A., Turin (Italy). Flight Test Development.
ACQUISITION AND RECORDING AN AMX A/C. AERITALIA EXPERIENCE AND PRESENT TRENDS
S. Cattunar 1987 13 p Presented at the European Telemetry Conference, Aix-en-Provence, France, 1987
(ETN-89-95217) Avail: NTIS HC A03/MF A01

Experimentation with the BUS 1553 B as the active link for all avionic, navigation and armament equipment in an AMX prototype A03 aircraft is described. The system allows for acquisition of 256 parameters from transducer and analog sources. Two different acquisition techniques, through a PCM (pulse code modulation) acquisition system and directly on a magnetic tape recorder, are used. The results of the experimentation helped in developing a unit allowing for considerable savings in track usage. ESA

N90-12599# Deutsche Forschungsanstalt fuer Luft- und Raumfahrt, Brunswick (Germany, F.R.). Abteilung Flugversuchstechnik.
AUTOMATIC PROCESSING OF IMAGES FROM THE GRATE FLIGHT TEST TOOL
Klaus Alvermann 24 May 1989 50 p In GERMAN; ENGLISH summary
(DLR-FB-89-28; ISSN-0171-1342; ETN-89-95837) Avail: NTIS HC A03/MF A01; DLR, VB-PL-DO, Postfach 40 60 58, 5000 Cologne, Fed. Republic of Germany, 21 Deutsche marks

The GRATE flight test tool is described. It produces a film, the pictures of which are processed automatically. Objects in the image are identified and their exact position determined. An algorithm necessary for the identification of objects is developed. A tracker (a pipper in a head-up display) and a target (a light on the ground) are developed. The mathematical elements of the algorithms are presented and discussed in detail. The operating efficiency is evaluated. ESA

07 AIRCRAFT PROPULSION AND POWER

Includes prime propulsion systems and systems components, e.g., gas turbine engines and compressors; and onboard auxilliary power plants for aircraft.

For related information see also *20 Spacecraft Propulsion and Power, 28 Propellants and Fuels,* and *44 Energy Production and Conversion.*

N90-12600 Iowa Univ., Iowa City.
STAGE EFFECTS ON STALLING AND RECOVERY OF A HIGH-SPEED 10-STAGE AXIAL-FLOW COMPRESSOR Ph.D. Thesis
William Ward Copenhaver 1988 400 p
Avail: Univ. Microfilms Order No. DA8909139

Results of a high speed 10-stage axial flow compressor test involving overall compressor and individual stage performance while stalling and operating in quasi-steady rotating stall are described. Test procedures and data acquisition methods used to obtain the dynamic stalling and quasi-steady in-stall data are explained. Unstalled and in-stall time averaged data obtained from the compressor operating at five different shaft speeds and one off-schedule variable vane condition are presented. The effects of compressor speed and variable geometry on overall compressor in-stall pressure rise and hysteresis extent are illustrated through the use of quasi-steady stage temperature rise and pressure rise characteristics. The results indicate that individual stage performance during overall compressor rotating stall operation varies considerably throughout the length of the compressor. Time resolved in-stall data acquired at two different shaft speeds are presented in support of the notion that stage operation varies significantly from entrance to exit of the compressor. Both time-averaged and time-resolved individual stage results suggest that stage matching is important, not only for unstalled performance but also for in-stall performance and recoverability from stall. The measured high speed 10-stage test compressor individual stage pressure and temperature characteristics were input into a stage-by-stage dynamic compressor performance model. The analytical model had been previously validated for the prediction of low-speed compressor stalling and in-stall performance. Dynamic pressures measured during stalling of the high speed 10-stage test compressor are compared during stalling of the high speed 10-stage test compressor are compared with analytical model results. The comparison of the model results and with analytical model results. The comparison of the model results and the measured pressures provided the additional validation necessary to demonstrate the model's ability to predict high speed multistage compressor stalling and in-stall performance. Dissert. Abstr.

N90-12601# Rolls-Royce Ltd., Derby (England).
ADVANCED CLEARANCE CONTROL SYSTEMS
P. F. Neal and W. E. Green 15 Jun. 1987 9 p Presented at the 8th International Symposium on Air Breathing Engines, Cincinnati, OH, 15-19 Jun. 1987
(PNR90553; ETN-89-95546) Copyright Avail: NTIS HC A02/MF A01

Ways of improving component efficiency, aerodynamics, and mechanical design, while keeping cost low as concerns clearance control systems, are discussed. Major improvements in component efficiencies clearly cannot be obtained and maintained in service without effective control of rotor tip clearance and seals inside and outside the aerodynamic flowpath. Reasonably good control of tip and seal clearances can be obtained by either careful thermal design for passive systems or by open-loop (scheduled) systems where casing radius is controlled using fixed rules and simple indications of engine power level. As running tip clearances continue to reduce, accurate control becomes more important in achieving and retaining increased performance. ESA

N90-12602# Rolls-Royce Ltd., Derby (England).
DEVELOPMENT OF TEXTURE ANALYSIS AND ITS APPLICATIONS TO TITANIUM AERO ENGINE COMPONENTS

K. Clay 22 Sep. 1988 30 p Presented at the 7th X Ray Diffraction Conference, Exeter, England, 22 Sep. 1988
(PNR90561; ETN-89-95548) Copyright Avail: NTIS HC A03/MF A01

The principles of the various options of texture assessment are discussed, from simple peak height analysis to fully quantitative three dimensional models of the Crystal Orientation Distribution Function (CODF). The need to match the level of sophistication of measurement and data presentation to the applications of the texture statement is covered. The practical development of digital pole figure generation system, ongoing since 1983, is described, including details of practical problems and limitations. The application of pole figure texture assessment in linking texture/anisotropy differences to changes in manufacturing routes for rolled titanium plate (used in wide chord fan blade production) is illustrated and the implication of texture assessment on other titaniun products is discussed. ESA

N90-12603# Rolls-Royce Ltd., Derby (England).
A VISION OF THE FUTURE: THE NEW ENGINE TECHNOLOGY
P. C. Ruffles 21 Aug. 1988 9 p Presented at the Financial Times Conference on Commercial Aviation to the End of the Century, London, England, 31 Aug. 1988
(PNR90566; ETN-89-95551) Copyright Avail: NTIS HC A02/MF A01

Predictions of future trends in engine design and technology are presented. These include reduction of fuel consumption with further improvement to current high bypass ratio engines and later by application of ultrahigh bypass ratio technology. Aircraft and engines are predicted as becoming larger. Large twin engine aircraft will require ever larger thrusts. The need for new materials in order to develop a light weight ultrahigh bypass ratio engine is stressed. Computer integration of design and manufacture processes is predicted for the lowering of development and production costs of such an engine. ESA

N90-12604# Rolls-Royce Ltd., Derby (England).
DESIGNING FOR RELIABLE AND LOW MAINTENANCE COST AERO ENGINES
S. P. Q. Byworth 15 Dec. 1988 25 p Presented at the Frank Radcliffe Bequest Seminar, 9 Dec. 1988
(PNR90570; MISS-2144; ETN-89-95553) Copyright Avail: NTIS HC A03/MF A01

The major engine factors influencing airline operating costs and the balance the engine designer has to make between the often conflicting requirements of improvements in fuel consumption, initial cost and maintenance costs are briefly reviewed. Operating costs are broken down, fuel burn trends are analyzed, and comparisons in operating costs are made between different Rolls Royce turbojet and turbofan engines. Modularity is investigated as a means of lowering costs, and typical maintenance cost forecasts are made. ESA

N90-12605# Rolls-Royce Ltd., Derby (England).
THE NEXT GENERATION SUPERSONIC TRANSPORT ENGINE: CRITICAL ISSUES
B. W. Lowrie, R. M. Denning, and P. C. Gupta 19 Apr. 1989 25 p Presented at the Royal Aeronautical Society Symposium on Aerodynamics Design for Supersonic Flight, London, England, 19 Apr. 1988
(PNR90576; E/BLO/163; ETN-89-95556) Copyright Avail: NTIS HC A03/MF A01

The design of a successor to the Concorde with a longhaul range of 5500 nautical miles is discussed. The ability of the engine and airframe to produce this range economically is briefly examined. Some offdesign implications of choice of cruise Mach number on matching and subsonic performance are outlined. Environmental requirements which can be controlled or influenced by engine design are discussed and the key issues noted. Consequent requirements for engine cycle variability are defined and two possibilities assessed. ESA

N90-12606# Rolls-Royce Ltd., Derby (England). Civil Powerplant Technology Engineering.
RE-ENGINE WITH THE ROLLS-ROYCE TAY 670, THE ROUTE TO SIGNIFICANT NOISE REDUCTION
V. M. Szewczyk 31 Jan. 1989 19 p Presented at the Avmark Noise Conference, Washington, DC, 31 Jan. 1989
(PNR90585; ETN-89-95560) Copyright Avail: NTIS HC A03/MF A01

The use of the Tay 670 engine to re-engine B 737-200, B 727-200 and DC 9 aircraft is described. The Tay engine has low jet velocities consistent with low noise production. Studies predicting that older aircraft re-engined with the Tay 670 will be competitive on noise with modern stage three turbofan powered aircraft are shown. The necessity for such engine changes due to ever increasing noise restrictions is described. ESA

N90-12607# Rolls-Royce Ltd., Derby (England).
A THEORETICAL STUDY OF INGRESS FOR SHROUDED ROTATING DISK SYSTEMS WITH RADIAL OUTFLOW
Theoretical Science Group Report
John W. Chew 2 Feb. 1989 10 p Presented at the 34th ASME International Gas Turbine and Aeroengine Congress, Toronto, Ontario, 4-8 Jun. 1989
(PNR90586; ETN-89-95561) Copyright Avail: NTIS HC A02/MF A01

Sealing of the cavity formed between a stationary disk and a rotating disk under axisymmetric conditions is considered. A mathematical model of the flow in the cavity based on momentum integral methods is described. A simple model of the seal for the case when no ingress occurs is presented. Predictions of the minimum imposed flow required to prevent ingress are obtained and shown to be in reasonable agreement with the data of Bayley and Owen (1970), Owen and Phadke (1982), Phadke (1982), and Phadke and Owen (1982, 1983, 1988). With an empirical constant in the model chosen to match this, data predictions for the minimum sealing flow are shown to be in good agreement with Graber et al's (1987) measurements. The analysis of Phadke's data also indicates the measurements for small seal clearances must be viewed with caution due to errors in setting the seal clearance. These errors are estimated to be twice the minimum clearance considered. Seal behavior when ingress occurs is also considered and estimates of the amount of ingress are made from the available data. ESA

N90-12608# Rolls-Royce Ltd., Derby (England). Materials and Mechanical Technology Dept.
THE ROLE OF COMPONENT TESTING
G. Asquith 26 Apr. 1989 14 p Presented at the 68th AGARD Structures and Materials Panel Meeting, Ottawa, Ontario, 26 Apr. 1989
(PNR90589; ETN-89-95562) Copyright Avail: NTIS HC A03/MF A01

The importance of component testing in ensuring that design and life goals of engines are met is addressed. The integration of component testing and material data generation into a material data bank is described. The techniques of stress and fracture mechanics analysis, crack monitoring, metallography and probabilistic approaches are used in establishing this data bank. The use of data on the material behavior of components in the development of new and improved materials is stressed. ESA

N90-12609# Rolls-Royce Ltd., Derby (England).
FLANGED JOINTS OF AEROENGINES
L. V. Lewis, H. Fessler, and T. H. Hyde (Nottingham Univ., England) 4 Sep. 1989 12 p Presented at the 9th International Symposium on Air Breathing Engines, Athens, Greece, 4-9 Sep. 1989
(PNR90594; ETN-89-95565) Copyright Avail: NTIS HC A03/MF A01

The design of a metal-to-metal bolted joint between two aeroengine casings is described. The joint has to achieve structural integrity and perform a sealing function. It must be light and have a small number of bolts. It is shown that present joints often fail

to seal, and suffer high cyclic stresses in the bolts and in the flange profiles. A way of pre-loading the joint on assembly is presented. It involves machining a cone angle onto the flange faces, so that a high-intensity line reaction is generated at the inside diameter on assembly. It is shown that perfect sealing can be achieved, and maintained at ratios of axial joint load/assembly bolt load that exceed present practice. Cyclic stresses are reduced to negligible proportions, so that low cycle fatigue is no longer a potential failure mode. It is shown that assembly stresses can be kept within elastic limits with acceptably light flange profiles. ESA

N90-12610# Rolls-Royce Ltd., Derby (England).
MATERIAL REQUIREMENTS FOR FUTURE AEROENGINES
G. E. Kirk 4 Sep. 1989 8 p Presented at the 9th International Symposium on Air Breathing Engines, Athens, Greece, 4-9 Sep. 1989
(PNR90595; ETN-89-95566) Copyright Avail: NTIS HC A02/MF A01

Improvements made in aeroengine technology are summarized. Performance gains, longer engine lives and higher thrust to weight ratio obtained through materials and process technology which made a significant contribution to this progress are outlined. For materials with higher temperature capability, lower cost and increased strength and stiffness in the future is stressed. Planned aeroengine configurations will not be viable without improvements in material properties and manufacturing technology. The developmental potential of titanium and nickel, and that of newer composite materials is outlined in terms of their use in future aeroengines. The problems that must be solved before they can be effectively used are identified. ESA

N90-12611# Rolls-Royce Ltd., Derby (England).
A COMPUTER INTEGRATED APPROACH TO DIMENSIONAL INSPECTION
S. A. Lee, N. Tsabourakis, M. Ristic, and C. B. Besant 3 Sep. 1989 10 p Presented at the 9th International Symposium on Air Breathing Engines, Athens, Greece, 4-9 Sep. 1988
(PNR90596; ETN-89-95567) Copyright Avail: NTIS HC A02/MF A01

A computer integrated dimensional inspection system supporting contact and noncontact methods of surface digitization is described. An extensive error handling facility enables errors to be found between nominal and actual surfaces. These errors may be presented, for example as contours of error, or be used in a three dimensional best-fitting process which minimizes error between actual and nominal surfaces. The design and development of the system are given in outline with a resume of its use. The system proves to be very powerful in dealing with the inspection of the highly complex forms involved in turbine blading. ESA

N90-12612# Rolls-Royce Ltd., Derby (England).
DYNAMIC TIP CLEARANCE MEASUREMENTS IN AXIAL FLOW COMPRESSORS
C. J. Parrish 15 Sep. 1989 6 p Presented at the COMADEM 89 International, Birmingham, England, Sep. 1989
(PNR90597; ETN-89-95568) Copyright Avail: NTIS HC A02/MF A01

Techniques used in measurement of tip clearance and the detection of tip rubs between rotor blade tips and rotor path lining in the compressors of jet engines are described. The importance of such measurements in obtaining engine efficiency is stressed. Tip clearance results broken down into closure, surge, and orbit types, are discussed. It is concluded that tip rubs occur during surge with a resultant loss in compressor efficiency. Closures are measured with rotor orbit to obtain the best cold build clearances for maximum compressor efficiency. ESA

N90-12613# Rolls-Royce Ltd., Derby (England).
THE DEVELOPMENT OF A HIGH RESPONSE AERODYNAMIC WEDGE PROBE AND USE ON A HIGH-SPEED RESEARCH COMPRESSOR Ph.D. Thesis - Cranfield Inst. of Technology
S. C. Cook 4 Sep. 1989 14 p Presented at the 9th International Air Breathing Engines, Athens, Greece, 4-9 Sep. 1988 Sponsored by the Ministry of Defence, London, England and the United Kingdom Science and Engineering Research Council
(PNR90598; ETN-89-95569) Copyright Avail: NTIS HC A03/MF A01

A high response aerodynamic wedge probe developed for use in performance testing of high-speed, axial-flow, research compressors and fans is described. The miniature probe incorporates flush-mounted high response silicon piezo-resistive pressure transducers, with both a dynamic and steady state measurement capability. New information on wedge probe aerodynamic sensitivity is given and details of important improvements to an iterative data reduction algorithm, facilitating successful use on dynamic data, are included. An electronic compensation scheme is employed to overcome the inherent temperature sensitivity of the transducers. Using this system, previously unreported transducer output nonlinearities are revealed. The 30 degree included angle wedge probe has a frequency response in excess of 100 kHz. The wedge probe was applied to a highspeed (9 kHz blade passing frequency), single-stage, axial-flow, research compressor at rotor trailing edge. Time resolved rotor wakes were measured using the wedge probe and compared with rotating wake data obtained using a crossed hot wire anemometer probe. The rotor wakes were found to be highly unsteady in terms of both amplitude and spatial location. ESA

N90-12614# Rolls-Royce Ltd., Derby (England).
GAS TURBINE PERFORMANCE ANALYSIS
A. J. B. Jackson 20 Jun. 1989 74 p Lecture presented at the Warwick Univ. IGDS Course, Warwick, England
(PNR90599; ETN-89-95570) Copyright Avail: NTIS HC A03/MF A01

The present state of gas turbine development is summarized. The history of gas turbine development is reviewed. The component parts of a gas turbine engine and their performance are outlined. Typical gas turbine overall characteristics are discussed, with attention given to power setting, atmospheric temperature, altitude and forward speed. Transient turbine behavior and overall aircraft performance are examined. ESA

N90-12615# Rolls-Royce Ltd., Derby (England).
ROLLS-ROYCE AND ERCOFTAC
P. Stow 20 Jun. 1989 4 p
(PNR90600; ETN-89-95571) Copyright Avail: NTIS HC A02/MF A01

How Rolls-Royce views the role of ERCOFTAC with respect to the company's needs and research and development strategies in CFD (charge flow devices) and turbulence and transition modeling is outlined. The company's interest in CFD stems from an initiative in computer aided engineering and manufacture aimed at reducing overall design and development times and costs. With CFD models that are a good representation of the physical processes involved in turbomachinery flows, one should be able to produce better design and development time and costs. Installation aerodynamics, intakes, nozzles, afterbodies, compressor and turbine blade steady and unsteady aerodynamics, turbine blade heat transfer, combustion and noise are all areas in which CFD applications have been found. ESA

N90-12616# Rolls-Royce Ltd., Derby (England). Theoretical Science Group.
BLADING DESIGN FOR MULTI-STORAGE HP COMPRESSOR
P. Stow 13 Mar. 1989 43 p Presented at the AGARD LS167 on Blading Design for Axial Turbomachines, Jun. 1987
(PNR90602; TSG0428; ETN-89-95573) Copyright Avail: NTIS HC A03/MF A01

Computer aided turbomachinery blade design is discussed with the emphasis on the mathematical models needed to account for physical phenomena. The various aspects of a typical blade design system are presented covering through-flow and blade-to-blade analysis. The through-flow aspects such as linked through-flow-blade-to-blade analysis, blade loss models, end-wall boundary layers, secondary flow analysis and spanwise mixing

models are discussed. Blade section design using mixed design and analysis methods is covered. Loss prediction using coupled inviscid boundary layer approaches is carried out. Limitations of the coupled approach are discussed together with the emerging role of Reynolds averaged Navier-Stokes methods aimed at removing these limitations. The need for fully three dimensional methods and their incorporation into the design system are discussed. Areas for future development and application are discussed. ESA

N90-12617*# Hamilton Standard Div., United Aircraft Corp., Windsor Locks, CT.
LARGE-SCALE ADVANCED PROP-FAN (LAP) STATIC ROTOR TEST REPORT
Charles L. DeGeorge, Jay E. Turnberg, and Harry S. Wainauski 1987 156 p
(Contract NAS3-23051)
(NASA-CR-180848; NAS 1.26:180848; HSER-116227) Avail: NTIS HC A08/MF A01 CSCL 21E

Discussed is Static Rotor Testing of the SR-7L Large Scale Advanced Prop-Fan (LAP). The LAP is an advanced 9 foot diameter, 8 bladed propeller designed and built by Hamilton Standard under contract to the NASA Lewis Research Center. The Prop-Fan employs thin swept blades to provide efficient propulsion at flight speeds up to Mach .85. Static Testing was conducted on a 10,000 HP whirl rig at Wright Patterson Air Force Base. The test objectives were to investigate the Prop-Fan static aerodynamic and structural dynamic performance, determine the blade steady state stressers and deflections and to measure steady and unsteady pressures on the SR-7L blade surface. The measured performance of the LAP correlated well with analytical predictions at blade pitch angles below 30 deg. A stall buffet phenomenon was observed at blade pitch angles above 30 deg. This phenomenon manifested itself by elevated blade vibratory stress levels and lower than expected thrust produced and power absorbed by the Prop-Fan for a given speed and blade angle. Author

N90-12618*# National Aeronautics and Space Administration. Lewis Research Center, Cleveland, OH.
REAL-TIME SIMULATION OF AN F110/STOVL TURBOFAN ENGINE
Colin K. Drummond and Peter J. Ouzts Nov. 1989 24 p Presented at the Central/Northeastern ADIUS Conference, Cleveland, OH, 16-17 Oct. 1989; sponsored by Applied Dynamics International
(NASA-TM-102409; E-5162; NAS 1.15:102409) Avail: NTIS HC A03/MF A01 CSCL 21E

A traditional F110-type turbofan engine model was extended to include a ventral nozzle and two thrust-augmenting ejectors for Short Take-Off Vertical Landing (STOVL) aircraft applications. Development of the real-time F110/STOVL simulation required special attention to the modeling approach to component performance maps, the low pressure turbine exit mixing region, and the tailpipe dynamic approximation. Simulation validation derives by comparing output from the ADSIM simulation with the output for a validated F110/STOVL General Electric Aircraft Engines FORTRAN deck. General Electric substantiated basic engine component characteristics through factory testing and full scale ejector data. Author

N90-12619# Royal Aerospace Establishment, Farnborough (England).
PRELIMINARY EXPERIENCE WITH HIGH RESPONSE PRESSURE MEASUREMENTS IN A MULTISTAGE, HIGH SPEED COMPRESSOR
M. A. Cherrett and J. D. Bryce 24 May 1988 26 p Presented at the 9th International Symposium on Measuring Techniques for Transonic and Supersonic Flows in Cascades and Turbomachines, Oxford, England, 21-22 Mar. 1988
(RAE-TM-P-1141; BR108489; ETN-89-94999) Copyright Avail: NTIS HC A03/MF A01

The unsteady aerodynamic phenomena within high speed axial turbomachines is investigated. A measuring system with a frequency bandwidth of 100 to 150 kHz is applied. Experiments to commission and prove a realtime digital data acquisition system are detailed. The strategy adopted for data analysis is described, particularly the facility to lock the data capture process to the rotating frame of the machine to carry out phase locked analysis on-line. Miniature high frequency response pressure transducers are used to measure the unsteady total and wall static pressures within a high speed axial core compressor. Successful protection of the transducer diaphragm is achieved. Experiments regarding the use of such transducers in this environment is described. ESA

N90-12620# Minnesota Univ., Minneapolis.
STUDIES OF GAS TURBINE HEAT TRANSFER AIRFOIL SURFACES AND END-WALL COOLING EFFECTS Final Report, 1 Mar. 1986 - 28 Feb. 1989
E. R. Eckert, R. J. Goldstein, S. V. Patankar, and T. W. Simon Jul. 1989 90 p
(Contract F49620-85-C-0049)
(AD-A212451; AFOSR-89-1225TR) Avail: NTIS HC A05/MF A01 CSCL 21/5

Understanding and prediction of the heat transfer in a turbine is dependent first on understanding the complex three-dimensional flow that occurs around a blade. In a turbine passage there are complex (interacting) vortices, significant variation in surface curvature, flow separation, transition from laminar to turbulent flow and perhaps relaminarization, and the influence of high turbulence level in the free stream flow. Heat or mass transfer measurements, aside from providing the needed design information, can also tells a great deal about the flow. The transport of heat or mass was used to detect characteristics of flow which were not readily detectable by other means. Modeling for computation of the flow and heat transfer, also, require knowledge of the flow as well as transport data to check the validity of models and their accuracy. GRA

08 AIRCRAFT STABILITY AND CONTROL

Includes aircraft handling qualities; piloting; flight controls; and autopilots.

For related information see also *05 Aircraft Design, Testing and Performance.*

N90-12621# European Space Agency, Paris (France).
A ROBUST DIGITAL MODEL FOLLOWING CONTROLLER FOR HELICOPTERS
Gerhard Bouwer (Deutsche Forschungs- und Versuchsanstalt fuer Luft- und Raumfahrt, Brunswick, Germany, F.R.) Apr. 1989 159 p Transl. into ENGLISH of Ein Robuster Digitaler Modellfolgeregler fuer Hubschrauber (Brunswick, Fed. Republic of Germany, DFVLR), Jan. 1988 157 p Original language document was announced as N88-27203
(ESA-TT-1041; DFVLR-FB-88-07; ETN-89-95389) Avail: NTIS HC A08/MF A01; original German version available from DFVLR, VB-PL-DO, Postfach 90 60 58, 5000 Cologne, Fed. Republic of Germany, 40.50 Deutsche marks

The development, design and testing of a model following control system for helicopters is reported. In order to comply with the operating limits, a special actuator simulation system is developed. The investigations are based on a model with simple dynamics and a model for flight simulation. Numerical simulation is applied to investigate the effectiveness of the closed loop control system both in model following control and in disturbance rejection. The limits of model following control are illustrated by variation in model parameters. The possibilities of inflight simulation are demonstrated. ESA

N90-12622# Systemes et Audio Frequences, Paris (France).
INTEGRATION OF A CENTRALIZED MULTIPLEXED CONTROL UNIT INTO THE COCKPIT OF AN AIRCRAFT Final Report [INTEGRATION DANS UN POSTE DE PILOTAGE D'AERONEF D'UN ORGANE DE COMMANDE CENTRALISEE MULTIPLEXEE]
16 Feb. 1989 113 p In FRENCH
(Contract DRET-84-34-481-00-470-75-01)
(F6150-DT410-1-88329; ETN-89-95276) Avail: NTIS HC A06/MF A01

A centralized multiplexed command unit developed for the cockpit of an aircraft is described. The unit includes a screen which displays information usually available on a wide variety of dashboard instruments. An optimization of the man/machine interface is achieved by minimizing the number of hand movements, body movements and eye movements necessary for operation of the aircraft. The unit has a keyboard of twenty multifunctional keys and eleven unifunctional keys. Details of the operation of such a command unit are given. ESA

N90-12623# Advisory Group for Aerospace Research and Development, Neuilly-Sur-Seine (France).
GUIDANCE AND CONTROL PANEL SYMPOSIUM ON GUIDANCE AND CONTROL OF UNMANNED AIR VEHICLES Technical Evaluation Report
Charles T. Elliott (Semcor, Inc., Farmingdale, NJ.) Jul. 1989 20 p Presented at the Guidance and Control Panel 47th Symposium, San Francisco, CA, 4-7 Oct. 1988
(AGARD-AR-260; ISBN-92-835-0521-2) Copyright Avail: NTIS HC A03/MF A01

Papers were presented covering the following headings: operational concepts, requirements and systems, vehicle guidance and control, optical systems, systems external to the vehicles, and evaluation and test. Author

N90-12624# Dynamic Controls, Inc., Dayton, OH.
ADVANCED ACTUATION SYSTEMS DEVELOPMENT, VOLUME 1 Final Report, May 1983 - Jan. 1987
Gavin D. Jenney, Harry W. Schreadley, John A. Anderson, William G. Talley, and Carl A. Allbright Aug. 1989 233 p
(Contract F33615-83-C-3600)
(AD-A213334; WRDC-TR-89-3076-Vol-1) Avail: NTIS HC A11/MF A02 CSCL 01/4

Six different research and development activities in flight control actuation are described. The activities are: (1) the development and test of a unique linear actuator sealing system for high-pressure systems, (2) the development and test of a digital servovalve using piezo-controlled high-speed solenoid valves, (3) the performance evaluation of an F-15 rudder actuator under applied loads, (4) the performance evaluation of a Mission Adaptive Wing section under different load conditions, (5) the evaluation of output impedance modification of an electrohydraulic actuator for flutter suppression, and (6) the development and test of a direct drive valve and electronics (analog and digital) for an F-16 Horizontal Tail/FlapeRon actuator. This volume presents activities 1, 2, and 3. Volume 2 presents activities 4, 5, and 6. GRA

09 RESEARCH AND SUPPORT FACILITIES (AIR)

Includes airports, hangars and runways; aircraft repair and overhaul facilities; wind tunnels; shock tubes; and aircraft engine test stands.

For related information see also *14 Ground Support Systems and Facilities (Space).*

N90-12625*# Vigyan Research Associates, Inc., Hampton, VA.
RESIDUAL INTERFERENCE ASSESSMENT IN ADAPTIVE WALL WIND TUNNELS
A. V. Murthy Sep. 1989 32 p
(Contract NAS1-18585)
(NASA-CR-181896; NAS 1.26:181896) Avail: NTIS HC A03/MF A01 CSCL 14B

A two-variable method is presented which is suitable for on-line calculation of residual interference in airfoil testing in the Langley 0.3-Meter Transonic Cryogenic Tunnel (0.3-M TCT). The method applies the Cauchy's integral formula to the closed contour formed by the contoured top and bottom walls, and the upstream and downstream ends. The measured top and bottom wall pressures and position are used to calculate the correction to the test Mach number and the airfoil angle of attack. Application to specific data obtained in the 0.3-M TCT adaptive wall test section demonstrates the need to assess residual interference to ensure that the desired level of wall streamlining is achieved. A FORTRAN computer program was developed for on-line calculation of the residual corrections during airfoil tests in the 0.3-M TCT. Author

N90-12626# European Space Agency, Paris (France).
DYNAMIC ROBOT MODELS USING THE MANUTEC r3 AS AN EXAMPLE
Stefan Tuerck Jul. 1989 84 p Transl. into ENGLISH of Dynamische Robotermodelle am Beispiel des Manutec r3 (Oberpfaffenhofen, Fed. Republic of Germany, DFVLR) 83 p Original language document was announced as N89-11444
(ESA-TT-1132; DFVLR-Mitt-88-16; ETN-89-95762) Avail: NTIS HC A05/MF A01; original German version available from DFVLR, VB-PL-DO, Postfach 90 60 58, 5000 Cologne, Fed. Republic of Germany

A mathematical, dynamical model for the description of the motions of a robot is presented. The Manutec r3 robot is used as an example. The components of the robot are assumed to be rigid bodies. The movements of the individual bodies are described by the equations of motion. The effects such as a variable moment of inertia, and terms covering centrifugal, Coriolis and weight forces are included. Elasticity, backlash and friction in the joints are represented by force laws. The inputs of the model are the nominal values of the motor's current controllers. The torques in the joints via the dynamics of the motors are determined. ESA

N90-12627# Pennsylvania Transportation Inst., University Park.
ANALYTICAL AND EXPERIMENTAL STUDY OF RUNWAY RUNOFF WITH WIND EFFECTS Final Report, Feb. 1986 - Jun. 1989
J. R. Reed, D. F. Kibler, and G. A. Krallis Oct. 1989 65 p Prepared for Naval Air Engineering Center, Lakehurst, NJ
(Contract DOT-FA74WAI-432)
(PTI-8948; DOT/FAA/CT-TN89/59) Avail: NTIS HC A04/MF A01

This study is an extension of an earlier study that investigated the drainage efficiency of rectangular runway grooves in reducing runoff depths and the potential for hydroplaning. A mathematical model based on kinematic wave theory was developed and compared to the results of experiments conducted on a concrete slab subject to artificially produced rainfall. Parallel grooves were cut in the slab along its 30-ft length, which sloped at a typical 1.5 percent normal to the flight path. The 30-ft dimension models only the central portion of a single runway lane perhaps 100 ft wide. It was concluded that the grooves decreased runoff depths appreciably, more so as the spacing between grooves decreased. The current investigation adds wind velocity (15 mph) and direction to the variables considered in the previous study, with all other conditions essentially the same. This final report describes: (1) a kinematic wave model with wind superimposed (Phase 1); and (2) experiments conducted to calibrate the model (Phase 2). The hydraulic resistance of the slab and the calibration constants of the models were determined from the experiment. Curves of water depths versus position on a runway were predicted from the model and plotted out to 100 ft. Data points in the first 26 ft were plotted on the same graphs as a comparison. A conservative estimate of the runoff depth increase due to a direct cross wind to the runway is 0.04 inch for all conditions. Increases that are somewhat larger are restricted to smaller runoff depths. The breakout point for runoff in grooves appears to shift upstream about 25 percent of the breakout distance without wind. Author

N90-12628# National Aerospace Lab., Amsterdam (Netherlands).
DEVELOPMENT OF A MULTI-COMPONENT INTERNAL STRAIN-GAUGE BALANCE FOR MODEL TESTS IN A CRYOGENIC WIND TUNNEL
J. F. Baljeu 1988 99 p
(NLR-TR-88157-U) Avail: NTIS HC A05/MF A01

A three-component internal strain-gauge balance for use in a cryogenic wind tunnel has been developed by National Aerospace Laboratory NLR. With this balance model tests were performed in the NASA Langley 0.3-m Transonic Cryogenic Tunnel. The results are discussed with a view to the development of strain-gauge balances for the European Transonic Wind Tunnel (ETW).
Author

N90-12629 Physics and Electronics Lab. TNO, The Hague (Netherlands).
THE COMPARISON OF THE AIRBASE SIMULATION MODELS AIRBASE AND SUSTAINED
P. Schulein and E. A. M. Theunissen Sep. 1988 41 p In DUTCH; ENGLISH summary
(Contract A84/KLU/046)
(FEL-1988-66; TD88-1107; ETN-89-94470) Copyright Avail: TNO Physics and Electronics Lab., P.O. Box 96864, 2509 JG The Hague, Netherlands

The results of the comparison between two airbase simulation models are reported. A successor of the airbase model, named sustained, is constructed. Based on this comparison the sustained model is considered to be a useful tool and is designed to replace airbase.
ESA

N90-12630# Office National d'Etudes et de Recherches Aerospatiales, Paris (France). Direction de la Physique Generale.
DEVELOPMENT OF AN ANTI-STOKES COHERENT RAMAN DIFFUSION SYSTEM FOR MEASURING HYPERSONIC FLOW Final Report [REALISATION D'UN MONTAGE DRASC POUR MESURER LES VITESSES DES ECOULEMENTS HYPERSONIQUES]
M. Lefebvre and M. Pealat Jan. 1989 32 p In FRENCH
(Contract DRET-87-001-51)
(ONERA-RSF-1/7301-PY; ETN-89-95016) Avail: NTIS HC A03/MF A01

A new technique for measuring the speed of hypersonic flow is described. The method involves measuring the Doppler delay between two signals produced simultaneously, one in a container where the gas is at rest, the other in the hypersonic flow. Difficulties involved in finding the right laser modes for creating the signal are outlined. Solutions are proposed. A test project, set up on a mini wind tunnel, and used to test the validity of the technique, is described.
ESA

N90-12631# Italian Aerospace Research Center, Naples. Hypersonics Section.
HERMES PLASMA WIND TUNNEL. PRELIMINARY STUDY, PHASE A1: TEXT Final Report
A. Garrone, G. Russo, V. Particco, and F. Tammaro 29 Aug. 1988 90 p
(Contract AMD.BA-08W00022)
(DVG-HER-TN-002-Pt-1; ETN-89-95205) Avail: NTIS HC A05/MF A01

The development of the plasma arc heater to be used in the Hermes plasma wind tunnel is described. The proposed plasma generator has 70 MW of power, enthalpy up to 20 MJ/kg, tunnel stagnation pressure up to 16.6 atm, and a mass flow rate of 0.2 to 2 kg/s. It is equipped with a conical nozzle for testing nose tips and leading edges, and a semi-elliptical nozzle for testing flat plates, fuselage panels, flaps, and air brakes. Future developments and demands placed on the heater are discussed.
ESA

N90-12632# Italian Aerospace Research Center, Naples. Hypersonics Section.
HERMES PLASMA WIND TUNNEL. PRELIMINARY STUDY, PHASE A1: ANNEXES, TABLES, FIGURES Final Report
A. Garrone, G. Russo, V. Particco, and F. Tammaro 29 Aug. 1988 101 p
(Contract AMD.BA-08W00022)
(DVG-HER-TN-002-Pt-2; ETN-89-95206) Avail: NTIS HC A06/MF A01

Progress made in the design and planning of the Hermes plasma wind tunnel are described. Reports from the different sectors working on the project are included. Data, figures and charts from these different facilities are provided. Future plans for each of the sections are identified. The areas of research covered are aerodynamics, hypersonics, plasma arc jet technology, and thermal performance.
ESA

N90-12633# Ballistic Research Labs., Aberdeen Proving Ground, MD.
SPARK CAMERA ANNOTATION AND CONTROL SYSTEM FOR THE BRL (BALLISTIC RESEARCH LABORATORY) TRANSONIC RANGE FACILITY
Wallace H. Clay, Lawrence W. Burke, Jr., James B. Harmon, Eugene M. Ferguson, and Kenneth A. Willan Sep. 1989 47 p
(AD-A212266; BRL-TR-3036) Avail: NTIS HC A03/MF A01 CSCL 14/4

New cameras were recently installed into the Transonic Range Facility of the Ballistic Research Laboratory as part of a range modification program. An automated annotation and control system was designed and fabricated by the Electronics Team of the Free Flight Aerodynamics Branch, Launch and Flight Division, to interface with the new cameras. This annotation system consists of electronic instrumentation and custom built circuits installed into the cameras themselves. It provides for remote opening and closing of the shutter on all cameras and for transmitting data, round number, and station identification information to each camera to be photographically impressed upon the film at each station. It also has features for determining a variety of status conditions such as shutter status and film load-unload conditions. Details of the design and fabrication of this system are given.
GRA

N90-12634# Dayton Univ., OH. Research Inst.
FIELD-OF-VIEW VARIATIONS AND STRIPE-TEXTURING EFFECTS ON ASSAULT LANDING PERFORMANCE IN THE C-130 WEAPON SYSTEM TRAINER Final Report, Feb. 1986 - Dec. 1988
Robert S. Kellogg, David C. Hubbard, and Michael J. Sieverding (Aeronautical Systems Div., Wright-Patterson AFB, OH.) Aug. 1989 24 p
(Contract F33615-87-C-0012)
(AD-A212763; AFHRL-TR-89-3) Avail: NTIS HC A03/MF A01 CSCL 01/2

Two experiments were conducted using the C-130 Weapon System Trainer (WST) located at Little Rock AFB, Arkansas. These experiments were the first of a series of R and D efforts designed to provide input to specification of the visual requirements for the C-17 flight simulator. Both studies assessed the effect of an experimental manipulation upon pilot performance of an assault landing. The basic experimental design for each was randomized block repeated measures. For each study, ten experienced C-130 pilots served as subjects. The first study investigated the effect of limiting the field of view (FOV) of the WST by reducing the five-channel, six-window visual system to two channels and two windows. The second study investigated the effect of data base texturing upon pilot performance. No strongly significant FOV effects were obtained in the first study. However, the results of the second study indicated that data base texturing improved the pilots' ability to fly at lower altitudes and place the aircraft closer to the center line during landing and touchdown.
GRA

N90-12522*# National Aeronautics and Space Administration. Langley Research Center, Hampton, VA.
HOT-FILM SYSTEM FOR TRANSITION DETECTION IN CRYOGENIC WIND TUNNELS
Charles B. Johnson, Debra L. Carraway, P. Calvin Stainback, and M. F. Fancher (Douglas Aircraft Co., Inc., Long Beach, CA.) *In its* Research in Natural Laminar Flow and Laminar-Flow Control,

Part 2 Dec. 1987 p 358-376 (For primary document see N90-12519 04-02)
Avail: NTIS HC A15/MF A02 CSCL 14B

N90-12526*# National Aeronautics and Space Administration. Langley Research Center, Hampton, VA.
BASIC AERODYNAMIC RESEARCH FACILITY FOR COMPARATIVE STUDIES OF FLOW DIAGNOSTIC TECHNIQUES
Gregory S. Jones, Luther R. Gartrell, and P. Calvin Stainback *In its* Research in Natural Laminar Flow and Laminar-Flow Control, Part 2 Dec. 1987 p 401-406 (For primary document see N90-12519 04-02)
Avail: NTIS HC A15/MF A02 CSCL 14B

N90-12528*# National Aeronautics and Space Administration. Langley Research Center, Hampton, VA.
RECENT FLOW VISUALIZATION STUDIES IN THE 0.3-m TCT
Walter L. Snow, Alpheus W. Burner, and William K. Goad *In its* Research in Natural Laminar Flow and Laminar-Flow Control, Part 2 Dec. 1987 p 412-419 (For primary document see N90-12519 04-02)
Avail: NTIS HC A15/MF A02 CSCL 14B

N90-12555*# National Aeronautics and Space Administration. Langley Research Center, Hampton, VA.
DESIGN AND FABRICATION REQUIREMENTS FOR LOW NOISE SUPERSONIC/HYPERSONIC WIND TUNNELS
Ivan E. Beckwith, Fang-Jeng Chen, and Mujeeb R. Malik (High Technology Corp., Hampton, VA.) *In its* Research in Natural Laminar Flow and Laminar-Flow Control, Part 3 Dec. 1987 p 947-964 (For primary document see N90-12539 04-02)
Avail: NTIS HC A17/MF A03 CSCL 14B

12 ASTRONAUTICS (GENERAL)

For extraterrestrial exploration see *91 Lunar and Planetary Exploration.*

N90-12635*# National Aeronautics and Space Administration, Washington, DC.
REPORT ON ORBITAL DEBRIS
Feb. 1989 74 p Prepared in cooperation with Air Force Systems Command, Bolling AFB, Washington, DC Original contains color illustrations
(NASA-TM-101855; NAS 1.15:101855) Avail: NTIS HC A04/MF A01 CSCL 22A

The success of space endeavors depends upon a space environment sufficiently free of debris to enable the safe and dependable operation of spacecraft. An environment overly cluttered with debris would threaten the ability to utilize space for a wide variety of scientific, technological, military, and commercial purposes. Man made space debris (orbital debris) differs from natural meteoroids because it remains in earth orbit during its lifetime and is not transient through the space around the Earth. The orbital debris environment is considered. The space environment is described along with sources of orbital debris. The current national space policy is examined, along with ways to minimize debris generation and ways to survive the debris environment. International efforts, legal issues and commercial regulations are also examined. E.R.

N90-12636# Commission on Integrated Long-Term Strategy, Washington, DC. Working Group on Technology.
RECOMMENDED CHANGES IN US MILITARY SPACE POLICIES AND PROGRAMS: A PAPER SUBMITTED TO THE COMMISSION ON INTEGRATED LONG-TERM STRATEGY
Charles Herzfeld Oct. 1988 15 p Sponsored by DOD, Washington, DC
(PB89-219364) Avail: NTIS HC A03/MF A01 CSCL 22A

Recommendations by the Commission on Integrated Long Term Strategy's Working Group on Technology are outlined for revisions in the United States' military space policies and programs. Author

N90-12637# Naval Postgraduate School, Monterey, CA. Dept. of Physics.
CURRENT LIMITING MECHANISMS IN ELECTRON AND ION BEAMS EXPERIMENTS Technical Report, period ending Aug. 1989
R. C. Olsen 7 Aug. 1989 67 p
(AD-A212295; NPS61-89-013) Avail: NTIS HC A04/MF A01 CSCL 22/1

The emission and collection of current from satellites or rockets in the ionosphere is a process which, at equilibrium, requires a balance between inward and outward currents. In most active experiments in the ionosphere and magnetosphere, the emitted current exceeds the integrated thermal current by one or more orders of magnitude. The system response is typically for the emitted current to be limited by processes such as differential charging of insulating surfaces, interactions between an emitted beam and the local plasma, and interactions between the beam and local neutral gas. These current limiting mechanisms have been illustrated for 20 years in sounding rocket and satellite experiments, which are reviewed here. Detailed presentations of the SCATHA electron and ion gun experiments are used to demonstrate the general range of observed phenomena. GRA

N90-12638# Naval Postgraduate School, Monterey, CA.
A SURVEY OF PERMANENTLY-MANNED LUNAR BASE CONCEPTS M.S. Thesis
Lorenzo S. Hiponia Jun. 1989 164 p
(AD-A212575; AD-E501149) Avail: NTIS HC A08/MF A01 CSCL 22/1

This thesis is a comparative evaluation of various lunar base concepts advocated by leading experts in the field of manned space exploration. Additionally, original design concepts are presented in four appendices. The emphasis is on the impact of mission strategy and objectives on lunar base design concepts. Three candidate mission scenarios involving a lunar base are compared: (1) a scientific research station, (2) a mining and manufacturing facility based on lunar resources, (3) a permanent, autonomous manned base or staging point for space exploration. The lunar base development stages are related to the evolution of the various mission alternatives. In addition, several lunar base design concepts are compared and evaluated in terms of function and construction techniques suitable for the lunar environment. Lunar base power sources are compared in terms of power output, complexity, and feasibility. Particular attention is given to the role of solar and nuclear power and the possible role of superconducting technology. Finally, the transportation infrastructure and logistics required to support an operational Moon base are examined, the primary focus being on mission modes, transportation costs, and supply logistics. This thesis concludes with a feasibility appraisal of a lunar base endeavor and surveys current lunar base study efforts. GRA

13 ASTRODYNAMICS

Includes powered and free-flight trajectories; and orbital and launching dynamics.

N90-12639# European Space Agency, Paris (France).
TROPOSPHERIC INFLUENCES ON SATELLITE-EARTH PATHS AND THEIR DETERMINATION BY MEANS OF RADAR MEASUREMENTS
Gottfried Schnabl Jul. 1989 218 p Transl. into ENGLISH of Bestimmung Troposphaerischer Stoerungen der Wellenausbreitung auf Erde-Satellit-Verbindungen mit Hilfe von Radarmessungen (Oberpfaffenhofen, Fed. Republic of Germany, DFVLR) 166 p Original language document was announced as N89-25250
(ESA-TT-1143; DFVLR-FB-88-53; ETN-89-95764) Avail: NTIS HC A10/MF A01; original German version available from

DFVLR, VB-PL-DO, Postfach 90 60 58, 5000 Cologne, Fed. Republic of Germany

A method to determine the influence of rain, snow and ice clouds on the propagation of electromagnetic waves along satellite-Earth paths, is described. Radar measurements are applied to evaluate the influence of those parameters, in the gigahertz region, in the troposphere. The attenuation, the depolarization and the phase shift are taken into account. The results did not provide any indication that scattering volumes of ice cause high degrees of depolarization. No long term continuous measurements are made and a temporary occurrence of higher degrees of depolarization due to scattering volumes of ice cannot be excluded. They are covered in every case by the models and methods developed here for radar data analysis. ESA

N90-12640# Royal Aerospace Establishment, Farnborough (England).
EVALUATION OF 15TH- AND 30TH-ORDER GEOPOTENTIAL HARMONIC COEFFICIENTS FROM 26 RESONANT SATELLITE ORBITS
D. G. King-Hele and Doreen M. C. Walker 24 Jun. 1989 38 p (RAE-TR-88045; RAE-SS-7; BR108723; ETN-89-94830)
Copyright Avail: NTIS HC A03/MF A01

The results of resonance analysis concerning the obtention of harmonic coefficients of order 15 and 30 are presented. They are determined by the analysis of the satellite orbits. Great improvements in the standard deviations of many of the 15th order coefficients of even degree are otained. For the 30th order and odd degree 15th order coefficients only small changes are observed. The obtained values are compared to those of geoid models. The results lead to the conclusion that for orders 15 and 30 the nominal standard deviations are quite realistic. ESA

N90-12641# Royal Aerospace Establishment, Farnborough (England).
ORBIT DETERMINATION AND ANALYSIS FOR COSMOS 236 AT 15TH-ORDER RESONANCE
A. N. Winterbottom Sep. 1988 29 p
(RAE-TR-88058; RAE-SS-9; BR108923; ETN-89-94832)
Copyright Avail: NTIS HC A03/MF A01

The orbital parameters of Cosmos 236, determined for 77 epochs between July 1983 and October 1984, are examined. The effects of 15th order resonance and the Earth's gravitational field are considered. The orbital accuracy achieved is consistent. The standard deviation in orbital inclination and eccentricity correspond on average to positional accuracies of 85 m and 65 m respectively. Analysis of the changes in inclination and in eccentricity are effectuated. The values of three pairs of lumped harmonics of order 15 and three pairs of order 30, are obtained. The values from inclination has standard deviations equivalent to accuracies in geoid height of 0.6 and 2.0 cm for orders 15 and 30 respectively. The equivalent accuracies for the values from eccentricity are 1.6 and 6.0 cm. ESA

N90-12642# Royal Aerospace Establishment, Farnborough (England).
ON MEAN ELEMENTS FOR SATELLITE ORBITS PERTURBED BY THE ZONAL HARMONICS OF THE GEOPOTENTIAL
R. H. Gooding Jul. 1989 9 p Presented at the 27th COSPAR Meeting, Espoo, Finland, 21 Jul. 1988 Submitted for publication
(AD-A212322; RAE-TM-371; DRIC-BR-110918) Avail: NTIS HC A02/MF A01 CSCL 22/3

Users of orbital elements are often puzzled by the different ways in which mean elements are defined. This applies to all the standard elements, but the difficulty is most pronounced in regard to semi-major axis and mean motion. Mean elements are related to the perturbations of a satellite caused by the earth's zonal harmonic J2, and it is shown how elements can be defined so that perturbations in spherical coordinates take an especially simple form. The emphasis is on the first-order effects of J2, with formulae given to connect the preferred elements to the elements of Kozai, but the extension to second order in J2 and first order in the general zonal harmonic is also considered. GRA

N90-12787*# Jet Propulsion Lab., California Inst. of Tech., Pasadena.
AN ANALYTIC DEVELOPMENT OF ORBIT DETERMINATION FOR A DISTANT, PLANETARY ORBITER
R. K. Russell and S. W. Thurman *In its* The Telecommunications and Data Acquisition Report 15 Aug. 1989 p 1-25 (For primary document see N90-12786 04-32)
Avail: NTIS HC A11/MF A02 CSCL 22A

14 GROUND SUPPORT SYSTEMS AND FACILITIES (SPACE)

Includes launch complexes, research and production facilities; ground support equipment, e.g., mobile transporters; and simulators.

For related information see also *09 Research and Support Facilities (Air).*

No abstracts in this category.

15 LAUNCH VEHICLES AND SPACE VEHICLES

Includes boosters; operating problems of launch/space vehicle systems; and reusable vehicles.

For related information see also *20 Spacecraft Propulsion and Power.*

N90-12643# Aerospace Corp., El Segundo, CA.
BATCH LCAP2-LINEAR CONTROL ANALYSIS, VERSION 2.0: USER'S MANUAL
Eugene A. Lee 31 Jan. 1989 467 p
(Contract F04701-88-C-0089)
(AD-A211670; TR-0089(9975)-1; SSD-TR-89-48) Avail: NTIS HC A20/MF A03 CSCL 22/4

Batch LCAP2 (Linear Controls Analysis Program) is a FORTRAN program which provides the controls analyst with a set of easy to use FORTRAN subroutines which implements classical SISO control analysis techniques such as transfer function evaluation, transfer function algebra, frequency response, root locus, inverse time response, and sampled-data transforms. It can handle continuous systems and continuous- and continuous discrete multirate systems with the use of s, z, and w transforms. Recent additions to LCAP2 include: (1) the capability for connecting transfer function blocks for both continuous and continuous-discrete multirate systems, and (2) a precompiler to aid the user in writing FORTRAN code. The methodology used for connecting transfer function blocks takes into consideration the dimensionality problem associated with the use of nondynamic blocks or algebraic variables used in modeling the connection of dynamic blocks. In the formulation of the system matrix used in LCAP2, the dimension of the system matrix is not increased by the use of nondynamic blocks. The automated analysis of continuous-discrete multirate systems modeled by a connection of transfer function blocks uses the Kalman-Bertram state space method. It is the primary frequency domain analysis program used for stability verification of launch vehicles. GRA

N90-12644# Air Force Systems Command, Wright-Patterson AFB, OH. Foreign Technology Div.
PRESENT AND FUTURE US AND SOVIET CHEMICAL MISSILES AND CHEMICAL ROCKET PROJECTILES
Guochang Zhang 16 Jun. 1989 11 p Transl. into ENGLISH from Military World (China), v. 1, no. 1, 1988 p 33-34
(AD-A212199; FTD-ID(RS)T-0677-89) Avail: NTIS HC A03/MF A01 CSCL 15/6

In the Soviet and U.S. arsenal of chemical weapons, chemical missiles and chemical rocket projectiles occupy an especially

important position. The missiles are a kind of risk-free remote chemical assault device, while the rocket projectiles are powerful antipersonnel weapons effective at close range and over a large area. Both countries have devoted a great effort to the development of chemical missiles and rocket projectiles. Currently, the U.S.S.R. has a clear superiority in the field, but the U.S. is rousing itself to catch up, thanks to its development and broad deployment of dual chemical weapons. GRA

16 SPACE TRANSPORTATION

Includes passenger and cargo space transportation, e.g., shuttle operations; and space rescue techniques.

For related information see also *03 Air Transportation and Safety* and *18 Spacecraft Design, Testing and Performance.* For space suits see *54 Man/System Technology and Life Support.*

No abstracts in this category.

17 SPACE COMM., SPACECRAFT COMM., COMMAND & TRACKING

Includes telemetry; space communications networks; astronavigation and guidance; and radio blackout.

For related information see also *04 Aircraft Communications and Navigation* and *32 Communications and Radar.*

No abstracts in this category.

18 SPACECRAFT DESIGN, TESTING AND PERFORMANCE

Includes satellites; space platforms; space stations; spacecraft systems and components such as thermal and environmental controls; and attitude controls.

For life support systems see *54 Man/System Technology and Life Support.* For related information see also *05 Aircraft Design, Testing and Performance, 39 Structural Mechanics,* and *16 Space Transportation.*

N90-12645*# Wyle Labs., Inc., Huntsville, AL.
ADVANCED SPACECRAFT FIRE SAFETY: PROPOSED PROJECTS AND PROGRAM PLAN Final Report
Wallace W. Youngblood and M. Vedha-Nayagam Oct. 1989 176 p
(Contract NAS3-25367)
(NASA-CR-185147; NAS 1.26:185147; Wyle-60300-1) Avail: NTIS HC A09/MF A01 CSCL 22B

A detailed review identifies spacecraft fire safety issues and the efforts for their resolution, particularly for the threats posed by the increased on-orbit duration, size, and complexity of the Space Station Freedom. Suggestions provided by a survey of Wyle consultants and outside fire safety experts were combined into 30 research and engineering projects. The projects were then prioritized with respect to urgency to meet Freedom design goals, status of enabling technology, cost, and so on, to yield 14 highest priority projects, described in terms of background, work breakdown structure, and schedule. These highest priority projects can be grouped into the thematic areas of fire detection, fire extinguishment, risk assessment, toxicology and human effects, and ground based testing. Recommendations for overall program management stress the need for NASA Headquarters and field center coordination, with information exchange through spacecraft fire safety oversight committees. Author

N90-12646*# Virginia Polytechnic Inst. and State Univ., Blacksburg. Dept. of Aerospace and Ocean Engineering.
NASA/USRA ADVANCED SPACE DESIGN PROGRAM: THE LASER POWERED INTERORBITAL VEHICLE
Jun. 1989 164 p Sponsored by USRA
(Contract NASw-4435)
(NASA-CR-186044; NAS 1.26:186044) Avail: NTIS HC A08/MF A01 CSCL 22B

A preliminary design is presented for a low-thrust Laser Powered Interorbital Vehicle (LPIV) intended for cargo transportation between an earth space station and a lunar base. The LPIV receives its power from two iodide laser stations, one orbiting the earth and the other located on the surface of the moon. The selected mission utilizes a spiral trajectory, characteristic of a low-thrust spacecraft, requiring 8 days for a lunar rendezvous and an additional 9 days for return. The ship's configuration consists primarily of an optical train, two hydrogen plasma engines, a 37.1 m box beam truss, a payload module, and fuel tanks. The total mass of the vehicle fully loaded is 63300 kg. A single plasma, regeneratively cooled engine design is incorporated into the two 500 N engines. These are connected to the spacecraft by turntables which allow the vehicle to thrust tangentially to the flight path. Proper collection and transmission of the laser beam to the thrust chambers is provided through the optical train. This system consists of the 23 m diameter primary mirror, a convex parabolic secondary mirror, a beam splitter and two concave parabolic tertiary mirrors. The payload bay is capable of carrying 18000 kg of cargo. The module is located opposite the primary mirror on the main truss. Fuel tanks carrying a maximum of 35000 kg of liquid hydrogen are fastened to tracks which allow the tanks to be moved perpendicular to the main truss. This capability is required to prevent the center of mass from moving out of the thrust vector line. The laser beam is located and tracked by means of an acquisition, pointing and tracking system which can be locked onto the space-based laser station. Correct orientation of the spacecraft with the laser beam is maintained by control moment gyros and reaction control rockets. Additionally an aerobrake configuration was designed to provide the option of using the atmospheric drag in place of propulsion for a return trajectory. Author

N90-12647# Air Force Geophysics Lab., Hanscom AFB, MA.
OPTICAL DETECTION OF SPACE DEBRIS USING A LARGE ACHROMATIC CORONAGRAPH
S. Koutchmy and C. Nitschelm (Centre National de la Recherche Scientifique, Paris, France) 1988 10 p Submitted for publication
(AD-A211362; AFGL-TR-89-0201) Avail: NTIS HC A02/MF A01 CSCL 17/5

The threat of space debris seems to increase steadily. Accordingly, new methods of detection are needed. We present a theoretical approach to this problem, assuming the use of a new generation large achromatic ground based coronagraph. Some interesting results are presented, including the estimation of the probability of being able to systematically observe small size space debris in a large range of altitudes. GRA

N90-12648# Missouri Univ., Rolla. Dept. of Mechanical and Aerospace Engineering.
PHASE CHANGE MATERIAL FOR SPACECRAFT THERMAL MANAGEMENT Interim Report, 15 Mar. 1987 - 31 Mar. 1988
John W. Sheffield and Chudong Wen Apr. 1989 72 p
(Contract F33615-86-C-2721; AF Proj. 3145)
(AD-A211404; WRDC-TR-89-2038) Avail: NTIS HC A04/MF A01 CSCL 20/13

Heat transfer problems involving phase change are encountered extensively in technical and natural processes. Latent heat storage, which possess the advantages of high density of energy and isothermal behavior during charging and discharging, is one application of using phase change material (PCM). A computational model is presented for the prediction of the heat

transfer between a heat transfer fluid (HTF) and PCM of latent heat storage unit. Two models of flow, hydrodynamically fully developed flow and developing flow, of the HTF were proposed in this study. A two-dimensional enthalpy method was used for the computation of the phase change heat transfer in the PCM. A fully implicit finite difference scheme was used for the calculation of convective heat transfer in the HTF. The unknown time dependent boundary condition between the HTF and the PCM was found iteratively. The predictions are substantiated by their fair agreement with experimental data. Factors which affect the heat transfer rates between the HTF and the PCM were studied numerically for both hydrodynamically fully developed flow and developing flow. It is found that the Nusselt number is significantly increased by the developing temperature profiles. GRA

N90-12649# European Space Agency, Paris (France). Space Science Dept.
REPORT ON ESA'S SCIENTIFIC SATELLITES
V. Domingo, U. O. Frisk, R. Grard, P. Jakobsen, M. F. Kessler, J.-P. Lebreton, R. Marsden, A. Peacock, M. A. C. Perryman, and R. Reinhard et al May 1989 120 p Original contains color illustrations
(ESA-SP-1110; ISSN-0379-6566; ETN-89-95386) Copyright
Avail: NTIS HC A06/MF A01

The missions and scientific results obtained by ESA's scientific satellite program for the period from May 1988 to April 1989 are described. During this period, ESA operated only one scientific satellite, the International Ultraviolet Explorer in collaboration with NASA. The Giotto spacecraft, still in orbit around the Sun, in hibernation mode, could potentially investigate the comet Grigg-Skellerup in 1992. Hipparcos, the astrometry satellite is ready for launch in July 1989, and the main development phase of ISO is well under way. Future missions, planned or in preparation are discussed and the future of the overall program is evaluated.
ESA

19 SPACECRAFT INSTRUMENTATION

For related information see also *06 Aircraft Instrumentation* and *35 Instrumentation and Photography.*

No abstracts in this category.

20 SPACECRAFT PROPULSION AND POWER

Includes main propulsion systems and components, e.g., rocket engines; and spacecraft auxilliary power sources.

For related information see also *07 Aircraft Propulsion and Power, 28 Propellants and Fuels, 44 Energy Production and Conversion,* and *15 Launch Vehicles and Space Vehicles.*

N90-12650*# Lockheed Missiles and Space Co., Huntsville, AL. Engineering Center.
SSME STRUCTURAL DYNAMIC MODEL DEVELOPMENT Final Report
Michael J. Foley Mar. 1989 117 p
(Contract NAS8-37302)
(NASA-CR-183671; NAS 1.26:183671; LMSC-HEC-TR-F268627)
Avail: NTIS HC A06/MF A01 CSCL 21H

The high pressure fuel turbopump (HPFTP) is a major component of the Space Shuttle Main Engine (SSME) powerhead. The device is a three stage centrifugal pump that is directly driven by a two stage hot gas turbine. The purpose of the pump is to deliver fuel (liquid hydrogen) from the low pressure fuel turbopump (LPFTP) through the main fuel valve (MFV) to the thrust chamber coolant circuits. In doing so, the pump pressurizes the fuel from an inlet pressure of approximately 178 psi to a discharge pressure of over 6000 psi. At full power level (FPL), the pump rotates at a speed of over 37,000 rpm while generating approximately 77,000 horsepower. Obviously, a pump failure at these speeds and power levels could jeopardize the mission. Results are summarized for work in which the solutions obtained from analytical models of the fuel turbopump impellers are compared with the results obtained from dynamic tests. Author

N90-12651*# Morton Thiokol, Brigham City, UT. Aerospace Group.
RSRM-3 (360L003) BALLISTICS/MASS PROPERTIES REPORT Final Report
B. A. Laubacher and M. C. Richards 5 May 1989 66 p
(Contract NAS8-30490)
(NASA-CR-183716; NAS 1.26:183716; TWR-17541-10; L211-FY89-M086) Avail: NTIS HC A04/MF A01 CSCL 21H

The propulsion performance and reconstructed mass properties data from Morton Thiokol's RSRM-3 motors which were assigned to the STS-29 launch are presented. The composite type solid propellant burn rates were close to predicted. The performance of the pair of motors were compared to some CEI Specifications. The performance from each motor as well as matched pair performance values were well within the CEI specification requirements. The nominal thrust time curve and impulse gate information is included. Post flight reconstructed Redesigned Solid Rocket Motor (RSRM) mass properties are within expected values for the lightweight configuration. E.R.

N90-12652*# Morton Thiokol, Brigham City, UT. Aerospace Group.
BALLISTICS/MASS PROPERTIES Final Report
Albert S. Drendel and M. C. Richards 23 Jun. 1989 20 p
(Contract NAS8-30490)
(NASA-CR-183723; NAS 1.26:183723; TWR-17543-10; ECS-SS-1012) Avail: NTIS HC A03/MF A01 CSCL 21H

The propulsion performance and reconstructed mass properties data from Morton Thiokol's RSRM-4 motors, which were assigned to the STS-30R launch, are presented. The composite type solid propellant burn rates were close to predicted. The performance of the pair of motors were compared to some CEI Specification CPW1-3600 for compliance. Some aspects of the CEI Specification could not be compared because of low sampling of data. The performance of the motors were well within the CEI specification requirements. Post flight reconstructured RSRM mass properties are within expected values for the RSRM quarterweight and halfweight configurations. E.R.

N90-12653 Virginia Polytechnic Inst. and State Univ., Blacksburg.
ANALYSIS AND SIMULATION OF DYNAMICS OF SPACECRAFT POWER SYSTEMS Ph.D. Thesis
Jae Ryong Lee 1988 219 p
Avail: Univ. Microfilms Order No. DA8907514

Comprehensive analyses, including dc, small-signal, and large-signal analyses, of the dynamics of various spacecraft power systems were performed. Systems dynamics are analyzed for various operating modes, such as the shunt, battery-charge and battery discharge modes, as well as the transition mode. Computer models using the EASY5 program were developed for the Direct Energy Transfer (DET) system, solar array switching system, and partial shunt system to facilitate design, analysis, and performance verification. Large-signal analyses were performed to identify stability conditions and to predict large-signal dynamic behavior for each mode of operation. Small-signal analyses of the DET system were performed for the three modes of operation. Various spacecraft power systems, such as solar array switching systems, a partial shunt system, a peak power tracking system, and the Cosmic Background Explorer (COBE) power system were analyzed and simulated. Design guidelines of the power conditioning equipment for each system were provided. Dissert. Abstr.

N90-12654*# Tennessee Univ. Space Inst., Tullahoma.
THE FAULT MONITORING AND DIAGNOSIS KNOWLEDGE-BASED SYSTEM FOR SPACE POWER SYSTEMS: AMPERES, PHASE 1 Final Report
S. C. Lee Nov. 1989 44 p
(Grant NAG8-721)
(NASA-CR-185486; NAS 1.26:185486) Avail: NTIS HC A03/MF A01 CSCL 10B

The objective is to develop a real time fault monitoring and diagnosis knowledge-based system (KBS) for space power systems which can save costly operational manpower and can achieve more reliable space power system operation. The proposed KBS was developed using the Autonomously Managed Power System (AMPS) test facility currently installed at NASA Marshall Space Flight Center (MSFC), but the basic approach taken for this project could be applicable for other space power systems. The proposed KBS is entitled Autonomously Managed Power-System Extendible Real-time Expert System (AMPERES). In Phase 1 the emphasis was put on the design of the overall KBS, the identification of the basic research required, the initial performance of the research, and the development of a prototype KBS. In Phase 2, emphasis is put on the completion of the research initiated in Phase 1, and the enhancement of the prototype KBS developed in Phase 1. This enhancement is intended to achieve a working real time KBS incorporated with the NASA space power system test facilities. Three major research areas were identified and progress was made in each area. These areas are real time data acquisition and its supporting data structure; sensor value validations; development of inference scheme for effective fault monitoring and diagnosis, and its supporting knowledge representation scheme. Author

N90-12655*# Rensselaer Polytechnic Inst., Troy, NY. Dept. of Mechanical Engineering, Aeronautical Engineering, and Mechanics.
APOLLO LIGHTCRAFT PROJECT
Leik N. Myrabo, Mark A. Atonison, ed., Sammy G. Chen, ed., Casimer DeCusatis, ed., Karl P. Kusche, ed., Marco A. Minucci, ed., Jeffrey P. Moder, ed., Ciro Morales, ed., Caroline V. Nelson, ed., and Jacques C. Richard, ed. et al Jun. 1989 258 p Presented at the 5th Annual Summer Conference on the NASA/USRA Advanced Design Program, Huntsville, AL, 12-16 Jun. 1989
(Contract NASw-4435)
(NASA-CR-186055; NAS 1.26:186055) Avail: NTIS HC A12/MF A02 CSCL 21H

The ultimate goal for this NASA/USRA-sponsored Apollo Lightcraft Project is to develop a revolutionary manned launch vehicle technology which can potentially reduce payload transport costs by a factor of 1000 below the Space Shuttle Orbiter. The Rensselaer design team proposes to utilize advanced, highly energetic, beamed-energy sources (laser, microwave) and innovative combined-cycle (airbreathing/rocket) engines to accomplish this goal. The research effort focuses on the concept of a 100 MW-class, laser-boosted Lightcraft Technology Demonstrator (LTD) drone. The preliminary conceptual design of this 1.4 meter diameter microspacecraft involved an analytical performance analysis of the transatmospheric engine in its two modes of operation (including an assessment of propellant and tankage requirements), and a detailed design of internal structure and external aeroshell configuration. The central theme of this advanced propulsion research was to pick a known excellent working fluid (i.e., air or LN sub 2), and then to design a combined-cycle engine concept around it. Also, a structural vibration analysis was performed on the annular shroud pulsejet engine. Finally, the sensor satellite mission was examined to identify the requisite subsystem hardware: e.g., electrical power supply, optics and sensors, communications and attitude control systems. Author

N90-12656*# Morton Thiokol, Brigham City, UT. Aerospace Group.
FLIGHT MOTOR SET 360L001 (STS-26R). (RECONSTRUCTED DYNAMIC LOADS ANALYSIS) Final Report
V. B. Call Jun. 1989 372 p
(Contract NAS8-30490)
(NASA-CR-183811; NAS 1.26:183811; TRW-17271-Vol-11)
Avail: NTIS HC A16/MF A02 CSCL 21H

A transient analysis was performed to correlate the predicted versus measured behavior of the Redesigned Solid Rocket Booster (RSRB) during Flight 360L001 (STS-26R) liftoff. Approximately 9 accelerometers, 152 strain gages, and 104 girth gages were bonded to the motors during this event. Prior to Flight 360L001, a finite element model of the RSRB was analyzed to predict the accelerations, strains, and displacements measured by this developmental flight instrumentation (DFI) within an order of magnitude. Subsequently, an analysis has been performed which uses actual Flight 360L001 liftoff loading conditions, and makes more precise predictions for the RSRB structural behavior. Essential information describing the analytical model, analytical techniques used, correlation of the predicted versus measured RSRB behavior, and conclusions, are presented. A detailed model of the RSRB was developed and correlated for use in analyzing the motor behavior during liftoff loading conditions. This finite element model, referred to as the RSRB global model, uses super-element techniques to model all components of the RSRB. The objective of the RSRB global model is to accurately predict deflections and gap openings in the field joints to an accuracy of approximately 0.001 inch. The model of the field joint component was correlated to Referee and Joint Environment Simulation (JES) tests. The accuracy of the assembled RSRB global model was validated by correlation to static-fire tests such DM-8, DM-9, QM-7, and QM-8. This validated RSRB global model was used to predict RSRB structural behavior and joint gap opening during Flight 360L001 liftoff. The results of a transient analysis of the RSRB global model with imposed liftoff loading conditions are presented. Rockwell used many gage measurements to reconstruct the load parameters which were imposed on the RSRB during the Flight 360L001 liftoff. Each load parameter, and its application, is described. Also presented are conclusions and recommendations based on the analysis of this load case and the resulting correlation between predicted and measured RSRB structural behavior. Author

N90-12657# Air Force Systems Command, Wright-Patterson AFB, OH. Foreign Technology Div.
A DATA ACQUISITION AND PROCESSING SYSTEM FOR SIX COMPONENT SOLID ROCKET MOTOR TESTING
Zhaomin Li, Jing Liu, Baojiang Li, and Zhuping Xu 16 Aug. 1989 9 p Transl. into ENGLISH from Binggong Xuebao (China), v. 3, Aug. 1987 p 73-75
(AD-A212200; FTD-ID(RS)T-0053-89) Avail: NTIS HC A02/MF A01 CSCL 21/8

This article introduces the PDP-11/03 microcomputer for the collection and processing of data from six component tests of solid rocket motors. It discusses the components of this system, its capabilities and special characteristics. Finally, it gives measured values for the static precision of the system in test measurements. GRA

23 CHEMISTRY AND MATERIALS (GENERAL)

N90-12658*# National Aeronautics and Space Administration. Lewis Research Center, Cleveland, OH.
TRIBOLOGICAL PROPERTIES OF CERAMIC/Ti3Al-Nb SLIDING COUPLES FOR USE AS CANDIDATE SEAL MATERIALS TO 700 DEG C
Christopher DellaCorte, Bruce M. Steinetz, and Pamela K. Brindley 1989 21 p Proposed for presentation at the International Conference on Metallurgical Coatings, San Diego, CA, 2-6 Apr. 1990; sponsored by American Vacuum Society
(NASA-TM-102401; E-5048; NAS 1.15:102401) Avail: NTIS HC A03/MF A01 CSCL 07A

Tribological properties of Ti3Al-Nb intermetallic disks sliding

against alumina-boria-silicate fabric were ascertained in air at temperatures from 25 to 700 C. These materials are candidates for sliding seal applications for the National AeroSpace Plane. The tests were done using a pin on disk tribometer. Sliding was unidirectional at 0.27 m/sec under a nominal contact stress of 340 kPa. Gold sputter or ion plating deposited films were used to reduce friction and wear. Rhodium and palladium films were used beneath the gold lubricating films to prevent diffusion of the substrate into the gold at high temperature. The friction and wear of the unlubricated specimens was unacceptable. Friction coefficients were generally greater than 1.0. The ion plated gold films, when used with a rhodium diffusion barrier reduced friction by almost a factor of 2. Wear was also substantially reduced. The sputter deposited films were not adherent unless the substrate was sputter cleaned immediately prior to film deposition. Palladium did not function as a diffusion barrier. Author

N90-12659*# National Aeronautics and Space Administration. Lewis Research Center, Cleveland, OH.
TRIBOLOGICAL PROPERTIES OF PM212: A HIGH-TEMPERATURE, SELF-LUBRICATING, POWDER METALLURGY COMPOSITE
Christopher DellaCorte and Harold E. Sliney 1989 22 p Proposed for presentation at the Annual Meeting of the Society of Tribologists and Lubrication Engineers, Denver, CO, 7-11 May 1990
(NASA-TM-102355; E-5066; NAS 1.15:102355) Avail: NTIS HC A03/MF A01 CSCL 07A

This paper describes a research program to develop and evaluate a new high temperature, self-lubricating powder metallurgy composite, PM212. PM212 has the same composition as the plasma-sprayed coating, PS212, which contains 70 wt percent metal-bonded chromium carbide, 15 wt percent silver and 15 wt percent barium fluoride/calcium fluoride eutectic. The carbide acts as a wear resistant matrix and the silver and fluorides act as low and high temperature lubricants, respectively. The material is prepared by sequential cold press, cold isostatic pressing and sintering techniques. In this study, hemispherically tipped wear pins of PM212 were prepared and slid against superalloy disks at temperatures from 25 to 850 C in air in a pin-on-disk tribometer. Friction coefficients range from 0.29 to 0.38 and the wear of both the composite pins and superalloy disks was moderate to low in the 10(exp -5) to 10(exp -6) cubic mm/N-m range. Preliminary tests indicate that the material has a compressive strength of at least 130 MPa over the entire temperature range of 25 to 900 C. This material has promise for use as seal inserts, bushings, small inside diameter parts and other applications where plasma-sprayed coatings are impractical or too costly. Author

24 COMPOSITE MATERIALS

Includes physical, chemical, and mechanical properties of laminates and other composite materials.
For ceramic materials see *27 Nonmetallic Materials*.

N90-12660 City Univ., London (England).
OPTICAL FIBRE WITNESSES OF FATIGUE DAMAGE IN COMPOSITE MATERIALS Ph.D. Thesis
Simon Roy Waite 1988 304 p
Avail: Univ. Microfilms Order No. BRDX84911

The use of embedded optical fiber to detect fatigue damage in woven glass epoxy composite material is described. An optical fiber attenuation measurement technique was used to detect the damage in fatigue 3 point bend specimens. A polarimetric technique was used to establish the effectiveness of the optical fiber strain recovery for the selected fiber. Specimens designed to produce through the thickness crack development were studied. The undamaged and damaged composite specimen stresses were theoretically represented by using laminate analysis and the finite element method. The embedded fiber was represented by using a concentric cylinder model. Dissert. Abstr.

N90-12661# Materials Research Labs., Ascot Vale (Australia).
BALLISTIC PROPERTIES OF COMPOSITE MATERIALS FOR PERSONNEL PROTECTION
Jim R. Brown and Graeme T. Egglestone 1989 17 p
(MRL-TR-89-6; AR-005-690) Avail: NTIS HC A03/MF A01

The Australian Army currently has requirements for new combat and vehicle crewman helmets. Various polymer materials in the form of fiber reinforced organic matrix composites were shown to have sufficient resistance to ballistic impact to be regarded as attractive construction materials for personnel protective helmets. The relative ballistic properties of those organic matrix composite materials which are considered as prime candidates to meet the requirements of the Army's new combat and vehicle crewman helmets are discussed. Author

N90-12662# Office National d'Etudes et de Recherches Aerospatiales, Paris (France).
HARDENING MECHANISMS AND ANALYSIS OF THE STRUCTURE OF THE TGDDM/DDS EPOXY RESIN SYSTEM (TETRAGLYCIDYL-4,4' DIAMINODIPHENYLMETHANE/4,4' DIAMINODIPHENYLSULFONE) Ph.D. Thesis - Paris VI Univ.
Andre-Jean Attias [1988] 211 p In FRENCH; ENGLISH summary
(NOTE-TECHNIQUE-1988-8; ISSN-0078-3781) Avail: NTIS HC A10/MF A02

Chemical as well as spectroscopic methods were used to try to describe as quantitatively as possible the different kinds of chemical bonds constituting the network of a cured epoxy matrix, the TGDDM/DDS system. The chemical approach consisted of putting together model compounds typifying the hypotheses that can be made about reactions taking place during the cure. This study confirms the possibility of intramolecular reactions during curing processes and, more specifically, of the formation of morpholine and also 7-membered cyclic ethers. Other non-ether cyclic products can also be formed. All detected structures were characterized by GPC, HPLC and C-13 NMR spectroscopy. These results excluded direct intermolecular hydroxyl-epoxide addition. On the other hand, model reactions from diepoxy and amino compounds were followed by chemical, chromatographic methods and spectroscopic analysis, in order to correlate the structure of the products with reactivity of the initial molecules, temperature of cure, and proportion of the reagents. The spectroscopic method that was found most useful to investigate the structure of the crosslinked epoxy resin is the high-resolution solid state C-13 NMR spectroscopy. Since these contained poorly resolved peaks, the aliphatic carbon region was decomposed into elementary lines; structural assignments of these lines were made using C-13 solution NMR data of model compounds. On the basis of the anticipated mechanisms, the structural groups of the network, as well as their variations during curing processes, were quantified. A detailed picture of the network is given. Author

N90-12663# MSNW, Inc., San Marcos, CA.
LASER PROBE VAPORIZATION/OXIDATION TESTING OF HIGH TEMPERATURE COMPOSITES Final Report, 22 Jun. - 22 Dec. 1987
J. T. Porter, G. H. Reynolds, T. D. Kunz, and M. J. Berry 11 Jul. 1989 103 p
(Contract F33615-87-C-5275; AF Proj. 3005)
(AD-A211410; WRDC-TR-89-4081) Avail: NTIS HC A06/MF A01 CSCL 11/4

A laser probe technique for the determination of vaporization/oxidation processes of high temperature ceramics was investigated. The technique was found to provide meaningful data on the vapor species near the specimen surface. These data were correlated with changes in specimen microstructure and analyzed by thermochemical and kinetic modeling. Results were found to be in general agreement with the modeling. GRA

N90-12664# Aeronautical Research Inst. of Sweden, Stockholm. Dept. of Structures.
DAMAGE TOLERANCE OF CFRP SANDWICH PANELS
Klas Levin Dec. 1988 14 p Presented at the ECCM, Bordeaux,

France, 20-23 Mar. 1989
(Contract FMV-FFL-82250-85-273-25-001)
(FFA-TN-1988-70; ETN-89-95151) Avail: NTIS HC A03/MF A01

An experimental evaluation of static strength and damage growth resistance under spectrum loading of impacted carbon fiber reinforced plastic (CFRP) epoxy sandwich panels is presented. The influence of impact energy on damage visibility, damage size and distribution, and strength losses with respect to different skin thicknesses and core densities is determined. In the case of barely visible impact damage, the susceptibility of sandwich panels to impacts is reflected in large strength reduction and damage growth during fatigue loading. The visibility of damage during the fatigue loading is subsequently reduced. ESA

N90-12665# Aeritalia S.p.A., Turin (Italy).
PROJECT, IMPLEMENTATION, AND UTILIZATION OF COMPOSITE STRUCTURES [PROGETTAZIONE, REALIZZAZIONE E IMPIEGO DI STRUTTURE IN COMPOSITO]
L. Casalegno 1987 31 p In ITALIAN Presented at a conference, Turin, Italy, 20 Nov. 1987
(ETN-89-95209) Avail: NTIS HC A03/MF A01

The most significant aspects of Aeritalia experience in designing and testing composite structures for aircrafts are described. The materials employed include Kevlar, glass and carbon fibers. The evolution of the mechanical properties of the commercial products is discussed. The software used to optimize the structural design of the composites is detailed. ESA

N90-12666# Institut National des Sciences Appliquees de Lyon, Villeurbanne (France). Lab. des Materiaux Macromoleculaires.
INFLUENCE OF THE STRUCTURE OF EPOXY NETWORK MODELS ON THE VOLUMETRIC, MECHANICAL AND VISCOELASTIC PROPERTIES Ph.D. Thesis
Yong-Gu Won 1989 237 p In FRENCH; ENGLISH summary
(ISAL-89-0024; ETN-89-95266) Avail: NTIS HC A11/MF A02

The relationship between the microstructures of the epoxy network and its volumetric, mechanical and viscoelastic properties is studied. The basic network consists of the prepolymer diglycidylether of bisphenol A and the hardner cycloaliphatic amine isophoronediamine and was modified by applying two different methods. The characterization of the tridimensional networks is accomplished by measuring the specific volume, dilation coefficient, glass transition temperature, mechanical properties, and relaxation of viscoelastic properties. These values are correlated with the various structural parameters such as crosslinking density, packing density, cohesive energy, and free volume. ESA

N90-12667# Rolls-Royce Ltd., Derby (England).
COMPOSITE MATERIALS FOR FUTURE AEROENGINES
G. E. Kirk 4 Jun. 1989 8 p Presented at the ASME Gas Turbine and Aeroengine Congress, Toronto, Ontario, 4-8 Jun. 1989
(PNR90584; ETN-89-95559) Copyright Avail: NTIS HC A02/MF A01

The need for advances in material and manufacturing technology in order that aeroengines can satisfy future market requirements is stressed. The potential of composite materials to meet the increased requirements is discussed. The use of resin composites and further improvements needed in that technology are summarized. The use of metal and ceramic composites where higher temperature capability is required is discussed. Problems that must be solved before these composites can be used to their full potential with confidence are described. ESA

N90-12668# Cranfield Inst. of Tech., Bedford (England). College of Aeronautics.
SHEAR FATIGUE TESTING AND LIFE PREDICTION OF FIBRE COMPOSITES
R. J. Butler, C. H. Edge, and P. M. Barnard May 1984 92 p
(Rept-8519; ISBN-0-947767-89-4; ETN-89-95574) Avail: NTIS HC A05/MF A01; Cranfield Inst. of Tech., Coll. of Aeronautics, Cranfield, Bedford MK43 0AL, England 7.50 sterling pounds

The methods used in providing shear fatigue test results using flat coupons are reviewed and investigated. The rail shear test and the slotted tension test were chosen after review of existing literature. The rail shear test is examined using finite element techniques in a static loading environment and, an exhaustive series of test work. Results of the work are used in a glass/epoxy laminate curve. Problems encountered during these tests have prompted the design of a modified rail shear rig and a slotted tension rig. ESA

N90-12669*# National Aeronautics and Space Administration. Hugh L. Dryden Flight Research Facility, Edwards, CA.
MULTILAYER THEORY FOR DELAMINATION ANALYSIS OF A COMPOSITE CURVED BAR SUBJECTED TO END FORCES AND END MOMENTS
William L. Ko and Raymond H. Jackson Sep. 1989 29 p Presented at the 5th International Conference on Composite Structures, Paisley, Scotland, 24-26 July 1989
(NASA-TM-4139; H-1490; NAS 1.15:4139) Avail: NTIS HC A03/MF A01 CSCL 11D

A composite test specimen in the shape of a semicircular curved bar subjected to bending offers an excellent stress field for studying the open-mode delamination behavior of laminated composite materials. This is because the open-mode delamination nucleates at the midspan of the curved bar. The classical anisotropic elasticity theory was used to construct a multilayer theory for the calculations of the stress and deformation fields induced in the multilayered composite semicircular curved bar subjected to end forces and end moments. The radial location and intensity of the open-mode delamination stress were calculated and were compared with the results obtained from the anisotropic continuum theory and from the finite element method. The multilayer theory gave more accurate predictions of the location and the intensity of the open-mode delamination stress than those calculated from the anisotropic continuum theory. Author

N90-12670*# National Aeronautics and Space Administration. Lewis Research Center, Cleveland, OH.
A NEW TEST MACHINE FOR MEASURING FRICTION AND WEAR IN CONTROLLED ATMOSPHERES TO 1200 C
Harold E. Sliney and Christopher DellaCorte 1989 23 p Proposed for presentation at the Annual Meeting of the Society of Tribologists and Lubrication Engineers, Denver, CO, 7-11 May 1990
(NASA-TM-102405; E-5093; NAS 1.15:102405) Avail: NTIS HC A03/MF A01 CSCL 11D

This paper describes a new high temperature friction and wear test apparatus (tribometer) at NASA Lewis Research Center, Cleveland, Ohio. The tribometer can be used as a pin-on-disk or pin-on-ring configuration and is specially designed to measure the tribological properties of ceramics and high temperature metallic alloys from room temperature to 1200 C. Sliding mode can be selected to be either unidirectional at velocities up to 22 m/sec or oscillating at frequencies up 4.5 Hz and amplitudes up to + or - 60 deg. The test atmosphere is established by a controlled flow rate of a purge gas. All components within the test chamber are compatible with oxidizing, inert, or reducing gases. Author

N90-12671# Royal Signals and Radar Establishment, Malvern (England).
SPECTROSCOPIC ELLIPSOMETRY CHARACTERIZATION OF CVD DEPOSITION AND DOPING OF POLYSILICON MULTILAYER STRUCTURES
S. Sharma, C. Pickering, A. Morpeth, and G. R. Terry Oct. 1988 44 p
(RSRE-Memo-4258; BR109060; ETN-89-94666) Copyright Avail: NTIS HC A03/MF A01

Polysilicon multilayer structures, prepared by a chemical vapor deposition (CVD) process, were studied. Spectroscopic ellipsometry supported by a computer modeling facility was used to synthesize models of the polysilicon-on-oxidized-silicon multilayer structures. Two deposition temperatures, 580 C and 617 C, were considered. Recrystallization and doping were studied on both bulk and

silicon-on-sapphire wafers. The accuracy of interferometry as a film thickness measurement technique on polysilicon was assessed. ESA

N90-12672# Office National d'Etudes et de Recherches Aerospatiales, Paris (France). Direction Scientifique de la Resistance des Structures.
NONLINEAR THEORIES CONCERNING LAMINATED COMPOSITES UNDER COMPRESSION WITH DELAMINATION Final Report [THEORIES NON LINEAIRES DES STRATIFIES COMPOSITES EN COMPRESSION AVEC DELAMINAGE]
D. Gilletta Jan. 1989 65 p In FRENCH
(Contract DRET-88-34-001)
(ONERA-RT-19/3542-RY-081-R; ETN-89-95020) Avail: NTIS HC A04/MF A01

The progression of delamination due to local flame heating of a multilayered plate under compression is described. The interaction between local flaming and the progression of cracks in the composite plate is studied. A calculation of energy release along the crack line is carried out. A mathematical simulation test shows strong agreement with experimental results. Its use as a tool in predicting the main phenomena involved is demonstrated. ESA

N90-12673# Etablissement Technique Central de l'Armement, Arcueil (France). Dept. Comportement des Materiaux.
A STUDY OF THE IMPACT OF A BALL BEARING ON A LONG FIBER COMPOSITE PLATE WITH A CARBON MATRIX, PART 2 [ETUDE DE L'IMPACT D'UNE BILLE SUR UNE PLAQUE COMPOSITE A FIBRES LONGUES ET A MATRICE ORGANIQUE, (2EME PARTIE)]
N. Beaumont, L. Penazzi, and C. Cazeneuve 12 Sep. 1988 16 p In FRENCH Presented at the 6th Journees Nationales sur les Composites, Paris, France, 11-13 Oct. 1988 Sponsored by the Direction des Recherches, Etudes et Techniques, Paris, France
(ETCA-88-R-088-Pt-2; ETN-89-95023-Pt-2) Avail: NTIS HC A03/MF A01

The behavior of long fiber composite materials on impact is studied. The speeds of impacts are between 100 and 300 meters per second. The main parameters of impact are identified and a two-dimensional analytic model developed. Using this model, the impact is simulated and changes in the speed of the ball bearing and plate show close agreement with experimental results. These experimental results were obtained in the first part of this research as described in part 1 of the report. ESA

N90-12674# Centre d'Etudes et de Recherches, Toulouse (France). Dept. d'Etudes et de Recherches en Micro-Ondes.
MODELING OF THE DIELECTRIC BEHAVIOR OF COMPOSITE MATERIALS Final Report [MODELISATION DU COMPORTEMENT DIELECTRIQUE DE MATERIAUX COMPOSITES]
Alain Priou Dec. 1988 59 p In FRENCH
(Contract DRET-87-1383/DS/SR)
(CERT-1/1398-MO; ETN-89-95025) Avail: NTIS HC A04/MF A01

The different mixtures used in composite materials are reviewed and the most appropriate laws for studying such heterogeneous materials are established. Based on experimental results which show that the variation in permittivity of a complex mixture follows a third order law based on the volumetric fraction, a study of such laws is carried out. In the case of dispersed distributions, a correction method is developed allowing the use of appropriate mixture laws. A comparison between theoretical and experimental values shows good agreement. ESA

N90-12675# Centre Technique des Industries Mecaniques, Senlis (France). Dept. of Calcul.
NUMERICAL ANALYSIS OF NOTCH TEST DAMAGE TO LAMINATED COMPOSITE PLATES SUBMITTED TO UNIAXIAL TRACTION Final Report [SUIVI NUMERIQUE DE L'ENDOMMAGEMENT DE PLAQUES COMPOSITES STRATIFIEES TROUEES SOUMISES A UNE TRACTION UNIAXIALE MONOTONE]
Yves Ousset Dec. 1988 43 p In FRENCH
(Contract MRES-86A-0526)
(CETIM-107310; NTI-88/53; ETN-89-95046) Copyright Avail: NTIS HC A03/MF A01

Computer software developed to carry out two-dimensional linear elasticity analysis of laminated materials is described. The software has yet to take damage analysis into consideration. Tests carried out to test an algorithm to be used in damage analysis are presented. These tests are for the moment totally numeric in nature. The numerical analysis of damage to composite plates submitted to uniaxial traction are to be compared to results of actual notch tests. ESA

N90-12676# Aerospatiale, Suresnes (France).
A STUDY OF PROGRESSIVE CRACKING DAMAGE TO CARBON-EPOXY COMPOSITES AND METHODS OF CRACK REDUCTION Final Report [ETUDE DES PROCESSUS D'ENDOMMAGEMENT PAR FISSURATION PROGRESSIVE DES COMPOSITES CARBONE-EPOXY ET DES METHODES DE CONTROLE ASSOCIEES]
B. Grimault and D. Lang 27 Jan. 1989 72 p In FRENCH
(Contract STPA-86-96-024-00-471-75-86)
(Rept-RE-49-324/F; ETN-89-95280) Avail: NTIS HC A04/MF A01

The influence of absorbed humidity and other complimentary factors causing cracking of carbon-epoxy composites is described. X ray radiography and static acoustic emission methods are used to study the progressive cracking of the composites. Ply type and internal fiber rupture are given particular attention. Two different surface types are studied in terms of their resistance to delamination, by static traction at the edge of the composite plates. ESA

N90-12677# Office National d'Etudes et de Recherches Aerospatiales, Paris (France). Direction Scientifique des Materiaux.
CRACK PROPAGATION FAILURE OF CARBON/RESIN COMPOSITES [ENDOMMAGEMENT DES COMPOSITES CARBONE/RESINE: PROPAGATION DES FISSURES EN MODES 1 ET 2]
C. Marais and P. Sigety Feb. 1987 53 p Partly in ENGLISH and FRENCH
(Contract DRET-86-34-001)
(ONERA-RT-45/7086-M; ETN-89-95283) Avail: NTIS HC A04/MF A01

Research on crack propagation in laminated carbon/resin composites is supplemented by research on the influence of such parameters as the thickness of samples, fiber content, and the speed of pressure application. Bend tests, notch tests, and shear tests are carried out to test the properties of the composites. Preliminary results indicate that these methods of mechanical testing give accurate results. ESA

N90-12678# Office National d'Etudes et de Recherches Aerospatiales, Paris (France). Direction des Materiaux.
MECHANICAL BEHAVIOR OF CARBON/RESIN COMPOSITES UNDER DELAMINATION AND CRACKING OF TRANSVERSE LAYERS [COMPORTEMENT MECANIQUE DES COMPOSITES CARBONE/RESINE: DELAMINAGE EN MODE I ET MULTIFISSURATION DES COUCHES TRANSVERSES]
J. P. Favre, C. Marais, and J. C. Laizet Jan. 1988 123 p In FRENCH
(Contract DRET-87-34-001)
(ONERA-RT-46/7086-M; ETN-89-95284) Avail: NTIS HC A06/MF A01

A study of crack propagation is described. The crack limit force is determined for several types of composite materials submitted to specific conditions. High temperature tests are used to determine the stability of the matrix. The role of interlinking fibers is tested by changing the orientation of the laminar layers. The micro fracturing of transverse layers is shown to be controlled by the initial fracture energy. Microfracture behavior is analyzed very accurately by means of acoustic emission. This involves choosing amongst the possible amplitude spectra those that are directly associated with the fracturing. ESA

N90-12679 Department of the Navy, Washington, DC.
CURABLE POLYETHER COMPOSITIONS Patent
Albert A. DeFusco, inventor (to Navy) and Eugene C. Martin, inventor (to Navy) 4 Oct. 1988 4 p Filed 4 Oct. 1988 Supersedes Pat-Appl-867660-86
(AD-D014200; US-Patent-4,775,729; US-Patent-Appl-SN-867660; US-Patent-Class-526-262) Avail: U.S. Patent and Trademark Office CSCL 07/6

Pentadienyl ether terminated polyethers and maleimidomethyl carbonate terminated polyethers are selectively combined via a Diels-Alder reaction at room temperature. The resulting aliphatic copolyethers are characterized by having at least two chemically combined halimido groups interposed between polyether radicals within the copolymer chain. The aliphatic polyether precursors terminated with pentadienyl ether groups are synthesized by reacting an aliphatic hydroxy terminated polyether with a metal alkoxide to form at least the bis alkoxide derivative. The alkoxide derivative is then reacted with a halogen substituted pentadiene yielding the bis or tris pentadiene ether terminated polyether for use in the copolymer synthesis. GRA

N90-12680# Institute for Defense Analyses, Alexandria, VA.
PROCEEDINGS OF THE DOD WORKSHOP ON THE MANUFACTURING/PRODUCIBILITY OF ORGANIC MATRIX COMPOSITES Final Report, May 1987 - May 1988
John E. Hove, ed., William S. Hong, ed., and Stanley L. Channon, ed. Jun. 1989 95 p Workshop held in Arlington, VA, 12-14 Apr. 1988
(Contract MDA903-84-C-0031)
(AD-A212577; AD-E501149; IDA-D-579; IDA/HQ-89-34363)
Avail: NTIS HC A05/MF A01 CSCL 11/4

This document summarizes the findings of a 1988 DOD Workshop concerned with enhancing the production of organic matrix composites (OMCs) for use in the aerospace industry. Present barriers to the greater use of these performance-enhancing structural materials are dominated by a reliance on expensive, labor-intensive manufacturing methods. Higher costs associated with OMCs relative to conventional aluminum alloys were also traced to conservative design approaches (taking inadequate advantage of superior OMC properties), the lack of standardization for materials, processing and testing, a lack of domestically sourced raw materials or precursors, and tooling and capital equipment technology inadequate for high rate production. Recommendations for changing the present situation are given which would affect all stages of the design and manufacturing process for OMCs. These include new design philosophies and worker training programs redirected for greater acceptance of OMCs, continued development of both raw materials and processing techniques with automation in mind, standardization of appropriate aspects of the technology, and increased use of computer aided manufacturing and tooling appropriate for automation. The steps required for implementing most of these recommendations are discussed in greater detail. GRA

N90-12681# Army Lab. Command, Watertown, MA. Materials Testing and Evaluation Branch.
BIAXIAL FLEXING OF A FIBER-REINFORCED ALUMINUM COMPOSITE Final Report
Nikos Tsangarakis and Marc S. Pepi Jul. 1989 23 p
(AD-A212742; MTL-TR-89-70) Avail: NTIS HC A03/MF A01 CSCL 11/4

Disks of silicon carbide continuous fiber reinforced (90 deg)4S aluminum were supported circumferentially on one side and the center of the other side with a pin. Maxima principal tensile surface were determined during flexing with strain gages. Failure under monotonic loading initiated on the convex side of the disks with the formation of multiple breaks in the first layer of fibers. With further flexing, cracking extended to inner fiber layers. Finally, fracture extended through the convex surface layer of the aluminum matrix. On cyclic flexing, fiber cracking was found to be the failure mechanism whenever the cyclic principal surface strain range was 0.0035 or greater. For cyclic strain ranges less than 0.0035, slip bands and cracks were formed in the matrix in addition to the cracks formed in the fibers. The cyclic strain range limit for 10(exp 6) cycles of life was found to approach 0.0015. The latter limit corresponded to a maximum cyclic fiber strain 0.00132, which is only 15 percent of the fiber strain to failure under monotonic uniaxial composite loading. GRA

25 INORGANIC AND PHYSICAL CHEMISTRY

Includes chemical analysis, e.g., chromatography; combustion theory; electrochemistry; and photochemistry.

For related information see also *77 Thermodynamics and Statistical Physics.*.

N90-12682# Department of Health and Human Services, Washington, DC.
CROSS-AXIS SYNCHRONOUS FLOW THROUGH COIL PLANET CENTRIFUGE FOR LARGE-SCALE PREPARATIVE COUNTERCURRENT CHROMATOGRAPHY Patent Application
Y. Ito, inventor (to Dept. of Health 30 Jan. 1989 56 p
(PB89-200174; US-Patent-Appl-SN-304853) Avail: NTIS HC A04/MF A01 CSCL 07D

Centrifugal countercurrent chromatography was used in high efficiency analytical separation with a variety of single and two phase systems. In separation, it was found that the geometry of the coiled column and the acting centrifugal force field play a major role in separation. The present invention relates to methods and apparatus for centrifugal separation, and more particularly to toroidal coil centrifugation for the separation of particles and solutes from liquids. A countercurrent chromatography apparatus and method where the column rotates about an axis spaced apart from, parallel to, and in the same radial plane as a radius extending from the central axis of revolution. The apparatus generates a unique force field which enables excellent separation. GRA

N90-12683 Princeton Univ., NJ.
ASYMPTOTIC ANALYSES OF THE STRUCTURES AND CHARACTERISTICS OF FLAMES Ph.D. Thesis
Harsha Kumar Chelliah 1989 208 p
Avail: Univ. Microfilms Order No. DA8908047

Asymptotic analyses are described for steady, planar, adiabatic laminar premixed and laminar diffusion flames with varying degrees of complexity in the description of transport and chemical kinetics. Simplified reaction mechanisms, derived by imposing the steady-state and partial-equilibrium approximations, were employed in the analysis of real flames. The most complete two-term expansions for burning velocity in activation energy asymptotics were derived for two-reactant flames with irreversible one-step chemistry. The analysis includes the general Stefan-Maxwell transport to describe the diffusion velocity. Activation-energy asymptotic methods were employed to investigate the combustion regimes of hydrogen-halogen premixed flames with detailed chemistry. Methods of obtaining simplified reaction schemes using the steady-state and partial-equilibrium approximations are described in detail. Methane-air diffusion flames, both with and without nitrogen dilution, at atmospheric pressure and with reactants at temperatures near room temperature were analyzed by asymptotic methods. Simplifications to the description of methane-air diffusion flames, with detailed chemical kinetics taken into account, were identified and compared with respect to their predictions of flame structure and extinction conditions. Deficiencies

are noted in earlier schemes for simplification on the basis of concepts of asymptotic analysis. Methods for correcting these deficiencies are discussed, and influences of selection of different sets of data for elementary rate constants are evaluated.
Dissert. Abstr.

N90-12684# EA-Mueller, Inc., Baltimore, MD.
RESEARCH AND DEVELOPMENT OPPORTUNITIES IN SUPERCRITICAL FLUID TECHNOLOGY Final Report
Aug. 1989 24 p Proceedings of Workshop held in Washington, DC, 2 Dec. 1988 Prepared in cooperation with Energetics, Inc., Columbia, MD
(Contract DE-AC01-87CE-40762)
(DE89-015320; CONF-881296-Summ) Avail: NTIS HC A03/MF A01

A special concern of the workshop was to determine the appropriate level of involvement for DOE and other organizations in order to develop commercial supercritical fluid technology. Group presentations and a general discussion were held to summarize the results. Comments on the general roles of DOE and industry in supercritical fluid R and D included: some industries (e.g., food processing) are already researching this technology; DOE should cooperate with industry in attempting to demonstrate this technology; and direct support of private-sector projects by DOE should be encouraged. It was also noted that productivity benefits may outweigh energy conservation benefits in some application areas. DOE

N90-12685# International Centre for Theoretical Physics, Trieste (Italy).
SYMMETRY BREAKING PHENOMENA IN LIQUID HELIUM-4
Mubarak Ahmad, S. K. Tikoo, and T. K. Raina (Government Coll. for Women, Srinagar, India) Dec. 1988 50 p
(DE89-618886; IC-88/413) Avail: NTIS (US Sales Only) HC A03/MF A01

Salient features of liquid Helium 2 are being analyzed in the light of a symmetry breaking mechanism. The excitation spectrum is derived by scaling transformation. A relation between roton excitation and Bogoliubov's quasi particles was established by giving different structures to the roton operators, similar to quasi boson approximation for phonon-like spectrum. This structure of the roton operators enables one to study the low temperature behavior of superfluid Helium-4 by introducing the idea of pairing for roton-like excitation for the onset of energy-gap. Superfluid Helium-4 is divided into the states of condensed bosons, oscillating condensed bosons, phonons, maxons, rotons and the states of vortices. The transition probabilities between these various states are considered. Coherent states of various superfluid regions of He 2 are being obtained and consistently analyzed which have deep inter-relationship. As higher excitations have also a group structure and their coherent behavior has been seen, this formalism seems to be more appropriate to deal with such an interesting problem. DOE

N90-12686# Bureau of Mines, Amarillo, TX. Helium Field Operations.
IMPROVED METHOD FOR DETERMINATION OF HELIUM-4 IN HELIUM-3 BY MASS SPECTROMETRY Report of Investigations, 1989
Samuel R. M. Burton and David E. Cornelius 1989 14 p
(PB89-201404; BUMINES-RI-9232; LC-88-600442) Avail: NTIS HC A03/MF A01 CSCL 07D

The U.S. Bureau of Mines report describes a method for determining parts per million (ppm) of helium-4 (He-4) in helium-3 (He-3) to an accuracy of + or - 5 percent by mass spectrometry. Gravimetrically prepared primary standards were used for the calibration of a Dempster 180 degrees magnetic section mass spectrometer. A comparison between a 2.49 percent He-4 in hydrogen mixture and a 2.49 percent He-4 in He-3 mixture shows that He-3 can be replaced with hydrogen as a diluent for standards with comparable mass spectrometry sensitivities for He-4. Using hydrogen as a diluent allows analysis of He-3 samples for He-4 when He-3 is not available for preparation of standards and also conserves the rare He-3 isotope. Standards of He-4 in H2 were prepared for calibration of the mass spectrometer for quantitative determinations of He-4 in the 2 to 100 ppm range. A minimum detectable limit of 2 ppm He-4 is obtained by the method. GRA

N90-12687# National Inst. of Standards and Technology, Boulder, CO. Center for Chemical Engineering.
VAPOR-LIQUID EQUILIBRIUM OF BINARY MIXTURES IN THE EXTENDED CRITICAL REGION. PART 1: THERMODYNAMIC MODEL
James C. Rainwater Apr. 1989 73 p
(PB89-218374; NIST/TN-1328-Pt-1) Avail: NTIS HC A04/MF A01; SOD HC $3.75 as 003-003-02945-9 CSCL 07D

The thermodynamic model of Leung and Griffiths for binary mixture vapor-liquid equilibrium near the critical locus, as modified by Moldover, Rainwater and others, is extended to accommodate fluid pairs of greater dissimilarity. GRA

N90-12688# Giner, Inc., Waltham, MA.
ADVANCED DOUBLE LAYER CAPACITOR Interim Technical Quarterly Report, No. 4
Anthony B. LaConti, Philip Lessner, and S. Saragapani Aug. 1989 18 p
(Contract N00014-88-C-0391; ARPA Order 9526)
(AD-A211977; C87A-25) Avail: NTIS HC A03/MF A01 CSCL 07/4

The overall goal of this project is to develop electrochemical capacitors with no liquid electrolyte present. The liquid electrolyte is replaced by a solid ionomer electrolyte. An advantage of these devices over conventional electrochemical capacitors containing free acid would be greater safety and reliability. Efforts were concentrated in three areas: (1) preparation and characterization of RuO(x) powders; (2) preparation of membrane and electrode (M and E) assemblies with high capacitance; and (3) scale-up of M and E structures to 2 x 2 size. GRA

N90-12689# Altex Technologies Corp., Santa Clara, CA.
CHARACTERIZATION OF NONPREMIXED TURBULENT BLUFF-BODY BURNER FLAMES Annual Report, Jan. - Dec. 1988
J. Kelly, M. Namazia, R. Schefer, and Marc Perrin (Gaz de France, La Plaine Saint Denis.) Apr. 1989 124 p
(Contract GRI-5086-260-1250)
(PB89-229447; GRI-89/0105) Avail: NTIS HC A06/MF A01 CSCL 21B

Methane concentration imaging data were analyzed for small and large diameter bluff-body burners. The data and simplified mixing models were used to correlate the recirculation zone (RZ) fuel concentration with the fuel to air diameter ratio (DR) and momentum flux ratio (MR). It is shown that the RZ fuel concentration varies with square of DR and increases linearly with MR, for MR much less than 1, and is inversely proportional to MR for MR much greater than 1. It is demonstrated that the varying RZ fuel concentration strongly influences flame regimes and flame stability. By diluting the fuel jet with air, and thereby modifying the RZ fuel concentration, flames were modified. Detached flames could be eliminated and the flame blowout limit could be significantly altered through dilution. A simple mixing model was used to correlate both small and large bluff-body flame length data. Author

N90-12690# National Inst. of Standards and Technology, Boulder, CO. Thermophysics Div.
TABLES FOR THE THERMOPHYSICAL PROPERTIES OF METHANE
Daniel G. Friend, James F. Ely, and Hepburn Ingham Apr. 1989 489 p
(PB89-222608; NIST/TN-1325) Avail: NTIS HC A21/MF A03; also available SOD HC $23.00 as 003-003-02947-5 CSCL 07D

The thermophysical properties of methane are tabulated for a large range of fluid states based on recently formulated correlations. For the thermodynamic properties, temperatures from 91 to 600 K at pressures less than 100 MPa are included. For the viscosity,

the corresponding range is 91 to 400 K with pressures to 55 MPa, while for the thermal conductivity the range is 91 to 600 K with pressures to 100 MPa. In addition to the tables of properties, algebraic expressions and associated tables of coefficients are given to allow additional property calculations. Tables of comparisons between experimental property determinations and the correlations are also given both for primary data used in the formulation of the correlations and for additional data. A listing of a FORTRAN program for the evaluation of methane thermophysical properties using the Schmidt-Wagner equation of state is included. Author

N90-12691# Pittsburgh Univ., PA. Surface Science Center.
THERMAL STABILITY OF THE CARBON-CARBON BOND IN ETHYLENE ADSORBED ON Si(100): AN ISOTOPIC MIXING STUDY
C. C. Cheng, W. J. Choyke, and J. T. Yates, Jr. 10 Aug. 1989 28 p Submitted for publication
(Contract N00014-82-K-0280)
(AD-A211591; TR-24) Avail: NTIS HC A03/MF A01 CSCL 07/6

The interaction of ethylene with the silicon surface has been studied in ultrahigh vacuum using a variety of surface science techniques to investigate the surface complex produced and the nature of the high temperature SiC thin film growth process on the Si(100) surface. Recent studies have shown that on a perfect Si(100) surface a single ethane molecule adsorbs on a silicon dimmer (Si2) site at saturation coverage and a surface bonding model has been proposed based on the absence of the C-C bond in this adsorbed species as determined by HREELS. GRA

N90-12692# Toulouse Univ. (France).
CHEMICAL AND PHOTOCHEMICAL REACTIVITY IN MICROEMULSIONS AND WATERLESS MICROEMULSIONS Final Report, Nov. 1985 - 7 May 1989
Armand Lattes and M. T. Maurette 7 May 1989 34 p
(Contract DAJA45-85-C-0024)
(AD-A211776; R/D-5037-CH-01) Avail: NTIS HC A03/MF A01 CSCL 07/4

Relatively little attention has been paid to molecular aggregation phenomena in structured nonaqueous solvents compared to that devoted to such processes in aqueous media. This paper is a review concerning our work with formamide in place of water. The following observations showed that formamide has sufficient cohesive force to favor molecular aggregation: (1) critical micellar concentrations (c.m.c.) were determined with various ionic and non-ionic surfactants; (2) the phase diagram of CTAB (cetyltrimethylammonium bromide) in formamide shows two mesomorphic phases closely resembling those found in aqueous systems; (3) x ray scattering demonstrated the presence of molecular aggregates, and gave an indication of their structure; and (4) a variety of microemulsions were prepared in formamide. Such non-aqueous microemulsions represent valuable media for synthetic purposes. For example, Diels-Alder reactions, photoamidation of olefins, and the Wacker process can be carried out readily in such media. The observed discontinuities in reaction selectivity indicate the presence of structured phases. GRA

N90-12693# ESDU International Ltd., London (England).
THERMOPHYSICAL PROPERTIES OF BENZENE. PART 1: THE IDEAL GAS AND THE SATURATED LIQUID AND VAPOUR
Apr. 1989 17 p
(ESDU-89002-Pt-1; ISBN-0-85679-673-9; ISSN-0141-4062; ISSN-0141-4070) Avail: ESDU

This data item gives equations obtained from a critical evaluation of experimental data in the literature for the variation along the saturation line with temperature, for both the liquid and the vapor, of: density, enthalpy, heat capacity at constant pressure, dynamic viscosity and thermal conductivity. Also given are equations for the variation with temperature along the saturation line of vapor pressure, latent heat of vaporization and surface tension, together with equations for the variation with temperature for the ideal gas of specific heat capacity at constant pressure, enthalpy, dynamic viscosity and thermal conductivity. Results on the saturation line evaluated in SI units using the equations are tabulated at 5 K intervals from the melting point to the critical point, or as close to it as possible for some properties. Results for the ideal gas evaluated also in SI units using the equations are tabulated at 10 K intervals from the melting point to 1000 K. In the absence of experimental values some of these results involve extrapolation and they are indicated in the tables. Conversion factors to facilitate use of the data in British units are included. ESDU 89003 provides thermodynamic data for the vapor at elevated pressures. ESDU

N90-12694# ESDU International Ltd., London (England).
THERMOPHYSICAL PROPERTIES OF BENZENE. PART 2: THERMODYNAMIC PROPERTIES AT ELEVATED PRESSURES
Mar. 1989 36 p Supersedes ESDU-73009
(ESDU-89003-Pt-2; ESDU-73009; ISBN-0-85679-674-3; ISSN-0141-4062) Avail: ESDU

ESDU 89003 tabulates in SI units from the melting point to the critical point along the saturation line at fixed pressures data for: saturation temperature, liquid density, vapor specific volume, liquid and vapor enthalpy and entropy, latent heat of vaporization and liquid specific heat capacity. In addition, for the vapor or liquid as appropriate, tables give along specific isobars for pressures up to 7 MN/sq m the variation with temperature of specific volume, compression factor, enthalpy, entropy, and specific heat capacities at constant pressure and volume. The data were generated from a single correlating function fitting selected experimental data drawn from the literature, and are therefore self-consistent. An estimate of the error in linear interpolation within the tables is included, and a computer-generated temperature-entropy chart representing the data is provided. To facilitate use of the data in British units, conversion factors are given. No equations for the values are included. Author

N90-12695# Laboratoire d'Automatique et d'Analyse des Systemes, Toulouse (France). Groupe Circuits et Composants a Effet de Champ.
STUDY OF PALLADIUM AND CHROMIUM SILICIDES FORMATION IN LIQUID PHASE AND IN SOLID PHASE Ph.D. Thesis - Toulouse Univ.
Catherine Seguelas 1989 212 p In FRENCH; ENGLISH summary
(LAAS-89040; ETN-89-95258) Avail: NTIS HC A10/MF A02

Attention is paid to metallic silicides and rapid annealing techniques. A synthesis of the principal thermodynamic and physico-chemical properties of metallic silicides is presented, together with the different annealing techniques currently used to obtain silicides. The characteristics of the phases obtained with these techniques are compared. The influence of pulsed electronic irradiations on metal/silicon bi-layer structures is evaluated. The heat equation is resolved in an unidimensional case in order to calculate the thermal profiles induced in these samples. Element concentration profiles are estimated by taking into account the occurrence of a liquid phase. The necessity of considering temporal modifications of the thermophysical properties of the structures is stressed. Rapid isothermal annealing is applied to form palladium and chromium silicides. The analysis is performed using secondary ion mass spectrometry. Palladium is fast diffusing and leads to well-controlled thicknesses, smooth surfaces, abrupt interfaces, and exhibits a diffusion-limited growth. Chromium reacts with persistent oxides, so several growth kinetics are observed according to treatment temperature. The Locker and Capio model is used to explain these results by considering the influence of nucleation barriers. Granular surfaces support this hypothesis. ESA

N90-12696*# National Aeronautics and Space Administration. Lewis Research Center, Cleveland, OH.
CHARACTERIZATION AND CYCLE TESTS OF LIGHTWEIGHT NICKEL ELECTRODES
Doris L. Britton 1989 13 p Presented at the Electrochemical Society Meeting, Hollywood, FL, 16-20 Oct. 1989

(NASA-TM-102399; E-5153; NAS 1.15:102399) Avail: NTIS HC A03/MF A01 CSCL 07D

Development of a high specific energy nickel electrode is the main goal of the lightweight nickel electrode program at NASA Lewis Research Center. The approach was to improve the nickel electrode by continuing combined in-house and contract efforts to develop a more efficient and lighter weight electrode for the nickel-hydrogen battery. High energy nickel electrodes suffer from having shorter lives than state-of-the-art electrode. However, these lightweight electrodes appear to be favorable for missions requiring moderate cycle lives and depth-of-discharge. Author

N90-12697# National Inst. of Standards and Technology, Gaithersburg, MD. Thermophysics Div.

PROPERTIES OF LENNARD-JONES MIXTURES AT VARIOUS TEMPERATURES AND ENERGY RATIOS WITH A SIZE RATIO OF TWO

Marcia L. Huber and James F. Ely May 1989 429 p

(PB89-235204; NIST/TN-1331) Avail: NTIS HC A19/MF A01; also available SOD HC $20.00 as 003-003-02952-1 CSCL 07D

Results are presented of molecular dynamics computer simulations for binary Lennard-Jones mixtures with a size ratio of two. A total of 84 state points were investigated at seven compositions ranging from 5 to 95 percent of the small molecule energy ratios from 0.5 to 3.0 and three reduced temperatures. In addition to the thermodynamic results, extensive tabular data are given for the radial distribution functions, local compositions and the direct correlation functions. Several theories of dense fluid mixtures are discussed and a new approximation is given for the radial distribution function of a pair in a mixture, which is called the modified mean density approximation. The predictions of various thermodynamic quantities from the different liquid mixture models are compared with simulation results. For mixtures with large size differencies, the modified mean density approximation was found to be competitive with first order, Lee-Levesque type statistical mechanical perturbation theory. Author

N90-12698# Office National d'Etudes et de Recherches Aerospatiales, Paris (France). Direction Scientifique des Materiaux.

SURFACE TREATMENTS OF CARBON FIBERS IN AN ORGANIC ENVIRONMENT. FINITE ELEMENT ANALYSIS OF PULL-OUT TESTS [TRAITEMENTS DE SURFACE DE FIBRES DE CARBONE EN MILIEU ORGANIQUE. ETUDE PAR ELEMENTS FINIS DE L'ESSAI DE DECHAUSSEMENT]

B. Barbier, M. F. Marmonier, and G. Desarmot Jan. 1988 102 p In FRENCH

(Contract DRET-87-34-001)

(ONERA-RT-7/3549-M; ETN-89-95282) Avail: NTIS HC A06/MF A01

Techniques of surface treating carbon fibers by varying different parameters controlling nitrogen link-up are described. Changes in temperature and anode potential play a large role in the creation of parasitic reactions. If possible, the solution within the fiber should be renewed periodically. Nitrogen concentrations of up to 22 percent can be obtained from fibers with initial concentrations of 2 percent. Pull-out tests are investigated and the Greszczuk model is verified. ESA

N90-12699# Army Cold Regions Research and Engineering Lab., Hanover, NH.

ESTIMATION OF TIME TO MAXIMUM SUPERCOOLING DURING DYNAMIC FRAZIL ICE FORMATION

Steven F. Daly and Kathleen D. Axelson Jul. 1989 16 p

(AD-A212204; CRREL-SR-89-26) Avail: NTIS HC A03/MF A01 CSCL 08/12

Time to maximum supercooling is a parameter that can be easily measured during experiments on the dynamic, nonequilibrium stage of frazil ice formation. Mercier has determined an analytical expression for the time to maximum supercooling that depends only on the four basic system parameters: the rates of heat loss, seeding, turbulent dissipation and secondary nucleation. Mercier's analytical expression is applied to a number of experiments. Heat loss rate and turbulent dissipation rate were reported or could be determined from the experiment description. The secondary nucleation was set at the value of 4x10 to the 10th power nuclei/erg suggested by Mercier, and the seeding rate optimized to reproduce the experimental results. An inverse relationship was found between the coldroom temperature at which the experiment was conducted and the seeding rate. The optimized seeding rates varied from 2.7 to 7.5 x .00001 crystals/sq cm s. The implications for frazil ice formation in rivers and streams are discussed. GRA

N90-12700# Ben Gurion Univ. of the Negev, Beersheva (Israel). Organic Metals Group.

ELECTRICALLY CONDUCTING ORGANIC MATERIALS: DESIGN, SYNTHESIS AND CHARACTERIZATION Interim Report No. 4

J. Bernstein, J. Y. Becker, S. Bittner, and S. S. Shaik Jul. 1989 6 p

(Contract DAJA45-87-C-0058)

(AD-A212214; R/D-5618-MS-01) Avail: NTIS HC A02/MF A01 CSCL 07/4

The activities during the last six months continue to be in five main research areas: Synthesis of D2A type molecules; Synthesis of rigid A2D type molecules; Electrochemical measurements and salt formation; Synthesis of telluro derivatives of TTF. Two quinones 1 and 2 were prepared and converted to the corresponding dicyanimines 3 and 4. The dicyanimine derivatives of 5 and 6 are currently being prepared and the solid state packing properties of all the compounds studied. A2D templates with sulfur atoms linking the moieties are being pursued. Some of those compounds exhibit a zig-zag type of stacking with considerable more overlap than usual. In the search for new organic conductors, it is convenient to match donors and acceptors by their electrochemistry. Cyclic voltametric data on some of the D2A molecules are shown. All experiments were carried out under argon in THF containing tetrabutylammonium tetrafluoroborate as electrolyte using platinum electrode as the working electrode and silver/silver chloride as the reference. The electrochemical potential was measured for all the other compounds described. Two new compounds were synthesized which are at the same time Te - TTF derivatives and TTF - dimers. GRA

N90-12701# Ballistic Research Labs., Aberdeen Proving Ground, MD.

STRUCTURES AND ENERGIES FOR SMALL BORANE COMPOUNDS: ONE AND TWO BORON COMPOUNDS Final Technical Report, Jun. 1985 - Jun. 1986

George F. Adams and Michael J. Page (Naval Research Lab., Washington, DC.) Aug. 1989 27 p Presented at the Army Science Conference, West Point, NY, Jun. 1986

(AD-A212264; BRL-TR-3027) Avail: NTIS HC A03/MF A01 CSCL 07/4

Optimized structures and harmonic vibrational frequencies at the Hartree Fock level of theory are reported with a double zeta plus polarization basis set for a number of B1 and B2 boranes. Atomization energies for these species are computed using full fourth order perturbation theory. Molecular heats of formation are then determined using the computed energies, vibrational frequencies and a system of additive bond correction factors. Due to the paucity of experimental thermochemical data on small boranes, these correction factors are determined from large basis set ab initio calculations on prototypical molecules. GRA

N90-12702# Ballistic Research Labs., Aberdeen Proving Ground, MD.

EXTENDED BASIS SET CALCULATIONS OF ATOMIZATION ENERGIES: COMPARISON OF ISOGYRIC AND DIRECT RESULTS Final Technical Report

George F. Adams, Mary M. Gallo, and Michael J. Page (Naval Research Lab., Washington, DC.) Sep. 1989 22 p

(AD-A212268; BRL-TR-3044) Avail: NTIS HC A03/MF A01 CSCL 07/4

With the development of software implementing quantum chemical techniques that employ energy gradient and Hessian data,

and the concurrent increase of access to modern supercomputers, systematic studies of molecular structures and properties have become routine. Recently, several groups have reported efforts to compute accurate values of molecular heats of formation. Researchers described a study of first-row hydrides using full fourth-order perturbation theory with a variety of basis sets. Also described are bond dissociation energies for a series of first-row diatomics. The results indicated that fourth-order perturbation theory calculations using extended basis sets provided generally excellent results for sigma-bonded systems, with less accurate results obtained for multiply bonded systems. We described the results of a series of extended basis set Moller-Plesset perturbation theory calculations of a series of first row hydrides. Analysis of atomization energy prediction obtained employing the isogyric reaction technique demonstrates that third-order perturbation theory results are virtually indistinguishable from the results using a full fourth order calculation. GRA

N90-12703# California Univ., Santa Barbara. Dept. of Chemical and Nuclear Engineering.
MEASUREMENT AND CORRELATION OF THE SOLUBILITY AND DIFFUSION COEFFICIENT FOR OXYGEN AND CHLORINE IN BASIC HYDROGEN PEROXIDE Final Report, 7 Apr. 1988 - 8 Mar. 1989
Orville C. Sandall, Gabriel Ruiz-Ibanez, Ali Bidarian, and Richard Davis Jun. 1989 52 p
(Contract F29601-88-K-0004; AF Proj. 3326)
(AD-A212348; WL-TR-89-14) Avail: NTIS HC A04/MF A01 CSCL 07/4

The reaction between chlorine (Cl) and basic hydrogen peroxide (BHP), a mixture of hydrogen peroxide (H2O2) and potassium hydroxide (KOH), is currently being utilized to provide a source of singlet delta oxygen for iodine chemical lasers. The byproducts of the reaction are potassium chloride (KCl) and water (H2O). Typically an excess of hydrogen peroxide is used. The physical solubilities and liquid diffusion coefficients of oxygen (O2) and Cl2 in BHP are important physicochemical parameters needed to model any generator designed to produce singlet delta oxygen based on the reaction between gaseous Cl2 and BHP solutions. The solubility and diffusion coefficient for oxygen and chlorine in aqueous alkaline hydrogen peroxide solutions were measured and correlated, in the range of -20 to 20 C. The solution of interest is an aqueous solution of 5 molar potassium hydroxide and 8 molar hydrogen peroxide (5 M KOH, 8 M H2O2 and 30 M H2O). This concentration of solution could be achieved by adding solid KOH to a 33 percent (wt) solution of hydrogen peroxide. GRA

N90-12704# National Inst. of Standards and Technology, Gaithersburg, MD.
FUNDAMENTAL MOLECULAR DATA TO SUPPORT CARS DIAGNOSTICS OF TEMPERATURE, PRESSURE, AND SPECIES CONCENTRATION Final Report, 17 Dec. 1985 - 30 Apr. 1989
Gregory J. Rosasco 10 Aug. 1989 113 p
(Contract MIPR-101-88)
(AD-A212411; ARO-23356.6-CH) Avail: NTIS HC A06/MF A01 CSCL 07/4

The J-, and T-dependence of line broadening and line shifting coefficients are reported for the A-branch spectra of Carbon Monoxide and various hydrogen diatomics. Experimental studies verify the ability to predict, using an energy-gap rate law description of the relaxation matrix equation, the collisionally narrowed A branch of self-broadened Carbon Monoxide. Line shifting is determined experimentally and accounted for by semi-classical calculation. This calculation also is shown to be very accurate for self-broadening in Carbon Monoxide and is used to predict line broadening in CO:N2 from 295 to 1500 K. The Q-branch line shape function for the hydrogen diatomics is studied for a range of collision partners and temperatures. In the low pressure, Dicke narrowed regime, the basic line shape function is understood; however, there is no reliable basis for prediction of the (in some cases complex) optical diffusion coefficient. In the pressure broadened regime, anomalous, asymmetric lineshapes are reported for the H2(D2): Air system. These are ascribed to inhomogeneous broadening associated with the speed dependence of dephasing cross-sections. This lineshape is shown to collisionally narrow and symmetrize with increasing H2(D2) concentration. The J-dependence of the line broadening for the hydrogen diatomics is described. GRA

N90-12705# State Univ. of New York, Binghamton. Dept. of Chemistry.
PHOTOCHEMICAL OBSERVATION OF ION FLOWS IN MEMBRANE CHANNELS Annual Report, Jul. 1988 - Jul. 1989
Michael E. Starzak Aug. 1989 7 p
(Contract N00014-87-K-0301; RR04108)
(AD-A212449) Avail: NTIS HC A02/MF A01 CSCL 06/1

Laser Doppler velocimetry and photochemical observation of Tl(I) ion flows are used to characterize the permeation properties of ions within gramicidin channels. The laser Doppler velocimetry provides a direct experimental determination of the distribution of ion velocities within these channels. For this information, it becomes possible to deduce the mechanism for ion transport, e.g., transport via discrete sites or continuum diffusion. The photochemical studies permit an experimental determination of the fraction of the total current carried by the Tl(I) ion in mixed cation systems using a dye molecule whose fluorescence is quenched by the permeating Tl(I) ion. This ion differentiation technique is utilized for a detailed study of Tl(I) ion in the gramicidin channel. This ion is a permeant ion at large mole fractions but becomes a channel blocker at small Tl(I) ion mole fractions. GRA

N90-12706# Arizona State Univ., Tempe. Dept. of Chemical, Bio and Materials Engineering.
HEAT PIPE AND THERMAL ENERGY STORAGE AND CORROSION STUDIES (1988) Final Report, Oct. 1987 - Sep. 1988
Mohan Krishnamurthy, Patrick Dalton, and Dean Jacobson Jun. 1989 138 p Prepared for Texas A and M Univ., College Station
(Contract F33615-86-C-2723)
(AD-A212655; WRDC-TR-89-2047) Avail: NTIS HC A07/MF A01 CSCL 07/1

Corrosion degradation analysis was performed on a set of three Inconel 617 Thermal Energy Storage capsules filled with different eutectic fluoride mixtures of LiF, MgF2, NaF and KF which were thermally cycled near 1000 K for 10,000 hours. These capsules were cut out and various sections were metallographically studied by Optical and Scanning Electron microscopy and by elemental x ray mapping. Chemical analyses on the metallic container were performed using the Electron Probe Micro-analyzer and that of the salts by Atomic Absorption Spectroscopy. It was determined that the container material did not suffer significant microstructural damage except for tiny pits near the edge in contact with the salts and some voids near the surface exposed to vacuum which could not be positively identified as due to corrosion. The region extending to about 50 microns form the inner edge is contact with salt and about 30 microns from the outer edge exposed to vacuum were found to be depleted mainly of Aluminum and to a lesser extent Chromium. GRA

N90-12707# Air Force Academy, CO. Research Lab.
HEAT CAPACITIES OF 1-METHYL-3-ETHYLIMIDAZOLIUM CHLORIDE-ALUMINUM CHLORIDE MOLTEN SALTS Technical Report, 1-22 Aug. 1989
Maureen K. Parrish and John R. Stuff Sep. 1989 13 p
(AD-A212790; FJSRL-TR-89-0007) Avail: NTIS HC A03/MF A01 CSCL 07/4

The addition of aluminum chloride to 1-methyl-3-ethyl-imidazolium chloride results in the formation of a room temperature molten salt. This ionic liquid has shown to be a useful electrolyte for battery applications. In practical situations, batteries are often subjected to extremes in temperatures, knowledge of the electrolytes' basic thermal properties, such as melting point, decomposition temperature and heat capacity, may help to predict how a battery containing the electrolyte of interest will behave under such conditions. The molar heat capacity, C(p)

is defined as the amount of heat needed to raise the temperature of one mole of a substance by one Kelvin. It is a measure of a system's ability to store heat through the vibrational and rotational motion of chemical bonds and through the translational motion of atoms and molecules in the system. A standard method for the determination of heat capacities using differential scanning calorimetry is described. The heat capacities for the molten salt system aluminum chloride 1-methyl-3-ethylimidazolium chloride were determined over the composition range 0.30 is less than N is less than 0.65 where N is the apparent mole fraction of aluminum chloride. GRA

N90-12708# Memphis State Univ., TN.
ELECTRON DENSITY MODULATION OF CATALYTIC METAL CENTERS BY SUBSTITUTED ARYL-ISOCYANIDE LIGANDS Final Report, 1 Jul. 1988 - 20 Aug. 1989
Randy F. Johnston 15 Sep. 1989 3 p
(Contract N00014-88-K-0385)
(AD-A212875) Avail: NTIS HC A02/MF A01 CSCL 07/3

Several substituted-aryl-isocyanide ligands were synthesized. The corresponding isocyanide pentacarbonyl chromium complexes were synthesized photolytically to evaluate the electronic properties of the isocyanide ligands. The chromium compounds were characterized by elemental analysis, infrared, H-1 and C-13 NMR, and cyclic voltammetry. The infrared and C-13 NMR data contained only small differences between all the investigated ligands. This result indicated that only small perturbations in the electron density at the metal center had occurred. The cyclic voltammetry data had a larger variation with a oxidation potential range of 106 mV. This range could prove to be important if a catalytic cycle of interest included an oxidative procell. To completely determine the potential utility of these ligands more work needs to be done. GRA

N90-12709# United Technologies of New Mexico, Inc., East Hartford, CT.
INVESTIGATION OF FUEL ADDITIVE EFFECTS ON SOOTING FLAMES Final Report, 1 Jun. 1986 - 31 May 1989
Paul A. Bonczyk 28 Jul. 1989 140 p
(Contract F49620-86-C-0054)
(AD-A212925; UTRC/R89-957464-F; AFOSR-89-1247TR) Avail: NTIS HC A07/MF A01 CSCL 21/4

Research was conducted to clarify the mechanisms responsible for the suppression of soot in flames by selected fuel additives. Measurements were limited to well defined prevaporized liquid and gaseous fueled hydrocarbon/air flames. Emphasis was given to ferrocene in a diffusion flame fueled by prevaporized iso-octane, as well as to alkali and alkaline earth additives in premixed ethylene/air flames. Nonperturbing laser optical diagnostic techniques were used to measure flame temperature, as well as to relate changes in soot particulate size, number density, and volume fraction to additive type and concentration. Quartz probe sampling and gas chromatography were used to determine the additive's effect on soot precursor hydrocarbon and other species. For the diffusion flame, the time of the first appearance of soot is shortened when ferrocene is present. Following its appearance, the particulate's size and number density are perturbed by ferrocene. Ferrocene accelerates acetylene oxidation. Ferrocene is very effective at late stages, appearing to enhance soot burnout. Attempts were not successful to find iron occluded by soot as a possible mechanism of enhanced soot oxidation. Alkali metals were effective. GRA

N90-12710# Naval Research Lab., Washington, DC. Lab. for Computational Physics and Fluid Dynamics.
FLIC (FLAME WITH IMPLICIT CONVECTION): A DETAILED, TWO-DIMENSIONAL FLAME MODEL Interim Report, Oct. 1986 - Sep. 1989
G. Patnaik, K. J. Laskey, K. Kailasanath, E. Oran, and T. Brun (Harvard Univ., Cambridge, MA.) 27 Sep. 1989 41 p
(AD-A212953; NRL-MR-6555) Avail: NTIS HC A03/MF A01 CSCL 21/2

This report describes the new computer code FLame with Implicit Convection (FLIC), a two-dimensional time-dependent program developed specifically to compute and study the behavior of flames and other subsonic chemically reactive flows. In order to describe a flame in enough detail to simulate its initiation, propagation, and extinction, FLIC combines algorithms for subsonic convective transport with buoyancy, detailed chemical reaction processes, and diffusive transport processes such as molecular diffusion, thermal conduction, and viscosity. Several new numerical techniques had to be developed specifically for multi-dimensional flame modeling, and these are highlighted. The numerical implementation of the flame model is described here, and a typical application is provided for illustration. FLIC is currently the state-of-the-art in detailed two-dimensional, time dependent flame models. GRA

N90-12711# Michigan Univ., Ann Arbor.
SMALL PARTICLE SCATTERING AND ABSORPTION Contractor Report, Jun. 1986 - Dec. 1988
Herschel Weil Jul. 1989 72 p
(Contract DAAA15-86-K-0022)
(AD-A213168; CRDEC-CR-045) Avail: NTIS HC A04/MF A01 CSCL 07/4

The aim is to extend the knowledge of the scattering and absorption of electromagnetic energy by aerosol particles. Particular interest is in mm wave, infrared and optical scattering for particles of dimensions ranging from much smaller than to comparable with the incident wavelengths. The work proposed and accomplished was all theoretical and computational. An overview is given of the theoretical and computational research on electromagnetic scattering by small particles. Results that were published in journal articles are described concisely. These include various special techniques to treat particles which are very thin compared to the incident wavelength, Lo. Also in this group of published results, is a study of the internal, surface, and near fields for capped cylindrical particles, all of whose dimensions are small compared to Lo and for which Lo is in a wavelength range such as to excite plasmon or polariton resonances in the particle. Unpublished work along these lines is described in detail in an appendix. This more recent work considers the effects on the resonant modes of particle proximity and aggregation and also considers individual spheres with spherical holes either inside the spheres or forming bites in the sphere surface. GRA

N90-12712# SRI International Corp., Menlo Park, CA.
MECHANISMS OF CO2 REDUCTION METAL AND METAL MODIFIED SEMICONDUCTOR ELECTRODES Final Report, Dec. 1985 - Dec. 1988
K. W. Frese, Jr. 20 Sep. 1989 16 p
(Contract N00014-86-C-0121)
(AD-A213169) Avail: NTIS HC A03/MF A01 CSCL 07/4

Fundamental studies were made to elucidate the factors that control the rate of electrochemical reduction of carbon dioxide. The reorganization energies for Carbon dioxide and Hydrogen cation reduction were 3.1 and 1.95 eV, respectively. Models were developed that allow prediction of binding energies of adsorbed intermediates on electrode surfaces. Palladium, Molybdenum and Gallium arsenide (111) were found to be among the best materials that catalyzed the reduction of CO2 to Methanol. GRA

N90-12713# Chemical Research and Development Center, Aberdeen Proving Ground, MD.
INFRARED SPECTROMETRY OF AEROSOLS Technical Report, Jan. 1979 - Dec. 1982
Hugh R. Carlon Aug. 1989 40 p
(AD-A213303; CRDEC-TR-046) Avail: NTIS HC A03/MF A01 CSCL 17/5

Aerosol spectrometry denotes a methodology for describing spectral effects of atmospheric constituents in quantitative, standardized, basic terms. This methodology is based on the premise that most atmospheric constituents, can be described (albeit in some cases very unconventionally) as specialized kinds of aerosols, some of which exhibit complex changes in spectral behavior between physical phases. Aerosol spectrometry permits

an intuitive understanding of the spectral properties of atmospheric constituents and, very importantly, allows insights not found in traditional or purely mathematical treatments. Liquid and solid particulate aerosols, special cases including Christiansen effects and isobestics, and the phase transitional behavior of liquid droplets in vapor were all studied. A study of this behavior led to the finding that anomalous (continuum) infrared absorption in water vapor could be attributed to liquid-like intermolecular hydrogen bonds in molecular complexes (clusters) long before this observation was made using traditional vapor spectrometric techniques. In two appendices, IR spectra are given with absorption coefficients for gases SF6 and CCl2F2, and extinction by nonabsorbing spheres is considered. GRA

N90-12714# Aerospace Corp., El Segundo, CA. Lab. Operations.
STANDARD METHOD FOR MEASUREMENT OF NONVOLATILE RESIDUE ON SURFACES
Eugene N. Borson, Ethel J. Watts, and Gloria A. To 10 Aug. 1989 65 p
(Contract F04701-88-C-0089)
(AD-A213324; TR-0089(4530-02)-1; SD-TR-89-63) Avail: NTIS HC A04/MF A01 CSCL 25/5

Contamination analyses are used to determine if material, components, and subsystems can be expected to meet the performance requirements of a system. Of particular concern is the quantity of molecular contaminants which might be deposited on critical payload surfaces from these sources. This would include all time periods from fabrication, through loading into the vehicle, launching, and during the lifetime of the spacecraft in orbit. A method for determining the mass of nonvolatile residue (NVR) was generated, and was accepted by the ASTM as Standard E1235. The standard applies to the mass of NVR deposited on 1 sq ft witness plates exposed in clean rooms, clean work areas, and clean enclosures. A wipe method is described for collecting molecular contaminants from any surface and procedures for gravimetric analysis of the NVR so obtained. GRA

26 METALLIC MATERIALS

Includes physical, chemical, and mechanical properties of metals, e.g., corrosion; and metallurgy.

N90-12715*# National Aeronautics and Space Administration. Marshall Space Flight Center, Huntsville, AL.
DETERMINATION OF THE GASEOUS HYDROGEN DUCTILE-BRITTLE TRANSITION IN COPPER-NICKEL ALLOYS
R. A. Parr, M. H. Johnston, J. H. Davis, and T. K. OH (Alabama Univ., Huntsville.) Feb. 1985 17 p
(NASA-TM-86494; NAS 1.15:86494) Avail: NTIS HC A03/MF A01 CSCL 11F

A series of copper-nickel alloys were fabricated, notched tensile specimens machined for each alloy, and the specimens tested in 34.5 MPa hydrogen and in air. A notched tensile ratio was determined for each alloy and the hydrogen environment embrittlement (HEE) determined for the alloys of 47.7 weight percent nickel to 73.5 weight percent nickel. Stacking fault probability and stacking fault energies were determined for each alloy using the x ray diffraction line shift and line profiles technique. Hydrogen environment embrittlement was determined to be influenced by stacking fault energies; however, the correlation is believed to be indirect and only partially responsible for the HEE behavior of these alloys. Author

N90-12716# Los Alamos National Lab., NM.
TEMPERATURE EFFECTS IN SHOCK CONSOLIDATION OF METAL POWDERS
K. P. Staudhammer (Fraunhofer-Inst. fuer Angewandte Material Forschung, Bremen, Germany, F.R.) 1989 5 p Presented at the American Physical Society Topical Conference on Shock Compression of Condensed Matter, Albuquerque, NM, 14-17 Aug. 1989 Sponsored by Alexander von Humboldt Stiftung, Fed. Republic of Germany
(Contract W-7405-eng-36)
(DE89-016782; LA-UR-89-2967; CONF-890812-34) Avail: NTIS HC A01/MF A01

The understanding of residual microstructure and properties of shock consolidated metal powders, knowledge of specific temperature effects pertinent to and resulting from shock events are important parameters. These temperature parameters can be described as the ambient, adiabatic, residual, and strain temperatures. To know these temperatures would be extremely desirable, particularly their sources, magnitudes and method or degree of control so as to optimize the consolidation process. In this work, temperature effects are obtained under conditions which investigates each variable relative to the overall temperature time history. DOE

N90-12717# Westinghouse Savannah River Co., Aiken, SC.
RAPID HEATING TENSILE TESTS OF HIGH-ENERGY-RATE-FORGED 316L STAINLESS STEEL CHARGED WITH HYDROGEN AND TRITIUM
W. C. Mosley 1989 47 p Presented at the Metallurgical Society Fall Meeting: Materials Week, Indianapolis, IN, 1-5 Oct. 1989
(Contracts DE-AC09-89SR-18035; DE-AC09-76SR-00001)
(DE89-017869; DP-MS-89-9; CONF-891024-1) Avail: NTIS HC A03/MF A01

Rapid heating tensile tests of uncharged, hydrogen-charged, and tritium-charged-and-aged stainless steels are being used to determine effects of internal hydrogen and helium on fracture modes and mechanical properties at elevated temperatures. Testing of high-energy-rate-forged (HERF) 316L stainless steel at temperatures up to near 1200 C revealed that internal hydrogen has only slight effects on mechanical properties whereas internal helium from radioactive decay of tritium causes severe embrittlement at temperatures above 500 C. DOE

N90-12718*# Grumman Aerospace Corp., Bethpage, NY.
SUPERPLASTIC FORMING AND DIFFUSION BONDING OF RAPIDLY SOLIDIFIED, DISPERSION STRENGTHENED ALUMINUM ALLOYS FOR ELEVATED TEMPERATURE STRUCTURAL APPLICATIONS
E. Y. Ting and J. R. Kennedy Sep. 1989 149 p
(Contract NAS1-18533)
(NASA-CR-181849; NAS 1.26:181849) Avail: NTIS HC A07/MF A01 CSCL 11F

Rapidly solidified alloys, based upon the Al-Fe-V-Si system and designed for elevated temperature applications, were evaluated for superplasticity and diffusion bonding behavior. Alloys with 8, 16, 27, and 36 volume percent silicide dispersoids were produced; dispersoid condition was varied by rolling at 300, 400, and 500 C (572, 752, and 932 F). Superplastic behavior was evaluated at strain rates from 1 x 10(exp -6)/s to 8.5/s at elevated temperatures. The results indicate that there was a significant increase in elongation at higher strain rates and at temperatures above 600 C (1112 F). However, the exposure of the alloys to temperatures greater than 600 C (1112 F) resulted in the coarsening of the strengthening dispersoid and the degradation of mechanical properties. Diffusion bonding was possible using low gas pressure at temperatures greater than 600 C (1112 F) which also resulted in degraded properties. The bonding of Al-Fe-V-Si alloys to 7475 aluminum alloy was performed at 516 C (960 F) without significant degradation in microstructure. Bond strengths equal to 90 percent that of the base metal shear strength were achieved. The mechanical properties and microstructural characteristics of the alloys were investigated. Author

N90-12719# Westinghouse Electric Corp., Pittsburgh, PA. Advanced Energy Systems.
AN INVESTIGATION OF THE IRRADIATION SWELLING MECHANISMS IN REFRACTORY METALS AT HIGH TEMPERATURES Final Scientific Report, 1 Mar. 1985 - 31 Jul. 1988
R. Bajaj, B. O. Hall, G. R. Fenske, J. C. Greggi, and A. T. Taylor

Jun. 1989 267 p
(Contract F49620-85-C-0060; AF Proj. 2301)
(AD-A211406; WAES-TR-89-0010; AFOSR-89-1051TR) Avail: NTIS HC A12/MF A01 CSCL 11/6

This report presents the results of an investigation of elevated temperature irradiation swelling in refractory metals with an objective of understanding swelling mechanisms in these materials and demonstrating practicality of swelling-resistant materials. The study was divided into three phases. During the first phase, a theoretical model was developed for the swelling in body-centered cubic (bcc) metals. The model was based on chemical reaction rate formalism. Calculations were carried out on on a model material, niobium, which was selected for the study. Experimental and theoretical work was conducted to determine the swelling mechanism. Niobium was irradiated with Nb(++) ions to a dose of 50 dpa and swelling was determined by transmission electron microscopy. A peak swelling at 900 C of 7 percent was observed. No swelling was observed above 1300 C. The experimental data were compared to those predicted by the theoretical model. Reasonable agreements were obtained between the experimental and theoretical swelling curve when niobium-oxygen interaction was included. Sink strength ratios were also calculated from the data. The theoretical model was extended during the second phase to include loop growth/shrinkage in bcc metals. During the third phase of the program, two alloys, Nb-5Hf and Nb-5W, were irradiated with Nb(++) alone and with Nb(++) + He(+) over a temperature range of 800 to 1350 C. GRA

N90-12720# Rolls-Royce Ltd., Derby (England).
THE FUTURE OF NON FERROUS METALS IN AEROSPACE ENGINES
P. J. Postans and R. H. Jeal 6 Oct. 1988 11 p Presented at Eurometaux, Luxembourg, 5-6 Oct. 1988
(PNR90572; ETN-89-95554) Copyright Avail: NTIS HC A03/MF A01

Trends in nonferrous metals use in aerospace engines in the past, and future uses of such metals are discussed. Nickel and titanium have played a key role in the continuing improvement of aero engines since the 1940s and 1950s. The 1990s will see these materials being further developed, but they are now approaching the limit of their capabilities. For engines beyond the year 2000, conventional metallic materials will not have sufficient strength, stiffness or temperature capability. The development of reinforced or composite materials with metal, glass or ceramic matrices and concurrent work and appropriate new design and manufacturing technology is called for. ESA

N90-12721# Helsinki Univ. of Technology, Espoo (Finland). Lab. of Physics.
COMPUTER SIMULATION STUDIES OF THE CATALYTIC OXIDATION OF CARBON MONOXIDE ON PLATINUM METALS
H. P. Kaukonen and R. M. Nieminen 1989 26 p
(PB89-223739; Rept-189) Avail: NTIS HC A03/MF A01 CSCL 11F

The steady state catalytic oxidation process of carbon monoxide on platinum metal surfaces is studied using two irreversible kinetic computer simulation models. An extended version of the model introduced by Ziff, Gulari, and Barshad (ZGB) with the effects of CO desorption and diffusion as well as finite reaction probability taken into account. The different physical processes, diffusion and desorption are studied independently and their effect on the equilibrium window, i.e., the regime where steady CO2 formation occurs is determined. An interaction model where adatom-adatom nearest neighbor (nn) interactions are taken explicitly into account through Boltzmann terms J1, J2, and J3 which are energies of the CO-CO, O-O, and CO-O interactions, respectively. The phase diagrams in the temperature-CO partial pressure (T, P sub co-) plane are determined for different values of the nn-interactions. The behavior of the system is dependent on the sign of J1 (=J2 in the simulations) as well as the sign of the difference J1-J3. There is thus a clear analogy with a two component equilibrium lattice gas with nn-interactions. Author

N90-12722# Helsinki Univ. of Technology, Espoo (Finland). Lab. of Physics.
TEMPERATURE DEPENDENCE OF POSITRON DIFFUSION IN CUBIC METALS
E. Soininen, H. Huomo, P. A. Huttunen, J. Maekinen, A. Vehanen, and P. Hautojarvi 1989 26 p
(PB89-222020; Rept-188) Avail: NTIS HC A03/MF A01 CSCL 11F

A slow positron beam technique was applied to extract quantitative results for the position diffusion coefficient in high purity defect free Mo, Al, Cu and Ag single crystal samples in the temperature range 20 to 1400 K. The values of the diffusion coefficient D+300 K is 1 to 2 sq cm/s and it follows a power law D+ varies as 1/Talpha as a function of the temperature T, with alpha = 0.5 to 0.6 in the studied temperature range. The results show that positron diffusion is largely limited by scattering from longitudinal acoustic phonons. A good agreement with band structure calculations is obtained with the positron effective mass m* approximately 1.5. The terms affecting the temperature dependence of the sum of the positron and electron chemical potentials are extracted. Author

N90-12723# Centre Technique des Industries Mecaniques, Senlis (France).
THE RELATIONSHIP BETWEEN THE MECHANICAL PROPERTIES OF MATERIALS AFTER PRESS FORMING AND THEIR IN-SERVICE PROPERTIES Final Report [LIAISON ENTRE LES PROPRIETES MECANIQUES DES MATERIAUX APRES MISE EN FORME ET LES PROPRIETES EN SERVICE]
R. Coutin, J. P. Doche, and V. Escalup Oct. 1988 70 p In FRENCH
(CETIM-101530; ETN-89-95035) Copyright Avail: NTIS HC A04/MF A01

The changes in mechanical properties of metal plates submitted to press forming are studied. The increased fragility of these pressed plates can lead to failure. Optimal heat treatment conditions designed to give these pressed plates their initial resilience and strength are investigated. Manufacturing techniques which allow the plates to maintain their good mechanical characteristics are studied. Maximum deformation coefficients, below which no post-pressing heat treatment is needed, are established. Full results of the research is given in graphic and tabular form. ESA

N90-12724# Centre Technique des Industries Mecaniques, Nantes (France).
THE EFFECTS OF HEAT TREATMENT AFTER WELDING ON THE FUNCTIONAL PROPERTIES OF ASSEMBLIES OF CrMo ALLOYS. HEAT TREATMENT OF A MIXED ASSEMBLY OF A48 AND 10CD9.10 ALLOYS Final Report [EFFETS DU TRAITEMENT THERMIQUE APRES SOUDAGE SUR LES PROPRIETES D'EMPLOI DES ASSEMBLAGES DE NUANCES FAIBLEMENT ALLIEES AU CRMO -- TRAITEMENT D'UN ASSEMBLAGE MIXTE A48-10CD9.10]
S. Debiez and D. Cartaud (Institut de Soudure, Paris, France) 23 Nov. 1988 45 p In FRENCH
(Contract CETIM-86-3191-B)
(CETIM-104320; IS-22-786; ETN-89-95036) Copyright Avail: NTIS HC A03/MF A01

Homogenous assemblies of 10CD9.10 and 15CD2.05 alloys submitted to heat treatment after welding are studied. The best heat treatment methods for mixed assemblies of A48 and 10CD9.10 are investigated. It is shown that homogenous assemblies of 10CD9.10 alloys benefit from heat treatment at 730C. The heat treatment is not as beneficial for the 15CD2.05 alloy due to strength reduction in the melted zone. Mixed assemblies benefit from heat treatment at 670C especially if a classic C-Mn weld is chosen rather than 0.5Cr to 0.5Mo. ESA

N90-12725# Centre Technique des Industries Mecaniques, Nantes (France).
HOW THE COMMON PRACTICE OF HEATING PLATES OF AUSTENITIC STAINLESS STEEL DURING COOLING AFFECTS THEIR MECHANICAL PROPERTIES Final Report [INFLUENCE DE LA PRATIQUE COURANTE DES CHAUDES DE RETRAIT SUR LES PROPRIETES D'EMPLOI DES TOLES D'ACIERS INOXYDABLES AUSTENITIQUES]
R. Gaillard and P. Roguin (Institut de Soudure, Paris, France) Mar. 1989 41 p In FRENCH
(Contract CETIM-87-2618-D)
(CETIM-104500; IS-23-471; ETN-89-95037) Copyright Avail: NTIS HC A03/MF A01

The influence of heating plates of austenitic stainless steel on their corrosion resistance and their microstructural and mechanical properties is described. Different thickness of plate and different alloy mixes were studied, submitted to heating by acetylene torches to temperatures between 600C and 1050C. The plates were cooled using compressed air and water. The results indicate that the acetylene flames are best adjusted to be rich in oxygen to avoid carbon deposits. No important changes in mechanical characteristics, corrosion or resiliency were found for plates heated to 600 to 800C. On a micro structural level no increase in grain size was noticed until the heating went beyond 1200C. ESA

N90-12726# Centre Technique des Industries Mecaniques, Nantes (France).
INFLUENCE OF THE COMPOSITION OF THE METAL DEPOSITED ON CARBON MANGANESE WELDS ON THE WORK PROPERTIES OF THE MELTED AREA DEPENDING ON THE OPERATING MODE OF THE WELD Final Report [INFLUENCE DE LA COMPOSITION DU METAL DEPOSE DES SOUDURES DE NUANCE CMN SUR LES PROPRIETES D'EMPLOI DE LA ZONE FONDUE, EN FONCTION DU MODE OPERATOIRE DE SOUDAGE]
Y. Darou and S. Debiez (Institut de Soudure, Paris, France) Sep. 1988 66 p In FRENCH
(Contract CETIM-87-2618-B)
(CETIM-104530; IS-88-358; ETN-89-95038) Copyright Avail: NTIS HC A04/MF A01

Experiments carried out to improve the quality of multi-pass carbon-manganese welds are described. These welds are studied on several levels: the actual operating mode of the weld, the speed and thickness of the weld, and a microstructural analysis of the weld after cooling to determine its chemical composition and most importantly its manganese content. Experiments carried out using two electrodes, one with 0.8 percent manganese, the other with 1.5 percent are described. The results are combined with those of a previous study using a 1.1 percent manganese electrode. The highest manganese concentration gives the strongest welds, as long as the weld layers are kept thin by keeping the passing speed of the weld high. ESA

N90-12727# Centre Technique des Industries Mecaniques, Senlis (France).
IMPROVEMENT IN PRE-CONSTRAINT FATIGUE RESISTANCE OF MODULAR FERRETIC AND BAINITIC STEEL BY SHOT PEENING TREATMENTS Final Report [AMELIORATION PAR GRENAILLAGE DE PRECONTRAINTE DE LA RESISTANCE A LA FATIGUE DES FONTES NODULAIRES FERRITIQUES, PERLITIQUES ET BAINITIQUES]
S. Parent-Simonin, J. Fargues (Centre Technique des Industries de la Fonderie, France), and J. F. Flavenot Dec. 1988 12 p In FRENCH
(CETIM-106370; ETN-89-95042) Copyright Avail: NTIS HC A03/MF A01

The use of shot peening in increasing the fatigue resistance of nodular cast steel is described. Such a treatment increases fatigue resistance by seven to thirty percent for ferritic steel, but can decrease fatigue resistance by up to twenty five percent for bainitic cast steel. The residual constraints caused by shot peening are all the greater, the greater the resistance of the cast steel treated. These residual constraints remain stable under fatigue conditions. ESA

N90-12728# Centre Technique des Industries Mecaniques, Senlis (France).
CARBONITRITION RESPONSE OF STEEL PLATES NOT DESTINED FOR HEAT TREATMENTS Final Report [REPONSE EN CARBONITRURATION DE TOLES EN ACIERS NON DESTINES AU TRAITEMENT THERMIQUE]
A. Bernard, D. Ghiglione, and C. Tournier Aug. 1988 89 p In FRENCH
(CETIM-106960; ETN-89-95044) Copyright Avail: NTIS HC A05/MF A01

Microstructure analysis of steel plates carried out to investigate failure problems in plates not destined for heat treatment is described. Low superficial lifetime and shallow carbonitrition penetration are the problems investigated. Metallographic photographs are taken of cross-sections of such plates. Investigation of grain size in the steel ran into problems of abnormalities in the microstructure. A better understanding of the formation processes and of the energy equilibrium within the steel is needed in order to improve the durability of these plates. ESA

N90-12729# Centre Technique des Industries Mecaniques, Senlis (France).
THE QUALITY OF VACUUM DEPOSITED SURFACE TREATMENTS Final Report [QUALITE DES DEPOTS SOUS VIDE]
C. Bournicon, R. Coutin, E. Grosset, J. Gasnier, M. Lefebvre, J. C. Crapart, C. Tournier, J. P. Peyre, P. Cherry, and J. C. Pavy et al Sep. 1988 374 p In FRENCH
(CETIM-107040; ETN-89-95045) Copyright Avail: NTIS HC A16/MF A01

Mechanical tests carried out to determine the best surface coatings for tools used in cutting, molding and forging are described. The lifetimes of surface treated and nontreated tools are compared. The lifetimes of different surface coatings (TiN, TiC, etc.) are compared. The breakdown of surface treated tools is studied. The results of this study are intended to help in the choice of a surface coating for a tool which will be best suited to the function of the tool. ESA

N90-12730# Centre Technique des Industries Mecaniques, Senlis (France).
A FEASIBILITY STUDY OF HYDROGEN DOSAGE ESTIMATION IN SCREW THREADS SUBMITTED TO SURFACE ELECTROLYTIC TREATMENT Final Report [ETUDE DE FAISABILITE DU DOSAGE D'HYDROGENE DANS LA VISSERIE SUBISSANT UN TRAITEMENT DE SURFACE ELECTROLYTIQUE]
Jerome Suchier Feb. 1989 45 p In FRENCH
(CETIM-110110; ETN-89-95049) Copyright Avail: NTIS HC A03/MF A01

A quantitative approach to studying the effects of hydrogen on the mechanical properties of highly resistant steel is described. Hydrogen produced during the chemical cleaning and electrolytic degreasing of steel parts can cause reversible and irreversible damage to the part, leading to increased fragility. Steel bolts being prepared for an electrolytic zinc surface treatment are studied in terms of fracture strength compared to hydrogen concentration. The behavior of hydrogen at different temperatures is studied. The link between different surface treatments and corresponding increases in fragility is described. ESA

N90-12731# Naval Postgraduate School, Monterey, CA. Dept. of Mechanical Engineering.
AN APPROACH TO LOW TEMPERATURE HIGH STRAIN RATE SUPERPLASTICITY IN ALUMINUM ALLOY 2090 M.S. Thesis
Michael W. Reedy Jun. 1989 80 p
(AD-A212271) Avail: NTIS HC A05/MF A01 CSCL 11/6

Successful study of processing microstructural development and superplasticity in Al-Mg alloys was extended to the Lithium-containing 2090 alloy. Attainment of superior superplastic

response in the 2090 alloy proved more difficult. Successive reductions in the temperature at which rolling was conducted resulted in moderate improving to superplastic response. Modification to the rolling schedule resulted in a continuously increasing strain rate during rolling while recovery temperature and rolling speed are unaltered from previous work. GRA

N90-12732# Defence Research Establishment Atlantic, Dartmouth (Nova Scotia).
IBM PC ANALYSIS OF POLARIZATION RESISTANCE DATA
A. E. Hardy and C. M. Hanham Jul. 1989 55 p
(AD-A212294; DREA-TC-89/307) Avail: NTIS HC A04/MF A01 CSCL 12/5

An IBM PC was set up to control an EG and G PARC M273 potentiostat to perform electrochemical corrosion experiments using PARC's M342 corrosion measurement software. Modifications to the software permit the measurement of corrosion current over long periods of time using the Polarization Resistance measurement technique. A computer program, PCCORROS, was used to analyze the polarization resistance data to determine the polarization resistance, corrosion current, anodic and cathodic tafel constants, and the corrosion potential. GRA

N90-12733# Dayton Univ., OH. School of Engineering.
GRADUATE FELLOWSHIPS IN THE FIELD OF HARD MAGNETIC MATERIALS Final Summary Report, 1 Mar. 1983 - 31 Dec. 1988
Karl J. Strnat 15 Jul. 1989 15 p
(Contract DAAG29-83-G-0007)
(AD-A212303; UDR-TR-62; ARO-20377.4-MS) Avail: NTIS HC A03/MF A01 CSCL 20/3

The report describes research performed by four Fellows who based their M.S. theses in Electrical or Materials Engineering on this effort. All work related to rare-earth permanent magnets and their applications in microwave or mm-wave devices. It prepared the candidates for employment in the permanent magnet-producing or the microwave tube industries. The specific topics of the four sub-projects were: (1) Design Analysis of Permanent Magnet Field Sources; (2) Study of the Effects of Heat Treatment Variables on Microstructural, Physical and Magnetic Properties of Sm(Co, Fe, Cu, Zr)z Alloys; (3) Interfacing Instruments for Magnetic Measurements to a Computer; and (4) Characterization of Modified Nd-Fe-B Magnets for Application in Microwave Devices at Elevated Temperatures. GRA

N90-12734# Army Lab. Command, Watertown, MA. Material Technology Lab.
CORROSION AND CORROSION INHIBITION OF METALS/ALLOYS IN METHYLPHOSPHONIC DIFLUORIDE AND DECONTAMINATING SOLUTIONS Final Report
Chester V. Zabielski, Milton Levy, and James Scanlon Jul. 1989 26 p Presented at the US Army Chemical Research, Development and Engineering Center Scientific Conference on Chemical Research, Aberdeen, MD, 15-18 Nov. 1988
(AD-A212404; MTL-TR-89-61) Avail: NTIS HC A03/MF A01 CSCL 11/6

Electrochemical potentiodynamic polarization studies were carried out for a variety of ferrous and nonferrous metals in methylphosphonic difluoride. Studies of the effect of organic inhibitors on the corrosion rate of 1020 steel, 316 and 304 stainless steel and magnesium in methylphosphonic difluoride were also carried out. In addition, electrochemical studies were conducted in Decon solutions of sodium carbonate, DS2, and STB. General corrosion rates are reported for ferrous alloys, titanium, aluminum alloys, magnesium, and two metal matrix composites in full strength and diluted Decon solutions. GRA

N90-12735# Washington Univ., Seattle. Dept. of Mechanical Engineering.
SPALL RESISTANCE OF ALUMINA
L. R. Deobald, M. Taya, A. S. Kobayashi, and H. S. Yoon Sep. 1989 17 p
(Contract N00014-87-K-0326)
(AD-A213213; UWA/DME/TR-89/1) Avail: NTIS HC A03/MF A01 CSCL 11/6

The spall strength of alumina bars was determined using a bar impact apparatus. The fracture morphology in the region of maximum tensile stress caused by the transient wave was investigated using a scanning electron microscope. No microcracking was detected away from the spall plane and the fracture toughness of the unspalled bar remained unchanged with increasing velocity. The ultimate goal is to study the residual strength of monolithic ceramics and ceramic/ceramic composites. The results of such a study can be used to design engineered ceramic composites with higher impact resistance. In order to achieve this goal, an impact test, which is a variation of the plate impact test, was developed. The plate impact test produces a 1-D compressive square stress pulse, which neglects the effects of lateral inertia caused by Poisson's effect, propagating from the impact face at the speed of sound. The impactor is made of the same material and its length is half of the specimen length. A stress pulse, with a length equal to the specimen length, is thus produced. GRA

27 NONMETALLIC MATERIALS

Includes physical, chemical, and mechanical properties of plastics, elastomers, lubricants, polymers, textiles, adhesives, and ceramic materials.

For composite materials see *24 Composite Materials*.

N90-12736# Washington Univ., Seattle. Dept. of Materials Science and Engineering.
SYNTHESIS AND HIGH TEMPERATURE CHEMISTRY OF METHYLSILSESQUIOXANE POLYMERS PRODUCED BY TITANIUM CATALYZED REDISTRIBUTION OF METHYLHYDRIDOOLIGO- AND POLYSILOXANES
Richard M. Laine, Kay A. Youngdahl, Florence Babonneau, John F. Harrod (Paris VI Univ., France), Martin Hoppe, and Jeffrey A. Rahn 1989 29 p
(Contract N00014-89-K-0305)
(AD-A212000; TR-19) Avail: NTIS HC A03/MF A01 CSCL 07/6

The synthetic utility of homogeneous titanium catalyzed redistribution of the cyclomers -(MeHSiO)(x)- (where x = 4 or 5) and the linear oligomer -MeHSiO(x)- (M sub n is approx. = 2,200 D) was explored as a route to MeSiH3 and a methylsilsesquioxane-methylhydridopolysiloxane copolymer of approximate composition -(MeHSiO)0.35(MeSi(O)1.5)0.65-. The high temperature behavior of the titanium derived methylsilisesquioxane copolymer follows closely that of similar polymers prepared by sol-gel processing. Heating under nitrogen to 800 to 1000 C at a heating rate of 5 C/min gives a black glass with an apparent composition of: SiO2 (70 percent); SiC (19 percent); and C (10 percent). The apparent composition belies the true nature of the material which is probably a metastable glass, best described by the various Si-X bonding arrangements (X = O, C, H). Thus, MAS NMR and DRIFT spectroscopy show the existence of species containing 4, 3, and 2 Si-O bonds with the remaining bonds either Si-C or SiH. At 600 C and below (under N2), the Si-C bonds are almost exclusively Si-H3, which is an indication of the extraordinary thermal stability of silsesquioxane polymers. Above 600 C, the CH3 groups react with Si-O bonds to generate Si-OH bonds, new Si-C bonds and Si-H bonds. This type of reactivity is illustrative of the basic chemistry involved in the carbothermal reduction of SiO2 to Si and/or SiC as well as the degradation mechanisms of the polymer. GRA

N90-12737# Minnesota Univ., Minneapolis. Corrosion Research Center.
ELECTROACTIVE POLYANILINE FILM DEPOSITED FROM NON-AQUEOUS MEDIA. 2: EFFECT OF ACID CONCENTRATION IN SOLUTIONS Technical Report No. 11, Jul. 1988 - Jun. 1989

Tetsuya Osaka, Toshiki Nakajima (Waseda Univ., Tokyo, Japan), Katsuhiko Naoi, and Boone B. Owens 15 Jun. 1989 16 p
(Contract N00014-88-K-0360)
(AD-A212084) Avail: NTIS HC A03/MF A01 CSCL 09/1

Polyaniline films electro-deposited from acidified non-aqueous media were investigated for their electropolymerization behavior and charge-discharge characteristics. The solution system used for the electropolymerization of polyaniline films was CF3COOH acidified propylene carbonate, which was previously found to be the best system for the preparation of highly electroactive conducting polymer film. Electroactive polyaniline films only form in solutions wherein the mole ratio of acid (CF3COOH) to aniline monomer is greater than one. As the acidity is increased, the resultant polyaniline film exhibits greater electroactivity and better charge-discharge performance. GRA

N90-12738# Pennsylvania Univ., Philadelphia. Dept. of Materials Science and Engineering.
THE MULTIVALENT BETA'-ALUMINAS Technical Report No. 27, 1987 - 1988
G. C. Farrington, B. Dunn, and J. O. Thomas (Uppsala Univ., Sweden) 7 Jun. 1989 10 p Submitted for publication
(Contract N00014-81-K-0526)
(AD-A212103) Avail: NTIS HC A02/MF A01 CSCL 07/1

The multivalent beta'-aluminas are a rich and diverse family of fast ion conductors. Their potential applications range from the traditional (batteries and sensors) to the unexpected (optoelectronic devices and lasers). The preparation and properties of beta'-aluminas containing Lead(II), Neodymium(III), and Copper(I) ions are briefly reviewed. GRA

N90-12739# Tennessee Univ., Knoxville. Dept. of Chemistry.
POLYMER CHARACTERIZATION BY ELECTROHYDRODYNAMIC IONIZATION MASS SPECTROMETRY Final Report, Jun. 1984 - Apr. 1989
Kelsey D. Cook 10 Aug. 1989 9 p
(Contract MIPR-129-86)
(AD-A212130; ARO-22574.9-CH) Avail: NTIS HC A02/MF A01 CSCL 07/6

Polymer molecular weight distribution, ionic interactions in solution, and impurities were characterized. Several factors affecting matrix-assisted desorption ionization were identified, and their effects on sensitivity compared. GRA

N90-12740# Washington Univ., Seattle. Dept. of Materials Science and Engineering.
TRANSITION METAL CATALYZED SYNTHESIS OF ORGANMETALLIC POLYMERS
Richard M. Laine 1989 28 p
(Contract N00014-88-K-0305)
(AD-A212133; TR-20) Avail: NTIS HC A03/MF A01 CSCL 07/6

Transition metal catalysts were recently used to synthesize organo-metallic oligomers and polymers containing boron or silicon in the polymer backbone. Three types of transition metal catalyzed reactions have proven useful for organometallic polymer synthesis: dehydrocoupling by self-reaction or by reaction with an acidic hydrogen redistribution of Si-H bonds with Si-O bonds, and, ring opening polymerization. The potential utility of these catalytic methods for the synthesis of organometallic polymers is examined. In each instance, an effort is made to illustrate the generality or lack thereof for reaction types. Relevant literature and proposed reaction mechanisms for each reaction are discussed. GRA

N90-12741# Arizona Univ., Tucson.
SYNTHESIS AND CRYSTALLIZATION BEHAVIOR OF FLUORIDE GLASSES Final Report, 1 Sep. 1985 - 30 Sep. 1988
Donald R. Uhlmann 22 Aug. 1989 42 p
(Grant AF-AFOSR-0350-86; AF Proj. 2303)
(AD-A212142; AFOSR-89-1203TR) Avail: NTIS HC A03/MF A01 CSCL 07/4

The objectives of the program were as follows: exploration of wet chemical synthesis routes to the preparation of metal-organic precursors for heavy metal fluoride glasses, exploration of synthesis conditions for converting precursors to multicomponent oxide gels for conversion to heavy metal fluoride glasses; exploration of chemistries and conditions for converting multicomponent oxide gels to heavy metal fluoride glasses; exploration of chemical approaches to passivating the surfaces of heavy metal fluoride glasses; and exploration of the possibility of developing a computer model to describe crystallization during a cycle of cooling-reheating-recooling a liquid to form a glass (the cycle used in forming fluoride glass fibers). GRA

N90-12742# California Univ., Los Angeles. Dept. of Materials Science Engineering.
OXIDE CERAMIC FIBERS BY THE SOL-GEL METHODS Final Report, Dec. 1986 - Feb. 1988
J. D. Mackenzie and K. Ono 10 Feb. 1989 79 p
(Contract F33615-86-C-5141; AF Proj. 2420)
(AD-A211315; AFWAL-TR-88-4199) Avail: NTIS HC A05/MF A01 CSCL 11/2

Sol-gel processing has many advantages over traditional powder based ceramic processing. These advantages include better homogeneity, higher purity and low temperature synthesis. Additionally, the sol-gel process is the only low temperature process available to make high temperature stable oxide fibers. Most of these fibers cannot be formed by drawing via the traditional melt method. Included is the research conducted on the preparation of lanthanum chromite fibers. Lanthanum chromite's high temperature stability was enhanced by coating with alumina. Additionally, a test rig was developed to measure the mechanical properties of fibers at high temperatures. Several commercial fibers, including alumina fibers were tested with this rig. GRA

N90-12743# Massachusetts Univ., Amherst. Dept. of Polymer Science and Engineering.
ULTRASTRUCTURE PROCESSING AND CHARACTERIZATION OF POLYMERS Final Report, 1 Oct. 1986 - 30 Sep. 1988
Frank E. Karasz 1988 20 p
(Grants AF-AFOSR-0033-87; AF-AFOSR-0046-88; AF Proj. 2303)
(AD-A211460; AFOSR-89-1185TR) Avail: NTIS HC A02/MF A01 CSCL 07/6

During this period the research program contained components dealing inter alia with polymer blends, electro- and optically-active polymers, computer simulation of blend phenomena, dynamic light scattering measuring diffusion in porous media, and aspects of ultrastructural processing. New state-of-the-art instrumentation was developed, including a two-dimensional x ray system and solid state NMR. In the area of polymer blends the continued emphasis is on the effect of chain microstructure on miscibility in multi-component systems. This has involved phase behavior studies of copolymer-containing blends, where the structure of the copolymer have been varied in terms of chemistry, tacticity and/or sequence distribution. In the electro-active polymer area, we have concentrated on research involving poly(p-phenylene vinylene) (PPV) and its derivatives, copolymers, and blends. The electrical and, more recently, the non-linear optical properties of this family of conjugated polymers has proved to be of particular interest and potential applicability. GRA

N90-12744# Laboratoire Marcel Mathieu, Pau (France).
TEXTURAL AND STRUCTURAL ORGANIZATION OF THE HEAT TREATED POLYMERS: MECHANICAL PROPERTIES RELATIONSHIPS Final Report [ORGANISATION STRUCTURALE ET TEXTURALE DE POLYMERES TRAITES THERMIQUEMENT, RELATIONS AVEC LES PROPRIETES MECANIQUES]
A. Oberlin and M. Monthioux 1989 113 p In FRENCH
(Contract DRET-86-106)
(ETN-89-95711) Avail: NTIS HC A06/MF A01

The microstructure and the texture of ceramics obtained from organometallic polymer manufacturing are investigated. The interfaces and the bulk structure of the carbon fiber resin composite materials are studied. The transmission electron microscopy and x ray diffraction are the basic applied techniques. Concerning

microstructure and texture characterization, the results obtained can be explained by the fact that the first atomic layers adsorbed on a surface, tend to grow following the bulk structure. In the carbon fiber resin composite investigations, the interphase gradients between the fibers, submitted to a surface treatment and greased, and the different resins, are not detected. ESA

N90-12745 National Physical Lab., Teddington (England). Div. of Materials Applications.
PHYSICAL AGEING AND SHORT TERM CREEP IN AMORPHOUS AND SEMICRYSTALLINE POLYMERS
B. E. Read, P. E. Tomlins, and G. D. Dean Jul. 1989 39 p (NPL-DMA(A)-185; ISSN-0143-7313; ETN-89-95933) Copyright Avail: National Physical Lab., Teddington, Middlesex, TW11 0LW, England

The effect of physical aging at 23C on the short term creep of polycarbonate (PC), polybutylene terephthalate (PBT) and high density polyethylene (HDPE) at creep times between 10 to the minus 8th power and 10 to the 5th power seconds is studied. With increasing age, a decrease is observed in the relaxed compliance of the beta-retardation process in each polymer and relationships between the relaxed compliance and the time elapsed are derived quantitative analysis of the data. For the amorphous PC and semicrystalline PBT, this decrease reflects a redution in the number of groups participating in the localized secondary process. In the case of HDPE, the small decrease in, the relaxed compliance with increasing time elapsed, for the glass-rubber beta-process, is similar to that found for polypropylene and probably involves conformational changes of amorphous tie molecules. The results for HDPE deviate from the predictions of Struik's model of aging in semicrystalline polymers. It is suggested that for the crystal related alpha-process, changes in retardation magnitude, or shape of the retardation time distribution, may occur with increasing age. ESA

N90-12746# Etablissement Technique Central de l'Armement, Arcueil (France). Dept. Comportement des Materiaux.
PYROLYTIC PRODUCTION OF CERAMIC COMPOSITES FROM SILICATES [ELABORATION PAR PYROLYSE DE COMPOSITES CERAMIQUES A PARTIR DE PRODUITS SILYLES]
J. Francillette, B. Mortaigne, and P.-A. Hoarau 24 Jan. 1989 74 p In FRENCH
(Contracts DRET/ETCA/CREA-CI-047683; DRET/ETCA/CREA-CI-048064)
(ETCA-89-R-012; ETN-89-95275) Avail: NTIS HC A04/MF A01

A study of the biproducts of the formation reactions in the synthesis of ceramic-ceramic composites is presented. Different analytic techniques: infrared spectrometry, gas phase chromatography, nuclear magnetic resonance and a combined pyrolysis, gas phase chromatography and a mass detection method are used in studying these biproducts. The influence of temperature in the pyrolitic process of obtaining silicon carbide fibers from other silicate-containing compounds is described. ESA

N90-12747# National Inst. of Standards and Technology, Gaithersburg, MD. Ceramics Div.
NBS/BAM (NATIONAL BUREAU OF STANDARDS/BUNDESANSTALT FUER MATERIALPRUFUNG) 1986 SYMPOSIUM ON ADVANCED CERAMICS Final Report
S. M. Hsu, ed. and H. Czichos, ed. (Bundesanstalt fuer Materialpruefung, Berlin, Germany, F.R.) May 1989 171 p Symposium held in Berlin, Fed. Republic of Germany, Apr. 1986
(PB89-229074; NIST/SP-766; LC-89-600737) Avail: NTIS HC A08/MF A01; also available SOD HC $9.00 as 003-003-02936-0 CSCL 11C

Advanced ceramics offer many advantages that other materials do not possess. They have high strength, dimensional stability, are chemically inert, lightweight, wear resistant, and have desirable properties in electrical, optical, and thermal applications. At high temperatures, they are the only class of material with reasonable properties. Worldwide production of advanced ceramics is growing rapidly. Since ceramics are based on alumina and silica, the most abundant minerals on earth, effective utilization of ceramics carries implications into the next several centuries. One of the major technical barriers to widespread use of ceramics is the inability of industry to manufacture reliable ceramics reproducibly and economically. Advanced ceramics are sensitive to small defects introduced during processing and generated during use. The symposium provides timely exchange of technical information on a very significant subject area of achieving reliable manufacturing through standards. Author

N90-12748# Centre Technique des Industries Mecaniques, Saint Etienne (France). Lab. Collage.
BEHAVIOR OF THE ADHESIVE A2 SUBMITTED TO MECHANICAL TRACTION Final Report [COMPORTEMENT AU FLUAGE DE L'ADHESIF A2]
Jean-Pierre Jeandrau Jan. 1989 73 p In FRENCH
(Contract MRES-86-A-0721)
(CETIM-105290; ETN-89-95040) Copyright Avail: NTIS HC A04/MF A01

The resistance of the A2 epoxy resin adhesive to mechanical traction under a variety of situations is described. The influence of temperature on its adhesive properties is studied. Deformation of the adhesive submitted to constant loads is studied. Glued-together assemblies are submitted to a variety of load stresses. Correlations are made between the results of these tests. Results of these tests are given in graphic and tabular form. ESA

N90-12749# Centre Technique des Industries Mecaniques, Senlis (France).
CHARACTERIZATION OF SELF-LUBRICATING SURFACE MATERIALS Final Report [CARACTERISATION DES REVETEMENTS AUTOLUBRIFIANTS]
G. Colin Mar. 1989 11 p In FRENCH
(CETIM-108060; ETN-89-95048) Copyright Avail: NTIS HC A03/MF A01

A survey carried out amongst companies producing or using self-lubricating surface materials is presented. The result of the survey indicates that tests carried out on a Dow Corning test bench are needed for a better understanding of the subject. The nature of antogonistic surfaces, contact geometry, applied load and sliding speed and environmental factors are some of the factors that will be taken into consideration when these tests are carried out. ESA

N90-12750# Universiteit Twente, Enschede (Netherlands). Faculty of Applied Mathematics.
A GRAPH-THEORETICAL APPROACH TO BLOCK-COPOLYMER COMPLEXES. PART 3: LOOPS AND CYCLES
Ruud vanDamme and Bernard J. Geurts Apr. 1989 27 p
(MEMO-778-Pt-3; ISSN-0169-2690; ETN-89-95669) Avail: NTIS HC A03/MF A01

In a continuing series the rheological properties of block-copolymers in solution are studied. Graph theory is used to determine the statistical properties of block-copolymers in solution. These complexes are assumed to have the topological structure of connected graphs with non-nested loops and cycles. The generating function method is used to determine the number of topologically different complexes containing a given number of block-copolymers. At sufficiently high concentration the system is shown to undergo a transition to a gel phase. The average number of polymers per complex is calculated and the relative increase in viscosity is found under the assumption that the complexes can be treated as porous spheres. ESA

N90-12751 Department of the Navy, Washington, DC.
HIGH TEMPERATURE INSULATORS Patent
James P. Newhouse, inventor (to Navy) and Robert A. Rhein, inventor (to Navy) 18 Oct. 1988 5 p Filed 25 Aug. 1987 Supersedes Pat-Appl-089120-87

(AD-D014193; US-Patent-4,778,871; US-Patent-Appl-SN-089120) Avail: U.S. Patent and Trademark Office CSCL 07/6

An object of this invention is to provide an ablative, high-temperature silphenylene vinylmethylsiloxane elastomer having good thermal stability as well as good mechanical properties. Another object of this invention is a process for producing a high temperature, high impact, erosion resistant silphenylene vinylmethylsiloxane elastomer. This patent describes a high temperature, high impact, erosion resistant silphenylene vinylmethylsiloxane elastomer and a process for making the same in which a liquid hydroxyl-terminated silphenylene vinylmethylsiloxane polymer is cured using a combination of hydrosilylation cure and urethane cure techniques. GRA

N90-12752# Air Force Systems Command, Wright-Patterson AFB, OH. Foreign Technology Div.

ANALYSIS OF CARBON FIBER'S X RAY MICROSCOPIC STRUCTURE

Yuxing Yang, Jiarong Wang, and Changlin Liu 16 Aug. 1989 18 p Transl. into ENGLISH from Shanghai Jiaotong Baxue Xuebac, (China), v. 22, no. 5, 1988 p 20-28

(AD-A212215; FTD-ID(RS)T-0665-89) Avail: NTIS HC A03/MF A01 CSCL 11/5

In this paper, we have used the x ray diffraction method (including the small angle scatter method) to study the microscopic structure of four kinds of carbon fibers. We include the measurement of interlayer distance C for random-layer graphite, average height L of layer surface stacks, average width L of layer surfaces, degree of orientation W1/2, and carbon fiber's average microscopic holes. We also propose a calculation procedure for handling small angle scattering. GRA

N90-12753# Missouri Univ., Rolla. Dept. of Chemistry.

MAGNETIC RESONANCE OF POLYMERS AT SURFACES

Frank D. Blum 28 Aug. 1989 30 p

(Contract N00014-88-K-0109)

(AD-A212225; UMR-FDB-11) Avail: NTIS HC A03/MF A01 CSCL 07/6

In most of the applications where polymers are used, more than one phase is present. In addition to the polymer matrix, the second phase may be comprised of the same or a different polymer, or of some type of filler or fiber which is typically a solid or solid-like. Typical applications of these materials include use in structural composites, adhesives, chromatography, protective coatings, elastomers, and particle stabilization and separation. A brief review of the use of magnetic resonance of polymer molecules attached to solid surfaces is given with examples from the author's laboratory. Liquid, solid (including wide-line and magic angle spinning), and two-dimensional magnetic resonance experiments have all been performed on surface polymers. The results suggest how magnetic resonance techniques can be used to probe the dynamics and structure of the polymer in composites, dispersions, surface treatments and the drying of a coating. GRA

N90-12754# Brookhaven National Lab., Upton, NY. Dept. of Applied Science.

POLYELECTROLYTE-DIFFUSED ZINC PHOSPHATE CONVERSION COATINGS AND POLYACID COUPLING PRIMERS FOR CORROSION PROTECTION OF STEEL AND ALUMINUM, AND ALKALI-CATALYZED HYDROLYSIS OF POLYIMIDE-BASED MATERIALS Final Report, Aug. 1985 - Aug. 1989

T. Sugama, L. E. Kukacka, N. R. Carciello, J. B. Warren, and C. R. Clayton (State Univ. of New York, Stony Brook.) Aug. 1989 108 p

(Contracts MIPR-ARO-112-86; MIPR-112-87; DE-AC02-76CH-00016; MIPR-ARO-102-89; MIPR-ARO-103-88)

(AD-A212240; BNL-43186; ARO-22732.14-MS) Avail: NTIS HC A06/MF A01 CSCL 11/3

The segmental adsorption of polyelectrolyte macromolecules either on newly precipitated crystal nuclei or on crystal growth sites during the primary zinc phosphate (Zn.Ph) conversion process on cold-rolled steel surfaces, acts to array a uniformly packed fine crystal topography brought about by the suppression and delay of the crystal growth. This adsorption is due to charge transfer from the Zn atoms in the crystalline conversion coatings to the electron accepting oxygen portion of functional pendent groups such as carboxylic acid, -COOH, and sulfonic acid, -SO3H, in the polyectrolytes. The formation of ZN-OOC or OSO2 complexes yielded by charge transfer reactions at the polyelectrolyte-Zn.Ph crystal interfaces, not only provides the stiffness and ductility of the normally brittle Zn.Ph layers. GRA

N90-12755# Minnesota Univ., Minneapolis. Corrosion Research Center.

QUARTZ CRYSTAL MICROBALANCE ANALYSIS. 1: EVIDENCE OF ANION OR CATION INSERTION INTO ELECTROPOLYMERIZED CONDUCTING POLYMERS Technical Report, Jul. 1988 - Jun. 1989

Katsuhiko Naoi, Mary M. Lien, and William H. Smyrl 15 Jun. 1989 6 p

(Contract N00014-88-K-0360)

(AD-A212304; TR-13-ONR-1) Avail: NTIS HC A02/MF A01 CSCL 07/6

The mass change during electropolymerization and redox process was monitored for polypyrrole films using Quartz Crystal Microbalance Gravimetry. During the reduction process the polypyrrole films which had incorporated large poly(4-styrenesulfonate) anions showed a mass increase instead of decrease (cation doping). On the other hand, the polypyrrole film formed with a small ClO4 anion showed a mass decrease (anion doping). GRA

N90-12756# Cornell Univ., Ithaca, NY. Dept. of Materials Science and Engineering.

ION BEAM ANALYSIS OF DIFFUSION IN POLYMER GLASSES Final Report, 6 May 1985 - 5 May 1989

Edward J. Kramer 6 Aug. 1989 29 p

(Contract DAAG29-85-K-0120)

(AD-A212339; ARO-22644.8-MS) Avail: NTIS HC A03/MF A01 CSCL 11/2

Rutherford backscattering spectrometry (RBS) and forward recoil spectrometry (FRES) were used to the fundamentals of Case 2 diffusion of organic molecules (solvent) into glassy polymers. These ion beam techniques were employed to measure the velocity V of the Case 2 diffusion front, the diffusion coefficient D of the solvent ahead of the front and the rate of swelling of the surface of the sample as well as the solvent diffusion profiles during the period before Case 2 diffusion has begun. The results indicate that Case 2 diffusion results from a physico-chemically (osmotic pressure) driven yielding of the polymer glass analogous to the familiar mechanical yielding; the almost discontinuous increase in diffusion coefficient that accompanies the yielding accounts for the formation of the front. GRA

N90-12757# Ohio State Univ., Columbus. Dept. of Chemistry.

THE CHEMISTRY OF HEXAAZATRIPHENYLENE HEXANITRILE, A POLYFUNCTIONAL HETEROCYCLE WITH POTENTIAL UTILITY IN THE FORMULATION OF THERMOSTABLE POLYMERS Final Report

Anthony W. Czarnik Jun. 1989 32 p

(Contract DAAG29-85-K-0200)

(AD-A212353; ARO-22825.7-CH) Avail: NTIS HC A03/MF A01 CSCL 07/6

Research results are contained in the publications listed below: Synthesis and Some Reactions of Hexaazatriphenylene Hexanitrile; a Hydrogen-Free Polyfunctional Heterocycle with D3h Symmetry; Decarboxylative Synthesis of Hexaazatriphenylene; Nitrozations in Anhydrous Trifluoroacetic Acid Media (A Modification for Insoluble or Deactivated Amine and Amide Precursors); Materials Derived from the Hydrogen Free Heterocycle Hexaazatriphenylene Hexacarbonitrile Syntheses and High Temperature Properties of Polyimides; A Highly Crosslinked, Thermally Stable Polyimide Film Derived From Hexaazatriphenylene; Syntheses of Some Hexacarboxylic Acid Derivatives of Hexaazatriphenylene; and

Synthesis and Thermogravimetric Analyses of Trisimides and Polyimides Derived from Hexaazatriphenylene. GRA

N90-12758# North Carolina State Univ., Raleigh.
CHEMICAL TREATMENT OF EPOXY RESINS TO REDUCE MOISTURE SENSITIVITY AND TO IMPROVE THE MECHANICAL PROPERTIES Final Report, 1 May 1985 - 31 Jul. 1989
Richard D. Gilbert and Raymond E. Fornes 15 Sep. 1989 5 p
(Contract DAAG29-85-K-0128)
(AD-A212360; Rept-4; ARO-22388.8-MS) Avail: NTIS HC A01/MF A01 CSCL 11/9

Epoxy resin/graphite fiber composites absorb moisture which has a deleterious effect on composite mechanical properties. The moisture results from the electrostatic attraction between residual functional groups on the epoxy resin molecules and water, blocking the functional groups with various reactants decreases the epoxy resin equilibrium moisture absorption as much as 75 percent. Marked isocyanates incorporated into the resin prior to curing permits in situ blocking of the functional groups, reduces moisture absorption up to 65 percent without affecting the elastic modulus. The resin Tg is lowered, but the stress-strain properties are generally unaffected. GRA

N90-12759# Aerospace Corp., El Segundo, CA. Chemistry and Physics Lab.
STRUCTURAL STUDIES OF SPUTTER-DEPOSITED MoS2 SOLID LUBRICANT FILMS
Michael R. Hilton and Paul D. Fleischauer 11 Sep. 1989 24 p
(Contract F04701-88-C-0089)
(AD-A212407; TR-0089(4064)-2; SD-TR-89-58) Avail: NTIS HC A03/MF A01 CSCL 11/8

The relationship between the morphologies and crystal structures of sputter-deposited MoS2 films and their lubricating capabilities is discussed. In particular, aspects of plastic deformation processes are presented. Scanning electron microscopy (top surface and cross sectional), transmission electron microscopy (lattice imaging and dark field), and x ray diffraction techniques were used to characterize film structure. The as-deposited morphology, which can be described in terms of zone models, was found to influence the initial nature of the wear debris and the load-bearing capabilities of the films. In many cases a highly deformed region confined to the films was found. Applied stress was found to reorient crystallites and to induce crystallization, with the degree of both processes being related to the initial structure of the film. Criteria are presented for selecting the film type and preparation conditions to fit various application. GRA

N90-12760# Minnesota Univ., Minneapolis. Corrosion Research Center.
CAPACITIVE BEHAVIOR IN CONDUCTING POLYMERS Technical Report No. 9, Jul. 1988 - Jun. 1989
Katsuhiko Naoi, Mary M. Lien, William H. Smyrl, and Boone B. Owens 15 Jun. 1989 18 p
(Contract N00014-88-K-0360)
(AD-A212448) Avail: NTIS HC A03/MF A01 CSCL 07/6

The over-all differential capacitance for conducting polymers like polypyrrole and polyvinylferrocene which show a very high redox capacity for the oxidation/reduction process was modeled as a function of applied voltage from the cyclic voltammetric data. The capacitance values are compared with various types of carbon double layer and conventional capacitor devices. Also, the theoretical capacitance values for a cell was estimated by assuming a hypothetical minimum equivalent cell consisting of an anode (Li), a cathode (polypyrrole) and an electrolyte solution (2 mol/cu. dm Lithium Perchlorate (PC)) without any hardware. The charge/discharge process or doping/undoping process was determined by impedance analysis and the limiting capacitance was estimated. Also, an attempt was made to separate the faradaic and capacitive currents according to the theory of the impedance of diffusion in a layer of finite thickness. GRA

N90-12761# Naval Surface Warfare Center, Silver Spring, MD. Dept. of Research and Technology.
SYNTHESIS OF ENERGETIC SINGLE PHASE AND MULTI-PHASE POLYMERS Annual Progress Report, 1 Jan. - 31 Dec. 1988
H. G. Adolph, J. M. Goldwasser, L. A. Nock, and D. A. Cichra May 1989 73 p
(Contracts N00014-89-WX-24004; N00014-88-WX-24148; N00014-89-WX-24; N00014-89-WX-20010)
(AD-A212539) Avail: NTIS HC A04/MF A01 CSCL 07/6

The synthesis of polyformals from fluoro- and nitrodiols was continued at a low level. New polyformals were prepared from octafluoro triethylene glycol and hexadeca fluoorodecanediol. Polyformals of a tetranitrodioxatridecanediol with molecular weights as high as 6000 were prepared. Additional copolyformals were prepared from fluoro- and nitrodiols with the objective to obtain polymers with the lowest glass transition temperature and highest energy possible for use as soft blocks in TPE (thermoplastic elastomer) synthesis. Copolymers of a hexanitrodiox adiazapentagecanediol and of dinitrodi azaoctanediol with several fluorodiols appear to be the most promising of the new polymers synthesized. GRA

N90-12762# Army Materials Technology Lab., Watertown, MA.
EFFECTS OF HOT CORROSION ON THE ROOM TEMPERATURE STRENGTH OF STRUCTURAL CERAMICS Final Report
Jeffrey J. Swab and Gary L. Leatherman (Worcester Polytechnic Inst., MA.) Jul. 1989 20 p
(DA Proj. 1L1-62105-AH-84)
(AD-A212568; MTL-TR-89-68) Avail: NTIS HC A02/MF A01 CSCL 11/2

A variety of advanced structural ceramics were treated in air at 1000C for 500 hours with and without various amounts of sodium sulfate. Room temperature flexure strength was determined before and after treatments. Results show that Ce-=TZP and alumina are resistant to strength degradation after exposure to sodium sulfate; however Si3N4 and, to a lesser degree, Y-TZP are not. The Y-TZP had a strength loss of 25 percent after 500 hours at 1000C with 10 to 20 mg/sq cm of Na2S04. This loss is about 10 percent greater than that experienced by specimens when treated at 1000C for 500 hours without sodium sulfate present, and is probably due to the leaching of Y2O3 from the zirconia which allows the tetragonal zirconia to transform to the monoclinic phase. Under similar conditions, the silicon nitride experienced a loss of 655 when sodium sulfate was added. This strength loss is 25 percent greater than the loss after thermal exposure in the absence of sodium sulfate. The additional strength loss here is due to the formation of larger corrosion pits. GRA

N90-12763# Cincinnati Univ., OH. Dept. of Materials Science and Engineering.
STRUCTURE AND PROPERTIES OF POLYMER INTERPHASES Final Report, 1 Jul. 1985 - 30 Jun. 1989
F. James Boerio 15 Sep. 1989 45 p
(Contract N00014-85-K-0459)
(AD-A212796) Avail: NTIS HC A03/MF A01 CSCL 11/1

The effect of metal substrates on the molecular structure of gamma-aminopropyl triethoxysilane (gamma-APS) primers during drying at elevated temperatures was determined using infrared spectroscopy. When drying was carried out at 110 C, the amino groups in primer films formed on 2024 aluminum and copper were oxidized to form imine groups but those in films formed on iron, titanium, and 1100 aluminum were not. When drying was carried out at 150 C, the films formed on iron, copper, titanium, and 2024 aluminum were oxidized to form imine structures but films formed on 1100 aluminum were not. These results indicate that copper-containing substrates catalyzed oxidation of the primer but the oxide on 1100 aluminum, which contained no copper, inhibited the free-radical oxidation. The molecular structure of interphases between model adhesive systems and metal substrates was determined by using x ray photoelectron spectroscopy and infrared spectroscopy to characterize the fracture surfaces of adhesive

joints prepared by curing beams of epoxies against metal beams. The structure of the interphase depended strongly on the curing agent, metal substrate, and use of an aminosilane primer on the substrate. When joints were prepared by curing an epoxy with a tertiary amine curing agent at 75 C against a steel substrate primed with gamma-APS, there was little reaction between the primer and adhesive, and failure occurred near the primer/adhesive interface. GRA

N90-12764# Massachusetts Univ., Amherst. Dept. of Polymer Science and Engineering.
A CENTER FOR ADVANCED ELECTRICAL AND STRUCTURAL POLYMERS Final Report, 1 Dec. 1986 - 31 Oct. 1988
Frank E. Karasz 31 Oct. 1988 47 p
(Contract F49620-87-C-0027)
(AD-A212853; AFOSR-89-1239TR) Avail: NTIS HC A03/MF A01 CSCL 07/6

Electrical and optical properties were investigated in which the main focus of attention was the conjugated macromolecule, poly-p-phenylene vinylene, its analogues, derivatives, copolymers and blends. The potential of PPV as a conducting polymer was amply demonstrated and more recently it was shown that this polymer has relatively high third order non-linear optical characteristics and, of equal importance, can be fabricated into oriented films and into blends with silica glass which have optical transmittances commensurate with device fabrication. New advanced ultrastructural polymer blends were developed. GRA

28 PROPELLANTS AND FUELS

Includes rocket propellants, igniters, and oxidizers; their storage and handling procedures; and aircraft fuels.

For related information see also *07 Aircraft Propulsion and Power, 20 Spacecraft Propulsion and Power,* and *44 Energy Production and Conversion.*

N90-12765# Ballistic Research Labs., Aberdeen Proving Ground, MD.
CONTINUING STUDIES OF LIQUID PROPELLANT DROPS IN HOT, HIGH-PRESSURE ENVIRONMENTS Final Technical Report, Jan. - Nov. 1987
Richard A. Beyer Sep. 1989 20 p
(AD-A212265; BRL-TR-3038) Avail: NTIS HC A03/MF A01 CSCL 14/1

Drops of LP 1846 have been heated in the gases and flames above burning solid propellants at pressures up to 20 MPa (3000 psi). Semi-quantitative measurements of drop lifetime versus pressure and drip diameter have been made. Although limited by uncertainty in the visualization, these observations show that the trend toward shorter drop lifetime with increasing pressure seen at lower pressures continues in this regime. Visible light emission from the evolved gases and near the drops was recorded during heating under some conditions. Microexplosions of the drops were not observed. GRA

N90-12766# Imperial Coll. of Science and Technology, London (England). Dept. of Chemical Engineering and Chemical Technology.
LASER INITIATED IGNITION OF LIQUID PROPELLANT Interim Report No. 5, 31 Dec. 1988 - 30 Jun. 1989
F. B. Carleton, K. Krallis, and F. J. Weinberg 30 Jun. 1989 7 p
(Contract DAJA45-87-C-0014)
(AD-A212342; R/D-5462-AN-01) Avail: NTIS HC A02/MF A01 CSCL 21/2

The 4th Interim Report included the first high speed movie sequence, albeit of rather optical quality, of the interaction between laser generated plasma and a droplet. This was a first step in a more extensive series of studies. Figure 1 shows three sequences illustrating the various parameters under investigations. These include the energy of the laser beam and the distance between the position of the laser focus and the droplet. Moreover, double firing the laser can be used to inject a second plasma kernel into the environment of a drop that is already disintegrating. The records show interaction with the propellant droplet of a rapidly expanding shock wave as well as the more slowly developing plasma kernel and illustrate the wide variation in the rate and completeness of the burning of the droplet that can be achieved. The provisional interpretation is that the shock wave emanating from the laser-generated plasma shatters the droplet and the fine filaments of liquid propellant which result are ignited when they become engulfed by the plasma. This makes the intensity of burning very dependent on the relative positioning of the droplet and laser focus. A second laser pulse (e.g., 200us, 3rd sequence) interacting with the disintegrating and burning fragments from the first in an additional means of promoting rapid decomposition. Comparative experiments with water droplets show shattering without combustion. GRA

N90-12767# Naval Research Lab., Washington, DC. Directed Energy Effects Branch.
THERMAL INITIATION OF CONFINED PRIMARY EXPLOSIVES WITH A PROTON BEAM Final Report, Oct. 1988 - Sep. 1989
A. Stolovy and J. M. Kidd 22 Sep. 1989 16 p
(AD-A212954; NRL-MR-6558) Avail: NTIS HC A03/MF A01 CSCL 21/2

The thermal initiation characteristics of the primary explosives lead azide and lead styphnate were studied by heating confined samples with a 200-MeV proton beam. Values were obtained for thermal initiation thresholds, explosion temperatures, and average specific heats. Thresholds and explosion temperatures, and average specific heats. Thresholds and explosion temperatures were found to depend strongly on the beam heating rate. GRA

N90-12774# Naval Weapons Center, China Lake, CA.
PYROTECHNIC SHOCK STRUCTURAL RESPONSE
R. G. Merritt *In* Vibration Inst., The Shock and Vibraiton Digest, Volume 21, No. 10 Oct. 1989 p 13-23 (For primary document see N90-12771 04-31)
Avail: NTIS HC A04/MF A01

29 MATERIALS PROCESSING

Includes space-based development of products and processes for commercial applications.

For biological materials see *55 Space Biology.*

N90-12768*# Alabama Univ., Huntsville. Center for Microgravity and Materials Research.
VIBRATION ISOLATION TECHNOLOGY: SENSITIVITY OF SELECTED CLASSES OF SPACE EXPERIMENTS TO RESIDUAL ACCELERATIONS Annual Report No. 1, 1 Jul. 1988 - 30 Jun. 1989
J. Iwan D. Alexander, Y. Q. Zhang, and Adebimpe Adebiyi 1989 67 p
(Grant NAG8-724)
(NASA-CR-185443; NAS 1.26:185443) Avail: NTIS HC A04/MF A01 CSCL 22A

Progress performed on each task is described. Order of magnitude analyses related to liquid zone sensitivity and thermo-capillary flow sensitivity are covered. Progress with numerical models of the sensitivity of isothermal liquid zones is described. Progress towards a numerical model of coupled buoyancy-driven and thermo-capillary convection experiments is also described. Interaction with NASA personnel is covered. Results to date are summarized and they are discussed in terms of the predicted space station acceleration environment. Work planned for the second year is also discussed. B.G.

N90-12769# European Space Agency, Paris (France).
BIOLOGY IN MICROGRAVITY: A GUIDE FOR EXPERIMENTERS
L. G. Briarty (Nottingham Univ., England) and B. Kaldeich, ed.

May 1989 128 p Original contains color illustrations
(ESA-TM-02; ISSN-1013-7076; ETN-89-95387) Copyright Avail: NTIS HC A07/MF A01

The techniques that were developed for studying the effects of spaceflight (principally microgravity) on living systems are discussed. The effects of weightlessness on plant and animal cells are given particular attention. The areas of whole animal physiology, space medicine and human physiology are not covered. The goal of the paper is to serve as a handbook for biologists embarking on studies in the field, and to provide data on some of the particular problems that may be encountered. The specialized hardware used in spaceborne biology experiments is described in detail. ESA

N90-12770*# Stanford Univ., CA. Center for Materials Research.
PROTEIN CRYSTAL GROWTH IN LOW GRAVITY Semiannual Technical Report, 27 Apr. - 26 Oct. 1989
Robert S. Feigelson Nov. 1989 21 p
(Grant NAG8-774)
(NASA-CR-186082; NAS 1.26:186082; CMR-89-9) Avail: NTIS HC A03/MF A01 CSCL 22A

The mechanisms involved in protein crystallization and those parameters which influence the growth process and crystalline perfection were studied. The analysis of the flows around growing crystals is detailed. The preliminary study of the growth of isocitrate lyase and the crystal morphologies found are discussed. Preliminary results of controlled nucleation studies are presented. Author

31 ENGINEERING (GENERAL)

Includes vacuum technology; control engineering; display engineering; cryogenics; and fire prevention.

N90-12771# Vibration Inst., Clarendon Hills, IL.
THE SHOCK AND VIBRATION DIGEST, VOLUME 21, NO. 10 Monthly Report
Vicki M. Pate, ed. Oct. 1989 72 p
Avail: NTIS HC A04/MF A01

The feature article of this volume of the digest is entitled: The Computer Age and Traditional Approximate, Analytical Methods. the literature review article is entitled: A Survey on Nonproportional Damping. A third article is entitled: Testing Technology - Pyrotechnic Shock Structural Response. For individual titles, see N90-12772 through N90-12774.

N90-12772# Universidad Nacional del Sur, Bahia Blanca (Argentina). Dept. of Engineering.
THE COMPUTER AGE AND TRADITIONAL APPROXIMATE, ANALYTICAL METHODS **c61**
P. A. A. Laura *In* Vibration Inst., The Shock and Vibration Digest, Volume 21, No. 10 Oct. 1989 p 3-6 Sponsored by CONICET Research and Development Program (For primary document see N90-12771 04-31)
Avail: NTIS HC A04/MF A01

A simple optimization approach is presented that improves the accuracy of the classical Kantorovich method. The method is illustrated in determining the fundamental frequency of plates of nonuniform thickness, and it is shown that in some cases the results are more accurate than those obtained by a finite element code or more cumbersome analytical procedures. Author

N90-12773# State Univ. of New York, Buffalo. Dept. of Mechanical and Aerospace Engineering.
A SURVEY ON NONPROPORTIONAL DAMPING **c39**
J. Bellos and D. J. Inman *In* Vibration Inst., The Shock and Vibration Digest, Volume 21, No. 10 Oct. 1989 p 7-12 (For primary document see N90-12771 04-31)
Avail: NTIS HC A04/MF A01

A literature survey is presented on lumped and distributed parameter, linear, viscously damped, dynamic systems, possessing non-classical modes. The different aspects of modal analysis for such systems are interpreted, and their advantages, as well as their disadvantages, are discussed. The proportional damping assumption and the errors associated with this assumption are stated. A summary of the literature on approximate decoupling techniques is given, emphasizing the extent of the applicability of each approximate method. Criteria and error bounds on predicting and quantifying the response errors due to decoupling approximations are also provided. Author

N90-12774# Naval Weapons Center, China Lake, CA.
PYROTECHNIC SHOCK STRUCTURAL RESPONSE **c28**
R. G. Merritt *In* Vibration Inst., The Shock and Vibraiton Digest, Volume 21, No. 10 Oct. 1989 p 13-23 (For primary document see N90-12771 04-31)
Avail: NTIS HC A04/MF A01

The measurement of structural response of a structure subjected to a pyrotechnic event is presented. The term structural response means the response of a dynamic mechanical structure in the 100 to 2,000 Hz range. The problem in measuring structural response involves a need to obtain acceleration measurement close to the source of the pyrotechnic shock. Some of what was learned about the collection, signal conditioning, and processing of the data is discussed. E.R.

N90-12775# Materials Research Labs., Ascot Vale (Australia).
PRELIMINARY REPORT ON THE FEASIBILITY OF HIGH POWER ELECTRONIC WARFARE (EW) USING EXPLOSIVE ENERGY SOURCES
Gregory A. Clark and David R. Sadedin 1989 26 p
(MRL-TR-89-3; AR-005-688) Avail: NTIS HC A03/MF A01

Electronic warfare (EW) is an extremely important element in modern military conflicts. One form of EW involves jamming, where in general the effectiveness increases with the power level that can be employed. Within the constraints of the upper power limit it would seem to be possible to raise power levels to the point where components are damaged. The required high powers for such EW functions can be produced by compact magnetohydrodynamic (MHD) power sources using fuels such as explosives and propellants. Some indicative applications are discussed and areas for research are identified. Author

N90-12776# National Inst. of Standards and Technology, Gaithersburg, MD. Office of Standards Code and Information.
DIRECTORY OF INTERNATIONAL AND REGIONAL ORGANIZATIONS CONDUCTING STANDARDS-RELATED ACTIVITIES, MAY 1989 Final Report
Maureen Breitenberg, ed. May 1989 443 p Supersedes NBS-SP-649
(PB89-221147; NIST/SP-767) Avail: NTIS HC A19/MF A03; also available SOD HC $22.00 as 003-003-02937-8 CSCL 13B

The directory contains information on 338 international and regional organizations which conduct standardization, certification, laboratory accreditation, or other standards-related activities. The volume describes their work in these areas, the scope of each organization, national affliations of members, U.S. participants, restrictions on membership, as well as the availability of any standards in English. The volume is designed to serve the needs of Federal agencies and standards writers for information on international and regional organizations involved in standardization and related activities. It may also be useful to manufacturers, engineers, purchasing agents, and others. Author

N90-12777# Naval Research Lab., Washington, DC. Chemistry Div.
AVIATION ENGINE TEST FACILITIES (AETF) FIRE PROTECTION STUDY Interim Report, Apr. 1986 - Apr. 1987
R. C. Beller, R. E. Burns (Hughes Associates, Inc., Wheaton, MD.), and J. T. Leonard 13 Jul. 1989 118 p
(AD-A211483; NRL-MR-6505) Avail: NTIS HC A06/MF A01 CSCL 01/3

An analysis is presented to the effectiveness of various types of fire fighting agents in extinguishing the kinds of fires anticipated in Aviation Engine Test Facilities (AETF), otherwise known as Hush Houses. The agents considered include Aqueous Film-Forming

Foam, Halon 1301, Halon 1211 and water. Previous test work has shown the rapidity with which aircraft, especially high performance aircraft, can be damaged by fire. Based on this, tentative criteria for this evaluation included a maximum time of 20 s from fire detection to extinguishment and a period of 30 min in which the agent would prevent reignition. Other issues examined included: toxicity, corrosivity, ease of personnel egress, system reliability, and cost effectiveness. The agents were evaluated for their performance in several fire scenarios, including: under frame fire, major engine fire, engine disintegration fire, high-volume pool fire with simultaneous spill fire, internal electrical fire, and runaway engine fire. GRA

N90-12778# Technische Univ., Delft (Netherlands). Faculty of Aerospace Engineering.
ROLLING OF ARALL LAMINATES (AN ALTERNATIVE METHOD FOR POST-STRETCHING ARALL LAMINATES)
D. Chen, F. E. H. M. Smulders, and L. B. Vogelesang Jul. 1988 23 p
(LR-560; ETN-89-95606) Avail: NTIS HC A03/MF A01

A rolling process is presented as an alternative to post stretching aramide reinforced aluminum laminates (ARALL) in order to set fibers under tension and the aluminum layers under compression. It is found that the reversion of the thermal residual stress system in ARALL laminates can easily be achieved by rolling the material to a permanent setting (for instance 0.4 percent). The fatigue properties of the material are as good as the post-stretched version and some of the mechanical properties show significant improvement without losing any advantage. The main advantage of this process is that conventional rolling equipment can be used which means lower costs and higher productivity for the materials manufacturer. The process may be used to treat wide panels which is essential if the ARALL laminates are to be used as aircraft fuselage skin materials. Test results are presented. ESA

N90-12779# MMR Technologies, Inc., Mountain View, CA.
DEVELOPMENT OF A LOW NOISE 10 K J-T REFRIGERATION SYSTEM Progress Report
Robert L. Paugh 15 Sep. 1989 4 p
(Contract N00014-86-C-0301)
(AD-A213347) Avail: NTIS HC A02/MF A01 CSCL 13/1

The purpose of this contract extension is the continuation of the development of a compact, microminiature, low noise, closed cycle, Joule-Thomson refrigeration system for 10 K operation for use in infra-red sensing, low noise microwave signal detection and high speed superconducting electronic data processing. Work is continuing in the following areas: ongoing refrigerator design and development; compressor assembly and test, implementation of gas cleansing techniques, and system integration. GRA

N90-12797*# Jet Propulsion Lab., California Inst. of Tech., Pasadena.
A CLOSED-CYCLE REFRIGERATOR FOR COOLING MASER AMPLIFIERS BELOW 4 KELVIN
M. Britcliffe *In its* The Telecommunications and Data Acquisition Report 15 Aug. 1989 p 141-149 (For primary document see N90-12786 04-32)
Avail: NTIS HC A11/MF A02 CSCL 13B

32 COMMUNICATIONS AND RADAR

Includes radar; land and global communications; communications theory; and optical communications.

For related information see also *04 Aircraft Communications and Navigation* and *17 Space Communications, Spacecraft Communications, Command and Tracking.* For search and rescue see *03 Air Transportation and Safety,* and *16 Space Transportation.*

N90-12780 Heriot-Watt Univ., Edinburgh (Scotland).
APPLICATION OF THE MOMENT METHOD TO THE DESIGN OF SLOTTED WAVEGUIDE ARRAY ANTENNAS Ph.D. Thesis
A. H. I. McCormick 1988 296 p
Avail: Univ. Microfilms Order No. BRDX84787

Slotted waveguide array antennas, which are widely used in radar systems, are becoming increasingly more amenable to computer aided design/synthesis procedures, since the scattering characteristics of a slot in a waveguide can be predicted to a high degree of accuracy. An improved theoretical CAD package is presented to design arrays of this type. It differs from earlier such packages in that the reliance on measured data was avoided with a theoretical technique termed the moment method being used to provide the self admittance data for the slots. The efficient implementation of this package and in particular the incorporation of the moment method into it was aided considerably by using this method to make a prior study of nature of certain critical slot characteristics. Most of the more significant waveguide slot relationships were discussed in literature in one form or another except for those relating to slot width. A study employing the moment method was performed to eliminate this oversight and the functional relationship between this parameter and the slot resonance was determined. The moment method solution was also extended to permit the examination of round end slots, which are commonly used in practice, by developing a novel axis sectioning procedure. The evolution of the computer aided array design package is described in detail. The package was subsequently employed to design array examples, one of which was constructed. The experimental and theoretical results for this antenna were presented to demonstrate the plausibility of this technique. Some less conventional array configurations were also synthesized to demonstrate design flexibility. Dissert. Abstr.

N90-12781# Federal Aviation Administration, Atlantic City, NJ. Technical Center.
AIRCRAFT REPLY AND INTERFERENCE ENVIRONMENT SIMULATOR (ARIES) HARDWARE PRINCIPLES OF OPERATION. VOLUME 2: APPENDIXES
Edward Mancus Oct. 1989 131 p
(DOT/FAA/CT-TN88/4-2) Avail: NTIS HC A07/MF A01

The Aircraft Reply and Interference Environment Simulator (ARIES) makes possible the performance assessment of the Mode Select (Mode S) sensor under its specific maximum aircraft load. To do this, ARIES operates upon disk files for traffic model and interference to generate simulated aircraft replies and fruit, feeding them to the sensor at radio frequency. Support documentation for ARIES consists of: (1) ARIES Hardware Maintenance Manual: Volume 1 (DOT/FAA/CT-TN88/3); (2) Appendixes of the Hardware Maintenance Manual: Volume 2; (3) ARIES Hardware Principles of Operation: Volume 1 (DOT/FAA/CT-TN88/4); (4) Appendices of the Hardware Principles of Operation: Volume 2; (5) ARIES Software Principles of Operation (DOT/FAA/CT-TN87/16); and (6) ARIES Software User's Manual (DOT/FAA/CT-TN88/15). The Appendices to the Hardware Principles of Operation provide: (1) the acronyms and abbreviations used within the document; (2) detailed information covering the development and implementation of controller microcode; and (3) uplink receiver digital alignment. Author

N90-12782# Federal Aviation Administration, Atlantic City, NJ. Technical Center.
AIRCRAFT REPLY AND INTERFERENCE ENVIRONMENT SIMULATOR (ARIES) HARDWARE PRINCIPLES OF OPERATION, VOLUME 1
Edward Mancus Oct. 1989 276 p
(DOT/FAA/CT-TN88/4-1) Avail: NTIS HC A13/MF A02

The Aircraft Reply and Interference Environment Simulator (ARIES) makes possible the performance assessment of the Mode Select (Mode S) sensor under its specific maximum aircraft load. To do this, ARIES operates upon disk files for traffic model and interference to generate simulated aircraft replies and fruit, feeding them to the sensor at radio frequency. Support documentation for ARIES consists of: (1) the ARIES Hardware Maintenance Manual: Volume 1 (DOT/FAA/CT-TN88/3); (2) Appendixes of the Hardware Maintenance Manual: Volume 2; (3) the ARIES Hardware Principles

of Operation: Volume 1 (DOT/FAA/CT-TN88/4-1); (4) Appendixes of the Hardware Principles of Operation: Volume 2; (5) ARIES Software Principles of Operation (DOT/FAA/CT-TN87/16); and (6) ARIES Software User's Manual (DOT/FAA/CT-TN88/15). This document, the ARIES Hardware Principles of Operation, Volume 1, explains the theory of operation of the ARIES special purpose hardware designed and fabricated at the Federal Aviation Administration Technical Center. Each hardware device is discussed. Functional block diagrams, signal timing diagrams, and state timing diagrams are included where appropriate. Author

N90-12783# International Centre for Theoretical Physics, Trieste (Italy).
PHYSICS OF THE TROPOSPHERIC RADIOPROPAGATION
G. O. Ajayi (Obafemi Awoiowo Univ., Ile-Ife, Nigeria) Feb. 1989 54 p Presented at the ICTP Coll. on Theoretical and Experimental Radiopropagation Physics, Trieste, Italy, 6-24 Feb. 1989 Submitted for publication
(DE89-619726; IC-89/23) Avail: NTIS (US Sales Only) HC A04/MF A01

The physics of the tropospheric radiopropagation is presented considering the atmospheric radio refractive index and taking into account the influence of precipitation and the attenuation due to the atmospheric gases. DOE

N90-12784*# Ohio State Univ., Columbus. ElectroScience Lab.
ADAPTIVE ANTENNA ARRAYS FOR SATELLITE COMMUNICATION Final Report
Inder J. Gupta Sep. 1989 139 p
(Grant NAG3-536)
(NASA-CR-185989; Rept-716111-09; NAS 1.26:185989) Avail: NTIS HC A07/MF A01 CSCL 20N

The feasibility of using adaptive antenna arrays to provide interference protection in satellite communications was studied. The feedback loops as well as the sample matric inversion (SMI) algorithm for weight control were studied. Appropriate modifications in the two were made to achieve the required interference suppression. An experimental system was built to test the modified feedback loops and the modified SMI algorithm. The performance of the experimental system was evaluated using bench generated signals and signals received from TVRO geosynchronous satellites. A summary of results is given. Some suggestions for future work are also presented. Author

N90-12785# Foersvarets Forskningsantalt, Linkoeping (Sweden).
DIGITAL RADIO LINK: WAVE PROPAGATION INVESTIGATIONS ON A 13 GHz LINE-OF-SIGHT PATH
Stefan Mattsson Oct. 1988 159 p In SWEDISH; ENGLISH summary
(PB89-213128; FOA-C-30516-3.5) Avail: NTIS HC A08/MF A01 CSCL 20N

Propagation investigations on two high capacity (34 mb/s) 13 GHz-paths (28 km and 46 km) were performed during the period 1983, 1984 and 1985. The main purpose of the measurements were to examine the activity of frequency selective fading and rain attenuation. The event-controlled measurements described where the power spectrum and signal levels are recorded in the case of a spectral slope or a fade depth exceeding a specific threshold. The suitable types of fading, such as rain- and Rayleigh-fading, are described with corresponding statistical models. A fit is made of the models to experimental cumulative distributions. A least-square fit is made of the reduced 3-way model to measured transfer functions. The resulting distribution of corresponding parameters of the model is presented together with the correlation between them. Finally, a model is proposed for the calculation of unavailability caused by rain, Rayleigh- and frequency selective fading. Author

N90-12786*# Jet Propulsion Lab., California Inst. of Tech., Pasadena.
THE TELECOMMUNICATIONS AND DATA ACQUISITION REPORT Progress Report, Apr. - Jun. 1989
E. C. Posner, ed. 15 Aug. 1989 234 p
(NASA-CR-185093; JPL-TDA-PR-42-98; NAS 1.26:185093) Avail: NTIS HC A11/MF A02 CSCL 17B

Archival reports on developments in programs managed by JPL's Office of Telecommunications and Data Acquisition (TDA) are presented. Activities of the Deep Space Network (DSN) and its associated Ground Communications Facility (GCF) related to DSN advanced systems, systems implementation, and DSN operations are addressed. In addition, recent developments in the NASA SETI (Search for Extraterrestrial Intelligence) sky survey are summarized. For individual titles, see N90-12787 through N90-12804.

N90-12787*# Jet Propulsion Lab., California Inst. of Tech., Pasadena.
AN ANALYTIC DEVELOPMENT OF ORBIT DETERMINATION FOR A DISTANT, PLANETARY ORBITER **c13**
R. K. Russell and S. W. Thurman *In its* The Telecommunications and Data Acquisition Report 15 Aug. 1989 p 1-25 (For primary document see N90-12786 04-32)
Avail: NTIS HC A11/MF A02 CSCL 22A

With the advent of the Mariner '71 Mission, NASA has been sending spacecraft to orbit various distant bodies within the solar system. At present, there is still no adequate theory describing the inherent state estimation accuracy, based on two-way, coherent range-rate data. It is the purpose of this article to lay the groundwork for a general elliptic theory, and in addition to provide an analytic solution for the special case of circular orbits. It is shown that circular orbits about distant planets may suffer singularities in over-all position error estimation. These singularities are due to orbit inclination, placement of the line-of-nodes, and insignificant cross-velocity at the start and end of retrograde motion when orbiting a superior planet. Even though these conclusions appear to yield poor state estimation, one should not be unduly alarmed inasmuch as the stated conditions for singularity are not maintained for extended periods during typical mission scenarios. However, mission analysts should be aware of these potential pitfalls and realize that spuriously large results for circular orbiters can be obtained and are not the result of incorrect assumptions or faulty software. The general elliptic problem appears so involved that analytic inversion at this time is just not feasible, and in any case the resulting expression for the position error would likely be so lengthy that any understanding would be lost in the maze.
Author

N90-12788*# Jet Propulsion Lab., California Inst. of Tech., Pasadena.
A STATISTICAL STUDY OF RADIO-SOURCE STRUCTURE EFFECTS ON ASTROMETRIC VERY LONG BASELINE INTERFEROMETRY OBSERVATIONS
J. S. Ulvestad *In its* The Telecommunications and Data Acquisition Report 15 Aug. 1989 p 26-56 (For primary document see N90-12786 04-32)
Avail: NTIS HC A11/MF A02 CSCL 17B

Errors from a number of sources in astrometric very long baseline interferometry (VLBI) have been reduced in recent years through a variety of methods of calibration and modeling. Such reductions have led to a situation in which the extended structure of the natural radio sources used in VLBI is a significant error source in the effort to improve the accuracy of the radio reference frame. In the past, work has been done on individual radio sources to establish the magnitude of the errors caused by their particular structures. The results of calculations on 26 radio sources are reported in which an effort is made to determine the typical delay and delay-rate errors for a number of sources having different types of structure. It is found that for single observations of the types of radio sources present in astrometric catalogs, group-delay and phase-delay scatter in the 50 to 100 psec range due to source structure can be expected at 8.4 GHz on the intercontinental baselines available in the Deep Space Network (DSN). Delay-rate scatter of approx. 5 x 10(exp -15) sec sec(exp -1) (or approx. 0.002 mm sec (exp -1) is also expected. If such errors mapped directly into source position errors, they would correspond to

position uncertainties of approx. 2 to 5 nrad, similar to the best position determinations in the current JPL VLBI catalog. With the advent of wider bandwidth VLBI systems on the large DSN antennas, the system noise will be low enough so that the structure-induced errors will be a significant part of the error budget. Several possibilities for reducing the structure errors are discussed briefly, although it is likely that considerable effort will have to be devoted to the structure problem in order to reduce the typical error by a factor of two or more. Author

N90-12789*# Jet Propulsion Lab., California Inst. of Tech., Pasadena.

AN APPARATUS FOR THE ELECTRODYNAMIC CONTAINMENT OF CHARGED MACROPARTICLES **c72**

A. Williams, R. Melbourne, L. Maleki, G. Janik, and J. Prestage *In its* The Telecommunications and Data Acquisition Report 15 Aug. 1989 p 57-62 (For primary document see N90-12786 04-32)

Avail: NTIS HC A11/MF A02 CSCL 20H

The dynamic motion of the ions contained in the trapped (199)Hg+ frequency standard contributes to the stability of the standard. In order to study these dynamics, a macroscopic analog of the (199)Hg+ trap is constructed. Containment of micron-sized particles in this trap allows direct visual observation of the particles' motion. Influenced by the confining fields and their own Coulomb repulsion, the particles can form stable arrays. Author

N90-12790*# Jet Propulsion Lab., California Inst. of Tech., Pasadena.

SPIN-LATTICE RELAXATION AND THE CALCULATION OF GAIN, PUMP POWER, AND NOISE TEMPERATURE IN RUBY **c76**

J. R. Lyons *In its* The Telecommunications and Data Acquisition Report 15 Aug. 1989 p 63-85 (For primary document see N90-12786 04-32)

Avail: NTIS HC A11/MF A02 CSCL 20L

The use of a quantitative analysis of the dominant source of relaxation in ruby spin systems to make predictions of key maser amplifier parameters is described. The spin-lattice Hamiltonian which describes the interaction of the electron spins with the thermal vibrations of the surrounding lattice is obtained from the literature. Taking into account the vibrational anisotropy of ruby, Fermi's rule is used to calculate the spin transition rates between the maser energy levels. The spin population rate equations are solved for the spin transition relaxation times, and a comparison with previous calculations is made. Predictions of ruby gain, inversion ratio, and noise temperature as a function of physical temperature are made for 8.4-GHz and 32-GHz maser pumping schemes. The theory predicts that ruby oriented at 90 deg will have approximately 50 percent higher gain in dB and slightly lower noise temperature than a 54.7-deg ruby at 32 GHz (assuming pump saturation). A specific calculation relating pump power to inversion ratio is given for a single channel of the 32-GHz reflected wave maser. Author

N90-12791*# Jet Propulsion Lab., California Inst. of Tech., Pasadena.

PERFORMANCE EFFECTS OF TIE-TRUSS MODIFICATIONS FOR A 70-METER CENTERLINE BEAM WAVEGUIDE ANTENNA

J. J. Cucchissi *In its* The Telecommunications and Data Acquisition Report 15 Aug. 1989 p 86-94 (For primary document see N90-12786 04-32)

Avail: NTIS HC A11/MF A02 CSCL 17B

The elevation-axis tie truss of the 70-m antennas would have to be modified to accommodate a centerline beam waveguide. To accomplish this, the center section of the tie truss has to be altered, causing a change in the tie-truss compliance and affecting structural performance. Even with the center section completely removed, the worst-case rms pathlength error due to gravity load is increased from 0.025 to only 0.030 inches. Using a simple postprocessor technique, the effects of modifying the compliance can be predicted without resorting to multiple and costly re-analyses of large finite-element models on a mainframe computer. Author

N90-12792*# Jet Propulsion Lab., California Inst. of Tech., Pasadena.

A PERFORMANCE COMPARISON BETWEEN BLOCK INTERLEAVED AND HELICALLY INTERLEAVED CONCATENATED CODING SYSTEMS

K.-M. Cheung and L. Swanson *In its* The Telecommunications and Data Acquisition Report 15 Aug. 1989 p 95-103 (For primary document see N90-12786 04-32)

Avail: NTIS HC A11/MF A02 CSCL 17B

The performance (bit-error rate vs. signal-to-noise ratio) of two different interleaving systems, block interleaving and the newer helical interleaving are compared. Both systems are studied with and without error forecasting. Without error forecasting, the two systems have identical performance. When error forecasting is used with shallow interleaving, helical interleaving gains, but less than 0.05 dB, over block interleaving. For higher interleaving depth, the systems have almost indistinguishable performance. Author

N90-12793*# Jet Propulsion Lab., California Inst. of Tech., Pasadena.

ON THE DECODER ERROR PROBABILITY OF LINEAR CODES

K.-M. Cheung *In its* The Telecommunications and Data Acquisition Report 15 Aug. 1989 p 104-109 (For primary document see N90-12786 04-32)

Avail: NTIS HC A11/MF A02 CSCL 17B

By using coding and combinatorial techniques, an approximate formula for the weight distribution of decodable words of most linear block codes is evaluated. This formula is then used to give an approximate expression for the decoder error probability P(sub E)(u) of linear block codes, given that an error pattern of weight u has occurred. It is shown that P(sub E)(u) approaches the constant Q as u gets large, where Q is the probability that a completely random error pattern will cause decoder error. Author

N90-12794*# Jet Propulsion Lab., California Inst. of Tech., Pasadena.

AUTOMATED MONITOR AND CONTROL FOR DEEP SPACE NETWORK SUBSYSTEMS

P. Smyth *In its* The Telecommunications and Data Acquisition Report 15 Aug. 1989 p 110-120 (For primary document see N90-12786 04-32)

Avail: NTIS HC A11/MF A02 CSCL 17B

The problem of automating monitor and control loops for Deep Space Network (DSN) subsystems is considered and an overview of currently available automation techniques is given. The use of standard numerical models, knowledge-based systems, and neural networks is considered. It is argued that none of these techniques alone possess sufficient generality to deal with the demands imposed by the DSN environment. However, it is shown that schemes that integrate the better aspects of each approach and are referenced to a formal system model show considerable promise, although such an integrated technology is not yet available for implementation. Frequent reference is made to the receiver subsystem since this work was largely motivated by experience in developing an automated monitor and control loop for the advanced receiver. Author

N90-12795*# Jet Propulsion Lab., California Inst. of Tech., Pasadena.

FRAME SYNCHRONIZATION METHODS BASED ON CHANNEL SYMBOL MEASUREMENTS

S. Dolinar and K.-M. Cheung *In its* The Telecommunications and Data Acquisition Report 15 Aug. 1989 p 121-137 (For primary document see N90-12786 04-32)

Avail: NTIS HC A11/MF A02 CSCL 17B

The current DSN frame synchronization procedure is based on monitoring the decoded bit stream for the appearance of a sync marker sequence that is transmitted once every data frame. The possibility of obtaining frame synchronization by processing the raw received channel symbols rather than the decoded bits is

explored. Performance results are derived for three channel symbol sync methods, and these are compared with results for decoded bit sync methods reported elsewhere. It is shown that each class of methods has advantages or disadvantages under different assumptions on the frame length, the global acquisition strategy, and the desired measure of acquisition timeliness. It is shown that the sync statistics based on decoded bits are superior to the statistics based on channel symbols, if the desired operating region utilizes a probability of miss many orders of magnitude higher than the probability of false alarm. This operating point is applicable for very large frame lengths and minimal frame-to-frame verification strategy. On the other hand, the statistics based on channel symbols are superior if the desired operating point has a miss probability only a few orders of magnitude greater than the false alarm probability. This happens for small frames or when frame-to-frame verifications are required. Author

N90-12796*# Jet Propulsion Lab., California Inst. of Tech., Pasadena.

PERFORMANCE OF THE IMAGE STATISTICS DECODER IN CONJUNCTION WITH THE GOLDSTONE-VLA ARRAY

H. C. Wang and G. H. Pitt, III *In its* The Telecommunications and Data Acquisition Report 15 Aug. 1989 p 138-140 (For primary document see N90-12786 04-32)

Avail: NTIS HC A11/MF A02 CSCL 17B

During Voyager's Neptune encounter, the National Radio Astronomy Observatory's Very Large Array (VLA) will be arrayed with Goldstone antennas to receive the transmitted telemetry data from the spacecraft. The telemetry signal from the VLA will drop out periodically, resulting in a periodic drop in the received signal-to-noise ratio (SNR). The Image Statistics Decoder (ISD), which assumes a correlation between pixels, can improve the bit error rate (BER) for images during these dropout periods. Simulation results have shown that the ISD, in conjunction with the Goldstone-VLA array can provide a 3-dB gain for uncompressed images at a BER of 5.0 x 10(exp -3). Author

N90-12797*# Jet Propulsion Lab., California Inst. of Tech., Pasadena.

A CLOSED-CYCLE REFRIGERATOR FOR COOLING MASER AMPLIFIERS BELOW 4 KELVIN **c31**

M. Britcliffe *In its* The Telecommunications and Data Acquisition Report 15 Aug. 1989 p 141-149 (For primary document see N90-12786 04-32)

Avail: NTIS HC A11/MF A02 CSCL 13B

A helium refrigerator utilizing the Gifford-McMahon/Joule-Thomson (GM/JT) cycle was designed and tested to demonstrate the feasibility of using small closed-cycle refrigerators as an alternative to batch-filled cryostats for operating temperatures below 4 K. The systems could be used to cool low-noise microwave maser amplifiers located in large parabolic antennas. These antennas tilt vertically, making conventional liquid-filled dewars difficult to use. The system could also be used for a non-tilting beam waveguide antenna to reduce the helium consumption of a liquid helium cryostat. The prototype system is adjustable to provide 700 mW of cooling at 2.5 K to 3 W at 4.3 K. Performance of the unit is not significantly affected by physical orientation. The volume occupied by the refrigerator is less than 0.1 cu m. Two JT expansion stages are used to maximize cooling capacity per unit mass flow. The heat exchangers were designed to produce minimum pressure drop in the return gas stream. Pressure drop for the entire JT return circuit is less than 5 kpa at a mass flow of 0.06 g/sec when operating at 2.5 K. Author

N90-12798*# Jet Propulsion Lab., California Inst. of Tech., Pasadena.

WIDEBAND PHASE-LOCKED ANGULAR MODULATOR

L. Nguyen *In its* The Telecommunications and Data Acquisition Report 15 Aug. 1989 p 150-156 (For primary document see N90-12786 04-32)

Avail: NTIS HC A11/MF A02 CSCL 17B

A phase-locked loop (PLL) angular modulator scheme has been proposed which has the characteristics of wideband modulation frequency response. The modulator design is independent of the PLL closed-loop transfer function H(s), thereby allowing independent optimization of the loop's parameters as well as the modulator's parameters. A phase modulator implementing the proposed scheme was built to phase modulate a low-noise phase-locked signal source at the output frequency of 2290 MHz. The measurement results validated the analysis by demonstrating that the resulting baseband modulation bandwidth exceeded that of the phase-locked loop by over an order of magnitude. However, it is expected to be able to achieve much wider response still. Author

N90-12799*# Jet Propulsion Lab., California Inst. of Tech., Pasadena.

PERFORMANCE OF THE SPLIT-SYMBOL MOMENTS SNR ESTIMATOR IN THE PRESENCE OF INTER-SYMBOL INTERFERENCE

B. Shah and S. Hinedi *In its* The Telecommunications and Data Acquisition Report 15 Aug. 1989 p 157-173 (For primary document see N90-12786 04-32)

Avail: NTIS HC A11/MF A02 CSCL 17B

The Split-Symbol Moments Estimator (SSME) is an algorithm that is designed to estimate symbol signal-to-noise ratio (SNR) in the presence of additive white Gaussian noise (AWGN). The performance of the SSME algorithm in band-limited channels is examined. The effects of the resulting inter-symbol interference (ISI) are quantified. All results obtained are in closed form and can be easily evaluated numerically for performance prediction purposes. Furthermore, they are validated through digital simulations. Author

N90-12800*# Jet Propulsion Lab., California Inst. of Tech., Pasadena.

DSN 70-METER ANTENNA MICROWAVE OPTICS DESIGN AND PERFORMANCE IMPROVEMENTS. PART 2: COMPARISON WITH MEASUREMENTS **c74**

D. A. Bathker and S. D. Slobin *In its* The Telecommunications and Data Acquisition Report 15 Aug. 1989 p 174-189 (For primary document see N90-12786 04-32)

Avail: NTIS HC A11/MF A02 CSCL 20F

The measured Deep Space Network (DSN) 70-meter antenna performance at S- and X-bands is compared with the design expectations. A discussion of natural radio-source calibration standards is given. New estimates of DSN 64-meter antenna performance are given, based on improved values of calibration source flux and size correction. A comparison of the 64- and 70-meter performances shows that average S-band peak gain improvement is 1.94 dB, compared with a design expectation of 1.77 dB. At X-band, the average peak gain improvement is 2.12 dB, compared with the (coincidentally similar) design expectation of 1.77 dB. The average measured 70-meter S-band peak gain exceeds the nominal design-expected gain by 0.02 dB; the average measured 70-meter X-band peak gain is 0.14 dB below the nominal design-expected gain. Author

N90-12801*# Jet Propulsion Lab., California Inst. of Tech., Pasadena.

STABLE KALMAN FILTERS FOR PROCESSING CLOCK MEASUREMENT DATA **c33**

P. A. Clements, B. P. Gibbs, and J. S. Vandergraft (Computational Engineering, Inc., Laurel, MD.) *In its* The Telecommunications and Data Acquisition Report 15 Aug. 1989 p 190-201 (For primary document see N90-12786 04-32)

Avail: NTIS HC A11/MF A02 CSCL 09C

Kalman filters have been used for some time to process clock measurement data. Due to instabilities in the standard Kalman filter algorithms, the results have been unreliable and difficult to obtain. During the past several years, stable forms of the Kalman filter have been developed, implemented, and used in many diverse applications. These algorithms, while algebraically equivalent to the standard Kalman filter, exhibit excellent numerical properties. Two of these stable algorithms, the Upper triangular-Diagonal (UD) filter and the Square Root Information Filter (SRIF), have been

implemented to replace the standard Kalman filter used to process data from the Deep Space Network (DSN) hydrogen maser clocks. The data are time offsets between the clocks in the DSN, the timescale at the National Institute of Standards and Technology (NIST), and two geographically intermediate clocks. The measurements are made by using the GPS navigation satellites in mutual view between clocks. The filter programs allow the user to easily modify the clock models, the GPS satellite dependent biases, and the random noise levels in order to compare different modeling assumptions. The results of this study show the usefulness of such software for processing clock data. The UD filter is indeed a stable, efficient, and flexible method for obtaining optimal estimates of clock offsets, offset rates, and drift rates. A brief overview of the UD filter is also given. Author

N90-12802*# Jet Propulsion Lab., California Inst. of Tech., Pasadena.

A SIMPLE MODEL FOR DSS-14 OUTAGE TIMES **c38**

H. C. Rumsey, R. Stevens, and E. C. Posner *In its* The Telecommunications and Data Acquisition Report 15 Aug. 1989 p 202-206 (For primary document see N90-12786 04-32)
Avail: NTIS HC A11/MF A02 CSCL 14D

A model is proposed to describe DSS-14 outage times. Discrepancy Reporting System outage data for the period from January 1986 through September 1988 are used to estimate the parameters of the model. The model provides a probability distribution for the duration of outages, which agrees well with observed data. The model depends only on a small number of parameters, and has some heuristic justification. This shows that the Discrepancy Reporting System in the Deep Space Network (DSN) can be used to estimate the probability of extended outages in spite of the discrepancy reports ending when the pass ends. The probability of an outage extending beyond the end of a pass is estimated as around 5 percent. Author

N90-12803*# Jet Propulsion Lab., California Inst. of Tech., Pasadena.

Ka-BAND MMIC BEAM STEERED TRANSMITTER ARRAY

D. L. Rascoe, A. L. Riley, J. Huang, V. Lubecke, and L. Duffy *In its* The Telecommunications and Data Acquisition Report 15 Aug. 1989 p 207-217 Previously announced in IAA as A89-53326 (For primary document see N90-12786 04-32)
Avail: NTIS HC A11/MF A02 CSCL 17B

A 32-GHz six-element linear transmitter array utilizing monolithic microwave integrated circuit (MMIC) phase shifters and power amplifiers was designed and tested as part of the development of a spacecraft array feed for NASA deep-space communications applications. Measurements of the performance of individual phase shifters, power amplifiers, and microstrip radiators were carried out, and electronic beam steering of the linear array was demonstrated. The switched-line phase shifters were accurate to within 7 percent on average and the power amplifier 1-dB compressed output power varied over 0.3 dB. The array had a beamwidth of 7.5 deg and demonstrated acceptable beam steering over + or - 8 deg. From the results, it can be concluded that this MMIC phased array has adequate beam-scanning capability for use in the two-dimensional array. The areas that need to be improved are the efficiency of the MMIC power amplifier and the insertion loss of the MMIC phase shifter. Author

N90-12804*# Jet Propulsion Lab., California Inst. of Tech., Pasadena.

THE NASA SETI SKY SURVEY: RECENT DEVELOPMENTS **c55**

M. J. Klein, S. Gulkis, E. T. Olsen, and N. A. Renzetti *In its* The Telecommunications and Data Acquisition Report 15 Aug. 1989 p 218-226 Previously announced in IAA as A89-17852 (For primary document see N90-12786 04-32)
Avail: NTIS HC A11/MF A02 CSCL 06C

NASA's Search for Extraterrestrial Intelligence (SETI) project utilizes two complementary search strategies: a sky survey and a targeted search. The SETI team at the Jet Propulsion Laboratory (JPL) in Pasadena, California, has primary responsibility to develop and carry out the sky survey part. Described here is progress that has been made developing the major elements of the survey including a 2-million channel wideband spectrum analyzer system that is being designed and constructed by JPL for the Deep Space Network (DSN). The system will be a multiuser instrument; it will serve as a prototype for the SETI sky survey processor. This prototype system will be used to test the signal detection and observational strategies on DSN antennas in the near future. Author

N90-12805# Helsinki Univ. of Technology, Espoo (Finland). Electromagnetics Lab.

SCALAR GREEN FUNCTION METHOD FOR MICROSTRIP ANTENNA ANALYSIS BASED ON THE EXACT IMAGE THEORY

Ismo V. Lindell, Keijo I. Nikoskinen, E. Alanen, and A. T. Hujanen Dec. 1988 32 p
(PB89-218838; Rept-38; ISBN-951-754-722-6) Avail: NTIS HC A03/MF A01 CSCL 20N

Exact image theory, applicable to the analysis of plane-stratified structures, is reviewed in general form, and expressions corresponding to the microstrip geometry are given. Essential in this method is the calculation of two scalar Green functions, responsible for the effect of the geometry for the field. Exact expressions for these Green functions are found for the microstrip in terms of integrals of special functions. The Green functions are needed in the formulation of electric field integral equations for the surface currents of the microstrip. The Green functions possess the same type of singularity as the free-space Green function and also a similar limit when the distance grows larger, with the exception of a waveguide-mode term, which can be easily evaluated separately. Simple approximate expressions for the Green functions are evaluated, suitable for practical analysis of microstrip structures. GRA

N90-12806# Danish Research Center for Applied Electronics, Hoersholm.

PRELIMINARY INVESTIGATION OF FARADAY ROTATION EFFECTS AND DESCRIPTION OF POLARIZATION MEASUREMENTS ON THE AFGL HIGH LATITUDE METEOR SCATTER TEST BED Final Report, Jun. 1988 - May 1989

Jens C. Ostergaard 1 Jan. 1989 57 p
(Contract F61101-88-C-0015)
(AD-A211298; AFGL-TR-89-0123) Avail: NTIS HC A04/MF A01 CSCL 20/14

The background, methodology and preliminary results of an investigation of Faraday rotation effects on the Meteor Scatter High Latitude Test Bed in Greenland are presented. A short review of polarization theory for radio waves, presenting basic properties and changes when reflected from the surface of the earth or propagated through the ionosphere is included. Material published by other workers is presented to give the background for the current interest in Faraday rotation on meteor scatter links. Propagation losses for meteor scatter paths originate from spatial spreading of RF energy, scattering losses at the meteor trail, ionospheric absorption and polarization mismatch at the receiving antenna. That part of the polarization mismatch generated by the ionosphere, the Faraday rotation, is described and evaluated. A method to compute the Faraday rotation is presented and results obtained for the AFGL MSHL Test Bed are given. An experiment, including the measurement of signal strength and polarization throughout the lifetime of the individual meteor scatter return is needed to fully assess the combined affects of absorption and depolarization during both quiet and disturbed ionospheric conditions. The measurement accuracy to be expected from a proposed experiment is evaluated. A few examples of meteor scatter returns obtained with a prototype experiment in Greenland are shown and discussed. GRA

N90-12807 Civil Aviation Authority, London (England). Air Traffic Control Evaluation Unit.
ASSESSMENT OF VOICE CODERS FOR ATC/PILOT VOICE COMMUNICATIONS VIA SATELLITE DIGITAL COMMUNICATION CHANNELS
N. L. Troll Mar. 1989 34 p Original contains color illustrations
(DEPE(CNA)-Proj. EU650)
(CAA-Paper-89004; Rept-550; ETN-89-95248) Copyright Avail: Civil Aviation Authority, Greville House, 37 Gratton Road, Cheltenham, England

An Air Traffic Control (ATC) simulation testbench constructed for the purpose of assessing the use of voice coding equipment (vocoders) for relaying voice communications between air traffic controllers and pilots via satellite digital communication channels is described. The development of the testbench and the analysis procedures is described. Several vocoders employing different coding algorithms which have been proposed for use over satellite data channels are assessed. Within the limitations imposed by the simulation, the assessment suggests that voice coded speech at 8 to 9.6 k bit/sec would be acceptable for some ATC tasks. The assessment results were also used to rank the vocoders for acceptability to support ATC voice communications under various bit error rates over the digital communication channel. ESA

N90-12808# European Space Agency, Paris (France).
ON A FAST TWO-DIMENSIONAL RADAR IMAGING PROCESS FOR ROTATING TARGETS, AND AN ANALYSIS OF ITS IMAGE QUALITY
Karl-Heinz Bethke (Deutsche Forschungs- und Versuchsanstalt fuer Luft- und Raumfahrt, Oberpfaffenhofen, West Germany) Jul. 1989 121 p Transl. into ENGLISH of Ein Schnelles Zweidimensionales Radarabbildungsverfahren fuer Rotierende, Objekte und Eine Analyse der Abbildungsqualitaet (Oberpfaffenhofen, Fed. Republic of Germany, DFVLR) 101 p Original language document was announced as N89-25376 Original contains color illustrations
(ESA-TT-1142; DFVLR-FB-88-51; ETN-89-95763) Avail: NTIS HC A06/MF A01; original German version available from DFVLR, VB-PL-DO, Postfach 90 60 58, 5000 Cologne, Fed. Republic of Germany

A fast method for generating two dimensional radar images is presented. The range resolution is obtained in real time by the hardware of a coherent short pulse radar. The cross range resolution is generated by offline data processing means using efficient fast imaging algorithms in accordance with the synthetic aperture principle. Image degradations resulting from approximations in the imaging algorithm and from the movement of the scattering centers through the resolution cells are discussed. A defined weighting function, together with the window functions, compensate this amplitude degradation. Target structures of wide crossrange dimension are discussed. The performance achieved by the imaging procedure is demonstrated. ESA

N90-12809# Royal Inst. of Tech., Stockholm (Sweden). Dept. of Plasma Physics and Fusion Research.
ON THE EXTREMUM ELECTRIC CHARGE PROBLEM OF STEADY ELECTROMAGNETIC EQUILIBRIA
B. Lehnert 14 May 1989 18 p
(TRITA-EPP-89-04; ISSN-0348-7539; ETN-89-95924) Avail: NTIS HC A03/MF A01

The variational problem of finding extremum values of the electric charge of steady electromagnetic equilibria is investigated. The analysis is effectuated in terms of axisymmetric configurations and a generating function F is applied. The variational procedure is simplified by incorporation of the field equations of the electric and magnetic potentials into the integrals of the charge, the magnetic moment, the mass, and the angular momentum of the system. In these conditions, the variational procedure reduces to find extremum values of the charge, by varying F under the constraints of a given asymptotic form of F at infinity, and of one quantum condition. It seems possible for a set of extremum values of the charge to arise from such a procedure. ESA

N90-12810# Royal Signals and Radar Establishment, Malvern (England).
PROPERTIES OF DENSITY TAPERED ARRAYS
G. J. Ball Mar. 1988 15 p
(RSRE-Memo-4210; BR108280; ETN-89-94330) Copyright Avail: Defence Research Information Centre, Kentigern House, 65 Brown Street, Glasgow, G2 8EX, Scotland

The properties of density tapered arrays designed with deterministic and statistical techniques are reviewed. The properties of statistically designed arrays are described as a function of main beam scan, average sidelobe level, model amplitude distribution, thinning, and array and aperture size. It is found that without additional signal processing large apertures are needed to produce low sidelobe levels. For example, the minimum circular aperture needed to produce a 40 dB peak sidelobe level has a diameter of 178 wavelengths. Statistical density tapering should be used to design arrays for applications with scanned main beams, since their peak sidelobe levels remain approximately constant as the main beam is scanned. The sidelobe levels of the deterministic array increase as the mainbeam is scanned. ESA

N90-12811# Ecole Nationale Superieure des Telecommunications, Paris (France). Dept. Signal.
SIMULATION OF CIRCUITS ADAPTED TO SIGNAL PROCESSING Ph.D. Thesis [SIMULATION DE CIRCUITS ADAPTES AU TRAITEMENT DU SIGNAL]
Jamal Guennouni Feb. 1989 274 p In FRENCH Sponsored by the Ministere de la Recherche et de la Technologie, Paris, France and CNRS
(Telecom-Paris-89-E001; ISSN-0751-1353; ETN-89-95267) Avail: NTIS HC A12/MF A02

Simulation tools developed to study integrated circuits to be used in a voice synthesizer/analyzer are described. These tools allow a signal processor to obtain the functional specifications of the circuit needed for a specified application. These tools are also able to validate circuit choices at an algorithmic level and permit temporal analysis of a circuit from the very beginning of the conception phase. The practical applications of these tools are outlined. ESA

N90-12812# Ecole Nationale Superieure des Telecommunications, Paris (France).
GROUND EFFECTS ON MULTIPATH FADING Ph.D. Thesis [INFLUENCE DU SOL SUR LA SELECTIVITE DUE AUX TRAJETS MULTIPLES]
Xing-Ya Pan Nov. 1988 180 p In FRENCH; ENGLISH summary
(Telecom-Paris-88-E017; ISSN-0751-1353; ETN-89-95268) Avail: NTIS HC A09/MF A01

Ground effects on multipath fading of digital microwave systems are investigated. A method of qualitatively evaluating the ground effects on the selectivity of signals for radio links is described. The method involves dividing the problem into several parts so as to be more easily treated using diffraction and diffusion theories. The interrelationship between atmospheric and ground effects is demonstrated. The use of the method in the planning of microwave links is described. ESA

N90-12813*# National Aeronautics and Space Administration. Lewis Research Center, Cleveland, OH.
SATELLITE RANGE DELAY SIMULATOR FOR A MATRIX-SWITCHED TIME DIVISION MULTIPLE-ACCESS NETWORK SIMULATOR
Lawrence A. Nagy 1989 14 p Proposed for presentation at the 13th International Communications Satellite Systems Conference, Los Angeles, CA, 11-15 Mar. 1990; sponsored by AIAA
(NASA-TM-102407; E-5159; NAS 1.15:102407) Avail: NTIS HC A03/MF A01 CSCL 17B

The Systems Integration, Test, and Evaluation (SITE) facility at NASA Lewis Research Center is presently configured as a satellite-switched time division multiple access (SS-TDMA) network simulator. The purpose of SITE is to demonstrate and evaluate

advanced communication satellite technologies, presently embodied by POC components developed under NASA contracts in addition to other hardware, such as ground terminals, designed and built in-house at NASA Lewis. Each ground terminal in a satellite communications system will experience a different aspect of the satellite's motion due mainly to daily tidal effects and station keeping, hence a different duration and rate of variation in the range delay. As a result of this and other effects such as local oscillator instability, each ground terminal must constantly adjust its transmit burst timing so that data bursts from separate ground terminals arrive at the satellite in their assigned time slots, preventing overlap and keeping the system in synchronism. On the receiving end, ground terminals must synchronize their local clocks using reference transmissions received through the satellite link. A feature of the SITE facility is its capability to simulate the varying propagation delays and associated Doppler frequency shifts that the ground terminals in the network have to cope with. Delay is achieved by means of two NASA Lewis designed and built range delay simulator (RDS) systems, each independently controlled locally with front panel switches or remotely by an experiment control and monitor (EC/M) computer. Author

N90-12814# Wisconsin Univ., Madison. Water Resources Center.

USE OF GROUND PENETRATING RADAR TO DEFINE RECHARGE AREAS IN THE CENTRAL SAND PLAIN

Geoffrey C. Bohling, Mary P. Anderson, and Charles R. Bentley 1989 72 p

(Grant DI-14-08-0001-G-1458)

(PB89-224885; WIS-WRC-89-01; USGS/G-1458-03) Avail: NTIS HC A04/MF A01 CSCL 17I

Contamination of groundwater by agricultural chemicals in the Central Sand Plain (Portage County in Wisconsin) has prompted studies of groundwater flow in the region. Because the groundwater system is particularly susceptible to contamination in areas where groundwater recharge occurs, identification of recharge zones can contribute significantly to the effective management of agricultural chemical use. An accurate map of water table elevation (groundwater head) is crucial to identifying the distribution of recharge. The reliability of ground penetrating radar as a total for obtaining high resolution maps of water table elevation was assessed. Sparse subsets of wells in the area were used to calibrate the radar. Water table depths obtained from these calibrations were compared to known water table depths in the remaining wells. Three wells are the minimum needed to obtain an estimate of uncertainty in calibration parameters; specifically the radar signal velocity in the subsurface materials and the return time correction factor. If several wells distributed throughout a region of interest yield consistent calibration results, radar can be used to produce a map of water table elevation for that region. GRA

N90-12815# Royal Signals and Radar Establishment, Malvern (England).

MODE S DATA LINK TRIALS, 10-11 JANUARY 1989

A. J. Hughes, R. J. Larkin, M. J. Rose, M. F. Worsley, and T. Alcock 21 Feb. 1989 23 p Sponsored by the Civil Aviation Authority, London, England

(RSRE-Memo-4267; BR109773; ETN-89-94727) Copyright Avail: NTIS HC A03/MF A01

The results and the analysis of the data link experiments are reported. Two flights, on 10 and 11 January 1989, of mode S surveillance, are performed. All message protocols are tested. Software errors are detected. No problems are found with transponder operation. No real time applications processes are run during the flights. Some discrepancies are observed between data downlinked by different means. The importance of ground based applications for the understanding of the aircraft date sources characteristics is emphasized. ESA

N90-12816# Royal Signals and Radar Establishment, Malvern (England).

FINE RESOLUTION ERRORS IN SECONDARY SURVEILLANCE RADAR ALTITUDE REPORTING AMONGST AIRCRAFT TRANSMITTING THE CONSPICUITY CODES 4321 AND 4322

P. Banks, B. A. Wyndham, and D. B. Jenkins Jun. 1988 13 p Sponsored by the Civil Aviation Authority, London, England

(RSRE-88004; BR108924; ETN-89-94834) Copyright Avail: NTIS HC A03/MF A01

The incidence of Secondary Surveillance Radar (SSR) mode C pressure altitude encoding faults are examined. It is caused by stuck/shorted C bits, investigated amongst aircraft transmitting the SSR mode A conspicuity codes 4321 and 4322. The 6808 aircraft trajectories are studied. The 152 trajectories displayed C bit faults on the SSR mode C replies. The proportion of SSR plots bearing conspicuity codes is found to vary with geographical location and time. The measured frequency for similar mode C faults and the presently measured frequencies of SSR plots mode C faults for conspicuity code aircraft are compared. The results show the overall frequency for stuck/shorted C bit faults ranging 0.49 percent for the airspace covered by the Civil Aviation Authority Heathrow tower radar to 0.70 percent for similar equipment. ESA

N90-12817# Royal Signals and Radar Establishment, Malvern (England).

SPECIFICATION OF VIPER1 IN Z

D. H. Kemp Sep. 1988 36 p

(RSRE-Memo-4195; BR108630; ETN-89-94837) Copyright Avail: NTIS HC A03/MF A01

The specification of the Viper1 microprocessor, in the Z (specification) language, is reported. No attempt to explain the primary constructs of Z is made. The following topics are presented: the basic, the bitwise, the logical, and the arithmetic functions; the word lengths, the memory, the registers, the clock, the stop and the Viper1 state. The Viper1 operations are described. It is shown that Z can give a high level specification and that it is a useful language. ESA

N90-12818# Royal Signals and Radar Establishment, Malvern (England).

STATISTICAL DENSITY AND AMPLITUDE TAPERED ARRAYS

G. J. Ball Mar. 1988 19 p

(RSRE-Memo-4211; BR108312; ETN-89-94838) Copyright Avail: NTIS HC A03/MF A01

The improvement of the radiation characteristics of thinned, density tapered arrays, is studied. The combination of statistical density and amplitude tapering is applied. The changes in both element density and amplitude weight are allowed. Statistical density tapering is extended: to each element one value of amplitude weight is allocated. It is shown that increasing the number of possible values, the sidelobe levels of an array are reduced. The properties of arrays designed using equi-space amplitude levels with binominally distributed selection probabilities are calculated and described as a function of the number of levels and aperture size. It is found that density and amplitude tapering cannot reduce the sidelobe levels without an accompanying increase in the number of elements, and that it cannot lower the sidelobes of a thinned, density tapered array to equal the lowest obtainable from the comparable fully filled, amplitude tapered array. It is also found that density and amplitude tapering can reduce the minimum aperture size and number of elements required to achieve a given sidelobe level. ESA

N90-12819# Royal Signals and Radar Establishment, Malvern (England).

SPECIFICATION OF VIPER2 IN Z

D. H. Kemp Oct. 1988 67 p

(RSRE-Memo-4217; BR108860; ETN-89-94839) Copyright Avail: NTIS HC A04/MF A01

The proposed Viper2 microprocessor, using the specification language Z, is described. No attempt to explain the primary constructs of Z, is made. The specification is type checked. No proof of correspondence between this specification and the one

in higher order logic is found. The following topics are presented: the basic, the bitwise, the logical, and the arithmetic functions; the word lengths, the memory, the registers, the clock, the stop and the Viper2 state. The Viper2 operations are described. It is shown that Z can give a high level specification and that it is a useful language. ESA

N90-12820# Royal Signals and Radar Establishment, Malvern (England).
AUTOMATIC COMMUNICATIONS CHANNEL INTERFERENCE MONITORING
N. G. Smith Apr. 1988 43 p
(RSRE-Memo-4243; BR108667; ETN-89-94843) Copyright Avail: NTIS HC A03/MF A01

A system that monitors a communications channel and logs details of interfering signals, is described. The system hardware configuration and a detailed description of the software are provided. The system consists of software for logging signals that occur in the channel and independent software for analysis of the logged data. The system's workability and adequacy is proven. Its development possibilities, including assessment of the present system and identifying restrictions, are discussed. ESA

N90-12821 Physics and Electronics Lab. TNO, The Hague (Netherlands).
DEDICATED TRACKING OF CROSSING TARGETS WITH A PHASED ARRAY MONOPULSE RADAR
R. vanSweeden and J. H. deVlieger Nov. 1988 63 p
(FEL-1988-95; TD88-5415; ETN-89-94990) Copyright Avail: TNO Physics and Electronics Lab., P.O. Box 96864, 2509 JG The Hague, Netherlands

The problem of tracking independent targets which cross at a short mutual distance is discussed. Procedures with application to multitarget tracking by a phased array monopulse radar are proposed. These procedures are developed in order to predict and detect the beginning and length of the interference period of target echoes. During the interference period only predictions of the target positions are used. A Monte Carlo approach is used to evaluate the interference handling software package procedures. The experiments performed, their results, and recommendations are given. ESA

N90-12822 Physics and Electronics Lab. TNO, The Hague (Netherlands).
A METHOD TO MODEL FUZE PERFORMANCE. PART 2: CALCULATION OF TARGET REFLECTIONS WITH PHYSICAL OPTICS
M. H. Vogel Jan. 1989 49 p
(FEL-1989-21-Pt-2; TD89-0952; ETN-89-94993) Copyright Avail: TNO Physics and Electronics Lab., P.O. Box 96864, 2509 JG The Hague, Netherlands

The derivation of (departing from the Maxwell equations) the electromagnetic fields, scattered by a perfectly conducting surface, is discussed. The expression of the scattered fields far from this surface in the total fields is given. The scattered fields are also expressed in terms of the incident magnetic field, which is assumed to be a known quantity. An integral over the scattering surface is performed. A simple expression for this integral is obtained by approximating the scattering surface by many small (planar) triangular surface patches. ESA

N90-12823 Physics and Electronics Lab. TNO, The Hague (Netherlands).
AIRCRAFT SAR SIMULATION SARGEN 1.0
M. P. G. Otten 8 Feb. 1989 66 p
(FEL-1989-44; TD89-0953; ETN-89-94994) Copyright Avail: TNO Physics and Electronics Lab., P.O. Box 96864, 2509 JG The Hague, Netherlands

An aircraft Synthetic Aperture Radar (SAR) simulation program which generates raw data (Sargen) is described. The purpose of the simulation is to investigate the effects of unwanted aircraft motions on SAR imaging. Deliberate maneuvering is not included. Both range and azimuth compressed data are considered. The range compression itself is assumed, not simulated. The azimuth compression, which is needed to form the image is not part of Sargen. The aircraft motion is specified by discrete time sequences of three position and three attitude variables. Validation runs are done, including image formation with existing azimuth compression algorithms. The observed effects corresponded to theoretical approximations. ESA

N90-12824 Physics and Electronics Lab. TNO, The Hague (Netherlands).
DESCRIPTION AND RESULTS OF A MULTIHOP NACS SIMULATION
A. J. Ruizenaar Oct. 1988 83 p
(Contract A86/KL/045)
(FEL-1988-46; TD88-5302; ETN-89-94995) Copyright Avail: TNO Physics and Electronics Lab., P.O. Box 96864, 2509 JG The Hague, Netherlands

The structure, the parameters which can be defined by the user, and the results obtained by a multihop packet radio network, the Nodeless Area Communication System (NACS) simulator, are described. The purposes of developing this simulator are: to obtain knowledge of the influence of the parameters on the performance and the behavior of a multihop packet radio system; to develop recommendations about multihop packet radio systems without developing expensive laboratory models; and to obtain and investigate the similarities and differences between singlehop and multihop packet radio systems. The results obtained from a lot of simulated configurations are discussed. The conclusions about multihop packet radio systems, formulated in accordance with the simulation results are given. ESA

N90-12825 Physics and Electronics Lab. TNO, The Hague (Netherlands).
A LITERATURE STUDY OF WAVE PROPAGATION IN THE 1-60 GHz RANGE. APPLICATION TO TRANSPORTABLE MILITARY COMMUNICATION SYSTEMS
W. Barendswaard Sep. 1988 86 p
(Contract A88/KL/608)
(FEL-1988-47; TD88-4850; ETN-89-94996) Copyright Avail: TNO Physics and Electronics Lab., P.O. Box 96864, 2509 JG The Hague, Netherlands

An overview of the existing literature about microwave and mm wave propagation (1 to 60 GHz) over rolling hilly terrain, is presented. The aim of the work is to study the usefulness of these waves for the short radio links in a transportable network. Physical aspects, important when low antenna heights are applied in rolling hilly terrain, are considered. Indicative (model) calculations of propagation loss are carried out. Frequencies within the 1 to 60 GHz range are considered, to evaluate the possibilities and limitations of the applications of different frequencies within this range. ESA

N90-12826 Physics and Electronics Lab. TNO, The Hague (Netherlands).
ANGLE ESTIMATION IN A MULTIPATH ENVIRONMENT WITH AN EIGHT ELEMENT LINEAR ARRAY OPERATING AT 10.5 GHz Final Report
A. Theil, A. G. Huizing, and M. P. G. Otten 18 Jan. 1989 103 p
(Contract A88/KM/627)
(FEL-1989-15; TD89-1200; ETN-89-95082) Copyright Avail: TNO Physics and Electronics Lab., P.O. Box 96864, 2509 JG The Hague, Netherlands

The applicability of enhanced angular resolution by means of high resolution angle estimation methods is studied. An environment in which multipath reflections occur is considered. These signal processing techniques can be applied in array radars and may improve the tracking of low flying targets above sea. The measurements are performed with a linear antenna array having eight horizontally polarized antenna elements. The antenna array operates at a frequency of 10.5 GHz. The measurements took place at an inland lake, and at a coastal site. The high resolution methods estimate the angles of incidence of the direct

and the reflected rays. Several angle estimation methods are judged on the angular accuracy and on the resolving capability. It is found that a maximum likelihood estimator is promising. ESA

N90-12827# Deutsche Forschungs- und Versuchsanstalt fuer Luft- und Raumfahrt, Oberpfaffenhofen (Germany, F.R.). Abteilung HF-Verfahren.
CONCEPTION AND RESULTS OF THE DLR REALTIME AZIMUTH PROCESSOR FOR THE E-SAR SYSTEM
Alberto Moreira Jun. 1989 71 p In GERMAN; ENGLISH summary Report will also be announced as translation (ESA-TT-1184)
(DLR-FB-89-30; ISSN-0171-1342; ETN-89-95839) Avail: NTIS HC A04/MF A01; DLR, VB-PL-DO, Postfach 40 60 58, 5000 Cologne, Fed. Republic of Germany, 26 Deutsche marks

A realtime azimuth processor developed for the airborne E-SAR (experimental synthetic aperture radar) system of DLR is described. The processor works with an unfocused compression method. This method simplifies data processing and is easily performed in realtime by the moving average approach. A SAR image processed by a traditional unfocused processing method has lower contrast, higher sidelobes and worse resolution than in the focused mode. An algorithm is developed, so that an amplitude weighting can be implemented into the unfocused processing method without additional complications. The image quality is significantly improved with exception of the resolution and is comparable to the conventional focused processing method. Several images processed in realtime with postprocessing techniques are presented. The results of the image analysis agree with the expected values and prove the validity of this approach. ESA

N90-12828 Department of the Navy, Washington, DC.
IMAGE PREPROCESSING BY MODIFIED MEDIAN FILTER Patent
Bruce O. May, inventor (to Navy) 5 Apr. 1989 6 p Filed 5 Apr. 1988 Supersedes Pat-Appl-737606-85
(AD-D014199; US-Patent-4,736,439; US-Patent-Appl-SN-737606) Avail: U.S. Patent and Trademark Office CSCL 17/11

Preprocessing of a noisy image, such as is obtained by a raster scan, by subtracting the median of the pixel values of one or more lines from the medians of predetermined pixel neighborhoods, is presented. GRA

N90-12829# Massachusetts Inst. of Tech., Cambridge. Lab. for Information and Decision Systems.
REQUIREMENTS SPECIFICATION WITH PETRI NETS USING THE CUBE TOOL METHODOLOGY
Didier M. Perdu Aug. 1989 79 p
(Contract N00014-85-K-0782)
(AD-A212190; LIDS-R-1901) Avail: NTIS HC A05/MF A01 CSCL 25/5

The distributed nature of command and control requires the consideration of both processes and communications in the formulation of requirements. Cube Tool is a methodology used to derive the processing and communication needs for each system function. An approach is introduced for extending the applicability of Cube Tool to the determination of requirements for C3I systems. First, using Cube Tool for each function, a Petri Net is derived that models all processes and communications for the correct execution of the function. Then, for a given scenario, these nets are interconnected and the steps of the methodology are applied again to derive the Petri Net that represents the mission-dependent requirements for the system. For different modes of operation are considered, different Petri Net are obtained which can then be folded together to obtain a Colored Petri Net representation of the processes and communications needs. GRA

N90-12830# Pennsylvania State Univ., University Park.
RADAR POLARIMETRIC STUDIES BASED ON THE MAYPOLE 1983 AND 1984 FIELD EXPERIMENTS Final Report
Kultegin Aydin and Thomas A. Seliga 10 Aug. 1989 21 p
(Contract DAAL03-87-K-0031)
(AD-A212226; ARO-24706.4-GS) Avail: NTIS HC A03/MF A01 CSCL 17/9

This research was conducted for the purpose of evaluating and improving the interpretation of multiparameter radar measurements (dual-linear polarization and dual wavelength) in rainfall and hail. The specific aspects of this research involved case studies from MAYPOLE comparing estimates of rainfall rate obtained from radar and ground based raingauge measurements and the development of analysis techniques for this purpose. Understanding and interpreting multiparameter radar measurements in hail was another problem which required analyzing radar data within the hail regions of a storm identified using the differential reflectively hail signal. GRA

N90-12831# Rome Air Development Center, Griffiss AFB, NY.
APPLICATION OF A GENERALIZED LEIBNIZ RULE FOR CALCULATING ELECTROMAGNETIC FIELDS WITHIN CONTINUOUS SOURCE REGIONS In-House Report, Sep. 1987 - Jan. 1988
Marian Silberstein Jan. 1989 40 p
(AD-A212470; RADC-TR-88-333) Avail: NTIS HC A03/MF A01 CSCL 20/3

In deriving the electric and magnetic fields in a continuous source region by differentiating the vector potential, the central obstacle is the dependence of the integration limits on the differentiation variable. Here, an alternative derivation is presented which evaluates the curl of the vector potential volume integral directly, retaining the dependence of the limits of the differentiation variable. It involves deriving a 3-D version of the Leibniz rule for differentiating an integral with variable limits of integration, and using the generalized rule to find the Maxwellian and cavity fields in the source region. A correction term is introduced for each variable integration limit. The extension to a 3-D volume integral presented here holds for any function of r and r, and shows that, analogously, one correction term is required per functional limit of the triple integral in each of the derivatives in the curl expression. This generalized 3-D Leibniz rule is then tailored to solve the specific problem of determining electromagnetic fields in the source region by direct differentiation of the vector potential. GRA

N90-12832# Gallaudet Coll., Washington, DC.
THE EFFECTS OF HEARING PROTECTORS ON SPEECH COMMUNICATION AND THE PERCEPTION OF WARNING SIGNALS Final Report
Alice H. Suter Jun. 1989 36 p
(DA Proj. 1L1-61102-B-74-A)
(AD-A212521; HEL-TM-2-89) Avail: NTIS HC A03/MF A01 CSCL 23/2

Because hearing protectors attenuate the noise and signal by equal amounts within a given frequency range, reducing both to a level where there is less likelihood of distortion, they often provide improved listening conditions. The crossover level from disadvantage to advantage usually occurs between 80 and 90 dB. However, hearing protectors may adversely affect speech recognition under a variety of conditions. For hearing-impaired listeners, whose average hearing levels at 2000, 3000, and 4000 Hz exceed 30 dB, certain speech sounds will fall below the level of audibility. Visual cues may decrease the disadvantage imposed by hearing protectors. However, the Occlusion Effect, which decreases vocal output when the talker wears protection, adversely affects the listener's speech recognition. The poorest performance occurs when both talkers and listeners wear protectors. Hearing protectors affect warning signal perception in a similar manner. Again the crossover level seems to be between 80 and 90 dB, and there is greater degradation for individuals with impaired hearing. Earmuffs appear to pose greater problems than plugs, and this is especially true of difficulties in signal localization. Earplugs produce mainly front-back localization errors, while earmuffs produce left-right localization errors as well. Earmuffs also drastically impede localization in the vertical plane. GRA

N90-12833# Naval Ocean Systems Center, San Diego, CA.
DIRECTION-OF-ARRIVAL CALCULATIONS AT VLF/LF (VERY LOW FREQUENCY/LOW FREQUENCY) Final Report, Jan. 1989 - Aug. 1989
R. A. Pappert and L. R. Hitney Aug. 1989 115 p
(AD-A212620; NOSC/TD-1602) Avail: NTIS HC A06/MF A01 CSCL 17/11

A modification of an earlier program has been used to calculate direction-of-arrival (DOA) errors due to geomagnetic field effects at San Diego for the following VLF/LF transmitters; Annapolis (21.4 kHz), Lualualei (23.4 kHz), Cutler (24 kHz), Jim Creek (24.8 kHz), and Silver Creek (48.5 kHz). The calculations have been compared with corresponding measurements of Stang and Davis. The program can be used for both laterally homogeneous and inhomogeneous guides and allows for airborne as well as ground transmissions. Essential features of the program are reviewed and a program listing is given. GRA

N90-12834# Naval Weapons Center, China Lake, CA.
ANALYSIS OF THREE- AND FOUR-SIDED UNIFORM WAVEGUIDES WITH UNUSUAL CROSS-SECTION/BOUNDARY CONDITIONS Interim Report, Jan. 1985 - Jan. 1989
P. L. Overfelt Jan. 1989 54 p
(AD-A212653; AD-E900917; NWC-TP-6989) Avail: NTIS HC A04/MF A01 CSCL 09/1

Closed-form expressions are given for the transverse electric and transverse magnetic modes of eight uniform waveguides with unusual cross-sectional geometry/boundary conditions. GRA

N90-12835# Ohio State Univ., Columbus. Electroscience Lab.
PROGRESS IN THE IDENTIFICATION OF AIRBORNE RADAR TARGETS
R. Carrier, F. D. Garber, I. Jouny, R. L. Moses, O. S. Sands, W. M. Steedly, and E. K. Walton Jun. 1989 103 p
(Contract N00014-86-K-0202)
(AD-A212749; ESL-718048-12) Avail: NTIS HC A06/MF A01 CSCL 17/11

During the first six months of this project, accomplishments reported include: (1) the development of techniques to estimate and parameterize canonical scattering centers of a radar object; (2) the development and evaluation of a signal processing technique that estimates the polarization characteristics of target scattering centers; (3) the evaluation of the feasibility of using bispectrum processing techniques for the purpose of radar target characterization and classification; and (4) the developement of improved techniques for target identification based on structural pattern recognition. GRA

N90-12836# Pacifica-Sierra Research Corp., Los Angeles, CA.
LONG WAVE ATMOSPHERIC NOISE MODEL, PHASE 1. VOLUME 1: LIGHTNING OCCURRENCE RATES AND PROPAGATION THEORY Technical Report, 18 Sep. 1987 - 14 Oct. 1988
Chris R. Warber, Lynda R. Kies, and Edward C. Field, Jr. 14 Oct. 1988 112 p
(Contract DNA001-87-C-0171)
(AD-A212794; PSR-1877-Vol-1; DNA-TR-88-239-V1) Avail: NTIS HC A06/MF A01 CSCL 20/14

Progress on a model that predicts how long wave atmospheric noise is affected by distortions in the earth ionosphere waveguide caused by high altitude nuclear bursts is described. When complete, the model will also represent worldwide noise under ambient conditions. The model comprises two submodels: source, which describes the occurrence rate of lightning flashes throughout the world; and propagation, which describes the propagation of energy radiated from centers of lightning activity. The new model is an improvement over existing ones. First, it uses recent data on the actual occurrence rate of lightning flashes as a function of time of day, latitude, and season. Second, it includes extremely low frequency and low frequency noise. Third, it uses new data on the altitude and orientation of individual strokes to model transverse electric noise. Finally, the model incorporates new propagation algorithms that are nearly as accurate as full wave algorithms, but they reduce computer running time by as much as fivefold. It would be costly to recalculate mode parameters for the earth ionosphere waveguide each time the model is exercised. Instead, attenuation rate, excitation factor, phase velocity, and eigencosine are precalculated and stored for a wide range of modes, frequency, ground conductivity, and spread debris nuclear environments. GRA

N90-12837# Pacifica-Sierra Research Corp., Los Angeles, CA.
LONG WAVE ATMOSPHERIC NOISE MODEL, PHASE 1. VOLUME 2: MODE PARAMETERS Technical Report, 18 Sep. 1987 - 14 Oct. 1988
Chris R. Warber 10 Apr. 1989 184 p
(Contract DNA001-87-C-0171)
(AD-A212795; DNA-TR-88-239-V2) Avail: NTIS HC A09/MF A01 CSCL 20/14

The full wave propagation code is used to calculate waveguide mode parameters in spread debris environments in order to develop a long wave atmospheric noise model. The parameters are stored for retrieval whenever the model is exercised. Because the noise-model data encompass parameters of all significant modes for a wide range of ground conductivities, frequencies, and nuclear environment intensities, graphs of those parameters are presented in this volume handbook format. GRA

N90-12838# Kansas Univ. Center for Research, Inc., Lawrence. Radar Systems and Remote Sensing Lab.
INVESTIGATION OF THE PROPERTIES OF RADAR BACKSCATTER FROM SEA ICE Final Report
R. K. Moore Sep. 1989 6 p
(Contract N00014-85-K-0200)
(AD-A212808; RSL-TR-331-9) Avail: NTIS HC A02/MF A01 CSCL 17/9

Measurements of the radar backscatter from sea ice have been made during the years 1985 through 1988 using specialized radar scatterometers developed for the purpose. Most of the experiments during this period have involved artificial sea ice grown at CRREL, but measurements also were made during LIMEX in the Labrador Sea during March, 1989. Much of the work involved use of a very fine resolution scatterometer to determine the sources of scattering from the ice and its overlying snow cover. Considerable insight into the mechanisms of scattering of radar signals from sea ice has resulted. Recently we have developed a polarimetric scatterometer capable of measuring the full scattering matrix, and this was used in two seasons of work. GRA

N90-12839# Naval Ocean Systems Center, San Diego, CA.
ATMOSPHERIC HORIZONTAL-INHOMOGENEITY EFFECTS ON THE OPTICAL DEPTHS DETERMINED BY THE DOUBLE-ELEVATION-ANGLE LIDAR TECHNIQUE Final Report, Apr. - Jun. 1989
Merle R. Paulson Aug. 1989 33 p
(AD-A212836; NOSC-TD-1600) Avail: NTIS HC A03/MF A01 CSCL 17/5

The proposals of dual, or multiple, elevation angle lidar measurements to determine integrated extinction, or optical depth, in the vertical are considered. Atmospheric conditions have to be horizontally homogeneous for this to be a usable technique. Additionally, the ratio of backscatter coefficient to extinction coefficient must be constant over the height range of interest. The results indicate that this is not a usable technique, since the atmosphere is not sufficiently horizontally homogeneous. GRA

N90-12840# National Academy of Sciences - National Research Council, Washington, DC. Panel on Removal of Noise from a Speech/Noise Signal.
REMOVAL OF NOISE FROM NOISE-DEGRADED SPEECH SIGNALS Technical Report, 1 Oct. 1988 - 30 Sep. 1989
1 Jun. 1989 42 p Workshop on Noise Removal held in Washington, DC, 26-27 Feb. 1987
(Contract MDA904-87-H-2009)
(AD-A212876) Avail: NTIS HC A03/MF A01 CSCL 25/4

Techniques for the removal of noise from noise-degraded

speech signals were reviewed and evaluation with special emphasis on live radio and telephone communications and the extraction of information from similar noisy recordings. The related area on the development of speech-enhancement devices for hearing-impaired people was reviewed. Evaluation techniques were reviewed to determine their suitability, particularly for the assessment of changes in the performance of workers who might use noise-reduction equipments on a daily basis in the applications cited above. The main conclusion was that noise-reduction methods may be useful in improving the performance of human operators who extract information from noisy speech material despite a lack of improvement found in using conventional closed-response intelligibility tests to assess those methods. GRA

N90-12841# Ohio State Univ., Columbus. ElectroScience Lab.
PERFORMANCE ANALYSIS OF LARGE ADAPTIVE SIDELOBE CANCELLER ARRAYS WITH REUSED ELEMENTS Final Report
J. Ward and R. T. Compton, Jr. Jun. 1989 228 p
(Contract N00014-87-K-2011)
(AD-A212888; Rept-719111-1) Avail: NTIS HC A11/MF A02 CSCL 17/4

This report considers adaptive sidelobe canceller arrays (SLCs) in which the mainbeam and auxiliary signals are obtained from the same set of elements. The SLC with element reuse is different from the conventional SLC in that thermal noise components of the mainbeam and auxiliary signals are correlated. This correlation causes sidelobe degradation when the number of degrees of freedom exceeds the number necessary to cancel a given jammer scenario. The equations for a general planar array with an arbitrary signal scenario are first formulated. These equations are then used to examine array performance with different auxiliary configurations. Both auxiliaries form from a single array element and auxiliaries form from subarrays of elements are studied. Various auxiliary configurations are investigated to determine how the auxiliaries should be chosen to provide good cancellation of multiple jammers while retaining low sidelobes in the mainbeam. It is shown that using single-element auxiliaries may result in serious SLL degradation whenever there are extra degrees of freedom. This degradation can be overcome by using subarray auxiliaries that satisfy an orthogonality condition on their patterns. Excellent cancellation and sidelobe level performance can be attained with small subarrays chosen to satisfy this orthogonality condition. GRA

N90-12842# Naval Postgraduate School, Monterey, CA.
WIRE GRID MODELING OF THE LINEAR TAPERED SLOT ANTENNA M.S. Thesis
Daniel K. Miller Jun. 1989 90 p
(AD-A212977) Avail: NTIS HC A05/MF A01 CSCL 09/1

The linearly Tapered Slot Antenna (LTSA) was the subject of considerable study and experimentation. Accurate theoretical models base on the Method of moments (MOM) were developed to study the radiation characteristics of this antenna. however, these models are limited due to the great amount of Central Processing Unit (CPU) time required to obtain the solution. Employing the Numerical Electromagnetics Code (NEC) an accurate wire-grid model of the LTSA is developed here in order to reduce the CPU time needed to obtain the solution. Numerical results are presented for the radiation pattern and compared with experimental results of the actual planar structure to validate the model and optimize the wire-grid. Once the model was optimized, effects of variable design parameters on radiation pattern are studied. Conclusions are made regarding optimum designs for the LTSA. GRA

N90-12843# Naval Ocean Systems Center, San Diego, CA.
SPECIFICATION FOR RADAR FREE-SPACE DETECTION RANGE AND FREE-SPACE INTERCEPT RANGE CALCULATIONS Final Report, Jan. - Jun. 1989
C. P. Hattan Jul. 1989 27 p
(AD-A213158; NOSC/TD-1598) Avail: NTIS HC A03/MF A01 CSCL 17/9

General purpose utility programs were developed to calculate the free-space ranges of a pulse radar and an Electronic Support Measure (ESM) receiver. These utility programs are written in ANSI FORTRAN. The radar utility program allows the user to calculate radar free-space ranges for arbitrary radar cross sections, for any probability of detection between 0.1 and 0.9, and for any probability of false alarm between 10(exp 12) and 10(exp -4). A similar program to calculate the free-space intercept range for ESM receivers allows the user to input receiver sensitivity, transmitted power, and transmitter antenna gain to obtain a free-space intercept range value. These programs are subroutines of simple driver programs the user can modify. The programs, as provided, will prompt the user to provide specific input values, and will print a list of the input values as well as the calculated free-space range value at the conclusion of the calculation of that range value. The equivalent one-way free-space path loss for isotropic antennas at the free-space range is also provided. This path loss value can be used with transmission-loss codes or diagrams to assess actual electromagnetic system performance in a real world environment. GRA

33 ELECTRONICS AND ELECTRICAL ENGINEERING

Includes test equipment and maintainability; components, e.g., tunnel diodes and transistors; microminiaturization; and integrated circuitry.

For related information see also *60 Computer Operations and Hardware* and *76 Solid-State Physics*.

N90-12844# Stanford Linear Accelerator Center, CA.
A 2-MeV MICROWAVE THERMIONIC GUN
E. Tanabe, M. Borland, M. C. Green, R. H. Miller, L. V. Nelson, J. N. Weaver, and H. Wiedemann (Stanford Univ., CA.) Aug. 1989 4 p Presented at the 14th Meeting on Linear Accelerators, Nara, Japan, 7-9 Sep. 1989
(Contract DE-AC03-76SF-00515)
(DE89-015640; SU-SLAC-PUB-5054; CONF-8909183-1) Avail: NTIS HC A01/MF A01

A high gradient, S-band microwave gun with a thermionic cathode is being developed in a collaborative effort by AET, Varian, and SSRL. A prototype design using an upgraded Varian dispenser cathode mounted with thermal isolation directly in the first half-cell of a 1-1/2 cell, side coupled, standing-wave cavity was fabricated and is being tested. Optimization of the cavity shape and beam formation was done using SUPERFISH, MASK, and PARMELA. An overview of design details, as well as the status of in-progress beam tests, is presented. DOE

N90-12845# National Inst. of Standards and Technology, Gaithersburg, MD. Center for Basic Standards.
NIST (NATIONAL INSTITUTE OF STANDARDS AND TECHNOLOGY) MEASUREMENT SERVICES: THE ac-dc DIFFERENCE CALIBRATIONS Final Report
Joseph R. Kinard, John R. Hastings, Thomas E. Lipe, and Clifton B. Childers May 1989 311 p
(PB89-222616; NIST/SP-250/27; LC-89-600736) Avail: NTIS HC A14/MF A02; SOD HC $2.50 as 003-003-02950-5 CSCL 09C

The publication collects and summarizes the specialized information needed to operate the ac-dc difference laboratory and calibration service at the National Institude of Standards and Technology (NIST) in Gaithersburg. It also serves as a convenient reference source for the users of this calibration service and other interested people by documenting the service and its underlying background in considerable detail. It contains the following: (1) an annotated table of contents; (2) a topical index with a glossary of common ac-dc acronyms; (3) an overview of the service; (4) selected published papers; (5) instructions for the operation of the comparator systems; (6) a schedule for the recalibration and periodic checks of the NIST thermal converters; and (7) a sample report of calibration. GRA

N90-12846# Tel-Aviv Univ. (Israel). Authority for Research and Industrial Development Ltd.
ADVANCED CALCIUM-THIONYL CHLORIDE HIGH-POWER BATTERY Periodic Report No. 1, 15 May - 15 Jul. 1989
Emanuel Peled 15 Jul. 1989 16 p
(Contract DAJA45-89-C-0013)
(AD-A211856; R/D-5899A-CH-01) Avail: NTIS HC A03/MF A01 CSCL 10/3

Recently, a breakthrough was made in the development of two advanced Ca-TC systems which have much better electric storage properties than the state-of-the-art Ca-SOC cell. This was done by replacing the CaX2 (X=AlCl4) electrolyte by SrX2 (type A), or BaX2 (type B). The project's goals are to gain a better understanding of the electrochemistry of the advanced systems and to establish their safety and performance. In this phase, the cell performance was improved significantly. An improved C-size A7 type cell delivers 4.4 Ah at 0.9 A rate and room temperature which is 50 percent more than similar size commercial lithium cells have. The SAFT LSH14 lithium-thionyl chloride and the Duracell L028SH lithium-SO2 cells have at this rate only 2.9 and 2.7 Ah respectively. During one year of storage at room temperature the heat generation rate of 150 sq cm C-size A7 type cells decreased to a level of 60 to 70 microwatts. A cell lost 0.3 Ah after this storage period. The effect of several parameters on the corrosion rate of calcium in TC solutions was studied. Preliminary results indicate: SO2 decreases corrosion, there is no stress corrosion due to twisting of Ca foils, the native oxide layer helps in preventing corrosion, Ca foils as received contain only about 90 percent metallic calcium. The role native calcium oxide layer plays depends on the type of electrolyte used. GRA

N90-12847# Massachusetts Inst. of Tech., Cambridge. Microsystems Research Center.
A 2d-1 LOWER BOUND 2-LAYER KNOCK-KNEE CHANNEL ROUTING
Tom Leighton May 1989 15 p
(Contracts DAAL03-86-K-0171; N00014-87-K-0825; N00014-80-C-0622; AF-AFOSR-0078-86)
(AD-A211948; VLSI-MEMO-89-544) Avail: NTIS HC A03/MF A01 CSCL 09/1

In this paper, we describe a 2-point net channel routing problem with density d that requires channel width 2d - 1 in the 2-layer knock-knee channel routing model. This means that the (2d - 1)-track algorithms of Rivest, Baratz and Miller, Bolognesi and Brown, Frank, Mehlhorn, Preparata and Sarrafzadeh and Berger, Brady, Brown and Leigton are, in some cases, optimal. Thus any improvement of these algorithms must rely on problem features other than density (such as flux), or must make fundamental changes in the wiring model (such as increasing the number of layers or allowing wires to overlap.) GRA

N90-12848# Air Force Armament Lab., Eglin AFB, FL.
DESIGN AND COMMISSIONING TEST RESULTS FOR THE HYPERVELOCITY LAUNCHER RESEARCH COMPLEX BATTERY POWER SUPPLY Final Report, Sep. 1987 - Sep. 1988
James B. Cornette, John D. Sterrett, Jack R. Lippert, and Robert W. Williams (Computer Science and Applications, Inc., Fort Walton Beach, FL.) Aug. 1989 12 p
(AD-A211320; AFATL-TP-89-14) Avail: NTIS HC A02/MF A01 CSCL 10/2

The preliminary design of the battery power supply (BPS) was reported to the 6th IEEE Pulsed Power conference. In 1987, the final design was completed, assembled, and sequentially verified during approximately 1750 operational verification tests. These experiments consisted of single string verifications at 1000 amperes to a system discharge of 2,150,000 amperes. Final system design is very similar to the preliminary design previously presented. System fabrication is complete and at the present time consists of 858, 16 battery series strings resulting in 13,728 operational batteries. The final switching design has evolved into several levels of redundancy at varying current levels. These include 36 pneumatic, 100,000 ampere switches that control 24, 16 battery strings in parallel. These switches are used for the primary make and break of system current to charge the inductor. There are also 18 pneumatic crowbar switches at the 24 string level that are used to short the inductor from the BPS prior to system opening. At the string level there are 2000 ampere dc contactors that are used as a secondary current break and to pre-set the BPS in the appropriate parallel/series configuration prior to a discharge sequence. Explosively driven opening and closing switches are also employed at the interface junction to any Hypervelocity launcher test article. GRA

N90-12849# Purdue Univ., West Lafayette, IN. Lab. for Electroceramics.
METALLO-ORGANIC DECOMPOSITION PROCESS FOR DIELECTRIC FILMS Annual Report, 1 Apr. 1988 - 31 Mar. 1989
R. W. Vest and G. M. Vest 15 Jun. 1989 66 p
(Contract N00014-83-K-0321)
(AD-A211590) Avail: NTIS HC A04/MF A01 CSCL 09/1

The metallo-organic decomposition (MOC) process is a technique for producing inorganic films without processing in vacuum or going through a gel or powder step. The processing starts with metallo-organic compounds of the desired elements dissolved in an appropriate solvent. These solutions of individual metallo-organic compounds are then mixed in the appropriate ratio to give the desired cation stoichiometry for the final film to produce a formulation, which is itself a true solution, This formulation is deposited on a substrate by any of a variety of techniques to produce a wet film, which is then heated to first remove any solvent that did not evaporate during the deposition step and then to decompose the metallo-organic compounds to produce an inorganic film. A significant volume change occurs in going from the wet film to the inorganic film; if the inorganic film produced by a single pass through the process is not as thick as desired, the deposition and pyrolysis steps can be repeated as many times as necessary to produce a multilayer film of the required thickness. After the desired film thickness is achieved, the films are often subjected to a further heat treatment to control features such as oxygen stoichiometry, grain size or preferred orientation. GRA

N90-12850# Mission Research Corp., Albuquerque, NM.
AIRBORNE/SPACEBORNE PULSED POWER SOURCE Final Report, 15 Aug. 1988 - 14 Apr. 1989
George Z. Hutcheson Aug. 1989 85 p
(Contract F33615-88-C-2855)
(AD-A211762; WRDC-TR-89-2120) Avail: NTIS HC A05/MF A01 CSCL 09/1

Mission Research Corporation (MRC) has completed a design study for a compact lightweight pulsed power source for airborne and spaceborne applications. Two designs were developed during the contract. Both design were constrained to -500 kV output pluses, 10 Hz repetition rates, and 2 ft. diameters. The designs utilized high voltage pulse-forming networks and (PFN) composed of liquid capacitors and air-core inductors. Dual resonance spiral strip transformers were incorporated into the designs for charging the PFNs from lower voltage capacitor banks. A mixture of water and ethylene glycol was used in the capacitor designs in order that the operating temperatures (-45 C to +110 C) of the designs could be extended beyond that of pure water. A pulser built from the final design would be capable of nominally producing -500 kV, 100 ns, 10 ohms pulses (i.e., 3 kJ). Such a pulser would be 10.9 ft. long (without prime power, power conditioning, and load) and would weigh 1300 lbs (with power conditioning but without prime power and load). The design has the unique advantage of being mechanically tunable to any desired pulse length (100 ns to 500 ns) or impedance (10 ohms to 50 ohms) as long as the output energy of the pulser is not changed from 3 kJ. GRA

N90-12851# Messerschmitt-Boelkow-Blohm G.m.b.H., Ottobrunn (Germany, F.R.). Dienstleistungsbereich.
MICROSYSTEMS TECHNIQUES: CONCEPT, SIGNIFICANCE, STATUS OF DEVELOPMENT [MIKROSYSTEMTECHNIK. BEGRIFFSBILDUNG BEDEUTUNG ENTWICKLUNGSSTAND]

Burkhart Kuehl and Hans Jochen Icoellner 1988 16 p In GERMAN Previously announced in IAA as A89-42929
(MBB-UA-1110/88-PUB; ETN-89-94616) Avail: NTIS HC A03/MF A01

The microsystems technique for electronic systems is introduced. The purpose of microsystems technique is the realization of sensors with data processing intelligence and, as far as energetically possible, actuators as electronic and mechanical microstructures in silicon solid state technology. Microsystem techniques comprise essentially the conception, design, and manufacture of miniaturized intelligent sensor systems. The microminiaturization of sensor systems in silicon becomes increasingly important in defense systems, aeronautics and astronautics, robotics, process engineering and automotive engineering. Pressure sensors, acceleration measuring systems, chemical probes, gas flow sensors, gas chromatographs, and microoptical signal processors are to be developed. ESA

N90-12852 Politecnico di Milano (Italy). Dipartimento di Elettronica.
FEEDBACK CHARGE AMPLIFIER INTEGRATED ON THE DETECTOR WAFER
P. Rehak, S. Rescia, V. Radeka, E. Gatti, A. Longoni, M. Sampietro, G. Bertuccio, P. Holl, and L. Strueder 1989 37 p
(Rept-89-037; ETN-89-95725) Avail: Politecnico di Milano, Piazza Leonardo da Vinci 32, 20133 Milan, Italy

The performance of a charge sensitive preamplifier is discussed. The preamplifier is realized on high resistivity detector grade silicon. The amplifier operates on a fully depleted bulk of a silicon wafer. The possibility of direct integration of the preamplifier close to the detector anode is demonstrated. It is shown that the production steps are compatible with production steps for radiation detectors. The implementation of the preamplifier is based on a type of single sided field effect transistor. ESA

N90-12853# Universiteit Twente, Enschede (Netherlands). Dept. of Mechanical Engineering.
MATHEMATICAL MODELS FOR THE LINEAR INDUCTION MOTOR
D. J. DeGroot Sep. 1988 81 p
(RR-WB-88-17; ETN-89-95744) Avail: NTIS HC A05/MF A01

Several mathematical models concerning the design of linear induction motors with low to zero speed applications, clamping devices, shortstroke servo actuators, conveyorbelt drives and capsule transport systems are discussed. The effect of typical motor dimensions on force and power limits is investigated. The study also includes: the calculation and measurement of the magnetic field ground wave and its harmonics in the airgap; the motor's dimensional analysis; the flux and force expressions, analyzed with two-dimensional Maxwell field equations and with the equivalent circuit method. ESA

N90-12854# Nationaal Inst. voor Kernfysica en Hoge Energiefysica, Amsterdam (Netherlands).
BUNCH LENGTH IN INTERNAL TARGET MODE
R. Maas May 1989 13 p
(NIKHEF-AmPS/89/04; ETN-89-95402) Avail: NTIS HC A03/MF A01

Bunching of stored electron beams in internal target mode is described. The electrons are bunched, or captured, and a voltage replenishes the synchrotron radiation losses. Due to this bunching the microscopic duty factor of the stored beam is in general much smaller than one hundred percent. Tables of bunch parameters as a function of frequency are provided. ESA

N90-12855# Grenoble-1 Univ. (France). Lab. des Techniques de l'Informatique, des Mathematiques, de la Microelectronique et de la Microscop
BUILT-IN GENERATION FOR CMOS CIRCUITS
F. Darlay, D. Baschiera, and B. Courtois Jun. 1988 28 p
(IMAG-RR-736-I; ETN-89-95491) Avail: NTIS HC A03/MF A01

In Complementary Metal Oxide Semiconductor (CMOS) devices stuck-open faults convert a combinational network into a sequential one. Test vector sequences are needed. A built-in test generator for CMOS circuits is described. The generator proves useful in detecting all single stuck-open faults in Internal Fan Out Free (IFOF) and Non Reconvergent Fan Out (NRFO) networks. The generator also detects multiple stuck-open faults in IFOF and NRFO networks. For Reconvergent Fan Out (RFO) networks a Design For Testability (DFT) solution is proposed, using additional test points. ESA

N90-12856# Quaid-i-Azam Univ., Islamabad (Pakistan). Dept. of Physics.
RESISTIVITY MEASUREMENTS OF SUPERCONDUCTING MATERIALS M.S. Thesis
Ghulam Akhtar 1988 139 p
(PB89-225700) Avail: NTIS HC A07/MF A01 CSCL 09C

A four-probe set up was constructed to study the electrical resistivity of high temperature superconductors. Resistivity measurements as a function of temperature (77-300K) were studied for the systems R-Ba-Cu-O (R=Ho,Dy). The superconducting transition was observed for DyBa2Cu3O7 and HoBa2Cu3O7 around 90K. GRA

N90-12857# Royal Aerospace Establishment, Farnborough (England).
THE DESIGN, CONSTRUCTION, PERFORMANCE AND CALIBRATION OF PULSE GENERATORS TO FULFILL THE REQUIREMENTS OF SPECIFICATIONS DEFENCE STANDARD 59-41, FS(F) 510 AND FS(S) 457
R. A. Hobbs 22 Aug. 1988 67 p
(RAE-TM-FS(F)-550; BR108479; ETN-89-94828) Copyright Avail: NTIS HC A04/MF A01

The construction, performance, and calibration of pulse generators are reported. The pulse generators are designed to fulfill the electromagnetic transient test requirements of the Defense Standard 59-41, FS(F)510 and FS(F)457. Three pulse generators are described. One produces damped sinusoidal waveforms in the frequency range 2 to 30 MHz, the second one is a fixed frequency 100 kHz generator, and the third one produces two waveforms for ground voltage lightning effects simulation. The generators are designed to enable electronic systems to be assessed for immunity to the effects of the electromagnetic compatibility, the nuclear electromagnetic pulse and the lightning effects of the electromagnetic pulse. ESA

N90-12858# Royal Signals and Radar Establishment, Malvern (England).
A WELL CONDITIONED FORMULATION FOR THE ANALYSIS OF MULTI-LAYERED FREQUENCY SELECTIVE SURFACES USING A CASCADED MATRIX APPROACH
A. J. Mackay and J. G. Gallagher May 1989 28 p
(RSRE-Memo-4289; BR111531; ETN-89-94893) Copyright Avail: NTIS HC A03/MF A01

A general method to analyze multilayered frequency selective surfaces is given. A coupling of evanescent and decaying modes in a conditoned manner are included. The method is capable of analyzing arbitrary lossy dielectric and magnetic materials used as supports with partially conducting surfaces. It is valid for incident plane waves with arbitrary polarization and angles of incidence. The solution, obtained by modal matching of the fields in the apertures of each surface, is shown. The manner in which the cascaded matrices are put together avoids numerical problems. Theoretical predictions are made and tested with satisfactory results. ESA

N90-12859# Department of the Army, Washington, DC.
NULL OFFSET VOLTAGE COMPENSATOR FOR OPERATIONAL AMPLIFIER Patent Application
Lawrence R. Groehl, inventor (to Army) 14 Aug. 1989 13 p
(AD-D014189; US-Patent-Appl-SN-393610) Avail: NTIS CSCL 09/1

This invention relates generally to operational amplifiers and more particularly, to such amplifiers which are utilized in circuitry where low level signals are common, for example, digital circuitry.

The null offset voltage of an operational amplifier is compensated with diodes connected at the output terminal thereof. These diodes are either forward biased and/or backbiased to block current flow from the operational amplifier until the output voltage thereof exceeds the offset voltage level. GRA

N90-12860 Department of the Navy, Washington, DC.
THIN-FILM INTEGRATED INJECTION LOGIC Patent
Graham A. Garcia, inventor (to Navy) and Ronald E. Reedy, inventor (to Navy) 27 Jun. 1989 13 p Filed 18 Apr. 1988
(AD-D014190; US-Patent-4,843,448; US-Patent-Appl-SN-183965) Avail: U.S. Patent and Trademark Office CSCL 09/1

An integrated injection logic device formed on an insulating substrate is disclosed. A lateral, load transistor and an adjacent, vertical switching transistor are formed in the semiconductor layer such that the collector region of the lateral transistor coincides with the base region of the switching transistor. The emitter of the switching transistor is located at the surface of the semiconductor injecting carriers downward into the collector. Isolated multiple collector contacts required for wired-AND logic are obtained by using separate Schottky-Barrier contacts for each collector output. GRA

N90-12861 Department of the Navy, Washington, DC.
VIDEO LINE PROCESSOR Patent
Daryl E. Hinman, inventor (to Navy), Vernon A. Anderson, inventor (to Navy), and Jon H. Bumgardner, inventor (to Navy) 4 Apr. 1989 16 p Filed 4 Apr. 1989 Supersedes Pat-Appl-875892-86
(AD-D014198; US-Patent-4,819,190; US-Patent-Appl-SN-875892) Avail: U.S. Patent and Trademark Office CSCL 09/1

A video line processor is described for varying the size of a video image portion along a video line in an image processor. In this image processor, image size variation occurs first along horizontal lines and then along vertical lines. Intermediate and final frames are stored in memories in which row and column addressing is interchanged on alternate frames. The line processor has a line memory for storing pixel values along each video line, has a pair of arithmetic circuits, one of which receives pixel values delayed in relation to pixel values received by the other, and has a coefficient memory with memory locations corresponding to pixel values along a video line. Each of these locations is loaded between video frames with an address for the line memory and with coefficients for the arithmetic circuits to control, respectively, the position of each pixel value along a line and the transformation of the value. GRA

N90-12862# Department of the Navy, Washington, DC.
RF AND dc DESENSITIZED ELECTROEXPLOSIVE DEVICE Patent Application
John W. Krainiak, inventor (to Navy), Paul D. Speaks, inventor (to Navy), and Michael S. Cornett, inventor (to Navy) 24 Jul. 1989 19 p
(AD-D014206; US-Patent-Appl-SN-385375) Avail: NTIS CSCL 09/1

This patent application relates to electroexplosive devices (EEDs) such as detonators, blasting caps and squibs, in particular to a method and device for desensitizing EEDs to electromagnetic radiation and electrostatic charges with the added ability to desensitize the device to essentially dc currents. An insensitive electroexplosive device to electrically ignite explosive is disclosed. This device is inherently immune to radio frequency (RF) radiation, and also provides protection against dc or very low frequency RF induced by arcing. A central feature is use of zeners and capacitors to form a reactively balanced bridge circuit. When constructed in semiconductor form, as described in this application, the device is capable of incorporation in small caliber ordnance. GRA

N90-12863# Minnesota Univ., Minneapolis. Corrosion Research Center.
THE USE OF LITHIUM BATTERIES IN BIOMEDICAL DEVICES Technical Report No. 14, Jul. 1988 - Jun. 1989
Boone B. Owens and P. S. S. Prasad 15 Jun. 1989 11 p Presented at the 9th Discussion Meeting of New Battery Conceptive Division, Kyoto, Japan, 25 Sep. 1989; sponsored by Electrochemical Society of Japan
(Contract N00014-88-K-0360)
(AD-A212187) Avail: NTIS HC A03/MF A01 CSCL 10/3

The market for lithium batteries has been growing steadily during the past fifteen years as these new types of power sources have been developed into reliable sources of power. Primary lithium batteries have been used in military, commercial and biomedical applications for over ten years and they have proven to be an increasingly important class within the battery industry. Rechargeable lithium batteries are the subject of considerable development activity, with some small cells having been already commercialized. However, the implementation of rechargeable lithium batteries on a wide spread basis still awaits the further development and qualification of new designs. GRA

N90-12864# Illinois Univ., Urbana. Coordinated Science Lab.
JOINT SERVICES ELECTRONICS PROGRAM Annual Progress Report, 1 Apr. 1988 - 31 Mar. 1989
W. K. Jenkins 30 Jun. 1989 96 p
(Contract N00014-84-C-0149)
(AD-A212309) Avail: NTIS HC A05/MF A01 CSCL 09/1

The third annual progress report of the research conducted at the Coordinated Science Laboratory is presented. The research areas include Solid State Electronics, Quantum Electronics, Electromagnetics, Information Systems, and Electronics Research (discretionary Director's unit). The areas of research are summarized, the most significant results are identified, and the publications sponsored by JSEP and other agencies are listed. GRA

N90-12865# Thermacore, Inc., Lancaster, PA.
HEAT PIPES FOR SODIUM-SULFUR BATTERIES Final Report, 29 Aug. 1988 - 1 May 1989
John R. Hartenstine Aug. 1989 70 p Original contains color illustrations
(Contract F33615-88-C-2892)
(AD-A212523; WRDC-TR-89-2122) Avail: NTIS HC A04/MF A01 CSCL 10/3

The objective of this program was to develop a variable conductance heat pipe (VCHP) for the thermal management of sodium-sulfur batteries. The VCHP maintains the sodium sulfur battery within a specified temperature rise limit (20 C) while the battery discharges a thermal load from 0 watts to 500 watts. A preliminary full scale thermal management design was developed for the sodium-sulfur battery, incorporating the VCHPs and supporting integration hardware. The feasibility of the VCHPs for this application was proved by test. The VCHP developed in Phase 1 utilized titanium as the heat pipe envelope material, and cesium as the heat pipe working fluid. The wick structure was axial grooves. Analysis and test indicate that the VCHP can provide the passive thermal control necessary for the sodium-sulfur battery. Test data show that with the heat input from Q = 0 watts to Q = 500 watts, the VCHP evaporator temperature increased from 350 C to 385 C. The temperature control range was higher than predicted due to working fluid vapor diffusion into the noncondensible gas and thermal axial conduction into the VCHP reservoir. Analysis has shown that by utilizing VCHPs for passive temperature control, the sodium-sulfur battery cells will have a lower axial delta-T during discharge than a current louver design. The VCHP thermal management package has the potential to be used in geosynchronous earth orbits (GEO) and low earth orbits (LEO). GRA

N90-12866# Air Force Inst. of Tech., Wright-Patterson AFB, OH.
THE ANALYSIS OF CURRENT-MIRROR MOSFETS FOR USE IN RADIATION ENVIRONMENTS M.S. Thesis - Arizona Univ.
Marino J. Martinez 1988 78 p
(AD-A212527; AFIT/CI/CIA-88-237) Avail: NTIS HC A05/MF A01 CSCL 09/1

Experiments were conducted on current-mirror MOSFETs to

examine their suitability for use in radiation environments. These devices, which allow low loss load current sensing (defined by a current-ratio n'), are an important element of many power integrated circuits (PICs). Total-dose testing demonstrated that the current ratio was virtually unaffected for many operating conditions. In all cases, changes were largest when sense resistance was largest and minimal when sense voltage was approximately equal to the load source's voltage. In addition, testing verified the feasibility of using sense-cell MOSFETs for applications which require radiation exposure. A constant-current op-amp circuit showed minimal current shifts, using proper circuit design, following total-dose exposure. Dose-rate testing showed the feasibility of using sense voltage to trigger gamma-dot protection through drain-source voltage clamping, providing a relatively inexpensive alternative to voltage derating. GRA

N90-12867# Naval Research Lab., Washington, DC. Plasma Theory Branch.

ELECTRON BEAM PROPAGATION THROUGH A MAGNETIC WIGGLER WITH RANDOM FIELD ERRORS Interim Report

E. Esarey, W. Marable (Maryland Univ., College Park.), and C. M. Tang 21 Aug. 1989 60 p

(AD-A212705; NRL-MR-6523) Avail: NTIS HC A04/MF A01 CSCL 09/3

The effects of random field errors on the propagation of a relativistic electron beam through a wiggler magnet is analyzed both theoretically and numerically. Random field errors give rise to detrimental effects such as a random walk in the transverse position of the beam centroid as well as fluctuations in the parallel energy of the electron beam. This random beam motion is analyzed both for a single realization of a wiggler magnet (a particular arrangement of field errors) and for an ensemble of wiggler magnets with identical statistical properties. Both helical and planar wiggler configurations are studied, with and without the effects of transverse focusing forces. Theoretical expressions are derived for the random electron motion and these results are then confirmed through 3-D particle simulations of electron beam transport including the effects of finite emittance. Without transverse focusing, the rms transverse centroid displacement scales as z to the 3/2 power and the variance of the parallel energy deviation scales as the square root of z, z being the axial propagation distance. Transverse focusing inhibits the random walk of the centroid so that its rms value scales as the square root of z, but the variance of the parallel energy is only reduced by a factor of the square root of 2. In a free electron laser (FEL) it may be possible for the random walk of the electrons to become large enough so that the centroids of the radiation and electron beams no longer overlap, thus destroying the FEL interaction and reducing the FEL gain. GRA

N90-12868# Naval Research Lab., Washington, DC. Beam Physics Branch.

COLD TESTS OF QUASI-OPTICAL GYROTRON RESONATORS Interim Report

R. P. Fischer, T. A. Hargreaves (Mission Research Corp., Newington, VA.), and A. W. Fliflet 7 Sep. 1989 30 p

(AD-A212707; NRL-MR-6531) Avail: NTIS HC A03/MF A01 CSCL 09/1

Cold test are performed on a number of quasi-optical gyrotron resonators at 94 and 120 GHz to determine the variation of cavity Q with mirror separation. The separation between the resonator mirrors is varied between 15 and 35 cm, with measured quality factors ranging from 10,000 to 100,000. Good agreement is obtained between the measured data and values calculated from scalar diffraction theory. The effect of misaligning the mirrors is also examines experimentally. GRA

N90-12869# Aerospace Corp., El Segundo, CA. Chemistry and Physics Lab.

THERMIONIC EMISSION INCLUDING BOTH SPACE CHARGE AND IMAGE FORCES

T. P. Lin and G. Eng 1 Sep. 1989 35 p

(Contract F04701-85-C-0086)

(AD-A212732; TR-0086A(2945-02)-2; SD-TR-89-64) Avail: NTIS HC A03/MF A01 CSCL 09/1

The net emission current for a uniform planar thermionic emitter is determined for a range of voltages, temperatures, and various values of the work function. Poisson's equation is self consistently solved, using numerical techniques, without any additional phenomenological assumptions. The net current is accurately specified in the transition region between space charge limited and temperature limited emission, and the first determination of the shape of the interelectrode potential there is presented. A comparison with earlier approximate techniques is also included. GRA

N90-12870# Aerospace Corp., El Segundo, CA. Electronics Research Lab.

STRONG-INVERSION MODEL OF THRESHOLD VOLTAGE IN MODULATION DOPED FIELD EFFECT TRANSISTORS: THE ROLE OF UNINTENTIONAL ACCEPTORS

Richard J. Krantz and Walter L. Bloss Jun. 1989 22 p

(Contract F04701-88-C-9989)

(AD-A212750; TR-0089(4925-07)-2; SD-TR-89-61) Avail: NTIS HC A03/MF A01 CSCL 20/12

A strong inversion model, in the depletion layer approximation, of the threshold voltage for modulation doped field effect transistors (MODFETs) was developed. It was shown that for a range of unintentional acceptor doping densities from 10(exp 13) to 10(exp 15)/cu cm in typical molecular beam epitaxy (MBE) grown structures, threshold voltages may increase by as much as 200 mV. The contributions of AlGaAs and GaAs to the threshold voltage were isolated. The model was verified by comparing predicted threshold voltages with those measured in typical MBE grown MODFET structures. GRA

N90-12871# North Carolina Univ., Chapel Hill. Dept. of Chemistry.

SYNTHESIS AND CHARACTERIZATION OF NEW LOW-DIMENSIONAL METAL COMPLEX CONDUCTORS Final Report, 1 May 1986 - 30 Apr. 1989

William E. Hatfield 1 Oct. 1989 12 p

(Contract N00014-86-K-0608)

(AD-A213189) Avail: NTIS HC A03/MF A01 CSCL 20/3

The synthesis and characterization of new transition metal complex electrical conductors is considered. Guidelines were developed which will lead to the rational synthesis of electrical conductors with desired properties, a secondary mandate was to solve important scientific problems that are encountered in the research. GRA

N90-12801*# Jet Propulsion Lab., California Inst. of Tech., Pasadena.

STABLE KALMAN FILTERS FOR PROCESSING CLOCK MEASUREMENT DATA

P. A. Clements, B. P. Gibbs, and J. S. Vandergraft (Computational Engineering, Inc., Laurel, MD.) *In its* The Telecommunications and Data Acquisition Report 15 Aug. 1989 p 190-201 (For primary document see N90-12786 04-32)

Avail: NTIS HC A11/MF A02 CSCL 09C

34 FLUID MECHANICS AND HEAT TRANSFER

Includes boundary layers; hydrodynamics; fluidics; mass transfer; and ablation cooling.

For related information see also *02 Aerodynamics* and *77 Thermodynamics and Statistical Physics.*

N90-12872*# Pennsylvania State Univ., University Park. Dept. of Aerospace Engineering.

A COMPUTATIONALLY EFFICIENT MODELLING OF LAMINAR SEPARATION BUBBLES Semiannual Status Report, Jan. - Jun. 1989

Paolo Dini and Mark D. Maughmer 1989 15 p

(Grant NAG1-778)

(NASA-CR-185854; NAS 1.26:185854) Avail: NTIS HC A03/MF A01 CSCL 20D

In order to predict the aerodynamic characteristics of airfoils operating at low Reynolds numbers, it is necessary to accurately account for the effects of laminar (transitional) separation bubbles. Generally, the greatest difficulty comes about when attempting to determine the increase in profile drag that results from the presence of separation bubbles. While a number of empirically based separation bubble models have been introduced in the past, the majority assume that the bubble development is fully predictable from upstream conditions. One way of accounting for laminar separation bubbles in airfoil design is the bubble analog used in the design and analysis program of Eppler and Somers. A locally interactive separation bubble model was developed and incorporated into the Eppler and Somers program. Although unable to account for strong interactions such as the large reduction in suction peak sometimes caused by leading edge bubbles, it is able to predict the increase in drag and the local alteration of the airfoil pressure distribution that is caused by bubbles occurring in the operational range which is of most interest. E.R.

N90-12873 Johns Hopkins Univ., Baltimore, MD.

STABILITY CONDITIONS FOR STEADY SHEARING. STABILITY CONDITIONS FOR SIMPLE SHEAR UNDER MIXED THERMAL BOUNDARY CONDITIONS Ph.D. Thesis

Howard Tz. Chen 1988 108 p

Avail: Univ. Microfilms Order No. DA8908093

The shearing of a slab of thermoviscoplastic material by the application of traction in the presence of heat conduction is examined. When the thermoviscoplastic constitutive law is given in general functional form, an integral expression for the analytic steady solutions of an inhomogeneous simple shear problem is obtained. A perturbation method, which gives rise to a set of linear partial differential equations (with spatially dependent coefficients), is then used to examine the stability of the steady-state solution of the governing equations. After separation of variables, the existence of eigenvalues and eigenfunctions of the resulting fourth-order system is demonstrated. An integral method is then used to obtain a sufficient condition for stability. The governing equations are set up for the quasi-static simple shear of a general thermoviscoplastic material with mixed thermal boundary conditions, where both temperature and temperature gradient can be specified at the boundary. The stability of this system is examined by means of a perturbation. Dissert. Abstr.

N90-12874*# Institute for Computer Applications in Science and Engineering, Hampton, VA.

NUMERICAL STUDY OF THREE-DIMENSIONAL SPATIAL INSTABILITY OF A SUPERSONIC FLAT PLATE BOUNDARY LAYER Final Report

Lucio Maestrello, A. Bayliss, and R. Krishnan (Vigyan Research Associates, Inc., Hampton, VA.) Oct. 1989 20 p

(Contracts NAS1-18107; NAS1-18605)

(NASA-CR-181931; NAS 1.26:181931; ICASE-89-74) Avail: NTIS HC A03/MF A01 CSCL 20D

The behavior of spatially growing three-dimensional waves in a supersonic boundary layer was studied numerically by solving the complete Navier-Stokes equations. Satisfactory comparison with linear parallel and non-parallel stability theories, and experiment are obtained when a small amplitude inflow disturbance is used. The three-dimensional unsteady Navier-Stokes equations are solved by a finite difference method which is fourth-order and second-order accurate in the convection and viscous terms respectively, and second-order accurate in time. Spanwise periodicity is assumed. The inflow disturbance is composed of eigenfunctions from linear stability theory. By increasing the amplitude of the inflow disturbance, nonlinear effects in the form of a relaxation type oscillation of the time signal of rho(u) are observed. Author

N90-12875# Stanford Linear Accelerator Center, CA.

SURVEY OF THE RESPONSE OF STANDARD LIMITED STREAMER TUBES OVER THE COMPLETE RANGE OF THREE-COMPONENT GAS MIXTURES OF ISOBUTANE, CO(SUB 2), ARGON

A. Calcaterra, R. DeSangro, P. DeSimone, P. Burrows, S. L. Cartwright, S. Gonzalez, A. Lath, U. Schneekloth, D. C. Williams, and J. M. Yamartino (Massachusetts Inst. of Tech., Cambridge.) et al Jul. 1989 11 p Presented at the 4th Pisa Meeting on Advanced Detectors: Frontier Detectors from Frontier Physics, La Biodola, Italy, 21-26 May 1989 Prepared in cooperation with INFN, Perugia, Italy; Padua Univ., Italy; INFN, Pisa, Italy; INFN, Padua, Italy; Pisa Univ., Italy; Wisconsin Univ., Madison and Perugia Univ., Italy

(Contracts DE-AC03-76SF-00515; DE-AC02-76ER-03069; DE-AC02-76ER-00881)

(DE89-016692; SU-SLAC-PUB-5016; CONF-8905194-4) Avail: NTIS HC A03/MF A01

The results are presented of a systematic study of three component gas mixtures containing argon, isobutane, and carbon dioxide. The study used production-type chambers from the SLD Warm Iron Calorimeter (WIC), instrumented with standard pleastic streamert tubes, and triggered by cosmic ray muons. Pulse height spectra are presented as a function of high voltage, over a wide range of mixtures of these three gases. Various features and similarities observed throughout this 3-D mixture space are important clues to understanding the underlying physics of discharge mechanisms in wire detectors. DOE

N90-12876# Technische Univ., Delft (Netherlands). Faculty of Technical Mathematics and Informatics.

FREE-FIELD RESPONSE FROM INCLINED BODY WAVES IN VISCOELASTIC RANDOM MEDIUM

Z. Hryniewicz (Technical Univ. of Koszalin, Poland) and A. J. Hermans 1988 50 p

(Rept-88-99; ISSN-0922-5641; ETN-89-95110) Copyright Avail: NTIS HC A03/MF A01

The free field response of the inplane motion resulting from a combination of inclined incident body waves is addressed. The amplification of waves in a viscoelastic layer with stochastic changes in the elastic properties and density is investigated. The Karal and Keller method, based on the idea of the fundamental matrix, is used. Third order correlations are neglected. The resulting integro-differential equation for the average displacements are solved by Laplace transform. Analysis indicates that the stochastic changes in the shear modulus and density enhance the damping in a significant manner. Increase in wave amplification is shown to arise in the case of a small dimensionless frequency and uncorrelated stochastic changes of material parameters. ESA

N90-12877# Cornell Univ., Ithaca, NY.

VORTEX DYNAMICS Final Technical Report, 1 Jun. 1987 - 31 May 1989

Sidney Leibovich 7 Aug. 1989 72 p

(Grant AF-AFOSR-0255-87; AF Proj. 2307)

(AD-A212119; AFOSR-89-1205TR) Avail: NTIS HC A04/MF A01 CSCL 20/4

A theoretical description of vortex breakdown, suitable for design and control purposes, is under development. The objective is to incorporate the essential physical processes governing the

occurrence, location, and strength of the phenomenon. It was shown, under sponsorship of this grant, that the axisymmetric Euler equations possess solutions describing flow structures creating very strong disruptions of concentrated vortex flows having axial streaming. The nature of four classes of flow structures of this character was described, and the interrelationships between them explained. Numerical analytical tools needed to treat the very large algebraic eigenvalue problems encountered in stability analyses of flows such as those found were developed. In other tasks: (1) the linear instability characteristics of the Hall-Stewartson model of the leading-edge vortex were determined asymptotically for large Reynolds numbers, and (2) nonlinear transitions and mode interactions were studied for viscous rotating pipe flow. GRA

N90-12878# Helsinki Univ. of Technology, Espoo (Finland). Nuclear Engineering Lab.
IMPROVED 2D NUMERICAL SIMULATION MODEL FOR STRONGLY COUPLED HEAT AND FLUID FLOW IN A THERMAL STORAGE
O. Kymaelaeinen and P. D. Lund Jan. 1989 46 p
(PB89-218879; TKK-F-A640; ISBN-951-754-798-6) Avail: NTIS HC A03/MF A01 CSCL 20D

A simulation program for heat and fluid flow in a water heat storage was developed. The simplified 2D flow equations are solved numerically using the vorticity-stream function approach. The problem is characterized by strong coupling between momentum and temperature equations. Thus, special emphasis needs to be given to the speed of the solution algorithm to enable in practice the simulation of water heat storages with a reasonable throughput time. The general objective was to develop a problem oriented simulation tool with much faster performance than the commercially available programs such as PHOENICS. The main application of the program is the visualization of flow fields. GRA

N90-12879# Helsinki Univ. of Technology, Espoo (Finland). Lab. of Aerodynamics.
SOLUTION OF THE THIN-LAYER NAVIER-STOKES EQUATIONS FOR LAMINAR TRANSONIC FLOW
Timo Siikonen and Jaakko Hoffren 28 Feb. 1989 60 p
(PB89-221600; SER-A-89-A11; ISBN-951-754-855-9) Avail: NTIS HC A04/MF A01 CSCL 20D

A finite-volume-based numerical method for the solution of the thin-layer Navier-Stokes equations is presented. The convective part of the fluxes is solved using a flux-vector splitting method and the diffusive part is solved using central differences. The equations are integrated in time with an approximately factored bidiagonal scheme. Convergence is accelerated by applying a multigrid technique. Results are presented for laminar transonic flows over a NACA 0012 airfoil. GRA

N90-12880# National Inst. of Standards and Technology, Boulder, CO. Chemical Engineering Science Div.
EFFECT OF PIPE ROUGHNESS ON ORIFICE FLOW MEASUREMENT
J. A. Brennan, S. E. McFaddin, C. F. Sindt, and R. R. Wilson Jul. 1989 66 p
(Contracts GRI-5081-353-0422; GRI-5081-271-1680)
(PB89-231484; NIST/TN-1329) Avail: NTIS HC A04/MF A01; also available SOD HC $3.50 as 003-003-02951-3 CSCL 20D

Flow measurement with orifice flowmeters is simple in concept and can be accurate, but, as demonstrated in flow measurement test facilities, can also result in large errors if any of the significant parameters are not controlled. Many of these parameters are well known and particular care is taken to ensure that they do not cause measurement errors. Others are more subtle and not so easily detected or controlled. One such parameter is the surface finish of the pipe immediately upstream of the orifice plate. Results of an experimental investigation into the effects of this pipe roughtness on the orifice discharge are presented, along with a review of some of the pertinent literature. Measurement errors of approximately 1 percent can result from using meter tubes that are too rough but still within the specification of the standards. Author

N90-12881# Fluid Jet Associates, Spring Valley, OH.
TWO DIMENSIONAL ORIFICE ARRAY, MONODISPERSE DROP SOURCE, PHASE 1 Final Report
John L. Dressler Feb. 1989 38 p
(Contract F33615-88-C-2865)
(AD-A211319; WRDC-TR-89-2044) Avail: NTIS HC A03/MF A01 CSCL 13/9

An acoustically driven drop generator was constructed. It differs from other such devices in that it generates drops in a two-dimensional array. Further, the generator can break the liquid jets into uniformly-sized drops with diameters smaller than the minimum sized predicted by Rayleigh's theory. One or two sizes of drops can be produced with diameters between 70 to 200 microns. The liquid jets are formed by liquid flowing from a constant pressure manifold through openings in a plate. The plate is made of laminated nickel and copper. Several plates with different hole patterns were constructed. The number of openings in the plates varied from 24 to 1010. The diameter of the openings ranged from 38 to 112 microns. A piezoelectric transducer creates pressure perturbations in the jets' velocity, forcing them to break into drops at the perturbation frequency. A signal generator provides one, two, or three sinusoidal signals for generating the input acoustic signal. A power amplifier boosts the signal and feeds it to the piezoelectric transducer. The jet breakup is observed and photographed through a microscope. GRA

N90-12882*# California Univ., Berkeley. Dept. of Mechanical Engineering.
INVESTIGATION OF TURBULENT FLOW IN HIGHLY CURVED DUCTS WITH APPLICATION TO TURBOMACHINERY COMPONENTS Final Report
J. A. C. Humphrey and M. P. Arnal 1987 166 p
(Grants NAG3-624; NAG3-735)
(NASA-CR-186060; NAS 1.26:186060) Avail: NTIS HC A08/MF A01 CSCL 20D

Numerical predictions were performed using a semi-elliptic calculation procedure for the case of turbulent flow in passage through a 90 deg bend of square cross section. Two versions of the isotropic turbulent viscosity two equation k-epsilon model were used. The first, the wall function model (WFM), employs the logarithmic law-of-the-wall relation and the notion of equilibrium flow to set all the necessary boundary conditions at the first grid point adjacent to a solid wall. The second model, the Van Driest model (VDM), employs Prandtl's original mixing length formulation, in conjunction with Van Driest's semi-empirical relation for the mixing length, to calculate the turbulent viscosity in the near wall regions of the flow. In this case, boundary conditions for k and epsilon, required to calculate these quantities in the core of the flow, are obtained by matching the mixing length and Reynolds number model formulations in an overlapping region of the flow near the walls. In both cases the results obtained show an improvement over earlier calculations using an elliptic numerical procedure. This is attributed to the finer grids possible in the present work. Of the two models, the VDM formulation shows better overall conformity with the mean flow measurements. Neither model reproduces well the details of the stress distribution as a result of the implied isotropic turbulent viscosity. Author

N90-12883# ESDU International Ltd., London (England).
TWO-PHASE FLOW PRESSURE LOSSES IN PIPELINE FITTINGS
Jun. 1989 30 p
(ESDU-89012; ISBN-0-85679-683-2; ISSN-0141-4011) Avail: ESDU

This data item presents the loss data for sudden contractions and expansions, orifice plates, valves (gate, globe, ball and diaphragm) and bends. In each case an equation is given for the two phase multiplier which, when it is applied as a factor to the single phase pressure loss calculated at the same mass flow rate, yields the two phase pressure loss. Data for the single phase loss are also included and, as in the case of multipliers, are based on semi-empirical methods. The choice of equation for the multiplier is recommended as a result of correlating predicted pressure loss

with a very wide range of experimental measurements drawn from the literature. For each component that correlation is shown graphically and details are given of the geometry, flow orientation, fluids involved and inlet pressure appropriate to the test results used. The influence of flow regime and pipe orientation is discussed for each component. An approximate iterative method of allowing for flashing is given and is illustrated in one of the two worked examples showing practical uses of the prediction methods.
ESDU

N90-12884# Gesellschaft fuer Reaktorsicherheit, Garching (Germany, F.R.).
ANALYTICAL CONTROL OF SPECIAL NUMERICAL CALCULATIONS OF PRESSURE PROPAGATION IN A FLUID [ANALYTISCHE UEBERPRUEFUNG SPEZIELLER NUMERISCHER RECHNUNGEN DER DRUCKAUSBREITUNG IM FLUID]
Karl Drittler Feb. 1989 83 p In GERMAN; ENGLISH summary
(GRS-70; ISBN-3-923875-20-7; ETN-89-94984) Avail: NTIS HC A05/MF A01

The results of numerical pressure propagation calculations are checked using the so-called one-dimensional wave propagation method. It is assumed that the propagation of the pressure wave in a fluid filled system can be approximated by a function that, in addition to time and other parameters, depends only on the wave propagation direction. Satisfactory approximations are obtained if the averaging of certain parameters in the direction perpendicular to the propagation is sufficient with regard to the mathematical evaluation of essential effects. The application of the method is strongly influenced by the interaction of the pressure pulses with the elastic fluid boundaries. The results agree well with those of extensive numerical calculations. The analytical methods lead to a better understanding of the essential physical effects. ESA

N90-12885# Technische Univ., Delft (Netherlands). Faculty of Technical Mathematics and Informatics.
A LINEARIZED SURFACE CONDITION IN LOW SPEED HYDRODYNAMICS
P. H. vanGemert and A. J. Hermans 1989 31 p
(Rept-89-04; ISSN-0922-5641; ETN-89-95438) Copyright Avail: NTIS HC A03/MF A01

The nonlinear character of sea surface condition, which poses a problem in the calculation of wave pattern and the wave resistance part of the total resistance working on a ship, is studied. The problem is mathematically formulated, and approximation theory applied in the approach to a solution. Approximation methods are described and difficulties encountered are noted. A discussion on some surface conditions is included and comparisons made. An iterative scheme to improve on the approximation is suggested and the applicability of the approach to other problems is described. ESA

N90-12886# Technische Univ., Delft (Netherlands). Faculty of Technical Mathematics and Informatics.
A MULTIGRID METHOD FOR THE NAVIER-STOKES AND BOUSSINESQ EQUATIONS
Zeng Shi and P. Wesseling 1989 68 p
(Rept-89-17; ISSN-0922-5641; ETN-89-95449) Copyright Avail: NTIS HC A04/MF A01

A nonlinear multigrid method is developed for the Navier-Stokes and Boussinesq equations using a discretization of finite volume type on Cartesian staggered grids and a nonlinear collective Gauss-Seidel method for smoothing. A simple multigrid algorithm incorporating the cycles V, F, W and an adaptive multigrid cycle (A cycle) is presented. Numerical experiments are described for a driven square cavity problem and a free convection problem in a rectangular cavity. Of the three cycles tested, namely V, W and A, the A cycle is found to be most efficient. The rate of convergence is shown to improve slightly when the mesh size is decreased. The multigrid method is found to be very much faster than single grid iteration with the smoother. ESA

N90-12887# Poitiers Univ. (France). Lab. de Mecanique des Fluides.
AUTOMATIC ANALYSIS AND EXPLOITATION OF THE FLOW VISUALIZATION IMAGES Final Report [ANALYSE ET EXPLOITATION AUTOMATISEES D'IMAGES DE VISUALISATION D'ECOULEMENTS]
Marie-France Collin 1988 40 p In FRENCH
(Contract DRET-88-1404/DS/SR)
(ETN-89-95712) Avail: NTIS HC A03/MF A01

The automatic system for the quantitative investigation of the flow images are described. The radioactive isotope technique is applied. The flow structure and evolution are studied by means of the Navier-Stokes equation. The results show that the flow velocity field, distributed in the knots of a regular network pattern, can be evaluated with an error below 7 percent. The automatic image analysis allows the identification of the linear and nonlinear tracks with 2 percent accuracy. The quantitative and qualitative results from the automatic and manual analyses, are compared and show the reliability of the designed automatic (chain) system. ESA

N90-12888# Centre d'Etudes et de Recherches, Toulouse (France). Dept. d'Etudes et de Recherches en Aerothermodynamique.
THREE-DIMENSIONAL SHEAR FLOWS: ANALYSIS OF THE TRACK AND ANGLE OF INCIDENCE [ECOULEMENTS CISAILLES TRIDIMENSIONNELS. ANALYSE DU SILLAGE D'UNE AILE EN FLECHE ET EN INCIDENCE]
G. Pailhas Mar. 1989 45 p In FRENCH
(Contract STPA-85-95-004-35)
(CERT-RTS-OA-31/5025-AYD; DERAT-31/5025.20;
ETN-89-95713) Avail: NTIS HC A03/MF A01

The characterization of a turbulent track, under the effect of a transversal pressure gradient, is investigated. The mean velocity and the turbulent field measurements are effectuated by means of a four wire anemometer. The results show that the transversal velocity profiles are not the same as those obtained in the classical three dimensional track studies. A relaxation track state cannot be established from the velocity fluctuation profiles. However, the results show that the flow behavior is driven by the presence of the pressure gradient. ESA

N90-12889# Centre d'Etudes et de Recherches, Toulouse (France). Dept. d'Etudes et de Recherches en Aerothermodynamique.
REDUCTION OF TURBULENT DRAG: BOUNDARY LAYER MANIPULATORS Final Report [REDUCTION DE TRAINEE DE FROTTEMENT TURBULENT: MANIPULATEURS DE COUCHE LIMITE]
E. Coustols Mar. 1989 55 p In FRENCH
(CERT-RSF-OA-74/2259-AYD; DERAT-59/5004.25;
ETN-89-95714) Avail: NTIS HC A04/MF A01

The drag reduction on airbus profiles is investigated. External and internal boundary layer manipulators are applied. The wind tunnel wall geometry and the model surface geometry are modified, carving riblets in the sense of the main flow. The change induced in the flow are studied using hotwire anemometry and spectral analysis. Direct drag measurements on Airbus profiles indicate a drag reduction of 3.5 percent. Experiments using cylindrical bodies in transonic flow show a drag reduction of 8 percent. ESA

N90-12890# Von Karman Inst. for Fluid Dynamics, Rhode-Saint-Genese (Belgium).
AN IMPLICIT NAVIER-STOKES SOLVER OPTIMISED FOR A VECTOR-PARALLEL COMPUTER
K. G. Ruddick and C. Benocci Feb. 1989 48 p
(Grant SERC-87-600212)
(VKI-TN-169; ETN-89-95742) Avail: NTIS HC A03/MF A01

A numerical method for the solution of the incompressible Navier-Stokes equations in the primitive variable formulation is presented. Space discretization is performed by centered finite differences on a curvilinear, nonorthogonal, staggered mesh. An implicit time discretization with a fractional step method is applied. Numerical results for the flow over a backward facing step and

flow in a curved channel are presented. Experimental data and numerical results are compared. Optimization of the algorithm for a vector parallel computer is discussed. ESA

N90-12891# Center for Mathematics and Computer Science, Amsterdam (Netherlands). Dept. of Numerical Mathematics.
UPWIND DISCRETIZATION OF THE STEADY NAVIER-STOKES EQUATIONS
Barry Koren Aug. 1988 16 p Submitted for publications
Sponsored by ESA and Avions Marcel Dassault-Breguet Aviation, Saint-Cloud, France
(CWI-NM-R8810; ETN-89-95621) Copyright Avail: NTIS HC A03/MF A01

A discretization method for the full, steady, compressible Navier-Stokes equations is presented, which makes use of quadrilateral finite volumes and consists of an upwind discretization of the convective part, and a central discretization of the diffusive part, with emphasis on the former. The steady equations are solved directly by means of a nonlinear relaxation method accelerated by multigrid, which requires the discretization to be continuously differentiable. Results of a quantitative error analysis for Osher's and van Leer's upwind schemes, which satisfy this requirement, are presented. Osher's scheme is shown to be increasingly more accurate with increasing Reynolds number. A higher order accurate discretization of the convection terms is derived and a limiter constructed to preserve monotonicity. Numerical results are presented for subsonic and supersonic flat plate flows, with oblique shock wave/boundary layer interaction, which agree with predictions. Useful properties of the method are the easy checking of false diffusion and that parameters need no tuning. ESA

N90-12892# National Inst. of Standards and Technology, Gaithersburg, MD. Chemical Process Metrology Div.
MEASUREMENTS OF COEFFICIENTS OF DISCHARGE FOR CONCENTRIC FLANGE-TAPPED SQUARE-EDGED ORIFICE METERS IN WATER OVER THE REYNOLDS NUMBER RANGE 600 TO 2,700,000 Final Technical Report
James R. Whetstone, William G. Cleveland, George P. Baumgarten, Samuel Woo, and M. Carroll Croarkin Jun. 1989 544 p
Sponsored by American Petroleum Inst., Washington, DC
(PB89-235147; NIST/TN-1264) Avail: NTIS HC A23/MF A03; also available SOD HC $26.00 as 003-003-02942-4 CSCL 20D

A description is presented of the measurement procedures and standards, data acquisition systems, and data bases developed in the American Petroleum Institute-sponsored orifice discharge coefficient data base project performed at the National Bureau of Standards primary water flow rate measurement facility. Measurements were performed on five orifice meter sizes, 2, 3, 4, 6, and 10 inches, over the beta ratio range of 0.08 to 0.75. The measurement systems and procedures were designed to provide full documentation of the relation between the observations comprising the data base developed and U.S. national measurement standards. GRA

N90-12893# Royal Aerospace Establishment, Farnborough (England).
NUMERICAL EVALUATION OF A SOLUTION REPRESENTING A JET IN CROSS-FLOW
C. C. Lytton and J. H. B. Smith 4 Aug. 1988 51 p
(RAE-TM-AERO-2137; BR108488; ETN-89-95000) Copyright Avail: NTIS HC A04/MF A01

The analytical results for the flow of an inviscid incompressible jet emerging from a circular pipe into a weak cross-flow, are presented. In particular, expressions in the form of infinite series or integrals are provided for the velocity potential in the following regions: inside the pipe, inside the jet and outside both, upstream and downstream of the orifice plane. The results show that the solutions in the pipe and jet are continuous across the orifice plane. The behavior of the solution near the orifice is displayed in graphical form. The consequences of the failure to satisfy a Kutta condition of smooth outflow at the lip is emphasized. ESA

N90-12894# Office National d'Etudes et de Recherches Aerospatiales, Paris (France). Direction de l'Aerodynamique.
EXPERIMENTAL STUDY OF HOMOGENEOUS TURBULENCE SUBMITTED TO ROTATIONAL EFFECTS Final Report [ETUDE EXPERIMENTALE DE LA TURBULENCE HOMOGENE SOUMISE A DES EFFETS DE ROTATION]
O. Leuchter and L. Jacquin Jul. 1988 213 p Partly in ENGLISH and FRENCH
(Contract DRET-8-34-001)
(ONERA-RSF-10/1145-AY-164A; ETN-89-95017) Avail: NTIS HC A10/MF A02

A hot wire probe anemometer and digital signal processing techniques used in the study of rotational turbulence are described. A method using four wires is given particular attention. Other means of improving the accuracy and operating ease of the experiments are given particular attention. The measurements are mainly of Reynolds tension, integral scales and spectral distributions. Their evolution during movement down the tube is recorded for several rotational speeds. Characteristic two dimensional behavior patterns of rotational turbulence are identified. ESA

N90-12895# Office National d'Etudes et de Recherches Aerospatiales, Paris (France). Direction de l'Aerodynamique.
FLOW IN THE NEIGHBORHOOD OF AN ELLIPSOID CYLINDER OF REVOLUTION MODEL [ETUDE EXPERIMENTALE DE L'ECOULEMENT AU VOISINAGE DU PLAN DE SYMETRIE EXTRADOS D'UNE MAQUETTE D'ELLIPSOIDE CYLINDRE DE REVOLUTION]
D. Barberis Oct. 1988 79 p In FRENCH
(ONERA-RT-22/7252-AN-000A; ETN-89-95021) Avail: NTIS HC A05/MF A01

The use of a laser velocimeter in a wind tunnel to study the surface layer effects of an ellipsoid cylinder of revolution is described. Good flow symmetry is obtained allowing for investigation of how a choppy boundary flow changes into a swirling flow when specific changes occur along wall boundaries. The need for further tests of flow motion closer to the wall boundaries is stressed. ESA

N90-12896# Centre Technique des Industries Mecaniques, Senlis (France).
A THEORETICAL METHOD FOR THE MECHANICAL CALCULATION OF HEAT EXCHANGERS WITH SLIDING HEADS, PHASE 1 STUDY Final Report [METHODE THEORIQUE POUR LE CALCUL MECANIQUE DES ECHANGEURS A TETE GLISSANTE, ETUDE DE PHASE 1]
F. Osweiller 1 Dec. 1988 53 p In FRENCH
(CETIM-110240-Phase-1; NTI-88/56-Phase-1; ETN-89-95043-Phase-1) Copyright Avail: NTIS HC A04/MF A01

The behavior of heat exchangers with tubular plates is analyzed for exchangers with stationary and mobile plates. Mathematical analysis of the behavior is fully illustrated. Solution of the problems involved calls for the use of a computer, as six equations with six unknowns must be solved to calculate the six integration constraints involved in the calculations. The problem can be simplified by supposing that the two tubular plates have the same diameter. This is in fact the case in most practical applications. ESA

N90-12897# Centre d'Etudes et de Recherches, Toulouse (France). Dept. d'Etudes et de Recherches en Aerothermodynamique.
TRANSITION IN SURFACE BOUNDARY LAYERS Final Report [TRANSITION DE LA COUCHE LIMITE]
D. Arnal, F. Vignau, and J. C. Juillen Feb. 1989 32 p In FRENCH
(Contract DRET-84-002)
(CERT-RSF-OA-43/5018-AYD; DERAT-43/5018.29; DERAT-43/5018.30; ETN-89-95279) Avail: NTIS HC A03/MF A01

Transition from laminar to turbulent flow at the boundary layer at supersonic speeds is investigated. Techniques of maintaining laminar flow by aspiration are described. Theoretical two

dimensional flow models are proposed. Experimental results of airfoil tests are provided. The maintenance of laminar flow by aspiration proves to be much more difficult to achieve in practice than the theoretical model suggests. This is due to the difficulty of determining the speed of flow perpendicular to the airfoil.
ESA

N90-12898# Wright State Univ., Dayton, OH. Dept. of Mechanical Systems Engineering.
ANALYSIS OF THE PERFORMANCE OF HEAT PIPES AND PHASE-CHANGE MATERIALS WITH MULTIPLE LOCALIZED HEAT SOURCES FOR SPACE APPLICATIONS Final Report, Jan. - Dec. 1988
Amir Faghri, Won S. Chang, and Edward T. Mahefkey (Air Force Wright Research and Development Center, Wright-Patterson AFB, OH.) May 1989 344 p
(Contract F33615-86-C-2720)
(AD-A212232; WSU-TR-88-001; WRDC-TR-89-2077) Avail: NTIS HC A15/MF A02 CSCL 20/13

The objective of this report is to examine the performance characteristics of heat pipes and phase-change materials with multiple localized heat sources as well as the fundamental problems related to their specific applications. A numerical analysis is presented for the overall performance of heat pipes with single or multiple heat sources. The analysis includes the heat conduction in the wall and liquid-wick regions as well as the compressibility effect of the vapor flow inside the heat pipe. The solutions are compared with existing experimental data for the vapor and wall temperatures at both low and high temperatures. In addition, the performance of heat pipes with localized heat input including the effects of axial and circumferential heat conduction under high and low working temperatures was investigated. The numerical results for block heating a heat pipe with low working temperatures indicate a good agreement with existing experimental data. GRA

N90-12899# Air Force Armament Lab., Eglin AFB, FL. Aerodynamics Branch.
UNSTEADY THREE-DIMENSIONAL THIN-LAYER NAVIER STOKES SOLUTIONS ON DYNAMIC BLOCKED GRIDS Final Report, Aug. 1986 - Dec. 1988
L. Bruce Simpson May 1989 157 p
(AD-A212377; AFATL-TR-89-19) Avail: NTIS HC A08/MF A01 CSCL 20/4

An efficient scheme for calculating steady and unsteady solutions on blocked grids for several airfoils and wings is presented. Two algorithms are presented, both of which are based on upwind, finite-volume, flux splitting for the convective terms, and an explicit treatment of the diffusive terms. The first algorithm is based on a flux difference split (FDS) scheme. The two algorithms are compared for steady thin-layer Navier-Stokes solutions on a laminar flat plate, RAE 2822 airfoil, and the ONERA M6 wing. The FDS scheme proved to be superior to the FVS in all cases, due to the excessive numerical dissipation in the FVS scheme. A flat plate laminar boundary layer profile is shown with the FDS scheme correctly modeling the boundary layer (compared to a Blasius solution) with only three grid cells internal to the boundary layer; the FVS scheme was not capable of correctly modeling the boundary layer profile. The FDS algorithm was used to evaluate the scheme for unsteady viscous calculations. The diffusive terms are time-lagged in the solution process and therefore are treated as source terms to the convective terms, which behave as a hyperbolic set of equations. The scheme is second order accurate in space and first order accurate in time due to the explicit treatment of the diffusive terms. A Newton subiteration technique was implemented to allow for larger time step sizes and second order temporal accuracy. GRA

N90-12900# Naval Research Lab., Washington, DC.
CALCULATION OF THE ODD AND EVEN INTEGRAL COMPONENTS OF THE WAVE RESISTANCE GREEN'S FUNCTION Interim Report, Jun. 1987 - Apr. 1989
Henry T. Wang and Joel C. Rogers 5 Sep. 1989 41 p
(AD-A212384; NRL-MR-6411) Avail: NTIS HC A03/MF A01 CSCL 20/4

This report presents a computerized method for calculating the total Green's function for the wave resistance case of a source in steady translation below the free surface. Starting with a representation of this function in the complex plane given by Bessho, a series of transformations of variables are used to reduce it to three real single integrals. The integrands are regular and are entirely in terms of elementary functions. Two of the integrals are even about $x=0$ while the remaining integral is odd. The even and odd integrals may also be conveniently expressed in terms of the near and far field components. The method is robust, except for the well known difficulties at the limiting cases when the source is located near the free surface, or the field point is close to the source. A computer code has been written to implement the above method. Sample calculated results are given in several forms to illustrate usage, accuracy, and computer time requirements of the code, as well as to show the relative behavior of the component integrals. GRA

N90-12901# Naval Postgraduate School, Monterey, CA.
FREE SURFACE SCARS AND STRIATIONS M.S. Thesis
Douglas H. Rau Jun. 1989 59 p
(AD-A212429) Avail: NTIS HC A04/MF A01 CSCL 20/4

A numerical and experimental investigation of the interaction of a pair of vortices with a free surface has been undertaken. The analysis is based on the vortex-sheet representation of the free surface and the use of the appropriate boundary conditions. The experiments were performed in a large basin and the vortices were generated through the use of a special nozzle. The rise of the resulting Kelvin oval, the trajectories of the vortices, and the instantaneous shape of the free surface were recorded on a video tape and then carefully analyzed through the use of a Motion Analysis system. The results have shown that the rise of the vortices not only gives rise to two scars, with a pronounced hump in the middle, but also, and more importantly, to a three-dimensional instability heretofore unknown. The measured and calculated vortex trajectories and the free-surface shapes at the corresponding times and Froude numbers are found to be in reasonable agreement. The new instability will form the basis of future investigations.
GRA

N90-12902# Naval Postgraduate School, Monterey, CA.
SEMI-LAGRANGIAN, SEMI-IMPLICIT SOLUTIONS OF THE SHALLOW WATER EQUATIONS IN ONE DIMENSION M.S. Thesis
Kristina B. Monk Jun. 1989 48 p
(AD-A212658) Avail: NTIS HC A03/MF A01 CSCL 20/4

The semi-Lagrangian, semi-implicit method is used to model the one dimensional shallow water system of equations with surface topography. The forecasts are compared to finite difference and semi-Lagrangian, explicit forecasts. In the first experiment, a non-rotating system is considered. The semi-Lagrangian, semi-implicit model agrees very well with hydraulic jump theory, while the semi-Lagrangian, explicit model exhibits excessive smoothing and the finite difference model breaks down when the nonlinear interactions become too large. In the second experiment, the system is allowed to rotate to examine the effect of rotation on the formation of topographically induced hydraulic jumps. Although further study is necessary, it is clear that rotation retards the development of the low pressure to the lee of the obstacle. A larger domain and higher spatial resolution are needed for more detailed simulation of hydraulic jumps. GRA

N90-12903# Naval Research Lab., Washington, DC. Lab. for Computational Physics and Fluid Dynamics.
EVALUATION OF THE NEAR-WALL k-EPSILON TURBULENCE MODEL BY COMPARISON WITH DIRECT SIMULATIONS OF TURBULENT CHANNEL FLOW Interim Report
E. Wade Miner, Thomas F. Swean, Jr., Robert A. Handler, and Richard I. Leighton 7 Sep. 1989 36 p
(AD-A212674; NRL-MR-6499) Avail: NTIS HC A03/MF A01 CSCL 20/4

Results have been reported for the direct numerical simulation (DNS) of a turbulent channel flow at moderate Reynolds number. These data are used to evaluate the terms in the exact and modeled transport equations for the turbulence kinetic energy, k, and the isotropic dissipation function, epsilon. Both transport equations show significant imbalances in the sums of the modeled terms in the high shear region near the channel walls. The model for the eddy viscosity is found to yield distributions for the modeled shear and production terms which do not agree well with the distributions calculated from the DNS data. The source of the imbalance is attributed to the wall damping function, f sub mu, which is required in eddy viscosity models for turbulent flows near walls. Several models for f sub mu are examined, and it is found that the models do not vary across the channel as does f sub mu when evaluated from the DNS data. The Lam-Bremhorst model is found to give reasonable agreement with the DNS data. The standard van Driest model is found to give better agreement with the DNS data. Modification of the van Driest model to include an effective origin improves agreement and gives very good agreement between the modeled shear and the shear calculated from the DNS data. GRA

35 INSTRUMENTATION AND PHOTOGRAPHY

Includes remote sensors; measuring instruments and gages; detectors; cameras and photographic supplies; and holography.

For aerial photography see *43 Earth Resources and Remote Sensing*. For related information see also *06 Aircraft Instrumentation*, and *19 Spacecraft Instrumentation*.

N90-12904*# National Aeronautics and Space Administration. Ames Research Center, Moffett Field, CA.

CATADIOPTRIC OPTICS FOR LASER DOPPLER VELOCIMETER APPLICATIONS

Stephen E. Dunagan 1 Oct. 1989 28 p

(NASA-TM-102210; A-89201; NAS 1.15:102210) Avail: NTIS HC A03/MF A01 CSCL 20E

In the design of a laser velocimeter system, attention must be given to the performance of the optical elements in their two principal tasks: focusing laser radiation into the probe volume, and collecting the scattered light. For large aperture applications, custom lens design and fabrication costs, long optical path requirements, and chromatic aberration (for two color operation) can be problematic. The adaptation of low cost Schmidt-Cassegrain astronomical telescopes to perform these laser beam manipulation and scattered light collection tasks is examined. A generic telescope design is analyzed using ray tracing and Gaussian beam propagation theory, and a simple modification procedure for converting from infinite to near unity conjugate ratio operation with image quality near the diffraction limit was identified. Modification requirements and performance are predicted for a range of geometries. Finally, a 200-mm-aperture telescope was modified for f/10 operation; performance data for this modified optic for both laser beam focusing and scattered light collection tasks agree well with predictions. Author

N90-12905# Royal Signals and Radar Establishment, Malvern (England).

READOUT AND SIGNAL CONDITIONING FOR A LINEAR PYROELECTRIC ARRAY

P. A. Manning Aug. 1988 23 p

(RSRE-Memo-4102; BR109769; ETN-89-95003) Copyright Avail: NTIS HC A03/MF A01

An infrared imaging system using a pyroelectric detector and image difference processing is designed, built and assessed. A sensitivity of 0.25 K at 50 Hz, is obtained. No cooling and low electrical power input are required. It is a low cost system. It has the ability to simply trade off chopping rate against sensitivity. It is shown that the sensitivity extends to a few tens of milli-degrees. The techniques described make the use of thermal imaging possible in a wide range of applications ESA

N90-12906# Institut Franco-Allemand de Recherches, Saint-Louis (France).

IMPROVEMENT OF ULTRASHORT PULSED LASER SHADOWGRAPH PHOTOGRAPHY BY MEANS OF OPTICAL FILTERS [AMELIORATION DES OMBROSCOPIES COHERENTES PAR FILTRAGE OPTIQUE]

H. Royer 22 Jun. 1988 8 p In FRENCH Presented at the Conference on Visualization et Traitement d'Images, Belfort, France, 20 May 1988

(ISL-CO-215/88; ETN-89-95030) Avail: NTIS HC A02/MF A01

The use of optical filters to diminish the perturbations caused by reflected light of laser beams is described. Techniques of reducing diffraction perturbations at the edge of images in shadowgraph photography are investigated. It is concluded that the use of optical filters to overcome both of these problems can be carried out simply even by someone with very little experience. A comparison between manual and computer choice of filtration is presented. ESA

N90-12907# Centre Technique des Industries Mecaniques, Senlis (France).

VIBRATION INTENSITY. EVALUATION OF A REMOTE MEASURING SYSTEM Final Report [INTENSITE VIBRATOIRE. EVALUATION D'UN SYSTEME DE MESURE SANS CONTACT]

Xavier Carniel 15 Mar. 1989 82 p Partly in ENGLISH and FRENCH

(CETIM-110430; ETN-89-95050) Copyright Avail: NTIS HC A05/MF A01

Two differential laser vibrometers are compared to more classic vibration measuring instruments. A prototype differential laser vibrometer produced by the Centre Technique des Industries Mechaniques (CETIM) and the Photonetics company is tested. A system made up of two Polytec vibrometers is also tested. The Polytec vibrometer is the most accurate. It is a compact tool and uses fiber optic technology which allows positioning of the receptor heads at two neighboring points at the surface of the liquid studied. This type of differential laser vibrometer is shown to give better results than any inductor capacitor or ultrasound system. ESA

N90-12908# Massachusetts Inst. of Tech., Cambridge. Artificial Intelligence Lab.

HEIGHT AND GRADIENT FROM SHADING Memorandum Report

Berthold K. P. Horn May 1989 65 p

(Contract N00014-85-K-0124)

(AD-A212338; AI-M-1105) Avail: NTIS HC A04/MF A01 CSCL 08/2

The method described here for recovering the shape of a surface from a shaded image can deal with complex, wrinkled surfaces. Integrability can be enforced easily because both surface height and gradient are represented (A gradient field is integrable if it is the gradient of some surface height function). The robustness of the method stems in part from linearization of the reflectance map about the current estimate of the surface orientation at each picture cell (The reflectance map gives the dependence of scene radiance on the gradient; or, equivalently, surface orientation). The new scheme can find an extract solution of a given shape-from-shading problem even though a regularizing term is scheduled. GRA

N90-12909# Naval Research Lab., Washington, DC. Beam Physics Branch.

SCALING OF AN 85 GHz GYROTRON TO OPERATE AT 94 GHz

G. Bergeron, M. Czarnaski (JAYCOR, Vienna, VA.), and M. Rhinewine 6 Sep. 1989 36 p

(AD-A212756; NRL-MR-6513) Avail: NTIS HC A03/MF A01 CSCL 09/1

A description is presented for a 94 GHz, 70 kV gyrotron operating in the TE13 mode was designed and built. The novel

feature of the design is that it was based to a large degree on a previously built gyrotron that operated at a lower frequency. The highest efficiency achieved was 32 percent at 4A which agrees well with theoretical predictions. The highest power measured was 135 kW at 12 A. GRA

N90-12910# Rome Air Development Center, Griffiss AFB, NY.
CHARACTERIZATION OF LIQUID CRYSTAL DISPLAYS FOR OPTICAL SIGNAL PROCESSING APPLICATIONS Final Report
Dennis M. Blanchard and Michael J. Ward Aug. 1989 29 p
(AD-A212832; RADC-TR-89-226) Avail: NTIS HC A03/MF A01 CSCL 09/5

Characterization and analysis of the liquid crystal displays (LCD) used in liquid crystal televisions for possible use as economical spatial light modulators has been performed. Results are presented of research into LCDs with recommendations for possible applications. This study measured pixel array dimensions; transmission as a function of wavelength, bias voltage, and video voltage; response time; and the optical losses and phase distortion of the LCD. We discuss the usefulness of the LCD as a variable attenuator and as an adaptive wavefront compensator, and ongoing efforts to use the device as a 1-D spatial light modulator in an optical signal processing system. GRA

N90-12911# Massachusetts Inst. of Tech., Cambridge. Research Lab. of Electronics.
MARK-3 INTERFEROMETER Progress Report, 1 Apr. 1988 - 30 Jun. 1989
David H. Staelin, John W. Barrett, Edward J. Kim, and Howard R. Stuart 25 Sep. 1989 8 p
(Contract N00014-88-K-2016)
(AD-A213155) Avail: NTIS HC A02/MF A01 CSCL 03/1

The development and testing of the Mark-3 stellar interferometer is considered. The instrument employs a two color technique to reduce position errors due to atmospheric turbulence, and can operate with four possible baseline configurations ranging from 9 to 20 meters. Despite its function as a technology development platform, it is also capable of stellar separation and stellar diameter measurements with nearly unprecedented accuracy and sensitivity. The major contributions are the development of a dispersed-fringe group delay measurement system which can boost the system sensitivity by several stellar magnitudes, and the initial stages of development of an infrared capability, which should increase the future scientific interest of the facility. GRA

N90-12912# San Diego State Univ., CA.
PHOTOELECTRON PUMPED PHOSPHORS Final Report, 25 Apr. 1987 - 31 Jan. 1988
Jul. 1989 82 p
(Contract N66001-85-D-0203)
(AD-A213202; NOSC-TD-1601) Avail: NTIS HC A05/MF A01 CSCL 14/2

The investigation of cathodophosphors was undertaken in connection with the development of optical devices for the detection of long wavelength photons in which the initial photon-to-electron detection is performed by an optical diode. Then the photoelectrons being accelerated by the electric field penetrate into a phosphor screen and the screen produces multiple photons which are detected by a (close coupled) photomultiplier. The results are presented of a comprehensive analysis and systematization of the data relevant to the fast and very fast commercially available phosphors and developmental works on improved materials and processes in the field of phosphors, especially cathodophosphors. The investigation included analysis of II-VI phosphors, alkaline-earth chalcogenides, silicates, garnets, halides, and some ternary compounds with diamond-like crystal structure. The investigation included, also, analysis of data regarding the activators and coactivators as well as mixtures of phosphors with optically transparent conductive powders for the low energy electron cathodoluminescence. GRA

N90-12527*# National Aeronautics and Space Administration. Langley Research Center, Hampton, VA.
RECENT TESTS AT LANGLEY WITH A UNIVERSITY OF TENNESSEE SPACE INSTITUTE (UTSI) SKIN FRICTION BALANCE
Pierce L. Lawing, A. D. Vakili, and J. M. Wu (Tennessee Univ. Space Inst., Tullahoma.) *In its* Research in Natural Laminar Flow and Laminar-Flow Control, Part 2 Dec. 1987 p 407-411
(For primary document see N90-12519 04-02)
Avail: NTIS HC A15/MF A02 CSCL 14B

36 LASERS AND MASERS

Includes parametric amplifiers.
For related information see also *76 Solid-State Physics.*

N90-12913# Naval Weapons Center, China Lake, CA.
LASER INDUCED DAMAGE IN OPTICAL MATERIALS: 1987 Final Report
Harold E. Bennett, ed., Arthur H. Guenther, ed., David Milam, ed., Brian E. Newnam, ed., and M. J. Soileau, ed. (University of Central Florida, Orlando.) Oct. 1988 653 p Proceedings of Symposium on Optical Materials for High-Power Lasers, Boulder, CO, 26-28 Oct. 1987 Sponsored by National Inst. of Standards and Technology, Boulder, CO; ONR, Washington, DC; DOE, Washington, DC; DARPA, Washington, DC; AFOSR, Washington, DC Prepared in cooperation with ASTM, Philadelphia, PA
(PB89-221162; NIST/SP-756; LC-88-600576) Avail: NTIS HC A99/MF A04; also available SOD HC $30.00 as 003-003-02929-7 CSCL 20E

The Nineteenth Annual Symposium on Optical Materials for High-Power Lasers (Boulder Damage Symposium) was divided into sessions concerning Materials and Measurements, Mirrors and Surfaces, Thin Films, and, finally, Fundamental Mechanisms. As in previous years, the emphasis of the papers presented at the Symposium was directed toward new frontiers and new developments. Particular emphasis was given to materials for high power systems. The wavelength range of prime interest was from 10.6 micrometers to the UV region. Highlights included surface characterization, thin film substrate boundaries, and advances in fundamental laser-matter threshold interactions and mechanisms. The scaling of damage thresholds with pulse duration, focal area, and wavelength was discussed in detail. GRA

N90-12914# Argonne National Lab., IL.
B FACTORY VIA CONVERSION OF 1 TeV ELECTRON BEAMS INTO 1 TeV PHOTON BEAMS
Sekazi K. Mtingwa and Mark Strikman (Leningrad Nuclear Physics Inst., USSR) 1989 10 p Presented at the Workshop on B-factories and Related Issues, Blois, France, 26 Jun. - 1 Jul. 1989
(Contract W-31-109-eng-38)
(DE89-017692; CONF-8906210-2) Avail: NTIS HC A02/MF A01

Formulae were derived which describe the interaction of laser beams with electron beams. Specializing to the case of 1 TeV electron beams from the future generation of electron linear accelerators, the production rate of backscattered 1 TeV photons was calculated, and using these photons, it is shown that it is possible to organize the photoproduction of beauty particles so as to measure 10 sup 9 b(bar b) pairs per year. This should be adequate to study rare decays and CP violation in B meson decay. DOE

N90-12915# Massachusetts Inst. of Tech., Lexington. Lincoln Lab.
DESIGN AND PERFORMANCE OF AN ON-SATELLITE LASER DIAGNOSTIC SYSTEM FOR A FREE SPACE OPTICAL HETERODYNE FREQUENCY-SHIFT-KEYED COMMUNICATION SYSTEM
V. Jayaraman, E. S. Kintzer, J. G. Garcia, and A. D. Pillsbury 11

Jul. 1989 20 p
(AD-A211986; TR-850; ESD-TR-89-111) Avail: NTIS HC A03/MF A01 CSCL 25/5

The advent of space-based coherent diode laser communication systems requires development of space-qualified laser diagnostics to make these systems robust in face of aging laser parameters. This report describes the packaging and performance of a diagnostic system which sets the wavelength, tone spacing, and optical power of a directly modulated frequency-shift-keyed GaAlAs laser transmitter. GRA

N90-12916# Aerospace Corp., El Segundo, CA. Aerophysics Lab.
PHOTODISSOCIATION OF XeF2 (XENON DIFLUORIDE) AT 193 nm
Jerry F. Bott, Raymond F. Heidner, John S. Holloway, and John B. Koffend 30 Jun. 1989 24 p
(Contract F04701-88-C-0089)
(AD-A211663; TR-0089(4930-04)-1; SD-TR-89-41) Avail: NTIS HC A03/MF A01 CSCL 07/5

Interest in the spectroscopy of xenon difluoride (XeF2) was stimulated by the xenon fluoride (XeF) laser, which operates on the B-X transitions at 351 and 353 nm and the C-A transitions at 483 nm. The vacuum ultraviolet (VUV) photolysis of XeF2 can be used either to obtain laser action on these transitions or to produce the several electronic states of XeF for kinetic studies. The XeF2 photodissociation laser has been pumped by UV sources, such as discharges initiated by exploding wires, UV radiation emitted by Xe2 excited by an electron beam, and sliding surface discharges. Modeling the performance of the XeF laser, requires rate coefficients for the kinetic processes that produce and remove the vibronic levels of the upper electronic state. The absorption coefficient of XeF2 has been measured at 193, 206, and 253 nm. The present measurements of XeF2 absorption of 193 and 253 nm appear to resolve the discrepancy in those absorption measurements. Adjusting the data of the two previous investigations to match the values at these two wavelengths brings the two sets of measured absorption coefficients into agreement in the overlapping wavelength interval, 203 to 210 nm. It was determined experimentally that one molecule of XeF2 is dissociated for each photon absorbed at 193 nm. GRA

N90-12917# National Facility for Use of Intensive Lasers, Palaiseau (France).
LECTURES ON X RAY LASERS
Pierre Jaegle 1988 37 p Presented at the Conference on Atomic Physics of Highly-Ionized Atoms, Cargese, Italy, 5-17 Jun. 1988
(Contract DRET-85-1437)
(ETN-89-95516) Avail: NTIS HC A03/MF A01

The x ray emission from the multicharged ions in laser produced plasmas is discussed. Experiments and calculations on plasma temperature, density distribution, time evolution, integrated radiative properties, and line shape perturbation are presented. Regarding x ray laser pumping, experiments set off two types of mechanisms amongst many possible theoretical schemes. Experiments with Ne- and Ni-like ions are considered. It is shown that Ne-like selenium provides a gain coefficient of 5 cm; that Ni-like ions allow this scheme to be extended to wavelengths below 100 angstroms. X ray lasers are up to now the brightest available x ray sources in laboratory. ESA

N90-12918# Rolls-Royce Ltd., Derby (England). Advanced Research Lab.
APPLICATION OF A COPPER VAPOUR LASER TO INVESTIGATION OF SHOCK AND BLADE INTERACTION IN A SHOCK TUBE
R. J. Parker and J. B. Brownell 15 Mar. 1989 17 p Presented at the 9th Symposium on Measuring Techniques for Transonic and Supersonic Flows in Cascades and Turbomachines, Oxford, England, Mar. 1988
(PNR90578; ETN-89-95558) Copyright Avail: NTIS HC A03/MF A01

A shock tube is used to simulate the behavior of an aeroengine compressor stator vane during surge. Stator vanes are tested both singly and in a cascade to observe their dynamic behavior under loading from a backward traveling shockwave. Conventional instrumentation is augmented by two optical techniques. Shadowgraph flow visualization allows the shock front transition through the cascade to be visualized, while optical grid projection allows the dynamic reaction of the vane to be measured. For both optical techniques a novel light source is employed. A copper vapor laser is used, providing an intense train of short optical pulses capable of freezing these fast-moving phenomena. The experimental optical equipment is described and the results of the optical measurements are presented and briefly discussed. ESA

N90-12919# Deutsche Forschungs- und Versuchsanstalt fuer Luft- und Raumfahrt, Stuttgart (Germany, F.R.). Inst. fuer Technische Physik.
MICROWAVE EXCITATION OF OXYGEN O2 (DELTA 1) FOR AN OXYGEN-IODINE LASER
Kerry Swift Mar. 1989 42 p
(DFVLR-FB-89-23; ISSN-0171-1342; ETN-89-95832) Avail: NTIS HC A03/MF A01; DFVLR, VB-PL-DO, Postfach 90 60 58, 5000 Cologne, Fed. Republic of Germany, 17.50 Deutsche marks

Supersonic cooling of laser gas to allow operation of an oxygen-iodine laser is investigated. The amount of oxygen that can be excited to a metastable state by an electric discharge is measured spectroscopically. Careful optimization of operation parameters could result in sufficiently high values of metastable oxygen molecules. A subsequent supersonic expansion would make the operation of such an oxygen-iodine laser possible. Uses of these lasers in material processing, inertial confinement fusion, and weapons applications, are discussed. ESA

N90-12920# Optical Society of America, Washington, DC.
TUNABLE SOLID STATE LASERS CONFERENCE EDITION: TUNABLE SOLID STATE LASERS TOPICAL MEETING Final Report, 30 Aug. 1988 - 30 Aug. 1989
30 Aug. 1989 243 p Meeting held in North Falmouth, MA, 1-3 May 1989; sponsored by Optical Society of America and Lasers and Electro-Optics Society of IEEE
(Contract N00014-88-J-1207; AF-AFOSR-0012-84)
(AD-A212292; ISBN-1-55752-090-9; LC-88-62706) Avail: NTIS HC A11/MF A01 CSCL 09/3

Progress and interest in solid state lasers generally, and in tunable solid state lasers specifically, continues to expand. Applications of these lasers include spectroscopy, remote sensing, ranging and imaging, and medicine. New solid state materials are providing lasers with higher output power, broader tunability, and more efficient pumping schemes. The quantum electronics and crystal chemistry properties of these new materials are leading to enhanced laser performance. At the meeting, topics included sapphire, novel laser schemes, Cr lasers, forsterite and excited state absorption, solid state lasers for specialized applications, alexandrite lasers, Cr related issues, diode pumped lasers, nonlinear frequency conversion, 1.3 micron Nd lasers, infrared lasers and energy transfer, 2-micron lasers, rare earth laser materials, and Er lasers. GRA

N90-12921# Texas Univ., Dallas. Center for Quantum Electronics.
PROOF OF THE FEASIBILITY OF COHERENT AND INCOHERENT SCHEMES FOR PUMPING A GAMMA-RAY LASER Annual Technical Progress Report, 1 Apr. 1988 - 31 Mar. 1989
Carl B. Collins Jun. 1989 223 p
(Contract N00014-86-C-2488)
(AD-A212315; GRL/8805) Avail: NTIS HC A10/MF A02 CSCL 09/3

This report continues to focus upon the approach that is the nuclear analog to the ruby laser. It embodies the simplest concepts for a gamma-ray laser and not surprisingly, the greatest rate of achievement in the quest for a subAngstrom laser continues in

that direction. For ruby the identification and exploitation of a band width funnel were the critical keys in the development of the first laser. There was a broad absorption band linked through efficient cascading to the narrow laser level. Determination of Gateway States in 197Au with a Compton Gamma Ray; Determination of Photoexcitation Cross Sections for 176Lu (Gamma Gamma) 176Lu(m) using A 6 MeV Bremsstrahlung Source; Accelerated Decay of 180a (m) and 176Lu in Stellar Interiors through (Gamma Gamma) Reactions; Spectral Characterization of Intense, Short Duration Bremsstrahlung Pulses with Nuclear Photoactivation Techniques; The use of a Compton Spectrograph/Monochromator for the Photoactivation of Nuclei Into Metastable States; Photoexcitation of Nuclear Isomers by (Gamma Gamma) Reactions through Relatively Unhindered Transitions Accessed with Bremsstrahlung from Medical Linear Accelerators; and Limits on Neutron Activation Interferences in Photoactivation Cross-Section Measurements in the 1.5 to 6 MeV Range are examined. GRA

N90-12922# Naval Research Lab., Washington, DC. Beam Physics Branch.

RADIO FREQUENCY LINAC DRIVEN FREE-ELECTRON LASER CONFIGURATIONS Memorandum Report

C. M. Tang, P. Sprangle, A. Ting, and B. Hafizi (Science Applications International Corp., McLean, VA.) 7 Sep. 1989 33 p Sponsored by ONR

(AD-A212572; NRL-MR-6390) Avail: NTIS HC A03/MF A01 CSCL 09/3

Recent developments in accelerator technology and the optical guiding property of the Free Electron Laser (FEL) radiation indicate that the RF linacs may be a strong contender for driving high energy power FEL amplifiers. We discuss two RF linac driven FEL configurations: the Master Oscillator Power Amplifier (MOPA) and the Single Stage Power Amplifier (SSPA). Our numerical results are obtained using the Source Dependent Expansion (SDE) method in the computer SHERA. The SDE method and the code SHERA are discussed and illustrations of the MOPA and SSPA configurations presented. GRA

N90-12923# Naval Research Lab., Washington, DC. Plasma Theory Branch.

CAVITY EIGENMODES FOR THE NIST/NRL (NATIONAL INSTITUTE OF STANDARDS AND TECHNOLOGY/NAVAL RESEARCH LABORATORY) FREE ELECTRON LASER Interim Report

S. Riyopoulos (Science Applications International Corp., McLean, VA.) and C. M. Tang 5 Sep. 1989 43 p

(AD-A212706; NRL-MR-6522) Avail: NTIS HC A03/MF A01 CSCL 09/3

The cavity transfer matrix for the round trip of a light pulse in the optical resonator of the National Institute of Standards and Technology (NIST)/Naval Research Laboratory (NRL) Free Electron Laser (FEL) oscillator is derived. The cavity eigenmodes and the corresponding eigenvalues are obtained, using an expansion in Gaussian-Laguerre vacuum modes, by numerical diagonalization. The fraction power loss per eigenmode, caused by the finite sizes of the cavity mirrors and apertures are determined. It is found that the losses are very small over the entire wavelength regime of operation. GRA

N90-12924# Texas Univ. at Dallas, Richardson. Center for Quantum Electronics.

PROOF OF THE FEASIBILITY OF COHERENT AND INCOHERENT SCHEMES FOR PUMPING A GAMMA-RAY LASER Quarterly Progress Report, 1 Apr. - 30 Jun. 1989

Carl B. Collins Jul. 1989 62 p

(Contract N00014-86-C-2488)

(AD-A212882; GRL/8901) Avail: NTIS HC A04/MF A01 CSCL 09/3

Recent approaches to the problem of the gamma ray laser have focused upon upconversion techniques in which metastable nuclei are pumped with long wavelength radiation. At the nuclear level the storage of energy can approach tera-Joules per liter for thousands of years. However, any plan to use such a resource for a gamma ray laser poses problems of a broad interdisciplinary nature requiring the fusion of concepts taken from relatively unrelated fields of physics. Areas of discussion are: photoexcitation of nuclear isomers with the DNA/aurora nuclear; and adaptation of a fixed energy electron accelerator to produce variable endpoint bremsstrahlung. GRA

N90-12925# Columbia Univ., New York, NY. Plasma Physics Lab.

THEORETICAL AND EXPERIMENTAL RESEARCH ON A MILLIMETER-WAVELENGTH FREE-ELECTRON LASER Final Report, 1979 - 1988

Thomas C. Marshall Sep. 1989 96 p

(Contract N00014-79-C-0769)

(AD-A213321; Rept-115) Avail: NTIS HC A05/MF A01 CSCL 09/3

The Columbia Free Electron Laser is summarized with a selection of key reprints. Topics include: gain and wavelength studies, Thomson-scattering diagnostics for electron beam momentum-spread, efficiency-enhancement experiments, theory and experiments on optical guiding and sidebands; papers describing the first results from the new FEL facility and other being a theory of beam temperature effects upon the gain of an FEL (one of the first of several such studies that have been made by several groups); a pair of papers discussing results from a type of FEL which has since become known as a CARM; the results of a CO2 laser - Thomson backscattering experiment determined the momentum spread of the electron beam in the FEL; and the operation of the FEL oscillator with a tapered undulator is reported in which not only efficiency enhancement but also sideband power reduction was obtained. The theory of optical guiding is covered in the Raman REL presenting experimental evidence that the optical power profile is modified by optical guiding as it occurs in the overmoded waveguide system. GRA

N90-12525*# National Aeronautics and Space Administration. Langley Research Center, Hampton, VA.

THREE-COMPONENT LASER DOPPLER VELOCIMETER MEASUREMENTS IN A JUNCTURE FLOW

L. R. Kubendran and Jim F. Meyers *In its* Research in Natural Laminar Flow and Laminar-Flow Control, Part 2 Dec. 1987 p 389-400 (For primary document see N90-12519 04-02)

Avail: NTIS HC A15/MF A02 CSCL 20E

37 MECHANICAL ENGINEERING

Includes auxiliary systems (nonpower); machine elements and processes; and mechanical equipment.

N90-12926 Ohio State Univ., Columbus.

ANALYSIS OF HIGH SPEED PNEUMATIC ACTUATION SYSTEMS UNDER ROTARY DIRECTIONAL ON-OFF FLOW CONTROL Ph.D. Thesis

Cengiz Osman Kunt 1988 154 p

Avail: Univ. Microfilms Order No. DA8907250

The open loop, pneumatic motion control system comprising a high speed on-off directional control valve (DCV), a linear actuator, and an inertial load was studied experimentally and theoretically. Due to the inherent limitations of the conventional sliding spool type DCVs at high cyclic speeds, new rotary valve (RV) prototypes are developed and examined. A nonlinear lumped-parameter dynamic model of the overall system with general RV kinematics and realistic fluid flow characteristics is developed to determine the controlled load motion in response to a specified RV spool displacement. A linear time varying (LTV) model is formulated for the analysis of such periodically excited pneumatic actuation systems. RV flow area variations as well as system operating points are approximated by staircase profiles. Using this model along with the Floquet Theory, a new and computationally efficient expanded state space approach is devised for the determination of the dynamic response. Using the LTV model and the expanded

state space approach, frequency response and stability characteristics of the 2 way RV controlled single acting cylinder are determined, and useful design information is obtained.
Dissert. Abstr.

N90-12927 Florida Univ., Gainesville.
KINEMATICS, SPECIAL CONFIGURATIONS AND PERFORMANCE EVALUATION OF SERIAL MANIPULATORS Ph.D. Thesis
Resit Soylu 1988 201 p
Avail: Univ. Microfilms Order No. DA8908283

The first major topic covered is the special (or singular) configurations of N degree of freedom (DOF) serial manipulators. These configurations are classified according to the number of degrees of freedom lost. This classification yields hypersurfaces in the joint space, the union of which is designated by HSC. An efficient methodology is developed for the identification of each such hypersurface via Screw Theory and Linear Algebra. The efficiency of this methodology stems from a novel theorem and the utilization of the minimal reference frames which depend on the type and sequence of the joints. Various novel concepts associated with the HSC are also introduced and it is demonstrated that these concepts are useful in the kinematic design, analysis, motion planning and control of manipulators. The second major topic discussed is the quantification of the freedom of the end effector for a 6 DOF manipulator. A computable measure, which includes joint limitations and scale, is introduced for this purpose. The computation of this measure is considerably simplified if the forward displacement mapping is one-to-one when restricted to a region which is, loosely speaking, bounded by the HSC. Sufficient conditions are derived for this useful property and simple expressions are obtained for the upper bound of the number of these regions. The reverse velocity analysis of 6 DOF manipulators constitutes the third topic. Efficient and systematic methods, applicable to any type of manipulator with or without any special geometry, are developed. The relations between the dimensions of the manipulator and the complexity of the reverse velocity analysis are also investigated. Further, an indepth analysis is presented of the Planar Wrist manipulators including workspace and closed-form reverse displacement analyses. Dissert. Abstr.

N90-12928# BDM Corp., Austin, TX.
A ROBOT WHICH WILL INVESTIGATE THE CONDITION OF UNDERGROUND PIPE Final Report, Mar. 1986 - Apr. 1988
J. P. Coose, B. Firey, and C. D. Zinsmeyer 17 Jun. 1988 43 p
(Contract GRI-5086-271-1226)
(PB89-230650; GRI-88/0258) Avail: NTIS HC A03/MF A01
CSCL 13I

The development of a robotic tool (mouse) to investigate the condition of underground pipe will reduce the maintenance cost and improve the safety of gas distribution systems by inspecting pipe from the inside and finding damage before leaks develop. The mouse is intended, eventually, to operate autonomously, traveling through a gas distribution system along a prescribed route. It will be configured to inspect for pipe defects appropriate to the type of pipe under inspection (cast iron, steel, or plastic) and will report defects and position to repair crews. The mouse may also be configured for other pipe activities such as distribution system mapping, visual inspection, or sensor deployment. Author

N90-12929# Lawrence Livermore National Lab., CA.
DESIGN AND PERFORMANCE OF AN OPTICAL MOUNT USING CROSS-FLEXURE PIVOTS
William J. Rundle (Martin Marietta Energy Systems, Inc., Livermore, CA.) 1 Jul. 1989 10 p Presented at the 33rd SPIE Annual International Technical Symposium on Optical and Optoelectronic Applied Science and Engineering, San Diego, CA, 6-11 Aug. 1989
(Contract W-7405-eng-48)
(DE89-017551; UCRL-100403; CONF-890836-13) Avail: NTIS HC A02/MF A01

The design of an optical mount using commercially available cross-flexure steel pivots is described. The pivots and their incorporation into a 5- (times) 10-inch rectangular optical mount are illustrated. Test data on this mount show acceptable thermal stability and thermal hysteresis for use in a laboratory optical system. The design is easily scaled to other optic sizes. DOE

N90-12930# Unilever Research, Merseyside (England). Dept. of Control Engineering.
SELF-TUNING CONTROL OF NONLINEAR ARMAX MODELS
K. R. Sales and S. A. Billings (Sheffield Univ., England) May 1989 28 p
(RR-362; ETN-89-95229) Avail: NTIS HC A03/MF A01

A control weighted self-tuning minimum-variance controller with a nonlinear difference equation structure is described. An extended recursive least squares estimation algorithm is employed to provide the adaptiveness. Performance analysis of the controller is discussed in terms of a cumulative loss function and high order correlation functions of the system input, output and residual sequences. Simulation results from an experiment using a model identified from a real system are provided. ESA

N90-12931# Sheffield Univ. (England). Dept. of Control Engineering.
NONLINEAR SYSTEMS AND KOLMOGOROV'S REPRESENTATION THEOREM
S. P. Banks May 1989 16 p
(RR-363; ETN-89-95230) Avail: NTIS HC A03/MF A01

A representation for discrete dynamical systems is presented by applying Komolgorov's representation theorem to the system functions. It is shown that any discrete system defined by continuous functions may be written in a separable form in which the defining equations consist of sum of functions of single variables. The stability of such systems is discussed while representing them in a quasi-linear form. Systems with controls are considered and a similar separable representation is obtained. The stability results are applied to this representation. ESA

N90-12932# Rolls-Royce Ltd., Derby (England).
DEMONSTRATION EPICYCLIC GEARBOX
Helen J. Travers, Andy Geer, Darren Shirley, and Richard Brooks 1 Nov. 1988 14 p Submitted for publication
(PNR90567; ETN-89-95552) Copyright Avail: NTIS HC A03/MF A01

The production of a simple model which accurately simulates the dynamic behavior of an epicyclic gear train is described. The analytical data concerning the selfaligning properties of the floating gear train are extracted. The goal of the model is to study how to avoid breakdown of the force system, ensuring load sharing under conditions of light or zero torque load. Once a breakdown occurs the gearbox begins to run out of alignment, leading to high unbalance forces. ESA

N90-12933# Rolls-Royce Ltd., Derby (England).
THE NATURE AND CONTROL OF SKIDDING IN LIGHTLY LOADED INTERSHAFT BEARINGS
K. V. Blanchard and G. A. Halls 17 May 1989 17 p Presented at the I. Mech. E. Aerospace Bearing Technology, Solihull, England, 17 May 1989
(PNR90591; ETN-89-95563) Copyright Avail: NTIS HC A03/MF A01

The dynamics of skid failure in the intershaft mainline bearing of an aero gas turbine engine are described. The test rig and research program are outlined. The effects of axial load, radial load, shaft speeds, oil flow and shaft and cage out of balance are analyzed in terms of their effect on skid failure of the bearing. A solution to the skidding problem using case out of balance is presented. The solution is demonstrated on the test rig and substantiated by service records. ESA

N90-12934# Rolls-Royce Ltd., Derby (England).
NON LINEAR VIBRATIONS IN A DRIVE TRAIN WHEN COUPLED TO CONSTANT TORQUE AND CONSTANT POWER LOADS
D. M. Gainford 10 Jul. 1989 7 p Presented at the 25th AIAA/ASME/SAE/ASEE Joint Propulsion Conference, Monterey,

CA, 10-12 Jul. 1989
(PNR90593; ETN-89-95564) Copyright Avail: NTIS HC A02/MF A01

A generalized model for a gearbox having a flexible element and a backlash component is presented. The dynamics of such a system when coupled to a constant torque load are analyzed using the phase-plane technique, and it is shown that the frequency of vibrations is amplitude-dependent but lies between predictable upper and lower bounds. When coupled to a contant power load (which is reflected into the system as having a negative damping characteristic), large amplitude vibrations can build up. Ways of reducing such vibrations and establishing a criterion for matching a gearbox to a constant power load are investigated. ESA

N90-12935*# Mechanical Technology, Inc., Latham, NY.
CRYOSTATLESS HIGH TEMPERATURE SUPERCURRENT BEARINGS FOR ROCKET ENGINE TURBOPUMPS
Dantam K. Rao and James F. Dill Sep. 1989 97 p
(NASA Order H-80591-B)
(NASA-CR-183807; NAS 1.26:183807; MTI-89TR40) Avail: NTIS HC A05/MF A01 CSCL 13I

The rocket engine systems examined include SSME, ALS, and CTV systems. The liquid hydrogen turbopumps in the SSME and ALS vehicle systems are identified as potentially attractive candidates for development of Supercurrent Bearings since the temperatures around the bearings is about 30 K, which is considerably lower than the 95 K transition temperatures of HTS materials. At these temperatures, the current HTS materials are shown to be capable of developing significantly higher current densities. This higher current density capability makes the development of supercurrent bearings for rocket engines an attractive proposition. These supercurrent bearings are also shown to offer significant advantages over conventional bearings used in rocket engines. They can increase the life and reliability over rolling element bearings because of noncontact operation. They offer lower power loss over conventional fluid film bearings. Compared to conventional magnetic bearings, they can reduce the weight of controllers significantly, and require lower power because of the use of persistent currents. In addition, four technology areas that require further attention have been identified. These are: Supercurrent Bearing Conceptual Design Verification; HTS Magnet Fabrication and Testing; Cryosensors and Controller Development; and Rocket Engine Environmental Compatibility Testing. Author

N90-12936*# Ohio State Univ., Columbus. Dept. of Mechanical Engineering.
VIBRATION TRANSMISSION THROUGH ROLLING ELEMENT BEARINGS IN GEARED ROTOR SYSTEM, PART 1 Ph.D. Thesis Final Report
Rajendra Singh and Teik Chin Lim Dec. 1989 146 p
(Grant NAG3-773)
(NASA-CR-186093; NAS 1.26:186093) Avail: NTIS HC A07/MF A01 CSCL 13I

A mathematical model is proposed to examine the vibration transmission through rolling element bearings in geared rotor systems. Current bearing models, based on either ideal boundary conditions for the shaft or purely translational stiffness element description, cannot explain how the vibratory motion may be transmitted from the rotating shaft to the casing. This study clarifies this issue qualitatively and quantitatively by developing a comprehensive bearing stiffness matrix of dimension 6 model for the precision rolling element bearings from basic principles. The proposed bearing formulation is extended to analyze the overall geared rotor system dynamics including casing and mounts. The bearing stiffness matrix is included in discrete system models using lumped parameter and/or dynamic finite element techniques. Eigensolution and forced harmonic response due to rotating mass unbalance or kinematic transmission error excitation for a number of examples are computed. Author

N90-12937# National Telecommunications and Information Administration, Boulder, CO. Inst. for Telecommunication Sciences.
AUTOMATED STEERABLE NULLING ANTENNA PROCESSOR (SNAP) MODEL
Nicholas DeMinco Jul. 1989 27 p Sponsored by Army Signal Center, Fort Gordon, GA
(PB89-231740; NTIA-89-245) Avail: NTIS HC A03/MF A01 CSCL 13I

An adaptive antenna computer model that simulates the behavior of a steerable-nulling antenna processor (SNAP) in a jamming or interference environment is described. The model predicts the signal-to-(interference-plus-noise) ratio as a function of antenna parameters and interference environment. The model can be used to demonstrate the application of antennas with the SNAP implementation for obtaining increased spectrum utilization or improved performance in an interference or jamming environment. Author

N90-12938# Centre Technique des Industries Mecaniques, Saint Etienne (France).
COLD PRESS LUBRICATION: FINE TUNING OF THE CETIM FORGELUB TEST Final Report [LUBRIFICATION EN FORGE A FROID: MISE AU POINT DE L'ESSAI CETIM-FORGELUB]
G. Batit Feb. 1989 49 p In FRENCH
(CETIM-105160; ETN-89-95039) Copyright Avail: NTIS HC A03/MF A01

A series of tests carried out to determine the efficiency of different lubricants used in cold press operations are described. These lubricant tests, grouped under the name CETIM (Centre Technique des Industries Mechaniques) Forgelub involve submitting a lubricant to conditions one would find in an industrial cold press environment. High pressure, significant spreading of the initially lubricated surface, and shear forces caused by the displacement of the metal sheet in relation to the tool press, are all conditions reproduced in these tests. After the test, the properties of the residual lubricant films are analyzed. Complete results of the testing of several solid lubricants commonly used in cold pressing are provided. ESA

N90-12939# Centre Technique des Industries Mecaniques, Senlis (France).
IMPROVEMENT OF RULES RELATING TO CLAMP CALCULATIONS [AMELIORATION DES REGLES RELATIVES AUX CALCULS DES BRIDES]
M. Robert 2 Dec. 1988 46 p In FRENCH
(CETIM-110610; NTI-88/55; ETN-89-95051) Copyright Avail: NTIS HC A03/MF A01

A summary of research carried out since 1974 in trying to develop new joint clamp codes is described. The increasing diversity in joint types and the increased seal requirements led the Welding Research Council (WRC) in 1974 to call for a complete experimental program in order to develop new codes. This Milestone Gasket Test Program (MGTP) identified three intrinsic parameters on a joint, B, d and S, from which it is possible to deduct the coefficients m and y to be used in clamp calculations. The research carried out in establishing these parameters is described. ESA

N90-12940# Department of the Navy, Washington, DC.
STRUCTURAL VIBRATION AND SHOCK ISOLATOR Patent Application
Ronald E. Waclawik, inventor (to Navy) 1 Jun. 1989 16 p
(AD-D014202; US-Patent-Appl-SN-360179) Avail: NTIS CSCL 13/13

This patent application is co-pending with related patent application entitled Structural Vibration and Shock Isolation in a High Pressure Environment by the same inventor filed on the same date as this application. The present invention generally relates to piping systems and more particularly a piping system wherein one end is isolated from the shock and vibration of the other end. The present invention provides structural vibration and shock isolation between inlet and outlet sections of a fluid system

having high axial loads. The outlet section has flanged arrangement in which isolation material components are placed both above and below the flange. The inlet section comprises a fluid conducting pipe. GRA

N90-12941# Massachusetts Inst. of Tech., Cambridge. Artificial Intelligence Lab.
SQUIRT: THE PROTOTYPICAL MOBILE ROBOT FOR AUTONOMOUS GRADUATE STUDENTS Memorandum Report
Anita M. Flynn, Rodney A. Brooks, William M. Wells, III, and David S. Barrett Jul. 1989 33 p
(Contracts N00014-86-K-0685; N00014-85-K-0124)
(AD-A212337; AI-M-1120) Avail: NTIS HC A03/MF A01 CSCL 12/9

An exercise is described in building a complete robot aimed at being as small as possible but using off the shelf components exclusively. The results is an autonomous mobile robot slightly larger than one cubic inch which incorporates sensing, actuation, onboard computation and onboard power supplies. Nicknamed Squirt, this robot acts as a bug, hiding in dark corners and venturing out in the direction of last heard noises, only moving after the noises are long gone. GRA

N90-12942# Leeds Univ. (England). Industrial Unit of Tribology.
THE 4TH US ARMY WORKSHOP ON LOW HEAT REJECTION ENGINES Sessions Report
31 Mar. 1989 15 p Workshop held in Leeds, England, 29-31 Mar. 1989
(Contract DAJA45-89-M-0043)
(AD-A212378; R/D-6149-AN-03) Avail: NTIS HC A03/MF A01 CSCL 21/7

There are a number of characteristics exhibited by ceramic materials which may provide potential benefits for the reciprocating internal combustion engine. However, the brittle nature of these materials together with a variability in strength has created difficulties in applying ceramic materials to the engine environment. Although a wide range of physical properties is available from contemporary ceramic materials, a material offering consistently high strength has yet to be developed. For sliding contact applications, desirable characteristics include good wear resistance, low friction, ability to join metals and good heat dissipation. Test results have shown that cam/follower components with cast iron cam sliding on a silicon nitride follower exhibit very low wear rates. The application of silicon carbide to face seals has also shown substantial reductions in both friction and wear when compared with conventional materials. The use of ceramic materials for in-cylinder components requires additional material characteristics such as high strength and low thermal conductivity. Another attractive application for ceramic materials has been the exhaust port liner. The primary requirements for this application are high thermal shock resistance and low thermal conductivity. Of all the materials evaluated, aluminum titanate has been found to exhibit the most attractive characteristics. GRA

N90-12943# Leeds Univ. (England). Industrial Unit of Tribology.
THE 4TH US ARMY WORKSHOP ON LOW HEAT REJECTION ENGINES
31 Mar. 1989 41 p Workshop held in Leeds, England, 29-31 Mar. 1989
(Contract DAJA45-89-M-0043)
(AD-A212379; R/D-6149-AN-03) Avail: NTIS HC A03/MF A01 CSCL 21/7

The paper describes the basic principles underlying the operation of low heat loss engines, and the magnitude of the efficiency improvements which are theoretically achievable. The effect of varying degrees of thermal insulation on various operating parameters is examined in some detail, as is the relationship between degree of insulation and ceramic coating thickness. The effect on ceramic materials of severe surface temperature oscillations and the resultant thermal stress gradients is also discussed. In the following section, the paper describes methods of construction adopted both for ceramic inserts and coatings, and rig tests for the assessment of thermal fatigue under both load and firing cycling. The paper does not attempt to draw any general conclusions. GRA

N90-12944# Carnegie-Mellon Univ., Pittsburgh, PA. Robotics Inst.
DEVELOPMENT OF AN INTEGRATED MOBILE ROBOT SYSTEM AT CMU (CARNEGIE-MELLON UNIVERSITY) Annual Report, Jul. 1987 - Jun. 1988
Steve Shafer and William Whittaker Jul. 1989 65 p
(Contract DACA76-86-C-0019; DARPA Order 5682)
(AD-A212555; CMU-RI-TR-89-22; ETL-0546) Avail: NTIS HC A04/MF A01 CSCL 12/9

The development is described of an integrated mobile robot system. This program includes a broad agenda of research in the development of mobile robot vehicles, focused on the NAVLAB computer controlled van. The NAVLAV mobile robot vehicle was built previously, by outfitting a commercial truck chassis with computer controlled drive and steering controls and a set of on-board computer workstations. The NAVLAB serves as a mobile navigation laboratory that allows researchers to interact intensive with the system during testing and execution. This year has seen a continued evolution and improvement of the NAVLAB mechanism, sensors, controller, and Virtual Vehicle interface to higher level planning and perception software. Last year, as part of this research program, the CODGER Blackboard system was designed and implemented for robot perception and reasoning on a distributed collection of processors. This year, in response to the experience in using CODGER for mobile robot control, it was upgraded to deal with geometric models and uncertainty in perception and map data. To control the NAVLAB and Terregator mobile robot vehicles, the Driving Pipeline architecture last year was developed for coordinating road following, obstacle avoidance, and vehicle motion control. This hardware and software is the basis for the New Generation System (NGS) for robot vision and navigation, which integrates many independent technologies to produce an integrated mobile robot system. GRA

N90-12945# Carnegie-Mellon Univ., Pittsburgh, PA. Robotics Inst.
ACCELERATION SETS OF PLANAR MANIPULATORS. PART 1: THEORY
Yong-yil Kim and Subhas Desa Jul. 1989 57 p
(AD-A213162; CMU-RI-TR-89-16-Pt-1) Avail: NTIS HC A04/MF A01 CSCL 13/9

A systematic approach is developed for determining the acceleration capability and the acceleration properties of the end effector of a planar two degree-of-freedom manipulator. The acceleration of the end effector at a given configuration of the manipulator is a linear function of the actuator torques and a (nonlinear) quadratic function of the joint-velocities. By decomposing the functional relationships between the inputs (actuator torques and joint velocities) and the output (acceleration of the end effector into two fundamental mappings, a linear mapping between the actuator torque space and the acceleration space of the end effector and a quadratic (nonlinear) mapping between the joint velocity space and the mapping acceleration space of the end effector, and by deriving the properties of these two mappings, it is possible to determine the properties of all acceleration sets which are the images of the appropriate inputs sets under the two fundamental mappings. The determination of the properties of the quadratic mapping allows one to obtain analytic expressions relating important acceleration properties of the end effector to all the manipulator parameters and input variables of interest. GRA

38 QUALITY ASSURANCE AND RELIABILITY

Includes product sampling procedures and techniques; and quality control.

N90-12946# Chalmers Univ. of Technology, Goeteborg (Sweden). Dept. of Hydraulics.
ESTIMATING THE TIME TO FATIGUE FAILURE OF MOORING CABLES
Wilhelm Rankka 1989 102 p
(PB89-220677; SER-A-20) Avail: NTIS HC A06/MF A01 CSCL 14D

Two methods of calculating the time to fatigue failure of mooring cables are analyzed. The methods are based on the theory of cumulative damage and they are applied to the fatigue of catenary cables of wire rope caused by fluctuating axial load. To calculate the cable load, a time domain approach is used which includes a simple model of the viscous damping of the platform heave motion. The cable load time history is analyzed with the rain flow counting algorithm. GRA

N90-12947# Precision Acoustic Devices, Inc., Freemont, CA.
AN AIR COUPLED TRANSMISSION MODE ACOUSTIC MICROSCOPE FOR ON-LINE NON-DESTRUCTIVE EVALUATION Final Report, 1 Sep. 1988 - 28 Feb. 1989
John D. Fraser Aug. 1989 18 p
(Contract DAAL03-88-C-0025)
(AD-A211416; ARO-26007.1-EG-SBI) Avail: NTIS HC A03/MF A01 CSCL 14/2

The feasibility of using a transmission type ultrasonic microscope operating in air in the 1 MHz frequency range was demonstrated. Such systems can be used for in-process evaluation of many structural materials such as composites and green ceramics. Specialized ultrasonic transducers were built that are coupled to air using low acoustic impedance quarter wave plates made of silicone rubber. The feasibility of manufacturing more optimum materials for quarter wave matching was demonstrated. These transducers were capable of being driven at high voltage levels (1500 V) for highest possible transmission efficiency. The minimum insertion loss of these devices is 48 dB, and the 6 dB bandwidth is 6 percent. Experiments were begun on imaging in transmission mode with two transducers. It was possible to transmit and receive over distances of up to 8 inches in air. Although no actual imaging was done with the air transducers, the measured signal-to-noise ratio demonstrates that there is sufficient dynamic range to provide useful images of graphite epoxy laminates. A material with close to the correct acoustic impedance for quarter wave matching to air was made, and further process development will improve its uniformity. GRA

N90-12948 Department of the Navy, Washington, DC.
DEVICE FOR INSPECTION OF MATERIALS BY EDDY CURRENT METHODS Patent Application
Susan N. Vernon, inventor (to Navy) and Stephen S. Lane, inventor (to Navy) 30 Jun. 1989 17 p
(AD-D014205; US-Patent-Appl-SN-374212) Avail: NTIS HC A03/MF A01 CSCL 14/2

With the growing application of filament-wound conductive fiber reinforced composites, particularly in aerospace, there is an increasing demand for nondestructive methods to detect and measure fiber anomalies such as service-incurred broken fibers and fabrication-related variations in fiber volume fraction or fiber density. Eddy current technology is ideally suited to these tasks since it is the conductive fibers which carry most of the current (carbon-carbons) or all of the current (graphite epoxies). Eddy current transducers may be used alone or in various combinations. A particular transducer may be both the transmitter and the receiver if the transducer is operating in the reflection mode. GRA

N90-12802*# Jet Propulsion Lab., California Inst. of Tech., Pasadena.
A SIMPLE MODEL FOR DSS-14 OUTAGE TIMES
H. C. Rumsey, R. Stevens, and E. C. Posner *In its* The Telecommunications and Data Acquisition Report 15 Aug. 1989 p 202-206 (For primary document see N90-12786 04-32)
Avail: NTIS HC A11/MF A02 CSCL 14D

39 STRUCTURAL MECHANICS

Includes structural element design and weight analysis; fatigue; and thermal stress.

For applications see *05 Aircraft Design, Testing and Performance* and *18 Spacecraft Design, Testing and Performance.*

N90-12949 Florida Univ., Gainesville.
A TWO-DIMENSIONAL HYBRID EXPERIMENTAL-NUMERICAL TECHNIQUE FOR ELASTIC-PLASTIC STRESS ANALYSIS Ph.D. Thesis
James Sanford Sirkis 1988 163 p
Avail: Univ. Microfilms Order No. DA8908281

A 2-D hybrid experimental-numerical technique for elastic-plastic stress analysis is presented. This technique results from merging two relatively new technologies in engineering mechanics: boundary element methods and image processing. A syntactic pattern recognition scheme termed Displacement Pattern Matching (DPM) determines displacement boundary conditions to be used in an elastic-plastic boundary element (EPBEM) code. The result is an automated stress analysis tool. Displacement pattern matching is a process where displacements are measured by tracking an arbitrary array of black spots on a white specimen. The digitized images of the specimen are compared in a double exposure format to determine displacements. Displacement pattern matching is a full field technique, with spatial resolution on the order of .0001 inch. Displacement pattern matching supplies the actual specimen displacement increments to the von Mises, isotropic work hardening, boundary element code. Given these displacements and free surface conditions, EPBEM is able to incrementally calculate the internal state of stress at selected locations. Results obtained for a variety of geometries and loading conditions compared well with ANSYS finite element and selected published experimental solutions and therefore are encouraging.
Dissert. Abstr.

N90-12950*# National Aeronautics and Space Administration. Lewis Research Center, Cleveland, OH.
A THERMOELASTIC TRANSVERSELY ISOTROPIC THICK WALLED CYLINDER/DISK APPLICATION: AN ANALYTICAL SOLUTION AND STUDY
S. M. Arnold Oct. 1989 46 p
(NASA-TM-102320; E-5016; NAS 1.15:102320) Avail: NTIS HC A03/MF A01 CSCL 20K

A continuum theory is utilized to represent the thermoelastic behavior of a thick walled composite cylinder that can be idealized as transversely isotropic. A multiaxial statement of the constitutive theory employed is presented, as well as the out of the plane of isotropy, plane stress, and plane strain reductions. The derived analytical solution presented is valid for a cylindrical tube or thin disk with a concentric hole, subjected to internal and/or external pressure and a general radial temperature distribution. A specific problem examined is that of a thick walled cylinder subjected to an internal and external pressure loading and a linear radial temperature distribution. The results are expressed in nondimensional form and the effects on the response behavior are examined for various material properties, fiber orientation and types of loadings. Author

N90-12951# Army Lab. Command, Watertown, MA. Material Technology Lab.
PROCEEDINGS OF THE ARMY SYMPOSIUM ON SOLID MECHANICS, 1989: MECHANICS OF ENGINEERED MATERIALS AND APPLICATIONS Final Report
Apr. 1989 233 p Symposium held in Newport, RI, 16-18 May

1989
(AD-A211954; MTL-MS-89-1) Avail: NTIS HC A11/MF A02 CSCL 20/11

The 1989 Army Symposium on Solid Mechanics: Mechanics of Engineered Materials and Applications was the eleventh in a series of biennial symposia which has focused on solid mechanics research achievements impacting defense systems needs. The committee endeavored to organize a symposium which would emphasize the synergistic interplay between solid mechanics and materials science in the development and effective utilization of advanced structural materials. The plan called for papers on the wide range of advanced materials to include structural ceramics, metal matrix composites, organic matrix composites, modern metallic alloys, polymers, and hybrids. The goal was to have technical sessions comprised of contributed papers and presentations by invited researchers who have made substantial contributions to the theme area. GRA

N90-12952# Aeronautical Research Inst. of Sweden, Stockholm. Dept. of Structures.
POTENTIAL DIFFERENCE APPLIED TO THE MEASUREMENT OF SMALL FATIGUE CRACK GROWTH AT NOTCHES IN TI-6AL-4V
M. D. Halliday, A. F. Blom, and C. J. Beevers (Birmingham Univ., England) Feb. 1989 28 p
(Contract STU-88-89)
(FFA-TN-1989-09; ETN-89-95152) Avail: NTIS HC A03/MF A01

Several fatigue tests carried out on a Ti-6Al-4V alloy containing machined and polished notches to evaluate the growth of short cracks are described. The potential difference method is used, together with a surface replication technique, to characterize the crack growth. A range of current and potential probe geometries is examined and the results show that when conventional point contact probes are used the sensitivity is dependent upon the relative positions of the crack and the probes. Line contact probes along the edge of the notch provide a relatively constant sensitivity of the signal to crack area independent of crack position and so simplify calibration. Differences in fatigue crack growth response are obtained at different positions on the crack front and are interpreted in terms of crack closure. ESA

N90-12953# Aeronautical Research Inst. of Sweden, Stockholm. Dept. of Structures.
MULTILEVEL OPTIMIZATION WITH SYSTEM OPTSYS
Dag Wiklander Dec. 1988 82 p
(Contract STU-87-88)
(FFA-TN-1988-60; ETN-89-95163) Avail: NTIS HC A05/MF A01

A multilevel formulation is implemented in the structural optimization system (Optsys). This formulation decomposes local buckling of stiffened panels problems into a number of smaller optimization problems, which can be independently analyzed on a sub level. The main reason for using a multilevel optimization scheme is the increased efficiency in the solution of large optimization problems where very detailed structural modeling is needed. The multilevel system is well suited to match future computer architectures due to the parallel structure of the decomposed optimization problem. The Optsys system is ready for multilevel analysis of problems other than local buckling problems. ESA

N90-12954# Aeritalia S.p.A., Turin (Italy).
FATIGUE BEHAVIOR OF SPECIMENS UNDER COMPRESSION LOAD SPECTRA [COMPORTAMENTO A FATICA DI PROVINI INTAGLIATI SOTTOPOSTI A SPETTRO PREVALENTEMENTE IN COMPRESSIONE]
F. Staropoli 1987 18 p In ITALIAN Presented at the Associazione Italiana per la Fatica in Aeronautica, Milan, Italy, 16-17 Mar. 1987
(ETN-89-95207) Avail: NTIS HC A03/MF A01

The fatigue behavior of the Al-7075-T73 aluminum alloy used in structural elements of the Tornado aircraft is studied. The goal was to understand cracks developed on the upper skin panel of the aircraft, in regions of high stress concentration. The load spectra were mainly compression loads, and the specimens were designed for high stress concentration factor. The analysis of the cracks confirms the hypothesis that crack propagation will cease on exit from the high Kt region. ESA

N90-12955# Etablissement Technique Central de l'Armement, Arcueil (France). Dept. Physique des Surfaces.
ELASTIC INDENTATION FRACTURES Thesis - Ecole Nationale des Mines [FRACTURE D'INDENTATION ELASTIQUE]
Remi Mouginot 22 Nov. 1988 109 p In FRENCH
(Contract ETCA/CREA/PS-CI-048190)
(ETCA-88-R-116; ETN-89-95274) Avail: NTIS HC A06/MF A01

Cracking of fragile materials submitted to elastic impact is studied. The conditions of crack initiation and elastic deformation are discussed. The Griffith thermoelastic criterium is used to determine the site of crack initiation. To calculate the load that needs to be applied to initiate cracking and to take into account the material characteristics, the Poisson ratio is used. The limit in size beyond which the material is no longer elastic fragile, but becomes elastoplastic fragile is determined using the Kendall method. ESA

N90-12956# Institut National des Sciences Appliquees de Lyon, Villeurbanne (France). Lab. de Mecanique des Contacts.
UNILATERAL CONTACT ANALYSIS OF A CRACK WITH FRICTION. APPLICATIONS
M. C. Dubourg 1989 12 p In FRENCH; ENGLISH summary
(ETN-89-95511) Avail: NTIS HC A03/MF A01

The results of the unilateral contact analysis of a crack are reported. The aim of the study is a better understanding and modeling of phenomena such as crack initiation and propagation. Crack behavior is predicted using a mixed approach based on fracture and contact mechanics. The applications concern the propagation mode 2 and the stress intensity factor is given for different load natures. The influence of the crack angle, of its length, of the friction coefficient between the crack lips and of the loading are determined. ESA

N90-12957# Rolls-Royce Ltd., Derby (England). Advanced Research Lab.
OPTICAL TECHNIQUES FOR IN-PLANE STRAIN ANALYSIS IN AN INDUSTRIAL ENVIRONMENT
J. B. Brownell and R. J. Parker 14 Apr. 1989 18 p Presented at the Stress and Vibration Conference, London, England, 14 Mar. 1989 Submitted for publication Sponsored by the Ministry of Defence Procurement Executive, London, England
(PNR90601; RR(OH)1054; ETN-89-95572) Copyright Avail: NTIS HC A03/MF A01

In-plane strain analysis techniques are summarized. Results of some laboratory work with optical methods and the development of a software analysis package are described. The optical techniques are all interferometric in nature and generate fringe maps which contour the surface displacement of the test piece. The techniques are non-contacting, full field and very sensitive. Analysis of the fringes gives data on the surface displacement field and this data can be differentiated to yield strain data with very short gage lengths. The techniques are applicable to actual components and may provide data where other methods fail, such as residual creep strain measurement on turbine disk rig tests. ESA

N90-12958# Technische Univ., Delft (Netherlands). Faculty of Aerospace Engineering.
AN INVESTIGATION ON COMBINED EXTENSION AND BENDING OF THIN SHEETS WITH A CENTRAL CRACK
D. Chen Aug. 1988 39 p
(LR-561; ETN-89-95607) Avail: NTIS HC A03/MF A01

An engineering method for predicting fracture behavior of thin metal sheets in combined extension and bending stress conditions

using a new testing method called curvature effect testing system (CETS) is described. This method may contribute to a better understanding of the effects of the bending moment in the aircraft fuselage skin introduced by bending the skin sheets elastically from a flat condition into a curved condition during the assembly process. An improved fracture criteria for combined extension and bending of thin sheet is outlined. The bulge-out phenomenon is discussed. ESA

N90-12959*# Purdue Univ., West Lafayette, IN. Composite Materials Lab.
ORTHOTROPIC ELASTO-PLASTIC BEHAVIOR OF AS4/APC-2 THERMOPLASTIC COMPOSITE IN COMPRESSION
C. T. Sun and Y. Rui Apr. 1989 37 p
(Grant NAG1-825)
(NASA-CR-186080; NAS 1.26:186080; CML-89-2) Avail: NTIS HC A03/MF A01 CSCL 20K

Uniaxial compression tests were performed on off-axis coupon specimens of unidirectional AS4/APC-2 thermoplastic composite at various temperatures. The elasto-plastic and strength properties of AS4/APC-2 composite were characterized with respect to temperature variation by using a one-parameter orthotropic plasticity model and a one-parameter failure criterion. Experimental results show that the orthotropic plastic behavior can be characterized quite well using the plasticity model, and the matrix-dominant compressive strengths can be predicted very accurately by the one-parameter failure criterion. Author

N90-12960# Institut Franco-Allemand de Recherches, Saint-Louis (France).
MATHEMATICAL SIMULATION OF DYNAMIC COMPRESSION TESTS USING THE HOPKINSON BAR METHOD [SIMULATION NUMERIQUE DU TEST DE COMPRESSION DYNAMIQUE UTILISANT DES BARRES D'HOPKINSON]
G. Gazeaud 16 Dec. 1987 34 p In FRENCH
(ISL-R-128/87; ETN-89-95027) Avail: NTIS HC A03/MF A01

Mathematical simulations of dynamic compression tests carried out with the help of the Lagrangian HEMP code are described. A brief summary of the method and it's principles are presented. The feasibility of such calculations is shown. The limits of this experimental technique are identified. The mathematical simulation results are compared with actual results of impact tests on samples of copper bars. Neither deformations nor constraints are shown to be homogeneous in the sample during the tests, but a good agreement is shown between the final average deformation and the elastic waves detected on the bars. ESA

N90-12961# Centre Technique des Industries Mecaniques, Senlis (France).
FATIGUE TESTING OF WELDED STEEL ASSEMBLIES WITH OR WITHOUT FINISHING TREATMENTS Final Report [TENUE EN FATIGUE D'ASSEMBLAGES SOUDES EN ACIER HLE AVEC OU SANS TRAITEMENT DE PARACHEVEMENT]
C. Bouhelier and G. Bel Nov. 1988 73 p In FRENCH
(CETIM-107900; ETN-89-95047) Copyright Avail: NTIS HC A04/MF A01

Fatigue tests carried out on welded steel assemblies are described. These tests involve impact tests, bending tests of welded joints, notch tests and load tests of welded sections of steel plate. Detailed descriptions of the testing methods are provided. Full test results are provided both in graphic and tabular form. Comparisons between test results of steel with and without finishing treatment are presented. ESA

N90-12962# Centre Technique des Industries Mecaniques, Senlis (France).
INCREASED FRAGILITY OF DEEP PRESSED THIN PLATES Final Report [FRAGILISATION DES EMBOUTIS PROFONDS EN TOLES MINCES]
R. Coutin and V. Escalup Oct. 1988 91 p In FRENCH
(CETIM-13-Y-313; ETN-89-95052) Copyright Avail: NTIS HC A05/MF A01

Mechanical testing of the fragility of pressed thin plates is described. The goal of the research is to see if heat treatment of pressed plates must necessarily be carried out to restore the mechanical characteristics and resiliency of the plates lost during the pressing process. Destructive and nondestructive tests are carried out. At temperatures of -20 C to -40 C, the risk of failure due to the increased fragility of pressed thin plates after pressing, is shown to be virtually nil. The results suggest that heat treatment of the pressed plates is not required for restoration of their mechanical and resilient characteristics. ESA

N90-12963# Ballistic Research Labs., Aberdeen Proving Ground, MD.
STRESS WAVES THROUGH PROJECTILE JOINTS AND INTERFACES
James M. Bender Jan. 1989 82 p
(AD-A212201; BRL-TR-2980) Avail: NTIS HC A05/MF A01 CSCL 20/11

The response to stress waves of a hollow cylinder containing a threaded joint is studied using the finite element method of dynamic stress analysis. These types of joints are common in many current cargo-carrying artillery projectiles. Sharp rise-time loads, which generate stress waves, can occur with electromagnetic launch and can occasionally result from a poorly behaved chemical charge (solid and liquid propellant) which creates pressure waves. The joint studied has 2 types of discontinuities: (1) a change of medium - the interface between aluminum and steel; and (2) a non-closing gap, typically found at a cylindrical joint with two closing faces. Analysis of a bimetallic rod is performed to verify aspects of the finite element code such as time step, element size and type, and analysis type. Response of a rod to stress waves can be easily compared to well-known analytical predictions. Next, a hollow homogeneous cylinder is analyzed to evaluate radial motion induced by the forcing function. This oscillatory motion disturbs the uniformity of the stress patterns. Only the initial pass of the stress wave is clear, and is similar in appearance to that of the rod. Thereafter, stress gradients through the wall thickness are evident with the onset of vibration modes, excited by the short-duration forcing function and appear to be a function of the duration of the applied transient load. Then, a non-closing notch discontinuity is introduced at the midsection of the hollow cylinder. GRA

N90-12964# Naval Ship Research and Development Center, Bethesda, MD. Computation Mathematics/Logistics Dept.
A MECHANICAL POWER FLOW CAPABILITY FOR THE FINITE ELEMENT CODE NASTRAN
Stephen A. Hambric Jul. 1989 39 p
(AD-A212202; DTRC/CMLD-89/07) Avail: NTIS HC A03/MF A01 CSCL 20/1

Structure-borne sound is the vibrational energy which travels through dynamically loaded mechanical systems. This vibrational energy is radiated eventually into an acoustic medium as noise. An example cited by Wohlever and Bernhard is an airplane wing loaded by engine vibrations. The vibrational energy travels along the wing to the fuselage and is radiated as sound into the cabin. The identification of power flow paths in dynamically loaded structures is an important, but currently unavailable, capability for the finite element analyst. For this reason, methods for calculating power flows and mechanical intensities in finite element models are developed here. Formulations for calculating input and output powers, power flows, mechanical intensities, and power dissipations for beam, plate, and solid element types are derived. NASTRAN is used to calculate the required velocity, force, and stress results of an analysis, which a post-processor then uses to calculate power flow quantities. The SDRC I-deas Supertab module is used to view the final results. Test models include a simple truss and a beam-stiffened cantilever plate. Both test cases show reasonable power flow fields over low to medium frequencies. GRA

N90-12965# Ballistic Research Labs., Aberdeen Proving Ground, MD.
THE EFFECT OF A RIGID ELLIPTICAL INCLUSION ON A STRAIGHT CRACK

E. M. Patton and M. H. Santare (Delaware Univ., Newark.) Aug. 1989 21 p
(AD-A212263; BRL-TR-3031) Avail: NTIS HC A03/MF A01 CSCL 20/11

The general problem of a straight crack near a rigid elliptical inclusion is solved. Complex potentials presented in a previous paper for the interaction of an edge dislocation with rigid ellipse are used to formulate the Green's function for this problem. The solution is written as a set of singular integral equations for crack opening displacement that are solved numerically. Stress intensity factors are presented for a variety of crack/inclusion geometries. GRA

N90-12966# Virginia Univ., Charlottesville. Dept. of Materials Science.
MODELING THE TEMPERATURE RISE AT THE TIP OF A FAST CRACK
Kasi Jagannadham and Heinz G. Wilsdorf Aug. 1989 52 p
(Contract N00014-88-K-0111)
(AD-A212418; UVA/525425/MS89/104) Avail: NTIS HC A04/MF A01 CSCL 20/11

Temperature changes that take place ahead of a crack tip in the plastic zone were analyzed using dislocation modeling of the plastic zone. The development of the process zone and that of the plastic zone is described in terms of dislocation generation and their movement at high strain rates of deformation. Among the various terms contributing to the total energy, the energy dissipation terms were identified. In particular, the plastic work dissipation rate was calculated using the phonon viscous drag forces acting on the dislocations. In the analysis, the transition from the heavily deformed process zone to the less heavily deformed plastic zone is gradual and continuous. GRA

N90-12773# State Univ. of New York, Buffalo. Dept. of Mechanical and Aerospace Engineering.
A SURVEY ON NONPROPORTIONAL DAMPING
J. Bellos and D. J. Inman *In* Vibration Inst., The Shock and Vibration Digest, Volume 21, No. 10 Oct. 1989 p 7-12 (For primary document see N90-12771 04-31)
Avail: NTIS HC A04/MF A01

42 GEOSCIENCES (GENERAL)

N90-12967# National Meteorological Center, Washington, DC.
COMPENDIUM OF MARINE METEOROLOGICAL AND OCEANOGRAPHIC PRODUCTS OF THE OCEAN PRODUCTS CENTER, REVISION 1
David M. Feit Jun. 1989 89 p Revised Prepared in cooperation with Ocean Products Center, Washington, DC
(PB89-230684; NOAA-TM-NMC-68-Rev-1; CONTRIB-38-Rev-1)
Avail: NTIS HC A05/MF A01 CSCL 04B

Brief descriptions of the current operational and experimental marine meteorological and oceanographic products of the Ocean Products Center (OPC) are presented. Included is information on: (1) marine meteorology, (2) ocean waves, (3) ocean thermal structure, and (4) polar seas and Great Lakes ice. Author

43 EARTH RESOURCES AND REMOTE SENSING

Includes remote sensing of earth resources by aircraft and spacecraft; photogrammetry; and aerial photography.

For instrumentation see *35 Instrumentation and Photography.*

N90-12968# National Oceanographic Instrumentation Center, Washington, DC. Satellite Research Lab.
REMOVING STRIPES IN GOES (GEOSTATIONARY OPERATIONAL ENVIRONMENTAL SATELLITES) IMAGES BY MATCHING EMPIRICAL DISTRIBUTION FUNCTIONS
M. P. Weinreb, R. Xie, J. H. Lienesch, and D. S. Crosby (American Univ., Washington, DC.) May 1989 33 p Sponsored by American Univ., Washington, DC Prepared in cooperation with Satellite Meteorological Center, Beijing, China
(PB89-213359; NOAA-TM-NESDIS-26) Avail: NTIS HC A03/MF A01 CSCL 05B

The current and future geostationary operational environmental satellites (GOES) are designed to produce visible images of the earth with linear arrays of eight detectors. Because the visible channels are not calibrated radiometrically in orbit, differences among instrument gains associated with the different detectors may cause artificial stripes to appear in the images. In the data processing on the ground, the images are normalized to remove the stripes. Images from future geostationary satellites, GOES I-M, will be normalized by the method of matching empirical distribution functions (EDF's). A study was made of EDF matching with data from GOES-7. The technique was used to generate a normalization look-up table from data taken on May 18, 1988 and the table was applied to image data obtained two weeks later, on June 1, 1988. This successfully removed the stripes from the image. The severity of striping was assessed qualitatively with numerical measures of striping derived from the EDF matching technique. The technique is expected to be even more effective with data from GOES I-M because of improvements in instrumentation. Author

N90-12969# Foersvarets Forskningsantalt, Linkoeping (Sweden). Dept. of Information Technology.
PROBLEM-DEPENDENT TRANSFORMATIONS OF 3D TERRAIN ELEVATION MAPS INTO COST PRECURSOR MAPS
Erik Tengvald (Linkoeping Univ., Sweden) and Erland Jungert Dec. 1988 15 p Submitted for publication
(PB89-218127; FOA-B-30135-3.4; ISSN-0281-0263) Avail: NTIS HC A03/MF A01 CSCL 08B

A method intended for reducing the complexity of 3-D path planning tasks is described, where such planning is restricted to terrain-going vehicles. Two classes of problems are addressed. Both classes share the property that different regions of terrain impose different costs during path traversal. The first problem class concerns traversal costs within a single region which are independent of the direction of motion. In the second problem class, however costs within a single region vary depending upon the direction in which the vehicle is travelling. Hence, 3-D terrain maps can be transformed into what are called cost precursor maps, which provide an abstraction of the 3-D terrain information into a 2-D reference frame. Author

N90-12970# Defense Mapping Agency Systems Center, Reston, VA.
GEODETIC POINT POSITIONING WITH GPS (GLOBAL POSITIONING SYSTEM) CARRIER BEAT PHASE DATA FROM THE CASA UNO EXPERIMENT
Stephen Malys and Peter A. Jensen (Royal Australian Survey Corps.) 1 Aug. 1989 13 p
(AD-A211955) Avail: NTIS HC A03/MF A01 CSCL 08/5

The Global Positioning System (GPS) carrier beat phase data collected by the T14100 GPS receiver was successfully utilized by the U.S. Defense Mapping Agency in an algorithm which is designed to estimate individual absolute geodetic point positions from data collected over a few hours. The algorithm uses

differenced data from one station and two to four GPS satellites at a series of epochs separated by 30 seconds intervals. The precise GPS ephemerides and satellite clock states, held fixed in the estimation process, are those estimated by the Naval Surface Warfare Center (NSWC). Broadcast ephemerides and clock states are also utilized for comparative purposes. An outline of the applied data corrections, the mathematical model and the estimation algorithm are present. Point positioning results and statistics are presented for a globally distributed set of stations which contributed to the CASA UNO experiment. GRA

N90-12971# Naval Postgraduate School, Monterey, CA.
VISUALIZATION OF HIGH-RESOLUTION DIGITAL TERRAIN M.S. Thesis
William O. Breden and James J. Zanoli Jun. 1989 74 p
(AD-A212149; NPS52-89-38) Avail: NTIS HC A04/MF A01 CSCL 08/2

Two methods are explored for real-time generation of more realistic two and three-dimensional terrain displays than what are currently available on relatively inexpensive graphics workstations. The first method involves using a high-resolution terrain elevation database. The second method involves coloring and shading the terrain with gray-scale data obtained from associated aerial photography. Both methods were implemented with a three-dimensional simulator using a high resolution digital terrain database that was generated from processed F-14 stereo imagery. The simulator, the High-Resolution Digital Terrain Model (HRDTM), was described listing its capabilities and graphics features. How the system performs on a high-performance graphics workstation was also presented. Topics discussed include: database manipulation; user interface; the magnification capability; the variable gamma ramp capability; the camera (laser printing) capability; file input/output; elevation contour map; and aerial photo display; and data panel performance measurements. GRA

N90-12972# Technische Univ., Delft (Netherlands).
REALIZATION OF A DIFFERENT NAVSTAR GLOBAL POSITIONING SYSTEM FOR HYDROGRAPHIC SURVEYING
R. vanDam Dec. 1988 99 p
(ETN-89-95720) Avail: NTIS HC A05/MF A01

The research program on a differential navigation system by timing and ranging (NAVSTAR) global positioning system (GPS) conception is reported. The system provides a worldwide coverage. It is shown that: the positions provided by GPS are contaminated by systematic errors due to delay of the transmitted signals in the ionosphere and troposphere, orbital deviations of the satellites, and clock drift. Only six of the intended 18 satellites are used, and positioning is not possible throughout the day. The GPS is developed for three coordinates and the clock-offset t sub b positioning. The systematical drift in all coordinates propagates in the horizontal position. Both drift and offset determination and propagation of delta h, phi and lambda are studied and tested. ESA

N90-12973*# California Univ., Santa Barbara. Dept. of Geography.
IMPROVEMENT AND EXTENSION OF A RADAR FOREST BACKSCATTERING MODEL Final Report
David S. Simonett and Yong Wang Oct. 1989 12 p
(Grant NAG5-1010)
(NASA-CR-186083; NAS 1.26:186083) Avail: NTIS HC A03/MF A01 CSCL 02F

Radar modeling of mangal forest stands, in the Sundarbans area of Southern Bangladesh, was developed. The modeling employs radar system parameters such as wavelength, polarization, and incidence angle, with forest data on tree height, spacing, biomass, species combinations, and water content (including slightly conductive water) both in leaves and trunks of the mangal. For Sundri and Gewa tropical mangal forests, five model components are proposed, which are required to explain the contributions of various forest species combinations in the attenuation and scattering of mangal vegetated nonflooded or flooded surfaces. Statistical data of simulated images (HH components only) were compared with those of SIR-B images both to refine the modeling procedures and to appropriately characterize the model output. The possibility of delineation of flooded or non-flooded boundaries is discussed. Author

N90-12974# Deutsche Forschungs- und Versuchsanstalt fuer Luft- und Raumfahrt, Oberpfaffenhofen (West Germany). Abteilung Fernerkundung.
AN ATTEMPT TO DRAW CONCLUSIONS FROM THE VEGETATION TO THE GEOLOGICAL UNDERGROUND IN THE AREA OF AMBERG (GERMANY, F.R.) BY MEANS OF DIGITAL IMAGE PROCESSING OF TM DATA
Tobias Wever (Ludwig-Maximilians-Universitaet, Munich, Germany, F.R.) Aug. 1988 95 p In GERMAN; ENGLISH summary Original contains color illustrations
(DFVLR-FB-89-24; ISSN-0171-1342; ETN-89-95833) Avail: NTIS HC A05/MF A01; DFVLR, VB-PL-DO, Postfach 90 60 58, 5000 Cologne, Fed. Republic of Germany, 36.50 Deutsche marks

Image processing of LANDSAT Thematic Mapper (TM) scenes is used to determine the lithology and techtonic units underlying vegetation in Central Europe. A photogeological interpretation of qualified color composites is developed of the Amberg (Germany F.R.) area. The causal connections between lithology, soil, and vegetation are discussed in detail. Anthropological effects such as intensive agriculture can modify the parameters of such a study. Such influences and the limitations of the technique are demonstrated and discussed. ESA

N90-12975# Louisiana State Univ., Baton Rouge.
A HYBRID ARCHITECTURE FOR FEATURE LABELLING OF OCEANOGRAPHIC SATELLITE IMAGES Report, for Oct. 1988 - May 1989
S. Sitharama Iyengar May 1989 29 p
(Contract N00014-88-K-6002; Proj. RM35G87)
(AD-A212236) Avail: NTIS HC A03/MF A01 CSCL 08/3

An automatic oceanographic image interpretation system was developed. This system will aid the operator in identifying various oceanic features and will predict the dynamic behavior of these features. Presently these tasks are handled by experts in oceanography and obviously, a time consuming process. The proposed project was divided into 3 phases: (1) the features present in the oceanographic image are identified (In this phase an efficient feature labeling algorithm were implemented); (2) an Expert System that helps in predicting the dynamic behavior of the oceanic features will be developed; and (3) these two modules will be integrated and the system will be tested with real time data. The design and development of Phase 1 started in May 1988. Various techniques for feature labeling were studied. It was decided to use nonlinear probabilistic relaxation labeling scheme for the oceanographic feature labeling problem. GRA

44 ENERGY PRODUCTION AND CONVERSION

Includes specific energy conversion systems, e.g., fuel cells; global sources of energy; geophysical conversion; and windpower.

For related information see also *07 Aircraft Propulsion and Power, 20 Spacecraft Propulsion and Power,* and *28 Propellants and Fuels.*

N90-12976# Minnesota Univ., Minneapolis. Dept. of Chemical Engineering and Materials Science.
ASSESSMENT OF THIN FILM BATTERIES BASED ON POLYMER ELECTROLYTES. PART 3: SPECIFIC ENERGY VERSUS SPECIFIC POWER Technical Report, Jul. 1988 - Jun. 1989
M. Z. A. Munshi and Boone B. Owens 15 Jun. 1989 16 p
(Contract N00014-88-K-0360)
(AD-A212141; ONR-TR-17) Avail: NTIS HC A03/MF A01 CSCL 10/3

The feasibility of solid state polymer electrolyte batteries for

applications such as the electric vehicle depends on the variation in the performance levels of the specific energy and specific power. Efforts were centered mainly on rechargeable lithium batteries with electrolyte complexes formed between polyethylene oxide and lithium salts having an ionic conductivity of .0001 Ohms/cm and V6O13 insertion cathodes. Prismatic unit cells of variable cathode thicknesses have been modeled and calculated results indicate that high specific energies (approx. 700 W/kg) are possible for this battery system utilizing metallic current collectors. Considerably higher values result for low density metallized plastic current collectors. GRA

N90-12977# Celgene Corp., Warren, NJ.
BIOLOGICAL AND BIOCHEMICAL METHANE REACTIONS Final Report, Mar. 1986 - Mar. 1989
H. Dalton, P. T. Pienkos, and D. I. Stirling Apr. 1989 50 p Prepared in cooperation with Warwick Univ., Coventry, England
(Contract GRI-5086-260-1209)
(PB89-232615; GRI-89/0101) Avail: NTIS HC A03/MF A01 CSCL 10A

The purpose of the project was to characterize the nature of the active site involved in methane activation by enzymes from well characterized and newly isolated methane-oxidizing bacteria. Kinetic and structural studies provided an initial picture of how the soluble methane monooxygenase (MMO) enzyme is structured and operates to selectively oxidize methane to methanol under ambient conditions. Cloning and sequencing of gene coding for some of the sMMO proteins were completed, and 72 strains of methanotrophs were isolated from extreme environments. Author

N90-12978# Technische Univ., Delft (Netherlands). Faculty of Technical Mathematics and Informatics.
A DEVICE TO EXTRACT ENERGY FROM WATER WAVES
A. J. Hermans, E. vanSabben, and J. A. Pinkster (Maritime Research Inst. Netherlands, Wageningen.) 1989 16 p
(Rept-89-34; ISSN-0922-5641; ETN-89-95592) Copyright Avail: NTIS HC A03/MF A01

The fundamental characteristics of a device to transform wave energy directly into rotational mechanical energy are discussed, and a mathematical model which describes the properties of the device is verified by results of model tests. The device consists of a profile rotating around an axis. Mathematical formulations are shown and diagrams included. Conclusions are detailed, including the observation that waves are generated downstream only. ESA

45 ENVIRONMENT POLLUTION

Includes atmospheric, noise, thermal, and water pollution.

N90-12979# Oak Ridge National Lab., TN.
CONTRIBUTION OF DEFORESTATION TO ATMOSPHERIC CO2 AND REFORESTATION AS AN OPTION TO CONTROL CO2
John D. Kinsman (Edison Electric Inst., Washington, DC.) and Greg Marland 1989 29 p Presented at the 82nd Air and Waste Management Association Annual Meeting and Exhibition, Anaheim, CA, 25-30 Jun. 1989
(Contract DE-AC05-84OR-21400)
(DE89-017255; CONF-890692-20) Avail: NTIS HC A03/MF A01

Various aspects are discussed of global climate change as related to forests: the rate of deforestation; CO2 emissions resulting from deforestation; and reforestation as a means to control atmospheric CO2. For perspective, a discussion is included of current policy considerations related to methods for reducing deforestation or promoting reforestation. DOE

N90-12980*# National Academy of Sciences - National Research Council, Washington, DC. Committee on Global Change.
TOWARD AN UNDERSTANDING OF GLOBAL CHANGE: INITIAL PRIORITIES FOR US CONTRIBUTIONS TO THE INTERNATIONAL GEOSPHERE-BIOSPHERE PROGRAM Final Report
Dec. 1988 226 p Sponsored by NASA, Washington, DC; NOAA, Rockville, MD and Geological Survey, Reston, VA
(Grant NSF OCE-87-13699)
(NASA-CR-185873; NAS 1.26:185873; PB89-231344) Avail: NTIS HC A11/MF A02 CSCL 13B

A limited number of high-priority research initiatives are recommended for early implementation as part of the U.S. contribution to the preparatory phase of the International Geosphere-Biosphere Program. The recommendations are based on the committee's analysis of the most critical gaps in the scientific knowledge needed to understand the changes that are occurring in the earth system not being addressed by existing programs. The report articulates a number of important key issues and interactions that characterize global change in the geosphere-biosphere system on time scales of decades to centuries; identifies the knowledge that is the most urgently needed to improve understanding of those issues and interactions; and formulates initial priorities for initial U.S. contributions to the IGBP, recognizing the contributions of other ongoing and proposed programs. Author

N90-12981# Systems Applications, Inc., San Rafael, CA.
SENSITIVITY OF A REGIONAL OXIDANT MODEL TO VARIATIONS IN CLIMATE PARAMETERS, VOLUME 1 AND 2 Final Report
R. E. Morris, M. W. Gery, M. K. Liu, G. E. Moore, C. Daley, and S. M. Greenfield Jul. 1989 149 p Sponsored by EPA, Research Triangle Park, NC
(PB89-224943; EPA/600/3-89/068-Vol-1/2) Avail: NTIS HC A07/MF A01 CSCL 13B

In order to investigate the sensitivity of ozone concentrations to future climate variations, a regional oxidant model was applied for future climate scenarios to two regions: one covering central California (San Joaquin Valley, Sierra Nevada mountains and the San Francisco Bay Area) and the other covering the midwestern and southeastern United States. Based on model calculations, the effects of increased temperature on ambient ozone concentrations results in an increase of the area of exceedances of the ozone air quality standard, a movement of the peak ozone concentration closer to the urban areas, and the resultant increase in the exposure of people to harmful levels of ozone concentrations. The calculations for California indicate that the maximum daily ozone concentrations may increase from 2 to 20 percent and the number of people exposed to hourly ozone concentrations in excess of the air quality standard may triple as a result of a temperature increase. Similar, although less dramatic, results were seen for the midwestern and southeastern applications. GRA

N90-12982# Valley Research Corp., Van Nuys, CA.
DEVELOPMENT OF AN INVENTORY OF MATERIALS POTENTIALLY SENSITIVE TO AMBIENT ATMOSPHERIC ACIDITY IN THE SOUTH COAST AIR BASIN Final Report
Yuji Horie, Arthur Shrope, and Richard Ellefsen (San Jose State Univ., CA.) Mar. 1989 234 p
(Contract ARB-A6-079-32)
(PB89-224604; ARB-R-89/399) Avail: NTIS HC A11/MF A02 CSCL 13B

An inventory of exposed materials for residential and nonresidential buildings and nonbuildings was developed. The inventory of the residential buildings was developed by conducting telephone surveys of 1,200 households and field surveys of 200 households. The inventory of multi-family residential buildings and nonresidential buildings was conducted by aerial photo analysis. The inventory of nonbuilding materials (infrastructure) was developed by conducting a limited survey and by using engineering calculations. The inventory was extrapolated to the entire South Coast Air Basin using the building-count method. Author

N90-12983# Colorado State Univ., Fort Collins. Dept. of Atmospheric Science.
A NEW GENERATION OF ATMOSPHERIC TRACERS: THE BIOLOGICAL CONNECTION Final Report, 1 May 1986 - 30 Apr. 1989
Peter C. Sinclair and Louis B. Bjostad 7 Aug. 1989 38 p
(Contract DAAL03-86-K-0065)
(AD-A212285; ARO-23019.1-GS) Avail: NTIS HC A03/MF A01 CSCL 04/1

The use of atmospheric tracers can provide information on air flow features that cannot be directly observed by meteorological instrumentation systems. Even in the special situations where remote sensing systems can operate, sufficient aerosol-hydrometer backscatter is required before relatively short range volume scans of the velocity field are possible. However, all measurement systems (standard or research) are deficient in being able to directly measure the Lagrangian features of the atmosphere. Tracers, on the other hand, can be designed and used to specifically document many of the actual flow characteristics (transport/diffusion) of the atmosphere. A prototype atmospheric tracer system (ABS-1) was developed that utilizes insect pheromones as the tracer and a live insect as the atmospheric biosensor (ABS-1). The laboratory experiments indicate that not only the presence of the pheromone tracer can be detected, but also an estimate can be made of the tracer concentration. Thus, atmospheric transport and diffusion estimates should now be possible with the ABS-1. GRA

46 GEOPHYSICS

Includes aeronomy; upper and lower atmosphere studies; ionospheric and magnetospheric physics; and geomagnetism.

For space radiation see *93 Space Radiation.*

N90-12984*# National Aeronautics and Space Administration. Lewis Research Center, Cleveland, OH.
THE GEM-T2 GRAVITATIONAL MODEL
J. G. Marsh, F. J. Lerch, B. H. Putney, T. L. Felsentreger, B. V. Sanchez, S. M. Klosko, G. B. Patel, J. W. Robbins, R. G. Williamson, and T. E. Engelis (ST Systems Corp., Lanham, MD.) et al Oct. 1989 91 p Prepared in cooperation with Maryland Univ., College Park
(NASA-TM-100746; Rept-89B00244; NAS 1.15:100746) Avail: NTIS HC A05/MF A01 CSCL 08E

The GEM-T2 is the latest in a series of Goddard Earth Models of the terrestrial field. It was designed to bring modeling capabilities one step closer towards ultimately determining the TOPEX/Poseidon satellite's radial position to an accuracy of 10-cm RMS (root mean square). It also improves models of the long wavelength geoid to support many oceanographic and geophysical applications. The GEM-T2 extends the spherical harmonic field to include more than 600 coefficients above degree 36 (which was the limit for its predecessor, GEM-T1). Like GEM-T1, it was produced entirely from satellite tracking data, but it now uses nearly twice as many satellites (31 vs. 17), contains four times the number of observations (2.4 million), has twice the number of data arcs (1132), and utilizes precise laser tracking from 11 satellites. The estimation technique for the solution has been augmented to include an optimum data weighting procedure with automatic error calibration for the gravitational parameters. Results for the GEM-T2 error calibration indicate significant improvement over previous satellite-only models. The error of commission in determining the geoid has been reduced from 155 cm in GEM-T1 to 105 cm for GEM-T2 for the 36 x 36 portion of the field, and 141 cm for the entire model. The orbital accuracies achieved using GEM-T2 are likewise improved. Also, the projected radial error on the TOPEX satellite orbit indicates 9.4 cm RMS for GEM-T2, compared to 24.1 cm for GEM-T1. Author

N90-12985*# National Aeronautics and Space Administration. Goddard Space Flight Center, Greenbelt, MD.
OPTIMUM DATA WEIGHTING AND ERROR CALIBRATION FOR ESTIMATION OF GRAVITATIONAL PARAMETERS
F. J. Lerch Jul. 1989 31 p
(NASA-TM-100737; Rept-89B00158; NAS 1.15:100737) Avail: NTIS HC A03/MF A01 CSCL 08E

A new technique was developed for the weighting of data from satellite tracking systems in order to obtain an optimum least squares solution and an error calibration for the solution parameters. Data sets from optical, electronic, and laser systems on 17 satellites in GEM-T1 (Goddard Earth Model, 36x36 spherical harmonic field) were employed toward application of this technique for gravity field parameters. Also, GEM-T2 (31 satellites) was recently computed as a direct application of the method and is summarized here. The method employs subset solutions of the data associated with the complete solution and uses an algorithm to adjust the data weights by requiring the differences of parameters between solutions to agree with their error estimates. With the adjusted weights the process provides for an automatic calibration of the error estimates for the solution parameters. The data weights derived are generally much smaller than corresponding weights obtained from nominal values of observation accuracy or residuals. Independent tests show significant improvement for solutions with optimal weighting as compared to the nominal weighting. The technique is general and may be applied to orbit parameters, station coordinates, or other parameters than the gravity model. Author

N90-12986# Atmospheric Radiation Consultants, Acton, MA.
RETRIEVAL OF ATOMIC OXYGEN AND TEMPERATURE IN THE THERMOSPHERE. PART 1: FEASIBILITY OF AN EXPERIMENT BASED ON THE SPECTRALLY RESOLVED 147 MICROMETER LIMB EMISSION Scientific Report No. 1, Feb. 1987 - Nov. 1988
A. S. Zachor, R. D. Sharma, B. K. Yap, and J. P. Riehl (Missouri Univ., Saint Louis.) 10 Apr. 1989 39 p
(Contract F19628-87-C-0053)
(AD-A211987; ARC-TR-89-011; GL-TR-89-0144) Avail: NTIS HC A03/MF A01 CSCL 04/1

The importance of atomic oxygen and translational temperature in mesospheric/thermospheric processes is the motivation to study the feasibility of recovering vertical profiles of the temperature and O-atom density from limb scan data obtained near 147 micrometer and/or 63 micrometer wavelength, corresponding to the oxygen atom ground electronic state (OI) transitions. The limb radiance data must be spectrally resolved to recover both temperature and atomic oxygen density if only one of the OI lines is used, which is the approach investigated in this report. We show how the two vertical profiles can be recovered by applying an onion-peeling method to synthetic data. The temperature and O-atom density in each peeled layer are obtained simultaneously by nonlinear least-squares spectrum fitting. Spectral data in the 147 micrometer line was found to yield reasonably accurate and stable profiles from 300 km down to an altitude between 130 and 90 km, depending on the noise level and spectral resolution, and gave better results than the stronger 63 micrometer data below 140 km. We estimate that the S/N and spectral resolution required for successful retrievals could be provided by a confocal Fabry-Perot system operating near 147 micrometer although retrievals down to 90 km from data obtained at orbital altitude would require cooled foreoptics roughly a meter in diameter. GRA

N90-12987# Alaska Univ., Fairbanks. Geophysical Inst.
DEVELOPMENT OF COMPUTER CODES TO MODEL DYNAMICS OF THE EARTH'S MAGNETOSPHERE Final Report, 1 Dec. 1985 - 31 May 1989
Daniel W. Swift Apr. 1989 21 p
(Grant AF-AFOSR-0037-86; AF Proj. 2311)
(AD-A211532; AFOSR-89-1108TR) Avail: NTIS HC A02/MF A01 CSCL 04/1

The objective of the research has been to develop models of plasma processes in the earth's magnetosphere and ionosphere

to understand processes responsible for auroral and magnetic phenomena. One major accomplishment has been the tentative identification of the process for generation of the electric potentials that accelerate auroral electrons. Another major accomplishment is a numerical model of auroral precipitation. The simulation indicates that anomalous resistivity plays little role in electron acceleration processes. The auroral simulation model indicates that the auroral beam may excite upper hybrid electrostatic waves, which may stochastically accelerate a portion of the electron beam to many tens of KeV. GRA

N90-12988# Cambridge Univ. (England). Dept. of Applied Mathematics and Theoretical Physics.
FUNDAMENTALS OF MIDDLE ATMOSPHERIC DYNAMICS Annual Letter Report, 1 Apr. 1988 - 31 Mar. 1989
M. E. McIntyre 31 Mar. 1989 10 p
(Contract N00014-87-J-1170)
(AD-A211747) Avail: NTIS HC A02/MF A01 CSCL 04/1

The middle atmosphere is a highly nonlinear dynamical system whose variability, and forecastability, is very poorly understood. The state of the mesosphere should be highly sensitive to the propagation of both gravity and Rossby waves from below, and that propagation can be sensitive to various kinds of wave-mean, wave-wave, and wave-turbulence interactions that occur on the way up. On longer timescales, there are trends in, for example, temperatures, chemical composition, and thresholds for aerosol and cloud formation, that may significantly change mean and extreme conditions in the middle atmosphere from year to year. These trends are partly a result of man-made perturbations and involve an intricate interplay of chemical, radiative and dynamical processes over a vast range of space and time scales, depending for example on the statistical properties of the wave-turbulence interactions. The problems thus posed are of formidable technical and conceptual difficulty. Progress is hindered by a lack of knowledge at the most fundamental level, particularly regarding the scale-interactive dynamical processes. The long-term aim of this project is to develop, test and exploit new theoretical concepts and modeling techniques to achieve a radically improved understanding of these processes. GRA

N90-12989# Air Force Geophysics Lab., Hanscom AFB, MA.
ROLE OF CHEMICAL EFFECTS IN DAYTIME HIGH LATITUDE TROUGH FORMATION
Christopher Sherman and Robert E. Daniell, Jr. 31 Jan. 1989 17 p Prepared in cooperation with Computational Physics, Inc., Newton, MA
(AD-A211772; AFGL-TR-89-0029; AFGL-ERP-1020) Avail: NTIS HC A03/MF A01 CSCL 04/1

The role of enhanced chemical reaction rates in the formation of the daytime F-region trough is examined. A simple convection model is used to estimate the maximum likely elevation of effective temperature for the ion reaction O+ + N2 yields NO(+)+ N. Under extreme conditions the effective temperature can reach 4000 K resulting in a 30-fold increase in the reaction rate. However, the resulting reduction in F-region electron density is only a factor of 4. Under more usual conditions, the reduction is less than a factor of 2. The actual density reduction factor in the daytime trough is observed to vary between 3 and 10 under normal conditions. Therefore, we conclude that under most circumstances, convection-enhanced chemistry contributes very little to the formation of the daytime trough. GRA

N90-12990# Ohio State Univ., Columbus. Dept. of Geodetic Science and Surveying.
A SIMULATION STUDY OF THE OVERDETERMINED GEODETIC BOUNDARY VALUE PROBLEM USING COLLOCATION
Lucia Tsaoussi Mar. 1989 143 p
(Contract F19628-86-K-0016)
(AD-A211785; OSU/DGSS-398; GL-TR-89-0109; SR-6) Avail: NTIS HC A07/MF A01 CSCL 08/5

This problem is defined in general by the Laplacian and at least two different boundary conditions holding on a spherical boundary, or overlapping parts of it. The least-squares collocation method is applied to estimate spherical harmonic coefficients for the disturbing potential. An algorithm was developed and the method was tested using simulated gravity anomaly and undulation signals. Point as well as mean boundary values were used, both with and without random noise added. The OSU86F spherical harmonic coefficient set was used to generate the simulated data and the required covariances. By computing statistics of the input field recovery, the applicability of the method is judged. Several problems were encountered while applying least-squares collocation to this problem. A theoretical singularity of the covariance matrix, caused by truncation in the summation of the covariance function at a finite degree, is found to be eliminated numerically when summing to degree 180. Instability and singularity due to the data distribution are treated successfully by applying Tikhonov regularization. Inversion of a large covariance matrix resulting from global data coverage limits the feasibility of the solution. To make the computation manageable, the block-Toeplitz pattern of the auto-covariance matrices is exploited in forming and inverting them. GRA

N90-12991 Physics and Electronics Lab. TNO, The Hague (Netherlands).
SURVEY OF THE CLUSE MAIN EXPERIMENT GRAND-CLUSE, MAY 1 - JUNE 15, 1988
G. deLeeuw Jul. 1988 25 p
(Contract N00014-87-G-0212)
(FEL-1988-43; TD88-3856; ETN-89-95077) Copyright Avail: TNO Physics and Electronics Lab., P.O. Box 96864, 2509 JG The Hague, Netherlands

The measurements made during the CLUSE main experiment Grand-CLUSE, are reported. The aim is to derive the influence of spray droplets on the atmospheric water vapor content. A homogeneous distribution of spray droplets is created in the tunnel boundary layer by means of a 24 m long spray bubbler net submersed at 50 cm below the water surface. With this model whitecap the bubble-mediated aerosol production and the interactions between the spray droplets and the turbulent fields of air flow, humidity and temperature are studied. The determination of the bubble spectra, the spray surface source function, spray droplet size distribution profiles, and profiling of the turbulence characteristics by various methods, is effectuated. The influence of waves on turbulent fluctuations of particle concentrations is confirmed. A better understanding of the processes in the open ocean is achieved. The model may be applied to the fields of satellite surveillance, electro-optical transmission, detection of sea-skimmers, meteorology and climatology and air pollution. ESA

N90-12992# Stockholm Univ. (Sweden). Dept. of Meteorology.
ZONAL AVERAGE CLOUD CHARACTERISTICS FOR GLOBAL ATMOSPHERIC CHEMISTRY MODELING
Jos Lelieveld, Paul J. Crutzen (Max-Planck-Inst. fuer Chemie, Mainz, Germany, F.R.), and Henning Rodhe Jun. 1989 57 p Sponsored by the Swedish National Environment Protection Board
(CM-76; GLOMAC-89/1; ISSN-0280-445X; ETN-89-95925) Avail: NTIS HC A04/MF A01

The zonal average cloud distribution for the lower (approximately six km) troposphere is studied. It is derived from surface observations of cloud occurrence and the average vertical extent of clouds. Assessments of updraft velocities through convective clouds and lifetime estimates of stratiform clouds are used to calculate the average time that air spends in clouds and the time between successive cloud encounters, as a function of latitude and altitude. The inferred cloud data and satellite observations are compared. Data derived from calculations with a general circulation model and satellite observations do not show a good fit. The results lead to the conclusion that for such models an effort must be devoted to develop cloud parameterizations in order to produce cloud distributions as needed for global atmospheric chemistry modeling. ESA

N90-12993# National Oceanic and Atmospheric Administration, Silver Spring, MD. Air Resources Lab.
SOUTH POLE SURFACE RADIATION BALANCE MEASUREMENTS, APRIL 1986 TO FEBRUARY 1988
Elizabeth G. Dutton, Robert S. Stone (Colorado Univ., Boulder.), and John J. DeLuisi Apr. 1989 55 p
(PB89-224018; NOAA-DR-ERL-ARL-17) Avail: NTIS HC A04/MF A01 CSCL 04A

Measured radiation budget (or balance) components with daily time resolution are presented for the U.S South Pole station. The measurement project and the data reduction and summary procedures are described. Useful plots and tables are used to present data in final form. Additionally, meteorological data, which could be useful in interpretation of the radiation measurement are included. It is seen that, during the peak solar months, there is a radiative gain of about 20 W sq m. Many transitory events of one to several days duration are also seen in the record. Radiation budget measurements are continuing at the site on an ongoing basis in an effort to establish a climatological record. Author

N90-12994# Chemical Research and Development Center, Aberdeen Proving Ground, MD.
INFRARED WATER VAPOR CONTINUUM ABSORPTION: NEW ATMOSPHERIC ELECTRICAL MEASUREMENTS AND THEORY Technical Report, Jan. 1979 - May 1987
Hugh R. Carlon Jul. 1989 30 p
(AD-A212594; CRDEC-TR-098) Avail: NTIS HC A03/MF A01 CSCL 04/1

The infrared (IR) continuum absorption, and probably similar absorption at longer wavelengths, can be attributed to populations of electrically-neutral water clusters that are present in near-Gaussian size distributions in water vapor and moist air. These neutral water clusters exist in equilibrium with much smaller populations of their water ions. Therefore, behavior of the ions and their equilibrium, IR-absorbing neutral clusters can be studied by careful measurements of the electrical conductivity of atmospheric moist air. Some results from a year of such measurements are presented and discussed. The most significant conclusions are: (1) the vapor continuum absorption almost certainly is due to water clusters; (2) prime sources of such clusters include fine water droplets, and finely-structured water films on surfaces, at higher relative humidities (RH) in electric fields typical of those in the earth's atmosphere; (3) the variability of the continuum absorption arises from many factors, some of the most important of which are vapor RH, state of equilibrium, and fineness of droplets and surface water film structure; and (4) the continuum absorption at any wavelength is due only to these clusters of the distribution that absorb there, and therefore, the total vapor cluster population cannot be estimated by measurements at a single wavelength. GRA

N90-12995# Air Force Geophysics Lab., Hanscom AFB, MA.
COMMENTS ON THE USE OF LOWTRAN IN TRANSMISSION CALCULATIONS FOR SITES WITH THE GROUND ELEVATED RELATIVE TO SEA LEVEL
Eric P. Shettle 15 Apr. 1989 3 p
(AD-A212724; GL-TR-89-0165) Avail: NTIS HC A01/MF A01 CSCL 04/1

The adjustment of the amount of aerosol to calculate atmospheric transmittance when the ground is higher than sea level is discussed. GRA

47 METEOROLOGY AND CLIMATOLOGY

Includes weather forecasting and modification.

N90-12996*# Alabama Univ., Huntsville. Atmospheric Science and Remote Sensing Lab.
ANALYSIS AND MODELING OF SUMMERTIME CONVECTIVE CLOUD AND PRECIPITATION STRUCTURE OVER THE SOUTHEASTERN UNITED STATES Semiannual Report, 15 Sep. 1988 - 14 Jun. 1989
Kevin R. Knupp Jun. 1989 12 p
(Grant NAG8-654)
(NASA-CR-185436; NAS 1.26:185436) Avail: NTIS HC A03/MF A01 CSCL 04B

Data analysis and numerical modeling efforts that are related to the 1986 Satellite Precipitation and Cloud Experiment (SPACE) are discussed. Progress during this period includes the following: further testing and development of the RAMS numerical modeling system on the Alabama CRAY X-MP/24; a continuation of the observational analysis of the 13 July 1986 mesoscale convective system (MCS); and an initial investigation of a small MCS that formed over the COHMEX region on 15 July 1986. Details for each of these individual tasks are given. Author

N90-12997# Meteorological Satellite Center, Tokyo (Japan).
METEOROLOGICAL SATELLITE CENTER TECHNICAL NOTE, NO. 18, 1989
Mar. 1989 87 p In ENGLISH and JAPANESE Original contains color illustrations
(MSC-TN-18; ISSN-0388-9653) Avail: NTIS HC A05/MF A01

In RA-II area (Asia), the meteorological satellite date from both geostationary and polar orbiting satellites are widely used by most Members. The authors sent questionnaire to Members in RA-II to investigate the status of the use of satellite data. The answers to the questionnaire are summarized as: (1) most Members receive both geostationary and polar orbiting satellite data; (2) for continuous operation of receiving stations, there are two fundamental factors (operators skill and availability of back-up system); (3) direct broadcast pictures are used for weather forecast and for the general and specified purposes by most Members; (4) the extracted meteorological parameter data transmitted through GTS are used for numerical weather prediction (NWP) by a few Members; and (5) a few dozens of Data Collection Platforms (DCPs) are installed in RA-II area and the observed data are collected by geostationary and polar orbiting satellites. Author

N90-12998# Naval Postgraduate School, Monterey, CA.
AIR FLOW OVER LARGE SCALE TOPOGRAPHY Final Report, 1 Oct. 1986 - 31 Mar. 1989
Mary A. Rennick and Roger T. Williams Jun. 1989 106 p
(Grants NSF ATM-84-05276; NSF ATM-86-10354)
(AD-A211779; NPS63-89-003) Avail: NTIS HC A06/MF A01 CSCL 04/2

This project studied the two aspects of topographic influence on transient atmospheric motions: (1) Lee Cyclogenesis. It is observed that cyclones frequently form on the lee side of mid-latitude mountain ranges. This problem is investigated with a long mountain range which is perpendicular to a vertically sheared basic current. The prediction equations are solved with both analytic and numerical methods. It is found that lee cyclogenesis can be partially explained by a superposition effect involving a counterclockwise rotating cyclone and a clockwise rotation circulation forced by the mountain range. (2) Effects of topography on fronts. It is often observed that fronts are strongly affected by topography. A two-dimensional numerical model is used for this study. The model predicts the formation of fronts through the effects of a confluent horizontal wind field. When a front is placed on the upwind side of a mountain range, it weakens relative to the no-mountain solution as it moves up the slope, and it strengthens as it moves down the lee slope. The collapse of a front to very small scales is studied with a non-hydrrostatic numerical model. It is found that this process excites gravity waves. GRA

N90-12999# Calspan Corp., Buffalo, NY.
INVESTIGATION OF NORTH ATLANTIC FOG AND DEVELOPMENT OF A MARINE FOG FORECAST SYSTEM Final Report, Jun. 1987 - Jun. 1989
C. William Rogers Apr. 1989 58 p
(Contract N00014-87-C-0232)
(AD-A211780; CALSPAN-7589-1; NEPRF-CR-89-11) Avail: NTIS HC A04/MF A01 CSCL 04/2

Ocean fog and haze were studied to provide additional

expertise for An Expert-system for Shipboard Obscuration Prediction (AESOP). Task 1 studied fog occurrence in the N. Atlantic and developed an AESOP rule base for these fogs, Task 2 evaluated forecast errors generated during a test of AESOP, and modified and extended the rule base to correct for these errors. Fog is primarily a summertime phenomenon in the N. Atlantic. Taylor fog forms at midlatitudes (40 to 50 N) in the stable, relatively shallow marine boundary layer which is located at the western end of the semi-permanent anticyclone. In the eastern N. Atlantic, extratropical anticyclogenesis occasionally occurs, which can produce stratus lowering fog along its eastern side and Taylor fog in the southerly flow at its western end. At 50 to 60 N in the track of the transient synoptic systems, much of the fog is advected in from the Taylor fog formation regions to the S and W. Fog dissipation is driven primarily by heating produced by absorption of solar radiation and mixing of warm air from above the inversion which caps the fog layer. These two dissipation processes are abetted by the mixing of the lower humidity of the warm air. Over the open ocean, the aerosol concentration is generally too low to provide even the minimum concentration required to produce a maximum haze visibility of 5 n mi. GRA

N90-13000 Royal Netherlands Meteorological Inst., De Bilt. Physical Meteorology Dept.

CENTRAL SUDAN SURFACE WIND DATA AND CLIMATE CHARACTERISTIC

E. H. AbuBakr 1988 59 p Sponsored by the Netherlands Foundation for the Advancement of Tropical Research and the Netherlands Organization for the Advancement of Pure Research
(KNMI-WR-88-01; ISSN-0169-1651; ETN-89-95598) Copyright
Avail: Royal Netherlands Meteorological Inst., P.O. Box 201, 3730 de Bilt, Wilhelminalaan 10, Netherlands

A representative data set from a reference data base used for developing a boundary layer model for tropical regions, is shown. The region selected for investigation is an area of 56,000 sq km around Kartoum (Sudan). The purpose of the investigation is the wind speed estimation, using the tropical boundary layer physics. The procedures applied to obtain a homogeneous wind data base are presented (reliability checks, azimuth-dependent exposure correction, and correction for standard height). The characteristics of climate in this region, especially the passage of the intertropical convergence zone and its influence on the wind regime, are discussed. ESA

N90-13001 Royal Netherlands Meteorological Inst., De Bilt. Dynamical Meteorology Dept.

INSTABILITY MECHANISMS IN A BAROTROPIC ATMOSPHERE Ph.D. Thesis - Vrije Univ., Amsterdam, Netherlands

R. J. Haarsma 1989 134 p
(KNMI-WR-89-01; ISSN-0169-1651; ETN-89-95600) Copyright
Avail: Royal Netherlands Meteorological Inst., P.O. Box 201, 3730 de Bilt, Wilhelminalaan 10, Netherlands

The relevance of barotropic instability for the observed low frequency variability in the atmosphere is investigated. The stability properties of the shallow water equations on a sphere are computed for small values of Lamb's parameter (F). The stability of simple zonal flows, as well as free and forced planetary Rossby waves are evaluated as a function of F. The results show that for increasing F, the instability critical amplitudes decrease. In the area of instability both growth rate and frequency of the perturbations decrease with increasing F. The horizontal structure of the perturbations changes slightly. The instability process occurs within one triad which is the triad closest to resonance. The stability properties of the observed 400 mb Northern Hemisphere winter climatological flow show both growth rate and frequency (of the perturbations) decrease for increasing F. ESA

N90-13002 Royal Netherlands Meteorological Inst., De Bilt. Div. of Oceanographic Research.

CLIMATOLOGICAL DATA FOR THE NORTH SEA BASED ON OBSERVATIONS BY VOLUNTARY OBSERVING SHIPS OVER THE PERIOD 1961-1980

C. G. Korevaar 1989 135 p
(KNMI-WR-89-02; ISSN-0169-1651; ETN-89-95601) Copyright
Avail: Royal Netherlands Meteorological Inst., P.O. Box 201, 3730 de Bilt, Wilhelminalaan 10, Netherlands

A selection of data about the North Sea climate is given. The data, assembled from voluntary observing ships, concerns temperature, wind, wave, visibility, air pressure, cloud cover, and precipitation. An average number of at least one observation per day for a great number of one degree squares (squares of one degree latitude by one degree longitude), and for other one degree squares an average of at least one observation in two days, is recorded. The observations are stored on magnetic tape and are subjected to a quality control program. The observations of the selected ships are at six-hourly intervals (standard times are 00, 06, 12 and 18 hours). Most observations are found along the main shipping routes, and a safisfactory coverage in space and time is obtained. ESA

N90-13003*# Colorado Univ., Boulder. Cooperative Inst. for Research in Environmental Sciences.

CLOUD COVER DETERMINATION IN POLAR REGIONS FROM SATELLITE IMAGERY Final Report

R. G. Barry and J. Key 15 Dec. 1989 269 p Prepared in cooperation with NOAA, Boulder, CO
(Grant NAG5-898)
(NASA-CR-186096; NAS 1.26:186096) Avail: NTIS HC A12/MF A02 CSCL 04B

The objectives are to develop a suitable validation data set for evaluating the effectiveness of the International Satellite Cloud Climatology Project (ISCCP) algorithm for cloud retrieval in polar regions, to identify limitations of current procedures and to explore potential means to remedy them using textural classifiers, and to compare synoptic cloud data from model runs with observations. Toward the first goal, a polar data set consisting of visible, thermal, and passive microwave data was developed. The AVHRR and SMMR data were digitally merged to a polar stereographic projection with an effective pixel size of 5 sq km. With this data set, two unconventional methods of classifying the imagery for the analysis of polar clouds and surfaces were examined: one based on fuzzy sets theory and another based on a trained neural network. An algorithm for cloud detection was developed from an early test version of the ISCCP algorithm. This algorithm includes the identification of surface types with passive microwave, then temporal tests at each pixel location in the cloud detection phase. Cloud maps and clear sky radiance composites for 5 day periods are produced. Algorithm testing and validation was done with both actural AVHRR/SMMR data, and simulated imagery. From this point in the algorithm, groups of cloud pixels are examined for their spectral and textural characteristics, and a procedure is developed for the analysis of cloud patterns utilizing albedo, IR temperature, and texture. In a completion of earlier work, empirical analyses of arctic cloud cover were explored through manual interpretations of DMSP imagery and compared to U.S. Air Force 3D-nephanalysis. Comparisons of observed cloudiness from existing climatologies to patterns computed by the GISS climate model were also made. Author

N90-13004# National Oceanic and Atmospheric Administration, Boulder, CO. Program for Regional Observing and Forecasting Services.

SUBJECTIVE USES OF WIND PROFILER DATA IN WARM SEASON ANALYSIS AND FORECASTING: WIND PROFILER TRAINING MANUAL NUMBER 3

Raymond H. Brady and Keith A. Brewster Apr. 1989 109 p Sponsored by National Weather Service, Silver Spring, MD
(PB89-223333) Avail: NTIS HC A06/MF A01 CSCL 04B

The training manual illustrates, through concise case studies, how the subjective analysis of profiler derived winds can be used in detecting mesoscale and synoptic scale upper air features which affect the analysis and forecasting of warm season weather events. Occasional references to conceptual models of profiler wind interpretation are included. Every signature detected in the data is not explained or commented on because several features are not

fully understood. The focus of the manual is to introduce the data to the forecaster. Other routinely available products essential in forecasting and analysis (e.g., radar and satellite data) are shown, and the incorporation and assimilation of all these data is stressed. Some of the attributes of the profiling system and data are described. The characteristics of the summer environment and its impact on the forecast problem are discussed, and specific cases are illustrated. Author

N90-13005# Royal Signals and Radar Establishment, Malvern (England).
A REAL-TIME WIND MODEL USING DIGITAL DATA FROM AIRCRAFT
M. F. Worsley and A. J. Hughes 28 Jul. 1989 25 p Sponsored by the Civil Aviation Authority, London, England
(RSRE-Memo-4309; BR111666; ETN-89-94869) Copyright
Avail: NTIS HC A03/MF A01

An approach to modeling upper atmospheric winds is described. The input data is obtained automatically from aircraft via a digital data link. A statistical method is used to combine the observational data. The realization of the one-dimensional implementation of the model is shown. The results of operating this model in real time are presented. The input data is obtained during ascents and descents of flights effectuated on January 10th and 11th 1989. ESA

N90-13006# Reading Univ. (England).
PROJECT WIND: EXPERIMENTS WITH THE UK METEOROLOGICAL OFFICE MESOSCALE MODEL Final Report, Jun. 1987 - Dec. 1988
R. P. Pearce 5 Sep. 1989 44 p
(Contract DAJA45-87-C-0035; DA Proj. 1L1-61102-BH-57)
(AD-A212291; R/D-5733-EN-01) Avail: NTIS HC A03/MF A01
CSCL 04/2

A preliminary report describing the first three numerical experiments carried out on the UK Meteorological Office (UKMO) mesoscale model using project WIND (Phase 1) data was prepared in Sept. 1987. This present report incorporates the results described in that report and goes on to describe subsequent work carried out between Oct. 1987 and March 1989. This included: (1) further analysis of the results of experiments 1, 2, and 3; (2) experiment 4, incorporating a change of surface albedo; (3) experiments with a single-column version of the MO model; and (4) the developement of a computer program to carry out three-dimensional objective analyses of project WIND data. Conclusions drawn from these experiments stress the implications of the results for future development of the heirarchy of models, particularly SIGMET, at the Atmospheric Sciences Lab (ASL). GRA

N90-13007# Colorado State Univ., Fort Collins.
MULTIPARAMETER RADAR ESTIMATION OF RAINDROP SIZE DISTRIBUTION Final Report
V. N. Bringi and V. Chandrasekar 7 Aug. 1989 3 p
(Contract DAAL03-86-K-0117)
(AD-A212410; ARO-23935.5-GS) Avail: NTIS HC A02/MF A01
CSCL 04/2

The error structure of multiparameter radar and surface disdrometer measurements of rainfall has been studied in detail. The radar observables studied were reflectivity, differential reflectivity and X-band specific attenuation. These radar observables were simulated from fundamental considerations which incorporated statistical fluctuations due to the Doppler spectrum and the cross-correlation between H and V-polarized signals at zero time lag. Surface disdrometer measurements were also simulated accounting for the Poisson and Gamma distributed nature of the drop samples. Sampling fluctuation as well as physical variabilities of the drop size distribution were incorporated into the radar and disdrometer simulations. An intercomparison of these simulated variables revealed the nature and reason for certain inconsistencies. The use of differential reflectivity does indeed improve the characterization of the median drop size, and that its use in rainfall rate estimation will increase the accuracy by approximately a factor of 2 over conventional reflectivity based methods. The axis ratio of raindrops is analyzed as functions of their size using 2D-PMS probe images of drops in convective rainshafts. Axis ratios were estimated for about 3500 drops using the Fourier descriptor technique. GRA

N90-13008# Naval Research Lab., Washington, DC. Atmospheric Physics Branch.
CATALOG OF ABSOLUTELY CALIBRATED, RANGE NORMALIZED, WIDEBAND, ELECTRIC FIELD WAVEFORMS FROM LOCATED LIGHTNING FLASHES IN FLORIDA: JULY 24 AND AUGUST 14, 1985 DATA
J. C. Bailey and J. C. Willett 1 Aug. 1989 322 p
(AD-A212708; NRL-MR-6497) Avail: NTIS HC A14/MF A01
CSCL 20/14

The electric field and its time derivative from located intra-cloud and cloud to ground lightning discharges were measured in Florida over salt water paths with flat plate antennas mounted on the roof of a metallic trailer. Also recorded was the HF energy spectral density within a 1.45 microsecs time window at either 5, 10, or 15 MHz averaged over a 1 MHz bandwidth. In this report we present range-normalized waveforms of all located lightning events in two storms occurring on 24 July and 14 August 1985. These events are classified into 15 categories according to previously identified electric field waveforms. Statistical and spectral analyses of these data will be presented in forthcoming papers. One result became evident from the data. Approximately 57 percent of the first return strokes had HF radiation preceding them indicative of the characteristic pulses described by Beasley et al., 1984. It was unclear if this result indicates that characteristic pulses do not always precede first return strokes. GRA

48 OCEANOGRAPHY

Includes biological, dynamic, and physical oceanography; and marine resources.

For related information see also *43 Earth Resources and Remote Sensing.*

N90-13009# National Weather Service, Silver Spring, MD. Climate Analysis Center.
ATLAS OF TROPICAL SEA SURFACE TEMPERATURE AND SURFACE WINDS
Michael S. Halpert and C. F. Ropelewski Jun. 1989 214 p
(PB89-223598; NOAA-ATLAS-8) Avail: NTIS HC A10/MF A02
CSCL 08C

An atlas of sea surface temperatures (SSTs) and surface winds over the global tropical oceans based on the Comprehensive Ocean Atmosphere Data Set (COADS) is presented. The emphasis of the atlas is the evolution of the annual cycle and variations about it. Mean SST, zonal and meridional wind means, standard deviations, differences from the annual mean and differences from the zonal mean are presented for the period 1950 to 1979, along with the vector wind means and differences from the annual mean. Time-longitude cross sections from 1950 to 1987 are shown for the mean, anomaly, and difference from the annual mean for the zonal wind, meridional wind and SST. Mean and anomalous ENSO composites for the vector wind and SST based on the years 1951, 1953, 1957, 1965, 1969, 1972, and 1976 are presented. Author

N90-13010# National Oceanic and Atmospheric Administration, Miami, FL. Oceanographic and Meteorological Labs.
CURRENT VELOCITY AND HYDROGRAPHIC OBSERVATIONS IN THE SOUTHWESTERN NORTH ATLANTIC OCEAN: SUBTROPICAL ATLANTIC CLIMATE STUDIES (STACS), 1988
Anne Marie Wilburn, Elizabeth Johns, and Mark Bushnell Jun. 1989 89 p
(PB89-230825; NOAA-DR-ERL-AOML-13) Avail: NTIS HC A05/MF A01 CSCL 08C

The primary objectives of the Subtropical Atlantic Climate Studies (STACS) program are to increase our understanding of the dynamics of the North Atlantic circulation and the role of ocean circulation in global climate, to develop the capability to

monitor the climatically important processes, and to provide data needed in the development of the coupled ocean-atmosphere general circulation models to be used for global climate prediction. In particular, the mechanisms by which the ocean transports heat to balance the net radiation deficit at northerly latitudes are being studied. Author

N90-13011# Naval Ocean Research and Development Activity, Bay Saint Louis, MS.
SURFACE CURRENT AND WAVE MODULATION MEASUREMENTS OVER BOTTOM TOPOGRAPHY: A COMPARISON WITH THEORY
Peter Smith and Donald Johnson 14 Jul. 1989 5 p Repr. from Proceedings of the 12th Canadian Symposium, Remote Sensing, 10-14 Jul. 1989 p 2710-2713
(AD-A212469; NORDA-PR-89; Rept-031; Rept-321) Avail: NTIS HC A02/MF A01 CSCL 08/3

The wave-current interaction model of Hughes (1978) is applied to the case of flow over bottom topography. The surface current is prescribed using data from four surface-following current meters positioned over a bottom feature on Nantucket Shoals. The ambient wave spectrum is prescribed using data collected by a drifting spar buoy. The current profiles across the submerged sill exhibits minima in both components of current. The dominating wave growth mechanism is the refraction of waves near the minimum in the along isobath component of flow. The spikey nature of the wave modulation dictates that finite amplitude together with wave-wave interaction terms should be included in the action transport equation. GRA

N90-13012# Naval Ocean Research and Development Activity, Bay Saint Louis, MS.
THE REGIONAL POLAR ICE PREDICTION SYSTEM, BERENTS SEA (RPIPS-B): A TECHNICAL DESCRIPTION Final Report
Ruth H. Preller, Shelley Riedlinger, and Pamela G. Posey May 1989 42 p
(AD-A213159; NORDA-182) Avail: NTIS HC A03/MF A01 CSCL 08/12

The hydraulic/thermodynamic Artic sea-ice model is designed by W. D. Hibler of the Cold Regions Research and Engineering Laboratory (CREEL) was adapted to the Barents Sea. This model is driven by atmospheric forcing from the Naval Operational Global Atmospheric Prediction System (NOGAPS) and oceanic forcing from the Hibler and Bryan coupled ice-ocean model. This high resolution model (25 km), which covers the entire Barents Sea and the western half of the Kara Sea, uses a 6-hour time step. Model results show good agreement with such data as the Naval Polar Oceanography Center's (NPOC) analysis of ice concentration and concentrations derived from passive microwave data. The model has a tendency, however, to melt ice too quickly in summer and to grow it back too slowly in the fall. Planned improvements in the atmospheric and oceanic forcing should correct this problem. The high resolution of the Barents Sea model enables it to predict the ice edge, ice growth and decay, and the movement of ice near land boundaries with greater accuracy than does the PIPS model. The Regional Polar Ice Prediction System for the Barents Sea (RPIPS-B) is the forecast system designed to run at the Fleet Numerical Oceanography Center (FNOC) based on the Barents Sea Ice model. RPIPS-B is updated weekly by the NPOC analysis of ice concentration. The forecast system, presently in its operational checkout phase, is being made ready for a winter-spring operational test. GRA

51 LIFE SCIENCES (GENERAL)

No abstracts in this category.

52 AEROSPACE MEDICINE

Includes physiological factors; biological effects of radiation; and effects of weightlessness on man and animals.

N90-13013*# National Aeronautics and Space Administration. Ames Research Center, Moffett Field, CA.
CARDIOVASCULAR, RENAL, ELECTROLYTE, AND HORMONAL CHANGES IN MAN DURING GRAVITATIONAL STRESS, WEIGHTLESSNESS, AND SIMULATED WEIGHTLESSNESS: LOWER BODY POSITIVE PRESSURE APPLIED BY THE ANTIGRAVITY SUIT Thesis - Oslo Univ.
Stein E. Kravik Oct. 1989 142 p Sponsored in part by NAS-NRC, Washington, DC; Joint Medical Service, HQ Defense Command, Norway and the Norwegian Research Council for Science and the Humanities
(NASA-TM-102232; A-89084; NAS 1.15:102232) Avail: NTIS HC A01/MF A01 CSCL 06S

Because of their erect posture, humans are more vulnerable to gravitational changes than any other animal. During standing or walking man must constantly use his antigravity muscles and his two columns, his legs, to balance against the force of gravity. At the same time, blood is surging downward to the dependent portions of the body, draining blood away from the brain and heart, and requiring a series of complex cardiovascular adjustments to maintain the human in a bipedal position. It was not until 12 April 1961, when Yuri Gagarin became the first human being to orbit Earth, that we could confirm man's ability to maintain vital functions in space -- at least for 90 min. Nevertheless, man's adaptation to weightlessness entails the deconditioning of various organs in the body. Muscles atrophy, and calcium loss leads to loss of bone strength as the demands on the musculoskeletal system are almost nonexistent in weightlessness. Because of the lack of hydrostatic pressures in space, blood rushes to the upper portions of the body, initiating a complex series of cardioregulatory responses. Deconditioning during spaceflight, however, first becomes a potentially serious problem in humans returning to Earth, when the cardiovascular system, muscles and bones are suddenly exposed to the demanding counterforce of gravity -- weight. One of the main purposes of our studies was to test the feasibility of using Lower Body Positive Pressure, applied with an antigravity suit, as a new and alternative technique to bed rest and water immersion for studying cardioregulatory, renal, electrolyte, and hormonal changes in humans. The results suggest that Lower Body Positive Pressure can be used as an analog of microgravity-induced physiological responses in humans. Author

N90-13014# Army Research Inst. of Environmental Medicine, Natick, MA.
HEAT EXHAUSTION
Lawrence E. Armstrong 30 Jun. 1989 4 p
(AD-A212128; USARIEM-M61-89) Avail: NTIS HC A01/MF A01 CSCL 06/10

Heat exhaustion is the most common heat illness, among soldiers and athletes. This manuscript is written in an ask the expert format, per request of the journal editor, to describe heat exhaustion for the athletes and practitioner. This manuscript describes the signs/symptoms, physiological cause, treatment, and measures which can be taken to prevent heat exhaustion. GRA

N90-13015# Health Effects Research Lab., Research Triangle Park, NC. Neurotoxicology Div.
EFFECTS OF ATMOSPHERIC MIX AND TOXIC FUMES ON MILITARY PERFORMANCE
Vernon A. Benignus 1989 85 p
(PB89-223630; EPA/600/D-89/060) Avail: NTIS HC A05/MF A01 CSCL 06P

The individual and combined neurobehavioral effects of carbon monoxide, hydrogen cyanide, carbon dioxide and hypoxic hypoxia were studied. The literature of the effects of combined exposures were covered. This is a relatively sparse literature. The empirical and physiological information available was encoded as a series of dose-effects and pharmacokinetic equations. Assuming additive effects, a mathematical model was proposed for the combined

exposure. Several pharmacokinetic interactions make the received dose of the combined pollutants nonadditive, however, and thus introduce nonadditivity into the combined model. The model was useful in pointing out the kind of information still needed to make predictions. The model thus serves a mainly heuristic purpose. GRA

N90-13016# Michigan Univ., Ann Arbor. Dept. of Electrical Engineering and Computer Science.
TIME-FREQUENCY FACTORS IN AUDITORY PERCEPTION Annual Report, 15 Apr. 1988 - 14 Apr. 1989
Gregory H. Wakefield 30 Jun. 1989 13 p
(Grant AF-AFOSR-0193-87; AF Proj. 2313)
(AD-A211491; AFOSR-89-1081TR) Avail: NTIS HC A02/MF A01 CSCL 06/4

This research investigates how the human auditory system processes temporal properties of a complex signal across two or more regions of the frequency spectrum. Much of the primary research from the original proposal on envelope phase disparity using AM carriers is complete. Several findings are outlined. A computer model has also been developed and analyzed to consider issues of cross-spectral temporal disparities. The model is based on localization by Colburn, among others. GRA

N90-13017# Air Force Occupational and Environmental Health Lab., Brooks AFB, TX.
BASE LEVEL MANAGEMENT OF RADIO FREQUENCY RADIATION PROTECTION PROGRAM Final Report
Steven E. Rademacher and Noel D. Montgomery Apr. 1989 111 p
(AD-A211759; USAFOEHL-89-023RC0111DRA) Avail: NTIS HC A06/MF A01 CSCL 25/2

Assistance is being developed for the base level aerospace medical team to manage their radio frequency radiation protection program. This report supersedes USAFOEHL Report 80-42, A practical R-F Guide for BEES. GRA

N90-13018# Deutsche Forschungsanstalt fuer Luft- und Raumfahrt, Cologne (Germany, F.R.). Inst. fuer. Flugmedizin.
BIOCHEMICAL AND PHYSIOLOGICAL CHANGES IN GLIDER PILOTS DURING MULTIHOUR FLIGHTS Thesis - Bonn Univ.
Klaus Gerecht Jun. 1989 118 p In GERMAN; ENGLISH summary Report will also be announced as translation (ESA-TT-1183)
(DLR-FB-89-29; ISSN-0171-1342; ETN-89-95838) Avail: NTIS HC A06/MF A01; DLR, VB-PL-DO, Postfach 40 60 58, 5000 Cologne, Fed. Republic of Germany, 40 Deutsche marks

Nine male glider pilots were studied during 12 multi-hour glider flights. Blood and urine samples were taken before, during and after each flight. The results revealed a high sympathetic, adrenomedullary and adrenocortical activity. Findings included a reduction in numbers of eosinophils, changes in blood lipid fractions due to induced lipolysis and an elevation of blood sugar concentrations during the flight, going back to normal shortly after landing. Excretion of adrenaline was highest during the preflight period showing a high level of anticipatory stress, followed by moderate reductions during the flight as opposed to increasing excretion rates of noradrenaline and 17-hydroxycorticosteroids. This pattern is related to increasing fatigue with length of flight. Subsequently loss of weight and elevated packed cell volumes were noted. Reduced serum potassium concentrations associated with more alkaline urine are sequels of hyperventilation, a common condition in pilots under flight stress. ESA

N90-13019# Deutsche Forschungsanstalt fuer Luft- und Raumfahrt, Cologne (Germany, F.R.). Inst. fuer Flugmedizin.
EFFECTS OF A TIME ZONE SHIFT OF NINE HOURS ON THE CIRCADIAN RHYTHMS IN COCKPIT AIRCREW MEMBERS ON LONGHAUL FLIGHTS Ph.D. Thesis - Tech. Hochschule Aachen
Silke Ruth Hasenclever Jun. 1989 94 p In GERMAN; ENGLISH summary Report will also be announced as translation (ESA-TT-1185)
(DLR-FB-89-31; ISSN-0171-1342; ETN-89-95840) Avail: NTIS HC A05/MF A01; DLR, VB-PL-DO, Postfach 40 60 58, 5000 Cologne, Fed. Republic of Germany, 32 Deutsche marks

Twelve aircrew members on a flight schedule crossing nine time zones are tested for heart rate, temperature, and excretion of certain hormone metabolites and electrolytes in the urine over a period of seven days. The data is analyzed regarding circadian rhythmicity. The results of this analysis are demonstrated and the possible effects of disturbing body rhythms of members of this profession are discussed. ESA

N90-13020# Army Research Inst. of Environmental Medicine, Natick, MA.
EXERTIONAL HEATSTROKE: AN INTERNATIONAL PERSPECTIVE. AN INTRODUCTION: THE ROLE OF EXERCISE IN THE ETIOLOGY OF EXERTIONAL HEATSTROKE Report, May - Jun. 1989
Roger W. Hubbard 12 Jun. 1989 17 p
(AD-A212242; USARIEM-M60-8968) Avail: NTIS HC A03/MF A01 CSCL 06/10

Exertional heatstroke usually occurs among healthy, fit individuals who are motivated to perform strenuous exercise because of peer pressure, discipline, or athletic competition. In fact, exertional heatstroke deaths among high school athletes in the United States ranked only third to head and neck injuries and heart failures. The reluctance of race directors to cancel or postpone mass participation road races during periods of severe heat and humidity, emphasize a continuing need for widespread dissemination of information. The purposes of this symposium are to: (1) convey essential information to the members of ACSM who are involved in exercise prescription, patient care, or athletic training, and (2) to disseminate recent scientific theories and research concerning exertional heatstroke. GRA

N90-13021# Virginia Univ., Charlottesville. Dept. of Materials Science.
SHAPE INSTABILITIES OF PLATE-LIKE STRUCTURES. 1: EXPERIMENTAL OBSERVATIONS IN HEAVILY COLD WORKED IN SITU COMPOSITES
T. H. Courtney (Naval Research Lab., Washington, DC.), J. C. Malzahn Kampe, and Y. Leng 1989 12 p Submitted for publication
(Contract DAAL03-88-K-0091)
(AD-A212251; ARO-25177.4-MS-1) Avail: NTIS HC A03/MF A01 CSCL 23/2

Because hearing protectors attenuate the noise and signal by equal amounts within a given frequency range, reducing both to a level where there is less likelihood of distortion, they often provide improved listening conditions. The crossover level from disadvantage to advantage usually occurs between 80 and 90 dB. However, hearing protectors may adversely affect speech recognition under a variety of conditions. For hearing-impaired listeners, whose average hearing levels at 2000, 3000, and 4000 Hz exceed 30 dB, certain speech sounds will fall below the level of audibility. Visual cues may decrease the disadvantage imposed by hearing protectors. However, the Occlusion Effect, which decreases vocal output when the talker wears protection, adversely affects the listener's speech recognition. The poorest performance occurs when both talkers and listeners wear protectors. Hearing protectors affect warning signal perception in a similar manner. Again the crossover level seems to be between 80 and 90 dB, and there is greater degradation for individuals with impaired hearing. Earmuffs appear to pose greater problems than plugs, and this is especially true of difficulties in signal localization. Earplugs produce mainly front-back localization errors, while earmuffs produce left-right localization errors as well. Earmuffs also drastically impede localization in the vertical plane. GRA

N90-13022# Arizona State Univ., Tempe. Coll. of Liberal Arts and Sciences.
PREDICTION OF THERMAL STRESS CASUALTIES Final Report, Mar. 1986 - Sep. 1988
Gary S. Krahenbuhl, Joseph Harris, Stefan H. Constable (School

of Aerospace Medicine, Brooks AFB, TX.), Don W. Morgan, and Jeffrey K. Allen May 1989 44 p
(Contract F33615-83-D-0602; AF Proj. 2729)
(AD-A212356; USAFSAM-TR-88-23) Avail: NTIS HC A03/MF A01 CSCL 06/10

Young adult male subjects (n=15) were monitored under conditions featuring various combinations of three factors: work (rest or treadmill walking at 50 percent VO2), clothing (USAF flight suit or USAF flight suit plus the MOPP-IV chemical defense ensemble (CDE)), and environment (in an air conditioned laboratory or outside in the desert summer). Biogenic amine and metabolite responses were determined from timed urine samples using the high performance liquid chromatography (HPLC) with electrochemical detection. The response profiles of subjects (n=9) able to persist in their exercise while wearing CDE outdoors in the heat were compared with those (n=6) unable to persist (those who voluntarily terminated exercise at 50 percent VO2 max before they had worked for 30 min or reached a rectal temperature of 38.5 C (101.3 F)). The data supports the conclusion that subjects who persisted in their exercise did so because they pushed themselves harder. In doing so, they experienced a higher level of physiological stress as indicated by the alteration in the excretion rates of the biogenic amines and metabolites. GRA

N90-13023# Science Applications International Corp., McLean, VA.
CALCIUM DISPLACEMENT CAUSED BY ELECTROMAGNETIC FIELDS Final Report, 1 Nov. 1982 - 31 Aug. 1989
James D. Bond and Carol A. Jordan 31 Aug. 1989 9 p
(Contract N00014-83-C-0008; RR04108)
(AD-A212690; SAIC-89/1587) Avail: NTIS HC A02/MF A01 CSCL 06/7

The research effort was to determine theoretically a physical basis for the interaction of low intensity externally applied electromagnetic fields with biological tissue. The primary aim of the investigation was to establish a molecular basis for the class of interactions commonly referred to as nonthermal effects of electromagnetic fields with biological systems. In particular, the biological structure of interest was the plasma membrane since it had been either directly or indirectly implicated in numerous experimental studies. It was demonstrated how a membrane undergoing a phase transition could qualitatively account for the release and/or uptake of divalent calcium ions. A characterization of changes in the structure of the membrane/electrolyte interface due to field induced changes in enzymatic activity was demonstrated. The role of critical phenomena was shown analytically to be able to account for the unique sensitivity of biomembranes to weak external field perturbations, and describe alterations in the passive transport of sodium ions in rabbit erythrocytes. GRA

N90-13024# Naval Medical Research Inst., Bethesda, MD.
RADIO FREQUENCY (13.56 MHz) ENERGY ENHANCES REWARMING FROM MILD HYPOTHERMIA Interim Report
R. L. Hesslink, R. G. Olsen (Naval Aerospace Medical Research Lab., Pensacola, FL.), L. D. Allen, L. D. Homer, S. B. Lewis, and V. Harmon 9 May 1989 13 p
(AD-A212703; NMRI-89-46) Avail: NTIS HC A03/MF A01 CSCL 06/5

The rate of warming after hypothermia depends on the method of rewarming. The effectiveness is compared of radio frequency (RF) energy against hot (41 C) water immersion (HW) and an insulated cocoon (IC) for rewarming hypothermic men. Six men fasted overnight and were rewarmed for one hour after attaining a 0.5 reduction in rectal temperature (Tre). Tre and esophageal temperature (Tes) were recorded every 5 minutes with non-metallic thermal probes. The baseline value for Tre and Tes just prior to rewarming was subtracted from each 5 minute Tre and Tes during rewarming to delta Tre and delta Tes. The twelve delta Tes values were average for each individual and compared using ANOVA. The superiority of radio frequency energy for rewarming mildly hypothermic men is shown. GRA

N90-13025# Naval Medical Research Inst., Bethesda, MD.
EFFECTS OF SERIAL WET-DRY-WET COLD EXPOSURE: THERMAL BALANCE, PHYSICAL ACTIVITY, AND COGNITIVE PERFORMANCE Final Report, Jan. - Mar. 1988
T. J. Doubt, R. P. Weinberg, R. L. Hesslink, and S. T. Ahlers Mar. 1989 52 p
(AD-A212704; NMRI-89-35) Avail: NTIS HC A04/MF A01 CSCL 06/10

Thermal balance, physical performance, and cognitive function were examined in 7 U.S. Navy divers who each performed two 7-hour cold exposures while wearing a TLS dry suit with M-400 Thinsulate insulation for thermal protection. The exposures consisted of 2.5 h immersed in 5 C water, followed by 2 h in 5 C air, and then reentering the water for another 2.5 h. This exposure paradigm was intended to simulate an operational mission involving a wet-dry-wet cold exposure. During each exposure, leg exercise at 50 W was performed for the last 30 min of the first immersion and the first 30 min of the second immersion. In the course of one cold exposure, the subject walked 90 min on a treadmill at 2 mph during the dry phase, while during the other exposure he remained seated at rest for the dry phase. Cognitive function, measured at rest during the midpoint of each dry phase, was assessed by a battery of 7 NMRI-PAB tests. GRA

N90-13026# National Academy of Sciences - National Research Council, Washington, DC. Committee on Hearing, Bioacoustics and Biomechanics.
SOUND LOCALIZATION BY HUMAN OBSERVERS SYMPOSIUM PROCEEDINGS Technical Report, 1 Oct. 1988 - 30 Sep. 1989
1 Jul. 1989 68 p Symposium held in Washington, DC, 14-16 Oct. 1988
(Contract N00014-87-C-0342)
(AD-A212877) Avail: NTIS HC A04/MF A01 CSCL 06/4

The relation between binaural perception of actual sounds in space and of stimuli presented over headphones, base on head-related transfer functions, showed a high correlation. Listeners reported that the sound image presented over headphones remained internal to the head and not external in space, as with natural sound. Head movement, context, bias, experience, and integration of information across senses remain probable contributions to externalizing headphone-delivered sounds at their real-world positions. Sensory information provided by one sense modality may modulate that received by another modality via motor and/or efferent control. Interest was expressed in the possibility of constructing, and adapting to, super localization systems. The symposium focused on mammalian research but crucial insights were reported on other animal models. Thus there was demonstration that auditory space for the cat may be coded by spatial maps within the superior colliclus. Some human data were presented on the poorer accuracy of locating a source in the presence of multiple sources. Monaural localization, and the coding of sound movement were discussed. GRA

N90-13027# Naval Aerospace Medical Research Lab., Pensacola, FL.
A SCHEINER-PRINCIPLE POCKET OPTOMETER FOR SELF-EVALUATION AND BIOFEEDBACK ACCOMMODATION TRAINING Interim Report, 1987 - 1988
William B. Cushman 19 Apr. 1989 14 p
(AD-A213171; NAMRL-1344) Avail: NTIS HC A03/MF A01 CSCL 20/6

Most humans tend toward myopia when presented with a visual field without sufficient detail to stimulate focusing mechanisms. This means that a pilot flying in darkness, or in an empty field such as empty sky, will be likely to focus nearer the windscreen than at the optical infinity required to focus on visual targets of probable interest. Biofeedback training to counter this problem is limited in practical application by expensive and cumbersome instrumentation. A Scheiner-principle optometer was developed for self-evaluation of accommodative state and biofeedback training. The specific advantages of the new invention over earlier optometers are: (1) simplicity of design; (2) hand held,

portable implementation; (3) light weight; (4) small size; (5) low manufacturing cost; (6) the use of a monochromatic light source to eliminate the effects of chromatic aberrations in the subject's eye; and (6) effectiveness as a training aid. Four prototypes of the pocket optometer have built and were used to implement biofeedback training to correct night myopia in 12 Navy aviation candidates. All subjects were emmotropic in full light. Training was limited in duration due to the transient nature of subject availability but was reasonably successful in 10 out of the 12 cases. GRA

N90-13028# Defence and Civil Inst. of Environmental Medicine, Downsview (Ontario).
THE EFFECT OF CONCURRENT STRENGTH AND ENDURANCE TRAINING ON ELECTROMECHANICAL DELAY, MAXIMUM VOLUNTARY CONTRACTION, AND RATE OF FORCE DEVELOPMENT
D. G. Bell, I. Jacobs, D. G. Sale, and J. D. MacDougall Aug. 1989 25 p
(AD-A213316; DCIEM-88-RR-33) Avail: NTIS HC A03/MF A01 CSCL 06/10

The effect of strength and endurance training and their combination on electromechanical delays (EMD), rate of force development (RFD) and maximum voluntary isometric contraction force (MVC) of the knee extensors in male and female subjects is compared. The seven male and six female subjects were separated into a strength trained group (SG), 3 males and 3 females, and an endurance group (EG), 4 males and 3 females. The SG performed strength training solely with one leg and combined strength and endurance training with the other leg. The EG performed endurance training solely in one leg and combined strength and endurance training in the other leg. Strength training consisted of one legged work on a leg press weight machine. Endurance training consisted of one legged cycling on a cycle ergometer. EMD values were derived from electromyographic activity (EMG) recorded from the vastus laterialis muscle during MVC. MVC forces was measured with a force transducer. Rate of force development (RFD) was determined form the MVC/time curves using computer software. The EMG, MVC/time curves and light signal data were simultaneously recorded on FM tape and later sampled at 2Khz and stored digitally. The results showed that EMD was significantly reduced only in the SG females. Post training data showed that the EMD values for the SG females had increased and were not different from initial levels. EMD times for the males were significantly shorter that the females. GRA

53 BEHAVIORAL SCIENCES

Includes psychological factors; individual and group behavior; crew training and evaluation; and psychiatric research.

N90-13029# Yale Univ., New Haven, CT. School of Medicine.
FEAR-POTENTIATED STARTLE AS A MODEL SYSTEM FOR ANALYZING LEARNING AND MEMORY Annual Report, 1 Jul. 1988 - 30 Jun. 1989
Michael Davis 25 Jul. 1989 7 p
(Grant AF-AFOSR-0336-87; AF Proj. 2312)
(AD-A212131; AFOSR-89-1221TR) Avail: NTIS HC A02/MF A01 CSCL 05/8

Previous research has shown that the acoustic startle response, a simple reflex mediated by four synapses in the brainstem and spinal cord, can be increased when elicited in the presence of a light previously paired with a footshock. This fear-potentiated startle effect can be selectively blocked by drugs that decrease anxiety in humans as well as by lesions of the central nucleus of the amygdala, an area of the brain known to be critical for fear. This year it was found that local infusion of N-methyl-D-aspartate (NMDA) selective antagonists such as AP5 or CPP completely block the acquisition of fear-potentiated startle. This effect could not be attributed to a decrease in shock sensitivity or vision and did not occur when these compounds were infused into the cerebellum. These data indicate that an NMDA-dependent mechanism in the amygdala is involved in fear conditioning and that fear-potentiated startle may provide an excellent behavioral model system to analyze cellular and biochemical mechanisms of learning and memory. GRA

N90-13030# California Univ., San Diego. Dept. of Neurosciences.
ELECTROPHYSIOLOGICAL STUDIES OF VISUAL ATTENTION AND RESOURCE ALLOCATION Final Report, 1 Jun. 1986 - 31 May 1989
Steven A. Hillyard, G. R. Mangun, and S. J. Luck 30 Aug. 1989 48 p
(Contract N00014-86-K-0291; RR04209)
(AD-A212287; SDEPL-002) Avail: NTIS HC A03/MF A01 CSCL 05/8

The objective of this project was to better understand mechanisms of visual selective attention in humans, both at the level of perceptual processing and at the level of the underlying brain mechanisms. The main approach was to record event related brain potentials (EPRs) from the intact scalp using multielectrode arrays. Selective attention to stimulus location was found to enhance short latency brain evoked activity, analysis of current source densities indicated that visual inputs were subject to attentional control at or before the level of the pre-striate occipital cortex. Stimuli patterns of early sensory modulation were found during spatially focussed attention to rapid sequences of unilateral stimuli, to single stimuli occurring at precued locations, and to bilateral stimulus arrays. Applications of these techniques for evaluating how human operators allocate their attention to visual displays are discussed. GRA

N90-13031# Air Force Inst. of Tech., Wright-Patterson AFB, OH.
A COMPARISON OF TWO SUBJECT-CONTROLLED ATTITUDE MEASURES DURING SOMATOGRAVIC ILLUSION EXPOSURE M.S. Thesis - Saint Mary's Univ.
John F. Thompson May 1989 82 p
(AD-A212528; AFIT/CI/CIA-88-236) Avail: NTIS HC A05/MF A01 CSCL 06/10

The United States Air Force School of Aerospace Medicine (USAFSAM) has a requirement for a performance evaluation and comparison of two subject-controlled attitude indicators during exposure to the somatogravic or posturogravic illusion. This illusion is well known for giving aircraft pilots a false sensation of excessive pitch-up during take-off. With a lack of visual stimuli, the pilot misinterprets the resultant gravitoinertial force vector as approximating the vertical force vector of gravity. Accidents occur when pilots adjust to what they feel is level flight, when they are, in fact, pitched down toward the ground. The USAFSAM Vertifuge (spatial disorientation device) was used to generate this illusion in 16 subjects (8 experienced pilots and 8 nonpilots) by varying gravitoinertial and actual (cabin) pitch positions. Each subject rode the Vertifuge twice. During one session, the subject used a canopy-mounted downpointer to estimate position in space relative to the ground, and in other session the subject used a joystick-controlled inside-out aircraft attitude indicator. As expected, the results clearly indicate that the canopy-mounted downpointer is better at quantifying the somatogravic illusion in this Vertifuge study. Furthermore, it is apparent that there are no significant differences in performance between pilots and nonpilots using either device. GRA

N90-13032# New York Univ., New York. Dept. of Psychology.
THREE STAGES AND TWO SYSTEMS OF VISUAL PROCESSING
George Sperling 1989 35 p
(Grant AF-AFOSR-0140-88; AF Proj. 2313)
(AD-A212670; AFOSR-89-1131TR) Avail: NTIS HC A03/MF A01 CSCL 20/6

Three stages of visual processing determine how internal noise appears to an external observer: light adaptation, contrast gain control, and a postsensory/decision stage. Dark noise occurs prior

to adaptation, determines dark-adapted absolute thresholds, and mimics stationary external noise. Sensory noise occurs after dark adaptation, determines contrast thresholds for sine gratings and similar stimuli, and mimics external noise that increases with mean luminance. Postsensory noise incorporates perceptual, decision, and mnemonic process. It occurs after contrast-gain control and mimics external noise that increases with stimulus contrast (i.e., multiplicative noise). Dark noise and sensory noise are frequently specific and primarily affect weak signals. Only postsensory noise significantly affects to strong signals, and it has constant power over a wide spatial frequency range in which sensory noise varies enormously. GRA

N90-13033# Southeastern Center for Electrical Engineering Education, Inc., Saint Cloud, FL.
EFFECTS OF TYPE OF RESPONDING ON MEMORY/VISUAL SEARCH: RESPONDING JUST YES OR JUST NO CAN LEAD TO INFLEXIBLE PERFORMANCE Final Report, May - Sep. 1986
Arthur D. Fisk and Phillip L. Ackerman Aug. 1989 10 p
(Contract F30602-81-C-0193)
(AD-A212764; AFHRL-TR-88-75) Avail: NTIS HC A02/MF A01 CSCL 05/8

Interactions of stimulus consistency and type of responding were examined during perceptual learning. Subjects performed hybrid memory-visual search tasks over extended consistent and varied mapping process. Response conditions required subjects to respond to both the presence and absence of a target, only when a target is not present. After training, the subjects were transferred to a different response condition. The results indicate that: (1) performance on search tasks with stimuli that are variably mapped shows no qualitative changes attributable to manipulation of response format; (2) improvement due to consistent mapping (CM) practice is attenuated in the no-only response condition; (3) yes-only CM training attenuates the subjects' ability to transfer to no-only responding; and (4) yes/no CM training leads to the greatest improvement and transfer when compared with other responding conditions. The practice and transfer data support and extend previous research investigating effects of response set in memory/visual search and help to delineate factors that facilitate or inhibit reduction of load effects in memory and visual search. GRA

N90-13034# Air Force Human Resources Lab., Brooks AFB, TX. Manpower and Personnel Div.
INDIVIDUAL DIFFERENCES IN ASSOCIATIVE LEARNING AND FORGETTING Interim Report, Nov. 1985 - Nov. 1988
Patrick C. Kyllonen and William C. Tirre Aug. 1989 36 p
(AD-A212765; AFHRL-TP-89-46) Avail: NTIS HC A03/MF A01 CSCL 05/8

Individual differences in retention were examimed, with particular emphasis on its relationship with item-specific learning speed, general learning speed, and general cognitive factors. Young adults (N=710) were taught 13 name number pairs to varying successive success criteria using an item dropout procedure to ensure equal learning. Subjects were then taught re-pairings to varying criteria, in an A-B, A-Br design, so as to produce a range of forgetting conditions. Subjects then were asked to recall and relearn the original pairs. Item-specific learning speed predicted retention and reacquisition speed: The fastest learners, despite having the fewest number of study opportunities, remembered more and relearned faster. This relationship held over all forgetting conditions, and after statistically equating for within-list interference. General learning speed, as indicated by performance on an independent set of items administered in a variety of formats, also predicted retention and relearning. To examine the effects of other cognitive factors on learning and retention, various latent-variable path models were fit to the data. Results are contrasted with those of other investigators who, by employing different procedures for equating degree of learning, have concluded that there are no individual differences in retention. Implications for the discrepancy in conclusions are discussed. GRA

54 MAN/SYSTEM TECHNOLOGY AND LIFE SUPPORT

Includes human engineering; biotechnology; and space suits and protective clothing.

For related information see also *16 Space Transportation.*

N90-13035*# Johns Hopkins Univ., Baltimore, MD. Injury Prevention Center.
FATIGUE, PILOT DEVIATIONS AND TIME OF DAY Report, 15 Jul. 1988 - 30 Jun. 1989
Susan P. Baker 23 Jun. 1989 36 p
(Contract NCC2-555)
(NASA-CR-185369; NAS 1.26:185369) Avail: NTIS HC A03/MF A01 CSCL 05H

The relationships between pilot fatigue, pilot deviations, reported incidents, and time of day are examined. A sample of 200 Aviation Safety Reporting System (ASRS) reports were analyzed from 1985 and 200 reports from 1987, plus 100 reports from late 1987 and early 1988 that were selected because of possible association with fatigue. The FAA pilot deviation data and incident data were analyzed in relation to denominator data that summarized the hourly operations (landings and takeoffs of scheduled flights) at major U.S. airports. Using as numerators FAA data on pilot deviations and incidents reported to the FAA, the rates by time of day were calculated. Pilot age was also analyzed in relation to the time of day, phase of flight, and type of incident. B.G.

N90-13036*# Auburn Univ., AL. Dept. of Aerospace Engineering.
PROPOSAL FOR A ZERO-GRAVITY TOILET FACILITY FOR THE SPACE STATION Final Report
Edgar L. Fleri, Jr., Paul A. Galliano, Mark E. Harrison, William B. Johnson, and Gregory J. Meyer Jun. 1989 56 p Sponsored by USRA
(Contract NASw-4435)
(NASA-CR-183151; NAS 1.26:183151) Avail: NTIS HC A04/MF A01 CSCL 06K

This proposed toilet facility has a straightforward design. It has few moving parts and is easily maintained. Air and water flow provide sanitary movement of the waste. The toilet's chambers are coated with Teflon which, along with the water flow, makes it self-cleaning. An added disinfectant called Betadiene kills any bacteria that may form on the chamber walls. The chair is contoured to take into account the neutral body position and the necessary strain position for defecation. Restraints at the ankles, knees, and midsection hold the body in the chair. The waste is stored in discs of Gortex material which are inside a replaceable storage chamber. This chamber can be removed, capped and stored until eventual return to earth. Author

N90-13037# Advanced Decision Systems, Mountain View, CA.
TELEROBOTIC CONTROL FOR TEAMS OF SEMI-AUTONOMOUS AGENTS, PHASE 1 Final Report, 19 Jul. 1988 - 27 Feb. 1989
Marcel Schoppers and Daniel Shapiro 20 Apr. 1989 37 p
(Contract DAAE07-88-C-R076)
(AD-A211648; ADS-TR-3213-01) Avail: NTIS HC A03/MF A01 CSCL 23/2

A Robotic Command Center is to be developed to allow a commander and two drivers (three people) to control four remote vehicles. The drivers will be attempting to control two vehicles each, a difficult task. Giving vehicles a measure of autonomy is one way to simplify that task. On the other hand, deployed vehicles must not be hampered by software with limited competence or reliability. The only solution available soon is a vehicle control interface that allows for the entire range of possibilities between autonomous behavior and continuous teleoperation. Ideas are fused from telerobotics and from the Reaction Planning subfield of Artificial Intelligence, to develop a technology that permits vehicles to react autonomously to expected circumstances, while also permitting the human operator to instruct vehicles about what to

do and how to do it. This study will program some examples of behaviors for the vehicles to perform semi-autonomously, and those behaviors by running them in the Team Works I environment. An interface was designed and built that allows the vehicle driver to communicate with the intelligent software controlling any and all of the vehicles. A single person is capable of controlling four simulated vehicles at the same time. The competence of the vehicle is to be expanded to give the operator new ways of instructing the vehicles, and to push those capabilities toward deployment in the real world. GRA

N90-13038# Ecole Nationale Superieure des Telecommunications, Paris (France).
STATE OF THE ART OF HUMAN/MACHINE DIALOG TOOL PROTOTYPES [ETAT DE L'ART SUR LES OUTILS DE PROTOTYPAGE DE DIALOGUE HOMME-MACHINE]
Francois Cornec Jun. 1989 66 p In FRENCH
(Telecom-Paris-89-H001; ISSN-0751-1361; ETN-89-95505) Avail: NTIS HC A04/MF A01

Computer man/machine interfaces available on the market are investigated and criticized. The need to develop interfaces with good graphic quality is stressed. The need for portable work stations directed the researcher to use a bitmap screen, and use of a Macintosh was not excluded. The ideal tool is identified as one capable of operating on a wide variety of interface levels. The theory and function of different interface systems are outlined. ESA

N90-13039 Institute for Perception RVO-TNO, Soesterberg (Netherlands). Speech and Hearing Group.
PRE- AND POSTFLIGHT POSTURAL CONTROL OF THE D1 SPACELAB MISSION ASTRONAUTS EXAMINED WITH A TILTING ROOM
W. Bles and J. L. vanRaaij Dec. 1988 26 p
(IZF-1988-25; TD89-0532; ETN-89-94462) Copyright Avail: TNO Inst. for Perception, P.O. Box 23, 3769 ZG Soesterberg, Netherlands

The postural stability of the astronauts, examined with stabilometry in a tilting room, is examined. Postural control is effectuated again, on the preflight level, on the day after their return from space. Two of the astronauts are examined a few hours after their spaceflight and their postural control is affected. In one of them a preference for the visual information is found, resulting in a large body sway and disturbed spatial orientation. The other astronaut preferred otolith information and maintained postural control with effort. Theoretical background, experimental set up and consequences are discussed. No correlation is found between the behavior in the tilting room and spacesickness susceptibility. ESA

N90-13040# Laboratoire de Psychologie Experimentale, Grenoble (France).
PSYCHOLOGICAL MECHANISMS INVOLVED IN THE DISORIENTATION OF PILOTS DUE TO FLIGHT CONDITIONS Final Report [MECANISMES PSYCHOLOGIQUES IMPLIQUES PAR LE PILOTAGE DES SYSTEMES DE POINTAGE]
Christian Marendaz and Theophile Ohlmann 1988 20 p In FRENCH
(Contract DRET-86-047-00-470-75-01)
(ETN-89-95014) Avail: NTIS HC A03/MF A01

A flight simulation apparatus designed to test the disorientation effects of flight conditions is described. A pilot seat on a tri-axial mounting with a variety of visual simulation accessories is described. Tests carried out to determine what type of movements cause flight motion sickness are described. Different visual illusions are used to test pilots ability to deal with situations in which there is no horizon line reference. The use of such a simulation bench to select individuals best suited for fighter pilot service or space flight is stressed. ESA

N90-13041 Institute for Perception RVO-TNO, Soesterberg (Netherlands). Human Performance Group.
SPATIAL TESTS FOR AVIATORS
L. C. Boer Aug. 1988 24 p
(Contract A85/K/077)
(IZF-1988-15; TD88-4123; ETN-89-95090) Copyright Avail: TNO Inst. for Perception, P.O. Box 23, 3769 ZG Soesterberg, Netherlands

The spatial ability measured by tests and required in the cockpit of a fighter plane is discussed and new tests are proposed. They are based on tasks occurring in the cockpit, and include aspects such as the conflict between cognition and sensation, and the use of wide visual fields and moving objects. The spatial efficiency in the actual flying performance can be approximated by the use of checklists or rating scales for spatial performances in the air. Sense of direction, or navigation ability in real life are suggested as a secondary criterion. ESA

N90-13042 Institute for Perception RVO-TNO, Soesterberg (Netherlands). Audiology Group.
APPLICATION OF ACTIVE NOISE REDUCTION FOR HEARING PROTECTION AND SPEECH INTELLIGIBILITY IMPROVEMENT
H. J. M. Steeneken and J. G. vanVelden Dec. 1988 24 p
(Contract A87/K/048)
(IZF-1988-21; TD89-0321; ETN-89-96005) Copyright Avail: TNO Inst. for Perception, P.O. Box 23, 3769 ZG Soesterberg, Netherlands

Two active noise reduction systems for improving the sound attenuation of earmuffs are evaluated. The sound attenuation is objectively and subjectively measured. The speech intelligibility of the intercom facility is measured in combination with noise. The system increases the sound attenuation at frequencies below 500Hz up with 10 to 20 dB. The intelligibility in noise with a level of 110 dB increases with 0.2 speech transmission index. A field evaluation experiment revealed that the active noise reduction systems do not work at noise levels above 120 dB. Below this level, most subjects preferred the active noise reduction systems to their earmuffs. ESA

N90-13043# Army Natick Research and Development Command, MA.
AIR FORCE FLIGHT FEEDING. VOLUME 1: EVALUATION OF CURRENT SYSTEM AND ALTERNATIVE CONCEPTS Final Report, Oct. 1982 - Jan. 1985
Robert OBrien, Barbara Bell, and Christopher Rees Jul. 1989 157 p
(Contract DAAK60-83-C-0055)
(AD-A212789; NATICK/TR-89/039-Vol-1) Avail: NTIS HC A08/MF A01 CSCL 06/8

This report covers the initial phase of the project, during which the current Air Force flight feeding system was evaluated via an extensive data collection and analysis effort. Project objectives included development of a new flight feeding system concept to meet the needs of current flight missions as well as those of the coming decade, improved flight meal customer acceptance, and increased operating efficiency of flight kitchens. Crew opinions were obtained through 2,811 mail survey and 146 on-site surveys. Feedback was received on availability and acceptability of menu items, adequacy of galley equipment on board the aircraft, and flight feeding issues in general. Project team members visited several Air Force bases to observe flight kitchens in operation, to collect technical data on selected aircraft, and to meet with key personnel (crew members, food service personnel, aircraft maintenance representatives) to determine current flight feeding deficiencies and to identify possible solutions. Structured telephone surveys of 40 Air Force flight kitchens were conducted to determine equipment inventories, work space, storage space, and personnel resources. GRA

55 SPACE BIOLOGY

Includes exobiology; planetary biology; and extraterrestrial life.

N90-12804*# Jet Propulsion Lab., California Inst. of Tech., Pasadena.
THE NASA SETI SKY SURVEY: RECENT DEVELOPMENTS
M. J. Klein, S. Gulkis, E. T. Olsen, and N. A. Renzetti *In its* The Telecommunications and Data Acquisition Report 15 Aug. 1989 p 218-226 Previously announced in IAA as A89-17852
(For primary document see N90-12786 04-32)
Avail: NTIS HC A11/MF A02 CSCL 06C

59 MATHEMATICAL AND COMPUTER SCIENCES (GENERAL)

No abstracts in this category.

60 COMPUTER OPERATIONS AND HARDWARE

Includes hardware for computer graphics, firmware, and data processing.

For components see *33 Electronics and Electrical Engineering.*

N90-13044# Technische Univ., Delft (Netherlands). Faculty of Technical Mathematics and Informatics.
THE M/G/1 PROCESSOR SHARING QUEUE AS THE ALMOST SURE LIMIT OF FEEDBACK QUEUES
J. A. C. Resing, Gerard Hooghiemstra, and M. S. Keane 1989 16 p
(Rept-89-32; ISSN-0922-5641; ETN-89-95591) Copyright Avail: NTIS HC A03/MF A01

A probalilistic coupling between the M/G/1 processor sharing queue and the M/M/1 feedback queue, with general feedback probabilities, is established. This coupling is used to prove the almost sure convergence of sojourn times in the feedback model to sojourn times in the M/G/1 processor sharing queue. Using the theory of generative processes it follows that for stable queues the stationary distribution of the sojourn time in the feedback model converges in law to the corresponding distribution in the processor sharing model. The results do not depend on Poisson arrival times, but are also valid for general arrival processes. ESA

N90-13045# Technische Univ., Delft (Netherlands). Faculty of Technical Mathematics and Informatics.
AN EXPERT SYSTEM FOR VM PERFORMANCE ANALYSIS
D. H. J. Epema 1989 74 p
(Rept-89-30; ISSN-0922-5641; ETN-89-95589) Avail: NTIS HC A04/MF A01

A diagnostic expert system for the analysis of the performance of computer systems running the Virtual Machine (VM) operating system is described. The aim of the system, called BOTTLE, is to augment the system programmer and performance analyst in the task of analyzing manually reports with data on the performance and resource utilization of the system components. An overview of, and performance measurement and reporting of, VM systems is given. The expert system environment is explained and a general design methodology for diagnostic expert systems which is applied to BOTTLE is given. Design issues of performance analysis expert systems, and the structure and capabilities of BOTTLE are discussed. Opportunities for fuzzy control in BOTTLE and the use of other expert system languages are addressed. E.R.

N90-13046# Naval Postgraduate School, Monterey, CA.
PERFORMANCE EVALUATIONS OF A PARALLEL AND EXPANDABLE DATABASE COMPUTER: THE MULTI-BACKEND DATABASE COMPUTER M.S. Thesis
James E. Hall Jun. 1989 100 p
(AD-A212761) Avail: NTIS HC A05/MF A01 CSCL 12/5

The actual application of a performance evaluation technique known as benchmarking to an experimental database management system (DBMS) is presented. The specific DBMS evaluated is the Multi-Backend Database System (MBDS) which is a software multiple backend database system. The unconventional nature of a multiple backend computer system required the development of a special performance evaluation methodology which was the topic of several related thesis. A previously developed performance evaluation methodology had only been applied to MBDS on a very small scale and had not been used with the current set of modern MBDS hardware. The current focus is the verification of the performance claims made by the implementor of MBDS. These performance claims were, in fact, validated by conducting a series of relatively large scale benchmarking experiments in which MBDS performed, generally, as predicted by its implementor. While the results are encouraging, future benchmarking experiments need to be conducted on an even larger database to examine MBDS performance under an extreme load. This will require the developement of a high-speed database loading utility which is not the current focus. Here, the test databases is reported along with test transactions and test results (which constitute the benchmarks) used to verify the MBDS implementor's claims of response time reduction and response time invariance. GRA

61 COMPUTER PROGRAMMING AND SOFTWARE

Includes computer programs, routines, alogorithms, and specific applications, e.g., CAD/CAM.

N90-13047*# Research Inst. for Advanced Computer Science, Moffett Field, CA.
TELESCIENCE TESTBED PILOT PROGRAM Quarterly Report No. 4, 1 Mar. 1988 - 31 Aug. 1988
Maria L. Gallagher, ed. and Barry M. Leiner, ed. 1 Jun. 1988 74 p
(Contract NASw-4234)
(NASA-CR-184997; NAS 1.26:184997; RIACS-M88.4) Avail: NTIS HC A04/MF A01 CSCL 09B

The Telescience Testbed Pilot Program (TTPP) is intended to develop initial recommendations for requirements and design approaches for the information system of the Space Station era. Multiple scientific experiments are being performed, each exploring advanced technologies and technical approaches and each emulating some aspect of Space Station era science. The aggregate results of the program will serve to guide the development of future NASA information systems. Author

N90-13048*# National Aeronautics and Space Administration. Ames Research Center, Moffett Field, CA.
A KNOWLEDGE-BASED APPROACH TO AUTOMATED FLOW-FIELD ZONING FOR COMPUTATIONAL FLUID DYNAMICS
Alison Andrews Vogel Apr. 1989 150 p
(NASA-TM-101072; A-89044; NAS 1.15:101072) Avail: NTIS HC A07/MF A01 CSCL 09B

An automated three-dimensional zonal grid generation capability for computational fluid dynamics is shown through the development of a demonstration computer program capable of automatically zoning the flow field of representative two-dimensional (2-D) aerodynamic configurations. The applicability of a knowledge-based programming approach to the domain of flow-field zoning is examined. Several aspects of flow-field zoning make the application of knowledge-based techniques challenging: the need for perceptual information, the role of individual bias in the design

and evaluation of zonings, and the fact that the zoning process is modeled as a constructive, design-type task (for which there are relatively few examples of successful knowledge-based systems in any domain). Engineering solutions to the problems arising from these aspects are developed, and a demonstration system is implemented which can design, generate, and output flow-field zonings for representative 2-D aerodynamic configurations.
Author

N90-13049# Helsinki Univ. of Technology, Espoo (Finland). Lab. of Computer and Information Science.
SELF-ORGANIZING SEMANTIC MAPS
Helge Ritter (Technische Univ., Munich, Germany, F.R.) and Teuvo Kohonen 31 Mar. 1989 30 p
(PB89-212609; A-8; ISBN-951-754-842-7; ISSN-0783-7445)
Avail: NTIS HC A03/MF A01 CSCL 09B

Self-organized formation of topographic maps for abstract data, such as words, is demonstrated. The semantic relationships in the data are reflected by their relative distances in the map. Two different simulations are given. Both are based on a neural network model that implements the algorithm of the self-organizing feature maps. For both, an essential, new ingredient is the inclusion of the contexts, in which each symbol appears, into the input data. This enables the network to detect the logical similarity between words from the statistics of their contexts. In the first demonstration, the context simply consists of a set of attribute values that occur in conjunction with the words. In the second demonstration, the context is defined by the sequences in which the words occur, without consideration of any associated attributes. Simple verbal statements consisting of nouns, verbs, and adverbs were analyzed in this way. GRA

N90-13050*# Computer Sciences Corp., Hampton, VA.
SPACECRAFT ORBIT DESIGN AND ANALYSIS (SODA), VERSION 1.0 USER'S GUIDE
Scott S. Stallcup and John S. Davis Aug. 1989 42 p
(Contract NAS1-17999)
(NASA-CR-181932; NAS 1.26:181932; TAO 50342) Avail: NTIS HC A03/MF A01 CSCL 09B

The Spacecraft Orbit Design and Analysis (SODA) computer program, Version 1.0 is described. SODA is a spaceflight mission planning system which consists of five program modules integrated around a common database and user interface. SODA runs on a VAX/VMS computer with an EVANS & SUTHERLAND PS300 graphics workstation. BOEING RIM-Version 7 relational database management system performs transparent database services. In the current version three program modules produce an interactive three dimensional (3D) animation of one or more satellites in planetary orbit. Satellite visibility and sensor coverage capabilities are also provided. One module produces an interactive 3D animation of the solar system. Another module calculates cumulative satellite sensor coverage and revisit time for one or more satellites. Currently Earth, Moon, and Mars systems are supported for all modules except the solar system module.
Author

N90-13051# Thomson-CSF, Palo Alto, CA.
A TRANSFORMATIONAL METHOD FOR VERIFYING SAFETY PROPERTIES IN REAL TIME SYSTEMS
Matthew K. Franklin and Armen Gaberielian Jul. 1989 21 p
(Contract N00014-89-C-0022)
(AD-A211925; TR-89-12) Avail: NTIS HC A03/MF A01 CSCL 12/7

The behavior of systems with hard real-time constraints can be specified in terms of Hierarchical Multi-State (HMS) abstract machines, which are generalizations of finite-state automata. A two-step method is presented for verifying that safety properties are not violated by an HMS specification of a system. In the first step, the safety verification question is recast as a reachability problem in an extension of the HMS machine. In the second step, reachability is determined by the use of correctness-preserving and partial correctness-preserving transformations. The method is shown to be complete, and it is illustrated by verifying that a safety property holds for a simple railroad-crossing system if all of its deadlines are met. GRA

N90-13052# Yale Univ., New Haven, CT. Dept. of Computer Science.
A FAST ALGORITHM FOR THE EVALUATION OF HEAT POTENTIALS
Leslie Greengard and John Strain (New York Univ., New York.) May 1989 18 p Sponsored by IBM and NSF
(Contracts N00014-89-J-1527; F49620-87-C-0065)
(AD-A211316; YALEU/DCS/RR-700) Avail: NTIS HC A02/MF A01 CSCL 20/13

Numerical methods for solving the heat equation via potential theory were ampered by the high cost of evaluating heat potentials. When M points are used in the discretization of the boundary and N time steps are computed, an amount of work of the order O(N-sq Msq) has traditionally been required. An algorithm was presented which requires an amount of work of the order O(NM), and speedups were observed for five orders of magnitude for large-scale problems. Thus, the method makes it possible to solve the heat equation by potential theory in practical situations. GRA

N90-13053# University of Southern California, Marina del Rey. Information Sciences Inst.
ISI'S (INFORMATION SCIENCES INSTITUTE) SDI ARCHITECTURE SIMULATOR: INITIAL PROTOTYPE USER INTERFACE
Susan Coatney and David Mizell Jul. 1989 20 p
(Contract N00014-87-K-0022)
(AD-A211325; ISI/RR-89-225) Avail: NTIS HC A02/MF A01 CSCL 12/5

The software design of the initial prototype user interface for the strategic defense architecture simulation system at ISI is described. The user interface was designed to satisfy several requirements. First, it should provide a means for the contractors to easily specify new simulation parameters, including candidate defense system architectures and threat scenarios. Second, it should not be necessary for users to be familiar with the internal workings of the simulator in order to execute the simulator and examine the simulation results. The design and implementation and software components are documented, and example interactive session to demonstrate use of the system is presented along with some suggestions for future improvements to the software.
GRA

N90-13054# Yale Univ., New Haven, CT. Dept. of Computer Science.
A FAN-IN ALGORITHM FOR DISTRIBUTED SPARSE NUMERICAL FACTORIZATION
Cleve Ashcraft, Stanley C. Eisenstat, and Joseph W. Liu 15 May 1989 8 p
(Contract N00014-86-K-0310; NSF DCR-85-21451)
(AD-A211569; YALEU/DCS/RR-706) Avail: NTIS HC A02/MF A01 CSCL 12/6

A column-oriented distributed algorithm is presented for factoring a large sparse symmetric positive definite matrix on a local-memory parallel processor. Processors co-operate in computing each column of the Cholesky factor by calculating independent updates to the corresponding column of the original matrix. These updates are sent in a fan- in manner to the processor assigned to the column, which then completes the computation. Experimental results on an Intel iPSC/2 hypercube demonstrate that the method is effective and achieves good speedups. GRA

N90-13055# Naval War Coll., Newport, RI. Dept. of Operations.
BUILDING A SOFTWARE PACKAGE FOR SOLVING LARGE SPARSE NONLINEAR SYSTEMS OF EQUATIONS Final Report
Robert T. Pavlak 16 Jun. 1989 27 p
(AD-A211758) Avail: NTIS HC A03/MF A01 CSCL 12/5

A preliminary version of a general purpose code based on a nonlinear version of GMRES, a method for solving nonsymmetric

linear systems was developed. Using the Jacobian-free approach, relatively hard problems were solved in a short period of time and with a minimum of programming effort, thus demonstrating the viability of the proposed code. Among the strongest points of the projected package are its ease of use and the variety of proposed techniques. Author

N90-13056# Technische Univ., Delft (Netherlands). Faculty of Technical Mathematics and Informatics.
SOLVING THREE DIMENSIONAL BLOCK BIDIAGONAL LINEAR SYSTEMS ON VECTOR COMPUTERS
J. J. F. M. Schlichting and H. A. vanderVorst 1989 14 p
(Rept-89-14; ISSN-0922-5641; ETN-89-95447) Copyright Avail: NTIS HC A03/MF A01

Different techniques for the vectorization of the solution of three dimensional block bidiagonal systems are discussed. The potentially most powerful of the vectorization techniques is shown to lead to long vector operations, at the cost, however, of strides and indirect addressing. Since the CYBER 205 is generally believed to stay behind in performance under such circumstances, this machine is selected for demonstration, to show in detail how these vectorization techniques can be implemented with almost equal performance as in the contiguous vector case. The methods presented are directly applicable to the ETA-10 family of supercomputers and may be adapted to other vector computers as well. ESA

N90-13057# Royal Signals and Radar Establishment, Malvern (England).
ALGORITHMIC FAULT TOLERANCE
I. K. Proudler Sep. 1988 28 p
(RSRE-Memo-4212; BR108109; ETN-89-94331) Copyright Avail: Defence Research Information Centre, Kentigern House, 65 Brown Street, Glasgow, G2 8EX, Scotland

The concept of algorithmic fault tolerance is explained and various techniques are reviewed with regard to their suitability for providing fault tolerance for signal processing algorithms in very large scale integration. Despite problems with the use of AN codes for protecting complicated algebra, it is argued that the advantages of such a technique are such that more effort could be justified in this direction. It must be remembered that (useful) AN codes are only single error correcting and that for higher error protection a switch to the use of residue codes is required. The latter are at least as good as, and often better than, AN codes in all respects except for the complexity of the arithmetic (vector instead of scalar). ESA

N90-13058# Royal Signals and Radar Establishment, Malvern (England).
NON-SEPARATE ARITHMETIC CODES
I. K. Proudler Sep. 1988 32 p
(RSRE-Memo-4215; BR108110; ETN-89-94332) Copyright Avail: Defence Research Information Centre, Kentigern House, 65 Brown Street, Glasgow, G2 8EX, Scotland

It is shown that a nonseparate arithmetic code that preserves both addition and multiplication must be an AN code where the generator A is an idempotent element of the ring being used. An idempotent element is one that satisfies the equation x sq = x. Given this type of code, its ability to detect errors in arithmetic expressions is explored and shown to be poor, due to error masking in multipliers. The constraints placed on a nonseparate multiplication-preserving arithmetic code that avoids such problems are discussed. The simplest code satisfying these conditions turns out to be an AN+B code where both A and B are idempotent elements. Conditions for the existence of this type of code are given along with examples. The fault tolerance provided by these codes is considered for a specific example. ESA

N90-13059 National Physical Lab., Teddington (England). Div. of Information Technology and Computing.
A FORMATTING STYLE FOR TYPESETTING AND DISTRIBUTING DRAFT INTERNATIONAL STANDARDS
R. S. Scowen and N. D. North Jun. 1989 8 p
(NPL-DITC-143/89; ISSN-0262-5369; ETN-89-95541) Copyright Avail: National Physical Laboratory, Teddington, Middlesex, TW11 0LW, United Kingdom

The adopted format and appearance of draft Prolog standards is illustrated. The advantages of this formatting style are that it is completely portable by electronic mail, or on magnetic tape to a wide number of computers. The syle is based on Latex which is widely available. But it uses only a small number of different commands, so it is simple to convert the source file for use with other word processors or desk top publishing systems. Double column output significantly improves the readability and also reduces the number of pages required for each draft. More information and full details of the formatting software are provided. ESA

N90-13060# Technische Univ., Delft (Netherlands). Faculty of Technical Mathematics and Informatics.
BINARY GRAY CODES AND INDEX SYSTEMS
A. J. vanZanten 1989 61 p
(Rept-89-29; ISSN-0922-5641; ETN-89-95588) Copyright Avail: NTIS HC A04/MF A01

A study of binary Gray codes is presented. Binary-reflected Gray codes are defined and some elementary properties given. The Gray index of a codeword and constant weight Gray codes are discussed, and a comparison made with a lexicographic code. In order to develop an index system, two number systems based on binomial coefficients are discussed. Two index systems are introduced, and the relationship between two codewords differing in bits is studied. Bounds are derived under this condition which give an indication for the error in the analog signal of a transmitted message required to cause this difference in bits. A sharp lower bound and maximal value are studied. Codewords are enumerated according to Gray order to provide the possibility of illustrating the various properties by non-trivial examples. ESA

N90-13061# Center for Mathematics and Computer Science, Amsterdam (Netherlands). Dept. of Numerical Mathematics.
SOLVING 3D BLOCK BIDIAGONAL LINEAR SYSTEMS ON VECTOR COMPUTERS
J. J. F. M. Schlichting and H. A. vanderVorst Dec. 1988 11 p Submitted for publication
(CWI-NM-R8819; ETN-89-95622) Copyright Avail: NTIS HC A03/MF A01

Techniques for the vectorization of the solution of three-dimensional block bidiagonal systems are discussed with a view to reduction in iteration steps and therefore improved computational speed on vector computers. The implementation of these vectorization techniques, with almost equal performance as in the contiguous vector case, is demonstrated using a CYBER 205. The methods are directly applicable to the ETA-10 family of supercomputers and can be adapted to other vector computers. A preconditioning algorithm is given which reduces iteration steps and reflects the same reduction in CPU (central processing unit) time. ESA

N90-13062# Universiteit Twente, Enschede (Netherlands). Dept. of Computer Science.
LOTOS TOOLS BASED ON THE CORNELL SYNTHESIZER GENERATOR
Peter vanEijk 1989 15 p
(MEMO-INF-89-5; ISSN-0923-1714; ETN-89-95686) Avail: NTIS HC A03/MF A01

A variety of interactive tools for the specification language LOTOS are constructed using the Cornell synthesizer generator, a system for constructing language based editors, which enables correct tools to be generated faster. Two examples are discussed in detail, an editor for the full LOTOS language, which incorporates static semantics checks and a menu function and allows investigation of the dynamic behavior of a specification, and a tool that supports interactive equivalence proof by transformation. A Calculus of Communicating Systems (CCS) is used for presentation purposes. ESA

N90-13063# Universiteit Twente, Enschede (Netherlands). Dept. of Computer Science.
ABSTRACT GRAMMARS BASED ON TRANSDUCTIONS
Peter R. J. Asveld 1989 21 p Revised
(MEMO-INF-89-7-Rev; ISSN-0923-1714; ETN-89-95687) Avail: NTIS HC A03/MF A01

An abstract grammatical model in which the effect or application of a production, determined by a so-called transduction, plays the main part, rather than the notion of production itself, is studied. Under appropriately chosen assumptions on the underlying family Tau of transductions, elementary, decidability, and complexity properties of the corresponding family of languages generated by Tau-grammars are established. These results are special instances of slightly more general properties of so-called Gamma-controlled Tau-grammars, since regular control does not increase the generating power of Tau-grammars. In a Gamma-controlled Tau-grammar the iteration of Tau-transductions is restricted to those sequences to transductions that belong to a given control language, taken from a family Gamma of control languages.
ESA

N90-13064# Universiteit Twente, Enschede (Netherlands). Dept. of Computer Science.
TRUTH MAINTENANCE SYSTEMS AND THEIR IMPLEMENTATION IN PROLOG
Huang Guoxing 22 Feb. 1989 69 p
(MEMO-INF-89-13; UT-KBS-89-01; ISBN-90-365-0259-4; ISSN-0923-1714; ETN-89-95688) Avail: NTIS HC A04/MF A01

In the field of artificial intelligence, the implementation of an assumption-based truth maintenance system (ATMS) in PROLOG is described. An overview of truth maintenance systems is given with a view on their efficiency. Datastructure is detailed and a simple testing program outlined. An N-queens program is used to test the ATMS and results are included. A full program listing is given.
ESA

N90-13065*# Virginia Polytechnic Inst. and State Univ., Blacksburg. Dept. of Engineering Science and Mechanics.
RTM USER'S GUIDE Interim Report
Steven J. Claus and Alfred C. Loos May 1989 71 p
(Grant NAG1-343)
(NASA-CR-186091; NAS 1.26:186091; CCMS-89-11; VPI-E-89-14) Avail: NTIS HC A04/MF A01 CSCL 09B

RTM is a FORTRAN '77 computer code which simulates the infiltration of textile reinforcements and the kinetics of thermosetting polymer resin systems. The computer code is based on the process simulation model developed by the author. The compaction of dry, woven textile composites is simulated to describe the increase in fiber volume fraction with increasing compaction pressure. Infiltration is assumed to follow D'Arcy's law for Newtonian viscous fluids. The chemical changes which occur in the resin during processing are simulated with a thermo-kinetics model. The computer code is discussed on the basis of the required input data, output files and some comments on how to interpret the results. An example problem is solved and a complete listing is included.
Author

N90-13066# Royal Signals and Radar Establishment, Malvern (England).
MATHEMATICAL EQUIVALENCE IN A PRIMITIVE ELLA
M. B. Davies Aug. 1988 25 p
(RSRE-Memo-4225; BR108440; ETN-89-94840) Copyright
Avail: NTIS HC A03/MF A01

The mathematical language L is defined. It represents circuits in a primitive subset of Ella programs containing delays, pairing, expressions (multiplexor), and recursive or feedback expressions. It is shown how by reduction of expressions in this language to an approximated finite form, equivalence between expressions can be tested in finite time. The theory application problems concerning the complexity, the data refinement and the undefined values are discussed.
ESA

N90-13067# Royal Signals and Radar Establishment, Malvern (England).
A Z SPECIFICATION OF THE MaCHO INTERFACE EDITOR
A. W. Wood Nov. 1988 56 p
(RSRE-Memo-4247; BR108668; ETN-89-94844) Copyright
Avail: NTIS HC A04/MF A01

The basic editor part of the MaCHO (mouse and cartouches for handling objects) user interface for a secure computer architecture, is described. The mathematical notation known as Z, is applied. Operations that are available to the user, and their effects on the screen display, are specified. Descriptions of the auxiliary functions and data structures necessary to support them, are provided. They are used to implement a powerful yet trustworthy interface for the initiation and control of security related transactions.
ESA

N90-13068# Royal Signals and Radar Establishment, Malvern (England).
THE INTEGRATION OF STRUCTURED AND FORMAL METHODS
G. P. Randell Jun. 1989 21 p
(RSRE-Memo-4293; BR111533; ETN-89-94969) Copyright
Avail: NTIS HC A03/MF A01

Five structured methods, in the development of software based systems, are studied. The possibilities for integration with a formal notation to produce a usable formal method combining the best of both formal and structured approaches, are considered. The definition of the rules to convert a data flow diagram into an outline Z specification, and those for translating a Z specification into diagrams, are outlined. The requirements, concerning acquisition, expression, and analysis, for further work improvements, are underlined.
ESA

N90-13069 Physics and Electronics Lab. TNO, The Hague (Netherlands).
USER MANUAL OF THE FORCE STRUCTURE MODEL SCENARIO EDITOR SCENE
P. A. B. vanSchagen Dec. 1988 143 p
(Contract A84/KL/065)
(FEL-1988-101; TD89-0346; ETN-89-94991) Copyright Avail: TNO Physics and Electronics Lab., P.O. Box 96864, 2509 JG The Hague, Netherlands

The scenarios made with the help of the scenario editor Scene are studied. The Scene editor is part of the Force Structure Model (FSM). Both the structure of an FSM scenario and the working of Scene are explained. The Scene editor makes use of the wargame construction set philosophy, implying that no software changes are needed. The default state of the model dependent parts are given, and the format of the scenario is explained.
ESA

N90-13070# Royal Signals and Radar Establishment, Malvern (England).
A MAPPING FOR CONVERTING MASCOT DESIGNS TO ADA PROGRAMS
T. Dean 19 Jul. 1988 25 p
(RSRE-Memo-4244; BR109214; ETN-89-95005) Copyright
Avail: NTIS HC A03/MF A01

The main characteristics of the method for mapping Mascot designs into Ada programs, are presented. Mascot is a software engineering methodology applicable to real time systems. The changes which are needed in order to solve specific problems are discussed. Mascot templates (both algorithmic and structure) are represented as generic packages. It is shown that: (1) the software is well structured and easy to maintain; (2) the Mascot idea of active and passive design elements makes deadlock situations easy to detect; and (3) the large library of reusable templates can be built up, producing reliable and maintainable programs.
ESA

N90-13071# Centre Technique des Industries Mecaniques, Saint Etienne (France).
WHAT IS THE BALANCE SHEET FOR INVESTMENT IN AUTOMATED MANUFACTURING Final Report [QUEL BILAN ECONOMIQUE POUR UN INVESTISSEMENT EN FABRICATION AUTOMATISEE]
R. Malosse Sep. 1988 29 p In FRENCH
(CETIM-105490; ETN-89-95041) Copyright Avail: NTIS HC A03/MF A01

Economic evaluation methods are applied to determining when it is worthwhile for a company to invest in an automated manufacturing system. The different parameters involved in making such a decision are analyzed. Feasibility evaluations based on annual salary costs, annual maintenance costs, the frequency of break downs, employee training costs, interest rates, and operation delays are presented. A conclusion is that there is no general formula for such a decision. Each case must be analyzed according to its own set of parameters. ESA

N90-13072# Center for Mathematics and Computer Science, Amsterdam (Netherlands). Dept. of Applied Mathematics.
MULTIPLICATIVE ITERATIVE ALGORITHMS FOR CONVEX PROGRAMMING
P. P. B. Eggermont (Delaware Univ., Newark.) Jul. 1988 12 p
(CWI-AM-R8808; ETN-89-95640) Copyright Avail: NTIS HC A03/MF A01

Multiplicative iterative algorithms for the minimization of a differentiable, convex function defined on the positive orthant of the set of real numbers are studied. If the objective function has compact level sets and has a locally Lipschitz continuous gradient then these algorithms are shown to converge to a solution of the minimization problem. The convergence is shown nearly monotone in the sense of Kullback-Leibler divergence. Special cases of these algorithms are applied in position emission tomography and are formally related to the maximum likelihood estimation (EM) algorithm for positron emission tomography. ESA

N90-13073# Center for Mathematics and Computer Science, Amsterdam (Netherlands). Dept. of Software Technology.
EXPERT SYSTEMS AS DEDUCTIVE SYSTEMS
A. Eliens Jul. 1988 23 p Sponsored in part by the Dutch Stimulerings Projectteam Informatica-Onderzoek
(CWI-CS-R8825; ETN-89-95647) Copyright Avail: NTIS HC A03/MF A01

A case study in the semantics of rule-based systems is presented. Rule-based expert systems are characterized as deductive systems. Deduction is viewed as an operator transforming a given state of knowledge into a new state containing as least as much knowledge. The meaning of a knowledge base can then be defined as the deductive closure obtained by applying the rules to a set of initial facts. An interpreter is defined that models the operational aspects of the inference engine of Mycin-like expert systems. The interpreter is proven complete provided that the dependencies between the attributes occurring in the rules are acyclic. First, the knowledge representation language will be restricted in such a way that the reasoning capabilities of the system do not transcend a positive logic. Later the knowledge representation language will be extended to adequately capture the functionality of existent rule-based expert systems. To model these extensions a four-valued logic is used, similar to the logic of Belnap. ESA

N90-13074# Center for Mathematics and Computer Science, Amsterdam (Netherlands). Dept. of Software Technology.
A SIMPLE DEFINITION FOR PARALLEL COMPOSITION OF PRIME EVENT STRUCTURES
Frits W. Vaandrager Mar. 1989 15 p Sponsored in part by the Commission of European Communities ESPRIT Project 432 METEOR
(CWI-CS-R8903; ETN-89-95650) Copyright Avail: NTIS HC A03/MF A01

The parallel composition of prime event structures as an intuitive model of concurrent processes is studied. A simple, non-inductive construction is presented for parallel composition of prime event structures with binary conflict. It is shown that the construction determines the same operation as the categorical construction of Winskel by proving that it is a product in the category of prime event structures with binary conflict. An application is the semantics of concurrent systems languages. ESA

N90-13075# Center for Mathematics and Computer Science, Amsterdam (Netherlands). Dept. of Software Technology.
PROVING TOTAL CORRECTNESS OF RECURSIVE PROCEDURES
Pierre America (Philips International B.V., Eindhoven, Netherlands) and Frank S. deBoer 15 Mar. 1989 36 p Sponsored in part by the Commission of European Communities ESPRIT Project 415
(CWI-CS-R8904; ETN-89-95651) Copyright Avail: NTIS HC A03/MF A01

Some well-known rules in a Hoare-style proof system for total correctness of recursive procedures are shown to interact in such a way that they yield incorrect results. The problem is connected to the quantification scope of certain variables in the proof rules. By defining some restrictions on the applicability of the rules a system is obtained that is sound and complete. However, the completeness proof differs substantially from the original one. This technique is also applied to dynamic logic, where it is shown that the original proof rules for recursive procedures are replaced by simpler and more natural ones, and that it is not necessay to extend the programming language in order to arrive at a sound and complete proof system. ESA

N90-13076# Center for Mathematics and Computer Science, Amsterdam (Netherlands). Dept. of Software Technology.
PROCESS EXPRESSIONS AND HOARE'S LOGIC
Alban Ponse Mar. 1989 22 p Sponsored by the Commission of European Communities ESPRIT Project 432 METEOR
(CWI-CS-R8905; ETN-89-95652) Copyright Avail: NTIS HC A03/MF A01

Processes specifiable over a non-uniform language are considered. The language contains constants for a set of atomic actions and constructs for alternative composition and sequential composition and it provides a mechanism for specifying processes by a form of guarded recursion (including nested applications). Processes are considered as having side-effects: atomic actions are to be specified in terms of observability and state transformations. The execution of a process having some initial state is formally described as a transition system containing information about observability and state transformations and is shown to lead to an operational semantics in the style of Plotkin. A logic in the style of Hoare and a proof system for deriving partial correctness assertions are presented. This proof system is complete (relative to all true assertions about the states), so any partial correctness assertion can be evaluated by investigating its derivability. Techniques concerning the construction of derivations or proofs of their absence are not discussed. ESA

N90-13077# Center for Mathematics and Computer Science, Amsterdam (Netherlands). Dept. of Software Technology.
CHARACTERIZING TERMINATION OF LOGIC PROBLEMS WITH LEVEL MAPPINGS
Marc Bezem Apr. 1989 13 p
(CWI-CS-R8912; ETN-89-95656) Copyright Avail: NTIS HC A03/MF A01

A large class of logic programs which terminate with respect to a natural class of goals is studied. Both classes are characterized in terms of level mappings and the class of logic programs is shown as strong enough to compute every total recursive function. The class of goals considerably extends the variable-free ones. Based on the ideas developed, a technique which improves the termination behavior of Prolog programs is presented. ESA

N90-13078# Groningen Rijksuniv. (Netherlands). Dept. of Mathematics and Computing Sciences.
TOWARDS A PARALLEL ALGORITHM FOR THE MANY BODY PROBLEM
Klaas Esselink 10 Oct. 1988 22 p
(CS-8813; ETN-89-95679) Avail: NTIS HC A03/MF A01

Research done in order to find out whether a known sequential algorithm for the many body problem was suitable for parallelization is reported. The many body problem tries to simulate the behavior of a universe containing a lot of objects influencing each others movement. The sequential algorithm has a time complexity believed to be O(N log N). The main issue is how to transform this algorithm into an efficient parallel one. The problem of how to distribute the work evenly among the different processors for this particular problem is considered. The data structure plays an important role, since it tends to be very big for a problem like this and special constructs are necessary to manage it while it it distributed among various processors. Some results from tests with not-many-but-still-a-lot-of-bodies on a 16 transputer system are shown and suggestions on how to proceed and improve the algorithm are given. The work presented is an example of how to approach a large parallel computing task. ESA

N90-13079# Groningen Rijksuniv. (Netherlands). Dept. of Mathematics and Computing Sciences.
POLYMORPHISM AND INFORMATION LOSS IN MARTIN-LOEF'S TYPE THEORY
Grant Malcolm and Paul Chisholm 1988 30 p
(CS-8814; ETN-89-95680) Avail: NTIS HC A03/MF A01

A type of polymorphic object is examined and it is shown how this type allows the derivation of concise programs in type theory. The head function on lists is presented as an example. The relationship between polymorphism and information loss is captured in some derived rules which allow inductive reasoning over restricted domains. An example is given of how these rules may be used in defining new data types such as balanced trees. ESA

N90-13080# Deutsche Forschungs- und Versuchsanstalt fuer Luft- und Raumfahrt, Oberpfaffenhofen (West Germany). Abteilung Mehrkoerperdynamik.
COMPUTER ORIENTED METHODS OF MULTIBODY DYNAMICS FOR APPLICATION IN VEHICLE TECHNOLOGY Ph.D. Thesis - Tech. Univ. Berlin
Oskar Wallrapp Apr. 1989 168 p In GERMAN; ENGLISH summary
(DFVLR-FB-89-17; ISSN-0171-1342; ETN-89-95831) Avail: NTIS HC A08/MF A01; DFVLR, VB-PL-DO, Postfach 90 60 58, 5000 Cologne, Fed. Republic of Germany, 53.50 Deutsche marks

A formalism for the computer oriented generation of the static and dynamic equations of multibody systems is presented. This formalism provides the core of the Medyna program for design, evaluation and simulation of tracked vehicles. The elements of the multibody systems considered are rigid and flexible bodies with arbitrary interconnections. The system motion is subdivided into a known large overall motion of the vehicle and a small relative motion of the individual bodies. The system kinematics are linearized with respect to the overall motions. To generate the complete system equations, nominal loads resulting in geometrical stiffness terms are considered. Various alternatives for incorporating these terms are discussed. A method which avoids the development of quadratic terms in kinematical relations, is presented. ESA

N90-13081# Deutsche Forschungsanstalt fuer Luft- und Raumfahrt, Stuttgart (Germany, F.R.). Inst. fuer Technische Thermodynamik.
INTERACTIVE COMPUTER PROGRAM FOR THE GENERATION OF ENTHALPY-ENTROPY AND TEMPERATURE-ENTROPY CHARTS OF NITROGEN AND HYDROGEN
Willi Nieratschker and Steffen Hauff Apr. 1989 64 p In GERMAN; ENGLISH summary Original contains color illustrations
(DLR-FB-89-27; ISSN-0171-1342; ETN-89-95836) Avail: NTIS HC A04/MF A01; DLR, VB-PL-DO, Postfach 40 60 58, 5000 Cologne, Fed. Republic of Germany, 35 Deutsche marks

Based on an interactive computer program for the calculation of thermophysical properties of nitrogen and hydrogen, the properties of liquid-vapor mixtures are computed to complete the calculated values for the generation of enthalpy-entropy and temperature-entropy charts. An appropriate interactive plot program is created and presented. In the temperature range between 14.0 and 400 K for hydrogen or 63.2 and 1900 K for nitrogen, users are enabled to generate corresponding coordinates for the two-phase boundaries, curves of equal pressure, density, enthalpy, temperature and equal liquid-vapor mass ratios. The plot program converts and combines the tables to any chart. A representative series of complete charts as well as a short users introduction are given. ESA

N90-13082# RAND Corp., Santa Monica, CA.
A TABLE-DRIVEN APPROACH TO FAST CONTEXT-FREE PARSING Interim Report
James R. Kipps Dec. 1988 55 p
(Contract MDA903-85-C-0030)
(AD-A212210; RAND/N-2841-DARPA) Avail: NTIS HC A04/MF A01 CSCL 12/5

This Note describes a parsing system developed for the ROSIE programming language and loosely based on Tomita's algorithm for general context-free parsing. Tomita's algorithm is unique in that it defines a bottom-up parser that uses an extended left-to-right (LR) parse table. While this algorithm does no better than the theoretical time bound of other general context-free parsing algorithms, its use of parse tables eliminates a component common to these algorithms. This makes Tomita's algorithm efficient enough for practical application. The parsing system described in this note has been implemented in LISP for distribution with the ROSIE programming language, which has a highly ambiguous English-like syntax. The note describes an approach to disambiguation and code generation, as well as an algorithm for constructing the extended LR parse table. GRA

N90-13083# Air Force Wright Aeronautical Labs., Wright-Patterson AFB, OH.
SUBSPACE ITERATION ALGORITHMS IN FORTRAN 77 AND FORTRAN 8x Final Report, Feb. - Dec. 1988
Paul J. Nidkolai 30 Dec. 1988 22 p
(AD-A212275; AFWAL-TR-88-3120; DOD/SW/DK-89/021A)
Avail: NTIS HC A03/MF A01 CSCL 12/5

This report describes a USA FORTRAN ANSI X3.9-1978 implementation of the Rutishauser-Reinsch subspace iteration algorithm for partial solution of the algebraic eigenvalue problem for a real matrix symmetric relative to a prescribed inner product. Also included is a corresponding description of the algorithm in the proposed FORTRAN 8x standard using the CFT77 compiler and the CRAY X-MP processor of Cray Research, Inc. Source code for both algorithms will be available to DOD qualified requestors in the form of a 5-1/4 in. diskette formatted under MS/DOS. GRA

N90-13084# Massachusetts Inst. of Tech., Lexington. Lincoln Lab.
PARALLEL AND DETERMINISTIC ALGORITHMS FROM MRF (MARKOV RANDOM FIELDS): SURFACE RECONSTRUCTION AND INTEGRATION
Davi Geiger and Federico Girosi May 1989 39 p
(Contracts DACA76-85-C-0010; N00014-85-K-0124)
(AD-A212457; AI-M-1114; CBIP-PAPER-35) Avail: NTIS HC A03/MF A01 CSCL 12/5

In recent years many researchers have investigated the use of Markov random fields (MRFs) for computer vision. They can be applied for example in the output of the visual processes to reconstruct surfaces from sparse and noisy depth data, or to integrate early vision processes to label physical discontinuities. Drawbacks of MRFs models have been the computational

complexity of the implementation and the difficulty in estimating the parameters of the model. Deterministic approximations are derived to MRFs models. One of the considered models is shown to give in a natural way the graduate non convexity (GNC) algorithm. This model can be applied to smooth a field preserving its discontinuities. A new model is then proposed: it allows the gradient of the field to be enhanced at the discontinuities and smoothed elsewhere. All the theoretical results are obtained in the framework of the mean field theory, that is a well known statistical mechanics technique. A fast, parallel and iterative algorithm to solve the deterministic equations of the two models is presented, together with experiments on synthetic and real images. The algorithm is applied to the problem of surface reconstruction is in the case of sparse data. A fast algorithm is also described that solves the problem of aligning the discontinuities of different visual models with intensity edges via integration. GRA

N90-13085# Mitre Corp., Bedford, MA.
SOFTWARE ENGINEERING EXERCISE (SEE) GUIDELINES Final Report
Herman P. Schultz Jul. 1989 27 p
(Contract F19628-89-C-0001)
(AD-A212510; M89-32; ESD-TR-89-199) Avail: NTIS HC A03/MF A01 CSCL 12/5

This Software Engineering Exercise (SEE) was found to be an effective discriminator in reducing the risks normally associated with a software acquisition. It is designed to be used during the source selection process as part of the technical evaluation of offerors and encompasses the development and administration of a well defined exercise (test problem) that is implemented by an offeror in a restricted time period (usually less than a month). The exercise problem typically addresses one or more software risk areas and is designed to be evaluated quickly to minimize its impact on the source selection schedule. Guidance is provided to acquisition offices in the planning and tasking required to implement a SEE and the flexibility that may be occasioned by tailoring the SEE to each program's needs. GRA

N90-13086# Stanford Univ., CA. Dept. of Operations Research.
ON THE IDENTIFICATION OF LOCAL MINIMIZERS IN INERTIA-CONTROLLING METHODS FOR QUADRATIC PROGRAMMING
Anders L. Forsgren, Philip E. Gill (California Univ., San Diego, La Jolla.), and Walter Murray Jul. 1989 25 p Sponsored by Goeran Gustafsson Foundation
(Contracts DE-FG03-87ER-25030; N00014-87-K-0142; NSF CCR-84-13211)
(AD-A212514; SU-SOL-89-11) Avail: NTIS HC A02/MF A01 CSCL 12/4

The verification of a local minimizer of a general (i.e., nonconvex) quadratic program is in general an NP-hard problem. The difficulty concerns the optimality of certain points (which are called dead points) at which the first-order necessary conditions for optimality are satisfied, but strict complementarity does not hold. One important class of methods for solving general quadratic programming problems are called intertia-controlling quadratic programming (ICQP) methods. A computational scheme is derived for proceeding at a dead point that is appropriate for general ICQP method. GRA

N90-13087# Kestrel Inst., Palo Alto, CA.
TOWARD A FORMAL MODEL OF THE DESIGN AND EVOLUTION OF SOFTWARE Final Report, 1 Dec. 1987 - 31 May 1989
Cordell Green and Douglas R. Smith 20 Dec. 1988 45 p
(Contract F49620-88-C-0033; AF Proj. 2304)
(AD-A212533; AFOSR-89-1253TR) Avail: NTIS HC A03/MF A01 CSCL 12/5

This report summarizes recent activities on the development of a formal model of the design and evolution of software. The model is intended to be both descriptive and prescriptive. It is descriptive in that we are attempting to capture known design processes in the model. The model is also intended to be prescriptive in the sense that it provides the conceptual basis for the sophisticated knowledge-based software design environments of the future. It should have the flexibility to support a variety of design methodologies, be comprehensive enough to encompass the gamut of software lifecycle activities, and be precise enough to provide the conceptual foundations for an open yet rigorous development environment. We also present recent work on the structure and design of a class of algorithms called global search. The design tactic for global search algorithms provides a rich example of the kind of design process that the abstract model is intended to capture. We present a tactic for designing global search algorithms and illustrate it with the derivation of an algorithm for enumerating cyclic difference sets - a rare kind of set that bear some similarities to the prime numbers. The design tactic has been implemented and used to derivation dozens of global search algorithms including one for enumerating cyclic difference sets. GRA

N90-13088# Stanford Univ., CA. Systems Optimization Lab.
SEQUENTIAL QUADRATIC PROGRAMMING ALGORITHMS FOR OPTIMIZATION
Francisco J. Prieto Aug. 1989 158 p
(Contracts DE-FG03-87ER-25030; N00014-87-K-0142; NSF ECS-87-15153)
(AD-A212800; SOL-89-7) Avail: NTIS HC A08/MF A01 CSCL 12/4

The problem considered in this dissertation is that of finding local minimizers for a function subject to general nonlinear inequality constraints, when first and perhaps second derivatives are available. The methods studied belong to the class of the sequential quadratic programming (SQP) algorithm embodied in the code NPSOL, which was developed at the Systems Optimization Laboratory, Stanford University. The goal of the dissertation is to develop SQP algorithms that allow some flexibility in their design. Specifically, we are interested in introducing modifications that enable the algorithms to solve large-scale problems efficiently. The following issues are considered in detail: Instead of trying to obtain the search direction as a minimizer for the QP, the solution process is terminated after a limited number of iterations. Suitable termination criteria are defined that ensure convergence for an algorithm that use a quasi-Newton approximation for the full Hessian. Theorems concerning the rate of convergence are also given. For many problems the reduced Hessian is considerably smaller than the full Hessian. Consequently, there are considerable practical benefits to be gained by only requiring an approximation to the reduced Hessian. Theorems are proved concerning the convergence and rate of convergence for an algorithm that uses a quasi-Newton approximation for the reduced Hessian when early termination of the QP subproblem is enforced. GRA

N90-13089# Missouri Univ., Columbia. Dept. of Mathematics and Computer Science.
ITERATIVE METHODS FOR LINEAR COMPLEMENTARY AND RELATED PROBLEMS Final Report, 15 May 1986 - 14 May 1989
Tzong H. Shiau 14 May 1989 26 p
(Grants AF-AFOSR-0124-86; NSF MCS-82-00632; AF Proj. 2304)
(AD-A212848; AFOSR-89-1254TR) Avail: NTIS HC A03/MF A01 CSCL 12/4

A sparsity preserving LP-based SOR method for solving classes of linear complementary problems including the case where the given matrix is positive semidefinite is proposed. The LP subproblems need be solved only approximately by a SOR method. Heuristic enhancement is discussed. Numerical results for a special class of problems are presented, which show that the heuristic enhancement is very effective and the resulting program can solve problems of more than 100 variables in a few seconds even on a personal computer. GRA

N90-13090# Systems Engineering Labs., Inc., Greenbelt, MD.
ALGORITHM DEVELOPMENT FOR SDI WEAPONS SYSTEM ALLOCATION Final Report, Dec. 1987 - May 1989

Gilmer L. Blankenship and William Bennett 1 Jun. 1989 60 p (Contract F49620-88-C-0026)
(AD-A212973; AFOSR-89-1255TR) Avail: NTIS HC A04/MF A01 CSCL 15/3

While several SDI weapons systems can provide adequate defense in a one-on-one basis, a coordinated attack by several enemy missiles launched over a substantial volume will be difficult to resist without an efficient command and control system for warfare coordination. The study of weapons allocation - coordination algorithms, is based on dynamical models for the missile/decoy systems including noise effects and uncertainties in the model parameters. Performance of the weapons targeting system may be measured in terms of the expected number of targets eliminated in a given interval (phase of operations) or the expected time to eliminate all the targets in a given region. Scheduling weapons deployment is a problem of constrained optimal (weapons) and state variables. The selection of weapons deployment tactics is based on solution of a complex optimization problem. An investigation was conducted on advanced modeling, stochastic control, and scheduling methodologies for aspects of the SDI weapons allocation problem; several platforms with assets of different character defending against a diverse collection of targets. The models for such scenarios lead to stochastic scheduling problems which can not be handled by conventional analytical methods. Several different analytical approaches are described which have the potential for synthesis of effective engagement algorithms. GRA

N90-13091# Prospective Computer Analysts, Inc., Arlington, VA.
EXPERT SYSTEM FOR TEST PROGRAM SET FAULT CANDIDATE SELECTION Final Report, Sep. 1986 - Mar. 1987
R. Glenn Wright and Mary Blanchard Sep. 1989 41 p Prepared in cooperation with Army Armament Munitions and Chemical Command, Dover, NJ
(Contract DAAA21-76-C-0225)
(AD-A213338) Avail: NTIS HC A03/MF A01 CSCL 23/2

An application of expert system technology to test program set (TPS) verification and validation is described. The goals of this project are to reduce the complexity and time requirements for testing test program software, and at the same time reduce the level of expertise required by acceptance test personnel. This work effort was funded by the U.S. Army Armament Research, Developement and Engineering Center (ARDEC) in Dover, NJ. GRA

N90-12772# Universidad Nacional del Sur, Bahia Blanca (Argentina). Dept. of Engineering.
THE COMPUTER AGE AND TRADITIONAL APPROXIMATE, ANALYTICAL METHODS
P. A. A. Laura *In* Vibration Inst., The Shock and Vibration Digest, Volume 21, No. 10 Oct. 1989 p 3-6 Sponsored by CONICET Research and Development Program (For primary document see N90-12771 04-31)
Avail: NTIS HC A04/MF A01

62 COMPUTER SYSTEMS

Includes computer networks and special application computer systems.

N90-13092# Massachusetts Inst. of Tech., Cambridge. Lab. for Computer Science.
AREA-UNIVERSAL NETWORKS Memorandum Report
Ronald I. Greenberg 1 Mar. 1989 13 p Sponsored by Fannie and John Hertz Foundation Fellowship
(Contracts N00014-87-K-0825; N00014-86-K-0593)
(AD-A211883; VLSI-MEMO-89-524) Avail: NTIS HC A03/MF A01 CSCL 12/7

An area-universal network is one which can efficiently simulate any other network of comparable area. This paper extends previous results on area-universal networks in several ways. First, it considers the size (amount of attached memory) of processors comprising the networks being compared. It shows that an appropriate universal network of area theta(A) built from processors of size lg A requires only O(lg squared A) slowdown in bit-times to simulate any network of area A, without any restriction on processor size or number of processors in the competing network. Furthermore, the universal network can be designed so that any message traversing a path of length d in the competing network need follow a path of only O(d + lg A) length in the universal network. Thus, the results are almost entirely insensitive to removal of the unit wire delay assumption used in previous work. This paper also derives upper bounds on the slowdown required by a universal network to simulate a network of larger area and shows that all of the simulation results are valid even without the usual assumption that computation and communication of the competing network proceed in separate phases. GRA

N90-13093# Massachusetts Inst. of Tech., Cambridge. Microsystems Research Center.
WORK-PRESERVING EMULATIONS OF FIXED-CONNECTION NETWORKS
Richard Koch, Tom Leighton, Bruce Maggs, Satish Rao, and Arnold Rosenberg (Massachusetts Univ., Amherst.) May 1989 16 p Submitted for publication Sponsored in part by International Business Machines, Armonk, NY
(Contracts N00014-87-K-0825; DAAL03-86-K-0171; N00014-86-K-0593; AF-AFOSR-0076-86; NSF CCR-88-12567)
(AD-A211915; VLSI-MEMO-89-531) Avail: NTIS HC A03/MF A01 CSCL 12/7

In this paper, we study the problem of emulating T sub G steps of an N sub G-node guest network on an N sub H-node host network. Although many isolated emulation results have been proved for specific networks in the past, and measures such as dilation and congestion were known to be important, the field has lacked a model within which general results and meaningful lower bounds can be proved. We attempt to provide such a model, along with corresponding general techniques and specific results in this paper. GRA

N90-13094# Grenoble-1 Univ. (France). Lab. des Techniques de l'Informatique, des Mathematiques, de la Microelectronique et de la Microscop
NAUTILE: A PHYSICAL DESIGN ENVIRONMENT BASED ON AN OBJECT-ORIENTED DATA MANAGER
A. A. Jerraya, P. Bondono, J. P. Geronimi, A. Hornik, and B. Courtois Jun. 1988 9 p
(IMAG-RR-737-I; ETN-89-95492) Avail: NTIS HC A02/MF A01

A physical design environment called NAUTILE is described. The NAUTILE system is built around an object oriented data manager that handles hierarchical design, and whose originality is to propose multiple views of the different elements composing the whole circuit, while maintaining links between each of these representations. Each circuit or subcircuit is defined by an external view, a construction view, and several physical views. Physical views may be given in external description languages which allows the use of circuits or subcircuits designed for other systems. NAUTILE provides other features of technology independence, full graphical and textual description, virtual grid symbolic design, and automatic routing and assembling. ESA

N90-13095# Universiteit Twente, Enschede (Netherlands). Dept. of Computer Science.
ON MODELING RESOURCES IN MULTIPROCESSOR SYSTEMS
E. G. Zondag Oct. 1988 29 p
(MEMO-INF-88-33; ETN-89-95683) Avail: NTIS HC A03/MF A01

The importance of resources in data processing systems, especially at levels where implementation concerns matter, is addressed. Several resource classifications applicable to multiprocessor systems are given. A survey of resource interaction schemes leads to the conclusion that there is hardly a way to unify them into a single model that is able to describe how resources and their interactions are implemented. The association of attributes with (the specification of) resources is proposed in

order to specify characteristics deviating from default ones. An implementation language kernel is given that offers attribution and several other extensions to Hoare's communicating sequential processes. ESA

N90-13096# Universiteit Twente, Enschede (Netherlands). Dept. of Computer Science.
AN IMPLEMENTATION-ORIENTED SPECIFICATION OF THE TUMULT COMMUNICATION PRIMITIVES
E. G. Zondag Oct. 1988 31 p
(MEMO-INF-88-34; ETN-89-95684) Avail: NTIS HC A03/MF A01

A possible implementation of the set of mailbox based TUMULT IPC (interprocess communication) primitives is given. It is expressed in a SCP (communicating sequential processes) type language which allows an efficient specification of the involved resources and their interactions. Global and local mailbox managers are presented as components of a two-level hierarchical operating subsystem. The TUMULT IPC scheme is characterized and criticized in several respects. The CSP based language used is proposed as very suitable for implementation-oriented specifications. ESA

N90-13097# Universiteit Twente, Enschede (Netherlands). Dept. of Computer Science.
PATH EXPRESSION BASED OPERATING SYSTEMS
Albert L. Schoute Dec. 1988 34 p
(MEMO-INF-88-68; ISBN-90-365-0240-3; ETN-89-95685) Avail: NTIS HC A03/MF A01

The use of path expressions at the command level of an interactive, multitasking system, both for the specification of user commands, by which tasks are evoked, and for the formulation of rules, which determine additional execution conditions is demonstrated. The operating system dynamically controls the task execution so that the system behavior conforms to the parallel, sequential and optional orders as specified. Total system evolution is the result of simultaneous evaluation of the path, and is explained, and evolution control based on tree-evaluation is shown. A prototype path based operating system is detailed, and experiences relating to potential in the area of intelligent, rule-based, parallel systems are described. ESA

N90-13098# Institut National Polytechnique, Grenoble (France). Techniques de l'Informatique, des Math., de la Microelectronique et de la Microscopie Quantitative.
FORMAL CALCULATIONS AND PARALLESISM. SOLVING LINEAR SYSTEMS Ph.D. Thesis [CALCUL FORMEL ET PARALLELISME. RESOLUTION DE SYSTEMES LINEAIRES]
Gilles Villard 23 Dec. 1988 162 p In FRENCH Sponsored by PRC Mathematiques et Informatique; the CNRS; and the Societe Floating Point Systems
(ETN-89-95499) Avail: NTIS HC A08/MF A01

Exact solutions for parallel linear systems are investigated. Two basic aspects of such solutions are addressed: calculating the nucleus of a matrix of which the coefficients are in a finite body and the solution of systems with real coefficients. A theoretic cost estimation for the use of the different algorithms proposed is presented. An experimental comparison of the algorithmic methods is carried out on a hypercube with sixteen processors. The Chinese remainder theorem proved to be the only one capable of finding solutions to rational systems in less than four hours. ESA

N90-13099# Universiteit Twente, Enschede (Netherlands). Dept. of Computer Science.
EXTENDED PERFORMABILITY MODELING USING DYNAMIC QUEING NETWORKS
Boudewijn R. Haverkort and Ignas G. Niemegeers Feb. 1989 27 p Submitted for publication
(Memo-INF-89-15; ISSN-0923-1714; ETN-89-95689) Avail: NTIS HC A03/MF A01

Dynamic queuing networks, a modeling approach for computer systems of dynamic structure, are presented. Product-form queuing networks are used for modeling performance aspects, and generalized stochastic Petri nets for fault-tolerance aspects. A Markovian model that describes the dynamic structure of the computer system is constructed using the Petri net, and parameters of the product-form queuing network possibly depend on the Petri net. An algorithm is used to obtain performance metrics and a Markov reward model is constructed that can be analyzed for steady state and transient measures. The proposed model allows existing performability models, and more complicated performability aspects of distributed systems, such as recovery, routing and reconfiguration, to be assessed. ESA

N90-13100# Universiteit Twente, Enschede (Netherlands). Dept. of Computer Science.
TRACE THEORY
Gerrit Niemeijer 1989 22 p
(Memo-INF-89-16; ISSN-0923-1714; ETN-89-95690) Avail: NTIS HC A03/MF A01

Trace theory attempts to solve the problem of the description of concurrent program behavior, where actions are executed in parallel and cannot therefore be described sequentially. An introduction to trace theory is presented, including details of trace structures and their composition, states and state graphs, and a worked out example. A trace theory based method for compiling concurrent compilations into VLSI (very large scale integration) circuits is described, and this application illustrates conclusions as to the advantages of trace theory, including better correctness proofs and the inviting of an ambiguous design by use of formal techniques. A discussion on further conclusions is included. ESA

63 CYBERNETICS

Includes feedback and control theory, artificial intelligence, robotics and expert systems.

For related information see also *54 Man/System Technology and Life Support.*

N90-13101# National Inst. of Standards and Technology, Gaithersburg, MD. Intelligent Controls Group.
VISUAL PERCEPTION PROCESSING IN A HIERARCHICAL CONTROL SYSTEM: LEVEL 1 Final Technical Report
Karen Chaconas and Marilyn Nashman Jun. 1989 53 p
(PB89-221188; NIST/TN-1260) Avail: NTIS HC A04/MF A01; also available SOD HC $3.00 as 003-003-02949-1 CSCL 09B

The interfaces and functionality of the first level of the visual perception branch of a real time hierarchical manipulator control system is described. It includes a description of the scope of the processing performed and the outputs generated. It defines the interfaces and the information exchanged between the modules at this level, as well as interfaces to a camera, a human operator, and to higher levels of the system. Author

N90-13102# Sheffield Univ. (England). Dept. of Control Engineering.
AN ON-LINE DISTRIBUTED MINIMUM-TIME TRAJECTORY GENERATOR FOR INTELLIGENT ROBOT MANIPULATORS
Ali M. S. Zalzala and Alan S. Morris Apr. 1988 48 p
(RR-358; ETN-89-95141) Avail: NTIS HC A03/MF A01

An algorithm is presented for the on-line generation of minimum time trajectories for robot manipulators. The algorithm is designed for intelligent robots with advanced on-board sensory equipment which can provide the position and orientation of the end-effector. Planning is performed in the configuration (joint) space by the use of optimized combined polynomial splines, along with a search technique to identify the best minimum time trajectory. The method proposed considers all physical and dynamical limitations inherent in the manipulator design, in addition to any geometric path constraints. Meeting the demands of the heavy computations involved leads to a distributed formulation on a multiprocessor system, for which an intelligent control unit is created to supervise its proper and practical implementation. Simulation results of a proposed case study are presented for a Puma 560 robot manipulator. ESA

N90-13103# Sheffield Univ. (England). Dept. of Control Engineering.
IDENTIFICATION OF ROBOT DYNAMICS: A PARALLEL PROCESSING APPROACH
A. Y. Zomaya and Alan S. Morris May 1989 23 p
(RR-361; ETN-89-95228) Avail: NTIS HC A03/MF A01

On-line estimation of the link inertial parameters using a semi-customized symbolic representation of the dynamic equations based on the Lagrangian formulation carried out using recursive least squares techniques is described. The algorithm is distributed over a network of parallel processors using OCCAM as its associated programming language. An example is given for the case of the first three links of the Stanford arm and good real-time results are demonstrated. The importance of including complicated behavior, such as varying inertia depending on the arm configuration, uncertain load effects, nonlinear effects such as the Coriolis and centripetal forces, and interactions among joints in designing such an arm, is stressed. ESA

N90-13104# Sheffield Univ. (England). Dept. of Control Engineering.
REAL-TIME ROBOT MOTION: THE VLSI IMPLEMENTATION VIA TRANSPUTERS
Ali M. S. Zalzala and Alan S. Morris Jun. 1989 21 p
(RR-364; ETN-89-95231) Avail: NTIS HC A03/MF A01

An on-line trajectory generator implemented for the control of robot manipulators is described. The computational complexities associated with such a task are reduced through distribution over a multiprocessor system, where the minimum-time motion of the robot is planned in real-time. The distributed structure of the transputer machines emphasizes the practicality and efficiency of the proposed system. Simulation results of a case study are presented for a Puma 560 robot manipulator. ESA

N90-13105# Ecole Nationale Superieure des Telecommunications, Paris (France).
THE APPLICATION OF ARTIFICIAL INTELLIGENCE TECHNIQUES TO TRACING THE INTERCONNECTIONS IN AN INTEGRATED CIRCUIT Ph.D. Thesis [APPLICATION DE TECHNIQUES D'INTELLIGENCE ARTIFICIELLE AU TRACE DES INTERCONNEXIONS D'UN CIRCUIT INTEGRE]
Pierre-Francois Dubois Mar. 1989 113 p In FRENCH; ENGLISH summmary
(Telecom-Paris-89-E002; ISSN-0751-1353; ETN-89-95503) Avail: NTIS HC A06/MF A01

A new approach to the routing of a layout system is proposed. This routing system can handle rectangular blocks with pins on the boundary. The local router is a 2-D router made up of two layers. Its strategy can be described as follows: all nets are first partitioned into a set of subnets, and can be considered as solving a set of subproblems which are interdependent; the contraints between these subproblems are analyzed by a set of experts, which together enable the system to decide in which order and how each subnet should be routed. The global routing is carried out on a new decomposition of the routing space. This decomposition and the local enable the system to solve the channel intersections efficiently. The properties of this decomposition are analyzed. The ability to shift blocks at any moment during the routing is described. A new technique for the routing of the power and ground nets is proposed. It ensures that both will be routed on the same layer. The two nets are first routed separately. Crossings are then examined and eliminated iteratively by modifying one net or the other. Some details of the data structures are given and discussed. Several routing examples are tested against the system. The test results are provided and comparisons made. ESA

N90-13106# Technische Univ., Delft (Netherlands). Faculty of Technical Mathematics and Informatics.
CONCEPTUAL DEPENDENCY THEORY AND ROBOT PROGRAMMING
Afke vanRijn 1989 44 p
(Rept-89-20; ISSN-0922-5641; ETN-89-95579) Copyright Avail: NTIS HC A03/MF A01

The programming of a flexible assembly, consisting of one or more robots, to assemble a product is addressed. The study seeks a knowledge representation that can be used both as a representation of assembly instructions and as an intermediate representation to let human beings conduct a dialogue with the system when problems occur in programming the assembly cell. Existing knowledge representations do not contain every property needed for the purpose. To this effect a known knowledge representation, the conceptual dependency theory, that contains some important concepts is started from. To make this representation suitable for the purpose the theory is formalized and generalized. The knowledge representation obtained is called conceptual dependency graphs, and these are considered as very suitable for the representation of robot programs or any other other representation in a limited domain. ESA

N90-13107 Physics and Electronics Lab. TNO, The Hague (Netherlands).
ARTIFICIAL INTELLIGENCE FOR COMMUNICATION PROSPECTS
E. H. Hakvoort Jan. 1989 123 p In DUTCH; ENGLISH summary
(FEL-1989-1; TD89-0393; ETN-89-94992) Copyright Avail: TNO Physics and Electronics Lab., P.O. Box 96864, 2509 JG The Hague, Netherlands

The prospects of Artificial Intelligence (AI) to improve the efficiency and effectiveness of military network management are reported. Using AI, decision procedures can be supported and completed more quickly. Optimization of the communication system is performed. Concerning the military network management, the Facilities Control (FC), the Operational Systems Control (OSC) and the system executive and planning, are considered. It is shown that the AI can be applied at the FC level for analyzing information streams and suggesting actions, and that at the OSC layer AI can ease the planning of the communication system by evaluating the situation. ESA

N90-13108# Etablissement Technique Central de l'Armement, Arcueil (France). Dept. Systeme de Perception.
RADAR AND SENSOR ARRAY DESIGN PLANNING FOR A NAVAL MISSILE TESTING CENTER. ARTIFICIAL INTELLIGENCE APPLICATIONS Final Report [AIDE A LA CONFIGURATION RADAR ET CAPTEURS DU DISPOSITIF DE MESURES DU FUTUR BEM: APPLICATIONS DE L'INTELLIGENCE ARTIFICIELLE]
IA Xavier Merlo and M. Jean-Michel Frecaut 10 Oct. 1988 68 p In FRENCH
(Contract ETCA/CTME/CME-042345)
(ETCA-88-R-099; ETN-89-95022) Avail: NTIS HC A04/MF A01

The stages involved in planning for a missile tracking network are described. A hierarchy of tasks in carrying out such planning is presented. The speed of operation of the different components of the tracking network are analyzed in order to optimize the efficiency of interactions. Sequencing of receptor and effector mechanisms is analyzed using simulations. The interdependence of computer software and radar and telemetry is stressed. Problem areas are identified and solutions proposed. ESA

N90-13109# Institut National Polytechnique, Grenoble (France). Techniques de l'Informatique, des Math., de la Microelectronique et de la Microscopie Quantitative.
LAIOS: A MULTIPROCESSOR NETWORK FOR ARTIFICIAL INTELLIGENCE APPLICATIONS Ph.D. Thesis
Jean Duprat 1988 154 p In FRENCH; ENGLISH summary
(ETN-89-95498) Avail: NTIS HC A08/MF A01

A massive multiprocessor network, named LAIOS, designed for parallel processing in artificial intelligence applications is presented. The PROLOG dialect programming language is described. The internal format uses self-defined objects structured in blocks. The research AND/OR tree of PROLOG is dynamically

spread. The AND pipe-line and the OR parallelism are ensured by the data copy and synchronized by the anticipation mechanism. The architecture of the network is described and simulation results are given. The network simulation demonstrates that, without sufficient parallelism, the multiple data copies handicap performance. Several ways of overcoming this problem are considered. ESA

N90-13110# Massachusetts Inst. of Tech., Cambridge. Artificial Intelligence Lab.
A THEORY OF NETWORKS FOR APPROXIMATION AND LEARNING
Tomaso Poggio and Federico Girosi Jul. 1989 88 p
(Contracts N00014-85-K-0124; DACA76-85-C-0010)
(AD-A212359; AI-M-1140; CBIP-PAPER-31) Avail: NTIS HC A05/MF A01 CSCL 12/9

Learning an input-output mapping from a set of examples, of the type that many neural networks have been constructed to perform, can be regarded as synthesizing an approximation of a multi-dimensional function, that is solving the problem of hypersurface reconstruction. From this point of view, this form of learning is closely related to classical approximation techniques. This paper considers the problems of an exact representation of the approximation of linear and nonlinear mappings in terms of simpler functions of fewer variables. Kolmogorov's theorem concerning the representation of functions of several variables in terms of functions of one variable turns out to be almost irrelevant in the context of networks for learning. We develop a theoretical framework for approximation based on regularization techniques that leads to a class of three-layer networks that we call Generalized Radial Basis Function (GRBF), since they are mathematically related to the well-known Radial Basis Functions, mainly used for strict interpolation tasks. GRBF networks are not only equivalent to generalized splines, but are also closely related to pattern recognition methods such as Parzen windows and potential functions and to several neural network algorithms, such as Kanerva's associative memory, backpropagation and Kohonen's topology preserving map. GRA

N90-13111# Advanced Decision Systems, Mountain View, CA.
SPATIAL DATA STRUCTURES FOR ROBOTIC VEHICLE ROUTE PLANNING Final Technical Report, Sep. 1987 - Oct. 1988
Michael J. Black, David L. Milgram, Sharon O. Cioffi, and Patrice Gelband Dec. 1988 117 p
(Contract DACA72-87-C-0015)
(AD-A212806; ADS-TR-3185-01; ETL-0520) Avail: NTIS HC A06/MF A01 CSCL 12/5

The goal of the Phase 2 SBIR contract was to investigate techniques and tradeoffs for representing digital terrain information in a computer environment. The long term goal of this research is to build a Spatial Data Structure Development System (SDSDS) to serve as the infrastructure base for terrain analysis applications. The Phase 2 contract addressed the following issues: (1) implementation of common terrain representations; (2) implementation of common spatial operations; (3) design of a methodology for evaluating the performance of spatial operations; (4) evaluation of the implemented representations and operations; and (5) initial design of testbed on which the SDSDS would be built. GRA

N90-13112# JAYCOR, San Diego, CA.
NTRFACE FOR MAGIC Final Report, 1 Jul. 1987 - 31 Jul. 1989
N. T. Gladd 31 Jul. 1989 39 p
(Contract F49620-87-C-0062)
(AD-A212858; AFOSR-89-1235TR) Avail: NTIS HC A03/MF A01 CSCL 12/5

The NTRFACE system was developed to demonstrate the utility of contemporary computing technologies for facilitating the operation of highly complex, but more traditional scientific computational models. To this end, NTRFACE makes use of the user friendliness of personal computers, the flexibility and expressiveness of modern languages such as LISP and C, the power and extensibility of object-oriented programming and also borrows some techniques from artificial intelligence. The NTRFACE system is made concrete by applying it to a specific application (a mature, highly complex plasma physics particle in cell simulation code name MAGIC). This document is intended to be the user manual for the beta test version of NTRFACE for MAGIC. It is not intended to be a finished product. Indeed, the purpose of this release is to distribute NTRFACE for MAGIC to various MAGIC users who will field test it. It is anticipated that bugs, oversights, and conceptual errors will be discovered and any comments and constructive criticism will be most welcome. GRA

64 NUMERICAL ANALYSIS

Includes iteration, difference equations, and numerical approximation.

N90-13113*# Illinois Univ., Chicago.
LABELED TREES AND THE EFFICIENT COMPUTATION OF DERIVATIONS
Robert Grossman and Richard G. Larson [1989] 7 p
(Grants NAG2-513; NSF DMS-87-01085)
(NASA-CR-185386; NAS 1.26:185386) Avail: NTIS HC A02/MF A01 CSCL 12A

The effective parallel symbolic computation of operators under composition is discussed. Examples include differential operators under composition and vector fields under the Lie bracket. Data structures consisting of formal linear combinations of rooted labeled trees are discussed. A multiplication on rooted labeled trees is defined, thereby making the set of these data structures into an associative algebra. An algebra homomorphism is defined from the original algebra of operators into this algebra of trees. An algebra homomorphism from the algebra of trees into the algebra of differential operators is then described. The cancellation which occurs when noncommuting operators are expressed in terms of commuting ones occurs naturally when the operators are represented using this data structure. This leads to an algorithm which, for operators which are derivations, speeds up the computation exponentially in the degree of the operator. It is shown that the algebra of trees leads naturally to a parallel version of the algorithm. Author

N90-13114# Institute of Theoretical Physics, Amsterdam (Netherlands).
MULTIGRID MONTE CARLO IN AN EXTERNAL U(1) GAUGE FIELD
Arjan Hulsebos, Jan Smit, and Jeroen C. Vink (Nationaal Inst. voor Kernfysica en Hoge Energiefysica, Amsterdam, Netherlands) Nov. 1988 4 p Presented at the Symposium on Lattice Field Theory, Batavia, IL, 22-25 Sep. 1988 Submitted for publication Sponsored by the Stichting voor Fundamenteel Onderzoek der Materie, Amsterdam, Netherlands
(NIKHEF-ITFA-88-52; ETN-89-95404) Avail: NTIS HC A01/MF A01

A multigrid Monte Carlo algorithm of two dimensional scalar field is tested, in a U(1) gauge field. A pure gauge case is considered. The algorithms are free of systematic errors and the original action of the system determines the acceptance probability of a proposed field configuration. The algorithm is efficient for the computer with respect to vectorization or parallelism. Beta greater than 2, for scaling behavior, and beta greater than 4 to the third power, for asymptotic scaling behavior are found. ESA

N90-13115# Helsinki Univ. of Technology, Espoo (Finland). Inst. of Mathematics.
STABLE AND UNSTABLE SUBSPACES OF A CRITICAL FUNCTIONAL DIFFERENTIAL EQUATION
Olof J. Staffans Feb. 1989 15 p
(PB89-220651; MAT-A265; ISBN-951-754-778-1) Avail: NTIS HC A03/MF A01 CSCL 12A

The asymptotic behavior of a linear infinite delay, autonomous system of functional differential equations is studied. Conditions

are found that ensure that a state space can be written as a direct sum of a stable subspace, characterized by the fact that solutions are small at infinity, a finite dimensional central subspace in which solutions are neither small nor large at infinity, and a finite dimensional exponentially unstable subspace consisting of exponentially growing solutions. Author

N90-13116# Helsinki Univ. of Technology, Espoo (Finland). Lab. of Aerodynamics.
MULTIGRID SOLUTION METHOD FOR THE EULER EQUATIONS
Timo Siikonen and Jaakko Hoffren 12 Jan. 1989 41 p
(PB89-219463; SER-A-89-A10; ISBN-951-754-766-8) Avail: NTIS HC A03/MF A01 CSCL 12A

A multigrid method for the two-dimensional Euler equations is described. The spatial discretization is based on the flux vector splitting of Van Leer. A finite volume form of the equations is used. Time integration is performed with an approximately factored implicit scheme. Convergence rate is enhanced by a multigrid algorithm. Results are presented for subsonic, transonic and supersonic flows over two airfoil sections. GRA

N90-13117# Helsinki Univ. of Technology, Espoo (Finland). Electromagnetics Lab.
TIME-DOMAIN GREEN FUNCTION CORRESPONDING TO A TIME-HARMONIC POINT SOURCE IN COMPLEX SPACE
Ismo V. Lindell and Keijo I. Nikoskinen Feb. 1989 21 p
(PB89-218846; Rept-42; ISBN-951-754-786-2) Avail: NTIS HC A03/MF A01 CSCL 12A

The time-domain counterpart of the scalar field arising from a time-harmonic point source in the complex space is derived. The solution corresponds to the complex-space source Green function, which has grown very important in various electromagnetic problems, because it can be applied to approximate the narrow radiation of the Gaussian beam type. The time-domain counterpart presented is seen to be real and causal. The solution is demonstrated to an asymptotic case of the Sommerfeld half-space problem in time domain. GRA

N90-13118# Howard Univ., Washington, DC.
STABLE SUMMABILITY AND APPROXIMATION THEORY Final Report, 1 Jul. 1984 - 30 Jun. 1989
Louise A. Raphael 25 Jul. 1989 11 p
(Contract DAAG29-84-G-0004)
(AD-A211379; ARO-21235.23-MA-H) Avail: NTIS HC A02/MF A01 CSCL 12/2

Research activity in the following areas is summarized: eigenfunctions expansions associated with elliptic operators; best data approximation; and multivariate splines. Results were published in 21 papers in research journals and conference proceedings. Fourteen of the papers are on elliptic and abstract operators, two on best data approximation, and five on splines. GRA

N90-13119# Technische Univ., Delft (Netherlands). Faculty of Technical Mathematics and Informatics.
DOMAIN OF ATTRACTION OF AN OPERATOR BETWEEN SUPREMUM AND SUM
Priscilla E. Greenwood and Gerard Hooghiemstra 1989 24 p
(Rept-89-05; ISSN-0922-5641; ETN-89-95439) Copyright Avail: NTIS HC A03/MF A01

Convergence and limit distributions for sums of independent random variables are investigated. In a sequence of independent random variables, the limiting behavior of normed sequences is shown to be parallel to the extreme value case. For approximate initial values the sequence is proved to be tight on the interior of the support of a limit law. A limit density is shown to exist, which is the unique density solution of a functional equation. ESA

N90-13120# Technische Univ., Delft (Netherlands). Faculty of Technical Mathematics and Informatics.
ON THE EXISTENCE OF A MAXIMAL WEAK SOLUTION FOR A SEMILINEAR ELLIPTIC EQUATION
E. N. Dancer (New England Univ., Armidale, Australia) and G. Sweers 1989 14 p
(Rept-89-06; ISSN-0922-5641; ETN-89-95440) Copyright Avail: NTIS HC A03/MF A01

Investigations on the solution of semilinear elliptic equations are presented. Classical proofs are extended to functions which are Lipschitz, and results are shown to hold true even if the function is not Lipschitz. Super(sub) solutions are used which allow general bounded domains. ESA

N90-13121# Sheffield Univ. (England). Dept. of Control Engineering.
A FUNCTIONAL EXPANSION AND STABILITY FOR NONLINEAR INPUT-OUTPUT MAPS
S. P. Banks and B. Chanane Apr. 1989 14 p
(RR-359; ETN-89-95142) Avail: NTIS HC A03/MF A01

Global bilinearization of a linear analytic system using the tensor operator approach is described. The results are generalized on finite dimensional bilinear systems. The idea of diagonal dominance for tensor operators is used to derive an exponential stability result. Examples are presented to illustrate the theory. ESA

N90-13122# Sheffield Univ. (England). Dept. of Control Engineering.
A NEW DECISION RULE FOR MODEL STRUCTURE IDENTIFICATION OF A CLASS OF NONLINEAR DYNAMIC SYSTEMS
Hong Gan and S. A. Billings Apr. 1989 13 p
(RR-360; ETN-89-95143) Avail: NTIS HC A03/MF A01

The problem of deriving a statistical decision rule for model structure identification of a class of nonlinear dynamic systems is addressed. A basis on which to describe the model structure is introduced and the model structure space and corresponding algebra structure are defined. Based on the Kullback-Leibler mean information, a model structure decision rule is developed by maximizing the average log-likelihood function. Some analytical and simulated comparisons of this decision rule with Akaike's and Bayes aposteriori decision rules are given. ESA

N90-13123# Sheffield Univ. (England). Dept. of Control Engineering.
A RECURSIVE ALGORITHM FOR COMPUTING THE FREQUENCY RESPONSE OF A CLASS OF NONLINEAR DIFFERENCE EQUATION MODELS
J. C. PeytonJones and S. A. Billings May 1988 21 p
(RR-354; ETN-89-95227) Avail: NTIS HC A03/MF A01

A recursive algorithm is developed which is both computationally compact, and which enables the nth order frequency response functions of a large class of nonlinear difference equation models to be found without restriction on the order n. To do this, the parameters of a Nonlinear Auto Regressive Moving Average with exogeneous inputs (NARMAX) model are estimated. The model is then used to generate the generalized frequency response characteristics. The advantage of using the polynomial NARMAX model rather than directly estimating the Volterra series is the reduced number of parameters and smaller data set which are required for identification purposes. How such an algorithm can be used in a variety of signal processing applications is described. ESA

N90-13124# Max-Planck-Institut fuer Stroemungsforschung, Goettingen (Germany, F.R.).
NUMERICAL ANALYSIS OF CHAOTIC SYMBOL SEQUENCES GENERATED BY PARABOLIC AND TRIANGLE MAPS OF THE INTERVAL
H. U. Vogel and W. Moehring Dec. 1987 48 p
(MPIS-22/1987; ISSN-0436-1199; ETN-89-95329) Avail: NTIS HC A03/MF A01

Important properties of dynamical systems (iterated maps of a phase space) are reflected by an associated symbol dynamics, i.e., the dynamical rules for symbols, which label the subsets of a partition of the phase space. Non-linear equations of motion are a necessary condition for self-exited oscillations and chaos to

occur in the phase space of a dynamical system. Many features of stability, bifurcation and chaos, known from more involved maps and even from turbulence are discussed. The degree of topological chaos present in a system as a whole is determined by counting the number of sequences of symbols admitted under the map. ESA

N90-13125# Grenoble-1 Univ. (France). Techniques de l'Informatique, des Mathematiques, de la Microelectronique et de la Microscopie Quanti

AN ERROR ESTIMATOR FOR PARAMETER CHOICE IN REGULATING LEAST SQUARE PROBLEMS. APPLICATION TO REGULARIZED DECONVOLUTION [UN NOUVEL ESTIMATEUR D'ERREUR POUR LE CHOIX DE PARAMETRES DANS LA REGULARISATION DE PROBLEMES DE MOINDRES CARRES. APPLICATION A LA DECONVOLUTION REGULARISEE]

Laurent Desbat (Centre National de la Recherche Scientifique, Grenoble, France) and Didier Girard Oct. 1988 25 p In FRENCH

(IMAG-RR-744-M; ETN-89-95494) Avail: NTIS HC A03/MF A01

A modified estimator, based on that proposed by Rice, but more reliable, is described. Elaboration of this estimator required an a priori knowledge of the desired function. This approach could find applications in solving least squares problems where calculation of the estimator is stable. In this improved form the estimator proposed by Rice can be compared to other methods of regulating parameter choice. ESA

N90-13126# Technische Univ., Delft (Netherlands). Faculty of Technical Mathematics and Informatics.

A GENERALIZATION OF MOAK'S q-LAGUERRE POLYNOMIALS

Roelof Koekoek 1989 33 p

(Rept-89-21; ISSN-0922-5641; ETN-89-95580) Copyright Avail: NTIS HC A03/MF A01

A study of polynomials which are generalization of the classical generalized Laguerre polynomials is presented. They are shown to be orthogonal on an interval with respect to an inner product. Two equivalent definitions of a q-analog of the polynomials are given. Two orthogonality relations are proved and a representation as a basic hypergeometric series is given. A five term recurrence relation is derived, with a Christoffel-Darboux type formula and a q-difference equation. Results about the zeros are given. ESA

N90-13127# Technische Univ., Delft (Netherlands). Faculty of Technical Mathematics and Informatics.

A POINT IN BETAZ/Z NOT CONTAINED IN A MAXIMAL ORBIT CLOSURE

Jan vanMill and Petr Simon (Univerzita Karolina, Prague, Czechoslovakia) 1989 16 p

(Rept-89-26; ISSN-0922-5641; ETN-89-95585) Copyright Avail: NTIS HC A03/MF A01

In the field of combinatorial number theory the question of whether every point in betaZ/Z is contained in a maximal orbit closure is addressed. As a partial answer to this question the existence of a strictly increasing chain of orbit closures in betaZ/Z is proved. Under a consequence of the continuum hypothesis a point in betaZ/Z is proved to exist, which is not contained in any maximal orbit closure. ESA

N90-13128# Technische Univ., Delft (Netherlands). Faculty of Technical Mathematics and Informatics.

A CELL-CENTERED MULTIGRID METHOD FOR THREE-DIMENSIONAL ANISOTROPIC-DIFFUSION AND INTERFACE PROBLEMS

M. Khalil and P. Wesseling 1989 24 p

(Rept-89-35; ISSN-0922-5641; ETN-89-95593) Copyright Avail: NTIS HC A03/MF A01

Three dimensional interpolatory prolongation and restriction operators for cell centered multigrid and a new smoother are presented. This smoother is based on a modification of incomplete point factorization. The multigrid method is applied to three dimensional anisotropic interface problems. Numerical results show good performance of the method in all cases when accelerated by a Lanczos type method. Comparison of storage and computing work required by cell centered and vertex centered multigrid methods is given. ESA

N90-13129# Technische Univ., Delft (Netherlands). Faculty of Technical Mathematics and Informatics.

LOCAL MODE SMOOTHING ANALYSIS OF VARIOUS INCOMPLETE FACTORIZATION ITERATIVE METHODS IN TWO DIMENSIONS

M. Khalil 1989 25 p

(Rept-89-36; ISSN-0922-5641; ETN-89-95594) Copyright Avail: NTIS HC A03/MF A01

The smoothing efficiency of some iterative methods based on incomplete factorizations are assessed by local mode analysis. The analysis consists of an analytic and numerical study of a simple two dimensional problem discretized by finite differences. Dirichlet boundary conditions are assumed and are taken into account in an approximate way in the analysis. This analysis is done for pointwise and blockwise incomplete factorizations. A simple and robust smoother is found. Simple expressions for the smoothing factors for the methods studied are given. The analysis gives a good prediction of the multigrid convergence behavior. ESA

N90-13130# Technische Univ., Delft (Netherlands). Faculty of Technical Mathematics and Informatics.

ANAPHORIC TREES AND AN EXTENSION OF THE MODEL OF ANAPHORA RESOLUTION

Maria Polkowska-Semeniuk and Lech T. Polkowski 1989 21 p

(Rept-89-37; ISSN-0922-5641; ETN-89-95595) Copyright Avail: NTIS HC A03/MF A01

In a continuing study, anaphora resolution in algebraic linguistics is addressed. Anaphoric trees are defined and by means of an ordering of such a tree some anaphoric resolutions which seem to have intuitive appeal are selected. A previous model of anophora resolution is extended to a larger class of occurrences covering some cases of singular reflexive pronoun anaphora. ESA

N90-13131# Center for Mathematics and Computer Science, Amsterdam (Netherlands). Dept. of Numerical Mathematics.

SMOOTHED PREDICTOR-CORRECTOR METHODS FOR SOLVING PARTIAL DIFFERENTIAL EQUATIONS

P. J. vanderHouwen and B. P. Sommeijer Jul. 1988 23 p

(CWI-NM-R8808; ETN-89-95619) Copyright Avail: NTIS HC A03/MF A01

Special predictor-corrector methods employing residue smoothing for solving semidiscrete partial differential equations are analyzed. Additional computational effort involved by the explicit smoothing technique used is low compared with its stabilizing effect, although overall accuracy may be decreased. The effect of residue smoothing on accuracy is investigated. ESA

N90-13132# Center for Mathematics and Computer Science, Amsterdam (Netherlands). Dept. of Numerical Mathematics.

ITERATED THETA METHOD FOR HYPERBOLIC EQUATIONS

P. J. vanderHouwen and B. P. Sommeijer Jul. 1988 23 p

(CWI-NM-R8809; ETN-89-95620) Copyright Avail: NTIS HC A03/MF A01

Iterated theta methods employing residue smoothing for solving semidiscrete hyperbolic differential equations are analyzed. The stability condition is considerably relaxed under residue smoothing technique, and the additional computational effort involved is low when compared with its stabilizing effect, although overall accuracy may be decreased. The effects on stability and accuracy under residue smoothing are investigated, and a number of explicitly given methods based on the iterated implicit midpoint rule are presented. Numerical examples confirm theoretical results. ESA

N90-13133# Center for Mathematics and Computer Science, Amsterdam (Netherlands). Dept. of Numerical Mathematics.
AN ALGEBRAIC CHARACTERIZATION OF B-CONVERGENT RUNGE-KUTTA METHODS
Willem H. Hundsdorfer and Josef Schneid (Technische Univ., Vienna, Austria) Jan. 1989 12 p Sponsored in part by the Fonds zur Foerderung der Wissenschaftlichen Forschung, Austria
(CWI-NM-R8901; ETN-89-95623) Copyright Avail: NTIS HC A03/MF A01

The analysis of discretization methods for stiff initial value problems is addressed. B-stability is already a known concept for Runge-Kutta methods applied to dissipative problems, but is not sufficient on its own for B-convergence. For the derivation of B-convergence results, that is, error bounds not affected by stiffness, necessary and sufficient conditions for B-convergence are determined. ESA

N90-13134# Center for Mathematics and Computer Science, Amsterdam (Netherlands). Dept. of Numerical Mathematics.
INCREASING THE REAL STABILITY BOUNDARY OF EXPLICIT METHODS
B. P. Sommeijer Jan. 1989 22 p
(CWI-NM-R8902; ETN-89-95624) Copyright Avail: NTIS HC A03/MF A01

Based on the simplest well-known integration rules (such as the forward Euler scheme and Runge-Kutta method), an extension to enlarge the real stability boundary is proposed. The method involves bridging a substantial part of a large time step by extrapolating approximations obtained in previous step points and applying a simple explicit integrator to perform actual integration over the remaining small part of the step. The ideas are outlined and methods of orders one to four are construed and analyzed. Numerical results and comparisons are presented. Conclusions are formulated, the main characteristic of the scheme being that computational complexity is hardly increased. ESA

N90-13135# Center for Mathematics and Computer Science, Amsterdam (Netherlands). Dept. of Numerical Mathematics.
NUMVEC FORTRAN LIBRARY MANUAL CHAPTER: SIMULTANEOUS LINEAR EQUATIONS
W. Hoffmann (Amsterdam Univ., Netherlands) and K. Potma Jan. 1989 20 p
(CWI-NM-R8903; ETN-89-95625) Copyright Avail: NTIS HC A03/MF A01

A set of NUMVEC FORTRAN (numerical software for vector and parallel computers in FORTRAN) library routines dealing with the full-rank linear least-squares problem and the orthogonal basis problem are described. A subroutine for calculating the factors of a matrix factorization decomposition with a compactly stored orthogonal factor is induced. This storage scheme is customary when Householder reflections are used. It contains subroutines for calculating the product of a coded orthogonal matrix (or its transposed) with a vector, and a subroutine for calculating the explicit form of this orthogonal matrix. ESA

N90-13136# Center for Mathematics and Computer Science, Amsterdam (Netherlands). Dept. of Numerical Mathematics.
A MOVING-GRID INTERFACE FOR SYSTEMS OF ONE-DIMENSIONAL TIME-DEPENDENT PARTIAL DIFFERENTIAL EQUATIONS
J. G. Blom and P. A. Zegeling Jan. 1989 40 p
(Contract CWI-55-092)
(CWI-NM-R8904; ETN-89-95626) Copyright Avail: NTIS HC A03/MF A01

A software interface is described for the spatial discretization of systems of one dimensional time dependent partial differential equations. A moving-grid interface is developed as a more successful method of solving models with steep spatial and temporal gradients. A finite-element discretization for Lagrangian forms of PDEs (partial differential equations) is implemented. The interface itself is discussed and an example shows its ease of use in the SPRINT environment. Numerical examples underline the performance of the moving grid method applied to problems possessing moving transition-layers. Subroutines, test functions, trial functions, and quadrative points used are described. ESA

N90-13137*# National Aeronautics and Space Administration. Ames Research Center, Moffett Field, CA.
AN EIGENVALUE ANALYSIS OF FINITE-DIFFERENCE APPROXIMATIONS FOR HYPERBOLIC IBVPS
Robert F. Warming and Richard M. Beam Oct. 1989 15 p Presented at the 8th GAMM Conference on Numerical Methods in Fluid Mechanics, Delft, Netherlands, 27-29 Sep. 1989
(NASA-TM-102241; A-89259; NAS 1.15:102241) Avail: NTIS HC A03/MF A01 CSCL 12A

The eigenvalue spectrum associated with a linear finite-difference approximation plays a crucial role in the stability analysis and in the actual computational performance of the discrete approximation. The eigenvalue spectrum associated with the Lax-Wendroff scheme applied to a model hyperbolic equation was investigated. For an initial-boundary-value problem (IBVP) on a finite domain, the eigenvalue or normal mode analysis is analytically intractable. A study of auxiliary problems (Dirichlet and quarter-plane) leads to asymptotic estimates of the eigenvalue spectrum and to an identification of individual modes as either benign or unstable. The asymptotic analysis establishes an intuitive as well as quantitative connection between the algebraic tests in the theory of Gustafsson, Kreiss, and Sundstrom and Lax-Richtmyer L(sub 2) stability on a finite domain. Author

N90-13138# Center for Mathematics and Computer Science, Amsterdam (Netherlands). Dept. of Pure Mathematics.
MEIXNER-POLLACZEK POLYNOMIALS AND THE HEISENBERG ALGEBRA
Tom H. Koornwinder Jul. 1988 9 p Submitted for publication
(CWI-PM-R8806; ETN-89-95627) Copyright Avail: NTIS HC A02/MF A01

An alternative proof is given for the connection between a system of continuous Hahn polynomials and identities for symmetric elements in the Heisenberg algebra which was first observed by Bender, Mead and Pinsky. The continuous Hahn polynomials turn out to be Meixner-Pollaczek polynomials. Use is made of the connection between Laguerre polynomials and Meixner-Pollaczek polynomials, the Rodrigues formula for Laguerre polynomials, an operational formula involving Meixner-Pollaczek polynomials and the Schroedinger model for the irreducible unitary representations of the three dimensional Heisenberg group. ESA

N90-13139# Center for Mathematics and Computer Science, Amsterdam (Netherlands). Dept. of Pure Mathematics.
JACOBI FUNCTIONS AS LIMIT CASES OF q-ULTRASPHERICAL POLYNOMIALS
Tom H. Koornwinder Jul. 1988 12 p Submitted for publication
(CWI-PM-R8807; ETN-89-95628) Copyright Avail: NTIS HC A03/MF A01

Jacobi functions of equal indices are obtained as limit cases of q-ultraspherical polynomials as q tends to 1. In particular, if the Jacobi function can be interpreted as a spherical function on a hyperboloid then the degree of the q-ultraspherical polynomial tends in the limit to the geodesic distance to a fixed point on the hyperboloid. Two appendices are given containing rigorous proofs of the limit formulas as q tends to 1 for the q-binomial series and the q-gamma function. ESA

N90-13140# Center for Mathematics and Computer Science, Amsterdam (Netherlands). Dept. of Pure Mathematics.
REPRESENTATIONS OF THE TWISTED SU(2) QUANTUM GROUP AND SOME q-HYPERGEOMETRIC ORTHOGONAL POLYNOMIALS
Tom H. Koornwinder Sep. 1988 21 p Submitted for publication
(CWI-PM-R8809; ETN-89-95629) Copyright Avail: NTIS HC A03/MF A01

The matrix elements of the irreducible unitary representations

of the twisted SU(2) quantum group are computed explicitly. Their identification with two different classes of q-hypergeometric orthogonal polynomials: with the little q-Jacobi polynomials and with certain q-analogs of Krawtchouk polynomials is shown. The orthogonality relations for these polynomials correspond to Schur type orthogonally relations in the first case and to the unitarity conditions for the representations in the second case. A new proof of Woronowicz' classification of the unitary irreducible representations of this quantum group which avoids infinitesimal methods is given. Symmetries of the matrix elements of the irreducible unitary representations are proved without using the explicit expressions. ESA

N90-13141# Center for Mathematics and Computer Science, Amsterdam (Netherlands). Dept. of Pure Mathematics.
INDEX FORMULAS FOR GENERALIZED WIENER-HOPF OPERATORS AND BOSON-FERMION CORRESPONDENCE IN 2N DIMENSIONS
S. N. M. Ruijsenaars Dec. 1988 39 p Submitted for publication Sponsored by the Netherlands Organization for the Advancement of Research
(CWI-PM-R8811; ETN-89-95630) Copyright Avail: NTIS HC A03/MF A01

The kernels of operators associated with special chiral gauge transformations (kinks) in the 2N (space-time) dimensional Dirac theory are explicitly determined. The result is used to obtain index formulas for Fredholm operators corresponding to continuous chiral gauge transformations. The Fock space quadratic forms corresponding to the kinks are proved to converge to the Dirac field as the kink size goes to zero. The Majorana field is reached in a similar fashion under conditions. ESA

N90-13142# Center for Mathematics and Computer Science, Amsterdam (Netherlands). Dept. of Mathematical Statistics.
A KERNEL APPROACH TO ESTIMATION OF THE SPHERE RADIUS DENSITY IN WICKSELL'S CORPUSCLE PROBLEM
A. J. vanEs (Amsterdam Univ., Netherlands) and A. W. Hoogendoorn Jun. 1988 25 p
(CWI-MS-R8809; ETN-89-95632) Copyright Avail: NTIS HC A03/MF A01

The estimation of the probability density function of the radii of spheres in a medium, given the radii of their profiles in a random slice, known as Wicksell's corpuscle problem is considered. An estimator related to the classical kernel density estimator is given and its properties are discussed. A comparison is made with two other estimators related to the kernel estimator. ESA

N90-13143# Center for Mathematics and Computer Science, Amsterdam (Netherlands). Dept. of Mathematical Statistics.
TAIL TRIVIALITY FOR SUMS OF STATIONARY RANDOM VARIABLES
H. C. P. Berbee and W. Th. F. denHollander (Technische Univ., Delft, Netherlands) Jun. 1988 15 p
(CWI-MS-R8810; ETN-89-95633) Copyright Avail: NTIS HC A03/MF A01

A study of tail sigma-fields and loss of memory associated with sums of stationary integer-valued random variables is presented. An application concerns convergence in distribution of interarrival times in 0 to 1 sequences. Proofs of theorems are presented and a proof of corollary using coupling is given. ESA

N90-13144# Center for Mathematics and Computer Science, Amsterdam (Netherlands). Dept. of Mathematical Statistics.
ON A RATE OF CONVERGENCE OF THE MULTIKNAPSACK VALUE FUNCTION
Sara A. vanderGeer and Leen Stougie (Amsterdam Univ., Netherlands) Jul. 1988 8 p
(CWI-MS-R8812; ETN-89-95634) Copyright Avail: NTIS HC A02/MF A01

The almost sure asymptotic characterization for the optimal solution of the Knapsack capacities, when the profit and requirement coefficients of items to be selected from are random variables, which was derived in Meanti et al., 1988, is studied. A rate of convergence for this process is established using results from the theory of empirical processes. ESA

N90-13145# Center for Mathematics and Computer Science, Amsterdam (Netherlands). Dept. of Mathematical Statistics.
A SEMIPARAMETRIC MODEL FOR CITATION COUNTS
Adriaan P. vanderPlas Sep. 1988 25 p
(CWI-MS-R8814; ETN-89-95636) Copyright Avail: NTIS HC A03/MF A01

The pattern of yearly citation counts of a scientific paper, which expresses in some way its importance, is modeled as a discrete time stochastic process with a conditional distribution dependent on a few parameters characterizing the particular scientific field. For a particular data set the parameters are estimated and several tests of the model performed. The estimates are shown to fit the test data quite well. Possible improvements to the model, and applications to scientometry, are discussed. ESA

N90-13146# Center for Mathematics and Computer Science, Amsterdam (Netherlands). Dept. of Mathematical Statistics.
ON THE HELLINGER TYPE DISTANCES FOR FILTERED EXPERIMENTS
K. O. Dzhaparidze and E. Valkeila (Helsinki Univ., Finland) Nov. 1988 12 p Sponsored in cooperation with the Finnish Academy and the Ella and Georg Ehrnooth Foundation
(CWI-MS-R8818; ETN-89-95638) Copyright Avail: NTIS HC A03/MF A01

Hellinger type distances on a filtered space are studied. Lower and upper bounds are given in predictable terms by a theorem. Applications to sequences of binary experiments and to a parametric family of experiments are discussed. Necessary and sufficient conditions for the convergence to a limiting Gaussian experiment are given by theorem. Evaluation, based on certain modulus of continuity needed in statistical applications, is demonstrated. ESA

N90-13147# Center for Mathematics and Computer Science, Amsterdam (Netherlands). Dept. of Mathematical Statistics.
ON THE SMOOTH FIT BOUNDARY CONDITIONS IN THE OPTIMAL STOPPING PROBLEM FOR SEMIMARTINGALES
R. J. Chitashvili (Academy of Sciences of the Georgian SSR, Tbilisi.) Dec. 1988 12 p Submitted for publication
(CWI-MS-R8819; ETN-89-95639) Copyright Avail: NTIS HC A03/MF A01

The well known smooth fit boundary conditions in the optimal stopping problem of Markov diffusion processes are generalized for the optimal stopping problem of semimartingales. The construction of the optimal stopping rule is connected with the construction of the value process, which is in turn based on characterization theorems. The most general supermartingale characterization is given, and all supermartingales considered are right continuous admitting left-hand limits and having special decompositions. ESA

N90-13148# Center for Mathematics and Computer Science, Amsterdam (Netherlands). Dept. of Algebra, Analysis, and Geometry.
LIE-ALGEBRAIC ASPECTS OF THE CLASSICAL NONRELATIVISTIC CALOGERO-MOSER MODELS
J. K. Scholma Jan. 1989 43 p
(CWI-AM-R8901; ETN-89-95641) Copyright Avail: NTIS HC A03/MF A01

A Lie-algebraic construction of the phase space and Poisson structure of the classical nonrelativistic Calogero-Moser models is given. The construction uses a real noncompact semisimple Lie algebra set with an involutive automorphism, and requires the existence of an element in the set with some special properties. The Lax equation is derived and a Lie-algebraic proof that the Ad-invariant functions on the set are in involution is given. Two well-known examples are described from this point of view and a possible generalization is discussed. Construction is compared with that of Kostant-Adler-Symes. ESA

N90-13149# Center for Mathematics and Computer Science, Amsterdam (Netherlands). Dept. of Algebra, Analysis, and Geometry.
HAHN-BANACH TYPE THEOREMS FOR DUAL SEMIGROUPS
J. M. A. M. vanNeerven Jan. 1989 13 p
(CWI-AM-R8903; ETN-89-95642) Copyright Avail: NTIS HC A03/MF A01

A study of the theories of Banach spaces and subspaces is presented. For most of the Hahn-Banach theorems it is shown that analagons exist between the theories of spaces and their subspaces. Invariance under the semigroup is shown to be the relevant extra hypothesis to be imposed. The theory presented is applied to study sun-reflexivity and a proof of de Pagter's characterization of sun-reflexivity is given. ESA

N90-13150# Center for Mathematics and Computer Science, Amsterdam (Netherlands). Dept. of Algebra, Analysis, and Geometry.
THE ALGEBRAIC BASIS OF MATHEMATICAL MORPHOLOGY. PART 2: OPENINGS AND CLOSINGS
C. Ronse (Philips Research Labs., Brussels, Belgium) and H. J. A. M. Heijmans Feb. 1989 45 p
(CWI-AM-R8904-Pt-2; ETN-89-95643-Pt-2) Copyright Avail: NTIS HC A03/MF A01

In a continuation of study, an abstract algebraic framework for mathematical morphology is investigated. The main assumption is that the object space is a complete lattice. Of interest are all (increasing) operators which are invariant under a given abelian group of automorphisms on the lattice. Openings and closings, which are very special classes of idempotent operators are investigated. Much attention is given to specific methods for building openings and closings. Some examples are given which illustrate the abstract theory. ESA

N90-13151# Center for Mathematics and Computer Science, Amsterdam (Netherlands). Dept. of Algebra, Analysis, and Geometry.
THE ADDITION FORMULA FOR LITTLE q-LEGENDRE POLYNOMIALS AND THE SU(2) QUANTUM GROUP
Tom H. Koornwinder Mar. 1989 12 p
(CWI-AM-R8906; ETN-89-95644) Copyright Avail: NTIS HC A03/MF A01

From the interpretation of little q-Jacobi polynomials as matrix elements of the irreducible unitary representations of the SU(2) quantum group, an addition formula is derived for the little q-Legendre polynomials. This involves an expansion in terms of Wall polynomials. A product formula for little q-Legendre polynomials is given in consequence by q-integration. ESA

N90-13152# Center for Mathematics and Computer Science, Amsterdam (Netherlands). Dept. of Software Technology.
MODULAR SPECIFICATIONS IN PROCESS ALGEBRA WITH CURIOUS QUEUES
Rob J. vanGlabbeek and Frits W. Vaandrager May 1988 52 p Sponsored by the Commission of European Communities ESPRIT Project 432 METEOR and RACE Project 1046 SPECS
(CWI-CS-R8821; ETN-89-95645) Copyright Avail: NTIS HC A04/MF A01

The semantical reality of a large number of closely related process algebras is reflected, and even used, on the level of algebraic specifications and in process verifications, by means of the notion of a module. The simplest modules are building blocks of operators and axioms, each block describing a feature of concurrency in a certain semantical setting. These modules are then combined by means of a union operator, an export operator which allows discounting of some operators in a module, an operator which changes semantics by taking homomorphic images, and an operator which takes subalgebras. These operators enable combination of a module in a subtle way, when the direct combination would be inconsistent. It is demonstrated how new process combinators can be defined in terms of the more elementary ones in a clean way. As an illustration of the approach, a methodology is presented that can be used to specify FIFO (first in first out) queues, and that facilitates verification of concurrent systems containing these queues. ESA

N90-13153# Center for Mathematics and Computer Science, Amsterdam (Netherlands). Dept. of Software Technology.
SEMANTICS AND CONSISTENCY OF RULE-BASED EXPERT SYSTEMS
Marc Bezem Jul. 1988 17 p Sponsored in part by the Dutch Stimulerings Projectteam Informatica-Onderzoek
(CWI-CS-R8824; ETN-89-95646) Copyright Avail: NTIS HC A03/MF A01

Consistency of a knowledge-based system which has become a topic of growing concern is addressed. Every notion of consistency presupposes a notion of semantics. A theoretical framework in which both the semantics and the consistency of a knowledge base can be studied is presented. This framework is based on first order flat many-sorted predicate logic and is sufficiently rich to capture an interesting class of rule-based expert systems and deductive databases. The feasibility of the consistency test is analyzed and this test is proved feasible for knowledge bases in Horn format without quantification. The use of expressions in rules is studied. ESA

N90-13154# Center for Mathematics and Computer Science, Amsterdam (Netherlands). Dept. of Algorithmics and Achitecture.
PLACING MIRRORS IN GRIDS
Evangelos Kranakis, Danny D. M. Krizanc, and Lambert G. L. T. Meertens Mar. 1989 14 p Submitted for publication
(CWI-CS-R8906; ETN-89-95653) Copyright Avail: NTIS HC A03/MF A01

Instances of a mirror placement problem on a (multidimensional) grid are studied. Given a light source S to be located at a node of the grid which is emitting a light beam in a single direction (e.g. a laser), the problem is to determine the minimum number of mirrors that must be placed on individual nodes of the grid in such a way that the light beam emanating from the source S will eventually hit all the vertices of the grid by traversing only edges of the grid. An asymptotically optimal algorithm for placing mirrors on the vertices of complete multidimensional grids is developed and worst-case behavior of any possible mirror-placement algorithm are analyzed. ESA

N90-13155# Center for Mathematics and Computer Science, Amsterdam (Netherlands). Dept. of Software Technology.
AN ALGEBRA FOR PROCESS CREATION
Frits W. Vaandrager and Jos C. M. Baeten Mar. 1989 27 p Sponsored in part by the Commission of European Communities ESPRIT Project 432 METEOR and RACE Project 1046 SPECS
(CWI-CS-R8907; ETN-89-95654) Copyright Avail: NTIS HC A03/MF A01

The issue of process creation from an algebraic perspective is studied. The key to the approach consists of giving a new interpretation to the sequential composition operator symbol in the axiom system basic process algebra (BPA). Other models for BPA are presented and the new interpretation is shown to naturally generalize the usual interpretation in algebra for process creation (ACP). An operational semantics based on Plotkin style inductive rules for a simple language with process creation and communication and a complete finite axiomatization of the associated bisimulation model are given. ESA

N90-13156# Center for Mathematics and Computer Science, Amsterdam (Netherlands). Dept. of Interactive Systems.
FASTER PHONG SHADING VIA ANGULAR INTERPOLATION
A. A. M. Kuijk and E. H. Blake Mar. 1989 21 p
(CWI-CS-R8909; ETN-89-95655) Copyright Avail: NTIS HC A03/MF A01

An angular interpolation for Phong shading planar polygons is presented as an efficient method to reduce artifacts when displaying moving objects. A shading algorithm which imposes no need for subdivision of patches as presented by the solid modeling system is yielded by shading calculation via angular interpolation. Two

alternative evaluation methods that trade off evaluation cost against level of accuracy are described which can both handle light source and view point at arbitrary distances, but differ in level of accuracy and therefore both impose restrictions on the topology of patches and light sources. The limitations imposed by these alternative shading methods are more liberal than the limitations on patch size imposed by the geometry. The most economic evaluation method presented can incrementally compute the color intensity along a scanline by two additions per pixel. The methods presented are generally applicable and can be easily implemented in hardware. ESA

N90-13157# Universiteit Twente, Enschede (Netherlands). Faculty of Applied Mathematics.
LONG DOMINATING CYCLES AND PATHS IN GRAPHS WITH LARGE NEIGHBORHOOD UNIONS
H. J. Broersma and H. J. Veldman Feb. 1989 22 p
(MEMO-769; ISSN-0169-2690; ETN-89-95660) Avail: NTIS HC A03/MF A01

Hamiltonian properties of graphs with large neighborhood unions and cycles and paths are investigated. Results are combined with a known sufficient condition for the existence of a D-cycle and a common generalization of Ore's theorem and several neighborhood union results' are obtained. Analogous results on long D-paths are established. Results, consequences and proofs are given. ESA

N90-13158# Universiteit Twente, Enschede (Netherlands). Faculty of Applied Mathematics.
REMARKS ON THE CONTROL OF DISCRETE TIME NONLINEAR SYSTEMS
Henk Nijmeijer Feb. 1989 20 p Submitted for publication
(MEMO-770; ISSN-0169-2690; ETN-89-95661) Avail: NTIS HC A03/MF A01

The (dynamic) input-output decoupling problem and the problem of right-invertibility for discrete-time nonlinear systems are studied. It is shown that under generic conditions these problems are solvable around an equilibrium point if and only if the same problems are solvable for the linearization of the nonlinear system. The results typically apply to well known questions in economics and an example stemming from economic modeling is given. ESA

N90-13159# Universiteit Twente, Enschede (Netherlands). Faculty of Applied Mathematics.
ON THE MAXIMUM PERIOD OF A PERMUTATION OF N ELEMENTS
H. J. Broersma and F. Goebel Feb. 1989 13 p Revised
(MEMO-771; MEMO-743; ISSN-0169-2690; ETN-89-95662)
Avail: NTIS HC A03/MF A01

A study on the maximum period of a permutation of n (where n is a natural number) elements is presented. Upper and lower bounds for the maximum period mu(n) of a permutation of n elements, and results from the study of the asymptotic behavior of mu are given. Tables are included. ESA

N90-13160# Universiteit Twente, Enschede (Netherlands). Faculty of Applied Mathematics.
MULTIVARIABLE DIVIDED DIFFERENCE AND B-SPLINES
M. Neamtu Mar. 1989 8 p
(MEMO-772; ISSN-0169-2690; ETN-89-95663) Avail: NTIS HC A02/MF A01

A definition of the multivariate divided difference functional, which is consistent with the corresponding univariate notion, is given. It is based on the pointwise evaluation of a certain multivariate function. A close relation to the multivariate (simplex) B-splines is shown. Remarks on the B-spline evaluation are made. ESA

N90-13161# Universiteit Twente, Enschede (Netherlands). Faculty of Applied Mathematics.
ASYMPTOTIC EXPANSIONS FOR TWO-STAGE RANK TESTS
Willem Albers Mar. 1989 34 p
(MEMO-773; ISSN-0169-2690; ETN-89-95664) Avail: NTIS HC A03/MF A01

In a study of asymptotic expansions, a nonparametric competitor of Stein's two stage procedure is realized by replacing the t-test by a rank test. For rank tests, the most precise information available are asymptotic expansions for their power to order n to the minus 1st power, where n is the sample size. Using results on combinations of rank tests for subsamples, the same level of precision is obtained for the two-stage case. In this way the size of the additional sample to the natural order is determined and the nonparametric and the classical procedure are compared in terms of expected additional numbers of observations required. ESA

N90-13162# Universiteit Twente, Enschede (Netherlands). Faculty of Applied Mathematics.
NOTE ON THE CONVERGENCE OF SIMULATED ANNEALING ALGORITHMS
U. Faigle and W. Kern Mar. 1989 15 p
(MEMO-774; ISSN-0169-2690; ETN-89-95665) Avail: NTIS HC A03/MF A01

An inductive proof for the fact that the stationary distributions of a simulated annealing algorithm converge to a distribution, where non-optimal elements are generated with probability zero, provided that a weak reversability condition holds, is given. Simulated annealing algorithms in terms of Markov processes are discussed. ESA

N90-13163# Universiteit Twente, Enschede (Netherlands). Faculty of Applied Mathematics.
INTERPRETATION AND MANIPULATION OF EDGEWORTH EXPANSIONS
W. C. M. Kallenberg Mar. 1989 21 p
(MEMO-775; ISSN-0169-2690; ETN-89-95666) Avail: NTIS HC A03/MF A01

With a given Edgeworth expansion independent random variables are associated such that the Edgeworth expansion for the standardized sum of these random variables agrees with the given Edgeworth expansion. This facilitates interpretation and manipulation of Edgeworth expansions. The theory is applied to the power of one and two sample linear rank statistics and to the combination of such statistics based on subsamples. Complicated expressions for the power are shown to become more transparent. As a consequence of the sum-structure it is seen why splitting the sample causes no loss of first order efficiency and only a small loss of second order efficiency. ESA

N90-13164# Universiteit Twente, Enschede (Netherlands). Faculty of Applied Mathematics.
TRANSFORMATIONS AND REPRESENTATIONS OF NONLINEAR SYSTEMS
A. J. vanderSchaft Mar. 1989 22 p Submitted for publication
(MEMO-776; ISSN-0169-2690; ETN-89-95667) Avail: NTIS HC A03/MF A01

Nonlinear systems described by sets of smooth algebraic and (higher-order) differential equations in the external variables (inputs and outputs), as well as auxiliary variables (states, driving variables) are studied. A general theorem for transforming such a system into a locally equivalent one, assuming constant rank conditions, is formulated. With the aid of this theorem the elimination of the auxiliary variables in the system description is shown. Conversely, necessary and sufficient conditions for representing a system only involving inputs and outputs as a state space system are derived. The techniques are applied to the construction of inverse systems. ESA

N90-13165# Universiteit Twente, Enschede (Netherlands). Faculty of Applied Mathematics.
THE DISCRETE-TIME SINGLE-SERVER QUEUEING MODEL
J. C. W. vanOmmeren Apr. 1989 38 p
(MEMO-780; ISSN-0169-2690; ETN-89-95671) Avail: NTIS HC A03/MF A01

In a study of the discrete-time single-server queueing model, an exact representation for the generating function of the waiting-time distribution in the case of general interarrival-time and service-time distributions is given. Once this relation is established more explicit results are given concerning when the generating function of the interarrival-time distribution or the generating function of the service-time distribution is rational. Some results on the asymptotic behavior for the waiting-time distribution are given. ESA

N90-13166# Universiteit Twente, Enschede (Netherlands). Faculty of Applied Mathematics.
TOWARDS A COMPLETE LOCAL SOLUTION OF THE NONLINEAR MODEL MATCHING PROBLEM
H. J. C. Huijberts and Henk Nijmeijer Apr. 1989 20 p
(MEMO-781; ISSN-0169-2690; ETN-89-95672) Avail: NTIS HC A03/MF A01

The model matching problem, which consists of designing a compensator for a given system, called the plant, in such a way that the resulting input-output behavior matches that of a prespecified model, is studied. A local solution to the nonlinear model matching problem is given for the case that the model is decouplable by static state feedback. The main theorem states that under generic conditions on the plant the problem is solvable around an equilibrium point if and only if it is solvable for the linearization of plant and model. The generic conditions are identified. They naturally appear in the solution of the input-output decoupling problem for the plant. The theory is illustrated by means of two examples. ESA

N90-13167# Groningen Rijksuniv. (Netherlands). Dept. of Mathematics and Computing Sciences.
EXPLICIT FORMULAS FOR HANKEL NORM APPROXIMATIONS OF INFINITE-DIMENSIONAL SYSTEMS
Ruth F. Curtain and A. C. M. Ran 1989 18 p
(TW-289; ETN-89-95681) Avail: NTIS HC A03/MF A01

Hankel norm approximation for finite dimensional systems has been studied extensively, both for continuous time systems and discrete time systems. One of the approaches is to combine the work of J. A. Ball and J. W. Helton with results on Wiener-Hopf factorization to produce explicit formulas for the solutions. This has been done by J. A. Ball and A. C. M. Ran for the finite dimensional case and for a class of infinite dimensional systems by A. C. M. Ran. This approach is shown to be extendable to a much larger class of infinite dimensional systems, those with an exponentially stable semigroup and unbounded input and output operators which satisfy a smoothness condition. This class is larger than the nuclear class for with this problem was solved by K. Glover, R. F. Curtain and J. R. Partington by an approximation approach. ESA

N90-13168# Groningen Rijksuniv. (Netherlands). Dept. of Mathematics and Computing Sciences.
WELL POSEDNESS OF TRIPLES OF OPERATORS (IN THE SENSE OF LINEAR SYSTEMS THEORY)
Ruth F. Curtain and George Weiss (Weizmann Inst. of Science, Rehovoth, Israel) 1988 22 p Presented at the 4th International Conference on Control of Distributed Parameter Systems, Vorau, Austria, Jul. 1988
(TW-292; ETN-89-95682) Avail: NTIS HC A03/MF A01

A triple of operators (A, B, C) is called well posed if an abstract linear system exists where A is the generator of its semigroup, B its control operator and C its observation operator. A set of necessary and sufficient conditions for (A, B, C) to be well posed are presented. Essential use is made of the concept of transfer function and the theory is illustrated by two examples. ESA

N90-13169# Ohio State Univ., Columbus. ElectroScience Lab.
EXPONENTIAL MODELING USING COMBINED FORWARD AND BACKWARD PREDICTION
W. M. Steedly and R. L. Moses Mar. 1989 39 p
(Contract N00014-86-K-0202)
(AD-A212317; ESL-718048-10) Avail: NTIS HC A03/MF A01 CSCL 20/14

A sequence of complex data can be modeled using a damped exponential model. Forward or backward linear prediction can be used to estimate poles, and then total least squares can be used to estimate amplitudes for each pole. When model order is larger than true order, extraneous poles appear. These poles generally appear inside or outside the unit circle, depending on whether forward or backward prediction is used, respectively. Since true poles appear in approximately the same place for both methods, use of combined forward and backward pole estimation can be used to distinguish true poles from extraneous ones. GRA

N90-13170# Maryland Univ., College Park.
INTERNATIONAL CONFERENCE ON OPERATOR THEORY: ADVANCES AND APPLICATIONS Final Report, 1 Jun. 1988 - 31 May 1989
Seymour Goldberg Aug. 1989 13 p Conference held 22-26 Aug. 1988
(Contract DAAL03-88-G-0024)
(AD-A212341; ARO-25301.1-MA-CF) Avail: NTIS HC A02/MF A01 CSCL 12/2

The conference attracted 93 participants from 17 different countries and included 13 graduate students. The very latest developments in operator and matrix theory, and their uses in modern control and systems engineering were presented and discussed by many of the world's leading investigators. There were 13 plenary speakers, 36 invited papers, and 16 contributed papers. GRA

N90-13171# Limoges Univ. (France).
INTERNATIONAL CONFERENCE ON FIXED POINT THEORY AND APPLICATIONS
Jean-Bernard Baillon, ed. and Michel Thera, ed. 9 Jun. 1989 226 p In FRENCH; ENGLISH summary Conference held in Marseilles, France, 5-9 Jun. 1989
(Contract DAJA45-88-M-0409)
(AD-A212369; R/D-6117-MA-02) Avail: NTIS HC A11/MF A02 CSCL 12/2

The idea for this symposium at CIRM originated after the special session on fixed points at the ICM at Berkeley in 1986. This collection of abstracts summarized the presentations given at the symposium by experts from 17 different countries. It represents active current research on problems in at least the following areas: Nonexpansive mappings; Set-valued mappings; Minimax theorems and other abstract inequalities; Topological methods and degree theory; Ordered structures; Applications to economic analysis, partial differential equations, optimization, game theory, etc. GRA

N90-13172# Rensselaer Polytechnic Inst., Troy, NY. Dept. of Mechanical Engineering.
ANALYSIS OF THE NON-PLANAR RESPONSE OF A CANTILEVER, WITH THE AID OF COMPUTERIZED SYMBOLIC MANIPULATION
M. R. CrespodaSilva 1988 8 p
(AD-A212421; ARO-24456.2-EG) Avail: NTIS HC A02/MF A01 CSCL 12/2

The nonlinear differential equations governing the static deformations of a cantilever with a tip mass are formulated and analyzed with the aid of computerized symbolic manipulation. The nonlinearities in the equations are geometric and include terms such as nonlinear contributions to the curvature expression. All the algebra in this work is relegated to the computer. Most of the work presented in the literature dealing with the response of structural elements such as beams is restricted to planar response. In addition, much of the work is also restricted to the cases where the deformations are very small and are analyzed by linear theory. In general, a structure can undergo flexure in any direction in space, and torsion. For infinitesimally small deformations, flexural and torsional motions are uncoupled. In this paper the flexural-flexural-torsional deformations on a cantilever with a tip mass are determined. GRA

N90-13173# Old Dominion Coll., Norfolk, VA. Dept. of Mathematical Sciences.
STRONG MODERATE DEVIATION THEOREMS FOR m-DEPENDENT RANDOM VARIABLES Interim Technical Report, period ending 30 Jun. 1989
Narasinga Rao Chaganty Aug. 1989 11 p
(Contract DAAL03-88-K-0076)
(AD-A212618; ARO-24834.2-MA) Avail: NTIS HC A03/MF A01 CSCL 12/3

A stationary sequence of m-dependent random variables is considered. Under some moment conditions, asymptotic expression are obtained for the probability of moderate deviations. This result extends some well known results obtained for independent and identically distributed sequences of random variables. GRA

N90-13174# Stanford Univ., CA. Systems Optimization Lab.
A MODIFIED NEWTON METHOD FOR UNCONSTRAINED MINIMIZATION
Anders L. Forsgren, Philip E. Gill (California Univ., San Diego, La Jolla.), and Walter Murray Jul. 1989 38 p Sponsored in part by Goran Gustafsson Foundation, Sweden and Swedish National Board for Technical Development
(Contracts N00014-87-K-0142; DE-FG03-87ER-25030; NSF ECS-87-15153)
(AD-A212752; SU-SOL-89-12) Avail: NTIS HC A03/MF A01 CSCL 12/4

Newton's method has proved to be a very efficient method for solving strictly convex unconstrained minimization problems. For the nonconvex case, various modified Newton methods were proposed. A new modified Newton method is presented. The method is a line search method, utilizing the Cholesky factorization of a positive-definite portion of the Hessian matrix. The search direction is defined as a linear combination of a descent direction and a direction of negative curvature. Theoretical properties of the method are established and its behavior is studied when applied to a set of test problems. GRA

N90-13175# Massachusetts Inst. of Tech., Cambridge. Artificial Intelligence Lab.
A COMPILATION STRATEGY FOR NUMERICAL PROGRAMS BASED ON PARTIAL EVALUATION
Andrew A. Berlin Jul. 1989 81 p
(Contract N00014-86-K-0180)
(AD-A212759; AI-TR-1144) Avail: NTIS HC A05/MF A01 CSCL 12/5

How partial evaluation can be put to practical use in the domain of high performance numerical computation is demonstrated. A technique was developed for performing partial evaluation by using placeholders to propagate intermediate results, and a prototype compiler based on this technique was implemented. For an important class of numerical programs, this compiler improves performance by an order of magnitude over conventional compilation techniques. It is also shown that by eliminating inherently sequential data structure references, partial evaluation exposes the low level parallelism inherent in a computation. A parallel program generator was implemented, as well as several analysis programs that study the tradeoffs involved in the design of an architecture that can effectively utilize this parallelism. These results are presented using the 9-body gravitational attraction problem as an example. GRA

N90-13176# Naval Research Lab., Washington, DC. Center for Fluid/Structure Interactions.
NUMERICAL EVALUATION OF THE FAR FIELD WAVE PATTERN OF THE RADIATION GREEN'S FUNCTION Memorandum Report, Jan. 1987 - Oct. 1988
Henry T. Wang and E. Wade Miner 5 Sep. 1989 27 p
(AD-A212839; NRL-MR-6478) Avail: NTIS HC A03/MF A01 CSCL 13/10

Computer program RADGREEN has been developed to calculate the far field wave pattern of the radiation Green's function corresponding to an oscillating source translating below the free surface. The program has the capability of calculating the Green's function and its derivatives, or the associated wave elevation and slopes. The far field analysis is based on an asymptotic formulation which neglects terms which are of order 1/R and higher. Techniques for removing and attenuating singularities in the formulation and eliminating short noise-like waves are described in some detail. A number of three dimensional and contour plots are given to show sample radiation wave patterns for a single source and for a line of sources whose strengths are adjusted to approximate those for a ship hull undergoing heave or pitch motions. GRA

N90-13177# Wisconsin Univ., Madison. Center for Mathematical Sciences.
THE PAINLEVE TEST FOR NONLINEAR ORDINARY AND PARTIAL DIFFERENTIAL EQUATIONS Technical Summary Report
Willy Hereman and Sigurd Angenent Jan. 1989 15 p
(Grant AF-AFOSR-0263-85)
(AD-A212894; CMS-TSR-89-23) Avail: NTIS HC A03/MF A01 CSCL 12/5

A MACSYMA program is presented which determines whether a given single nonlinear ODE or PDE with (real) polynomial terms fulfills the necessary conditions for having the Painleve property. Together with some mathematical background, a synopsis is given of the algorithm for the computer program, its scope and limitations. Various examples of typical output of the program are provided. GRA

65 STATISTICS AND PROBABILITY

Includes data sampling and smoothing; Monte Carlo method; and stochastic processes.

N90-13178# Royal Signals and Radar Establishment, Malvern (England).
EXPLICIT MODELLING OF STATE DURATION CORRELATIONS IN HIDDEN MARKOV MODELS
M. J. Russell and L. Sime Sep. 1988 30 p Original contains color illustrations
(RSRE-Memo-4152; BR108108; ETN-89-94329) Copyright Avail: Defence Research Information Centre, Kentigern House, 65 Brown Street, Glasgow, G2 8EX, Scotland

Correlated duration hidden Markov models (CDHMM) as a framework for modeling local state duration correlations in HMMs are presented. Experiments were conducted in which CDHMMs were constructed using examples of sentences spoken at different rates. The resulting models were then used to investigate, in terms of HMM state duration, the strategies which speakers adopt to change their speaking rate, the potential usefulness of measures of local state duration correlation for rate-independent speech recognition, the effect of using the rate meter to control speaking rate, and the invariance of a measure of state duration ratio to changes in speaking rate. Although the CDHMM method provides insights into the effects of speaking rate on HMM state duration structure, the results suggest that the extent to which information about local state duration correlations can be useful in achieving good recognition accuracy across speaking rates depends critically on the nature of the states themselves. The characteristics of the states were determined by the mathematical techniques which were used to construct the models. Consequently, although some states correspond to phonetically identifiable segments of the acoustic pattern, others are used to obtain piecewise stationary approximations to nonstationary regions of the speech pattern. ESA

N90-13179# Center for Mathematics and Computer Science, Amsterdam (Netherlands). Dept. of Mathematical Statistics.
BERRY-ESSEEN RATES AND BOOTSTRAP RESULTS FOR GENERALIZED L-STATISTICS
R. Helmers, P. Janssen, and R. Serfling (Johns Hopkins Univ., Baltimore, MD.) Jun. 1988 12 p

(Contracts N00014-79-C-0801; NATO-0034/87)
(CWI-MS-R8808; ETN-89-95631) Copyright Avail: NTIS HC A03/MF A01

The rate of convergence of the distribution of a generalized L-statistic to its normal limit is established. Based on this result the corresponding bootstrap approximation is shown to be asymptotically valid, thus providing an alternative to the use of the normal approximation. By the same method of proof the asymptotic accuracy of the bootstrap approximation of generalized L-statistics is obtained. ESA

N90-13180# Center for Mathematics and Computer Science, Amsterdam (Netherlands). Dept. of Mathematical Statistics.
A STATISTICAL ANALYSIS OF SPATIAL POINT PATTERNS, A CASE STUDY
M. J. Rottschaefer and L. G. Barendregt Sep. 1988 26 p
(CWI-MS-R8813; ETN-89-95635) Copyright Avail: NTIS HC A03/MF A01

Within the context of a statistical image analysis project, some spatial point patterns that originated from biological observations are studied. These observations were the positions of so called EGF (epidermal growth factor) receptors on the surface of human carcinoma cells. A stochastic model for these point patterns is proposed. Since the EGF receptors appear in clusters on the cell surface, the Poisson-cluster process is employed as the model. The three parameters in this process are estimated by means of a method described by Diggle. Work in assessing the statistical reliability of estimates is described. ESA

N90-13181# Center for Mathematics and Computer Science, Amsterdam (Netherlands). Dept. of Mathematical Statistics.
RANDOM TRUNCATION MODELS AND MARKOV PROCESSES
N. Keiding (Copenhagen Univ., Denmark) and R. D. Gill Nov. 1988 63 p Revised
(CWI-MS-R8817; CWI-MS-R8702; ETN-89-95637) Copyright Avail: NTIS HC A04/MF A01

Random left truncation is modeled by the conditional distribution of the random variable X of interest, given that it is larger than the truncating random variable Y, assuming X and Y are independent, based on a simple reparametrization of the left truncation model as a three-state Markov process. The derivation of a nonparametric estimator of a distribution function under random truncation is achieved as a special case of results on the statistical theory of counting processes by Aalen and Johansen. The status of the estimator as a nonparametric maximum likelihood estimator is clarified, and consistency, asymptotic normality and efficiency may be derived directly as special cases of Aalen and Johansen's general theorems and later work. The method improves the interpretability of the results, considerably shortens proofs and derivations, and allows several generalizations. ESA

N90-13182# Center for Mathematics and Computer Science, Amsterdam (Netherlands). Dept. of Software Technology.
DIFFERENT NOTIONS OF UNCERTAINTY IN QUASI-PROBABILISTIC MODELS
L. C. vanderGaag Dec. 1988 14 p
(CWI-CS-R8847; ETN-89-95648) Copyright Avail: NTIS HC A03/MF A01

Investigations into early quasi-probabilistic models which are employed frequently in present day rule-based expert systems, but which were not justified mathematically, are presented. Two of these models, the certainty factor model and the subjective Bayesian method are shown to model different notions of uncertainty. The difference in the interpretation and application of production rules in the respective models is discussed. ESA

N90-13183# Universiteit Twente, Enschede (Netherlands). Faculty of Applied Mathematics.
ON NEW METHODS FOR COMPUTING WITH MULTIVARIATE B-SPLINES
M. Neamtu Apr. 1989 24 p
(Memo-783; ISSN-0169-2690; ETN-89-95674) Avail: NTIS HC A03/MF A01

New methods for computing with multivariate B-splines are studied as a follow up to the derivation of a recurrence relation for multivariate (simplex) B-splines. Extensions of these ideas yield new recurrence relations for directional derivatives and inner products of B-splines. Algorithms for these new methods are outlined. The approach presented is discussed and compared with the readily established one. ESA

N90-13184# Center for Mathematics and Computer Science, Amsterdam (Netherlands). Dept. of Pure Mathematics.
NONGAUSSIAN LINEAR FILTERING, IDENTIFICATION OF LINEAR SYSTEMS, AND THE SYMPLECTIC GROUP
Michiel Hazewinkel Oct. 1988 16 p Submitted for publication
(CWI-PM-R8810; ETN-89-95753) Copyright Avail: NTIS HC A03/MF A01

A study is carried out concerning stochastic linear dynamical systems. Two problems are considered, the calculation of the conditioned probability density of x at time t given specific observations in the case of x(O) not necessarily Gaussian, and identification, that is the joint conditional probability density of (x, A, B, C) at time t (where A, B, C are matrices), given the same observations. The methods used rely on Wei-Norman theory, the Duncan-Mortensen-Zakai equation, and a real form of the Segal-Shale-Weil representation of a symplectic group. ESA

N90-13185# Michigan Univ., Ann Arbor.
STOCHASTIC PROCESS MODELS IN DEVICE PHYSICS Final Report, Jun. 1986 - Aug. 1989
Fred M. Hoppe 20 Aug. 1989 7 p
(Grant AF-AFOSR-0047-86; AF Proj. 2304)
(AD-A212284; AFOSR-89-1252TR) Avail: NTIS HC A02/MF A01 CSCL 12/3

A statistical study of Monte Carlo methods in device physics was undertaken using tools from the modern theory of probability and stochastic processes. The Monte Carlo approach was used to obtain numerical estimates of parameters by simulating the physical process on a computer rather than attempting to solve the integrodifferential equations which arise. Thus this method estimates averages and can be applied to any quantity expressible as such but may require an enormous number of simulations before statistically reliable results are obtained, especially if the quantity of interest is subject of very low probability of occurrence. A probabilistic study was undertaken of the behavior of individual electrons, complementing the Monte Carlo approach. The methodology required the formulation of some novel stochastic processes and suggested new types of conditions for ergodicity of Markov processes. GRA

N90-13186# Stanford Univ., CA. Dept. of Operations Research.
SMOOTHED LIMIT THEOREMS FOR EQUILIBRIUM PROCESSES
Peter W. Glynn and Donald L. Iglehart Jun. 1989 17 p
(Contract DAAL03-88-K-0063)
(AD-A212321; ARO-25839.11-MA) Avail: NTIS HC A03/MF A01 CSCL 12/2

Renewal ideas play a fundamental rule in applied probability. In particular, renewal methods are powerful tools for dealing with the asymptotic behavior of the regenerative processes that are typical of queueing and operations research applications. The main results of the theory were surveyed and some smoothed versions of the convergence theorems were developed. These smoothed versions typically have much weaker associated regularity hypotheses than the classical version. These smoothed limit theorems are established under minimal conditions that are essentially necessary. GRA

N90-13187# Stanford Univ., CA. Dept. of Statistics.
ILLUSTRATION OF BAYESIAN INFERENCE IN NORMAL DATA MODELS USING GIBBS SAMPLING
Alan E. Gelfand, Susan E. Hills, Amy Racine-Poon, and Adrian F. Smith 6 Sep. 1989 38 p

(Contract N00014-89-J-1627)
(AD-A212630; TR-421) Avail: NTIS HC A03/MF A01 CSCL 06/10

Use of the Gibbs sampler as a method for calculating Bayesian marginal posterior and predictive densities is reviewed and illustrated with a range of normal data models, including: variance components; unordered and ordered means; hierarchial growth curves; and missing data in a cross-over trial. In all cases the approach is straightforward to specify distributionally, trivial to implement computationally, with output readily adapted for required inference summaries. GRA

N90-13188# Defence Research Establishment Suffield, Ralston (Alberta).
THE SHAPE OF THE PROBABILITY DENSITY FUNCTION OF SHORT-TERM CONCENTRATION FLUCTUATIONS OF PLUMES IN THE ATMOSPHERIC BOUNDARY LAYER
E. Yee Jul. 1989 45 p
(AD-A212632; DRES-SR-525; PCN-051SP) Avail: NTIS HC A03/MF A01 CSCL 12/3

The shape of the probability distribution of a set of high-resolution concentration fluctuation measurements from ion plume is studied using order statistics and certain selected quantities derived from them. A number of graphical techniques are applied, from underlying distribution of concentration. These graphical techniques are applied, from both a descriptive and a computational point of view, to elucidate the underlying distributional shape of concentration and to assess the characterization efficacy of the probability distributions that have been proposed as models for concentration fluctuations. None of the commonly used models for the concentration probability distribution is able to accurately characterize the extreme upper end of the concentration frequency distribution (i.e., the end of the distribution that is critical for the prediction of the probability of exposure to peak levels). The clipped-normal distribution is shown to provide a reasonably conservative model for the prediction of the exceedances of critical concentration levels. The g and h distribution yields a bimodal form for the total probability density function for concentration whereas the clipped-normal distribution provides a unimodal form. It is shown that the bimodal form of the total concentration probability density function is consistent with both the data and certain theoretical results. GRA

N90-13189# Stanford Univ., CA. Systems Optimization Lab.
MONTE CARLO (IMPORTANCE) SAMPLING WITHIN A BENDERS' DECOMPOSITION ALGORITHM FOR STOCHASTIC LINEAR PROGRAMS
Gerd Infanger Sep. 1989 34 p
(Contracts N00014-89-J-1659; DE-FG03-87ER-25028; NSF DDM-88-14253; NSF DMS-89-13089)
(AD-A212854; SU-SOL-89-13) Avail: NTIS HC A03/MF A01 CSCL 12/4

A method employing decomposition techniques and Monte Carlo sampling (importance sampling) to solve stochastic linear programs is described and applied to capacity expansion planning problems of electric utilities. Uncertain availability of generators is considered along with transmission lines and uncertain demand. Numerical results are presented. GRA

66 SYSTEMS ANALYSIS

Includes mathematical modeling; network analysis; and operations research.

No abstracts in this category.

67 THEORETICAL MATHEMATICS

Includes topology and number theory.

N90-13190# Technische Univ., Delft (Netherlands). Faculty of Technical Mathematics and Informatics.
JULIA-FATOU-SULLIVAN THEORY FOR REAL ONE-DIMENSIONAL DYNAMICS
Marco Martens, Welington deMelo (IMPA, Rio de Janeiro, Brazil), and Sebastian vanStrien 1989 47 p Sponsored in part by the Netherlands Scientific Organization
(Rept-88-100; ISSN-0922-5641; ETN-89-95436) Copyright Avail: NTIS HC A03/MF A01

The Julia-Fatou-Sullivan structure theory for the dynamics of rational maps is investigated, with the aim of validating the theory further. Smooth maps of the circle or of the interval, whose critical points are non-flat, are shown not to be able to have wandering intervals, and the period of attracting periodic orbits is shown to be uniformly bounded. ESA

N90-13191# Center for Mathematics and Computer Science, Amsterdam (Netherlands). Dept. of Algorithmics and Architecture.
KOLMOGOROV COMPLEXITY AND ITS APPLICATIONS
Ming Li and Paul M. B. Vitanyi (Amsterdam Univ., Netherlands) Feb. 1989 112 p Revised
(Contracts N00014-85-K-0445; DAAL03-86-K-0171; NSF DCR-86-06366; NSERC-OGP-0036747)
(CWI-CS-R8901; ETN-89-95649) Copyright Avail: NTIS HC A06/MF A01

An introduction to the mathematical theory of Kolmogorov complexity is presented which includes notions of randomness. Many applications are discussed including: (1) lower bound arguments that use the fact that certain strings cannot be compressed at all with applications ranging from Turing machines and formal languages to electronic chips; (2) some strings can be compressed more than by any computable function, applied in a version of Goedel's incompleteness theorem; (3) applications in probability theory of the individual compressibility (or simplicity) of strings, for instance, Bayesian inference and a universal a priori probability, with applications ranging from foundational issues to the theory of learning and inductive inference in artificial intelligence; and (4) resource-bounded Kolmogorov complexity, with applications ranging from NP-completeness and the P versus NP question to cryptography. ESA

70 PHYSICS (GENERAL)

For precision time and time interval (PTTI) see *35 Instrumentation and Photography;* for geophysics, astrophysics or solar physics see *46 Geophysics, 90 Astrophysics,* or *92 Solar Physics.*

N90-13192# Helsinki Univ. of Technology, Espoo (Finland). Lab. of Physics.
SEMINARS OF APPLIED PHYSICS, MATERIALS PHYSICS AND BIOMEDICAL ENGINEERING, 1989
T. Katila, ed. and M. Hautala, ed. May 1989 122 p Seminars held in Espoo, Finland, 1989
(PB89-218572; Rept-187) Avail: NTIS HC A06/MF A01 CSCL 20C

The seminars of Applied Physics, Materials Physics and Biomedical Engineering were arranged in 1989 as one common seminar. This report consists of the talks prepared by students as partial fulfillment of their M.Sc. degrees. Topics include: (1) High temperature superconductors; (2) Solid state surface analysis methods; (3) Dispersion in Poiseuille flow; (4) Identification of the ion channel types (Medical applications); (5) Hyperthermia; (6) Resolving of tone frequencies in the vertebrate ear; and (7) Noninvasive electromagnetic location (Medical applications). GRA

N90-13193# KJS Associates, Dayton, OH.
A SURVEY OF THE CURRENT STATE-OF-THE-ART IN HIGH-ENERGY-PRODUCT PERMANENT MAGNETS Final Report, Jul. 1988 - Apr. 1989
Reinhold M. Strnat and Karl J. Strnat Jun. 1989 74 p
(Contract F33615-88-C-2868)
(AD-A211761; WRDC-TR-89-2096) Avail: NTIS HC A04/MF A01 CSCL 20/3

The current state-of-the-art of high energy permanent magnets (HEPM, with (BH max) is greater than or = 10MGOe) was surveyed to inform design engineers about presently available magnetic material types. Users of HEPM's were asked to provide information about their current and future requirements on the properties of permanent magnets for their devices. The responses were divided into six application categories, and are presented in the form of specifications. An up-to-date list of HEPM manufacturers, their addresses, and a summary of the materials they make is included, and cross-referenced. A functioning prototype fixture was built to perform demagnetization curve testing at temperature between -197 and +300 C. Design considerations are discussed. Example demagnetization curve sets as functions of temperature were measured and are presented. GRA

N90-13194# Groningen Rijksuniv. (Netherlands). Kernfysisch Versneller Inst.
DIMENSIONAL REDUCTION AT HIGH TEMPERATURE REVISITED
E. L. M. Koopman and N. P. Landsman (Amsterdam Univ., Netherlands) Jan. 1989 6 p Submitted for publication
(KVI-791; ETN-89-95748) Avail: NTIS HC A02/MF A01

A perturbative analysis of dimensional reduction in the infinite temperature limit of thermal field theory, in the imaginary time formalism, is given. In analogy with the decoupling theorem, a class of renormalization schemes in which the heavy (nonstatic) modes decouple is obtained. The appropriate context to study dimensional reduction at high T is shown to be the finite temperature renormalization group. It is also shown that dimensional reduction to all orders occurs only in exceptional cases. The results lead to the conclusion that a four dimensional theory cannot apply the extrapolation of the results from the three dimensional theory. ESA

N90-13195# Massachusetts Inst. of Tech., Cambridge. Artificial Intelligence Lab.
DIRECT COMPUTATION OF 3D SHAPE INVARIANTS AND THE FOCUS OF EXPANSION
Daphna Weinshall (Weizmann Inst. of Science, Rehovoth, Israel) May 1989 28 p
(Contracts DACA76-85-C-0010; N00014-85-K-0124; NSF IRI-87-19394)
(AD-A212386; AI-M-1131; CBIP-Paper-38) Avail: NTIS HC A03/MF A01 CSCL 20/5

Structure from motion often refers to the computation of 3D structure from a matched sequence of images. However, a (relative) depth map of a surface may not be a good representation for storage and recognition; a more concise representation seems necessary. The sign of the Gaussian curvature of a surface is one candidate to be a part of a useful representation of the surface. It is shown that in order to compute the sign of the Gaussian curvature it is not necessary first to go through the computationally expensive and error sensitive process of recovering the exact function of the surface and the motion parameters. GRA

N90-13196# Air Force Academy, CO. Research Lab.
MAGNETICALLY INSULATED ELECTRON FLOWS IN PULSED POWER SYSTEMS Final Report, Jan. 1987 - Jan. 1988
Robert I. Lawconnell Aug. 1989 166 p
(AD-A212746; FJSRL-TR-89-0008) Avail: NTIS HC A08/MF A01 CSCL 20/3

Magnetic insulation is crucial in the operation of large pulsed power systems. Particular attention will be paid to describing magnetic insulation in realistic pulsed power systems. A theoretical model is developed that allows the production of self consistent magnetically insulated laminar flows in perturbed cylindrical systems given only the electron density profile. The theory is checked and justified by detailed comparisons with results from a 2-dimensional electromagnetic code, MASK. The procedure followed in the theoretical development is to use the relativistic Vlasov equation, Ampere's law and Gauss' law, to obtain a relation between the density profile and the velocity profile for insulated flows. Given the density profile and the corresponding derived velocity profile, a self consistent flow solution is obtained by means of Maxwell's equations. It is checked by taking a special case (corresponding to no perturbations) which results in the well known Brillouin flow theory. Emphasis is placed on determining the magnetic insulation threshold of a pulsed power system employing a plasma erosion opening switch. The procedure employed in the computational study is to vary critical aspects of the pulsed power system and then note whether magnetic insulation breaks down. The point at which magnetic insulation breaks down (as a function of geometry, load impedance, and applied voltage) is the magnetic insulation threshold for the system. GRA

N90-13197# Naval Postgraduate School, Monterey, CA.
A NUMERICAL STUDY OF RAIN-INDUCED SURFACE GRAVITY WAVE ATTENUATION M.S. Thesis
David W. Howell Jun. 1989 38 p
(AD-A212762) Avail: NTIS HC A03/MF A01 CSCL 08/3

Strong rain induced mixing in a thin surface layer is numerically shown to greatly increase surface gravity wave attenuation. This case study uses a single wavelength (2.8 m) together with two mixed layer depths (10 and 20 cm). The rain induced mixing is simulated by varying kinematic viscosity within the mixed layer from 0.000001 to 0.01 sq m per sec, molecular to strong turbulent mixing, respectively. The results indicate that surface gravity wave attenuation in the presence of a thin rain induced mixed layer can increase by a factor of up to 6000 times the attenuation rate due to molecular viscosity alone. This indicates that rain need only mix the top 10 to 20 cm surface layer to effectively dampen short surface gravity waves. GRA

71 ACOUSTICS

Includes sound generation, transmission and attenuation. For noise pollution see *45 Environmental Pollution.*

N90-13198*# Douglas Aircraft Co., Inc., Long Beach, CA.
UHB DEMONSTRATOR INTERIOR NOISE CONTROL FLIGHT TESTS AND ANALYSIS Final Report
M. A. Simpson, P. M. Druez, A. J. Kimbrough, M. P. Brock, P. L. Burge, G. P. Mathur, M. R. Cannon, and B. N. Tran Oct. 1989 188 p
(Contract NAS1-18037)
(NASA-CR-181897; NAS 1.26:181897) Avail: NTIS HC A09/MF A01 CSCL 20A

The measurement and analysis of MD-UHB (McDonnell Douglas Ultra High Bypass) Demonstrator noise and vibration flight test data are described as they relate to passenger cabin noise. The analyses were done to investigate the interior noise characteristics of advanced turboprop aircraft with aft-mounted engines, and to study the effectiveness of selected noise control treatments in reducing passenger cabin noise. The UHB Demonstrator is an MD-80 test aircraft with the left JT8D engine replaced with a prototype UHB engine. For these tests, the UHB engine was a General Electric Unducted Fan, with either 8x8 or 10x8 counter-rotating propeller configurations. Interior noise level characteristics were studied for several altitudes and speeds, with emphasis on high altitude (35,000 ft), high speed (0.75 Mach) cruise conditions. The effectiveness of several noise control treatments was evaluated based on cabin noise measurements. The important airborne and structureborne transmission paths were identified for both tonal and broadband sources using the results of a sound intensity survey, exterior and interior noise and vibration data, and partial coherence analysis techniques. Estimates of the

turbulent boundary layer pressure wavenumber-frequency spectrum were made, based on measured fuselage noise levels. Author

N90-13199# Office National d'Etudes et de Recherches Aerospatiales, Paris (France).
BULK ACOUSTIC WAVES RESONATORS MADE OF AMORPHOUS MATERIALS Ph.D. Thesis - Paris VI Univ.
Michel Breuzet [1989] 181 p In FRENCH; ENGLISH summary
(NOTE-TECHNIQUE-1989-4; ISSN-0078-3781) Avail: NTIS HC A09/MF A01 CSCL 20A

Characterization of radiofrequency vibrating plates made of amorphous conductive or insulating materials was studied theoretically and experimentally. Capacitive excitation was used for these nonpiezoelectric resonators, taking advantage of the long experience of ONERA in highly sensitive capacitive sensors. The theoretical analysis is composed of two parts. First, the advantage of using contour modes and more especially the so-called Lame mode, is demonstrated. These modes are more adapted to isotropic materials and to electrostatic excitation than the thickness shear mode, generally used in quartz resonators. Then, an analysis of the resonator attachment is made, in order to minimize resonator mounting coupling and increase the quality factor. To this end, finite element method calculations are used. The experimental work was carried out on aluminum alloy (2017) and vitreous silica (SiO2) vibrating plates. A high quality factor of 4 x 10(exp 6) was obtained at room temperature with a vitreous silica resonator vibrating in Lame mode at a frequency of 200 kHz. A value close to 5 x 10(exp 6) was measured with a Lame resonator made of aluminum alloy (2017) at cryogenic temperature (40 K) and at a frequency of 170 kHz. Author

N90-13200# Texas Univ., Austin. Dept. of Mechanical Engineering.
PROBLEMS IN NONLINEAR ACOUSTICS: SCATTERING OF SOUND BY SOUND, PARAMETRIC RECEIVING ARRAYS, NONLINEAR EFFECTS IN ASYMMETRIC SOUND BEAMS AND PULSED FINITE AMPLITUDE SOUND BEAMS Annual Summary Report No. 1, 1 Jul. 1988 - 31 Jul. 1989
Mark F. Hamilton 1 Aug. 1989 18 p
(Contract N00014-89-J-1003)
(AD-A211756; ASR-1) Avail: NTIS HC A03/MF A01 CSCL 20/1

Four projects are discussed in this annual summary report, all of which involve basic research in nonlinear acoustics: Scattering of Sound by Sound, a theoretical study of two nonconlinear Gaussian beams which interact to produce sum and difference frequency sound; Parametric Receiving Arrays, a theoretical study of parametric reception in a reverberant environment; Nonlinear Effects in Asymmetric Sound Beams, a numerical study of two dimensional finite amplitude sound fields; and Pulsed Finite Amplitude Sound Beams, a numerical time domain solution of the KZK equation. GRA

N90-13201# Centre Scienctifique et Technique du Batiment, Saint-Martin-d'Heres (France).
WIND EFFECT ON SOUND WAVE PROPAGATION AT GROUND VICINITY Final Report [EFFET DU VENT SUR LA PROPAGATION DU SON AU VOISINAGE DU SOL]
M. Rosen Dec. 1988 104 p In FRENCH
(Contract DRET-87-34-141)
(CSTB-2-87-008; GA/88-655-MR/CB; ETN-89-95273) Avail: NTIS HC A06/MF A01

Sound wave propagation in a moving, inhomogeneous media is investigated. The experiments are carried out in a wind tunnel, on a 1/20 scale. The interference observed in the response plot, is displaced towards the low frequencies by the effect of the wind (when both the wind and the sound waves travel in the same direction). In the case where the wind and the sound waves propagate in opposite directions, the signal attenuation at high frequencies, and the effect of turbulence on the penetration of the zone of shadow, are observed. A model is proposed and tested for wind velocities of 5 m/s traveling in the some sound wave direction. ESA

N90-13202# Rolls-Royce Ltd., Derby (England). Powerplant Technology Div.
THE DESIGN AND DEVELOPMENT OF AN ACOUSTIC TEST SECTION FOR THE ARA TRANSONIC WIND TUNNEL
M. E. Wood and D. A. Newman 15 Nov. 1988 63 p
(PNR90574; INR90259; ETN-89-95555) Copyright Avail: NTIS HC A04/MF A01

The structural, aerodynamic and acoustic design of a lined test section necessary to produce a sufficiently reflection-free environment for noise tests in the Aircraft Research Association (ARA) tunnel at Mach numbers up to 0.85 are described. The aerodynamic design was aided by computational fluid dynamics methods and the acoustic design by a ray-theory model. Results of the aerodynamic calibration of the liner and preliminary acoustic and performance tests on two model propellers are presented. Development work carried out to improve the liner acoustically and aerodynamically is described. ESA

N90-13203# Rolls-Royce Ltd., Derby (England).
THE COMMERCIAL AIRCRAFT NOISE PROBLEM
M. J. T. Smith 15 Jan. 1989 11 p Presented at the Interdependenzen von Luftfahrt-Staedtebau-Umwelt, Fed. Republic of Germany, Jan. 1988
(PNR90577; ETN-89-95557) Copyright Avail: NTIS HC A03/MF A01

The history and future developments of commercial aircraft noise are discussed. The use of the turbofan engine to replace the louder turbojet engine is identified as a step forward in reducing noise. The increasing use of two engine planes for medium and even long hauls is seen as a positive trend. An increase in the number of aircraft movements is predicted. An upturn in noise exposure around the end of the century is predicted. The development goals of Rolls Royce in meeting the noise reduction challenges of the next decades are discussed. ESA

N90-13204*# Georgia Inst. of Tech., Atlanta. School of Mechanical Engineering.
AN INVESTIGATION OF THE DIFFRACTION OF AN ACOUSTIC PLANE WAVE BY A CURVED SURFACE OF FINITE IMPEDANCE Ph.D. Thesis Final Technical Report, 1 Feb. 1985 - 1 Sep. 1989
James A. Kearns Dec. 1989 244 p
(Grant NAG1-566)
(NASA-CR-186069; NAS 1.26:186069) Avail: NTIS HC A11/MF A02 CSCL 20A

Phenomena associated with long range propagation of sound over irregular topography motivated this work, which was to analyze the diffraction effects which would occur near the tops of hills and ridges. The diffraction of a high frequency plane wave due to its grazing of a two-dimensional curved surface of finite impedance was also studied. Laboratory scale models were constructed and measurements were made of the field on, above, and behind either of two curved surfaces possessing distinctly different impedances; that is, one was soft while the other was hard. The experimental technique consisted of simultaneously measuring the pressure at a reference point and at a field point due to a transient pulse generated by an electric spark. The pressure waveforms were digitized and processed. The ratio of the discrete Fourier transforms of the two waveforms provided an estimate of the insertion loss between them. The results of the measurements were compared with the predictions of a theory which was derived by Pierce using the method of Matched Asymptotic Expansions (MAE). The predictions relied upon the experimental evaluation of the impedance of each surface at grazing angles of incidence. This evaluation was achieved by a fairly standard technique involving empirical models of various generic types of surfaces. An example was shown of the important role that the structural intricacies of a surface play in the determination of an appropriate model. The comparison between the measurements and predictions indicated that the theory gives an excellent description of the

field anywhere near a curved surface. Further, with a simple modification, the theory was also shown to give nearly as good of a description of the field surrounding a curved surface even at distances far behind the surface yet near the line of sight.
Author

N90-13205# Royal Aerospace Establishment, Farnborough (England).
A FREQUENCY DOMAIN TECHNIQUE FOR IMPROVING SOUND FIELD REPRODUCTION
J. B. Collister 9 Nov. 1988 13 p
(RAE-TM-MM-10; BR108877; ETN-89-94825) Copyright Avail: NTIS HC A03/MF A01

A method for minimizing the third octave errors existing between a target sound field and its reproduction elsewhere, is described. The spectrum is iteratively modified by the error spectrum. This method of operating in the frequency domain is essentially the dual of the method, which uses digital filtering in the time domain.
ESA

N90-13206# Royal Aerospace Establishment, Farnborough (England).
PERCEIVED URGENCY OF WARNING SIGNALS DETERMINED USING A FORCED CHOICE PAIR COMPARISON TECHNIQUE
J. A. Chillery and J. B. Collister 24 Nov. 1988 18 p
(RAE-TM-MM-12; BR108876; ETN-89-94826) Copyright Avail: NTIS HC A03/MF A01

The spectral content of 40 high urgency warning signals is discussed. They are designed to compensate the acoustic characteristics of the aircraft, flight helmet and communication system. An experiment to select the six signals which are perceived as conveying the greatest urgency, is effectuated. The results confirmed that those signals are ranked correctly and that the relationships, amongst the complete set of ten signals are as predicted. The performed experiment showed that the signals are easily learned and that there is no confusion amongst them.
ESA

N90-13207# Royal Aerospace Establishment, Farnborough (England).
ACOUSTIC RECORDING SYSTEMS FOR USE IN MILITARY AIRCRAFT
K. Harpur 24 Nov. 1988 25 p
(RAE-TM-MM-11; BR109026; ETN-89-95002) Copyright Avail: NTIS HC A03/MF A01

The recording systems used for inflight noise measurements inside military aircraft are described. The details of the equipment, its method of operation, possible measurement configurations and capabilities, are included. In particular, the following equipment is presented: the tape recorder, the microphone and microphone box, the telephone box, the alternative systems and the active noise reduction power supply unit.
ESA

N90-13208 Physics and Electronics Lab. TNO, The Hague (Netherlands).
MODIFIED NEWTON-TYPE METHODS FOR LONG-RANGE TARGET MOTION ANALYSIS
R. H. J. GmeligMeyling Apr. 1989 54 p
(Contract A87/KM/172)
(FEL-1989-82; TD89-1654; ETN-89-95085) Copyright Avail: TNO Physics and Electronics Lab., P.O. Box 96864, 2509 JG The Hague, Netherlands

An interactive solution method for the problem of long range Target Motion Analysis (TMA), is reported. It is based on Newton type interactions. The aim is to estimate position, course, speed, and emitted frequencies of a maneuvering target, given a time sequence of measurements. For the long range case, the passive sonar measurements are obtained by a ship equipped with a towed array. The noise, which contaminates data, is assumed to be zero mean Gaussian. Attempts are made to minimize a nonlinear cost function, which is a sum of squared residuals. Long range TMA is a difficult problem, due to the inaccurate measurements and the low data rates.
ESA

N90-13209# Gallaudet Coll., Washington, DC.
THE EFFECTS OF NOISE ON PERFORMANCE Final Report
Alice H. Suter Jun. 1989 56 p
(DA Proj. 1L1-61102-B-74-A)
(AD-A212519; HEL-TM-3-89) Avail: NTIS HC A04/MF A01 CSCL 20/1

The effects of noise on task performance are quite complex, and not as predictable as other noise effects. They are often affected by non-acoustical factors, such as biological and psychological state, as well as external factors such as task complexity and the presence of other stressors. This report describes the rationale and some of the problems inherent in noise and performance research, as well as theories on the mechanisms of effects, and summarizes the various effects. Research on noise and vision suggests some effects from high noise levels on thresholds of sensitivity, critical flicker fusion, and visual field shifts. Small but reliable effects have been demonstrated on vestibular function, expecially with asymmetric exposures. Motor performance usually adapts with repeated or prolonged exposure, but high noise levels can show persistent decrements. Some startle responses, notably the eye-blink response, do not habituate. With respect to task variables, noise has little effect on simple tasks, and can even improve performance on monotonous tasks. Tasks requiring continuous performance may be disrupted, especially by noise levels over 100 dB and if the job requires a high level of sustained performance. Intellectual function is not usually affected, but vigilance tasks are susceptible to noise, particularly under certain conditions. Complex tasks requiring more than one activity are much more likely to be disrupted than simple tasks.
GRA

N90-13210# Gallaudet Coll., Washington, DC.
THE EFFECTS OF NOISE ON SPEECH AND WARNING SIGNALS Final Report
Alice H. Suter Jun. 1989 57 p
(DA Proj. 1L1-61102-B-74-A)
(AD-A212520) Avail: NTIS HC A04/MF A01 CSCL 23/2

To assess the effects of noise on speech communication it is necessary to examine certain characteristics of the speech signal. Speech level can be measured by a variety of methods, none of which has yet been standardized, and it should be kept in mind that vocal effort increases with background noise level and with different types of activity. Noise and filtering commonly degrade the speech signal, especially as it is transmitted through communications systems. Intelligibility is also adversely affected by distance, reverberation, and monaural listening. Communication systems currently in use may cause strain and delays on the part of the listener, but there are many possibilities for improvement. Individuals who need to communicate in noise may be subject to voice disorders. Shouted speech becomes progressively less intelligible at high voice levels, but improvements can be realized when talkers use clear speech. Tolerable listening levels are lower for negative than for positive S/Ns, and comfortable listening levels should be at a S/N of at least 5 dB, and preferably above 10 dB. Popular methods to predict speech intelligibility in noise include the Articulation Index, Speech Interference Level, Speech Transmission Index, and the sound level meter's A-weighting network. This report describes these methods, discussing certain advantages and disadvantages of each, and shows their interrelations.
GRA

N90-13211# Naval Postgraduate School, Monterey, CA.
MEASUREMENTS OF BUBBLE PROPERTIES USING A MULTI-FREQUENCY SOUND FIELD M.S. Thesis
Robert A. Perron Jun. 1989 62 p
(AD-A212591) Avail: NTIS HC A04/MF A01 CSCL 20/1

An apparatus was designed, constructed, and tested to measure properties of single bubbles in a fluid by use of a multi-frequency sound field. The theoretical background on the dual frequency method for obtaining bubble properties such as resonance frequency, rectified diffusion thresholds and rates, rise-time sizing, and damping coefficients are discussed. Specifications and design of the device are presented. Sizes of single air bubbles in water determined from dual frequency methods are compared to rise-time

sizing for radii from 30 to 100 microns. These two methods are shown to agree within 1 percent. Rectified diffusion rates measured above, at, and below threshold for an initial bubble radius of 50 microns in air-saturated water over a period of 700 seconds were measured and the results demonstrated the reliability of the system. The potential of this device to measure damping coefficient is discussed. GRA

N90-13212# Massachusetts Inst. of Tech., Cambridge. Dept. of Mechanical Engineering.
FUNDAMENTAL STUDIES OF TURBULENT WALL PRESSURE FLUCTUATIONS WITH APPLICATIONS TO ADVANCED ACOUSTIC SENSOR SYSTEMS Final Report, 1 Nov. 1982 - 30 Apr. 1986
Patrick Leehey 25 Jul. 1989 6 p
(Contract N00014-83-K-0227)
(AD-A213041; MIT-OSP-93019-2) Avail: NTIS HC A02/MF A01 CSCL 20/1

The work is considered which was done under the Hydroacoustic Special Research Opportunity (SRO) in computation of turbulent boundary layer wall pressure fluctuations, analyses of boundary layer flow noise and receptivity to sound, measurements of wall pressure fluctuations and computations of structural response. GRA

N90-12538*# PRC Kentron, Inc., Hampton, VA.
NEAR-FIELD NOISE PREDICTIONS OF AN AIRCRAFT IN CRUISE
John W. Rawls, Jr. *In* NASA, Langley Research Center, Research in Natural Laminar Flow and Laminar-Flow Control, Part 2 Dec. 1987 p 617-636 (For primary document see N90-12519 04-02)
Avail: NTIS HC A15/MF A02 CSCL 20A

N90-12553*# National Aeronautics and Space Administration. Langley Research Center, Hampton, VA.
EFFECTS OF ACOUSTIC SOURCES
James A. Schoenster and Michael G. Jones (PRC Kentron, Inc., Hampton, VA.) *In its* Research in Natural Laminar Flow and Laminar-Flow Control, Part 3 Dec. 1987 p 914-921 (For primary document see N90-12539 04-02)
Avail: NTIS HC A17/MF A03 CSCL 20A

72 ATOMIC AND MOLECULAR PHYSICS

Includes atomic structure, electron properties, and molecular spectra.

N90-13213# State Univ. of New York at Buffalo, Amherst. Dept. of Chemistry and Physics.
DYNAMICS OF AN M-LEVEL ATOM INTERACTING WITH CAVITY FIELDS: PROPERTIES OF PHOTON STATISTICS
Fu-Li Li, Xiao-Shen Li (Center of Theoretical Physics, Beijing, China), D. L. Lin, and Thomas F. George Aug. 1989 31 p Submitted for publication
(Contracts N00014-86-K-0043; F49620-86-C-0009; NSF CHE-86-20274)
(AD-A211321; TR-108) Avail: NTIS HC A03/MF A01 CSCL 20/5

For a system of an M-level atom interacting with cavity fields, the statistical properties of the field are investigated numerically. The variation of photon antibunching and probability distribution with the atomic level number and initial field intensity are discussed for both resonance and off-resonance cases. GRA

N90-13214# Naval Research Lab., Washington, DC.
MOLECULAR DYNAMICS OF LIPID BILAYERS Final Report, 1 Oct. 1987 - 30 Sep. 1988
Mark Nagumo 9 Aug. 1989 9 p
(AD-A211492) Avail: NTIS HC A02/MF A01 CSCL 06/2

The aim of this work is to study, by molecular dynamics simulations, the properties of lipid bilayers. We have applied the vectorizable, order-N Monotonic Lagrangian Grid near-neighbors algorithm and have developed a novel constraint algorithm to a simple model bilayer system. We have developed fast angle-dependent force/potential algorithms to treat angle bending and torsion. GRA

N90-13215# Groningen Rijksuniv. (Netherlands). Kernfysisch Versneller Inst.
THE INTERACTING BOSON APPROXIMATION
Olaf Scholten 1988 17 p Presented at the Int. School Recent Advances in Experimental Nuclear Physics, Poiana Brason, Romania, 30 Aug. - 10 Sep. 1988
(KVI-774; ETN-89-95746) Avail: NTIS HC A03/MF A01

The equivalence between the bosons and collective fermions pair states is discussed. The microscopic approach to the interacting boson model and the S and D pairs, are considered. The general structure of the Hamiltonian in the interacting boson fermion approach is obtained. It is shown that the Hamiltonian can account for most of the observed features in the spectra of odd-mass nuclei. Parameters extracted from calculations for isotopic chains show that the extracted mass dependence of the parameters is in agreement with the predictions, but in some cases violations are observed. The validity limits of the approach are analyzed. A variety of other mapping procedures are developed but a satisfactory answer is not yet found. ESA

N90-13216# Groningen Rijksuniv. (Netherlands). Kernfysisch Versneller Inst.
EXPLORING ASYMMETRIC HEAVY-ION REACTIONS AT THE KX-RAY METHOD: THE Ne20 + Tb159 REACTION AT 15 MeV/UNIT
B. Kotlinski, P. C. N. Crouzen, R. Kaper, E. E. Koldenhof, H. K. W. Leegte, R. H. Siemssen, H. W. Wilschut, and X. Y. Xie 1989 8 p Presented at the International Seminar on Direct Nuclear Reactions, Bangalore, India, 12-16 Jan. 1989
(KVI-777; ETN-89-95747) Avail: NTIS HC A02/MF A01

The Ne20 + Tb159 reaction is studied at 294 MeV with the KX-ray method. Partial cross sections are obtained for the quasi-elastic as well as the deep inelastic components. By measuring particle-particle KX-ray triple coincidences it is possible to correct the results for charged particle evaporation from the heavy residual nucleus. Primary cross sections are constructed for the quasi-elastic and the strongly damped components. Large cross sections are found for a component in which light paticles only are emitted. The results are possibly the remnants of deep inelastic processes. ESA

N90-13217# Groningen Rijksuniv. (Netherlands). Kernfysisch Versneller Inst.
COMPRESSIBILITY OF HEAVY NUCLEI AT HIGH TEMPERATURES
J. C. Bacelar, A. vanderWoude, J. vanKlinken, A. Buda, Th. Steenbergen, and M. deBoer 1989 8 p Presented at the 27th International Meeting on Nuclear Physics, Bormio, Italy, Jan. 1989
(KVI-792; ETN-89-95749) Avail: NTIS HC A02/MF A01

The monopole vibrations which occur in higly excited nuclear states after compound fusion reactions are investigated. To detect the monopole vibrations a way to measure its characteristic decay width for pair production is proposed. The compressibility of nuclear matter is studied as a function of the temperature. A pair spectrometer, is applied for the detection of both electrons and positrons, resulting from the decay of the monopole vibrations (in the 5 to 20 MeV range). The results are of interest in nuclear physics and in supernovae models. ESA

N90-13218# Groningen Rijksuniv. (Netherlands). Kernfysisch Versneller Inst.
ELEMENTS OF A RELATIVISTIC MICROSCOPIC THEORY OF HADRONIC MATTER IN EQUILIBRIUM AND NON-EQUILIBRIUM
Rudi Malfliet 1989 16 p Presented at the Winter School on Nuclear Matter and Heavy Ion Collisions, Les Houches, France,

7-16 Feb. 1989
(KVI-796; ETN-89-95750) Avail: NTIS HC A03/MF A01

The relativistic many body problem is discussed. The Dirac-Brueckner approximation is emphasized. A unified treatment of equilibrium and nonequilibrium is achieved. It is based on the time dependent Green's function formalism in the Keldysh representation. The results obtained are shown to be in agreement with a number of experimental equilibrium observables: saturation properties for symmetric and asymmetric nuclear matter, optical potential properties and compressibility of nuclear matter. The formalism can be applied to a fundamental understanding of the properties of many hadron systems. However, problems like the role of the form factor, the neglect of negative energy states and the question of convergence of the Brueckner approximation are not yet satisfactorily understood. ESA

N90-13219# Groningen Rijksuniv. (Netherlands). Kernfysisch Versneller Inst.
[ACTIVITIES REPORT OF THE KERNFYSISCH VERSNELLER INSTITUUT] Annual Report, 1988
1988 205 p
(ETN-89-95752) Avail: NTIS HC A10/MF A01

The experimental results and theoretical studies performed in the Kernfysisch Versneller Institute (KVI) are reported. The following topics are presented: giant resonances, direct reaction studies, nuclei and high spin, light and heavy mass systems, models of reaction mechanism, relativistic heavy ions, nuclear matter and structure, Bhabha scattering, surface and atomic Physics, environmental radiation research, nuclear Medicine, the AGOR group, cyclotron and ionic sources, electronics, computer systems, detectors and target laboratory. The publications, the seminars and the Institute's staff personnel are listed. ESA

N90-13220 National Physical Lab., Teddington (England). Div. of Materials Applications.
UNSTEADY DIFFUSION FROM A HEMISPHERICAL PIT
D. H. Ferriss Aug. 1989 11 p
(NPL-DMA(A)-190; ISSN-0143-7313; ETN-89-95934) Copyright Avail: National Physical Lab., Teddington, Middlesex, TW11 OLW, England

The solution to a problem involving unsteady radial diffusion, in a region bounded by hemispheres, is discussed. The analysis can be applied to the case of a hydrogen atom diffusing into steel, from a surface pit. The formulae derived enable the estimation of the hydrogen concentration and its dependence on time. The differences in pit radius with time and the concentration on the pit wall are taken into account. These effects affect the time dependence of the solution. The variation of the concentration on the pit wall renders the unsteady problem two dimensional. ESA

N90-13221# Helsinki Univ. of Technology, Espoo (Finland). Low Temperature Lab.
PERSISTENT CURRENT, NMR, AND ION TRANSMISSION EXPERIMENTS IN ROTATING He-3 SUPERFLUIDS Ph.D. Thesis
Kaj Nummila 1989 79 p Sponsored by Emil Aaltonen Foundation and the Juho Leino Foundation
(ISBN-952-90056-1-X; ETN-89-95181; PB89-223176) Avail: NTIS HC A05/MF A01

The behavior of rotating helium isotopes, He-3 and He-4, superfluids and the vortices therein are studied. Three different techniques are used. Magnetic resonance is used to obtain detailed information about the vortices. The superfluids are characterized by an ac-gyroscopic technique which facilitates non-destructive measurement of persistent currents. The third technique makes use of the strong orbital anisotropy in He-3. These techniques and the main results are described in detail. ESA

N90-13222# Nationaal Inst. voor Kernfysica en Hoge Energiefysica, Amsterdam (Netherlands).
MINIMAL TOTAL CROSS SECTION FOR E(+)E(-) YIELDS W(+)W(-)
K. J. F. Gaemers Sep. 1988 16 p
(NIKHEF-H/88-12; ETN-89-95609) Avail: NTIS HC A03/MF A01

The total cross section with the most general form for the gauge boson vertices is given at tree level for the process e(+)e(-) giving W(+)W(-). Each vertex is parameterized with seven couplings and the minimum of the total cross section is studied over a wide energy range. Although there are large cancellations between the neutrino exchange diagram and the photon and Z annihilation diagrams, it is not possible to get significantly below the standard model cross section for any value of the parameters. ESA

N90-13223# Nationaal Inst. voor Kernfysica en Hoge Energiefysica, Amsterdam (Netherlands).
THE PROCESS E(-)P GIVING GAMMA E(-)P AS A FAST LUMINOSITY FOR THE HERA COLLIDER
K. J. F. Gaemers (Amsterdam Univ., Netherlands) and M. vanderHorst Sep. 1988 27 p
(NIKHEF-H/88-13; ETN-89-95610) Avail: NTIS HC A03/MF A01

The process e(-)p giving gamma e(-)p is considered as a candidate for a fast luminosity monitor for Hera. Results are given and discussed for the differential cross sections and the integrated cross section. It is possible to use the expressions derived in the form of an event generator. The results for a sample of one hundred thousand events are shown. The use of this event generator makes it possible to use the results obtained in a detector simulation. ESA

N90-13224# Nationaal Inst. voor Kernfysica en Hoge Energiefysica, Amsterdam (Netherlands).
OPERATOR PRODUCT COEFFICIENTS IN NON-DIAGONAL CONFORMAL FIELD THEORIES
Juergen Fuchs Nov. 1988 9 p
(NIKHEF-H/88-19; ETN-89-95611) Avail: NTIS HC A02/MF A01

The problems involved in the determination of operator product coefficients in nondiagonal conformal field theories are explained. Dotsenko and Fateev methods are used to derive formulae which allows computation of these coefficients. A careful treatment of the issue of uniqueness of the results is shown to be necessary. The formulae derived can be easily evaluated on a computer. The results apply directly to the case of c less than 1 RCFT's (rational conformal field theories) and to A sub 1 Wess Zumino Witten (WZW) theories where the differential equations for the four point functions are known explicitly. Analogous considerations are valid for any RCFT. ESA

N90-13225# Groningen Rijksuniv. (Netherlands). Kernfysisch Versneller Inst.
AN EXPLICIT PARTITION OF THE FUSION-LIKE CROSS SECTION
J. D. Hinnefeld, H. K. W. Leegte, E. E. Koldenhof, R. H. Siemssen, Z. Sosin, H. W. Wilschut, and Z. Zhang (Academia Sinica, Lanzhou, China) 1989 8 p Submitted for publication Sponsored by Stichting Fundamenteel der Materie and the Netherlands Organization of Scientific Research
(KVI-797; ETN-89-95751) Avail: NTIS HC A02/MF A01

The results obtained by combining the KX-ray method, with a plastic wall, for the detection of fast light particles, are reported. The aim of the experiment is to study the cross sections of the 309 MeV N20 + Tb159 reactions. It is achieved by decomposing them into cross sections for complete fusion and a number of specific incomplete fusion channels. With this partition it is possible to successfully describe the incomplete momentum transfer observed in velocity spectra of evaporation residues from similar system. ESA

N90-13226# State Univ. of New York, Buffalo. Dept. of Chemistry.
GROUND STATES OF A TWO-DIMENSIONAL CHARGED-BOSON SYSTEM
C. I. Um, W. H. Kahng, E. S. Yim, and Thomas F. George Aug.

1989 28 p
(Contract N00014-86-K-0043)
(AD-A212363; UBUFFALO/DC/89/TR-110) Avail: NTIS HC A03/MF A01 CSCL 20/8

The ground state of a two-dimensional charged-boson system is investigated over the range of densities 1 somewhat greater than Rs somewhat greater than 10 in the self-consistent field approximation: R sub s = Sqrt(1/((a sub o) sq rho pi)), where a is the Bohr radius and rho is the number density. Starting with numerical self-consistent calculations of the static structure factor, the elementary excitation, pair-correlation functions, pressure and ground-state energy are evaluated. These results are compared with those of the two-dimensional and three-dimensional systems obtained from other methods. The ground-state energy is given sub as E0 = -1.2918 Rs-2/3 + 0.03, which improves the result from the ring-diagram approximation. GRA

N90-13227# Air Force Astronautics Lab., Edwards AFB, CA.
PROCEEDINGS OF THE 10 MAY 1989 ANTIPROTON TECHNOLOGY WORKSHOP: ADDENDUM
Gerald D. Nordley, ed. Sep. 1989 41 p Workshop held in Upton, NY, 10 May 1989; sponsored by Brookhaven National Lab. and DOE
(AD-A212804; AL-CP-89-001A-Add) Avail: NTIS HC A03/MF A01 CSCL 20/8

Antiprotons are particles of antimatter which release highly penetrating radiation when they are stopped in normal matter. According to presentations at the Antiproton Technology Workshop this radiation can be used, in very small quantities, to image objects and determine their composition and density. In larger amounts, the radiation could be used to kill cancer tumors or produce highly localized heating and shock waves. Titles of presentations include: Stopping Power of MeV Proton and Antiproton Beams; Recent Simulation Results of ASTER; Pbar Testing of Hydrogen Effects in Sealed Carbon-Carbon Composites; Potential for Antiprotons in Radiation Oncology; Prospects for a Commercial Antiproton Source; Prospects for Exciting Extreme States in Nuclear Matter with Intense Antiproton Beams; Status of AL Studies Relating to condensed Antimatter; Electromagnetic Traps for Atomic Antihydrogen; Antihydrogen Production; Antiproton Catalyzed Fusion; Antiproton Induced Fusion Reaction; Modeling Antiproton-Plasma Interactions; Introduction to CP Violation Studies with Pbars; and Antiproton Production Calculation by the Multistring Model VENUS. GRA

N90-12789*# Jet Propulsion Lab., California Inst. of Tech., Pasadena.
AN APPARATUS FOR THE ELECTRODYNAMIC CONTAINMENT OF CHARGED MACROPARTICLES
A. Williams, R. Melbourne, L. Maleki, G. Janik, and J. Prestage *In its* The Telecommunications and Data Acquisition Report 15 Aug. 1989 p 57-62 (For primary document see N90-12786 04-32)
Avail: NTIS HC A11/MF A02 CSCL 20H

73 NUCLEAR AND HIGH-ENERGY PHYSICS

Includes elementary and nuclear particles; and reactor theory.
For space radiation see *93 Space Radiation.*

N90-13228*# Mesoscale Environmental Simulations and Operations, Inc., Hampton, VA.
MESOSCALE ACID DEPOSITION MODELING STUDIES Final Report, Jul. 1986 - Jul. 1989
Michael L. Kaplan, F. H. Proctor, John W. Zack, V. Mohan Karyampudi, P. E. Price, M. D. Bousquet, and G. D. Coats Washington Dec. 1989 114 p
(Contract NAS1-18336)
(NASA-CR-4262; NAS 1.26:4262) Avail: NTIS HC A06/MF A01 CSCL 04B

The work performed in support of the EPA/DOE MADS (Mesoscale Acid Deposition) Project included the development of meteorological data bases for the initialization of chemistry models, the testing and implementation of new planetary boundary layer parameterization schemes in the MASS model, the simulation of transport and precipitation for MADS case studies employing the MASS model, and the use of the TASS model in the simulation of cloud statistics and the complex transport of conservative tracers within simulated cumuloform clouds. The work performed in support of the NASA/FAA Wind Shear Program included the use of the TASS model in the simulation of the dynamical processes within convective cloud systems, the analyses of the sensitivity of microburst intensity and general characteristics as a function of the atmospheric environment within which they are formed, comparisons of TASS model microburst simulation results to observed data sets, and the generation of simulated wind shear data bases for use by the aviation meteorological community in the evaluation of flight hazards caused by microbursts. Author

74 OPTICS

Includes light phenomena; and optical devices.
For lasers see *36 Lasers and Masers.*

N90-13229# Helsinki Univ. of Technology, Espoo (Finland). Electromagnetics Lab.
VARIATIONAL AND ASYMPTOTIC METHODS IN OPEN AND CLOSED WAVEGUIDE ANALYSIS Ph.D. Thesis
Markku Ilmari Oksanen Nov. 1988 21 p Sponsored by the Academy of Finland; the Emil Aaltonen Foundation; the Jenny and Antti Wihuri Foundation; and the Walter Ahlstroem Foundation
(Rept-34; ISBN-951-754-671-8; ISSN-0784-848X; ETN-89-95178) Avail: NTIS HC A03/MF A01

Two different approximative variational and asymptotic methods, are employed for determining propagation constants, attenuation and field distributions in open anisotropic optical fibers and in closed waveguides or resonators surrounded by metal walls. These methods are used in three ways. When exact solutions do not exist, or by using an approximative method, a simpler analysis can be performed. New theories or methods are developed and tested for known waveguides. ESA

N90-13230 Institute for Perception RVO-TNO, Soesterberg (Netherlands). Vision Group.
A VALIDATION OF THE PROPOSED NATO STANDARD METHOD TO DETERMINE TARGET ACQUISITION DISTANCES WITH IMAGE INTENSIFIERS
J. J. Vos and J. Boogaard Apr. 1988 33 p
(Contract R87/KL/094)
(IZF-1988-8; TD88-2608; ETN-89-94459) Copyright Avail: TNO Inst. for Perception, P.O. Box 23, 3769 ZG Soesterberg, Netherlands

Two methods to determine the nominal recognition distance are compared. Experiments with an 8 per 50 image intensifier and an 8 per 40 optical telescope are performed. The first method is the vehicle scene method, and the second is the three bar pattern method, considered by NATO, and the two methods give different results. Questions about the applicability of the so called Johnson criterion and the reliability of the related predicted recognition distances in operations research studies are raised. ESA

N90-13231# Royal Signals and Radar Establishment, Malvern (England).
A REVIEW OF FOCAL REDUCER INTERFEROMETER SYSTEMS
C. J. Baddiley Jun. 1986 22 p
(RSRE-Memo-3486; BR108558; ETN-89-94835) Copyright Avail: NTIS HC A03/MF A01

The development of focal reducer imaging systems for use with interferometers and telescopes is reviewed, and designs are

discussed. The importance of this type of optical system is outlined. The development of image intensifiers and electronic detector arrays are considered. The designs are shown to be of interest wherever image reduction is required. ESA

N90-13232# Office National d'Etudes et de Recherches Aerospatiales, Paris (France). Direction des Etudes de Synthese.
ENHANCEMENT OF INFRARED THERMOGRAPHIC IMAGERY: LOCAL SMOOTHING AND TIME-BASED INTERPOLATION [TRAITEMENT D'IMAGES DE THERMOGRAPHIE INFRA-ROUGE: LISSAGE LOCAL ET INTERPOLATION TEMPORELLE]
C. Enault and F. Bretaudeau 1 Jun. 1989 40 p In FRENCH
(ONERA-RT-8/7254-SN; ETN-89-95018) Avail: NTIS HC A03/MF A01

An interpolation and smoothing technique for treatment of thermographic images is described. The images are first converted to isochronous images, then segmented for simpler transfer of the image. An example of such an image segmentation process is provided. ESA

N90-13233 Physics and Electronics Lab. TNO, The Hague (Netherlands).
SMOOTH TRACK GENERATION FOR TARGET MOTION ANALYSIS
R. H. J. GmeligMeyling Mar. 1989 37 p
(Contract A87/KM/172)
(FEL-1989-83; TD89-1655; ETN-89-95086) Copyright Avail: TNO Physics and Electronics Lab., P.O. Box 96864, 2509 JG The Hague, Netherlands

The generation of artificial sonar data for computer simulation of target motion analysis is investigated. The aim of the work is to estimate the position, speed, course and source of frequencies of a maneuvering target from a given time sequence consisting of bearing and frequency measurements. A realistic mathematical model for the trajectories of a moving target is developed. Piecewise polynomial functions (or splines) are employed to represent smooth trajectories of arbitrary shape. ESA

N90-13234 Physics and Electronics Lab. TNO, The Hague (Netherlands).
THE PHYSICAL OPTICS APPROXIMATION IN THE NEAR-FIELD REGION
M. H. Vogel Apr. 1989 41 p
(FEL-1989-100; TD89-1653; ETN-89-95087) Copyright Avail: TNO Physics and Electronics Lab., P.O. Box 96864, 2509 JG The Hague, Netherlands

The calculation of monostatic electromagnetic reflections from some smooth, perfectly conducting objects, is carried out with the Physical Optics (PO) method. The field is calculated in the near field of the object. The surface of the object is approximated by flat surface patches. For each individual patch the far field approximation is applied. The integration over each surface patch is effectuated. The reflection from the entire object is calculated by vectorial summation of all individual patch contributions. The PO predictions of the reflections and experimental data, are compared. ESA

N90-13235# Purdue Univ., West Lafayette, IN. School of Electrical Engineering.
RESEARCH IN COMPUTER VISION FOR AUTONOMOUS SYSTEMS Progress Report, Jun. - Sep. 1988
Avi Kak, Mark Yoder, Keith Andress, Steve Blask, and Tom Underwood 15 Sep. 1988 532 p
(Contract DAAL01-85-C-0456)
(AD-A212420) Avail: NTIS HC A23/MF A03 CSCL 12/9

This report addresses FLIR processing, LADAR processing and electronic terrain board modeling. In our discussion on FLIR processing, issues were analyzed for classifiability of FLIR features, computationally efficient algorithms for target segmentation, metrics, etc. The discussion on LADAR includes a comparison of a number of different approaches to the segmentation of target surfaces from range images, extraction of silhouettes at different ranges, and reasoning strategies for the recognition of targets and estimation of their aspects. Regarding electronic terrain board modeling, it was shown how the readily available wire-frame data for strategic targets can be converted into volumetric models utilizing the concepts of constructive solid geometry; then is was shown how from the resulting volumetric models it is possible to generate synthetic range images that are very similar to real LADAR images. Also shown is how sensor noise can be added to these synthetic images to make them even more realistic. GRA

N90-13236# Consejo Superior de Investigaciones Cientificas, Madrid (Spain). Inst. of Optics.
WORKSHOP ON RECENT PROGRESS IN SURFACE AND VOLUME SCATTERING
16 Sep. 1988 36 p Workshop held in Madrid, Spain, 14-16 Sep. 1988
(Contract DAJA45-88-M-0137)
(AD-A212455) Avail: NTIS HC A03/MF A01 CSCL 20/14

Topics covered at the workshop include: Surface scattering; Limitations of physical optics; Surface plasmon effects; Enhanced backscattering; Numerical solutions; Polarization effects; Inverse problems; Periodic structures; Volume scattering; Enhancement and photon localization; Polarization and anysotropy effects; Dynamic scattering by dense media; and Double pass effects through phase screens. GRA

N90-13237# California Univ., Santa Barbara. Dept. of Electrical and Computer Engineering.
HIGH SPEED QUANTUM-WELL OPTOELECTRONIC DEVICES BY MBE Final Report, 23 Oct. 1986 - 31 Jul. 1989
Larry A. Coldren May 1989 52 p
(Contract DAAL03-87-K-0012)
(AD-A212585; CU-ECE-TR-89-07; ARO-24480.25-EL) Avail: NTIS HC A04/MF A01 CSCL 20/10

The work has involved the use of Molecular Beam Epitaxy to grow precisely controlled thin layers of III-V compound semiconductors for applications in high-speed optoelectronics devices. The program was intended to serve as a hardware complement to optical computing and high-speed signal processing systems work funded elsewhere under SDIO. The focus of the work has been on the growth, processing and characterization of novel quantum-confined structures. In the past, such quantum-well or quantum-wire structures had been shown to hold great promise for advanced device applications, but until recently very little of this promise had been fulfilled. Partly as a result of this program, some of the desirable characteristics of such structures have been realized for the first time. For example, the first clear measurements of lateral quantum-confinement in quantum-wire arrays were obtained on layers grown by sub-atomic layer epitaxy on off-axis substrates. The body of work had been concerned with creating and evaluating novel wave guided as well as surface-emitting (transverse) device structures. In both areas, significant advances have resulted as well. Surface-emitting lasers with segmented periodic-gain have led to record low threshold pumping levels. GRA

N90-13238# Aerospace Corp., El Segundo, CA. Lab. Operations.
DESIGN AND TESTS OF SIMPLE, INEXPENSIVE OPTICAL BEACON FOR USE ON SMALL SATELLITES
Thomas L. Hayhurst, Marcus N. Osibov, Ray W. Russell, Robert J. Maulfair, and Rick Fleeter 28 Aug. 1989 35 p
(Contract F04701-88-C-0089)
(AD-A213325; TR-0089(4051-01)-1; SD-TR-89-67) Avail: NTIS HC A03/MF A01 CSCL 14/4

A standard photography flash unit modified for automatic repetitive flashing and presetable pulse duration was tested for its utility as an aid for optically acquiring a target in low earth orbit. The relative visibility of the flash with respect to repetition rate and pulse duration was measured with two types of low-light-level TV camera systems over a range of effective distances. Optimal operating parameters for the flash were determined for its application as an optical beacon on the small satellites used in

the Chemical Release Observation (CRO) experiments, part of the Infrared Backgrounds and Signatures Survey (IBSS) Space Shuttle mission. GRA

N90-12524*# National Aeronautics and Space Administration. Langley Research Center, Hampton, VA.
REMOTE DETECTION OF BOUNDARY-LAYER TRANSITION BY AN OPTICAL SYSTEM
Robert M. Hall, Medhat Azzazy, and Dariush Modarress (Spectron Development Labs., Inc., Costa Mesa, CA.) *In its* Research in Natural Laminar Flow and Laminar-Flow Control, Part 2 Dec. 1987 p 381-388 (For primary document see N90-12519 04-02)
Avail: NTIS HC A15/MF A02 CSCL 20F

N90-12800*# Jet Propulsion Lab., California Inst. of Tech., Pasadena.
DSN 70-METER ANTENNA MICROWAVE OPTICS DESIGN AND PERFORMANCE IMPROVEMENTS. PART 2: COMPARISON WITH MEASUREMENTS
D. A. Bathker and S. D. Slobin *In its* The Telecommunications and Data Acquisition Report 15 Aug. 1989 p 174-189 (For primary document see N90-12786 04-32)
Avail: NTIS HC A11/MF A02 CSCL 20F

75 PLASMA PHYSICS

Includes magnetohydrodynamics and plasma fusion.
For ionospheric plasmas see *46 Geophysics*. For space plasmas see *90 Astrophysics*.

N90-13239# Oak Ridge National Lab., TN.
THREE-DIMENSIONAL EQUILIBRIA AND MERCIER STABILITY CALCULATIONS
V. E. Lynch, N. Dominguez, B. A. Carreras, A. Varias, C. Alejaldre, and A. L. Fraguas (Centro de Investigaciones Energeticas, Madrid, Spain) 1989 4 p Presented at the 13th Conference on the Numerical Simulation of Plasmas, Santa Fe, NM, 17-20 Sep. 1989
(Contract DE-AC05-84OR-21400)
(DE89-015907; CONF-890931-2) Avail: NTIS HC A01/MF A01

It is well known that an equilibrium to be used for stability calculations must be extremely accurate. These high accuracy requirements, in a fixed boundary calculation, are translated into high accuracy in the representation of the boundary. These requirements are even stricter for stellarator configurations, for which all the information about the magnetic configuration is given externally through the boundary. Many Fourier components are required to accurately represent the boundary input from a realistic coil system. For torsatron-type configurations, as many as 50 components can be needed to describe the last closed magnetic surface for the vacuum field. For a heliac configuration, the number of components can go up to 200. For 3-D calculations, there is another question of accuracy that does not apply to stability calculations for axisymmetric systems. This is the role of resonant components in the calculation of the geodesic curvature or the Pfirsch-Schlueter current. As Boozer argues, local flattening of the pressure profile eliminates the singularities generated by the resonant components. However, to implement it in a numerical calculation and to eliminate the resonant components, it is necessary to work in a coordinate system with straight magnetic field lines. This creates another problem, since the equilibrium representation in a straight magnetic field lines coordinate system requires many more components than the optimal equilibrium representation developed by Hirshman and co-workers over the last decade and implemented in the VMEC equilibrium code. The VMEC equilibrium code is used and the results to the straight magnetic field line coordinate system are transformed to calculate the input for the stability analysis. The accuracy of the transformation and the convergence of the equilibrium in the new coordinate system are the major points discussed. DOE

N90-13240# Ceskoslovenska Akademie Ved, Prague. Inst. of Plasma Physics.
EFFECT OF THE LENGTH OF THE MULTIJUNCTION GRILL ON ITS LOWER HYBRID CURRENT DRIVE EFFICIENCY
J. Preinhaelter Jun. 1988 15 p
(IPPCZ-283) Avail: NTIS HC A03/MF A01

The distance between the junction of the subsidiary waveguides in the main waveguide and the grill mouth has great influence upon: (1) the spectrum of radiated waves; (2) the total reflection coefficient; (3) the distribution of the power among the separate waveguides; and (4) the actual phases of incident waves. This effect is nearly as important as that of the phase shift between the adjacent waveguides and it is necessary to carry out the optimization over this parameter at grill design. Author

N90-13241# Ceskoslovenska Akademie Ved, Prague. Inst. of Plasma Physics.
ON OPTIMIZATION OF THE MULTIJUNCTION GRILL FOR THE LOWER HYBRID CURRENT DRIVE
J. Preinhaelter Apr. 1988 37 p
(IPPCZ-280) Avail: NTIS HC A03/MF A01

The design of a multijunction grill for use in current drive experiments calls for the optimization of three important parameters: (1) the phase shift Delta Phi among the adjacent waveguides; (2) the length of the multi-junction grill L sub g (from the junction to the mouth); and (3) the surface density N sub o. This optimization was demonstrated through the numerical investigation of a four-waveguide grill designed for a small tokamak. It was shown that current drive efficiency (or the directivity) can reach 50 percent for practically arbitrary Delta Phi (not equal to 0 deg, 180 deg), if we choose angle g properly. The enhanced current drive efficiency at Delta Phi not equal to 90 deg follows from an unevenly distributed power among the separate waveguides and from the self-adjustment of the phases of the incident waves. The risk of the power overloading of the waveguides grows with the decreasing N sub o. A short description of the author's variant of the theory of the wave diffraction on the junction is also given. Author

N90-13242# TRW Space Technology Labs., Redondo Beach, CA.
PLASMA SEPARATION PROCESS: MAGNET MOVE TO OAK RIDGE NATIONAL LABORATORY
Jul. 1989 70 p
(Contract DE-AC03-77ET-33006)
(DE89-017457; DOE/ET-33006/042; PSP-1969) Avail: NTIS HC A04

This is the final report on the series of operations which culminated with the delivery of the Plasma Separation Process prototype magnet system (PMS) to Building K1432 at Oak Ridge National Laboratory (ORNL). This procedure included real time monitoring of the cold mass support strut strain gauges and an in-cab rider to monitor the instrumentation and direct the driver. The primary technical consideration for these precautions was the possibility of low frequency resonant vibration of the cold mass when excited by symmetrical rough road conditions at specific speeds causing excess stress levels in the support struts and consequent strut failure. A secondary consideration was the possibility of high acceleration loads due to sudden stops, severe road conditions, of impacts. The procedure for moving and transportation to ORNL included requirements for real time continuous monitoring of the eight strut stain gauges and three external accelerometers. Because the strain gauges had not been used since the original magnet cooldown, it was planned to verify their integrity during magnet warmup. The measurements made from the strut strain gauges resulted in stress values that were physically impossible. It was concluded that further evaluation was necessary to verify the usefulness of these gauges and whether they might be faulty. DOE

N90-13243# Tennessee Univ., Knoxville. Plasma Science Lab.
RESEARCH ON HEATING, INSTABILITIES, TURBULENCE AND RF EMISSION FROM ELECTRIC FIELD DOMINATED PLASMAS Final Report, 15 Mar. 1986 - 14 May 1989
J. R. Roth and Igor Alexeff 1 Jul. 1989 238 p
(Grant AF-AFOSR-0100-86; AF Proj. 2301)
(AD-A212122; UTK-PSL-89-2; AFOSR-89-1226TR) Avail: NTIS HC A11/MF A02 CSCL 20/9

This contract has supported four research programs: (1) a program of research on plasma turbulence; (2) a program of research on plasma heating by collisional magnetic pumping; (3) a research program on the Orbitron submillimeter maser; and (4) the initial phase of a program on plasma cloaking of military targets for protection against radar and directed microwave energy weapons. Progress in these areas is documented in the text of this final report and in the twenty archival publications included in the appendices to this report. In addition to the above four research areas, work was continued on plasma diagnostic development, and the development of new state-of-the-art data analysis and reduction methods, including software development for online reduction of Langmuir probe, capacitive probe, and other diagnostic information. Also being developed is the capability to analyze electrostatic potential fluctuations by the methods of nonlinear dynamics. An important part of the research program was the training of graduate and undergraduate research assistants in state-of-the-art methods in the fields of high temperature plasma physics, plasma diagnostics, communications, and related areas. GRA

N90-13244# National Inst. of Standards and Technology, Boulder, CO.
LIQUID AND SOLID ION PLASMAS
D. J. Wineland and J. J. Bollinger 10 Sep. 1989 11 p
(Contract N00014-89-F-00020)
(AD-A212415) Avail: NTIS HC A03/MF A01 CSCL 20/9

Atomic ions which are stored in electromagnetic fields are an example of nonneutral plasmas. Laser techniques allow control of plasma angular momentum and provide plasma cooling to temperatures much less than 1 K. Using imaging techniques, plasma spatial information is achieved. Laser spectroscopic techniques allow measurement of plasma velocity distribution functions. Liquid and solid behavior of ion plasmas is studied. GRA

N90-13245# Stanford Univ., CA. Dept. of Applied Physics.
ADVANCED SOURCE DEVELOPMENT AND APPLICATIONS. LASER-PRODUCED PLASMAS: A COMPACT SOFT X RAY SOURCE WITH HIGH PEAK BRIGHTNESS Final Technical Report, 1 Oct. 1986 - 30 Sep. 1988
Robert L. Byer Jul. 1989 26 p
(Contract F49620-86-K-0019)
(AD-A212677; AFOSR-89-1245TR) Avail: NTIS HC A03/MF A01 CSCL 09/3

The development of high average power pulsed solid-state lasers and the application of these lasers to the generation of laser produced plasmas for soft-x ray generation is described. A 44-W average power moving slab neodymium glass laser was demonstrated. In a separate experiment, injection seeding of this laser to produce 500-MW 11-ps pulses was attained. Soft-x ray generation has been investigated with the moving slab laser, a fix slab laser, and commercial rod-geometry lasers. The techniques that were demonstrated show the feasibility of scaling the operation of slab lasers to the kilowatt level. The rapid development of diode-laser pumping techniques suggests the potential for remarkable efficient, compact and economical laser systems for short wavelength lithography and microscopy applications. GRA

N90-13246# Naval Research Lab., Washington, DC. Center for Computational Physics Development.
FLUX-CORRECTED TRANSPORT ALGORITHMS FOR TWO-DIMENSIONAL COMPRESSIBLE MAGNETOHYDRODYNAMICS Interim Report, Jan. 1987 - Jun. 1989
C. R. DeVore 7 Sep. 1989 24 p
(AD-A212757; NRL-MR-6544) Avail: NTIS HC A03/MF A01 CSCL 20/9

Flux corrected transport (FCT) algorithms for conservatively integrating generalized continuity and hydromagnetic equations in two spatial dimensions are described. By placing the magnetic field components at the interface locations of the finite difference grid, the field is kept divergence-free to within machine roundoff error. The new algorithms are particularly well suited for magnetohydrodynamical problems involving shocks and other discontinuities. GRA

N90-13247# Mission Research Corp., Santa Barbara, CA.
TIME EVOLUTION OF THE ELECTRON SWARM ENERGY DISTRIBUTION FUNCTION Final Report, 1 Jan. 1986 - 30 Apr. 1989
N. J. Carron 28 Jun. 1989 67 p
(Contract F49620-86-C-0019)
(AD-A212967; MRC-R-1240; AFOSR-89-1234TR) Avail: NTIS HC A04/MF A01 CSCL 20/9

The approximate theory of the Boltzmann Equation for the energy distribution function of swarm electrons is reviewed. The L, M approximation (essentially the Fokker-Planck approximation) is developed, being valid when average fractional energy loss per energy transfer collision is small, as is approximately the case in N2 and O2. A summary comparison with N2 and O2 swarm transport coefficients is presented showing excellent agreement over more than four orders of magnitude in the reduced electric field E.No. The spread of energy loss rate about the mean in determining the spectrum is shown. The physical reason for the deficiency of the Continuous Slowing Down Approximation (CSDA) is clarified. It is further shown that the CSDA violates detailed balance. The physical meaning of the function forms is made clear by showing its relation to ordinary diffusion convection theory. The time dependent Boltzmann Equation in the L, M approximation is solved numerically for illustrative cases, demonstrating spectral time lag effects when the electric field varies on a time scale comparable with the swarm energy transfer collision frequency. GRA

76 SOLID-STATE PHYSICS

Includes superconductivity.

For related information, see also *33 Electronics and Electrical Engineering* and *36 Lasers and Masers.*

N90-13248 California Univ., Riverside.
FRACTIONAL CHARGING AND REENTRANCE IN GRANULAR SUPERCONDUCTORS Ph.D. Thesis
Harold Martin Cooper 1988 77 p
Avail: Univ. Microfilms Order No. DA8909860

Quantum mechanical states corresponding to non-integer numbers of superconducting pairs are discussed within the context of granular superconductors. There are two cases of non-integer quantization discussed. The first correspond to states that appear to be half-pairs. The physical consistency of such states is established on the basis of the Anderson pseudo-spin picture of superconductivity. In the second case, it appears that the number of pairs in a given system may range over a continuum. In this case, the continuum arises in connection with a modification the usual Hubbard-Stratonovich transformation used to discuss superconductivity. Physically, a situation occurs in which coupling to external degrees of freedom break the symmetry associated with an integer counting of pairs. A formal device, called a frustrated H-S transformation, allows the discussion of this symmetry breaking as a charge continuum. A pair sensitive device making a measurement on such a continuum, would always measure an integer pair number, the average over an ensemble of identical systems yielding a new quantum number, which is called the crystal charge, corresponding to the continuum. These continuous states give rise to a reentrant phase transition in a granular superconductor. It is shown that intergranular charge-phase

fluctuations that wipe out or severely diminish reentrance in discrete charge models, only weakly effect reentrance in the continuous model. It is also shown that under appropriate circumstances, the presence of dissipation may enhance reentrance. Finally, it is argued that the reentrance reported in BaPb.75Bi.25O3 is due to the existence of continuous charging states, augmented by dissipation. Dissert. Abstr.

N90-13249 North Carolina State Univ., Raleigh.
STRUCTURAL AND ELECTRICAL PROPERTIES OF THIN FILMS AND SUPERLATTICES COMPOSED OF II-VI SEMICONDUCTORS Ph.D. Thesis
Shyang Hwang 1988 231 p
Avail: Univ. Microfilms Order No. DA8909222

Double crystal x ray diffraction (DCXD) and Hall effect (HE) were used to study the structural and electrical properties, respectively of selected II-VI semiconductor thin films and superlattices prepared by photoassisted molecular beam epitaxy (PAMBE). Epitaxial films of CdTe grown by PAMBE exhibit good structural and electrical properties. Electron concentration analysis indicate that these samples are lightly compensated. Theoretical mobility calculations were made. The results show that polar optical phonun scattering and impurity scattering are the dominating scattering mechanisms at high and low temperatures, respectively. HgCdTe epitaxial films grown by PAMBE also exhibit good structural and electrical properties. Carrier concentration analysis shows good agreement between theoretical and experimental data for n-type samples. The properties of p-type modulation-doped HgCdTe samples were studies. These samples exibited outstanding structural and electrical properties as determined by DCXD and HE. HgTe-CdTe superlattices grown by PAMBE exhibit a high structural quality. The structural properties of HgTe-CdTe superlattices were analyzed using a kinematical model. Both n- and p-type superlattices were studied. The carrier concentrations of n-type superlattices exhibit an intrinsic behavior in the temperature range from 50 to 300 K. P-type samples exhibit high mobilities. The properties of thin films and superlattices containing CdMnTe and HgMnTe were also studied. Dissert. Abstr.

N90-13250# Montpellier Univ. (France).
EUROPEAN SOLID STATE DEVICE RESEARCH CONFERENCE (18TH) ESSDERC 88 HELD IN MONTPELLIER, FRANCE ON 13-16 SEPTEMBER 1988
J. P. Nougier, ed. and D. Gasquet, ed, 16 Sep. 1988 812 p
Proceedings of the 18th European Solid State Device Research Conference, held in Montpellier, France, 13-16 Sep. 1988
(Contract DAJA45-88-M-0151)
(AD-A210618; R/D-5983-EE-02) Avail: NTIS HC A99/MF E06 CSCL 20/12

A broad spectrum of scientific topics were covered within the general scope of the physics and terminology of logic and analog solid state devices, including fabrication, modeling, and characterization. Author

N90-13251# International Centre for Theoretical Physics, Trieste (Italy).
COMPOSITE VS CONSTITUENT PARTICLE ASPECTS OF HOLE MOTION IN THE CuO2 PLANE
Su Zhaobin (Academia Sinica, Beijing, China) and Lu Yu Dec. 1988 11 p
(DE89-618864; IC-88/427) Avail: NTIS (US Sales Only) HC A03/MF A01

The question whether the basic physics related to Hi-Tc Superconductivity can be described in terms of the one-band Hubbard model, or an oxygen-copper two-band model, is a question under active discussion. A theoretical scheme is developed to consider the oxygen-copper singlet state as a composite particle. It appears as a bound state in low-frequency phenomena such as conductivity and IR absorption. On the contrary, the oxygen and copper states appear as constituent particles in high-frequency phenomena such as high-energy electron spectroscopy. Depending on the values of the parameters involved, a two-band Fermi-liquid type behavior, or an one-band Hubbard type behavior, should be expected. On the one band, a p-wave pairing of holes induced by antiferromagnetic spin fluctuations, is discussed in the Fermi-liquid picture. On the other hand, the oxygen propagation effect, the renormalization of the hole hopping integral, as well as the possible interpretation of the conductivity, are considered in the composite particle picture. A possible scenario for superconductivity, differing both from the BCS pairing and the holon condensation, is speculated. DOE

N90-13252# Joint Inst. for Nuclear Research, Dubna (USSR). Lab. of Neutron Physics.
ANALYSIS OF HIGH TEMPERATURE SUPERCONDUCTORS BY MEANS OF PIXE AND RBS METHODS
R. A. Ilkhamov (Taskent V. I. Lenin State Univ., USSR), A. P. Kobzev, R. Sandrik, and D. Valentovic 1988 8 p Presented at the 7th Conference on Analytical Spectroscopy, Torun, Poland, Sep. 1988
(DE89-630241; JINR-E-14-88-568) Avail: NTIS (US Sales Only) HC A02/MF A01

The non-destructive ion beam element analyses of the high temperature superconductors are presented. The bulk analysis of materials of Y-Ba-Cu-O composition by the particle induced x ray emission (PIXE) method and study of thin films of these materials by Rutherford Backscattering (RBS) method are proposed. The concentrations of the elements have been calculated by means of external standards technique in the case of PIXE method and by means of experimental spectrum modeling in the case of RBS. The elemental composition can be measured with accuracy not less than 4.5, 4.0 and 4.5 percent for Cu,Y and Ba respectively. DOE

N90-13253# National Inst. of Standards and Technology, Gaithersburg, MD. Semiconductor Electronics Div.
SEMICONDUCTOR MEASUREMENT TECHNOLOGY: DATABASE FOR AND STATISTICAL ANALYSIS OF THE INTERLABORATORY DETERMINATION OF THE CONVERSION COEFFICIENT FOR THE MEASUREMENT OF THE INTERSTITIAL OXYGEN CONTENT OF SILICON BY INFRARED ABSORPTION Final Report
Aslan Baghdadi, ed., Robert I. Scace, ed., and E. Jane Walters, ed. Jul. 1989 183 p
(PB89-221170; NIST/SP-400/82; LC-89-600739) Avail: NTIS HC A09/MF A01; also available SOD HC $9.50 as 003-003-02943-2 CSCL 20L

The data collected for the worldwide, double-round-robin determination of the conversion coefficient used to calculate the interstitial oxygen content of silicon from infrared absorption measurements is presented. Detailed statistical of the data is also presented. The approach taken to determine the conversion coefficient was to conduct inter-laboratory round robins for both the infrared measurements and the absolute measurements. The infrared measurements were carried out at 18 laboratories in China, Europe, Japan, and the United States, using either dispersive infrared or Fourier transform infrared spectrometers. The absolute measurements were carried out at eight laboratories in Europe, Japan, and the United States, using either charged-particle activation analysis, photon activation analysis, or inert gas fusion analysis. Author

N90-13254# Case Western Reserve Univ., Cleveland, OH. Center for Electrochemical Sciences.
THE EFFECTS OF TRACE ANIONS ON THE VOLTAMMETRY OF SINGLE CRYSTAL GOLD SURFACES Technical Report, 1988 - 1989
B. D. Cahan, H. M. Villullas, and E. B. Yeager 18 Aug. 1989 36 p Submitted for publication
(Contract N00014-83-K-0343)
(AD-A211886; TR-68) Avail: NTIS HC A03/MF A01 CSCL 09/1

The development of a new technique for mounting single crystals as a Hanging Meniscus Rotating Disk (HMRD) electrode has facilitated the study of the effect of traces of anionic impurities on the voltammetry of gold single crystals. It is shown that the

cause of most of the differences between voltammetry curves reported in the literature for the same crystal face is the presence in the solution of low levels of Chloride and sulfate ions which were present in the original reagent. Variation of the rotation rate from 0 to 10,000 r.p.m. permitted a change of the effective concentrations of these impurities by a factor of 100. The resultant curves are compared to those produced by purposeful addition of these anions. GRA

N90-13255# Royal Holloway and Bedford New Coll., Egham (England).
DIELECTRIC SPECTROSCOPY OF SEMICONDUCTORS Progress Report No. 5
Andrew K. Jonscher, Mohammad A. Bari, and Najeeb Siddiqui Jul. 1989 8 p
(Contract DAJA45-87-C-0011)
(AD-A211989; R/D-5119-EE-01-05) Avail: NTIS HC A02/MF A01 CSCL 20/12

Our understanding of the frequency dependence of transport in a two-dimensional electron gas (2-DEG) as seen in a nearly-cut-off Field-Effect Transistor (FET) is now reasonably complete, earlier difficulties having been due to confusing experimental artifacts. The result is a confirmation of our prediction that 2-DEG should show strong Low-Frequency Dispersion (LFD), which has some fundamental significance. We are expanding our studies to the investigation of the decay of photo-voltages in p-n junctions on high-resistivity silicon, the dielectric spectra of which were described in the 3rd Progress Report. We believe that the results will be of some interest for the better understanding of the recombination processes in these devices. The new many-body theory of the fractional power-law time-dependence of trapping/generation processes in deep levels in space charge regions of p-n junctions and Schottky barriers has now been accepted by Solid State Electronics. This theory departs radically from previously accepted interpretations which predict near exponential decay, while our experimental evidence shows that this is only a limiting case of a much more general form of dependence. GRA

N90-13256# Cornell Univ., Ithaca, NY. Dept. of Chemistry.
SYNTHESIS AND PROPERTIES OF NdNiO(3) PREPARED BY LOW TEMPERATURE METHODS
John K. Vassiliou, Marc Hornbostel, Robin P. Ziebarth, and Francis J. DiSalvo 16 Aug. 1989 20 p
(Contract N00014-88-K-0139)
(AD-A212117; TR-1) Avail: NTIS HC A03/MF A01 CSCL 09/1

NdNiO3 was prepared with a rhombohedral perovskite structure by low temperature methods, and its magnetic and electric properties were studied between 4 K and 300 K. The temperature coefficient of the resistivity changes at 130 K from positive (i.e., metal-like) to negative (i.e., semiconductor-like), with some thermal hysteresis at this transition. The magnetic susceptibility shows Curie-Weiss behavior, modified by the changing thermal occupation of the Nd+3 crystal field levels, over the whole temperature range. Differential thermal analysis and thermogravimetric analysis showed oxygen loss beginning at 900 C in an N2 atmosphere. Subsequent x ray analysis at room temperature showed the presence of Nd2NiO4 and NiO. The electrical resistivity of sintered polycrystalline samples is somewhat above the expected minimum metallic conductivity, but the observation of a positive constant term in the susceptibility above 100 K suggests metallic band behavior. GRA

N90-13257# Texas Univ., Austin. Dept. of Physics.
TUNNELING MICROSCOPY OF SUPERCONDUCTORS AND TUNNELING BARRIERS Final Report, 1 Jun. 1988 - 31 May 1989
Alex DeLozanne 9 Aug. 1989 4 p
(Grant AF-AFOSR-0228-87; AF Proj. 2306)
(AD-A212120; AFOSR-89-1204TR) Avail: NTIS HC A01/MF A01 CSCL 20/3

A cold stage was built for in-situ UPS measurements. Preliminary results show a fermi edge that disappears as the sample is warmed up in a vacuum. This surface degradation is reversible by annealing at 400 C in pure oxygen. The films made by co-evaporation have improved. Films on bare silicon have zero resistance by 73 K. The best films grow on SrTiO3 (110) with zero resistance by 84 K and critical current densities greater than 1 million A/sq cm below 67 K. A unique system of loadlocks was implemented that allows the transfer of a film from the synthesis chamber to the low temperature STM for analysis. This has yielded, for the first time, good images of the YBCO surface. Spectroscopic measurements indicate thus far that most of the surface is normal, with a few spots showing superconducting behavior and a large superconducting gap. GRA

N90-13258# Helsinki Univ. of Technology, Espoo (Finland). Low Temperature Lab.
SUPERFLUID PHASE SLIPPAGE IN (3)He-B FLOW THROUGH A NARROW CHANNEL
N. B. Kopnin (Academy of Sciences, USSR, Moscow) and M. M. Salomaa Feb. 1989 17 p
(PB89-218986; TKK-F-A639; ISBN-951-754-791-9) Avail: NTIS HC A03/MF A01 CSCL 20L

Phase slippage in flowing superfluid (3)He is presented, based on the numerical integration of time-dependent Ginzburg-Landau equations. The quantum-dynamical phase-slip processes in (3)He are found to be associated with superfluid-core phase-slip centers, in contrast with the resistive state for superconductors where phase-slip centers have normal cores. GRA

N90-13259# Institut National des Sciences Appliquees de Lyon, Villeurbanne (France). Lab. de Physique de la Matiere.
STUDY OF THE ELECTRICAL AND OPTICAL PROPERTIES OF THE VANADIUM AND NICKEL IMPURITIES IN GaAs Ph.D. Thesis [ETUDE DES PROPRIETES ELECTRO-OPTIQUES DES IMPURETES VANADIUM ET NICKEL DANS GAAS]
Neila Hizem 1989 155 p In FRENCH
(ISAL-89-0028; ETN-89-95709) Avail: NTIS HC A08/MF A01

The influence of nickel (NI) and vanadium (V) addition on the electrical and optical behavior of GaAs, is investigated. Capacitance and optical techniques are applied to characterize the GaAs properties. The minimization of the GaAs carbon contamination, during the GaAs: V production, is obtained. The existence of a low spin orbital configuration (type 2E) for the 0.15 eV level of V, is demonstrated. Concerning the Ni addition, it is shown that a high resistivity interface appears under the Au-Ge-Ni contact. A method for the Schottky diodes manufacture on GaSb is included. ESA

N90-13260 Politecnico di Milano (Italy). Dipt. di Elettronica.
INSTABILITY OF THE BEHAVIOR OF HIGH RESISTIVITY SILICON DETECTORS DUE TO THE PRESENCE OF OXIDE CHARGES
A. Longoni, M. Sampietro, and L. Strueder (Max-Planck-Inst. fuer Plasmaphysik, Munich, Germany, F.R.) 1989 27 p
(Rept-89-038; ETN-89-95724) Avail: Politecnico di Milano, Piazza Leonardo da Vinci 32, 20133 Milan, Italy

The combined effect of the positive oxide charges and of the negative ones, which reach the outer surface of SiO2, in high resistivity detectors, is investigated. The measurement of the mutual capacitance between two contiguous reverse biased p(+) junctions, separated by a region covered by a non metalized oxide, is effectuated. The presence of an accumulation layer of electrons under the oxide is verified. The width of the depleted gap between the accumulation layer and the p(+) junction is measured. Instabilities due to the migration of charges over the external surface of the oxide are detected. It is shown that the equilibrium charge distribution, can be reached in a short time if the mobility of the surface charges is increased. ESA

N90-13261# National Inst. of Standards and Technology, Gaithersburg, MD. Semiconductor Electronics Div.
SEMICONDUCTOR MEASUREMENT TECHNOLOGY: A SOFTWARE PROGRAM FOR AIDING THE ANALYSIS OF ELLIPSOMETRIC MEASUREMENTS, SIMPLE MODELS
J. F. Marchiando Jul. 1989 256 p
(PB89-235923; NIST/SP-400/83; LC-89-600743) Avail: NTIS HC A12/MF A01; also available SOD HC $13.00 as 003-003-02954-8 CSCL 20L

MAIN1 is a software program for aiding the analysis of ellipsometric measurements. MAIN1 consists of a suite of routines written in FORTRAN that are used to invert the standard reflection ellipsometric equations for simple systems. Here a system is said to be simple if the solid material sample may be adequately characterized by models which assume at least the following: materials are nonmagnetic; samples exhibit depth dependent optical properties, such as one with layered or laminar structure atop a substrate that behaves like a semi-infinite half-space; layers are flat and of uniform thickness; and the dielectric function within each layer/substrate is isotropic, homogeneous, local, and linear. Each layer is characterized in part by a thickness, while the optical properties for a given material and wavelength are expressed in terms of a refractive index and extinction coefficient. The ellipsometric equations are formulated as a standard damped nonlinear least squares problem and then solved by an iterative method when possible. Estimates of the uncertainties associated with assigning numerical values to the model parameters are calculated as well. Author

N90-13262 Department of the Navy, Washington, DC.
METHOD FOR GROWING PATTERNED THIN FILMS OF SUPERCONDUCTORS Patent
Howard Lessoff, inventor (to Navy) and Richard F. Greene, inventor (to Navy) 27 Jun. 1989 6 p Filed 23 Nov. 1987 Supersedes US-Patent-Appl-SN-123629
(AD-D014195; US-Patent-4,843,060; US-Patent-Appl-SN-123629; US-Patent-Class-505-1) Avail: U.S. Patent and Trademark Office CSCL 20/2

A method for growing a patterned superconductive oxide film of the general formula XZ2Cu3O(6+x) is disclosed, wherein X is yttrium, a lanthanide or a mixture thereof, Z is one or more alkaline earth elements and x is a number between 0 and 1. This patterned superconductive oxide film of XZ2Cu3O(6+x) is formed by preparing an aqueous solution of the nitrates of X, Z and Cu in the X;Z;Cu stoichiometric ratio of 1;2;3; spraying the aqueous nitrate solution onto a heated substrate to form on the substrate a thin film of XZ2Cu3Oy material, wherein y is an undefined number; spot-heating preselected portions of the thin film in an oxygen-rich atmosphere to convert the preselected portions into the patterned superconductive oxide film of XZ2Cu3O(6+x) and removing the unheated thin film of XZ2Cu3Oy material with a solvent. GRA

N90-13263# North Carolina State Univ., Raleigh. Dept. of Materials Science and Engineering.
A TWO-PARAMETER REPRESENTATION OF DYNAMIC DISLOCATION DISTRIBUTIONS
Kasi Jagannadham and Hans Conrad 1989 11 p Submitted for publication
(Contract DAAL03-86-K-0015)
(AD-A212249; ARO-23090.16-MS) Avail: NTIS HC A03/MF A01 CSCL 20/2

A two-parameter representation of the dislocation segment length distribution is offered to represent the plastically deformed state of a material. This distribution function represents the radii to which dislocations are bowed during plastic deformation. It is based on the premise that both a minimum and a maximum value of radius exists. Various quantities associated with the plastically deformed state, namely the fraction of mobile dislocations, the stress dependence of strain rate and of the dislocation velocity are derived from the two-parameter distribution function. The distribution function is also applied to the plastic deformation behavior of polycrystalline copper in tension, in torsion and in tension plus torsion. The results illustrate that the two-parameter distribution explains different characteristic features of plastic deformation and also distinguishes the different forms of plastic deformation of solids. GRA

N90-13264# Stanford Univ., CA. Information Systems Lab.
OPTICAL CLOCK DISTRIBUTION TO VLSI CHIPS Final Report, 1 Aug. 1985 - 30 Jun. 1987
Joseph W. Goodman Jul. 1989 176 p
(Contract DAAG29-85-K-0211)
(AD-A212269; ARO-22908.5-PH) Avail: NTIS HC A09/MF A01 CSCL 20/12

Investigations of the use of optical for distributing the clock to a CMOS chip are reported. Two chips were designed, the first incorporating a set of integrated detectors followed by transimpedance amplifiers. The clock was distributed as an optical square wave. The detected clock signals were then amplified, distributed on polysilicon, and applied to digital logic. The chips were fabricated at the MOSIS facility. Testing of this family of chips yielded a maximum clock rate of about 20 MHz. A second chip was designed in which the optical clock was used only to synchronize a series of free-running electronic clocks distributed about the chip. Again the fabrication was performed at MOSIS. While theory and simulations predicted a maximum clock frequency of 100 MHz, it proved impossible to actually lock the clocks, due to nonuniformities in the fabrication parameters across the chip. Future work should aim at modifying the design for greater tolerance to fabrication nonuniformities. GRA

N90-13265# Princeton Univ., NJ. Dept. of Electrical Engineering.
ELECTRON TRANSPORT IN HETEROJUNCTION SUPERLATTICES Final Report, 15 Apr. 1985 - 14 May 1989
D. C. Tsui 1 Aug. 1989 12 p
(Contract DAAG29-85-K-0098)
(AD-A212366; ARO-22592.5-PH) Avail: NTIS HC A03/MF A01 CSCL 20/12

This final report describes briefly three accomplishments in the area of resonant tunneling through double-barrier devices made of GaAs/Al(x)Ga(1-x)As heterostructures. They are: (1) the first experimental demonstration of the importance of many-electron effect in transport through such devices, (2) a self consistent calculation to take into account the space charge effect and thus to extract spectroscopic information from the experimentally measured I-V characteristics, and (3) the first observation of an intrinsic electrical bistability. GRA

N90-13266# Purdue Univ., West Lafayette, IN. School of Electrical Engineering.
GaAs GATE DYNAMIC MEMORY TECHNOLOGY Final Report, 1 Jun. 1986 - 31 May 1989
Michael R. Melloch, James A. Cooper, Jr., Thomas E. Dungan, Philip G. Neudeck, and John W. Pabst 1 Aug. 1989 154 p
(Contract N00014-86-K-0350)
(AD-A212387; TR-EE-89-47) Avail: NTIS HC A08/MF A01 CSCL 20/12

The expected performance characteristics of GaAs dynamic memories are compared with the capabilities of existing technologies to establish a speed capacity window for possible applications. The design of GaAs dynamic memories using FET direct access of PN-junction based storage capacitors is developed. The leakage mechanisms in PN-junction capacitors are considered theoretically, and experimental performance of mesa-isolated capacitors in GaAs and AlGaAs is reported. Optimization of storage time performance and charge capacity by selection of materials and dopings is discussed, and the limitations of optimized capacitors with respect to temperature and scaling are examined experimentally, MBE-grown mesa-isolated PN-junction capacitors are demonstrated to have both sufficient storage time and sufficient capacity for high density GaAs DRAMs operating above 100 C. Design of access transistors for optimal subthreshold performance is discussed. A 2-D harmonic solution for the potential in subthreshold FETs is presented. The harmonic solution is used to calculate the relationships between physical FET design parameters

and subthreshold performance. Trade-offs between design for best subthreshold characteristics versus manufacturability and circuit requirements are considered. The design of complete DRAM cells combining a capacitor and an access transistor is developed. Required operating voltages for read, write, and storage sequences are established. GRA

N90-13267# Wayne State Univ., Detroit, MI. Dept. of Physics.
INTERSTITIAL FORMATION, NON-EQUILIBRIUM AND MACROSCOPIC PROCESSES IN MERCURY CADMIUM TELLURIDE Final Report, 1 May 1985 - 30 Jun. 1989
C. G. Morgan-Pond 28 Aug. 1989 20 p
(Contract DAAG29-85-K-0119)
(AD-A212412) Avail: NTIS HC A03/MF A01 CSCL 20/2

Several issues of major importance for the crystal quality of mercury cadmium telluride and related materials (cadmium telluride and cadmium zinc telluride) were investigated during the course of this contract. These issues are: the effects of defect interactions, including complex formation and possible changes in defect diffusion, the role of interstitial defects, and the magnitude and effects of lattice relaxation around defects. A new technique (the local matrix method) was developed to obtain estimates of point defect total energies, electronic levels, and the character of the localized states for ionic and metallic tetrahedrally bonded materials, such as mercury cadmium telluride. Preliminary work on a more accurate tight-binding supercell method has given encouraging results. GRA

N90-13268# Stanford Univ., CA. High Temperature Gasdynamics Lab.
AN INVESTIGATION OF DIAMOND FILM DEPOSITION IN A PREMIXED OXYACETYLENE FLAME
Mark A. Cappelli and P. H. Paul 11 Sep. 1989 27 p
(Contract N00014-89-J-1197)
(AD-A212595; TR-1) Avail: NTIS HC A03/MF A01 CSCL 11/3

Polycrystalline diamond film synthesis has been demonstrated using a wide variety of enhanced chemical vapor deposition (CVD) techniques. The method of choice depends on the end application of the deposited film or coating. Diamond film has been deposited in a single-nozzle pre-mixed oxy-acetylene flame. Results of runs of varying duration suggest that diamond is deposited via the transport of hydrocarbon fragments produced at the secondary flame front. Planar laser induced photodissociation fluorescence suggests that this region is rich in C2H species. Emission studies also suggest that the post primary flame zone presents a source of C2 radicals which may account for the observed graphite and diamond-like carbon deposited on the substrate exposed to this region of the flame. The results on the pre-mixed flame suggest that it would be possible and more convenient to attempt large area deposition using a multi-nozzle diffusion flame. GRA

N90-13269# PCO, Inc., Chatsworth, CA.
THE GROWTH OF EPITAXIAL GaAs AND GaAlAs ON SILICON SUBSTRATES BY OMVPE Quarterly Report No. 9, Sep. - Nov. 1988
R. R. Bradley, J. A. Beswick, D. J. Stirland, D. J. Warner, and P. Kightley 1989 38 p
(Contract N00014-86-C-2432)
(AD-A212873) Avail: NTIS HC A03/MF A01 CSCL 20/12

This report covers the reporting period September to November 1988, quarter 9 in the program. Further heteroepitaxial and homo-epitaxial FET structures were grown and assessed. CV profiles and mesa isolation tests have revealed difficulties in obtaining GaAs buffer layers with sufficiently high resistance to provide adequate mesa isolation to enable FETs to be processed to completion. A Further series of silicon substrates were submitted for processing to give linear features orientated in the 110, 010 and 100, directions. GRA

N90-13270# Massachusetts Inst. of Tech., Cambridge.
SYNTHESIS AND STUDY OF MATERIALS FOR SUPERCONDUCTING ELECTRONICS Final Report, 15 Oct. 1987 - 14 Oct. 1988
P. M. Tedrow 15 Sep. 1988 7 p
(Grant AF-AFOSR-0035-88; AF Proj. 2306)
(AD-A212966; AFOSR-89-1241TR) Avail: NTIS HC A02/MF A01 CSCL 20/12

Thin films of BiSrCaCuO superconductor were made by RF magnetron sputtering onto sapphire and MgO substrates. The use of MgO substrates produced better films. Good tunnel junctions were fabricated using YBa2Cu3O7 films with Pb counterelectrodes. No gap was seen for the YBCO film. Critical field anistropy was studied in single crystals of YBCO and NdBa2Cu3O7. Measurements of the Fermi-liquid effects in Ga and V were completed. GRA

N90-13271# Brown Univ., Providence, RI. Dept. of Chemistry.
GROWTH AND CHARACTERIZATION OF ZINC SULFIDE FILMS BY CONVERSION OF ZINC OXIDE FILMS WITH H2S
Y. M. Gao, P. Wu, J. Baglio (GTE Labs., Inc., Waltham, MA.), K. Dwight, and Aaron Wold 26 Sep. 1989 9 p Submitted for publication
(Contract N00014-85-K-0177)
(AD-A213345; TR-12) Avail: NTIS HC A02/MF A01 CSCL 07/2

Zinc sulfide is an IR window material and a transparent semiconductor with a large direct band gap. It also possesses piezoelectric, photoconductive and electroluminescent properties. Thin films of zinc sulfide can be utilized for infrared antireflection coatings, light-emitting diodes (LEDs), electroluminescent (EL) displays, multilayer dielectric filters, optical phase modulation and light guiding in integrated optics. In recent years, there was a large effort directed at the growth of high quality films of ZnS. Various fabrication techniques were employed, such as ion beam epitaxy sputtering atomic layer epitaxy (ALE), molecular beam (MBE), metal-organic chemical vapor deposition and spray pyrolysis. Zinc sulfide films were prepared by conversion of zinc oxide films in the presence of hydrogen sulfide. The films which contained both the hexagonal and cubic forms of zinc sulfide were shown to be uniform and gave a measured band gap of 3.65 eV. GRA

N90-12790*# Jet Propulsion Lab., California Inst. of Tech., Pasadena.
SPIN-LATTICE RELAXATION AND THE CALCULATION OF GAIN, PUMP POWER, AND NOISE TEMPERATURE IN RUBY
J. R. Lyons *In its* The Telecommunications and Data Acquisition Report 15 Aug. 1989 p 63-85 (For primary document see N90-12786 04-32)
Avail: NTIS HC A11/MF A02 CSCL 20L

77 THERMODYNAMICS AND STATISTICAL PHYSICS

Includes quantum mechanics; theoretical physics; and Bose and Fermi statistics.

For related information see also *25 Inorganic and Physical Chemistry* and *34 Fluid Mechanics and Heat Transfer.*

N90-13272# Nationaal Inst. voor Kernfysica en Hoge Energiefysica, Amsterdam (Netherlands).
ON THE SPECTRUM OF THE STAGGERED DIRAC OPERATOR AT FINITE CHEMICAL POTENTIAL
Jeroen C. Vink (CHEAF, Amsterdam, Netherlands) Dec. 1988 17 p
(ITFA-88-53; ETN-89-95754) Avail: NTIS HC A03/MF A01

The spectrum of the staggered Dirac operator in two-dimensional quantum electrodynamics is investigated at finite chemical potential. In the quenched model, it is shown that lattice artifacts cause a spurious scattering of eigenvalues. This scattering disappears when the lattice distance is taken to zero. In the

unquenched model, a new approach is used to show that similar effects are absent. In the scope of the work, the following topics are studied: the exact results for the spectrum of the Dirac operator; the lattice and the gauge fields; the lattice artefacts in the eigenvalue distribution; and the unquenched theory. The relevance of the results in quantum chromodynamics is discussed. ESA

N90-13273# Nationaal Inst. voor Kernfysica en Hoge Energiefysica, Amsterdam (Netherlands).
MORE ON THE SUPER WZW THEORY
Juergen Fuchs (Heidelberg Univ., Germany, F.R.) Sep. 1988 27 p
(NIKHEF-H/88-11; HD-THEP-88-27; ETN-89-95608) Avail: NTIS HC A03/MF A01

The super Weiss, Zumino, Witten (WZW) theory is analyzed further. The quantum equivalence to a bosonic WZW theory supplemented by free fermions is proven and implications of this equivalence are investigated both in the Neveu-Schwartz and in the Ramond sector of the theory. The goal is to prove that the equivalence holds at a quantum level, especially in view of the fact that the lowest component of the supercurrent is a primary field of the Virasoro algebra with conformal dimension and spin and thus essentially a free fermion. A proof is presented. ESA

N90-13274*# Fermi National Accelerator Lab., Batavia, IL. Astrophysics Center.
CORRECTIONS TO THE THIN WALL APPROXIMATION IN GENERAL RELATIVITY
David Garfinkle (Florida Univ., Gainesville.) and Ruth Gregory Oct. 1989 18 p Sponsored in part by DOE
(Grants NAGw-1340; NSF PHY-85-0498; NSF PHY-85-06686)
(NASA-CR-186078; NAS 1.26:186078; FERMILAB-Pub-89/225-A)
Avail: NTIS HC A03/MF A01 CSCL 20C

The question is considered whether the thin wall formalism of Israel applies to the gravitating domain walls of a lambda phi(exp 4) theory. The coupled Einstein-scalar equations that describe the thick gravitating wall are expanded in powers of the thickness of the wall. The solutions of the zeroth order equations reproduce the results of the usual Israel thin wall approximation for domain walls. The solutions of the first order equations provide corrections to the expressions for the stress-energy of the wall and to the Israel thin wall equations. The modified thin wall equations are then used to treat the motion of spherical and planar domain walls. Author

N90-13275# Royal Signals and Radar Establishment, Malvern (England).
TWISTONS
B. D. Bramson Oct. 1988 33 p
(RSRE-Memo-4234; BR108686; ETN-89-94841) Copyright
Avail: NTIS HC A03/MF A01

A new kind of particle, defined in the context of non relativistic quantum mechanics, the twiston, is investigated. It possesses mass, charge, spin and magnetic moment. The gyromagnetic ratio classical analog is that of a rapidly rotating, charged black hole with naked singularity. The electromagnetostatic field of such a particle is shown to be non-singular except at a single point, and contains finite self energy. It is also shown that its electrostatic potential violates the law (like charges repel, unlike charges attract) at small distances. Interactions between twistons of spin 1/2 are considered. Identical twistons in the triplet state are included. The existence of a nonlinear relationship between the twiston field and vector potential, suggestive of a non Abelian gauge theory, is revealed. ESA

80 SOCIAL SCIENCES (GENERAL)

Includes educational matters.

N90-13276# European Space Agency, Paris (France).
WIDER HORIZONS: POTENTIAL CONTRIBUTIONS BY SPACE SYSTEMS TO SOCIO-ECONOMIC ADVANCEMENT IN DEVELOPING COUNTRIES
Norman Longdon, ed. Jun. 1989 63 p Original contains color illustrations
(ESA-SP-1106; ISBN-92-9092-028-9; ETN-89-95705) Copyright
Avail: NTIS HC A04/MF A01; ESA Publications Div., ESTEC, Noordwijk, Netherlands, 30 Dutch guilders

The main topics of the June 1989 Wider Horizons edition are: the ESA (European Space Agency) involvement with satellite applications in developing countries; generational programs in remote sensing and satellite communications in India and in Brazil; the Earth observation programs and perspectives; the Asian and African development banks. The prospects of cooperation with developing countries in the sphere of telecommunications are underlined. Concerning computer data base systems, one-off operations on a considerable scale, and operations to provide support to documentation centers are recommended. ESA

81 ADMINISTRATION AND MANAGEMENT

Includes management planning and research.

N90-13277*# National Aeronautics and Space Administration, Washington, DC.
ISSUES IN NASA PROGRAM AND PROJECT MANAGEMENT
Francis T. Hoban, ed. 1989 57 p
(NASA-SP-6101(02); NAS 1.21:6101(02)) Avail: NTIS HC A04/MF A01; SOD HC $15.00 as 033-000-010-64-8 CSCL 05A

This new collection of papers on aerospace management issues contains a history of NASA program and project management, some lessons learned in the areas of management and budget from the Space Shuttle Program, an analysis of tools needed to keep large multilayer programs organized and on track, and an update of resources for NASA managers. A wide variety of opinions and techniques are presented. Author

N90-13278# Office National d'Etudes et de Recherches Aerospatiales, Paris (France). Direction des Grands Moyens d'Essais.
STUDIES OF THE EUROPEAN TRANSONIC WIND TUNNEL Final Report [ETUDES DE LA SOUFFLERIE TRANSSONIQUE EUROPEENNE]
X. Bouis Dec. 1988 16 p In FRENCH
(Contract DRET-88-817)
(ONERA-RSF-12/0694-GY; ETN-89-95019) Avail: NTIS HC A03/MF A01

The stages of planning and development of the European transonic wind tunnel are described. Progress in resolving budgetary and technical problems is outlined. Changes in administration and personnel involved in the project are listed. Contracts and costs involved in the project are outlined. An operating scenario is presented. An hierarchical list of the different sectors and managers involved in the project is provided. ESA

82 DOCUMENTATION AND INFORMATION SCIENCE

Includes information management; information storage and retrieval technology; technical writing; graphic arts; and micrography.

For computer documentation see *61 Computer Programming and Software.*

N90-13279# National Inst. of Standards and Technology, Gaithersburg, MD. Information Resources and Services Div.
PUBLICATIONS OF THE NATIONAL INSTITUTE OF STANDARDS AND TECHNOLOGY, 1988 CATALOG Report, Jan. - Dec. 1988
Rebecca J. Pardee, ed. Jun. 1989 348 p
(PB89-218382; NIST/SP-305-Suppl-20; LC-48-47112) Avail: NTIS HC A15/MF A02; also available SOD HC $17.00 as 003-003-02940-8 CSCL 05B

The 20th Supplement to Special Publication 305 contains full bibliographic citations including keywords and abstracts for National Institute of Standards and Technology (NIST) (formerly National Bureau of Standards (NBS)) 1988 papers published and entered into the National Technical Information Service (NTIS) collection. Also included are NBS/NIST papers published prior to 1988 but not reported in previous supplements of this annual catalog. Four indexes are included to allow the user to identify NBS/NIST papers by author, keywords, title, and NTIS order/report number. GRA

N90-13280# North Carolina Univ., Chapel Hill.
FELLOWSHIPS IN INFORMATION AND STOCHASTIC SYSTEMS Final Report, 1 Jul. 1986 - 30 Jun. 1989
Charles R. Baker Aug. 1989 3 p
(Contract DAAL03-86-C-0022)
(AD-A212385; ARO-23779.2-MA-F) Avail: NTIS HC A01/MF A01 CSCL 05/2

The most extensive results obtained were on the capacity of Poisson communication channels. Such channels are central to optical communications. The results obtained included information capacity and coding capacity when the channel noise intensity was permitted to be time-varying and random. Previous research on these problems was limited to channels with constant encoder intensity. In this same area, the information capacity of a Poisson channel subject to jamming was determined. GRA

83 ECONOMICS AND COST ANALYSIS

Includes cost effectiveness studies.

No abstracts in this category.

84 LAW, POLITICAL SCIENCE AND SPACE POLICY

Includes NASA appropriation hearings; aviation law; space law and policy; international law; international cooperation; and patent policy.

N90-13281# Committee on Appropriations (U.S. House).
DEPARTMENTS OF VETERANS AFFAIRS AND HOUSING AND URBAN DEVELOPMENT, AND INDEPENDENT AGENCIES APPROPRIATIONS BILL, 1990
Bob Traxler GPO 1989 95 p Report to accompany H.R. 2916 presented by the Committee on Appropriations to the Committee of the Whole House on the State of the Union, 101st Congress, 1st Session, 17 Jul. 1989
(H-Rept-101-150; GPO-19-437) Avail: Document Room, House of Representatives, Washington, DC 20515 HC free

The explanation of the accompanying bill making appropriations for the Department of Veterans Affairs and Housing and Urban Development, and for sundry independent agencies, boards, commissions, corporations, and offices for the fiscal year ending September 30, 1990, and for other purposes is presented by the House Committee on Appropriations. For individual titles, see N90-13282 through N90-13282.

N90-13282# Committee on Appropriations (U.S. House).
NATIONAL AERONAUTICS AND SPACE ADMINISTRATION
In its Departments of Veterans Affairs and Housing and Urban Development, and Independent Agencies Appropriations Bill, 1990 1989 p 60-67 (For primary document see N90-13281 04-84)
Avail: Document Room, House of Representatives, Washington, DC 20515 HC free

The House budget recommendations are presented for appropriations for the National Aeronautics and Space Administration for the fiscal year 1990. The recommendations cover research and development, construction of facilities, space flight and communications, and research and program management. B.G.

N90-13283# Committee on Science, Space and Technology (U.S. House).
FISCAL YEAR 1990 AUTHORIZATION REQUEST AND BUDGET ESTIMATES FOR THE NATIONAL AERONAUTICS AND SPACE ADMINISTRATION
1989 367 p
(GPO-96-945) Avail: Document Room, House of Representatives, Washington, D.C. 20515 HC free; SOD HC $11.00 as 552-070-06558-0

A draft bill was submitted to the subcommittee on the House Committee on Science, Space, and Technology to authorize appropriations to the National Aeronautics and Space Administration for research and development; space flight, control, and data communications; construction of facilities; and research and program management. B.G.

N90-13284# Committee on Appropriations (U.S. Senate).
DEPARTMENTS OF VETERANS AFFAIRS AND HOUSING AND URBAN DEVELOPMENT, AND INDEPENDENT AGENCIES APPROPRIATION BILL, 1990
Barbara Mikulski GPO 1989 156 p Report to accompany H.R. 2916 presented by the Committee on Appropriations, 101st Congress, 1st Session, 13 Sep. 1989
(S-Rept-101-128; GPO-21-609) Avail: Document Room, Senate, Washington, DC 20510 HC free

The House Committee on Appropriations presents the various ammendments with an explanation of the contents of the bill for the Departments of Veterans Affairs and Housing and Urban Development, and for sundry independent agencies, boards, commissions, corporations, and offices for the fiscal year ending 30 September 1990. B.G.

N90-13285# Committee on Science, Space and Technology (U.S. House).
THE 1990 NATIONAL AERONAUTICS AND SPACE ADMINISTRATION AUTHORIZATION
1989 1287 p
(GPO-98-466) Avail: Subcommittee on Space Science and Applications, House of Representatives, Washington, DC 20515 HC free; SOD HC $31.00 as 552-070-068-50-3

Hearings before a subcommittee of the House Committee on Science, Space, and Technology are presented along with the budget estimates for the National Aeronautics and Space Administration for the fiscal year 1990. All written testimony and submittals for the record are also included. The budget estimates provide a detailed outline of budgetary information and justifications for research and development, construction of facilities, space flight and communications, and research and program management. B.G.

N90-13286# Congress of the United States, Washington, DC.
DEPARTMENT OF VETERANS AFFAIRS AND HOUSING AND URBAN DEVELOPMENT, AND INDEPENDENT AGENCIES APPROPRIATIONS ACT, 1990
GPO 28 Sep. 1989 98 p H.R. 2916 enacted by the Senate and House of Representatives, 101st Congress, 1st Session, 28 Sep. 1989
(HR-2916-PP) Avail: Document Room, House of Representatives, Washington, DC 20515 HC free

A bill was submitted to the House of Representatives for appropriations for the Departments of Veterans Affairs and Housing and Urban Development, and for sundry independent agencies, boards, commissions, corporations, and offices for the fiscal year ending September 30, 1990, and for other purposes. For individual titles, see N90-13287 through N90-13287.

N90-13287# Congress of the United States, Washington, DC.
NATIONAL AERONAUTICS AND SPACE ADMINISTRATION
In its Department of Veterans Affairs and Housing and Urban Development, and Independent Agencies Appropriations Act, 1990 28 Sep. 1989 p 67-76 (For primary document see N90-13286 04-84)
Avail: Document Room, House of Representatives, Washington, DC 20515 HC free

House committee recommendations for appropriations for the National Aeronautics and Space Administration for the fiscal year ending September 30, 1990 are presented. The budget recommendations provide an outline of budgetary information for research and development, construction of facilities, space flight and communications, and research and program management. B.G.

N90-13288# Committee on Commerce, Science, and Transportation (U.S. Senate).
NATIONAL AERONAUTICS AND SPACE ADMINISTRATION AUTHORIZATION ACT, FISCAL YEAR 1990
Washington GPO 3 Jan. 1989 32 p A bill, S.916, referred to the Committee on Commerce, Science and Transportation, 101st Congress, 1st Session, 3 May 1989
(S-Rept-101-157) Avail: Document Room, Senate, Washington, DC 20510 HC free

A bill was presented to the Senate to authorize appropriations to the National Aeronautics and Space Administration for research and development, space flight, control and data communications, construction of facilities, and research and program management, and for other purposes. B.G.

N90-13289# Committee on Commerce, Science, and Transportation (U.S. Senate).
NATIONAL AERONAUTICS AND SPACE ADMINISTRATION AUTHORIZATION ACT, FISCAL YEAR 1990
Washington GPO 1989 70 p Report on S.916 presented to the Committee on Commerce, Science and Transportation, 101st Congress, 1st Session, 3 Oct. 1989
(S-Rept-101-157; GPO-22-382) Avail: Document Room, Senate, Washington, DC 20510 HC free

The report on the appropriations to the National Aeronautics and Space Administration by the Committee on Commerce, Science, and Transportation was submitted to the Senate. The budgetary estimates provide a detailed outline of budgetary information and justifications for research and development, construction of facilities, space flight and communications, and research and program management. B.G.

85 URBAN TECHNOLOGY AND TRANSPORTATION

Includes applications of space technology to urban problems; technology transfer; technology assessment; and surface and mass transportation.

For related information see also *03 Air Transportation and Safety, 16 Space Transportation,* and *44 Energy Production and Conversion.*

N90-13290# Committee on Science and Technology (U.S. House).
NASA TECHNOLOGY APPLICATIONS
1989 107 p
(GPO-99-412) Avail: Subcommittee on Space Science and Applications, House of Representatives, Washington, D.C. 20510 HC free; SOD HC $6.00 as 552-070-070-32-0

Hearings before a subcommittee of the House Committee on Science, Space, and Technology are presented for the National Aeronautics and Space Administration Technology Utilization program. All written testimony and submittals for the record are included. B.G.

N90-13291# Office of Technology Assessment, Washington, DC.
TECHNOLOGY TRANSFER TO THE UNITED STATES: THE MIT (MASSACHUSETTS INSTITUTE OF TECHNOLOGY) JAPAN SCIENCE AND TECHNOLOGY PROGRAM. A BACKGROUND PAPER OF OTA'S (OFFICE OF TECHNOLOGY ASSESSMENT'S) ASSESSMENT ON TECHNOLOGY, INNOVATION, AND US TRADE
Apr. 1989 24 p
(PB89-224711) Avail: NTIS HC A03/MF A01 CSCL 05A

A brief description is given of the MIT-Japan Science and Technology Program. The principal themes and issues raised at a workshop held September 1988 are noted. Author

88 SPACE SCIENCES (GENERAL)

No abstracts in this category.

89 ASTRONOMY

Includes radio, gamma-ray, and infrared astronomy, and astrometry.

N90-13292# Royal Aerospace Establishment, Farnborough (England). Space Dept.
PARTICLE TRANSPORT SIMULATION FOR SPACEBORNE, NaI GAMMA-RAY SPECTROMETERS
C. S. Dyer, P. R. Truscott, A. J. Sims, C. Comber, and N. D. A. Hammond (Scicon Consultancy International Ltd., London, England) 24 Nov. 1988 11 p Presented at the IEEE Nuclear and Space Radiation Effects Conference, Portland, OR, 11-15 Jul. 1988 Previously announced in IAA as A89-25740
(AD-A205150; RAE-TM-SPACE-365; BR108793; ETN-89-94827)
Copyright Avail: NTIS HC A03/MF A01

Spaceborne gamma-ray spectrometers sensitivity is investigated. Monte Carlo transport codes are employed to simulate particle transport of cosmic rays and inner-belt protons in representations of the gamma-ray observatory spacecraft and the oriented scintillation spectrometer experiment. Results are used to quantify the contributions to the radioactive background, assess shielding options and examine the effect of detector and spacecraft orientation in anisotropic trapped proton fluxes. ESA

90 ASTROPHYSICS

Includes cosmology; celestial mechanics; space plasmas; and interstellar and interplanetary gases and dust.
For related information see also *75 Plasma Physics*.

N90-13293 Newcastle-upon-Tyne Univ. (England).
STRINGS, p-BRANES AND SKYRMIONS IN CURVED SPACE Ph.D. Thesis
H. C. Luckock 1988 134 p
Avail: Univ. Microfilms Order No. BRDX84887

The behavior of extended objects in curved spacetime is examined. The first such object which is considered is the nucleon, as described by the nonlinear sigma model of T. H. R. Skyrme. When in the gravitational field of a Schwarzschild black hole, it is found that the classical field equations of the Skyrmion admit stable non-trivial solutions. As a consequence, the black hole can have a measurable baryonic charge. However, configurations of this sort decay by quantum tunnelling; an expression is obtained for the decay rate. The quantum theory of bosonic strings and spinning strings were considered and it was shown that string theories are generally renormalizable and are finite when spacetime has the critical dimensionality. The analysis applies to strings with or without boundaries, in a general curved spacetime. These results are used to calculate the ground state string wave-function, and a probability distribution for string configurations at finite temperatures. A similar analysis is then applied to a class of bosonic theories which describe the motion through space of p-dimensional extended objects, referred to as p-branes. A description of the spinning membrane, which can be thought of as a supersymmetric extension of the bosonic 2-brane is contained. To ensure full supersymmetry, the action includes a boundary term. It is then possible to calculate the one-loop divergences of the spinning membrane with boundary, and it is shown that this model is also non-renormalizable in an arbitrary number of spacetime dimensions. Dissert. Abstr.

N90-13294# International Centre for Theoretical Physics, Trieste (Italy).
RELATIONSHIP BETWEEN THE CURRENT AND THE WIDTH OF THE POGO ELECTROJET DURING THE SOLSTICES
P. C. Ozoemena and C. A. Onwumechili (Cardiff Univ., Wales) Dec. 1988 20 p
(DE89-619725; IC-88/399) Avail: NTIS (US Sales Only) HC A03/MF A01

A detailed study of the POGO data, obtained in the northern winter and summer seasons, all over the earth, has elucidated the relationship between the width and current intensity of equatorial electrojet. By employing regression and correlation analysis to these data, we find that, the width and current intensity of the equatorial electrojet are inversely correlated in such a manner that constriction in the width occurs whenever the current is highly intense. This therefore, demonstrates qualitatively that the solstitial electrojet is: (1) wider in the morning hours when it is less intense, (2) narrower around local noon when it is most intense, and (3) broader again in the afternoon and evening hours when it is decaying. For this inverse relationship, we present an argument in favor of channelling arising from differences in conductivities at various local times, winds and pinch effects among other factors. DOE

N90-13295 Max-Planck-Inst. fuer Physik und Astrophysik, Garching (Germany, F.R.). Inst. fuer Extraterrestrische Physik.
NONEQUILIBRIUM IONIZATION IN SUPERNOVA REMNANTS: THE CASE OF TYCHO
W. Brinkmann, H. H. Fink, A. Smith, and F. Haberl (European Space Agency. European Space Research and Technology Center, ESTEC, Noordwijk, Netherlands) May 1989 37 p Submitted for publication
(MPE-Preprint-153; ETN-89-95855) Copyright Avail: Fachinformationszentrum Karlsruhe 7514
Eggenstein-Leopoldshafen 2, Fed. Republic of Germany

A numerical study of the x ray emission of Tycho's supernova remnant which at an age of approximately 430 years did not reach its adiabatic phase of expansion is reported. The carbon deflagration of a C+O white dwarf, which influences the hydrodynamical evolution of the remnant, is studied. Using Nomoto's W7 model of an exploding white dwarf as initial condition, the hydrodynamical and ionizational evolution for different densities of the interstellar medium are followed. They are compared to the emitted spectra with EXOSAT GSPC observations. To match the fluxes of the observed x ray lines a partial mixing is required. The results indicate that the density of the ambient medium is between 0.5 and 10/cu cm, and the distance to Tycho is about 3kpc. The actual physical uncertainties in modeling supernova remnants are discussed. They are related to the magnitude of the possible errors of the derived parameters. ESA

N90-13296*# Max-Planck-Inst. fuer Physik und Astrophysik, Garching (Germany, F.R.). Inst. fuer Extraterrestrische Physik.
FAR INFRARED, submm AND mm SPECTROSCOPY OF THE GALACTIC CENTER: RADIO ARC AND +20/+50 km s (EXP -1) CLOUDS
R. Genzel, G. J. Stacey, A. I. Harris, C. H. Townes (California Univ., Berkeley.), N. Geis, U. U. Graf, A. Poglitsch, and J. Stutzki Jul. 1989 52 p Submitted for publication
(Grant NAG2-208)
(NASA-CR-185497; NAS 1.26:185497; MPE-Preprint-155; ETN-89-95857) Copyright Avail: NTIS HC A04/MF A01 CSCL 03B

The observations of the par improved spectroscopy and the molecular clouds at the galactic center are reported. The results show: the spatial distributions of C(II) 158 microns and molecular line radiation and of the thermal radio continuum emission in the arched filaments of the radio arc are similar; about 2 x 10(exp 4) of the solar mass, or 10 percent of the total gas mass in the radio arc, are contained in C(+) regions; the H(+)/C(+) regions are probably located at the surfaces of the dense molecular clouds in the arc. Profiles, fluxes and spatial distributions of the C(II) fine structure and CO rotational lines are reported. It is demonstrated that the data does not fit models in which the neutral interstellar clouds in the arc are ionized by shocks or by magnetohydrodynamic phenomena. Moreover, that the high temperatures and densities derived previously from NH3 and CS observations may not be characteristic of the bulk of the molecular gas. ESA

N90-13297*# Fermi National Accelerator Lab., Batavia, IL. Astrophysics Center.
EVOLUTION OF DOMAIN WALLS IN THE EARLY UNIVERSE Ph.D. Thesis - Chicago Univ.
Lawrence Kawano (Chicago Univ., IL.) Oct. 1989 30 p Sponsored in part by DOE
(Grant NAGw-1340)
(NASA-CR-186076; NAS 1.26:186076; FERMILAB-Pub-89/208-A) Avail: NTIS HC A03/MF A01 CSCL 03B

The evolution of domain walls in the early universe is studied via 2-D computer simulation. The walls are initially configured on a triangular lattice and then released from the lattice, their evolution driven by wall curvature and by the universal expansion. The walls attain an average velocity of about 0.3c and their surface area per volume (as measured in comoving coordinates) goes down with a slope of -1 with respect to conformal time, regardless of whether the universe is matter or radiation dominated. The additional influence of vacuum pressure causes the energy density to fall away from this slope and steepen, thus allowing a situation in which domain walls can constitute a significant portion of the energy density of the universe without provoking an unacceptably large perturbation upon the microwave background. Author

N90-13298*# Fermi National Accelerator Lab., Batavia, IL. Astrophysics Center.
SMALL SCALE STRUCTURE ON COSMIC STRINGS
Andreas Albrecht 30 Oct. 1989 20 p Submitted for publication Sponsored in part by DOE
(Grant NAGw-1340)
(NASA-CR-186075; NAS 1.26:186075; FERMILAB-Conf-89/221-A) Avail: NTIS HC A03/MF A01 CSCL 03B

The current understanding of cosmic string evolution is discussed, and the focus placed on the question of small scale structure on strings, where most of the disagreements lie. A physical picture designed to put the role of the small scale structure into more intuitive terms is presented. In this picture it can be seen how the small scale structure can feed back in a major way on the overall scaling solution. It is also argued that it is easy for small scale numerical errors to feed back in just such a way. The intuitive discussion presented here may form the basis for an analytic treatment of the small scale structure, which argued in any case would be extremely valuable in filling the gaps in the present understanding of cosmic string evolution. Author

N90-13299*# Fermi National Accelerator Lab., Batavia, IL. Theoretical Astrophysics Group.
COSMIC STRINGS AND BARYON DECAY CATALYSIS
Ruth Gregory, W. B. Perkins, A.-C. Davis, and R. H. Brandenberger (Brown Univ., Providence, RI.) Sep. 1989 25 p Presented at the Symposium on the Formation and Evolution of Cosmic Strings, Cambridge, England, 2-7 Jul. 1989 Sponsored by U.K. SERC; Kings College, Cambridge, England; and A. P. Sloan Foundation
(Contract NAGw-1340; DE-AC02-76ER-03130)
(NASA-CR-186074; NAS 1.26:186074; FERMILAB-Conf-89/215-A; BROWN-HET-725; DOE/ER-03130/433) Avail: NTIS HC A03/MF A01 CSCL 03B

Cosmic strings, like monopoles, can catalyze proton decay. For integer charged fermions, the cross section for catalysis is not amplified, unlike in the case of monopoles. The catalysis processes are reviewed both in the free quark and skyrmion pictures and the implications for baryogenesis are discussed. A computation of the cross section for monopole catalyzed skyrmion decay is presented using classical physics. Also discussed are some effects which can screen catalysis processes. Author

91 LUNAR AND PLANETARY EXPLORATION

Includes planetology; and manned and unmanned flights.
For spacecraft design or space stations see *18 Spacecraft Design, Testing and Performance.*

No abstracts in this category.

92 SOLAR PHYSICS

Includes solar activity, solar flares, solar radiation and sunspots.
For related information see *93 Space Radiation.*

N90-13300 National Geophysical Data Center, Boulder, CO.
SOLAR-GEOPHYSICAL DATA NUMBER 537, MAY 1989. PART 2: COMPREHENSIVE REPORTS, DATA FOR NOV. 1988 AND MISCELLANEOUS
Helen E. Coffey, ed. Jul. 1987 96 p
(PB89-207401; SGD-537-Pt-2; LC-79-640375; ISSN-0038-0911)
Avail: NTIS HC A05/MF A01 CSCL 03B

Solar data are presented for Novembver 1988. The data include solar flares in the H-alpha line; solar radio bursts at fixed frequencies; interplanetary solar particles and plasma; solar x ray radiation as seen from the GOES-7 artificial satellite; mass ejections from the sun; and active prominences and filaments. GRA

N90-13301# Bern Univ. (Switzerland). Div. of Solar Observations.
BERNE SOLAR OBSERVATIONS Progress Report, Jan. 1989 - Jun. 1989
A. Magun, M. Fuhrer, G. Bruggmann, M. Graeter, F. Blanchoud, S. Eder, and R. Herrmann 1989 136 p
(Rept-55; ETN-89-95758) Avail: NTIS HC A07/MF A01

The solar flare (at H-alpha) and solar radio observations for January to June 1989 are reported. The specifications for the solar radio observations are: 3.1 to 92.5 GHz frequency range, 200 to 1000 MHz bandwidth, 100 ms time of integration, and 2.5 degrees to 8 minutes beamwidth. Concerning the solar flare data obtention, at H-alpha, the telescope aperture and focal length are respectively 15 and 194 cm, and charged coupled devices are applied in the line center and line profile observations. ESA

N90-13302# European Space Agency, Paris (France).
THE SOHO MISSION. SCIENTIFIC AND TECHNICAL ASPECTS OF THE INSTRUMENTS
T. D. Guyenne, comp. Nov. 1988 85 p SOHO Science Working Team held 27-30 Jun. 1988
(ESA-SP-1104; ISSN-0379-6566; ETN-89-94988) Avail: NTIS HC A05/MF A01; ESA Publications Div., ESTEC, Noordwijk, Netherlands, 25 Dutch guilders or 12 U.S. dollars

The different instruments to be included in the SOHO (solar and heliospheric observatory) payload are described. The instruments include: a coronal diagnostic spectrometer, an extreme ultraviolet imaging telescope, a wide-field white light and spectrometric coronagraph. Other experiments to be carried out on SOHO are described. These include a study of solar wind anisotropies, a charge, element and isotope analysis system, a comprehensive suprathermal and energetic particle analyzer and an energetic and relativistic nuclei and electron experiment. All these experiments and the instruments involved are described. For individual titles, see N90-13303 through N90-13315.

N90-13303# National Aeronautics and Space Administration. Goddard Space Flight Center, Greenbelt, MD.
SOHO: AN OBSERVATORY TO STUDY THE SOLAR INTERIOR AND THE SOLAR ATMOSPHERE
V. Domingo (European Space Agency. European Space Research and Technology Center, ESTEC, Noordwijk, Netherlands) and A. I. Poland *In* ESA, The SOHO Mission. Scientific and Technical Aspects of the Instruments Nov. 1988 p 7-12 (For primary document see N90-13302 04-92)
Avail: NTIS HC A05/MF A01; ESA Publications Div., ESTEC, Noordwijk, Netherlands, 25 Dutch guilders or 12 U.S. dollars

The Solar and Heliospheric Observatory (SOHO) is described. The two main objectives of SOHO are to improve understanding of solar coronal phenomena and to study solar structure and interior dynamics from its core to the photosphere. The primary goals of the coronal and solar wind studies are to understand the coronal heating mechanism and its expansion into the solar wind. These goals will be achieved both by remote sensing of the solar atmosphere with high resolution spectrometers and telescopes and by in situ measurement of the composition and energy of the resulting solar wind and the energetic particles that propagate through it. The structure and interior dynamics are to be studied by helioseismological methods and the measurement of solar irradiance variations. The SOHO spacecraft will be three-axis stabilized and located in a halo orbit around the L1 Lagrangian point (approximately 1 percent of the distance from the Earth to the Sun). It is currently scheduled for launch in July 1995. ESA

N90-13304# Centre National de la Recherche Scientifique, Verrieres-Le Buisson (France). Lab. de Physique Stellaire et Planetaire.
GOLF: GLOBAL OSCILLATIONS AT LOW FREQUENCIES FOR THE SOHO MISSION
A. H. Gabriel, R. Bocchia, R. M. Bonnet, C. Cesarsky, J. Christensen-Dalsgaard, L. Dame, Ph. Delache, F. L. Deubner, B. Foing, and E. Fossat (Nice Univ., France) et al *In* ESA, The SOHO Mission. Scientific and Technical Aspects of the Instruments Nov. 1988 p 13-17 (For primary document see N90-13302 04-92)
Avail: NTIS HC A05/MF A01; ESA Publications Div., ESTEC, Noordwijk, Netherlands, 25 Dutch guilders or 12 U.S. dollars

The GOLF (global oscillations at low frequencies) SOHO (solar

heliospheric observatory) mission is described. It aims to study the internal structure of the Sun by measuring the spectrum of free global oscillations. GOLF will measure both p and g mode oscillations, with emphasis on low order long period waves which penetrate the solar core. The instrument aims to measure frequencies between 10-7 and 6 10-3 Hz, with a sensitivity of 1 mm/s. The method involves an extension to space of the ground based technique for measuring the mean line-of-sight velocity of the solar surface. A sodium vapor resonance scattering filter is used in a longitudinal magnetic field to sample the two wings of the solar absorption line. The use of a modulating magnetic field provides a continuous internal calibration of the sensitivity. By adding an additional rotating polarizer, measurements are also made of the average solar magnetic field. Efforts are made to correct the data for the spurious effects caused by solar magnetic active regions. ESA

N90-13305# Physikalisch-Meteorologisches Observatorium, Davos (Switzerland).
VIRGO: THE SOLAR MONITOR EXPERIMENT ON SOHO
C. Froehlich, B. N. Andersen, G. Berthomieu, D. Crommelynck, Ph. Delache, V. Domingo, A. Jimenez, A. R. Jones, T. RocaCortes (Consejo Superior de Investigaciones Cientificas, Tenerife, Spain), and Ch. Wehrli *In* ESA, The SOHO Mission. Scientific and Technical Aspects of the Instruments Nov. 1988 p 19-23 Previously announced as N89-25884 (For primary document see N90-13302 04-92)
Avail: NTIS HC A05/MF A01; ESA Publications Div., ESTEC, Noordwijk, Netherlands, 25 Dutch guilders or 12 U.S. dollars

The Variability of solar IRradiance and Gravity Oscillations (VIRGO) experiment contains two types of active cavity radiometers for monitoring of the solar constant, two three channel sunphotometers for the measurement of spectral irradiance at 335, 500 and 865 nm and a low resolution imager with 12 pixels. The main scientific objective is probing the solar interior by helioseismology with p and g mode solar oscillations determined from spectral irradiance and radiance variations on time scales of minutes to the mission time. Information about the convection zone is thus obtained. The comparison of the amplitudes and phases of the oscillations as manifested in irradiance and radiance (from VIRGO) and velocity as measured by the GOLF (global oscillations at low frequencies) experiment are also used in analyzing the convection zone. ESA

N90-13306# Stanford Univ., CA. Center for Space Science and Astrophysics.
SOI: THE SOLAR OSCILLATIONS IMAGER ON SOHO
P. H. Scherrer, J. T. Hoeksema, R. S. Bogart, A. B. C. Walker, Jr., A. M. Title, T. D. Tarbell, C. J. Wolfson, T. M. Brown, Jr., J. Christensen-Dalsgaard, and D. O. Gough (Cambridge Univ., England) et al *In* ESA, The SOHO Mission. Scientific and Technical Aspects of the Instruments Nov. 1988 p 25-30 (For primary document see N90-13302 04-92)
Avail: NTIS HC A05/MF A01; ESA Publications Div., ESTEC, Noordwijk, Netherlands, 25 Dutch guilders or 12 U.S. dollars

The Solar Oscillations Imager (SOI) program for SOHO (solar and heliospheric observatory) is described. It will consist of a Michelson Doppler Imager (MDI) instrument, a facility providing data reduction and analysis capability, and a coordinated set of investigations designed to address a set of science objectives. The MDI is designed to take advantage of the anticipated SOHO telemetry by organizing the observations into four observation programs: structure (at all times), dynamics (two months per year), campaign (eight hours per day, ten months per year), and magnetic fields (few minutes per day). The MDI will measure line-of-sight velocity by Doppler shift, transverse velocity by local correlation tracking, line and continuum intensity, and line-of-sight magnetic fields with both 4 and 1.4 arc-second resolution (2 and 0.7 arc-sec pixels respectively). ESA

N90-13307# National Aeronautics and Space Administration. Goddard Space Flight Center, Greenbelt, MD.
SUMER: SOLAR ULTRAVIOLET MEASUREMENTS OF EMITTED RADIATION
K. Wilhelm, W. I. Axford, W. Curdt, A. H. Gabriel, M. Grewing, M. C. E. Huber, M. C. E. Jordan, P. Lemaire, E. Marsch (Max-Planck-Inst. fuer Aeronomie, Katlenburg-Lindau, Germany, F.R.), and A. I. Poland et al *In* ESA, The SOHO Mission. Scientific and Technical Aspects of the Instruments Nov. 1988 p 31-37 (For primary document see N90-13302 04-92)
Avail: NTIS HC A05/MF A01; ESA Publications Div., ESTEC, Noordwijk, Netherlands, 25 Dutch guilders or 12 U.S. dollars

The SUMER (solar ultraviolet measurements of emitted radiation) experiment is described. It will study flows, turbulent motions, waves, temperatures and densities of the plasma in the upper atmosphere of the Sun. Structures and events associated with solar magnetic activity will be observed on various spatial and temporal scales. This will contribute to the understanding of coronal heating processes and the solar wind expansion. The instrument will take images of the Sun in EUV (extreme ultra violet) light with high resolution in space, wavelength and time. The spatial resolution and spectral resolving power of the instrument are described. Spectral shifts can be determined with subpixel accuracy. The wavelength range extends from 500 to 1600 angstroms. The integration time can be as short as one second. Line profiles, shifts and broadenings are studied. Ratios of temperature and density sensitive EUV emission lines are established. ESA

N90-13308# Rutherford High Energy Lab., Chilton (England).
CDS: THE CORONAL DIAGNOSTIC SPECTROMETER
B. E. Patchett, R. A. Harrison, E. C. Sawyer, B. Aschenbach, J. L. Culhane, G. A. Doschek, A. H. Gabriel, M. C. E. Huber, C. Jordan, and O. Kjeldseth-Moe (Oslo Univ., Norway) et al *In* ESA, The SOHO Mission. Scientific and Technical Aspects of the Instruments Nov. 1988 p 39-42 (For primary document see N90-13302 04-92)
Avail: NTIS HC A05/MF A01; ESA Publications Div., ESTEC, Noordwijk, Netherlands, 25 Dutch guilders or 12 U.S. dollars

The prime objective of the Coronal Diagnostic Spectrometer (CDS) is to obtain intensity ratios of selected extreme-ultraviolet line pairs, with spatial and temporal scales appropriate to the fine-scale features of the solar atmosphere. This will be done simultaneously across a large portion of the solar atmosphere. From this, density and temperature information will be derived which coupled with a modest capability for the detection of flows will be used to study the energy and mass balance of the atmosphere. Understanding the heating of the solar corona and the acceleration of the solar wind are the ultimate goals of this research. ESA

N90-13309# National Aeronautics and Space Administration. Goddard Space Flight Center, Greenbelt, MD.
EIT: SOLAR CORONA SYNOPTIC OBSERVATIONS FROM SOHO WITH AN EXTREME-ULTRAVIOLET IMAGING TELESCOPE
J. P. Delaboudiniere, A. H. Gabriel, G. E. Artzner, D. J. Michels, K. P. Dere, R. A. Howard, R. Catura, R. Stern, J. Lemen (Lockheed Aircraft Corp., Palo Alto, CA.), and W. Neupert et al *In* ESA, The SOHO Mission. Scientific and Technical Aspects of the Instruments Nov. 1988 p 43-48 (For primary document see N90-13302 04-92)
Avail: NTIS HC A05/MF A01; ESA Publications Div., ESTEC, Noordwijk, Netherlands, 25 Dutch guilders or 12 U.S. dollars

The Extreme-ultraviolet Imaging Telescope (EIT) of SOHO (solar and heliospheric observatory) will provide full disk images in emission lines formed at temperatures that map solar structures ranging from the chromospheric network to the hot magnetically confined plasma in the corona. Images in four narrow bandpasses will be obtained using normal incidence multilayered optics deposited on quadrants of a Ritchey-Chretien telescope. The EIT is capable of providing a uniform one arc second resolution over its entire 50 by 50 arc min field of view. Data from the EIT will be

extremely valuable for identifying and interpreting the spatial and temperature fine structures of the solar atmosphere. Temporal analysis will provide information on the stability of these structures and identify dynamical processes. EIT images, issued daily, will provide the global corona context for aid in unifying the investigations and in forming the observing plans for SOHO coronal instruments. ESA

N90-13310# Harvard-Smithsonian Center for Astrophysics, Cambridge, MA.
UVCS: AN ULTRAVIOLET CORONAGRAPH SPECTROMETER FOR SOHO
J. L. Kohl, L. W. Hartmann, A. A. vanBallegooijen, G. L. Withbroe, J. C. Raymond, H. Weiser, G. Noci, E. Antonucci, J. Geiss, and G. Gloeckler (Maryland Univ., College Park.) et al *In* ESA, The SOHO Mission. Scientific and Technical Aspects of the Instruments Nov. 1988 p 49-54 (For primary document see N90-13302 04-92)
Avail: NTIS HC A05/MF A01; ESA Publications Div., ESTEC, Noordwijk, Netherlands, 25 Dutch guilders or 12 U.S. dollars

The UltraViolet Coronagraph Spectrometer (UVCS) of SOHO (solar and heliospheric observatory) provides ultraviolet spectroscopic observations of the solar corona out to ten solar radii from sun-center. This capability is expected to greatly expand the number of plasma parameters that can be specified by remote sensing techniques. Plasma diagnostic techniques are expected to provide a sufficient number of empirically derived parameters to significantly constrain theories of solar wind acceleration, coronal heating, and solar wind composition. The spectral line profiles and intensities are sensitive to random velocity distributions and to the effective temperatures of protons, minor ions, and electrons. Ion densities, chemical abundances, and outflow velocities of coronal protons and ions into the solar wind are also taken into consideration. ESA

N90-13311# Hulburt (E. O.) Center for Space Research, Washington, DC.
LASCO: A WIDE-FIELD WHITE LIGHT AND SPECTROMETRIC CORONAGRAPH FOR SOHO
D. J. Michels, R. Schwenn (Max-Planck-Inst. fuer Aeronomie, Katlenburg-Lindau, Germany, F.R.), R. A. Howard, J.-D. F. Bartoe, S. K. Antiochos, G. E. Brueckner, C.-C. Cheng, K. P. Dere, G. A. Doschek, and J. T. Mariska et al *In* ESA, The SOHO Mission. Scientific and Technical Aspects of the Instruments Nov. 1988 p 55-61 (For primary document see N90-13302 04-92)
Avail: NTIS HC A05/MF A01; ESA Publications Div., ESTEC, Noordwijk, Netherlands, 25 Dutch guilders or 12 U.S. dollars

The scientific objectives of the LASCO (light and spectrometric coronagraph) project in the SOHO (solar and heliospheric observatory) mission are described. These include investigation of mechanisms for heating of the corona and acceleration of the solar wind, causes of coronal transients, and their role in development of large scale coronal patterns and interplanetary disturbances. The distribution and properties of dust particles, including those released from sun-grazing comets are investigated. Interactions of coronal plasma with the dust are studied. The corona is analyzed spectroscopically by a high-resolution scanning, imaging interferometer. The spectral profiles of three emission lines and one Fraunhofer line are measured for each picture point, giving temperatures, velocities, turbulent motions and volume densities. Polarization analysis yields the direction of coronal magnetic fields. ESA

N90-13312# Centre National de la Recherche Scientifique, Verrieres-Le Buisson (France). Service d'Aeronomie.
SWAN: A STUDY OF SOLAR WIND ANISOTROPIES
J. L. Bertaux, R. Pellinen, E. Chassefiere, E. Dimarellis, F. Goutail, T. E. Holzer, V. Kelha, S. Korpela, E. Kyrola (Finnish Meteorological Inst., Helsinki.), and R. Lallement et al *In* ESA, The SOHO Mission. Scientific and Technical Aspects of the Instruments Nov. 1988 p 63-68 (For primary document see N90-13302 04-92)
Avail: NTIS HC A05/MF A01; ESA Publications Div., ESTEC, Noordwijk, Netherlands, 25 Dutch guilders or 12 U.S. dollars

The SWAN (solar wind anisotropies) Lyman photometer project is described. It will map the interplanetary hydrogen emission every other day. From these sky maps, the latitude distribution of the solar wind mass flux from equator to pole can be measured, as well as the variation of this distribution. Solar wind mass flux at high latitude is a key boundary condition to the dynamics of the expansion of the solar wind, particularly in the coronal holes, and correlatives studies conducted with other SOHO (solar and heliospheric observatory) coronal instruments. Secondary objectives include the monitoring of known comets, the possible discovery of new comets, and coronal observations. ESA

N90-13313# Max-Planck-Inst. fuer Physik und Astrophysik, Garching (Germany, F.R.).
CELIAS: CHARGE, ELEMENT AND ISOTOPE ANALYSIS SYSTEM FOR SOHO
D. Hovestadt, J. Geiss, G. Gloeckler, E. Moebius, P. Bochsler, F. Gliem, F. M. Ipavich, B. Wilken, W. I. Axford, and H. Balsiger (Bern Univ., Switzerland) et al *In* ESA, The SOHO Mission. Scientific and Technical Aspects of the Instruments Nov. 1988 p 69-74 (For primary document see N90-13302 04-92)
Avail: NTIS HC A05/MF A01; ESA Publications Div., ESTEC, Noordwijk, Netherlands, 25 Dutch guilders or 12 U.S. dollars

The CELIAS (charge, element, and isotope analysis system) experiment on SOHO (solar and heliospheric observatory) is described. It is designed to measure the mass, ionic charge and energy of the low and high speed solar wind, of suprathermal ions, and of low energy flare particles. Through analysis of the elemental and isotopic abundances, the ionic charge state and velocity distributions of ions originating in the solar atmosphere, the investigation focuses on studying the plasma processes on various temporal and spatial scales in the solar chromosphere, transition zone, and corona. CELIAS includes three mass and charge discriminating sensors based on the time-of-flight technique. These intruments provide detailed in situ diagnostics of the solar wind and of accelerated particles, which complement the optical and spectroscopic investigations of the solar atmosphere carried out by SOHO. ESA

N90-13314# National Aeronautics and Space Administration. Goddard Space Flight Center, Greenbelt, MD.
COSTEP: A COMPREHENSIVE SUPRATHERMAL AND ENERGETIC PARTICLE ANALYZER FOR SOHO
Horst Kunow, Harald Fischer, Guenter Green, Reinhold Mueller-Mellin, Gerd Wibberenz, Hartmut Holweger, Paul Evenson, Jean-Paul Meyer, Nabuyuki Hasebe (Ehime Univ., Matsuyama, Japan), and Tycho vonRosenvinge et al *In* ESA, The SOHO Mission. Scientific and Technical Aspects of the Instruments Nov. 1988 p 75-80 (For primary document see N90-13302 04-92)
Avail: NTIS HC A05/MF A01; ESA Publications Div., ESTEC, Noordwijk, Netherlands, 25 Dutch guilders or 12 U.S. dollars

The group of instruments involved in the COSTEP (comprehensive suprathermal and energetic particle analyzer) project are described. Three sensors, the LION (low energy ion and electron) instrument, the MEICA (medium energy ion composition analyzer) and the EPHIN (electron proton helium instrument) are described. They are designed to analyze particle emissions from the sun over a wide range of species (electrons through iron) and energies (60 KeV/particle to 500 MeV/nucleon). The data collected is used in studying solar and space plasma physics. ESA

N90-13315# Turku Univ. (Finland). Wihuri Physical Lab.
ERNE: ENERGETIC AND RELATIVISTIC NUCLEI AND ELECTRON EXPERIMENT
J. Torsti, A. Aurela, V. Kelha, G. Leppelmeier, K. Leppala, I. Liede, M. Lumme, J. L. Osborne, R. Pellinen, and H. Saarikko (Helsinki Univ. of Technology, Espoo, Finland) et al *In* ESA, The SOHO Mission. Scientific and Technical Aspects of the Instruments Nov. 1988 p 81-84 (For primary document see N90-13302 04-92)
Avail: NTIS HC A05/MF A01; ESA Publications Div., ESTEC, Noordwijk, Netherlands, 25 Dutch guilders or 12 U.S. dollars

The Energetic and Relativistic Nuclei and Electron (ERNE)

experiment is described. It will investigate the solar atmosphere and outer heliosphere by detecting particles produced in various kinds of solar energy release processes. The scientific objectives include the measurement of elemental and isotopic abundances in solar flares, investigation of acceleration processes and physical conditions in the solar atmosphere, and investigation of particle propagation in interplanetary space. The ERNE instrument was designed to measure solar particles from about 1 MeV/nucleon upwards. Electrons, protons and all nuclei, including their isotopes, up to the iron group of elements can be identified. Differential energy spectrum measurements for the heaviest nuclei extend up to 540 MeV/nucleon. ESA

93 SPACE RADIATION

Includes cosmic radiation; and inner and outer earth's radiation belts.

For biological effects of radiation see *52 Aerospace Medicine*. For theory see *73 Nuclear and High-Energy Physics*.

N90-13316*# California Inst. of Tech., Pasadena. Space Radiation Lab.
RESEARCH IN COSMIC AND GAMMA RAY ASTROPHYSICS Annual Status Report
E. C. Stone, L. Davis, Jr., R. A. Mewaldt, and T. A. Prince Mar. 1989 31 p
(Grant NGR-05-002-160)
(NASA-CR-185451; NAS 1.26:185451) Avail: NTIS HC A03/MF A01 CSCL 03B

Research activities in cosmic rays, gamma rays, and astrophysical plasmas are covered. The activities are divided into sections and described, followed by a bibliography. The astrophysical aspects of cosmic rays, gamma rays, and of the radiation and electromagnetic field environment of the Earth and other planets are investigated. These investigations are performed by means of energetic particle and photon detector systems flown on spacecraft and balloons. B.G.

N90-13317# Royal Aerospace Establishment, Farnborough (England). Space Dept.
RADIOACTIVITY INDUCED IN GAMMA-RAY SPECTROMETERS
C. S. Dyer, P. R. Truscott, N. D. A. Hammond, and C. Comber (Scicon Consultancy International Ltd., London, England) 29 Feb. 1988 13 p
(RAE-TM-SPACE-363; BR107145; ETN-89-94997) Copyright Avail: NTIS HC A03/MF A01

The data and the methods used in the prediction of radioactivity, induced in spaceborne gamma ray spectrometers by the space radiation environment are reviewed. Due to large masses of current the application of particle transport codes are required. The results from such codes are given for scintillator detectors. Calculations and irradiation data are presented for germanium and bismuth germanate. ESA

N90-13318# Royal Aerospace Establishment, Farnborough (England). Space Dept.
THE COSMIC RADIATION EFFECTS AND ACTIVATION MONITOR
C. S. Dyer, A. J. Sims, R. J. Hutchings, D. Mapper, J. H. Stephen, and J. Farren (Atomic Energy Research Establishment, Harwell, England) 29 Feb. 1988 13 p
(RAE-TM-SPACE-364; BR107144; ETN-89-94998) Copyright Avail: NTIS HC A03/MF A01

The cosmic radiation effects and activation monitor is described. It is designed to monitor real time linear energy transfer spectra together with mission integrated particle fluences and radioactivity. The aim of the work is to improve the predictive models used to define the aerospace environment. The experiment, together with the expected environments and ground calibration data, are presented. ESA

99 GENERAL

N90-13319*# National Aeronautics and Space Administration. Ames Research Center, Moffett Field, CA.
RESEARCH AND TECHNOLOGY ANNUAL REPORT, 1988
Aug. 1989 263 p Original contains color illustrations
(NASA-TM-101070; A-89034; NAS 1.15:101070) Avail: NTIS HC A12/MF A02 CSCL 05D

Selected research and technology activities at Ames-Moffett and Ames-Dryden are summarized. These accomplishments exemplify the Center's varied and highly productive research efforts for 1988. Author

N90-13320# National Science Foundation, Washington, DC.
NATIONAL SCIENCE FOUNDATION Annual Report, 1988
1988 58 p Original contains color illustrations
Avail: NTIS HC A04/MF A01; SOD HC $4.00 as 038-000-00581-2

The mission of the National Science Foundation is to support and encourage research, both collaborative and independent. The NSF also promotes broad-based science and mathematics education programs, as well as special efforts to ensure that a continuing supply of talented scientists and engineers is available for research. In addition, the Foundation supports the basic equipment needs of researchers and the institutions in which they work. Such projects include a major upgrade of the University of Michigan cyclotron, use of an x ray crystallography technique to obtain some of the first images of viruses, and operation of a wide array of radio, x ray, and light telescopes. All these activities, described in this report, aim to boost economic competitiveness as well as nurture the intellect and awaken our natural curiosity. Author

N90-13321# Joint Research Centre of the European Communities, Ispra (Italy).
[ACTIVITIES REPORT OF THE JOINT RESEARCH CENTER] Annual Report, 1987
1988 92 p Original contains color illustrations
(ETN-89-95757) Avail: NTIS HC A05/MF A01

The scientific and technical achievements of the Joint Research Center carried out under the 1984 to 1987 multiannual program are reported. Details of the management of resources, program execution and the results obtained are included. The following subjects are presented: industrial technologies; fusion; fission; non nuclear energies; environment; exploitation of the high flux reactor; general support cooperation and mutual assistance in case of disaster; international cooperation and development; social, common agricultural, environmental and energy policies; and customs union. ESA

N90-13322# European Space Agency, Paris (France).
EUROPEAN SPACE TECHNOLOGY: CELEBRATING TWENTY-FIVE YEARS OF RESEARCH AND DEVELOPMENT
M. Briscoe, J. Toussaint, H. Kummer, and Norman Longdon, ed. Jun. 1989 105 p Original contains color illustrations
(ESA-BR-55; ISBN-92-9092-003-3; ISSN-0250-1589; ETN-89-95388) Copyright Avail: NTIS HC A06/MF A01; ESA Publications Div., ESTEC, Noordwijk, Netherlands, 30 Dutch guilders

The research and development history of the European community since 1965 is described. Special attention is given to specific spacecraft components developed by the European Space Agency since is was formed in 1975. Momentum wheels, tribology, thermal control and life support, propulsion, solar power generation, spacecraft power distribution systems, energy storage and batteries are some of the research and development areas covered. Spinoffs of European space research such as solar cells, heat pipes and carbon fiber technology are discussed. Future programs and developments are presented. ESA

Typical Subject Index Listing

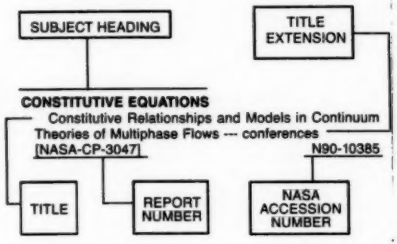

The subject heading is a key to the subject content of the document. Titles, report numbers, and accession numbers of pertinent documents are provided under each subject heading. When the title is insufficiently descriptive of the document content, a title extension has been added, separated from the title by three hyphens. The report number helps to indicate the type of document cited (e.g., NASA report, NASA translation, NASA contractor report). The NASA accession number is the number by which the document abstracts are arranged in this journal and by which the document is sold or requested. The titles, with title extensions if present, are arranged under each subject heading in ascending accession number order. The subject headings have been selected from the latest revision of the *NASA Thesaurus* (NASA SP-7064).

A

ABLATIVE MATERIALS
High temperature insulators
[AD-D014193] N90-12751

ABSORPTIVITY
Photodissociation of XeF2 (xenon difluoride) at 193 nm
[AD-A211663] N90-12916

ABSTRACTS
Publications of the National Institute of Standards and Technology, 1988 catalog
[PB89-218382] N90-13279

ABUNDANCE
Research in cosmic and gamma ray astrophysics
[NASA-CR-185451] N90-13316

ACCELERATION (PHYSICS)
Vibration isolation technology: Sensitivity of selected classes of space experiments to residual accelerations
[NASA-CR-185443] N90-12768
Acceleration sets of planar manipulators. Part 1: Theory
[AD-A213162] N90-12945

ACCEPTOR MATERIALS
Electrically conducting organic materials: Design, synthesis and characterization
[AD-A212214] N90-12700
Strong-inversion model of threshold voltage in modulation doped field effect transistors: The role of unintentional acceptors
[AD-A212750] N90-12870

ACETYLENE
Investigation of fuel additive effects on sooting flames
[AD-A212925] N90-12709

ACID RAIN
Development of an inventory of materials potentially sensitive to ambient atmospheric acidity in the South Coast Air Basin
[PB89-224604] N90-12982
Mesoscale acid deposition modeling studies
[NASA-CR-4262] N90-13228

ACOUSTIC ATTENUATION
Application of active noise reduction for hearing protection and speech intelligibility improvement
[IZF-1988-21] N90-13042

ACOUSTIC EXCITATION
Bulk acoustic waves resonators made of amorphous materials
[NOTE-TECHNIQUE-1989-4] N90-13199

ACOUSTIC IMPEDANCE
An investigation of the diffraction of an acoustic plane wave by a curved surface of finite impedance
[NASA-CR-186069] N90-13204

ACOUSTIC MEASUREMENT
A frequency domain technique for improving sound field reproduction
[RAE-TM-MM-10] N90-13205

ACOUSTIC MICROSCOPES
An air coupled transmission mode acoustic microscope for on-line non-destructive evaluation
[AD-A211416] N90-12947

ACOUSTIC PROPAGATION
Wind effect on sound wave propagation at ground vicinity
[CSTB-2-87-008] N90-13201

ACOUSTIC PROPERTIES
Problems in nonlinear acoustics: Scattering of sound by sound, parametric receiving arrays, nonlincar effects in asymmetric sound beams and pulsed finite amplitude sound beams
[AD-A211756] N90-13200

ACOUSTIC SCATTERING
Problems in nonlinear acoustics: Scattering of sound by sound, parametric receiving arrays, nonlinear effects in asymmetric sound beams and pulsed finite amplitude sound beams
[AD-A211756] N90-13200

ACOUSTIC SOUNDING
Acoustic recording systems for use in military aircraft
[RAE-TM-MM-11] N90-13207

ACOUSTICS
Bulk acoustic waves resonators made of amorphous materials
[NOTE-TECHNIQUE-1989-4] N90-13199
Problems in nonlinear acoustics: Scattering of sound by sound, parametric receiving arrays, nonlinear effects in asymmetric sound beams and pulsed finite amplitude sound beams
[AD-A211756] N90-13200

ACOUSTO-OPTICS
An air coupled transmission mode acoustic microscope for on-line non-destructive evaluation
[AD-A211416] N90-12947
Sound Localization by Human Observers symposium proceedings
[AD-A212877] N90-13026

ACTIVATION ANALYSIS
Proof of the feasibility of coherent and incoherent schemes for pumping a gamma-ray laser
[AD-A212315] N90-12921
Semiconductor measurement technology: Database for and statistical analysis of the interlaboratory determination of the conversion coefficient for the measurement of the interstitial oxygen content of silicon by infrared absorption
[PB89-221170] N90-13253

ACTIVATION ENERGY
Asymptotic analyses of the structures and characteristics of flames N90-12683

ACTIVE CONTROL
Application of sound and temperature to control boundary-layer transition N90-12537

ACTUATORS
Advanced actuation systems development, volume 1
[AD-A213334] N90-12624
Acceleration sets of planar manipulators. Part 1: Theory
[AD-A213162] N90-12945

ADA (PROGRAMMING LANGUAGE)
A mapping for converting Mascot designs to Ada programs
[RSRE-MEMO-4244] N90-13070

ADAPTATION
Performance analysis of large adaptive sidelobe canceller arrays with reused elements
[AD-A212888] N90-12841

ADDITIVES
Spectroscopic ellipsometry characterization of CVD deposition and doping of polysilicon multilayer structures
[RSRE-MEMO-4258] N90-12671

ADHESION TESTS
Behavior of the adhesive A2 submitted to mechanical traction
[CETIM-105290] N90-12748

ADHESIVE BONDING
Behavior of the adhesive A2 submitted to mechanical traction
[CETIM-105290] N90-12748
Structure and properties of polymer interphases
[AD-A212796] N90-12763

ADHESIVES
Behavior of the adhesive A2 submitted to mechanical traction
[CETIM-105290] N90-12748

ADJOINTS
Hahn-Banach type theorems for dual semigroups
[CWI-AM-R8903] N90-13149

ADSORPTION
Thermal stability of the carbon-carbon bond in ethylene adsorbed on Si(100): An isotopic mixing study
[AD-A211591] N90-12691

AERIAL PHOTOGRAPHY
Visualization of high-resolution digital terrain
[AD-A212149] N90-12971

AEROACOUSTICS
Effects of acoustic sources N90-12553
Acoustic design considerations: Review of rotor acoustic sources N90-12585

AERODYNAMIC CHARACTERISTICS
Nacelle aerodynamic performance N90-12552
Aerodynamic test and analysis of a slender generic missile configuration
[AD-A212522] N90-12567
The development of a high response aerodynamic wedge probe and use on a high-speed research compressor
[PNR90598] N90-12613
Large-scale Advanced Prop-fan (LAP) static rotor test report
[NASA-CR-180848] N90-12617

AERODYNAMIC COEFFICIENTS
Design and test of a natural laminar flow/large Reynolds number airfoil with a high design cruise lift coefficient N90-12543
Effects of acoustic sources N90-12553
Powered-lift aircraft technology
[NASA-SP-501] N90-12589

AERODYNAMIC LOADS
Rotor blade structural design N90-12584

AERODYNAMIC NOISE
Acoustic design considerations: Review of rotor acoustic sources N90-12585

AERODYNAMIC STABILITY
Rotor blade dynamic design N90-12583
Airframe design considerations: Overview --- rotor design optimization N90-12586

AERODYNAMIC STALLING
Some observations on transitory stall in conical diffusers
[NASA-TM-102387] N90-12561

AERODYNAMICS
Aeronautical engineering: A continuing bibliography with indexes (supplement 245)
[NASA-SP-7037(245)] N90-12497
Development of a VSAERO (Vortex Separation Aerodynamics) model of the F/A-18
[AD-A212442] N90-12566
Chordwise loading and camber for two-dimensional thin sections
[AD-A213318] N90-12568

Vortex dynamics
[AD-A212119] N90-12877
Research and Technology annual report, 1988
[NASA-TM-101070] N90-13319
AEROELASTICITY
Numerical simulation of unsteady rotational flow over propfan configurations
[NASA-CR-186037] N90-12500
AERONAUTICAL ENGINEERING
Aeronautical engineering: A continuing bibliography with indexes (supplement 245)
[NASA-SP-7037(245)] N90-12497
AEROSOLS
Small particle scattering and absorption
[AD-A213168] N90-12711
Infrared spectrometry of aerosols
[AD-A213303] N90-12713
Comments on the use of LOWTRAN in transmission calculations for sites with the ground elevated relative to sea level
[AD-A212724] N90-12995
AEROSPACE ENGINEERING
Project, implementation, and utilization of composite structures
[ETN-89-95209] N90-12665
Research and Technology annual report, 1988
[NASA-TM-101070] N90-13319
AEROSPACE ENVIRONMENTS
Biology in microgravity: A guide for experimenters
[ESA-TM-02] N90-12769
AEROSPACE INDUSTRY
Issues in NASA program and project management
[NASA-SP-6101(02)] N90-13277
AEROSPACE MEDICINE
Biochemical and physiological changes in glider pilots during multihour flights
[DLR-FB-89-29] N90-13018
AEROSPACE SYSTEMS
Airborne/spaceborne pulsed power source
[AD-A211762] N90-12850
AEROSPACE TECHNOLOGY TRANSFER
NASA technology applications
[GPO-99-412] N90-13290
AGING
Physical ageing and short term creep in amorphous and semicrystalline polymers
[NPL-DMA(A)-185] N90-12745
AIR
An air coupled transmission mode acoustic microscope for on-line non-destructive evaluation
[AD-A211416] N90-12947
AIR BREATHING ENGINES
Apollo lightcraft project
[NASA-CR-186055] N90-12655
AIR FLOW
Air flow over large scale topography
[AD-A211779] N90-12998
AIR LAUNCHING
Low Earth Orbit Raider (LER) winged air launch vehicle concept
[NASA-CR-186057] N90-12590
AIR POLLUTION
Contribution of deforestation to atmospheric CO2 and reforestation as an option to control CO2
[DE89-017255] N90-12979
Development of an inventory of materials potentially sensitive to ambient atmospheric acidity in the South Coast Air Basin
[PB89-224604] N90-12982
AIR QUALITY
Sensitivity of a regional oxidant model to variations in climate parameters, volume 1 and 2
[PB89-224943] N90-12981
AIR TRAFFIC
FAA air traffic activity: Fiscal year 1988
[AD-A211338] N90-12570
AIR TRAFFIC CONTROL
FAA air traffic activity: Fiscal year 1988
[AD-A211338] N90-12570
Development and evaluation at ATCEU of executive and support operations, phase 4A/3D --- ATCEU (Air Traffic Control Evaluation Unit)
[CAA-PAPER-88017] N90-12572
Operational trial of effect of raising minimum stack level in Heathrow stacks
[CAA-PAPER-89003] N90-12573
Parallel approach separation and controller performance: A study of the impact of two separation standards
[DOT/FAA/CT-TN89/50] N90-12574
Software fault tolerance
[RSRE-MEMO-4237] N90-12575
Aircraft Reply and Interference Environment Simulator (ARIES) hardware principles of operation. Volume 2: Appendixes
[DOT/FAA/CT-TN88/4-2] N90-12781
Aircraft Reply and Interference Environment Simulator (ARIES) hardware principles of operation, volume 1
[DOT/FAA/CT-TN88/4-1] N90-12782
Assessment of voice coders for ATC/pilot voice communications via satellite digital communication channels
[CAA-PAPER-89004] N90-12807
Fine resolution errors in secondary surveillance radar altitude reporting amongst aircraft transmitting the conspicuity codes 4321 and 4322
[RSRE-88004] N90-12816
AIR WATER INTERACTIONS
Current velocity and hydrographic observations in the southwestern North Atlantic Ocean: Subtropical Atlantic Climate Studies (STACS), 1988
[PB89-230825] N90-13010
AIRCRAFT APPROACH SPACING
Parallel approach separation and controller performance: A study of the impact of two separation standards
[DOT/FAA/CT-TN89/50] N90-12574
AIRCRAFT COMMUNICATION
Fine resolution errors in secondary surveillance radar altitude reporting amongst aircraft transmitting the conspicuity codes 4321 and 4322
[RSRE-88004] N90-12816
AIRCRAFT COMPARTMENTS
UHB demonstrator interior noise control flight tests and analysis
[NASA-CR-181897] N90-13198
AIRCRAFT CONSTRUCTION MATERIALS
A vision of the future: The new engine technology
[PNR90586] N90-12603
Material requirements for future aeroengines
[PNR90595] N90-12610
Composite materials for future aeroengines
[PNR90584] N90-12667
The future of non ferrous metals in aerospace engines
[PNR90572] N90-12720
Fatigue behavior of specimens under compression load spectra
[ETN-89-95207] N90-12954
An investigation on combined extension and bending of thin sheets with a central crack
[LR-561] N90-12958
AIRCRAFT CONTROL
Integration of a centralized multiplexed control unit into the cockpit of an aircraft
[F6150-DT410-1-88329] N90-12622
Aircraft SAR simulation Sargen 1.0
[FEL-1989-44] N90-12823
AIRCRAFT DESIGN
LFC: A maturing concept
[DOUGLAS-PAPER-7878] N90-12505
Lockheed laminar-flow control systems development and applications N90-12506
Laminar flow: The Cessna perspective N90-12507
Long-range LFC transport N90-12508
Development flight tests of JetStar LFC leading-edge flight test experiment N90-12509
The right wing of the LEFT airplane N90-12510
Research in Natural Laminar Flow and Laminar-Flow Control, part 2
[NASA-CP-2487-PT-2] N90-12519
Research in Natural Laminar Flow and Laminar-Flow Control, part 3
[NASA-CP-2487-PT-3] N90-12539
The design of an airfoil for a high-altitude, long-endurance remotely piloted vehicle N90-12545
The 757 NLF glove flight test results N90-12546
Nacelle design N90-12551
Project, implementation, and utilization of composite structures
[ETN-89-95209] N90-12665
AIRCRAFT ENGINES
Flanged joints of aeroengines
[PNR90594] N90-12609
Aviation Engine Test Facilities (AETF) fire protection study
[AD-A211483] N90-12777
AIRCRAFT EQUIPMENT
Acoustic recording systems for use in military aircraft
[RAE-TM-MM-11] N90-13207
AIRCRAFT LANDING
Field-of-View variations and stripe-texturing effects on assault landing performance in the C-130 weapon system trainer
[AD-A212763] N90-12634
AIRCRAFT MANEUVERS
FPG2: A flight profile generator program
[AD-A212408] N90-12595
AIRCRAFT NOISE
The NASA experience in aeronautical R and D: Three case studies with analysis
[AD-A211486] N90-12496
Near-field noise predictions of an aircraft in cruise N90-12538
Acoustic design considerations: Review of rotor acoustic sources N90-12585
UHB demonstrator interior noise control flight tests and analysis
[NASA-CR-181897] N90-13198
AIRCRAFT PILOTS
A comparison of two subject-controlled attitude measures during somatogravic illusion exposure
[AD-A212528] N90-13031
AIRCRAFT SAFETY
A comparison of two subject-controlled attitude measures during somatogravic illusion exposure
[AD-A212528] N90-13031
AIRCRAFT WAKES
Development of a VSAERO (Vortex Separation Aerodynamics) model of the F/A-18
[AD-A212442] N90-12566
AIRFOIL PROFILES
Design of the low-speed NLF(1)-0414F and the high-speed HSNLF(1)-0213 airfoils with high-lift systems N90-12540
Wind tunnel results of the high-speed NLF(1)-0213 airfoil N90-12542
Design and test of a natural laminar flow/large Reynolds number airfoil with a high design cruise lift coefficient N90-12543
Residual interference assessment in adaptive wall wind tunnels
[NASA-CR-181896] N90-12625
AIRFOILS
Goertler instability on an airfoil N90-12517
The design of an airfoil for a high-altitude, long-endurance remotely piloted vehicle N90-12545
Studies of gas turbine heat transfer airfoil surfaces and end-wall cooling effects
[AD-A212451] N90-12620
AIRFRAMES
Airframe design considerations: Overview --- rotor design optimization N90-12586
AIRPORT PLANNING
Development and evaluation at ATCEU of executive and support operations, phase 4A/3D --- ATCEU (Air Traffic Control Evaluation Unit)
[CAA-PAPER-88017] N90-12572
AIRPORT TOWERS
FAA air traffic activity: Fiscal year 1988
[AD-A211338] N90-12570
AIRPORTS
Development and evaluation at ATCEU of executive and support operations, phase 4A/3D --- ATCEU (Air Traffic Control Evaluation Unit)
[CAA-PAPER-88017] N90-12572
ALGEBRA
Anaphoric trees and an extension of the model of anaphora resolution
[REPT-89-37] N90-13130
An algebra for process creation
[CWI-CS-R8907] N90-13155
ALGORITHMS
Numerical algorithms for steady and unsteady incompressible Navier-Stokes equations
[NASA-CR-186039] N90-12499
Chordwise loading and camber for two-dimensional thin sections
[AD-A213318] N90-12568
Automatic processing of images from the GRATE flight test tool
[DLR-FB-89-28] N90-12599
Numerical analysis of notch test damage to laminated composite plates submitted to uniaxial traction
[CETIM-107310] N90-12675
FLIC (FLame with Implicit Convection): A detailed, two-dimensional flame model
[AD-A212953] N90-12710
Stable Kalman filters for processing clock measurement data N90-12801
On a fast two-dimensional radar imaging process for rotating targets, and an analysis of its image quality
[ESA-TT-1142] N90-12808
Automatic analysis and exploitation of the flow visualization images
[ETN-89-95712] N90-12887
Self-tuning control of nonlinear Armax models --- Autoregressive Moving Average with eXogeneous (ARMAX) inputs
[RR-362] N90-12930
Geodetic point positioning with GPS (Global Positioning System) carrier beat phase data from the CASA UNO experiment
[AD-A211955] N90-12970
Cloud cover determination in polar regions from satellite imagery
[NASA-CR-186096] N90-13003

A fast algorithm for the evaluation of heat potentials [AD-A211316] N90-13052
A fan-in algorithm for distributed sparse numerical factorization [AD-A211569] N90-13054
Algorithmic fault tolerance [RSRE-MEMO-4212] N90-13057
Solving 3D block bidiagonal linear systems on vector computers [CWI-NM-R8819] N90-13061
Multiplicative iterative algorithms for convex programming [CWI-AM-R8808] N90-13072
Towards a parallel algorithm for the many body problem [CS-8813] N90-13078
Subspace iteration algorithms in FORTRAN 77 and FORTRAN 8x [AD-A212275] N90-13083
Parallel and deterministic algorithms from MRF (Markov Random Fields): Surface reconstruction and integration [AD-A212457] N90-13084
Sequential quadratic programming algorithms for optimization [AD-A212800] N90-13088
Algorithm development for SDI weapons system allocation [AD-A212973] N90-13090
Formal calculations and parallesism. Solving linear systems [ETN-89-95499] N90-13098
Labeled trees and the efficient computation of derivations [NASA-CR-185386] N90-13113
Multigrid Monte Carlo in an external U(1) gauge field [NIKHEF-ITFA-88-52] N90-13114
A recursive algorithm for computing the frequency response of a class of nonlinear difference equation models [RR-354] N90-13123
Placing mirrors in grids [CWI-CS-R8906] N90-13154
Note on the convergence of simulated annealing algorithms [MEMO-774] N90-13162
The Painleve test for nonlinear ordinary and partial differential equations [AD-A212894] N90-13177
Monte Carlo (importance) sampling within a Benders' decomposition algorithm for stochastic linear programs [AD-A212854] N90-13189
Molecular dynamics of lipid bilayers [AD-A211492] N90-13214
Research in computer vision for autonomous systems [AD-A212420] N90-13235
Flux-corrected transport algorithms for two-dimensional compressible magnetohydrodynamics [AD-A212757] N90-13246

ALIGNMENT
Cold tests of quasi-optical gyrotron resonators [AD-A212707] N90-12868

ALUMINUM
Tribological properties of ceramic/Ti3Al-Nb sliding couples for use as candidate seal materials to 700 deg C [NASA-TM-102401] N90-12658
Biaxial flexing of a fiber-reinforced aluminum composite [AD-A212742] N90-12681
Rolling of ARALL laminates (an alternative method for post-stretching ARALL laminates) [LR-560] N90-12778

ALUMINUM ALLOYS
Superplastic forming and diffusion bonding of rapidly solidified, dispersion strengthened aluminum alloys for elevated temperature structural applications [NASA-CR-181849] N90-12718
An approach to low temperature high strain rate superplasticity in aluminum alloy 2090 [AD-A212271] N90-12731
Corrosion and corrosion inhibition of metals/alloys in methylphosphonic difluoride and decontaminating solutions [AD-A212404] N90-12734

ALUMINUM CHLORIDES
Heat capacities of 1-methyl-3-ethylimidazolium chloride-aluminum chloride molten salts [AD-A212790] N90-12707

ALUMINUM GALLIUM ARSENIDES
Electron transport in heterojunction superlattices [AD-A212366] N90-13265
GaAs gate dynamic memory technology [AD-A212387] N90-13266
The growth of epitaxial GaAs and GaAlAs on silicon substrates by OMVPE [AD-A212873] N90-13269

ALUMINUM OXIDES
Spall resistance of alumina [AD-A213213] N90-12735
The multivalent beta'-aluminas [AD-A212103] N90-12738
NBS/BAM (National Bureau of Standards/Bundesanstalt fuer Materialprufung) 1986 Symposium on Advanced Ceramics [PB89-229074] N90-12747

AMIDES
Chemical and photochemical reactivity in microemulsions and waterless microemulsions [AD-A211776] N90-12692

AMORPHOUS MATERIALS
Physical ageing and short term creep in amorphous and semicrystalline polymers [NPL-DMA(A)-185] N90-12745
Bulk acoustic waves resonators made of amorphous materials [NOTE-TECHNIQUE-1989-4] N90-13199

ANALYSIS (MATHEMATICS)
A thermoelastic transversely isotropic thick walled cylinder/disk application: An analytical solution and study [NASA-TM-102320] N90-12950

ANALYZERS
COSTEP: A comprehensive suprathermal and energetic particle analyzer for SOHO N90-13314

ANGLE OF ATTACK
Prediction of unsteady blade surface pressures on an advanced propeller at an angle of attack [NASA-TM-102374] N90-12560

ANGULAR RESOLUTION
Angle estimation in a multipath environment with an eight element linear array operating at 10.5 GHz [FEL-1989-15] N90-12826
Faster Phong shading via angular interpolation [CWI-CS-R8909] N90-13156

ANGULAR VELOCITY
Hybrid angular velocity reference system for the investigation of dynamic properties of strapdown gryos [DFVLR-FB-89-25] N90-12577
RTSIN1: A model of a strapdown INS on a two-axis rate table [AD-A212406] N90-12579

ANILINE
Electroactive polyaniline film deposited from non-aqueous media. 2: Effect of acid concentration in solutions [AD-A212084] N90-12737

ANIONS
Quartz crystal microbalance analysis. 1: Evidence of anion or cation insertion into electropolymerized conducting polymers [AD-A212304] N90-12755
The effects of trace anions on the voltammetry of single crystal gold surfaces [AD-A211886] N90-13254

ANISOTROPY
Development of texture analysis and its applications to titanium aero engine components [PNR90561] N90-12602
A cell-centered multigrid method for three-dimensional anisotropic-diffusion and interface problems [REPT-89-35] N90-13128
SWAN: A study of solar wind anisotropies N90-13312

ANNEALING
Study of palladium and chromium silicides formation in liquid phase and in solid phase [LAAS-89040] N90-12695
Note on the convergence of simulated annealing algorithms [MEMO-774] N90-13162

ANNIHILATION REACTIONS
Minimal total cross section for e(+)e(-) yields W(+)W(-) [NIKHEF-H/88-12] N90-13222

ANNUAL VARIATIONS
Atlas of tropical sea surface temperature and surface winds [PB89-223598] N90-13009

ANOMALIES
Device for inspection of materials by eddy current methods [AD-D014205] N90-12948

ANTENNA ARRAYS
Application of the moment method to the design of slotted waveguide array antennas N90-12780
Adaptive antenna arrays for satellite communication [NASA-CR-185989] N90-12784
Properties of density tapered arrays [RSRE-MEMO-4210] N90-12810
Statistical density and amplitude tapered arrays [RSRE-MEMO-4211] N90-12818
Performance analysis of large adaptive sidelobe canceller arrays with reused elements [AD-A212888] N90-12841

ANTENNA COMPONENTS
Performance effects of tie-truss modifications for a 70-meter centerline beam waveguide antenna N90-12791

ANTENNA DESIGN
Application of the moment method to the design of slotted waveguide array antennas N90-12780
Performance effects of tie-truss modifications for a 70-meter centerline beam waveguide antenna N90-12791
DSN 70-meter antenna microwave optics design and performance improvements. Part 2: Comparison with measurements N90-12800
Properties of density tapered arrays [RSRE-MEMO-4210] N90-12810

ANTENNA FEEDS
Ka-band MMIC beam steered transmitter array N90-12803

ANTENNA RADIATION PATTERNS
Scalar Green function method for microstrip antenna analysis based on the exact image theory [PB89-218838] N90-12805
Properties of density tapered arrays [RSRE-MEMO-4210] N90-12810
Statistical density and amplitude tapered arrays [RSRE-MEMO-4211] N90-12818

ANTIMISSILE DEFENSE
Algorithm development for SDI weapons system allocation [AD-A212973] N90-13090

ANTIPARTICLES
Minimal total cross section for e(+)e(-) yields W(+)W(-) [NIKHEF-H/88-12] N90-13222

ANTIPROTONS
Proceedings of the 10 May 1989 Antiproton Technology Workshop: Addendum [AD-A212804] N90-13227

ANXIETY
Fear-potentiated startle as a model system for analyzing learning and memory [AD-A212131] N90-13029

APERTURES
Properties of density tapered arrays [RSRE-MEMO-4210] N90-12810

APPLICATIONS PROGRAMS (COMPUTERS)
Development of computer codes to model dynamics of the earth's magnetosphere [AD-A211532] N90-12987
Building a software package for solving large sparse nonlinear systems of equations [AD-A211758] N90-13055
A moving-grid interface for systems of one-dimensional time-dependent partial differential equations [CWI-NM-R8904] N90-13136

APPROACH CONTROL
Operational trial of effect of raising minimum stack level in Heathrow stacks [CAA-PAPER-89003] N90-12573
Parallel approach separation and controller performance: A study of the impact of two separation standards [DOT/FAA/CT-TN89/50] N90-12574

APPROPRIATIONS
Departments of Veterans Affairs and Housing and Urban Development, and Independent Agencies Appropriations Bill, 1990 [H-REPT-101-150] N90-13281
National Aeronautics and Space Administration N90-13282
Fiscal year 1990 authorization request and budget estimates for the National Aeronautics and Space Administration [GPO-96-945] N90-13283
Departments of Veterans Affairs and Housing and Urban Development, and Independent Agencies Appropriation Bill, 1990 [S-REPT-101-128] N90-13284
The 1990 National Aeronautics and Space Administration Authorization [GPO-98-466] N90-13285
Department of Veterans Affairs and Housing and Urban Development, and Independent Agencies Appropriations Act, 1990 [HR-2916-PP] N90-13286
National Aeronautics and Space Administration N90-13287
National Aeronautics and Space Administration Authorization Act, fiscal year 1990 [S-REPT-101-157] N90-13288
National Aeronautics and Space Administration Authorization Act, fiscal year 1990 [S-REPT-101-157] N90-13289

APPROXIMATION
A linearized surface condition in low speed hydrodynamics
[REPT-89-04] N90-12885
Multiplicative iterative algorithms for convex programming
[CWI-AM-R8808] N90-13072
Stable summability and approximation theory
[AD-A211379] N90-13118
A generalization of Moak's q-Laguerre polynomials
[REPT-89-21] N90-13126
An Eigenvalue Analysis of finite-difference approximations for hyperbolic IBVPs
[NASA-TM-102241] N90-13137
Explicit formulas for Hankel norm approximations of infinite-dimensional systems
[TW-289] N90-13167
Berry-Esseen rates and bootstrap results for generalized L-statistics
[CWI-MS-R8808] N90-13179
Random truncation models and Markov processes
[CWI-MS-R8817] N90-13181
On new methods for computing with multivariate B-splines
[MEMO-783] N90-13183
The physical optics approximation in the near-field region
[FEL-1989-100] N90-13234
Time evolution of the electron swarm energy distribution function
[AD-A212967] N90-13247
Small scale structure on cosmic strings
[NASA-CR-186075] N90-13298
ARC HEATING
Hermes plasma wind tunnel. Preliminary study, phase A1: Text
[DVG-HER-TN-002-PT-1] N90-12631
ARCHITECTURE (COMPUTERS)
Development of an integrated mobile robot system at CMU (Carnegie-Mellon University)
[AD-A212555] N90-12944
A hybrid architecture for feature labelling of oceanographic satellite images
[AD-A212236] N90-12975
ISI's (Information Sciences Institute) SDI architecture simulator: Initial prototype user interface
[AD-A211325] N90-13053
A Z specification of the MaCHO interface editor
[RSRE-MEMO-4247] N90-13067
Area-universal networks
[AD-A211883] N90-13092
LAIOS: A multiprocessor network for artificial intelligence applications
[ETN-89-95498] N90-13109
A compilation strategy for numerical programs based on partial evaluation
[AD-A212759] N90-13175
AREA
Area-universal networks
[AD-A211883] N90-13092
ARGON
Survey of the response of standard limited streamer tubes over the complete range of three-component gas mixtures of isobutane, CO(sub 2), argon
[DE89-016692] N90-12875
ARITHMETIC
Non-separate arithmetic codes
[RSRE-MEMO-4215] N90-13058
ARMED FORCES (UNITED STATES)
Proceedings of the Army Symposium on Solid Mechanics, 1989: Mechanics of Engineered Materials and Applications
[AD-A211954] N90-12951
ARTICULATION (SPEECH)
The effects of noise on speech and warning signals
[AD-A212520] N90-13210
ARTIFICIAL INTELLIGENCE
Telerobotic control for teams of semi-autonomous agents, phase 1
[AD-A211648] N90-13037
A knowledge-based approach to automated flow-field zoning for computational fluid dynamics
[NASA-TM-101072] N90-13048
Truth maintenance systems and their implementation in PROLOG
[MEMO-INF-89-13] N90-13064
Expert system for test program set fault candidate selection
[AD-A213338] N90-13091
An on-line distributed minimum-time trajectory generator for intelligent robot manipulators
[RR-358] N90-13102
Artificial intelligence for communication prospects
[FEL-1989-1] N90-13107
Radar and sensor array design planning for a naval missile testing center. Artificial intelligence applications
[ETCA-88-R-099] N90-13108
LAIOS: A multiprocessor network for artificial intelligence applications
[ETN-89-95498] N90-13109
A theory of networks for approximation and learning
[AD-A212359] N90-13110
NTRFACE for MAGIC
[AD-A212858] N90-13112
Research in computer vision for autonomous systems
[AD-A212420] N90-13235
ASSEMBLIES
Fatigue testing of welded steel assemblies with or without finishing treatments
[CETIM-107900] N90-12961
ASSESSMENTS
Assessment of voice coders for ATC/pilot voice communications via satellite digital communication channels
[CAA-PAPER-89004] N90-12807
ASSOCIATIVE PROCESSING (COMPUTERS)
On modeling resources in multiprocessor systems
[MEMO-INF-88-33] N90-13095
An implementation-oriented specification of the TUMULT communication primitives
[MEMO-INF-88-34] N90-13096
ASTRODYNAMICS
On mean elements for satellite orbits perturbed by the zonal harmonics of the geopotential
[AD-A212322] N90-12642
ASTROMETRY
A statistical study of radio-source structure effects on astrometric very long baseline interferometry observations N90-12788
ASTRONAUT PERFORMANCE
Pre- and postflight postural control of the D1 Spacelab mission astronauts examined with a tilting room
[IZF-1988-25] N90-13039
ASTRONOMY
National Science Foundation N90-13320
ASTROPHYSICS
Research in cosmic and gamma ray astrophysics
[NASA-CR-185451] N90-13316
ASYMMETRY
Building a software package for solving large sparse nonlinear systems of equations
[AD-A211758] N90-13055
Exploring asymmetric heavy-ion reactions at the KX-ray method: The Ne20 + Tb159 reaction at 15 MeV/unit
[KVI-777] N90-13216
ASYMPTOTES
On the maximum period of a permutation of N elements
[MEMO-771] N90-13159
ASYMPTOTIC METHODS
Asymptotic analyses of the structures and characteristics of flames N90-12683
Berry-Esseen rates and bootstrap results for generalized L-statistics
[CWI-MS-R8808] N90-13179
Variational and asymptotic methods in open and closed waveguide analysis
[REPT-34] N90-13229
ASYMPTOTIC PROPERTIES
Stable and unstable subspaces of a critical functional differential equation
[PB89-220651] N90-13115
On a rate of convergence of the multiknapsack value function
[CWI-MS-R8812] N90-13144
Asymptotic expansions for two-stage rank tests
[MEMO-773] N90-13161
Interpretation and manipulation of Edgeworth expansions
[MEMO-775] N90-13163
ASYMPTOTIC SERIES
Smoothed limit theorems for equilibrium processes
[AD-A212321] N90-13186
ATLANTIC OCEAN
Investigation of North Atlantic fog and development of a marine fog forecast system
[AD-A211780] N90-12999
Current velocity and hydrographic observations in the southwestern North Atlantic Ocean: Subtropical Atlantic Climate Studies (STACS), 1988
[PB89-230825] N90-13010
ATMOSPHERIC ATTENUATION
Tropospheric influences on satellite-Earth paths and their determination by means of radar measurements
[ESA-TT-1143] N90-12639
ATMOSPHERIC BOUNDARY LAYER
Central Sudan surface wind data and climate characteristic
[KNMI-WR-88-01] N90-13000
The shape of the probability density function of short-term concentration fluctuations of plumes in the atmospheric boundary layer
[AD-A212632] N90-13188
ATMOSPHERIC CHEMISTRY
Fundamental molecular data to support CARS diagnostics of temperature, pressure, and species concentration
[AD-A212411] N90-12704
Infrared spectrometry of aerosols
[AD-A213303] N90-12713
Retrieval of atomic oxygen and temperature in the thermosphere. Part 1: Feasibility of an experiment based on the spectrally resolved 147 micrometer limb emission
[AD-A211987] N90-12986
Fundamentals of middle atmospheric dynamics
[AD-A211747] N90-12988
Role of chemical effects in daytime high latitude trough formation
[AD-A211772] N90-12989
Zonal average cloud characteristics for global atmospheric chemistry modeling
[CM-76] N90-12992
Infrared water vapor continuum absorption: New atmospheric electrical measurements and theory
[AD-A212594] N90-12994
Mesoscale acid deposition modeling studies
[NASA-CR-4262] N90-13228
ATMOSPHERIC CIRCULATION
A new generation of atmospheric tracers: The biological connection
[AD-A212285] N90-12983
Air flow over large scale topography
[AD-A211779] N90-12998
ATMOSPHERIC COMPOSITION
Contribution of deforestation to atmospheric CO2 and reforestation as an option to control CO2
[DE89-017255] N90-12979
ATMOSPHERIC DIFFUSION
A new generation of atmospheric tracers: The biological connection
[AD-A212285] N90-12983
ATMOSPHERIC EFFECTS
Atmospheric horizontal-inhomogeneity effects on the optical depths determined by the double-elevation-angle lidar technique
[AD-A212836] N90-12839
ATMOSPHERIC ELECTRICITY
Infrared water vapor continuum absorption: New atmospheric electrical measurements and theory
[AD-A212594] N90-12994
ATMOSPHERIC GENERAL CIRCULATION MODELS
Analysis and modeling of summertime convective cloud and precipitation structure over the Southeastern United States
[NASA-CR-185436] N90-12996
ATMOSPHERIC MODELS
Sensitivity of a regional oxidant model to variations in climate parameters, volume 1 and 2
[PB89-224943] N90-12981
Development of computer codes to model dynamics of the earth's magnetosphere
[AD-A211532] N90-12987
Air flow over large scale topography
[AD-A211779] N90-12998
Cloud cover determination in polar regions from satellite imagery
[NASA-CR-186096] N90-13003
Project WIND: Experiments with the UK Meteorological Office mesoscale model
[AD-A212291] N90-13006
Mesoscale acid deposition modeling studies
[NASA-CR-4262] N90-13228
ATMOSPHERIC MOISTURE
Survey of the CLUSE main experiment Grand-CLUSE, May 1 - June 15, 1988 --- Humidity Exchange Over the Sea (HEXOS) experiment
[FEL-1988-43] N90-12991
Infrared water vapor continuum absorption: New atmospheric electrical measurements and theory
[AD-A212594] N90-12994
ATMOSPHERIC OPTICS
Atmospheric horizontal-inhomogeneity effects on the optical depths determined by the double-elevation-angle lidar technique
[AD-A212836] N90-12839
ATMOSPHERIC PHYSICS
A new generation of atmospheric tracers: The biological connection
[AD-A212285] N90-12983
Fundamentals of middle atmospheric dynamics
[AD-A211747] N90-12988
Infrared water vapor continuum absorption: New atmospheric electrical measurements and theory
[AD-A212594] N90-12994

Comments on the use of LOWTRAN in transmission calculations for sites with the ground elevated relative to sea level
[AD-A212724] N90-12995
The shape of the probability density function of short-term concentration fluctuations of plumes in the atmospheric boundary layer
[AD-A212632] N90-13188

ATMOSPHERIC PRESSURE
Instability mechanisms in a barotropic atmosphere
[KNMI-WR-89-01] N90-13001

ATMOSPHERIC TEMPERATURE
Retrieval of atomic oxygen and temperature in the thermosphere. Part 1: Feasibility of an experiment based on the spectrally resolved 147 micrometer limb emission
[AD-A211987] N90-12986

ATMOSPHERICS
Long wave atmospheric noise model, phase 1. Volume 1: Lightning occurrence rates and propagation theory
[AD-A212794] N90-12836
Long wave atmospheric noise model, phase 1. Volume 2: Mode parameters
[AD-A212795] N90-12837

ATOM CONCENTRATION
Retrieval of atomic oxygen and temperature in the thermosphere. Part 1: Feasibility of an experiment based on the spectrally resolved 147 micrometer limb emission
[AD-A211987] N90-12986

ATOMIC COLLISIONS
The process e(-)p giving gamma e(-)p as a fast luminosity for the HERA collider
[NIKHEF-H/88-13] N90-13223

ATOMIC ENERGY LEVELS
Dynamics of an M-level atom interacting with cavity fields: Properties of photon statistics
[AD-A211321] N90-13213

ATOMIZING
Structures and energies for small borane compounds: One and two boron compounds
[AD-A212264] N90-12701
Extended basis set calculations of atomization energies: Comparison of isogyric and direct results
[AD-A212268] N90-12702

ATTACK AIRCRAFT
Estimating the relationships between the state of the art of technology and production cost for the US aircraft
[AD-A212127] N90-12495
Evaluation of a damaged F/A-18 horizontal stabilator
[AD-A212573] N90-12597

ATTACKING (ASSAULTING)
Field-of-View variations and stripe-texturing effects on assault landing performance in the C-130 weapon system trainer
[AD-A212763] N90-12634

ATTENTION
Electrophysiological studies of visual attention and resource allocation
[AD-A212287] N90-13030

ATTITUDE (INCLINATION)
A comparison of two subject-controlled attitude measures during somatogravic illusion exposure
[AD-A212528] N90-13031

ATTITUDE CONTROL
Aircraft SAR simulation Sargen 1.0
[FEL-1989-44] N90-12823

AUDIO SIGNALS
Perceived urgency of warning signals determined using a forced choice pair comparison technique
[RAE-TM-MM-12] N90-13206

AUDITORY PERCEPTION
The effects of hearing protectors on speech communication and the perception of warning signals
[AD-A212521] N90-12832
Removal of noise from noise-degraded speech signals
[AD-A212876] N90-12840
Time-frequency factors in auditory perception
[AD-A211491] N90-13016
Shape instabilities of plate-like structures. 1: Experimental observations in heavily cold worked in situ composites
[AD-A212251] N90-13021
Seminars of Applied Physics, Materials Physics and Biomedical Engineering, 1989
[PB89-218572] N90-13192

AUDITORY SIGNALS
Time-frequency factors in auditory perception
[AD-A211491] N90-13016

AUDITORY STIMULI
Sound Localization by Human Observers symposium proceedings
[AD-A212877] N90-13026

AURORAS
Development of computer codes to model dynamics of the earth's magnetosphere
[AD-A211532] N90-12987

AUSTENITIC STAINLESS STEELS
How the common practice of heating plates of austenitic stainless steel during cooling affects their mechanical properties
[CETIM-104500] N90-12725

AUTOMATED EN ROUTE ATC
Route data representation for ATC simulation experiments
[RSRE-MEMO-4133] N90-12576

AUTOMATIC CONTROL
Batch LCAP2-linear control analysis, version 2.0: User's manual
[AD-A211670] N90-12643
Automated monitor and control for deep space network subsystems N90-12794
Automatic communications channel interference monitoring
[RSRE-MEMO-4243] N90-12820
Automated Steerable Nulling Antenna Processor (SNAP) model
[PB89-231740] N90-12937

AUTOMATIC CONTROL VALVES
Analysis of high speed pneumatic actuation systems under rotary directional on-off flow control N90-12926

AUTOMATIC TEST EQUIPMENT
Expert system for test program set fault candidate selection
[AD-A213338] N90-13091

AUTOMORPHISMS
The algebraic basis of mathematical morphology. Part 2: Openings and closings
[CWI-AM-R8904-PT-2] N90-13150

AUTONOMY
Squirt: The prototypical mobile robot for autonomous graduate students
[AD-A212337] N90-12941
Research in computer vision for autonomous systems
[AD-A212420] N90-13235

AUTOREGRESSIVE PROCESSES
Self-tuning control of nonlinear Armax models --- Autoregressive Moving Average with eXogeneous (ARMAX) inputs
[RR-362] N90-12930

AVIONICS
Acquisition and recording an AMX A/C. Aeritalia experience and present trends
[ETN-89-95217] N90-12598

AXIAL FLOW
Stage effects on stalling and recovery of a high-speed 10-stage axial-flow compressor N90-12600

B

BACKGROUND NOISE
The effects of noise on speech and warning signals
[AD-A212520] N90-13210

BACKGROUND RADIATION
Design and tests of simple, inexpensive optical beacon for use on small satellites
[AD-A213325] N90-13238

BACKSCATTERING
Ion beam analysis of diffusion in polymer glasses
[AD-A212339] N90-12756
Investigation of the properties of radar backscatter from sea ice
[AD-A212808] N90-12838
Improvement and extension of a radar forest backscattering model
[NASA-CR-186083] N90-12973
Workshop on Recent Progress in Surface and Volume Scattering
[AD-A212455] N90-13236
Analysis of high temperature superconductors by means of PIXE and RBS methods
[DE89-630241] N90-13252

BAINITIC STEEL
Improvement in pre-constraint fatigue resistance of modular ferretic and bainitic steel by shot peening treatments
[CETIM-106370] N90-12727

BALLISTIC RANGES
Spark camera annotation and control system for the BRL (Ballistic Research Laboratory) Transonic Range Facility
[AD-A212266] N90-12633

BALLISTICS
RSRM-3 (360L003) ballistics/mass properties report
[NASA-CR-183716] N90-12651
Ballistics/mass properties
[NASA-CR-183723] N90-12652
Ballistic properties of composite materials for personnel protection
[MRL-TR-89-6] N90-12661

BANACH SPACE
Hahn-Banach type theorems for dual semigroups
[CWI-AM-R8903] N90-13149

BARENTS SEA
The Regional Polar Ice Prediction System, Berents Sea (RPIPS-B): A technical description
[AD-A213159] N90-13012

BARIUM OXIDES
Resistivity measurements of superconducting materials
[PB89-225700] N90-12856

BAROCLINIC INSTABILITY
Instability mechanisms in a barotropic atmosphere
[KNMI-WR-89-01] N90-13001

BAROTROPIC FLOW
Instability mechanisms in a barotropic atmosphere
[KNMI-WR-89-01] N90-13001

BARS
Multilayer theory for delamination analysis of a composite curved bar subjected to end forces and end moments
[NASA-TM-4139] N90-12669

BARYONS
Cosmic strings and baryon decay catalysis
[NASA-CR-186074] N90-13299

BAYES THEOREM
Different notions of uncertainty in quasi-probabilistic models
[CWI-CS-R8847] N90-13182
Illustration of Bayesian inference in normal data models using Gibbs sampling
[AD-A212630] N90-13187

BEACON SATELLITES
Design and tests of simple, inexpensive optical beacon for use on small satellites
[AD-A213325] N90-13238

BEAM WAVEGUIDES
Performance effects of tie-truss modifications for a 70-meter centerline beam waveguide antenna N90-12791

BEARING (DIRECTION)
Optimal observer motion for bearings-only localization and tracking N90-12569

BEARINGS
The nature and control of skidding in lightly loaded intershaft bearings
[PNR90591] N90-12933
Vibration transmission through rolling element bearings in geared rotor system, part 1
[NASA-CR-186093] N90-12936

BEND TESTS
Crack propagation failure of carbon/resin composites
[ONERA-RT-45/7086-M] N90-12677

BENDING
Multilayer theory for delamination analysis of a composite curved bar subjected to end forces and end moments
[NASA-TM-4139] N90-12669

BENDING FATIGUE
An investigation on combined extension and bending of thin sheets with a central crack
[LR-561] N90-12958

BENZENE
Thermophysical properties of benzene. Part 1: The ideal gas and the saturated liquid and vapour
[ESDU-89002-PT-1] N90-12693
Thermophysical properties of benzene. Part 2: Thermodynamic properties at elevated pressures
[ESDU-89003-PT-2] N90-12694

BIBLIOGRAPHIES
Aeronautical engineering: A continuing bibliography with indexes (supplement 245)
[NASA-SP-7037(245)] N90-12497
A semiparametric model for citation counts
[CWI-MS-R8814] N90-13145
Publications of the National Institute of Standards and Technology, 1988 catalog
[PB89-218382] N90-13279

BINARY CODES
Binary Gray codes and index systems
[REPT-89-29] N90-13060

BINARY MIXTURES
Vapor-liquid equilibrium of binary mixtures in the extended critical region. Part 1: Thermodynamic model
[PB89-218374] N90-12687

BIOASTRONAUTICS
Biology in microgravity: A guide for experimenters
[ESA-TM-02] N90-12769

BIOCHEMISTRY
Biological and biochemical methane reactions
[PB89-232615] N90-12977
Fear-potentiated startle as a model system for analyzing learning and memory
[AD-A212131] N90-13029

BIOCONTROL SYSTEMS
A Scheiner-principle pocket optometer for self-evaluation and biofeedback accommodation training [AD-A213171] N90-13027
BIOELECTRIC POTENTIAL
Electrophysiological studies of visual attention and resource allocation [AD-A212287] N90-13030
BIOFEEDBACK
A Scheiner-principle pocket optometer for self-evaluation and biofeedback accommodation training [AD-A213171] N90-13027
BIOINSTRUMENTATION
A new generation of atmospheric tracers: The biological connection [AD-A212285] N90-12983
BIOLOGICAL EFFECTS
Biology in microgravity: A guide for experimenters [ESA-TM-02] N90-12769
BIOMAGNETISM
Seminars of Applied Physics, Materials Physics and Biomedical Engineering, 1989 [PB89-218572] N90-13192
BIT ERROR RATE
A performance comparison between block interleaved and helically interleaved concatenated coding systems N90-12792
Performance of the image statistics decoder in conjunction with the Goldstone-VLA array N90-12796
Binary Gray codes and index systems [REPT-89-29] N90-13060
BIT SYNCHRONIZATION
Frame synchronization methods based on channel symbol measurements N90-12795
BLACK HOLES (ASTRONOMY)
Twistons [RSRE-MEMO-4234] N90-13275
BLADE TIPS
Advanced clearance control systems — blade tips [PNR90553] N90-12601
Dynamic tip clearance measurements in axial flow compressors [PNR90597] N90-12612
BLADE-VORTEX INTERACTION
Application of a copper vapour laser to investigation of shock and blade interaction in a shock tube [PNR90578] N90-12918
BLOWING
Numerical experiments on transition control in wall-bounded shear flows N90-12536
BLUFF BODIES
Characterization of nonpremixed turbulent bluff-body burner flames [PB89-229447] N90-12689
BODIES OF REVOLUTION
Flow in the neighborhood of an ellipsoid cylinder of revolution model [ONERA-RT-22/7252-AN-000A] N90-12895
BODY TEMPERATURE
Prediction of thermal stress casualties [AD-A212356] N90-13022
Radio frequency (13.56 MHz) energy enhances rewarming from mild hypothermia [AD-A212703] N90-13024
BODY-WING CONFIGURATIONS
Three-component laser Doppler velocimeter measurements in a juncture flow N90-12525
Pivotal mono wing cruise missile with wing deployment and fastener mechanism [AD-D014191] N90-12594
BOLTED JOINTS
Flanged joints of aeroengines [PNR90594] N90-12609
BOLTZMANN TRANSPORT EQUATION
Time evolution of the electron swarm energy distribution function [AD-A212967] N90-13247
BOMBS (ORDNANCE)
Pivotal mono wing cruise missile with wing deployment and fastener mechanism [AD-D014191] N90-12594
BOOLEAN ALGEBRA
Modular specifications in process algebra with curious queues [CWI-CS-R8821] N90-13152
BORANES
Structures and energies for small borane compounds: One and two boron compounds [AD-A212264] N90-12701
BOSONS
The interacting boson approximation [KVI-774] N90-13215
Ground states of a two-dimensional charged-boson system [AD-A212363] N90-13226
BOUNDARIES
On the Hellinger type distances for filtered experiments [CWI-MS-R8818] N90-13146
On the smooth fit boundary conditions in the optimal stopping problem for semimartingales [CWI-MS-R8819] N90-13147
On the maximum period of a permutation of N elements [MEMO-771] N90-13159
BOUNDARY ELEMENT METHOD
A two-dimensional hybrid experimental-numerical technique for elastic-plastic stress analysis N90-12949
BOUNDARY LAYER CONTROL
Research in Natural Laminar Flow and Laminar-Flow Control, part 1 [NASA-CP-2487-PT-1] N90-12503
Laminar flow: Challenge and potential N90-12504
LFC: A maturing concept [DOUGLAS-PAPER-7878] N90-12505
Lockheed laminar-flow control systems development and applications N90-12506
Laminar flow: The Cessna perspective N90-12507
Long-range LFC transport N90-12508
Development flight tests of JetStar LFC leading-edge flight test experiment N90-12509
The right wing of the LEFT airplane N90-12510
Performance of laminar-flow leading-edge test articles in cloud encounters N90-12511
Simulated airline service experience with laminar-flow control leading-edge systems N90-12512
Stability theory applications to laminar-flow control N90-12513
Nonparallel stability of boundary layers N90-12514
Goertler instability on an airfoil N90-12517
Effect of roughness on the stability of boundary layers N90-12518
Research in Natural Laminar Flow and Laminar-Flow Control, part 2 [NASA-CP-2487-PT-2] N90-12519
Advanced measurement techniques, part 1 N90-12520
Experimental studies on Goertler vortices N90-12529
An experimental evaluation of slots versus porous strips for laminar-flow applications N90-12530
Boundary-layer stability analysis of Langley Research Center 8-foot LFC experimental data N90-12532
Sensitivity of LFC techniques in the non-linear regime N90-12533
Numerical solutions of the compressible 3-D boundary-layer equations for aerospace configurations with emphasis on LFC N90-12534
Theoretical methods and design studies for NLF and HLFC swept wings at subsonic and supersonic speeds N90-12535
Numerical experiments on transition control in wall-bounded shear flows N90-12536
Application of sound and temperature to control boundary-layer transition N90-12537
Research in Natural Laminar Flow and Laminar-Flow Control, part 3 [NASA-CP-2487-PT-3] N90-12539
Design and test of an NLF wing glove for the variable-sweep transition flight experiment N90-12544
F-14 VSTFE and results of the cleanup flight test program N90-12547
Status report on a natural laminar-flow nacelle flight experiment N90-12550
Nacelle design N90-12551
Nacelle aerodynamic performance N90-12552
Supersonic laminar-flow control N90-12554
The effects of wall surface defects on boundary-layer transition in quiet and noisy supersonic flow N90-12556
Supersonic boundary-layer transition on the LaRC F-106 and the DFRF F-15 aircraft. Part 1: Transition measurements and stability analysis N90-12558
BOUNDARY LAYER EQUATIONS
Boundary-layer receptivity and laminar-flow airfoil design N90-12516
Numerical solutions of the compressible 3-D boundary-layer equations for aerospace configurations with emphasis on LFC N90-12534
Theoretical methods and design studies for NLF and HLFC swept wings at subsonic and supersonic speeds N90-12535
Unsteady three-dimensional thin-layer Navier Stokes solutions on dynamic blocked grids [AD-A212377] N90-12899
BOUNDARY LAYER FLOW
Three-component laser Doppler velocimeter measurements in a juncture flow N90-12525
Recent tests at Langley with a University of Tennessee Space Institute (UTSI) skin friction balance N90-12527
Experimental and numerical analyses of laminar boundary-layer flow stability over an aircraft fuselage forebody N90-12549
Reduction of turbulent drag: Boundary layer manipulators [CERT-RSF-OA-74/2259-AYD] N90-12889
Fundamental studies of turbulent wall pressure fluctuations with applications to advanced acoustic sensor systems [AD-A213041] N90-13212
BOUNDARY LAYER SEPARATION
Some observations on transitory stall in conical diffusers [NASA-TM-102387] N90-12561
A computationally efficient modelling of laminar separation bubbles [NASA-CR-185854] N90-12872
BOUNDARY LAYER STABILITY
Nonparallel stability of boundary layers N90-12514
Interaction of Tollmien-Schlichting waves and Goertler vortices N90-12515
Boundary-layer receptivity and laminar-flow airfoil design N90-12516
Effect of roughness on the stability of boundary layers N90-12518
Predicted and hot-film measured Tollmien-Schlichting wave characteristics N90-12523
Experimental studies on Goertler vortices N90-12529
An experimental evaluation of slots versus porous strips for laminar-flow applications N90-12530
Results of LFC experiment on slotted swept supercritical airfoil in Langley's 8-foot transonic pressure tunnel N90-12531
Boundary-layer stability analysis of Langley Research Center 8-foot LFC experimental data N90-12532
Sensitivity of LFC techniques in the non-linear regime N90-12533
Numerical solutions of the compressible 3-D boundary-layer equations for aerospace configurations with emphasis on LFC N90-12534
Theoretical methods and design studies for NLF and HLFC swept wings at subsonic and supersonic speeds N90-12535
Research in Natural Laminar Flow and Laminar-Flow Control, part 3 [NASA-CP-2487-PT-3] N90-12539
Design of the low-speed NLF(1)-0414F and the high-speed HSNLF(1)-0213 airfoils with high-lift systems N90-12540
Design and test of an NLF wing glove for the variable-sweep transition flight experiment N90-12544
Variable-Sweep Transition Flight Experiment (VSTFE): Stability code development and clean-up glove data analysis N90-12548
Experimental and numerical analyses of laminar boundary-layer flow stability over an aircraft fuselage forebody N90-12549
Experimental and theoretical investigation of boundary-layer instability mechanisms on a swept leading edge at Mach 3.5 N90-12557
Supersonic boundary-layer transition on the LaRC F-106 and the DFRF F-15 aircraft. Part 1: Transition measurements and stability analysis N90-12558
BOUNDARY LAYER TRANSITION
Research in Natural Laminar Flow and Laminar-Flow Control, part 1 [NASA-CP-2487-PT-1] N90-12503
Performance of laminar-flow leading-edge test articles in cloud encounters N90-12511
Stability theory applications to laminar-flow control N90-12513
Boundary-layer receptivity and laminar-flow airfoil design N90-12516
Research in Natural Laminar Flow and Laminar-Flow Control, part 2 [NASA-CP-2487-PT-2] N90-12519
Advanced measurement techniques, part 1 N90-12520
Flow quality measurements in compressible subsonic flows N90-12521
Hot-film system for transition detection in cryogenic wind tunnels N90-12522
Remote detection of boundary-layer transition by an optical system N90-12524
Theoretical methods and design studies for NLF and HLFC swept wings at subsonic and supersonic speeds N90-12535
Numerical experiments on transition control in wall-bounded shear flows N90-12536
Application of sound and temperature to control boundary-layer transition N90-12537
Research in Natural Laminar Flow and Laminar-Flow Control, part 3 [NASA-CP-2487-PT-3] N90-12539
Wind tunnel results of the low-speed NLF(1)-0414F airfoil N90-12541
Design and test of an NLF wing glove for the variable-sweep transition flight experiment N90-12544
The 757 NLF glove flight test results N90-12546

F-14 VSTFE and results of the cleanup flight test program N90-12547
Variable-Sweep Transition Flight Experiment (VSTFE): Stability code development and clean-up glove data analysis N90-12548
Experimental and numerical analyses of laminar boundary-layer flow stability over an aircraft fuselage forebody N90-12549
Status report on a natural laminar-flow nacelle flight experiment N90-12550
Nacelle design N90-12551
Nacelle aerodynamic performance N90-12552
Supersonic laminar-flow control N90-12554
Design and fabrication requirements for low noise supersonic/hypersonic wind tunnels N90-12555
The effects of wall surface defects on boundary-layer transition in quiet and noisy supersonic flow N90-12556
Supersonic boundary-layer transition on the LaRC F-106 and the DFRF F-15 aircraft. Part 1: Transition measurements and stability analysis N90-12558
Supersonic boundary-layer transition on the LaRC F-106 and the DFRF F-15 aircraft. Part 2: Aerodynamic predictions N90-12559
A computationally efficient modelling of laminar separation bubbles [NASA-CR-185854] N90-12872
Transition in surface boundary layers [CERT-RSF-OA-43/5018-AYD] N90-12897

BOUNDARY LAYERS
Upwind discretization of the steady Navier-Stokes equations [CWI-NM-R8810] N90-12891

BOUNDARY LUBRICATION
Cold press lubrication: Fine tuning of the CETIM Forgelub test [CETIM-105160] N90-12938

BOUNDARY VALUE PROBLEMS
Goertler instability on an airfoil N90-12517
Analysis of three- and four-sided uniform waveguides with unusual cross-section/boundary conditions [AD-A212653] N90-12834
A 2d-1 lower bound 2-layer knock-knee channel routing [AD-A211948] N90-12847
Stability conditions for steady shearing. Stability conditions for simple shear under mixed thermal boundary conditions N90-12873
A simulation study of the overdetermined geodetic boundary value problem using collocation [AD-A211785] N90-12990
Smoothed predictor-corrector methods for solving partial differential equations [CWI-NM-R8808] N90-13131
Iterated theta method for hyperbolic equations [CWI-NM-R8809] N90-13132
An algebraic characterization of B-convergent Runge-Kutta methods [CWI-NM-R8901] N90-13133
Increasing the real stability boundary of explicit methods [CWI-NM-R8902] N90-13134
An Eigenvalue Analysis of finite-difference approximations for hyperbolic IBVPs [NASA-TM-102241] N90-13137

BOUSSINESQ APPROXIMATION
A multigrid method for the Navier-Stokes and Boussinesq equations [REPT-89-17] N90-12886

BRANCHING (MATHEMATICS)
Numerical analysis of chaotic symbol sequences generated by parabolic and triangle maps of the interval [MPIS-22/1987] N90-13124

BREMSSTRAHLUNG
Proof of the feasibility of coherent and incoherent schemes for pumping a gamma-ray laser [AD-A212315] N90-12921

BRILLOUIN ZONES
Magnetically insulated electron flows in pulsed power systems [AD-A212746] N90-13196

BROADBAND
Wideband phase-locked angular modulator N90-12798

BROKEN SYMMETRY
Symmetry breaking phenomena in liquid Helium-4 [DE89-618886] N90-12685
Fractional charging and reentrance in granular superconductors N90-13248

BUBBLES
A computationally efficient modelling of laminar separation bubbles [NASA-CR-185854] N90-12872
Measurements of bubble properties using a multi-frequency sound field [AD-A212591] N90-13211

BUCKLING
Multilevel optimization with system Optsys [FFA-TN-1988-60] N90-12953

BUDGETING
Studies of the European transonic wind tunnel [ONERA-RSF-12/0694-GY] N90-13278

BURNERS
Characterization of nonpremixed turbulent bluff-body burner flames [PB89-229447] N90-12689

BURNING RATE
RSRM-3 (360L003) ballistics/mass properties report [NASA-CR-183716] N90-12651
Ballistics/mass properties [NASA-CR-183723] N90-12652

BUTANES
Survey of the response of standard limited streamer tubes over the complete range of three-component gas mixtures of isobutane, CO(sub 2), argon [DE89-016892] N90-12875

C

C-140 AIRCRAFT
The right wing of the LEFT airplane N90-12510
Simulated airline service experience with laminar-flow control leading-edge systems N90-12512

CABLES (ROPES)
Estimating the time to fatigue failure of mooring cables [PB89-220677] N90-12946

CALCIUM
Calcium displacement caused by electromagnetic fields [AD-A212690] N90-13023

CALCIUM CHLORIDES
Advanced calcium-thionyl chloride high-power battery [AD-A211856] N90-12846

CALCIUM COMPOUNDS
Advanced calcium-thionyl chloride high-power battery [AD-A211856] N90-12846

CALIBRATING
DSN 70-meter antenna microwave optics design and performance improvements. Part 2: Comparison with measurements N90-12800
NIST (National Institute of Standards and Technology) measurement services: The ac-dc difference calibrations [PB89-222616] N90-12845
Optimum data weighting and error calibration for estimation of gravitational parameters [NASA-TM-100737] N90-12985
Catalog of absolutely calibrated, range normalized, wideband, electric field waveforms from located lightning flashes in Florida: July 24 and August 14, 1985 data [AD-A212708] N90-13008

CANCELLATION
Performance analysis of large adaptive sidelobe canceller arrays with reused elements [AD-A212888] N90-12841

CANCER
Proceedings of the 10 May 1989 Antiproton Technology Workshop: Addendum [AD-A212804] N90-13227

CANTILEVER BEAMS
Analysis of the non-planar response of a cantilever, with the aid of computerized symbolic manipulation [AD-A212421] N90-13172

CAPACITANCE
Capacitive behavior in conducting polymers [AD-A212448] N90-12760

CAPACITORS
Advanced double layer capacitor [AD-A211977] N90-12688
Capacitive behavior in conducting polymers [AD-A212448] N90-12760
GaAs gate dynamic memory technology [AD-A212387] N90-13266

CAPILLARY FLOW
Vibration isolation technology: Sensitivity of selected classes of space experiments to residual accelerations [NASA-CR-185443] N90-12768

CAPTIVE TESTS
Pivotal mono wing cruise missile with wing deployment and fastener mechanism [AD-D014191] N90-12594

CARBON
An investigation of diamond film deposition in a premixed oxyacetylene flame [AD-A212595] N90-13268

CARBON DIOXIDE
Mechanisms of CO2 reduction metal and metal modified semiconductor electrodes [AD-A213169] N90-12712
Survey of the response of standard limited streamer tubes over the complete range of three-component gas mixtures of isobutane, CO(sub 2), argon [DE89-016892] N90-12875
Contribution of deforestation to atmospheric CO2 and reforestation as an option to control CO2 [DE89-017255] N90-12979
Effects of atmospheric mix and toxic fumes on military performance [PB89-223630] N90-13015

CARBON FIBER REINFORCED PLASTICS
Damage tolerance of CFRP sandwich panels [FFA-TN-1988-70] N90-12664
Textural and structural organization of the heat treated polymers: Mechanical properties relationships [ETN-89-95711] N90-12744

CARBON FIBERS
Project, implementation, and utilization of composite structures [ETN-89-95209] N90-12665
Surface treatments of carbon fibers in an organic environment. Finite element analysis of pull-out tests [ONERA-RT-7/3549-M] N90-12698
Analysis of carbon fiber's x ray microscopic structure [AD-A212215] N90-12752

CARBON MONOXIDE
Fundamental molecular data to support CARS diagnostics of temperature, pressure, and species concentration [AD-A212411] N90-12704
Computer simulation studies of the catalytic oxidation of carbon monoxide on platinum metals [PB89-223739] N90-12721
Effects of atmospheric mix and toxic fumes on military performance [PB89-223630] N90-13015

CARBON STEELS
Carbonitrition response of steel plates not destined for heat treatments [CETIM-106960] N90-12728

CARBON-CARBON COMPOSITES
Thermal stability of the carbon-carbon bond in ethylene adsorbed on Si(100): An isotopic mixing study [AD-A211591] N90-12691

CARBOXYLIC ACIDS
Electroactive polyaniline film deposited from non-aqueous media. 2: Effect of acid concentration in solutions [AD-A212084] N90-12737

CARDIOVASCULAR SYSTEM
Cardiovascular, renal, electrolyte, and hormonal changes in man during gravitational stress, weightlessness, and simulated weightlessness: Lower body positive pressure applied by the antigravity suit [NASA-TM-102232] N90-13013

CARRIER FREQUENCIES
Time-frequency factors in auditory perception [AD-A211491] N90-13016

CASE HISTORIES
The NASA experience in aeronautical R and D: Three case studies with analysis [AD-A211486] N90-12496

CASUALTIES
Prediction of thermal stress casualties [AD-A212356] N90-13022

CATALOGS
Publications of the National Institute of Standards and Technology, 1988 catalog [PB89-218382] N90-13279

CATALYSIS
Electron density modulation of catalytic metal centers by substituted aryl-isocyanide ligands [AD-A212875] N90-12708
Mechanisms of CO2 reduction metal and metal modified semiconductor electrodes [AD-A213169] N90-12712
Computer simulation studies of the catalytic oxidation of carbon monoxide on platinum metals [PB89-223739] N90-12721
Synthesis and high temperature chemistry of methylsilsesquioxane polymers produced by titanium catalyzed redistribution of methylhydridooligo- and polysiloxanes [AD-A212000] N90-12736
Transition metal catalyzed synthesis of organmetallic polymers [AD-A212133] N90-12740
Cosmic strings and baryon decay catalysis [NASA-CR-186074] N90-13299

CATHODOLUMINESCENCE
Photoelectron pumped phosphors [AD-A213202] N90-12912

CATIONS
Quartz crystal microbalance analysis. 1: Evidence of anion or cation insertion into electropolymerized conducting polymers
[AD-A212304] N90-12755
CAVITIES
Dynamics of an M-level atom interacting with cavity fields: Properties of photon statistics
[AD-A211321] N90-13213
CAVITY RESONATORS
Cold tests of quasi-optical gyrotron resonators
[AD-A212707] N90-12868
Cavity eigenmodes for the NIST/NRL (National Institute of Standards and Technology/Naval Research Laboratory) free electron laser
[AD-A212706] N90-12923
CDC CYBER 205 COMPUTER
Solving 3D block bidiagonal linear systems on vector computers
[CWI-NM-R8819] N90-13061
CELESTIAL MECHANICS
On mean elements for satellite orbits perturbed by the zonal harmonics of the geopotential
[AD-A212322] N90-12642
CELLS (BIOLOGY)
A statistical analysis of spatial point patterns, a case study
[CWI-MS-R8813] N90-13180
CENTRAL PROCESSING UNITS
The M/G/1 processor sharing queue as the almost sure limit of feedback queues
[REPT-89-32] N90-13044
Solving 3D block bidiagonal linear systems on vector computers
[CWI-NM-R8819] N90-13061
Area-universal networks
[AD-A211883] N90-13092
CENTRIFUGES
Cross-axis synchronous flow through coil planet centrifuge for large-scale preparative countercurrent chromatography
[PB89-200174] N90-12682
CERAMIC FIBERS
Oxide ceramic fibers by the sol-gel methods
[AD-A211315] N90-12742
CERAMICS
Tribological properties of ceramic/Ti3Al-Nb sliding couples for use as candidate seal materials to 700 deg C
[NASA-TM-102401] N90-12658
Laser probe vaporization/oxidation testing of high temperature composites
[AD-A211410] N90-12663
Spall resistance of alumina
[AD-A213213] N90-12735
Synthesis and high temperature chemistry of methylsilsesquioxane polymers produced by titanium catalyzed redistribution of methylhydridooligo- and polysiloxanes
[AD-A212000] N90-12736
Oxide ceramic fibers by the sol-gel methods
[AD-A211315] N90-12742
Pyrolytic production of ceramic composites from silicates
[ETCA-89-R-012] N90-12746
NBS/BAM (National Bureau of Standards/Bundesanstalt fuer Materialprufung) 1986 Symposium on Advanced Ceramics
[PB89-229074] N90-12747
Ion beam analysis of diffusion in polymer glasses
[AD-A212339] N90-12756
Effects of hot corrosion on the room temperature strength of structural ceramics
[AD-A212568] N90-12762
The 4th US Army Workshop on Low Heat Rejection Engines
[AD-A212378] N90-12942
The 4th US Army Workshop on Low Heat Rejection Engines
[AD-A212379] N90-12943
An air coupled transmission mode acoustic microscope for on-line non-destructive evaluation
[AD-A211416] N90-12947
Proceedings of the Army Symposium on Solid Mechanics, 1989: Mechanics of Engineered Materials and Applications
[AD-A211954] N90-12951
CERTIFICATION
Directory of International and Regional Organizations Conducting Standards-Related Activities, May 1989
[PB89-221147] N90-12776
CESSNA AIRCRAFT
Laminar flow: The Cessna perspective N90-12507
CHANNEL CAPACITY
Fellowships in information and stochastic systems
[AD-A212385] N90-13280
CHANNEL FLOW
Numerical experiments on transition control in wall-bounded shear flows N90-12536
Investigation of turbulent flow in highly curved ducts with application to turbomachinery components
[NASA-CR-186060] N90-12882
Evaluation of the near-wall k-epsilon turbulence model by comparison with direct simulations of turbulent channel flow
[AD-A212674] N90-12903
Superfluid phase slippage in (3)He-B flow through a narrow channel
[PB89-218986] N90-13258
CHANNELS (DATA TRANSMISSION)
Automatic communications channel interference monitoring
[RSRE-MEMO-4243] N90-12820
CHARACTERIZATION
Characterization and cycle tests of lightweight nickel electrodes
[NASA-TM-102399] N90-12696
Polymer characterization by electrohydrodynamic ionization mass spectrometry
[AD-A212130] N90-12739
CHARGE FLOW DEVICES
Rolls-Royce and ERCOFTAC
[PNR90600] N90-12615
Feedback charge amplifier integrated on the detector wafer
[REPT-89-037] N90-12852
CHARGED PARTICLES
Twistons
[RSRE-MEMO-4234] N90-13275
CHECKOUT
Truth maintenance systems and their implementation in PROLOG
[MEMO-INF-89-13] N90-13064
CHEMICAL ANALYSIS
Heat pipe and thermal energy storage and corrosion studies (1988)
[AD-A212655] N90-12706
CHEMICAL BONDS
Synthesis and high temperature chemistry of methylsilsesquioxane polymers produced by titanium catalyzed redistribution of methylhydridooligo- and polysiloxanes
[AD-A212000] N90-12736
Molecular dynamics of lipid bilayers
[AD-A211492] N90-13214
Interstitial formation, non-equilibrium and macroscopic processes in mercury cadmium telluride
[AD-A212412] N90-13267
CHEMICAL COMPOSITION
Fundamentals of middle atmospheric dynamics
[AD-A211747] N90-12988
Semiconductor measurement technology: Database for and statistical analysis of the interlaboratory determination of the conversion coefficient for the measurement of the interstitial oxygen content of silicon by infrared absorption
[PB89-221170] N90-13253
CHEMICAL EFFECTS
Role of chemical effects in daytime high latitude trough formation
[AD-A211772] N90-12989
CHEMICAL ENERGY
On the spectrum of the staggered Dirac operator at finite chemical potential
[ITFA-88-53] N90-13272
CHEMICAL EQUILIBRIUM
Rotational and vibrational nonequilibrium effects in rarefied, hypersonic flow
[NASA-CR-182559] N90-12498
CHEMICAL PROPERTIES
The multivalent beta'-aluminas
[AD-A212103] N90-12738
CHEMICAL PROPULSION
Present and future US and Soviet chemical missiles and chemical rocket projectiles
[AD-A212199] N90-12644
CHEMICAL REACTIONS
Chemical and photochemical reactivity in microemulsions and waterless microemulsions
[AD-A211776] N90-12692
Measurement and correlation of the solubility and diffusion coefficient for oxygen and chlorine in basic hydrogen peroxide
[AD-A212348] N90-12703
FLIC (FLame with Implicit Convection): A detailed, two-dimensional flame model
[AD-A212953] N90-12710
An investigation of the irradiation swelling mechanisms in refractory metals at high temperatures
[AD-A211406] N90-12719
Chemical treatment of epoxy resins to reduce moisture sensitivity and to improve the mechanical properties
[AD-A212360] N90-12758
Role of chemical effects in daytime high latitude trough formation
[AD-A211772] N90-12989
Growth and characterization of zinc sulfide films by conversion of zinc oxide films with H2S
[AD-A213345] N90-13271
CHIPS (ELECTRONICS)
Optical clock distribution to VLSI chips
[AD-A212269] N90-13264
CHIRAL DYNAMICS
Index formulas for generalized Wiener-Hopf operators and Boson-Fermion correspondence in 2N dimensions
[CWI-PM-R8811] N90-13141
CHLORINE
Measurement and correlation of the solubility and diffusion coefficient for oxygen and chlorine in basic hydrogen peroxide
[AD-A212348] N90-12703
CHROMATOGRAPHY
Cross-axis synchronous flow through coil planet centrifuge for large-scale preparative countercurrent chromatography
[PB89-200174] N90-12682
CHROMIUM ALLOYS
The effects of heat treatment after welding on the functional properties of assemblies of CrMo alloys. Heat treatment of a mixed assembly of A48 and 10CD9.10 alloys
[CETIM-104320] N90-12724
CHROMIUM COMPOUNDS
Study of palladium and chromium silicides formation in liquid phase and in solid phase
[LAAS-89040] N90-12695
CIRCADIAN RHYTHMS
Effects of a time zone shift of nine hours on the circadian rhythms in cockpit aircrew members on longhaul flights
[DLR-FB-89-31] N90-13019
CIRCUIT DIAGRAMS
Built-in generation for CMOS circuits
[IMAG-RR-736-I] N90-12855
The application of artificial intelligence techniques to tracing the interconnections in an integrated circuit
[TELECOM-PARIS-89-E002] N90-13105
CIRCUITS
Simulation of circuits adapted to signal processing
[TELECOM-PARIS-89-E001] N90-12811
CIRCULAR ORBITS
An analytic development of orbit determination for a distant, planetary orbiter N90-12787
CIRCULATION DISTRIBUTION
A formatting style for typesetting and distributing draft international standards
[NPL-DITC-143/89] N90-13059
CIVIL AVIATION
Simulated airline service experience with laminar-flow control leading-edge systems N90-12512
Fine resolution errors in secondary surveillance radar altitude reporting amongst aircraft transmitting the conspicuity codes 4321 and 4322
[RSRE-88004] N90-12816
CLAMPS
Improvement of rules relating to clamp calculations
[CETIM-110610] N90-12939
CLEARANCES
Advanced clearance control systems --- blade tips
[PNR90553] N90-12601
Dynamic tip clearance measurements in axial flow compressors
[PNR90597] N90-12612
CLIMATE
Toward an understanding of global change: Initial priorities for US contributions to the International Geosphere-Biosphere Program
[NASA-CR-185873] N90-12980
Central Sudan surface wind data and climate characteristic
[KNMI-WR-88-01] N90-13000
Current velocity and hydrographic observations in the southwestern North Atlantic Ocean: Subtropical Atlantic Climate Studies (STACS), 1988
[PB89-230825] N90-13010
CLIMATE CHANGE
Contribution of deforestation to atmospheric CO2 and reforestation as an option to control CO2
[DE89-017255] N90-12979
Toward an understanding of global change: Initial priorities for US contributions to the International Geosphere-Biosphere Program
[NASA-CR-185873] N90-12980
Sensitivity of a regional oxidant model to variations in climate parameters, volume 1 and 2
[PB89-224943] N90-12981

South Pole surface radiation balance measurements, April 1986 to February 1988
[PB89-224018] N90-12993
CLIMATOLOGY
Climatological data for the North Sea based on observations by voluntary observing ships over the period 1961-1980
[KNMI-WR-89-02] N90-13002
Cloud cover determination in polar regions from satellite imagery
[NASA-CR-186096] N90-13003
Current velocity and hydrographic observations in the southwestern North Atlantic Ocean: Subtropical Atlantic Climate Studies (STACS), 1988
[PB89-230825] N90-13010
CLOCKS
Stable Kalman filters for processing clock measurement data N90-12801
Optical clock distribution to VLSI chips
[AD-A212269] N90-13264
CLOSED CYCLES
Development of a low noise 10 K J-T refrigeration system
[AD-A213347] N90-12779
CLOSURE LAW
A point in betaZ/Z not contained in a maximal orbit closure
[REPT-89-26] N90-13127
CLOUD COVER
Cloud cover determination in polar regions from satellite imagery
[NASA-CR-186096] N90-13003
CLOUDS (METEOROLOGY)
Performance of laminar-flow leading-edge test articles in cloud encounters N90-12511
Zonal average cloud characteristics for global atmospheric chemistry modeling
[CM-76] N90-12992
Analysis and modeling of summertime convective cloud and precipitation structure over the Southeastern United States
[NASA-CR-185436] N90-12996
Mesoscale acid deposition modeling studies
[NASA-CR-4262] N90-13228
CLUSTER ANALYSIS
A statistical analysis of spatial point patterns, a case study
[CWI-MS-R8813] N90-13180
CMOS
Built-in generation for CMOS circuits
[IMAG-RR-736-I] N90-12855
European Solid State Device Research Conference (18th) ESSDERC 88 held in Montpellier, France on 13-16 September 1988
[AD-A210618] N90-13250
COATINGS
The 4th US Army Workshop on Low Heat Rejection Engines
[AD-A212379] N90-12943
An investigation of diamond film deposition in a premixed oxyacetylene flame
[AD-A212595] N90-13268
COCKPIT SIMULATORS
Spatial tests for aviators
[IZF-1988-15] N90-13041
COCKPITS
Integration of a centralized multiplexed control unit into the cockpit of an aircraft
[F6150-DT410-1-88329] N90-12622
CODING
Wire grid modeling of the linear tapered slot antenna
[AD-A212977] N90-12842
Subspace iteration algorithms in FORTRAN 77 and FORTRAN 8x
[AD-A212275] N90-13083
Magnetically insulated electron flows in pulsed power systems
[AD-A212746] N90-13196
COEFFICIENTS
A simulation study of the overdetermined geodetic boundary value problem using collocation
[AD-A211785] N90-12990
Operator product coefficients in non-diagonal conformal field theories
[NIKHEF-H/88-19] N90-13224
COGNITION
Individual differences in associative learning and forgetting
[AD-A212765] N90-13034
Spatial tests for aviators
[IZF-1988-15] N90-13041
COHERENT RADIATION
Proof of the feasibility of coherent and incoherent schemes for pumping a gamma-ray laser
[AD-A212882] N90-12924
COLD PRESSING
Cold press lubrication: Fine tuning of the CETIM Forgelub test
[CETIM-105160] N90-12938
Increased fragility of deep pressed thin plates
[CETIM-13-Y-313] N90-12962
COLD SURFACES
Tunneling microscopy of superconductors and tunneling barriers
[AD-A212120] N90-13257
COLD WEATHER
Effects of serial wet-dry-wet cold exposure: Thermal balance, physical activity, and cognitive performance
[AD-A212704] N90-13025
COLLISIONAL PLASMAS
Research on heating, instabilities, turbulence and RF emission from electric field dominated plasmas
[AD-A212122] N90-13243
Time evolution of the electron swarm energy distribution function
[AD-A212967] N90-13247
COLLOCATION
A simulation study of the overdetermined geodetic boundary value problem using collocation
[AD-A211785] N90-12990
COMBINATORIAL ANALYSIS
On the decoder error probability of linear codes N90-12793
COMMAND AND CONTROL
Requirements specification with Petri nets using the cube tool methodology
[AD-A212190] N90-12829
Design and performance of an on-satellite laser diagnostic system for a free space optical heterodyne frequency-shift-keyed communication system
[AD-A211986] N90-12915
Telerobotic control for teams of semi-autonomous agents, phase 1
[AD-A211648] N90-13037
Algorithm development for SDI weapons system allocation
[AD-A212973] N90-13090
COMMUNICATION NETWORKS
A literature study of wave propagation in the 1-60 GHz range. Application to transportable military communication systems
[FEL-1988-47] N90-12825
COMPACTING
RTM user's guide
[NASA-CR-186091] N90-13065
COMPARISON
Perceived urgency of warning signals determined using a forced choice pair comparison technique
[RAE-TM-MM-12] N90-13206
COMPENSATORS
Null offset voltage compensator for operational amplifier
[AD-D014189] N90-12859
Towards a complete local solution of the nonlinear model matching problem
[MEMO-781] N90-13166
COMPILERS
A compilation strategy for numerical programs based on partial evaluation
[AD-A212759] N90-13175
COMPLETENESS
Proving total correctness of recursive procedures
[CWI-CS-R8904] N90-13075
COMPLEX COMPOUNDS
A graph-theoretical approach to block-copolymer complexes. Part 3: Loops and cycles
[MEMO-778-PT-3] N90-12750
Synthesis and characterization of new low-dimensional metal complex conductors
[AD-A213189] N90-12871
COMPLEX SYSTEMS
Explicit formulas for Hankel norm approximations of infinite-dimensional systems
[TW-289] N90-13167
COMPLEXITY
Kolmogorov complexity and its applications
[CWI-CS-R8901] N90-13191
COMPONENT RELIABILITY
The role of component testing
[PNR90589] N90-12608
COMPOSITE MATERIALS
Material requirements for future aeroengines
[PNR90595] N90-12610
Optical fibre witnesses of fatigue damage in composite materials N90-12660
Laser probe vaporization/oxidation testing of high temperature composites
[AD-A211410] N90-12663
Multilayer theory for delamination analysis of a composite curved bar subjected to end forces and end moments
[NASA-TM-4139] N90-12669
A study of the impact of a ball bearing on a long fiber composite plate with a carbon matrix, part 2
[ETCA-88-R-088-PT-2] N90-12673
Modeling of the dielectric behavior of composite materials
[CERT-1/1398-MO] N90-12674
Oxide ceramic fibers by the sol-gel methods
[AD-A211315] N90-12742
Pyrolytic production of ceramic composites from silicates
[ETCA-89-R-012] N90-12746
An air coupled transmission mode acoustic microscope for on-line non-destructive evaluation
[AD-A211416] N90-12947
Proceedings of the Army Symposium on Solid Mechanics, 1989: Mechanics of Engineered Materials and Applications
[AD-A211954] N90-12951
RTM user's guide
[NASA-CR-186091] N90-13065
COMPOSITE PROPELLANTS
RSRM-3 (360L003) ballistics/mass properties report
[NASA-CR-183716] N90-12651
Ballistics/mass properties
[NASA-CR-183723] N90-12652
COMPOSITE STRUCTURES
Evaluation of a damaged F/A-18 horizontal stabilator
[AD-A212573] N90-12597
Project, implementation, and utilization of composite structures
[ETN-89-95209] N90-12665
A thermoelastic transversely isotropic thick walled cylinder/disk application: An analytical solution and study
[NASA-TM-102320] N90-12950
COMPOSITION (PROPERTY)
Modeling of the dielectric behavior of composite materials
[CERT-1/1398-MO] N90-12674
COMPRESSIBILITY
Compressibility of heavy nuclei at high temperatures
[KVI-792] N90-13217
COMPRESSIBLE BOUNDARY LAYER
Numerical solutions of the compressible 3-D boundary-layer equations for aerospace configurations with emphasis on LFC N90-12534
COMPRESSIBLE FLOW
Flow quality measurements in compressible subsonic flows N90-12521
Flux-corrected transport algorithms for two-dimensional compressible magnetohydrodynamics
[AD-A212757] N90-13246
COMPRESSING
Temperature effects in shock consolidation of metal powders
[DE89-016782] N90-12716
COMPRESSION TESTS
Nonlinear theories concerning laminated composites under compression with delamination
[ONERA-RT-19/3542-RY-081-R] N90-12672
Orthotropic elasto-plastic behavior of AS4/APC-2 thermoplastic composite in compression
[NASA-CR-186080] N90-12959
Mathematical simulation of dynamic compression tests using the Hopkinson bar method
[ISL-R-128/87] N90-12960
COMPRESSIVE STRENGTH
Orthotropic elasto-plastic behavior of AS4/APC-2 thermoplastic composite in compression
[NASA-CR-186080] N90-12959
COMPRESSOR BLADES
Blading design for multi-storage HP compressor
[PNR90602] N90-12616
COMPRESSOR EFFICIENCY
Dynamic tip clearance measurements in axial flow compressors
[PNR90597] N90-12612
COMPRESSORS
Stage effects on stalling and recovery of a high-speed 10-stage axial-flow compressor N90-12600
COMPTON EFFECT
Proof of the feasibility of coherent and incoherent schemes for pumping a gamma-ray laser
[AD-A212315] N90-12921
COMPUTATION
Analysis of carbon fiber's x ray microscopic structure
[AD-A212215] N90-12752
Direction-of-arrival calculations at VLF/LF (Very Low Frequency/Low Frequency)
[AD-A212620] N90-12833

Comments on the use of LOWTRAN in transmission calculations for sites with the ground elevated relative to sea level
[AD-A212724] N90-12995
Labeled trees and the efficient computation of derivations
[NASA-CR-185386] N90-13113
Multivariable divided difference and B-splines
[MEMO-772] N90-13160
On new methods for computing with multivariate B-splines
[MEMO-783] N90-13183
Direct computation of 3D shape invariants and the focus of expansion
[AD-A212386] N90-13195
Ground states of a two-dimensional charged-boson system
[AD-A212363] N90-13226

COMPUTATIONAL FLUID DYNAMICS
Rotational and vibrational nonequilibrium effects in rarefied, hypersonic flow
[NASA-CR-182559] N90-12498
Numerical algorithms for steady and unsteady incompressible Navier-Stokes equations
[NASA-CR-186039] N90-12499
Research in Natural Laminar Flow and Laminar-Flow Control, part 2
[NASA-CP-2487-PT-2] N90-12519
Sensitivity of LFC techniques in the non-linear regime N90-12533
Numerical solutions of the compressible 3-D boundary-layer equations for aerospace configurations with emphasis on LFC N90-12534
Numerical experiments on transition control in wall-bounded shear flows N90-12536
CFD methods for drag prediction and analysis currently in use in UK
[RAE-TM-AERO-2146] N90-12563
Aerodynamic test and analysis of a slender generic missile configuration
[AD-A212522] N90-12567
Numerical study of three-dimensional spatial instability of a supersonic flat plate boundary layer
[NASA-CR-181931] N90-12874
A multigrid method for the Navier-Stokes and Boussinesq equations
[REPT-89-17] N90-12886
An implicit Navier-Stokes solver optimised for a vector-parallel computer
[VKI-TN-169] N90-12890
A knowledge-based approach to automated flow-field zoning for computational fluid dynamics
[NASA-TM-101072] N90-13048

COMPUTATIONAL GRIDS
Solution of the thin-layer Navier-Stokes equations for laminar transonic flow
[PB89-221600] N90-12879
A multigrid method for the Navier-Stokes and Boussinesq equations
[REPT-89-17] N90-12886
Multigrid Monte Carlo in an external U(1) gauge field
[NIKHEF-ITFA-88-52] N90-13114
Multigrid solution method for the Euler equations
[PB89-219483] N90-13116
Local mode smoothing analysis of various incomplete factorization iterative methods in two dimensions
[REPT-89-36] N90-13129

COMPUTER AIDED DESIGN
The design of an airfoil for a high-altitude, long-endurance remotely piloted vehicle N90-12545
Supersonic boundary-layer transition on the LaRC F-106 and the DFRF F-15 aircraft. Part 2: Aerodynamic predictions N90-12559
On the precision and reliability of GPS networks computed using the double difference observable
[ETN-89-95719] N90-12571
Case study on rapid software prototyping and automated software generation: An inertial navigation system
[AD-A212272] N90-12578
A vision of the future: The new engine technology
[PNR90566] N90-12603
A computer integrated approach to dimensional inspection
[PNR90596] N90-12611
Rolls-Royce and ERCOFTAC
[PNR90600] N90-12615
Application of the moment method to the design of slotted waveguide array antennas N90-12780
A theoretical method for the mechanical calculation of heat exchangers with sliding heads, phase 1 study
[CETIM-110240-PHASE-1] N90-12896
Computer oriented methods of multibody dynamics for application in vehicle technology
[DFVLR-FB-89-17] N90-13060
NAUTILE: A physical design environment based on an object-oriented data manager
[IMAG-RR-737-I] N90-13094
The application of artificial intelligence techniques to tracing the interconnections in an integrated circuit
[TELECOM-PARIS-89-E002] N90-13105

COMPUTER AIDED MANUFACTURING
A vision of the future: The new engine technology
[PNR90566] N90-12603
What is the balance sheet for investment in automated manufacturing
[CETIM-105490] N90-13071

COMPUTER AIDED MAPPING
Characterizing termination of logic problems with level mappings
[CWI-CS-R8912] N90-13077

COMPUTER DESIGN
Area-universal networks
[AD-A211883] N90-13092

COMPUTER GRAPHICS
Visualization of high-resolution digital terrain
[AD-A212149] N90-12971
Research in computer vision for autonomous systems
[AD-A212420] N90-13235

COMPUTER INFORMATION SECURITY
A Z specification of the MaCHO interface editor
[RSRE-MEMO-4247] N90-13067

COMPUTER NETWORKS
Telescience Testbed Pilot Program
[NASA-CR-184997] N90-13047
A formatting style for typesetting and distributing draft international standards
[NPL-DITC-143/89] N90-13059
Area-universal networks
[AD-A211883] N90-13092
Work-preserving emulations of fixed-connection networks
[AD-A211915] N90-13093
Extended performability modeling using dynamic queing networks
[MEMO-INF-89-15] N90-13099
Activities report of the Kernfysisch Versneller Instituut
[ETN-89-95752] N90-13219

COMPUTER PROGRAM INTEGRITY
Proving total correctness of recursive procedures
[CWI-CS-R8904] N90-13075

COMPUTER PROGRAMMING
Case study on rapid software prototyping and automated software generation: An inertial navigation system
[AD-A212272] N90-12578
An expert system for VM performance analysis
[REPT-89-30] N90-13045
ISI's (Information Sciences Institute) SDI architecture simulator: Initial prototype user interface
[AD-A211325] N90-13053
Building a software package for solving large sparse nonlinear systems of equations
[AD-A211758] N90-13055
Mathematical equivalence in a primitive Ella
[RSRE-MEMO-4225] N90-13066
A table-driven approach to fast context-free parsing
[AD-A212210] N90-13082
Software Engineering Exercise (SEE) guidelines
[AD-A212510] N90-13085
Toward a formal model of the design and evolution of software
[AD-A212533] N90-13087
NTRFACE for MAGIC
[AD-A212858] N90-13112
A modified Newton method for unconstrained minimization
[AD-A212752] N90-13174

COMPUTER PROGRAMS
Additions and corrections to SUPER: A program for calculating steady and oscillatory supersonic flow over a thin wing, tail plane and fin
[AD-A211771] N90-12501
Development of a VSAERO (Vortex Separation Aerodynamics) model of the F/A-18
[AD-A212442] N90-12566
FPG2: A flight profile generator program
[AD-A212408] N90-12595
Rolls-Royce and ERCOFTAC
[PNR90600] N90-12615
Numerical analysis of notch test damage to laminated composite plates submitted to uniaxial traction
[CETIM-107310] N90-12675
IBM PC analysis of polarization resistance data
[AD-A212294] N90-12732
Specification of Viper1 in Z
[RSRE-MEMO-4195] N90-12817
Specification of Viper2 in Z
[RSRE-MEMO-4217] N90-12819
Aircraft SAR simulation Sargen 1.0
[FEL-1989-44] N90-12823
Specification for radar free-space detection range and free-space intercept range calculations
[AD-A213158] N90-12843
Automated Steerable Nulling Antenna Processor (SNAP) model
[PB89-231740] N90-12937
Improvement of rules relating to clamp calculations
[CETIM-110610] N90-12939
Visualization of high-resolution digital terrain
[AD-A212149] N90-12971
A hybrid architecture for feature labelling of oceanographic satellite images
[AD-A212236] N90-12975
Cloud cover determination in polar regions from satellite imagery
[NASA-CR-186096] N90-13003
The effect of concurrent strength and endurance training on electromechanical delay, maximum voluntary contraction, and rate of force development
[AD-A213316] N90-13028
Spacecraft Orbit Design and Analysis (SODA), version 1.0 user's guide
[NASA-CR-181932] N90-13050
Characterizing termination of logic problems with level mappings
[CWI-CS-R8912] N90-13077
Interactive computer program for the generation of enthalpy-entropy and temperature-entropy charts of nitrogen and hydrogen
[DLR-FB-89-27] N90-13081
Subspace iteration algorithms in FORTRAN 77 and FORTRAN 8x
[AD-A212275] N90-13083
Software Engineering Exercise (SEE) guidelines
[AD-A212510] N90-13085
NAUTILE: A physical design environment based on an object-oriented data manager
[IMAG-RR-737-I] N90-13094
On modeling resources in multiprocessor systems
[MEMO-INF-88-33] N90-13095
Numerical evaluation of the far field wave pattern of the radiation Green's function
[AD-A212839] N90-13176
The Painleve test for nonlinear ordinary and partial differential equations
[AD-A212894] N90-13177
Research on heating, instabilities, turbulence and RF emission from electric field dominated plasmas
[AD-A212122] N90-13243
Semiconductor measurement technology: A software program for aiding the analysis of ellipsometric measurements, simple models
[PB89-235923] N90-13261

COMPUTER SYSTEMS DESIGN
State of the art of human/machine dialog tool prototypes
[TELECOM-PARIS-89-H001] N90-13038
NAUTILE: A physical design environment based on an object-oriented data manager
[IMAG-RR-737-I] N90-13094
A compilation strategy for numerical programs based on partial evaluation
[AD-A212759] N90-13175

COMPUTER SYSTEMS PERFORMANCE
The computer age and traditional approximate, analytical methods N90-12772
Specification of Viper2 in Z
[RSRE-MEMO-4217] N90-12819
An expert system for VM performance analysis
[REPT-89-30] N90-13045
Performance evaluations of a parallel and expandable database computer: The multi-backend database computer
[AD-A212761] N90-13046
Software Engineering Exercise (SEE) guidelines
[AD-A212510] N90-13085
Extended performability modeling using dynamic queing networks
[MEMO-INF-89-15] N90-13099
A compilation strategy for numerical programs based on partial evaluation
[AD-A212759] N90-13175

COMPUTER SYSTEMS PROGRAMS
Truth maintenance systems and their implementation in PROLOG
[MEMO-INF-89-13] N90-13064

COMPUTER SYSTEMS SIMULATION
The comparison of the airbase simulation models airbase and sustained
[FEL-1988-66] N90-12629

COMPUTER TECHNIQUES
Calculation of the odd and even integral components of the wave resistance Green's function
[AD-A212384] N90-12900
Abstract grammars based on transductions
[MEMO-INF-89-7-REV] N90-13063

Trace theory --- concurrent processing
[MEMO-INF-89-16] N90-13100
NTRFACE for MAGIC
[AD-A212858] N90-13112

COMPUTER VISION
Development of an integrated mobile robot system at CMU (Carnegie-Mellon University)
[AD-A212555] N90-12944
Parallel and deterministic algorithms from MRF (Markov Random Fields): Surface reconstruction and integration
[AD-A212457] N90-13084
Research in computer vision for autonomous systems
[AD-A212420] N90-13235

COMPUTERIZED SIMULATION
Development and evaluation at ATCEU of executive and support operations, phase 4A/3D --- ATCEU (Air Traffic Control Evaluation Unit)
[CAA-PAPER-88017] N90-12572
Route data representation for ATC simulation experiments
[RSRE-MEMO-4133] N90-12576
RTSIN1: A model of a strapdown INS on a two-axis rate table
[AD-A212406] N90-12579
Real-time simulation of an F110/STOVL turbofan engine
[NASA-TM-102409] N90-12618
Analysis and simulation of dynamics of spacecraft power systems N90-12653
A study of the impact of a ball bearing on a long fiber composite plate with a carbon matrix, part 2
[ETCA-88-R-088-PT-2] N90-12673
Properties of Lennard-Jones mixtures at various temperatures and energy ratios with a size ratio of two
[PB89-235204] N90-12697
FLIC (FLame with Implicit Convection): A detailed, two-dimensional flame model
[AD-A212953] N90-12710
Computer simulation studies of the catalytic oxidation of carbon monoxide on platinum metals
[PB89-223739] N90-12721
Synthesis and crystallization behavior of fluoride glasses
[AD-A212142] N90-12741
Ultrastructure processing and characterization of polymers
[AD-A211460] N90-12743
Simulation of circuits adapted to signal processing
[TELECOM-PARIS-89-E001] N90-12811
Aircraft SAR simulation Sargen 1.0
[FEL-1989-44] N90-12823
Description and results of a multihop NACS simulation
[FEL-1988-46] N90-12824
A 2-MeV microwave thermionic gun
[DE89-015640] N90-12844
Improved 2D numerical simulation model for strongly coupled heat and fluid flow in a thermal storage
[PB89-218879] N90-12878
Analysis of high speed pneumatic actuation systems under rotary directional on-off flow control N90-12926
Mathematical simulation of dynamic compression tests using the Hopkinson bar method
[ISL-R-128/87] N90-12960
Telerobotic control for teams of semi-autonomous agents, phase 1
[AD-A211648] N90-13037
ISI's (Information Sciences Institute) SDI architecture simulator: Initial prototype user interface
[AD-A211325] N90-13053
RTM user's guide
[NASA-CR-186091] N90-13065
Computer oriented methods of multibody dynamics for application in vehicle technology
[DFVLR-FB-89-17] N90-13080
Formal calculations and parallesism. Solving linear systems
[ETN-89-95499] N90-13098
Real-time robot motion: The VLSI implementation via transputers
[RR-364] N90-13104
LAIOS: A multiprocessor network for artificial intelligence applications
[ETN-89-95498] N90-13109
Analysis of the non-planar response of a cantilever, with the aid of computerized symbolic manipulation
[AD-A212421] N90-13172
The process e(-)p giving gamma e(-)p as a fast luminosity for the HERA collider
[NIKHEF-H/88-13] N90-13223
Particle transport simulation for spaceborne, NaI gamma-ray spectrometers
[AD-A205150] N90-13292
Evolution of domain walls in the early universe
[NASA-CR-186076] N90-13297

CONCATENATED CODES
A performance comparison between block interleaved and helically interleaved concatenated coding systems N90-12792

CONCENTRATION (COMPOSITION)
Electroactive polyaniline film deposited from non-aqueous media. 2: Effect of acid concentration in solutions
[AD-A212084] N90-12737

CONCORDE AIRCRAFT
The next generation supersonic transport engine: Critical issues
[PNR90576] N90-12605

CONCURRENT PROCESSING
A simple definition for parallel composition of prime event structures
[CWI-CS-R8903] N90-13074
Trace theory --- concurrent processing
[MEMO-INF-89-16] N90-13100
Modular specifications in process algebra with curious queues
[CWI-CS-R8821] N90-13152
An algebra for process creation
[CWI-CS-R8907] N90-13155

CONDITIONING (LEARNING)
Individual differences in associative learning and forgetting
[AD-A212765] N90-13034

CONFERENCES
Research in Natural Laminar Flow and Laminar-Flow Control, part 1
[NASA-CP-2487-PT-1] N90-12503
Research in Natural Laminar Flow and Laminar-Flow Control, part 2
[NASA-CP-2487-PT-2] N90-12519
Research in Natural Laminar Flow and Laminar-Flow Control, part 3
[NASA-CP-2487-PT-3] N90-12539
Guidance and Control Panel Symposium on Guidance and Control of Unmanned Air Vehicles
[AGARD-AR-260] N90-12623
Proceedings of the DOD Workshop on the Manufacturing/Producibility of Organic Matrix Composites
[AD-A212577] N90-12680
NBS/BAM (National Bureau of Standards/Bundesanstalt fuer Materialprufung) 1986 Symposium on Advanced Ceramics
[PB89-229074] N90-12747
Laser Induced Damage in Optical Materials: 1987
[PB89-221162] N90-12913
The 4th US Army Workshop on Low Heat Rejection Engines
[AD-A212379] N90-12943
Proceedings of the Army Symposium on Solid Mechanics, 1989: Mechanics of Engineered Materials and Applications
[AD-A211954] N90-12951
Exertional heatstroke: An international perspective. An introduction: The role of exercise in the etiology of exertional heatstroke
[AD-A212242] N90-13020
Sound Localization by Human Observers symposium proceedings
[AD-A212877] N90-13026
International Conference on Operator Theory: Advances and applications
[AD-A212341] N90-13170
International Conference on Fixed Point Theory and Applications
[AD-A212369] N90-13171
Seminars of Applied Physics, Materials Physics and Biomedical Engineering, 1989
[PB89-218572] N90-13192
Proceedings of the 10 May 1989 Antiproton Technology Workshop: Addendum
[AD-A212804] N90-13227
Workshop on Recent Progress in Surface and Volume Scattering
[AD-A212455] N90-13236
European Solid State Device Research Conference (18th) ESSDERC 88 held in Montpellier, France on 13-16 September 1988
[AD-A210618] N90-13250

CONFINEMENT
Thermal initiation of confined primary explosives with a proton beam
[AD-A212954] N90-12767

CONFORMAL MAPPING
Operator product coefficients in non-diagonal conformal field theories
[NIKHEF-H/88-19] N90-13224

CONGRESSIONAL REPORTS
Departments of Veterans Affairs and Housing and Urban Development, and Independent Agencies Appropriations Bill, 1990
[H-REPT-101-150] N90-13281
National Aeronautics and Space Administration N90-13282
Fiscal year 1990 authorization request and budget estimates for the National Aeronautics and Space Administration
[GPO-96-945] N90-13283
Departments of Veterans Affairs and Housing and Urban Development, and Independent Agencies Appropriation Bill, 1990
[S-REPT-101-128] N90-13284
The 1990 National Aeronautics and Space Administration Authorization
[GPO-98-466] N90-13285
Department of Veterans Affairs and Housing and Urban Development, and Independent Agencies Appropriations Act, 1990
[HR-2916-PP] N90-13286
National Aeronautics and Space Administration N90-13287
National Aeronautics and Space Administration Authorization Act, fiscal year 1990
[S-REPT-101-157] N90-13288
National Aeronautics and Space Administration Authorization Act, fiscal year 1990
[S-REPT-101-157] N90-13289
NASA technology applications
[GPO-99-412] N90-13290

CONICAL FLOW
Some observations on transitory stall in conical diffusers
[NASA-TM-102387] N90-12561

CONSISTENCY
Semantics and consistency of rule-based expert systems
[CWI-CS-R8824] N90-13153

CONSOLIDATION
Temperature effects in shock consolidation of metal powders
[DE89-016782] N90-12716

CONTAINMENT
An apparatus for the electrodynamic containment of charged macroparticles N90-12789

CONTAMINANTS
Standard method for measurement of nonvolatile residue on surfaces
[AD-A213324] N90-12714
Effects of atmospheric mix and toxic fumes on military performance
[PB89-223630] N90-13015

CONTINUITY (MATHEMATICS)
An algebra for process creation
[CWI-CS-R8907] N90-13155

CONTINUUMS
A point in betaZ/Z not contained in a maximal orbit closure
[REPT-89-26] N90-13127

CONTRACT MANAGEMENT
Studies of the European transonic wind tunnel
[ONERA-RSF-12/0694-GY] N90-13278

CONTRACTION
The effect of concurrent strength and endurance training on electromechanical delay, maximum voluntary contraction, and rate of force development
[AD-A213316] N90-13028

CONTROL EQUIPMENT
Integration of a centralized multiplexed control unit into the cockpit of an aircraft
[F6150-DT410-1-88329] N90-12622

CONTROL STABILITY
Wind tunnel results of the low-speed NLF(1)-0414F airfoil N90-12541

CONTROL SYSTEMS DESIGN
Advanced clearance control systems --- blade tips
[PNR90553] N90-12601
Spark camera annotation and control system for the BRL (Ballistic Research Laboratory) Transonic Range Facility
[AD-A212266] N90-12633
Automated monitor and control for deep space network subsystems N90-12794
Self-tuning control of nonlinear Armax models --- Autoregressive Moving Average with eXogeneous (ARMAX) inputs
[RR-362] N90-12930
Visual perception processing in a hierarchical control system: Level 1
[PB89-221188] N90-13101
Identification of robot dynamics: A parallel processing approach
[RR-361] N90-13103

CONTROLLERS
Automated monitor and control for deep space network subsystems N90-12794
Self-tuning control of nonlinear Armax models — Autoregressive Moving Average with eXogeneous (ARMAX) inputs
[RR-362] N90-12930
CONVECTIVE HEAT TRANSFER
Phase change material for spacecraft thermal management
[AD-A211404] N90-12648
FLIC (FLame with Implicit Convection): A detailed, two-dimensional flame model
[AD-A212953] N90-12710
Prediction of thermal stress casualties
[AD-A212356] N90-13022
CONVERGENCE
An algebraic characterization of B-convergent Runge-Kutta methods
[CWI-NM-R8901] N90-13133
Tail triviality for sums of stationary random variables
[CWI-MS-R8810] N90-13143
On a rate of convergence of the multiknapsack value function
[CWI-MS-R8812] N90-13144
On the Hellinger type distances for filtered experiments
[CWI-MS-R8818] N90-13146
Note on the convergence of simulated annealing algorithms
[MEMO-774] N90-13162
Berry-Esseen rates and bootstrap results for generalized L-statistics
[CWI-MS-R8808] N90-13179
COOLING
Estimation of time to maximum supercooling during dynamic frazil ice formation
[AD-A212204] N90-12699
A closed-cycle refrigerator for cooling maser amplifiers below 4 Kelvin N90-12797
COPOLYMERIZATION
Curable polyether compositions
[AD-D014200] N90-12679
COPOLYMERS
Curable polyether compositions
[AD-D014200] N90-12679
Ultrastructure processing and characterization of polymers
[AD-A211460] N90-12743
A graph-theoretical approach to block-copolymer complexes. Part 3: Loops and cycles
[MEMO-778-PT-3] N90-12750
Synthesis of energetic single phase and multi-phase polymers
[AD-A212539] N90-12761
A center for advanced electrical and structural polymers
[AD-A212853] N90-12764
COPPER ALLOYS
Determination of the gaseous hydrogen ductile-brittle transition in copper-nickel alloys
[NASA-TM-86494] N90-12715
COPPER OXIDES
Resistivity measurements of superconducting materials
[PB89-225700] N90-12656
Composite vs constituent particle aspects of hole motion in the CuO2 plane
[DE89-618864] N90-13251
CORONAGRAPHS
Optical detection of space debris using a large achromatic coronagraph
[AD-A211362] N90-12647
The SOHO mission. Scientific and technical aspects of the instruments
[ESA-SP-1104] N90-13302
UVCS: An Ultraviolet Coronagraph Spectrometer for SOHO N90-13310
LASCO: A wide-field white light and spectrometric coronagraph for SOHO N90-13311
CORROSION
Heat pipe and thermal energy storage and corrosion studies (1988)
[AD-A212655] N90-12706
Development of an inventory of materials potentially sensitive to ambient atmospheric acidity in the South Coast Air Basin
[PB89-224604] N90-12982
CORROSION PREVENTION
Corrosion and corrosion inhibition of metals/alloys in methylphosphonic difluoride and decontaminating solutions
[AD-A212404] N90-12734
Polyelectrolyte-diffused zinc phosphate conversion coatings and polyacid coupling primers for corrosion protection of steel and aluminum, and alkali-catalyzed hydrolysis of polyimide-based materials
[AD-A212240] N90-12754
CORROSION RESISTANCE
How the common practice of heating plates of austenitic stainless steel during cooling affects their mechanical properties
[CETIM-104500] N90-12725
Corrosion and corrosion inhibition of metals/alloys in methylphosphonic difluoride and decontaminating solutions
[AD-A212404] N90-12734
COSMIC RAYS
Research in cosmic and gamma ray astrophysics
[NASA-CR-185451] N90-13316
The cosmic radiation effects and activation monitor
[RAE-TM-SPACE-364] N90-13318
COSMOLOGY
Evolution of domain walls in the early universe
[NASA-CR-186076] N90-13297
Small scale structure on cosmic strings
[NASA-CR-186075] N90-13298
Cosmic strings and baryon decay catalysis
[NASA-CR-186074] N90-13299
COSMOS SATELLITES
Orbit determination and analysis for Cosmos 236 at 15th-order resonance
[RAE-TR-88058] N90-12641
COST ANALYSIS
What is the balance sheet for investment in automated manufacturing
[CETIM-105490] N90-13071
COST EFFECTIVENESS
Designing for reliable and low maintenance cost aero engines
[PNR90570] N90-12604
Guidance and Control Panel Symposium on Guidance and Control of Unmanned Air Vehicles
[AGARD-AR-260] N90-12623
Aviation Engine Test Facilities (AETF) fire protection study
[AD-A211483] N90-12777
COST ESTIMATES
Estimating the relationships between the state of the art of technology and production cost for the US aircraft
[AD-A212127] N90-12495
COUNTERS
Instability of the behavior of high resistivity silicon detectors due to the presence of oxide charges
[REPT-89-038] N90-13260
COUPLED MODES
A well conditioned formulation for the analysis of multi-layered frequency selective surfaces using a cascaded matrix approach
[RSRE-MEMO-4289] N90-12858
An air coupled transmission mode acoustic microscope for on-line non-destructive evaluation
[AD-A211416] N90-12947
COVARIANCE
A simulation study of the overdetermined geodetic boundary value problem using collocation
[AD-A211785] N90-12990
CRACK GEOMETRY
Potential difference applied to the measurement of small fatigue crack growth at notches in Ti-6Al-4V
[FFA-TN-1989-09] N90-12952
Unilateral contact analysis of a crack with friction. Applications
[ETN-89-95511] N90-12956
CRACK INITIATION
Elastic indentation fractures
[ETCA-88-R-116] N90-12955
Unilateral contact analysis of a crack with friction. Applications
[ETN-89-95511] N90-12956
CRACK OPENING DISPLACEMENT
The effect of a rigid elliptical inclusion on a straight crack
[AD-A212263] N90-12965
CRACK PROPAGATION
A study of progressive cracking damage to carbon-epoxy composites and methods of crack reduction
[REPT-RE-49-324/F] N90-12676
Crack propagation failure of carbon/resin composites
[ONERA-RT-45/7086-M] N90-12677
Mechanical behavior of carbon/resin composites under delamination and cracking of transverse layers
[ONERA-RT-46/7086-M] N90-12678
Biaxial flexing of a fiber-reinforced aluminum composite
[AD-A212742] N90-12681
Potential difference applied to the measurement of small fatigue crack growth at notches in Ti-6Al-4V
[FFA-TN-1989-09] N90-12952
Elastic indentation fractures
[ETCA-88-R-116] N90-12955
Unilateral contact analysis of a crack with friction. Applications
[ETN-89-95511] N90-12956
An investigation on combined extension and bending of thin sheets with a central crack
[LR-561] N90-12958
CRACK TIPS
Modeling the temperature rise at the tip of a fast crack
[AD-A212418] N90-12966
CRACKING (FRACTURING)
Nonlinear theories concerning laminated composites under compression with delamination
[ONERA-RT-19/3542-RY-081-R] N90-12672
A study of progressive cracking damage to carbon-epoxy composites and methods of crack reduction
[REPT-RE-49-324/F] N90-12676
Elastic indentation fractures
[ETCA-88-R-116] N90-12955
CRACKS
The effect of a rigid elliptical inclusion on a straight crack
[AD-A212263] N90-12965
CREATIVITY
An algebra for process creation
[CWI-CS-R8907] N90-13155
CREEP ANALYSIS
Physical ageing and short term creep in amorphous and semicrystalline polymers
[NPL-DMA(A)-185] N90-12745
CREWS
Air Force flight feeding. Volume 1: Evaluation of current system and alternative concepts
[AD-A212789] N90-13043
CRITICAL PRESSURE
Vapor-liquid equilibrium of binary mixtures in the extended critical region. Part 1: Thermodynamic model
[PB89-218374] N90-12687
CRITICAL TEMPERATURE
Vapor-liquid equilibrium of binary mixtures in the extended critical region. Part 1: Thermodynamic model
[PB89-218374] N90-12687
CROSS FLOW
Design and test of an NLF wing glove for the variable-sweep transition flight experiment N90-12544
The 757 NLF glove flight test results N90-12546
Cross-axis synchronous flow through coil planet centrifuge for large-scale preparative countercurrent chromatography
[PB89-200174] N90-12682
Numerical evaluation of a solution representing a jet in cross-flow
[RAE-TM-AERO-2137] N90-12893
CRUISE MISSILES
Pivotal mono wing cruise missile with wing deployment and fastener mechanism
[AD-D014191] N90-12594
CRYOGENIC EQUIPMENT
A closed-cycle refrigerator for cooling maser amplifiers below 4 Kelvin N90-12797
Cryostatless high temperature supercurrent bearings for rocket engine turbopumps
[NASA-CR-183807] N90-12935
CRYOGENIC WIND TUNNELS
Hot-film system for transition detection in cryogenic wind tunnels N90-12522
Residual interference assessment in adaptive wall wind tunnels
[NASA-CR-181896] N90-12625
CRYSTAL GROWTH
Estimation of time to maximum supercooling during dynamic frazil ice formation
[AD-A212204] N90-12699
Method for growing patterned thin films of superconductors
[AD-D014195] N90-13262
CRYSTAL STRUCTURE
Development of texture analysis and its applications to titanium aero engine components
[PNR90561] N90-12602
Electrically conducting organic materials: Design, synthesis and characterization
[AD-A212214] N90-12700
Structural studies of sputter-deposited MoS2 solid lubricant films
[AD-A212407] N90-12759
CRYSTAL SURFACES
The effects of trace anions on the voltammetry of single crystal gold surfaces
[AD-A211886] N90-13254
CRYSTALLIZATION
Synthesis and crystallization behavior of fluoride glasses
[AD-A212142] N90-12741

CUBIC LATTICES
Temperature dependence of positron diffusion in cubic metals
[PB89-222020] N90-12722
CUMULATIVE DAMAGE
Evaluation of a damaged F/A-18 horizontal stabilator
[AD-A212573] N90-12597
CURING
Curable polyether compositions
[AD-D014200] N90-12679
Structure and properties of polymer interphases
[AD-A212796] N90-12763
CURL (VECTORS)
Application of a generalized Leibniz rule for calculating electromagnetic fields within continuous source regions
[AD-A212470] N90-12831
CURRENT CONVERTERS (AC TO DC)
NIST (National Institute of Standards and Technology) measurement services: The ac-dc difference calibrations
[PB89-222616] N90-12845
CYANO COMPOUNDS
Electron density modulation of catalytic metal centers by substituted aryl-isocyanide ligands
[AD-A212875] N90-12708
CYBERNETICS
Conceptual dependency theory and robot programming
[REPT-89-20] N90-13106
CYCLES
Long dominating cycles and paths in graphs with large neighborhood unions
[MEMO-769] N90-13157
CYCLONES
Air flow over large scale topography
[AD-A211779] N90-12998
CYCLOTRON RESONANCE DEVICES
Cold tests of quasi-optical gyrotron resonators
[AD-A212707] N90-12868
Scaling of an 85 GHz gyrotron to operate at 94 GHz
[AD-A212756] N90-12909
CYCLOTRONS
National Science Foundation N90-13320
CYLINDRICAL BODIES
Small particle scattering and absorption
[AD-A213168] N90-12711
Stress waves through projectile joints and interfaces
[AD-A212201] N90-12963
CYLINDRICAL SHELLS
A thermoelastic transversely isotropic thick walled cylinder/disk application: An analytical solution and study
[NASA-TM-102320] N90-12950

D

DAMAGE ASSESSMENT
Optical fibre witnesses of fatigue damage in composite materials N90-12660
Damage tolerance of CFRP sandwich panels
[FFA-TN-1988-70] N90-12664
DAMPING
Non linear vibrations in a drive train when coupled to constant torque and constant power loads
[PNR90593] N90-12934
DARK ADAPTATION
Three stages and two systems of visual processing
[AD-A212670] N90-13032
DARKNESS
A Scheiner-principle pocket optometer for self-evaluation and biofeedback accommodation training
[AD-A213171] N90-13027
DATA ACQUISITION
Preliminary experience with high response pressure measurements in a multistage, high speed compressor
[RAE-TM-P-1141] N90-12619
A data acquisition and processing system for six component solid rocket motor testing
[AD-A212200] N90-12657
The Telecommunications and Data Acquisition Report
[NASA-CR-185093] N90-12786
Mode S data link trials, 10-11 January 1989
[RSRE-MEMO-4267] N90-12815
Climatological data for the North Sea based on observations by voluntary observing ships over the period 1961-1980
[KNMI-WR-89-02] N90-13002
A real-time wind model using digital data from aircraft
[RSRE-MEMO-4309] N90-13005
Air Force flight feeding. Volume 1: Evaluation of current system and alternative concepts
[AD-A212789] N90-13043
Berne solar observations
[REPT-55] N90-13301
DATA BASE MANAGEMENT SYSTEMS
Performance evaluations of a parallel and expandable database computer: The multi-backend database computer
[AD-A212761] N90-13048
The integration of structured and formal methods
[RSRE-MEMO-4293] N90-13068
DATA BASES
The role of component testing
[PNR90589] N90-12808
Central Sudan surface wind data and climate characteristic
[KNMI-WR-88-01] N90-13000
Mesoscale acid deposition modeling studies
[NASA-CR-4262] N90-13228
DATA FLOW ANALYSIS
The integration of structured and formal methods
[RSRE-MEMO-4293] N90-13068
The application of artificial intelligence techniques to tracing the interconnections in an integrated circuit
[TELECOM-PARIS-89-E002] N90-13105
DATA LINKS
Mode S data link trials, 10-11 January 1989
[RSRE-MEMO-4267] N90-12815
DATA MANAGEMENT
The integration of structured and formal methods
[RSRE-MEMO-4293] N90-13068
NAUTILE: A physical design environment based on an object-oriented data manager
[IMAG-RR-737-I] N90-13094
Illustration of Bayesian inference in normal data models using Gibbs sampling
[AD-A212630] N90-13187
DATA PROCESSING
Stable Kalman filters for processing clock measurement data N90-12801
Conception and results of the DLR realtime azimuth processor for the E-SAR system
[DLR-FB-89-30] N90-12827
Automatic analysis and exploitation of the flow visualization images
[ETN-89-95712] N90-12887
A Z specification of the MaCHO interface editor
[RSRE-MEMO-4247] N90-13067
User manual of the force structure model scenario editor SCENE
[FEL-1988-101] N90-13069
Process expressions and Hoare's logic
[CWI-CS-R8905] N90-13076
DATA RECORDING
Acoustic recording systems for use in military aircraft
[RAE-TM-MM-11] N90-13207
DATA SIMULATION
Route data representation for ATC simulation experiments
[RSRE-MEMO-4133] N90-12576
Aircraft SAR simulation Sargen 1.0
[FEL-1989-44] N90-12823
DATA SMOOTHING
A cell-centered multigrid method for three-dimensional anisotropic-diffusion and interface problems
[REPT-89-35] N90-13128
Local mode smoothing analysis of various incomplete factorization iterative methods in two dimensions
[REPT-89-36] N90-13129
Smoothed predictor-corrector methods for solving partial differential equations
[CWI-NM-R8808] N90-13131
Iterated theta method for hyperbolic equations
[CWI-NM-R8809] N90-13132
DATA STRUCTURES
Route data representation for ATC simulation experiments
[RSRE-MEMO-4133] N90-12576
Spatial data structures for robotic vehicle route planning
[AD-A212806] N90-13111
DAYTIME
Role of chemical effects in daytime high latitude trough formation
[AD-A211772] N90-12989
DECAY
Cosmic strings and baryon decay catalysis
[NASA-CR-186074] N90-13299
DECISION MAKING
Three stages and two systems of visual processing
[AD-A212670] N90-13032
DECISION THEORY
A new decision rule for model structure identification of a class of nonlinear dynamic systems
[RR-360] N90-13122
DECODERS
On the decoder error probability of linear codes N90-12793
Performance of the image statistics decoder in conjunction with the Goldstone-VLA array N90-12796
DECODING
On the decoder error probability of linear codes N90-12793
Frame synchronization methods based on channel symbol measurements N90-12795
DECOMPOSITION
Metallo-organic decomposition process for dielectric films
[AD-A211590] N90-12849
DECONTAMINATION
Corrosion and corrosion inhibition of metals/alloys in methylphosphonic difluoride and decontaminating solutions
[AD-A212404] N90-12734
DEDUCTION
Expert systems as deductive systems
[CWI-CS-R8825] N90-13073
DEEP SPACE NETWORK
The Telecommunications and Data Acquisition Report
[NASA-CR-185093] N90-12786
Automated monitor and control for deep space network subsystems N90-12794
Frame synchronization methods based on channel symbol measurements N90-12795
DSN 70-meter antenna microwave optics design and performance improvements. Part 2: Comparison with measurements N90-12800
Stable Kalman filters for processing clock measurement data N90-12801
A simple model for DSS-14 outage times N90-12802
The NASA SETI sky survey: Recent developments N90-12804
DEFECTS
A robot which will investigate the condition of underground pipe
[PB89-230650] N90-12928
DEFENSE COMMUNICATIONS SYSTEM (DCS)
Artificial intelligence for communication prospects
[FEL-1989-1] N90-13107
DEFENSE PROGRAM
Recommended changes in US military space policies and programs: A paper submitted to the Commission on Integrated Long-Term Strategy
[PB89-219364] N90-12636
DEFINITION
A simple definition for parallel composition of prime event structures
[CWI-CS-R8903] N90-13074
DEFORESTATION
Contribution of deforestation to atmospheric CO2 and reforestation as an option to control CO2
[DE89-017255] N90-12979
DEGRADATION
Effects of hot corrosion on the room temperature strength of structural ceramics
[AD-A212568] N90-12762
Shape instabilities of plate-like structures. 1: Experimental observations in heavily cold worked in situ composites
[AD-A212251] N90-13021
Tunneling microscopy of superconductors and tunneling barriers
[AD-A212120] N90-13257
DEHYDRATION
Heat exhaustion
[AD-A212128] N90-13014
DELAMINATING
Multilayer theory for delamination analysis of a composite curved bar subjected to end forces and end moments
[NASA-TM-4139] N90-12669
Nonlinear theories concerning laminated composites under compression with delamination
[ONERA-RT-19/3542-RY-081-R] N90-12672
DELAY LINES
Satellite range delay simulator for a matrix-switched time division multiple-access network simulator
[NASA-TM-102407] N90-12813
DEMAGNETIZATION
A survey of the current state-of-the-art in high-energy-product permanent magnets
[AD-A211761] N90-13193
DEPOSITION
Metallo-organic decomposition process for dielectric films
[AD-A211590] N90-12849
Mesoscale acid deposition modeling studies
[NASA-CR-4262] N90-13228
DEPTH MEASUREMENT
Use of ground penetrating radar to define recharge areas in the Central Sand Plain
[PB89-224885] N90-12814
DESIGN ANALYSIS
On the precision and reliability of GPS networks computed using the double difference observable
[ETN-89-95719] N90-12571

Low Earth Orbit Raider (LER) winged air launch vehicle concept
[NASA-CR-186057] N90-12590
Rolls-Royce and ERCOFTAC
[PNR90600] N90-12615
Blading design for multi-storage HP compressor
[PNR90602] N90-12616
Analysis and simulation of dynamics of spacecraft power systems N90-12653
Mathematical models for the linear induction motor
[RR-WB-88-17] N90-12853
The design, construction, performance and calibration of pulse generators to fulfil the requirements of specifications defence standard 59-41, FS(F) 510 and FS(S) 457
[RAE-TM-FS(F)-550] N90-12857
A review of focal reducer interferometer systems
[RSRE-MEMO-3486] N90-13231

DESYNCHRONIZATION (BIOLOGY)
Effects of a time zone shift of nine hours on the circadian rhythms in cockpit aircrew members on longhaul flights
[DLR-FB-89-31] N90-13019

DETONATION
Thermal initiation of confined primary explosives with a proton beam
[AD-A212954] N90-12767

DETONATORS
RF and dc desensitized electroexplosive device
[AD-D014206] N90-12862

DEVELOPING NATIONS
Wider horizons: Potential contributions by space systems to socio-economic advancement in developing countries
[ESA-SP-1106] N90-13276

DEVIATION
Strong moderate deviation theorems for m-dependent random variables
[AD-A212618] N90-13173

DIAMONDS
An investigation of diamond film deposition in a premixed oxyacetylene flame
[AD-A212595] N90-13268

DIATOMIC MOLECULES
Extended basis set calculations of atomization energies: Comparison of isogyric and direct results
[AD-A212268] N90-12702

DIELECTRICS
Metallo-organic decomposition process for dielectric films
[AD-A211590] N90-12849
Dielectric spectroscopy of semiconductors
[AD-A211989] N90-13255
Growth and characterization of zinc sulfide films by conversion of zinc oxide films with H2S
[AD-A213345] N90-13271

DIELS-ALDER REACTIONS
Curable polyether compositions
[AD-D014200] N90-12679

DIENES
Curable polyether compositions
[AD-D014200] N90-12679

DIFFERENCES
Multivariable divided difference and B-splines
[MEMO-772] N90-13160

DIFFERENTIAL EQUATIONS
Vortex dynamics
[AD-A212119] N90-12877
Stable and unstable subspaces of a critical functional differential equation
[PB89-220651] N90-13115
A recursive algorithm for computing the frequency response of a class of nonlinear difference equation models
[RR-354] N90-13123
Increasing the real stability boundary of explicit methods
[CWI-NM-R8902] N90-13134
Transformations and representations of nonlinear systems
[MEMO-776] N90-13164
Operator product coefficients in non-diagonal conformal field theories
[NIKHEF-H/88-19] N90-13224

DIFFERENTIAL INTERFEROMETRY
Remote detection of boundary-layer transition by an optical system N90-12524

DIFFERENTIAL PRESSURE
Measurements of coefficients of discharge for concentric flange-tapped square-edged orifice meters in water over the Reynolds number range 600 to 2,700,000
[PB89-235147] N90-12892

DIFFUSION
Some observations on transitory stall in conical diffusers
[NASA-TM-102387] N90-12561
Ion beam analysis of diffusion in polymer glasses
[AD-A212339] N90-12756

DIFFUSION COEFFICIENT
Measurement and correlation of the solubility and diffusion coefficient for oxygen and chlorine in basic hydrogen peroxide
[AD-A212348] N90-12703
Temperature dependence of positron diffusion in cubic metals
[PB89-222020] N90-12722

DIFFUSION FLAMES
Asymptotic analyses of the structures and characteristics of flames N90-12683
Investigation of fuel additive effects on sooting flames
[AD-A212925] N90-12709
FLIC (FLame with Implicit Convection): A detailed, two-dimensional flame model
[AD-A212953] N90-12710

DIFFUSION THEORY
Time evolution of the electron swarm energy distribution function
[AD-A212967] N90-13247

DIFFUSION WELDING
Superplastic forming and diffusion bonding of rapidly solidified, dispersion strengthened aluminum alloys for elevated temperature structural applications
[NASA-CR-181849] N90-12718

DIFLUORIDES
Corrosion and corrosion inhibition of metals/alloys in methylphosphonic difluoride and decontaminating solutions
[AD-A212404] N90-12734

DIGITAL COMPUTERS
The Shock and Vibration Digest, volume 21, no. 10 N90-12771
The computer age and traditional approximate, analytical methods N90-12772

DIGITAL DATA
A real-time wind model using digital data from aircraft
[RSRE-MEMO-4309] N90-13005

DIGITAL SIMULATION
A robust digital model following controller for helicopters
[ESA-TT-1041] N90-12621
Performance of the split-symbol moments SNR estimator in the presence of inter-symbol interference N90-12799
Analytical control of special numerical calculations of pressure propagation in a fluid
[GRS-70] N90-12884
Visualization of high-resolution digital terrain
[AD-A212149] N90-12971

DIGITAL SYSTEMS
Advanced actuation systems development, volume 1
[AD-A213334] N90-12624
Height and gradient from shading
[AD-A212338] N90-12908

DIMENSIONS
Dimensional reduction at high temperature revisited
[KVI-791] N90-13194

DIMERS
Electrically conducting organic materials: Design, synthesis and characterization
[AD-A212214] N90-12700
Structures and energies for small borane compounds: One and two boron compounds
[AD-A212264] N90-12701

DIODES
Null offset voltage compensator for operational amplifier
[AD-D014189] N90-12859

DIRAC EQUATION
On the spectrum of the staggered Dirac operator at finite chemical potential
[ITFA-88-53] N90-13272

DIRECTION
Direction-of-arrival calculations at VLF/LF (Very Low Frequency/Low Frequency)
[AD-A212620] N90-12833

DIRECTORIES
Directory of International and Regional Organizations Conducting Standards-Related Activities, May 1989
[PB89-221147] N90-12776

DISCHARGE COEFFICIENT
Effect of pipe roughness on orifice flow measurement
[PB89-231484] N90-12880
Measurements of coefficients of discharge for concentric flange-tapped square-edged orifice meters in water over the Reynolds number range 600 to 2,700,000
[PB89-235147] N90-12892

DISCRETE ADDRESS BEACON SYSTEM
Aircraft Reply and Interference Environment Simulator (ARIES) hardware principles of operation. Volume 2: Appendixes
[DOT/FAA/CT-TN88/4-2] N90-12781
Aircraft Reply and Interference Environment Simulator (ARIES) hardware principles of operation, volume 1
[DOT/FAA/CT-TN88/4-1] N90-12782

DISCRETE FUNCTIONS
The discrete-time single-server queueing model
[MEMO-780] N90-13165

DISKS (SHAPES)
A thermoelastic transversely isotropic thick walled cylinder/disk application: An analytical solution and study
[NASA-TM-102320] N90-12950

DISLOCATIONS (MATERIALS)
A two-parameter representation of dynamic dislocation distributions
[AD-A212249] N90-13263

DISORIENTATION
Spatial tests for aviators
[IZF-1988-15] N90-13041

DISPERSIONS
Superplastic forming and diffusion bonding of rapidly solidified, dispersion strengthened aluminum alloys for elevated temperature structural applications
[NASA-CR-181849] N90-12718

DISPLACEMENT
Calcium displacement caused by electromagnetic fields
[AD-A212690] N90-13023

DISPLAY DEVICES
Integration of a centralized multiplexed control unit into the cockpit of an aircraft
[F6150-DT410-1-88329] N90-12622
Characterization of liquid crystal displays for optical signal processing applications
[AD-A212832] N90-12910
State of the art of human/machine dialog tool prototypes
[TELECOM-PARIS-89-H001] N90-13038
A Z specification of the MaCHO interface editor
[RSRE-MEMO-4247] N90-13067

DISTANCE
Jacobi functions as limit cases of q-ultraspherical polynomials
[CWI-PM-R8807] N90-13139
On the Hellinger type distances for filtered experiments
[CWI-MS-R8818] N90-13146
A validation of the proposed NATO standard method to determine target acquisition distances with image intensifiers
[IZF-1988-8] N90-13230

DISTORTION
A Scheiner-principle pocket optometer for self-evaluation and biofeedback accommodation training
[AD-A213171] N90-13027

DISTRIBUTED PROCESSING
A fan-in algorithm for distributed sparse numerical factorization
[AD-A211569] N90-13054

DISTRIBUTION
Tail triviality for sums of stationary random variables
[CWI-MS-R8810] N90-13143

DISTRIBUTION FUNCTIONS
A simple model for DSS-14 outage times N90-12802
Removing stripes in GOES (Geostationary Operational Environmental Satellites) images by matching empirical distribution functions
[PB89-213359] N90-12968
Domain of attraction of an operator between supremum and sum
[REPT-89-05] N90-13119

DIVIDING (MATHEMATICS)
Multivariable divided difference and B-splines
[MEMO-772] N90-13160

DIVING (UNDERWATER)
Effects of serial wet-dry-wet cold exposure: Thermal balance, physical activity, and cognitive performance
[AD-A212704] N90-13025

DOCUMENTATION
A semiparametric model for citation counts
[CWI-MS-R8814] N90-13145

DOCUMENTS
Publications of the National Institute of Standards and Technology, 1988 catalog
[PB89-218382] N90-13279

DOMAIN WALL
Evolution of domain walls in the early universe
[NASA-CR-186076] N90-13297

DOMAINS
Time-domain Green function corresponding to a time-harmonic point source in complex space
[PB89-218846] N90-13117
Corrections to the thin wall approximation in general relativity
[NASA-CR-186078] N90-13274

DOPED CRYSTALS
Strong-inversion model of threshold voltage in modulation doped field effect transistors: The role of unintentional acceptors
[AD-A212750] N90-12870
DOPPLER EFFECT
Development of an anti-Stokes coherent Raman diffusion system for measuring hypersonic flow
[ONERA-RSF-1/7301-PY] N90-12630
Photochemical observation of ion flows in membrane channels
[AD-A212449] N90-12705
Multiparameter radar estimation of raindrop size distribution
[AD-A212410] N90-13007
DOPPLER RADAR
Subjective uses of wind profiler data in warm season analysis and forecasting: Wind profiler training manual number 3
[PB89-223333] N90-13004
DOWNTIME
A simple model for DSS-14 outage times N90-12802
DRAG REDUCTION
Application of sound and temperature to control boundary-layer transition N90-12537
Design of the low-speed NLF(1)-0414F and the high-speed HSNLF(1)-0213 airfoils with high-lift systems N90-12540
Experimental and numerical analyses of laminar boundary-layer flow stability over an aircraft fuselage forebody N90-12549
Status report on a natural laminar-flow nacelle flight experiment N90-12550
Nacelle design N90-12551
Reduction of turbulent drag: Boundary layer manipulators
[CERT-RSF-OA-74/2259-AYD] N90-12889
DRAINAGE
Analytical and experimental study of runway runoff with wind effects
[PTI-8948] N90-12627
DROP SIZE
Two dimensional orifice array, monodisperse drop source, phase 1
[AD-A211319] N90-12881
Multiparameter radar estimation of raindrop size distribution
[AD-A212410] N90-13007
DROPS (LIQUIDS)
Continuing studies of liquid propellant drops in hot, high-pressure environments
[AD-A212265] N90-12765
Two dimensional orifice array, monodisperse drop source, phase 1
[AD-A211319] N90-12881
Survey of the CLUSE main experiment Grand-CLUSE, May 1 - June 15, 1988 --- Humidity Exchange Over the Sea (HEXOS) experiment
[FEL-1988-43] N90-12991
DRYING
Structure and properties of polymer interphases
[AD-A212796] N90-12763
DUALITY THEOREM
Hahn-Banach type theorems for dual semigroups
[CWI-AM-R8903] N90-13149
DUCTED FLOW
Investigation of turbulent flow in highly curved ducts with application to turbomachinery components
[NASA-CR-186060] N90-12882
DYADICS
Scalar Green function method for microstrip antenna analysis based on the exact image theory
[PB89-218838] N90-12805
DYNAMIC CHARACTERISTICS
Analysis and simulation of dynamics of spacecraft power systems N90-12653
DYNAMIC CONTROL
Path expression based operating systems
[MEMO-INF-88-68] N90-13097
Remarks on the control of discrete time nonlinear systems
[MEMO-770] N90-13158
DYNAMIC LOADS
Flight motor set 360L001 (STS-26R). (Reconstructed dynamic loads analysis)
[NASA-CR-183811] N90-12656
DYNAMIC MODELS
Dynamic robot models using the Manutec r3 as an example
[ESA-TT-1132] N90-12626
Analysis of high speed pneumatic actuation systems under rotary directional on-off flow control N90-12926
Fundamentals of middle atmospheric dynamics
[AD-A211747] N90-12988
Extended performability modeling using dynamic queing networks
[MEMO-INF-89-15] N90-13099
DYNAMIC RESPONSE
Rotor blade dynamic design N90-12583
The Shock and Vibration Digest, volume 21, no. 10 N90-12771
A survey on nonproportional damping N90-12773
Pyrotechnic shock structural response N90-12774
A recursive algorithm for computing the frequency response of a class of nonlinear difference equation models
[RR-354] N90-13123
DYNAMIC STABILITY
Vortex dynamics
[AD-A212119] N90-12877
DYNAMIC STRUCTURAL ANALYSIS
RAN (Royal Australian Navy) vibration analysis system operator's guide
[AD-A212441] N90-12596
Flight motor set 360L001 (STS-26R). (Reconstructed dynamic loads analysis)
[NASA-CR-183811] N90-12656
Julia-Fatou-Sullivan theory for real one-dimensional dynamics
[REPT-88-100] N90-13190
DYNAMICAL SYSTEMS
Nonlinear systems and Kolmogorov's representation theorem
[RR-363] N90-12931
A new decision rule for model structure identification of a class of nonlinear dynamic systems
[RR-360] N90-13122
Numerical analysis of chaotic symbol sequences generated by parabolic and triangle maps of the interval
[MPIS-22/1987] N90-13124
Remarks on the control of discrete time nonlinear systems
[MEMO-770] N90-13158
DYSPROSIUM COMPOUNDS
Resistivity measurements of superconducting materials
[PB89-225700] N90-12856

E

EAR PROTECTORS
The effects of hearing protectors on speech communication and the perception of warning signals
[AD-A212521] N90-12832
Shape instabilities of plate-like structures. 1: Experimental observations in heavily cold worked in situ composites
[AD-A212251] N90-13021
Application of active noise reduction for hearing protection and speech intelligibility improvement
[IZF-1988-21] N90-13042
EARTH GRAVITATION
Optimum data weighting and error calibration for estimation of gravitational parameters
[NASA-TM-100737] N90-12985
EARTH LIMB
Retrieval of atomic oxygen and temperature in the thermosphere. Part 1: Feasibility of an experiment based on the spectrally resolved 147 micrometer limb emission
[AD-A211987] N90-12986
EARTH MAGNETOSPHERE
Development of computer codes to model dynamics of the earth's magnetosphere
[AD-A211532] N90-12987
Relationship between the current and the width of the POGO electrojet during the solstices
[DE89-619725] N90-13294
EARTH ORBITS
On mean elements for satellite orbits perturbed by the zonal harmonics of the geopotential
[AD-A212322] N90-12642
EARTH RADIATION BUDGET
South Pole surface radiation balance measurements, April 1986 to February 1988
[PB89-224018] N90-12993
EARTH ROTATION
RTSIN1: A model of a strapdown INS on a two-axis rate table
[AD-A212406] N90-12579
EATING
Air Force flight feeding. Volume 1: Evaluation of current system and alternative concepts
[AD-A212789] N90-13043
ECONOMIC ANALYSIS
What is the balance sheet for investment in automated manufacturing
[CETIM-105490] N90-13071
International Conference on Fixed Point Theory and Applications
[AD-A212369] N90-13171
ECONOMICS
Remarks on the control of discrete time nonlinear systems
[MEMO-770] N90-13158
EDDY CURRENTS
Device for inspection of materials by eddy current methods
[AD-D014205] N90-12948
EDITING ROUTINES (COMPUTERS)
A Z specification of the MaCHO interface editor
[RSRE-MEMO-4247] N90-13067
User manual of the force structure model scenario editor SCENE
[FEL-1988-101] N90-13069
EDUCATION
National Science Foundation N90-13320
EFFICIENCY
Scaling of an 85 GHz gyrotron to operate at 94 GHz
[AD-A212756] N90-12909
EIGENVALUES
An Eigenvalue Analysis of finite-difference approximations for hyperbolic IBVPs
[NASA-TM-102241] N90-13137
ELASTIC DEFORMATION
Mathematical simulation of dynamic compression tests using the Hopkinson bar method
[ISL-R-128/87] N90-12960
Analysis of the non-planar response of a cantilever, with the aid of computerized symbolic manipulation
[AD-A212421] N90-13172
ELASTIC PROPERTIES
Free-field response from inclined body waves in viscoelastic random medium
[REPT-88-99] N90-12876
Elastic indentation fractures
[ETCA-88-R-116] N90-12955
ELASTIC WAVES
Analytical control of special numerical calculations of pressure propagation in a fluid
[GRS-70] N90-12884
Bulk acoustic waves resonators made of amorphous materials
[NOTE-TECHNIQUE-1989-4] N90-13199
ELASTOMERS
High temperature insulators
[AD-D014193] N90-12751
Synthesis of energetic single phase and multi-phase polymers
[AD-A212539] N90-12761
ELASTOPLASTICITY
A two-dimensional hybrid experimental-numerical technique for elastic-plastic stress analysis N90-12949
Orthotropic elasto-plastic behavior of AS4/APC-2 thermoplastic composite in compression
[NASA-CR-186080] N90-12959
ELECTRIC BATTERIES
Design and commissioning test results for the hypervelocity launcher research complex battery power supply
[AD-A211320] N90-12848
Assessment of thin film batteries based on polymer electrolytes. Part 3: Specific energy versus specific power
[AD-A212141] N90-12976
ELECTRIC CHARGE
On the extremum electric charge problem of steady electromagnetic equilibria
[TRITA-EPP-89-04] N90-12809
Instability of the behavior of high resistivity silicon detectors due to the presence of oxide charges
[REPT-89-038] N90-13260
ELECTRIC CONDUCTORS
Synthesis and characterization of new low-dimensional metal complex conductors
[AD-A213189] N90-12871
ELECTRIC FIELDS
Scalar Green function method for microstrip antenna analysis based on the exact image theory
[PB89-218838] N90-12805
Catalog of absolutely calibrated, range normalized, wideband, electric field waveforms from located lightning flashes in Florida: July 24 and August 14, 1985 data
[AD-A212708] N90-13008
ELECTRIC NETWORKS
A 2d-1 lower bound 2-layer knock-knee channel routing
[AD-A211948] N90-12847
ELECTRIC POTENTIAL
Capacitive behavior in conducting polymers
[AD-A212448] N90-12760

Strong-inversion model of threshold voltage in modulation doped field effect transistors: The role of unintentional acceptors
[AD-A212750] N90-12870
ELECTRIC PROPULSION
Assessment of thin film batteries based on polymer electrolytes. Part 3: Specific energy versus specific power
[AD-A212141] N90-12976
ELECTRICAL FAULTS
Built-in generation for CMOS circuits
[IMAG-RR-736-I] N90-12855
ELECTRICAL IMPEDANCE
Magnetically insulated electron flows in pulsed power systems
[AD-A212746] N90-13196
ELECTRICAL MEASUREMENT
Infrared water vapor continuum absorption: New atmospheric electrical measurements and theory
[AD-A212594] N90-12994
The effects of trace anions on the voltammetry of single crystal gold surfaces
[AD-A211886] N90-13254
ELECTRICAL PROPERTIES
Ultrastructure processing and characterization of polymers
[AD-A211460] N90-12743
A center for advanced electrical and structural polymers
[AD-A212853] N90-12764
Structural and electrical properties of thin films and superlattices composed of II-VI semiconductors N90-13249
Study of the electrical and optical properties of the vanadium and nickel impurities in GaAs
[ISAL-89-0028] N90-13259
ELECTRICAL RESISTIVITY
Electrically conducting organic materials: Design, synthesis and characterization
[AD-A212214] N90-12700
Capacitive behavior in conducting polymers
[AD-A212448] N90-12760
Resistivity measurements of superconducting materials
[PB89-225700] N90-12856
Synthesis and characterization of new low-dimensional metal complex conductors
[AD-A213189] N90-12871
Assessment of thin film batteries based on polymer electrolytes. Part 3: Specific energy versus specific power
[AD-A212141] N90-12976
ELECTRO-OPTICS
The multivalent beta''-aluminas
[AD-A212103] N90-12738
Workshop on Recent Progress in Surface and Volume Scattering
[AD-A212455] N90-13236
European Solid State Device Research Conference (18th) ESSDERC 88 held in Montpellier, France on 13-16 September 1988
[AD-A210618] N90-13250
ELECTROCHEMICAL CORROSION
IBM PC analysis of polarization resistance data
[AD-A212294] N90-12732
Corrosion and corrosion inhibition of metals/alloys in methylphosphonic difluoride and decontaminating solutions
[AD-A212404] N90-12734
Advanced calcium-thionyl chloride high-power battery
[AD-A211856] N90-12846
ELECTROCHEMISTRY
Advanced double layer capacitor
[AD-A211977] N90-12688
Electrically conducting organic materials: Design, synthesis and characterization
[AD-A212214] N90-12700
Mechanisms of CO2 reduction metal and metal modified semiconductor electrodes
[AD-A213169] N90-12712
ELECTRODEPOSITION
Electroactive polyaniline film deposited from non-aqueous media. 2: Effect of acid concentration in solutions
[AD-A212084] N90-12737
ELECTRODES
Characterization and cycle tests of lightweight nickel electrodes
[NASA-TM-102399] N90-12696
Influence of the composition of the metal deposited on carbon manganese welds on the work properties of the melted area depending on the operating mode of the weld
[CETIM-104530] N90-12726
The effects of trace anions on the voltammetry of single crystal gold surfaces
[AD-A211886] N90-13254
ELECTROHYDRODYNAMICS
Polymer characterization by electrohydrodynamic ionization mass spectrometry
[AD-A212130] N90-12739
ELECTROJETS
Relationship between the current and the width of the POGO electrojet during the solstices
[DE89-619725] N90-13294
ELECTROLUMINESCENCE
Growth and characterization of zinc sulfide films by conversion of zinc oxide films with H2S
[AD-A213345] N90-13271
ELECTROLYTE METABOLISM
Cardiovascular, renal, electrolyte, and hormonal changes in man during gravitational stress, weightlessness, and simulated weightlessness: Lower body positive pressure applied by the antigravity suit
[NASA-TM-102232] N90-13013
ELECTROLYTES
Heat capacities of 1-methyl-3-ethylimidazolium chloride-aluminum chloride molten salts
[AD-A212790] N90-12707
Assessment of thin film batteries based on polymer electrolytes. Part 3: Specific energy versus specific power
[AD-A212141] N90-12976
Heat exhaustion
[AD-A212128] N90-13014
ELECTROLYTIC CELLS
Capacitive behavior in conducting polymers
[AD-A212448] N90-12760
Assessment of thin film batteries based on polymer electrolytes. Part 3: Specific energy versus specific power
[AD-A212141] N90-12976
ELECTROMAGNETIC COMPATIBILITY
The design, construction, performance and calibration of pulse generators to fulfil the requirements of specifications defence standard 59-41, FS(F) 510 and FS(S) 457
[RAE-TM-FS(F)-550] N90-12857
ELECTROMAGNETIC FIELDS
On the extremum electric charge problem of steady electromagnetic equilibria
[TRITA-EPP-89-04] N90-12809
Application of a generalized Leibniz rule for calculating electromagnetic fields within continuous source regions
[AD-A212470] N90-12831
Wire grid modeling of the linear tapered slot antenna
[AD-A212977] N90-12842
Calcium displacement caused by electromagnetic fields
[AD-A212690] N90-13023
Time-domain Green function corresponding to a time-harmonic point source in complex space
[PB89-218846] N90-13117
Liquid and solid ion plasmas
[AD-A212415] N90-13244
Research in cosmic and gamma ray astrophysics
[NASA-CR-185451] N90-13316
ELECTROMAGNETIC NOISE
Performance analysis of large adaptive sidelobe canceller arrays with reused elements
[AD-A212688] N90-12841
Sound Localization by Human Observers symposium proceedings
[AD-A212877] N90-13026
Numerical evaluation of the far field wave pattern of the radiation Green's function
[AD-A212839] N90-13176
ELECTROMAGNETIC PULSES
The design, construction, performance and calibration of pulse generators to fulfil the requirements of specifications defence standard 59-41, FS(F) 510 and FS(S) 457
[RAE-TM-FS(F)-550] N90-12857
ELECTROMAGNETIC RADIATION
Specification for radar free-space detection range and free-space intercept range calculations
[AD-A213158] N90-12843
Catalog of absolutely calibrated, range normalized, wideband, electric field waveforms from located lightning flashes in Florida: July 24 and August 14, 1985 data
[AD-A212708] N90-13008
ELECTROMAGNETIC SCATTERING
Small particle scattering and absorption
[AD-A213168] N90-12711
The physical optics approximation in the near-field region
[FEL-1989-100] N90-13234
Workshop on Recent Progress in Surface and Volume Scattering
[AD-A212455] N90-13236
ELECTROMAGNETIC WAVE TRANSMISSION
Long wave atmospheric noise model, phase 1. Volume 1: Lightning occurrence rates and propagation theory
[AD-A212794] N90-12836
Long wave atmospheric noise model, phase 1. Volume 2: Mode parameters
[AD-A212795] N90-12837
ELECTROMAGNETISM
Joint Services Electronics Program
[AD-A212309] N90-12864
ELECTROMECHANICAL DEVICES
The effect of concurrent strength and endurance training on electromechanical delay, maximum voluntary contraction, and rate of force development
[AD-A213316] N90-13028
ELECTRON ACCELERATION
Development of computer codes to model dynamics of the earth's magnetosphere
[AD-A211532] N90-12987
ELECTRON ACCELERATORS
Bunch length in internal target mode
[NIKHEF-AMPS/89/04] N90-12854
Electron beam propagation through a magnetic wiggler with random field errors
[AD-A212705] N90-12867
ELECTRON BEAMS
Current limiting mechanisms in electron and ion beams experiments
[AD-A212295] N90-12637
Bunch length in internal target mode
[NIKHEF-AMPS/89/04] N90-12854
B factory via conversion of 1 TeV electron beams into 1 TeV photon beams
[DE89-017692] N90-12914
ELECTRON BUNCHING
Bunch length in internal target mode
[NIKHEF-AMPS/89/04] N90-12854
ELECTRON DENSITY (CONCENTRATION)
Electron density modulation of catalytic metal centers by substituted aryl-isocyanide ligands
[AD-A212875] N90-12708
ELECTRON DENSITY PROFILES
Magnetically insulated electron flows in pulsed power systems
[AD-A212746] N90-13196
ELECTRON EMISSION
COSTEP: A comprehensive suprathermal and energetic particle analyzer for SOHO N90-13314
ELECTRON ENERGY
Structures and energies for small borane compounds: One and two boron compounds
[AD-A212264] N90-12701
Time evolution of the electron swarm energy distribution function
[AD-A212967] N90-13247
ELECTRON GAS
Dielectric spectroscopy of semiconductors
[AD-A211989] N90-13255
ELECTRON GUNS
A 2-MeV microwave thermionic gun
[DE89-015640] N90-12844
ELECTRON PARAMAGNETIC RESONANCE
Magnetic resonance of polymers at surfaces
[AD-A212225] N90-12753
ELECTRON SCATTERING
Proof of the feasibility of coherent and incoherent schemes for pumping a gamma-ray laser
[AD-A212315] N90-12921
ELECTRON TRANSFER
Electron transport in heterojunction superlattices
[AD-A212366] N90-13265
ELECTRON TUNNELING
Tunneling microscopy of superconductors and tunneling barriers
[AD-A212120] N90-13257
Electron transport in heterojunction superlattices
[AD-A212366] N90-13265
ELECTRONIC COUNTERMEASURES
Research on heating, instabilities, turbulence and RF emission from electric field dominated plasmas
[AD-A212122] N90-13243
ELECTRONIC EQUIPMENT TESTS
Built-in generation for CMOS circuits
[IMAG-RR-736-I] N90-12855
ELECTRONIC MAIL
A formatting style for typesetting and distributing draft international standards
[NPL-DITC-143/89] N90-13059
ELECTRONIC WARFARE
Preliminary report on the feasibility of high power Electronic Warfare (EW) using explosive energy sources
[MRL-TR-89-3] N90-12775
ELECTRONS
Minimal total cross section for e(+)e(-) yields W(+)W(-)
[NIKHEF-H/88-12] N90-13222

ELECTROPHYSIOLOGY
Seminars of Applied Physics, Materials Physics and Biomedical Engineering, 1989
[PB89-218572] N90-13192
ELECTROPOLISHING
A feasibility study of hydrogen dosage estimation in screw threads submitted to surface electrolytic treatment
[CETIM-110110] N90-12730
ELECTROSTATIC CHARGE
RF and dc desensitized electroexplosive device
[AD-D014206] N90-12862
ELEMENTARY PARTICLES
Twistons
[RSRE-MEMO-4234] N90-13275
ELEVATION
Height and gradient from shading
[AD-A212338] N90-12908
ELLIPSOIDS
Flow in the neighborhood of an ellipsoid cylinder of revolution model
[ONERA-RT-22/7252-AN-000A] N90-12895
ELLIPSOMETRY
Spectroscopic ellipsometry characterization of CVD deposition and doping of polysilicon multilayer structures
[RSRE-MEMO-4258] N90-12671
ELLIPTIC DIFFERENTIAL EQUATIONS
On the existence of a maximal weak solution for a semilinear elliptic equation
[REPT-89-06] N90-13120
ELLIPTICAL ORBITS
An analytic development of orbit determination for a distant, planetary orbiter N90-12787
ELLIPTICAL POLARIZATION
Semiconductor measurement technology: A software program for aiding the analysis of ellipsometric measurements, simple models
[PB89-235923] N90-13261
EMBEDDED COMPUTER SYSTEMS
Work-preserving emulations of fixed-connection networks
[AD-A211915] N90-13093
EMBEDDING
Optical fibre witnesses of fatigue damage in composite materials N90-12660
EMISSION
Analysis of high temperature superconductors by means of PIXE and RBS methods
[DE89-630241] N90-13252
EMULSIONS
Chemical and photochemical reactivity in microemulsions and waterless microemulsions
[AD-A211776] N90-12692
END EFFECTORS
Kinematics, special configurations and performance evaluation of serial manipulators N90-12927
Acceleration sets of planar manipulators. Part 1: Theory
[AD-A213162] N90-12945
ENERGETIC PARTICLES
CELIAS: Charge, element and isotope analysis system for SOHO N90-13313
COSTEP: A comprehensive suprathermal and energetic particle analyzer for SOHO N90-13314
ERNE: Energetic and Relativistic Nuclei and Electron experiment N90-13315
ENERGY BANDS
Composite vs constituent particle aspects of hole motion in the CuO2 plane
[DE89-618864] N90-13251
ENERGY DISSIPATION
A mechanical power flow capability for the finite element code NASTRAN
[AD-A212202] N90-12964
ENERGY DISTRIBUTION
Time evolution of the electron swarm energy distribution function
[AD-A212967] N90-13247
ENERGY STORAGE
Phase change material for spacecraft thermal management
[AD-A211404] N90-12648
Heat pipe and thermal energy storage and corrosion studies (1988)
[AD-A212655] N90-12706
ENERGY TRANSFER
Rotational and vibrational nonequilibrium effects in rarefied, hypersonic flow
[NASA-CR-182559] N90-12498
Analysis and simulation of dynamics of spacecraft power systems N90-12653
A mechanical power flow capability for the finite element code NASTRAN
[AD-A212202] N90-12964
Time evolution of the electron swarm energy distribution function
[AD-A212967] N90-13247
ENGINE AIRFRAME INTEGRATION
Re-engine with the Rolls-Royce Tay 670, the route to significant noise reduction
[PNR90585] N90-12606
ENGINE DESIGN
Advanced clearance control systems --- blade tips
[PNR90553] N90-12601
A vision of the future: The new engine technology
[PNR90566] N90-12603
Designing for reliable and low maintenance cost aero engines
[PNR90570] N90-12604
The next generation supersonic transport engine: Critical issues
[PNR90576] N90-12605
Material requirements for future aeroengines
[PNR90595] N90-12610
A computer integrated approach to dimensional inspection
[PNR90596] N90-12611
Gas turbine performance analysis
[PNR90599] N90-12614
Rolls-Royce and ERCOFTAC
[PNR90600] N90-12615
Blading design for multi-storage HP compressor
[PNR90602] N90-12616
NASA/USRA advanced space design program: The laser powered interorbital vehicle
[NASA-CR-186044] N90-12646
Composite materials for future aeroengines
[PNR90584] N90-12667
The future of non ferrous metals in aerospace engines
[PNR90572] N90-12720
Cryostatless high temperature supercurrent bearings for rocket engine turbopumps
[NASA-CR-183807] N90-12935
The commercial aircraft noise problem
[PNR90577] N90-13203
ENGINE INLETS
Development of a VSAERO (Vortex Separation Aerodynamics) model of the F/A-18
[AD-A212442] N90-12566
ENGINE NOISE
Near-field noise predictions of an aircraft in cruise N90-12538
The 757 NLF glove flight test results N90-12546
Re-engine with the Rolls-Royce Tay 670, the route to significant noise reduction
[PNR90585] N90-12606
The commercial aircraft noise problem
[PNR90577] N90-13203
ENGINE PARTS
Development of texture analysis and its applications to titanium aero engine components
[PNR90561] N90-12602
The role of component testing
[PNR90589] N90-12608
Real-time simulation of an F110/STOVL turbofan engine
[NASA-TM-102409] N90-12618
The 4th US Army Workshop on Low Heat Rejection Engines
[AD-A212378] N90-12942
ENGINE TESTS
The role of component testing
[PNR90589] N90-12608
Flight motor set 360L001 (STS-26R). (Reconstructed dynamic loads analysis)
[NASA-CR-183811] N90-12656
A data acquisition and processing system for six component solid rocket motor testing
[AD-A212200] N90-12657
Aviation Engine Test Facilities (AETF) fire protection study
[AD-A211483] N90-12777
ENTHALPY
Interactive computer program for the generation of enthalpy-entropy and temperature-entropy charts of nitrogen and hydrogen
[DLR-FB-89-27] N90-13081
ENTROPY
Interactive computer program for the generation of enthalpy-entropy and temperature-entropy charts of nitrogen and hydrogen
[DLR-FB-89-27] N90-13081
ENVIRONMENT EFFECTS
The next generation supersonic transport engine: Critical issues
[PNR90576] N90-12605
Development of an inventory of materials potentially sensitive to ambient atmospheric acidity in the South Coast Air Basin
[PB89-224604] N90-12982
ENVIRONMENT MODELS
The Regional Polar Ice Prediction System, Berents Sea (RPIPS-B): A technical description
[AD-A213159] N90-13012
ENVIRONMENT SIMULATORS
Aircraft Reply and Interference Environment Simulator (ARIES) hardware principles of operation. Volume 2: Appendixes
[DOT/FAA/CT-TN88/4-2] N90-12781
Aircraft Reply and Interference Environment Simulator (ARIES) hardware principles of operation, volume 1
[DOT/FAA/CT-TN88/4-1] N90-12782
ENVIRONMENTAL TESTS
Biology in microgravity: A guide for experimenters
[ESA-TM-02] N90-12769
ENZYMES
Biological and biochemical methane reactions
[PB89-232615] N90-12977
EPICYCLOIDS
Demonstration epicyclic gearbox
[PNR90567] N90-12932
EPITAXY
The growth of epitaxial GaAs and GaAlAs on silicon substrates by OMVPE
[AD-A212873] N90-13269
EPOXY COMPOUNDS
Influence of the structure of epoxy network models on the volumetric, mechanical and viscoelastic properties
[ISAL-89-0024] N90-12666
Structure and properties of polymer interphases
[AD-A212796] N90-12783
EPOXY MATRIX COMPOSITES
Hardening mechanisms and analysis of the structure of the TGDDM/DDS epoxy resin system (tetraglycidyl-4,4' diaminodiphenylmethane/4,4' diaminodiphenylsulfone)
[NOTE-TECHNIQUE-1988-8] N90-12662
Influence of the structure of epoxy network models on the volumetric, mechanical and viscoelastic properties
[ISAL-89-0024] N90-12666
A study of progressive cracking damage to carbon-epoxy composites and methods of crack reduction
[REPT-RE-49-324/F] N90-12676
EPOXY RESINS
Hardening mechanisms and analysis of the structure of the TGDDM/DDS epoxy resin system (tetraglycidyl-4,4' diaminodiphenylmethane/4,4' diaminodiphenylsulfone)
[NOTE-TECHNIQUE-1988-8] N90-12662
Behavior of the adhesive A2 submitted to mechanical traction
[CETIM-105290] N90-12748
Chemical treatment of epoxy resins to reduce moisture sensitivity and to improve the mechanical properties
[AD-A212360] N90-12758
EQUATIONS OF MOTION
Corrections to the thin wall approximation in general relativity
[NASA-CR-186078] N90-13274
EQUILIBRIUM EQUATIONS
On the extremum electric charge problem of steady electromagnetic equilibria
[TRITA-EPP-89-04] N90-12809
EQUIVALENCE
Mathematical equivalence in a primitive Ella
[RSRE-MEMO-4225] N90-13066
Transformations and representations of nonlinear systems
[MEMO-776] N90-13164
ERROR ANALYSIS
The fault monitoring and diagnosis knowledge-based system for space power systems: AMPERES, phase 1
[NASA-CR-185486] N90-12654
A statistical study of radio-source structure effects on astrometric very long baseline interferometry observations N90-12788
On the decoder error probability of linear codes N90-12793
ERROR DETECTION CODES
Fine resolution errors in secondary surveillance radar altitude reporting amongst aircraft transmitting the conspicuity codes 4321 and 4322
[RSRE-88004] N90-12816
Non-separate arithmetic codes
[RSRE-MEMO-4215] N90-13058
ERRORS
A performance comparison between block interleaved and helically interleaved concatenated coding systems N90-12792
Direction-of-arrival calculations at VLF/LF (Very Low Frequency/Low Frequency)
[AD-A212620] N90-12833
Optimum data weighting and error calibration for estimation of gravitational parameters
[NASA-TM-100737] N90-12985
Multiparameter radar estimation of raindrop size distribution
[AD-A212410] N90-13007

An error estimator for parameter choice in regulating least square problems. Application to regularized deconvolution
[IMAG-RR-744-M] N90-13125
A frequency domain technique for improving sound field reproduction
[RAE-TM-MM-10] N90-13205
ESTIMATING
Estimating the time to fatigue failure of mooring cables
[PB89-220677] N90-12946
Optimum data weighting and error calibration for estimation of gravitational parameters
[NASA-TM-100737] N90-12985
ETHANE
Thermal stability of the carbon-carbon bond in ethylene adsorbed on Si(100): An isotopic mixing study
[AD-A211591] N90-12691
ETHERS
Curable polyether compositions
[AD-D014200] N90-12679
ETHYLENE
Thermal stability of the carbon-carbon bond in ethylene adsorbed on Si(100): An isotopic mixing study
[AD-A211591] N90-12691
ETIOLOGY
Exertional heatstroke: An international perspective. An introduction: The role of exercise in the etiology of exertional heatstroke
[AD-A212242] N90-13020
EULER EQUATIONS OF MOTION
Numerical simulation of unsteady rotational flow over propfan configurations
[NASA-CR-186037] N90-12500
Improvements in the formulations and numerical solution of the Euler problem for swept wings
[RAE-TM-AERO-2139] N90-12562
Euler equation solutions applied to a helicopter rotor in forward moving flight
[ONERA-RSF-32/1285-AY-346A] N90-12592
Multigrid solution method for the Euler equations
[PB89-219463] N90-13116
EUROPEAN SPACE AGENCY
European space technology: Celebrating twenty-five years of research and development
[ESA-BR-55] N90-13322
EUROPEAN SPACE PROGRAMS
European space technology: Celebrating twenty-five years of research and development
[ESA-BR-55] N90-13322
EUTECTIC COMPOSITES
Tribological properties of PM212: A high-temperature, self-lubricating, powder metallurgy composite
[NASA-TM-102355] N90-12659
EUTECTICS
Heat pipe and thermal energy storage and corrosion studies (1988)
[AD-A212655] N90-12706
EVALUATION
On the Hellinger type distances for filtered experiments
[CWI-MS-R8818] N90-13146
EVENTS
A simple definition for parallel composition of prime event structures
[CWI-CS-R8903] N90-13074
EVOKED RESPONSE (PSYCHOPHYSIOLOGY)
Electrophysiological studies of visual attention and resource allocation
[AD-A212287] N90-13030
EVOLUTION (DEVELOPMENT)
Small scale structure on cosmic strings
[NASA-CR-186075] N90-13298
EXCITATION
Symmetry breaking phenomena in liquid Helium-4
[DE89-618886] N90-12685
Ground states of a two-dimensional charged-boson system
[AD-A212363] N90-13226
EXERCISE PHYSIOLOGY
Exertional heatstroke: An international perspective. An introduction: The role of exercise in the etiology of exertional heatstroke
[AD-A212242] N90-13020
Prediction of thermal stress casualties
[AD-A212356] N90-13022
EXHAUST GASES
Effects of atmospheric mix and toxic fumes on military performance
[PB89-223630] N90-13015
EXPERIMENTATION
On the Hellinger type distances for filtered experiments
[CWI-MS-R8818] N90-13146
EXPERT SYSTEMS
The fault monitoring and diagnosis knowledge-based system for space power systems: AMPERES, phase 1
[NASA-CR-185486] N90-12654
Automated monitor and control for deep space network subsystems N90-12794
Investigation of North Atlantic fog and development of a marine fog forecast system
[AD-A211780] N90-12999
An expert system for VM performance analysis
[REPT-89-30] N90-13045
A knowledge-based approach to automated flow-field zoning for computational fluid dynamics
[NASA-TM-101072] N90-13048
Expert systems as deductive systems
[CWI-CS-R8825] N90-13073
Expert system for test program set fault candidate selection
[AD-A213338] N90-13091
Path expression based operating systems
[MEMO-INF-88-68] N90-13097
Semantics and consistency of rule-based expert systems
[CWI-CS-R8824] N90-13153
EXPLOSIVE DEVICES
RF and dc desensitized electroexplosive device
[AD-D014206] N90-12862
EXPLOSIVES
Thermal initiation of confined primary explosives with a proton beam
[AD-A212954] N90-12767
Preliminary report on the feasibility of high power Electronic Warfare (EW) using explosive energy sources
[MRL-TR-89-3] N90-12775
EXTERNAL SURFACE CURRENTS
Scalar Green function method for microstrip antenna analysis based on the exact image theory
[PB89-218838] N90-12805
EXTINCTION
Atmospheric horizontal-inhomogeneity effects on the optical depths determined by the double-elevation-angle lidar technique
[AD-A212836] N90-12839
EXTRATERRESTRIAL INTELLIGENCE
The NASA SETI sky survey: Recent developments N90-12804
EXTRATERRESTRIAL RADIATION
Radioactivity induced in gamma-ray spectrometers
[RAE-TM-SPACE-363] N90-13317
EXTREME ULTRAVIOLET RADIATION
The SOHO mission. Scientific and technical aspects of the instruments
[ESA-SP-1104] N90-13302
SUMER: Solar Ultraviolet Measurements of Emitted Radiation N90-13307
CDS: The Coronal Diagnostic Spectrometer N90-13308
EIT: Solar corona synoptic observations from SOHO with an Extreme-ultraviolet Imaging Telescope N90-13309
EXTREMELY HIGH FREQUENCIES
Ka-band MMIC beam steered transmitter array N90-12803
EXTREMUM VALUES
On the extremum electric charge problem of steady electromagnetic equilibria
[TRITA-EPP-89-04] N90-12809

F

F REGION
Role of chemical effects in daytime high latitude trough formation
[AD-A211772] N90-12989
F-14 AIRCRAFT
F-14 VSTFE and results of the cleanup flight test program N90-12547
FABRICATION
Scaling of an 85 GHz gyrotron to operate at 94 GHz
[AD-A212756] N90-12909
Optical clock distribution to VLSI chips
[AD-A212269] N90-13264
FACTOR ANALYSIS
A fan-in algorithm for distributed sparse numerical factorization
[AD-A211569] N90-13054
FACTORIZATION
A fan-in algorithm for distributed sparse numerical factorization
[AD-A211569] N90-13054
Local mode smoothing analysis of various incomplete factorization iterative methods in two dimensions
[REPT-89-36] N90-13129
NUMVEC FORTRAN library manual chapter: Simultaneous linear equations
[CWI-NM-R8903] N90-13135
FAILURE ANALYSIS
RAN (Royal Australian Navy) vibration analysis system operator's guide
[AD-A212441] N90-12596
SSME structural dynamic model development
[NASA-CR-183671] N90-12650
Numerical analysis of notch test damage to laminated composite plates submitted to uniaxial traction
[CETIM-107310] N90-12675
The nature and control of skidding in lightly loaded intershaft bearings
[PNR90591] N90-12933
Estimating the time to fatigue failure of mooring cables
[PB89-220677] N90-12946
FAR FIELDS
A method to model fuze performance. Part 2: Calculation of target reflections with physical optics
[FEL-1989-21-PT-2] N90-12822
Calculation of the odd and even integral components of the wave resistance Green's function
[AD-A212384] N90-12900
Numerical evaluation of the far field wave pattern of the radiation Green's function
[AD-A212839] N90-13178
FAR INFRARED RADIATION
Far infrared, submm and mm spectroscopy of the galactic center: Radio arc and +20/+50 km s (exp -1) clouds
[NASA-CR-185497] N90-13296
FARADAY EFFECT
Preliminary investigation of Faraday rotation effects and description of polarization measurements on the AFGL high latitude meteor scatter test bed
[AD-A211298] N90-12806
FASTENERS
Pivotal mono wing cruise missile with wing deployment and fastener mechanism
[AD-D014191] N90-12594
FATIGUE (BIOLOGY)
Heat exhaustion
[AD-A212128] N90-13014
The effect of concurrent strength and endurance training on electromechanical delay, maximum voluntary contraction, and rate of force development
[AD-A213316] N90-13028
Fatigue, pilot deviations and time of day
[NASA-CR-185369] N90-13035
FATIGUE (MATERIALS)
Improvement in pre-constraint fatigue resistance of modular ferretic and bainitic steel by shot peening treatments
[CETIM-106370] N90-12727
Estimating the time to fatigue failure of mooring cables
[PB89-220677] N90-12946
Proceedings of the Army Symposium on Solid Mechanics, 1989: Mechanics of Engineered Materials and Applications
[AD-A211954] N90-12951
FATIGUE TESTS
Optical fibre witnesses of fatigue damage in composite materials N90-12660
Damage tolerance of CFRP sandwich panels
[FFA-TN-1988-70] N90-12664
Shear fatigue testing and life prediction of fibre composites
[REPT-8519] N90-12668
Potential difference applied to the measurement of small fatigue crack growth at notches in Ti-6Al-4V
[FFA-TN-1989-09] N90-12952
Fatigue behavior of specimens under compression load spectra
[ETN-89-95207] N90-12954
Fatigue testing of welded steel assemblies with or without finishing treatments
[CETIM-107900] N90-12961
FAULT TOLERANCE
Software fault tolerance
[RSRE-MEMO-4237] N90-12575
Algorithmic fault tolerance
[RSRE-MEMO-4212] N90-13057
FEAR
Fear-potentiated startle as a model system for analyzing learning and memory
[AD-A212131] N90-13029
FEASIBILITY ANALYSIS
A survey of permanently-manned lunar base concepts
[AD-A212575] N90-12638
Proof of the feasibility of coherent and incoherent schemes for pumping a gamma-ray laser
[AD-A212315] N90-12921
An air coupled transmission mode acoustic microscope for on-line non-destructive evaluation
[AD-A211416] N90-12947
What is the balance sheet for investment in automated manufacturing
[CETIM-105490] N90-13071

FEDERAL BUDGETS
Departments of Veterans Affairs and Housing and Urban Development, and Independent Agencies Appropriations Bill, 1990
[H-REPT-101-150] N90-13281
National Aeronautics and Space Administration N90-13282
Fiscal year 1990 authorization request and budget estimates for the National Aeronautics and Space Administration
[GPO-96-945] N90-13283
Departments of Veterans Affairs and Housing and Urban Development, and Independent Agencies Appropriation Bill, 1990
[S-REPT-101-128] N90-13284
The 1990 National Aeronautics and Space Administration Authorization
[GPO-98-466] N90-13285
Department of Veterans Affairs and Housing and Urban Development, and Independent Agencies Appropriations Act, 1990
[HR-2916-PP] N90-13286
National Aeronautics and Space Administration N90-13287
National Aeronautics and Space Administration Authorization Act, fiscal year 1990
[S-REPT-101-157] N90-13288
National Aeronautics and Space Administration Authorization Act, fiscal year 1990
[S-REPT-101-157] N90-13289

FEEDBACK AMPLIFIERS
Feedback charge amplifier integrated on the detector wafer
[REPT-89-037] N90-12852

FEEDBACK CONTROL
A robust digital model following controller for helicopters
[ESA-TT-1041] N90-12621
Wideband phase-locked angular modulator N90-12798
The M/G/1 processor sharing queue as the almost sure limit of feedback queues
[REPT-89-32] N90-13044

FERMI SURFACES
Tunneling microscopy of superconductors and tunneling barriers
[AD-A212120] N90-13257

FERMIONS
The interacting boson approximation
[KVI-774] N90-13215
More on the super WZW theory
[NIKHEF-H/88-11] N90-13273

FERRITIC STAINLESS STEELS
Improvement in pre-constraint fatigue resistance of modular ferretic and bainitic steel by shot peening treatments
[CETIM-106370] N90-12727

FERROCENES
Investigation of fuel additive effects on sooting flames
[AD-A212925] N90-12709

FERROELECTRICITY
Metallo-organic decomposition process for dielectric films
[AD-A211590] N90-12849

FIBER COMPOSITES
Ballistic properties of composite materials for personnel protection
[MRL-TR-89-6] N90-12661
Shear fatigue testing and life prediction of fibre composites
[REPT-8519] N90-12668
Biaxial flexing of a fiber-reinforced aluminum composite
[AD-A212742] N90-12681
Device for inspection of materials by eddy current methods
[AD-D014205] N90-12948
Orthotropic elasto-plastic behavior of AS4/APC-2 thermoplastic composite in compression
[NASA-CR-186080] N90-12959

FIELD EFFECT TRANSISTORS
The analysis of current-mirror MOSFETs for use in radiation environments
[AD-A212527] N90-12866
Strong-inversion model of threshold voltage in modulation doped field effect transistors: The role of unintentional acceptors
[AD-A212750] N90-12870
Dielectric spectroscopy of semiconductors
[AD-A211989] N90-13255
GaAs gate dynamic memory technology
[AD-A212387] N90-13266
The growth of epitaxial GaAs and GaAlAs on silicon substrates by OMVPE
[AD-A212873] N90-13269

FIELD OF VIEW
Field-of-View variations and stripe-texturing effects on assault landing performance in the C-130 weapon system trainer
[AD-A212763] N90-12634

FIELD THEORY (PHYSICS)
Dimensional reduction at high temperature revisited
[KVI-791] N90-13194
Operator product coefficients in non-diagonal conformal field theories
[NIKHEF-H/88-19] N90-13224
Corrections to the thin wall approximation in general relativity
[NASA-CR-186078] N90-13274

FIGHTER AIRCRAFT
Estimating the relationships between the state of the art of technology and production cost for the US aircraft
[AD-A212127] N90-12495
Development and applications of reliability and maintainability design criteria in military aircraft
[ETN-89-95208] N90-12591
Spatial tests for aviators
[IZF-1988-15] N90-13041

FINITE DIFFERENCE THEORY
An Eigenvalue Analysis of finite-difference approximations for hyperbolic IBVPs
[NASA-TM-102241] N90-13137
Flux-corrected transport algorithms for two-dimensional compressible magnetohydrodynamics
[AD-A212757] N90-13246

FINITE ELEMENT METHOD
SSME structural dynamic model development
[NASA-CR-183671] N90-12650
Surface treatments of carbon fibers in an organic environment. Finite element analysis of pull-out tests
[ONERA-RT-7/3549-M] N90-12698
A mechanical power flow capability for the finite element code NASTRAN
[AD-A212202] N90-12964

FINNED BODIES
Aerodynamic test and analysis of a slender generic missile configuration
[AD-A212522] N90-12567

FINS
Additions and corrections to SUPER: A program for calculating steady and oscillatory supersonic flow over a thin wing, tail plane and fin
[AD-A211771] N90-12501

FIRE CONTROL
Algorithm development for SDI weapons system allocation
[AD-A212973] N90-13090

FIRE EXTINGUISHERS
Advanced spacecraft fire safety: Proposed projects and program plan
[NASA-CR-185147] N90-12645
Aviation Engine Test Facilities (AETF) fire protection study
[AD-A211483] N90-12777

FIRE PREVENTION
Advanced spacecraft fire safety: Proposed projects and program plan
[NASA-CR-185147] N90-12645
Aviation Engine Test Facilities (AETF) fire protection study
[AD-A211483] N90-12777

FIRES
Aviation Engine Test Facilities (AETF) fire protection study
[AD-A211483] N90-12777

FISSION
Activities report of the Joint Research Center
[ETN-89-95757] N90-13321

FLAME PROBES
Investigation of fuel additive effects on sooting flames
[AD-A212925] N90-12709

FLAME PROPAGATION
FLIC (FLame with Implicit Convection): A detailed, two-dimensional flame model
[AD-A212953] N90-12710

FLAME TEMPERATURE
Investigation of fuel additive effects on sooting flames
[AD-A212925] N90-12709

FLAMMABILITY
Advanced spacecraft fire safety: Proposed projects and program plan
[NASA-CR-185147] N90-12645

FLANGES
Flanged joints of aeroengines
[PNR90594] N90-12609

FLAT PLATES
Effect of roughness on the stability of boundary layers N90-12518
Unsteady three-dimensional thin-layer Navier Stokes solutions on dynamic blocked grids
[AD-A212377] N90-12899

FLEXIBILITY
Numerical simulation of unsteady rotational flow over propfan configurations
[NASA-CR-186037] N90-12500
Analysis of the non-planar response of a cantilever, with the aid of computerized symbolic manipulation
[AD-A212421] N90-13172

FLEXING
Biaxial flexing of a fiber-reinforced aluminum composite
[AD-A212742] N90-12681

FLIGHT CONTROL
Advanced actuation systems development, volume 1
[AD-A213334] N90-12624

FLIGHT FATIGUE
Biochemical and physiological changes in glider pilots during multihour flights
[DLR-FB-89-29] N90-13018
Psychological mechanisms involved in the disorientation of pilots due to flight conditions
[ETN-89-95014] N90-13040

FLIGHT MANAGEMENT SYSTEMS
Development and evaluation at ATCEU of executive and support operations, phase 4A/3D --- ATCEU (Air Traffic Control Evaluation Unit)
[CAA-PAPER-88017] N90-12572
Operational trial of effect of raising minimum stack level in Heathrow stacks
[CAA-PAPER-89003] N90-12573

FLIGHT OPERATIONS
Research and Technology annual report, 1988
[NASA-TM-101070] N90-13319

FLIGHT PATHS
Operational trial of effect of raising minimum stack level in Heathrow stacks
[CAA-PAPER-89003] N90-12573
FPG2: A flight profile generator program
[AD-A212408] N90-12595

FLIGHT SAFETY
Report on orbital debris
[NASA-TM-101855] N90-12635

FLIGHT SIMULATION
FPG2: A flight profile generator program
[AD-A212408] N90-12595
The comparison of the airbase simulation models airbase and sustained
[FEL-1988-66] N90-12629
Fatigue, pilot deviations and time of day
[NASA-CR-185369] N90-13035
Psychological mechanisms involved in the disorientation of pilots due to flight conditions
[ETN-89-95014] N90-13040

FLIGHT SIMULATORS
A robust digital model following controller for helicopters
[ESA-TT-1041] N90-12621
Field-of-View variations and stripe-texturing effects on assault landing performance in the C-130 weapon system trainer
[AD-A212763] N90-12634

FLIGHT STRESS (BIOLOGY)
Biology in microgravity: A guide for experimenters
[ESA-TM-02] N90-12769
Effects of a time zone shift of nine hours on the circadian rhythms in cockpit aircrew members on longhaul flights
[DLR-FB-89-31] N90-13019

FLIGHT TEST INSTRUMENTS
Automatic processing of images from the GRATE flight test tool
[DLR-FB-89-28] N90-12599

FLIGHT TESTS
Development flight tests of JetStar LFC leading-edge flight test experiment N90-12509
The right wing of the LEFT airplane N90-12510
Performance of laminar-flow leading-edge test articles in cloud encounters N90-12511
Simulated airline service experience with laminar-flow control leading-edge systems N90-12512
Flow quality measurements in compressible subsonic flows N90-12521
Design and test of an NLF wing glove for the variable-sweep transition flight experiment N90-12544
F-14 VSTFE and results of the cleanup flight test program N90-12547
Status report on a natural laminar-flow nacelle flight experiment N90-12550
Pivotal mono wing cruise missile with wing deployment and fastener mechanism
[AD-D014191] N90-12594
Air Force flight feeding. Volume 1: Evaluation of current system and alternative concepts
[AD-A212789] N90-13043
UHB demonstrator interior noise control flight tests and analysis
[NASA-CR-181897] N90-13198

FLIR DETECTORS
Research in computer vision for autonomous systems
[AD-A212420] N90-13235
FLOQUET THEOREM
A well conditioned formulation for the analysis of multi-layered frequency selective surfaces using a cascaded matrix approach
[RSRE-MEMO-4289] N90-12858
FLORIDA
Catalog of absolutely calibrated, range normalized, wideband, electric field waveforms from located lightning flashes in Florida: July 24 and August 14, 1985 data
[AD-A212708] N90-13008
FLOW DISTRIBUTION
Rotational and vibrational nonequilibrium effects in rarefied, hypersonic flow
[NASA-CR-182559] N90-12498
Experimental and theoretical investigation of boundary-layer instability mechanisms on a swept leading edge at Mach 3.5 N90-12557
Improved 2D numerical simulation model for strongly coupled heat and fluid flow in a thermal storage
[PB89-218879] N90-12878
Investigation of turbulent flow in highly curved ducts with application to turbomachinery components
[NASA-CR-186060] N90-12882
Two-phase flow pressure losses in pipeline fittings
[ESDU-89012] N90-12883
Reduction of turbulent drag: Boundary layer manipulators
[CERT-RSF-OA-74/2259-AYD] N90-12889
Numerical evaluation of a solution representing a jet in cross-flow
[RAE-TM-AERO-2137] N90-12893
A mechanical power flow capability for the finite element code NASTRAN
[AD-A212202] N90-12964
A knowledge-based approach to automated flow-field zoning for computational fluid dynamics
[NASA-TM-101072] N90-13048
Multigrid solution method for the Euler equations
[PB89-219463] N90-13116
FLOW EQUATIONS
CFD methods for drag prediction and analysis currently in use in UK
[RAE-TM-AERO-2146] N90-12563
Surface current and wave modulation measurements over bottom topography: A comparison with theory
[AD-A212469] N90-13011
FLOW GEOMETRY
A theoretical study of ingress for shrouded rotating disk systems with radial outflow
[PNR90586] N90-12607
Automatic analysis and exploitation of the flow visualization images
[ETN-89-95712] N90-12887
Flow in the neighborhood of an ellipsoid cylinder of revolution model
[ONERA-RT-22/7252-AN-000A] N90-12895
A knowledge-based approach to automated flow-field zoning for computational fluid dynamics
[NASA-TM-101072] N90-13048
Julia-Fatou-Sullivan theory for real one-dimensional dynamics
[REPT-88-100] N90-13190
FLOW MEASUREMENT
Advanced measurement techniques, part 1 N90-12520
Flow quality measurements in compressible subsonic flows N90-12521
Hot-film system for transition detection in cryogenic wind tunnels N90-12522
Predicted and hot-film measured Tollmien-Schlichting wave characteristics N90-12523
Remote detection of boundary-layer transition by an optical system N90-12524
Three-component laser Doppler velocimeter measurements in a juncture flow N90-12525
Basic aerodynamic research facility for comparative studies of flow diagnostic techniques N90-12526
Recent tests at Langley with a University of Tennessee Space Institute (UTSI) skin friction balance N90-12527
Development of an anti-Stokes coherent Raman diffusion system for measuring hypersonic flow
[ONERA-RSF-1/7301-PY] N90-12630
Effect of pipe roughness on orifice flow measurement
[PB89-231484] N90-12880
Measurements of coefficients of discharge for concentric flange-tapped square-edged orifice meters in water over the Reynolds number range 600 to 2,700,000
[PB89-235147] N90-12892
Experimental study of homogeneous turbulence submitted to rotational effects
[ONERA-RSF-10/1145-AY-164A] N90-12894
FLOW STABILITY
Research in Natural Laminar Flow and Laminar-Flow Control, part 1
[NASA-CP-2487-PT-1] N90-12503
Long-range LFC transport N90-12508
Stability theory applications to laminar-flow control N90-12513
Numerical study of three-dimensional spatial instability of a supersonic flat plate boundary layer
[NASA-CR-181931] N90-12874
FLOW VELOCITY
Three-component laser Doppler velocimeter measurements in a juncture flow N90-12525
Experimental studies on Goertler vortices N90-12529
Stage effects on stalling and recovery of a high-speed 10-stage axial-flow compressor N90-12600
Development of an anti-Stokes coherent Raman diffusion system for measuring hypersonic flow
[ONERA-RSF-1/7301-PY] N90-12630
Measurements of coefficients of discharge for concentric flange-tapped square-edged orifice meters in water over the Reynolds number range 600 to 2,700,000
[PB89-235147] N90-12892
A new generation of atmospheric tracers: The biological connection
[AD-A212285] N90-12983
FLOW VISUALIZATION
Advanced measurement techniques, part 1 N90-12520
Recent flow visualization studies in the 0.3-m TCT N90-12528
Experimental studies on Goertler vortices N90-12529
Improved 2D numerical simulation model for strongly coupled heat and fluid flow in a thermal storage
[PB89-218879] N90-12878
FLOWMETERS
Measurements of coefficients of discharge for concentric flange-tapped square-edged orifice meters in water over the Reynolds number range 600 to 2,700,000
[PB89-235147] N90-12892
FLUID FILMS
Structural studies of sputter-deposited MoS2 solid lubricant films
[AD-A212407] N90-12759
FLUID FLOW
Vortex dynamics
[AD-A212119] N90-12877
Improved 2D numerical simulation model for strongly coupled heat and fluid flow in a thermal storage
[PB89-218879] N90-12878
Analysis of high speed pneumatic actuation systems under rotary directional on-off flow control N90-12926
FLUID JETS
Two dimensional orifice array, monodisperse drop source, phase 1
[AD-A211319] N90-12881
FLUID MANAGEMENT
Vibration isolation technology: Sensitivity of selected classes of space experiments to residual accelerations
[NASA-CR-185443] N90-12768
FLUORIDES
Synthesis and crystallization behavior of fluoride glasses
[AD-A212142] N90-12741
FLUORINE
The chemistry of hexaazatriphenylene hexanitrile, a polyfunctional heterocycle with potential utility in the formulation of thermostable polymers
[AD-A212353] N90-12757
FLUX DENSITY
Ground states of a two-dimensional charged-boson system
[AD-A212363] N90-13226
SWAN: A study of solar wind anisotropies N90-13312
FLUX VECTOR SPLITTING
Solution of the thin-layer Navier-Stokes equations for laminar transonic flow
[PB89-221600] N90-12879
Multigrid solution method for the Euler equations
[PB89-219463] N90-13116
FOAMS
Aviation Engine Test Facilities (AETF) fire protection study
[AD-A211483] N90-12777
FOCAL PLANE DEVICES
A review of focal reducer interferometer systems
[RSRE-MEMO-3486] N90-13231
FOCUSING
Electron beam propagation through a magnetic wiggler with random field errors
[AD-A212705] N90-12867
Catadioptric Optics for laser Doppler velocimeter applications
[NASA-TM-102210] N90-12904
A Scheiner-principle pocket optometer for self-evaluation and biofeedback accommodation training
[AD-A213171] N90-13027
Direct computation of 3D shape invariants and the focus of expansion
[AD-A212386] N90-13195
FOG
Investigation of North Atlantic fog and development of a marine fog forecast system
[AD-A211780] N90-12999
FOG DISPERSAL
Investigation of North Atlantic fog and development of a marine fog forecast system
[AD-A211780] N90-12999
FOREBODIES
Experimental and numerical analyses of laminar boundary-layer flow stability over an aircraft fuselage forebody N90-12549
FORECASTING
The Regional Polar Ice Prediction System, Berents Sea (RPIPS-B): A technical description
[AD-A213159] N90-13012
FORESTS
Improvement and extension of a radar forest backscattering model
[NASA-CR-186083] N90-12973
FORMALISM
The integration of structured and formal methods
[RSRE-MEMO-4293] N90-13068
Computer oriented methods of multibody dynamics for application in vehicle technology
[DFVLR-FB-89-17] N90-13080
Corrections to the thin wall approximation in general relativity
[NASA-CR-186078] N90-13274
FORMAT
A formatting style for typesetting and distributing draft international standards
[NPL-DITC-143/89] N90-13059
FORMING TECHNIQUES
Superplastic forming and diffusion bonding of rapidly solidified, dispersion strengthened aluminum alloys for elevated temperature structural applications
[NASA-CR-181849] N90-12718
FORMULAS (MATHEMATICS)
Process expressions and Hoare's logic
[CWI-CS-R8905] N90-13076
Jacobi functions as limit cases of q-ultrasphericel polynomials
[CWI-PM-R8807] N90-13139
Index formulas for generalized Wiener-Hopf operators and Boson-Fermion correspondence in 2N dimensions
[CWI-PM-R8811] N90-13141
The addition formula for little q-Legendre polynomials and the SU(2) quantum group
[CWI-AM-R8906] N90-13151
Explicit formulas for Hankel norm approximations of infinite-dimensional systems
[TW-289] N90-13167
FORTRAN
Subspace iteration algorithms in FORTRAN 77 and FORTRAN 8x
[AD-A212275] N90-13083
NUMVEC FORTRAN library manual chapter: Simultaneous linear equations
[CWI-NM-R8903] N90-13135
FORWARD SCATTERING
Ion beam analysis of diffusion in polymer glasses
[AD-A212339] N90-12756
FRACTURE MECHANICS
Rapid heating tensile tests of high-energy-rate-forged 316L stainless steel charged with hydrogen and tritium
[DE89-017869] N90-12717
Spall resistance of alumina
[AD-A213213] N90-12735
Unilateral contact analysis of a crack with friction. Applications
[ETN-89-95511] N90-12956
The effect of a rigid elliptical inclusion on a straight crack
[AD-A212263] N90-12965
FRACTURE STRENGTH
Crack propagation failure of carbon/resin composites
[ONERA-RT-45/7086-M] N90-12677
Increased fragility of deep pressed thin plates
[CETIM-13-Y-313] N90-12962
FRACTURES (MATERIALS)
Proceedings of the Army Symposium on Solid Mechanics, 1989: Mechanics of Engineered Materials and Applications
[AD-A211954] N90-12951
FRAMING CAMERAS
Video line processor
[AD-D014198] N90-12861

FRAUNHOFER LINES
LASCO: A wide-field white light and spectrometric coronagraph for SOHO N90-13311
FREDHOLM EQUATIONS
Index formulas for generalized Wiener-Hopf operators and Boson-Fermion correspondence in 2N dimensions [CWI-PM-R8811] N90-13141
FREE ELECTRON LASERS
Electron beam propagation through a magnetic wiggler with random field errors
[AD-A212705] N90-12867
Radio frequency linac driven free-electron laser configurations
[AD-A212572] N90-12922
Cavity eigenmodes for the NIST/NRL (National Institute of Standards and Technology/Naval Research Laboratory) free electron laser
[AD-A212706] N90-12923
Theoretical and experimental research on a millimeter-wavelength free-electron laser
[AD-A213321] N90-12925
FREQUENCY CONTROL
Three stages and two systems of visual processing
[AD-A212670] N90-13032
FREQUENCY MEASUREMENT
A well conditioned formulation for the analysis of multi-layered frequency selective surfaces using a cascaded matrix approach
[RSRE-MEMO-4289] N90-12858
A frequency domain technique for improving sound field reproduction
[RAE-TM-MM-10] N90-13205
Smooth track generation for target motion analysis
[FEL-1989-83] N90-13233
FREQUENCY RANGES
A literature study of wave propagation in the 1-60 GHz range. Application to transportable military communication systems
[FEL-1988-47] N90-12825
Angle estimation in a multipath environment with an eight element linear array operating at 10.5 GHz
[FEL-1989-15] N90-12826
Far infrared, submm and mm spectroscopy of the galactic center: Radio arc and +20/+50 km s (exp -1) clouds
[NASA-CR-185497] N90-13296
FREQUENCY STABILITY
An apparatus for the electrodynamic containment of charged macroparticles N90-12789
FREQUENCY STANDARDS
An apparatus for the electrodynamic containment of charged macroparticles N90-12789
FRICTION
A new test machine for measuring friction and wear in controlled atmospheres to 1200 C
[NASA-TM-102405] N90-12670
Unilateral contact analysis of a crack with friction. Applications
[ETN-89-95511] N90-12956
FRONTS (METEOROLOGY)
Air flow over large scale topography
[AD-A211779] N90-12998
FUEL CONSUMPTION
Supersonic boundary-layer transition on the LaRC F-106 and the DFRF F-15 aircraft. Part 1: Transition measurements and stability analysis N90-12558
FUEL INJECTION
Two dimensional orifice array, monodisperse drop source, phase 1
[AD-A211319] N90-12881
FUEL-AIR RATIO
Investigation of fuel additive effects on sooting flames
[AD-A212925] N90-12709
FUMES
Effects of atmospheric mix and toxic fumes on military performance
[PB89-223630] N90-13015
FUNCTION GENERATORS
A graph-theoretical approach to block-copolymer complexes. Part 3: Loops and cycles
[MEMO-778-PT-3] N90-12750
FUNCTIONAL ANALYSIS
A functional expansion and stability for nonlinear input-output maps
[RR-359] N90-13121
FUNCTIONS (MATHEMATICS)
Stable and unstable subspaces of a critical functional differential equation
[PB89-220651] N90-13115
FUSELAGES
Experimental and numerical analyses of laminar boundary-layer flow stability over an aircraft fuselage forebody N90-12549
FUSION
Activities report of the Joint Research Center
[ETN-89-95757] N90-13321

G

GALACTIC CLUSTERS
Far infrared, submm and mm spectroscopy of the galactic center: Radio arc and +20/+50 km s (exp -1) clouds
[NASA-CR-185497] N90-13296
GALLIUM ARSENIDES
Study of the electrical and optical properties of the vanadium and nickel impurities in GaAs
[ISAL-89-0028] N90-13259
Electron transport in heterojunction superlattices
[AD-A212366] N90-13265
The growth of epitaxial GaAs and GaAlAs on silicon substrates by OMVPE
[AD-A212873] N90-13269
GAME THEORY
International Conference on Fixed Point Theory and Applications
[AD-A212369] N90-13171
GAMMA RAY LASERS
Proof of the feasibility of coherent and incoherent schemes for pumping a gamma-ray laser
[AD-A212882] N90-12924
GAMMA RAY OBSERVATORY
Particle transport simulation for spaceborne, NaI gamma-ray spectrometers
[AD-A205150] N90-13292
GAMMA RAY SPECTROMETERS
Particle transport simulation for spaceborne, NaI gamma-ray spectrometers
[AD-A205150] N90-13292
Radioactivity induced in gamma-ray spectrometers
[RAE-TM-SPACE-363] N90-13317
GAMMA RAYS
Proof of the feasibility of coherent and incoherent schemes for pumping a gamma-ray laser
[AD-A212315] N90-12921
Research in cosmic and gamma ray astrophysics
[NASA-CR-185451] N90-13316
GAS DENSITY
Retrieval of atomic oxygen and temperature in the thermosphere. Part 1: Feasibility of an experiment based on the spectrally resolved 147 micrometer limb emission
[AD-A211987] N90-12986
GAS MIXTURES
Characterization of nonpremixed turbulent bluff-body burner flames
[PB89-229447] N90-12689
Properties of Lennard-Jones mixtures at various temperatures and energy ratios with a size ratio of two
[PB89-235204] N90-12697
Survey of the response of standard limited streamer tubes over the complete range of three-component gas mixtures of isobutane, CO(sub 2), argon
[DE89-016692] N90-12875
GAS PIPES
A robot which will investigate the condition of underground pipe
[PB89-230650] N90-12928
GAS TURBINE ENGINES
Gas turbine performance analysis
[PNR90599] N90-12614
The nature and control of skidding in lightly loaded intershaft bearings
[PNR90591] N90-12933
GAS TURBINES
Studies of gas turbine heat transfer airfoil surfaces and end-wall cooling effects
[AD-A212451] N90-12620
GAS VISCOSITY
Thermophysical properties of benzene. Part 1: The ideal gas and the saturated liquid and vapour
[ESDU-89002-PT-1] N90-12693
GAS-METAL INTERACTIONS
A feasibility study of hydrogen dosage estimation in screw threads submitted to surface electrolytic treatment
[CETIM-110110] N90-12730
GASES
Continuing studies of liquid propellant drops in hot, high-pressure environments
[AD-A212265] N90-12765
Development of a low noise 10 K J-T refrigeration system
[AD-A213347] N90-12779
GASKETS
Improvement of rules relating to clamp calculations
[CETIM-110610] N90-12939
GATES (CIRCUITS)
GaAs gate dynamic memory technology
[AD-A212387] N90-13266
GAUGE INVARIANCE
Multigrid Monte Carlo in an external U(1) gauge field
[NIKHEF-ITFA-88-52] N90-13114
GAUGE THEORY
Twistons
[RSRE-MEMO-4234] N90-13275
GAUSS EQUATION
A multigrid method for the Navier-Stokes and Boussinesq equations
[REPT-89-17] N90-12886
GEARS
RAN (Royal Australian Navy) vibration analysis system operator's guide
[AD-A212441] N90-12596
Demonstration epicyclic gearbox
[PNR90567] N90-12932
Non linear vibrations in a drive train when coupled to constant torque and constant power loads
[PNR90593] N90-12934
Vibration transmission through rolling element bearings in geared rotor system, part 1
[NASA-CR-186093] N90-12936
GELATION
A graph-theoretical approach to block-copolymer complexes. Part 3: Loops and cycles
[MEMO-778-PT-3] N90-12750
GENES
Biological and biochemical methane reactions
[PB89-232615] N90-12977
GEODESIC LINES
Jacobi functions as limit cases of q-ultraspherical polynomials
[CWI-PM-R8807] N90-13139
GEODESY
Geodetic point positioning with GPS (Global Positioning System) carrier beat phase data from the CASA UNO experiment
[AD-A211955] N90-12970
GEOMETRICAL ACOUSTICS
An investigation of the diffraction of an acoustic plane wave by a curved surface of finite impedance
[NASA-CR-186069] N90-13204
GEOMETRY
Analysis of three- and four-sided uniform waveguides with unusual cross-section/boundary conditions
[AD-A212653] N90-12834
GEOPOTENTIAL
Evaluation of 15th- and 30th-order geopotential harmonic coefficients from 26 resonant satellite orbits
[RAE-TR-88045] N90-12640
The GEM-T2 gravitational model
[NASA-TM-100745] N90-12984
GLASS
Project, implementation, and utilization of composite structures
[ETN-89-95209] N90-12665
Synthesis and high temperature chemistry of methylsilsesquioxane polymers produced by titanium catalyzed redistribution of methylhydridooligo- and polysiloxanes
[AD-A212000] N90-12736
Synthesis and crystallization behavior of fluoride glasses
[AD-A212142] N90-12741
GLASS LASERS
Advanced source development and applications. Laser-produced plasmas: A compact soft x ray source with high peak brightness
[AD-A212677] N90-13245
GLIDERS
Biochemical and physiological changes in glider pilots during multihour flights
[DLR-FB-89-29] N90-13018
GLOBAL POSITIONING SYSTEM
On the precision and reliability of GPS networks computed using the double difference observable
[ETN-89-95719] N90-12571
Stable Kalman filters for processing clock measurement data N90-12801
Geodetic point positioning with GPS (Global Positioning System) carrier beat phase data from the CASA UNO experiment
[AD-A211955] N90-12970
Realization of a different NAVSTAR global positioning system for hydrographic surveying
[ETN-89-95720] N90-12972
GLOBAL WARMING
Sensitivity of a regional oxidant model to variations in climate parameters, volume 1 and 2
[PB89-224943] N90-12981
National Science Foundation N90-13320
GOERTLER INSTABILITY
Stability theory applications to laminar-flow control N90-12513
Interaction of Tollmien-Schlichting waves and Goertler vortices N90-12515
Goertler instability on an airfoil N90-12517
Experimental studies on Goertler vortices N90-12529

GOLD
The effects of trace anions on the voltammetry of single crystal gold surfaces
[AD-A211886] N90-13254
GRADIENTS
Height and gradient from shading
[AD-A212338] N90-12908
GRAIN SIZE
Carbonitrition response of steel plates not destined for heat treatments
[CETIM-106960] N90-12728
Metallo-organic decomposition process for dielectric films
[AD-A211590] N90-12849
GRAMMARS
Abstract grammars based on transductions
[MEMO-INF-89-7-REV] N90-13063
A table-driven approach to fast context-free parsing
[AD-A212210] N90-13082
GRANULAR MATERIALS
Fractional charging and reentrance in granular superconductors N90-13248
GRAPH THEORY
A graph-theoretical approach to block-copolymer complexes. Part 3: Loops and cycles
[MEMO-778-PT-3] N90-12750
Placing mirrors in grids
[CWI-CS-R8906] N90-13154
Long dominating cycles and paths in graphs with large neighborhood unions
[MEMO-769] N90-13157
GRAPHITE
Analysis of carbon fiber's x ray microscopic structure
[AD-A212215] N90-12752
An investigation of diamond film deposition in a premixed oxyacetylene flame
[AD-A212595] N90-13268
GRAPHITE-EPOXY COMPOSITES
A study of progressive cracking damage to carbon-epoxy composites and methods of crack reduction
[REPT-RE-49-324/F] N90-12676
GRAPHS (CHARTS)
Long dominating cycles and paths in graphs with large neighborhood unions
[MEMO-769] N90-13157
GRAVIMETRY
Standard method for measurement of nonvolatile residue on surfaces
[AD-A213324] N90-12714
The GEM-T2 gravitational model
[NASA-TM-100746] N90-12984
GRAVITATIONAL EFFECTS
Orbit determination and analysis for Cosmos 236 at 15th-order resonance
[RAE-TR-88058] N90-12541
Cardiovascular, renal, electrolyte, and hormonal changes in man during gravitational stress, weightlessness, and simulated weightlessness: Lower body positive pressure applied by the antigravity suit
[NASA-TM-102232] N90-13013
GRAVITATIONAL FIELDS
The GEM-T2 gravitational model
[NASA-TM-100746] N90-12984
GRAVITATIONAL PHYSIOLOGY
Cardiovascular, renal, electrolyte, and hormonal changes in man during gravitational stress, weightlessness, and simulated weightlessness: Lower body positive pressure applied by the antigravity suit
[NASA-TM-102232] N90-13013
GRAVITY WAVES
Fundamentals of middle atmospheric dynamics
[AD-A211747] N90-12988
A numerical study of rain-induced surface gravity wave attenuation
[AD-A212762] N90-13197
GREEN'S FUNCTIONS
Scalar Green function method for microstrip antenna analysis based on the exact image theory
[PB89-218838] N90-12805
Calculation of the odd and even integral components of the wave resistance Green's function
[AD-A212384] N90-12900
The effect of a rigid elliptical inclusion on a straight crack
[AD-A212263] N90-12965
Time-domain Green function corresponding to a time-harmonic point source in complex space
[PB89-218846] N90-13117
Numerical evaluation of the far field wave pattern of the radiation Green's function
[AD-A212839] N90-13176
GREENHOUSE EFFECT
Sensitivity of a regional oxidant model to variations in climate parameters, volume 1 and 2
[PB89-224943] N90-12981
GRID GENERATION (MATHEMATICS)
A knowledge-based approach to automated flow-field zoning for computational fluid dynamics
[NASA-TM-101072] N90-13048
A cell-centered multigrid method for three-dimensional anisotropic-diffusion and interface problems
[REPT-89-35] N90-13128
A moving-grid interface for systems of one-dimensional time-dependent partial differential equations
[CWI-NM-R8904] N90-13136
GRIFFITH CRACK
Elastic indentation fractures
[ETCA-88-R-116] N90-12955
GROUND EFFECT (AERODYNAMICS)
Wind effect on sound wave propagation at ground vicinity
[CSTB-2-87-008] N90-13201
GROUND EFFECT (COMMUNICATIONS)
Ground effects on multipath fading
[TELECOM-PARIS-88-E017] N90-12812
GROUND STATE
Ground states of a two-dimensional charged-boson system
[AD-A212363] N90-13226
GROUND STATIONS
The Telecommunications and Data Acquisition Report
[NASA-CR-185093] N90-12786
GROUND WATER
Use of ground penetrating radar to define recharge areas in the Central Sand Plain
[PB89-224885] N90-12814
GROUND WIND
Central Sudan surface wind data and climate characteristic
[KNMI-WR-88-01] N90-13000
Atlas of tropical sea surface temperature and surface winds
[PB89-223598] N90-13009
GROUND-AIR-GROUND COMMUNICATION
Aircraft Reply and Interference Environment Simulator (ARIES) hardware principles of operation. Volume 2: Appendixes
[DOT/FAA/CT-TN88/4-2] N90-12781
Aircraft Reply and Interference Environment Simulator (ARIES) hardware principles of operation, volume 1
[DOT/FAA/CT-TN88/4-1] N90-12782
GROUP THEORY
Representations of the twisted SU(2) quantum group and some q-hypergeometric orthogonal polynomials
[CWI-PM-R8809] N90-13140
The addition formula for little q-Legendre polynomials and the SU(2) quantum group
[CWI-AM-R8906] N90-13151

H

HADRONS
Elements of a relativistic microscopic theory of hadronic matter in equilibrium and non-equilibrium
[KVI-796] N90-13218
HAIL
Radar polarimetric studies based on the MAYPOLE 1983 and 1984 field experiments
[AD-A212226] N90-12830
HAMILTONIAN FUNCTIONS
Long dominating cycles and paths in graphs with large neighborhood unions
[MEMO-769] N90-13157
HANKEL FUNCTIONS
Explicit formulas for Hankel norm approximations of infinite-dimensional systems
[TW-289] N90-13167
HARDENING
Hardening mechanisms and analysis of the structure of the TGDDM/DDS epoxy resin system (tetraglycidyl-4,4' diaminodiphenylmethane/4,4' diaminodiphenylsulfone)
[NOTE-TECHNIQUE-1988-8] N90-12662
HARMONIC FUNCTIONS
Orbit determination and analysis for Cosmos 236 at 15th-order resonance
[RAE-TR-88058] N90-12641
HAZARDS
Base level management of radio frequency radiation protection program
[AD-A211759] N90-13017
HAZE
Investigation of North Atlantic fog and development of a marine fog forecast system
[AD-A211780] N90-12999
HEAD-UP DISPLAYS
Automatic processing of images from the GRATE flight test tool
[DLR-FB-89-28] N90-12599
HEARING
The effects of hearing protectors on speech communication and the perception of warning signals
[AD-A212521] N90-12832
Shape instabilities of plate-like structures. 1: Experimental observations in heavily cold worked in situ composites
[AD-A212251] N90-13021
Application of active noise reduction for hearing protection and speech intelligibility improvement
[IZF-1988-21] N90-13042
The effects of noise on speech and warning signals
[AD-A212520] N90-13210
HEAT
Heat exhaustion
[AD-A212128] N90-13014
HEAT ACCLIMATIZATION
Exertional heatstroke: An international perspective. An introduction: The role of exercise in the etiology of exertional heatstroke
[AD-A212242] N90-13020
HEAT EXCHANGERS
A closed-cycle refrigerator for cooling maser amplifiers below 4 Kelvin N90-12797
HEAT MEASUREMENT
Studies of gas turbine heat transfer airfoil surfaces and end-wall cooling effects
[AD-A212451] N90-12620
Heat capacities of 1-methyl-3-ethylimidazolium chloride-aluminum chloride molten salts
[AD-A212790] N90-12707
HEAT PIPES
Heat pipe and thermal energy storage and corrosion studies (1988)
[AD-A212655] N90-12706
Heat pipes for sodium-sulfur batteries
[AD-A212523] N90-12865
Analysis of the performance of heat pipes and phase-change materials with multiple localized heat sources for space applications
[AD-A212232] N90-12898
HEAT RESISTANT ALLOYS
An investigation of the irradiation swelling mechanisms in refractory metals at high temperatures
[AD-A211406] N90-12719
HEAT SOURCES
Analysis of the performance of heat pipes and phase-change materials with multiple localized heat sources for space applications
[AD-A212232] N90-12898
HEAT STORAGE
Improved 2D numerical simulation model for strongly coupled heat and fluid flow in a thermal storage
[PB89-218879] N90-12878
HEAT STROKE
Exertional heatstroke: An international perspective. An introduction: The role of exercise in the etiology of exertional heatstroke
[AD-A212242] N90-13020
HEAT TRANSFER
Phase change material for spacecraft thermal management
[AD-A211404] N90-12648
South Pole surface radiation balance measurements, April 1986 to February 1988
[PB89-224018] N90-12993
A fast algorithm for the evaluation of heat potentials
[AD-A211316] N90-13052
HEAT TRANSMISSION
Studies of gas turbine heat transfer airfoil surfaces and end-wall cooling effects
[AD-A212451] N90-12620
A theoretical method for the mechanical calculation of heat exchangers with sliding heads, phase 1 study
[CETIM-110240-PHASE-1] N90-12896
Analysis of the performance of heat pipes and phase-change materials with multiple localized heat sources for space applications
[AD-A212232] N90-12898
HEAT TREATMENT
The relationship between the mechanical properties of materials after press forming and their in-service properties
[CETIM-101530] N90-12723
The effects of heat treatment after welding on the functional properties of assemblies of CrMo alloys. Heat treatment of a mixed assembly of A48 and 10CD9.10 alloys
[CETIM-104320] N90-12724
How the common practice of heating plates of austenitic stainless steel during cooling affects their mechanical properties
[CETIM-104500] N90-12725
Graduate fellowships in the field of hard magnetic materials
[AD-A212303] N90-12733

Stability conditions for steady shearing. Stability conditions for simple shear under mixed thermal boundary conditions N90-12873
Increased fragility of deep pressed thin plates [CETIM-13-Y-313] N90-12962
Method for growing patterned thin films of superconductors [AD-D014195] N90-13262

HEATING
Application of sound and temperature to control boundary-layer transition N90-12537
Rapid heating tensile tests of high-energy-rate-forged 316L stainless steel charged with hydrogen and tritium [DE89-017869] N90-12717
Thermal initiation of confined primary explosives with a proton beam [AD-A212954] N90-12767

HEAVY IONS
Exploring asymmetric heavy-ion reactions at the KX-ray method: The Ne20 + Tb159 reaction at 15 MeV/unit [KVI-777] N90-13216

HEAVY NUCLEI
Compressibility of heavy nuclei at high temperatures [KVI-792] N90-13217

HEIGHT
Height and gradient from shading [AD-A212338] N90-12908

HEISENBERG THEORY
Meixner-Pollaczek polynomials and the Heisenberg algebra [CWI-PM-R8806] N90-13138

HELICOPTER DESIGN
Integrated multidisciplinary optimization of rotorcraft: A plan for development [NASA-TM-101617] N90-12580
General approach and scope --- rotor blade design optimization N90-12581
Rotor blade aerodynamic design N90-12582
Airframe design considerations: Overview --- rotor design optimization N90-12586
Validation of the procedures --- integrated multidisciplinary optimization of rotorcraft N90-12587
Appendix: Results obtained to date --- integrated multidisciplinary optimization of rotorcraft N90-12588
Euler equation solutions applied to a helicopter rotor in forward moving flight [ONERA-RSF-32/1285-AY-346A] N90-12592

HELICOPTERS
RAN (Royal Australian Navy) vibration analysis system operator's guide [AD-A212441] N90-12596
A robust digital model following controller for helicopters [ESA-TT-1041] N90-12621

HELIOSEISMOLOGY
The SOHO mission. Scientific and technical aspects of the instruments [ESA-SP-1104] N90-13302
SOHO: An observatory to study the solar interior and the solar atmosphere N90-13303
VIRGO: The solar monitor experiment on SOHO N90-13305
SOI: The Solar Oscillations Imager on SOHO N90-13306

HELIUM
An investigation of the irradiation swelling mechanisms in refractory metals at high temperatures [AD-A211406] N90-12719

HELIUM ISOTOPES
Symmetry breaking phenomena in liquid Helium-4 [DE89-616886] N90-12685
Improved method for determination of helium-4 in helium-3 by mass spectrometry [PB89-201404] N90-12686
Persistent current, NMR, and ion transmission experiments in rotating He-3 superfluids --- Nuclear Magnetic Resonance (NMR) [ISBN-952-90056-1-X] N90-13221
Superfluid phase slippage in (3)He-B flow through a narrow channel [PB89-218986] N90-13258

HELMETS
Ballistic properties of composite materials for personnel protection [MRL-TR-89-6] N90-12661

HERMES MANNED SPACEPLANE
Hermes plasma wind tunnel. Preliminary study, phase A1: Annexes, tables, figures [DVG-HER-TN-002-PT-2] N90-12632

HETEROJUNCTIONS
Electron transport in heterojunction superlattices [AD-A212366] N90-13265

HEURISTIC METHODS
Iterative methods for linear complementary and related problems [AD-A212848] N90-13089

HIERARCHIES
A transformational method for verifying safety properties in real time systems [AD-A211925] N90-13051

HIGH LEVEL LANGUAGES
Mathematical equivalence in a primitive Ella [RSRE-MEMO-4225] N90-13066

HIGH POWER LASERS
Laser Induced Damage in Optical Materials: 1987 [PB89-221162] N90-12913
Tunable Solid State Lasers conference edition: Tunable Solid State Lasers Topical Meeting [AD-A212292] N90-12920

HIGH PRESSURE
Advanced actuation systems development, volume 1 [AD-A213334] N90-12624
Thermophysical properties of benzene. Part 2: Thermodynamic properties at elevated pressures [ESDU-89003-PT-2] N90-12694
Continuing studies of liquid propellant drops in hot, high-pressure environments [AD-A212265] N90-12765

HIGH RESOLUTION
Visualization of high-resolution digital terrain [AD-A212149] N90-12971

HIGH REYNOLDS NUMBER
Design and test of a natural laminar flow/large Reynolds number airfoil with a high design cruise lift coefficient N90-12543

HIGH SPEED
Analysis of high speed pneumatic actuation systems under rotary directional on-off flow control N90-12926
High speed quantum-well optoelectronic devices by MBE [AD-A212585] N90-13237

HIGH SPEED CAMERAS
Spark camera annotation and control system for the BRL (Ballistic Research Laboratory) Transonic Range Facility [AD-A212266] N90-12633

HIGH TEMPERATURE
Laser probe vaporization/oxidation testing of high temperature composites [AD-A211410] N90-12663
Synthesis and high temperature chemistry of methylsilsesquioxane polymers produced by titanium catalyzed redistribution of methylhydridooligo- and polysiloxanes [AD-A212000] N90-12736
High temperature insulators [AD-D014193] N90-12751
Dimensional reduction at high temperature revisited [KVI-791] N90-13194
Compressibility of heavy nuclei at high temperatures [KVI-792] N90-13217

HIGH TEMPERATURE PLASMAS
Research on heating, instabilities, turbulence and RF emission from electric field dominated plasmas [AD-A212122] N90-13243

HIGH TEMPERATURE SUPERCONDUCTORS
Resistivity measurements of superconducting materials [PB89-225700] N90-12856
Seminars of Applied Physics, Materials Physics and Biomedical Engineering, 1989 [PB89-218572] N90-13192
Analysis of high temperature superconductors by means of PIXE and RBS methods [DE89-630241] N90-13252

HIGH TEMPERATURE TESTS
A new test machine for measuring friction and wear in controlled atmospheres to 1200 C [NASA-TM-102405] N90-12670

HILBERT SPACE
Well posedness of triples of operators (in the sense of linear systems theory) [TW-292] N90-13168

HIPPARCOS SATELLITE
Report on ESA's scientific satellites [ESA-SP-1110] N90-12649

HISTORIES
LFC: A maturing concept [DOUGLAS-PAPER-7878] N90-12505

HOLMIUM
Resistivity measurements of superconducting materials [PB89-225700] N90-12856

HOMOGENEITY
Atmospheric horizontal-inhomogeneity effects on the optical depths determined by the double-elevation-angle lidar technique [AD-A212836] N90-12839

HOMOMORPHISMS
Modular specifications in process algebra with curious queues [CWI-CS-R8821] N90-13152

HORMONES
Cardiovascular, renal, electrolyte, and hormonal changes in man during gravitational stress, weightlessness, and simulated weightlessness: Lower body positive pressure applied by the antigravity suit [NASA-TM-102232] N90-13013

HOT CORROSION
Effects of hot corrosion on the room temperature strength of structural ceramics [AD-A212568] N90-12762

HOT-FILM ANEMOMETERS
Advanced measurement techniques, part 1 N90-12520
Hot-film system for transition detection in cryogenic wind tunnels N90-12522
Predicted and hot-film measured Tollmien-Schlichting wave characteristics N90-12523

HOT-WIRE ANEMOMETERS
Flow quality measurements in compressible subsonic flows N90-12521
Basic aerodynamic research facility for comparative studies of flow diagnostic techniques N90-12526
Experimental study of homogeneous turbulence submitted to rotational effects [ONERA-RSF-10/1145-AY-164A] N90-12894

HUMAN BEHAVIOR
Fear-potentiated startle as a model system for analyzing learning and memory [AD-A212131] N90-13029

HUMAN BEINGS
Individual differences in associative learning and forgetting [AD-A212765] N90-13034

HUMAN FACTORS ENGINEERING
Integration of a centralized multiplexed control unit into the cockpit of an aircraft [F6150-DT410-1-88329] N90-12622
Psychological mechanisms involved in the disorientation of pilots due to flight conditions [ETN-89-95014] N90-13040

HUMAN FACTORS LABORATORIES
Psychological mechanisms involved in the disorientation of pilots due to flight conditions [ETN-89-95014] N90-13040

HUMAN PERFORMANCE
Effects of atmospheric mix and toxic fumes on military performance [PB89-223630] N90-13015
Effects of serial wet-dry-wet cold exposure: Thermal balance, physical activity, and cognitive performance [AD-A212704] N90-13025
The effects of noise on performance [AD-A212519] N90-13209

HUMAN TOLERANCES
Heat exhaustion [AD-A212128] N90-13014

HUMAN WASTES
Proposal for a zero-gravity toilet facility for the space station [NASA-CR-183151] N90-13036

HUMIDITY MEASUREMENT
Survey of the CLUSE main experiment Grand-CLUSE, May 1 - June 15, 1988 --- Humidity Exchange Over the Sea (HEXOS) experiment [FEL-1988-43] N90-12991
Infrared water vapor continuum absorption: New atmospheric electrical measurements and theory [AD-A212594] N90-12994

HYDRIDES
Extended basis set calculations of atomization energies: Comparison of isogyric and direct results [AD-A212268] N90-12702

HYDROCYANIC ACID
Effects of atmospheric mix and toxic fumes on military performance [PB89-223630] N90-13015

HYDROGEN
Rapid heating tensile tests of high-energy-rate-forged 316L stainless steel charged with hydrogen and tritium [DE89-017869] N90-12717
Interactive computer program for the generation of enthalpy-entropy and temperature-entropy charts of nitrogen and hydrogen [DLR-FB-89-27] N90-13081
Unsteady diffusion from a hemispherical pit [NPL-DMA(A)-190] N90-13220

HYDROGEN EMBRITTLEMENT
Determination of the gaseous hydrogen ductile-brittle transition in copper-nickel alloys [NASA-TM-86494] N90-12715
A feasibility study of hydrogen dosage estimation in screw threads submitted to surface electrolytic treatment [CETIM-110110] N90-12730

HYDROGEN PEROXIDE
Measurement and correlation of the solubility and diffusion coefficient for oxygen and chlorine in basic hydrogen peroxide
[AD-A212348] N90-12703
HYDROGEN SULFIDE
Growth and characterization of zinc sulfide films by conversion of zinc oxide films with H2S
[AD-A213345] N90-13271
HYDROGRAPHY
Realization of a different NAVSTAR global positioning system for hydrographic surveying
[ETN-89-95720] N90-12972
Current velocity and hydrographic observations in the southwestern North Atlantic Ocean: Subtropical Atlantic Climate Studies (STACS), 1988
[PB89-230825] N90-13010
HYDROLYSIS
Polyelectrolyte-diffused zinc phosphate conversion coatings and polyacid coupling primers for corrosion protection of steel and aluminum, and alkali-catalyzed hydrolysis of polyimide-based materials
[AD-A212240] N90-12754
HYPERBOLIC DIFFERENTIAL EQUATIONS
Iterated theta method for hyperbolic equations
[CWI-NM-R8809] N90-13132
An Eigenvalue Analysis of finite-difference approximations for hyperbolic IBVPs
[NASA-TM-102241] N90-13137
HYPERCUBE MULTIPROCESSORS
Work-preserving emulations of fixed-connection networks
[AD-A211915] N90-13093
Formal calculations and parallesism. Solving linear systems
[ETN-89-95499] N90-13098
HYPERGEOMETRIC FUNCTIONS
Meixner-Pollaczek polynomials and the Heisenberg algebra
[CWI-PM-R8806] N90-13138
Jacobi functions as limit cases of q-ultraspherical polynomials
[CWI-PM-R8807] N90-13139
Representations of the twisted SU(2) quantum group and some q-hypergeometric orthogonal polynomials
[CWI-PM-R8809] N90-13140
The addition formula for little q-Legendre polynomials and the SU(2) quantum group
[CWI-AM-R8906] N90-13151
HYPERSONIC BOUNDARY LAYER
Hypersonic boundary layers. Viscous effects within the shock layer
[CERT-RSF-OA-25/5005-AYD] N90-12502
HYPERSONIC FLIGHT
The NASA experience in aeronautical R and D: Three case studies with analysis
[AD-A211486] N90-12496
HYPERSONIC FLOW
Rotational and vibrational nonequilibrium effects in rarefied, hypersonic flow
[NASA-CR-182559] N90-12498
Basic research on methods of calculating supersonic and hypersonic flow
[ONERA-RSF-19/1123-AY-234A] N90-12565
Development of an anti-Stokes coherent Raman diffusion system for measuring hypersonic flow
[ONERA-RSF-1/7301-PY] N90-12630
HYPERSONIC SHOCK
Hypersonic boundary layers. Viscous effects within the shock layer
[CERT-RSF-OA-25/5005-AYD] N90-12502
HYPERSONIC VEHICLES
Rotational and vibrational nonequilibrium effects in rarefied, hypersonic flow
[NASA-CR-182559] N90-12498
HYPERSONIC WIND TUNNELS
Design and fabrication requirements for low noise supersonic/hypersonic wind tunnels N90-12555
HYPERTHERMIA
Exertional heatstroke: An international perspective. An introduction: The role of exercise in the etiology of exertional heatstroke
[AD-A212242] N90-13020
Seminars of Applied Physics, Materials Physics and Biomedical Engineering, 1989
[PB89-218572] N90-13192
HYPERVELOCITY LAUNCHERS
Design and commissioning test results for the hypervelocity launcher research complex battery power supply
[AD-A211320] N90-12848
HYPOTHERMIA
Radio frequency (13.56 MHz) energy enhances rewarming from mild hypothermia
[AD-A212703] N90-13024
HYPOXIA
Effects of atmospheric mix and toxic fumes on military performance
[PB89-223630] N90-13015

I

ICE
Estimation of time to maximum supercooling during dynamic frazil ice formation
[AD-A212204] N90-12699
ICE FORMATION
Estimation of time to maximum supercooling during dynamic frazil ice formation
[AD-A212204] N90-12699
The Regional Polar Ice Prediction System, Berents Sea (RPIPS-B): A technical description
[AD-A213159] N90-13012
ICE MAPPING
The Regional Polar Ice Prediction System, Berents Sea (RPIPS-B): A technical description
[AD-A213159] N90-13012
IDEAL GAS
Thermophysical properties of benzene. Part 1: The ideal gas and the saturated liquid and vapour
[ESDU-89002-PT-1] N90-12693
IGNITION
Laser initiated ignition of liquid propellant
[AD-A212342] N90-12766
ILLUSIONS
A comparison of two subject-controlled attitude measures during somatogravic illusion exposure
[AD-A212528] N90-13031
IMAGE ANALYSIS
Conception and results of the DLR realtime azimuth processor for the E-SAR system
[DLR-FB-89-30] N90-12827
A hybrid architecture for feature labelling of oceanographic satellite images
[AD-A212236] N90-12975
The algebraic basis of mathematical morphology. Part 2: Openings and closings
[CWI-AM-R8904-PT-2] N90-13150
A review of focal reducer interferometer systems
[RSRE-MEMO-3486] N90-13231
IMAGE ENHANCEMENT
Enhancement of infrared thermographic imagery: Local smoothing and time-based interpolation
[ONERA-RT-8/7254-SN] N90-13232
IMAGE FILTERS
Image preprocessing by modified median filter
[AD-D014199] N90-12828
IMAGE INTENSIFIERS
A validation of the proposed NATO standard method to determine target acquisition distances with image intensifiers
[IZF-1988-8] N90-13230
IMAGE PROCESSING
On a fast two-dimensional radar imaging process for rotating targets, and an analysis of its image quality
[ESA-TT-1142] N90-12808
Conception and results of the DLR realtime azimuth processor for the E-SAR system
[DLR-FB-89-30] N90-12827
Image preprocessing by modified median filter
[AD-D014199] N90-12828
Video line processor
[AD-D014198] N90-12861
Readout and signal conditioning for a linear pyroelectric array
[RSRE-MEMO-4102] N90-12905
A two-dimensional hybrid experimental-numerical technique for elastic-plastic stress analysis N90-12949
Removing stripes in GOES (Geostationary Operational Environmental Satellites) images by matching empirical distribution functions
[PB89-213359] N90-12968
An attempt to draw conclusions from the vegetation to the geological underground in the area of Amberg (Germany, F.R.) by means of digital image processing of TM data
[DFVLR-FB-89-24] N90-12974
Three stages and two systems of visual processing
[AD-A212670] N90-13032
Visual perception processing in a hierarchical control system: Level 1
[PB89-221188] N90-13101
The algebraic basis of mathematical morphology. Part 2: Openings and closings
[CWI-AM-R8904-PT-2] N90-13150
IMAGE RECONSTRUCTION
Parallel and deterministic algorithms from MRF (Markov Random Fields): Surface reconstruction and integration
[AD-A212457] N90-13084
Faster Phong shading via angular interpolation
[CWI-CS-R8909] N90-13156
IMAGERY
Faster Phong shading via angular interpolation
[CWI-CS-R8909] N90-13156
IMAGES
Performance of the image statistics decoder in conjunction with the Goldstone-VLA array N90-12796
Video line processor
[AD-D014198] N90-12861
Direct computation of 3D shape invariants and the focus of expansion
[AD-A212386] N90-13195
IMAGING TECHNIQUES
On a fast two-dimensional radar imaging process for rotating targets, and an analysis of its image quality
[ESA-TT-1142] N90-12808
An air coupled transmission mode acoustic microscope for on-line non-destructive evaluation
[AD-A211416] N90-12947
An attempt to draw conclusions from the vegetation to the geological underground in the area of Amberg (Germany, F.R.) by means of digital image processing of TM data
[DFVLR-FB-89-24] N90-12974
Faster Phong shading via angular interpolation
[CWI-CS-R8909] N90-13156
Proceedings of the 10 May 1989 Antiproton Technology Workshop: Addendum
[AD-A212804] N90-13227
A review of focal reducer interferometer systems
[RSRE-MEMO-3486] N90-13231
Liquid and solid ion plasmas
[AD-A212415] N90-13244
IMPACT RESISTANCE
Ballistic properties of composite materials for personnel protection
[MRL-TR-89-6] N90-12661
Spall resistance of alumina
[AD-A213213] N90-12735
IMPACT STRENGTH
Damage tolerance of CFRP sandwich panels
[FFA-TN-1988-70] N90-12664
A study of the impact of a ball bearing on a long fiber composite plate with a carbon matrix, part 2
[ETCA-88-R-088-PT-2] N90-12673
IMPACT TESTS
Damage tolerance of CFRP sandwich panels
[FFA-TN-1988-70] N90-12664
A study of the impact of a ball bearing on a long fiber composite plate with a carbon matrix, part 2
[ETCA-88-R-088-PT-2] N90-12673
Mathematical simulation of dynamic compression tests using the Hopkinson bar method
[ISL-R-128/87] N90-12960
Fatigue testing of welded steel assemblies with or without finishing treatments
[CETIM-107900] N90-12961
IMPEDANCE
Capacitive behavior in conducting polymers
[AD-A212448] N90-12760
IMPELLERS
SSME structural dynamic model development
[NASA-CR-183671] N90-12650
IMPURITIES
The effects of trace anions on the voltammetry of single crystal gold surfaces
[AD-A211886] N90-13254
Study of the electrical and optical properties of the vanadium and nickel impurities in GaAs
[ISAL-89-0028] N90-13259
INCLUSIONS
The effect of a rigid elliptical inclusion on a straight crack
[AD-A212263] N90-12965
INCOHERENCE
Proof of the feasibility of coherent and incoherent schemes for pumping a gamma-ray laser
[AD-A212315] N90-12921
INCOMPRESSIBLE FLOW
Numerical algorithms for steady and unsteady incompressible Navier-Stokes equations
[NASA-CR-186039] N90-12499
Numerical evaluation of a solution representing a jet in cross-flow
[RAE-TM-AERO-2137] N90-12893
INDENTATION
Elastic indentation fractures
[ETCA-88-R-116] N90-12955
INDEPENDENT VARIABLES
Interpretation and manipulation of Edgeworth expansions
[MEMO-775] N90-13163

INDEXES (DOCUMENTATION)
Aeronautical engineering: A continuing bibliography with indexes (supplement 245)
[NASA-SP-7037(245)] N90-12497
INDEXES (RATIOS)
Index formulas for generalized Wiener-Hopf operators and Boson-Fermion correspondence in 2N dimensions
[CWI-PM-R8811] N90-13141
INDUCTION (MATHEMATICS)
Kolmogorov complexity and its applications
[CWI-CS-R8901] N90-13191
INDUCTION MOTORS
Mathematical models for the linear induction motor
[RR-WB-88-17] N90-12853
INDUSTRIAL PLANTS
The effects of noise on performance
[AD-A212519] N90-13209
INERTIA
On the identification of local minimizers in inertia-controlling methods for quadratic programming
[AD-A212514] N90-13086
INERTIAL GUIDANCE
Guidance and Control Panel Symposium on Guidance and Control of Unmanned Air Vehicles
[AGARD-AR-260] N90-12623
INERTIAL NAVIGATION
Case study on rapid software prototyping and automated software generation: An inertial navigation system
[AD-A212272] N90-12578
RTSIN1: A model of a strapdown INS on a two-axis rate table
[AD-A212406] N90-12579
FPG2: A flight profile generator program
[AD-A212408] N90-12595
INERTIAL REFERENCE SYSTEMS
Hybrid angular velocity reference system for the investigation of dynamic properties of strapdown gryos
[DFVLR-FB-89-25] N90-12577
INFERENCE
Illustration of Bayesian inference in normal data models using Gibbs sampling
[AD-A212630] N90-13187
Kolmogorov complexity and its applications
[CWI-CS-R8901] N90-13191
INFORMATION
Polymorphism and information loss in Martin-Loef's type theory
[CS-8814] N90-13079
INFORMATION DISSEMINATION
Activities report of the Kernfysisch Versneller Instituut
[ETN-89-95752] N90-13219
Activities report of the Joint Research Center
[ETN-89-95757] N90-13321
INFORMATION PROCESSING (BIOLOGY)
Electrophysiological studies of visual attention and resource allocation
[AD-A212287] N90-13030
Visual perception processing in a hierarchical control system: Level 1
[PB89-221188] N90-13101
INFORMATION SYSTEMS
Telescience Testbed Pilot Program
[NASA-CR-184997] N90-13047
Fellowships in information and stochastic systems
[AD-A212385] N90-13280
INFRARED ABSORPTION
Infrared water vapor continuum absorption: New atmospheric electrical measurements and theory
[AD-A212594] N90-12994
INFRARED DETECTORS
Readout and signal conditioning for a linear pyroelectric array
[RSRE-MEMO-4102] N90-12905
Photoelectron pumped phosphors
[AD-A213202] N90-12912
INFRARED IMAGERY
Enhancement of infrared thermographic imagery: Local smoothing and time-based interpolation
[ONERA-RT-8/7254-SN] N90-13232
INFRARED LASERS
Tunable Solid State Lasers conference edition: Tunable Solid State Lasers Topical Meeting
[AD-A212292] N90-12920
INFRARED RADIATION
Mark-3 interferometer
[AD-A213155] N90-12911
INFRARED SIGNATURES
Design and tests of simple, inexpensive optical beacon for use on small satellites
[AD-A213325] N90-13238
INFRARED SPACE OBSERVATORY (ISO)
Report on ESA's scientific satellites
[ESA-SP-1110] N90-12649
INFRARED SPECTRA
Infrared spectrometry of aerosols
[AD-A213303] N90-12713
INFRARED SPECTROMETERS
Infrared spectrometry of aerosols
[AD-A213303] N90-12713
INFRARED SPECTROSCOPY
Infrared spectrometry of aerosols
[AD-A213303] N90-12713
Semiconductor measurement technology: Database for and statistical analysis of the interlaboratory determination of the conversion coefficient for the measurement of the interstitial oxygen content of silicon by infrared absorption
[PB89-221170] N90-13253
INITIATION
Thermal initiation of confined primary explosives with a proton beam
[AD-A212954] N90-12767
INJECTION
Thin-film integrated injection logic
[AD-D014190] N90-12860
INJURIES
Exertional heatstroke: An international perspective. An introduction: The role of exercise in the etiology of exertional heatstroke
[AD-A212242] N90-13020
INPUT/OUTPUT ROUTINES
A functional expansion and stability for nonlinear input-output maps
[RR-359] N90-13121
INSPECTION
A computer integrated approach to dimensional inspection
[PNR90596] N90-12611
A robot which will investigate the condition of underground pipe
[PB89-230650] N90-12928
INSTRUCTION SETS (COMPUTERS)
User manual of the force structure model scenario editor SCENE
[FEL-1988-101] N90-13069
Modular specifications in process algebra with curious queues
[CWI-CS-R8821] N90-13152
INSTRUMENTS
National Science Foundation N90-13320
INSULATION
The 4th US Army Workshop on Low Heat Rejection Engines
[AD-A212379] N90-12943
Magnetically insulated electron flows in pulsed power systems
[AD-A212746] N90-13196
INSULATORS
High temperature insulators
[AD-D014193] N90-12751
INTAKE SYSTEMS
Structural vibration and shock isolator
[AD-D014202] N90-12940
INTEGRALS
Calculation of the odd and even integral components of the wave resistance Green's function
[AD-A212384] N90-12900
INTEGRATED CIRCUITS
Ka-band MMIC beam steered transmitter array N90-12803
A 2d-1 lower bound 2-layer knock-knee channel routing
[AD-A211948] N90-12847
INTEGRATED MISSION CONTROL CENTER
The cosmic radiation effects and activation monitor
[RAE-TM-SPACE-364] N90-13318
INTEGRATED OPTICS
Growth and characterization of zinc sulfide films by conversion of zinc oxide films with H2S
[AD-A213345] N90-13271
INTELLIGIBILITY
Removal of noise from noise-degraded speech signals
[AD-A212876] N90-12840
The effects of noise on speech and warning signals
[AD-A212520] N90-13210
INTERACTIVE CONTROL
On modeling resources in multiprocessor systems
[MEMO-INF-88-33] N90-13095
INTERFACES
Structure and properties of polymer interphases
[AD-A212796] N90-12763
Stress waves through projectile joints and interfaces
[AD-A212201] N90-12963
State of the art of human/machine dialog tool prototypes
[TELECOM-PARIS-89-H001] N90-13038
A cell-centered multigrid method for three-dimensional anisotropic-diffusion and interface problems
[REPT-89-35] N90-13128
A moving-grid interface for systems of one-dimensional time-dependent partial differential equations
[CWI-NM-R8904] N90-13136
INTERFERENCE
Residual interference assessment in adaptive wall wind tunnels
[NASA-CR-181896] N90-12625
INTERFEROMETERS
Mark-3 interferometer
[AD-A213155] N90-12911
A review of focal reducer interferometer systems
[RSRE-MEMO-3486] N90-13231
LASCO: A wide-field white light and spectrometric coronagraph for SOHO N90-13311
INTERMOLECULAR FORCES
Molecular dynamics of lipid bilayers
[AD-A211492] N90-13214
INTERNAL COMBUSTION ENGINES
The 4th US Army Workshop on Low Heat Rejection Engines
[AD-A212378] N90-12942
The 4th US Army Workshop on Low Heat Rejection Engines
[AD-A212379] N90-12943
INTERNATIONAL COOPERATION
Wider horizons: Potential contributions by space systems to socio-economic advancement in developing countries
[ESA-SP-1106] N90-13276
Technology transfer to the United States: The MIT (Massachusetts Institute of Technology) Japan Science and Technology Program. A background paper of OTA's (Office of Technology Assessment's) assessment on technology, innovation, and US trade
[PB89-224711] N90-13291
INTERPOLATION
A theory of networks for approximation and learning
[AD-A212359] N90-13110
Faster Phong shading via angular interpolation
[CWI-CS-R8909] N90-13158
Enhancement of infrared thermographic imagery: Local smoothing and time-based interpolation
[ONERA-RT-8/7254-SN] N90-13232
INTERPROCESSOR COMMUNICATION
An implementation-oriented specification of the TUMULT communication primitives
[MEMO-INF-88-34] N90-13096
INTERSTELLAR MATTER
Nonequilibrium ionization in supernova remnants: The case of Tycho
[MPE-PREPRINT-153] N90-13295
INTERSTITIALS
Interstitial formation, non-equilibrium and macroscopic processes in mercury cadmium telluride
[AD-A212412] N90-13267
INTERSYMBOLIC INTERFERENCE
Numerical analysis of chaotic symbol sequences generated by parabolic and triangle maps of the interval
[MPIS-22/1987] N90-13124
INVENTORIES
Air Force flight feeding. Volume 1: Evaluation of current system and alternative concepts
[AD-A212789] N90-13043
INVERSIONS
Batch LCAP2-linear control analysis, version 2.0: User's manual
[AD-A211670] N90-12643
INVISCID FLOW
Supersonic boundary-layer transition on the LaRC F-106 and the DFRF F-15 aircraft. Part 2: Aerodynamic predictions N90-12559
Numerical evaluation of a solution representing a jet in cross-flow
[RAE-TM-AERO-2137] N90-12893
IODINE LASERS
Microwave excitation of oxygen O2 (delta 1) for an oxygen-iodine laser
[DFVLR-FB-89-23] N90-12919
ION BEAMS
Current limiting mechanisms in electron and ion beams experiments
[AD-A212295] N90-12637
ION EMISSION
COSTEP: A comprehensive suprathermal and energetic particle analyzer for SOHO N90-13314
ION EXCHANGING
Photochemical observation of ion flows in membrane channels
[AD-A212449] N90-12705
ION TRAPS (INSTRUMENTATION)
An apparatus for the electrodynamic containment of charged macroparticles N90-12789
IONIC COLLISIONS
Exploring asymmetric heavy-ion reactions at the KX-ray method: The Ne20 + Tb159 reaction at 15 MeV/unit
[KVI-777] N90-13216
An explicit partition of the fusion-like cross section
[KVI-797] N90-13225

IONIZATION
Polymer characterization by electrohydrodynamic ionization mass spectrometry
[AD-A212130] N90-12739
IONS
The multivalent beta'-aluminas
[AD-A212103] N90-12738
Liquid and solid ion plasmas
[AD-A212415] N90-13244
IRRADIATION
An investigation of the irradiation swelling mechanisms in refractory metals at high temperatures
[AD-A211406] N90-12719
ISOCYANATES
Chemical treatment of epoxy resins to reduce moisture sensitivity and to improve the mechanical properties
[AD-A212360] N90-12758
ISOLATION
Vibration isolation technology: Sensitivity of selected classes of space experiments to residual accelerations
[NASA-CR-185443] N90-12768
Structural vibration and shock isolator
[AD-D014202] N90-12940
ISOTHERMAL PROCESSES
Vibration isolation technology: Sensitivity of selected classes of space experiments to residual accelerations
[NASA-CR-185443] N90-12768
ISOTOPES
CELIAS: Charge, element and isotope analysis system for SOHO N90-13313
ISOTROPIC TURBULENCE
Evaluation of the near-wall k-epsilon turbulence model by comparison with direct simulations of turbulent channel flow
[AD-A212674] N90-12903
ISOTROPY
A thermoelastic transversely isotropic thick walled cylinder/disk application: An analytical solution and study
[NASA-TM-102320] N90-12950
ITERATION
Multiplicative iterative algorithms for convex programming
[CWI-AM-R8808] N90-13072
Iterative methods for linear complementary and related problems
[AD-A212848] N90-13089
Local mode smoothing analysis of various incomplete factorization iterative methods in two dimensions
[REPT-89-36] N90-13129
Iterated theta method for hyperbolic equations
[CWI-NM-R8809] N90-13132
ITERATIVE SOLUTION
Solution of the thin-layer Navier-Stokes equations for laminar transonic flow
[PB89-221600] N90-12879
A linearized surface condition in low speed hydrodynamics
[REPT-89-04] N90-12885
Subspace iteration algorithms in FORTRAN 77 and FORTRAN 8x
[AD-A212275] N90-13083
Iterative methods for linear complementary and related problems
[AD-A212848] N90-13089
Multigrid solution method for the Euler equations
[PB89-219463] N90-13116

J

JAMMING
Preliminary report on the feasibility of high power Electronic Warfare (EW) using explosive energy sources
[MRL-TR-89-3] N90-12775
Performance analysis of large adaptive sidelobe canceller arrays with reused elements
[AD-A212888] N90-12841
Automated Steerable Nulling Antenna Processor (SNAP) model
[PB89-231740] N90-12937
Fellowships in information and stochastic systems
[AD-A212385] N90-13280
JAPAN
Technology transfer to the United States: The MIT (Massachusetts Institute of Technology) Japan Science and Technology Program. A background paper of OTA's (Office of Technology Assessment's) assessment on technology, innovation, and US trade
[PB89-224711] N90-13291
JET AIRCRAFT NOISE
What should be done with those noisy old aircraft
[PNR90562] N90-12593
Re-engine with the Rolls-Royce Tay 670, the route to significant noise reduction
[PNR90585] N90-12606
The commercial aircraft noise problem
[PNR90577] N90-13203
JET ENGINES
Dynamic tip clearance measurements in axial flow compressors
[PNR90597] N90-12612
JET FLOW
Numerical evaluation of a solution representing a jet in cross-flow
[RAE-TM-AERO-2137] N90-12893
JET LAG
Effects of a time zone shift of nine hours on the circadian rhythms in cockpit aircrew members on longhaul flights
[DLR-FB-89-31] N90-13019
JET MIXING FLOW
Characterization of nonpremixed turbulent bluff-body burner flames
[PB89-229447] N90-12689
JOINTS (JUNCTIONS)
Stress waves through projectile joints and interfaces
[AD-A212201] N90-12963
JOULE-THOMSON EFFECT
Development of a low noise 10 K J-T refrigeration system
[AD-A213347] N90-12779

K

K-EPSILON TURBULENCE MODEL
Investigation of turbulent flow in highly curved ducts with application to turbomachinery components
[NASA-CR-186060] N90-12882
Evaluation of the near-wall k-epsilon turbulence model by comparison with direct simulations of turbulent channel flow
[AD-A212674] N90-12903
KALMAN FILTERS
Stable Kalman filters for processing clock measurement data N90-12801
KERNEL FUNCTIONS
A kernel approach to estimation of the sphere radius density in Wicksell's corpuscle problem
[CWI-MS-R8809] N90-13142
KEVLAR (TRADEMARK)
Project, implementation, and utilization of composite structures
[ETN-89-95209] N90-12665
KINEMATIC EQUATIONS
Dynamic robot models using the Manutec r3 as an example
[ESA-TT-1132] N90-12626
KINEMATICS
Kinematics, special configurations and performance evaluation of serial manipulators N90-12927
KINETIC THEORY
Time evolution of the electron swarm energy distribution function
[AD-A212967] N90-13247
KINETICS
Photodissociation of XeF2 (xenon difluoride) at 193 nm
[AD-A211663] N90-12916
RTM user's guide
[NASA-CR-186091] N90-13065
KNOWLEDGE BASES (ARTIFICIAL INTELLIGENCE)
A knowledge-based approach to automated flow-field zoning for computational fluid dynamics
[NASA-TM-101072] N90-13048
KNOWLEDGE REPRESENTATION
The fault monitoring and diagnosis knowledge-based system for space power systems: AMPERES, phase 1
[NASA-CR-185486] N90-12654
Expert systems as deductive systems
[CWI-CS-R8825] N90-13073
Conceptual dependency theory and robot programming
[REPT-89-20] N90-13106
Semantics and consistency of rule-based expert systems
[CWI-CS-R8824] N90-13153
KOLMOGOROFF THEORY
Nonlinear systems and Kolmogorov's representation theorem
[RR-363] N90-12931
Kolmogorov complexity and its applications
[CWI-CS-R8901] N90-13191

L

LAGRANGE MULTIPLIERS
Semi-Lagrangian, semi-implicit solutions of the shallow water equations in one dimension
[AD-A212658] N90-12902
A moving-grid interface for systems of one-dimensional time-dependent partial differential equations
[CWI-NM-R8904] N90-13136
LAGRANGIAN EQUILIBRIUM POINTS
On a rate of convergence of the multiknapsack value function
[CWI-MS-R8812] N90-13144
LAGUERRE FUNCTIONS
A generalization of Moak's q-Laguerre polynomials
[REPT-89-21] N90-13126
Meixner-Pollaczek polynomials and the Heisenberg algebra
[CWI-PM-R8806] N90-13138
LAMINAR BOUNDARY LAYER
Research in Natural Laminar Flow and Laminar-Flow Control, part 1
[NASA-CP-2487-PT-1] N90-12503
Laminar flow: Challenge and potential N90-12504
LFC: A maturing concept
[DOUGLAS-PAPER-7878] N90-12505
Lockheed laminar-flow control systems development and applications N90-12506
Laminar flow: The Cessna perspective N90-12507
Long-range LFC transport N90-12508
Development flight tests of JetStar LFC leading-edge flight test experiment N90-12509
The right wing of the LEFT airplane N90-12510
Performance of laminar-flow leading-edge test articles in cloud encounters N90-12511
Simulated airline service experience with laminar-flow control leading-edge systems N90-12512
Stability theory applications to laminar-flow control N90-12513
Nonparallel stability of boundary layers N90-12514
Goertler instability on an airfoil N90-12517
Effect of roughness on the stability of boundary layers N90-12518
Research in Natural Laminar Flow and Laminar-Flow Control, part 2
[NASA-CP-2487-PT-2] N90-12519
Advanced measurement techniques, part 1 N90-12520
Flow quality measurements in compressible subsonic flows N90-12521
Predicted and hot-film measured Tollmien-Schlichting wave characteristics N90-12523
Experimental studies on Goertler vortices N90-12529
An experimental evaluation of slots versus porous strips for laminar-flow applications N90-12530
Results of LFC experiment on slotted swept supercritical airfoil in Langley's 8-foot transonic pressure tunnel N90-12531
Boundary-layer stability analysis of Langley Research Center 8-foot LFC experimental data N90-12532
Sensitivity of LFC techniques in the non-linear regime N90-12533
Numerical solutions of the compressible 3-D boundary-layer equations for aerospace configurations with emphasis on LFC N90-12534
Theoretical methods and design studies for NLF and HLFC swept wings at subsonic and supersonic speeds N90-12535
Near-field noise predictions of an aircraft in cruise N90-12538
Design and test of an NLF wing glove for the variable-sweep transition flight experiment N90-12544
Experimental and numerical analyses of laminar boundary-layer flow stability over an aircraft fuselage forebody N90-12549
Status report on a natural laminar-flow nacelle flight experiment N90-12550
Nacelle aerodynamic performance N90-12552
Supersonic laminar-flow control N90-12554
LAMINAR FLOW
Numerical algorithms for steady and unsteady incompressible Navier-Stokes equations
[NASA-CR-186039] N90-12499
Research in Natural Laminar Flow and Laminar-Flow Control, part 1
[NASA-CP-2487-PT-1] N90-12503
Laminar flow: Challenge and potential N90-12504
LFC: A maturing concept
[DOUGLAS-PAPER-7878] N90-12505
Research in Natural Laminar Flow and Laminar-Flow Control, part 2
[NASA-CP-2487-PT-2] N90-12519
Research in Natural Laminar Flow and Laminar-Flow Control, part 3
[NASA-CP-2487-PT-3] N90-12539
The design of an airfoil for a high-altitude, long-endurance remotely piloted vehicle N90-12545
F-14 VSTFE and results of the cleanup flight test program N90-12547
Variable-Sweep Transition Flight Experiment (VSTFE): Stability code development and clean-up glove data analysis N90-12548

Nacelle aerodynamic performance N90-12552
Effects of acoustic sources N90-12553
Supersonic laminar-flow control N90-12554
Supersonic boundary-layer transition on the LaRC F-106 and the DFRF F-15 aircraft. Part 1: Transition measurements and stability analysis N90-12558
Supersonic boundary-layer transition on the LaRC F-106 and the DFRF F-15 aircraft. Part 2: Aerodynamic predictions N90-12559
Asymptotic analyses of the structures and characteristics of flames N90-12683
A computationally efficient modelling of laminar separation bubbles [NASA-CR-185854] N90-12872
Solution of the thin-layer Navier-Stokes equations for laminar transonic flow [PB89-221600] N90-12879
Transition in surface boundary layers [CERT-RSF-OA-43/5018-AYD] N90-12897
Seminars of Applied Physics, Materials Physics and Biomedical Engineering, 1989 [PB89-218572] N90-13192

LAMINAR FLOW AIRFOILS
Research in Natural Laminar Flow and Laminar-Flow Control, part 1 [NASA-CP-2487-PT-1] N90-12503
Laminar flow: Challenge and potential N90-12504
Laminar flow: The Cessna perspective N90-12507
Long-range LFC transport N90-12508
Development flight tests of JetStar LFC leading-edge flight test experiment N90-12509
The right wing of the LEFT airplane N90-12510
Performance of laminar-flow leading-edge test articles in cloud encounters N90-12511
Simulated airline service experience with laminar-flow control leading-edge systems N90-12512
Boundary-layer receptivity and laminar-flow airfoil design N90-12516
Goertler instability on an airfoil N90-12517
Research in Natural Laminar Flow and Laminar-Flow Control, part 2 [NASA-CP-2487-PT-2] N90-12519
Predicted and hot-film measured Tollmien-Schlichting wave characteristics N90-12523
Results of LFC experiment on slotted swept supercritical airfoil in Langley's 8-foot transonic pressure tunnel N90-12531
Boundary-layer stability analysis of Langley Research Center 8-foot LFC experimental data N90-12532
Theoretical methods and design studies for NLF and HLFC swept wings at subsonic and supersonic speeds N90-12535
Research in Natural Laminar Flow and Laminar-Flow Control, part 3 [NASA-CP-2487-PT-3] N90-12539
Design of the low-speed NLF(1)-0414F and the high-speed HSNLF(1)-0213 airfoils with high-lift systems N90-12540
Wind tunnel results of the low-speed NLF(1)-0414F airfoil N90-12541
Wind tunnel results of the high-speed NLF(1)-0213 airfoil N90-12542
Design and test of a natural laminar flow/large Reynolds number airfoil with a high design cruise lift coefficient N90-12543
The 757 NLF glove flight test results N90-12546
Nacelle design N90-12551
Transition in surface boundary layers [CERT-RSF-OA-43/5018-AYD] N90-12897
Unsteady three-dimensional thin-layer Navier Stokes solutions on dynamic blocked grids [AD-A212377] N90-12899

LAMINAR HEAT TRANSFER
Studies of gas turbine heat transfer airfoil surfaces and end-wall cooling effects [AD-A212451] N90-12620

LAMINATES
Spectroscopic ellipsometry characterization of CVD deposition and doping of polysilicon multilayer structures [RSRE-MEMO-4258] N90-12671
Nonlinear theories concerning laminated composites under compression with delamination [ONERA-RT-19/3542-RY-081-R] N90-12672
Numerical analysis of notch test damage to laminated composite plates submitted to uniaxial traction [CETIM-107310] N90-12675
Analysis of carbon fiber's x ray microscopic structure [AD-A212215] N90-12752
Rolling of ARALL laminates (an alternative method for post-stretching ARALL laminates) [LR-560] N90-12778

LAND USE
Wider horizons: Potential contributions by space systems to socio-economic advancement in developing countries [ESA-SP-1106] N90-13276

LANDING SIMULATION
Route data representation for ATC simulation experiments [RSRE-MEMO-4133] N90-12576

LANGUAGE PROGRAMMING
Specification of Viper1 in Z [RSRE-MEMO-4195] N90-12817
Specification of Viper2 in Z [RSRE-MEMO-4217] N90-12819
LOTOS tools based on the Cornell synthesizer generator [MEMO-INF-89-5] N90-13062
A Z specification of the MaCHO interface editor [RSRE-MEMO-4247] N90-13067

LANGUAGES
Process expressions and Hoare's logic [CWI-CS-R8905] N90-13076
Anaphoric trees and an extension of the model of anaphora resolution [REPT-89-37] N90-13130

LARGE SPACE STRUCTURES
A closed-cycle refrigerator for cooling maser amplifiers below 4 Kelvin N90-12797

LASER ANEMOMETERS
Flow in the neighborhood of an ellipsoid cylinder of revolution model [ONERA-RT-22/7252-AN-000A] N90-12895

LASER APPLICATIONS
Volumetric analysis by spontaneous Raman diffusion in a supersonic wind tunnel [ISL-R-109/88] N90-12564
Vibration intensity. Evaluation of a remote measuring system [CETIM-110430] N90-12907
Design and performance of an on-satellite laser diagnostic system for a free space optical heterodyne frequency-shift-keyed communication system [AD-A211986] N90-12915
Lectures on x ray lasers [ETN-89-95516] N90-12917
Liquid and solid ion plasmas [AD-A212415] N90-13244

LASER BEAMS
Laser initiated ignition of liquid propellant [AD-A212342] N90-12766
Catadioptric Optics for laser Doppler velocimeter applications [NASA-TM-102210] N90-12904
B factory via conversion of 1 TeV electron beams into 1 TeV photon beams [DE89-017692] N90-12914

LASER CAVITIES
Cavity eigenmodes for the NIST/NRL (National Institute of Standards and Technology/Naval Research Laboratory) free electron laser [AD-A212706] N90-12923

LASER DAMAGE
Laser Induced Damage in Optical Materials: 1987 [PB89-221162] N90-12913

LASER DOPPLER VELOCIMETERS
Three-component laser Doppler velocimeter measurements in a juncture flow N90-12525
Basic aerodynamic research facility for comparative studies of flow diagnostic techniques N90-12526
Experimental studies on Goertler vortices N90-12529
Catadioptric Optics for laser Doppler velocimeter applications [NASA-TM-102210] N90-12904

LASER FUSION
Microwave excitation of oxygen O2 (delta 1) for an oxygen-iodine laser [DFVLR-FB-89-23] N90-12919

LASER GYROSCOPES
Hybrid angular velocity reference system for the investigation of dynamic properties of strapdown gryos [DFVLR-FB-89-25] N90-12577

LASER HEATING
Lectures on x ray lasers [ETN-89-95516] N90-12917

LASER INTERFEROMETRY
Remote detection of boundary-layer transition by an optical system N90-12524

LASER MATERIALS
Tunable Solid State Lasers conference edition: Tunable Solid State Lasers Topical Meeting [AD-A212292] N90-12920

LASER OUTPUTS
Tunable Solid State Lasers conference edition: Tunable Solid State Lasers Topical Meeting [AD-A212292] N90-12920

LASER PLASMA INTERACTIONS
Lectures on x ray lasers [ETN-89-95516] N90-12917

LASER PLASMAS
Liquid and solid ion plasmas [AD-A212415] N90-13244

LASER PROPULSION
NASA/USRA advanced space design program: The laser powered interorbital vehicle [NASA-CR-186044] N90-12646

LASER PUMPING
Photodissociation of XeF2 (xenon difluoride) at 193 nm [AD-A211663] N90-12916
Tunable Solid State Lasers conference edition: Tunable Solid State Lasers Topical Meeting [AD-A212292] N90-12920
Proof of the feasibility of coherent and incoherent schemes for pumping a gamma-ray laser [AD-A212882] N90-12924

LASERS
Apollo lightcraft project [NASA-CR-186055] N90-12655

LATTICES (MATHEMATICS)
The algebraic basis of mathematical morphology. Part 2: Openings and closings [CWI-AM-R8904-PT-2] N90-13150

LAUNCH VEHICLE CONFIGURATIONS
Low Earth Orbit Raider (LER) winged air launch vehicle concept [NASA-CR-186057] N90-12590

LAUNCH VEHICLES
Low Earth Orbit Raider (LER) winged air launch vehicle concept [NASA-CR-186057] N90-12590
Apollo lightcraft project [NASA-CR-186055] N90-12655

LAUNCHING
Stress waves through projectile joints and interfaces [AD-A212201] N90-12963

LAYOUTS
A 2d-1 lower bound 2-layer knock-knee channel routing [AD-A211948] N90-12847

LEADING EDGES
The right wing of the LEFT airplane N90-12510
Performance of laminar-flow leading-edge test articles in cloud encounters N90-12511
Simulated airline service experience with laminar-flow control leading-edge systems N90-12512
Experimental and theoretical investigation of boundary-layer instability mechanisms on a swept leading edge at Mach 3.5 N90-12557

LEARNING
Fear-potentiated startle as a model system for analyzing learning and memory [AD-A212131] N90-13029
Effects of type of responding on memory/visual search: Responding just yes or just no can lead to inflexible performance [AD-A212764] N90-13033

LEARNING THEORY
A theory of networks for approximation and learning [AD-A212359] N90-13110

LEAST SQUARES METHOD
Self-tuning control of nonlinear Armax models — Autoregressive Moving Average with eXogeneous (ARMAX) inputs [RR-362] N90-12930
An error estimator for parameter choice in regulating least square problems. Application to regularized deconvolution [IMAG-RR-744-M] N90-13125
NUMVEC FORTRAN library manual chapter: Simultaneous linear equations [CWI-NM-R8903] N90-13135
Exponential modeling using combined forward and backward prediction [AD-A212317] N90-13169

LENNARD-JONES GAS
Properties of Lennard-Jones mixtures at various temperatures and energy ratios with a size ratio of two [PB89-235204] N90-12697

LENS DESIGN
Catadioptric Optics for laser Doppler velocimeter applications [NASA-TM-102210] N90-12904

LIE GROUPS
Lie-algebraic aspects of the classical nonrelativistic Calogero-Moser models [CWI-AM-R8901] N90-13148

LIFE (DURABILITY)
Shear fatigue testing and life prediction of fibre composites [REPT-8519] N90-12668
The quality of vacuum deposited surface treatments [CETIM-107040] N90-12729

LIFT
Wind tunnel results of the low-speed NLF(1)-0414F airfoil N90-12541
Powered-lift aircraft technology [NASA-SP-501] N90-12589

LIFT DEVICES
Wind tunnel results of the high-speed NLF(1)-0213 airfoil N90-12542
LIFT DRAG RATIO
Design and test of a natural laminar flow/large Reynolds number airfoil with a high design cruise lift coefficient N90-12543
LIFTOFF (LAUNCHING)
Flight motor set 360L001 (STS-26R). (Reconstructed dynamic loads analysis) [NASA-CR-183811] N90-12656
LIGANDS
Electron density modulation of catalytic metal centers by substituted aryl-isocyanide ligands [AD-A212875] N90-12708
LIGHT MODULATION
Characterization of liquid crystal displays for optical signal processing applications [AD-A212832] N90-12910
LIGHT SCATTERING
Small particle scattering and absorption [AD-A213168] N90-12711
Semiconductor measurement technology: A software program for aiding the analysis of ellipsometric measurements, simple models [PB89-235923] N90-13261
LIGHTNING
Long wave atmospheric noise model, phase 1. Volume 1: Lightning occurrence rates and propagation theory [AD-A212794] N90-12836
Catalog of absolutely calibrated, range normalized, wideband, electric field waveforms from located lightning flashes in Florida: July 24 and August 14, 1985 data [AD-A212708] N90-13008
LIMITER CIRCUITS
Current limiting mechanisms in electron and ion beams experiments [AD-A212295] N90-12637
LIMITS (MATHEMATICS)
Domain of attraction of an operator between supremum and sum [REPT-89-05] N90-13119
Jacobi functions as limit cases of q-ultraspherical polynomials [CWI-PM-R8807] N90-13139
LINE OF SIGHT
A Scheiner-principle pocket optometer for self-evaluation and biofeedback accommodation training [AD-A213171] N90-13027
LINE SPECTRA
Far infrared, submm and mm spectroscopy of the galactic center: Radio arc and +20/+50 km s (exp -1) clouds [NASA-CR-185497] N90-13296
LINEAR ACCELERATORS
Radio frequency linac driven free-electron laser configurations [AD-A212572] N90-12922
LINEAR ARRAYS
Angle estimation in a multipath environment with an eight element linear array operating at 10.5 GHz [FEL-1989-15] N90-12826
LINEAR EQUATIONS
Kinematics, special configurations and performance evaluation of serial manipulators N90-12927
LINEAR FILTERS
On the Hellinger type distances for filtered experiments [CWI-MS-R8818] N90-13146
LINEAR OPERATORS
Well posedness of triples of operators (in the sense of linear systems theory) [TW-292] N90-13168
LINEAR PROGRAMMING
Iterative methods for linear complementary and related problems [AD-A212648] N90-13089
Monte Carlo (importance) sampling within a Benders' decomposition algorithm for stochastic linear programs [AD-A212854] N90-13189
LINEAR QUADRATIC GAUSSIAN CONTROL
Nongaussian linear filtering, identification of linear systems, and the symplectic group [CWI-PM-R8810] N90-13184
LINEAR SYSTEMS
Advanced actuation systems development, volume 1 [AD-A213334] N90-12624
Solving three dimensional block bidiagonal linear systems on vector computers [REPT-89-14] N90-13056
Solving 3D block bidiagonal linear systems on vector computers [CWI-NM-R8819] N90-13061
Formal calculations and parallelism. Solving linear systems [ETN-89-95499] N90-13098
Well posedness of triples of operators (in the sense of linear systems theory) [TW-292] N90-13168
Exponential modeling using combined forward and backward prediction [AD-A212317] N90-13169
Nongaussian linear filtering, identification of linear systems, and the symplectic group [CWI-PM-R8810] N90-13184
LINEARITY
On the existence of a maximal weak solution for a semilinear elliptic equation [REPT-89-06] N90-13120
LINEARIZATION
Towards a complete local solution of the nonlinear model matching problem [MEMO-781] N90-13166
LINGUISTICS
Self-organizing semantic maps [PB89-212609] N90-13049
Anaphoric trees and an extension of the model of anaphora resolution [REPT-89-37] N90-13130
LIPIDS
Molecular dynamics of lipid bilayers [AD-A211492] N90-13214
LIQUID ATOMIZATION
Survey of the CLUSE main experiment Grand-CLUSE, May 1 - June 15, 1988 --- Humidity Exchange Over the Sea (HEXOS) experiment [FEL-1988-43] N90-12991
LIQUID CHROMATOGRAPHY
Research and Development Opportunities in Supercritical Fluid Technology [DE89-015320] N90-12684
LIQUID CRYSTALS
Advanced measurement techniques, part 1 N90-12520
Characterization of liquid crystal displays for optical signal processing applications [AD-A212832] N90-12910
LIQUID HELIUM
Symmetry breaking phenomena in liquid Helium-4 [DE89-618886] N90-12685
Persistent current, NMR, and ion transmission experiments in rotating He-3 superfluids --- Nuclear Magnetic Resonance (NMR) [ISBN-952-90056-1-X] N90-13221
LIQUID ROCKET PROPELLANTS
Continuing studies of liquid propellant drops in hot, high-pressure environments [AD-A212265] N90-12765
LIQUID-SOLID INTERFACES
Interactive computer program for the generation of enthalpy-entropy and temperature-entropy charts of nitrogen and hydrogen [DLR-FB-89-27] N90-13081
LIQUID-VAPOR EQUILIBRIUM
Vapor-liquid equilibrium of binary mixtures in the extended critical region. Part 1: Thermodynamic model [PB89-218374] N90-12687
LITHIUM
The use of lithium batteries in biomedical devices [AD-A212187] N90-12863
LOAD DISTRIBUTION (FORCES)
Chordwise loading and camber for two-dimensional thin sections [AD-A213318] N90-12568
LOAD TESTS
Flight motor set 360L001 (STS-26R). (Reconstructed dynamic loads analysis) [NASA-CR-183811] N90-12656
Fatigue testing of welded steel assemblies with or without finishing treatments [CETIM-107900] N90-12961
LOADS (FORCES)
Multilayer theory for delamination analysis of a composite curved bar subjected to end forces and end moments [NASA-TM-4139] N90-12669
Fatigue behavior of specimens under compression load spectra [ETN-89-95207] N90-12954
LOGIC PROGRAMMING
Multiplicative iterative algorithms for convex programming [CWI-AM-R8808] N90-13072
Expert systems as deductive systems [CWI-CS-R8825] N90-13073
Process expressions and Hoare's logic [CWI-CS-R8905] N90-13076
Characterizing termination of logic problems with level mappings [CWI-CS-R8912] N90-13077
LOGISTICS
A survey of permanently-manned lunar base concepts [AD-A212575] N90-12638
LONG WAVE RADIATION
Proof of the feasibility of coherent and incoherent schemes for pumping a gamma-ray laser [AD-A212882] N90-12924
LOSSES
Polymorphism and information loss in Martin-Loef's type theory [CS-8814] N90-13079
LOW GRAVITY MANUFACTURING
Protein crystal growth in low gravity [NASA-CR-186082] N90-12770
LOW NOISE
Design and fabrication requirements for low noise supersonic/hypersonic wind tunnels N90-12555
Development of a low noise 10 K J-T refrigeration system [AD-A213347] N90-12779
LOW SPEED
Mathematical models for the linear induction motor [RR-WB-88-17] N90-12853
LOW TEMPERATURE
An approach to low temperature high strain rate superplasticity in aluminum alloy 2090 [AD-A212271] N90-12731
Synthesis and properties of NdNiO(3) prepared by low temperature methods [AD-A212117] N90-13256
LUBRICANT TESTS
Characterization of self-lubricating surface materials [CETIM-108060] N90-12749
Cold press lubrication: Fine tuning of the CETIM Forgelub test [CETIM-105160] N90-12938
LUBRICATION
Tribological properties of ceramic/Ti3Al-Nb sliding couples for use as candidate seal materials to 700 deg C [NASA-TM-102401] N90-12658
LUBRICATION SYSTEMS
Structural studies of sputter-deposited MoS2 solid lubricant films [AD-A212407] N90-12759
LUMINANCE
Three stages and two systems of visual processing [AD-A212670] N90-13032
LUMINOSITY
The process e(-)p giving gamma e(-)p as a fast luminosity for the HERA collider [NIKHEF-H/88-13] N90-13223
LUMINOUS INTENSITY
Design and tests of simple, inexpensive optical beacon for use on small satellites [AD-A213325] N90-13238
LUNAR BASES
A survey of permanently-manned lunar base concepts [AD-A212575] N90-12638

M

MACH NUMBER
Experimental and theoretical investigation of boundary-layer instability mechanisms on a swept leading edge at Mach 3.5 N90-12557
Transition in surface boundary layers [CERT-RSF-OA-43/5018-AYD] N90-12897
MACHINE TOOLS
The quality of vacuum deposited surface treatments [CETIM-107040] N90-12729
MAGNETIC BEARINGS
Cryostatless high temperature supercurrent bearings for rocket engine turbopumps [NASA-CR-183807] N90-12935
MAGNETIC FIELDS
Direction-of-arrival calculations at VLF/LF (Very Low Frequency/Low Frequency) [AD-A212620] N90-12833
Electron beam propagation through a magnetic wiggler with random field errors [AD-A212705] N90-12867
A survey of the current state-of-the-art in high-energy-product permanent magnets [AD-A211761] N90-13193
Three-dimensional equilibria and Mercier stability calculations [DE89-015907] N90-13239
MAGNETIC MATERIALS
Graduate fellowships in the field of hard magnetic materials [AD-A212303] N90-12733

MAGNETIC PROPERTIES
Graduate fellowships in the field of hard magnetic materials
[AD-A212303] N90-12733
Synthesis and properties of NdNiO(3) prepared by low temperature methods
[AD-A212117] N90-13256
MAGNETOHYDRODYNAMIC FLOW
Hermes plasma wind tunnel. Preliminary study, phase A1: Annexes, tables, figures
[DVG-HER-TN-002-PT-2] N90-12632
MAGNETOHYDRODYNAMIC GENERATORS
Preliminary report on the feasibility of high power Electronic Warfare (EW) using explosive energy sources
[MRL-TR-89-3] N90-12775
MAGNETOHYDRODYNAMIC STABILITY
Three-dimensional equilibria and Mercier stability calculations
[DE89-015907] N90-13239
MAGNETOHYDRODYNAMICS
Flux-corrected transport algorithms for two-dimensional compressible magnetohydrodynamics
[AD-A212757] N90-13246
MAGNETRON SPUTTERING
Synthesis and study of materials for superconducting electronics
[AD-A212966] N90-13270
MAGNETS
Plasma separation process: Magnet move to Oak Ridge National Laboratory
[DE89-017457] N90-13242
MAINTAINABILITY
Development and applications of reliability and maintainability design criteria in military aircraft
[ETN-89-95208] N90-12591
MAINTENANCE
Evaluation of a damaged F/A-18 horizontal stabilator
[AD-A212573] N90-12597
Designing for reliable and low maintenance cost aero engines
[PNR90570] N90-12604
MAMMALS
Sound Localization by Human Observers symposium proceedings
[AD-A212877] N90-13026
MAN-COMPUTER INTERFACE
Visualization of high-resolution digital terrain
[AD-A212149] N90-12971
State of the art of human/machine dialog tool prototypes
[TELECOM-PARIS-89-H001] N90-13038
ISI's (Information Sciences Institute) SDI architecture simulator: Initial prototype user interface
[AD-A211325] N90-13053
Conceptual dependency theory and robot programming
[REPT-89-20] N90-13106
MANAGEMENT
Base level management of radio frequency radiation protection program
[AD-A211759] N90-13017
MANAGEMENT METHODS
Issues in NASA program and project management
[NASA-SP-6101(02)] N90-13277
MANAGEMENT PLANNING
Development and evaluation at ATCEU of executive and support operations, phase 4A/3D --- ATCEU (Air Traffic Control Evaluation Unit)
[CAA-PAPER-88017] N90-12572
MANAGEMENT SYSTEMS
Artificial intelligence for communication prospects
[FEL-1989-1] N90-13107
MANGANESE
Influence of the composition of the metal deposited on carbon manganese welds on the work properties of the melted area depending on the operating mode of the weld
[CETIM-104530] N90-12726
MANIPULATORS
Kinematics, special configurations and performance evaluation of serial manipulators N90-12927
Acceleration sets of planar manipulators. Part 1: Theory
[AD-A213162] N90-12945
Visual perception processing in a hierarchical control system: Level 1
[PB89-221188] N90-13101
Identification of robot dynamics: A parallel processing approach
[RR-361] N90-13103
Real-time robot motion: The VLSI implementation via transputers
[RR-364] N90-13104
MANNED SPACECRAFT
A survey of permanently-manned lunar base concepts
[AD-A212575] N90-12638
Apollo lightcraft project
[NASA-CR-186055] N90-12655
MANUFACTURING
Proceedings of the DOD Workshop on the Manufacturing/Producibility of Organic Matrix Composites
[AD-A212577] N90-12680
MANY BODY PROBLEM
Towards a parallel algorithm for the many body problem
[CS-8813] N90-13078
Elements of a relativistic microscopic theory of hadronic matter in equilibrium and non-equilibrium
[KVI-796] N90-13218
MAPPING
Height and gradient from shading
[AD-A212338] N90-12908
A robot which will investigate the condition of underground pipe
[PB89-230650] N90-12928
Visualization of high-resolution digital terrain
[AD-A212149] N90-12971
A mapping for converting Mascot designs to Ada programs
[RSRE-MEMO-4244] N90-13070
Julia-Fatou-Sullivan theory for real one-dimensional dynamics
[REPT-88-100] N90-13190
MAPS
Problem-dependent transformations of 3D terrain elevation maps into cost precursor maps
[PB89-218127] N90-12969
Self-organizing semantic maps
[PB89-212609] N90-13049
Julia-Fatou-Sullivan theory for real one-dimensional dynamics
[REPT-88-100] N90-13190
Direct computation of 3D shape invariants and the focus of expansion
[AD-A212386] N90-13195
MARINE METEOROLOGY
Compendium of marine meteorological and oceanographic products of the Ocean Products Center, revision 1
[PB89-230684] N90-12967
Investigation of North Atlantic fog and development of a marine fog forecast system
[AD-A211780] N90-12999
MARKERS
Frame synchronization methods based on channel symbol measurements N90-12795
MARKOV PROCESSES
Parallel and deterministic algorithms from MRF (Markov Random Fields): Surface reconstruction and integration
[AD-A212457] N90-13084
Extended performability modeling using dynamic queing networks
[MEMO-INF-89-15] N90-13099
Note on the convergence of simulated annealing algorithms
[MEMO-774] N90-13162
Explicit modelling of state duration correlations in hidden Markov models --- speech recognition
[RSRE-MEMO-4152] N90-13178
Random truncation models and Markov processes
[CWI-MS-R8817] N90-13181
Stochastic process models in device physics
[AD-A212284] N90-13185
MARTINGALES
On the smooth fit boundary conditions in the optimal stopping problem for semimartingales
[CWI-MS-R8819] N90-13147
MASER OUTPUTS
Spin-lattice relaxation and the calculation of gain, pump power, and noise temperature in ruby N90-12790
MASER PUMPING
Spin-lattice relaxation and the calculation of gain, pump power, and noise temperature in ruby N90-12790
MASERS
A closed-cycle refrigerator for cooling maser amplifiers below 4 Kelvin N90-12797
Research on heating, instabilities, turbulence and RF emission from electric field dominated plasmas
[AD-A212122] N90-13243
MASS FLOW RATE
Two-phase flow pressure losses in pipeline fittings
[ESDU-89012] N90-12883
MASS SPECTROSCOPY
Improved method for determination of helium-4 in helium-3 by mass spectrometry
[PB89-201404] N90-12686
Polymer characterization by electrohydrodynamic ionization mass spectrometry
[AD-A212130] N90-12739
MASS TRANSFER
Studies of gas turbine heat transfer airfoil surfaces and end-wall cooling effects
[AD-A212451] N90-12620
MATCHING
Towards a complete local solution of the nonlinear model matching problem
[MEMO-781] N90-13166
MATERIALS HANDLING
Plasma separation process: Magnet move to Oak Ridge National Laboratory
[DE89-017457] N90-13242
MATERIALS RECOVERY
Research and Development Opportunities in Supercritical Fluid Technology
[DE89-015320] N90-12684
MATHEMATICAL LOGIC
Anaphoric trees and an extension of the model of anaphora resolution
[REPT-89-37] N90-13130
MATHEMATICAL MODELS
Basic research on methods of calculating supersonic and hypersonic flow
[ONERA-RSF-19/1123-AY-234A] N90-12585
Euler equation solutions applied to a helicopter rotor in forward moving flight
[ONERA-RSF-32/1285-AY-346A] N90-12592
Dynamic robot models using the Manutec r3 as an example
[ESA-TT-1132] N90-12626
Phase change material for spacecraft thermal management
[AD-A211404] N90-12648
SSME structural dynamic model development
[NASA-CR-183671] N90-12650
Modeling of the dielectric behavior of composite materials
[CERT-1/1398-MO] N90-12674
Vapor-liquid equilibrium of binary mixtures in the extended critical region. Part 1: Thermodynamic model
[PB89-218374] N90-12687
FLIC (FLame with Implicit Convection): A detailed, two-dimensional flame model
[AD-A212953] N90-12710
Vibration isolation technology: Sensitivity of selected classes of space experiments to residual accelerations
[NASA-CR-185443] N90-12768
Aircraft SAR simulation Sargen 1.0
[FEL-1989-44] N90-12823
Long wave atmospheric noise model, phase 1. Volume 1: Lightning occurrence rates and propagation theory
[AD-A212794] N90-12836
Long wave atmospheric noise model, phase 1. Volume 2: Mode parameters
[AD-A212795] N90-12837
Wire grid modeling of the linear tapered slot antenna
[AD-A212977] N90-12842
Mathematical models for the linear induction motor
[RR-WB-88-17] N90-12853
A computationally efficient modelling of laminar separation bubbles
[NASA-CR-185854] N90-12872
A theoretical method for the mechanical calculation of heat exchangers with sliding heads, phase 1 study
[CETIM-110240-PHASE-1] N90-12896
Evaluation of the near-wall k-epsilon turbulence model by comparison with direct simulations of turbulent channel flow
[AD-A212674] N90-12903
Automated Steerable Nulling Antenna Processor (SNAP) model
[PB89-231740] N90-12937
Mathematical simulation of dynamic compression tests using the Hopkinson bar method
[ISL-R-128/87] N90-12960
Modeling the temperature rise at the tip of a fast crack
[AD-A212418] N90-12966
Geodetic point positioning with GPS (Global Positioning System) carrier beat phase data from the CASA UNO experiment
[AD-A211955] N90-12970
Improvement and extension of a radar forest backscattering model
[NASA-CR-186083] N90-12973
Analysis and modeling of summertime convective cloud and precipitation structure over the Southeastern United States
[NASA-CR-185436] N90-12996
NTRFACE for MAGIC
[AD-A212858] N90-13112
A new decision rule for model structure identification of a class of nonlinear dynamic systems
[RR-360] N90-13122

Lie-algebraic aspects of the classical nonrelativistic Calogero-Moser models
[CWI-AM-R8901] N90-13148
The algebraic basis of mathematical morphology. Part 2: Openings and closings
[CWI-AM-R8904-PT-2] N90-13150
Semantics and consistency of rule-based expert systems
[CWI-CS-R8824] N90-13153
Remarks on the control of discrete time nonlinear systems
[MEMO-770] N90-13158
The discrete-time single-server queueing model
[MEMO-780] N90-13165
Towards a complete local solution of the nonlinear model matching problem
[MEMO-781] N90-13166
Exponential modeling using combined forward and backward prediction
[AD-A212317] N90-13169
Explicit modelling of state duration correlations in hidden Markov models --- speech recognition
[RSRE-MEMO-4152] N90-13178
Random truncation models and Markov processes
[CWI-MS-R8817] N90-13181
Different notions of uncertainty in quasi-probabilistic models
[CWI-CS-R8847] N90-13182
Stochastic process models in device physics
[AD-A212284] N90-13185
Corrections to the thin wall approximation in general relativity
[NASA-CR-186078] N90-13274
Strings, p-branes and Skyrmions in curved space N90-13293

MATHEMATICAL PROGRAMMING
Polymorphism and information loss in Martin-Loef's type theory
[CS-8814] N90-13079

MATRICES (MATHEMATICS)
A well conditioned formulation for the analysis of multi-layered frequency selective surfaces using a cascaded matrix approach
[RSRE-MEMO-4289] N90-12858
NUMVEC FORTRAN library manual chapter: Simultaneous linear equations
[CWI-NM-R8903] N90-13135

MATRIX MATERIALS
Proceedings of the DOD Workshop on the Manufacturing/Producibility of Organic Matrix Composites
[AD-A212577] N90-12680
Magnetic resonance of polymers at surfaces
[AD-A212225] N90-12753

MATRIX THEORY
International Conference on Operator Theory: Advances and applications
[AD-A212341] N90-13170

MAXIMUM LIKELIHOOD ESTIMATES
A simple model for DSS-14 outage times N90-12802
Multiplicative iterative algorithms for convex programming
[CWI-AM-R8808] N90-13072

MAXIMUM PRINCIPLE
On the existence of a maximal weak solution for a semilinear elliptic equation
[REPT-89-06] N90-13120

MAXWELL EQUATION
Application of a generalized Leibniz rule for calculating electromagnetic fields within continuous source regions
[AD-A212470] N90-12831
Magnetically insulated electron flows in pulsed power systems
[AD-A212746] N90-13196

MEASURE AND INTEGRATION
Basic research on methods of calculating supersonic and hypersonic flow
[ONERA-RSF-19/1123-AY-234A] N90-12565

MEASURING INSTRUMENTS
Advanced measurement techniques, part 1 N90-12520
Recent tests at Langley with a University of Tennessee Space Institute (UTSI) skin friction balance N90-12527

MECHANICAL DEVICES
A device to extract energy from water waves
[REPT-89-34] N90-12978

MECHANICAL PROPERTIES
Material requirements for future aeroengines
[PNR90595] N90-12610
Influence of the structure of epoxy network models on the volumetric, mechanical and viscoelastic properties
[ISAL-89-0024] N90-12666
Composite materials for future aeroengines
[PNR90584] N90-12667
The relationship between the mechanical properties of materials after press forming and their in-service properties
[CETIM-101530] N90-12723
The effects of heat treatment after welding on the functional properties of assemblies of CrMo alloys. Heat treatment of a mixed assembly of A48 and 10CD9.10 alloys
[CETIM-104320] N90-12724
How the common practice of heating plates of austenitic stainless steel during cooling affects their mechanical properties
[CETIM-104500] N90-12725
The multivalent beta'-aluminas
[AD-A212103] N90-12738
Textural and structural organization of the heat treated polymers: Mechanical properties relationships
[ETN-89-95711] N90-12744
Effects of hot corrosion on the room temperature strength of structural ceramics
[AD-A212568] N90-12762
A center for advanced electrical and structural polymers
[AD-A212853] N90-12764
Rolling of ARALL laminates (an alternative method for post-stretching ARALL laminates)
[LR-560] N90-12778
Structural vibration and shock isolator
[AD-D014202] N90-12940
Proceedings of the Army Symposium on Solid Mechanics, 1989: Mechanics of Engineered Materials and Applications
[AD-A211954] N90-12951
Increased fragility of deep pressed thin plates
[CETIM-13-Y-313] N90-12962
Synthesis and properties of NdNiO(3) prepared by low temperature methods
[AD-A212117] N90-13256

MEMBRANE STRUCTURES
Advanced double layer capacitor
[AD-A211977] N90-12688

MEMBRANES
Photochemical observation of ion flows in membrane channels
[AD-A212449] N90-12705
Calcium displacement caused by electromagnetic fields
[AD-A212690] N90-13023

MEMORY
Fear-potentiated startle as a model system for analyzing learning and memory
[AD-A212131] N90-13029
Effects of type of responding on memory/visual search: Responding just yes or just no can lead to inflexible performance
[AD-A212764] N90-13033
Individual differences in associative learning and forgetting
[AD-A212765] N90-13034

MEMORY (COMPUTERS)
GaAs gate dynamic memory technology
[AD-A212387] N90-13266

MENTAL PERFORMANCE
Effects of serial wet-dry-wet cold exposure: Thermal balance, physical activity, and cognitive performance
[AD-A212704] N90-13025

MERCURY CADMIUM TELLURIDES
Interstitial formation, non-equilibrium and macroscopic processes in mercury cadmium telluride
[AD-A212412] N90-13267

MERCURY ISOTOPES
An apparatus for the electrodynamic containment of charged macroparticles N90-12789

MEROMORPHIC FUNCTIONS
The Painleve test for nonlinear ordinary and partial differential equations
[AD-A212894] N90-13177

MESONS
Minimal total cross section for e(+)e(-) yields W(+)W(-)
[NIKHEF-H/88-12] N90-13222

MESOSCALE PHENOMENA
Analysis and modeling of summertime convective cloud and precipitation structure over the Southeastern United States
[NASA-CR-185436] N90-12996
Project WIND: Experiments with the UK Meteorological Office mesoscale model
[AD-A212291] N90-13006
Mesoscale acid deposition modeling studies
[NASA-CR-4262] N90-13228

MESOSPHERE
Fundamentals of middle atmospheric dynamics
[AD-A211747] N90-12988

MESSAGE PROCESSING
On modeling resources in multiprocessor systems
[MEMO-INF-88-33] N90-13095

METABOLITES
Prediction of thermal stress casualties
[AD-A212356] N90-13022

METAL COATINGS
The quality of vacuum deposited surface treatments
[CETIM-107040] N90-12729

METAL CRYSTALS
Temperature dependence of positron diffusion in cubic metals
[PB89-222020] N90-12722

METAL FLUORIDES
Corrosion and corrosion inhibition of metals/alloys in methylphosphonic difluoride and decontaminating solutions
[AD-A212404] N90-12734

METAL IONS
An apparatus for the electrodynamic containment of charged macroparticles N90-12789

METAL MATRIX COMPOSITES
Biaxial flexing of a fiber-reinforced aluminum composite
[AD-A212742] N90-12681
Corrosion and corrosion inhibition of metals/alloys in methylphosphonic difluoride and decontaminating solutions
[AD-A212404] N90-12734

METAL OXIDE SEMICONDUCTORS
The analysis of current-mirror MOSFETs for use in radiation environments
[AD-A212527] N90-12866
European Solid State Device Research Conference (18th) ESSDERC 88 held in Montpellier, France on 13-16 September 1988
[AD-A210618] N90-13250

METAL PLATES
The relationship between the mechanical properties of materials after press forming and their in-service properties
[CETIM-101530] N90-12723
Carbonitrition response of steel plates not destined for heat treatments
[CETIM-106960] N90-12728
Increased fragility of deep pressed thin plates
[CETIM-13-Y-313] N90-12962

METAL POWDER
Tribological properties of PM212: A high-temperature, self-lubricating, powder metallurgy composite
[NASA-TM-102355] N90-12659
Temperature effects in shock consolidation of metal powders
[DE89-016782] N90-12716

METAL SURFACES
Mechanisms of CO2 reduction metal and metal modified semiconductor electrodes
[AD-A213169] N90-12712

METAL WORKING
The relationship between the mechanical properties of materials after press forming and their in-service properties
[CETIM-101530] N90-12723
Rolling of ARALL laminates (an alternative method for post-stretching ARALL laminates)
[LR-560] N90-12778
Cold press lubrication: Fine tuning of the CETIM Forgelub test
[CETIM-105160] N90-12938

METALLOGRAPHY
Development of texture analysis and its applications to titanium aero engine components
[PNR90561] N90-12602

METALS
Electron density modulation of catalytic metal centers by substituted aryl-isocyanide ligands
[AD-A212875] N90-12708

METEOR TRAILS
Preliminary investigation of Faraday rotation effects and description of polarization measurements on the AFGL high latitude meteor scatter test bed
[AD-A211298] N90-12806

METEOROLOGICAL PARAMETERS
Radar polarimetric studies based on the MAYPOLE 1983 and 1984 field experiments
[AD-A212226] N90-12830
Meteorological Satellite Center Technical Note, no. 18, 1989
[MSC-TN-18] N90-12997
Project WIND: Experiments with the UK Meteorological Office mesoscale model
[AD-A212291] N90-13006

METEOROLOGICAL SATELLITES
Meteorological Satellite Center Technical Note, no. 18, 1989
[MSC-TN-18] N90-12997

METEOROLOGY
Semi-Lagrangian, semi-implicit solutions of the shallow water equations in one dimension
[AD-A212658] N90-12902
Project WIND: Experiments with the UK Meteorological Office mesoscale model
[AD-A212291] N90-13006
METHANE
Tables for the thermophysical properties of methane
[PB89-222608] N90-12690
Biological and biochemical methane reactions
[PB89-232615] N90-12977
MICROBALANCES
Quartz crystal microbalance analysis. 1: Evidence of anion or cation insertion into electropolymerized conducting polymers
[AD-A212304] N90-12755
MICROCRACKS
Mechanical behavior of carbon/resin composites under delamination and cracking of transverse layers
[ONERA-RT-46/7086-M] N90-12678
MICROELECTRONICS
Microsystems techniques: Concept, significance, status of development
[MBB-UA-1110/88-PUB] N90-12851
MICROPOROSITY
Carbonitrition response of steel plates not destined for heat treatments
[CETIM-106960] N90-12728
MICROPROCESSORS
Specification of Viper1 in Z
[RSRE-MEMO-4195] N90-12817
Specification of Viper2 in Z
[RSRE-MEMO-4217] N90-12819
MICROSTRIP ANTENNAS
Scalar Green function method for microstrip antenna analysis based on the exact image theory
[PB89-218838] N90-12805
MICROSTRUCTURE
Laser probe vaporization/oxidation testing of high temperature composites
[AD-A211410] N90-12663
Heat pipe and thermal energy storage and corrosion studies (1988)
[AD-A212655] N90-12706
Temperature effects in shock consolidation of metal powders
[DE89-016782] N90-12716
Rapid heating tensile tests of high-energy-rate-forged 316L stainless steel charged with hydrogen and tritium
[DE89-017869] N90-12717
How the common practice of heating plates of austenitic stainless steel during cooling affects their mechanical properties
[CETIM-104500] N90-12725
Carbonitrition response of steel plates not destined for heat treatments
[CETIM-106960] N90-12728
Ultrastructure processing and characterization of polymers
[AD-A211460] N90-12743
Textural and structural organization of the heat treated polymers: Mechanical properties relationships
[ETN-89-95711] N90-12744
Microsystems techniques: Concept, significance, status of development
[MBB-UA-1110/88-PUB] N90-12851
MICROWAVE AMPLIFIERS
Spin-lattice relaxation and the calculation of gain, pump power, and noise temperature in ruby N90-12790
A closed-cycle refrigerator for cooling maser amplifiers below 4 Kelvin N90-12797
MICROWAVE EQUIPMENT
A 2-MeV microwave thermionic gun
[DE89-015640] N90-12644
MICROWAVE TRANSMISSION
Ka-band MMIC beam steered transmitter array N90-12803
Ground effects on multipath fading
[TELECOM-PARIS-88-E017] N90-12812
MICROWAVES
Apollo lightcraft project
[NASA-CR-186055] N90-12655
DSN 70-meter antenna microwave optics design and performance improvements. Part 2: Comparison with measurements N90-12800
Microwave excitation of oxygen O2 (delta 1) for an oxygen-iodine laser
[DFVLR-FB-89-23] N90-12919
MIE SCATTERING
Infrared spectrometry of aerosols
[AD-A213303] N90-12713
MILITARY OPERATIONS
Recommended changes in US military space policies and programs: A paper submitted to the Commission on Integrated Long-Term Strategy
[PB89-219364] N90-12636
Algorithm development for SDI weapons system allocation
[AD-A212973] N90-13090
MILITARY TECHNOLOGY
Recommended changes in US military space policies and programs: A paper submitted to the Commission on Integrated Long-Term Strategy
[PB89-219364] N90-12636
A literature study of wave propagation in the 1-60 GHz range. Application to transportable military communication systems
[FEL-1988-47] N90-12825
Artificial intelligence for communication prospects
[FEL-1989-1] N90-13107
MILLIMETER WAVES
Theoretical and experimental research on a millimeter-wavelength free-electron laser
[AD-A213321] N90-12925
MIMD (COMPUTERS)
An implementation-oriented specification of the TUMULT communication primitives
[MEMO-INF-88-34] N90-13096
MINIATURE ELECTRONIC EQUIPMENT
Microsystems techniques: Concept, significance, status of development
[MBB-UA-1110/88-PUB] N90-12851
MINIATURIZATION
Squirt: The prototypical mobile robot for autonomous graduate students
[AD-A212337] N90-12941
MINIMAX TECHNIQUE
International Conference on Fixed Point Theory and Applications
[AD-A212369] N90-13171
MIRRORS
Placing mirrors in grids
[CWI-CS-R8906] N90-13154
MISSILE CONFIGURATIONS
Aerodynamic test and analysis of a slender generic missile configuration
[AD-A212522] N90-12567
MISSILE TESTS
Aerodynamic test and analysis of a slender generic missile configuration
[AD-A212522] N90-12567
MISSILES
Present and future US and Soviet chemical missiles and chemical rocket projectiles
[AD-A212199] N90-12644
MISSION PLANNING
Report on ESA's scientific satellites
[ESA-SP-1110] N90-12649
European space technology: Celebrating twenty-five years of research and development
[ESA-BR-55] N90-13322
MIXTURES
Airborne/spaceborne pulsed power source
[AD-A211762] N90-12850
MNEMONICS
Three stages and two systems of visual processing
[AD-A212670] N90-13032
MODAL RESPONSE
A survey on nonproportional damping N90-12773
MODELS
Development of a VSAERO (Vortex Separation Aerodynamics) model of the F/A-18
[AD-A212442] N90-12566
Studies of gas turbine heat transfer airfoil surfaces and end-wall cooling effects
[AD-A212451] N90-12620
The comparison of the airbase simulation models airbase and sustained
[FEL-1988-66] N90-12629
Laser probe vaporization/oxidation testing of high temperature composites
[AD-A211410] N90-12663
Photochemical observation of ion flows in membrane channels
[AD-A212449] N90-12705
An investigation of the irradiation swelling mechanisms in refractory metals at high temperatures
[AD-A211406] N90-12719
Structural studies of sputter-deposited MoS2 solid lubricant films
[AD-A212407] N90-12759
Height and gradient from shading
[AD-A212338] N90-12908
Visualization of high-resolution digital terrain
[AD-A212149] N90-12971
The GEM-T2 gravitational model
[NASA-TM-100746] N90-12984
MODULARITY
Modular specifications in process algebra with curious queues
[CWI-CS-R8821] N90-13152
MODULATION
Wideband phase-locked angular modulator N90-12798
Surface current and wave modulation measurements over bottom topography: A comparison with theory
[AD-A212469] N90-13011
MODULATION DOPING
Strong-inversion model of threshold voltage in modulation doped field effect transistors: The role of unintentional acceptors
[AD-A212750] N90-12870
MODULATORS
Wideband phase-locked angular modulator N90-12798
MOISTURE
Chemical treatment of epoxy resins to reduce moisture sensitivity and to improve the mechanical properties
[AD-A212360] N90-12758
MOLECULAR ABSORPTION
Chemical treatment of epoxy resins to reduce moisture sensitivity and to improve the mechanical properties
[AD-A212360] N90-12758
MOLECULAR BEAM EPITAXY
High speed quantum-well optoelectronic devices by MBE
[AD-A212585] N90-13237
MOLECULAR CHAINS
Ultrastructure processing and characterization of polymers
[AD-A211460] N90-12743
MOLECULAR COLLISIONS
Fundamental molecular data to support CARS diagnostics of temperature, pressure, and species concentration
[AD-A212411] N90-12704
MOLECULAR DIFFUSION
Photochemical observation of ion flows in membrane channels
[AD-A212449] N90-12705
MOLECULAR ENERGY LEVELS
Properties of Lennard-Jones mixtures at various temperatures and energy ratios with a size ratio of two
[PB89-235204] N90-12697
MOLECULAR INTERACTIONS
Properties of Lennard-Jones mixtures at various temperatures and energy ratios with a size ratio of two
[PB89-235204] N90-12697
Molecular dynamics of lipid bilayers
[AD-A211492] N90-13214
MOLECULAR OSCILLATIONS
Structures and energies for small borane compounds: One and two boron compounds
[AD-A212264] N90-12701
MOLECULAR RELAXATION
Fundamental molecular data to support CARS diagnostics of temperature, pressure, and species concentration
[AD-A212411] N90-12704
MOLECULAR STRUCTURE
Hardening mechanisms and analysis of the structure of the TGDDM/DDS epoxy resin system (tetraglycidyl-4,4' diaminodiphenylmethane/4,4' diaminodiphenylsulfone)
[NOTE-TECHNIQUE-1988-8] N90-12662
Electrically conducting organic materials: Design, synthesis and characterization
[AD-A212214] N90-12700
Extended basis set calculations of atomization energies: Comparison of isogyric and direct results
[AD-A212268] N90-12702
Magnetic resonance of polymers at surfaces
[AD-A212225] N90-12753
Structure and properties of polymer interphases
[AD-A212796] N90-12763
MOLECULES
Standard method for measurement of nonvolatile residue on surfaces
[AD-A213324] N90-12714
MOLTEN SALTS
Heat capacities of 1-methyl-3-ethylimidazolium chloride-aluminum chloride molten salts
[AD-A212790] N90-12707
MOLYBDENUM ALLOYS
The effects of heat treatment after welding on the functional properties of assemblies of CrMo alloys. Heat treatment of a mixed assembly of A48 and 10CD9.10 alloys
[CETIM-104320] N90-12724
MOLYBDENUM SULFIDES
Structural studies of sputter-deposited MoS2 solid lubricant films
[AD-A212407] N90-12759

MONITORS
The fault monitoring and diagnosis knowledge-based system for space power systems: AMPERES, phase 1
[NASA-CR-185486] N90-12654
Automated monitor and control for deep space network subsystems N90-12794
The process e(-)p giving gamma e(-)p as a fast luminosity for the HERA collider
[NIKHEF-H/88-13] N90-13223
Plasma separation process: Magnet move to Oak Ridge National Laboratory
[DE89-017457] N90-13242
The cosmic radiation effects and activation monitor
[RAE-TM-SPACE-364] N90-13318
MONOPOLES
Compressibility of heavy nuclei at high temperatures
[KVI-792] N90-13217
Cosmic strings and baryon decay catalysis
[NASA-CR-186074] N90-13299
MONOPULSE ANTENNAS
Dedicated tracking of crossing targets with a phased array monopulse radar
[FEL-1988-95] N90-12821
MONTE CARLO METHOD
Rotational and vibrational nonequilibrium effects in rarefied, hypersonic flow
[NASA-CR-182559] N90-12498
Multigrid Monte Carlo in an external U(1) gauge field
[NIKHEF-ITFA-88-52] N90-13114
Stochastic process models in device physics
[AD-A212284] N90-13185
Monte Carlo (importance) sampling within a Benders' decomposition algorithm for stochastic linear programs
[AD-A212854] N90-13189
MOORING
Estimating the time to fatigue failure of mooring cables
[PB89-220677] N90-12946
MORPHOLOGY
The algebraic basis of mathematical morphology. Part 2: Openings and closings
[CWI-AM-R8904-PT-2] N90-13150
MOTION PERCEPTION
Development of an integrated mobile robot system at CMU (Carnegie-Mellon University)
[AD-A212555] N90-12944
MOTION STABILITY
Free surface scars and striations
[AD-A212429] N90-12901
MOVING TARGET INDICATORS
Modified Newton-type methods for long-range target motion analysis
[FEL-1989-82] N90-13208
MTBF
Estimating the time to fatigue failure of mooring cables
[PB89-220677] N90-12946
MULTICHANNEL COMMUNICATION
Description and results of a multihop NACS simulation
[FEL-1988-46] N90-12824
MULTIPATH TRANSMISSION
Ground effects on multipath fading
[TELECOM-PARIS-88-E017] N90-12812
MULTIPLICATION
Non-separate arithmetic codes
[RSRE-MEMO-4215] N90-13058
MULTIPROCESSING (COMPUTERS)
On modeling resources in multiprocessor systems
[MEMO-INF-88-33] N90-13095
An implementation-oriented specification of the TUMULT communication primitives
[MEMO-INF-88-34] N90-13096
Path expression based operating systems
[MEMO-INF-88-68] N90-13097
Real-time robot motion: The VLSI implementation via transputers
[RR-364] N90-13104
LAIOS: A multiprocessor network for artificial intelligence applications
[ETN-89-95496] N90-13109
MULTIPROGRAMMING
Spark camera annotation and control system for the BRL (Ballistic Research Laboratory) Transonic Range Facility
[AD-A212266] N90-12633
MULTISTAGE ROCKET VEHICLES
Low Earth Orbit Raider (LER) winged air launch vehicle concept
[NASA-CR-186057] N90-12590
MULTIVARIATE STATISTICAL ANALYSIS
Stable summability and approximation theory
[AD-A211379] N90-13118
Multivariable divided difference and B-splines
[MEMO-772] N90-13160
On new methods for computing with multivariate B-splines
[MEMO-783] N90-13183

N

N-TYPE SEMICONDUCTORS
Dielectric spectroscopy of semiconductors
[AD-A211989] N90-13255
NACELLES
Status report on a natural laminar-flow nacelle flight experiment N90-12550
Nacelle design N90-12551
Nacelle aerodynamic performance N90-12552
Effects of acoustic sources N90-12553
NAKED SINGULARITIES
Twistons
[RSRE-MEMO-4234] N90-13275
NASA PROGRAMS
The NASA experience in aeronautical R and D: Three case studies with analysis
[AD-A211486] N90-12496
Issues in NASA program and project management
[NASA-SP-6101(02)] N90-13277
Departments of Veterans Affairs and Housing and Urban Development, and Independent Agencies Appropriations Bill, 1990
[H-REPT-101-150] N90-13281
National Aeronautics and Space Administration N90-13282
Fiscal year 1990 authorization request and budget estimates for the National Aeronautics and Space Administration
[GPO-96-945] N90-13283
Departments of Veterans Affairs and Housing and Urban Development, and Independent Agencies Appropriation Bill, 1990
[S-REPT-101-128] N90-13284
The 1990 National Aeronautics and Space Administration Authorization
[GPO-98-466] N90-13285
Department of Veterans Affairs and Housing and Urban Development, and Independent Agencies Appropriations Act, 1990
[HR-2916-PP] N90-13286
National Aeronautics and Space Administration N90-13287
National Aeronautics and Space Administration Authorization Act, fiscal year 1990
[S-REPT-101-157] N90-13288
National Aeronautics and Space Administration Authorization Act, fiscal year 1990
[S-REPT-101-157] N90-13289
NASA technology applications
[GPO-99-412] N90-13290
Research and Technology annual report, 1988
[NASA-TM-101070] N90-13319
NASTRAN
A mechanical power flow capability for the finite element code NASTRAN
[AD-A212202] N90-12964
NATIONAL AEROSPACE PLANE PROGRAM
National Aeronautics and Space Administration N90-13287
NATIONAL AIRSPACE UTILIZATION SYSTEM
Operational trial of effect of raising minimum stack level in Heathrow stacks
[CAA-PAPER-89003] N90-12573
NAVIER-STOKES EQUATION
Numerical algorithms for steady and unsteady incompressible Navier-Stokes equations
[NASA-CR-186039] N90-12499
Hypersonic boundary layers. Viscous effects within the shock layer
[CERT-RSF-OA-25/5005-AYD] N90-12502
Interaction of Tollmien-Schlichting waves and Goertler vortices N90-12515
Effect of roughness on the stability of boundary layers N90-12518
Application of sound and temperature to control boundary-layer transition N90-12537
Numerical study of three-dimensional spatial instability of a supersonic flat plate boundary layer
[NASA-CR-181931] N90-12874
Solution of the thin-layer Navier-Stokes equations for laminar transonic flow
[PB89-221600] N90-12879
A multigrid method for the Navier-Stokes and Boussinesq equations
[REPT-89-17] N90-12886
An implicit Navier-Stokes solver optimised for a vector-parallel computer
[VKI-TN-169] N90-12890
Upwind discretization of the steady Navier-Stokes equations
[CWI-NM-R8810] N90-12891
Unsteady three-dimensional thin-layer Navier Stokes solutions on dynamic blocked grids
[AD-A212377] N90-12899
NAVIGATION AIDS
Modified Newton-type methods for long-range target motion analysis
[FEL-1989-82] N90-13208
NAVIGATION INSTRUMENTS
Acquisition and recording an AMX A/C. Aeritalia experience and present trends
[ETN-89-95217] N90-12598
NAVIGATION SATELLITES
Stable Kalman filters for processing clock measurement data N90-12801
NAVIGATION TECHNOLOGY SATELLITES
Realization of a different NAVSTAR global positioning system for hydrographic surveying
[ETN-89-95720] N90-12972
NAVSTAR SATELLITES
Realization of a different NAVSTAR global positioning system for hydrographic surveying
[ETN-89-95720] N90-12972
NEAR FIELDS
Near-field noise predictions of an aircraft in cruise N90-12538
Calculation of the odd and even integral components of the wave resistance Green's function
[AD-A212384] N90-12900
The physical optics approximation in the near-field region
[FEL-1989-100] N90-13234
NEODYMIUM LASERS
Tunable Solid State Lasers conference edition: Tunable Solid State Lasers Topical Meeting
[AD-A212292] N90-12920
Advanced source development and applications. Laser-produced plasmas: A compact soft x ray source with high peak brightness
[AD-A212677] N90-13245
NETWORK ANALYSIS
On the precision and reliability of GPS networks computed using the double difference observable
[ETN-89-95719] N90-12571
Simulation of circuits adapted to signal processing
[TELECOM-PARIS-89-E001] N90-12811
Path expression based operating systems
[MEMO-INF-88-68] N90-13097
The application of artificial intelligence techniques to tracing the interconnections in an integrated circuit
[TELECOM-PARIS-89-E002] N90-13105
NETWORK CONTROL
Satellite range delay simulator for a matrix-switched time division multiple-access network simulator
[NASA-TM-102407] N90-12813
NEURAL NETS
Self-organizing semantic maps
[PB89-212609] N90-13049
A theory of networks for approximation and learning
[AD-A212359] N90-13110
NEUROLOGY
A theory of networks for approximation and learning
[AD-A212359] N90-13110
NEUTRINOS
Minimal total cross section for e(+)e(-) yields W(+)W(-)
[NIKHEF-H/88-12] N90-13222
NEUTRON PHYSICS
Proof of the feasibility of coherent and incoherent schemes for pumping a gamma-ray laser
[AD-A212315] N90-12921
NEWTON METHODS
A modified Newton method for unconstrained minimization
[AD-A212752] N90-13174
Modified Newton-type methods for long-range target motion analysis
[FEL-1989-82] N90-13208
NICKEL ALLOYS
Determination of the gaseous hydrogen ductile-brittle transition in copper-nickel alloys
[NASA-TM-86494] N90-12715
NICKEL HYDROGEN BATTERIES
Characterization and cycle tests of lightweight nickel electrodes
[NASA-TM-102399] N90-12696
NIGHT VISION
A Scheiner-principle pocket optometer for self-evaluation and biofeedback accommodation training
[AD-A213171] N90-13027
NITRILES
The chemistry of hexaazatriphenylene hexanitrile, a polyfunctional heterocycle with potential utility in the formulation of thermostable polymers
[AD-A212353] N90-12757
NITROGEN
Interactive computer program for the generation of enthalpy-entropy and temperature-entropy charts of nitrogen and hydrogen
[DLR-FB-89-27] N90-13081

NITROGEN IONS
An explicit partition of the fusion-like cross section
[KVI-797] N90-13225
NITROGENATION
Surface treatments of carbon fibers in an organic environment. Finite element analysis of pull-out tests
[ONERA-RT-7/3549-M] N90-12698
NOISE (SOUND)
The effects of noise on performance
[AD-A212519] N90-13209
NOISE GENERATORS
Effects of acoustic sources N90-12553
NOISE INTENSITY
The effects of noise on speech and warning signals
[AD-A212520] N90-13210
NOISE MEASUREMENT
The design and development of an acoustic test section for the ARA transonic wind tunnel
[PNR90574] N90-13202
Acoustic recording systems for use in military aircraft
[RAE-TM-MM-11] N90-13207
NOISE POLLUTION
The effects of noise on speech and warning signals
[AD-A212520] N90-13210
NOISE PREDICTION
Acoustic design considerations: Review of rotor acoustic sources N90-12585
NOISE PREDICTION (AIRCRAFT)
Near-field noise predictions of an aircraft in cruise N90-12538
NOISE REDUCTION
The NASA experience in aeronautical R and D: Three case studies with analysis
[AD-A211486] N90-12496
What should be done with those noisy old aircraft
[PNR90562] N90-12593
Re-engine with the Rolls-Royce Tay 670, the route to significant noise reduction
[PNR90585] N90-12606
Adaptive antenna arrays for satellite communication
[NASA-CR-185989] N90-12784
Removal of noise from noise-degraded speech signals
[AD-A212876] N90-12840
Application of active noise reduction for hearing protection and speech intelligibility improvement
[IZF-1988-21] N90-13042
UHB demonstrator interior noise control flight tests and analysis
[NASA-CR-181897] N90-13198
The commercial aircraft noise problem
[PNR90577] N90-13203
A frequency domain technique for improving sound field reproduction
[RAE-TM-MM-10] N90-13205
NOISE SPECTRA
Effects of acoustic sources N90-12553
A frequency domain technique for improving sound field reproduction
[RAE-TM-MM-10] N90-13205
NOISE TEMPERATURE
Spin-lattice relaxation and the calculation of gain, pump power, and noise temperature in ruby N90-12790
NONAQUEOUS ELECTROLYTES
Electroactive polyaniline film deposited from non-aqueous media. 2: Effect of acid concentration in solutions
[AD-A212084] N90-12737
NONDESTRUCTIVE TESTS
An air coupled transmission mode acoustic microscope for on-line non-destructive evaluation
[AD-A211416] N90-12947
Device for inspection of materials by eddy current methods
[AD-D014205] N90-12948
NONEQUILIBRIUM CONDITIONS
Rotational and vibrational nonequilibrium effects in rarefied, hypersonic flow
[NASA-CR-182559] N90-12498
Elements of a relativistic microscopic theory of hadronic matter in equilibrium and non-equilibrium
[KVI-796] N90-13218
NONEQUILIBRIUM IONIZATION
Nonequilibrium ionization in supernova remnants: The case of Tycho
[MPE-PREPRINT-153] N90-13295
NONFERROUS METALS
The future of non ferrous metals in aerospace engines
[PNR90572] N90-12720
NONLINEAR EQUATIONS
Self-tuning control of nonlinear Armax models --- Autoregressive Moving Average with eXogeneous (ARMAX) inputs
[RR-362] N90-12930
Building a software package for solving large sparse nonlinear systems of equations
[AD-A211758] N90-13055
A recursive algorithm for computing the frequency response of a class of nonlinear difference equation models
[RR-354] N90-13123
The Painleve test for nonlinear ordinary and partial differential equations
[AD-A212894] N90-13177
NONLINEAR FILTERS
Nongaussian linear filtering, identification of linear systems, and the symplectic group
[CWI-PM-R8810] N90-13184
NONLINEAR SYSTEMS
Optimal observer motion for bearings-only localization and tracking N90-12569
Nonlinear systems and Kolmogorov's representation theorem
[RR-363] N90-12931
Fundamentals of middle atmospheric dynamics
[AD-A211747] N90-12988
Building a software package for solving large sparse nonlinear systems of equations
[AD-A211758] N90-13055
A functional expansion and stability for nonlinear input-output maps
[RR-359] N90-13121
A new decision rule for model structure identification of a class of nonlinear dynamic systems
[RR-360] N90-13122
Remarks on the control of discrete time nonlinear systems
[MEMO-770] N90-13158
Transformations and representations of nonlinear systems
[MEMO-776] N90-13164
Towards a complete local solution of the nonlinear model matching problem
[MEMO-781] N90-13166
Nongaussian linear filtering, identification of linear systems, and the symplectic group
[CWI-PM-R8810] N90-13184
Problems in nonlinear acoustics: Scattering of sound by sound, parametric receiving arrays, nonlinear effects in asymmetric sound beams and pulsed finite amplitude sound beams
[AD-A211756] N90-13200
NONLINEARITY
Sensitivity of LFC techniques in the non-linear regime N90-12533
NONPARAMETRIC STATISTICS
Random truncation models and Markov processes
[CWI-MS-R8817] N90-13181
NONRELATIVISTIC MECHANICS
Twistons
[RSRE-MEMO-4234] N90-13275
NORMALIZING (STATISTICS)
Removing stripes in GOES (Geostationary Operational Environmental Satellites) images by matching empirical distribution functions
[PB89-213359] N90-12968
NORTH SEA
Climatological data for the North Sea based on observations by voluntary observing ships over the period 1961-1980
[KNMI-WR-89-02] N90-13002
NORTHERN HEMISPHERE
Current velocity and hydrographic observations in the southwestern North Atlantic Ocean: Subtropical Atlantic Climate Studies (STACS), 1988
[PB89-230825] N90-13010
NOTCH TESTS
Numerical analysis of notch test damage to laminated composite plates submitted to uniaxial traction
[CETIM-107310] N90-12675
Determination of the gaseous hydrogen ductile-brittle transition in copper-nickel alloys
[NASA-TM-86494] N90-12715
Fatigue testing of welded steel assemblies with or without finishing treatments
[CETIM-107900] N90-12961
NUCLEAR BINDING ENERGY
Mechanisms of CO2 reduction metal and metal modified semiconductor electrodes
[AD-A213169] N90-12712
NUCLEAR EXPLOSION EFFECT
Long wave atmospheric noise model, phase 1. Volume 2: Mode parameters
[AD-A212795] N90-12837
NUCLEAR EXPLOSIONS
Long wave atmospheric noise model, phase 1. Volume 1: Lightning occurrence rates and propagation theory
[AD-A212794] N90-12836
NUCLEAR FUSION
An explicit partition of the fusion-like cross section
[KVI-797] N90-13225
NUCLEAR MAGNETIC RESONANCE
Hardening mechanisms and analysis of the structure of the TGDDM/DDS epoxy resin system (tetraglycidyl-4,4' diaminodiphenylmethane/4,4' diaminodiphenylsulfone)
[NOTE-TECHNIQUE-1988-8] N90-12662
Magnetic resonance of polymers at surfaces
[AD-A212225] N90-12753
Persistent current, NMR, and ion transmission experiments in rotating He-3 superfluids --- Nuclear Magnetic Resonance (NMR)
[ISBN-952-90056-1-X] N90-13221
NUCLEAR MEDICINE
Activities report of the Kernfysisch Versneller Instituut
[ETN-89-95752] N90-13219
NUCLEAR RADIATION
Proof of the feasibility of coherent and incoherent schemes for pumping a gamma-ray laser
[AD-A212315] N90-12921
NUCLEAR REACTORS
Activities report of the Joint Research Center
[ETN-89-95757] N90-13321
NUCLEAR SCATTERING
Small particle scattering and absorption
[AD-A213168] N90-12711
NUCLEI (NUCLEAR PHYSICS)
Activities report of the Kernfysisch Versneller Instituut
[ETN-89-95752] N90-13219
NUCLEON-NUCLEON INTERACTIONS
The interacting boson approximation
[KVI-774] N90-13215
NULL ZONES
Null offset voltage compensator for operational amplifier
[AD-D014189] N90-12859
Characterization of liquid crystal displays for optical signal processing applications
[AD-A212832] N90-12910
NUMERICAL ANALYSIS
Numerical analysis of notch test damage to laminated composite plates submitted to uniaxial traction
[CETIM-107310] N90-12675
Unsteady three-dimensional thin-layer Navier Stokes solutions on dynamic blocked grids
[AD-A212377] N90-12899
Radio frequency linac driven free-electron laser configurations
[AD-A212572] N90-12922
Cavity eigenmodes for the NIST/NRL (National Institute of Standards and Technology/Naval Research Laboratory) free electron laser
[AD-A212706] N90-12923
A cell-centered multigrid method for three-dimensional anisotropic-diffusion and interface problems
[REPT-89-35] N90-13128
Local mode smoothing analysis of various incomplete factorization iterative methods in two dimensions
[REPT-89-36] N90-13129
Problems in nonlinear acoustics: Scattering of sound by sound, parametric receiving arrays, nonlinear effects in asymmetric sound beams and pulsed finite amplitude sound beams
[AD-A211756] N90-13200
Ground states of a two-dimensional charged-boson system
[AD-A212363] N90-13226
NUMERICAL CONTROL
Development of an integrated mobile robot system at CMU (Carnegie-Mellon University)
[AD-A212555] N90-12944
NUMERICAL INTEGRATION
Increasing the real stability boundary of explicit methods
[CWI-NM-R8902] N90-13134
NUMERICAL STABILITY
Development of a VSAERO (Vortex Separation Aerodynamics) model of the F/A-18
[AD-A212442] N90-12566
Vortex dynamics
[AD-A212119] N90-12877
Smoothed predictor-corrector methods for solving partial differential equations
[CWI-NM-R8808] N90-13131
Iterated theta method for hyperbolic equations
[CWI-NM-R8809] N90-13132
NUMERICAL WEATHER FORECASTING
Semi-Lagrangian, semi-implicit solutions of the shallow water equations in one dimension
[AD-A212658] N90-12902

O

OBSERVABILITY (SYSTEMS)
Optimal observer motion for bearings-only localization and tracking N90-12569

OBSERVATION AIRCRAFT
Mode S data link trials, 10-11 January 1989
[RSRE-MEMO-4267] N90-12815
OCEAN BOTTOM
Surface current and wave modulation measurements over bottom topography: A comparison with theory
[AD-A212469] N90-13011
OCEAN CURRENTS
Compendium of marine meteorological and oceanographic products of the Ocean Products Center, revision 1
[PB89-230684] N90-12967
OCEAN DATA ACQUISITIONS SYSTEMS
Climatological data for the North Sea based on observations by voluntary observing ships over the period 1961-1980
[KNMI-WR-89-02] N90-13002
OCEAN DYNAMICS
A linearized surface condition in low speed hydrodynamics
[REPT-89-04] N90-12885
A hybrid architecture for feature labelling of oceanographic satellite images
[AD-A212236] N90-12975
OCEANOGRAPHY
Compendium of marine meteorological and oceanographic products of the Ocean Products Center, revision 1
[PB89-230684] N90-12967
A hybrid architecture for feature labelling of oceanographic satellite images
[AD-A212236] N90-12975
ODD-ODD NUCLEI
The interacting boson approximation
[KVI-774] N90-13215
ON-LINE SYSTEMS
An air coupled transmission mode acoustic microscope for on-line non-destructive evaluation
[AD-A211416] N90-12947
ONE DIMENSIONAL FLOW
Julia-Fatou-Sullivan theory for real one-dimensional dynamics
[REPT-88-100] N90-13190
OPERATING COSTS
Designing for reliable and low maintenance cost aero engines
[PNR90570] N90-12604
OPERATING SYSTEMS (COMPUTERS)
An expert system for VM performance analysis
[REPT-89-30] N90-13045
A mapping for converting Mascot designs to Ada programs
[RSRE-MEMO-4244] N90-13070
Process expressions and Hoare's logic
[CWI-CS-R8905] N90-13076
Path expression based operating systems
[MEMO-INF-88-68] N90-13097
OPERATIONAL AMPLIFIERS
Null offset voltage compensator for operational amplifier
[AD-D014189] N90-12859
OPERATIONS RESEARCH
The comparison of the airbase simulation models airbase and sustained
[FEL-1988-66] N90-12629
Solving three dimensional block bidiagonal linear systems on vector computers
[REPT-89-14] N90-13056
Radar and sensor array design planning for a naval missile testing center. Artificial intelligence applications
[ETCA-88-R-099] N90-13108
Smoothed limit theorems for equilibrium processes
[AD-A212321] N90-13186
OPERATOR PERFORMANCE
Parallel approach separation and controller performance: A study of the impact of two separation standards
[DOT/FAA/CT-TN89/50] N90-12574
OPERATORS (MATHEMATICS)
Labeled trees and the efficient computation of derivations
[NASA-CR-185386] N90-13113
Stable summability and approximation theory
[AD-A211379] N90-13118
Modular specifications in process algebra with curious queues
[CWI-CS-R8821] N90-13152
International Conference on Operator Theory: Advances and applications
[AD-A212341] N90-13170
Operator product coefficients in non-diagonal conformal field theories
[NIKHEF-H/88-19] N90-13224
OPTICAL COMMUNICATION
Design and performance of an on-satellite laser diagnostic system for a free space optical heterodyne frequency-shift-keyed communication system
[AD-A211986] N90-12915
Three stages and two systems of visual processing
[AD-A212670] N90-13032
Fellowships in information and stochastic systems
[AD-A212385] N90-13280
OPTICAL CORRECTION PROCEDURE
Improvement of ultrashort pulsed laser shadowgraph photography by means of optical filters
[ISL-CO-215/88] N90-12906
OPTICAL DATA PROCESSING
Characterization of liquid crystal displays for optical signal processing applications
[AD-A212832] N90-12910
OPTICAL EQUIPMENT
Design and performance of an optical mount using cross-flexure pivots
[DE89-017551] N90-12929
OPTICAL FIBERS
Optical fibre witnesses of fatigue damage in composite materials N90-12660
Variational and asymptotic methods in open and closed waveguide analysis
[REPT-34] N90-13229
OPTICAL FILTERS
Improvement of ultrashort pulsed laser shadowgraph photography by means of optical filters
[ISL-CO-215/88] N90-12906
OPTICAL HETERODYNING
Design and performance of an on-satellite laser diagnostic system for a free space optical heterodyne frequency-shift-keyed communication system
[AD-A211986] N90-12915
OPTICAL MEASUREMENT
Remote detection of boundary-layer transition by an optical system N90-12524
Optical detection of space debris using a large achromatic coronagraph
[AD-A211362] N90-12647
OPTICAL MEASURING INSTRUMENTS
Catadioptric Optics for laser Doppler velocimeter applications
[NASA-TM-102210] N90-12904
Mark-3 interferometer
[AD-A213155] N90-12911
Application of a copper vapour laser to investigation of shock and blade interaction in a shock tube
[PNR90578] N90-12918
Optical techniques for in-plane strain analysis in an industrial environment
[PNR90601] N90-12957
OPTICAL PATHS
Catadioptric Optics for laser Doppler velocimeter applications
[NASA-TM-102210] N90-12904
OPTICAL PROPERTIES
Fundamental molecular data to support CARS diagnostics of temperature, pressure, and species concentration
[AD-A212411] N90-12704
Small particle scattering and absorption
[AD-A213168] N90-12711
Ultrastructure processing and characterization of polymers
[AD-A211460] N90-12743
Laser initiated ignition of liquid propellant
[AD-A212342] N90-12786
Cavity eigenmodes for the NIST/NRL (National Institute of Standards and Technology/Naval Research Laboratory) free electron laser
[AD-A212706] N90-12923
Comments on the use of LOWTRAN in transmission calculations for sites with the ground elevated relative to sea level
[AD-A212724] N90-12995
Direct computation of 3D shape invariants and the focus of expansion
[AD-A212386] N90-13195
Study of the electrical and optical properties of the vanadium and nickel impurities in GaAs
[ISAL-89-0028] N90-13259
Optical clock distribution to VLSI chips
[AD-A212269] N90-13264
Growth and characterization of zinc sulfide films by conversion of zinc oxide films with H2S
[AD-A213345] N90-13271
OPTICAL PUMPING
Photoelectron pumped phosphors
[AD-A213202] N90-12912
OPTICAL RADAR
Atmospheric horizontal-inhomogeneity effects on the optical depths determined by the double-elevation-angle lidar technique
[AD-A212836] N90-12839
OPTICAL RESONATORS
Variational and asymptotic methods in open and closed waveguide analysis
[REPT-34] N90-13229
OPTIMAL CONTROL
Optimal observer motion for bearings-only localization and tracking N90-12569
Integration of a centralized multiplexed control unit into the cockpit of an aircraft
[F6150-DT410-1-88329] N90-12622
OPTIMIZATION
Integrated multidisciplinary optimization of rotorcraft: A plan for development
[NASA-TM-101617] N90-12580
General approach and scope — rotor blade design optimization N90-12581
Validation of the procedures — integrated multidisciplinary optimization of rotorcraft N90-12587
Appendix: Results obtained to date — integrated multidisciplinary optimization of rotorcraft N90-12588
The computer age and traditional approximate, analytical methods N90-12772
Reduction of turbulent drag: Boundary layer manipulators
[CERT-RSF-OA-74/2259-AYD] N90-12889
An implicit Navier-Stokes solver optimised for a vector-parallel computer
[VKI-TN-169] N90-12890
Multilevel optimization with system Optsys
[FFA-TN-1988-60] N90-12953
Optimum data weighting and error calibration for estimation of gravitational parameters
[NASA-TM-100737] N90-12985
On the identification of local minimizers in inertia-controlling methods for quadratic programming
[AD-A212514] N90-13086
Sequential quadratic programming algorithms for optimization
[AD-A212800] N90-13088
Algorithm development for SDI weapons system allocation
[AD-A212973] N90-13090
On a rate of convergence of the multiknapsack value function
[CWI-MS-R8812] N90-13144
On the smooth fit boundary conditions in the optimal stopping problem for semimartingales
[CWI-MS-R8819] N90-13147
A modified Newton method for unconstrained minimization
[AD-A212752] N90-13174
Effect of the length of the multijunction grill on its lower hybrid current drive efficiency
[IPPCZ-283] N90-13240
On optimization of the multijunction grill for the lower hybrid current drive
[IPPCZ-280] N90-13241
OPTOELECTRONIC DEVICES
High speed quantum-well optoelectronic devices by MBE
[AD-A212585] N90-13237
OPTOMETRY
A Scheiner-principle pocket optometer for self-evaluation and biofeedback accommodation training
[AD-A213171] N90-13027
ORBIT CALCULATION
Evaluation of 15th- and 30th-order geopotential harmonic coefficients from 26 resonant satellite orbits
[RAE-TR-88045] N90-12640
Orbit determination and analysis for Cosmos 236 at 15th-order resonance
[RAE-TR-88058] N90-12641
An analytic development of orbit determination for a distant, planetary orbiter N90-12787
The GEM-T2 gravitational model
[NASA-TM-100746] N90-12984
Spacecraft Orbit Design and Analysis (SODA), version 1.0 user's guide
[NASA-CR-181932] N90-13050
ORBITAL MECHANICS
An analytic development of orbit determination for a distant, planetary orbiter N90-12787
Spacecraft Orbit Design and Analysis (SODA), version 1.0 user's guide
[NASA-CR-181932] N90-13050
ORGANIC CHEMISTRY
Electron density modulation of catalytic metal centers by substituted aryl-isocyanide ligands
[AD-A212875] N90-12708
Ion beam analysis of diffusion in polymer glasses
[AD-A212339] N90-12756

ORGANIC MATERIALS
Proceedings of the DOD Workshop on the Manufacturing/Producibility of Organic Matrix Composites
[AD-A212577] N90-12680
ORGANIZATIONS
Directory of International and Regional Organizations Conducting Standards-Related Activities, May 1989
[PB89-221147] N90-12776
National Science Foundation N90-13320
ORGANOMETALLIC COMPOUNDS
Metallo-organic decomposition process for dielectric films
[AD-A211590] N90-12849
ORGANOMETALLIC POLYMERS
Transition metal catalyzed synthesis of organmetallic polymers
[AD-A212133] N90-12740
ORIFICE FLOW
Effect of pipe roughness on orifice flow measurement
[PB89-231484] N90-12880
Measurements of coefficients of discharge for concentric flange-tapped square-edged orifice meters in water over the Reynolds number range 600 to 2,700,000
[PB89-235147] N90-12892
ORIFICES
Two dimensional orifice array, monodisperse drop source, phase 1
[AD-A211319] N90-12881
ORTHOGONALITY
A generalization of Moak's q-Laguerre polynomials
[REPT-89-21] N90-13126
NUMVEC FORTRAN library manual chapter: Simultaneous linear equations
[CWI-NM-R8903] N90-13135
Representations of the twisted SU(2) quantum group and some q-hypergeometric orthogonal polynomials
[CWI-PM-R8809] N90-13140
OSCILLATIONS
Additions and corrections to SUPER: A program for calculating steady and oscillatory supersonic flow over a thin wing, tail plane and fin
[AD-A211771] N90-12501
OTOLITH ORGANS
Pre- and postflight postural control of the D1 Spacelab mission astronauts examined with a tilting room
[IZF-1988-25] N90-13039
OXIDATION
Computer simulation studies of the catalytic oxidation of carbon monoxide on platinum metals
[PB89-223739] N90-12721
OXIDATION-REDUCTION REACTIONS
Capacitive behavior in conducting polymers
[AD-A212448] N90-12760
OXIDES
Synthesis and properties of NdNiO(3) prepared by low temperature methods
[AD-A212117] N90-13256
OXYACETYLENE
An investigation of diamond film deposition in a premixed oxyacetylene flame
[AD-A212595] N90-13268
OXYGEN
Measurement and correlation of the solubility and diffusion coefficient for oxygen and chlorine in basic hydrogen peroxide
[AD-A212348] N90-12703
Metallo-organic decomposition process for dielectric films
[AD-A211590] N90-12849
Microwave excitation of oxygen O2 (delta 1) for an oxygen-iodine laser
[DFVLR-FB-89-23] N90-12919
Semiconductor measurement technology: Database for and statistical analysis of the interlaboratory determination of the conversion coefficient for the measurement of the interstitial oxygen content of silicon by infrared absorption
[PB89-221170] N90-13253
OXYGEN ATOMS
Retrieval of atomic oxygen and temperature in the thermosphere. Part 1: Feasibility of an experiment based on the spectrally resolved 147 micrometer limb emission
[AD-A211987] N90-12986
OXYGEN CONSUMPTION
Prediction of thermal stress casualties
[AD-A212356] N90-13022
OZONE
Sensitivity of a regional oxidant model to variations in climate parameters, volume 1 and 2
[PB89-224943] N90-12981

P

P-TYPE SEMICONDUCTORS
Dielectric spectroscopy of semiconductors
[AD-A211989] N90-13255
PACKET TRANSMISSION
Description and results of a multihop NACS simulation
[FEL-1988-46] N90-12824
PALLADIUM COMPOUNDS
Study of palladium and chromium silicides formation in liquid phase and in solid phase
[LAAS-89040] N90-12695
PARABOLIC ANTENNAS
A closed-cycle refrigerator for cooling maser amplifiers below 4 Kelvin N90-12797
PARABOLIC REFLECTORS
Performance effects of tie-truss modifications for a 70-meter centerline beam waveguide antenna N90-12791
PARALLEL COMPUTERS
An implicit Navier-Stokes solver optimised for a vector-parallel computer
[VKI-TN-169] N90-12890
Performance evaluations of a parallel and expandable database computer: The multi-backend database computer
[AD-A212761] N90-13046
Area-universal networks
[AD-A211883] N90-13092
PARALLEL PROCESSING (COMPUTERS)
Multilevel optimization with system Optsys
[FFA-TN-1988-60] N90-12953
Performance evaluations of a parallel and expandable database computer: The multi-backend database computer
[AD-A212761] N90-13046
A fan-in algorithm for distributed sparse numerical factorization
[AD-A211569] N90-13054
Parallel and deterministic algorithms from MRF (Markov Random Fields): Surface reconstruction and integration
[AD-A212457] N90-13084
NAUTILE: A physical design environment based on an object-oriented data manager
[IMAG-RR-737-I] N90-13094
Formal calculations and parallesism. Solving linear systems
[ETN-89-95499] N90-13098
Identification of robot dynamics: A parallel processing approach
[RR-361] N90-13103
PARALLEL PROGRAMMING
A simple definition for parallel composition of prime event structures
[CWI-CS-R8903] N90-13074
Towards a parallel algorithm for the many body problem
[CS-8813] N90-13078
A compilation strategy for numerical programs based on partial evaluation
[AD-A212759] N90-13175
PARAMETER IDENTIFICATION
Improvement of rules relating to clamp calculations
[CETIM-110610] N90-12939
An error estimator for parameter choice in regulating least square problems. Application to regularized deconvolution
[IMAG-RR-744-M] N90-13125
A kernel approach to estimation of the sphere radius density in Wicksell's corpuscle problem
[CWI-MS-R8809] N90-13142
A semiparametric model for citation counts
[CWI-MS-R8814] N90-13145
PARAMETERIZATION
An error estimator for parameter choice in regulating least square problems. Application to regularized deconvolution
[IMAG-RR-744-M] N90-13125
PARSING ALGORITHMS
A table-driven approach to fast context-free parsing
[AD-A212210] N90-13082
PARTIAL DIFFERENTIAL EQUATIONS
Smoothed predictor-corrector methods for solving partial differential equations
[CWI-NM-R8808] N90-13131
A moving-grid interface for systems of one-dimensional time-dependent partial differential equations
[CWI-NM-R8904] N90-13136
The Painleve test for nonlinear ordinary and partial differential equations
[AD-A212894] N90-13177
PARTICLE DENSITY (CONCENTRATION)
Performance of laminar-flow leading-edge test articles in cloud encounters N90-12511
PARTICLE DIFFUSION
Temperature dependence of positron diffusion in cubic metals
[PB89-222020] N90-12722
PARTICLE EMISSION
ERNE: Energetic and Relativistic Nuclei and Electron experiment N90-13315
PARTICLE IN CELL TECHNIQUE
NTRFACE for MAGIC
[AD-A212858] N90-13112
PARTICLE MOTION
Composite vs constituent particle aspects of hole motion in the CuO2 plane
[DE89-618864] N90-13251
PARTICLES
Small particle scattering and absorption
[AD-A213168] N90-12711
PATHS
Long dominating cycles and paths in graphs with large neighborhood unions
[MEMO-769] N90-13157
PATTERN RECOGNITION
Automatic processing of images from the GRATE flight test tool
[DLR-FB-89-28] N90-12599
Progress in the identification of airborne radar targets
[AD-A212749] N90-12835
A robot which will investigate the condition of underground pipe
[PB89-230650] N90-12928
A two-dimensional hybrid experimental-numerical technique for elastic-plastic stress analysis N90-12949
A theory of networks for approximation and learning
[AD-A212359] N90-13110
PEEK
Orthotropic elasto-plastic behavior of AS4/APC-2 thermoplastic composite in compression
[NASA-CR-186080] N90-12959
PERCEPTION
Effects of type of responding on memory/visual search: Responding just yes or just no can lead to inflexible performance
[AD-A212764] N90-13033
PERFORMANCE PREDICTION
Numerical simulation of unsteady rotational flow over propfan configurations
[NASA-CR-186037] N90-12500
Analysis and simulation of dynamics of spacecraft power systems N90-12653
Optical fibre witnesses of fatigue damage in composite materials N90-12660
Multilayer theory for delamination analysis of a composite curved bar subjected to end forces and end moments
[NASA-TM-4139] N90-12669
Performance of the split-symbol moments SNR estimator in the presence of inter-symbol interference N90-12799
PERFORMANCE TESTS
Hybrid angular velocity reference system for the investigation of dynamic properties of strapdown gryos
[DFVLR-FB-89-25] N90-12577
The role of component testing
[PNR90589] N90-12608
SSME structural dynamic model development
[NASA-CR-183671] N90-12650
Oxide ceramic fibers by the sol-gel methods
[AD-A211315] N90-12742
Mode S data link trials, 10-11 January 1989
[RSRE-MEMO-4267] N90-12815
Removal of noise from noise-degraded speech signals
[AD-A212876] N90-12840
Performance analysis of large adaptive sidelobe canceller arrays with reused elements
[AD-A212888] N90-12841
Design and commissioning test results for the hypervelocity launcher research complex battery power supply
[AD-A211320] N90-12848
Feedback charge amplifier integrated on the detector wafer
[REPT-89-037] N90-12852
The analysis of current-mirror MOSFETs for use in radiation environments
[AD-A212527] N90-12866
Cold tests of quasi-optical gyrotron resonators
[AD-A212707] N90-12868
Pre- and postflight postural control of the D1 Spacelab mission astronauts examined with a tilting room
[IZF-1988-25] N90-13039
Expert system for test program set fault candidate selection
[AD-A213338] N90-13091
Design and tests of simple, inexpensive optical beacon for use on small satellites
[AD-A213325] N90-13238

PERIODIC FUNCTIONS
On the maximum period of a permutation of N elements
[MEMO-771] N90-13159
The discrete-time single-server queueing model
[MEMO-780] N90-13165
PERMANENT MAGNETS
Graduate fellowships in the field of hard magnetic materials
[AD-A212303] N90-12733
A survey of the current state-of-the-art in high-energy-product permanent magnets
[AD-A211761] N90-13193
PERMITTIVITY
Modeling of the dielectric behavior of composite materials
[CERT-1/1398-MO] N90-12674
PERMUTATIONS
On the maximum period of a permutation of N elements
[MEMO-771] N90-13159
PERTURBATION
On mean elements for satellite orbits perturbed by the zonal harmonics of the geopotential
[AD-A212322] N90-12642
Magnetically insulated electron flows in pulsed power systems
[AD-A212746] N90-13196
PERTURBATION THEORY
Extended basis set calculations of atomization energies: Comparison of isogyric and direct results
[AD-A212268] N90-12702
PETRI NETS
Requirements specification with Petri nets using the cube tool methodology
[AD-A212190] N90-12829
Extended performability modeling using dynamic queing networks
[MEMO-INF-89-15] N90-13099
PHASE CHANGE MATERIALS
Phase change material for spacecraft thermal management
[AD-A211404] N90-12648
PHASE DIAGRAMS
Interactive computer program for the generation of enthalpy-entropy and temperature-entropy charts of nitrogen and hydrogen
[DLR-FB-89-27] N90-13081
PHASE LOCKED SYSTEMS
Wideband phase-locked angular modulator
N90-12798
PHASE SHIFT
Effect of the length of the multijunction grill on its lower hybrid current drive efficiency
[IPPCZ-283] N90-13240
On optimization of the multijunction grill for the lower hybrid current drive
[IPPCZ-280] N90-13241
PHASE TRANSFORMATIONS
Analysis of the performance of heat pipes and phase-change materials with multiple localized heat sources for space applications
[AD-A212232] N90-12896
Synthesis and properties of NdNiO(3) prepared by low temperature methods
[AD-A212117] N90-13256
PHASE VELOCITY
Long wave atmospheric noise model, phase 1. Volume 1: Lightning occurrence rates and propagation theory
[AD-A212794] N90-12836
PHASE-SPACE INTEGRAL
Lie-algebraic aspects of the classical nonrelativistic Calogero-Moser models
[CWI-AM-R8901] N90-13145
PHASED ARRAYS
Dedicated tracking of crossing targets with a phased array monopulse radar
[FEL-1988-95] N90-12821
PHENYLS
High temperature insulators
[AD-D014193] N90-12751
PHOSPHATES
Polyelectrolyte-diffused zinc phosphate conversion coatings and polyacid coupling primers for corrosion protection of steel and aluminum, and alkali-catalyzed hydrolysis of polyimide-based materials
[AD-A212240] N90-12754
PHOSPHORS
Photoelectron pumped phosphors
[AD-A213202] N90-12912
PHOTOCHEMICAL REACTIONS
Chemical and photochemical reactivity in microemulsions and waterless microemulsions
[AD-A211776] N90-12692
Photochemical observation of ion flows in membrane channels
[AD-A212449] N90-12705
Small particle scattering and absorption
[AD-A213168] N90-12711
PHOTODISSOCIATION
Photodissociation of XeF2 (xenon difluoride) at 193 nm
[AD-A211663] N90-12916
PHOTOELECTRONS
Photoelectron pumped phosphors
[AD-A213202] N90-12912
PHOTOGEOLOGY
An attempt to draw conclusions from the vegetation to the geological underground in the area of Amberg (Germany, F.R.) by means of digital image processing of TM data
[DFVLR-FB-89-24] N90-12974
PHOTOLYSIS
Photodissociation of XeF2 (xenon difluoride) at 193 nm
[AD-A211663] N90-12916
PHOTOMAPS
Height and gradient from shading
[AD-A212338] N90-12908
PHOTOMETERS
SWAN: A study of solar wind anisotropies
N90-13312
PHOTOMULTIPLIER TUBES
Photoelectron pumped phosphors
[AD-A213202] N90-12912
PHOTON BEAMS
B factory via conversion of 1 TeV electron beams into 1 TeV photon beams
[DE89-017692] N90-12914
PHOTON-ELECTRON INTERACTION
B factory via conversion of 1 TeV electron beams into 1 TeV photon beams
[DE89-017692] N90-12914
PHOTOPRODUCTION
B factory via conversion of 1 TeV electron beams into 1 TeV photon beams
[DE89-017692] N90-12914
PHYSICAL EXERCISE
Exertional heatstroke: An international perspective. An introduction: The role of exercise in the etiology of exertional heatstroke
[AD-A212242] N90-13020
PHYSICAL FITNESS
The effect of concurrent strength and endurance training on electromechanical delay, maximum voluntary contraction, and rate of force development
[AD-A213316] N90-13028
PHYSICAL OPTICS
A method to model fuze performance. Part 2: Calculation of target reflections with physical optics
[FEL-1989-21-PT-2] N90-12822
The physical optics approximation in the near-field region
[FEL-1989-100] N90-13234
PHYSIOLOGICAL EFFECTS
Effects of atmospheric mix and toxic fumes on military performance
[PB89-223630] N90-13015
Biochemical and physiological changes in glider pilots during multihour flights
[DLR-FB-89-29] N90-13018
The effects of noise on performance
[AD-A212519] N90-13209
PHYSIOLOGICAL FACTORS
Pre- and postflight postural control of the D1 Spacelab mission astronauts examined with a tilting room
[IZF-1988-25] N90-13039
PHYSIOLOGICAL RESPONSES
Cardiovascular, renal, electrolyte, and hormonal changes in man during gravitational stress, weightlessness, and simulated weightlessness: Lower body positive pressure applied by the antigravity suit
[NASA-TM-102232] N90-13013
PILOT ERROR
Fatigue, pilot deviations and time of day
[NASA-CR-185369] N90-13035
PILOT PERFORMANCE
Field-of-View variations and stripe-texturing effects on assault landing performance in the C-130 weapon system trainer
[AD-A212763] N90-12634
Fatigue, pilot deviations and time of day
[NASA-CR-185369] N90-13035
Spatial tests for aviators
[IZF-1988-15] N90-13041
PILOT TRAINING
Field-of-View variations and stripe-texturing effects on assault landing performance in the C-130 weapon system trainer
[AD-A212763] N90-12634
A Scheiner-principle pocket optometer for self-evaluation and biofeedback accommodation training
[AD-A213171] N90-13027
A comparison of two subject-controlled attitude measures during somatogravic illusion exposure
[AD-A212528] N90-13031
PILOTS (PERSONNEL)
Biochemical and physiological changes in glider pilots during multihour flights
[DLR-FB-89-29] N90-13018
PIPE FLOW
Effect of pipe roughness on orifice flow measurement
[PB89-231484] N90-12880
Two-phase flow pressure losses in pipeline fittings
[ESDU-89012] N90-12883
PIPELINES
Two-phase flow pressure losses in pipeline fittings
[ESDU-89012] N90-12883
PITTING
Unsteady diffusion from a hemispherical pit
[NPL-DMA(A)-190] N90-13220
PIVOTS
Pivotal mono wing cruise missile with wing deployment and fastener mechanism
[AD-D014191] N90-12594
Design and performance of an optical mount using cross-flexure pivots
[DE89-017551] N90-12929
PIXELS
Image preprocessing by modified median filter
[AD-D014199] N90-12828
Video line processor
[AD-D014198] N90-12861
PLAINS
Use of ground penetrating radar to define recharge areas in the Central Sand Plain
[PB89-224885] N90-12814
PLANAR STRUCTURES
Acceleration sets of planar manipulators. Part 1: Theory
[AD-A213162] N90-12945
Analysis of the non-planar response of a cantilever, with the aid of computerized symbolic manipulation
[AD-A212421] N90-13172
PLANETARY MAGNETOSPHERES
Research in cosmic and gamma ray astrophysics
[NASA-CR-185451] N90-13316
PLANETARY ORBITS
An analytic development of orbit determination for a distant, planetary orbiter N90-12787
PLANNING
Problem-dependent transformations of 3D terrain elevation maps into cost precursor maps
[PB89-218127] N90-12969
PLASMA COOLING
Liquid and solid ion plasmas
[AD-A212415] N90-13244
PLASMA CURRENTS
Effect of the length of the multijunction grill on its lower hybrid current drive efficiency
[IPPCZ-283] N90-13240
On optimization of the multijunction grill for the lower hybrid current drive
[IPPCZ-280] N90-13241
PLASMA DENSITY
Magnetically insulated electron flows in pulsed power systems
[AD-A212746] N90-13196
PLASMA DIAGNOSTICS
Research on heating, instabilities, turbulence and RF emission from electric field dominated plasmas
[AD-A212122] N90-13243
PLASMA DYNAMICS
Development of computer codes to model dynamics of the earth's magnetosphere
[AD-A211532] N90-12987
Research on heating, instabilities, turbulence and RF emission from electric field dominated plasmas
[AD-A212122] N90-13243
PLASMA ENGINES
NASA/USRA advanced space design program: The laser powered interorbital vehicle
[NASA-CR-186044] N90-12646
PLASMA EQUILIBRIUM
Three-dimensional equilibria and Mercier stability calculations
[DE89-015907] N90-13239
PLASMA GENERATORS
Hermes plasma wind tunnel. Preliminary study, phase A1: Text
[DVG-HER-TN-002-PT-1] N90-12631
Hermes plasma wind tunnel. Preliminary study, phase A1: Annexes, tables, figures
[DVG-HER-TN-002-PT-2] N90-12632

PLASMA HEATING
Hermes plasma wind tunnel. Preliminary study, phase A1: Text
[DVG-HER-TN-002-PT-1] N90-12631
Hermes plasma wind tunnel. Preliminary study, phase A1: Annexes, tables, figures
[DVG-HER-TN-002-PT-2] N90-12632
Effect of the length of the multijunction grill on its lower hybrid current drive efficiency
[IPPCZ-283] N90-13240
Research on heating, instabilities, turbulence and RF emission from electric field dominated plasmas
[AD-A212122] N90-13243
PLASMA INTERACTIONS
Calcium displacement caused by electromagnetic fields
[AD-A212690] N90-13023
Proceedings of the 10 May 1989 Antiproton Technology Workshop: Addendum
[AD-A212804] N90-13227
PLASMA JET WIND TUNNELS
Hermes plasma wind tunnel. Preliminary study, phase A1: Text
[DVG-HER-TN-002-PT-1] N90-12631
Hermes plasma wind tunnel. Preliminary study, phase A1: Annexes, tables, figures
[DVG-HER-TN-002-PT-2] N90-12632
PLASMA OSCILLATIONS
GOLF: Global Oscillations at Low Frequencies for the SOHO mission N90-13304
PLASMA PHYSICS
Plasma separation process: Magnet move to Oak Ridge National Laboratory
[DE89-017457] N90-13242
Time evolution of the electron swarm energy distribution function
[AD-A212967] N90-13247
PLASMA POWER SOURCES
Magnetically insulated electron flows in pulsed power systems
[AD-A212746] N90-13196
PLASMA PROPULSION
NASA/USRA advanced space design program: The laser powered interorbital vehicle
[NASA-CR-186044] N90-12646
PLASMA RADIATION
Proceedings of the 10 May 1989 Antiproton Technology Workshop: Addendum
[AD-A212804] N90-13227
PLASMA TURBULENCE
Research on heating, instabilities, turbulence and RF emission from electric field dominated plasmas
[AD-A212122] N90-13243
PLASMAS (PHYSICS)
Advanced source development and applications. Laser-produced plasmas: A compact soft x ray source with high peak brightness
[AD-A212677] N90-13245
PLASMASPHERE
Development of computer codes to model dynamics of the earth's magnetosphere
[AD-A211532] N90-12987
PLASTIC COATINGS
Polyelectrolyte-diffused zinc phosphate conversion coatings and polyacid coupling primers for corrosion protection of steel and aluminum, and alkali-catalyzed hydrolysis of polyimide-based materials
[AD-A212240] N90-12754
PLASTIC DEFORMATION
A two-parameter representation of dynamic dislocation distributions
[AD-A212249] N90-13263
PLASTIC PROPERTIES
Modeling the temperature rise at the tip of a fast crack
[AD-A212418] N90-12966
PLASTICS
Modeling the temperature rise at the tip of a fast crack
[AD-A212418] N90-12966
PLATES (STRUCTURAL MEMBERS)
A study of the impact of a ball bearing on a long fiber composite plate with a carbon matrix, part 2
[ETCA-88-R-088-PT-2] N90-12673
PLATINUM
Computer simulation studies of the catalytic oxidation of carbon monoxide on platinum metals
[PB89-223739] N90-12721
PLUGS
The effects of hearing protectors on speech communication and the perception of warning signals
[AD-A212521] N90-12832
Shape instabilities of plate-like structures. 1: Experimental observations in heavily cold worked in situ composites
[AD-A212251] N90-13021
PLUMES
The shape of the probability density function of short-term concentration fluctuations of plumes in the atmospheric boundary layer
[AD-A212632] N90-13188
PLY ORIENTATION
Mechanical behavior of carbon/resin composites under delamination and cracking of transverse layers
[ONERA-RT-46/7086-M] N90-12678
PNEUMATIC CONTROL
Analysis of high speed pneumatic actuation systems under rotary directional on-off flow control N90-12926
POGO
Relationship between the current and the width of the POGO electrojet during the solstices
[DE89-619725] N90-13294
POINTS (MATHEMATICS)
A point in betaZ/Z not contained in a maximal orbit closure
[REPT-89-26] N90-13127
A statistical analysis of spatial point patterns, a case study
[CWI-MS-R8813] N90-13180
POISSON DENSITY FUNCTIONS
Lie-algebraic aspects of the classical nonrelativistic Calogero-Moser models
[CWI-AM-R8901] N90-13148
Fellowships in information and stochastic systems
[AD-A212385] N90-13280
POISSON EQUATION
Thermionic emission including both space charge and image forces
[AD-A212732] N90-12869
POLAR REGIONS
Role of chemical effects in daytime high latitude trough formation
[AD-A211772] N90-12989
Cloud cover determination in polar regions from satellite imagery
[NASA-CR-186096] N90-13003
POLARIMETRY
Radar polarimetric studies based on the MAYPOLE 1983 and 1984 field experiments
[AD-A212226] N90-12830
Investigation of the properties of radar backscatter from sea ice
[AD-A212808] N90-12838
POLARIZATION (CHARGE SEPARATION)
IBM PC analysis of polarization resistance data
[AD-A212294] N90-12732
POLARIZATION (WAVES)
Preliminary investigation of Faraday rotation effects and description of polarization measurements on the AFGL high latitude meteor scatter test bed
[AD-A211298] N90-12806
POLYATOMIC MOLECULES
Molecular dynamics of lipid bilayers
[AD-A211492] N90-13214
POLYCARBONATES
Physical ageing and short term creep in amorphous and semicrystalline polymers
[NPL-DMA(A)-185] N90-12745
POLYCRYSTALS
Spectroscopic ellipsometry characterization of CVD deposition and doping of polysilicon multilayer structures
[RSRE-MEMO-4258] N90-12671
Synthesis and properties of NdNiO(3) prepared by low temperature methods
[AD-A212117] N90-13256
A two-parameter representation of dynamic dislocation distributions
[AD-A212249] N90-13263
POLYETHYLENE TEREPHTHALATE
Physical ageing and short term creep in amorphous and semicrystalline polymers
[NPL-DMA(A)-185] N90-12745
POLYIMIDE RESINS
The chemistry of hexaazatriphenylene hexanitrile, a polyfunctional heterocycle with potential utility in the formulation of thermostable polymers
[AD-A212353] N90-12757
POLYMER BLENDS
A center for advanced electrical and structural polymers
[AD-A212853] N90-12764
POLYMER CHEMISTRY
Ultrastructure processing and characterization of polymers
[AD-A211460] N90-12743
The chemistry of hexaazatriphenylene hexanitrile, a polyfunctional heterocycle with potential utility in the formulation of thermostable polymers
[AD-A212353] N90-12757
POLYMER MATRIX COMPOSITES
Ballistic properties of composite materials for personnel protection
[MRL-TR-89-6] N90-12661
Magnetic resonance of polymers at surfaces
[AD-A212225] N90-12753
Orthotropic elasto-plastic behavior of AS4/APC-2 thermoplastic composite in compression
[NASA-CR-186080] N90-12959
POLYMERIC FILMS
Electroactive polyaniline film deposited from non-aqueous media. 2: Effect of acid concentration in solutions
[AD-A212084] N90-12737
POLYMERIZATION
Synthesis and high temperature chemistry of methylsilsesquioxane polymers produced by titanium catalyzed redistribution of methylhydridooligo- and polysiloxanes
[AD-A212000] N90-12736
Polymer characterization by electrohydrodynamic ionization mass spectrometry
[AD-A212130] N90-12739
Quartz crystal microbalance analysis. 1: Evidence of anion or cation insertion into electropolymerized conducting polymers
[AD-A212304] N90-12755
Synthesis of energetic single phase and multi-phase polymers
[AD-A212539] N90-12761
POLYMERS
Magnetic resonance of polymers at surfaces
[AD-A212225] N90-12753
POLYMORPHISM
Polymorphism and information loss in Martin-Loef's type theory
[CS-8814] N90-13079
POLYNOMIALS
A generalization of Moak's q-Laguerre polynomials
[REPT-89-21] N90-13126
POLYURETHANE RESINS
Polyelectrolyte-diffused zinc phosphate conversion coatings and polyacid coupling primers for corrosion protection of steel and aluminum, and alkali-catalyzed hydrolysis of polyimide-based materials
[AD-A212240] N90-12754
POPULATION INVERSION
Spin-lattice relaxation and the calculation of gain, pump power, and noise temperature in ruby N90-12790
POROUS BOUNDARY LAYER CONTROL
An experimental evaluation of slots versus porous strips for laminar-flow applications N90-12530
Results of LFC experiment on slotted swept supercritical airfoil in Langley's 8-foot transonic pressure tunnel N90-12531
POSITION (LOCATION)
Optimal observer motion for bearings-only localization and tracking N90-12569
Sound Localization by Human Observers symposium proceedings
[AD-A212877] N90-13026
POSITION ERRORS
RTSIN1: A model of a strapdown INS on a two-axis rate table
[AD-A212406] N90-12579
POSITION INDICATORS
Automatic processing of images from the GRATE flight test tool
[DLR-FB-89-28] N90-12599
POSITIONING
Geodetic point positioning with GPS (Global Positioning System) carrier beat phase data from the CASA UNO experiment
[AD-A211955] N90-12970
Placing mirrors in grids
[CWI-CS-R8906] N90-13154
POSITIVE IONS
Instability of the behavior of high resistivity silicon detectors due to the presence of oxide charges
[REPT-89-038] N90-13260
POSITRONS
Temperature dependence of positron diffusion in cubic metals
[PB89-222020] N90-12722
POSTURE
Cardiovascular, renal, electrolyte, and hormonal changes in man during gravitational stress, weightlessness, and simulated weightlessness: Lower body positive pressure applied by the antigravity suit
[NASA-TM-102232] N90-13013
Pre- and postflight postural control of the D1 Spacelab mission astronauts examined with a tilting room
[IZF-1988-25] N90-13039

POTENTIAL ENERGY
On the spectrum of the staggered Dirac operator at finite chemical potential
[ITFA-88-53] N90-13272
POTENTIAL THEORY
Application of a generalized Leibniz rule for calculating electromagnetic fields within continuous source regions
[AD-A212470] N90-12831
A fast algorithm for the evaluation of heat potentials
[AD-A211316] N90-13052
POWDER (PARTICLES)
Temperature effects in shock consolidation of metal powders
[DE89-016782] N90-12716
POWDER METALLURGY
Tribological properties of PM212: A high-temperature, self-lubricating, powder metallurgy composite
[NASA-TM-102355] N90-12659
POWER CONDITIONING
Analysis and simulation of dynamics of spacecraft power systems N90-12653
POWER SPECTRA
A mechanical power flow capability for the finite element code NASTRAN
[AD-A212202] N90-12964
POWERED LIFT AIRCRAFT
The NASA experience in aeronautical R and D: Three case studies with analysis
[AD-A211486] N90-12496
Powered-lift aircraft technology
[NASA-SP-501] N90-12589
PREAMPLIFIERS
Feedback charge amplifier integrated on the detector wafer
[REPT-89-037] N90-12852
PRECIPITATION (METEOROLOGY)
Analysis and modeling of summertime convective cloud and precipitation structure over the Southeastern United States
[NASA-CR-185436] N90-12996
PREDICTION ANALYSIS TECHNIQUES
Stability theory applications to laminar-flow control N90-12513
CFD methods for drag prediction and analysis currently in use in UK
[RAE-TM-AERO-2146] N90-12563
Exponential modeling using combined forward and backward prediction
[AD-A212317] N90-13169
PREDICTIONS
Aerodynamic test and analysis of a slender generic missile configuration
[AD-A212522] N90-12567
Shear fatigue testing and life prediction of fibre composites
[REPT-8519] N90-12668
Asymptotic analyses of the structures and characteristics of flames N90-12683
An investigation on combined extension and bending of thin sheets with a central crack
[LR-561] N90-12958
PREDICTOR-CORRECTOR METHODS
Smoothed predictor-corrector methods for solving partial differential equations
[CWI-NM-R8808] N90-13131
PREMIXED FLAMES
Asymptotic analyses of the structures and characteristics of flames N90-12683
Investigation of fuel additive effects on sooting flames
[AD-A212925] N90-12709
An investigation of diamond film deposition in a premixed oxyacetylene flame
[AD-A212595] N90-13268
PREPROCESSING
Image preprocessing by modified median filter
[AD-D014199] N90-12828
PRESSING (FORMING)
The relationship between the mechanical properties of materials after press forming and their in-service properties
[CETIM-101530] N90-12723
Cold press lubrication: Fine tuning of the CETIM Forgelub test
[CETIM-105160] N90-12938
PRESSURE DISTRIBUTION
Status report on a natural laminar-flow nacelle flight experiment N90-12550
Nacelle design N90-12551
Nacelle aerodynamic performance N90-12552
Effects of acoustic sources N90-12553
Supersonic boundary-layer transition on the LaRC F-106 and the DFRF F-15 aircraft. Part 2: Aerodynamic predictions N90-12559
Prediction of unsteady blade surface pressures on an advanced propeller at an angle of attack
[NASA-TM-102374] N90-12560
Development of a VSAERO (Vortex Separation Aerodynamics) model of the F/A-18
[AD-A212442] N90-12566
A computationally efficient modelling of laminar separation bubbles
[NASA-CR-185854] N90-12672
PRESSURE EFFECTS
Stage effects on stalling and recovery of a high-speed 10-stage axial-flow compressor N90-12600
PRESSURE GRADIENTS
Three-dimensional shear flows: Analysis of the track and angle of incidence
[CERT-RTS-OA-31/5025-AYD] N90-12888
PRESSURE MEASUREMENT
Preliminary experience with high response pressure measurements in a multistage, high speed compressor
[RAE-TM-P-1141] N90-12619
PRESSURE OSCILLATIONS
Fundamental studies of turbulent wall pressure fluctuations with applications to advanced acoustic sensor systems
[AD-A213041] N90-13212
PRESSURE RECOVERY
Some observations on transitory stall in conical diffusers
[NASA-TM-102387] N90-12561
PRESSURE REDUCTION
Two-phase flow pressure losses in pipeline fittings
[ESDU-89012] N90-12883
PRESSURE SENSORS
Advanced measurement techniques, part 1 N90-12520
PRIMARY BATTERIES
The use of lithium batteries in biomedical devices
[AD-A212187] N90-12863
PRIMERS (COATINGS)
Structure and properties of polymer interphases
[AD-A212796] N90-12763
PRIORITIES
Toward an understanding of global change: Initial priorities for US contributions to the International Geosphere-Biosphere Program
[NASA-CR-185873] N90-12980
PROBABILITY DENSITY FUNCTIONS
A kernel approach to estimation of the sphere radius density in Wicksell's corpuscle problem
[CWI-MS-R8809] N90-13142
Nongaussian linear filtering, identification of linear systems, and the symplectic group
[CWI-PM-R8810] N90-13184
The shape of the probability density function of short-term concentration fluctuations of plumes in the atmospheric boundary layer
[AD-A212632] N90-13188
PROBABILITY DISTRIBUTION FUNCTIONS
Dynamics of an M-level atom interacting with cavity fields: Properties of photon statistics
[AD-A211321] N90-13213
PROBABILITY THEORY
Optical detection of space debris using a large achromatic coronagraph
[AD-A211362] N90-12647
On the decoder error probability of linear codes N90-12793
A simple model for DSS-14 outage times N90-12802
On a rate of convergence of the multiknapsack value function
[CWI-MS-R8812] N90-13144
Different notions of uncertainty in quasi-probabilistic models
[CWI-CS-R8847] N90-13182
Stochastic process models in device physics
[AD-A212284] N90-13185
Smoothed limit theorems for equilibrium processes
[AD-A212321] N90-13186
The shape of the probability density function of short-term concentration fluctuations of plumes in the atmospheric boundary layer
[AD-A212632] N90-13188
PROBLEM SOLVING
Solving 3D block bidiagonal linear systems on vector computers
[CWI-NM-R8819] N90-13061
On the identification of local minimizers in inertia-controlling methods for quadratic programming
[AD-A212514] N90-13086
NTRFACE for MAGIC
[AD-A212858] N90-13112
Stable and unstable subspaces of a critical functional differential equation
[PB89-220651] N90-13115
On the existence of a maximal weak solution for a semilinear elliptic equation
[REPT-89-06] N90-13120
Remarks on the control of discrete time nonlinear systems
[MEMO-770] N90-13158
Towards a complete local solution of the nonlinear model matching problem
[MEMO-781] N90-13166
A modified Newton method for unconstrained minimization
[AD-A212752] N90-13174
PROCEDURES
An algebra for process creation
[CWI-CS-R8907] N90-13155
PRODUCTION ENGINEERING
Estimating the relationships between the state of the art of technology and production cost for the US aircraft
[AD-A212127] N90-12495
PROGRAM VERIFICATION (COMPUTERS)
Truth maintenance systems and their implementation in PROLOG
[MEMO-INF-89-13] N90-13064
Expert system for test program set fault candidate selection
[AD-A213338] N90-13091
PROGRAMMED INSTRUCTION
Conceptual dependency theory and robot programming
[REPT-89-20] N90-13106
PROGRAMMING (SCHEDULING)
Software Engineering Exercise (SEE) guidelines
[AD-A212510] N90-13085
PROGRAMMING LANGUAGES
LOTOS tools based on the Cornell synthesizer generator
[MEMO-INF-89-5] N90-13062
Abstract grammars based on transductions
[MEMO-INF-89-7-REV] N90-13063
A simple definition for parallel composition of prime event structures
[CWI-CS-R8903] N90-13074
PROJECT MANAGEMENT
Issues in NASA program and project management
[NASA-SP-6101(02)] N90-13277
SOI: The Solar Oscillations Imager on SOHO N90-13306
PROJECT PLANNING
Studies of the European transonic wind tunnel
[ONERA-RSF-12/0694-GY] N90-13278
PROJECT SETI
The NASA SETI sky survey: Recent developments N90-12804
PROJECTILES
Present and future US and Soviet chemical missiles and chemical rocket projectiles
[AD-A212199] N90-12644
Stress waves through projectile joints and interfaces
[AD-A212201] N90-12963
PROLOG (PROGRAMMING LANGUAGE)
A formatting style for typesetting and distributing draft international standards
[NPL-DITC-143/89] N90-13059
Truth maintenance systems and their implementation in PROLOG
[MEMO-INF-89-13] N90-13064
LAIOS: A multiprocessor network for artificial intelligence applications
[ETN-89-95498] N90-13109
PROP-FAN TECHNOLOGY
Numerical simulation of unsteady rotational flow over propfan configurations
[NASA-CR-186037] N90-12500
Large-scale Advanced Prop-fan (LAP) static rotor test report
[NASA-CR-180848] N90-12617
The design and development of an acoustic test section for the ARA transonic wind tunnel
[PNR90574] N90-13202
PROPELLANT COMBUSTION
Laser initiated ignition of liquid propellant
[AD-A212342] N90-12768
PROPELLANT DECOMPOSITION
Laser initiated ignition of liquid propellant
[AD-A212342] N90-12768
PROPELLER BLADES
Prediction of unsteady blade surface pressures on an advanced propeller at an angle of attack
[NASA-TM-102374] N90-12560
Large-scale Advanced Prop-fan (LAP) static rotor test report
[NASA-CR-180848] N90-12617
PROPELLER EFFICIENCY
The design and development of an acoustic test section for the ARA transonic wind tunnel
[PNR90574] N90-13202

PROPULSION SYSTEM CONFIGURATIONS
Large-scale Advanced Prop-fan (LAP) static rotor test report
[NASA-CR-180848] N90-12617
PROPULSION SYSTEM PERFORMANCE
Gas turbine performance analysis
[PNR90599] N90-12614
RSRM-3 (360L003) ballistics/mass properties report
[NASA-CR-183716] N90-12651
Ballistics/mass properties
[NASA-CR-183723] N90-12652
PROPULSIVE EFFICIENCY
RSRM-3 (360L003) ballistics/mass properties report
[NASA-CR-183716] N90-12651
Ballistics/mass properties
[NASA-CR-183723] N90-12652
PROTECTIVE CLOTHING
Prediction of thermal stress casualties
[AD-A212356] N90-13022
PROTECTIVE COATINGS
Surface treatments of carbon fibers in an organic environment. Finite element analysis of pull-out tests
[ONERA-RT-7/3549-M] N90-12698
The quality of vacuum deposited surface treatments
[CETIM-107040] N90-12729
Polyelectrolyte-diffused zinc phosphate conversion coatings and polyacid coupling primers for corrosion protection of steel and aluminum, and alkali-catalyzed hydrolysis of polyimide-based materials
[AD-A212240] N90-12754
PROTEIN CRYSTAL GROWTH
Protein crystal growth in low gravity
[NASA-CR-186082] N90-12770
PROTEIN SYNTHESIS
Protein crystal growth in low gravity
[NASA-CR-186082] N90-12770
PROTEINS
Protein crystal growth in low gravity
[NASA-CR-186082] N90-12770
PROTOCOL (COMPUTERS)
Analysis and modeling of summertime convective cloud and precipitation structure over the Southeastern United States
[NASA-CR-185436] N90-12996
PROTON BEAMS
Thermal initiation of confined primary explosives with a proton beam
[AD-A212954] N90-12767
PROTOTYPES
Case study on rapid software prototyping and automated software generation: An inertial navigation system
[AD-A212272] N90-12578
ISI's (Information Sciences Institute) SDI architecture simulator: Initial prototype user interface
[AD-A211325] N90-13053
PROVING
Validation of the procedures --- integrated multidisciplinary optimization of rotorcraft N90-12587
Proving total correctness of recursive procedures
[CWI-CS-R8904] N90-13075
Process expressions and Hoare's logic
[CWI-CS-R8905] N90-13076
Meixner-Pollaczek polynomials and the Heisenberg algebra
[CWI-PM-R8806] N90-13138
A validation of the proposed NATO standard method to determine target acquisition distances with image intensifiers
[IZF-1988-8] N90-13230
More on the super WZW theory
[NIKHEF-H/88-11] N90-13273
PROVISIONING
Air Force flight feeding. Volume 1: Evaluation of current system and alternative concepts
[AD-A212789] N90-13043
PSYCHOLOGICAL EFFECTS
Psychological mechanisms involved in the disorientation of pilots due to flight conditions
[ETN-89-95014] N90-13040
PULSE CODE MODULATION
Acquisition and recording an AMX A/C. Aeritalia experience and present trends
[ETN-89-95217] N90-12598
PULSE COMMUNICATION
Assessment of voice coders for ATC/pilot voice communications via satellite digital communication channels
[CAA-PAPER-89004] N90-12807
PULSE GENERATORS
The design, construction, performance and calibration of pulse generators to fulfil the requirements of specifications defence standard 59-41, FS(F) 510 and FS(S) 457
[RAE-TM-FS(F)-550] N90-12857
PULSE RADAR
Specification for radar free-space detection range and free-space intercept range calculations
[AD-A213158] N90-12843
PULSED LASERS
Advanced source development and applications. Laser-produced plasmas: A compact soft x ray source with high peak brightness
[AD-A212677] N90-13245
PULSES
Airborne/spaceborne pulsed power source
[AD-A211762] N90-12850
Magnetically insulated electron flows in pulsed power systems
[AD-A212746] N90-13196
PYROELECTRICITY
Readout and signal conditioning for a linear pyroelectric array
[RSRE-MEMO-4102] N90-12905
PYROLYSIS
Pyrolytic production of ceramic composites from silicates
[ETCA-89-R-012] N90-12746
Continuing studies of liquid propellant drops in hot, high-pressure environments
[AD-A212265] N90-12765
PYROLYTIC MATERIALS
Pyrolytic production of ceramic composites from silicates
[ETCA-89-R-012] N90-12746
Growth and characterization of zinc sulfide films by conversion of zinc oxide films with H2S
[AD-A213345] N90-13271
PYROTECHNICS
The Shock and Vibration Digest, volume 21, no. 10 N90-12771
Pyrotechnic shock structural response N90-12774
PYRROLES
Quartz crystal microbalance analysis. 1: Evidence of anion or cation insertion into electropolymerized conducting polymers
[AD-A212304] N90-12755

Q

QUADRATIC PROGRAMMING
On the identification of local minimizers in inertia-controlling methods for quadratic programming
[AD-A212514] N90-13086
Sequential quadratic programming algorithms for optimization
[AD-A212800] N90-13088
QUADRATURES
Faster Phong shading via angular interpolation
[CWI-CS-R8909] N90-13156
QUALITY CONTROL
The role of component testing
[PNR90589] N90-12608
QUANTITATIVE ANALYSIS
Improved method for determination of helium-4 in helium-3 by mass spectrometry
[PB89-201404] N90-12686
QUANTUM CHROMODYNAMICS
On the spectrum of the staggered Dirac operator at finite chemical potential
[ITFA-88-53] N90-13272
QUANTUM ELECTRODYNAMICS
On the spectrum of the staggered Dirac operator at finite chemical potential
[ITFA-88-53] N90-13272
QUANTUM ELECTRONICS
Joint Services Electronics Program
[AD-A212309] N90-12864
QUANTUM STATISTICS
More on the super WZW theory
[NIKHEF-H/88-11] N90-13273
QUANTUM THEORY
Representations of the twisted SU(2) quantum group and some q-hypergeometric orthogonal polynomials
[CWI-PM-R8809] N90-13140
The addition formula for little q-Legendre polynomials and the SU(2) quantum group
[CWI-AM-R8906] N90-13151
Strings, p-branes and Skyrmions in curved space N90-13293
QUANTUM WELLS
High speed quantum-well optoelectronic devices by MBE
[AD-A212585] N90-13237
QUARKS
Cosmic strings and baryon decay catalysis
[NASA-CR-186074] N90-13299
QUARTZ CRYSTALS
Quartz crystal microbalance analysis. 1: Evidence of anion or cation insertion into electropolymerized conducting polymers
[AD-A212304] N90-12755
QUEUEING THEORY
The M/G/1 processor sharing queue as the almost sure limit of feedback queues
[REPT-89-32] N90-13044
Extended performability modeling using dynamic queing networks
[MEMO-INF-89-15] N90-13099
Modular specifications in process algebra with curious queues
[CWI-CS-R8821] N90-13152
The discrete-time single-server queueing model
[MEMO-780] N90-13165
QUIET ENGINE PROGRAM
What should be done with those noisy old aircraft
[PNR90562] N90-12593
Re-engine with the Rolls-Royce Tay 670, the route to significant noise reduction
[PNR90585] N90-12606
The commercial aircraft noise problem
[PNR90577] N90-13203

R

RACKS (FRAMES)
Pivotal mono wing cruise missile with wing deployment and fastener mechanism
[AD-D014191] N90-12594
RADAR CROSS SECTIONS
Specification for radar free-space detection range and free-space intercept range calculations
[AD-A213158] N90-12843
The physical optics approximation in the near-field region
[FEL-1989-100] N90-13234
RADAR DATA
Specification of Viper1 in Z
[RSRE-MEMO-4195] N90-12817
Specification of Viper2 in Z
[RSRE-MEMO-4217] N90-12819
RADAR DETECTION
Specification for radar free-space detection range and free-space intercept range calculations
[AD-A213158] N90-12843
RADAR ECHOES
Investigation of the properties of radar backscatter from sea ice
[AD-A212808] N90-12838
Multiparameter radar estimation of raindrop size distribution
[AD-A212410] N90-13007
RADAR EQUIPMENT
Tropospheric influences on satellite-Earth paths and their determination by means of radar measurements
[ESA-TT-1143] N90-12039
RADAR IMAGERY
On a fast two-dimensional radar imaging process for rotating targets, and an analysis of its image quality
[ESA-TT-1142] N90-12808
Conception and results of the DLR realtime azimuth processor for the E-SAR system
[DLR-FB-89-30] N90-12827
Progress in the identification of airborne radar targets
[AD-A212749] N90-12835
RADAR MEASUREMENT
Use of ground penetrating radar to define recharge areas in the Central Sand Plain
[PB89-224885] N90-12814
Radar polarimetric studies based on the MAYPOLE 1983 and 1984 field experiments
[AD-A212226] N90-12830
RADAR SCATTERING
Improvement and extension of a radar forest backscattering model
[NASA-CR-186083] N90-12973
RADAR SIGNATURES
Progress in the identification of airborne radar targets
[AD-A212749] N90-12835
RADAR TARGETS
Dedicated tracking of crossing targets with a phased array monopulse radar
[FEL-1988-95] N90-12821
Progress in the identification of airborne radar targets
[AD-A212749] N90-12835
RADAR TRACKING
Multiparameter radar estimation of raindrop size distribution
[AD-A212410] N90-13007

RADAR TRANSMISSION
Radar polarimetric studies based on the MAYPOLE 1983 and 1984 field experiments
[AD-A212226] N90-12830
RADIAL FLOW
A theoretical study of ingress for shrouded rotating disk systems with radial outflow
[PNR90586] N90-12607
RADIATION ABSORPTION
Small particle scattering and absorption
[AD-A213168] N90-12711
RADIATION COUNTERS
Survey of the response of standard limited streamer tubes over the complete range of three-component gas mixtures of isobutane, CO(sub 2), argon
[DE89-016692] N90-12875
RADIATION DISTRIBUTION
Wire grid modeling of the linear tapered slot antenna
[AD-A212977] N90-12842
RADIATION DOSAGE
The analysis of current-mirror MOSFETs for use in radiation environments
[AD-A212527] N90-12866
RADIATION EFFECTS
Calcium displacement caused by electromagnetic fields
[AD-A212690] N90-13023
The cosmic radiation effects and activation monitor
[RAE-TM-SPACE-364] N90-13318
RADIATION PROTECTION
Base level management of radio frequency radiation protection program
[AD-A211759] N90-13017
RADIATION TRANSPORT
Particle transport simulation for spaceborne, NaI gamma-ray spectrometers
[AD-A205150] N90-13292
RADICALS
Electrically conducting organic materials: Design, synthesis and characterization
[AD-A212214] N90-12700
RADII
A kernel approach to estimation of the sphere radius density in Wicksell's corpuscle problem
[CWI-MS-R8809] N90-13142
Measurements of bubble properties using a multi-frequency sound field
[AD-A212591] N90-13211
A two-parameter representation of dynamic dislocation distributions
[AD-A212249] N90-13263
RADIO ANTENNAS
Performance effects of tie-truss modifications for a 70-meter centerline beam waveguide antenna N90-12791
RADIO ASTRONOMY
The Telecommunications and Data Acquisition Report
[NASA-CR-185093] N90-12786
A statistical study of radio-source structure effects on astrometric very long baseline interferometry observations N90-12788
Performance of the image statistics decoder in conjunction with the Goldstone-VLA array N90-12796
RADIO ATTENUATION
Ground effects on multipath fading
[TELECOM-PARIS-88-E017] N90-12812
RADIO COMMUNICATION
Preliminary investigation of Faraday rotation effects and description of polarization measurements on the AFGL high latitude meteor scatter test bed
[AD-A211298] N90-12806
A literature study of wave propagation in the 1-60 GHz range. Application to transportable military communication systems
[FEL-1988-47] N90-12825
RADIO EQUIPMENT
A literature study of wave propagation in the 1-60 GHz range. Application to transportable military communication systems
[FEL-1988-47] N90-12825
RADIO FREQUENCIES
Preliminary report on the feasibility of high power Electronic Warfare (EW) using explosive energy sources
[MRL-TR-89-3] N90-12775
RF and dc desensitized electroexplosive device
[AD-D014206] N90-12862
Radio frequency linac driven free-electron laser configurations
[AD-A212572] N90-12922
Synthesis and study of materials for superconducting electronics
[AD-A212966] N90-13270
RADIO FREQUENCY HEATING
Radio frequency (13.56 MHz) energy enhances rewarming from mild hypothermia
[AD-A212703] N90-13024
RADIO FREQUENCY INTERFERENCE
Adaptive antenna arrays for satellite communication
[NASA-CR-185989] N90-12784
Digital radio link: Wave propagation investigations on a 13 GHz line-of-sight path
[PB89-213128] N90-12785
Automatic communications channel interference monitoring
[RSRE-MEMO-4243] N90-12820
Long wave atmospheric noise model, phase 1. Volume 1: Lightning occurrence rates and propagation theory
[AD-A212794] N90-12836
Long wave atmospheric noise model, phase 1. Volume 2: Mode parameters
[AD-A212795] N90-12837
RADIO SOURCES (ASTRONOMY)
A statistical study of radio-source structure effects on astrometric very long baseline interferometry observations N90-12788
RADIO TRANSMITTERS
Description and results of a multihop NACS simulation
[FEL-1988-46] N90-12824
RADIO WAVES
Physics of the tropospheric radiopropagation
[DE89-619726] N90-12783
Preliminary investigation of Faraday rotation effects and description of polarization measurements on the AFGL high latitude meteor scatter test bed
[AD-A211298] N90-12806
Base level management of radio frequency radiation protection program
[AD-A211759] N90-13017
Far infrared, submm and mm spectroscopy of the galactic center: Radio arc and +20/+50 km s (exp -1) clouds
[NASA-CR-185497] N90-13296
RADIOACTIVE ISOTOPES
Automatic analysis and exploitation of the flow visualization images
[ETN-89-95712] N90-12887
RADIOACTIVITY
Radioactivity induced in gamma-ray spectrometers
[RAE-TM-SPACE-363] N90-13317
The cosmic radiation effects and activation monitor
[RAE-TM-SPACE-364] N90-13318
RADIOMETRIC RESOLUTION
Removing stripes in GOES (Geostationary Operational Environmental Satellites) images by matching empirical distribution functions
[PB89-213359] N90-12968
RAIN
Radar polarimetric studies based on the MAYPOLE 1983 and 1984 field experiments
[AD-A212226] N90-12830
A numerical study of rain-induced surface gravity wave attenuation
[AD-A212762] N90-13197
RAINDROPS
Multiparameter radar estimation of raindrop size distribution
[AD-A212410] N90-13007
RAMAN LASERS
Volumetric analysis by spontaneous Raman diffusion in a supersonic wind tunnel
[ISL-R-109/88] N90-12564
Development of an anti-Stokes coherent Raman diffusion system for measuring hypersonic flow
[ONERA-RSF-1/7301-PY] N90-12630
RAMAN SPECTROSCOPY
Volumetric analysis by spontaneous Raman diffusion in a supersonic wind tunnel
[ISL-R-109/88] N90-12564
Fundamental molecular data to support CARS diagnostics of temperature, pressure, and species concentration
[AD-A212411] N90-12704
Ion beam analysis of diffusion in polymer glasses
[AD-A212339] N90-12756
RANDOM ERRORS
On the decoder error probability of linear codes N90-12793
Electron beam propagation through a magnetic wiggler with random field errors
[AD-A212705] N90-12867
RANDOM NOISE
Performance of the split-symbol moments SNR estimator in the presence of inter-symbol interference N90-12799
RANDOM VARIABLES
Domain of attraction of an operator between supremum and sum
[REPT-89-05] N90-13119
Tail triviality for sums of stationary random variables
[CWI-MS-R8810] N90-13143
Strong moderate deviation theorems for m-dependent random variables
[AD-A212618] N90-13173
Random truncation models and Markov processes
[CWI-MS-R8817] N90-13181
RANDOM WALK
Electron beam propagation through a magnetic wiggler with random field errors
[AD-A212705] N90-12867
RANK TESTS
Asymptotic expansions for two-stage rank tests
[MEMO-773] N90-13161
RARE EARTH COMPOUNDS
Graduate fellowships in the field of hard magnetic materials
[AD-A212303] N90-12733
RATIONS
Air Force flight feeding. Volume 1: Evaluation of current system and alternative concepts
[AD-A212789] N90-13043
RAYLEIGH-RITZ METHOD
The Shock and Vibration Digest, volume 21, no. 10 N90-12771
The computer age and traditional approximate, analytical methods N90-12772
REACTION KINETICS
Measurement and correlation of the solubility and diffusion coefficient for oxygen and chlorine in basic hydrogen peroxide
[AD-A212348] N90-12703
FLIC (FLame with Implicit Convection): A detailed, two-dimensional flame model
[AD-A212953] N90-12710
Mechanisms of CO2 reduction metal and metal modified semiconductor electrodes
[AD-A213169] N90-12712
An investigation of the irradiation swelling mechanisms in refractory metals at high temperatures
[AD-A211406] N90-12719
Computer simulation studies of the catalytic oxidation of carbon monoxide on platinum metals
[PB89-223739] N90-12721
Role of chemical effects in daytime high latitude trough formation
[AD-A211772] N90-12989
REACTIVITY
Chemical and photochemical reactivity in microemulsions and waterless microemulsions
[AD-A211776] N90-12692
REACTOR TECHNOLOGY
Activities report of the Joint Research Center
[ETN-89-95757] N90-13321
REAL TIME OPERATION
Real-time simulation of an F110/STOVL turbofan engine
[NASA-TM-102409] N90-12618
Preliminary experience with high response pressure measurements in a multistage, high speed compressor
[RAE-TM-P-1141] N90-12619
On a fast two-dimensional radar imaging process for rotating targets, and an analysis of its image quality
[ESA-TT-1142] N90-12808
A real-time wind model using digital data from aircraft
[RSRE-MEMO-4309] N90-13005
A transformational method for verifying safety properties in real time systems
[AD-A211925] N90-13051
A mapping for converting Mascot designs to Ada programs
[RSRE-MEMO-4244] N90-13070
Visual perception processing in a hierarchical control system: Level 1
[PB89-221188] N90-13101
RECIRCULATIVE FLUID FLOW
Characterization of nonpremixed turbulent bluff-body burner flames
[PB89-229447] N90-12689
RECOGNITION
A validation of the proposed NATO standard method to determine target acquisition distances with image intensifiers
[IZF-1988-8] N90-13230
RECOMMENDATIONS
Toward an understanding of global change: Initial priorities for US contributions to the International Geosphere-Biosphere Program
[NASA-CR-185873] N90-12980
RECURSIVE FUNCTIONS
Mathematical equivalence in a primitive Ella
[RSRE-MEMO-4225] N90-13066
Proving total correctness of recursive procedures
[CWI-CS-R8904] N90-13075
Characterizing termination of logic problems with level mappings
[CWI-CS-R8912] N90-13077

A recursive algorithm for computing the frequency response of a class of nonlinear difference equation models
[RR-354] N90-13123
REDUCED GRAVITY
Biology in microgravity: A guide for experimenters
[ESA-TM-02] N90-12769
Protein crystal growth in low gravity
[NASA-CR-186082] N90-12770
REDUCTION (CHEMISTRY)
Mechanisms of CO2 reduction metal and metal modified semiconductor electrodes
[AD-A213169] N90-12712
REFERENCE STARS
A statistical study of radio-source structure effects on astrometric very long baseline interferometry observations N90-12788
REFLECTANCE
Hahn-Banach type theorems for dual semigroups
[CWI-AM-R8903] N90-13149
REFLECTED WAVES
Angle estimation in a multipath environment with an eight element linear array operating at 10.5 GHz
[FEL-1989-15] N90-12826
The physical optics approximation in the near-field region
[FEL-1989-100] N90-13234
REFORESTATION
Contribution of deforestation to atmospheric CO2 and reforestation as an option to control CO2
[DE89-017255] N90-12979
REFRACTIVITY
Recent flow visualization studies in the 0.3-m TCT N90-12528
REFRACTORY MATERIALS
Tribological properties of ceramic/Ti3Al-Nb sliding couples for use as candidate seal materials to 700 deg C
[NASA-TM-102401] N90-12658
Tribological properties of PM212: A high-temperature, self-lubricating, powder metallurgy composite
[NASA-TM-102355] N90-12659
Graduate fellowships in the field of hard magnetic materials
[AD-A212303] N90-12733
REFRACTORY METALS
An investigation of the irradiation swelling mechanisms in refractory metals at high temperatures
[AD-A211406] N90-12719
REFRIGERATING
Development of a low noise 10 K J-T refrigeration system
[AD-A213347] N90-12779
REFRIGERATORS
Development of a low noise 10 K J-T refrigeration system
[AD-A213347] N90-12779
A closed-cycle refrigerator for cooling maser amplifiers below 4 Kelvin N90-12797
REGRESSION ANALYSIS
Estimating the relationships between the state of the art of technology and production cost for the US aircraft
[AD-A212127] N90-12495
REINFORCING FIBERS
A study of the impact of a ball bearing on a long fiber composite plate with a carbon matrix, part 2
[ETCA-88-R-088-PT-2] N90-12673
Oxide ceramic fibers by the sol-gel methods
[AD-A211315] N90-12742
Rolling of ARALL laminates (an alternative method for post-stretching ARALL laminates)
[LR-560] N90-12778
RELATIVISTIC ELECTRON BEAMS
Electron beam propagation through a magnetic wiggler with random field errors
[AD-A212705] N90-12867
RELATIVISTIC THEORY
Elements of a relativistic microscopic theory of hadronic matter in equilibrium and non-equilibrium
[KVI-796] N90-13218
RELATIVITY
Corrections to the thin wall approximation in general relativity
[NASA-CR-186078] N90-13274
RELAXATION METHOD (MATHEMATICS)
Upwind discretization of the steady Navier-Stokes equations
[CWI-NM-R8810] N90-12891
Iterative methods for linear complementary and related problems
[AD-A212848] N90-13089
On a rate of convergence of the multiknapsack value function
[CWI-MS-R8812] N90-13144
RELIABILITY
On the precision and reliability of GPS networks computed using the double difference observable
[ETN-89-95719] N90-12571
Software fault tolerance
[RSRE-MEMO-4237] N90-12575
RELIABILITY ENGINEERING
Development and applications of reliability and maintainability design criteria in military aircraft
[ETN-89-95208] N90-12591
Flanged joints of aeroengines
[PNR90594] N90-12609
Aviation Engine Test Facilities (AETF) fire protection study
[AD-A211483] N90-12777
Telerobotic control for teams of semi-autonomous agents, phase 1
[AD-A211648] N90-13037
REMOTE CONTROL
Guidance and Control Panel Symposium on Guidance and Control of Unmanned Air Vehicles
[AGARD-AR-260] N90-12623
Spark camera annotation and control system for the BRL (Ballistic Research Laboratory) Transonic Range Facility
[AD-A212266] N90-12633
REMOTE SENSING
A new generation of atmospheric tracers: The biological connection
[AD-A212285] N90-12983
REMOTE SENSORS
The development of a high response aerodynamic wedge probe and use on a high-speed research compressor
[PNR90598] N90-12613
REMOTELY PILOTED VEHICLES
The design of an airfoil for a high-altitude, long-endurance remotely piloted vehicle N90-12545
Guidance and Control Panel Symposium on Guidance and Control of Unmanned Air Vehicles
[AGARD-AR-260] N90-12623
Telerobotic control for teams of semi-autonomous agents, phase 1
[AD-A211648] N90-13037
RENAL FUNCTION
Cardiovascular, renal, electrolyte, and hormonal changes in man during gravitational stress, weightlessness, and simulated weightlessness: Lower body positive pressure applied by the antigravity suit
[NASA-TM-102232] N90-13013
REPLACING
What should be done with those noisy old aircraft
[PNR90562] N90-12593
REPRESENTATIONS
Representations of the twisted SU(2) quantum group and some q-hypergeometric orthogonal polynomials
[CWI-PM-R8809] N90-13140
Transformations and representations of nonlinear systems
[MEMO-776] N90-13164
REQUIREMENTS
Requirements specification with Petri nets using the cube tool methodology
[AD-A212190] N90-12829
RESEARCH
National Science Foundation N90-13320
RESEARCH AND DEVELOPMENT
The NASA experience in aeronautical R and D: Three case studies with analysis
[AD-A211486] N90-12496
Acquisition and recording an AMX A/C. Aeritalia experience and present trends
[ETN-89-95217] N90-12598
Gas turbine performance analysis
[PNR90599] N90-12614
National Aeronautics and Space Administration N90-13282
Fiscal year 1990 authorization request and budget estimates for the National Aeronautics and Space Administration
[GPO-96-945] N90-13283
The 1990 National Aeronautics and Space Administration Authorization
[GPO-98-466] N90-13285
National Aeronautics and Space Administration N90-13287
National Aeronautics and Space Administration Authorization Act, fiscal year 1990
[S-REPT-101-157] N90-13288
National Aeronautics and Space Administration Authorization Act, fiscal year 1990
[S-REPT-101-157] N90-13289
NASA technology applications
[GPO-99-412] N90-13290
Research and Technology annual report, 1988
[NASA-TM-101070] N90-13319
European space technology: Celebrating twenty-five years of research and development
[ESA-BR-55] N90-13322
RESEARCH FACILITIES
Basic aerodynamic research facility for comparative studies of flow diagnostic techniques N90-12526
Research and Technology annual report, 1988
[NASA-TM-101070] N90-13319
RESEARCH MANAGEMENT
The NASA experience in aeronautical R and D: Three case studies with analysis
[AD-A211486] N90-12496
The integration of structured and formal methods
[RSRE-MEMO-4293] N90-13068
Research on heating, instabilities, turbulence and RF emission from electric field dominated plasmas
[AD-A212122] N90-13243
RESIDUES
Standard method for measurement of nonvolatile residue on surfaces
[AD-A213324] N90-12714
RESIN MATRIX COMPOSITES
Crack propagation failure of carbon/resin composites
[ONERA-RT-45/7086-M] N90-12677
Mechanical behavior of carbon/resin composites under delamination and cracking of transverse layers
[ONERA-RT-46/7086-M] N90-12678
Textural and structural organization of the heat treated polymers: Mechanical properties relationships
[ETN-89-95711] N90-12744
RESONANCE
Evaluation of 15th- and 30th-order geopotential harmonic coefficients from 26 resonant satellite orbits
[RAE-TR-88045] N90-12640
Orbit determination and analysis for Cosmos 236 at 15th-order resonance
[RAE-TR-88058] N90-12641
Measurements of bubble properties using a multi-frequency sound field
[AD-A212591] N90-13211
Dynamics of an M-level atom interacting with cavity fields: Properties of photon statistics
[AD-A211321] N90-13213
RESONANT FREQUENCIES
Measurements of bubble properties using a multi-frequency sound field
[AD-A212591] N90-13211
RESONATORS
Bulk acoustic waves resonators made of amorphous materials
[NOTE-TECHNIQUE-1989-4] N90-13199
RESOURCE ALLOCATION
Electrophysiological studies of visual attention and resource allocation
[AD-A212287] N90-13030
RESOURCES
On modeling resources in multiprocessor systems
[MEMO-INF-88-33] N90-13095
RESPONSE TIME (COMPUTERS)
Performance evaluations of a parallel and expandable database computer: The multi-backend database computer
[AD-A212761] N90-13046
RETENTION (PSYCHOLOGY)
Individual differences in associative learning and forgetting
[AD-A212765] N90-13034
RETRACTABLE EQUIPMENT
Pivotal mono wing cruise missile with wing deployment and fastener mechanism
[AD-D014191] N90-12594
RETROFITTING
What should be done with those noisy old aircraft
[PNR90562] N90-12593
REVERBERATION
Problems in nonlinear acoustics: Scattering of sound by sound, parametric receiving arrays, nonlinear effects in asymmetric sound beams and pulsed finite amplitude sound beams
[AD-A211756] N90-13200
RHEOLOGY
A graph-theoretical approach to block-copolymer complexes. Part 3: Loops and cycles
[MEMO-778-PT-3] N90-12750
RIEMANN WAVES
Basic research on methods of calculating supersonic and hypersonic flow
[ONERA-RSF-19/1123-AY-234A] N90-12565
RIGID STRUCTURES
Dynamic robot models using the Manutec r3 as an example
[ESA-TT-1132] N90-12626
RIVERS
Estimation of time to maximum supercooling during dynamic frazil ice formation
[AD-A212204] N90-12699

ROBOTICS
Dynamic robot models using the Manutec r3 as an example
[ESA-TT-1132] N90-12626
A robot which will investigate the condition of underground pipe
[PB89-230650] N90-12928
Squirt: The prototypical mobile robot for autonomous graduate students
[AD-A212337] N90-12941
Development of an integrated mobile robot system at CMU (Carnegie-Mellon University)
[AD-A212555] N90-12944
Telerobotic control for teams of semi-autonomous agents, phase 1
[AD-A211648] N90-13037
What is the balance sheet for investment in automated manufacturing
[CETIM-105490] N90-13071
An on-line distributed minimum-time trajectory generator for intelligent robot manipulators
[RR-358] N90-13102
Identification of robot dynamics: A parallel processing approach
[RR-361] N90-13103
Real-time robot motion: The VLSI implementation via transputers
[RR-364] N90-13104
Spatial data structures for robotic vehicle route planning
[AD-A212606] N90-13111
Research in computer vision for autonomous systems
[AD-A212420] N90-13235

ROBOTS
Dynamic robot models using the Manutec r3 as an example
[ESA-TT-1132] N90-12626
Squirt: The prototypical mobile robot for autonomous graduate students
[AD-A212337] N90-12941
Development of an integrated mobile robot system at CMU (Carnegie-Mellon University)
[AD-A212555] N90-12944
Identification of robot dynamics: A parallel processing approach
[RR-361] N90-13103
Conceptual dependency theory and robot programming
[REPT-89-20] N90-13106

ROCKET ENGINES
Apollo lightcraft project
[NASA-CR-186055] N90-12655

ROLLING
Rolling of ARALL laminates (an alternative method for post-stretching ARALL laminates)
[LR-560] N90-12778

ROTARY STABILITY
Vortex dynamics
[AD-A212119] N90-12877

ROTARY WING AIRCRAFT
Integrated multidisciplinary optimization of rotorcraft: A plan for development
[NASA-TM-101617] N90-12580
General approach and scope — rotor blade design optimization N90-12581
Validation of the procedures — integrated multidisciplinary optimization of rotorcraft N90-12587
Appendix: Results obtained to date — integrated multidisciplinary optimization of rotorcraft N90-12588

ROTARY WINGS
Rotor blade aerodynamic design N90-12582
Rotor blade dynamic design N90-12583
Rotor blade structural design N90-12584
Acoustic design considerations: Review of rotor acoustic sources N90-12585
Airframe design considerations: Overview — rotor design optimization N90-12586
Appendix: Results obtained to date — integrated multidisciplinary optimization of rotorcraft N90-12588
Euler equation solutions applied to a helicopter rotor in forward moving flight
[ONERA-RSF-32/1285-AY-346A] N90-12592
RAN (Royal Australian Navy) vibration analysis system operator's guide
[AD-A212441] N90-12596

ROTATING DISKS
A theoretical study of ingress for shrouded rotating disk systems with radial outflow
[PNR90586] N90-12607
The effects of trace anions on the voltammetry of single crystal gold surfaces
[AD-A211886] N90-13254

ROTATING SHAFTS
Vibration transmission through rolling element bearings in geared rotor system, part 1
[NASA-CR-186093] N90-12938

ROTATING STALLS
Stage effects on stalling and recovery of a high-speed 10-stage axial-flow compressor N90-12600

ROTATION
Rotational and vibrational nonequilibrium effects in rarefied, hypersonic flow
[NASA-CR-182559] N90-12498
Cross-axis synchronous flow through coil planet centrifuge for large-scale preparative countercurrent chromatography
[PB89-200174] N90-12682
Experimental study of homogeneous turbulence submitted to rotational effects
[ONERA-RSF-10/1145-AY-164A] N90-12894
A device to extract energy from water waves
[REPT-89-34] N90-12978

ROTOR AERODYNAMICS
Prediction of unsteady blade surface pressures on an advanced propeller at an angle of attack
[NASA-TM-102374] N90-12580
Integrated multidisciplinary optimization of rotorcraft: A plan for development
[NASA-TM-101617] N90-12580
General approach and scope — rotor blade design optimization N90-12581
Rotor blade aerodynamic design N90-12582

ROTOR BLADES (TURBOMACHINERY)
Numerical simulation of unsteady rotational flow over propfan configurations
[NASA-CR-186037] N90-12500
Dynamic tip clearance measurements in axial flow compressors
[PNR90597] N90-12612
Blading design for multi-storage HP compressor
[PNR90602] N90-12616

ROTOR DYNAMICS
Integrated multidisciplinary optimization of rotorcraft: A plan for development
[NASA-TM-101617] N90-12580
General approach and scope — rotor blade design optimization N90-12581
Rotor blade aerodynamic design N90-12582
Rotor blade dynamic design N90-12583

ROTORS
Large-scale Advanced Prop-fan (LAP) static rotor test report
[NASA-CR-180848] N90-12617
Vibration transmission through rolling element bearings in geared rotor system, part 1
[NASA-CR-186093] N90-12936

ROUTES
Route data representation for ATC simulation experiments
[RSRE-MEMO-4133] N90-12576
A 2d-1 lower bound 2-layer knock-knee channel routing
[AD-A211948] N90-12847
Spatial data structures for robotic vehicle route planning
[AD-A212606] N90-13111

RUBY
Spin-lattice relaxation and the calculation of gain, pump power, and noise temperature in ruby N90-12790

RUN TIME (COMPUTERS)
Solving 3D block bidiagonal linear systems on vector computers
[CWI-NM-R8819] N90-13061

RUNGE-KUTTA METHOD
An algebraic characterization of B-convergent Runge-Kutta methods
[CWI-NM-R8901] N90-13133
Increasing the real stability boundary of explicit methods
[CWI-NM-R8902] N90-13134

RUNWAYS
Analytical and experimental study of runway runoff with wind effects
[PTI-8948] N90-12627

RUTHENIUM COMPOUNDS
Advanced double layer capacitor
[AD-A211977] N90-12688

S

S MATRIX THEORY
A well conditioned formulation for the analysis of multi-layered frequency selective surfaces using a cascaded matrix approach
[RSRE-MEMO-4289] N90-12858

SAFETY FACTORS
Advanced spacecraft fire safety: Proposed projects and program plan
[NASA-CR-185147] N90-12645
A transformational method for verifying safety properties in real time systems
[AD-A211925] N90-13051

SAMPLING
Multiparameter radar estimation of raindrop size distribution
[AD-A212410] N90-13007
Asymptotic expansions for two-stage rank tests
[MEMO-773] N90-13161
Interpretation and manipulation of Edgeworth expansions
[MEMO-775] N90-13163
Illustration of Bayesian inference in normal data models using Gibbs sampling
[AD-A212630] N90-13187

SANDWICH STRUCTURES
Crack propagation failure of carbon/resin composites
[ONERA-RT-45/7086-M] N90-12677

SATELLITE COMMUNICATION
Adaptive antenna arrays for satellite communication
[NASA-CR-185989] N90-12784
Satellite range delay simulator for a matrix-switched time division multiple-access network simulator
[NASA-TM-102407] N90-12813
Design and performance of an on-satellite laser diagnostic system for a free space optical heterodyne frequency-shift-keyed communication system
[AD-A211986] N90-12915
Wider horizons: Potential contributions by space systems to socio-economic advancement in developing countries
[ESA-SP-1106] N90-13276

SATELLITE IMAGERY
Removing stripes in GOES (Geostationary Operational Environmental Satellites) images by matching empirical distribution functions
[PB89-213359] N90-12968
A hybrid architecture for feature labelling of oceanographic satellite images
[AD-A212236] N90-12975
Meteorological Satellite Center Technical Note, no. 18, 1989
[MSC-TN-18] N90-12997
Cloud cover determination in polar regions from satellite imagery
[NASA-CR-186096] N90-13003

SATELLITE NETWORKS
Satellite range delay simulator for a matrix-switched time division multiple-access network simulator
[NASA-TM-102407] N90-12813

SATELLITE OBSERVATION
Tropospheric influences on satellite-Earth paths and their determination by means of radar measurements
[ESA-TT-1143] N90-12639
Design and tests of simple, inexpensive optical beacon for use on small satellites
[AD-A213325] N90-13238

SATELLITE ORBITS
Evaluation of 15th- and 30th-order geopotential harmonic coefficients from 26 resonant satellite orbits
[RAE-TR-88045] N90-12640
Orbit determination and analysis for Cosmos 236 at 15th-order resonance
[RAE-TR-88058] N90-12641
On mean elements for satellite orbits perturbed by the zonal harmonics of the geopotential
[AD-A212322] N90-12642
The GEM-T2 gravitational model
[NASA-TM-100746] N90-12984

SATELLITE TRACKING
The GEM-T2 gravitational model
[NASA-TM-100746] N90-12984
Optimum data weighting and error calibration for estimation of gravitational parameters
[NASA-TM-100737] N90-12985

SCALE MODELS
Demonstration epicyclic gearbox
[PNR90567] N90-12932

SCATTER PROPAGATION
Preliminary investigation of Faraday rotation effects and description of polarization measurements on the AFGL high latitude meteor scatter test bed
[AD-A211298] N90-12806

SCATTERING
Analysis of carbon fiber's x ray microscopic structure
[AD-A212215] N90-12752
Problems in nonlinear acoustics: Scattering of sound by sound, parametric receiving arrays, nonlinear effects in asymmetric sound beams and pulsed finite amplitude sound beams
[AD-A211756] N90-13200

SCATTERING CROSS SECTIONS
An explicit partition of the fusion-like cross section
[KVI-797] N90-13225

SCATTEROMETERS
Investigation of the properties of radar backscatter from sea ice
[AD-A212808] N90-12838
SCHEDULING
Algorithm development for SDI weapons system allocation
[AD-A212973] N90-13090
SCIENTIFIC SATELLITES
Report on ESA's scientific satellites
[ESA-SP-1110] N90-12649
SCINTILLATION COUNTERS
Radioactivity induced in gamma-ray spectrometers
[RAE-TM-SPACE-363] N90-13317
SCREWS
A feasibility study of hydrogen dosage estimation in screw threads submitted to surface electrolytic treatment
[CETIM-110110] N90-12730
SEA ICE
Investigation of the properties of radar backscatter from sea ice
[AD-A212808] N90-12838
The Regional Polar Ice Prediction System, Berents Sea (RPIPS-B): A technical description
[AD-A213159] N90-13012
SEA ROUGHNESS
A linearized surface condition in low speed hydrodynamics
[REPT-89-04] N90-12885
SEA SURFACE TEMPERATURE
Atlas of tropical sea surface temperature and surface winds
[PB89-223598] N90-13009
SEALING
A theoretical study of ingress for shrouded rotating disk systems with radial outflow
[PNR90586] N90-12607
Flanged joints of aeroengines
[PNR90594] N90-12609
Advanced actuation systems development, volume 1
[AD-A213334] N90-12624
SEALS (STOPPERS)
A theoretical study of ingress for shrouded rotating disk systems with radial outflow
[PNR90586] N90-12607
SEARCHING
Effects of type of responding on memory/visual search: Responding just yes or just no can lead to inflexible performance
[AD-A212764] N90-13033
SEAS
Investigation of the properties of radar backscatter from sea ice
[AD-A212808] N90-12838
SECONDARY RADAR
Aircraft Reply and Interference Environment Simulator (ARIES) hardware principles of operation. Volume 2: Appendixes
[DOT/FAA/CT-TN88/4-2] N90-12781
Aircraft Reply and Interference Environment Simulator (ARIES) hardware principles of operation, volume 1
[DOT/FAA/CT-TN88/4-1] N90-12782
SELECTIVE SURFACES
A well conditioned formulation for the analysis of multi-layered frequency selective surfaces using a cascaded matrix approach
[RSRE-MEMO-4289] N90-12858
SELF ALIGNMENT
Demonstration epicyclic gearbox
[PNR90567] N90-12932
SELF LUBRICATING MATERIALS
Tribological properties of PM212: A high-temperature, self-lubricating, powder metallurgy composite
[NASA-TM-102355] N90-12659
Characterization of self-lubricating surface materials
[CETIM-108060] N90-12749
SELF ORGANIZING SYSTEMS
Self-organizing semantic maps
[PB89-212609] N90-13049
SEMANTICS
Self-organizing semantic maps
[PB89-212609] N90-13049
A simple definition for parallel composition of prime event structures
[CWI-CS-R8903] N90-13074
Semantics and consistency of rule-based expert systems
[CWI-CS-R8824] N90-13153
SEMICONDUCTOR DEVICES
European Solid State Device Research Conference (18th) ESSDERC 88 held in Montpellier, France on 13-16 September 1988
[AD-A210618] N90-13250
SEMICONDUCTOR JUNCTIONS
Dielectric spectroscopy of semiconductors
[AD-A211989] N90-13255
GaAs gate dynamic memory technology
[AD-A212387] N90-13266
SEMICONDUCTOR LASERS
Design and performance of an on-satellite laser diagnostic system for a free space optical heterodyne frequency-shift-keyed communication system
[AD-A211986] N90-12915
Tunable Solid State Lasers conference edition: Tunable Solid State Lasers Topical Meeting
[AD-A212292] N90-12920
SEMICONDUCTORS (MATERIALS)
Mechanisms of CO2 reduction metal and metal modified semiconductor electrodes
[AD-A213169] N90-12712
Thin-film integrated injection logic
[AD-D014190] N90-12860
RF and dc desensitized electroexplosive device
[AD-D014206] N90-12862
High speed quantum-well optoelectronic devices by MBE
[AD-A212585] N90-13237
Structural and electrical properties of thin films and superlattices composed of II-VI semiconductors N90-13249
Semiconductor measurement technology: A software program for aiding the analysis of ellipsometric measurements, simple models
[PB89-235923] N90-13261
Interstitial formation, non-equilibrium and macroscopic processes in mercury cadmium telluride
[AD-A212412] N90-13267
SENSITIVITY
Sensitivity of a regional oxidant model to variations in climate parameters, volume 1 and 2
[PB89-224943] N90-12981
SENSORY PERCEPTION
Sound Localization by Human Observers symposium proceedings
[AD-A212877] N90-13026
A comparison of two subject-controlled attitude measures during somatogravic illusion exposure
[AD-A212528] N90-13031
Three stages and two systems of visual processing
[AD-A212670] N90-13032
Spatial tests for aviators
[IZF-1988-15] N90-13041
SEQUENCING
Numerical analysis of chaotic symbol sequences generated by parabolic and triangle maps of the interval
[MPIS-22/1987] N90-13124
Direct computation of 3D shape invariants and the focus of expansion
[AD-A212386] N90-13195
SEQUENTIAL ANALYSIS
Sequential quadratic programming algorithms for optimization
[AD-A212800] N90-13088
Domain of attraction of an operator between supremum and sum
[REPT-89-05] N90-13119
SEQUENTIAL CONTROL
An algebra for process creation
[CWI-CS-R8907] N90-13155
SERIES EXPANSION
Asymptotic expansions for two-stage rank tests
[MEMO-773] N90-13161
Interpretation and manipulation of Edgeworth expansions
[MEMO-775] N90-13163
SERVOMECHANISMS
Advanced actuation systems development, volume 1
[AD-A213334] N90-12624
SET THEORY
Extended basis set calculations of atomization energies: Comparison of isogyric and direct results
[AD-A212268] N90-12702
A point in betaZ/Z not contained in a maximal orbit closure
[REPT-89-26] N90-13127
SHADOWGRAPH PHOTOGRAPHY
Recent flow visualization studies in the 0.3-m TCT N90-12528
Spark camera annotation and control system for the BRL (Ballistic Research Laboratory) Transonic Range Facility
[AD-A212266] N90-12633
Improvement of ultrashort pulsed laser shadowgraph photography by means of optical filters
[ISL-CO-215/88] N90-12906
SHAFTS (MACHINE ELEMENTS)
The nature and control of skidding in lightly loaded intershaft bearings
[PNR90591] N90-12933
SHALLOW WATER
Semi-Lagrangian, semi-implicit solutions of the shallow water equations in one dimension
[AD-A212658] N90-12902
Instability mechanisms in a barotropic atmosphere
[KNMI-WR-89-01] N90-13001
SHAPES
Development of a VSAERO (Vortex Separation Aerodynamics) model of the F/A-18
[AD-A212442] N90-12566
Direct computation of 3D shape invariants and the focus of expansion
[AD-A212386] N90-13195
SHEAR
Stability conditions for steady shearing. Stability conditions for simple shear under mixed thermal boundary conditions N90-12873
SHEAR FLOW
Numerical experiments on transition control in wall-bounded shear flows N90-12536
Three-dimensional shear flows: Analysis of the track and angle of incidence
[CERT-RTS-OA-31/5025-AYD] N90-12888
SHEAR PROPERTIES
Shear fatigue testing and life prediction of fibre composites
[REPT-8519] N90-12668
SHEAR STRENGTH
Behavior of the adhesive A2 submitted to mechanical traction
[CETIM-105290] N90-12748
SHIP HULLS
Calculation of the odd and even integral components of the wave resistance Green's function
[AD-A212384] N90-12900
Numerical evaluation of the far field wave pattern of the radiation Green's function
[AD-A212839] N90-13176
SHIPS
Climatological data for the North Sea based on observations by voluntary observing ships over the period 1961-1980
[KNMI-WR-89-02] N90-13002
SHOCK ABSORBERS
Structural vibration and shock isolator
[AD-D014202] N90-12940
SHOCK LOADS
Pyrotechnic shock structural response N90-12774
SHOCK TUBES
Preliminary report on the feasibility of high power Electronic Warfare (EW) using explosive energy sources
[MRL-TR-89-3] N90-12775
Application of a copper vapour laser to investigation of shock and blade interaction in a shock tube
[PNR90578] N90-12918
SHOCK WAVE INTERACTION
Upwind discretization of the steady Navier-Stokes equations
[CWI-NM-R8810] N90-12891
SHOCK WAVE PROFILES
A device to extract energy from water waves
[REPT-89-34] N90-12978
SHOCK WAVES
Hypersonic boundary layers. Viscous effects within the shock layer
[CERT-RSF-OA-25/5005-AYD] N90-12502
Laser initiated ignition of liquid propellant
[AD-A212342] N90-12766
The Shock and Vibration Digest, volume 21, no. 10 N90-12771
Pyrotechnic shock structural response N90-12774
SHORT TAKEOFF AIRCRAFT
The NASA experience in aeronautical R and D: Three case studies with analysis
[AD-A211486] N90-12496
Powered-lift aircraft technology
[NASA-SP-501] N90-12589
Real-time simulation of an F110/STOVL turbofan engine
[NASA-TM-102409] N90-12618
SHOT PEENING
Improvement in pre-constraint fatigue resistance of modular ferretic and bainitic steel by shot peening treatments
[CETIM-106370] N90-12727
SIDELOBE REDUCTION
Statistical density and amplitude tapered arrays
[RSRE-MEMO-4211] N90-12818
SIDELOBES
Performance analysis of large adaptive sidelobe canceller arrays with reused elements
[AD-A212888] N90-12841
SIGNAL DETECTION
The NASA SETI sky survey: Recent developments N90-12804

SIGNAL DETECTORS
Fundamental studies of turbulent wall pressure fluctuations with applications to advanced acoustic sensor systems
[AD-A213041] N90-13212
SIGNAL ENCODING
Binary Gray codes and index systems
[REPT-89-29] N90-13060
SIGNAL FADING
Digital radio link: Wave propagation investigations on a 13 GHz line-of-sight path
[PB89-213128] N90-12785
Ground effects on multipath fading
[TELECOM-PARIS-88-E017] N90-12812
SIGNAL PROCESSING
Simulation of circuits adapted to signal processing
[TELECOM-PARIS-89-E001] N90-12811
Specification of Viper1 in Z
[RSRE-MEMO-4195] N90-12817
Specification of Viper2 in Z
[RSRE-MEMO-4217] N90-12819
Progress in the identification of airborne radar targets
[AD-A212749] N90-12835
Characterization of liquid crystal displays for optical signal processing applications
[AD-A212832] N90-12910
Time-frequency factors in auditory perception
[AD-A211491] N90-13016
SIGNAL REFLECTION
A method to model fuze performance. Part 2: Calculation of target reflections with physical optics
[FEL-1989-21-PT-2] N90-12822
SIGNAL TO NOISE RATIOS
Adaptive antenna arrays for satellite communication
[NASA-CR-185989] N90-12784
A performance comparison between block interleaved and helically interleaved concatenated coding systems N90-12792
Performance of the image statistics decoder in conjunction with the Goldstone-VLA array N90-12796
Performance of the split-symbol moments SNR estimator in the presence of inter-symbol interference N90-12799
SIGNAL TRANSMISSION
Automatic communications channel interference monitoring
[RSRE-MEMO-4243] N90-12820
SILICATES
Pyrolytic production of ceramic composites from silicates
[ETCA-89-R-012] N90-12746
SILICIDES
Study of palladium and chromium silicides formation in liquid phase and in solid phase
[LAAS-89040] N90-12695
SILICON
Transition metal catalyzed synthesis of organmetallic polymers
[AD-A212133] N90-12740
Semiconductor measurement technology: Database for and statistical analysis of the interlaboratory determination of the conversion coefficient for the measurement of the interstitial oxygen content of silicon by infrared absorption
[PB89-221170] N90-13253
The growth of epitaxial GaAs and GaAlAs on silicon substrates by OMVPE
[AD-A212873] N90-13269
SILICON DIOXIDE
NBS/BAM (National Bureau of Standards/Bundesanstalt fuer Materialprufung) 1986 Symposium on Advanced Ceramics
[PB89-229074] N90-12747
SILICON FILMS
Spectroscopic ellipsometry characterization of CVD deposition and doping of polysilicon multilayer structures
[RSRE-MEMO-4258] N90-12671
Tunneling microscopy of superconductors and tunneling barriers
[AD-A212120] N90-13257
SILICON ISOTOPES
Thermal stability of the carbon-carbon bond in ethylene adsorbed on Si(100): An isotopic mixing study
[AD-A211591] N90-12691
SILICON NITRIDES
Effects of hot corrosion on the room temperature strength of structural ceramics
[AD-A212568] N90-12762
SILICON OXIDES
Instability of the behavior of high resistivity silicon detectors due to the presence of oxide charges
[REPT-89-038] N90-13260
SILOXANES
Synthesis and high temperature chemistry of methylsilsesquioxane polymers produced by titanium catalyzed redistribution of methylhydridooligo- and polysiloxanes
[AD-A212000] N90-12736
High temperature insulators
[AD-D014193] N90-12751
SIMULATION
Evaluation of the near-wall k-epsilon turbulence model by comparison with direct simulations of turbulent channel flow
[AD-A212674] N90-12903
A simulation study of the overdetermined geodetic boundary value problem using collocation
[AD-A211785] N90-12990
Work-preserving emulations of fixed-connection networks
[AD-A211915] N90-13093
Note on the convergence of simulated annealing algorithms
[MEMO-774] N90-13162
SIMULATORS
Satellite range delay simulator for a matrix-switched time division multiple-access network simulator
[NASA-TM-102407] N90-12813
SIMULTANEOUS EQUATIONS
NUMVEC FORTRAN library manual chapter: Simultaneous linear equations
[CWI-NM-R8903] N90-13135
SINGLE CRYSTALS
The effects of trace anions on the voltammetry of single crystal gold surfaces
[AD-A211886] N90-13254
SISO (CONTROL SYSTEMS)
Batch LCAP2-linear control analysis, version 2.0: User's manual
[AD-A211670] N90-12643
SIZE DETERMINATION
Measurements of bubble properties using a multi-frequency sound field
[AD-A212591] N90-13211
SIZE DISTRIBUTION
Multiparameter radar estimation of raindrop size distribution
[AD-A212410] N90-13007
SKIDDING
The nature and control of skidding in lightly loaded intershaft bearings
[PNR90591] N90-12933
SKIN FRICTION
Lockheed laminar-flow control systems development and applications N90-12506
Recent tests at Langley with a University of Tennessee Space Institute (UTSI) skin friction balance N90-12527
SKY SURVEYS (ASTRONOMY)
The NASA SETI sky survey: Recent developments N90-12804
SLENDER BODIES
Aerodynamic test and analysis of a slender generic missile configuration
[AD-A212522] N90-12567
SLIDING FRICTION
Tribological properties of ceramic/Ti3Al-Nb sliding couples for use as candidate seal materials to 700 deg C
[NASA-TM-102401] N90-12658
Characterization of self-lubricating surface materials
[CETIM-108060] N90-12749
SLOT ANTENNAS
Application of the moment method to the design of slotted waveguide array antennas N90-12780
Wire grid modeling of the linear tapered slot antenna
[AD-A212977] N90-12842
SODIUM IODIDES
Particle transport simulation for spaceborne, NaI gamma-ray spectrometers
[AD-A205150] N90-13292
SODIUM SULFATES
Effects of hot corrosion on the room temperature strength of structural ceramics
[AD-A212568] N90-12762
SODIUM SULFUR BATTERIES
Heat pipes for sodium-sulfur batteries
[AD-A212523] N90-12865
SOFTWARE ENGINEERING
Case study on rapid software prototyping and automated software generation: An inertial navigation system
[AD-A212272] N90-12578
Telescience Testbed Pilot Program
[NASA-CR-184997] N90-13047
Building a software package for solving large sparse nonlinear systems of equations
[AD-A211758] N90-13055
LOTOS tools based on the Cornell synthesizer generator
[MEMO-INF-89-5] N90-13062
A mapping for converting Mascot designs to Ada programs
[RSRE-MEMO-4244] N90-13070
Software Engineering Exercise (SEE) guidelines
[AD-A212510] N90-13085
Toward a formal model of the design and evolution of software
[AD-A212533] N90-13087
SOFTWARE TOOLS
Software fault tolerance
[RSRE-MEMO-4237] N90-12575
Automatic communications channel interference monitoring
[RSRE-MEMO-4243] N90-12820
LOTOS tools based on the Cornell synthesizer generator
[MEMO-INF-89-5] N90-13062
Truth maintenance systems and their implementation in PROLOG
[MEMO-INF-89-13] N90-13064
User manual of the force structure model scenario editor SCENE
[FEL-1988-101] N90-13069
Expert system for test program set fault candidate selection
[AD-A213338] N90-13091
SOL-GEL PROCESSES
Oxide ceramic fibers by the sol-gel methods
[AD-A211315] N90-12742
SOLAR ACTIVITY
Solar-geophysical data number 537, May 1989. Part 2: Comprehensive Reports, data for Nov. 1988 and miscellaneous
[PB89-207401] N90-13300
SOLAR ATMOSPHERE
SOHO: An observatory to study the solar interior and the solar atmosphere N90-13303
EIT: Solar corona synoptic observations from SOHO with an Extreme-ultraviolet Imaging Telescope N90-13309
CELIAS: Charge, element and isotope analysis system for SOHO N90-13313
ERNE: Energetic and Relativistic Nuclei and Electron experiment N90-13315
SOLAR CORONA
EIT: Solar corona synoptic observations from SOHO with an Extreme-ultraviolet Imaging Telescope N90-13309
UVCS: An Ultraviolet Coronagraph Spectrometer for SOHO N90-13310
SOLAR CORPUSCULAR RADIATION
ERNE: Energetic and Relativistic Nuclei and Electron experiment N90-13315
SOLAR FLARES
Solar-geophysical data number 537, May 1989. Part 2: Comprehensive Reports, data for Nov. 1988 and miscellaneous
[PB89-207401] N90-13300
Berne solar observations
[REPT-55] N90-13301
The SOHO mission. Scientific and technical aspects of the instruments
[ESA-SP-1104] N90-13302
SOLAR HEATING
SUMER: Solar Ultraviolet Measurements of Emitted Radiation N90-13307
CDS: The Coronal Diagnostic Spectrometer N90-13308
SOLAR INTERIOR
SOHO: An observatory to study the solar interior and the solar atmosphere N90-13303
GOLF: Global Oscillations at Low Frequencies for the SOHO mission N90-13304
VIRGO: The solar monitor experiment on SOHO N90-13305
SOLAR MAGNETIC FIELD
The SOHO mission. Scientific and technical aspects of the instruments
[ESA-SP-1104] N90-13302
GOLF: Global Oscillations at Low Frequencies for the SOHO mission N90-13304
SOI: The Solar Oscillations Imager on SOHO N90-13306
SOLAR OBSERVATORIES
Berne solar observations
[REPT-55] N90-13301
The SOHO mission. Scientific and technical aspects of the instruments
[ESA-SP-1104] N90-13302
SOHO: An observatory to study the solar interior and the solar atmosphere N90-13303
LASCO: A wide-field white light and spectrometric coronagraph for SOHO N90-13311
SWAN: A study of solar wind anisotropies N90-13312

SOLAR OSCILLATIONS
GOLF: Global Oscillations at Low Frequencies for the SOHO mission N90-13304
VIRGO: The solar monitor experiment on SOHO N90-13305
SOI: The Solar Oscillations Imager on SOHO N90-13306

SOLAR PHYSICS
Solar-geophysical data number 537, May 1989. Part 2: Comprehensive Reports, data for Nov. 1988 and miscellaneous
[PB89-207401] N90-13300
SOHO: An observatory to study the solar interior and the solar atmosphere N90-13303

SOLAR PLANETARY INTERACTIONS
Solar-geophysical data number 537, May 1989. Part 2: Comprehensive Reports, data for Nov. 1988 and miscellaneous
[PB89-207401] N90-13300

SOLAR RADIATION
SUMER: Solar Ultraviolet Measurements of Emitted Radiation N90-13307

SOLAR RADIO BURSTS
Solar-geophysical data number 537, May 1989. Part 2: Comprehensive Reports, data for Nov. 1988 and miscellaneous
[PB89-207401] N90-13300

SOLAR RADIO EMISSION
Berne solar observations
[REPT-55] N90-13301

SOLAR SPECTROMETERS
The SOHO mission. Scientific and technical aspects of the instruments
[ESA-SP-1104] N90-13302
VIRGO: The solar monitor experiment on SOHO N90-13305
SUMER: Solar Ultraviolet Measurements of Emitted Radiation N90-13307
CDS: The Coronal Diagnostic Spectrometer N90-13308
UVCS: An Ultraviolet Coronagraph Spectrometer for SOHO N90-13310

SOLAR WIND
SUMER: Solar Ultraviolet Measurements of Emitted Radiation N90-13307
CDS: The Coronal Diagnostic Spectrometer N90-13308
LASCO: A wide-field white light and spectrometric coronagraph for SOHO N90-13311
CELIAS: Charge, element and isotope analysis system for SOHO N90-13313

SOLAR WIND VELOCITY
The SOHO mission. Scientific and technical aspects of the instruments
[ESA-SP-1104] N90-13302
SWAN: A study of solar wind anisotropies N90-13312

SOLAR X-RAYS
Solar-geophysical data number 537, May 1989. Part 2: Comprehensive Reports, data for Nov. 1988 and miscellaneous
[PB89-207401] N90-13300

SOLID ELECTROLYTES
Advanced double layer capacitor
[AD-A211977] N90-12688
The multivalent beta'-aluminas
[AD-A212103] N90-12738

SOLID LUBRICANTS
Structural studies of sputter-deposited MoS2 solid lubricant films
[AD-A212407] N90-12759
Cold press lubrication: Fine tuning of the CETIM Forgelub test
[CETIM-105160] N90-12938

SOLID MECHANICS
Proceedings of the Army Symposium on Solid Mechanics, 1989: Mechanics of Engineered Materials and Applications
[AD-A211954] N90-12951

SOLID PROPELLANT ROCKET ENGINES
RSRM-3 (360L003) ballistics/mass properties report
[NASA-CR-183716] N90-12651
Ballistics/mass properties
[NASA-CR-183723] N90-12652
A data acquisition and processing system for six component solid rocket motor testing
[AD-A212200] N90-12657

SOLID STATE DEVICES
Joint Services Electronics Program
[AD-A212309] N90-12864
Assessment of thin film batteries based on polymer electrolytes. Part 3: Specific energy versus specific power
[AD-A212141] N90-12976
European Solid State Device Research Conference (18th) ESSDERC 88 held in Montpellier, France on 13-16 September 1988
[AD-A210618] N90-13250

SOLID STATE LASERS
Tunable Solid State Lasers conference edition: Tunable Solid State Lasers Topical Meeting
[AD-A212292] N90-12920
Advanced source development and applications. Laser-produced plasmas: A compact soft x ray source with high peak brightness
[AD-A212677] N90-13245

SOLIDIFICATION
Superplastic forming and diffusion bonding of rapidly solidified, dispersion strengthened aluminum alloys for elevated temperature structural applications
[NASA-CR-181849] N90-12718

SOLSTICES
Relationship between the current and the width of the POGO electrojet during the solstices
[DE89-619725] N90-13294

SOLUBILITY
Measurement and correlation of the solubility and diffusion coefficient for oxygen and chlorine in basic hydrogen peroxide
[AD-A212348] N90-12703

SONDES
The development of a high response aerodynamic wedge probe and use on a high-speed research compressor
[PNR90598] N90-12613

SOUND FIELDS
Measurements of bubble properties using a multi-frequency sound field
[AD-A212591] N90-13211

SOUND LOCALIZATION
Sound Localization by Human Observers symposium proceedings
[AD-A212877] N90-13026

SOUND PROPAGATION
An investigation of the diffraction of an acoustic plane wave by a curved surface of finite impedance
[NASA-CR-186069] N90-13204

SOUND RANGING
Modified Newton-type methods for long-range target motion analysis
[FEL-1989-82] N90-13208

SOUND TRANSMISSION
Sound Localization by Human Observers symposium proceedings
[AD-A212877] N90-13026
UHB demonstrator interior noise control flight tests and analysis
[NASA-CR-181897] N90-13198

SOUND WAVES
Application of sound and temperature to control boundary-layer transition N90-12537
A frequency domain technique for improving sound field reproduction
[RAE-TM-MM-10] N90-13205
Perceived urgency of warning signals determined using a forced choice pair comparison technique
[RAE-TM-MM-12] N90-13206
Measurements of bubble properties using a multi-frequency sound field
[AD-A212591] N90-13211

SOUNDING ROCKETS
Current limiting mechanisms in electron and ion beams experiments
[AD-A212295] N90-12637

SOUTHERN HEMISPHERE
South Pole surface radiation balance measurements, April 1986 to February 1988
[PB89-224018] N90-12993

SPACE ADAPTATION SYNDROME
Biology in microgravity: A guide for experimenters
[ESA-TM-02] N90-12769
Cardiovascular, renal, electrolyte, and hormonal changes in man during gravitational stress, weightlessness, and simulated weightlessness: Lower body positive pressure applied by the antigravity suit
[NASA-TM-102232] N90-13013

SPACE CHARGE
Thermionic emission including both space charge and image forces
[AD-A212732] N90-12869
Electron transport in heterojunction superlattices
[AD-A212366] N90-13265

SPACE COMMUNICATION
The Telecommunications and Data Acquisition Report
[NASA-CR-185093] N90-12786

SPACE DEBRIS
Report on orbital debris
[NASA-TM-101855] N90-12635
Optical detection of space debris using a large achromatic coronagraph
[AD-A211362] N90-12647

SPACE EXPLORATION
A survey of permanently-manned lunar base concepts
[AD-A212575] N90-12638

SPACE FLIGHT
Report on orbital debris
[NASA-TM-101855] N90-12635

SPACE PLASMAS
COSTEP: A comprehensive suprathermal and energetic particle analyzer for SOHO N90-13314
Research in cosmic and gamma ray astrophysics
[NASA-CR-185451] N90-13316

SPACE PROGRAMS
Recommended changes in US military space policies and programs: A paper submitted to the Commission on Integrated Long-Term Strategy
[PB89-219364] N90-12636

SPACE SHUTTLE BOOSTERS
Flight motor set 360L001 (STS-26R). (Reconstructed dynamic loads analysis)
[NASA-CR-183811] N90-12656

SPACE STATIONS
Advanced spacecraft fire safety: Proposed projects and program plan
[NASA-CR-185147] N90-12645
Proposal for a zero-gravity toilet facility for the space station
[NASA-CR-183151] N90-13036
Telescience Testbed Pilot Program
[NASA-CR-184997] N90-13047
National Aeronautics and Space Administration N90-13282
Fiscal year 1990 authorization request and budget estimates for the National Aeronautics and Space Administration
[GPO-96-945] N90-13283
The 1990 National Aeronautics and Space Administration Authorization
[GPO-98-466] N90-13285
National Aeronautics and Space Administration N90-13287
National Aeronautics and Space Administration Authorization Act, fiscal year 1990
[S-REPT-101-157] N90-13288
National Aeronautics and Space Administration Authorization Act, fiscal year 1990
[S-REPT-101-157] N90-13289

SPACE TRANSPORTATION
A survey of permanently-manned lunar base concepts
[AD-A212575] N90-12638

SPACE TRANSPORTATION SYSTEM
National Aeronautics and Space Administration N90-13282
Fiscal year 1990 authorization request and budget estimates for the National Aeronautics and Space Administration
[GPO-96-945] N90-13283
The 1990 National Aeronautics and Space Administration Authorization
[GPO-98-466] N90-13285
National Aeronautics and Space Administration Authorization Act, fiscal year 1990
[S-REPT-101-157] N90-13288
National Aeronautics and Space Administration Authorization Act, fiscal year 1990
[S-REPT-101-157] N90-13289

SPACE-TIME FUNCTIONS
Index formulas for generalized Wiener-Hopf operators and Boson-Fermion correspondence in 2N dimensions
[CWI-PM-R8811] N90-13141
Strings, p-branes and Skyrmions in curved space N90-13293

SPACEBORNE EXPERIMENTS
Current limiting mechanisms in electron and ion beams experiments
[AD-A212295] N90-12637
Biology in microgravity: A guide for experimenters
[ESA-TM-02] N90-12769

SPACECRAFT ANTENNAS
Ka-band MMIC beam steered transmitter array N90-12803

SPACECRAFT CHARGING
Current limiting mechanisms in electron and ion beams experiments
[AD-A212295] N90-12637

SPACECRAFT COMPONENTS
European space technology: Celebrating twenty-five years of research and development
[ESA-BR-55] N90-13322

SPACECRAFT CONFIGURATIONS
NASA/USRA advanced space design program: The laser powered interorbital vehicle
[NASA-CR-186044] N90-12646

SPACECRAFT CONTAMINATION
Standard method for measurement of nonvolatile residue on surfaces
[AD-A213324] N90-12714
SPACECRAFT DESIGN
Report on orbital debris
[NASA-TM-101855] N90-12635
NASA/USRA advanced space design program: The laser powered interorbital vehicle
[NASA-CR-186044] N90-12646
Apollo lightcraft project
[NASA-CR-186055] N90-12655
SPACECRAFT EQUIPMENT
Radioactivity induced in gamma-ray spectrometers
[RAE-TM-SPACE-363] N90-13317
SPACECRAFT INSTRUMENTS
Radioactivity induced in gamma-ray spectrometers
[RAE-TM-SPACE-363] N90-13317
SPACECRAFT ORBITS
An analytic development of orbit determination for a distant, planetary orbiter N90-12787
Spacecraft Orbit Design and Analysis (SODA), version 1.0 user's guide
[NASA-CR-181932] N90-13050
SPACECRAFT POWER SUPPLIES
Analysis and simulation of dynamics of spacecraft power systems N90-12653
The fault monitoring and diagnosis knowledge-based system for space power systems: AMPERES, phase 1
[NASA-CR-185486] N90-12654
Airborne/spaceborne pulsed power source
[AD-A211762] N90-12850
SPACECRAFT PROPULSION
Apollo lightcraft project
[NASA-CR-186055] N90-12655
SPACECRAFT SHIELDING
Report on orbital debris
[NASA-TM-101855] N90-12635
SPACECRAFT STABILITY
Flight motor set 360L001 (STS-26R). (Reconstructed dynamic loads analysis)
[NASA-CR-183811] N90-12656
SPACECRAFT TRACKING
The Telecommunications and Data Acquisition Report
[NASA-CR-185093] N90-12786
SPACECRAFT TRAJECTORIES
On mean elements for satellite orbits perturbed by the zonal harmonics of the geopotential
[AD-A212322] N90-12642
Three-dimensional shear flows: Analysis of the track and angle of incidence
[CERT-RTS-OA-31/5025-AYD] N90-12888
SPACELAB
Pre- and postflight postural control of the D1 Spacelab mission astronauts examined with a tilting room
[IZF-1988-25] N90-13039
SPALLING
Spall resistance of alumina
[AD-A213213] N90-12735
SPATIAL DISTRIBUTION
Survey of the CLUSE main experiment Grand-CLUSE, May 1 - June 15, 1988 — Humidity Exchange Over the Sea (HEXOS) experiment
[FEL-1988-43] N90-12991
Spatial data structures for robotic vehicle route planning
[AD-A212806] N90-13111
A statistical analysis of spatial point patterns, a case study
[CWI-MS-R8813] N90-13180
Liquid and solid ion plasmas
[AD-A212415] N90-13244
SPECIES DIFFUSION
Unsteady diffusion from a hemispherical pit
[NPL-DMA(A)-190] N90-13220
SPECIFIC HEAT
Heat capacities of 1-methyl-3-ethylimidazolium chloride-aluminum chloride molten salts
[AD-A212790] N90-12707
SPECIFICATIONS
Requirements specification with Petri nets using the cube tool methodology
[AD-A212190] N90-12829
An implementation-oriented specification of the TUMULT communication primitives
[MEMO-INF-88-34] N90-13096
SPECIMEN GEOMETRY
Fatigue behavior of specimens under compression load spectra
[ETN-89-95207] N90-12954
SPECTROSCOPIC ANALYSIS
Hardening mechanisms and analysis of the structure of the TGDDM/DDS epoxy resin system (tetraglycidyl-4,4' diaminodiphenylmethane/4,4' diaminodiphenylsulfone)
[NOTE-TECHNIQUE-1988-8] N90-12662
Spectroscopic ellipsometry characterization of CVD deposition and doping of polysilicon multilayer structures
[RSRE-MEMO-4258] N90-12671
Improved method for determination of helium-4 in helium-3 by mass spectrometry
[PB89-201404] N90-12686
SPECTROSCOPY
Dielectric spectroscopy of semiconductors
[AD-A211989] N90-13255
SPECTRUM ANALYSIS
Infrared spectrometry of aerosols
[AD-A213303] N90-12713
The NASA SETI sky survey: Recent developments N90-12804
SPEECH RECOGNITION
The effects of hearing protectors on speech communication and the perception of warning signals
[AD-A212521] N90-12832
Shape instabilities of plate-like structures. 1: Experimental observations in heavily cold worked in situ composites
[AD-A212251] N90-13021
Application of active noise reduction for hearing protection and speech intelligibility improvement
[IZF-1988-21] N90-13042
Explicit modelling of state duration correlations in hidden Markov models — speech recognition
[RSRE-MEMO-4152] N90-13178
SPHERES
A kernel approach to estimation of the sphere radius density in Wicksell's corpuscle problem
[CWI-MS-R8809] N90-13142
SPIN-LATTICE RELAXATION
Spin-lattice relaxation and the calculation of gain, pump power, and noise temperature in ruby N90-12790
SPLINE FUNCTIONS
Multivariable divided difference and B-splines
[MEMO-772] N90-13160
On new methods for computing with multivariate B-splines
[MEMO-783] N90-13183
Smooth track generation for target motion analysis
[FEL-1989-83] N90-13233
SPRAYERS
Continuing studies of liquid propellant drops in hot, high-pressure environments
[AD-A212265] N90-12765
Two dimensional orifice array, monodisperse drop source, phase 1
[AD-A211319] N90-12881
Survey of the CLUSE main experiment Grand-CLUSE, May 1 - June 15, 1988 — Humidity Exchange Over the Sea (HEXOS) experiment
[FEL-1988-43] N90-12991
SPRING (SEASON)
Subjective uses of wind profiler data in warm season analysis and forecasting: Wind profiler training manual number 3
[PB89-223333] N90-13004
STABILITY
Stable summability and approximation theory
[AD-A211379] N90-13118
Increasing the real stability boundary of explicit methods
[CWI-NM-R8902] N90-13134
Instability of the behavior of high resistivity silicon detectors due to the presence of oxide charges
[REPT-89-038] N90-13260
STABILITY DERIVATIVES
A functional expansion and stability for nonlinear input-output maps
[RR-359] N90-13121
STABILIZERS (FLUID DYNAMICS)
Evaluation of a damaged F/A-18 horizontal stabilator
[AD-A212573] N90-12597
STACKING FAULT ENERGY
Determination of the gaseous hydrogen ductile-brittle transition in copper-nickel alloys
[NASA-TM-86494] N90-12715
STAINLESS STEELS
Rapid heating tensile tests of high-energy-rate-forged 316L stainless steel charged with hydrogen and tritium
[DE89-017869] N90-12717
STANDARDIZATION
Directory of International and Regional Organizations Conducting Standards-Related Activities, May 1989
[PB89-221147] N90-12776
Interpretation and manipulation of Edgeworth expansions
[MEMO-775] N90-13163
STANDARDS
Directory of International and Regional Organizations Conducting Standards-Related Activities, May 1989
[PB89-221147] N90-12776
A formatting style for typesetting and distributing draft international standards
[NPL-DITC-143/89] N90-13059
Publications of the National Institute of Standards and Technology, 1988 catalog
[PB89-218382] N90-13279
STATE ESTIMATION
An analytic development of orbit determination for a distant, planetary orbiter N90-12787
STATIC STABILITY
Aerodynamic test and analysis of a slender generic missile configuration
[AD-A212522] N90-12567
STATIC TESTS
Large-scale Advanced Prop-fan (LAP) static rotor test report
[NASA-CR-180848] N90-12617
STATISTICAL ANALYSIS
Performance of the split-symbol moments SNR estimator in the presence of inter-symbol interference N90-12799
Vibration transmission through rolling element bearings in geared rotor system, part 1
[NASA-CR-186093] N90-12936
A real-time wind model using digital data from aircraft
[RSRE-MEMO-4309] N90-13005
Catalog of absolutely calibrated, range normalized, wideband, electric field waveforms from located lightning flashes in Florida: July 24 and August 14, 1985 data
[AD-A212708] N90-13008
Atlas of tropical sea surface temperature and surface winds
[PB89-223598] N90-13009
Parallel and deterministic algorithms from MRF (Markov Random Fields): Surface reconstruction and integration
[AD-A212457] N90-13084
Berry-Esseen rates and bootstrap results for generalized L-statistics
[CWI-MS-R8808] N90-13179
A statistical analysis of spatial point patterns, a case study
[CWI-MS-R8813] N90-13180
Stochastic process models in device physics
[AD-A212284] N90-13185
The shape of the probability density function of short-term concentration fluctuations of plumes in the atmospheric boundary layer
[AD-A212632] N90-13188
Semiconductor measurement technology: Database for and statistical analysis of the interlaboratory determination of the conversion coefficient for the measurement of the interstitial oxygen content of silicon by infrared absorption
[PB89-221170] N90-13253
STATISTICAL CORRELATION
Index formulas for generalized Wiener-Hopf operators and Boson-Fermion correspondence in 2N dimensions
[CWI-PM-R8811] N90-13141
STATISTICAL DISTRIBUTIONS
A semiparametric model for citation counts
[CWI-MS-R8814] N90-13145
A statistical analysis of spatial point patterns, a case study
[CWI-MS-R8813] N90-13180
STATISTICAL MECHANICS
A graph-theoretical approach to block-copolymer complexes. Part 3: Loops and cycles
[MEMO-778-PT-3] N90-12750
STATISTICS
Interpretation and manipulation of Edgeworth expansions
[MEMO-775] N90-13163
STATOR BLADES
Application of a copper vapour laser to investigation of shock and blade interaction in a shock tube
[PNR90578] N90-12918
STEADY FLOW
Numerical algorithms for steady and unsteady incompressible Navier-Stokes equations
[NASA-CR-186039] N90-12499
Additions and corrections to SUPER: A program for calculating steady and oscillatory supersonic flow over a thin wing, tail plane and fin
[AD-A211771] N90-12501
Unsteady three-dimensional thin-layer Navier Stokes solutions on dynamic blocked grids
[AD-A212377] N90-12899
STEADY STATE
Elements of a relativistic microscopic theory of hadronic matter in equilibrium and non-equilibrium
[KVI-796] N90-13218
STEELS
Fatigue testing of welded steel assemblies with or without finishing treatments
[CETIM-107900] N90-12961

STEERABLE ANTENNAS
Automated Steerable Nulling Antenna Processor (SNAP) model
[PB89-231740] N90-12937
STEERING
Ka-band MMIC beam steered transmitter array
N90-12803
STELLAR COLOR
Mark-3 interferometer
[AD-A213155] N90-12911
STIFFNESS MATRIX
An algebraic characterization of B-convergent Runge-Kutta methods
[CWI-NM-R8901] N90-13133
STOCHASTIC PROCESSES
Statistical density and amplitude tapered arrays
[RSRE-MEMO-4211] N90-12818
Free-field response from inclined body waves in viscoelastic random medium
[REPT-88-99] N90-12876
A semiparametric model for citation counts
[CWI-MS-R8814] N90-13145
Stochastic process models in device physics
[AD-A212284] N90-13185
Monte Carlo (importance) sampling within a Benders' decomposition algorithm for stochastic linear programs
[AD-A212854] N90-13189
Fellowships in information and stochastic systems
[AD-A212385] N90-13280
STOICHIOMETRY
Method for growing patterned thin films of superconductors
[AD-D014195] N90-13262
STOPPING
On the smooth fit boundary conditions in the optimal stopping problem for semimartingales
[CWI-MS-R8819] N90-13147
STORAGE BATTERIES
Advanced calcium-thionyl chloride high-power battery
[AD-A211856] N90-12846
The use of lithium batteries in biomedical devices
[AD-A212187] N90-12863
Assessment of thin film batteries based on polymer electrolytes. Part 3: Specific energy versus specific power
[AD-A212141] N90-12976
STORAGE STABILITY
Advanced calcium-thionyl chloride high-power battery
[AD-A211856] N90-12846
STORMS
Catalog of absolutely calibrated, range normalized, wideband, electric field waveforms from located lightning flashes in Florida: July 24 and August 14, 1985 data
[AD-A212708] N90-13008
STRAIN GAGE BALANCES
Development of a multi-component internal strain-gauge balance for model tests in a cryogenic wind tunnel
[NLR-TR-88157-U] N90-12628
STRAIN GAGES
Development of a multi-component internal strain-gauge balance for model tests in a cryogenic wind tunnel
[NLR-TR-88157-U] N90-12628
Optical techniques for in-plane strain analysis in an industrial environment
[PNR90601] N90-12957
Plasma separation process: Magnet move to Oak Ridge National Laboratory
[DE89-017457] N90-13242
STRAIN MEASUREMENT
Optical techniques for in-plane strain analysis in an industrial environment
[PNR90601] N90-12957
STRAIN RATE
An approach to low temperature high strain rate superplasticity in aluminum alloy 2090
[AD-A212271] N90-12731
STRAPDOWN INERTIAL GUIDANCE
Hybrid angular velocity reference system for the investigation of dynamic properties of strapdown gryos
[DFVLR-FB-89-25] N90-12577
RTSIN1: A model of a strapdown INS on a two-axis rate table
[AD-A212406] N90-12579
STRESS (PHYSIOLOGY)
Prediction of thermal stress casualties
[AD-A212356] N90-13022
Effects of serial wet-dry-wet cold exposure: Thermal balance, physical activity, and cognitive performance
[AD-A212704] N90-13025
The effects of noise on performance
[AD-A212519] N90-13209
STRESS ANALYSIS
Rotor blade structural design N90-12584
Optical fibre witnesses of fatigue damage in composite materials N90-12660
Multilayer theory for delamination analysis of a composite curved bar subjected to end forces and end moments
[NASA-TM-4139] N90-12669
Stress waves through projectile joints and interfaces
[AD-A212201] N90-12963
The effect of a rigid elliptical inclusion on a straight crack
[AD-A212263] N90-12965
STRESS INTENSITY FACTORS
Fatigue behavior of specimens under compression load spectra
[ETN-89-95207] N90-12954
Unilateral contact analysis of a crack with friction. Applications
[ETN-89-95511] N90-12956
The effect of a rigid elliptical inclusion on a straight crack
[AD-A212263] N90-12965
STRESS WAVES
Stress waves through projectile joints and interfaces
[AD-A212201] N90-12963
STRESSES
Plasma separation process: Magnet move to Oak Ridge National Laboratory
[DE89-017457] N90-13242
STRIATION
Free surface scars and striations
[AD-A212429] N90-12901
STRING THEORY
More on the super WZW theory
[NIKHEF-H/88-11] N90-13273
Strings, p-branes and Skyrmions in curved space
N90-13293
Evolution of domain walls in the early universe
[NASA-CR-186076] N90-13297
Small scale structure on cosmic strings
[NASA-CR-186075] N90-13298
Cosmic strings and baryon decay catalysis
[NASA-CR-186074] N90-13299
STRUCTURAL ANALYSIS
Integrated multidisciplinary optimization of rotorcraft: A plan for development
[NASA-TM-101617] N90-12580
General approach and scope --- rotor blade design optimization N90-12581
Rotor blade aerodynamic design N90-12582
Rotor blade structural design N90-12584
Validation of the procedures --- integrated multidisciplinary optimization of rotorcraft N90-12587
Appendix: Results obtained to date --- integrated multidisciplinary optimization of rotorcraft N90-12588
Evaluation of a damaged F/A-18 horizontal stabilator
[AD-A212573] N90-12597
SSME structural dynamic model development
[NASA-CR-183671] N90-12650
Influence of the structure of epoxy network models on the volumetric, mechanical and viscoelastic properties
[ISAL-89-0024] N90-12666
Structural studies of sputter-deposited MoS2 solid lubricant films
[AD-A212407] N90-12759
Effects of hot corrosion on the room temperature strength of structural ceramics
[AD-A212566] N90-12762
A center for advanced electrical and structural polymers
[AD-A212853] N90-12764
Structural vibration and shock isolator
[AD-D014202] N90-12940
Proceedings of the Army Symposium on Solid Mechanics, 1989: Mechanics of Engineered Materials and Applications
[AD-A211954] N90-12951
Multilevel optimization with system Optsys
[FFA-TN-1988-60] N90-12953
A mechanical power flow capability for the finite element code NASTRAN
[AD-A212202] N90-12964
Analysis of the non-planar response of a cantilever, with the aid of computerized symbolic manipulation
[AD-A212421] N90-13172
Structural and electrical properties of thin films and superlattices composed of II-VI semiconductors
N90-13249
STRUCTURAL DESIGN
Integrated multidisciplinary optimization of rotorcraft: A plan for development
[NASA-TM-101617] N90-12580
General approach and scope --- rotor blade design optimization N90-12581
Rotor blade aerodynamic design N90-12582
Rotor blade dynamic design N90-12583
Rotor blade structural design N90-12584
Acoustic design considerations: Review of rotor acoustic sources N90-12585
Airframe design considerations: Overview --- rotor design optimization N90-12586
Appendix: Results obtained to date --- integrated multidisciplinary optimization of rotorcraft N90-12588
Scaling of an 85 GHz gyrotron to operate at 94 GHz
[AD-A212756] N90-12909
STRUCTURAL DESIGN CRITERIA
Development and applications of reliability and maintainability design criteria in military aircraft
[ETN-89-95208] N90-12591
Project, implementation, and utilization of composite structures
[ETN-89-95209] N90-12665
STRUCTURAL FAILURE
Estimating the time to fatigue failure of mooring cables
[PB89-220677] N90-12946
STRUCTURAL STABILITY
Development of a VSAERO (Vortex Separation Aerodynamics) model of the F/A-18
[AD-A212442] N90-12566
Flight motor set 360L001 (STS-26R). (Reconstructed dynamic loads analysis)
[NASA-CR-183811] N90-12656
Performance effects of tie-truss modifications for a 70-meter centerline beam waveguide antenna
N90-12791
STRUCTURAL STRAIN
Evaluation of a damaged F/A-18 horizontal stabilator
[AD-A212573] N90-12597
STRUCTURAL VIBRATION
Airframe design considerations: Overview --- rotor design optimization N90-12586
The Shock and Vibration Digest, volume 21, no. 10
N90-12771
Pyrotechnic shock structural response N90-12774
Vibration transmission through rolling element bearings in geared rotor system, part 1
[NASA-CR-186093] N90-12936
Plasma separation process: Magnet move to Oak Ridge National Laboratory
[DE89-017457] N90-13242
STRUTS
Plasma separation process: Magnet move to Oak Ridge National Laboratory
[DE89-017457] N90-13242
SUBGROUPS
A point in betaZ/Z not contained in a maximal orbit closure
[REPT-89-26] N90-13127
SUBROUTINES
Batch LCAP2-linear control analysis, version 2.0: User's manual
[AD-A211670] N90-12643
SUBSONIC AIRCRAFT
Lockheed laminar-flow control systems development and applications N90-12506
SUBSONIC FLOW
Flow quality measurements in compressible subsonic flows N90-12521
CFD methods for drag prediction and analysis currently in use in UK
[RAE-TM-AERO-2146] N90-12563
Upwind discretization of the steady Navier-Stokes equations
[CWI-NM-R8810] N90-12891
Multigrid solution method for the Euler equations
[PB89-219463] N90-13116
SUBSTITUTES
Re-engine with the Rolls-Royce Tay 670, the route to significant noise reduction
[PNR90585] N90-12606
SUBSTRATES
Structure and properties of polymer interphases
[AD-A212796] N90-12763
Method for growing patterned thin films of superconductors
[AD-D014195] N90-13262
The growth of epitaxial GaAs and GaAlAs on silicon substrates by OMVPE
[AD-A212873] N90-13269
SUCTION
Numerical experiments on transition control in wall-bounded shear flows N90-12536
SUDAN
Central Sudan surface wind data and climate characteristic
[KNMI-WR-88-01] N90-13000
SULFUR COMPOUNDS
Advanced calcium-thionyl chloride high-power battery
[AD-A211856] N90-12846
SUMMER
Subjective uses of wind profiler data in warm season analysis and forecasting: Wind profiler training manual number 3
[PB89-223333] N90-13004

SUMS
Tail triviality for sums of stationary random variables [CWI-MS-R8810] N90-13143
SUPERCOMPUTERS
Solving three dimensional block bidiagonal linear systems on vector computers [REPT-89-14] N90-13056
Solving 3D block bidiagonal linear systems on vector computers [CWI-NM-R8819] N90-13061
SUPERCONDUCTIVITY
Resistivity measurements of superconducting materials [PB89-225700] N90-12856
Synthesis and characterization of new low-dimensional metal complex conductors [AD-A213189] N90-12871
Fractional charging and reentrance in granular superconductors N90-13248
Composite vs constituent particle aspects of hole motion in the CuO2 plane [DE89-618864] N90-13251
Tunneling microscopy of superconductors and tunneling barriers [AD-A212120] N90-13257
Method for growing patterned thin films of superconductors [AD-D014195] N90-13262
Synthesis and study of materials for superconducting electronics [AD-A212966] N90-13270
SUPERCONDUCTORS
Fractional charging and reentrance in granular superconductors N90-13248
Tunneling microscopy of superconductors and tunneling barriers [AD-A212120] N90-13257
Method for growing patterned thin films of superconductors [AD-D014195] N90-13262
Synthesis and study of materials for superconducting electronics [AD-A212966] N90-13270
SUPERCOOLING
Estimation of time to maximum supercooling during dynamic frazil ice formation [AD-A212204] N90-12699
SUPERCRITICAL FLUIDS
Research and Development Opportunities in Supercritical Fluid Technology [DE89-015320] N90-12684
SUPERCRITICAL WINGS
Results of LFC experiment on slotted swept supercritical airfoil in Langley's 8-foot transonic pressure tunnel N90-12531
Boundary-layer stability analysis of Langley Research Center 8-foot LFC experimental data N90-12532
SUPERFLUIDITY
Symmetry breaking phenomena in liquid Helium-4 [DE89-618886] N90-12685
Persistent current, NMR, and ion transmission experiments in rotating He-3 superfluids --- Nuclear Magnetic Resonance (NMR) [ISBN-952-90056-1-X] N90-13221
Superfluid phase slippage in (3)He-B flow through a narrow channel [PB89-218986] N90-13258
SUPERHIGH FREQUENCIES
DSN 70-meter antenna microwave optics design and performance improvements. Part 2: Comparison with measurements N90-12800
SUPERLATTICES
Structural and electrical properties of thin films and superlattices composed of II-VI semiconductors N90-13249
Electron transport in heterojunction superlattices [AD-A212366] N90-13265
SUPERNOVA REMNANTS
Nonequilibrium ionization in supernova remnants: The case of Tycho [MPE-PREPRINT-153] N90-13295
SUPERPLASTICITY
Superplastic forming and diffusion bonding of rapidly solidified, dispersion strengthened aluminum alloys for elevated temperature structural applications [NASA-CR-181849] N90-12718
An approach to low temperature high strain rate superplasticity in aluminum alloy 2090 [AD-A212271] N90-12731
SUPERSONIC BOUNDARY LAYERS
Supersonic laminar-flow control N90-12554
Supersonic boundary-layer transition on the LaRC F-106 and the DFRF F-15 aircraft. Part 1: Transition measurements and stability analysis N90-12558
Supersonic boundary-layer transition on the LaRC F-106 and the DFRF F-15 aircraft. Part 2: Aerodynamic predictions N90-12559
Numerical study of three-dimensional spatial instability of a supersonic flat plate boundary layer [NASA-CR-181931] N90-12874
SUPERSONIC COMBUSTION
The next generation supersonic transport engine: Critical issues [PNR90576] N90-12605
SUPERSONIC COMMERCIAL AIR TRANSPORT
The next generation supersonic transport engine: Critical issues [PNR90576] N90-12605
SUPERSONIC DRAG
CFD methods for drag prediction and analysis currently in use in UK [RAE-TM-AERO-2146] N90-12563
SUPERSONIC FLOW
Additions and corrections to SUPER: A program for calculating steady and oscillatory supersonic flow over a thin wing, tail plane and fin [AD-A211771] N90-12501
The effects of wall surface defects on boundary-layer transition in quiet and noisy supersonic flow N90-12556
Basic research on methods of calculating supersonic and hypersonic flow [ONERA-RSF-19/1123-AY-234A] N90-12565
Upwind discretization of the steady Navier-Stokes equations [CWI-NM-R8810] N90-12891
Multigrid solution method for the Euler equations [PB89-219463] N90-13116
SUPERSONIC WIND TUNNELS
Design and fabrication requirements for low noise supersonic/hypersonic wind tunnels N90-12555
Volumetric analysis by spontaneous Raman diffusion in a supersonic wind tunnel [ISL-R-109/88] N90-12564
SUPERSYMMETRY
Strings, p-branes and Skyrmions in curved space N90-13293
SUPPORTS
Design and performance of an optical mount using cross-flexure pivots [DE89-017551] N90-12929
SURFACE COOLING
Studies of gas turbine heat transfer airfoil surfaces and end-wall cooling effects [AD-A212451] N90-12620
SURFACE CRACKS
Biaxial flexing of a fiber-reinforced aluminum composite [AD-A212742] N90-12681
SURFACE DEFECTS
The effects of wall surface defects on boundary-layer transition in quiet and noisy supersonic flow N90-12556
SURFACE DISTORTION
Optical techniques for in-plane strain analysis in an industrial environment [PNR90601] N90-12957
SURFACE FINISHING
Design and fabrication requirements for low noise supersonic/hypersonic wind tunnels N90-12555
Surface treatments of carbon fibers in an organic environment. Finite element analysis of pull-out tests [ONERA-RT-7/3549-M] N90-12698
The quality of vacuum deposited surface treatments [CETIM-107040] N90-12729
A feasibility study of hydrogen dosage estimation in screw threads submitted to surface electrolytic treatment [CETIM-110110] N90-12730
SURFACE LAYERS
Thin-film integrated injection logic [AD-D014190] N90-12860
SURFACE NAVIGATION
Problem-dependent transformations of 3D terrain elevation maps into cost precursor maps [PB89-218127] N90-12969
Spatial data structures for robotic vehicle route planning [AD-A212806] N90-13111
SURFACE PROPERTIES
Characterization of self-lubricating surface materials [CETIM-108060] N90-12749
Seminars of Applied Physics, Materials Physics and Biomedical Engineering, 1989 [PB89-218572] N90-13192
Workshop on Recent Progress in Surface and Volume Scattering [AD-A212455] N90-13236
SURFACE ROUGHNESS
Effect of roughness on the stability of boundary layers N90-12518
Recent tests at Langley with a University of Tennessee Space Institute (UTSI) skin friction balance N90-12527
Effect of pipe roughness on orifice flow measurement [PB89-231484] N90-12880
SURFACE ROUGHNESS EFFECTS
The effects of wall surface defects on boundary-layer transition in quiet and noisy supersonic flow N90-12556
SURFACE TO SURFACE MISSILES
Present and future US and Soviet chemical missiles and chemical rocket projectiles [AD-A212199] N90-12644
SURFACE VEHICLES
Problem-dependent transformations of 3D terrain elevation maps into cost precursor maps [PB89-218127] N90-12969
Computer oriented methods of multibody dynamics for application in vehicle technology [DFVLR-FB-89-17] N90-13080
SURFACE WAVES
A linearized surface condition in low speed hydrodynamics [REPT-89-04] N90-12885
Surface current and wave modulation measurements over bottom topography: A comparison with theory [AD-A212469] N90-13011
A numerical study of rain-induced surface gravity wave attenuation [AD-A212762] N90-13197
SURFACES
Free surface scars and striations [AD-A212429] N90-12901
SURFACTANTS
Chemical and photochemical reactivity in microemulsions and waterless microemulsions [AD-A211776] N90-12692
SURVEILLANCE
Mode S data link trials, 10-11 January 1989 [RSRE-MEMO-4267] N90-12815
SURVEILLANCE RADAR
Aircraft Reply and Interference Environment Simulator (ARIES) hardware principles of operation. Volume 2: Appendixes [DOT/FAA/CT-TN88/4-2] N90-12781
Aircraft Reply and Interference Environment Simulator (ARIES) hardware principles of operation, volume 1 [DOT/FAA/CT-TN88/4-1] N90-12782
Fine resolution errors in secondary surveillance radar altitude reporting amongst aircraft transmitting the conspicuity codes 4321 and 4322 [RSRE-88004] N90-12816
SURVEYS
Characterization of self-lubricating surface materials [CETIM-108060] N90-12749
A survey of the current state-of-the-art in high-energy-product permanent magnets [AD-A211761] N90-13193
SWEEP EFFECT
Design of the low-speed NLF(1)-0414F and the high-speed HSNLF(1)-0213 airfoils with high-lift systems N90-12540
Experimental and theoretical investigation of boundary-layer instability mechanisms on a swept leading edge at Mach 3.5 N90-12557
SWEPT WINGS
Boundary-layer stability analysis of Langley Research Center 8-foot LFC experimental data N90-12532
Theoretical methods and design studies for NLF and HLFC swept wings at subsonic and supersonic speeds N90-12535
Experimental and theoretical investigation of boundary-layer instability mechanisms on a swept leading edge at Mach 3.5 N90-12557
Improvements in the formulations and numerical solution of the Euler problem for swept wings [RAE-TM-AERO-2139] N90-12562
SYMBOLS
Frame synchronization methods based on channel symbol measurements N90-12795
Performance of the split-symbol moments SNR estimator in the presence of inter-symbol interference N90-12799
Numerical analysis of chaotic symbol sequences generated by parabolic and triangle maps of the interval [MPIS-22/1987] N90-13124
SYNAPSES
Fear-potentiated startle as a model system for analyzing learning and memory [AD-A212131] N90-13029
SYNCHROTRONS
Bunch length in internal target mode [NIKHEF-AMPS/89/04] N90-12854
SYNOPTIC MEASUREMENT
EIT: Solar corona synoptic observations from SOHO with an Extreme-ultraviolet Imaging Telescope N90-13309
SYNOPTIC METEOROLOGY
Cloud cover determination in polar regions from satellite imagery [NASA-CR-186096] N90-13003

SYNTAX
A table-driven approach to fast context-free parsing
[AD-A212210] N90-13082
SYNTHESIS (CHEMISTRY)
Electrically conducting organic materials: Design, synthesis and characterization
[AD-A212214] N90-12700
The multivalent beta'-aluminas
[AD-A212103] N90-12738
Transition metal catalyzed synthesis of organmetallic polymers
[AD-A212133] N90-12740
Synthesis and crystallization behavior of fluoride glasses
[AD-A212142] N90-12741
The chemistry of hexaazatriphenylene hexanitrile, a polyfunctional heterocycle with potential utility in the formulation of thermostable polymers
[AD-A212353] N90-12757
Synthesis and characterization of new low-dimensional metal complex conductors
[AD-A213189] N90-12871
Synthesis and properties of NdNiO(3) prepared by low temperature methods
[AD-A212117] N90-13256
Synthesis and study of materials for superconducting electronics
[AD-A212966] N90-13270
SYNTHETIC APERTURE RADAR
Aircraft SAR simulation Sargen 1.0
[FEL-1989-44] N90-12823
Conception and results of the DLR realtime azimuth processor for the E-SAR system
[DLR-FB-89-30] N90-12827
SYSTEM EFFECTIVENESS
Characterization and cycle tests of lightweight nickel electrodes
[NASA-TM-102399] N90-12696
SYSTEMS ANALYSIS
Non linear vibrations in a drive train when coupled to constant torque and constant power loads
[PNR90593] N90-12934
The integration of structured and formal methods
[RSRE-MEMO-4293] N90-13068
Variational and asymptotic methods in open and closed waveguide analysis
[REPT-34] N90-13229
Semiconductor measurement technology: A software program for aiding the analysis of ellipsometric measurements, simple models
[PB89-235923] N90-13261
SYSTEMS ENGINEERING
Advanced actuation systems development, volume 1
[AD-A213334] N90-12624
Development of a low noise 10 K J-T refrigeration system
[AD-A213347] N90-12779
Performance evaluations of a parallel and expandable database computer: The multi-backend database computer
[AD-A212761] N90-13046
A transformational method for verifying safety properties in real time systems
[AD-A211925] N90-13051
Building a software package for solving large sparse nonlinear systems of equations
[AD-A211758] N90-13055
Toward a formal model of the design and evolution of software
[AD-A212533] N90-13087
International Conference on Operator Theory: Advances and applications
[AD-A212341] N90-13170
SYSTEMS STABILITY
Nonlinear systems and Kolmogorov's representation theorem
[RR-363] N90-12931

T

TABLES (DATA)
Tables for the thermophysical properties of methane
[PB89-222608] N90-12690
Berne solar observations
[REPT-55] N90-13301
TAIL ASSEMBLIES
Additions and corrections to SUPER: A program for calculating steady and oscillatory supersonic flow over a thin wing, tail plane and fin
[AD-A211771] N90-12501
TAPERING
Properties of density tapered arrays
[RSRE-MEMO-4210] N90-12810
Statistical density and amplitude tapered arrays
[RSRE-MEMO-4211] N90-12818
Wire grid modeling of the linear tapered slot antenna
[AD-A212977] N90-12842
TARGET ACQUISITION
Guidance and Control Panel Symposium on Guidance and Control of Unmanned Air Vehicles
[AGARD-AR-260] N90-12623
Dedicated tracking of crossing targets with a phased array monopulse radar
[FEL-1988-95] N90-12821
A method to model fuze performance. Part 2: Calculation of target reflections with physical optics
[FEL-1989-21-PT-2] N90-12822
Modified Newton-type methods for long-range target motion analysis
[FEL-1989-82] N90-13208
A validation of the proposed NATO standard method to determine target acquisition distances with image intensifiers
[IZF-1988-8] N90-13230
Smooth track generation for target motion analysis
[FEL-1989-83] N90-13233
TARGET RECOGNITION
Progress in the identification of airborne radar targets
[AD-A212749] N90-12835
Research in computer vision for autonomous systems
[AD-A212420] N90-13235
TARGET SIMULATORS
Smooth track generation for target motion analysis
[FEL-1989-83] N90-13233
TECHNOLOGICAL FORECASTING
A vision of the future: The new engine technology
[PNR90566] N90-12603
The next generation supersonic transport engine: Critical issues
[PNR90576] N90-12605
Material requirements for future aeroengines
[PNR90595] N90-12610
Composite materials for future aeroengines
[PNR90584] N90-12667
The future of non ferrous metals in aerospace engines
[PNR90572] N90-12720
TECHNOLOGIES
Publications of the National Institute of Standards and Technology, 1988 catalog
[PB89-218382] N90-13279
Technology transfer to the United States: The MIT (Massachusetts Institute of Technology) Japan Science and Technology Program. A background paper of OTA's (Office of Technology Assessment's) assessment on technology, innovation, and US trade
[PB89-224711] N90-13291
TECHNOLOGY ASSESSMENT
Estimating the relationships between the state of the art of technology and production cost for the US aircraft
[AD-A212127] N90-12495
LFC: A maturing concept
[DOUGLAS-PAPER-7878] N90-12505
Ultrastructure processing and characterization of polymers
[AD-A211460] N90-12743
A survey of the current state-of-the-art in high-energy-product permanent magnets
[AD-A211761] N90-13193
Research on heating, instabilities, turbulence and RF emission from electric field dominated plasmas
[AD-A212122] N90-13243
TECHNOLOGY TRANSFER
Technology transfer to the United States: The MIT (Massachusetts Institute of Technology) Japan Science and Technology Program. A background paper of OTA's (Office of Technology Assessment's) assessment on technology, innovation, and US trade
[PB89-224711] N90-13291
TECHNOLOGY UTILIZATION
Research and Development Opportunities in Supercritical Fluid Technology
[DE89-015320] N90-12684
Proceedings of the 10 May 1989 Antiproton Technology Workshop: Addendum
[AD-A212804] N90-13227
NASA technology applications
[GPO-99-412] N90-13290
European space technology: Celebrating twenty-five years of research and development
[ESA-BR-55] N90-13322
TELECOMMUNICATION
Requirements specification with Petri nets using the cube tool methodology
[AD-A212190] N90-12829
Removal of noise from noise-degraded speech signals
[AD-A212876] N90-12840
TELEMETRY
Performance of the image statistics decoder in conjunction with the Goldstone-VLA array N90-12796
Radar and sensor array design planning for a naval missile testing center. Artificial intelligence applications
[ETCA-88-R-099] N90-13108
TELEOPERATORS
Telerobotic control for teams of semi-autonomous agents, phase 1
[AD-A211648] N90-13037
TELEPHONY
Removal of noise from noise-degraded speech signals
[AD-A212876] N90-12840
TEMPERATURE
Modeling the temperature rise at the tip of a fast crack
[AD-A212418] N90-12966
TEMPERATURE CONTROL
Phase change material for spacecraft thermal management
[AD-A211404] N90-12648
Heat pipes for sodium-sulfur batteries
[AD-A212523] N90-12865
TEMPERATURE DEPENDENCE
Temperature dependence of positron diffusion in cubic metals
[PB89-222020] N90-12722
TEMPERATURE DISTRIBUTION
Dimensional reduction at high temperature revisited
[KVI-791] N90-13194
TEMPERATURE EFFECTS
Application of sound and temperature to control boundary-layer transition N90-12537
Nonlinear theories concerning laminated composites under compression with delamination
[ONERA-RT-19/3542-RY-081-R] N90-12672
Thermophysical properties of benzene. Part 1: The ideal gas and the saturated liquid and vapour
[ESDU-89002-PT-1] N90-12693
Temperature effects in shock consolidation of metal powders
[DE89-016782] N90-12716
Behavior of the adhesive A2 submitted to mechanical traction
[CETIM-105290] N90-12748
Heat exhaustion
[AD-A212128] N90-13014
TEMPERATURE GRADIENTS
The 4th US Army Workshop on Low Heat Rejection Engines
[AD-A212379] N90-12943
TEMPERATURE PROFILES
Phase change material for spacecraft thermal management
[AD-A211404] N90-12648
Retrieval of atomic oxygen and temperature in the thermosphere. Part 1: Feasibility of an experiment based on the spectrally resolved 147 micrometer limb emission
[AD-A211987] N90-12986
TEMPORAL DISTRIBUTION
The M/G/1 processor sharing queue as the almost sure limit of feedback queues
[REPT-89-32] N90-13044
The discrete-time single-server queueing model
[MEMO-780] N90-13165
TENSILE DEFORMATION
Biaxial flexing of a fiber-reinforced aluminum composite
[AD-A212742] N90-12681
TENSILE PROPERTIES
Rapid heating tensile tests of high-energy-rate-forged 316L stainless steel charged with hydrogen and tritium
[DE89-017869] N90-12717
TERBIUM COMPOUNDS
An explicit partition of the fusion-like cross section
[KVI-797] N90-13225
TERMINAL FACILITIES
FAA air traffic activity: Fiscal year 1988
[AD-A211338] N90-12570
TERRAIN
Problem-dependent transformations of 3D terrain elevation maps into cost precursor maps
[PB89-218127] N90-12969
TERRAIN ANALYSIS
Visualization of high-resolution digital terrain
[AD-A212149] N90-12971
Spatial data structures for robotic vehicle route planning
[AD-A212806] N90-13111
TERRESTRIAL RADIATION
South Pole surface radiation balance measurements, April 1986 to February 1988
[PB89-224018] N90-12993
TEST FACILITIES
The fault monitoring and diagnosis knowledge-based system for space power systems: AMPERES, phase 1
[NASA-CR-185486] N90-12654

TEST PATTERN GENERATORS
Built-in generation for CMOS circuits
[IMAG-RR-736-I] N90-12855
TEXTILES
RTM user's guide
[NASA-CR-186091] N90-13065
TEXTURES
Development of texture analysis and its applications to titanium aero engine components
[PNR90561] N90-12602
Textural and structural organization of the heat treated polymers: Mechanical properties relationships
[ETN-89-95711] N90-12744
THEMATIC MAPPERS (LANDSAT)
An attempt to draw conclusions from the vegetation to the geological underground in the area of Amberg (Germany, F.R.) by means of digital image processing of TM data
[DFVLR-FB-89-24] N90-12974
THEMATIC MAPPING
An attempt to draw conclusions from the vegetation to the geological underground in the area of Amberg (Germany, F.R.) by means of digital image processing of TM data
[DFVLR-FB-89-24] N90-12974
THEOREM PROVING
A generalization of Moak's q-Laguerre polynomials
[REPT-89-21] N90-13126
Well posedness of triples of operators (in the sense of linear systems theory)
[TW-292] N90-13168
THEOREMS
Hahn-Banach type theorems for dual semigroups
[CWI-AM-R8903] N90-13149
Strong moderate deviation theorems for m-dependent random variables
[AD-A212618] N90-13173
Smoothed limit theorems for equilibrium processes
[AD-A212321] N90-13188
THEORIES
Trace theory — concurrent processing
[MEMO-INF-89-16] N90-13100
THERAPY
Radio frequency (13.56 MHz) energy enhances rewarming from mild hypothermia
[AD-A212703] N90-13024
THERMAL ANALYSIS
A theoretical method for the mechanical calculation of heat exchangers with sliding heads, phase 1 study
[CETIM-110240-PHASE-1] N90-12896
THERMAL EMISSION
Evaluation of a damaged F/A-18 horizontal stabilator
[AD-A212573] N90-12597
THERMAL ENERGY
Heat pipe and thermal energy storage and corrosion studies (1988)
[AD-A212655] N90-12706
THERMAL FATIGUE
The 4th US Army Workshop on Low Heat Rejection Engines
[AD-A212379] N90-12943
THERMAL PROTECTION
Effects of serial wet-dry-wet cold exposure: Thermal balance, physical activity, and cognitive performance
[AD-A212704] N90-13025
THERMAL STABILITY
Thermal stability of the carbon-carbon bond in ethylene adsorbed on Si(100): An isotopic mixing study
[AD-A211591] N90-12691
High temperature insulators
[AD-D014193] N90-12751
The chemistry of hexaazatriphenylene hexanitrile, a polyfunctional heterocycle with potential utility in the formulation of thermostable polymers
[AD-A212353] N90-12757
THERMAL STRESSES
The 4th US Army Workshop on Low Heat Rejection Engines
[AD-A212379] N90-12943
Prediction of thermal stress casualties
[AD-A212356] N90-13022
THERMIONIC CATHODES
Thermionic emission including both space charge and image forces
[AD-A212732] N90-12869
THERMIONIC DIODES
A 2-MeV microwave thermionic gun
[DE89-015640] N90-12844
THERMIONIC EMISSION
Thermionic emission including both space charge and image forces
[AD-A212732] N90-12869
THERMOCHEMISTRY
Laser probe vaporization/oxidation testing of high temperature composites
[AD-A211410] N90-12663
THERMODYNAMIC EFFICIENCY
Theoretical and experimental research on a millimeter-wavelength free-electron laser
[AD-A213321] N90-12925
THERMODYNAMIC EQUILIBRIUM
Vapor-liquid equilibrium of binary mixtures in the extended critical region. Part 1: Thermodynamic model
[PB89-218374] N90-12687
THERMODYNAMIC PROPERTIES
Heat pipe and thermal energy storage and corrosion studies (1988)
[AD-A212655] N90-12706
Effects of hot corrosion on the room temperature strength of structural ceramics
[AD-A212568] N90-12762
Thermal initiation of confined primary explosives with a proton beam
[AD-A212954] N90-12767
A survey of the current state-of-the-art in high-energy-product permanent magnets
[AD-A211761] N90-13193
Synthesis and properties of NdNiO(3) prepared by low temperature methods
[AD-A212117] N90-13256
THERMOELASTICITY
A thermoelastic transversely isotropic thick walled cylinder/disk application: An analytical solution and study
[NASA-TM-102320] N90-12950
THERMOGRAPHY
Readout and signal conditioning for a linear pyroelectric array
[RSRE-MEMO-4102] N90-12905
Enhancement of infrared thermographic imagery: Local smoothing and time-based interpolation
[ONERA-RT-8/7254-SN] N90-13232
THERMOPHYSICAL PROPERTIES
Tables for the thermophysical properties of methane
[PB89-222608] N90-12690
Thermophysical properties of benzene. Part 2: Thermodynamic properties at elevated pressures
[ESDU-89003-PT-2] N90-12694
Study of palladium and chromium silicides formation in liquid phase and in solid phase
[LAAS-89040] N90-12695
THERMOPLASTIC RESINS
Synthesis of energetic single phase and multi-phase polymers
[AD-A212539] N90-12761
THERMOPLASTICITY
Stability conditions for steady shearing. Stability conditions for simple shear under mixed thermal boundary conditions N90-12873
THERMOSETTING RESINS
RTM user's guide
[NASA-CR-186091] N90-13065
THERMOSPHERE
Retrieval of atomic oxygen and temperature in the thermosphere. Part 1: Feasibility of an experiment based on the spectrally resolved 147 micrometer limb emission
[AD-A211987] N90-12986
THICK WALLS
A thermoelastic transversely isotropic thick walled cylinder/disk application: An analytical solution and study
[NASA-TM-102320] N90-12950
THIN FILMS
Spectroscopic ellipsometry characterization of CVD deposition and doping of polysilicon multilayer structures
[RSRE-MEMO-4258] N90-12671
Thermal stability of the carbon-carbon bond in ethylene adsorbed on Si(100): An isotopic mixing study
[AD-A211591] N90-12691
Metallo-organic decomposition process for dielectric films
[AD-A211590] N90-12849
Thin-film integrated injection logic
[AD-D014190] N90-12860
Laser Induced Damage in Optical Materials: 1987
[PB89-221162] N90-12913
Assessment of thin film batteries based on polymer electrolytes. Part 3: Specific energy versus specific power
[AD-A212141] N90-12976
High speed quantum-well optoelectronic devices by MBE
[AD-A212585] N90-13237
Structural and electrical properties of thin films and superlattices composed of II-VI semiconductors N90-13249
Method for growing patterned thin films of superconductors
[AD-D014195] N90-13262
Synthesis and study of materials for superconducting electronics
[AD-A212966] N90-13270
Growth and characterization of zinc sulfide films by conversion of zinc oxide films with H2S
[AD-A213345] N90-13271
THIN PLATES
The relationship between the mechanical properties of materials after press forming and their in-service properties
[CETIM-101530] N90-12723
An investigation on combined extension and bending of thin sheets with a central crack
[LR-561] N90-12958
Increased fragility of deep pressed thin plates
[CETIM-13-Y-313] N90-12962
THIN WALLS
Corrections to the thin wall approximation in general relativity
[NASA-CR-186078] N90-13274
THIN WINGS
Additions and corrections to SUPER: A program for calculating steady and oscillatory supersonic flow over a thin wing, tail plane and fin
[AD-A211771] N90-12501
Chordwise loading and camber for two-dimensional thin sections
[AD-A213318] N90-12568
THREADS
A feasibility study of hydrogen dosage estimation in screw threads submitted to surface electrolytic treatment
[CETIM-110110] N90-12730
THREE DIMENSIONAL BOUNDARY LAYER
Numerical solutions of the compressible 3-D boundary-layer equations for aerospace configurations with emphasis on LFC N90-12534
THREE DIMENSIONAL FLOW
Numerical study of three-dimensional spatial instability of a supersonic flat plate boundary layer
[NASA-CR-181931] N90-12874
Three-dimensional shear flows: Analysis of the track and angle of incidence
[CERT-RTS-OA-31/5025-AYD] N90-12888
THREE DIMENSIONAL MODELS
A cell-centered multigrid method for three-dimensional anisotropic-diffusion and interface problems
[REPT-89-35] N90-13128
Placing mirrors in grids
[CWI-CS-R8906] N90-13154
THRESHOLD VOLTAGE
Strong-inversion model of threshold voltage in modulation doped field effect transistors: The role of unintentional acceptors
[AD-A212750] N90-12870
TIME
Time-frequency factors in auditory perception
[AD-A211491] N90-13016
Fatigue, pilot deviations and time of day
[NASA-CR-185369] N90-13035
The discrete-time single-server queueing model
[MEMO-780] N90-13165
TIME DEPENDENCE
Time-domain Green function corresponding to a time-harmonic point source in complex space
[PB89-218846] N90-13117
A moving-grid interface for systems of one-dimensional time-dependent partial differential equations
[CWI-NM-R8904] N90-13136
Unsteady diffusion from a hemispherical pit
[NPL-DMA(A)-190] N90-13220
TIME DIVISION MULTIPLE ACCESS
Satellite range delay simulator for a matrix-switched time division multiple-access network simulator
[NASA-TM-102407] N90-12813
TIME FUNCTIONS
Berry-Esseen rates and bootstrap results for generalized L-statistics
[CWI-MS-R8808] N90-13179
TIME MEASUREMENT
Stable Kalman filters for processing clock measurement data N90-12801
TIME OF FLIGHT SPECTROMETERS
CELIAS: Charge, element and isotope analysis system for SOHO N90-13313
TIME SERIES ANALYSIS
Tail triviality for sums of stationary random variables
[CWI-MS-R8810] N90-13143
TIME SHARING
The M/G/1 processor sharing queue as the almost sure limit of feedback queues
[REPT-89-32] N90-13044
TISSUES (BIOLOGY)
Biology in microgravity: A guide for experimenters
[ESA-TM-02] N90-12769
TITANIUM
Development of texture analysis and its applications to titanium aero engine components
[PNR90561] N90-12602

Synthesis and high temperature chemistry of methylsilsesquioxane polymers produced by titanium catalyzed redistribution of methylhydridooligo- and polysiloxanes
[AD-A212000] N90-12736

TITANIUM ALLOYS
Tribological properties of ceramic/Ti3Al-Nb sliding couples for use as candidate seal materials to 700 deg C
[NASA-TM-102401] N90-12658
Potential difference applied to the measurement of small fatigue crack growth at notches in Ti-6Al-4V
[FFA-TN-1989-09] N90-12952

TOILETS
Proposal for a zero-gravity toilet facility for the space station
[NASA-CR-183151] N90-13036

TOKAMAK DEVICES
Effect of the length of the multijunction grill on its lower hybrid current drive efficiency
[IPPCZ-283] N90-13240
On optimization of the multijunction grill for the lower hybrid current drive
[IPPCZ-280] N90-13241

TOLERANCES (MECHANICS)
Dynamic tip clearance measurements in axial flow compressors
[PNR90597] N90-12612

TOLERANCES (PHYSIOLOGY)
Effects of serial wet-dry-wet cold exposure: Thermal balance, physical activity, and cognitive performance
[AD-A212704] N90-13025
The effects of noise on performance
[AD-A212519] N90-13209

TOLLMIEN-SCHLICHTING WAVES
Long-range LFC transport N90-12508
Interaction of Tollmien-Schlichting waves and Goertler vortices N90-12515
Boundary-layer receptivity and laminar-flow airfoil design N90-12516
Effect of roughness on the stability of boundary layers N90-12518
Predicted and hot-film measured Tollmien-Schlichting wave characteristics N90-12523
Sensitivity of LFC techniques in the non-linear regime N90-12533
Design and test of an NLF wing glove for the variable-sweep transition flight experiment N90-12544

TOPOGRAPHY
Semi-Lagrangian, semi-implicit solutions of the shallow water equations in one dimension
[AD-A212658] N90-12902
Surface current and wave modulation measurements over bottom topography: A comparison with theory
[AD-A212469] N90-13011
Self-organizing semantic maps
[PB89-212609] N90-13049
An investigation of the diffraction of an acoustic plane wave by a curved surface of finite impedance
[NASA-CR-186069] N90-13204

TOPOLOGY
A theory of networks for approximation and learning
[AD-A212359] N90-13110
International Conference on Fixed Point Theory and Applications
[AD-A212369] N90-13171
Julia-Fatou-Sullivan theory for real one-dimensional dynamics
[REPT-88-100] N90-13190

TORQUE
Non linear vibrations in a drive train when coupled to constant torque and constant power loads
[PNR90593] N90-12934

TOXICITY
Effects of atmospheric mix and toxic fumes on military performance
[PB89-223630] N90-13015

TRACE CONTAMINANTS
Study of the electrical and optical properties of the vanadium and nickel impurities in GaAs
[ISAL-89-0028] N90-13259

TRACKED VEHICLES
Computer oriented methods of multibody dynamics for application in vehicle technology
[DFVLR-FB-89-17] N90-13080

TRACKING (POSITION)
Optimal observer motion for bearings-only localization and tracking N90-12569
Dedicated tracking of crossing targets with a phased array monopulse radar
[FEL-1988-95] N90-12821
Modified Newton-type methods for long-range target motion analysis
[FEL-1989-82] N90-13208

TRACKING PROBLEM
Optimal observer motion for bearings-only localization and tracking N90-12569

TRACKING RADAR
Radar and sensor array design planning for a naval missile testing center. Artificial intelligence applications
[ETCA-88-R-099] N90-13108

TRACTION
Stability conditions for steady shearing. Stability conditions for simple shear under mixed thermal boundary conditions N90-12873

TRAINING DEVICES
Subjective uses of wind profiler data in warm season analysis and forecasting: Wind profiler training manual number 3
[PB89-223333] N90-13004

TRAJECTORY MEASUREMENT
Radar and sensor array design planning for a naval missile testing center. Artificial intelligence applications
[ETCA-88-R-099] N90-13108
Smooth track generation for target motion analysis
[FEL-1989-83] N90-13233

TRAJECTORY OPTIMIZATION
Optimal observer motion for bearings-only localization and tracking N90-12569
An on-line distributed minimum-time trajectory generator for intelligent robot manipulators
[RR-358] N90-13102

TRANSFER FUNCTIONS
Batch LCAP2-linear control analysis, version 2.0: User's manual
[AD-A211670] N90-12643
Wideband phase-locked angular modulator N90-12798
Mathematical equivalence in a primitive Ella
[RSRE-MEMO-4225] N90-13066
Well posedness of triples of operators (in the sense of linear systems theory)
[TW-292] N90-13168

TRANSFERRING
Effects of type of responding on memory/visual search: Responding just yes or just no can lead to inflexible performance
[AD-A212764] N90-13033

TRANSFORMATIONS (MATHEMATICS)
A transformational method for verifying safety properties in real time systems
[AD-A211925] N90-13051
Transformations and representations of nonlinear systems
[MEMO-776] N90-13164

TRANSISTOR CIRCUITS
GaAs gate dynamic memory technology
[AD-A212387] N90-13266

TRANSISTOR LOGIC
Thin-film integrated injection logic
[AD-D014190] N90-12860

TRANSITION METALS
Transition metal catalyzed synthesis of organmetallic polymers
[AD-A212133] N90-12740

TRANSITION POINTS
Design and fabrication requirements for low noise supersonic/hypersonic wind tunnels N90-12555

TRANSLATING
Abstract grammars based on transductions
[MEMO-INF-89-7-REV] N90-13063

TRANSMISSION EFFICIENCY
Binary Gray codes and index systems
[REPT-89-29] N90-13060

TRANSMISSIONS (MACHINE ELEMENTS)
Demonstration epicyclic gearbox
[PNR90567] N90-12932
Non linear vibrations in a drive train when coupled to constant torque and constant power loads
[PNR90593] N90-12934

TRANSMITTANCE
Comments on the use of LOWTRAN in transmission calculations for sites with the ground elevated relative to sea level
[AD-A212724] N90-12995

TRANSMITTERS
Ka-band MMIC beam steered transmitter array N90-12803
Direction-of-arrival calculations at VLF/LF (Very Low Frequency/Low Frequency)
[AD-A212620] N90-12833

TRANSONIC FLOW
Theoretical methods and design studies for NLF and HLFC swept wings at subsonic and supersonic speeds N90-12535
Improvements in the formulations and numerical solution of the Euler problem for swept wings
[RAE-TM-AERO-2139] N90-12562
Spark camera annotation and control system for the BRL (Ballistic Research Laboratory) Transonic Range Facility
[AD-A212266] N90-12633
Solution of the thin-layer Navier-Stokes equations for laminar transonic flow
[PB89-221600] N90-12879
Multigrid solution method for the Euler equations
[PB89-219463] N90-13116

TRANSONIC WIND TUNNELS
Basic aerodynamic research facility for comparative studies of flow diagnostic techniques N90-12526
Residual interference assessment in adaptive wall wind tunnels
[NASA-CR-181896] N90-12625
The design and development of an acoustic test section for the ARA transonic wind tunnel
[PNR90574] N90-13202
Studies of the European transonic wind tunnel
[ONERA-RSF-12/0694-GY] N90-13278

TRANSPORT AIRCRAFT
Laminar flow: Challenge and potential N90-12504
Lockheed laminar-flow control systems development and applications N90-12506
Long-range LFC transport N90-12508

TRANSPORT PROPERTIES
Flux-corrected transport algorithms for two-dimensional compressible magnetohydrodynamics
[AD-A212757] N90-13246

TRAPPED PARTICLES
An apparatus for the electrodynamic containment of charged macroparticles N90-12789

TREES (MATHEMATICS)
Labeled trees and the efficient computation of derivations
[NASA-CR-185386] N90-13113
Anaphoric trees and an extension of the model of anaphora resolution
[REPT-89-37] N90-13130

TRIBOLOGY
Tribological properties of ceramic/Ti3Al-Nb sliding couples for use as candidate seal materials to 700 deg C
[NASA-TM-102401] N90-12658
Tribological properties of PM212: A high-temperature, self-lubricating, powder metallurgy composite
[NASA-TM-102355] N90-12659
A new test machine for measuring friction and wear in controlled atmospheres to 1200 C
[NASA-TM-102405] N90-12670
Structural studies of sputter-deposited MoS2 solid lubricant films
[AD-A212407] N90-12759

TRITIUM
Rapid heating tensile tests of high-energy-rate-forged 316L stainless steel charged with hydrogen and tritium
[DE89-017869] N90-12717

TROPICAL METEOROLOGY
Atlas of tropical sea surface temperature and surface winds
[PB89-223598] N90-13009

TROPOSPHERE
Physics of the tropospheric radiopropagation
[DE89-619726] N90-12783
Zonal average cloud characteristics for global atmospheric chemistry modeling
[CM-76] N90-12992

TROPOSPHERIC SCATTERING
Tropospheric influences on satellite-Earth paths and their determination by means of radar measurements
[ESA-TT-1143] N90-12639

TRUSSES
Performance effects of tie-truss modifications for a 70-meter centerline beam waveguide antenna N90-12791

TUBE HEAT EXCHANGERS
A theoretical method for the mechanical calculation of heat exchangers with sliding heads, phase 1 study
[CETIM-110240-PHASE-1] N90-12896

TUNABLE LASERS
Tunable Solid State Lasers conference edition: Tunable Solid State Lasers Topical Meeting
[AD-A212292] N90-12920

TUNING
Airborne/spaceborne pulsed power source
[AD-A211762] N90-12850

TURBINE BLADES
A computer integrated approach to dimensional inspection
[PNR90596] N90-12611

TURBINE ENGINES
A computer integrated approach to dimensional inspection
[PNR90596] N90-12611

TURBINE PUMPS
SSME structural dynamic model development
[NASA-CR-183671] N90-12650
Cryostatless high temperature supercurrent bearings for rocket engine turbopumps
[NASA-CR-183807] N90-12935
TURBOCOMPRESSORS
The development of a high response aerodynamic wedge probe and use on a high-speed research compressor
[PNR90598] N90-12613
Blading design for multi-storage HP compressor
[PNR90602] N90-12616
Preliminary experience with high response pressure measurements in a multistage, high speed compressor
[RAE-TM-P-1141] N90-12619
TURBOFAN ENGINES
Near-field noise predictions of an aircraft in cruise N90-12538
The 757 NLF glove flight test results N90-12546
What should be done with those noisy old aircraft
[PNR90562] N90-12593
Designing for reliable and low maintenance cost aero engines
[PNR90570] N90-12604
Blading design for multi-storage HP compressor
[PNR90602] N90-12616
Real-time simulation of an F110/STOVL turbofan engine
[NASA-TM-102409] N90-12618
The commercial aircraft noise problem
[PNR90577] N90-13203
TURBOMACHINE BLADES
Advanced clearance control systems --- blade tips
[PNR90553] N90-12601
TURBOPROP ENGINES
UHB demonstrator interior noise control flight tests and analysis
[NASA-CR-181897] N90-13198
TURBULENCE
Experimental study of homogeneous turbulence submitted to rotational effects
[ONERA-RSF-10/1145-AY-164A] N90-12894
TURBULENCE EFFECTS
Experimental study of homogeneous turbulence submitted to rotational effects
[ONERA-RSF-10/1145-AY-164A] N90-12894
TURBULENT BOUNDARY LAYER
Reduction of turbulent drag: Boundary layer manipulators
[CERT-RSF-OA-74/2259-AYD] N90-12889
TURBULENT FLOW
Investigation of turbulent flow in highly curved ducts with application to turbomachinery components
[NASA-CR-186060] N90-12882
Transition in surface boundary layers
[CERT-RSF-OA-43/5018-AYD] N90-12897
Semi-Lagrangian, semi-implicit solutions of the shallow water equations in one dimension
[AD-A212658] N90-12902
Evaluation of the near-wall k-epsilon turbulence model by comparison with direct simulations of turbulent channel flow
[AD-A212674] N90-12903
A numerical study of rain-induced surface gravity wave attenuation
[AD-A212762] N90-13197
Fundamental studies of turbulent wall pressure fluctuations with applications to advanced acoustic sensor systems
[AD-A213041] N90-13212
TURBULENT MIXING
Characterization of nonpremixed turbulent bluff-body burner flames
[PB89-229447] N90-12689
TWO DIMENSIONAL FLOW
Nonparallel stability of boundary layers N90-12514
Design of the low-speed NLF(1)-0414F and the high-speed HSNLF(1)-0213 airfoils with high-lift systems N90-12540
Wind tunnel results of the low-speed NLF(1)-0414F airfoil N90-12541
Wind tunnel results of the high-speed NLF(1)-0213 airfoil N90-12542
TWO DIMENSIONAL MODELS
FLIC (FLame with Implicit Convection): A detailed, two-dimensional flame model
[AD-A212953] N90-12710
Improved 2D numerical simulation model for strongly coupled heat and fluid flow in a thermal storage
[PB89-218879] N90-12878
Local mode smoothing analysis of various incomplete factorization iterative methods in two dimensions
[REPT-89-36] N90-13129
Placing mirrors in grids
[CWI-CS-R8906] N90-13154
TWO PHASE FLOW
Two-phase flow pressure losses in pipeline fittings
[ESDU-89012] N90-12883

U

ULTRAHIGH FREQUENCIES
DSN 70-meter antenna microwave optics design and performance improvements. Part 2: Comparison with measurements N90-12800
ULTRAHIGH VACUUM
Thermal stability of the carbon-carbon bond in ethylene adsorbed on Si(100): An isotopic mixing study
[AD-A211591] N90-12691
ULTRASHORT PULSED LASERS
Improvement of ultrashort pulsed laser shadowgraph photography by means of optical filters
[ISL-CO-215/88] N90-12906
Application of a copper vapour laser to investigation of shock and blade interaction in a shock tube
[PNR90578] N90-12918
ULTRAVIOLET ASTRONOMY
UVCS: An Ultraviolet Coronagraph Spectrometer for SOHO N90-13310
ULTRAVIOLET TELESCOPES
EIT: Solar corona synoptic observations from SOHO with an Extreme-ultraviolet Imaging Telescope N90-13309
UNIVERSE
Evolution of domain walls in the early universe
[NASA-CR-186076] N90-13297
UNIVERSITIES
Technology transfer to the United States: The MIT (Massachusetts Institute of Technology) Japan Science and Technology Program. A background paper of OTA's (Office of Technology Assessment's) assessment on technology, innovation, and US trade
[PB89-224711] N90-13291
UNSTEADY AERODYNAMICS
Prediction of unsteady blade surface pressures on an advanced propeller at an angle of attack
[NASA-TM-102374] N90-12560
UNSTEADY FLOW
Numerical algorithms for steady and unsteady incompressible Navier-Stokes equations
[NASA-CR-186039] N90-12499
Numerical simulation of unsteady rotational flow over propfan configurations
[NASA-CR-186037] N90-12500
Unsteady three-dimensional thin-layer Navier Stokes solutions on dynamic blocked grids
[AD-A212377] N90-12899
Free surface scars and striations
[AD-A212429] N90-12901
UNSTEADY STATE
Unsteady diffusion from a hemispherical pit
[NPL-DMA(A)-190] N90-13220
URBAN DEVELOPMENT
Departments of Veterans Affairs and Housing and Urban Development, and Independent Agencies Appropriations Bill, 1990
[H-REPT-101-150] N90-13281
Departments of Veterans Affairs and Housing and Urban Development, and Independent Agencies Appropriation Bill, 1990
[S-REPT-101-128] N90-13284
Department of Veterans Affairs and Housing and Urban Development, and Independent Agencies Appropriations Act, 1990
[HR-2916-PP] N90-13286
USER MANUALS (COMPUTER PROGRAMS)
RAN (Royal Australian Navy) vibration analysis system operator's guide
[AD-A212441] N90-12596
Batch LCAP2-linear control analysis, version 2.0: User's manual
[AD-A211670] N90-12643
Spacecraft Orbit Design and Analysis (SODA), version 1.0 user's guide
[NASA-CR-181932] N90-13050
RTM user's guide
[NASA-CR-186091] N90-13065
User manual of the force structure model scenario editor SCENE
[FEL-1988-101] N90-13069
NUMVEC FORTRAN library manual chapter: Simultaneous linear equations
[CWI-NM-R8903] N90-13135
USER REQUIREMENTS
The design, construction, performance and calibration of pulse generators to fulfil the requirements of specifications defence standard 59-41, FS(F) 510 and FS(S) 457
[RAE-TM-FS(F)-550] N90-12857
State of the art of human/machine dialog tool prototypes
[TELECOM-PARIS-89-H001] N90-13038
Telescience Testbed Pilot Program
[NASA-CR-184997] N90-13047

V

VACUUM DEPOSITION
The quality of vacuum deposited surface treatments
[CETIM-107040] N90-12729
VALUE ENGINEERING
Designing for reliable and low maintenance cost aero engines
[PNR90570] N90-12604
VALVES
Advanced actuation systems development, volume 1
[AD-A213334] N90-12624
VANADIUM ALLOYS
Potential difference applied to the measurement of small fatigue crack growth at notches in Ti-6Al-4V
[FFA-TN-1989-09] N90-12952
VAPOR DEPOSITION
Spectroscopic ellipsometry characterization of CVD deposition and doping of polysilicon multilayer structures
[RSRE-MEMO-4258] N90-12671
An investigation of diamond film deposition in a premixed oxyacetylene flame
[AD-A212595] N90-13268
The growth of epitaxial GaAs and GaAlAs on silicon substrates by OMVPE
[AD-A212873] N90-13269
VAPOR PRESSURE
Thermophysical properties of benzene. Part 1: The ideal gas and the saturated liquid and vapour
[ESDU-89002-PT-1] N90-12693
VARIABLE SWEEP WINGS
Design and test of an NLF wing glove for the variable-sweep transition flight experiment N90-12544
F-14 VSTFE and results of the cleanup flight test program N90-12547
Variable-Sweep Transition Flight Experiment (VSTFE): Stability code development and clean-up glove data analysis N90-12548
VARIANCE (STATISTICS)
Multiparameter radar estimation of raindrop size distribution
[AD-A212410] N90-13007
VARIATIONAL PRINCIPLES
On the extremum electric charge problem of steady electromagnetic equilibria
[TRITA-EPP-89-04] N90-12809
VARIATIONS
Sensitivity of a regional oxidant model to variations in climate parameters, volume 1 and 2
[PB89-224943] N90-12981
VECTORS (MATHEMATICS)
Solving three dimensional block bidiagonal linear systems on vector computers
[REPT-89-14] N90-13056
VEGETATIVE INDEX
Improvement and extension of a radar forest backscattering model
[NASA-CR-186083] N90-12973
VELOCITY DISTRIBUTION
Supersonic boundary-layer transition on the LaRC F-106 and the DFRF F-15 aircraft. Part 2: Aerodynamic predictions N90-12559
Zonal average cloud characteristics for global atmospheric chemistry modeling
[CM-76] N90-12992
VERTICAL ORIENTATION
The effects of hearing protectors on speech communication and the perception of warning signals
[AD-A212521] N90-12832
A comparison of two subject-controlled attitude measures during somatogravic illusion exposure
[AD-A212528] N90-13031
VERTICAL TAKEOFF AIRCRAFT
Powered-lift aircraft technology
[NASA-SP-501] N90-12589
VERY LARGE ARRAY (VLA)
Performance of the image statistics decoder in conjunction with the Goldstone-VLA array N90-12796
VERY LARGE SCALE INTEGRATION
Algorithmic fault tolerance
[RSRE-MEMO-4212] N90-13057
Trace theory --- concurrent processing
[MEMO-INF-89-16] N90-13100
Real-time robot motion: The VLSI implementation via transputers
[RR-364] N90-13104
The application of artificial intelligence techniques to tracing the interconnections in an integrated circuit
[TELECOM-PARIS-89-E002] N90-13105

Optical clock distribution to VLSI chips
[AD-A212269] N90-13264

VERY LONG BASE INTERFEROMETRY
The Telecommunications and Data Acquisition Report
[NASA-CR-185093] N90-12786
A statistical study of radio-source structure effects on astrometric very long baseline interferometry observations N90-12788

VERY LOW FREQUENCIES
Direction-of-arrival calculations at VLF/LF (Very Low Frequency/Low Frequency)
[AD-A212620] N90-12833
Long wave atmospheric noise model, phase 1. Volume 2: Mode parameters
[AD-A212795] N90-12837

VIBRATION
Rotational and vibrational nonequilibrium effects in rarefied, hypersonic flow
[NASA-CR-182559] N90-12498
RAN (Royal Australian Navy) vibration analysis system operator's guide
[AD-A212441] N90-12596
Vibration isolation technology: Sensitivity of selected classes of space experiments to residual accelerations
[NASA-CR-185443] N90-12768

VIBRATION DAMPING
The Shock and Vibration Digest, volume 21, no. 10 N90-12771
A survey on nonproportional damping N90-12773

VIBRATION EFFECTS
Non linear vibrations in a drive train when coupled to constant torque and constant power loads
[PNR90593] N90-12934

VIBRATION ISOLATORS
Structural vibration and shock isolator
[AD-D014202] N90-12940

VIBRATION MEASUREMENT
Vibration intensity. Evaluation of a remote measuring system
[CETIM-110430] N90-12907

VIBRATION METERS
Vibration intensity. Evaluation of a remote measuring system
[CETIM-110430] N90-12907

VIBRATIONAL SPECTRA
Structures and energies for small borane compounds: One and two boron compounds
[AD-A212264] N90-12701

VIDEO EQUIPMENT
Video line processor
[AD-D014198] N90-12861

VIDEO SIGNALS
Video line processor
[AD-D014198] N90-12861

VIRTUAL MEMORY SYSTEMS
An expert system for VM performance analysis
[REPT-89-30] N90-13045

VISCOELASTIC DAMPING
Free-field response from inclined body waves in viscoelastic random medium
[REPT-88-99] N90-12876

VISCOELASTICITY
Free-field response from inclined body waves in viscoelastic random medium
[REPT-88-99] N90-12876

VISCOPLASTICITY
Stability conditions for steady shearing. Stability conditions for simple shear under mixed thermal boundary conditions N90-12873

VISCOSITY
A numerical study of rain-induced surface gravity wave attenuation
[AD-A212762] N90-13197

VISCOUS DAMPING
A survey on nonproportional damping N90-12773

VISCOUS FLOW
Numerical algorithms for steady and unsteady incompressible Navier-Stokes equations
[NASA-CR-186039] N90-12499
Hypersonic boundary layers. Viscous effects within the shock layer
[CERT-RSF-OA-25/5005-AYD] N90-12502

VISIBILITY
Atmospheric horizontal-inhomogeneity effects on the optical depths determined by the double-elevation-angle lidar technique
[AD-A212836] N90-12839
Design and tests of simple, inexpensive optical beacon for use on small satellites
[AD-A213325] N90-13238

VISION
Fear-potentiated startle as a model system for analyzing learning and memory
[AD-A212131] N90-13029
Three stages and two systems of visual processing
[AD-A212670] N90-13032

VISUAL ACUITY
A Scheiner-principle pocket optometer for self-evaluation and biofeedback accommodation training
[AD-A213171] N90-13027

VISUAL AIDS
Research in computer vision for autonomous systems
[AD-A212420] N90-13235

VISUAL FIELDS
Spatial tests for aviators
[IZF-1988-15] N90-13041

VISUAL PERCEPTION
Electrophysiological studies of visual attention and resource allocation
[AD-A212287] N90-13030
Pre- and postflight postural control of the D1 Spacelab mission astronauts examined with a tilting room
[IZF-1988-25] N90-13039
Visual perception processing in a hierarchical control system: Level 1
[PB89-221188] N90-13101

VISUAL STIMULI
Electrophysiological studies of visual attention and resource allocation
[AD-A212287] N90-13030
Three stages and two systems of visual processing
[AD-A212670] N90-13032
Effects of type of responding on memory/visual search: Responding just yes or just no can lead to inflexible performance
[AD-A212764] N90-13033

VISUAL TASKS
Spatial tests for aviators
[IZF-1988-15] N90-13041

VOCODERS
Assessment of voice coders for ATC/pilot voice communications via satellite digital communication channels
[CAA-PAPER-89004] N90-12807

VOICE COMMUNICATION
The effects of hearing protectors on speech communication and the perception of warning signals
[AD-A212521] N90-12832
Removal of noise from noise-degraded speech signals
[AD-A212876] N90-12840
The effects of noise on speech and warning signals
[AD-A212520] N90-13210

VOICE DATA PROCESSING
Simulation of circuits adapted to signal processing
[TELECOM-PARIS-89-E001] N90-12811

VOLTAGE AMPLIFIERS
Null offset voltage compensator for operational amplifier
[AD-D014189] N90-12859

VOLTAGE CONVERTERS (AC TO AC)
NIST (National Institute of Standards and Technology) measurement services: The ac-dc difference calibrations
[PB89-222616] N90-12845

VOLTAGE CONVERTERS (DC TO DC)
NIST (National Institute of Standards and Technology) measurement services: The ac-dc difference calibrations
[PB89-222616] N90-12845

VOLUME
Workshop on Recent Progress in Surface and Volume Scattering
[AD-A212455] N90-13236

VOLUMETRIC ANALYSIS
Volumetric analysis by spontaneous Raman diffusion in a supersonic wind tunnel
[ISL-R-109/88] N90-12564

VORTEX GENERATORS
Improvements in the formulations and numerical solution of the Euler problem for swept wings
[RAE-TM-AERO-2139] N90-12562

VORTEX SHEETS
Free surface scars and striations
[AD-A212429] N90-12901

VORTICES
Interaction of Tollmien-Schlichting waves and Goertler vortices N90-12515
Goertler instability on an airfoil N90-12517
Experimental studies on Goertler vortices N90-12529
Development of a VSAERO (Vortex Separation Aerodynamics) model of the F/A-18
[AD-A212442] N90-12566
Vortex dynamics
[AD-A212119] N90-12877
Free surface scars and striations
[AD-A212429] N90-12901
Persistent current, NMR, and ion transmission experiments in rotating He-3 superfluids --- Nuclear Magnetic Resonance (NMR)
[ISBN-952-90056-1-X] N90-13221
Superfluid phase slippage in (3)He-B flow through a narrow channel
[PB89-218986] N90-13258

W

WAFERS
Feedback charge amplifier integrated on the detector wafer
[REPT-89-037] N90-12852

WALL FLOW
Three-component laser Doppler velocimeter measurements in a juncture flow N90-12525
Investigation of turbulent flow in highly curved ducts with application to turbomachinery components
[NASA-CR-186060] N90-12882

WALL PRESSURE
Fundamental studies of turbulent wall pressure fluctuations with applications to advanced acoustic sensor systems
[AD-A213041] N90-13212

WARNING SYSTEMS
Shape instabilities of plate-like structures. 1: Experimental observations in heavily cold worked in situ composites
[AD-A212251] N90-13021
Perceived urgency of warning signals determined using a forced choice pair comparison technique
[RAE-TM-MM-12] N90-13206

WASTE DISPOSAL
Proposal for a zero-gravity toilet facility for the space station
[NASA-CR-183151] N90-13036

WATER FLOW
Measurements of coefficients of discharge for concentric flange-tapped square-edged orifice meters in water over the Reynolds number range 600 to 2,700,000
[PB89-235147] N90-12892

WATER IMMERSION
Effects of serial wet-dry-wet cold exposure: Thermal balance, physical activity, and cognitive performance
[AD-A212704] N90-13025

WATER TABLES
Use of ground penetrating radar to define recharge areas in the Central Sand Plain
[PB89-224885] N90-12814

WATER VAPOR
Infrared water vapor continuum absorption: New atmospheric electrical measurements and theory
[AD-A212594] N90-12994

WATER WAVES
A device to extract energy from water waves
[REPT-89-34] N90-12978

WATERWAVE ENERGY CONVERSION
A device to extract energy from water waves
[REPT-89-34] N90-12978

WAVE AMPLIFICATION
Free-field response from inclined body waves in viscoelastic random medium
[REPT-88-99] N90-12876

WAVE ATTENUATION
A numerical study of rain-induced surface gravity wave attenuation
[AD-A212762] N90-13197

WAVE DIFFRACTION
An investigation of the diffraction of an acoustic plane wave by a curved surface of finite impedance
[NASA-CR-186069] N90-13204

WAVE EQUATIONS
Semi-Lagrangian, semi-implicit solutions of the shallow water equations in one dimension
[AD-A212658] N90-12902

WAVE FUNCTIONS
Calculation of the odd and even integral components of the wave resistance Green's function
[AD-A212384] N90-12900

WAVE INTERACTION
Stability theory applications to laminar-flow control N90-12513
Interaction of Tollmien-Schlichting waves and Goertler vortices N90-12515
Surface current and wave modulation measurements over bottom topography: A comparison with theory
[AD-A212469] N90-13011

WAVE PROPAGATION
Tropospheric influences on satellite-Earth paths and their determination by means of radar measurements
[ESA-TT-1143] N90-12639
Physics of the tropospheric radiopropagation
[DE89-619726] N90-12783
Digital radio link: Wave propagation investigations on a 13 GHz line-of-sight path
[PB89-213126] N90-12785
A literature study of wave propagation in the 1-60 GHz range. Application to transportable military communication systems
[FEL-1988-47] N90-12825

Long wave atmospheric noise model, phase 1. Volume 2: Mode parameters
[AD-A212795] N90-12837
Electron beam propagation through a magnetic wiggler with random field errors
[AD-A212705] N90-12867
Analytical control of special numerical calculations of pressure propagation in a fluid
[GRS-70] N90-12884
Fundamentals of middle atmospheric dynamics
[AD-A211747] N90-12988
An investigation of the diffraction of an acoustic plane wave by a curved surface of finite impedance
[NASA-CR-186069] N90-13204

WAVE RESISTANCE
Calculation of the odd and even integral components of the wave resistance Green's function
[AD-A212384] N90-12900

WAVE SCATTERING
A method to model fuze performance. Part 2: Calculation of target reflections with physical optics
[FEL-1989-21-PT-2] N90-12822

WAVEGUIDE ANTENNAS
Performance effects of tie-truss modifications for a 70-meter centerline beam waveguide antenna N90-12791
A closed-cycle refrigerator for cooling maser amplifiers below 4 Kelvin N90-12797

WAVEGUIDES
Application of the moment method to the design of slotted waveguide array antennas N90-12780
Analysis of three- and four-sided uniform waveguides with unusual cross-section/boundary conditions
[AD-A212653] N90-12834
Theoretical and experimental research on a millimeter-wavelength free-electron laser
[AD-A213321] N90-12925
Effect of the length of the multijunction grill on its lower hybrid current drive efficiency
[IPPCZ-283] N90-13240
On optimization of the multijunction grill for the lower hybrid current drive
[IPPCZ-280] N90-13241

WAVELENGTHS
Laser Induced Damage in Optical Materials: 1987
[PB89-221162] N90-12913

WEAPON SYSTEMS
Field-of-View variations and stripe-texturing effects on assault landing performance in the C-130 weapon system trainer
[AD-A212763] N90-12634
Algorithm development for SDI weapons system allocation
[AD-A212973] N90-13090
Research on heating, instabilities, turbulence and RF emission from electric field dominated plasmas
[AD-A212122] N90-13243

WEAPONS
Present and future US and Soviet chemical missiles and chemical rocket projectiles
[AD-A212199] N90-12644

WEAR RESISTANCE
Tribological properties of ceramic/Ti3Al-Nb sliding couples for use as candidate seal materials to 700 deg C
[NASA-TM-102401] N90-12658
The quality of vacuum deposited surface treatments
[CETIM-107040] N90-12729
Spall resistance of alumina
[AD-A213213] N90-12735

WEAR TESTS
Tribological properties of PM212: A high-temperature, self-lubricating, powder metallurgy composite
[NASA-TM-102355] N90-12659
A new test machine for measuring friction and wear in controlled atmospheres to 1200 C
[NASA-TM-102405] N90-12670
Characterization of self-lubricating surface materials
[CETIM-108060] N90-12749

WEATHER FORECASTING
Investigation of North Atlantic fog and development of a marine fog forecast system
[AD-A211780] N90-12999
Subjective uses of wind profiler data in warm season analysis and forecasting: Wind profiler training manual number 3
[PB89-223333] N90-13004

WEIGHT REDUCTION
Characterization and cycle tests of lightweight nickel electrodes
[NASA-TM-102399] N90-12696

WEIGHTING FUNCTIONS
Optimum data weighting and error calibration for estimation of gravitational parameters
[NASA-TM-100737] N90-12985

WEIGHTLESSNESS
Cardiovascular, renal, electrolyte, and hormonal changes in man during gravitational stress, weightlessness, and simulated weightlessness: Lower body positive pressure applied by the antigravity suit
[NASA-TM-102232] N90-13013

WEIGHTLESSNESS SIMULATION
Cardiovascular, renal, electrolyte, and hormonal changes in man during gravitational stress, weightlessness, and simulated weightlessness: Lower body positive pressure applied by the antigravity suit
[NASA-TM-102232] N90-13013

WELD STRENGTH
Influence of the composition of the metal deposited on carbon manganese welds on the work properties of the melted area depending on the operating mode of the weld
[CETIM-104530] N90-12726

WELD TESTS
Influence of the composition of the metal deposited on carbon manganese welds on the work properties of the melted area depending on the operating mode of the weld
[CETIM-104530] N90-12726
Fatigue testing of welded steel assemblies with or without finishing treatments
[CETIM-107900] N90-12961

WELDED JOINTS
Improvement of rules relating to clamp calculations
[CETIM-110610] N90-12939

WELDING
Influence of the composition of the metal deposited on carbon manganese welds on the work properties of the melted area depending on the operating mode of the weld
[CETIM-104530] N90-12726

WELDING MACHINES
Influence of the composition of the metal deposited on carbon manganese welds on the work properties of the melted area depending on the operating mode of the weld
[CETIM-104530] N90-12726

WELLS
Use of ground penetrating radar to define recharge areas in the Central Sand Plain
[PB89-224885] N90-12814

WENTZEL-KRAMER-BRILLOUIN METHOD
Nonparallel stability of boundary layers N90-12514

WHITE DWARF STARS
Nonequilibrium ionization in supernova remnants: The case of Tycho
[MPE-PREPRINT-153] N90-13295

WHITE NOISE
Performance of the split-symbol moments SNR estimator in the presence of inter-symbol interference N90-12799

WIGGLER MAGNETS
Electron beam propagation through a magnetic wiggler with random field errors
[AD-A212705] N90-12867

WIND (METEOROLOGY)
Project WIND: Experiments with the UK Meteorological Office mesoscale model
[AD-A212291] N90-13006

WIND DIRECTION
Analytical and experimental study of runway runoff with wind effects
[PTI-8948] N90-12627

WIND EFFECTS
Analytical and experimental study of runway runoff with wind effects
[PTI-8948] N90-12627

WIND PROFILES
Subjective uses of wind profiler data in warm season analysis and forecasting: Wind profiler training manual number 3
[PB89-223333] N90-13004
A real-time wind model using digital data from aircraft
[RSRE-MEMO-4309] N90-13005

WIND SHEAR
Mesoscale acid deposition modeling studies
[NASA-CR-4262] N90-13228

WIND TUNNEL APPARATUS
Hot-film system for transition detection in cryogenic wind tunnels N90-12522
Basic aerodynamic research facility for comparative studies of flow diagnostic techniques N90-12526
Recent tests at Langley with a University of Tennessee Space Institute (UTSI) skin friction balance N90-12527
Development of a multi-component internal strain-gauge balance for model tests in a cryogenic wind tunnel
[NLR-TR-88157-U] N90-12628
Hermes plasma wind tunnel. Preliminary study, phase A1: Annexes, tables, figures
[DVG-HER-TN-002-PT-2] N90-12632
The design and development of an acoustic test section for the ARA transonic wind tunnel
[PNR90574] N90-13202

WIND TUNNEL CALIBRATION
The design and development of an acoustic test section for the ARA transonic wind tunnel
[PNR90574] N90-13202

WIND TUNNEL NOZZLES
Design and fabrication requirements for low noise supersonic/hypersonic wind tunnels N90-12555

WIND TUNNEL TESTS
Research in Natural Laminar Flow and Laminar-Flow Control, part 2
[NASA-CP-2487-PT-2] N90-12519
Flow quality measurements in compressible subsonic flows N90-12521
Results of LFC experiment on slotted swept supercritical airfoil in Langley's 8-foot transonic pressure tunnel N90-12531
Boundary-layer stability analysis of Langley Research Center 8-foot LFC experimental data N90-12532
Wind tunnel results of the low-speed NLF(1)-0414F airfoil N90-12541
Wind tunnel results of the high-speed NLF(1)-0213 airfoil N90-12542
Design and test of a natural laminar flow/large Reynolds number airfoil with a high design cruise lift coefficient N90-12543
Residual interference assessment in adaptive wall wind tunnels
[NASA-CR-181896] N90-12625
Development of a multi-component internal strain-gauge balance for model tests in a cryogenic wind tunnel
[NLR-TR-88157-U] N90-12628
Flow in the neighborhood of an ellipsoid cylinder of revolution model
[ONERA-RT-22/7252-AN-000A] N90-12895

WIND TUNNEL WALLS
The effects of wall surface defects on boundary-layer transition in quiet and noisy supersonic flow N90-12556
Residual interference assessment in adaptive wall wind tunnels
[NASA-CR-181896] N90-12625

WIND TUNNELS
Wind effect on sound wave propagation at ground vicinity
[CSTB-2-87-008] N90-13201

WIND VELOCITY
Analytical and experimental study of runway runoff with wind effects
[PTI-8948] N90-12627
Central Sudan surface wind data and climate characteristic
[KNMI-WR-88-01] N90-13000
Wind effect on sound wave propagation at ground vicinity
[CSTB-2-87-008] N90-13201

WING CAMBER
Chordwise loading and camber for two-dimensional thin sections
[AD-A213318] N90-12568

WING LOADING
Advanced actuation systems development, volume 1
[AD-A213334] N90-12624

WING PROFILES
Unsteady three-dimensional thin-layer Navier Stokes solutions on dynamic blocked grids
[AD-A212377] N90-12899

WING SLOTS
An experimental evaluation of slots versus porous strips for laminar-flow applications N90-12530

WINGS
Laminar flow: The Cessna perspective N90-12507

WIRE
Wire grid modeling of the linear tapered slot antenna
[AD-A212977] N90-12842

WISCONSIN
Use of ground penetrating radar to define recharge areas in the Central Sand Plain
[PB89-224885] N90-12814

WORDS (LANGUAGE)
Self-organizing semantic maps
[PB89-212609] N90-13049

WORK HARDENING
Improvement in pre-constraint fatigue resistance of modular ferretic and bainitic steel by shot peening treatments
[CETIM-106370] N90-12727

WORKSTATIONS
Telescience Testbed Pilot Program
[NASA-CR-184997] N90-13047

X

X RAY ANALYSIS
A study of progressive cracking damage to carbon-epoxy composites and methods of crack reduction
[REPT-RE-49-324/F] N90-12676
X RAY ASTRONOMY
Nonequilibrium ionization in supernova remnants: The case of Tycho
[MPE-PREPRINT-153] N90-13295
X RAY DENSITY MEASUREMENT
Exploring asymmetric heavy-ion reactions at the KX-ray method: The Ne20 + Tb159 reaction at 15 MeV/unit
[KVI-777] N90-13216
X RAY DIFFRACTION
Analysis of carbon fiber's x ray microscopic structure
[AD-A212215] N90-12752
X RAY LASERS
Lectures on x ray lasers
[ETN-89-95516] N90-12917
X RAY SOURCES
Advanced source development and applications. Laser-produced plasmas: A compact soft x ray source with high peak brightness
[AD-A212677] N90-13245
X RAYS
Analysis of high temperature superconductors by means of PIXE and RBS methods
[DE89-630241] N90-13252
XENON FLUORIDE LASERS
Photodissociation of XeF2 (xenon difluoride) at 193 nm
[AD-A211663] N90-12916

Z

ZINC COATINGS
Polyelectrolyte-diffused zinc phosphate conversion coatings and polyacid coupling primers for corrosion protection of steel and aluminum, and alkali-catalyzed hydrolysis of polyimide-based materials
[AD-A212240] N90-12754
ZINC OXIDES
Growth and characterization of zinc sulfide films by conversion of zinc oxide films with H2S
[AD-A213345] N90-13271
ZINC SULFIDES
Growth and characterization of zinc sulfide films by conversion of zinc oxide films with H2S
[AD-A213345] N90-13271
ZIRCONIUM OXIDES
Effects of hot corrosion on the room temperature strength of structural ceramics
[AD-A212568] N90-12762
ZONAL FLOW (METEOROLOGY)
Zonal average cloud characteristics for global atmospheric chemistry modeling
[CM-76] N90-12992
ZONAL HARMONICS
On mean elements for satellite orbits perturbed by the zonal harmonics of the geopotential
[AD-A212322] N90-12642

Typical Personal Author Index Listing

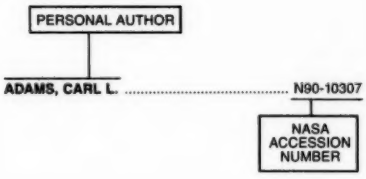

Listings in this index are arranged alphabetically by personal author. The NASA accession number denotes the number by which the citation is identified.

A

ABGRALL, R. N90-12565
ABUBAKR, E. H. N90-13000
ACKERMAN, PHILLIP L. N90-13033
ADAMS, GEORGE F. N90-12701
N90-12702
ADEBIYI, ADEBIMPE N90-12768
ADELMAN, HOWARD M. N90-12580
N90-12581
N90-12583
ADOLPH, H. G. N90-12761
AHLERS, S. T. N90-13025
AHMAD, MUBARAK N90-12685
AJAYI, G. O. N90-12783
AKHTAR, GHULAM N90-12856
AL-MAAITAH, AYMAN N90-12518
ALA, D. N90-12591
ALANEN, E. N90-12805
ALBERS, WILLEM N90-13161
ALBRECHT, ANDREAS N90-13298
ALCOCK, T. N90-12815
ALEJALDRE, C. N90-13239
ALEXANDER, J. IWAN D. N90-12768
ALEXEFF, IGOR N90-13243
ALLBRIGHT, CARL A. N90-12624
ALLEN, JEFFREY K. N90-13022
ALLEN, L. D. N90-13024
ALVERMANN, KLAUS N90-12599
AMERICA, PIERRE N90-13075
ANDERSEN, B. N. N90-13305
ANDERSON, JOHN A. N90-12624
ANDERSON, MARY P. N90-12814
ANDERSON, VERNON A. N90-12861
ANDRESS, KEITH N90-13235
ANGENENT, SIGURD N90-13177
ANTIOCHOS, S. K. N90-13311
ANTONUCCI, E. N90-13310
ARMSTRONG, LAWRENCE E. N90-13014
ARNAL, D. N90-12897
ARNAL, M. P. N90-12882
ARNOLD, S. M. N90-12950
ARTZNER, G. E. N90-13309
ASCHENBACH, B. N90-13308
ASHCRAFT, CLEVE N90-13054
ASHILL, P. R. N90-12563
ASQUITH, G. N90-12608
ASVELD, PETER R. J. N90-13063
ATONISON, MARK A. N90-12655
ATTIAS, ANDRE-JEAN N90-12662
AUPOIX, B. N90-12502
AURELA, A. N90-13315
AXELSON, KATHLEEN D. N90-12699
AXFORD, W. I. N90-13307
N90-13313
AYDIN, KULTEGIN N90-12830
AZZAZY, MEDHAT N90-12524

B

BABONNEAU, FLORENCE N90-12736
BACELAR, J. C. N90-13217
BADDILEY, C. J. N90-13231
BAETEN, JOS C. M. N90-13155
BAGHDADI, ASLAN N90-13253
BAGLIO, J. N90-13271
BAILEY, J. C. N90-13008
BAILLON, JEAN-BERNARD N90-13171
BAJAJ, R. N90-12719
BAKER, CHARLES R. N90-13280
BAKER, SUSAN P. N90-13035
BALJEU, J. F. N90-12628
BALL, G. J. N90-12810
N90-12818
BALSIGER, H. N90-13313
BANKS, P. N90-12816
BANKS, S. P. N90-12931
N90-13121
BARBERIS, D. N90-12895
BARBIER, B. N90-12698
BARENDREGT, L. G. N90-13180
BARENDSWAARD, W. N90-12825
BARI, MOHAMMAD A. N90-13255
BARNARD, P. M. N90-12668
BARRETT, DAVID S. N90-12941
BARRETT, JOHN W. N90-12911
BARRY, R. G. N90-13003
BARTLETT, DENNIS W. N90-12547
BARTOE, J.-D. F. N90-13311
BASCHIERA, D. N90-12855
BATHKER, D. A. N90-12600
BATIT, G. N90-12938
BAUMGARTEN, GEORGE P. N90-12892
BAYLISS, A. N90-12537
N90-12874
BEAM, RICHARD M. N90-13137
BEAUMONT, N. N90-12673
BECKER, J. Y. N90-12700
BECKWITH, IVAN E. N90-12555
N90-12557
BEEVERS, C. J. N90-12952
BEHBEHANI, R. A. N90-12546
BEL, G. N90-12961
BELL, BARBARA N90-13043
BELL, D. G. N90-13028
BELLER, R. C. N90-12777
BELLOS, J. N90-12773
BENDER, JAMES M. N90-12963
BENIGNUS, VERNON A. N90-13015
BENNETT, HAROLD E. N90-12913
BENNETT, WILLIAM N90-13090
BENOCCI, C. N90-12890
BENTLEY, CHARLES R. N90-12814
BERBEE, H. C. P. N90-13143
BERGERON, G. N90-12909
BERLIN, ANDREW A. N90-13175
BERNARD, A. N90-12728
BERNSTEIN, J. N90-12700
BERRY, M. J. N90-12663
BERRY, SCOTT N90-12532
BERTAUX, J. L. N90-13312
BERTHOMIEU, G. N90-13305
BERTUCCIO, G. N90-12852
BESANT, C. B. N90-12611
BESWICK, J. A. N90-13269
BETHKE, KARL-HEINZ N90-12808
BEYER, RICHARD A. N90-12765
BEZEM, MARC N90-13077
N90-13153
BIDARIAN, ALI N90-12703
BIELAK, G. W. N90-12546
BILLINGS, S. A. N90-12930
N90-13122
N90-13123
BIRINGEN, S. N90-12536
BITTNER, S. N90-12700
BJOSTAD, LOUIS B. N90-12983
BLACK, MICHAEL J. N90-13111
BLAKE, E. H. N90-13156
BLANCHARD, DENNIS M. N90-12910
BLANCHARD, K. V. N90-12933
BLANCHARD, MARY N90-13091
BLANCHOUD, F. N90-13301
BLANKENSHIP, GILMER L. N90-13090
BLASK, STEVE N90-13235
BLES, W. N90-13039
BLOM, A. F. N90-12952
BLOM, J. G. N90-13136
BLOSS, WALTER L. N90-12870
BLUM, FRANK D. N90-12753
BOBIN, L. N90-12564
BOCCHIA, R. N90-13304
BOCHSLER, P. N90-13313
BOER, L. C. N90-13041
BOERIO, F. JAMES N90-12763
BOGART, R. S. N90-13306
BOHLING, GEOFFREY C. N90-12814
BOLLINGER, J. J. N90-13244
BONCZYK, PAUL A. N90-12709
BOND, JAMES D. N90-13023
BONDONO, P. N90-13094
BONNET, R. M. N90-13304
BOOGAARD, J. N90-13230
BORLAND, M. N90-12844
BORSON, EUGENE N. N90-12714
BOTT, JERRY F. N90-12916
BOUHELIER, C. N90-12961
BOUIS, X. N90-13278
BOURNICON, C. N90-12729
BOUSQUET, M. D. N90-13228
BOUWER, GERHARD N90-12621
BOYD, IAIN D. N90-12498
BRADLEY, R. R. N90-13269
BRADY, RAYMOND H. N90-13004
BRAMSON, B. D. N90-13275
BRANDENBERGER, R. H. N90-13299
BREDEN, WILLIAM O. N90-12971
BREITENBERG, MAUREEN N90-12776
BRENNAN, J. A. N90-12880
BRETAUDEAU, F. N90-13232
BREUZET, MICHEL N90-13199
BREWSTER, KEITH A. N90-13004
BRIARTY, L. G. N90-12769
BRINDLEY, PAMELA K. N90-12658
BRINGI, V. N. N90-13007
BRINKMANN, W. N90-13295
BRISCOE, M. N90-13322
BRITCLIFFE, M. N90-12797
BRITTON, DORIS L. N90-12696
BROCK, M. P. N90-13198
BROERSMA, H. J. N90-13157
N90-13159
BROM, G. N90-12564
BROOKS, CUYLER W., JR. N90-12531
N90-12532
BROOKS, RICHARD N90-12932
BROOKS, RODNEY A. N90-12941
BROWN, JIM R. N90-12661
BROWN, T. M., JR. N90-13306
BROWNELL, J. B. N90-12918
N90-12957
BRUECKNER, G. E. N90-13311
BRUGGMANN, G. N90-13301
BRUN, T. N90-12710
BRYANT, T. D. N90-12537
BRYCE, J. D. N90-12619
BUDA, A. N90-13217
BUFFARDI, R. N90-12591
BUMGARDNER, JON H. N90-12861
BURGE, P. L. N90-13198
BURKE, LAWRENCE W., JR. N90-12633
BURNER, ALPHEUS W. N90-12528
BURNS, R. E. N90-12777
BURROWS, P. N90-12875
BURTON, SAMUEL R. M. N90-12686
BUSHNELL, DENNIS M. N90-12533
N90-12554
BUSHNELL, MARK N90-13010
BUTLER, R. J. N90-12668
BYER, ROBERT L. N90-13245
BYWORTH, S. P. Q. N90-12604

C

CAHAN, B. D. N90-13254
CALCATERRA, A. N90-12875
CALL, V. B. N90-12656
CAMPBELL, RICHARD L. N90-12540
N90-12544
CANNON, M. R. N90-13198
CAPPELLI, MARK A. N90-13268
CARCIELLO, N. R. N90-12754
CARLETON, F. B. N90-12786
CARLON, HUGH R. N90-12713
N90-12994
CARNIEL, XAVIER N90-12907
CARRAWAY, DEBRA L. N90-12520
N90-12522
CARRERAS, B. A. N90-13239
CARRIER, R. N90-12835
CARRON, N. J. N90-13247
CARTAUD, D. N90-12724
CARTWRIGHT, S. L. N90-12875
CARUSO, M. J. N90-12536
CASALEGNO, L. N90-12665
CATTUNAR, S. N90-12598
CATURA, R. N90-13309
CAZENEUVE, C. N90-12673
CESARSKY, C. N90-13304
CHACONAS, KAREN N90-13101
CHAGANTY, NARASINGA RAO N90-13173
CHANANE, B. N90-13121
CHANDRASEKAR, V. N90-13007
CHANG, WON S. N90-12898
CHANNON, STANLEY L. N90-12680
CHASSEFIERE, E. N90-13312
CHATTOPADHYAY, ADITI N90-12588
CHELLIAH, HARSHA KUMAR N90-12683
CHEN, A. W. N90-12546
CHEN, D. N90-12778
N90-12958
CHEN, FANG-JENG N90-12555
CHEN, HOWARD TZ. N90-12873
CHEN, SAMMY G. N90-12655
CHENG, C. C. N90-12691
CHENG, C.-C. N90-13311
CHERRETT, M. A. N90-12619
CHERRY, P. N90-12729
CHEUNG, K.-M. N90-12792
N90-12793
N90-12795
CHEW, JOHN W. N90-12607
CHILDERS, CLIFTON B. N90-12845
CHILLERY, J. A. N90-13206
CHISHOLM, PAUL N90-13079
CHITASHVILI, R. J. N90-13147
CHOYKE, W. J. N90-12691
CHRISTENSEN-DALSGAARD, J. N90-13304
N90-13306
CICHRA, D. A. N90-12761
CIOFFI, SHARON O. N90-13111
CIPOLLA, JOHN R. N90-12567
CLARK, GREGORY A. N90-12775
CLAUS, STEVEN J. N90-13065
CLAY, K. N90-12602
CLAY, WALLACE H. N90-12633
CLAYTON, C. R. N90-12754
CLEMENTS, P. A. N90-12801
CLEVELAND, WILLIAM G. N90-12892
COATNEY, SUSAN N90-13053
COATS, G. D. N90-13228
COFFEY, HELEN E. N90-13300
COLDREN, LARRY A. N90-13237
COLIN, G. N90-12749
COLLIER, FAYETTE S., JR. N90-12558
COLLIN, MARIE-FRANCE N90-12887
COLLINS, CARL B. N90-12921
N90-12924
COLLISTER, J. B. N90-13205
N90-13206
COMBER, C. N90-13292
N90-13317
COMPTON, R. T., JR. N90-12841
CONJERTI, SAMUEL N. N90-12594
CONRAD, HANS N90-13263
CONSTABLE, STEFAN H. N90-13022
COOK, KELSEY D. N90-12739
COOK, S. C. N90-12613
COOPER, HAROLD MARTIN N90-13248
COOPER, JAMES A., JR. N90-13266
COOSE, J. P. N90-12928
COPENHAVER, WILLIAM WARD N90-12600
CORNEC, FRANCOIS N90-13038
CORNELIUS, DAVID E. N90-12686
CORNELIUS, KENNETH C. N90-12530
CORNETT, MICHAEL S. N90-12862
CORNETTE, JAMES B. N90-12848
COURTNEY, T. H. N90-13021
COURTOIS, B. N90-12855
N90-13094
COUSTOLS, E. N90-12889
COUTIN, R. N90-12723
N90-12729
N90-12962
CRAPART, J. C. N90-12729
CREEL, THEODORE R., JR. N90-12556
N90-12557
CRESPODASILVA, M. R. N90-13172
CROARKIN, M. CARROLL N90-12892
CROMMELYNCK, D. N90-13305
CROOM, CYNTHIA C. N90-12520
CROSBY, D. S. N90-12968
CROUZEN, P. C. N. N90-13216
CRUTZEN, PAUL J. N90-12992
CUCCHISSI, J. J. N90-12791
CULHANE, J. L. N90-13308
CURDT, W. N90-13307
CURTAIN, RUTH F. N90-13167
N90-13168
CUSHMAN, WILLIAM B. N90-13027
CZARNASKI, M. N90-12909
CZARNIK, ANTHONY W. N90-12757
CZICHOS, H. N90-12747

D

DACLES, JENNIFER N90-12499
DAGENHART, J. RAY N90-12517
N90-12523
N90-12529
N90-12532
DAHL, M. D. N90-12561
DALEY, C. N90-12981
DALTON, H. N90-12977
DALTON, PATRICK N90-12706
DALY, STEVEN F. N90-12699
DAME, L. N90-13304
DANCER, E. N. N90-13120
DANIELL, ROBERT E., JR. N90-12969
DARLAY, F. N90-12855
DAROU, Y. N90-12726
DAVIES, M. B. N90-13066
DAVIS, A.-C. N90-13299
DAVIS, J. H. N90-12715
DAVIS, JOHN S. N90-13050
DAVIS, L., JR. N90-13316
DAVIS, MICHAEL N90-13029
DAVIS, PATRICK J. N90-12541
DAVIS, RICHARD N90-12703
DAVIS, RICHARD E. N90-12511
DEAN, G. D. N90-12745
DEAN, T. N90-13070
DEBIEZ, S. N90-12724
N90-12726
DEBOER, FRANK S. N90-13075
DEBOER, M. N90-13217
DECKERT, W. H. N90-12589
DECUSATIS, CASIMER N90-12655
DEFUSCO, ALBERT A. N90-12679
DEGEORGE, CHARLES L. N90-12617
DEGROOT, D. J. N90-12853
DELABOUDINIERE, J. P. N90-13309
DELACHE, PH. N90-13304
N90-13305
DELEEUW, G. N90-12991
DELLACORTE, CHRISTOPHER N90-12658
N90-12659
N90-12670
DELOZANNE, ALEX N90-13257
DELUISI, JOHN J. N90-12993
DEMELO, WELINGTON N90-13190
DEMINCO, NICHOLAS N90-12937
DENHOLLANDER, W. TH. F. N90-13143
DENNING, R. M. N90-12605
DEOBALD, L. R. N90-12735
DERE, K. P. N90-13309
N90-13311
DESA, SUBHAS N90-12945
DESANGRO, R. N90-12875
DESARMOT, G. N90-12698
DESBAT, LAURENT N90-13125
DESIMONE, P. N90-12875
DEUBNER, F. L. N90-13304
DEVLIEGER, J. H. N90-12821
DEVORE, C. R. N90-13246
DILL, JAMES F. N90-12935
DIMARELLIS, E. N90-13312
DINI, PAOLO N90-12872
DISALVO, FRANCIS J. N90-13256
DOCHE, J. P. N90-12723
DODBELE, S. S. N90-12550
N90-12552
DOLINAR, S. N90-12795
DOMINGO, V. N90-12649
N90-13303
N90-13305
DOMINGUEZ, N. N90-13239
DOSCHEK, G. A. N90-13308
N90-13311
DOUBT, T. J. N90-13025
DOWSETT, M. J. N90-12572
DRENDEL, ALBERT S. N90-12652
DRESSLER, JOHN L. N90-12881
DRITTLER, KARL N90-12884
DRUEZ, P. M. N90-13198
DRUMMOND, COLIN K. N90-12618
DUBOIS, PIERRE-FRANCOIS N90-13105
DUBOURG, M. C. N90-12956
DUFFY, L. N90-12803
DUNAGAN, STEPHEN E. N90-12904
DUNGAN, THOMAS E. N90-13266
DUNN, B. N90-12738
DUPRAT, JEAN N90-13109
DUTTON, ELIZABETH G. N90-12993
DWIGHT, K. N90-13271
DYER, C. S. N90-13292
N90-13317
N90-13318
DZHAPARIDZE, K. O. N90-13146

E

ECKERT, E. R. N90-12620
EDER, S. N90-13301
EDGE, C. H. N90-12668
EGGERMONT, P. P. B. N90-13072
EGGLESTONE, GRAEME T. N90-12661
EISENSTAT, STANLEY C. N90-13054
ELIENS, A. N90-13073
ELLEFSEN, RICHARD N90-12982
ELLIOTT, CHARLES T. N90-12623
ELY, JAMES F. N90-12690
N90-12697
ENAULT, C. N90-13232
ENG, G. N90-12869
ENGELIS, T. E. N90-12984
EPEMA, D. H. J. N90-13045
ESAREY, E. N90-12867
ESCALUP, V. N90-12723
N90-12962
ESSELINK, KLAAS N90-13078
EVENSON, PAUL N90-13314

F

FAGHRI, AMIR N90-12898
FAIGLE, U. N90-13162
FANCHER, M. F. N90-12522
FARGUES, J. N90-12727
FARREN, J. N90-13318
FARRINGTON, G. C. N90-12738
FAUST, G. K. N90-12550
N90-12551
FAVRE, J. P. N90-12678
FEAUX, KARL N90-12590
FEIGELSON, ROBERT S. N90-12770
FEIT, DAVID M. N90-12967
FELSENTREGER, T. L. N90-12984
FENSKE, G. R. N90-12719
FERGUSON, EUGENE M. N90-12633
FERRISS, D. H. N90-13220
FESSLER, H. N90-12609
FIELD, EDWARD C., JR. N90-12836
FINCH, W. N90-12576
FINK, H. H. N90-13295
FIREY, B. N90-12928
FISCHER, HARALD N90-13314
FISCHER, MARK A. N90-12567
FISCHER, MICHAEL C. N90-12509
N90-12512
FISCHER, R. P. N90-12868
FISHER, DAVID F. N90-12509
N90-12512
FISK, ARTHUR D. N90-13033
FLAVENOT, J. F. N90-12727
FLEETER, RICK N90-13238
FLEISCHAUER, PAUL D. N90-12759
FLERI, EDGAR L., JR. N90-13036
FLIFLET, A. W. N90-12868
FLYNN, ANITA M. N90-12941
FOING, B. N90-13304
FOLEY, MICHAEL J. N90-12650
FORNES, RAYMOND E. N90-12758
FORRESTER, B. D. N90-12596
FORSGREN, ANDERS L. N90-13086
N90-13174

FOSSAT, E. N90-13304
FRAGUAS, A. L. N90-13239
FRANCILLETTE, J. N90-12746
FRANKLIN, J. A. N90-12589
FRANKLIN, MATTHEW K. N90-13051
FRASER, JOHN D. N90-12947
FRECAUT, M. JEAN-MICHEL N90-13108
FRESE, K. W., JR. N90-12712
FRIEND, DANIEL G. N90-12690
FRISK, U. O. N90-12649
FROEHLICH, C. N90-13305
FUCHS, JUERGEN N90-13224
N90-13273
FUHRER, M. N90-13301

G

GABERIELIAN, ARMEN N90-13051
GABRIEL, A. H. N90-13304
N90-13307
N90-13308
N90-13309
GAEMERS, K. J. F. N90-13222
N90-13223
GAILLARD, R. N90-12725
GAINFORD, D. M. N90-12934
GALLAGHER, J. G. N90-12858
GALLAGHER, MARIA L. N90-13047
GALLIANO, PAUL A. N90-13036
GALLO, MARY M. N90-12702
GAN, HONG N90-13122
GAO, Y. M. N90-13271
GARBER, F. D. N90-12835
GARCIA, GRAHAM A. N90-12860
GARCIA, J. G. N90-12915
GARFINKLE, DAVID N90-13274
GARRONE, A. N90-12631
N90-12632
GARTRELL, LUTHER R. N90-12526
GASNIER, J. N90-12729
GASQUET, D. N90-13250
GATES, ROGER S. N90-12567
GATTI, E. N90-12852
GAZEAUD, G. N90-12960
GEER, ANDY N90-12932
GEIGER, DAVI N90-13084
GEIS, N. N90-13296
GEISS, J. N90-13310
N90-13313
GELBAND, PATRICE N90-13111
GELFAND, ALAN E. N90-13187
GENZEL, R. N90-13296
GEORGE, THOMAS F. N90-13213
N90-13226
GERECHT, KLAUS N90-13018
GERONIMI, J. P. N90-13094
GERY, M. W. N90-12981
GEURTS, BERNARD J. N90-12750
GHIGLIONE, D. N90-12728
GIBBS, B. P. N90-12801
GILBERT, RICHARD D. N90-12758
GILL, PHILIP E. N90-13086
N90-13174
GILL, R. D. N90-13181
GILLETTA, D. N90-12672
GIRARD, DIDIER N90-13125
GIROSI, FEDERICO N90-13084
N90-13110
GLADD, N. T. N90-13112
GLIEM, F. N90-13313
GLOECKLER, G. N90-13310
N90-13313
GLYNN, PETER W. N90-13186
GMELIGMEYLING, R. H. J. N90-13208
N90-13233
GOAD, WILLIAM K. N90-12528
GOEBEL, F. N90-13159
GOLDBERG, SEYMOUR N90-13170
GOLDSTEIN, R. J. N90-12620
GOLDWASSER, J. M. N90-12761
GONZALEZ, S. N90-12875
GOODING, R. H. N90-12642
GOODMAN, JOSEPH W. N90-13264
GORADIA, SURESH H. N90-12535
GOUGH, D. O. N90-13306
GOUTAIL, F. N90-13312
GRAETER, M. N90-13301
GRAF, U. U. N90-13296
GRARD, R. N90-12649
GREEN, CORDELL N90-13087
GREEN, GUENTER N90-13314
GREEN, M. C. N90-12844
GREEN, W. E. N90-12601
GREENBERG, RONALD I. N90-13092
GREENE, RICHARD F. N90-13262
GREENFIELD, S. M. N90-12981
GREENGARD, LESLIE N90-13052
GREENWOOD, PRISCILLA E. N90-13119
GREGGI, J. C. N90-12719
GREGORY, RUTH N90-13274
N90-13299
GREWING, M. N90-13307
GRIMAULT, B. N90-12676
GROEHL, LAWRENCE R. N90-12859
GROENEWEG, J. F. N90-12560
GROSSET, E. N90-12729
GROSSMAN, ROBERT N90-13113
GROUTAGE, FREDERICK D. N90-12594
GRUNDY, I. H. N90-12501
GUENNOUNI, JAMAL N90-12811
GUENTERBERG, HERBERT N90-12578
GUENTHER, ARTHUR H. N90-12913
GULKIS, S. N90-12804
GUOXING, HUANG N90-13064
GUPTA, INDER J. N90-12784
GUPTA, P. C. N90-12605
GUYENNE, T. D. N90-13302

H

HAARSMA, R. J. N90-13001
HABERL, F. N90-13295
HAFEZ, MOHAMMED N90-12499
HAFIZI, B. N90-12922
HAHNE, DAVID E. N90-12542
HAKVOORT, E. H. N90-13107
HALL, B. O. N90-12719
HALL, JAMES E. N90-13046
HALL, M. G. N90-12562
HALL, PHIL N90-12515
HALL, ROBERT M. N90-12524
HALLIDAY, M. D. N90-12952
HALLISSY, JAMES B. N90-12544
HALLS, G. A. N90-12933
HALPERT, MICHAEL S. N90-13009
HAMBRIC, STEPHEN A. N90-12964
HAMILTON, MARK F. N90-13200
HAMMEL, SHERRY ELIZABETH N90-12569
HAMMOND, N. D. A. N90-13292
N90-13317
HANDLER, ROBERT A. N90-12903
HANHAM, C. M. N90-12732
HARDY, A. E. N90-12732
HARGREAVES, T. A. N90-12868
HARMON, JAMES B. N90-12633
HARMON, V. N90-13024
HARPUR, K. N90-13207
HARRIS, A. I. N90-13296
HARRIS, CHARLES D. N90-12531
N90-12532
HARRIS, JOSEPH N90-13022
HARRIS, JULIUS E. N90-12534
HARRISON, MARK E. N90-13036
HARRISON, R. A. N90-13308
HARROD, JOHN F. N90-12736
HARTENSTINE, JOHN R. N90-12865
HARTMANN, L. W. N90-13310
HASEBE, NABUYUKI N90-13314
HASENCLEVER, SILKE RUTH N90-13019
HASTINGS, EARL C., JR. N90-12550
HASTINGS, JOHN R. N90-12845
HATFIELD, WILLIAM E. N90-12871
HATTAN, C. P. N90-12843
HAUFF, STEFFEN N90-13081
HAUTALA, M. N90-13192
HAUTOJARVI, P. N90-12722
HAVERKORT, BOUDEWIJN R. N90-13099
HAYHURST, THOMAS L. N90-13238
HAZEWINKEL, MICHIEL N90-13184
HEFNER, JERRY N. N90-12503
N90-12519
N90-12539
HEIDNER, RAYMOND F. N90-12916
HEIJMANS, H. J. A. M. N90-13150
HELMERS, R. N90-13179
HEREMAN, WILLY N90-13177
HERMANS, A. J. N90-12876
N90-12885
N90-12978
HERRMANN, R. N90-13301
HERZFELD, CHARLES N90-12636
HESSLINK, R. L. N90-13024
N90-13025
HILLS, SUSAN E. N90-13187
HILLYARD, STEVEN A. N90-13030
HILTON, MICHAEL R. N90-12759
HINEDI, S. N90-12799
HINMAN, DARYL E. N90-12861
HINNEFELD, J. D. N90-13225
HIPONIA, LORENZO S. N90-12638
HITNEY, L. R. N90-12833
HIZEM, NEILA N90-13259
HOARAU, P.-A. N90-12746
HOBAN, FRANCIS T. N90-13277
HOBBS, R. A. N90-12857
HOEKSEMA, J. T. N90-13306
HOFFMANN, W. N90-13135
HOFFREN, JAAKKO N90-12879
N90-13116
HOLL, P. N90-12852
HOLLOWAY, JOHN S. N90-12916
HOLMES, BRUCE J. N90-12520
N90-12549
HOLWEGER, HARTMUT N90-13314
HOLZER, T. E. N90-13312
HOMER, L. D. N90-13024
HONG, WILLIAM S. N90-12680
HOOGENDOORN, A. W. N90-13142
HOOGHIEMSTRA, GERARD N90-13044
N90-13119
HOPPE, FRED M. N90-13185
HOPPE, MARTIN N90-12736
HORIE, YUJI N90-12982
HORN, BERTHOLD K. P. N90-12908
HORNBOSTEL, MARC N90-13256
HORNIK, A. N90-13094
HOVE, JOHN E. N90-12680
HOVESTADT, D. N90-13313
HOWARD, R. A. N90-13309
N90-13311
HOWELL, DAVID W. N90-13197
HRYNIEWICZ, Z. N90-12876
HSU, S. M. N90-12747
HUANG, J. N90-12803
HUANG, L. S. N90-12537
HUBBARD, DAVID C. N90-12634
HUBBARD, ROGER W. N90-13020
HUBER, M. C. E. N90-13307
N90-13308
HUBER, MARCIA L. N90-12697
HUGHES, A. J. N90-12815
N90-13005
HUIJBERTS, H. J. C. N90-13166
HUIZING, A. G. N90-12826
HUJANEN, A. T. N90-12805
HULSEBOS, ARJAN N90-13114
HUMPHREY, J. A. C. N90-12882
HUNDSDORFER, WILLEM H. N90-13133
HUOMO, H. N90-12722
HUSSAINI, M. Y. N90-12533
HUTCHESON, GEORGE Z. N90-12850
HUTCHINGS, R. J. N90-13318
HUTTUNEN, P. A. N90-12722
HWANG, SHYANG N90-13249
HYDE, T. H. N90-12609

I

ICOELLNER, HANS JOCHEN N90-12851
IGLEHART, DONALD L. N90-13186
ILKHAMOV, R. A. N90-13252
INFANGER, GERD N90-13189
INGHAM, HEPBURN N90-12690
INGLESE, B. N90-12591
INMAN, D. J. N90-12773
IPAVICH, F. M. N90-13313
ITO, Y. N90-12682
IYENGAR, S. SITHARAMA N90-12975
IYER, VENKIT N90-12534

J

JACKSON, A. J. B. N90-12614
JACKSON, RAYMOND H. N90-12669
JACOBS, I. N90-13028
JACOBSON, DEAN N90-12706
JACQUIN, L. N90-12894
JAEGLE, PIERRE N90-12917
JAGANNADHAM, KASI N90-12966
N90-13263
JAKOBSEN, P. N90-12649
JANIK, G. N90-12789
JANSSEN, P. N90-13179
JAYARAMAN, V. N90-12915
JEAL, R. H. N90-12720
JEANDRAU, JEAN-PIERRE N90-12748
JENKINS, D. B. N90-12816
JENKINS, W. K. N90-12864
JENNETT, LISA A. N90-12512
JENNEY, GAVIN D. N90-12624
JENSEN, PETER A. N90-12970
JERRAYA, A. A. N90-13094
JIMENEZ, A. N90-13305
JOHNS, ELIZABETH N90-13010

JOHNSON, A. E. N90-12572
N90-12573
JOHNSON, CHARLES B. N90-12521
N90-12522
JOHNSON, DONALD N90-13011
JOHNSON, JOSEPH B. N90-12558
JOHNSON, WILLIAM B. N90-13036
JOHNSTON, M. H. N90-12715
JOHNSTON, RANDY F. N90-12708
JONES, A. R. N90-13305
JONES, GREGORY S. N90-12526
JONES, MICHAEL G. N90-12550
N90-12553
JONSCHER, ANDREW K. N90-13255
JOOSTEN, PETER N90-12571
JORDAN, C. N90-13308
JORDAN, CAROL A. N90-13023
JORDAN, FRANK L., JR. N90-12541
N90-12542
JORDAN, M. C. E. N90-13307
JORDAN, WILLIAM N90-12590
JOUNY, I. N90-12835
JUILLEN, J. C. N90-12897
JUNGERT, ERLAND N90-12969

K

KAHNG, W. H. N90-13226
KAILASANATH, K. N90-12710
KAK, AVI N90-13235
KALBURGI, VIJAY N90-12517
KALDEICH, B. N90-12769
KALLENBERG, W. C. M. N90-13163
KAMPE, J. C. MALZAHN N90-13021
KAPER, R. N90-13216
KAPLAN, MICHAEL L. N90-13228
KARASZ, FRANK E. N90-12743
N90-12764
KARYAMPUDI, V. MOHAN N90-13228
KATILA, T. N90-13192
KAUKONEN, H. P. N90-12721
KAWANO, LAWRENCE N90-13297
KEANE, M. S. N90-13044
KEARNS, JAMES A. N90-13204
KEIDING, N. N90-13181
KELHA, V. N90-13312
N90-13315
KELLOGG, ROBERT S. N90-12634
KELLY, J. N90-12689
KEMP, D. H. N90-12817
N90-12819
KENNEDY, J. R. N90-12718
KERN, W. N90-13162
KERSCHEN, EDWARD J. N90-12516
KESSLER, M. F. N90-12649
KEY, J. N90-13003
KHALIL, M. N90-13128
N90-13129
KIBLER, D. F. N90-12627
KIDD, J. M. N90-12767
KIES, LYNDA R. N90-12836
KIGHTLEY, P. N90-13269
KILLOUGH, GRAHAM N90-12590
KIM, EDWARD J. N90-12911
KIM, YONG-YIL N90-12945
KIMBROUGH, A. J. N90-13198
KINARD, JOSEPH R. N90-12845
KING-HELE, D. G. N90-12640
KINSMAN, JOHN D. N90-12979
KINTZER, E. S. N90-12915
KIPPS, JAMES R. N90-13082
KIRCHNER, MARK E. N90-12504
KIRK, G. E. N90-12610
N90-12667
KJELDSETH-MOE, O. N90-13308
KLEIN, M. J. N90-12804
KLOSKO, S. M. N90-12984
KNUPP, KEVIN R. N90-12996
KO, WILLIAM L. N90-12669
KOBAYASHI, A. S. N90-12735
KOBZEV, A. P. N90-13252
KOCH, RICHARD N90-13093
KOEKOEK, ROELOF N90-13126
KOFFEND, JOHN B. N90-12916
KOHL, J. L. N90-13310
KOHONEN, TEUVO N90-13049
KOLDENHOF, E. E. N90-13216
N90-13225
KOLESAR, C. E. N90-12543
KOOPMAN, E. L. M. N90-13194
KOORNWINDER, TOM H. N90-13138
N90-13139
N90-13140
N90-13151
KOPNIN, N. B. N90-13258
KOREN, BARRY N90-12891
KOREVAAR, C. G. N90-13002
KORPELA, S. N90-13312
KOTLINSKI, B. N90-13216
KOUTCHMY, S. N90-12647
KRAHENBUHL, GARY S. N90-13022
KRAINIAK, JOHN W. N90-12862
KRALLIS, G. A. N90-12627
KRALLIS, K. N90-12766
KRAMER, EDWARD J. N90-12756
KRANAKIS, EVANGELOS N90-13154
KRANTZ, RICHARD J. N90-12870
KRAVIK, STEIN E. N90-13013
KRISHNAMURTHY, MOHAN N90-12706
KRISHNAN, R. N90-12874
KRIZANC, DANNY D. M. N90-13154
KUBENDRAN, L. R. N90-12525
KUEHL, BURKHART N90-12851
KUIJK, A. A. M. N90-13156
KUKACKA, L. E. N90-12754
KUMMER, H. N90-13322
KUNOW, HORST N90-13314
KUNT, CENGIZ OSMAN N90-12926
KUNZ, T. D. N90-12663
KUSCHE, KARL P. N90-12655
KVATERNIK, RAYMOND G. N90-12586
KYLLONEN, PATRICK C. N90-13034
KYMAELAEINEN, O. N90-12878
KYROLA, E. N90-13312

L

LACONTI, ANTHONY B. N90-12688
LAFON, A. N90-12502
LAINE, RICHARD M. N90-12736
N90-12740
LAIZET, J. C. N90-12678
LALLEMENT, R. N90-13312
LANDSMAN, N. P. N90-13194
LANE, STEPHEN S. N90-12948
LANG, D. N90-12676
LANGE, ROY H. N90-12506
LANGFORD, JOHN S., III N90-12496
LARKIN, R. J. N90-12815
LARSON, RICHARD G. N90-13113
LASKEY, K. J. N90-12710
LATH, A. N90-12875
LATTES, ARMAND N90-12692
LAUBACHER, B. A. N90-12651
LAURA, P. A. A. N90-12772
LAWCONNELL, ROBERT I. N90-13196
LAWING, PIERCE L. N90-12527
LEATHERMAN, GARY L. N90-12762
LEBRETON, J.-P. N90-12649
LEE, EUGENE A. N90-12643
LEE, JAE RYONG N90-12653
LEE, S. A. N90-12611
LEE, S. C. N90-12654
LEEGTE, H. K. W. N90-13216
N90-13225
LEEHEY, PATRICK N90-13212
LEFEBVRE, M. N90-12630
N90-12729
LEHNERT, B. N90-12809
LEIBOVICH, SIDNEY N90-12877
LEIGHTON, RICHARD I. N90-12903
LEIGHTON, TOM N90-12847
N90-13093
LEINER, BARRY M. N90-13047
LELIEVELD, JOS N90-12992
LEMAIRE, P. N90-13307
LEMEN, J. N90-13309
LENG, Y. N90-13021
LEONARD, J. T. N90-12777
LEPPALA, K. N90-13315
LEPPELMEIER, G. N90-13315
LERCH, F. J. N90-12984
N90-12985
LESSNER, PHILIP N90-12688
LESSOFF, HOWARD N90-13262
LEUCHTER, O. N90-12894
LEVIN, KLAS N90-12664
LEVY, MILTON N90-12734
LEWIS, L. V. N90-12609
LEWIS, S. B. N90-13024
LI, BAOJIANG N90-12657
LI, FU-LI N90-13213
LI, MING N90-13191
LI, XIAO-SHEN N90-13213
LI, ZHAOMIN N90-12657
LIEDE, I. N90-13315
LIEN, MARY M. N90-12755
N90-12780
LIENESCH, J. H. N90-12968
LIM, TEIK CHIN N90-12936
LIN, D. L. N90-13213
LIN, T. P. N90-12869
LINDELL, ISMO V. N90-12805
N90-13117
LIPE, THOMAS E. N90-12845
LIPPERT, JACK R. N90-12848
LIU, CHANGLIN N90-12752
LIU, JING N90-12657
LIU, JOSEPH W. N90-13054
LIU, M. K. N90-12981
LONGDON, NORMAN N90-13276
N90-13322
LONGONI, A. N90-12852
N90-13260
LOOS, ALFRED C. N90-13065
LOWE, ROBERT E. N90-12495
LOWRIE, B. W. N90-12605
LUBECKE, V. N90-12803
LUCK, S. J. N90-13030
LUCKOCK, H. C. N90-13293
LUMME, M. N90-13315
LUND, P. D. N90-12878
LYNCH, V. E. N90-13239
LYONS, J. R. N90-12790
LYTTON, C. C. N90-12893

M

MAAS, R. N90-12854
MACDOUGALL, J. D. N90-13028
MACKAY, A. J. N90-12858
MACKAY, MICHAEL N90-12568
MACKENZIE, J. D. N90-12742
MADDALON, DAL V. N90-12511
N90-12512
MAEKINEN, J. N90-12722
MAESTRELLO, LUCIO N90-12537
N90-12874
MAGGS, BRUCE N90-13093
MAGUN, A. N90-13301
MAHEFKEY, EDWARD T. N90-12898
MALCOLM, GRANT N90-13079
MALEKI, L. N90-12789
MALFLIET, RUDI N90-13218
MALIK, MUJEEB R. N90-12513
N90-12554
N90-12555
N90-12557
MALOSSE, R. N90-13071
MALYS, STEPHEN N90-12970
MANCUS, EDWARD N90-12781
N90-12782
MANGALAM, SIVA M. N90-12517
N90-12529
MANGUN, G. R. N90-13030
MANNING, P. A. N90-12905
MANTAY, WAYNE R. N90-12580
N90-12581
N90-12583
N90-12587
MANUEL, GREGORY S. N90-12520
MAPPER, D. N90-13318
MARABLE, W. N90-12867
MARAIS, C. N90-12677
N90-12678
MARCHIANDO, J. F. N90-13261
MARENDAZ, CHRISTIAN N90-13040
MARISKA, J. T. N90-13311
MARLAND, GREG N90-12979
MARMONIER, M. F. N90-12698
MARSCH, E. N90-13307
MARSDEN, R. N90-12649
MARSH, J. G. N90-12984
MARSHALL, THOMAS C. N90-12925
MARTENS, MARCO N90-13190
MARTIN, EUGENE C. N90-12679
MARTIN, RUTH M. N90-12585
MARTINEZ, MARINO J. N90-12866
MATHUR, G. P. N90-13198
MATTSSON, STEFAN N90-12785
MAUGHMER, MARK D. N90-12545
N90-12872
MAULFAIR, ROBERT J. N90-13238
MAURETTE, M. T. N90-12692
MAY, BRUCE O. N90-12828
MCCORMICK, A. H. I. N90-12780
MCFADDIN, S. E. N90-12880
MCGHEE, ROBERT J. N90-12541
N90-12542
MCINTYRE, M. E. N90-12988
MEERTENS, LAMBERT G. L. T. N90-13154
MELBOURNE, R. N90-12789
MELLOCH, MICHAEL R. N90-13266
MERLO, IA XAVIER N90-13108
MERRITT, R. G. N90-12774

MEWALDT, R. A. N90-13316
MEYER, GREGORY J. N90-13036
MEYER, JEAN-PAUL N90-13314
MEYER, ROBERT R. N90-12547
MEYERS, JIM F. N90-12525
N90-12529
MICHELS, D. J. N90-13309
N90-13311
MIKULSKI, BARBARA N90-13284
MILAM, DAVID N90-12913
MILGRAM, DAVID L. N90-13111
MILLER, D. S. N90-12558
N90-12559
MILLER, DANIEL K. N90-12842
MILLER, R. B. N90-12579
N90-12595
MILLER, R. H. N90-12844
MILLER, ROBERT N90-12590
MINER, E. WADE N90-12903
N90-13176
MINUCCI, MARCO A. N90-12655
MIZELL, DAVID N90-13053
MODARRESS, DARIUSH N90-12524
MODER, JEFFREY P. N90-12655
MOEBIUS, E. N90-13313
MOEHRING, W. N90-13124
MONK, KRISTINA B. N90-12902
MONTGOMERY, NOEL D. N90-13017
MONTHIOUX, M. N90-12744
MOORE, G. E. N90-12981
MOORE, R. K. N90-12838
MORALES, CIRO N90-12655
MOREIRA, ALBERTO N90-12827
MORGAN-POND, C. G. N90-13267
MORGAN, DON W. N90-13022
MORGAN, HARRY L., JR. N90-12535
N90-12540
MORPETH, A. N90-12671
MORRIS, ALAN S. N90-13102
N90-13103
N90-13104
MORRIS, JOHN N90-12505
MORRIS, R. E. N90-12981
MORRISETTE, E. LEON N90-12556
MORTAIGNE, B. N90-12746
MOSES, R. L. N90-12835
N90-13169
MOSLEY, W. C. N90-12717
MOUGINOT, REMI N90-12955
MTINGWA, SEKAZI K. N90-12914
MUELLER-MELLIN, REINHOLD N90-13314
MUNGUR, PARMA N90-12550
N90-12551
MUNSHI, M. Z. A. N90-12976
MURRAY, WALTER N90-13086
N90-13174
MURRI, DANIEL G. N90-12541
MURTHY, A. V. N90-12625
MURTHY, T. SREEKANTA N90-12586
MYRABO, LEIK N. N90-12655

N

NAGUMO, MARK N90-13214
NAGY, LAWRENCE A. N90-12813
NAKAJIMA, TOSHIKI N90-12737
NALLASAMY, M. N90-12560
NAMAZIA, M. N90-12689
NAOI, KATSUHIKO N90-12737
N90-12755
N90-12760
NARBOROUGH-HALL, C. S. N90-12572
NASHMAN, MARILYN N90-13101
NAYFEH, ALI H. N90-12514
N90-12518
NEAL, P. F. N90-12601
NEAMTU, M. N90-13160
N90-13183
NELSON, CAROLINE V. N90-12655
NELSON, L. V. N90-12844
NEUDECK, PHILIP G. N90-13266
NEUPERT, W. N90-13309
NEWHOUSE, JAMES P. N90-12751
NEWMAN, D. A. N90-13202
NEWNAM, BRIAN E. N90-12913
NGUYEN, L. N90-12798
NIDKOLAI, PAUL J. N90-13083
NIEDERSTRASSER, HELMUT N90-12577
NIEMEGEERS, IGNAS G. N90-13099
NIEMEIJER, GERRIT N90-13100
NIEMINEN, R. M. N90-12721
NIERATSCHKER, WILLI N90-13081
NIJMEIJER, HENK N90-13158
N90-13166
NIKOSKINEN, KEIJO I. N90-12805
N90-13117
NITSCHELM, C. N90-12647
NIXON, MARK W. N90-12584
N90-12588
NOCI, G. N90-13310
NOCK, L. A. N90-12761
NOONAN, KEVIN W. N90-12582
NORDLEY, GERALD D. N90-13227
NORTH, N. D. N90-13059
NOUGIER, J. P. N90-13250
NUMMILA, KAJ N90-13221

O

OBARA, CLIFFORD J. N90-12550
N90-12552
OBERLIN, A. N90-12744
OBRIEN, ROBERT N90-13043
OH, T. K. N90-12715
OHLMANN, THEOPHILE N90-13040
OKSANEN, MARKKU ILMARI N90-13229
OLSEN, E. T. N90-12804
OLSEN, R. C. N90-12637
OLSEN, R. G. N90-13024
ONO, K. N90-12742
ONWUMECHILI, C. A. N90-13294
ORAN, E. N90-12710
OSAKA, TETSUYA N90-12737
OSBORNE, J. L. N90-13315
OSIBOV, MARCUS N. N90-13238
OSTERGAARD, JENS C. N90-12806
OSWEILLER, F. N90-12896
OTTEN, M. P. G. N90-12823
N90-12826
OUSSET, YVES N90-12675
OUZTS, PETER J. N90-12618
OVERFELT, P. L. N90-12834
OWENS, BOONE B. N90-12737
N90-12760
N90-12863
N90-12976
OZOEMENA, P. C. N90-13294

P

PABST, JOHN W. N90-13266
PAGE, MICHAEL J. N90-12701
N90-12702
PAILHAS, G. N90-12888
PAISLEY, M. F. N90-12562
PAN, XING-YA N90-12812
PAPPERT, R. A. N90-12833
PARDEE, REBECCA J. N90-13279
PARENT-SIMONIN, S. N90-12727
PARIKH, PARESH N90-12537
PARKER, R. J. N90-12918
N90-12957
PARR, R. A. N90-12715
PARRISH, C. J. N90-12612
PARRISH, MAUREEN K. N90-12707
PARTICCO, V. N90-12631
N90-12632
PATANKAR, S. V. N90-12620
PATCHETT, B. E. N90-13308
PATE, VICKI M. N90-12771
PATEL, G. B. N90-12984
PATNAIK, G. N90-12710
PATTON, E. M. N90-12965
PAUGH, ROBERT L. N90-12779
PAUL, J. N90-12597
PAUL, P. H. N90-13268
PAULSON, MERLE R. N90-12839
PAVLAK, ROBERT T. N90-13055
PAVY, J. C. N90-12729
PEACOCK, A. N90-12649
PEALAT, M. N90-12630
PEARCE, R. P. N90-13006
PELED, EMANUEL N90-12846
PELLINEN, R. N90-13312
N90-13315
PENAZZI, L. N90-12673
PEPI, MARC S. N90-12681
PERDU, DIDIER M. N90-12829
PERKINS, W. B. N90-13299
PERRIN, MARC N90-12689
PERRON, ROBERT A. N90-13211
PERRYMAN, M. A. C. N90-12649
PETERMAN, BRUCE E. N90-12507
PEYRE, J. P. N90-12729
PEYTONJONES, J. C. N90-13123
PFENNINGER, WERNER N90-12508
N90-12540
PHILLIPS, PAM S. N90-12544
PICKERING, C. N90-12671
PIENKOS, P. T. N90-12977
PILLSBURY, A. D. N90-12915
PINKSTER, J. A. N90-12978
PITT, G. H., III N90-12796
PLUNK, VONN N90-12590
POGGIO, TOMASO N90-13110
POGLITSCH, A. N90-13296
POLAND, A. I. N90-13303
N90-13307
POLKOWSKA-SEMENIUK, MARIA N90-13130
POLKOWSKI, LECH T. N90-13130
PONSE, ALBAN N90-13076
PORTER, J. T. N90-12663
POSEY, PAMELA G. N90-13012
POSNER, E. C. N90-12786
N90-12802
POSTANS, P. J. N90-12720
POTMA, K. N90-13135
POWELL, ARTHUR G. N90-12510
PRASAD, P. S. S. N90-12863
PREINHAELTER, J. N90-13240
N90-13241
PRELLER, RUTH H. N90-13012
PRESTAGE, J. N90-12789
PRICE, P. E. N90-13228
PRIETO, FRANCISCO J. N90-13088
PRINCE, T. A. N90-13316
PRIOU, ALAIN N90-12674
PRITCHARD, JOCELYN I. N90-12583
N90-12588
PROCTOR, F. H. N90-13228
PROUDLER, I. K. N90-13057
N90-13058
PUTNEY, B. H. N90-12984

R

RACINE-POON, AMY N90-13187
RADEKA, V. N90-12852
RADEMACHER, STEVEN E. N90-13017
RADWAN, SAMIR N90-12534
RAGAB, SAAD A. N90-12518
RAHN, JEFFREY A. N90-12736
RAINA, T. K. N90-12685
RAINWATER, JAMES C. N90-12687
RAN, A. C. M. N90-13167
RANDELL, G. P. N90-13068
RANKKA, WILHELM N90-12946
RAO, DANTAM K. N90-12935
RAO, SATISH N90-13093
RAPHAEL, LOUISE A. N90-13118
RASCOE, D. L. N90-12803
RAU, DOUGLAS H. N90-12901
RAWLS, JOHN W., JR. N90-12538
RAYMOND, J. C. N90-13310
READ, B. E. N90-12745
REED, J. R. N90-12627
REEDY, MICHAEL W. N90-12731
REEDY, RONALD E. N90-12860
REES, CHRISTOPHER N90-13043
REHAK, P. N90-12852
REINHARD, R. N90-12649
RENNICK, MARY A. N90-12998
RENZETTI, N. A. N90-12804
RESCIA, S. N90-12852
RESING, J. A. C. N90-13044
REYNOLDS, G. H. N90-12663
RHEIN, ROBERT A. N90-12751
RHINEWINE, M. N90-12909
RICHARD, JACQUES C. N90-12655
RICHARDS, M. C. N90-12651
N90-12652
RIEDLINGER, SHELLEY N90-13012
RIEHL, J. P. N90-12986
RILEY, A. L. N90-12803
RISTIC, M. N90-12611
RITTER, HELGE N90-13049
RIYOPOULOS, S. N90-12923
ROBBINS, J. W. N90-12984
ROBERT, M. N90-12939
ROCACORTES, T. N90-13305
RODHE, HENNING N90-12992
ROGERS, C. WILLIAM N90-12999
ROGERS, JOEL C. N90-12900
ROGUIN, P. N90-12725
RONSE, C. N90-13150
ROPELEWSKI, C. F. N90-13009
ROSASCO, GREGORY J. N90-12704
ROSE, M. J. N90-12815
ROSE, OLLIE J. N90-12558
N90-12559
ROSEN, M. N90-13201
ROSENBERG, ARNOLD N90-13093
ROTH, J. R. N90-13243
ROTTSCHAEFER, M. J. N90-13180
ROYER, H. N90-12906

ROZENDAAL, ROGER A. N90-12546
N90-12548
RUDDICK, K. G. N90-12890
RUFFLES, P. C. N90-12603
RUI, Y. N90-12959
RUIJSENAARS, S. N. M. N90-13141
RUIZ-IBANEZ, GABRIEL N90-12703
RUIZENAAR, A. J. N90-12824
RUMSEY, H. C. N90-12802
RUNDLE, WILLIAM J. N90-12929
RUNYAN, L. JIM N90-12546
RUSSELL, M. J. N90-13178
RUSSELL, R. K. N90-12787
RUSSELL, RAY W. N90-13238
RUSSO, G. N90-12631
N90-12632

S

SAARIKKO, H. N90-13315
SABO, FRANCES E. N90-12503
N90-12519
N90-12539
SADEDIN, DAVID R. N90-12775
SALE, D. G. N90-13028
SALES, K. R. N90-12930
SALOMAA, M. M. N90-13258
SAMPIETRO, M. N90-12852
N90-13260
SANCHEZ, B. V. N90-12984
SANDALL, ORVILLE C. N90-12703
SANDRIK, R. N90-13252
SANDS, O. S. N90-12835
SANKAR, L. N. N90-12500
SANTARE, M. H. N90-12965
SARAGAPANI, S. N90-12688
SAWYER, E. C. N90-13308
SCACE, ROBERT I. N90-13253
SCANLON, JAMES N90-12734
SCHEFER, R. N90-12689
SCHERRER, P. H. N90-13306
SCHLICHTING, J. J. F. M. N90-13056
N90-13061
SCHNABL, GOTTFRIED N90-12639
SCHNEEKLOTH, U. N90-12875
SCHNEID, JOSEF N90-13133
SCHOENSTER, JAMES A. N90-12550
N90-12553
SCHOLMA, J. K. N90-13148
SCHOLTEN, OLAF N90-13215
SCHOPPERS, MARCEL N90-13037
SCHOUTE, ALBERT L. N90-13097
SCHREADLEY, HARRY W. N90-12624
SCHULEIN, P. N90-12629
SCHULTZ, HERMAN P. N90-13085
SCHWENN, R. N90-13311
SCOWEN, R. S. N90-13059
SEGUELAS, CATHERINE N90-12695
SELIGA, THOMAS A. N90-12830
SERFLING, R. N90-13179
SEWALL, WILLIAM G. N90-12542
SHAFER, STEVE N90-12944
SHAH, B. N90-12799
SHAIK, S. S. N90-12700
SHAPIRO, DANIEL N90-13037
SHARMA, R. D. N90-12986
SHARMA, S. N90-12671
SHAW, LOCKBURN S. N90-12594
SHEFFIELD, JOHN W. N90-12648
SHERMAN, CHRISTOPHER N90-12989
SHETTLE, ERIC P. N90-12995
SHI, ZENG N90-12886
SHIAU, TZONG H. N90-13089
SHIRLEY, DARREN N90-12932
SHROPE, ARTHUR N90-12982
SIDDIQUI, NAJEEB N90-13255
SIDES, J. N90-12592
SIEMSSEN, R. H. N90-13216
N90-13225
SIEVERDING, MICHAEL J. N90-12634
SIGETY, P. N90-12677
SIIKONEN, TIMO N90-12879
N90-13116
SILBERSTEIN, MARIAN N90-12831
SIMCOX, L. N. N90-12575
SIME, L. N90-13178
SIMON, PETR N90-13127
SIMON, T. W. N90-12620
SIMONETT, DAVID S. N90-12973
SIMPSON, L. BRUCE N90-12899
SIMPSON, M. A. N90-13198
SIMS, A. J. N90-13292
N90-13318
SINCLAIR, PETER C. N90-12983
SINDT, C. F. N90-12880
SINGH, RAJENDRA N90-12936
SIRKIS, JAMES SANFORD N90-12949
SLINEY, HAROLD E. N90-12659
N90-12670
SLOBIN, S. D. N90-12800
SMIT, JAN N90-13114
SMITH, A. N90-13295
SMITH, ADRIAN F. N90-13187
SMITH, DOUGLAS R. N90-13087
SMITH, J. H. B. N90-12893
SMITH, M. J. T. N90-12593
N90-13203
SMITH, N. G. N90-12820
SMITH, PETER N90-13011
SMULDERS, F. E. H. M. N90-12778
SMYRL, WILLIAM H. N90-12755
N90-12760
SMYTH, P. N90-12794
SNOW, WALTER L. N90-12528
SOILEAU, M. J. N90-12913
SOININEN, E. N90-12722
SOMERS, DAN M. N90-12545
SOMMEIJER, B. P. N90-13131
N90-13132
N90-13134
SOSIN, Z. N90-13225
SOYLU, RESIT N90-12927
SPEAKS, PAUL D. N90-12862
SPERLING, GEORGE N90-13032
SPRANGLE, P. N90-12922
SRIVASTAVA, R. N90-12500
STACEY, G. J. N90-13296
STACK, JOHN P. N90-12523
STAELIN, DAVID H. N90-12911
STAFFANS, OLOF J. N90-13115
STAINBACK, P. CALVIN N90-12521
N90-12522
N90-12526
STALLCUP, SCOTT S. N90-13050
STAROPOLI, F. N90-12954
STARZAK, MICHAEL E. N90-12705
STAUDHAMMER, K. P. N90-12716
STEEDLY, W. M. N90-12835
N90-13169
STEENBERGEN, TH. N90-13217
STEENEKEN, H. J. M. N90-13042
STEIN, EARL S. N90-12574
STEINETZ, BRUCE M. N90-12658
STEPHEN, J. H. N90-13318
STERN, R. N90-13309
STERRETT, JOHN D. N90-12848
STEVENS, R. N90-12802
STIRLAND, D. J. N90-13269
STIRLING, D. I. N90-12977
STOLOVY, A. N90-12767
STONE, E. C. N90-13316
STONE, ROBERT S. N90-12993
STOUGIE, LEEN N90-13144
STOW, P. N90-12615
N90-12616
STRAIN, JOHN N90-13052
STRIKMAN, MARK N90-12914
STRNAT, KARL J. N90-12733
N90-13193
STRNAT, REINHOLD M. N90-13193
STRUEDER, L. N90-12852
N90-13260
STUART, HOWARD R. N90-12911
STUFF, JOHN R. N90-12707
STUTZKI, J. N90-13296
SUCHIER, JEROME N90-12730
SUGAMA, T. N90-12754
SUN, C. T. N90-12959
SUTER, ALICE H. N90-12832
N90-13209
N90-13210
SWAB, JEFFREY J. N90-12762
SWANSON, L. N90-12792
SWEAN, THOMAS F., JR. N90-12903
SWEERS, G. N90-13120
SWIFT, DANIEL W. N90-12987
SWIFT, KERRY N90-12919
SZEWCZYK, V. M. N90-12593
N90-12606

T

TALLEY, WILLIAM G. N90-12624
TAMMARO, F. N90-12631
N90-12632
TANABE, E. N90-12844
TANG, C. M. N90-12867
N90-12822
N90-12923
TARBELL, T. D. N90-13306
TAYA, M. N90-12735
TAYLOR, A. T. N90-12719
TEDROW, P. M. N90-13270
TENGVALD, ERIK N90-12969
TERRY, G. R. N90-12671
THEIL, A. N90-12826
THERA, MICHEL N90-13171
THEUNISSEN, E. A. M. N90-12629
THOMAS, J. O. N90-12738
THOMPSON, JOHN F. N90-13031
THURMAN, S. W. N90-12787
TIKOO, S. K. N90-12685
TING, A. N90-12922
TING, E. Y. N90-12718
TIRRE, WILLIAM C. N90-13034
TITLE, A. M. N90-13306
TIWARI, S. N. N90-12517
TO, GLORIA A. N90-12714
TOFFOLETTO, R. N90-12566
TOMLINS, P. E. N90-12745
TORSTI, J. N90-13315
TOURNIER, C. N90-12728
N90-12729
TOUSSAINT, J. N90-13322
TOWNES, C. H. N90-13296
TRAN, B. N. N90-13196
TRAVERS, HELEN J. N90-12932
TRAXLER, BOB N90-13281
TROLL, N. L. N90-12807
TRUJILLO, BIANCA M. N90-12547
TRUSCOTT, P. R. N90-13292
N90-13317
TSABOURAKIS, N. N90-12611
TSANGARAKIS, NIKOS N90-12681
TSAOUSSI, LUCIA N90-12990
TSUI, D. C. N90-13265
TUERCK, STEFAN N90-12626
TURNBERG, JAY E. N90-12617

U

UHLMANN, DONALD R. N90-12741
ULVESTAD, J. S. N90-12788
UM, C. I. N90-13226
UNDERWOOD, TOM N90-13235

V

VAANDRAGER, FRITS W. N90-13074
N90-13152
N90-13155
VAKILI, A. D. N90-12527
VALENTOVIC, D. N90-13252
VALKEILA, E. N90-13146
VANBALLEGOOIJEN, A. A. N90-13310
VANDAM, R. N90-12972
VANDAMME, RUUD N90-12750
VANDERGAAG, L. C. N90-13182
VANDERGEER, SARA A. N90-13144
VANDERGRAFT, J. S. N90-12801
VANDERHORST, M. N90-13223
VANDERHOUWEN, P. J. N90-13131
N90-13132
VANDERPLAS, ADRIAAN P. N90-13145
VANDERSCHAFT, A. J. N90-13164
VANDERVORST, H. A. N90-13056
N90-13061
VANDERWOUDE, A. N90-13217
VANEIJK, PETER N90-13062
VANES, A. J. N90-13142
VANGEMERT, P. H. N90-12885
VANGLABBEEK, ROB J. N90-13152
VANKLINKEN, J. N90-13217
VANMILL, JAN N90-13127
VANNEERVEN, J. M. A. M. N90-13149
VANOMMEREN, J. C. W. N90-13165
VANRAAIJ, J. L. N90-13039
VANRIJN, AFKE N90-13106
VANSABBEN, E. N90-12978
VANSCHAGEN, P. A. B. N90-13069
VANSTRIEN, SEBASTIAN N90-13190
VANSWEEDEN, R. N90-12821
VANVELDEN, J. G. N90-13042
VANZANTEN, A. J. N90-13060
VARIAS, A. N90-13239
VASSILIOU, JOHN K. N90-13256
VEDHA-NAYAGAM, M. N90-12645
VEHANEN, A. N90-12722
VELDMAN, H. J. N90-13157
VERNON, SUSAN N. N90-12948
VEST, G. M. N90-12849
VEST, R. W. N90-12849
VIGNAU, F. N90-12897
VIJGEN, PAUL M. H. W. N90-12549

VIKEN, JEFFREY K. N90-12540
N90-12541
VILLARD, GILLES N90-13098
VILLULLAS, H. M. N90-13254
VINK, JEROEN C. N90-13114
N90-13272
VITANYI, PAUL M. B. N90-13191
VOGEL, ALISON ANDREWS N90-13048
VOGEL, H. U. N90-13124
VOGEL, M. H. N90-12822
N90-13234
VOGELESANG, L. B. N90-12778
VONROSENVINGE, TYCHO N90-13314
VOS, J. J. N90-13230

W

WACLAWIK, RONALD E. N90-12940
WAGGONER, ED G. N90-12544
WAGNER, RICHARD D. N90-12511
WAINAUSKI, HARRY S. N90-12617
WAITE, SIMON ROY N90-12660
WAKEFIELD, GREGORY H. N90-13016
WALKER, A. B. C., JR. N90-13306
WALKER, DOREEN M. C. N90-12640
WALLRAPP, OSKAR N90-13080
WALSH, JOANNE L. N90-12582
N90-12588
WALTERS, E. JANE N90-13253
WALTON, E. K. N90-12835
WANG, H. C. N90-12796
WANG, HENRY T. N90-12900
N90-13176
WANG, JIARONG N90-12752
WANG, YONG N90-12973
WARBER, CHRIS R. N90-12836
N90-12837
WARD, J. N90-12841
WARD, MICHAEL J. N90-12910
WARMING, ROBERT F. N90-13137
WARNER, D. J. N90-13269
WARREN, J. B. N90-12754
WATSON-VIKEN, SALLY A. N90-12540
WATTS, ETHEL J. N90-12714
WEAVER, J. N. N90-12844
WEHRLI, CH. N90-13305
WEIL, HERSCHEL N90-12711
WEINBERG, F. J. N90-12766
WEINBERG, R. P. N90-13025
WEINREB, M. P. N90-12968
WEINSHALL, DAPHNA N90-13195
WEISER, H. N90-13310
WEISS, GEORGE N90-13168
WELLS, WILLIAM M., III N90-12941
WEN, CHUDONG N90-12648
WESSELING, P. N90-12886
N90-13128
WEVER, TOBIAS N90-12974
WHETSTONE, JAMES R. N90-12892
WHITTAKER, WILLIAM N90-12944
WIBBERENZ, GERD N90-13314
WIEDEMANN, H. N90-12844
WIKLANDER, DAG N90-12953
WILBURN, ANNE MARIE N90-13010
WILHELM, K. N90-13307
WILKEN, B. N90-13313
WILLAN, KENNETH A. N90-12633
WILLETT, J. C. N90-13008
WILLIAMS, A. N90-12789
WILLIAMS, D. C. N90-12875
WILLIAMS, ROBERT W. N90-12848
WILLIAMS, ROGER T. N90-12998
WILLIAMSON, R. G. N90-12984
WILSCHUT, H. W. N90-13216
N90-13225
WILSDORF, HEINZ G. N90-12966
WILSON, R. R. N90-12880
WINCHENBACH, G. L. N90-12567
WINELAND, D. J. N90-13244
WINTERBOTTOM, A. N. N90-12641
WITHBROE, G. L. N90-13310
WOLD, AARON N90-13271
WOLFSON, C. J. N90-13306
WON, YONG-GU N90-12666
WOO, SAMUEL N90-12892
WOOD, A. W. N90-13067
WOOD, M. E. N90-13202
WORSLEY, M. F. N90-12815
N90-13005
WRIGHT, R. GLENN N90-13091
WU, J. M. N90-12527
WU, P. N90-13271
WYNDHAM, B. A. N90-12816

X

XIE, R. N90-12968
XIE, X. Y. N90-13216
XU, ZHUPING N90-12657

Y

YAMARTINO, J. M. N90-12875
YANG, YUXING N90-12752
YAP, B. K. N90-12986
YATES, J. T., JR. N90-12691
YEAGER, E. B. N90-13254
YEATON, ROBERT B. N90-12523
YEE, E. N90-13188
YIM, E. S. N90-13226
YODER, MARK N90-13235
YOON, H. S. N90-12735
YOUNGBLOOD, WALLACE W. N90-12645
YOUNGDAHL, KAY A. N90-12736
YU, LU N90-13251

Z

ZABIELSKI, CHESTER V. N90-12734
ZACHOR, A. S. N90-12986
ZACK, JOHN W. N90-13228
ZALZALA, ALI M. S. N90-13102
N90-13104
ZAMAN, K. B. M. Q. N90-12561
ZANG, TOM A. N90-12533
ZANOLI, JAMES J. N90-12971
ZEGELING, P. A. N90-13136
ZHANG, GUOCHANG N90-12644
ZHANG, Y. Q. N90-12768
ZHANG, Z. N90-13225
ZHAOBIN, SU N90-13251
ZIEBARTH, ROBIN P. N90-13256
ZINSMEYER, C. D. N90-12928
ZOMAYA, A. Y. N90-13103
ZONDAG, E. G. N90-13095
N90-13096

Typical Corporate Source Index Listing

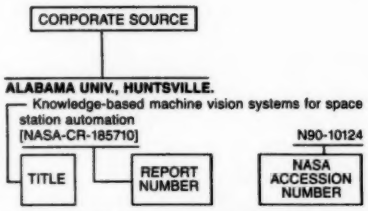

Listings in this index are arranged alphabetically by corporate source. The title of the document provides the user with a brief description of the subject matter. The report number helps to indicate the type of document cited (e.g., NASA report, translation, NASA contractor report). The NASA accession number denotes the number by which the citation is identified. The titles are arranged under each corporate source in ascending accession number order.

A

ADVANCED DECISION SYSTEMS, MOUNTAIN VIEW, CA.
Telerobotic control for teams of semi-autonomous agents, phase 1
[AD-A211648] N90-13037
Spatial data structures for robotic vehicle route planning
[AD-A212806] N90-13111

ADVISORY GROUP FOR AEROSPACE RESEARCH AND DEVELOPMENT, NEUILLY-SUR-SEINE (FRANCE).
Guidance and Control Panel Symposium on Guidance and Control of Unmanned Air Vehicles
[AGARD-AR-260] N90-12623

AERITALIA S.P.A., TURIN (ITALY).
Development and applications of reliability and maintainability design criteria in military aircraft
[ETN-89-95208] N90-12591
Acquisition and recording an AMX A/C. Aeritalia experience and present trends
[ETN-89-95217] N90-12598
Project, implementation, and utilization of composite structures
[ETN-89-95209] N90-12665
Fatigue behavior of specimens under compression load spectra
[ETN-89-95207] N90-12954

AERONAUTICAL RESEARCH INST. OF SWEDEN, STOCKHOLM.
Damage tolerance of CFRP sandwich panels
[FFA-TN-1988-70] N90-12664
Potential difference applied to the measurement of small fatigue crack growth at notches in Ti-6Al-4V
[FFA-TN-1989-09] N90-12952
Multilevel optimization with system Optsys
[FFA-TN-1988-60] N90-12953

AERONAUTICAL RESEARCH LABS., MELBOURNE (AUSTRALIA).
Additions and corrections to SUPER: A program for calculating steady and oscillatory supersonic flow over a thin wing, tail plane and fin
[AD-A211771] N90-12501
Development of a VSAERO (Vortex Separation Aerodynamics) model of the F/A-18
[AD-A212442] N90-12566
RTSIN1: A model of a strapdown INS on a two-axis rate table
[AD-A212406] N90-12579
FPG2: A flight profile generator program
[AD-A212408] N90-12595
RAN (Royal Australian Navy) vibration analysis system operator's guide
[AD-A212441] N90-12596
Evaluation of a damaged F/A-18 horizontal stabilator
[AD-A212573] N90-12597

AEROSPACE CORP., EL SEGUNDO, CA.
Batch LCAP2-linear control analysis, version 2.0: User's manual
[AD-A211670] N90-12643
Standard method for measurement of nonvolatile residue on surfaces
[AD-A213324] N90-12714
Structural studies of sputter-deposited MoS2 solid lubricant films
[AD-A212407] N90-12759
Thermionic emission including both space charge and image forces
[AD-A212732] N90-12869
Strong-inversion model of threshold voltage in modulation doped field effect transistors: The role of unintentional acceptors
[AD-A212750] N90-12870
Photodissociation of XeF2 (xenon difluoride) at 193 nm
[AD-A211663] N90-12916
Design and tests of simple, inexpensive optical beacon for use on small satellites
[AD-A213325] N90-13238

AEROSPATIALE, SURESNES (FRANCE).
A study of progressive cracking damage to carbon-epoxy composites and methods of crack reduction
[REPT-RE-49-324/F] N90-12676

AIR FORCE ACADEMY, CO.
Heat capacities of 1-methyl-3-ethylimidazolium chloride-aluminum chloride molten salts
[AD-A212790] N90-12707
Magnetically insulated electron flows in pulsed power systems
[AD-A212746] N90-13196

AIR FORCE ARMAMENT LAB., EGLIN AFB, FL.
Aerodynamic test and analysis of a slender generic missile configuration
[AD-A212522] N90-12567
Design and commissioning test results for the hypervelocity launcher research complex battery power supply
[AD-A211320] N90-12848
Unsteady three-dimensional thin-layer Navier Stokes solutions on dynamic blocked grids
[AD-A212377] N90-12899

AIR FORCE ASTRONAUTICS LAB., EDWARDS AFB, CA.
Proceedings of the 10 May 1989 Antiproton Technology Workshop: Addendum
[AD-A212804] N90-13227

AIR FORCE GEOPHYSICS LAB., HANSCOM AFB, MA.
Optical detection of space debris using a large achromatic coronagraph
[AD-A211362] N90-12647
Role of chemical effects in daytime high latitude trough formation
[AD-A211772] N90-12989
Comments on the use of LOWTRAN in transmission calculations for sites with the ground elevated relative to sea level
[AD-A212724] N90-12995

AIR FORCE HUMAN RESOURCES LAB., BROOKS AFB, TX.
Individual differences in associative learning and forgetting
[AD-A212765] N90-13034

AIR FORCE INST. OF TECH., WRIGHT-PATTERSON AFB, OH.
The analysis of current-mirror MOSFETs for use in radiation environments
[AD-A212527] N90-12866
A comparison of two subject-controlled attitude measures during somatogravic illusion exposure
[AD-A212528] N90-13031

AIR FORCE OCCUPATIONAL AND ENVIRONMENTAL HEALTH LAB., BROOKS AFB, TX.
Base level management of radio frequency radiation protection program
[AD-A211759] N90-13017

AIR FORCE SYSTEMS COMMAND, BOLLING AFB, WASHINGTON, DC.
Report on orbital debris
[NASA-TM-101855] N90-12635

AIR FORCE SYSTEMS COMMAND, WRIGHT-PATTERSON AFB, OH.
Present and future US and Soviet chemical missiles and chemical rocket projectiles
[AD-A212199] N90-12644
A data acquisition and processing system for six component solid rocket motor testing
[AD-A212200] N90-12657
Analysis of carbon fiber's x ray microscopic structure
[AD-A212215] N90-12752

AIR FORCE WRIGHT AERONAUTICAL LABS., WRIGHT-PATTERSON AFB, OH.
Subspace iteration algorithms in FORTRAN 77 and FORTRAN 8x
[AD-A212275] N90-13083

ALABAMA UNIV., HUNTSVILLE.
Vibration isolation technology: Sensitivity of selected classes of space experiments to residual accelerations
[NASA-CR-185443] N90-12768
Analysis and modeling of summertime convective cloud and precipitation structure over the Southeastern United States
[NASA-CR-185436] N90-12996

ALASKA UNIV., FAIRBANKS.
Development of computer codes to model dynamics of the earth's magnetosphere
[AD-A211532] N90-12987

ALTEX TECHNOLOGIES CORP., SANTA CLARA, CA.
Characterization of nonpremixed turbulent bluff-body burner flames
[PB89-229447] N90-12689

AMERICAN SOCIETY FOR TESTING AND MATERIALS, PHILADELPHIA, PA.
Laser Induced Damage in Optical Materials: 1987
[PB89-221162] N90-12913

ANALYTICAL SERVICES AND MATERIALS, INC., HAMPTON, VA.
Long-range LFC transport N90-12508

ARGONNE NATIONAL LAB., IL.
B factory via conversion of 1 TeV electron beams into 1 TeV photon beams
[DE89-017692] N90-12914

ARIZONA STATE UNIV., TEMPE.
Heat pipe and thermal energy storage and corrosion studies (1988)
[AD-A212655] N90-12706
Prediction of thermal stress casualties
[AD-A212356] N90-13022

ARIZONA UNIV., TUCSON.
Boundary-layer receptivity and laminar-flow airfoil design N90-12516
Synthesis and crystallization behavior of fluoride glasses
[AD-A212142] N90-12741

ARMY ARMAMENT MUNITIONS AND CHEMICAL COMMAND, DOVER, NJ.
Expert system for test program set fault candidate selection
[AD-A213338] N90-13091

ARMY AVIATION SYSTEMS COMMAND, HAMPTON, VA.
Rotor blade structural design N90-12584
Validation of the procedures N90-12587

ARMY COLD REGIONS RESEARCH AND ENGINEERING LAB., HANOVER, NH.
Estimation of time to maximum supercooling during dynamic frazil ice formation
[AD-A212204] N90-12699

ARMY LAB. COMMAND, WATERTOWN, MA.
Biaxial flexing of a fiber-reinforced aluminum composite
[AD-A212742] N90-12681
Corrosion and corrosion inhibition of metals/alloys in methylphosphonic difluoride and decontaminating solutions
[AD-A212404] N90-12734

Proceedings of the Army Symposium on Solid Mechanics, 1989: Mechanics of Engineered Materials and Applications
[AD-A211954] N90-12951

ARMY MATERIALS TECHNOLOGY LAB., WATERTOWN, MA.
Effects of hot corrosion on the room temperature strength of structural ceramics
[AD-A212568] N90-12762

ARMY NATICK RESEARCH AND DEVELOPMENT COMMAND, MA.
Air Force flight feeding. Volume 1: Evaluation of current system and alternative concepts
[AD-A212789] N90-13043

ARMY RESEARCH INST. OF ENVIRONMENTAL MEDICINE, NATICK, MA.
Heat exhaustion
[AD-A212128] N90-13014
Exertional heatstroke: An international perspective. An introduction: The role of exercise in the etiology of exertional heatstroke
[AD-A212242] N90-13020

ATMOSPHERIC RADIATION CONSULTANTS, ACTON, MA.
Retrieval of atomic oxygen and temperature in the thermosphere. Part 1: Feasibility of an experiment based on the spectrally resolved 147 micrometer limb emission
[AD-A211987] N90-12986

AUBURN UNIV., AL.
Low Earth Orbit Raider (LER) winged air launch vehicle concept
[NASA-CR-186057] N90-12590
Proposal for a zero-gravity toilet facility for the space station
[NASA-CR-183151] N90-13036

B

BALLISTIC RESEARCH LABS., ABERDEEN PROVING GROUND, MD.
Spark camera annotation and control system for the BRL (Ballistic Research Laboratory) Transonic Range Facility
[AD-A212266] N90-12633
Structures and energies for small borane compounds: One and two boron compounds
[AD-A212264] N90-12701
Extended basis set calculations of atomization energies: Comparison of isogyric and direct results
[AD-A212268] N90-12702
Continuing studies of liquid propellant drops in hot, high-pressure environments
[AD-A212265] N90-12765
Stress waves through projectile joints and interfaces
[AD-A212201] N90-12963
The effect of a rigid elliptical inclusion on a straight crack
[AD-A212263] N90-12965

BDM CORP., AUSTIN, TX.
A robot which will investigate the condition of underground pipe
[PB89-230650] N90-12928

BEN GURION UNIV. OF THE NEGEV, BEERSHEVA (ISRAEL).
Electrically conducting organic materials: Design, synthesis and characterization
[AD-A212214] N90-12700

BERN UNIV. (SWITZERLAND).
Berne solar observations
[REPT-55] N90-13301

BOEING COMMERCIAL AIRPLANE CO., SEATTLE, WA.
Laminar flow: Challenge and potential N90-12504
The 757 NLF glove flight test results N90-12546
Variable-Sweep Transition Flight Experiment (VSTFE): Stability code development and clean-up glove data analysis N90-12548

BOEING MILITARY AIRPLANE DEVELOPMENT, SEATTLE, WA.
Design and test of a natural laminar flow/large Reynolds number airfoil with a high design cruise lift coefficient N90-12543

BROOKHAVEN NATIONAL LAB., UPTON, NY.
Polyelectrolyte-diffused zinc phosphate conversion coatings and polyacid coupling primers for corrosion protection of steel and aluminum, and alkali-catalyzed hydrolysis of polyimide-based materials
[AD-A212240] N90-12754

BROWN UNIV., PROVIDENCE, RI.
Growth and characterization of zinc sulfide films by conversion of zinc oxide films with H2S
[AD-A213345] N90-13271

BUREAU OF MINES, AMARILLO, TX.
Improved method for determination of helium-4 in helium-3 by mass spectrometry
[PB89-201404] N90-12686

C

CALIFORNIA INST. OF TECH., PASADENA.
Research in cosmic and gamma ray astrophysics
[NASA-CR-185451] N90-13316

CALIFORNIA UNIV., BERKELEY.
Investigation of turbulent flow in highly curved ducts with application to turbomachinery components
[NASA-CR-186060] N90-12882

CALIFORNIA UNIV., DAVIS.
Numerical algorithms for steady and unsteady incompressible Navier-Stokes equations
[NASA-CR-186039] N90-12499

CALIFORNIA UNIV., LOS ANGELES.
Oxide ceramic fibers by the sol-gel methods
[AD-A211315] N90-12742

CALIFORNIA UNIV., RIVERSIDE.
Fractional charging and reentrance in granular superconductors N90-13248

CALIFORNIA UNIV., SAN DIEGO.
Electrophysiological studies of visual attention and resource allocation
[AD-A212287] N90-13030

CALIFORNIA UNIV., SANTA BARBARA.
Measurement and correlation of the solubility and diffusion coefficient for oxygen and chlorine in basic hydrogen peroxide
[AD-A212348] N90-12703
Improvement and extension of a radar forest backscattering model
[NASA-CR-186083] N90-12973
High speed quantum-well optoelectronic devices by MBE
[AD-A212585] N90-13237

CALSPAN CORP., BUFFALO, NY.
Investigation of North Atlantic fog and development of a marine fog forecast system
[AD-A211780] N90-12999

CAMBRIDGE UNIV. (ENGLAND).
Fundamentals of middle atmospheric dynamics
[AD-A211747] N90-12988

CARNEGIE-MELLON UNIV., PITTSBURGH, PA.
Development of an integrated mobile robot system at CMU (Carnegie-Mellon University)
[AD-A212555] N90-12944
Acceleration sets of planar manipulators. Part 1: Theory
[AD-A213162] N90-12945

CASE WESTERN RESERVE UNIV., CLEVELAND, OH.
The effects of trace anions on the voltammetry of single crystal gold surfaces
[AD-A211886] N90-13254

CELGENE CORP., WARREN, NJ.
Biological and biochemical methane reactions
[PB89-232615] N90-12977

CENTER FOR MATHEMATICS AND COMPUTER SCIENCE, AMSTERDAM (NETHERLANDS).
Upwind discretization of the steady Navier-Stokes equations
[CWI-NM-R8810] N90-12891
Solving 3D block bidiagonal linear systems on vector computers
[CWI-NM-R8819] N90-13061
Multiplicative iterative algorithms for convex programming
[CWI-AM-R8808] N90-13072
Expert systems as deductive systems
[CWI-CS-R8825] N90-13073
A simple definition for parallel composition of prime event structures
[CWI-CS-R8903] N90-13074
Proving total correctness of recursive procedures
[CWI-CS-R8904] N90-13075
Process expressions and Hoare's logic
[CWI-CS-R8905] N90-13076
Characterizing termination of logic problems with level mappings
[CWI-CS-R8912] N90-13077
Smoothed predictor-corrector methods for solving partial differential equations
[CWI-NM-R8808] N90-13131
Iterated theta method for hyperbolic equations
[CWI-NM-R8809] N90-13132
An algebraic characterization of B-convergent Runge-Kutta methods
[CWI-NM-R8901] N90-13133
Increasing the real stability boundary of explicit methods
[CWI-NM-R8902] N90-13134
NUMVEC FORTRAN library manual chapter: Simultaneous linear equations
[CWI-NM-R8903] N90-13135
A moving-grid interface for systems of one-dimensional time-dependent partial differential equations
[CWI-NM-R8904] N90-13136
Meixner-Pollaczek polynomials and the Heisenberg algebra
[CWI-PM-R8806] N90-13138
Jacobi functions as limit cases of q-ultraspherical polynomials
[CWI-PM-R8807] N90-13139
Representations of the twisted SU(2) quantum group and some q-hypergeometric orthogonal polynomials
[CWI-PM-R8809] N90-13140
Index formulas for generalized Wiener-Hopf operators and Boson-Fermion correspondence in 2N dimensions
[CWI-PM-R8811] N90-13141
A kernel approach to estimation of the sphere radius density in Wicksell's corpuscle problem
[CWI-MS-R8809] N90-13142
Tail triviality for sums of stationary random variables
[CWI-MS-R8810] N90-13143
On a rate of convergence of the multiknapsack value function
[CWI-MS-R8812] N90-13144
A semiparametric model for citation counts
[CWI-MS-R8814] N90-13145
On the Hellinger type distances for filtered experiments
[CWI-MS-R8818] N90-13146
On the smooth fit boundary conditions in the optimal stopping problem for semimartingales
[CWI-MS-R8819] N90-13147
Lie-algebraic aspects of the classical nonrelativistic Calogero-Moser models
[CWI-AM-R8901] N90-13148
Hahn-Banach type theorems for dual semigroups
[CWI-AM-R8903] N90-13149
The algebraic basis of mathematical morphology. Part 2: Openings and closings
[CWI-AM-R8904-PT-2] N90-13150
The addition formula for little q-Legendre polynomials and the SU(2) quantum group
[CWI-AM-R8906] N90-13151
Modular specifications in process algebra with curious queues
[CWI-CS-R8821] N90-13152
Semantics and consistency of rule-based expert systems
[CWI-CS-R8824] N90-13153
Placing mirrors in grids
[CWI-CS-R8906] N90-13154
An algebra for process creation
[CWI-CS-R8907] N90-13155
Faster Phong shading via angular interpolation
[CWI-CS-R8909] N90-13156
Berry-Esseen rates and bootstrap results for generalized L-statistics
[CWI-MS-R8808] N90-13179
A statistical analysis of spatial point patterns, a case study
[CWI-MS-R8813] N90-13180
Random truncation models and Markov processes
[CWI-MS-R8817] N90-13181
Different notions of uncertainty in quasi-probabilistic models
[CWI-CS-R8847] N90-13182
Nongaussian linear filtering, identification of linear systems, and the symplectic group
[CWI-PM-R8810] N90-13184
Kolmogorov complexity and its applications
[CWI-CS-R8901] N90-13191

CENTRE D'ETUDES ET DE RECHERCHES, TOULOUSE (FRANCE).
Hypersonic boundary layers. Viscous effects within the shock layer
[CERT-RSF-OA-25/5005-AYD] N90-12502
Modeling of the dielectric behavior of composite materials
[CERT-1/1398-MO] N90-12674
Three-dimensional shear flows: Analysis of the track and angle of incidence
[CERT-RTS-OA-31/5025-AYD] N90-12888
Reduction of turbulent drag: Boundary layer manipulators
[CERT-RSF-OA-74/2259-AYD] N90-12889
Transition in surface boundary layers
[CERT-RSF-OA-43/5018-AYD] N90-12897

CENTRE NATIONAL DE LA RECHERCHE SCIENTIFIQUE, VERRIERES-LE BUISSON (FRANCE).
GOLF: Global Oscillations at Low Frequencies for the SOHO mission N90-13304
SWAN: A study of solar wind anisotropies N90-13312

CENTRE SCIENCTIFIQUE ET TECHNIQUE DU BATIMENT, SAINT-MARTIN-D'HERES (FRANCE).
Wind effect on sound wave propagation at ground vicinity
[CSTB-2-87-008] N90-13201

CENTRE TECHNIQUE DES INDUSTRIES MECANIQUES, NANTES (FRANCE).
The effects of heat treatment after welding on the functional properties of assemblies of CrMo alloys. Heat treatment of a mixed assembly of A48 and 10CD9.10 alloys
[CETIM-104320] N90-12724
How the common practice of heating plates of austenitic stainless steel during cooling affects their mechanical properties
[CETIM-104500] N90-12725
Influence of the composition of the metal deposited on carbon manganese welds on the work properties of the melted area depending on the operating mode of the weld
[CETIM-104530] N90-12726
CENTRE TECHNIQUE DES INDUSTRIES MECANIQUES, SENLIS (FRANCE).
Numerical analysis of notch test damage to laminated composite plates submitted to uniaxial traction
[CETIM-107310] N90-12675
The relationship between the mechanical properties of materials after press forming and their in-service properties
[CETIM-101530] N90-12723
Improvement in pre-constraint fatigue resistance of modular ferretic and bainitic steel by shot peening treatments
[CETIM-106370] N90-12727
Carbonitriliion response of steel plates not destined for heat treatments
[CETIM-106960] N90-12728
The quality of vacuum deposited surface treatments
[CETIM-107040] N90-12729
A feasibility study of hydrogen dosage estimation in screw threads submitted to surface electrolytic treatment
[CETIM-110110] N90-12730
Characterization of self-lubricating surface materials
[CETIM-108060] N90-12749
A theoretical method for the mechanical calculation of heat exchangers with sliding heads, phase 1 study
[CETIM-110240-PHASE-1] N90-12896
Vibration intensity. Evaluation of a remote measuring system
[CETIM-110430] N90-12907
Improvement of rules relating to clamp calculations
[CETIM-110610] N90-12939
Fatigue testing of welded steel assemblies with or without finishing treatments
[CETIM-107900] N90-12961
Increased fragility of deep pressed thin plates
[CETIM-13-Y-313] N90-12962
CENTRE TECHNIQUE DES INDUSTRIES MECANIQUES, SAINT ETIENNE (FRANCE).
Behavior of the adhesive A2 submitted to mechanical traction
[CETIM-105290] N90-12748
Cold press lubrication: Fine tuning of the CETIM Forgelub test
[CETIM-105160] N90-12938
What is the balance sheet for investment in automated manufacturing
[CETIM-105490] N90-13071
CESKOSLOVENSKA AKADEMIE VED, PRAGUE.
Effect of the length of the multijunction grill on its lower hybrid current drive efficiency
[IPPCZ-283] N90-13240
On optimization of the multijunction grill for the lower hybrid current drive
[IPPCZ-280] N90-13241
CESSNA AIRCRAFT CO., WICHITA, KS.
Laminar flow: The Cessna perspective N90-12507
CHALMERS UNIV. OF TECHNOLOGY, GOETEBORG (SWEDEN).
Estimating the time to fatigue failure of mooring cables
[PB89-220677] N90-12946
CHEMICAL RESEARCH AND DEVELOPMENT CENTER, ABERDEEN PROVING GROUND, MD.
Infrared spectrometry of aerosols
[AD-A213303] N90-12713
Infrared water vapor continuum absorption: New atmospheric electrical measurements and theory
[AD-A212594] N90-12994
CINCINNATI UNIV., OH.
Structure and properties of polymer interphases
[AD-A212796] N90-12763
CITY UNIV., LONDON (ENGLAND).
Optical fibre witnesses of fatigue damage in composite materials N90-12660
CIVIL AVIATION AUTHORITY, LONDON (ENGLAND).
Development and evaluation at ATCEU of executive and support operations, phase 4A/3D
[CAA-PAPER-88017] N90-12572
Operational trial of effect of raising minimum stack level in Heathrow stacks
[CAA-PAPER-89003] N90-12573
Assessment of voice coders for ATC/pilot voice communications via satellite digital communication channels
[CAA-PAPER-89004] N90-12807
COLORADO STATE UNIV., FORT COLLINS.
A new generation of atmospheric tracers: The biological connection
[AD-A212285] N90-12983
Multiparameter radar estimation of raindrop size distribution
[AD-A212410] N90-13007
COLORADO UNIV., BOULDER.
Numerical experiments on transition control in wall-bounded shear flows N90-12536
Cloud cover determination in polar regions from satellite imagery
[NASA-CR-186096] N90-13003
COLUMBIA UNIV., NEW YORK, NY.
Theoretical and experimental research on a millimeter-wavelength free-electron laser
[AD-A213321] N90-12925
COMMISSION ON INTEGRATED LONG-TERM STRATEGY, WASHINGTON, DC.
Recommended changes in US military space policies and programs: A paper submitted to the Commission on Integrated Long-Term Strategy
[PB89-219364] N90-12636
COMMITTEE ON APPROPRIATIONS (U.S. HOUSE).
Departments of Veterans Affairs and Housing and Urban Development, and Independent Agencies Appropriations Bill, 1990
[H-REPT-101-150] N90-13281
National Aeronautics and Space Administration N90-13282
COMMITTEE ON APPROPRIATIONS (U.S. SENATE).
Departments of Veterans Affairs and Housing and Urban Development, and Independent Agencies Appropriation Bill, 1990
[S-REPT-101-128] N90-13284
COMMITTEE ON COMMERCE, SCIENCE, AND TRANSPORTATION (U.S. SENATE).
National Aeronautics and Space Administration Authorization Act, fiscal year 1990
[S-REPT-101-157] N90-13288
National Aeronautics and Space Administration Authorization Act, fiscal year 1990
[S-REPT-101-157] N90-13289
COMMITTEE ON SCIENCE, SPACE AND TECHNOLOGY (U.S. HOUSE).
Fiscal year 1990 authorization request and budget estimates for the National Aeronautics and Space Administration
[GPO-98-945] N90-13283
The 1990 National Aeronautics and Space Administration Authorization
[GPO-98-466] N90-13285
COMMITTEE ON SCIENCE AND TECHNOLOGY (U.S. HOUSE).
NASA technology applications
[GPO-99-412] N90-13290
COMPUTATIONAL PHYSICS, INC., NEWTON, MA.
Role of chemical effects in daytime high latitude trough formation
[AD-A211772] N90-12989
COMPUTER SCIENCES CORP., HAMPTON, VA.
Spacecraft Orbit Design and Analysis (SODA), version 1.0 user's guide
[NASA-CR-181932] N90-13050
CONGRESS OF THE UNITED STATES, WASHINGTON, DC.
Department of Veterans Affairs and Housing and Urban Development, and Independent Agencies Appropriations Act, 1990
[HR-2916-PP] N90-13286
National Aeronautics and Space Administration N90-13287
CONSEJO SUPERIOR DE INVESTIGACIONES CIENTIFICAS, MADRID (SPAIN).
Workshop on Recent Progress in Surface and Volume Scattering
[AD-A212455] N90-13236
CORNELL UNIV., ITHACA, NY.
Ion beam analysis of diffusion in polymer glasses
[AD-A212339] N90-12756
Vortex dynamics
[AD-A212119] N90-12877
Synthesis and properties of NdNiO(3) prepared by low temperature methods
[AD-A212117] N90-13256
CRANFIELD INST. OF TECH., BEDFORD (ENGLAND).
Shear fatigue testing and life prediction of fibre composites
[REPT-8519] N90-12668

D

DANISH RESEARCH CENTER FOR APPLIED ELECTRONICS, HOERSHOLM.
Preliminary investigation of Faraday rotation effects and description of polarization measurements on the AFGL high latitude meteor scatter test bed
[AD-A211298] N90-12806
DAYTON UNIV., OH.
Field-of-View variations and stripe-texturing effects on assault landing performance in the C-130 weapon system trainer
[AD-A212763] N90-12634
Graduate fellowships in the field of hard magnetic materials
[AD-A212303] N90-12733
DEFENCE AND CIVIL INST. OF ENVIRONMENTAL MEDICINE, DOWNSVIEW (ONTARIO).
The effect of concurrent strength and endurance training on electromechanical delay, maximum voluntary contraction, and rate of force development
[AD-A213316] N90-13028
DEFENCE RESEARCH ESTABLISHMENT ATLANTIC, DARTMOUTH (NOVA SCOTIA).
Chordwise loading and camber for two-dimensional thin sections
[AD-A213318] N90-12568
IBM PC analysis of polarization resistance data
[AD-A212294] N90-12732
DEFENCE RESEARCH ESTABLISHMENT SUFFIELD, RALSTON (ALBERTA).
The shape of the probability density function of short-term concentration fluctuations of plumes in the atmospheric boundary layer
[AD-A212632] N90-13188
DEFENSE MAPPING AGENCY SYSTEMS CENTER, RESTON, VA.
Geodetic point positioning with GPS (Global Positioning System) carrier beat phase data from the CASA UNO experiment
[AD-A211955] N90-12970
DEPARTMENT OF HEALTH AND HUMAN SERVICES, WASHINGTON, DC.
Cross-axis synchronous flow through coil planet centrifuge for large-scale preparative countercurrent chromatography
[PB89-200174] N90-12682
DEPARTMENT OF THE ARMY, WASHINGTON, DC.
Null offset voltage compensator for operational amplifier
[AD-D014189] N90-12859
DEPARTMENT OF THE NAVY, WASHINGTON, DC.
Pivotal mono wing cruise missile with wing deployment and fastener mechanism
[AD-D014191] N90-12594
Curable polyether compositions
[AD-D014200] N90-12679
High temperature insulators
[AD-D014193] N90-12751
Image preprocessing by modified median filter
[AD-D014199] N90-12828
Thin-film integrated injection logic
[AD-D014190] N90-12860
Video line processor
[AD-D014198] N90-12861
RF and dc desensitized electroexplosive device
[AD-D014206] N90-12862
Structural vibration and shock isolator
[AD-D014202] N90-12940
Device for inspection of materials by eddy current methods
[AD-D014205] N90-12948
Method for growing patterned thin films of superconductors
[AD-D014195] N90-13262
DEUTSCHE FORSCHUNGS- UND VERSUCHSANSTALT FUER LUFT- UND RAUMFAHRT, BRUNSWICK (GERMANY, F.R.).
Hybrid angular velocity reference system for the investigation of dynamic properties of strapdown gryos
[DFVLR-FB-89-25] N90-12577
DEUTSCHE FORSCHUNGS- UND VERSUCHSANSTALT FUER LUFT- UND RAUMFAHRT, OBERPFAFFENHOFEN (WEST GERMANY).
An attempt to draw conclusions from the vegetation to the geological underground in the area of Amberg (Germany, F.R.) by means of digital image processing of TM data
[DFVLR-FB-89-24] N90-12974
Computer oriented methods of multibody dynamics for application in vehicle technology
[DFVLR-FB-89-17] N90-13080

DEUTSCHE FORSCHUNGS- UND VERSUCHSANSTALT FUER LUFT- UND RAUMFAHRT, STUTTGART (GERMANY, F.R.).
Microwave excitation of oxygen O2 (delta 1) for an oxygen-iodine laser
[DFVLR-FB-89-23] N90-12919
DEUTSCHE FORSCHUNGSANSTALT FUER LUFT- UND RAUMFAHRT, BRUNSWICK (GERMANY, F.R.).
Automatic processing of images from the GRATE flight test tool
[DLR-FB-89-28] N90-12599
DEUTSCHE FORSCHUNGSANSTALT FUER LUFT- UND RAUMFAHRT, COLOGNE (GERMANY, F.R.).
Biochemical and physiological changes in glider pilots during multihour flights
[DLR-FB-89-29] N90-13018
Effects of a time zone shift of nine hours on the circadian rhythms in cockpit aircrew members on longhaul flights
[DLR-FB-89-31] N90-13019
DEUTSCHE FORSCHUNGS- UND VERSUCHSANSTALT FUER LUFT- UND RAUMFAHRT, OBERPFAFFENHOFEN (GERMANY, F.R.).
Conception and results of the DLR realtime azimuth processor for the E-SAR system
[DLR-FB-89-30] N90-12827
DEUTSCHE FORSCHUNGSANSTALT FUER LUFT- UND RAUMFAHRT, STUTTGART (GERMANY, F.R.).
Interactive computer program for the generation of enthalpy-entropy and temperature-entropy charts of nitrogen and hydrogen
[DLR-FB-89-27] N90-13081
DOUGLAS AIRCRAFT CO., INC., LONG BEACH, CA.
LFC: A maturing concept
[DOUGLAS-PAPER-7878] N90-12505
The right wing of the LEFT airplane N90-12510
UHB demonstrator interior noise control flight tests and analysis
[NASA-CR-181897] N90-13196
DYNAMIC CONTROLS, INC., DAYTON, OH.
Advanced actuation systems development, volume 1
[AD-A213334] N90-12624

E

EA-MUELLER, INC., BALTIMORE, MD.
Research and Development Opportunities in Supercritical Fluid Technology
[DE89-015320] N90-12684
ECOLE NATIONALE SUPERIEURE DES TELECOMMUNICATIONS, PARIS (FRANCE).
Simulation of circuits adapted to signal processing
[TELECOM-PARIS-89-E001] N90-12811
Ground effects on multipath fading
[TELECOM-PARIS-88-E017] N90-12812
State of the art of human/machine dialog tool prototypes
[TELECOM-PARIS-89-H001] N90-13038
The application of artificial intelligence techniques to tracing the interconnections in an integrated circuit
[TELECOM-PARIS-89-E002] N90-13105
ELORET CORP., SUNNYVALE, CA.
Rotational and vibrational nonequilibrium effects in rarefied, hypersonic flow
[NASA-CR-182559] N90-12498
ENERGETICS, INC., COLUMBIA, MD.
Research and Development Opportunities in Supercritical Fluid Technology
[DE89-015320] N90-12684
ESDU INTERNATIONAL LTD., LONDON (ENGLAND).
Thermophysical properties of benzene. Part 1: The ideal gas and the saturated liquid and vapour
[ESDU-89002-PT-1] N90-12693
Thermophysical properties of benzene. Part 2: Thermodynamic properties at elevated pressures
[ESDU-89003-PT-2] N90-12694
Two-phase flow pressure losses in pipeline fittings
[ESDU-89012] N90-12883
ETABLISSEMENT TECHNIQUE CENTRAL DE L'ARMEMENT, ARCUEIL (FRANCE).
A study of the impact of a ball bearing on a long fiber composite plate with a carbon matrix, part 2
[ETCA-88-R-088-PT-2] N90-12673
Pyrolytic production of ceramic composites from silicates
[ETCA-89-R-012] N90-12746
Elastic indentation fractures
[ETCA-88-R-116] N90-12955
Radar and sensor array design planning for a naval missile testing center. Artificial intelligence applications
[ETCA-88-R-099] N90-13108
EUROPEAN SPACE AGENCY, PARIS (FRANCE).
A robust digital model following controller for helicopters
[ESA-TT-1041] N90-12621
Dynamic robot models using the Manutec r3 as an example
[ESA-TT-1132] N90-12626
Tropospheric influences on satellite-Earth paths and their determination by means of radar measurements
[ESA-TT-1143] N90-12639
Report on ESA's scientific satellites
[ESA-SP-1110] N90-12649
Biology in microgravity: A guide for experimenters
[ESA-TM-02] N90-12769
On a fast two-dimensional radar imaging process for rotating targets, and an analysis of its image quality
[ESA-TT-1142] N90-12808
Wider horizons: Potential contributions by space systems to socio-economic advancement in developing countries
[ESA-SP-1106] N90-13276
The SOHO mission. Scientific and technical aspects of the instruments
[ESA-SP-1104] N90-13302
European space technology: Celebrating twenty-five years of research and development
[ESA-BR-55] N90-13322
EXETER UNIV. (ENGLAND).
Interaction of Tollmien-Schlichting waves and Goertler vortices N90-12515

F

FEDERAL AVIATION ADMINISTRATION, ATLANTIC CITY, NJ.
Parallel approach separation and controller performance: A study of the impact of two separation standards
[DOT/FAA/CT-TN89/50] N90-12574
Aircraft Reply and Interference Environment Simulator (ARIES) hardware principles of operation. Volume 2: Appendixes
[DOT/FAA/CT-TN88/4-2] N90-12781
Aircraft Reply and Interference Environment Simulator (ARIES) hardware principles of operation, volume 1
[DOT/FAA/CT-TN88/4-1] N90-12782
FEDERAL AVIATION ADMINISTRATION, WASHINGTON, DC.
FAA air traffic activity: Fiscal year 1988
[AD-A211338] N90-12570
FERMI NATIONAL ACCELERATOR LAB., BATAVIA, IL.
Corrections to the thin wall approximation in general relativity
[NASA-CR-186078] N90-13274
Evolution of domain walls in the early universe
[NASA-CR-186076] N90-13297
Small scale structure on cosmic strings
[NASA-CR-186075] N90-13298
Cosmic strings and baryon decay catalysis
[NASA-CR-186074] N90-13299
FLORIDA UNIV., GAINESVILLE.
Kinematics, special configurations and performance evaluation of serial manipulators N90-12927
A two-dimensional hybrid experimental-numerical technique for elastic-plastic stress analysis N90-12949
FLUID JET ASSOCIATES, SPRING VALLEY, OH.
Two dimensional orifice array, monodisperse drop source, phase 1
[AD-A211319] N90-12881
FOERSVARETS FORSKNINGSANTALT, LINKOEPING (SWEDEN).
Digital radio link: Wave propagation investigations on a 13 GHz line-of-sight path
[PB89-213128] N90-12785
Problem-dependent transformations of 3D terrain elevation maps into cost precursor maps
[PB89-218127] N90-12969

G

GALLAUDET COLL., WASHINGTON, DC.
The effects of hearing protectors on speech communication and the perception of warning signals
[AD-A212521] N90-12832
The effects of noise on performance
[AD-A212519] N90-13209
The effects of noise on speech and warning signals
[AD-A212520] N90-13210
GENERAL ELECTRIC CO., CINCINNATI, OH.
Nacelle design N90-12551
GEORGIA INST. OF TECH., ATLANTA.
Numerical simulation of unsteady rotational flow over propfan configurations
[NASA-CR-186037] N90-12500
An investigation of the diffraction of an acoustic plane wave by a curved surface of finite impedance
[NASA-CR-186069] N90-13204
GESELLSCHAFT FUER REAKTORSICHERHEIT, GARCHING (GERMANY, F.R.).
Analytical control of special numerical calculations of pressure propagation in a fluid
[GRS-70] N90-12884
GINER, INC., WALTHAM, MA.
Advanced double layer capacitor
[AD-A211977] N90-12688
GRENOBLE-1 UNIV. (FRANCE).
Built-in generation for CMOS circuits
[IMAG-RR-736-I] N90-12855
NAUTILE: A physical design environment based on an object-oriented data manager
[IMAG-RR-737-I] N90-13094
An error estimator for parameter choice in regulating least square problems. Application to regularized deconvolution
[IMAG-RR-744-M] N90-13125
GRONINGEN RIJKSUNIV. (NETHERLANDS).
Towards a parallel algorithm for the many body problem
[CS-8813] N90-13078
Polymorphism and information loss in Martin-Loef's type theory
[CS-8814] N90-13079
Explicit formulas for Hankel norm approximations of infinite-dimensional systems
[TW-289] N90-13167
Well posedness of triples of operators (in the sense of linear systems theory)
[TW-292] N90-13168
Dimensional reduction at high temperature revisited
[KVI-791] N90-13194
The interacting boson approximation
[KVI-774] N90-13215
Exploring asymmetric heavy-ion reactions at the KX-ray method: The Ne20 + Tb159 reaction at 15 MeV/unit
[KVI-777] N90-13216
Compressibility of heavy nuclei at high temperatures
[KVI-792] N90-13217
Elements of a relativistic microscopic theory of hadronic matter in equilibrium and non-equilibrium
[KVI-796] N90-13218
Activities report of the Kernfysisch Versneller Instituut
[ETN-89-95752] N90-13219
An explicit partition of the fusion-like cross section
[KVI-797] N90-13225
GRUMMAN AEROSPACE CORP., BETHPAGE, NY.
Superplastic forming and diffusion bonding of rapidly solidified, dispersion strengthened aluminum alloys for elevated temperature structural applications
[NASA-CR-181849] N90-12718

H

HAMILTON STANDARD DIV., UNITED AIRCRAFT CORP., WINDSOR LOCKS, CT.
Large-scale Advanced Prop-fan (LAP) static rotor test report
[NASA-CR-180848] N90-12617
HARVARD-SMITHSONIAN CENTER FOR ASTROPHYSICS, CAMBRIDGE, MA.
UVCS: An Ultraviolet Coronagraph Spectrometer for SOHO N90-13310
HEALTH EFFECTS RESEARCH LAB., RESEARCH TRIANGLE PARK, NC.
Effects of atmospheric mix and toxic fumes on military performance
[PB89-223630] N90-13015
HELSINKI UNIV. OF TECHNOLOGY, ESPOO (FINLAND).
Computer simulation studies of the catalytic oxidation of carbon monoxide on platinum metals
[PB89-223739] N90-12721
Temperature dependence of positron diffusion in cubic metals
[PB89-222020] N90-12722
Scalar Green function method for microstrip antenna analysis based on the exact image theory
[PB89-218838] N90-12805
Improved 2D numerical simulation model for strongly coupled heat and fluid flow in a thermal storage
[PB89-218879] N90-12878
Solution of the thin-layer Navier-Stokes equations for laminar transonic flow
[PB89-221600] N90-12879
Self-organizing semantic maps
[PB89-219609] N90-13049
Stable and unstable subspaces of a critical functional differential equation
[PB89-220651] N90-13115
Multigrid solution method for the Euler equations
[PB89-219463] N90-13116
Time-domain Green function corresponding to a time-harmonic point source in complex space
[PB89-218846] N90-13117

Seminars of Applied Physics, Materials Physics and Biomedical Engineering, 1989
[PB89-218572] N90-13192
Persistent current, NMR, and ion transmission experiments in rotating He-3 superfluids
[ISBN-952-90056-1-X] N90-13221
Variational and asymptotic methods in open and closed waveguide analysis
[REPT-34] N90-13229
Superfluid phase slippage in (3)He-B flow through a narrow channel
[PB89-218986] N90-13258

HERIOT-WATT UNIV., EDINBURGH (SCOTLAND).
Application of the moment method to the design of slotted waveguide array antennas N90-12780

HIGH TECHNOLOGY CORP., HAMPTON, VA.
Stability theory applications to laminar-flow control N90-12513

HOWARD UNIV., WASHINGTON, DC.
Stable summability and approximation theory
[AD-A211379] N90-13118

HULBURT (E. O.) CENTER FOR SPACE RESEARCH, WASHINGTON, DC.
LASCO: A wide-field white light and spectrometric coronagraph for SOHO N90-13311

I

ILLINOIS UNIV., CHICAGO.
Labeled trees and the efficient computation of derivations
[NASA-CR-185386] N90-13113

ILLINOIS UNIV., URBANA.
Joint Services Electronics Program
[AD-A212309] N90-12864

IMPERIAL COLL. OF SCIENCE AND TECHNOLOGY, LONDON (ENGLAND).
Laser initiated ignition of liquid propellant
[AD-A212342] N90-12766

INSTITUT FRANCO-ALLEMAND DE RECHERCHES, SAINT-LOUIS (FRANCE).
Volumetric analysis by spontaneous Raman diffusion in a supersonic wind tunnel
[ISL-R-109/88] N90-12564
Improvement of ultrashort pulsed laser shadowgraph photography by means of optical filters
[ISL-CO-215/88] N90-12906
Mathematical simulation of dynamic compression tests using the Hopkinson bar method
[ISL-R-128/87] N90-12960

INSTITUT NATIONAL DES SCIENCES APPLIQUEES DE LYON, VILLEURBANNE (FRANCE).
Influence of the structure of epoxy network models on the volumetric, mechanical and viscoelastic properties
[ISAL-89-0024] N90-12666
Unilateral contact analysis of a crack with friction. Applications
[ETN-89-95511] N90-12956
Study of the electrical and optical properties of the vanadium and nickel impurities in GaAs
[ISAL-89-0028] N90-13259

INSTITUT NATIONAL POLYTECHNIQUE, GRENOBLE (FRANCE).
Formal calculations and parallelism. Solving linear systems
[ETN-89-95499] N90-13098
LAIOS: A multiprocessor network for artificial intelligence applications
[ETN-89-95498] N90-13109

INSTITUTE FOR COMPUTER APPLICATIONS IN SCIENCE AND ENGINEERING, HAMPTON, VA.
Numerical study of three-dimensional spatial instability of a supersonic flat plate boundary layer
[NASA-CR-181931] N90-12874

INSTITUTE FOR DEFENSE ANALYSES, ALEXANDRIA, VA.
The NASA experience in aeronautical R and D: Three case studies with analysis
[AD-A211486] N90-12496
Proceedings of the DOD Workshop on the Manufacturing/Producibility of Organic Matrix Composites
[AD-A212577] N90-12680

INSTITUTE FOR PERCEPTION RVO-TNO, SOESTERBERG (NETHERLANDS).
Pre- and postflight postural control of the D1 Spacelab mission astronauts examined with a tilting room
[IZF-1988-25] N90-13039
Spatial tests for aviators
[IZF-1988-15] N90-13041
Application of active noise reduction for hearing protection and speech intelligibility improvement
[IZF-1988-21] N90-13042
A validation of the proposed NATO standard method to determine target acquisition distances with image intensifiers
[IZF-1988-8] N90-13230

INSTITUTE OF THEORETICAL PHYSICS, AMSTERDAM (NETHERLANDS).
Multigrid Monte Carlo in an external U(1) gauge field
[NIKHEF-ITFA-88-52] N90-13114

INTERNATIONAL CENTRE FOR THEORETICAL PHYSICS, TRIESTE (ITALY).
Symmetry breaking phenomena in liquid Helium-4
[DE89-618886] N90-12685
Physics of the tropospheric radiopropagation
[DE89-619726] N90-12783
Composite vs constituent particle aspects of hole motion in the CuO2 plane
[DE89-618864] N90-13251
Relationship between the current and the width of the POGO electrojet during the solstices
[DE89-619725] N90-13294

IOWA UNIV., IOWA CITY.
Stage effects on stalling and recovery of a high-speed 10-stage axial-flow compressor N90-12600

ISTITUTO NAZIONALE DI FISICA NUCLEARE, PADUA (ITALY).
Survey of the response of standard limited streamer tubes over the complete range of three-component gas mixtures of isobutane, CO(sub 2), argon
[DE89-016692] N90-12875

ISTITUTO NAZIONALE DI FISICA NUCLEARE, PERUGIA (ITALY).
Survey of the response of standard limited streamer tubes over the complete range of three-component gas mixtures of isobutane, CO(sub 2), argon
[DE89-016692] N90-12875

ISTITUTO NAZIONALE DI FISICA NUCLEARE, PISA (ITALY).
Survey of the response of standard limited streamer tubes over the complete range of three-component gas mixtures of isobutane, CO(sub 2), argon
[DE89-016692] N90-12875

ITALIAN AEROSPACE RESEARCH CENTER, NAPLES.
Hermes plasma wind tunnel. Preliminary study, phase A1: Text
[DVG-HER-TN-002-PT-1] N90-12631
Hermes plasma wind tunnel. Preliminary study, phase A1: Annexes, tables, figures
[DVG-HER-TN-002-PT-2] N90-12632

J

JAYCOR, SAN DIEGO, CA.
NTRFACE for MAGIC
[AD-A212858] N90-13112

JET PROPULSION LAB., CALIFORNIA INST. OF TECH., PASADENA.
The Telecommunications and Data Acquisition Report
[NASA-CR-185093] N90-12786
An analytic development of orbit determination for a distant, planetary orbiter N90-12787
A statistical study of radio-source structure effects on astrometric very long baseline interferometry observations N90-12788
An apparatus for the electrodynamic containment of charged macroparticles N90-12789
Spin-lattice relaxation and the calculation of gain, pump power, and noise temperature in ruby N90-12790
Performance effects of tie-truss modifications for a 70-meter centerline beam waveguide antenna N90-12791
A performance comparison between block interleaved and helically interleaved concatenated coding systems N90-12792
On the decoder error probability of linear codes N90-12793
Automated monitor and control for deep space network subsystems N90-12794
Frame synchronization methods based on channel symbol measurements N90-12795
Performance of the image statistics decoder in conjunction with the Goldstone-VLA array N90-12796
A closed-cycle refrigerator for cooling maser amplifiers below 4 Kelvin N90-12797
Wideband phase-locked angular modulator N90-12798
Performance of the split-symbol moments SNR estimator in the presence of inter-symbol interference N90-12799
DSN 70-meter antenna microwave optics design and performance improvements. Part 2: Comparison with measurements N90-12800
Stable Kalman filters for processing clock measurement data N90-12801
A simple model for DSS-14 outage times N90-12802
Ka-band MMIC beam steered transmitter array N90-12803
The NASA SETI sky survey: Recent developments N90-12804

JOHNS HOPKINS UNIV., BALTIMORE, MD.
Stability conditions for steady shearing. Stability conditions for simple shear under mixed thermal boundary conditions N90-12873
Fatigue, pilot deviations and time of day
[NASA-CR-185369] N90-13035

JOINT INST. FOR NUCLEAR RESEARCH, DUBNA (USSR).
Analysis of high temperature superconductors by means of PIXE and RBS methods
[DE89-630241] N90-13252

JOINT RESEARCH CENTRE OF THE EUROPEAN COMMUNITIES, ISPRA (ITALY).
Activities report of the Joint Research Center
[ETN-89-95757] N90-13321

K

KANSAS UNIV. CENTER FOR RESEARCH, INC., LAWRENCE.
Investigation of the properties of radar backscatter from sea ice
[AD-A212808] N90-12838

KESTREL INST., PALO ALTO, CA.
Toward a formal model of the design and evolution of software
[AD-A212533] N90-13087

KJS ASSOCIATES, DAYTON, OH.
A survey of the current state-of-the-art in high-energy-product permanent magnets
[AD-A211761] N90-13193

L

LABORATOIRE D'AUTOMATIQUE ET D'ANALYSE DES SYSTEMES, TOULOUSE (FRANCE).
Study of palladium and chromium silicides formation in liquid phase and in solid phase
[LAAS-89040] N90-12695

LABORATOIRE DE PSYCHOLOGIE EXPERIMENTALE, GRENOBLE (FRANCE).
Psychological mechanisms involved in the disorientation of pilots due to flight conditions
[ETN-89-95014] N90-13040

LABORATOIRE MARCEL MATHIEU, PAU (FRANCE).
Textural and structural organization of the heat treated polymers: Mechanical properties relationships
[ETN-89-95711] N90-12744

LAWRENCE LIVERMORE NATIONAL LAB., CA.
Design and performance of an optical mount using cross-flexure pivots
[DE89-017551] N90-12929

LEEDS UNIV. (ENGLAND).
The 4th US Army Workshop on Low Heat Rejection Engines
[AD-A212378] N90-12942
The 4th US Army Workshop on Low Heat Rejection Engines
[AD-A212379] N90-12943

LIMOGES UNIV. (FRANCE).
International Conference on Fixed Point Theory and Applications
[AD-A212369] N90-13171

LOCKHEED-GEORGIA CO., MARIETTA.
Lockheed laminar-flow control systems development and applications N90-12506
An experimental evaluation of slots versus porous strips for laminar-flow applications N90-12530

LOCKHEED MISSILES AND SPACE CO., HUNTSVILLE, AL.
SSME structural dynamic model development
[NASA-CR-183671] N90-12650

LOS ALAMOS NATIONAL LAB., NM.
Temperature effects in shock consolidation of metal powders
[DE89-016782] N90-12716

LOUISIANA STATE UNIV., BATON ROUGE.
A hybrid architecture for feature labelling of oceanographic satellite images
[AD-A212236] N90-12975

M

MARYLAND UNIV., COLLEGE PARK.
The GEM-T2 gravitational model
[NASA-TM-100746] N90-12984
International Conference on Operator Theory: Advances and applications
[AD-A212341] N90-13170

MASSACHUSETTS INST. OF TECH., CAMBRIDGE.
Requirements specification with Petri nets using the cube tool methodology
[AD-A212190] N90-12829
A 2d-1 lower bound 2-layer knock-knee channel routing
[AD-A211948] N90-12847
Height and gradient from shading
[AD-A212338] N90-12908
Mark-3 interferometer
[AD-A213155] N90-12911
Squirt: The prototypical mobile robot for autonomous graduate students
[AD-A212337] N90-12941
Area-universal networks
[AD-A211883] N90-13092
Work-preserving emulations of fixed-connection networks
[AD-A211915] N90-13093
A theory of networks for approximation and learning
[AD-A212359] N90-13110
A compilation strategy for numerical programs based on partial evaluation
[AD-A212759] N90-13175
Direct computation of 3D shape invariants and the focus of expansion
[AD-A212396] N90-13195
Fundamental studies of turbulent wall pressure fluctuations with applications to advanced acoustic sensor systems
[AD-A213041] N90-13212
Synthesis and study of materials for superconducting electronics
[AD-A212966] N90-13270

MASSACHUSETTS INST. OF TECH., LEXINGTON.
Design and performance of an on-satellite laser diagnostic system for a free space optical heterodyne frequency-shift-keyed communication system
[AD-A211986] N90-12915
Parallel and deterministic algorithms from MRF (Markov Random Fields): Surface reconstruction and integration
[AD-A212457] N90-13084

MASSACHUSETTS UNIV., AMHERST.
Ultrastructure processing and characterization of polymers
[AD-A211460] N90-12743
A center for advanced electrical and structural polymers
[AD-A212853] N90-12764

MATERIALS RESEARCH LABS., ASCOT VALE (AUSTRALIA).
Ballistic properties of composite materials for personnel protection
[MRL-TR-89-6] N90-12661
Preliminary report on the feasibility of high power Electronic Warfare (EW) using explosive energy sources
[MRL-TR-89-3] N90-12775

MAX-PLANCK-INST. FUER PHYSIK UND ASTROPHYSIK, GARCHING (GERMANY, F.R.).
Nonequilibrium ionization in supernova remnants: The case of Tycho
[MPE-PREPRINT-153] N90-13295
Far infrared, submm and mm spectroscopy of the galactic center: Radio arc and +20/+50 km s (exp -1) clouds
[NASA-CR-185497] N90-13296
CELIAS: Charge, element and isotope analysis system for SOHO N90-13313

MAX-PLANCK-INSTITUT FUER STROEMUNGSFORSCHUNG, GOETTINGEN (GERMANY, F.R.).
Numerical analysis of chaotic symbol sequences generated by parabolic and triangle maps of the interval
[MPIS-22/1987] N90-13124

MECHANICAL TECHNOLOGY, INC., LATHAM, NY.
Cryostatless high temperature supercurrent bearings for rocket engine turbopumps
[NASA-CR-183807] N90-12935

MEMPHIS STATE UNIV., TN.
Electron density modulation of catalytic metal centers by substituted aryl-isocyanide ligands
[AD-A212875] N90-12708

MESOSCALE ENVIRONMENTAL SIMULATIONS AND OPERATIONS, INC., HAMPTON, VA.
Mesoscale acid deposition modeling studies
[NASA-CR-4262] N90-13228

MESSERSCHMITT-BOELKOW-BLOHM G.M.B.H., OTTOBRUNN (GERMANY, F.R.).
Microsystems techniques: Concept, significance, status of development
[MBB-UA-1110/88-PUB] N90-12851

METEOROLOGICAL SATELLITE CENTER, TOKYO (JAPAN).
Meteorological Satellite Center Technical Note, no. 18, 1989
[MSC-TN-18] N90-12997

MICHIGAN UNIV., ANN ARBOR.
Small particle scattering and absorption
[AD-A213168] N90-12711
Time-frequency factors in auditory perception
[AD-A211491] N90-13016
Stochastic process models in device physics
[AD-A212284] N90-13185

MINNESOTA UNIV., MINNEAPOLIS.
Studies of gas turbine heat transfer airfoil surfaces and end-wall cooling effects
[AD-A212451] N90-12620
Electroactive polyaniline film deposited from non-aqueous media. 2: Effect of acid concentration in solutions
[AD-A212084] N90-12737
Quartz crystal microbalance analysis. 1: Evidence of anion or cation insertion into electropolymerized conducting polymers
[AD-A212304] N90-12755
Capacitive behavior in conducting polymers
[AD-A212448] N90-12760
The use of lithium batteries in biomedical devices
[AD-A212187] N90-12863
Assessment of thin film batteries based on polymer electrolytes. Part 3: Specific energy versus specific power
[AD-A212141] N90-12976

MISSION RESEARCH CORP., ALBUQUERQUE, NM.
Airborne/spaceborne pulsed power source
[AD-A211762] N90-12850

MISSION RESEARCH CORP., SANTA BARBARA, CA.
Time evolution of the electron swarm energy distribution function
[AD-A212967] N90-13247

MISSOURI UNIV., COLUMBIA.
Iterative methods for linear complementary and related problems
[AD-A212848] N90-13089

MISSOURI UNIV., ROLLA.
Phase change material for spacecraft thermal management
[AD-A211404] N90-12648
Magnetic resonance of polymers at surfaces
[AD-A212225] N90-12753

MITRE CORP., BEDFORD, MA.
Software Engineering Exercise (SEE) guidelines
[AD-A212510] N90-13085

MMR TECHNOLOGIES, INC., MOUNTAIN VIEW, CA.
Development of a low noise 10 K J-T refrigeration system
[AD-A213347] N90-12779

MONTPELLIER UNIV. (FRANCE).
European Solid State Device Research Conference (18th) ESSDERC 88 held in Montpellier, France on 13-16 September 1988
[AD-A210618] N90-13250

MORTON THIOKOL, BRIGHAM CITY, UT.
RSRM-3 (360L003) ballistics/mass properties report
[NASA-CR-183716] N90-12651
Ballistics/mass properties
[NASA-CR-183723] N90-12652
Flight motor set 360L001 (STS-26R). (Reconstructed dynamic loads analysis)
[NASA-CR-183811] N90-12656

MSNW, INC., SAN MARCOS, CA.
Laser probe vaporization/oxidation testing of high temperature composites
[AD-A211410] N90-12663

N

NATIONAAL INST. VOOR KERNFYSICA EN HOGE ENERGIEFYSICA, AMSTERDAM (NETHERLANDS).
Bunch length in internal target mode
[NIKHEF-AMPS/89/04] N90-12854
Minimal total cross section for e(+)e(-) yields W(+)W(-)
[NIKHEF-H/88-12] N90-13222
The process e(-)p giving gamma e(-)p as a fast luminosity for the HERA collider
[NIKHEF-H/88-13] N90-13223
Operator product coefficients in non-diagonal conformal field theories
[NIKHEF-H/88-19] N90-13224
On the spectrum of the staggered Dirac operator at finite chemical potential
[ITFA-88-53] N90-13272
More on the super WZW theory
[NIKHEF-H/88-11] N90-13273

NATIONAL ACADEMY OF SCIENCES - NATIONAL RESEARCH COUNCIL, WASHINGTON, DC.
Removal of noise from noise-degraded speech signals
[AD-A212876] N90-12840
Toward an understanding of global change: Initial priorities for US contributions to the International Geosphere-Biosphere Program
[NASA-CR-185873] N90-12980
Sound Localization by Human Observers symposium proceedings
[AD-A212877] N90-13026

NATIONAL AERONAUTICS AND SPACE ADMINISTRATION, WASHINGTON, DC.
Aeronautical engineering: A continuing bibliography with indexes (supplement 245)
[NASA-SP-7037(245)] N90-12497
Report on orbital debris
[NASA-TM-101855] N90-12635
Issues in NASA program and project management
[NASA-SP-6101(02)] N90-13277

NATIONAL AERONAUTICS AND SPACE ADMINISTRATION. AMES RESEARCH CENTER, MOFFETT FIELD, CA.
Powered-lift aircraft technology
[NASA-SP-501] N90-12589
Catadioptric Optics for laser Doppler velocimeter applications
[NASA-TM-102210] N90-12904
Cardiovascular, renal, electrolyte, and hormonal changes in man during gravitational stress, weightlessness, and simulated weightlessness: Lower body positive pressure applied by the antigravity suit
[NASA-TM-102232] N90-13013
A knowledge-based approach to automated flow-field zoning for computational fluid dynamics
[NASA-TM-101072] N90-13048
An Eigenvalue Analysis of finite-difference approximations for hyperbolic IBVPs
[NASA-TM-102241] N90-13137
Research and Technology annual report, 1988
[NASA-TM-101070] N90-13319

NATIONAL AERONAUTICS AND SPACE ADMINISTRATION. GODDARD SPACE FLIGHT CENTER, GREENBELT, MD.
Optimum data weighting and error calibration for estimation of gravitational parameters
[NASA-TM-100737] N90-12985
SOHO: An observatory to study the solar interior and the solar atmosphere N90-13303
SUMER: Solar Ultraviolet Measurements of Emitted Radiation N90-13307
EIT: Solar corona synoptic observations from SOHO with an Extreme-ultraviolet Imaging Telescope N90-13309
COSTEP: A comprehensive suprathermal and energetic particle analyzer for SOHO N90-13314

NATIONAL AERONAUTICS AND SPACE ADMINISTRATION. HUGH L. DRYDEN FLIGHT RESEARCH FACILITY, EDWARDS, CA.
Development flight tests of JetStar LFC leading-edge flight test experiment N90-12509
F-14 VSTFE and results of the cleanup flight test program N90-12547
Multilayer theory for delamination analysis of a composite curved bar subjected to end forces and end moments
[NASA-TM-4139] N90-12669

NATIONAL AERONAUTICS AND SPACE ADMINISTRATION. LANGLEY RESEARCH CENTER, HAMPTON, VA.
Research in Natural Laminar Flow and Laminar-Flow Control, part 1
[NASA-CP-2487-PT-1] N90-12503
Performance of laminar-flow leading-edge test articles in cloud encounters N90-12511
Simulated airline service experience with laminar-flow control leading-edge systems N90-12512
Interaction of Tollmien-Schlichting waves and Goertler vortices N90-12515
Goertler instability on an airfoil N90-12517
Research in Natural Laminar Flow and Laminar-Flow Control, part 2
[NASA-CP-2487-PT-2] N90-12519
Advanced measurement techniques, part 1 N90-12520
Flow quality measurements in compressible subsonic flows N90-12521
Hot-film system for transition detection in cryogenic wind tunnels N90-12522
Predicted and hot-film measured Tollmien-Schlichting wave characteristics N90-12523
Remote detection of boundary-layer transition by an optical system N90-12524
Three-component laser Doppler velocimeter measurements in a juncture flow N90-12525
Basic aerodynamic research facility for comparative studies of flow diagnostic techniques N90-12526
Recent tests at Langley with a University of Tennessee Space Institute (UTSI) skin friction balance N90-12527
Recent flow visualization studies in the 0.3-m TCT N90-12528

Experimental studies on Goertler vortices N90-12529
Results of LFC experiment on slotted swept supercritical airfoil in Langley's 8-foot transonic pressure tunnel N90-12531
Boundary-layer stability analysis of Langley Research Center 8-foot LFC experimental data N90-12532
Sensitivity of LFC techniques in the non-linear regime N90-12533
Numerical solutions of the compressible 3-D boundary-layer equations for aerospace configurations with emphasis on LFC N90-12534
Theoretical methods and design studies for NLF and HLFC swept wings at subsonic and supersonic speeds N90-12535
Application of sound and temperature to control boundary-layer transition N90-12537
Research in Natural Laminar Flow and Laminar-Flow Control, part 3
[NASA-CP-2487-PT-3] N90-12539
Design of the low-speed NLF(1)-0414F and the high-speed HSNLF(1)-0213 airfoils with high-lift systems N90-12540
Wind tunnel results of the low-speed NLF(1)-0414F airfoil N90-12541
Wind tunnel results of the high-speed NLF(1)-0213 airfoil N90-12542
Design and test of an NLF wing glove for the variable-sweep transition flight experiment N90-12544
The design of an airfoil for a high-altitude, long-endurance remotely piloted vehicle N90-12545
Experimental and numerical analyses of laminar boundary-layer flow stability over an aircraft fuselage forebody N90-12549
Status report on a natural laminar-flow nacelle flight experiment N90-12550
Effects of acoustic sources N90-12553
Supersonic laminar-flow control N90-12554
Design and fabrication requirements for low noise supersonic/hypersonic wind tunnels N90-12555
The effects of wall surface defects on boundary-layer transition in quiet and noisy supersonic flow N90-12556
Experimental and theoretical investigation of boundary-layer instability mechanisms on a swept leading edge at Mach 3.5 N90-12557
Supersonic boundary-layer transition on the LaRC F-106 and the DFRF F-15 aircraft. Part 1: Transition measurements and stability analysis N90-12558
Supersonic boundary-layer transition on the LaRC F-106 and the DFRF F-15 aircraft. Part 2: Aerodynamic predictions N90-12559
Integrated multidisciplinary optimization of rotorcraft: A plan for development
[NASA-TM-101617] N90-12580
General approach and scope N90-12581
Rotor blade aerodynamic design N90-12582
Rotor blade dynamic design N90-12583
Acoustic design considerations: Review of rotor acoustic sources N90-12585
Airframe design considerations: Overview N90-12586
Appendix: Results obtained to date N90-12588

NATIONAL AERONAUTICS AND SPACE ADMINISTRATION. LEWIS RESEARCH CENTER, CLEVELAND, OH.
Prediction of unsteady blade surface pressures on an advanced propeller at an angle of attack
[NASA-TM-102374] N90-12560
Some observations on transitory stall in conical diffusers
[NASA-TM-102387] N90-12561
Real-time simulation of an F110/STOVL turbofan engine
[NASA-TM-102409] N90-12618
Tribological properties of ceramic/TiGAl-Nb sliding couples for use as candidate seal materials to 700 deg C
[NASA-TM-102401] N90-12658
Tribological properties of PM212: A high-temperature, self-lubricating, powder metallurgy composite
[NASA-TM-102355] N90-12659
A new test machine for measuring friction and wear in controlled atmospheres to 1200 C
[NASA-TM-102405] N90-12670
Characterization and cycle tests of lightweight nickel electrodes
[NASA-TM-102399] N90-12696
Satellite range delay simulator for a matrix-switched time division multiple-access network simulator
[NASA-TM-102407] N90-12813
A thermoelastic transversely isotropic thick walled cylinder/disk application: An analytical solution and study
[NASA-TM-102320] N90-12950
The GEM-T2 gravitational model
[NASA-TM-100746] N90-12984

NATIONAL AERONAUTICS AND SPACE ADMINISTRATION. MARSHALL SPACE FLIGHT CENTER, HUNTSVILLE, AL.
Determination of the gaseous hydrogen ductile-brittle transition in copper-nickel alloys
[NASA-TM-86494] N90-12715

NATIONAL AEROSPACE LAB., AMSTERDAM (NETHERLANDS).
Development of a multi-component internal strain-gauge balance for model tests in a cryogenic wind tunnel
[NLR-TR-88157-U] N90-12628

NATIONAL FACILITY FOR USE OF INTENSIVE LASERS, PALAISEAU (FRANCE).
Lectures on x ray lasers
[ETN-89-95516] N90-12917

NATIONAL GEOPHYSICAL DATA CENTER, BOULDER, CO.
Solar-geophysical data number 537, May 1989. Part 2: Comprehensive Reports, data for Nov. 1988 and miscellaneous
[PB89-207401] N90-13300

NATIONAL INST. OF STANDARDS AND TECHNOLOGY, BOULDER, CO.
Vapor-liquid equilibrium of binary mixtures in the extended critical region. Part 1: Thermodynamic model
[PB89-218374] N90-12687
Tables for the thermophysical properties of methane
[PB89-222608] N90-12690
Effect of pipe roughness on orifice flow measurement
[PB89-231484] N90-12880
Liquid and solid ion plasmas
[AD-A212415] N90-13244

NATIONAL INST. OF STANDARDS AND TECHNOLOGY, GAITHERSBURG, MD.
Properties of Lennard-Jones mixtures at various temperatures and energy ratios with a size ratio of two
[PB89-235204] N90-12697
Fundamental molecular data to support CARS diagnostics of temperature, pressure, and species concentration
[AD-A212411] N90-12704
NBS/BAM (National Bureau of Standards/Bundesanstalt fuer Materialprufung) 1986 Symposium on Advanced Ceramics
[PB89-229074] N90-12747
Directory of International and Regional Organizations Conducting Standards-Related Activities, May 1989
[PB89-221147] N90-12776
NIST (National Institute of Standards and Technology) measurement services: The ac-dc difference calibrations
[PB89-222616] N90-12845
Measurements of coefficients of discharge for concentric flange-tapped square-edged orifice meters in water over the Reynolds number range 600 to 2,700,000
[PB89-235147] N90-12892
Visual perception processing in a hierarchical control system: Level 1
[PB89-221188] N90-13101
Semiconductor measurement technology: Database for and statistical analysis of the interlaboratory determination of the conversion coefficient for the measurement of the interstitial oxygen content of silicon by infrared absorption
[PB89-221170] N90-13253
Semiconductor measurement technology: A software program for aiding the analysis of ellipsometric measurements, simple models
[PB89-235923] N90-13261
Publications of the National Institute of Standards and Technology, 1988 catalog
[PB89-218382] N90-13279

NATIONAL METEOROLOGICAL CENTER, WASHINGTON, DC.
Compendium of marine meteorological and oceanographic products of the Ocean Products Center, revision 1
[PB89-230684] N90-12967

NATIONAL OCEANIC AND ATMOSPHERIC ADMINISTRATION, BOULDER, CO.
Cloud cover determination in polar regions from satellite imagery
[NASA-CR-186096] N90-13003
Subjective uses of wind profiler data in warm season analysis and forecasting: Wind profiler training manual number 3
[PB89-223333] N90-13004

NATIONAL OCEANIC AND ATMOSPHERIC ADMINISTRATION, MIAMI, FL.
Current velocity and hydrographic observations in the southwestern North Atlantic Ocean: Subtropical Atlantic Climate Studies (STACS), 1988
[PB89-230825] N90-13010

NATIONAL OCEANIC AND ATMOSPHERIC ADMINISTRATION, SILVER SPRING, MD.
South Pole surface radiation balance measurements, April 1986 to February 1988
[PB89-224018] N90-12993

NATIONAL OCEANOGRAPHIC INSTRUMENTATION CENTER, WASHINGTON, DC.
Removing stripes in GOES (Geostationary Operational Environmental Satellites) images by matching empirical distribution functions
[PB89-213359] N90-12968

NATIONAL PHYSICAL LAB., TEDDINGTON (ENGLAND).
Physical ageing and short term creep in amorphous and semicrystalline polymers
[NPL-DMA(A)-185] N90-12745
A formatting style for typesetting and distributing draft international standards
[NPL-DITC-143/89] N90-13059
Unsteady diffusion from a hemispherical pit
[NPL-DMA(A)-190] N90-13220

NATIONAL SCIENCE FOUNDATION, WASHINGTON, DC.
National Science Foundation N90-13320

NATIONAL TELECOMMUNICATIONS AND INFORMATION ADMINISTRATION, BOULDER, CO.
Automated Steerable Nulling Antenna Processor (SNAP) model
[PB89-231740] N90-12937

NATIONAL WEATHER SERVICE, SILVER SPRING, MD.
Atlas of tropical sea surface temperature and surface winds
[PB89-223598] N90-13009

NAVAL AEROSPACE MEDICAL RESEARCH LAB., PENSACOLA, FL.
A Scheiner-principle pocket optometer for self-evaluation and biofeedback accommodation training
[AD-A213171] N90-13027

NAVAL AIR ENGINEERING CENTER, LAKEHURST, NJ.
Analytical and experimental study of runway runoff with wind effects
[PTI-8948] N90-12627

NAVAL MEDICAL RESEARCH INST., BETHESDA, MD.
Radio frequency (13.56 MHz) energy enhances rewarming from mild hypothermia
[AD-A212703] N90-13024
Effects of serial wet-dry-wet cold exposure: Thermal balance, physical activity, and cognitive performance
[AD-A212704] N90-13025

NAVAL OCEAN RESEARCH AND DEVELOPMENT ACTIVITY, BAY SAINT LOUIS, MS.
Surface current and wave modulation measurements over bottom topography: A comparison with theory
[AD-A212469] N90-13011
The Regional Polar Ice Prediction System, Berents Sea (RPIPS-B): A technical description
[AD-A213159] N90-13012

NAVAL OCEAN SYSTEMS CENTER, SAN DIEGO, CA.
Direction-of-arrival calculations at VLF/LF (Very Low Frequency/Low Frequency)
[AD-A212620] N90-12833
Atmospheric horizontal-inhomogeneity effects on the optical depths determined by the double-elevation-angle lidar technique
[AD-A212836] N90-12839
Specification for radar free-space detection range and free-space intercept range calculations
[AD-A213158] N90-12843

NAVAL POSTGRADUATE SCHOOL, MONTEREY, CA.
Estimating the relationships between the state of the art of technology and production cost for the US aircraft
[AD-A212127] N90-12495
Case study on rapid software prototyping and automated software generation: An inertial navigation system
[AD-A212272] N90-12578
Current limiting mechanisms in electron and ion beams experiments
[AD-A212295] N90-12637
A survey of permanently-manned lunar base concepts
[AD-A212575] N90-12638
An approach to low temperature high strain rate superplasticity in aluminum alloy 2090
[AD-A212271] N90-12731
Wire grid modeling of the linear tapered slot antenna
[AD-A212977] N90-12842
Free surface scars and striations
[AD-A212429] N90-12901
Semi-Lagrangian, semi-implicit solutions of the shallow water equations in one dimension
[AD-A212658] N90-12902
Visualization of high-resolution digital terrain
[AD-A212149] N90-12971
Air flow over large scale topography
[AD-A211779] N90-12998

Performance evaluations of a parallel and expandable database computer: The multi-backend database computer
[AD-A212761] N90-13046
A numerical study of rain-induced surface gravity wave attenuation
[AD-A212762] N90-13197
Measurements of bubble properties using a multi-frequency sound field
[AD-A212591] N90-13211

NAVAL RESEARCH LAB., WASHINGTON, DC.
FLIC (FLame with Implicit Convection): A detailed, two-dimensional flame model
[AD-A212953] N90-12710
Thermal initiation of confined primary explosives with a proton beam
[AD-A212954] N90-12767
Aviation Engine Test Facilities (AETF) fire protection study
[AD-A211483] N90-12777
Electron beam propagation through a magnetic wiggler with random field errors
[AD-A212705] N90-12867
Cold tests of quasi-optical gyrotron resonators
[AD-A212707] N90-12868
Calculation of the odd and even integral components of the wave resistance Green's function
[AD-A212384] N90-12900
Evaluation of the near-wall k-epsilon turbulence model by comparison with direct simulations of turbulent channel flow
[AD-A212674] N90-12903
Scaling of an 85 GHz gyrotron to operate at 94 GHz
[AD-A212756] N90-12909
Radio frequency linac driven free-electron laser configurations
[AD-A212572] N90-12922
Cavity eigenmodes for the NIST/NRL (National Institute of Standards and Technology/Naval Research Laboratory) free electron laser
[AD-A212706] N90-12923
Catalog of absolutely calibrated, range normalized, wideband, electric field waveforms from located lightning flashes in Florida: July 24 and August 14, 1985 data
[AD-A212708] N90-13008
Numerical evaluation of the far field wave pattern of the radiation Green's function
[AD-A212839] N90-13176
Molecular dynamics of lipid bilayers
[AD-A211492] N90-13214
Flux-corrected transport algorithms for two-dimensional compressible magnetohydrodynamics
[AD-A212757] N90-13246

NAVAL SHIP RESEARCH AND DEVELOPMENT CENTER, BETHESDA, MD.
A mechanical power flow capability for the finite element code NASTRAN
[AD-A212202] N90-12964

NAVAL SURFACE WARFARE CENTER, SILVER SPRING, MD.
Synthesis of energetic single phase and multi-phase polymers
[AD-A212539] N90-12761

NAVAL WAR COLL., NEWPORT, RI.
Building a software package for solving large sparse nonlinear systems of equations
[AD-A211758] N90-13055

NAVAL WEAPONS CENTER, CHINA LAKE, CA.
Pyrotechnic shock structural response N90-12774
Analysis of three- and four-sided uniform waveguides with unusual cross-section/boundary conditions
[AD-A212653] N90-12834
Laser Induced Damage in Optical Materials: 1987
[PB89-221162] N90-12913

NEW YORK UNIV., NEW YORK.
Three stages and two systems of visual processing
[AD-A212670] N90-13032

NEWCASTLE-UPON-TYNE UNIV. (ENGLAND).
Strings, p-branes and Skyrmions in curved space N90-13293

NORTH CAROLINA STATE UNIV., RALEIGH.
Chemical treatment of epoxy resins to reduce moisture sensitivity and to improve the mechanical properties
[AD-A212360] N90-12758
Structural and electrical properties of thin films and superlattices composed of II-VI semiconductors N90-13249
A two-parameter representation of dynamic dislocation distributions
[AD-A212249] N90-13263

NORTH CAROLINA UNIV., CHAPEL HILL.
Synthesis and characterization of new low-dimensional metal complex conductors
[AD-A213189] N90-12671
Fellowships in information and stochastic systems
[AD-A212385] N90-13280

O

OAK RIDGE NATIONAL LAB., TN.
Contribution of deforestation to atmospheric CO2 and reforestation as an option to control CO2
[DE89-017255] N90-12979
Three-dimensional equilibria and Mercier stability calculations
[DE89-015907] N90-13239

OCEAN PRODUCTS CENTER, WASHINGTON, DC.
Compendium of marine meteorological and oceanographic products of the Ocean Products Center, revision 1
[PB89-230684] N90-12967

OFFICE NATIONAL D'ETUDES ET DE RECHERCHES AEROSPATIALES, PARIS (FRANCE).
Basic research on methods of calculating supersonic and hypersonic flow
[ONERA-RSF-19/1123-AY-234A] N90-12565
Euler equation solutions applied to a helicopter rotor in forward moving flight
[ONERA-RSF-32/1285-AY-346A] N90-12592
Development of an anti-Stokes coherent Raman diffusion system for measuring hypersonic flow
[ONERA-RSF-1/7301-PY] N90-12630
Hardening mechanisms and analysis of the structure of the TGDDM/DDS epoxy resin system (tetraglycidyl-4,4' diaminodiphenylmethane/4,4' diaminodiphenylsulfone)
[NOTE-TECHNIQUE-1988-8] N90-12662
Nonlinear theories concerning laminated composites under compression with delamination
[ONERA-RT-19/3542-RY-081-R] N90-12672
Crack propagation failure of carbon/resin composites
[ONERA-RT-45/7086-M] N90-12677
Mechanical behavior of carbon/resin composites under delamination and cracking of transverse layers
[ONERA-RT-46/7086-M] N90-12678
Surface treatments of carbon fibers in an organic environment. Finite element analysis of pull-out tests
[ONERA-RT-7/3549-M] N90-12698
Experimental study of homogeneous turbulence submitted to rotational effects
[ONERA-RSF-10/1145-AY-164A] N90-12894
Flow in the neighborhood of an ellipsoid cylinder of revolution model
[ONERA-RT-22/7252-AN-000A] N90-12895
Bulk acoustic waves resonators made of amorphous materials
[NOTE-TECHNIQUE-1989-4] N90-13199
Enhancement of infrared thermographic imagery: Local smoothing and time-based interpolation
[ONERA-RT-8/7254-SN] N90-13232
Studies of the European transonic wind tunnel
[ONERA-RSF-12/0694-GY] N90-13278

OFFICE OF TECHNOLOGY ASSESSMENT, WASHINGTON, DC.
Technology transfer to the United States: The MIT (Massachusetts Institute of Technology) Japan Science and Technology Program. A background paper of OTA's (Office of Technology Assessment's) assessment on technology, innovation, and US trade
[PB89-224711] N90-13291

OHIO STATE UNIV., COLUMBUS.
The chemistry of hexaazatriphenylene hexanitrile, a polyfunctional heterocycle with potential utility in the formulation of thermostable polymers
[AD-A212353] N90-12757
Adaptive antenna arrays for satellite communication
[NASA-CR-185989] N90-12784
Progress in the identification of airborne radar targets
[AD-A212749] N90-12835
Performance analysis of large adaptive sidelobe canceller arrays with reused elements
[AD-A212888] N90-12841
Analysis of high speed pneumatic actuation systems under rotary directional on-off flow control N90-12926
Vibration transmission through rolling element bearings in geared rotor system, part 1
[NASA-CR-186093] N90-12936
A simulation study of the overdetermined geodetic boundary value problem using collocation
[AD-A211785] N90-12990
Exponential modeling using combined forward and backward prediction
[AD-A212317] N90-13169

OLD DOMINION COLL., NORFOLK, VA.
Strong moderate deviation theorems for m-dependent random variables
[AD-A212618] N90-13173

OPTICAL SOCIETY OF AMERICA, WASHINGTON, DC.
Tunable Solid State Lasers conference edition: Tunable Solid State Lasers Topical Meeting
[AD-A212292] N90-12920

P

PACIFICA-SIERRA RESEARCH CORP., LOS ANGELES, CA.
Long wave atmospheric noise model, phase 1. Volume 1: Lightning occurrence rates and propagation theory
[AD-A212794] N90-12836
Long wave atmospheric noise model, phase 1. Volume 2: Mode parameters
[AD-A212795] N90-12837

PADUA UNIV. (ITALY).
Survey of the response of standard limited streamer tubes over the complete range of three-component gas mixtures of isobutane, CO(sub 2), argon
[DE89-016692] N90-12875

PCO, INC., CHATSWORTH, CA.
The growth of epitaxial GaAs and GaAlAs on silicon substrates by OMVPE
[AD-A212873] N90-13269

PENNSYLVANIA STATE UNIV., UNIVERSITY PARK.
Radar polarimetric studies based on the MAYPOLE 1983 and 1984 field experiments
[AD-A212226] N90-12830
A computationally efficient modelling of laminar separation bubbles
[NASA-CR-185854] N90-12872

PENNSYLVANIA TRANSPORTATION INST., UNIVERSITY PARK.
Analytical and experimental study of runway runoff with wind effects
[PTI-8948] N90-12627

PENNSYLVANIA UNIV., PHILADELPHIA.
The multivalent beta'-aluminas
[AD-A212103] N90-12738

PERUGIA UNIV. (ITALY).
Survey of the response of standard limited streamer tubes over the complete range of three-component gas mixtures of isobutane, CO(sub 2), argon
[DE89-016692] N90-12875

PHYSICS AND ELECTRONICS LAB. TNO, THE HAGUE (NETHERLANDS).
The comparison of the airbase simulation models airbase and sustained
[FEL-1988-66] N90-12629
Dedicated tracking of crossing targets with a phased array monopulse radar
[FEL-1988-95] N90-12821
A method to model fuze performance. Part 2: Calculation of target reflections with physical optics
[FEL-1989-21-PT-2] N90-12822
Aircraft SAR simulation Sargen 1.0
[FEL-1989-44] N90-12823
Description and results of a multihop NACS simulation
[FEL-1988-46] N90-12824
A literature study of wave propagation in the 1-60 GHz range. Application to transportable military communication systems
[FEL-1988-47] N90-12825
Angle estimation in a multipath environment with an eight element linear array operating at 10.5 GHz
[FEL-1989-15] N90-12826
Survey of the CLUSE main experiment Grand-CLUSE, May 1 - June 15, 1988
[FEL-1988-43] N90-12991
User manual of the force structure model scenario editor SC**NE
[F.L-1988-101] N90-13069
Artificial intelligence for communication prospects
[FEL-1989-1] N90-13107
Modified Newton-type methods for long-range target motion analysis
[FEL-1989-82] N90-13208
Smooth track generation for target motion analysis
[FEL-1989-83] N90-13233
The physical optics approximation in the near-field region
[FEL-1989-100] N90-13234

PHYSIKALISCH-METEOROLOGISCHES OBSERVATORIUM, DAVOS (SWITZERLAND).
VIRGO: The solar monitor experiment on SOHO N90-13305

PISA UNIV. (ITALY).
Survey of the response of standard limited streamer tubes over the complete range of three-component gas mixtures of isobutane, CO(sub 2), argon
[DE89-016692] N90-12875

PITTSBURGH UNIV., PA.
Thermal stability of the carbon-carbon bond in ethylene adsorbed on Si(100): An isotopic mixing study
[AD-A211591] N90-12691

POITIERS UNIV. (FRANCE).
Automatic analysis and exploitation of the flow visualization images
[ETN-89-95712] N90-12887

POLITECNICO DI MILANO (ITALY).
Feedback charge amplifier integrated on the detector wafer
[REPT-89-037] N90-12852
Instability of the behavior of high resistivity silicon detectors due to the presence of oxide charges
[REPT-89-038] N90-13260
PRC KENTRON, INC., HAMPTON, VA.
Near-field noise predictions of an aircraft in cruise N90-12538
Nacelle aerodynamic performance N90-12552
PRECISION ACOUSTIC DEVICES, INC., FREEMONT, CA.
An air coupled transmission mode acoustic microscope for on-line non-destructive evaluation
[AD-A211416] N90-12947
PRINCETON UNIV., NJ.
Asymptotic analyses of the structures and characteristics of flames N90-12683
Electron transport in heterojunction superlattices
[AD-A212366] N90-13265
PROSPECTIVE COMPUTER ANALYSTS, INC., ARLINGTON, VA.
Expert system for test program set fault candidate selection
[AD-A213338] N90-13091
PURDUE UNIV., WEST LAFAYETTE, IN.
Metallo-organic decomposition process for dielectric films
[AD-A211590] N90-12849
Orthotropic elasto-plastic behavior of AS4/APC-2 thermoplastic composite in compression
[NASA-CR-186080] N90-12959
Research in computer vision for autonomous systems
[AD-A212420] N90-13235
GaAs gate dynamic memory technology
[AD-A212387] N90-13266

Q

QUAID-I-AZAM UNIV., ISLAMABAD (PAKISTAN).
Resistivity measurements of superconducting materials
[PB89-225700] N90-12856

R

RAND CORP., SANTA MONICA, CA.
A table-driven approach to fast context-free parsing
[AD-A212210] N90-13082
READING UNIV. (ENGLAND).
Project WIND: Experiments with the UK Meteorological Office mesoscale model
[AD-A212291] N90-13006
RENSSELAER POLYTECHNIC INST., TROY, NY.
Apollo lightcraft project
[NASA-CR-186055] N90-12655
Analysis of the non-planar response of a cantilever, with the aid of computerized symbolic manipulation
[AD-A212421] N90-13172
RESEARCH INST. FOR ADVANCED COMPUTER SCIENCE, MOFFETT FIELD, CA.
Telescience Testbed Pilot Program
[NASA-CR-184997] N90-13047
RHODE ISLAND UNIV., KINGSTON.
Optimal observer motion for bearings-only localization and tracking N90-12569
ROLLS-ROYCE LTD., DERBY (ENGLAND).
What should be done with those noisy old aircraft
[PNR90562] N90-12593
Advanced clearance control systems
[PNR90553] N90-12601
Development of texture analysis and its applications to titanium aero engine components
[PNR90561] N90-12602
A vision of the future: The new engine technology
[PNR90566] N90-12603
Designing for reliable and low maintenance cost aero engines
[PNR90570] N90-12604
The next generation supersonic transport engine: Critical issues
[PNR90576] N90-12605
Re-engine with the Rolls-Royce Tay 670, the route to significant noise reduction
[PNR90585] N90-12606
A theoretical study of ingress for shrouded rotating disk systems with radial outflow
[PNR90586] N90-12607
The role of component testing
[PNR90589] N90-12608
Flanged joints of aeroengines
[PNR90594] N90-12609
Material requirements for future aeroengines
[PNR90595] N90-12610
A computer integrated approach to dimensional inspection
[PNR90596] N90-12611
Dynamic tip clearance measurements in axial flow compressors
[PNR90597] N90-12612
The development of a high response aerodynamic wedge probe and use on a high-speed research compressor
[PNR90598] N90-12613
Gas turbine performance analysis
[PNR90599] N90-12614
Rolls-Royce and ERCOFTAC
[PNR90600] N90-12615
Blading design for multi-storage HP compressor
[PNR90602] N90-12616
Composite materials for future aeroengines
[PNR90584] N90-12667
The future of non ferrous metals in aerospace engines
[PNR90572] N90-12720
Application of a copper vapour laser to investigation of shock and blade interaction in a shock tube
[PNR90578] N90-12918
Demonstration epicyclic gearbox
[PNR90567] N90-12932
The nature and control of skidding in lightly loaded intershaft bearings
[PNR90591] N90-12933
Non linear vibrations in a drive train when coupled to constant torque and constant power loads
[PNR90593] N90-12934
Optical techniques for in-plane strain analysis in an industrial environment
[PNR90601] N90-12957
The design and development of an acoustic test section for the ARA transonic wind tunnel
[PNR90574] N90-13202
The commercial aircraft noise problem
[PNR90577] N90-13203
ROME AIR DEVELOPMENT CENTER, GRIFFISS AFB, NY.
Application of a generalized Leibniz rule for calculating electromagnetic fields within continuous source regions
[AD-A212470] N90-12831
Characterization of liquid crystal displays for optical signal processing applications
[AD-A212832] N90-12910
ROYAL AEROSPACE ESTABLISHMENT, FARNBOROUGH (ENGLAND).
Improvements in the formulations and numerical solution of the Euler problem for swept wings
[RAE-TM-AERO-2139] N90-12562
CFD methods for drag prediction and analysis currently in use in UK
[RAE-TM-AERO-2146] N90-12563
Preliminary experience with high response pressure measurements in a multistage, high speed compressor
[RAE-TM-P-1141] N90-12619
Evaluation of 15th- and 30th-order geopotential harmonic coefficients from 26 resonant satellite orbits
[RAE-TR-88045] N90-12640
Orbit determination and analysis for Cosmos 236 at 15th-order resonance
[RAE-TR-88058] N90-12641
On mean elements for satellite orbits perturbed by the zonal harmonics of the geopotential
[AD-A212322] N90-12642
The design, construction, performance and calibration of pulse generators to fulfil the requirements of specifications defence standard 59-41, FS(F) 510 and FS(S) 457
[RAE-TM-FS(F)-550] N90-12857
Numerical evaluation of a solution representing a jet in cross-flow
[RAE-TM-AERO-2137] N90-12893
A frequency domain technique for improving sound field reproduction
[RAE-TM-MM-10] N90-13205
Perceived urgency of warning signals determined using a forced choice pair comparison technique
[RAE-TM-MM-12] N90-13206
Acoustic recording systems for use in military aircraft
[RAE-TM-MM-11] N90-13207
Particle transport simulation for spaceborne, NaI gamma-ray spectrometers
[AD-A205150] N90-13292
Radioactivity induced in gamma-ray spectrometers
[RAE-TM-SPACE-363] N90-13317
The cosmic radiation effects and activation monitor
[RAE-TM-SPACE-364] N90-13318
ROYAL HOLLOWAY AND BEDFORD NEW COLL., EGHAM (ENGLAND).
Dielectric spectroscopy of semiconductors
[AD-A211989] N90-13255
ROYAL INST. OF TECH., STOCKHOLM (SWEDEN).
On the extremum electric charge problem of steady electromagnetic equilibria
[TRITA-EPP-89-04] N90-12809
ROYAL NETHERLANDS METEOROLOGICAL INST., DE BILT.
Central Sudan surface wind data and climate characteristic
[KNMI-WR-88-01] N90-13000
Instability mechanisms in a barotropic atmosphere
[KNMI-WR-89-01] N90-13001
Climatological data for the North Sea based on observations by voluntary observing ships over the period 1961-1980
[KNMI-WR-89-02] N90-13002
ROYAL SIGNALS AND RADAR ESTABLISHMENT, MALVERN (ENGLAND).
Software fault tolerance
[RSRE-MEMO-4237] N90-12575
Route data representation for ATC simulation experiments
[RSRE-MEMO-4133] N90-12576
Spectroscopic ellipsometry characterization of CVD deposition and doping of polysilicon multilayer structures
[RSRE-MEMO-4258] N90-12671
Properties of density tapered arrays
[RSRE-MEMO-4210] N90-12810
Mode S data link trials, 10-11 January 1989
[RSRE-MEMO-4267] N90-12815
Fine resolution errors in secondary surveillance radar altitude reporting amongst aircraft transmitting the conspicuity codes 4321 and 4322
[RSRE-88004] N90-12816
Specification of Viper1 in Z
[RSRE-MEMO-4195] N90-12817
Statistical density and amplitude tapered arrays
[RSRE-MEMO-4211] N90-12818
Specification of Viper2 in Z
[RSRE-MEMO-4217] N90-12819
Automatic communications channel interference monitoring
[RSRE-MEMO-4243] N90-12820
A well conditioned formulation for the analysis of multi-layered frequency selective surfaces using a cascaded matrix approach
[RSRE-MEMO-4289] N90-12858
Readout and signal conditioning for a linear pyroelectric array
[RSRE-MEMO-4102] N90-12905
A real-time wind model using digital data from aircraft
[RSRE-MEMO-4309] N90-13005
Algorithmic fault tolerance
[RSRE-MEMO-4212] N90-13057
Non-separate arithmetic codes
[RSRE-MEMO-4215] N90-13058
Mathematical equivalence in a primitive Ella
[RSRE-MEMO-4225] N90-13066
A Z specification of the MaCHO interface editor
[RSRE-MEMO-4247] N90-13067
The integration of structured and formal methods
[RSRE-MEMO-4293] N90-13068
A mapping for converting Mascot designs to Ada programs
[RSRE-MEMO-4244] N90-13070
Explicit modelling of state duration correlations in hidden Markov models
[RSRE-MEMO-4152] N90-13178
A review of focal reducer interferometer systems
[RSRE-MEMO-3486] N90-13231
Twistons
[RSRE-MEMO-4234] N90-13275
RUTHERFORD HIGH ENERGY LAB., CHILTON (ENGLAND).
CDS: The Coronal Diagnostic Spectrometer N90-13308

S

SAN DIEGO STATE UNIV., CA.
Photoelectron pumped phosphors
[AD-A213202] N90-12912
SATELLITE METEOROLOGICAL CENTER, BEIJING (CHINA).
Removing stripes in GOES (Geostationary Operational Environmental Satellites) images by matching empirical distribution functions
[PB89-213359] N90-12968
SCIENCE APPLICATIONS INTERNATIONAL CORP., MCLEAN, VA.
Calcium displacement caused by electromagnetic fields
[AD-A212690] N90-13023

SHEFFIELD UNIV. (ENGLAND).
Nonlinear systems and Kolmogorov's representation theorem
[RR-363] N90-12931
An on-line distributed minimum-time trajectory generator for intelligent robot manipulators
[RR-358] N90-13102
Identification of robot dynamics: A parallel processing approach
[RR-361] N90-13103
Real-time robot motion: The VLSI implementation via transputers
[RR-364] N90-13104
A functional expansion and stability for nonlinear input-output maps
[RR-359] N90-13121
A new decision rule for model structure identification of a class of nonlinear dynamic systems
[RR-360] N90-13122
A recursive algorithm for computing the frequency response of a class of nonlinear difference equation models
[RR-354] N90-13123
SOUTHEASTERN CENTER FOR ELECTRICAL ENGINEERING EDUCATION, INC., SAINT CLOUD, FL.
Effects of type of responding on memory/visual search: Responding just yes or just no can lead to inflexible performance
[AD-A212764] N90-13033
SRI INTERNATIONAL CORP., MENLO PARK, CA.
Mechanisms of CO2 reduction metal and metal modified semiconductor electrodes
[AD-A213169] N90-12712
STANFORD LINEAR ACCELERATOR CENTER, CA.
A 2-MeV microwave thermionic gun
[DE89-015640] N90-12844
Survey of the response of standard limited streamer tubes over the complete range of three-component gas mixtures of isobutane, CO(sub 2), argon
[DE89-016692] N90-12875
STANFORD UNIV., CA.
Protein crystal growth in low gravity
[NASA-CR-186082] N90-12770
On the identification of local minimizers in inertia-controlling methods for quadratic programming
[AD-A212514] N90-13086
Sequential quadratic programming algorithms for optimization
[AD-A212800] N90-13088
A modified Newton method for unconstrained minimization
[AD-A212752] N90-13174
Smoothed limit theorems for equilibrium processes
[AD-A212321] N90-13186
Illustration of Bayesian inference in normal data models using Gibbs sampling
[AD-A212630] N90-13187
Monte Carlo (importance) sampling within a Benders' decomposition algorithm for stochastic linear programs
[AD-A212854] N90-13189
Advanced source development and applications. Laser-produced plasmas: A compact soft x ray source with high peak brightness
[AD-A212677] N90-13245
Optical clock distribution to VLSI chips
[AD-A212269] N90-13264
An investigation of diamond film deposition in a premixed oxyacetylene flame
[AD-A212595] N90-13268
SOI: The Solar Oscillations Imager on SOHO
N90-13306
STATE UNIV. OF NEW YORK, BINGHAMTON.
Photochemical observation of ion flows in membrane channels
[AD-A212449] N90-12705
STATE UNIV. OF NEW YORK, BUFFALO.
A survey on nonproportional damping N90-12773
Ground states of a two-dimensional charged-boson system
[AD-A212363] N90-13226
STATE UNIV. OF NEW YORK AT BUFFALO, AMHERST.
Dynamics of an M-level atom interacting with cavity fields: Properties of photon statistics
[AD-A211321] N90-13213
STOCKHOLM UNIV. (SWEDEN).
Zonal average cloud characteristics for global atmospheric chemistry modeling
[CM-76] N90-12992
SYSTEMES ET AUDIO FREQUENCES, PARIS (FRANCE).
Integration of a centralized multiplexed control unit into the cockpit of an aircraft
[F6150-DT410-1-88329] N90-12622
SYSTEMS APPLICATIONS, INC., SAN RAFAEL, CA.
Sensitivity of a regional oxidant model to variations in climate parameters, volume 1 and 2
[PB89-224943] N90-12981
SYSTEMS ENGINEERING LABS., INC., GREENBELT, MD.
Algorithm development for SDI weapons system allocation
[AD-A212973] N90-13090

T

TECHNISCHE UNIV., DELFT (NETHERLANDS).
On the precision and reliability of GPS networks computed using the double difference observable
[ETN-89-95719] N90-12571
Rolling of ARALL laminates (an alternative method for post-stretching ARALL laminates)
[LR-560] N90-12778
Free-field response from inclined body waves in viscoelastic random medium
[REPT-88-99] N90-12876
A linearized surface condition in low speed hydrodynamics
[REPT-89-04] N90-12885
A multigrid method for the Navier-Stokes and Boussinesq equations
[REPT-89-17] N90-12886
An investigation on combined extension and bending of thin sheets with a central crack
[LR-561] N90-12958
Realization of a different NAVSTAR global positioning system for hydrographic surveying
[ETN-89-95720] N90-12972
A device to extract energy from water waves
[REPT-89-34] N90-12978
The M/G/1 processor sharing queue as the almost sure limit of feedback queues
[REPT-89-32] N90-13044
An expert system for VM performance analysis
[REPT-89-30] N90-13045
Solving three dimensional block bidiagonal linear systems on vector computers
[REPT-89-14] N90-13056
Binary Gray codes and index systems
[REPT-89-29] N90-13060
Conceptual dependency theory and robot programming
[REPT-89-20] N90-13106
Domain of attraction of an operator between supremum and sum
[REPT-89-05] N90-13119
On the existence of a maximal weak solution for a semilinear elliptic equation
[REPT-89-06] N90-13120
A generalization of Moak's q-Laguerre polynomials
[REPT-89-21] N90-13126
A point in betaZ/Z not contained in a maximal orbit closure
[REPT-89-26] N90-13127
A cell-centered multigrid method for three-dimensional anisotropic-diffusion and interface problems
[REPT-89-35] N90-13128
Local mode smoothing analysis of various incomplete factorization iterative methods in two dimensions
[REPT-89-36] N90-13129
Anaphoric trees and an extension of the model of anaphora resolution
[REPT-89-37] N90-13130
Julia-Fatou-Sullivan theory for real one-dimensional dynamics
[REPT-88-100] N90-13190
TEL-AVIV UNIV. (ISRAEL).
Advanced calcium-thionyl chloride high-power battery
[AD-A211856] N90-12846
TENNESSEE UNIV., KNOXVILLE.
Polymer characterization by electrohydrodynamic ionization mass spectrometry
[AD-A212130] N90-12739
Research on heating, instabilities, turbulence and RF emission from electric field dominated plasmas
[AD-A212122] N90-13243
TENNESSEE UNIV. SPACE INST., TULLAHOMA.
The fault monitoring and diagnosis knowledge-based system for space power systems: AMPERES, phase 1
[NASA-CR-185486] N90-12654
TEXAS A&M UNIV., COLLEGE STATION.
Heat pipe and thermal energy storage and corrosion studies (1988)
[AD-A212655] N90-12706
TEXAS UNIV., AUSTIN.
Problems in nonlinear acoustics: Scattering of sound by sound, parametric receiving arrays, nonlinear effects in asymmetric sound beams and pulsed finite amplitude sound beams
[AD-A211756] N90-13200
Tunneling microscopy of superconductors and tunneling barriers
[AD-A212120] N90-13257
TEXAS UNIV., DALLAS.
Proof of the feasibility of coherent and incoherent schemes for pumping a gamma-ray laser
[AD-A212315] N90-12921
TEXAS UNIV. AT DALLAS, RICHARDSON.
Proof of the feasibility of coherent and incoherent schemes for pumping a gamma-ray laser
[AD-A212882] N90-12924
THERMACORE, INC., LANCASTER, PA.
Heat pipes for sodium-sulfur batteries
[AD-A212523] N90-12865
THOMSON-CSF, PALO ALTO, CA.
A transformational method for verifying safety properties in real time systems
[AD-A211925] N90-13051
TOULOUSE UNIV. (FRANCE).
Chemical and photochemical reactivity in microemulsions and waterless microemulsions
[AD-A211776] N90-12692
TRW SPACE TECHNOLOGY LABS., REDONDO BEACH, CA.
Plasma separation process: Magnet move to Oak Ridge National Laboratory
[DE89-017457] N90-13242
TURKU UNIV. (FINLAND).
ERNE: Energetic and Relativistic Nuclei and Electron experiment N90-13315

U

UNILEVER RESEARCH, MERSEYSIDE (ENGLAND).
Self-tuning control of nonlinear Armax models
[RR-362] N90-12930
UNITED TECHNOLOGIES OF NEW MEXICO, INC., EAST HARTFORD, CT.
Investigation of fuel additive effects on sooting flames
[AD-A212925] N90-12709
UNIVERSIDAD NACIONAL DEL SUR, BAHIA BLANCA (ARGENTINA).
The computer age and traditional approximate, analytical methods N90-12772
UNIVERSITEIT TWENTE, ENSCHEDE (NETHERLANDS).
A graph-theoretical approach to block-copolymer complexes. Part 3: Loops and cycles
[MEMO-778-PT-3] N90-12750
Mathematical models for the linear induction motor
[RR-WB-88-17] N90-12853
LOTOS tools based on the Cornell synthesizer generator
[MEMO-INF-89-5] N90-13062
Abstract grammars based on transductions
[MEMO-INF-89-7-REV] N90-13063
Truth maintenance systems and their implementation in PROLOG
[MEMO-INF-89-13] N90-13064
On modeling resources in multiprocessor systems
[MEMO-INF-88-33] N90-13095
An implementation-oriented specification of the TUMULT communication primitives
[MEMO-INF-88-34] N90-13096
Path expression based operating systems
[MEMO-INF-88-68] N90-13097
Extended performability modeling using dynamic queing networks
[MEMO-INF-89-15] N90-13099
Trace theory
[MEMO-INF-89-16] N90-13100
Long dominating cycles and paths in graphs with large neighborhood unions
[MEMO-769] N90-13157
Remarks on the control of discrete time nonlinear systems
[MEMO-770] N90-13158
On the maximum period of a permutation of N elements
[MEMO-771] N90-13159
Multivariable divided difference and B-splines
[MEMO-772] N90-13160
Asymptotic expansions for two-stage rank tests
[MEMO-773] N90-13161
Note on the convergence of simulated annealing algorithms
[MEMO-774] N90-13162
Interpretation and manipulation of Edgeworth expansions
[MEMO-775] N90-13163

Transformations and representations of nonlinear systems
[MEMO-776] N90-13164
The discrete-time single-server queueing model
[MEMO-780] N90-13165
Towards a complete local solution of the nonlinear model matching problem
[MEMO-781] N90-13166
On new methods for computing with multivariate B-splines
[MEMO-783] N90-13183

UNIVERSITY OF SOUTHERN CALIFORNIA, MARINA DEL REY.
ISI's (Information Sciences Institute) SDI architecture simulator: Initial prototype user interface
[AD-A211325] N90-13053

V

VALLEY RESEARCH CORP., VAN NUYS, CA.
Development of an inventory of materials potentially sensitive to ambient atmospheric acidity in the South Coast Air Basin
[PB89-224604] N90-12982

VIBRATION INST., CLARENDON HILLS, IL.
The Shock and Vibration Digest, volume 21, no. 10 N90-12771

VIGYAN RESEARCH ASSOCIATES, INC., HAMPTON, VA.
Residual interference assessment in adaptive wall wind tunnels
[NASA-CR-181896] N90-12625

VIRGINIA POLYTECHNIC INST. AND STATE UNIV., BLACKSBURG.
NASA/USRA advanced space design program: The laser powered interorbital vehicle
[NASA-CR-186044] N90-12646
Analysis and simulation of dynamics of spacecraft power systems N90-12653
RTM user's guide
[NASA-CR-186091] N90-13065

VIRGINIA UNIV., CHARLOTTESVILLE.
Nonparallel stability of boundary layers N90-12514
Effect of roughness on the stability of boundary layers N90-12518
Modeling the temperature rise at the tip of a fast crack
[AD-A212418] N90-12966
Shape instabilities of plate-like structures. 1: Experimental observations in heavily cold worked in situ composites
[AD-A212251] N90-13021

VON KARMAN INST. FOR FLUID DYNAMICS, RHODE-SAINT-GENESE (BELGIUM).
An implicit Navier-Stokes solver optimised for a vector-parallel computer
[VKI-TN-169] N90-12890

W

WARWICK UNIV., COVENTRY (ENGLAND).
Biological and biochemical methane reactions
[PB89-232615] N90-12977

WASHINGTON UNIV., SEATTLE.
Spall resistance of alumina
[AD-A213213] N90-12735
Synthesis and high temperature chemistry of methylsilsesquioxane polymers produced by titanium catalyzed redistribution of methylhydridooligo- and polysiloxanes
[AD-A212000] N90-12736
Transition metal catalyzed synthesis of organmetallic polymers
[AD-A212133] N90-12740

WAYNE STATE UNIV., DETROIT, MI.
Interstitial formation, non-equilibrium and macroscopic processes in mercury cadmium telluride
[AD-A212412] N90-13267

WESTINGHOUSE ELECTRIC CORP., PITTSBURGH, PA.
An investigation of the irradiation swelling mechanisms in refractory metals at high temperatures
[AD-A211406] N90-12719

WESTINGHOUSE SAVANNAH RIVER CO., AIKEN, SC.
Rapid heating tensile tests of high-energy-rate-forged 316L stainless steel charged with hydrogen and tritium
[DE89-017869] N90-12717

WISCONSIN UNIV., MADISON.
Use of ground penetrating radar to define recharge areas in the Central Sand Plain
[PB89-224885] N90-12814
Survey of the response of standard limited streamer tubes over the complete range of three-component gas mixtures of isobutane, CO(sub 2), argon
[DE89-016692] N90-12875
The Painleve test for nonlinear ordinary and partial differential equations
[AD-A212894] N90-13177

WRIGHT STATE UNIV., DAYTON, OH.
Analysis of the performance of heat pipes and phase-change materials with multiple localized heat sources for space applications
[AD-A212232] N90-12898

WYLE LABS., INC., HUNTSVILLE, AL.
Advanced spacecraft fire safety: Proposed projects and program plan
[NASA-CR-185147] N90-12645

Y

YALE UNIV., NEW HAVEN, CT.
Fear-potentiated startle as a model system for analyzing learning and memory
[AD-A212131] N90-13029
A fast algorithm for the evaluation of heat potentials
[AD-A211316] N90-13052
A fan-in algorithm for distributed sparse numerical factorization
[AD-A211589] N90-13054

Typical Contract Number Index Listing

Listings in this index are arranged alphanumerically by contract number. Under each contract number the NASA accession numbers denoting documents that have been produced as a result of research done under that contract are arranged in ascending order. The NASA accession number denotes the number by which the citation is identified.

AF PROJ. 2301 ..... N90-12719
N90-13243
AF PROJ. 2303 ..... N90-12741
N90-12743
AF PROJ. 2304 ..... N90-13087
N90-13089
N90-13185
AF PROJ. 2306 ..... N90-13257
N90-13270
AF PROJ. 2307 ..... N90-12877
AF PROJ. 2311 ..... N90-12987
AF PROJ. 2312 ..... N90-13029
AF PROJ. 2313 ..... N90-13016
N90-13032
AF PROJ. 2420 ..... N90-12742
AF PROJ. 2567 ..... N90-12567
AF PROJ. 2729 ..... N90-13022
AF PROJ. 3005 ..... N90-12663
AF PROJ. 3145 ..... N90-12648
AF PROJ. 3326 ..... N90-12703
AF-AFOSR-0012-84 ..... N90-12920
AF-AFOSR-0033-87 ..... N90-12743
AF-AFOSR-0035-88 ..... N90-13270
AF-AFOSR-0037-86 ..... N90-12987
AF-AFOSR-0046-88 ..... N90-12743
AF-AFOSR-0047-86 ..... N90-13185
AF-AFOSR-0076-86 ..... N90-13093
AF-AFOSR-0078-88 ..... N90-12847
AF-AFOSR-0100-86 ..... N90-13243
AF-AFOSR-0124-86 ..... N90-13089
AF-AFOSR-0140-88 ..... N90-13032
AF-AFOSR-0193-87 ..... N90-13016
AF-AFOSR-0228-87 ..... N90-13257
AF-AFOSR-0255-87 ..... N90-12877
AF-AFOSR-0263-85 ..... N90-13177
AF-AFOSR-0336-87 ..... N90-13029
AF-AFOSR-0350-86 ..... N90-12741
AMD.BA-08W00022 ..... N90-12631
N90-12632
ARB-A6-079-32 ..... N90-12982
ARPA ORDER 9526 ..... N90-12688
A84/KL/065 ..... N90-13069
A84/KLU/046 ..... N90-12629
A85/K/077 ..... N90-13041
A86/KL/045 ..... N90-12824
A87/K/048 ..... N90-13042
A87/KM/172 ..... N90-13208
N90-13233
A88/KL/608 ..... N90-12825
A88/KM/627 ..... N90-12826
CETIM-86-3191-B N90-12724
CETIM-87-2618-B N90-12726
CETIM-87-2618-D N90-12725
CWI-55-092 ..... N90-13136
DA PROJ. 1L1-61102-B-74-A N90-12832
N90-13209
N90-13210
DA PROJ. 1L1-61102-BH-57 ..... N90-13006
DA PROJ. 1L1-62105-AH-84 ..... N90-12762
DAAA15-86-K-0022 ..... N90-12711
DAAA21-76-C-0225 ..... N90-13091
DAAE07-88-C-R076 ..... N90-13037
DAAG29-83-G-0007 ..... N90-12733
DAAG29-84-G-0004 ..... N90-13118
DAAG29-85-K-0098 ..... N90-13265
DAAG29-85-K-0119 ..... N90-13267
DAAG29-85-K-0120 ..... N90-12756
DAAG29-85-K-0128 ..... N90-12758
DAAG29-85-K-0200 ..... N90-12757
DAAG29-85-K-0211 ..... N90-13264
DAAK60-83-C-0055 ..... N90-13043
DAAL01-85-C-0456 ..... N90-13235
DAAL03-86-C-0022 ..... N90-13280
DAAL03-86-K-0015 ..... N90-13263
DAAL03-86-K-0065 ..... N90-12983
DAAL03-86-K-0117 ..... N90-13007
DAAL03-86-K-0171 ..... N90-12847
N90-13093
N90-13191
DAAL03-87-K-0012 ..... N90-13237
DAAL03-87-K-0031 ..... N90-12830
DAAL03-88-C-0025 ..... N90-12947
DAAL03-88-G-0024 ..... N90-13170
DAAL03-88-K-0063 ..... N90-13186
DAAL03-88-K-0076 ..... N90-13173
DAAL03-88-K-0091 ..... N90-13021
DACA72-87-C-0015 ..... N90-13111
DACA76-85-C-0010 ..... N90-13084
N90-13110
N90-13195
DACA76-86-C-0019 ..... N90-12944
DAJA45-85-C-0024 ..... N90-12692
DAJA45-87-C-0011 ..... N90-13255
DAJA45-87-C-0014 ..... N90-12768
DAJA45-87-C-0035 ..... N90-13006
DAJA45-87-C-0058 ..... N90-12700
DAJA45-88-M-0137 ..... N90-13236
DAJA45-88-M-0151 ..... N90-13250
DAJA45-88-M-0409 ..... N90-13171
DAJA45-89-C-0013 ..... N90-12846
DAJA45-89-M-0043 ..... N90-12942
N90-12943
DARPA ORDER 5682 ..... N90-12944
DE-AC01-87CE-40762 ..... N90-12684
DE-AC02-76CH-00016 ..... N90-12754
DE-AC02-76ER-00881 ..... N90-12875
DE-AC02-76ER-03069 ..... N90-12875
DE-AC02-76ER-03130 ..... N90-13299
DE-AC03-76SF-00515 ..... N90-12844
N90-12875
DE-AC03-77ET-33006 ..... N90-13242
DE-AC05-84OR-21400 ..... N90-12979
N90-13239
DE-AC09-76SR-00001 ..... N90-12717
DE-AC09-89SR-18035 ..... N90-12717
DE-FG03-87ER-25028 ..... N90-13189
DE-FG03-87ER-25030 ..... N90-13086
N90-13088
N90-13174
DEPE(CNA)-PROJ. EU650 ..... N90-12807
DI-14-08-0001-G-1458 ..... N90-12814
DNA001-87-C-0171 ..... N90-12836
N90-12837
DOT-FA74WAI-432 ..... N90-12627
DRET-8-34-001 ..... N90-12894
DRET-84-34-481-00-470-75-01 ..... N90-12622
DRET-84-002 ..... N90-12897
DRET-85-1437 ..... N90-12917
DRET-86-34-001 ..... N90-12677
DRET-86-047-00-470-75-01 ..... N90-13040
DRET-86-106 ..... N90-12744
DRET-87-34-001 ..... N90-12678
N90-12698
DRET-87-34-141 ..... N90-13201
DRET-87-001-51 ..... N90-12630
DRET-87-068 ..... N90-12564
DRET-87-1383/DS/SR N90-12674
DRET-88-34-001 ..... N90-12565
N90-12592
N90-12672
DRET-88-002-19 ..... N90-12502
DRET-88-817 ..... N90-13278
DRET-88-1404/DS/SR N90-12887
DRET/ETCA/CREA-CI-047683 ..... N90-12746
DRET/ETCA/CREA-CI-048064 ..... N90-12746
ETCA/CREA/PS-CI-048190 ..... N90-12955
ETCA/CTME/CME-042345 ..... N90-13108
FMV-FFL-82250-85-273-25-001 ..... N90-12664
F2006D N90-12574
F04701-85-C-0086 ..... N90-12869
F04701-88-C-0089 ..... N90-12643
N90-12714
N90-12759
N90-12916
N90-13238
F04701-88-C-9989 ..... N90-12870
F19628-86-K-0016 ..... N90-12990
F19628-87-C-0053 ..... N90-12986
F19628-89-C-0001 ..... N90-13085
F29601-88-K-0004 ..... N90-12703
F30602-81-C-0193 ..... N90-13033
F33615-83-C-3600 ..... N90-12624
F33615-83-D-0602 ..... N90-13022
F33615-86-C-2720 ..... N90-12898
F33615-86-C-2721 ..... N90-12648
F33615-86-C-2723 ..... N90-12706
F33615-86-C-5141 ..... N90-12742
F33615-87-C-0012 ..... N90-12634
F33615-87-C-5275 ..... N90-12663
F33615-88-C-2855 ..... N90-12850
F33615-88-C-2865 ..... N90-12881
F33615-88-C-2868 ..... N90-13193
F33615-88-C-2892 ..... N90-12865
F49620-85-C-0049 ..... N90-12620
F49620-85-C-0060 ..... N90-12719
F49620-86-C-0009 ..... N90-13213
F49620-86-C-0019 ..... N90-13247
F49620-86-C-0054 ..... N90-12709
F49620-86-K-0019 ..... N90-13245
F49620-87-C-0027 ..... N90-12764
F49620-87-C-0062 ..... N90-13112
F49620-87-C-0065 ..... N90-13052
F49620-88-C-0026 ..... N90-13090
F49620-88-C-0033 ..... N90-13087
F61101-88-C-0015 ..... N90-12806
GRI-5081-271-1680 ..... N90-12880
GRI-5081-353-0422 ..... N90-12880
GRI-5086-260-1209 ..... N90-12977
GRI-5086-260-1250 ..... N90-12689
GRI-5086-271-1226 ..... N90-12928
MDA903-84-C-0031 ..... N90-12680
MDA903-85-C-0030 ..... N90-13082
MDA904-87-H-2009 ..... N90-12840
MIPR-ARO-102-89 ..... N90-12754
MIPR-ARO-103-88 ..... N90-12754
MIPR-ARO-112-86 ..... N90-12754
MIPR-101-88 ..... N90-12704
MIPR-112-87 ..... N90-12754
MIPR-129-86 ..... N90-12739
MRES-86-A-0721 ..... N90-12748
MRES-86A-0526 ..... N90-12675
NAGW-1340 ..... N90-13274
N90-13297
N90-13298
N90-13299
NAG1-343 ..... N90-13065
NAG1-566 ..... N90-13204
NAG1-778 ..... N90-12872
NAG1-825 ..... N90-12959
NAG2-208 ..... N90-13296
NAG2-513 ..... N90-13113
NAG3-536 ..... N90-12784
NAG3-624 ..... N90-12882
NAG3-730 ..... N90-12500
NAG3-735 ..... N90-12882
NAG3-773 ..... N90-12936
NAG5-898 ..... N90-13003
NAG5-1010 ..... N90-12973
NAG8-654 ..... N90-12996
NAG8-721 ..... N90-12654
NAG8-724 ..... N90-12768
NAG8-774 ..... N90-12770
NASA ORDER H-80591-B N90-12935
NASW-4234 ..... N90-13047
NASW-4435 ..... N90-12590
N90-12646
N90-12655

	N90-13036
NAS1-17999	N90-13050
NAS1-18037	N90-13198
NAS1-18107	N90-12874
NAS1-18336	N90-13228
NAS1-18533	N90-12718
NAS1-18585	N90-12625
NAS1-18605	N90-12874
NAS3-23051	N90-12617
NAS3-25266	N90-12560
NAS3-25367	N90-12645
NAS8-30490	N90-12651
	N90-12652
	N90-12656
NAS8-37302	N90-12650
NATO-0034/87	N90-13179
NCA2-210	N90-12499
NCC2-555	N90-13035
NCC2-582	N90-12498
NGR-05-002-160	N90-13316
NSERC-OGP-0036747	N90-13191
NSF ATM-84-05276	N90-12998
NSF ATM-86-10354	N90-12998
NSF CCR-84-13211	N90-13086
NSF CCR-88-12567	N90-13093
NSF CHE-86-20274	N90-13213
NSF DCR-85-21451	N90-13054
NSF DCR-86-06366	N90-13191
NSF DDM-88-14253	N90-13189
NSF DMS-87-01085	N90-13113
NSF DMS-89-13089	N90-13189
NSF ECS-87-15153	N90-13088
	N90-13174
NSF IRI-87-19394	N90-13195
NSF MCS-82-00632	N90-13089
NSF OCE-87-13699	N90-12980
NSF PHY-85-0498	N90-13274
NSF PHY-85-06686	N90-13274
N00014-79-C-0769	N90-12925
N00014-79-C-0801	N90-13179
N00014-80-C-0622	N90-12847
N00014-81-K-0526	N90-12738
N00014-82-K-0280	N90-12691
N00014-83-C-0008	N90-13023
N00014-83-K-0227	N90-13212
N00014-83-K-0321	N90-12849
N00014-83-K-0343	N90-13254
N00014-84-C-0149	N90-12864
N00014-85-K-0124	N90-12908
	N90-12941
	N90-13084
	N90-13110
	N90-13195
N00014-85-K-0177	N90-13271
N00014-85-K-0200	N90-12838
N00014-85-K-0445	N90-13191
N00014-85-K-0459	N90-12763
N00014-85-K-0782	N90-12829
N00014-86-C-0121	N90-12712
N00014-86-C-0301	N90-12779
N00014-86-C-2432	N90-13269
N00014-86-C-2488	N90-12921
	N90-12924
N00014-86-K-0043	N90-13213
	N90-13226
N00014-86-K-0180	N90-13175
N00014-86-K-0202	N90-12835
	N90-13169
N00014-86-K-0291	N90-13030
N00014-86-K-0310	N90-13054
N00014-86-K-0350	N90-13266
N00014-86-K-0593	N90-13092
	N90-13093
N00014-86-K-0608	N90-12871
N00014-86-K-0685	N90-12941
N00014-87-C-0232	N90-12999
N00014-87-C-0342	N90-13026
N00014-87-G-0212	N90-12991
N00014-87-J-1170	N90-12988
N00014-87-K-0022	N90-13053
N00014-87-K-0142	N90-13086
	N90-13088
	N90-13174
N00014-87-K-0301	N90-12705
N00014-87-K-0326	N90-12735
N00014-87-K-0825	N90-12847
	N90-13092
	N90-13093
N00014-87-K-2011	N90-12841
N00014-88-C-0391	N90-12688
N00014-88-J-1207	N90-12920
N00014-88-K-0109	N90-12753
N00014-88-K-0111	N90-12966
N00014-88-K-0139	N90-13256
N00014-88-K-0305	N90-12740
N00014-88-K-0360	N90-12737
N00014-88-K-0385	N90-12755
N00014-88-K-2016	N90-12760
N00014-88-K-6002	N90-12863
N00014-88-WX-24148	N90-12976
N00014-89-C-0022	N90-12708
N00014-89-F-00020	N90-12911
N00014-89-J-1003	N90-12975
N00014-89-J-1197	N90-12761
N00014-89-J-1527	N90-13051
N00014-89-J-1627	N90-13244
N00014-89-J-1659	N90-13200
N00014-89-K-0305	N90-13268
N00014-89-WX-24	N90-13052
N00014-89-WX-20010	N90-13187
N00014-89-WX-24004	N90-13189
N66001-85-D-0203	N90-12736
PROJ. RM35G87	N90-12761
RR04108	N90-12761
	N90-12761
RR04209	N90-12912
R87/KL/094	N90-12975
SERC-87-600212	N90-12705
STPA-85-95-004-35	N90-13023
STPA-86-96-024-00-471-75-86	N90-13030
STU-87-88	N90-13230
STU-88-89	N90-12890
W-31-109-ENG-38	N90-12888
W-7405-ENG-36	N90-12676
W-7405-ENG-48	N90-12953
055-40-01-00-96	N90-12952
146-90-04-52	N90-12914
199-18-12-01	N90-12716
199-50-62-07-02	N90-12929
310-10-60-60-00	N90-12802
310-10-62-15-00	N90-13228
310-10-63-50-00	N90-13013
310-20-65-86-04	N90-12804
310-20-66-87-02	N90-12788
310-30-70-89-02	N90-12789
310-30-71-83-02	N90-12787
	N90-12791
	N90-12790
310-30-71-83-04	N90-12794
314-30-42-01-34	N90-12792
314-30-56-44-01	N90-12793
314-30-56-57-17	N90-12795
314-30-56-57-33	N90-12796
	N90-12797
315-91-50-02-02	N90-12800
323-53-62	N90-12801
414-70-75-25	N90-12798
505-43-01	N90-12799
505-60-00	N90-12803
505-60-01	N90-12645
505-60-31-06	N90-12984
	N90-12589
	N90-13137
505-61-01-09	N90-13048
505-61-51	N90-12503
505-62-21	N90-12519
505-62-71	N90-12539
505-63-1A	N90-12625
	N90-12904
	N90-12561
505-63-01-02	N90-12618
505-63-51-10	N90-12658
505-90-21-01	N90-12659
506-41-21	N90-12670
506-49-21-02	N90-12718
510-01-0A	N90-12580
532-09-01	N90-12874
535-03-01	N90-12696
535-03-11-03	N90-13050
650-60-23	N90-12950
	N90-12669
	N90-12560
	N90-13198
	N90-12813

REPORT/ACCESSION NUMBER INDEX

Typical Report Number Index Listing

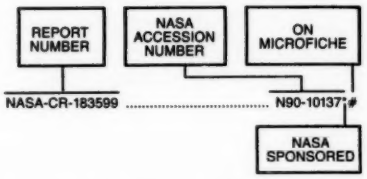

Listings in this index are arranged alphanumerically by report number. The NASA accession number denotes the number by which the citation is identified. An asterisk (*) indicates that the itemis a NASA report. A pound sign (#) indicates that the item is available on microfiche.

A-8 ..... N90-13049 #
A-89034 ..... N90-13319* #
A-89044 ..... N90-13048* #
A-89084 ..... N90-13013* #
A-89201 ..... N90-12904* #
A-89259 ..... N90-13137* #

AD-A205150 ..... N90-13292 #
AD-A210618 ..... N90-13250 #
AD-A211298 ..... N90-12806 #
AD-A211315 ..... N90-12742 #
AD-A211316 ..... N90-13052 #
AD-A211319 ..... N90-12881 #
AD-A211320 ..... N90-12848 #
AD-A211321 ..... N90-13213 #
AD-A211325 ..... N90-13053 #
AD-A211338 ..... N90-12570 #
AD-A211362 ..... N90-12647 #
AD-A211379 ..... N90-13118 #
AD-A211404 ..... N90-12648 #
AD-A211406 ..... N90-12719 #
AD-A211410 ..... N90-12663 #
AD-A211416 ..... N90-12947 #
AD-A211460 ..... N90-12743 #
AD-A211483 ..... N90-12777 #
AD-A211486 ..... N90-12496 #
AD-A211491 ..... N90-13016 #
AD-A211492 ..... N90-13214 #
AD-A211532 ..... N90-12987 #
AD-A211569 ..... N90-13054 #
AD-A211590 ..... N90-12849 #
AD-A211591 ..... N90-12691 #
AD-A211648 ..... N90-13037 #
AD-A211663 ..... N90-12916 #
AD-A211670 ..... N90-12643 #
AD-A211747 ..... N90-12988 #
AD-A211756 ..... N90-13200 #
AD-A211758 ..... N90-13055 #
AD-A211759 ..... N90-13017 #
AD-A211761 ..... N90-13193 #
AD-A211762 ..... N90-12850 #
AD-A211771 ..... N90-12501 #
AD-A211772 ..... N90-12989 #
AD-A211776 ..... N90-12692 #
AD-A211779 ..... N90-12998 #
AD-A211780 ..... N90-12999 #
AD-A211785 ..... N90-12990 #
AD-A211856 ..... N90-12846 #
AD-A211883 ..... N90-13092 #
AD-A211886 ..... N90-13254 #
AD-A211915 ..... N90-13093 #
AD-A211925 ..... N90-13051 #
AD-A211948 ..... N90-12847 #
AD-A211954 ..... N90-12951 #
AD-A211955 ..... N90-12970 #
AD-A211977 ..... N90-12688 #
AD-A211986 ..... N90-12915 #
AD-A211987 ..... N90-12986 #
AD-A211989 ..... N90-13255 #
AD-A212000 ..... N90-12736 #
AD-A212084 ..... N90-12737 #
AD-A212103 ..... N90-12738 #
AD-A212117 ..... N90-13256 #
AD-A212119 ..... N90-12877 #
AD-A212120 ..... N90-13257 #
AD-A212122 ..... N90-13243 #
AD-A212127 ..... N90-12495 #
AD-A212128 ..... N90-13014 #
AD-A212130 ..... N90-12739 #
AD-A212131 ..... N90-13029 #
AD-A212133 ..... N90-12740 #
AD-A212141 ..... N90-12976 #
AD-A212142 ..... N90-12741 #
AD-A212149 ..... N90-12971 #
AD-A212187 ..... N90-12863 #
AD-A212190 ..... N90-12829 #
AD-A212199 ..... N90-12644 #
AD-A212200 ..... N90-12657 #
AD-A212201 ..... N90-12963 #
AD-A212202 ..... N90-12964 #
AD-A212204 ..... N90-12699 #
AD-A212210 ..... N90-13082 #
AD-A212214 ..... N90-12700 #
AD-A212215 ..... N90-12752 #
AD-A212225 ..... N90-12753 #
AD-A212226 ..... N90-12830 #
AD-A212232 ..... N90-12898 #
AD-A212236 ..... N90-12975 #
AD-A212240 ..... N90-12754 #
AD-A212242 ..... N90-13020 #
AD-A212249 ..... N90-13263 #
AD-A212251 ..... N90-13021 #
AD-A212263 ..... N90-12965 #
AD-A212264 ..... N90-12701 #
AD-A212265 ..... N90-12765 #
AD-A212266 ..... N90-12633 #
AD-A212268 ..... N90-12702 #
AD-A212269 ..... N90-13264 #
AD-A212271 ..... N90-12731 #
AD-A212272 ..... N90-12578 #
AD-A212275 ..... N90-13083 #
AD-A212284 ..... N90-13185 #
AD-A212285 ..... N90-12983 #
AD-A212287 ..... N90-13030 #
AD-A212291 ..... N90-13006 #
AD-A212292 ..... N90-12920 #
AD-A212294 ..... N90-12732 #
AD-A212295 ..... N90-12637 #
AD-A212303 ..... N90-12733 #
AD-A212304 ..... N90-12755 #
AD-A212309 ..... N90-12864 #
AD-A212315 ..... N90-12921 #
AD-A212317 ..... N90-13169 #
AD-A212321 ..... N90-13186 #
AD-A212322 ..... N90-12642 #
AD-A212337 ..... N90-12941 #
AD-A212338 ..... N90-12908 #
AD-A212339 ..... N90-12756 #
AD-A212341 ..... N90-13170 #
AD-A212342 ..... N90-12766 #
AD-A212348 ..... N90-12703 #
AD-A212353 ..... N90-12757 #
AD-A212356 ..... N90-13022 #
AD-A212359 ..... N90-13110 #
AD-A212360 ..... N90-12758 #
AD-A212363 ..... N90-13226 #
AD-A212366 ..... N90-13265 #
AD-A212369 ..... N90-13171 #
AD-A212377 ..... N90-12899 #
AD-A212378 ..... N90-12942 #
AD-A212379 ..... N90-12943 #
AD-A212384 ..... N90-12900 #
AD-A212385 ..... N90-13280 #
AD-A212386 ..... N90-13195 #
AD-A212387 ..... N90-13266 #
AD-A212404 ..... N90-12734 #
AD-A212406 ..... N90-12579 #
AD-A212407 ..... N90-12759 #
AD-A212408 ..... N90-12595 #
AD-A212410 ..... N90-13007 #
AD-A212411 ..... N90-12704 #
AD-A212412 ..... N90-13267 #
AD-A212415 ..... N90-13244 #
AD-A212418 ..... N90-12966 #
AD-A212420 ..... N90-13235 #
AD-A212421 ..... N90-13172 #
AD-A212429 ..... N90-12901 #
AD-A212441 ..... N90-12596 #
AD-A212442 ..... N90-12566 #
AD-A212448 ..... N90-12760 #
AD-A212449 ..... N90-12705 #
AD-A212451 ..... N90-12620 #
AD-A212455 ..... N90-13236 #
AD-A212457 ..... N90-13084 #
AD-A212469 ..... N90-13011 #
AD-A212470 ..... N90-12831 #
AD-A212510 ..... N90-13085 #
AD-A212514 ..... N90-13086 #
AD-A212519 ..... N90-13209 #
AD-A212520 ..... N90-13210 #
AD-A212521 ..... N90-12832 #
AD-A212522 ..... N90-12567 #
AD-A212523 ..... N90-12865 #
AD-A212527 ..... N90-12866 #
AD-A212528 ..... N90-13031 #
AD-A212533 ..... N90-13087 #
AD-A212539 ..... N90-12761 #
AD-A212555 ..... N90-12944 #
AD-A212568 ..... N90-12762 #
AD-A212572 ..... N90-12922 #
AD-A212573 ..... N90-12597 #
AD-A212575 ..... N90-12638 #
AD-A212577 ..... N90-12680 #
AD-A212585 ..... N90-13237 #
AD-A212591 ..... N90-13211 #
AD-A212594 ..... N90-12994 #
AD-A212595 ..... N90-13268 #
AD-A212618 ..... N90-13173 #
AD-A212620 ..... N90-12833 #
AD-A212630 ..... N90-13187 #
AD-A212632 ..... N90-13188 #
AD-A212653 ..... N90-12834 #
AD-A212655 ..... N90-12706 #
AD-A212658 ..... N90-12902 #
AD-A212670 ..... N90-13032 #
AD-A212674 ..... N90-12903 #
AD-A212677 ..... N90-13245 #
AD-A212690 ..... N90-13023 #
AD-A212703 ..... N90-13024 #
AD-A212704 ..... N90-13025 #
AD-A212705 ..... N90-12867 #
AD-A212706 ..... N90-12923 #
AD-A212707 ..... N90-12868 #
AD-A212708 ..... N90-13008 #
AD-A212724 ..... N90-12995 #
AD-A212732 ..... N90-12869 #
AD-A212742 ..... N90-12681 #
AD-A212746 ..... N90-13196 #
AD-A212749 ..... N90-12835 #
AD-A212750 ..... N90-12870 #
AD-A212752 ..... N90-13174 #
AD-A212756 ..... N90-12909 #
AD-A212757 ..... N90-13246 #
AD-A212759 ..... N90-13175 #
AD-A212761 ..... N90-13046 #
AD-A212762 ..... N90-13197 #
AD-A212763 ..... N90-12634 #
AD-A212764 ..... N90-13033 #
AD-A212765 ..... N90-13034 #
AD-A212789 ..... N90-13043 #
AD-A212790 ..... N90-12707 #
AD-A212794 ..... N90-12836 #
AD-A212795 ..... N90-12837 #
AD-A212796 ..... N90-12763 #
AD-A212800 ..... N90-13088 #
AD-A212804 ..... N90-13227 #
AD-A212806 ..... N90-13111 #
AD-A212808 ..... N90-12838 #
AD-A212832 ..... N90-12910 #
AD-A212836 ..... N90-12839 #
AD-A212839 ..... N90-13176 #
AD-A212848 ..... N90-13089 #
AD-A212853 ..... N90-12764 #
AD-A212854 ..... N90-13189 #
AD-A212858 ..... N90-13112 #
AD-A212873 ..... N90-13269 #
AD-A212875 ..... N90-12708 #

AD-A212876 ..... N90-12840 #
AD-A212877 ..... N90-13026 #
AD-A212882 ..... N90-12924 #
AD-A212888 ..... N90-12841 #
AD-A212894 ..... N90-13177 #
AD-A212925 ..... N90-12709 #
AD-A212953 ..... N90-12710 #
AD-A212954 ..... N90-12767 #
AD-A212966 ..... N90-13270 #
AD-A212967 ..... N90-13247 #
AD-A212973 ..... N90-13090 #
AD-A212977 ..... N90-12842 #
AD-A213041 ..... N90-13212 #
AD-A213155 ..... N90-12911 #
AD-A213158 ..... N90-12843 #
AD-A213159 ..... N90-13012 #
AD-A213162 ..... N90-12945 #
AD-A213168 ..... N90-12711 #
AD-A213169 ..... N90-12712 #
AD-A213171 ..... N90-13027 #
AD-A213189 ..... N90-12871 #
AD-A213202 ..... N90-12912 #
AD-A213213 ..... N90-12735 #
AD-A213303 ..... N90-12713 #
AD-A213316 ..... N90-13028 #
AD-A213318 ..... N90-12568 #
AD-A213321 ..... N90-12925 #
AD-A213324 ..... N90-12714 #
AD-A213325 ..... N90-13238 #
AD-A213334 ..... N90-12624 #
AD-A213338 ..... N90-13091 #
AD-A213345 ..... N90-13271 #
AD-A213347 ..... N90-12779 #

AD-D014189 ..... N90-12859 #
AD-D014190 ..... N90-12860
AD-D014191 ..... N90-12594
AD-D014193 ..... N90-12751
AD-D014195 ..... N90-13262
AD-D014198 ..... N90-12861
AD-D014199 ..... N90-12828
AD-D014200 ..... N90-12679
AD-D014202 ..... N90-12940 #
AD-D014205 ..... N90-12948
AD-D014206 ..... N90-12862 #

AD-E501144 ..... N90-12496 #
AD-E501149 ..... N90-12638 #
AD-E501149 ..... N90-12680 #
AD-E900917 ..... N90-12834 #

ADS-TR-3185-01 ..... N90-13111 #
ADS-TR-3213-01 ..... N90-13037 #

AFATL-TP-89-14 ..... N90-12848 #
AFATL-TP-89-17 ..... N90-12567 #

AFATL-TR-89-19 ..... N90-12899 #

AFGL-ERP-1020 ..... N90-12989 #

AFGL-TR-89-0029 ..... N90-12989 #
AFGL-TR-89-0123 ..... N90-12806 #
AFGL-TR-89-0201 ..... N90-12647 #

AFHRL-TP-89-46 ..... N90-13034 #

AFHRL-TR-88-75 ..... N90-13033 #
AFHRL-TR-89-3 ..... N90-12634 #

AFIT/CI/CIA-88-236 ..... N90-13031 #
AFIT/CI/CIA-88-237 ..... N90-12866 #

AFOSR-89-1051TR ..... N90-12719 #
AFOSR-89-1081TR ..... N90-13016 #
AFOSR-89-1108TR ..... N90-12987 #
AFOSR-89-1131TR ..... N90-13032 #
AFOSR-89-1165TR ..... N90-12743 #
AFOSR-89-1203TR ..... N90-12741 #
AFOSR-89-1204TR ..... N90-13257 #
AFOSR-89-1205TR ..... N90-12877 #
AFOSR-89-1221TR ..... N90-13029 #
AFOSR-89-1225TR ..... N90-12620 #
AFOSR-89-1226TR ..... N90-13243 #
AFOSR-89-1234TR ..... N90-13247 #
AFOSR-89-1235TR ..... N90-13112 #
AFOSR-89-1239TR ..... N90-12764 #
AFOSR-89-1241TR ..... N90-13270 #
AFOSR-89-1245TR ..... N90-13245 #
AFOSR-89-1247TR ..... N90-12709 #
AFOSR-89-1252TR ..... N90-13185 #
AFOSR-89-1253TR ..... N90-13067 #
AFOSR-89-1254TR ..... N90-13089 #
AFOSR-89-1255TR ..... N90-13090 #

AFWAL-TR-88-3120 ..... N90-13083 #

AFWAL-TR-88-4199 ..... N90-12742 #

AGARD-AR-260 ..... N90-12623 #

AI-M-1105 ..... N90-12908 #
AI-M-1114 ..... N90-13084 #
AI-M-1120 ..... N90-12941 #
AI-M-1131 ..... N90-13195 #
AI-M-1140 ..... N90-13110 #

AI-TR-1144 ..... N90-13175 #

AIAA-89-1060 ..... N90-12560* #
AIAA-90-0048 ..... N90-12561* #

AL-CP-89-001A-ADD ..... N90-13227 #

AR-005-688 ..... N90-12775 #
AR-005-690 ..... N90-12661 #

ARB-R-89/399 ..... N90-12982 #

ARC-TR-89-011 ..... N90-12986 #

ARL-FLIGHT-MECH-TM-404 ..... N90-12566 #

ARL-PROP-TM-441 ..... N90-12596 #

ARL-STRUC-TM-503 ..... N90-12597 #
ARL-STRUC-TM-504 ..... N90-12501 #

ARL-SYS-TM-98 ..... N90-12595 #
ARL-SYS-TM-102 ..... N90-12579 #

ARO-20377.4-MS ..... N90-12733 #
ARO-21235.23-MA-H ..... N90-13118 #
ARO-22388.8-MS ..... N90-12758 #
ARO-22574.9-CH ..... N90-12739 #
ARO-22592.5-PH ..... N90-13265 #
ARO-22644.8-MS ..... N90-12756 #
ARO-22732.14-MS ..... N90-12754 #
ARO-22825.7-CH ..... N90-12757 #
ARO-22908.5-PH ..... N90-13264 #
ARO-23019.1-GS ..... N90-12983 #
ARO-23090.16-MS ..... N90-13263 #
ARO-23356.6-CH ..... N90-12704 #
ARO-23779.2-MA-F ..... N90-13280 #
ARO-23935.5-GS ..... N90-13007 #
ARO-24456.2-EG ..... N90-13172 #
ARO-24480.25-EL ..... N90-13237 #
ARO-24706.4-GS ..... N90-12830 #
ARO-24834.2-MA ..... N90-13173 #
ARO-25177.4-MS-1 ..... N90-13021 #
ARO-25301.1-MA-CF ..... N90-13170 #
ARO-25839.11-MA ..... N90-13186 #
ARO-26007.1-EG-SBI ..... N90-12947 #

ASR-1 ..... N90-13200 #

AVSCOM-TM-89-B-004 ..... N90-12580* #

BNL-43186 ..... N90-12754 #

BRL-TR-2980 ..... N90-12963 #
BRL-TR-3027 ..... N90-12701 #
BRL-TR-3031 ..... N90-12965 #
BRL-TR-3036 ..... N90-12633 #
BRL-TR-3038 ..... N90-12765 #
BRL-TR-3044 ..... N90-12702 #

BROWN-HET-725 ..... N90-13299* #

BR107144 ..... N90-13318 #
BR107145 ..... N90-13317 #
BR108108 ..... N90-13178 #
BR108109 ..... N90-13057 #
BR108110 ..... N90-13058 #
BR108280 ..... N90-12810 #
BR108312 ..... N90-12818 #
BR108362 ..... N90-12562 #
BR108440 ..... N90-13066 #
BR108479 ..... N90-12857 #
BR108488 ..... N90-12893 #
BR108489 ..... N90-12619 #
BR108558 ..... N90-13231 #
BR108630 ..... N90-12817 #
BR108667 ..... N90-12820 #
BR108668 ..... N90-13067 #
BR108686 ..... N90-13275 #
BR108723 ..... N90-12640 #
BR108793 ..... N90-13292 #
BR108860 ..... N90-12819 #
BR108876 ..... N90-13206 #
BR108877 ..... N90-13205 #
BR108878 ..... N90-12575 #
BR108923 ..... N90-12641 #

BR108924 ..... N90-12816 #
BR109026 ..... N90-13207 #
BR109060 ..... N90-12671 #
BR109148 ..... N90-12576 #
BR109214 ..... N90-13070 #
BR109769 ..... N90-12905 #
BR109770 ..... N90-12563 #
BR109773 ..... N90-12815 #
BR111531 ..... N90-12858 #
BR111533 ..... N90-13068 #
BR111686 ..... N90-13005 #

BUMINES-RI-9232 ..... N90-12686 #

CAA-PAPER-88017 ..... N90-12572
CAA-PAPER-89003 ..... N90-12573
CAA-PAPER-89004 ..... N90-12807

CALSPAN-7589-1 ..... N90-12999 #

CBIP-PAPER-31 ..... N90-13110 #
CBIP-PAPER-35 ..... N90-13084 #
CBIP-PAPER-38 ..... N90-13195 #

CCMS-89-11 ..... N90-13065* #

CERT-RSF-OA-25/5005-AYD ..... N90-12502 #
CERT-RSF-OA-43/5018-AYD ..... N90-12897 #
CERT-RSF-OA-74/2259-AYD ..... N90-12889 #

CERT-RTS-OA-31/5025-AYD ..... N90-12888 #

CERT-1/1398-MO ..... N90-12674 #

CETIM-13-Y-313 ..... N90-12962 #
CETIM-101530 ..... N90-12723 #
CETIM-104320 ..... N90-12724 #
CETIM-104500 ..... N90-12725 #
CETIM-104530 ..... N90-12726 #
CETIM-105160 ..... N90-12938 #
CETIM-105290 ..... N90-12748 #
CETIM-105490 ..... N90-13071 #
CETIM-106370 ..... N90-12727 #
CETIM-106960 ..... N90-12728 #
CETIM-107040 ..... N90-12729 #
CETIM-107310 ..... N90-12675 #
CETIM-107900 ..... N90-12961 #
CETIM-108060 ..... N90-12749 #
CETIM-110110 ..... N90-12730 #
CETIM-110240-PHASE-1 ..... N90-12896 #
CETIM-110430 ..... N90-12907 #
CETIM-110610 ..... N90-12939 #

CM-76 ..... N90-12992 #

CML-89-2 ..... N90-12959* #

CMR-89-9 ..... N90-12770* #

CMS-TSR-89-23 ..... N90-13177 #

CMU-RI-TR-89-16-PT-1 ..... N90-12945 #
CMU-RI-TR-89-22 ..... N90-12944 #

CONF-881296-SUMM ..... N90-12684 #
CONF-890692-20 ..... N90-12979 #
CONF-890812-34 ..... N90-12716 #
CONF-890836-13 ..... N90-12929 #
CONF-890931-2 ..... N90-13239 #
CONF-891024-1 ..... N90-12717 #
CONF-8905194-4 ..... N90-12875 #
CONF-8906210-2 ..... N90-12914 #
CONF-8909183-1 ..... N90-12844 #

CONTRIB-38-REV-1 ..... N90-12967 #

CRDEC-CR-045 ..... N90-12711 #

CRDEC-TR-046 ..... N90-12713 #
CRDEC-TR-098 ..... N90-12994 #

CRREL-SR-89-26 ..... N90-12699 #

CS-8813 ..... N90-13078 #
CS-8814 ..... N90-13079 #

CSTB-2-87-008 ..... N90-13201 #

CU-ECE-TR-89-07 ..... N90-13237 #

CWI-AM-R8808 ..... N90-13072 #
CWI-AM-R8901 ..... N90-13148 #
CWI-AM-R8903 ..... N90-13149 #
CWI-AM-R8904-PT-2 ..... N90-13150 #
CWI-AM-R8906 ..... N90-13151 #

CWI-CS-R8821 ..... N90-13152 #
CWI-CS-R8824 ..... N90-13153 #
CWI-CS-R8825 ..... N90-13073 #
CWI-CS-R8847 ..... N90-13182 #
CWI-CS-R8901 ..... N90-13191 #
CWI-CS-R8903 ..... N90-13074 #
CWI-CS-R8904 ..... N90-13075 #
CWI-CS-R8905 ..... N90-13076 #
CWI-CS-R8906 ..... N90-13154 #
CWI-CS-R8907 ..... N90-13155 #
CWI-CS-R8909 ..... N90-13156 #
CWI-CS-R8912 ..... N90-13077 #

CWI-MS-R8702 ..... N90-13181 #
CWI-MS-R8808 ..... N90-13179 #
CWI-MS-R8809 ..... N90-13142 #
CWI-MS-R8810 ..... N90-13143 #
CWI-MS-R8812 ..... N90-13144 #
CWI-MS-R8813 ..... N90-13180 #
CWI-MS-R8814 ..... N90-13145 #
CWI-MS-R8817 ..... N90-13181 #
CWI-MS-R8818 ..... N90-13146 #
CWI-MS-R8819 ..... N90-13147 #

CWI-NM-R8808 ..... N90-13131 #
CWI-NM-R8809 ..... N90-13132 #
CWI-NM-R8810 ..... N90-12891 #
CWI-NM-R8819 ..... N90-13061 #
CWI-NM-R8901 ..... N90-13133 #
CWI-NM-R8902 ..... N90-13134 #
CWI-NM-R8903 ..... N90-13135 #
CWI-NM-R8904 ..... N90-13136 #

CWI-PM-R8806 ..... N90-13138 #
CWI-PM-R8807 ..... N90-13139 #
CWI-PM-R8809 ..... N90-13140 #
CWI-PM-R8810 ..... N90-13184 #
CWI-PM-R8811 ..... N90-13141 #

C87A-25 ..... N90-12688 #

DCIEM-88-RR-33 ..... N90-13028 #

DERAT-25/5005.13 ..... N90-12502 #
DERAT-31/5025.20 ..... N90-12888 #
DERAT-43/5018.29 ..... N90-12897 #
DERAT-43/5018.30 ..... N90-12897 #
DERAT-59/5004.25 ..... N90-12889 #

DE89-015320 ..... N90-12684 #
DE89-015640 ..... N90-12844 #
DE89-015907 ..... N90-13239 #
DE89-016692 ..... N90-12875 #
DE89-016782 ..... N90-12716 #
DE89-017255 ..... N90-12979 #
DE89-017457 ..... N90-13242 #
DE89-017551 ..... N90-12929 #
DE89-017692 ..... N90-12914 #
DE89-017869 ..... N90-12717 #
DE89-618864 ..... N90-13251 #
DE89-618886 ..... N90-12685 #
DE89-619725 ..... N90-13294 #
DE89-619726 ..... N90-12783 #
DE89-630241 ..... N90-13252 #

DFVLR-FB-88-07 ..... N90-12621 #
DFVLR-FB-88-51 ..... N90-12808 #
DFVLR-FB-88-53 ..... N90-12639 #
DFVLR-FB-89-17 ..... N90-13080 #
DFVLR-FB-89-23 ..... N90-12919 #
DFVLR-FB-89-24 ..... N90-12974 #
DFVLR-FB-89-25 ..... N90-12577 #

DFVLR-MITT-88-16 ..... N90-12626 #

DLR-FB-89-27 ..... N90-13081 #
DLR-FB-89-28 ..... N90-12599 #
DLR-FB-89-29 ..... N90-13018 #
DLR-FB-89-30 ..... N90-12827 #
DLR-FB-89-31 ..... N90-13019 #

DNA-TR-88-239-V1 ..... N90-12836 #
DNA-TR-88-239-V2 ..... N90-12837 #

DOD/SW/DK-89/021A ..... N90-13083 #

DODA-AR-004-525 ..... N90-12596 #
DODA-AR-004-574 ..... N90-12595 #
DODA-AR-004-598 ..... N90-12579 #
DODA-AR-005-543 ..... N90-12566 #
DODA-AR-005-591 ..... N90-12501 #
DODA-AR-005590 ..... N90-12597 #

DOE/ER-03130/433 ..... N90-13299* #

DOE/ET-33006/042 ..... N90-13242 #

DOT/FAA/CT-TN88/4-1 ..... N90-12782 #
DOT/FAA/CT-TN88/4-2 ..... N90-12781 #
DOT/FAA/CT-TN89/50 ..... N90-12574 #
DOT/FAA/CT-TN89/59 ..... N90-12627 #

DOUGLAS-PAPER-7878 ..... N90-12505* #

DP-MS-89-9 ..... N90-12717 #

DREA-TC-89/307 ..... N90-12732 #

DREA-TM-89/219 ..... N90-12568 #

DRES-SR-525 ..... N90-13188 #

DRIC-BR-110918 ..... N90-12642 #

DTRC/CMLD-89/07 ..... N90-12964 #

DVG-HER-TN-002-PT-1 ..... N90-12631 #
DVG-HER-TN-002-PT-2 ..... N90-12632 #

E-5016 ..... N90-12950* #
E-5048 ..... N90-12658* #
E-5066 ..... N90-12659* #
E-5093 ..... N90-12670* #
E-5108 ..... N90-12560* #
E-5128 ..... N90-12561* #
E-5153 ..... N90-12696* #
E-5159 ..... N90-12813* #
E-5162 ..... N90-12618* #

E/BLO/163 ..... N90-12605 #

ECS-SS-1012 ..... N90-12652* #

EPA/600/D-89/060 ..... N90-13015 #
EPA/600/3-89/068-VOL-1/2 ..... N90-12981 #

ESA-BR-55 ..... N90-13322 #

ESA-SP-1104 ..... N90-13302 #
ESA-SP-1106 ..... N90-13276 #
ESA-SP-1110 ..... N90-12649 #

ESA-TM-02 ..... N90-12769 #

ESA-TT-1041 ..... N90-12621 #
ESA-TT-1132 ..... N90-12626 #
ESA-TT-1142 ..... N90-12808 #
ESA-TT-1143 ..... N90-12639 #

ESD-TR-89-111 ..... N90-12915 #
ESD-TR-89-199 ..... N90-13085 #

ESDU-73009 ..... N90-12694 #
ESDU-89002-PT-1 ..... N90-12693 #
ESDU-89003-PT-2 ..... N90-12694 #
ESDU-89012 ..... N90-12883 #

ESL-718048-10 ..... N90-13169 #
ESL-718048-12 ..... N90-12835 #

ETCA-88-R-088-PT-2 ..... N90-12673 #
ETCA-88-R-099 ..... N90-13108 #
ETCA-88-R-116 ..... N90-12955 #
ETCA-89-R-012 ..... N90-12748 #

ETL-0520 ..... N90-13111 #
ETL-0546 ..... N90-12944 #

ETN-89-94329 ..... N90-13178 #
ETN-89-94330 ..... N90-12810 #
ETN-89-94331 ..... N90-13057 #
ETN-89-94332 ..... N90-13058 #
ETN-89-94459 ..... N90-13230
ETN-89-94462 ..... N90-13039
ETN-89-94470 ..... N90-12629
ETN-89-94616 ..... N90-12851 #
ETN-89-94666 ..... N90-12671 #
ETN-89-94727 ..... N90-12815 #
ETN-89-94825 ..... N90-13205 #
ETN-89-94826 ..... N90-13206 #
ETN-89-94827 ..... N90-13292 #
ETN-89-94828 ..... N90-12857 #
ETN-89-94829 ..... N90-12562 #
ETN-89-94830 ..... N90-12640 #
ETN-89-94832 ..... N90-12641 #
ETN-89-94834 ..... N90-12816 #
ETN-89-94835 ..... N90-13231 #
ETN-89-94837 ..... N90-12817 #
ETN-89-94838 ..... N90-12818 #
ETN-89-94839 ..... N90-12819 #
ETN-89-94840 ..... N90-13066 #
ETN-89-94841 ..... N90-13275 #
ETN-89-94842 ..... N90-12575 #

ETN-89-94843 ..... N90-12820 #
ETN-89-94844 ..... N90-13067 #
ETN-89-94889 ..... N90-13005 #
ETN-89-94893 ..... N90-12858 #
ETN-89-94969 ..... N90-13068 #
ETN-89-94984 ..... N90-12884 #
ETN-89-94988 ..... N90-13302 #
ETN-89-94990 ..... N90-12821
ETN-89-94991 ..... N90-13069
ETN-89-94992 ..... N90-13107
ETN-89-94993 ..... N90-12822
ETN-89-94994 ..... N90-12823
ETN-89-94995 ..... N90-12824
ETN-89-94996 ..... N90-12825
ETN-89-94997 ..... N90-13317 #
ETN-89-94998 ..... N90-13318 #
ETN-89-94999 ..... N90-12619 #
ETN-89-95000 ..... N90-12893 #
ETN-89-95001 ..... N90-12563 #
ETN-89-95002 ..... N90-13207 #
ETN-89-95003 ..... N90-12905 #
ETN-89-95004 ..... N90-12576 #
ETN-89-95005 ..... N90-13070 #
ETN-89-95014 ..... N90-13040 #
ETN-89-95016 ..... N90-12630 #
ETN-89-95017 ..... N90-12894 #
ETN-89-95018 ..... N90-13232 #
ETN-89-95019 ..... N90-13278 #
ETN-89-95020 ..... N90-12672 #
ETN-89-95021 ..... N90-12895 #
ETN-89-95022 ..... N90-13108 #
ETN-89-95023-PT-2 ..... N90-12673 #
ETN-89-95025 ..... N90-12674 #
ETN-89-95027 ..... N90-12960 #
ETN-89-95028 ..... N90-12564 #
ETN-89-95030 ..... N90-12906 #
ETN-89-95035 ..... N90-12723 #
ETN-89-95036 ..... N90-12724 #
ETN-89-95037 ..... N90-12725 #
ETN-89-95038 ..... N90-12726 #
ETN-89-95039 ..... N90-12938 #
ETN-89-95040 ..... N90-12748 #
ETN-89-95041 ..... N90-13071 #
ETN-89-95042 ..... N90-12727 #
ETN-89-95043-PHASE-1 ..... N90-12896 #
ETN-89-95044 ..... N90-12728 #
ETN-89-95045 ..... N90-12729 #
ETN-89-95046 ..... N90-12675 #
ETN-89-95047 ..... N90-12961 #
ETN-89-95048 ..... N90-12749 #
ETN-89-95049 ..... N90-12730 #
ETN-89-95050 ..... N90-12907 #
ETN-89-95051 ..... N90-12939 #
ETN-89-95052 ..... N90-12962 #
ETN-89-95077 ..... N90-12991
ETN-89-95082 ..... N90-12826
ETN-89-95085 ..... N90-13208
ETN-89-95086 ..... N90-13233
ETN-89-95087 ..... N90-13234
ETN-89-95090 ..... N90-13041
ETN-89-95110 ..... N90-12876 #
ETN-89-95141 ..... N90-13102 #
ETN-89-95142 ..... N90-13121 #
ETN-89-95143 ..... N90-13122 #
ETN-89-95151 ..... N90-12664 #
ETN-89-95152 ..... N90-12952 #
ETN-89-95163 ..... N90-12953 #
ETN-89-95178 ..... N90-13229 #
ETN-89-95181 ..... N90-13221 #
ETN-89-95205 ..... N90-12631 #
ETN-89-95206 ..... N90-12632 #
ETN-89-95207 ..... N90-12954 #
ETN-89-95208 ..... N90-12591 #
ETN-89-95209 ..... N90-12665 #
ETN-89-95217 ..... N90-12598 #
ETN-89-95227 ..... N90-13123 #
ETN-89-95228 ..... N90-13103 #
ETN-89-95229 ..... N90-12930 #
ETN-89-95230 ..... N90-12931 #
ETN-89-95231 ..... N90-13104 #
ETN-89-95246 ..... N90-12572
ETN-89-95247 ..... N90-12573
ETN-89-95248 ..... N90-12807
ETN-89-95258 ..... N90-12695 #
ETN-89-95266 ..... N90-12666 #
ETN-89-95267 ..... N90-12811 #
ETN-89-95268 ..... N90-12812 #
ETN-89-95273 ..... N90-13201 #
ETN-89-95274 ..... N90-12955 #
ETN-89-95275 ..... N90-12746 #
ETN-89-95276 ..... N90-12622 #
ETN-89-95277 ..... N90-12502 #
ETN-89-95279 ..... N90-12897 #
ETN-89-95280 ..... N90-12676 #
ETN-89-95282 ..... N90-12698 #
ETN-89-95283 ..... N90-12677 #

ETN-89-95284 ..... N90-12678 #
ETN-89-95285 ..... N90-12565 #
ETN-89-95286 ..... N90-12592 #
ETN-89-95329 ..... N90-13124 #
ETN-89-95386 ..... N90-12649 #
ETN-89-95387 ..... N90-12769 #
ETN-89-95388 ..... N90-13322 #
ETN-89-95389 ..... N90-12621 #
ETN-89-95402 ..... N90-12854 #
ETN-89-95404 ..... N90-13114 #
ETN-89-95436 ..... N90-13190 #
ETN-89-95438 ..... N90-12885 #
ETN-89-95439 ..... N90-13119 #
ETN-89-95440 ..... N90-13120 #
ETN-89-95447 ..... N90-13056 #
ETN-89-95449 ..... N90-12886 #
ETN-89-95491 ..... N90-12855 #
ETN-89-95492 ..... N90-13094 #
ETN-89-95494 ..... N90-13125 #
ETN-89-95498 ..... N90-13109 #
ETN-89-95499 ..... N90-13096 #
ETN-89-95503 ..... N90-13105 #
ETN-89-95505 ..... N90-13038 #
ETN-89-95511 ..... N90-12956 #
ETN-89-95516 ..... N90-12917 #
ETN-89-95541 ..... N90-13059
ETN-89-95546 ..... N90-12601 #
ETN-89-95548 ..... N90-12602 #
ETN-89-95549 ..... N90-12593 #
ETN-89-95551 ..... N90-12603 #
ETN-89-95552 ..... N90-12932 #
ETN-89-95553 ..... N90-12604 #
ETN-89-95554 ..... N90-12720 #
ETN-89-95555 ..... N90-13202 #
ETN-89-95556 ..... N90-12605 #
ETN-89-95557 ..... N90-13203 #
ETN-89-95558 ..... N90-12916 #
ETN-89-95559 ..... N90-12667 #
ETN-89-95560 ..... N90-12606 #
ETN-89-95561 ..... N90-12607 #
ETN-89-95562 ..... N90-12608 #
ETN-89-95563 ..... N90-12933 #
ETN-89-95564 ..... N90-12934 #
ETN-89-95565 ..... N90-12609 #
ETN-89-95566 ..... N90-12610 #
ETN-89-95567 ..... N90-12611 #
ETN-89-95568 ..... N90-12612 #
ETN-89-95569 ..... N90-12613 #
ETN-89-95570 ..... N90-12614 #
ETN-89-95571 ..... N90-12615 #
ETN-89-95572 ..... N90-12957 #
ETN-89-95573 ..... N90-12616 #
ETN-89-95574 ..... N90-12668 #
ETN-89-95579 ..... N90-13106 #
ETN-89-95580 ..... N90-13126 #
ETN-89-95585 ..... N90-13127 #
ETN-89-95588 ..... N90-13060 #
ETN-89-95589 ..... N90-13045 #
ETN-89-95591 ..... N90-13044 #
ETN-89-95592 ..... N90-12978 #
ETN-89-95593 ..... N90-13128 #
ETN-89-95594 ..... N90-13129 #
ETN-89-95595 ..... N90-13130 #
ETN-89-95598 ..... N90-13000
ETN-89-95600 ..... N90-13001
ETN-89-95601 ..... N90-13002
ETN-89-95606 ..... N90-12778 #
ETN-89-95607 ..... N90-12958 #
ETN-89-95608 ..... N90-13273 #
ETN-89-95609 ..... N90-13222 #
ETN-89-95610 ..... N90-13223 #
ETN-89-95611 ..... N90-13224 #
ETN-89-95619 ..... N90-13131 #
ETN-89-95620 ..... N90-13132 #
ETN-89-95621 ..... N90-12891 #
ETN-89-95622 ..... N90-13061 #
ETN-89-95623 ..... N90-13133 #
ETN-89-95624 ..... N90-13134 #
ETN-89-95625 ..... N90-13135 #
ETN-89-95626 ..... N90-13136 #
ETN-89-95627 ..... N90-13138 #
ETN-89-95628 ..... N90-13139 #
ETN-89-95629 ..... N90-13140 #
ETN-89-95630 ..... N90-13141 #
ETN-89-95631 ..... N90-13179 #
ETN-89-95632 ..... N90-13142 #
ETN-89-95633 ..... N90-13143 #
ETN-89-95634 ..... N90-13144 #
ETN-89-95635 ..... N90-13180 #
ETN-89-95636 ..... N90-13145 #
ETN-89-95637 ..... N90-13181 #
ETN-89-95638 ..... N90-13146 #
ETN-89-95639 ..... N90-13147 #
ETN-89-95640 ..... N90-13072 #
ETN-89-95641 ..... N90-13148 #
ETN-89-95642 ..... N90-13149 #
ETN-89-95643-PT-2 ..... N90-13150 #
ETN-89-95644 ..... N90-13151 #
ETN-89-95645 ..... N90-13152 #
ETN-89-95646 ..... N90-13153 #
ETN-89-95647 ..... N90-13073 #
ETN-89-95648 ..... N90-13182 #
ETN-89-95649 ..... N90-13191 #
ETN-89-95650 ..... N90-13074 #
ETN-89-95651 ..... N90-13075 #
ETN-89-95652 ..... N90-13076 #
ETN-89-95653 ..... N90-13154 #
ETN-89-95654 ..... N90-13155 #
ETN-89-95655 ..... N90-13156 #
ETN-89-95656 ..... N90-13077 #
ETN-89-95660 ..... N90-13157 #
ETN-89-95661 ..... N90-13158 #
ETN-89-95662 ..... N90-13159 #
ETN-89-95663 ..... N90-13160 #
ETN-89-95664 ..... N90-13161 #
ETN-89-95665 ..... N90-13162 #
ETN-89-95666 ..... N90-13163 #
ETN-89-95667 ..... N90-13164 #
ETN-89-95669 ..... N90-12750 #
ETN-89-95671 ..... N90-13165 #
ETN-89-95672 ..... N90-13166 #
ETN-89-95674 ..... N90-13183 #
ETN-89-95679 ..... N90-13078 #
ETN-89-95680 ..... N90-13079 #
ETN-89-95681 ..... N90-13167 #
ETN-89-95682 ..... N90-13168 #
ETN-89-95683 ..... N90-13095 #
ETN-89-95684 ..... N90-13096 #
ETN-89-95685 ..... N90-13097 #
ETN-89-95686 ..... N90-13062 #
ETN-89-95687 ..... N90-13063 #
ETN-89-95688 ..... N90-13064 #
ETN-89-95689 ..... N90-13099 #
ETN-89-95690 ..... N90-13100 #
ETN-89-95705 ..... N90-13276 #
ETN-89-95709 ..... N90-13259 #
ETN-89-95711 ..... N90-12744 #
ETN-89-95712 ..... N90-12887 #
ETN-89-95713 ..... N90-12888 #
ETN-89-95714 ..... N90-12889 #
ETN-89-95719 ..... N90-12571 #
ETN-89-95720 ..... N90-12972 #
ETN-89-95724 ..... N90-13260
ETN-89-95725 ..... N90-12852
ETN-89-95742 ..... N90-12890 #
ETN-89-95744 ..... N90-12853 #
ETN-89-95746 ..... N90-13215 #
ETN-89-95747 ..... N90-13216 #
ETN-89-95748 ..... N90-13194 #
ETN-89-95749 ..... N90-13217 #
ETN-89-95750 ..... N90-13218 #
ETN-89-95751 ..... N90-13225 #
ETN-89-95752 ..... N90-13219 #
ETN-89-95753 ..... N90-13184 #
ETN-89-95754 ..... N90-13272 #
ETN-89-95757 ..... N90-13321 #
ETN-89-95758 ..... N90-13301 #
ETN-89-95762 ..... N90-12626 #
ETN-89-95763 ..... N90-12808 #
ETN-89-95764 ..... N90-12639 #
ETN-89-95831 ..... N90-13080 #
ETN-89-95832 ..... N90-12919 #
ETN-89-95833 ..... N90-12974 #
ETN-89-95834 ..... N90-12577 #
ETN-89-95836 ..... N90-13081 #
ETN-89-95837 ..... N90-12599 #
ETN-89-95838 ..... N90-13018 #
ETN-89-95839 ..... N90-12827 #
ETN-89-95840 ..... N90-13019 #
ETN-89-95855 ..... N90-13295
ETN-89-95857 ..... N90-13296* #
ETN-89-95924 ..... N90-12809 #
ETN-89-95925 ..... N90-12992 #
ETN-89-95933 ..... N90-12745
ETN-89-95934 ..... N90-13220
ETN-89-96005 ..... N90-13042
EU404 ..... N90-12572
EU656 ..... N90-12573
FEL-1988-43 ..... N90-12991
FEL-1988-46 ..... N90-12824
FEL-1988-47 ..... N90-12825
FEL-1988-66 ..... N90-12629
FEL-1988-95 ..... N90-12821
FEL-1988-101 ..... N90-13069
FEL-1989-1 ..... N90-13107
FEL-1989-15 ..... N90-12826
FEL-1989-21-PT-2 ..... N90-12822
FEL-1989-44 ..... N90-12823
FEL-1989-82 ..... N90-13208
FEL-1989-83 ..... N90-13233
FEL-1989-100 ..... N90-13234
FERMILAB-CONF-89/215-A ..... N90-13299* #
FERMILAB-CONF-89/221-A ..... N90-13298* #
FERMILAB-PUB-89/208-A ..... N90-13297* #
FERMILAB-PUB-89/225-A ..... N90-13274* #
FFA-TN-1988-60 ..... N90-12953 #
FFA-TN-1988-70 ..... N90-12664 #
FFA-TN-1989-09 ..... N90-12952 #
FJSRL-TR-89-0007 ..... N90-12707 #
FJSRL-TR-89-0008 ..... N90-13196 #
FOA-B-30135-3.4 ..... N90-12969 #
FOA-C-30518-3.5 ..... N90-12785 #
FTD-ID(RS)T-0053-89 ..... N90-12657 #
FTD-ID(RS)T-0665-89 ..... N90-12752 #
FTD-ID(RS)T-0677-89 ..... N90-12644 #
F6150-DT410-1-88329 ..... N90-12622 #
GA/88-655-MR/CB ..... N90-13201 #
GL-TR-89-0109 ..... N90-12990 #
GL-TR-89-0144 ..... N90-12986 #
GL-TR-89-0165 ..... N90-12995 #
GLOMAC-89/1 ..... N90-12992 #
GPO-19-437 ..... N90-13281 #
GPO-21-609 ..... N90-13284 #
GPO-22-382 ..... N90-13289 #
GPO-96-945 ..... N90-13283 #
GPO-98-466 ..... N90-13285 #
GPO-99-412 ..... N90-13290 #
GRI-88/0258 ..... N90-12928 #
GRI-89/0101 ..... N90-12977 #
GRI-89/0105 ..... N90-12689 #
GRL/8805 ..... N90-12921 #
GRL/8901 ..... N90-12924 #
GRS-70 ..... N90-12884 #
H-REPT-101-150 ..... N90-13281 #
H-1490 ..... N90-12669* #
HD-THEP-88-27 ..... N90-13273 #
HEL-TM-2-89 ..... N90-12832 #
HEL-TM-3-89 ..... N90-13209 #
HR-2916-PP ..... N90-13286 #
HSER-116227 ..... N90-12617* #
IC-88/399 ..... N90-13294 #
IC-88/413 ..... N90-12695 #
IC-88/427 ..... N90-13251 #
IC-89/23 ..... N90-12783 #
ICASE-89-74 ..... N90-12874* #
IDA-D-579 ..... N90-12680 #
IDA-R-319 ..... N90-12496 #
IDA/HQ-87-32596 ..... N90-12496 #
IDA/HQ-89-34363 ..... N90-12680 #
IMAG-RR-736-I ..... N90-12855 #
IMAG-RR-737-I ..... N90-13094 #
IMAG-RR-744-M ..... N90-13125 #
INR90259 ..... N90-13202 #
IPPCZ-280 ..... N90-13241 #
IPPCZ-283 ..... N90-13240 #
IS-22-786 ..... N90-12724 #
IS-23-471 ..... N90-12725 #
IS-88-358 ..... N90-12726 #
ISAL-89-0024 ..... N90-12666 #
ISAL-89-0028 ..... N90-13259 #
ISBN-0-85679-673-9 ..... N90-12693 #
ISBN-0-85679-674-3 ..... N90-12694 #
ISBN-0-85679-683-2 ..... N90-12883 #
ISBN-0-947767-89-4 ..... N90-12668 #

ISBN-1-55752-090-9 N90-12920 #
ISBN-3-923875-20-7 N90-12884 #
ISBN-90-365-0240-3 N90-13097 #
ISBN-90-365-0259-4 N90-13064 #
ISBN-92-835-0521-2 N90-12623 #
ISBN-92-9092-003-3 N90-13322 #
ISBN-92-9092-028-9 N90-13276 #
ISBN-951-754-671-8 N90-13229 #
ISBN-951-754-722-6 N90-12805 #
ISBN-951-754-766-8 N90-13116 #
ISBN-951-754-778-1 N90-13115 #
ISBN-951-754-786-2 N90-13117 #
ISBN-951-754-791-9 N90-13258 #
ISBN-951-754-798-6 N90-12878 #
ISBN-951-754-842-7 N90-13049 #
ISBN-951-754-855-9 N90-12879 #
ISBN-952-90056-1-X N90-13221 #

ISI/RR-89-225 N90-13053 #

ISL-CO-215/88 N90-12906 #

ISL-R-109/88 N90-12564 #
ISL-R-128/87 N90-12960 #

ISSN-0038-0911 N90-13300
ISSN-0078-3781 N90-12662 #
ISSN-0078-3781 N90-13199 #
ISSN-0141-4011 N90-12883 #
ISSN-0141-4062 N90-12693 #
ISSN-0141-4062 N90-12694 #
ISSN-0141-4070 N90-12693 #
ISSN-0143-7313 N90-12745
ISSN-0143-7313 N90-13220
ISSN-0169-1651 N90-13000
ISSN-0169-1651 N90-13001
ISSN-0169-1651 N90-13002
ISSN-0169-2690 N90-12750 #
ISSN-0169-2690 N90-13157 #
ISSN-0169-2690 N90-13158 #
ISSN-0169-2690 N90-13159 #
ISSN-0169-2690 N90-13160 #
ISSN-0169-2690 N90-13161 #
ISSN-0169-2690 N90-13162 #
ISSN-0169-2690 N90-13163 #
ISSN-0169-2690 N90-13164 #
ISSN-0169-2690 N90-13165 #
ISSN-0169-2690 N90-13166 #
ISSN-0169-2690 N90-13183 #
ISSN-0171-1342 N90-12577 #
ISSN-0171-1342 N90-12599 #
ISSN-0171-1342 N90-12827 #
ISSN-0171-1342 N90-12919 #
ISSN-0171-1342 N90-12974 #
ISSN-0171-1342 N90-13018 #
ISSN-0171-1342 N90-13019 #
ISSN-0171-1342 N90-13080 #
ISSN-0171-1342 N90-13081 #
ISSN-0250-1589 N90-13322 #
ISSN-0262-5369 N90-13059
ISSN-0280-445X N90-12992 #
ISSN-0281-0263 N90-12969 #
ISSN-0348-7539 N90-12809 #
ISSN-0379-6566 N90-12649 #
ISSN-0379-6566 N90-13302 #
ISSN-0388-9653 N90-12997 #
ISSN-0436-1199 N90-13124 #
ISSN-0751-1353 N90-12811 #
ISSN-0751-1353 N90-12812 #
ISSN-0751-1353 N90-13105 #
ISSN-0751-1361 N90-13038 #
ISSN-0783-7445 N90-13049 #
ISSN-0784-848X N90-13229 #
ISSN-0922-5641 N90-12876 #
ISSN-0922-5641 N90-12885 #
ISSN-0922-5641 N90-12886 #
ISSN-0922-5641 N90-12978 #
ISSN-0922-5641 N90-13044 #
ISSN-0922-5641 N90-13045 #
ISSN-0922-5641 N90-13056 #
ISSN-0922-5641 N90-13060 #
ISSN-0922-5641 N90-13106 #
ISSN-0922-5641 N90-13119 #
ISSN-0922-5641 N90-13120 #
ISSN-0922-5641 N90-13126 #
ISSN-0922-5641 N90-13127 #
ISSN-0922-5641 N90-13128 #
ISSN-0922-5641 N90-13129 #
ISSN-0922-5641 N90-13130 #
ISSN-0922-5641 N90-13190 #
ISSN-0923-1714 N90-13062 #
ISSN-0923-1714 N90-13063 #
ISSN-0923-1714 N90-13064 #
ISSN-0923-1714 N90-13099 #
ISSN-0923-1714 N90-13100 #
ISSN-1013-7076 N90-12769 #

ITFA-88-53 N90-13272 #

IZF-1988-8 N90-13230
IZF-1988-15 N90-13041
IZF-1988-21 N90-13042
IZF-1988-25 N90-13039

JINR-E-14-88-568 N90-13252 #

JPL-TDA-PR-42-98 N90-12786* #

KNMI-WR-88-01 N90-13000
KNMI-WR-89-01 N90-13001
KNMI-WR-89-02 N90-13002

KVI-774 N90-13215 #
KVI-777 N90-13216 #
KVI-791 N90-13194 #
KVI-792 N90-13217 #
KVI-796 N90-13218 #
KVI-797 N90-13225 #

L-16350-PT-1 N90-12503* #
L-16350-PT-2 N90-12519* #
L-16350-PT-3 N90-12539* #

LA-UR-89-2967 N90-12716 #

LAAS-89040 N90-12695 #

LC-48-47112 N90-13279 #
LC-79-640375 N90-13300
LC-88-62706 N90-12920 #
LC-88-600442 N90-12686 #
LC-88-600576 N90-12913 #
LC-89-39482 N90-12589* #
LC-89-600736 N90-12845 #
LC-89-600737 N90-12747 #
LC-89-600739 N90-13253 #
LC-89-600743 N90-13261 #

LIDS-R-1901 N90-12829 #

LMSC-HEC-TR-F268627 N90-12650* #

LR-560 N90-12778 #
LR-561 N90-12958 #

L211-FY89-M086 N90-12651* #

MAT-A265 N90-13115 #

MBB-UA-1110/88-PUB N90-12851 #

MEMO-INF-88-33 N90-13095 #
MEMO-INF-88-34 N90-13096 #
MEMO-INF-88-68 N90-13097 #
MEMO-INF-89-5 N90-13062 #
MEMO-INF-89-7-REV N90-13063 #
MEMO-INF-89-13 N90-13064 #
MEMO-INF-89-15 N90-13099 #
MEMO-INF-89-16 N90-13100 #

MEMO-743 N90-13159 #
MEMO-769 N90-13157 #
MEMO-770 N90-13158 #
MEMO-771 N90-13159 #
MEMO-772 N90-13160 #
MEMO-773 N90-13161 #
MEMO-774 N90-13162 #
MEMO-775 N90-13163 #
MEMO-776 N90-13164 #
MEMO-778-PT-3 N90-12750 #
MEMO-780 N90-13165 #
MEMO-781 N90-13166 #
MEMO-783 N90-13183 #

MISS-2144 N90-12604 #

MIT-OSP-93019-2 N90-13212 #

MPE-PREPRINT-153 N90-13295
MPE-PREPRINT-155 N90-13296* #

MPIS-22/1987 N90-13124 #

MRC-R-1240 N90-13247 #

MRL-TR-89-3 N90-12775 #
MRL-TR-89-6 N90-12661 #

MSC-TN-18 N90-12997 #

MTI-89TR40 N90-12935* #

MTL-MS-89-1 N90-12951 #

MTL-TR-89-61 N90-12734 #
MTL-TR-89-68 N90-12762 #
MTL-TR-89-70 N90-12681 #

M89-32 N90-13085 #

NAMRL-1344 N90-13027 #

NAS 1.15:4139 N90-12669* #
NAS 1.15:86494 N90-12715* #
NAS 1.15:100737 N90-12965* #
NAS 1.15:100746 N90-12984* #
NAS 1.15:101070 N90-13319* #
NAS 1.15:101072 N90-13048* #
NAS 1.15:101617 N90-12580* #
NAS 1.15:101855 N90-12635* #
NAS 1.15:102210 N90-12904* #
NAS 1.15:102232 N90-13013* #
NAS 1.15:102241 N90-13137* #
NAS 1.15:102320 N90-12950* #
NAS 1.15:102355 N90-12659* #
NAS 1.15:102374 N90-12560* #
NAS 1.15:102387 N90-12561* #
NAS 1.15:102399 N90-12696* #
NAS 1.15:102401 N90-12658* #
NAS 1.15:102405 N90-12670* #
NAS 1.15:102407 N90-12813* #
NAS 1.15:102409 N90-12618* #
NAS 1.21:501 N90-12589* #
NAS 1.21:6101(02) N90-13277* #
NAS 1.21:7037(245) N90-12497*
NAS 1.26:4262 N90-13228* #
NAS 1.26:180848 N90-12617* #
NAS 1.26:181849 N90-12718* #
NAS 1.26:181896 N90-12625* #
NAS 1.26:181897 N90-13198* #
NAS 1.26:181931 N90-12874* #
NAS 1.26:181932 N90-13050* #
NAS 1.26:182559 N90-12498* #
NAS 1.26:183151 N90-13036* #
NAS 1.26:183671 N90-12650* #
NAS 1.26:183716 N90-12651* #
NAS 1.26:183723 N90-12652* #
NAS 1.26:183807 N90-12935* #
NAS 1.26:183811 N90-12656* #
NAS 1.26:184997 N90-13047* #
NAS 1.26:185093 N90-12786* #
NAS 1.26:185147 N90-12645* #
NAS 1.26:185369 N90-13035* #
NAS 1.26:185386 N90-13113* #
NAS 1.26:185436 N90-12996* #
NAS 1.26:185443 N90-12768* #
NAS 1.26:185451 N90-13316* #
NAS 1.26:185486 N90-12654* #
NAS 1.26:185497 N90-13296* #
NAS 1.26:185854 N90-12872* #
NAS 1.26:185873 N90-12980* #
NAS 1.26:185989 N90-12784* #
NAS 1.26:186037 N90-12500* #
NAS 1.26:186039 N90-12499* #
NAS 1.26:186044 N90-12646* #
NAS 1.26:186055 N90-12655* #
NAS 1.26:186057 N90-12590* #
NAS 1.26:186060 N90-12882* #
NAS 1.26:186069 N90-13204* #
NAS 1.26:186074 N90-13299* #
NAS 1.26:186075 N90-13298* #
NAS 1.26:186076 N90-13297* #
NAS 1.26:186078 N90-13274* #
NAS 1.26:186080 N90-12959* #
NAS 1.26:186082 N90-12770* #
NAS 1.26:186083 N90-12973* #
NAS 1.26:186091 N90-13065* #
NAS 1.26:186093 N90-12936* #
NAS 1.26:186096 N90-13003* #
NAS 1.55:2487-PT-1 N90-12503* #
NAS 1.55:2487-PT-2 N90-12519* #
NAS 1.55:2487-PT-3 N90-12539* #

NASA-CP-2487-PT-1 N90-12503* #
NASA-CP-2487-PT-2 N90-12519* #
NASA-CP-2487-PT-3 N90-12539* #

NASA-CR-4262 N90-13228* #
NASA-CR-180848 N90-12617* #
NASA-CR-181849 N90-12718* #
NASA-CR-181896 N90-12625* #
NASA-CR-181897 N90-13198* #
NASA-CR-181931 N90-12874* #
NASA-CR-181932 N90-13050* #
NASA-CR-182559 N90-12498* #
NASA-CR-183151 N90-13036* #
NASA-CR-183671 N90-12650* #
NASA-CR-183716 N90-12651* #
NASA-CR-183723 N90-12652* #
NASA-CR-183807 N90-12935* #

NASA-CR-183811 N90-12656* #
NASA-CR-184997 N90-13047* #
NASA-CR-185093 N90-12786* #
NASA-CR-185147 N90-12645* #
NASA-CR-185369 N90-13035* #
NASA-CR-185386 N90-13113* #
NASA-CR-185436 N90-12996* #
NASA-CR-185443 N90-12768* #
NASA-CR-185451 N90-13316* #
NASA-CR-185486 N90-12654* #
NASA-CR-185497 N90-13296* #
NASA-CR-185854 N90-12872* #
NASA-CR-185873 N90-12980* #
NASA-CR-185989 N90-12784* #
NASA-CR-186037 N90-12500* #
NASA-CR-186039 N90-12499* #
NASA-CR-186044 N90-12646* #
NASA-CR-186055 N90-12655* #
NASA-CR-186057 N90-12590* #
NASA-CR-186060 N90-12682* #
NASA-CR-186069 N90-13204* #
NASA-CR-186074 N90-13299* #
NASA-CR-186075 N90-13298* #
NASA-CR-186076 N90-13297* #
NASA-CR-186078 N90-13274* #
NASA-CR-186080 N90-12959* #
NASA-CR-186082 N90-12770* #
NASA-CR-186083 N90-12973* #
NASA-CR-186091 N90-13065* #
NASA-CR-186093 N90-12936* #
NASA-CR-186096 N90-13003* #

NASA-SP-501 N90-12589* #
NASA-SP-6101(02) N90-13277* #
NASA-SP-7037(245) N90-12497*

NASA-TM-4139 N90-12669* #
NASA-TM-86494 N90-12715* #
NASA-TM-100737 N90-12985* #
NASA-TM-100746 N90-12984* #
NASA-TM-101070 N90-13319* #
NASA-TM-101072 N90-13048* #
NASA-TM-101617 N90-12580* #
NASA-TM-101855 N90-12635* #
NASA-TM-102210 N90-12904* #
NASA-TM-102232 N90-13013* #
NASA-TM-102241 N90-13137* #
NASA-TM-102320 N90-12950* #
NASA-TM-102355 N90-12659* #
NASA-TM-102374 N90-12560* #
NASA-TM-102387 N90-12561* #
NASA-TM-102399 N90-12696* #
NASA-TM-102401 N90-12658* #
NASA-TM-102405 N90-12670* #
NASA-TM-102407 N90-12813* #
NASA-TM-102409 N90-12618* #

NATICK/TR-89/039-VOL-1 N90-13043 #

NEPRF-CR-89-11 N90-12999 #

NIKHEF-AMPS/89/04 N90-12854 #

NIKHEF-H/88-11 N90-13273 #
NIKHEF-H/88-12 N90-13222 #
NIKHEF-H/88-13 N90-13223 #
NIKHEF-H/88-19 N90-13224 #

NIKHEF-ITFA-88-52 N90-13114 #

NIST/SP-250/27 N90-12845 #
NIST/SP-305-SUPPL-20 N90-13279 #
NIST/SP-400/82 N90-13253 #
NIST/SP-400/83 N90-13261 #
NIST/SP-756 N90-12913 #
NIST/SP-766 N90-12747 #
NIST/SP-767 N90-12776 #

NIST/TN-1260 N90-13101 #
NIST/TN-1264 N90-12892 #
NIST/TN-1325 N90-12690 #
NIST/TN-1328-PT-1 N90-12687 #
NIST/TN-1329 N90-12880 #
NIST/TN-1331 N90-12697 #

NLR-TR-88157-U N90-12628 #

NMRI-89-35 N90-13025 #
NMRI-89-46 N90-13024 #

NOAA-ATLAS-8 N90-13009 #

NOAA-DR-ERL-AOML-13 N90-13010 #

NOAA-DR-ERL-ARL-17 N90-12993 #

NOAA-TM-NESDIS-26 N90-12968 #

NOAA-TM-NMC-68-REV-1 N90-12967 #

NORDA-PR-89 N90-13011 #

NORDA-182 N90-13012 #

NOSC-TD-1600 N90-12839 #
NOSC-TD-1601 N90-12912 #

NOSC/TD-1598 N90-12843 #
NOSC/TD-1602 N90-12833 #

NOTE-TECHNIQUE-1988-8 N90-12662 #
NOTE-TECHNIQUE-1989-4 N90-13199 #

NPL-DITC-143/89 N90-13059

NPL-DMA(A)-185 N90-12745
NPL-DMA(A)-190 N90-13220

NPS52-89-38 N90-12971 #
NPS61-89-013 N90-12637 #
NPS63-89-003 N90-12998 #

NRL-MR-6390 N90-12922 #
NRL-MR-6411 N90-12900 #
NRL-MR-6478 N90-13176 #
NRL-MR-6497 N90-13008 #
NRL-MR-6499 N90-12903 #
NRL-MR-6505 N90-12777 #
NRL-MR-6513 N90-12909 #
NRL-MR-6522 N90-12923 #
NRL-MR-6523 N90-12867 #
NRL-MR-6531 N90-12868 #
NRL-MR-6544 N90-13246 #
NRL-MR-6555 N90-12710 #
NRL-MR-6558 N90-12767 #

NTI-88/53 N90-12675 #
NTI-88/55 N90-12939 #
NTI-88/56-PHASE-1 N90-12896 #

NTIA-89-245 N90-12937 #

NWC-TP-6989 N90-12834 #

ONERA-RSF-1/7301-PY N90-12630 #
ONERA-RSF-10/1145-AY-164A N90-12894 #
ONERA-RSF-12/0694-GY N90-13278 #
ONERA-RSF-19/1123-AY-234A N90-12565 #
ONERA-RSF-32/1285-AY-346A N90-12592 #

ONERA-RT-7/3549-M N90-12698 #
ONERA-RT-8/7254-SN N90-13232 #
ONERA-RT-19/3542-RY-081-R N90-12672 #
ONERA-RT-22/7252-AN-000A N90-12895 #
ONERA-RT-45/7086-M N90-12677 #
ONERA-RT-46/7086-M N90-12678 #

ONR-TR-17 N90-12976 #

OSU/DGSS-398 N90-12990 #

PB89-200174 N90-12682 #
PB89-201404 N90-12686 #
PB89-207401 N90-13300
PB89-212609 N90-13049 #
PB89-213128 N90-12785 #
PB89-213359 N90-12968 #
PB89-218127 N90-12969 #
PB89-218374 N90-12687 #
PB89-218382 N90-13279 #
PB89-218572 N90-13192 #
PB89-218838 N90-12805 #
PB89-218846 N90-13117 #
PB89-218879 N90-12878 #
PB89-218986 N90-13258 #
PB89-219364 N90-12636 #
PB89-219463 N90-13116 #
PB89-220651 N90-13115 #
PB89-220677 N90-12946 #
PB89-221147 N90-12776 #
PB89-221162 N90-12913 #
PB89-221170 N90-13253 #
PB89-221188 N90-13101 #
PB89-221600 N90-12879 #
PB89-222020 N90-12722 #
PB89-222608 N90-12690 #
PB89-222616 N90-12845 #
PB89-223176 N90-13221 #
PB89-223333 N90-13004 #
PB89-223598 N90-13009 #
PB89-223630 N90-13015 #
PB89-223739 N90-12721 #

PB89-224018 N90-12993 #
PB89-224604 N90-12982 #
PB89-224711 N90-13291 #
PB89-224885 N90-12814 #
PB89-224943 N90-12981 #
PB89-225700 N90-12856 #
PB89-229074 N90-12747 #
PB89-229447 N90-12689 #
PB89-230650 N90-12928 #
PB89-230684 N90-12967 #
PB89-230825 N90-13010 #
PB89-231344 N90-12980* #
PB89-231484 N90-12880 #
PB89-231740 N90-12937 #
PB89-232615 N90-12977 #
PB89-235147 N90-12892 #
PB89-235204 N90-12697 #
PB89-235923 N90-13261 #

PCN-051SP N90-13188 #

PNR90553 N90-12601 #
PNR90561 N90-12602 #
PNR90562 N90-12593 #
PNR90566 N90-12603 #
PNR90567 N90-12932 #
PNR90570 N90-12604 #
PNR90572 N90-12720 #
PNR90574 N90-13202 #
PNR90576 N90-12605 #
PNR90577 N90-13203 #
PNR90578 N90-12918 #
PNR90584 N90-12667 #
PNR90585 N90-12606 #
PNR90586 N90-12607 #
PNR90589 N90-12608 #
PNR90591 N90-12933 #
PNR90593 N90-12934 #
PNR90594 N90-12609 #
PNR90595 N90-12610 #
PNR90596 N90-12611 #
PNR90597 N90-12612 #
PNR90598 N90-12613 #
PNR90599 N90-12614 #
PNR90600 N90-12615 #
PNR90601 N90-12957 #
PNR90602 N90-12616 #

PSP-1989 N90-13242 #

PSR-1877-VOL-1 N90-12836 #

PTI-8948 N90-12627 #

R/D-5037-CH-01 N90-12692 #
R/D-5119-EE-01-05 N90-13255 #
R/D-5462-AN-01 N90-12766 #
R/D-5618-MS-01 N90-12700 #
R/D-5733-EN-01 N90-13006 #
R/D-5899A-CH-01 N90-12846 #
R/D-5983-EE-02 N90-13250 #
R/D-6117-MA-02 N90-13171 #
R/D-6149-AN-03 N90-12942 #
R/D-6149-AN-03 N90-12943 #

RADC-TR-88-333 N90-12831 #
RADC-TR-89-226 N90-12910 #

RAE-SS-7 N90-12640 #
RAE-SS-9 N90-12641 #

RAE-TM-AERO-2137 N90-12893 #
RAE-TM-AERO-2139 N90-12562 #
RAE-TM-AERO-2146 N90-12563 #

RAE-TM-FS(F)-550 N90-12857 #

RAE-TM-MM-10 N90-13205 #
RAE-TM-MM-11 N90-13207 #
RAE-TM-MM-12 N90-13206 #

RAE-TM-P-1141 N90-12619 #

RAE-TM-SPACE-363 N90-13317 #
RAE-TM-SPACE-364 N90-13318 #
RAE-TM-SPACE-365 N90-13292 #

RAE-TM-371 N90-12642 #

RAE-TR-88045 N90-12640 #
RAE-TR-88058 N90-12641 #

RAND/N-2841-DARPA N90-13082 #

REPT-RE-49-324/F N90-12676 #

REPT-4 ..... N90-12758 #
REPT-34 ..... N90-13229 #
REPT-38 ..... N90-12805 #
REPT-42 ..... N90-13117 #
REPT-55 ..... N90-13301 #
REPT-88-99 ..... N90-12876 #
REPT-88-100 ..... N90-13190 #
REPT-89-04 ..... N90-12885 #
REPT-89-05 ..... N90-13119 #
REPT-89-06 ..... N90-13120 #
REPT-89-14 ..... N90-13056 #
REPT-89-17 ..... N90-12886 #
REPT-89-20 ..... N90-13106 #
REPT-89-21 ..... N90-13126 #
REPT-89-26 ..... N90-13127 #
REPT-89-29 ..... N90-13060 #
REPT-89-30 ..... N90-13045 #
REPT-89-32 ..... N90-13044 #
REPT-89-34 ..... N90-12978 #
REPT-89-35 ..... N90-13128 #
REPT-89-36 ..... N90-13129 #
REPT-89-37 ..... N90-13130 #
REPT-89-037 ..... N90-12852
REPT-89-038 ..... N90-13260
REPT-89B00158 ..... N90-12985* #
REPT-89B00244 ..... N90-12984* #
REPT-031 ..... N90-13011 #
REPT-115 ..... N90-12925 #
REPT-187 ..... N90-13192 #
REPT-188 ..... N90-12722 #
REPT-189 ..... N90-12721 #
REPT-321 ..... N90-13011 #
REPT-508 ..... N90-12572
REPT-549 ..... N90-12573
REPT-550 ..... N90-12807
REPT-8519 ..... N90-12668 #
REPT-716111-09 ..... N90-12784* #
REPT-719111-1 ..... N90-12841 #

RIACS-M88.4 ..... N90-13047* #

RR(OH)1054 ..... N90-12957 #

RR-WB-88-17 ..... N90-12853 #

RR-354 ..... N90-13123 #
RR-358 ..... N90-13102 #
RR-359 ..... N90-13121 #
RR-360 ..... N90-13122 #
RR-361 ..... N90-13103 #
RR-362 ..... N90-12930 #
RR-363 ..... N90-12931 #
RR-364 ..... N90-13104 #

RSL-TR-331-9 ..... N90-12838 #

RSRE-MEMO-3486 ..... N90-13231 #
RSRE-MEMO-4102 ..... N90-12905 #
RSRE-MEMO-4133 ..... N90-12576 #
RSRE-MEMO-4152 ..... N90-13178 #
RSRE-MEMO-4195 ..... N90-12817 #
RSRE-MEMO-4210 ..... N90-12810 #
RSRE-MEMO-4211 ..... N90-12818 #
RSRE-MEMO-4212 ..... N90-13057 #
RSRE-MEMO-4215 ..... N90-13058 #
RSRE-MEMO-4217 ..... N90-12819 #
RSRE-MEMO-4225 ..... N90-13066 #
RSRE-MEMO-4234 ..... N90-13275 #
RSRE-MEMO-4237 ..... N90-12575 #
RSRE-MEMO-4243 ..... N90-12820 #
RSRE-MEMO-4244 ..... N90-13070 #
RSRE-MEMO-4247 ..... N90-13067 #
RSRE-MEMO-4258 ..... N90-12671 #
RSRE-MEMO-4267 ..... N90-12815 #
RSRE-MEMO-4289 ..... N90-12858 #
RSRE-MEMO-4293 ..... N90-13068 #
RSRE-MEMO-4309 ..... N90-13005 #

RSRE-88004 ..... N90-12816 #

S-REPT-101-128 ..... N90-13284 #
S-REPT-101-157 ..... N90-13288 #
S-REPT-101-157 ..... N90-13289 #

SAIC-89/1587 ..... N90-13023 #

SD-TR-89-41 ..... N90-12916 #
SD-TR-89-58 ..... N90-12759 #
SD-TR-89-61 ..... N90-12670 #
SD-TR-89-63 ..... N90-12714 #
SD-TR-89-64 ..... N90-12869 #
SD-TR-89-67 ..... N90-13238 #

SDEPL-002 ..... N90-13030 #

SER-A-20 ..... N90-12946 #
SER-A-89-A10 ..... N90-13116 #
SER-A-89-A11 ..... N90-12879 #

SGD-537-PT-2 ..... N90-13300

SOL-89-7 ..... N90-13088 #

SR-6 ..... N90-12990 #

SSD-TR-89-48 ..... N90-12643 #

SU-SLAC-PUB-5016 ..... N90-12875 #
SU-SLAC-PUB-5054 ..... N90-12844 #

SU-SOL-89-11 ..... N90-13086 #
SU-SOL-89-12 ..... N90-13174 #
SU-SOL-89-13 ..... N90-13189 #

TAO 50342 ..... N90-13050* #

TD88-1107 ..... N90-12629
TD88-2608 ..... N90-13230
TD88-3856 ..... N90-12991
TD88-4123 ..... N90-13041
TD88-4850 ..... N90-12825
TD88-5302 ..... N90-12824
TD88-5415 ..... N90-12821
TD89-0321 ..... N90-13042
TD89-0346 ..... N90-13069
TD89-0393 ..... N90-13107
TD89-0532 ..... N90-13039
TD89-0952 ..... N90-12822
TD89-0953 ..... N90-12823
TD89-1200 ..... N90-12826
TD89-1653 ..... N90-13234
TD89-1654 ..... N90-13208
TD89-1655 ..... N90-13233

TELECOM-PARIS-88-E017 ..... N90-12812 #
TELECOM-PARIS-89-E001 ..... N90-12811 #
TELECOM-PARIS-89-E002 ..... N90-13105 #
TELECOM-PARIS-89-H001 ..... N90-13038 #

TKK-F-A639 ..... N90-13258 #
TKK-F-A640 ..... N90-12878 #

TR-EE-89-47 ..... N90-13266 #

TR-1 ..... N90-13256 #
TR-1 ..... N90-13268 #
TR-12 ..... N90-13271 #
TR-13-ONR-1 ..... N90-12755 #
TR-19 ..... N90-12736 #
TR-20 ..... N90-12740 #
TR-24 ..... N90-12691 #
TR-68 ..... N90-13254 #
TR-89-12 ..... N90-13051 #
TR-108 ..... N90-13213 #
TR-421 ..... N90-13187 #
TR-850 ..... N90-12915 #
TR-0086A(2945-02)-2 ..... N90-12869 #
TR-0089(4051-01)-1 ..... N90-13238 #
TR-0089(4064)-2 ..... N90-12759 #
TR-0089(4530-02)-1 ..... N90-12714 #
TR-0089(4925-07)-2 ..... N90-12870 #
TR-0089(4930-04)-1 ..... N90-12916 #
TR-0089(9975)-1 ..... N90-12643 #

TRITA-EPP-89-04 ..... N90-12809 #

TRW-17271-VOL-11 ..... N90-12656* #

TSG0428 ..... N90-12616 #

TW-289 ..... N90-13167 #
TW-292 ..... N90-13168 #

TWR-17541-10 ..... N90-12651* #
TWR-17543-10 ..... N90-12652* #

UBUFFALO/DC/89/TR-110 ..... N90-13226 #

UCRL-100403 ..... N90-12929 #

UDR-TR-82 ..... N90-12733 #

UMR-FDB-11 ..... N90-12753 #

US-PATENT-APPL-SN-089120 ..... N90-12751
US-PATENT-APPL-SN-123629 ..... N90-13262
US-PATENT-APPL-SN-159423 ..... N90-12594
US-PATENT-APPL-SN-183965 ..... N90-12860
US-PATENT-APPL-SN-304853 ..... N90-12682 #
US-PATENT-APPL-SN-360179 ..... N90-12940 #
US-PATENT-APPL-SN-374212 ..... N90-12948
US-PATENT-APPL-SN-385375 ..... N90-12862 #
US-PATENT-APPL-SN-393610 ..... N90-12859 #
US-PATENT-APPL-SN-737606 ..... N90-12828
US-PATENT-APPL-SN-867660 ..... N90-12679
US-PATENT-APPL-SN-875892 ..... N90-12861

US-PATENT-CLASS-244-328 ..... N90-12594
US-PATENT-CLASS-505-1 ..... N90-13262
US-PATENT-CLASS-526-262 ..... N90-12679

US-PATENT-4,736,439 ..... N90-12828
US-PATENT-4,775,729 ..... N90-12679
US-PATENT-4,778,871 ..... N90-12751
US-PATENT-4,819,190 ..... N90-12861
US-PATENT-4,842,218 ..... N90-12594
US-PATENT-4,843,060 ..... N90-13262
US-PATENT-4,843,448 ..... N90-12860

USAFOEHL-89-023RC0111DRA ..... N90-13017 #

USAFSAM-TR-88-23 ..... N90-13022 #

USARIEM-M60-8968 ..... N90-13020 #
USARIEM-M61-89 ..... N90-13014 #

USGS/G-1458-03 ..... N90-12814 #

UT-KBS-89-01 ..... N90-13064 #

UTK-PSL-89-2 ..... N90-13243 #

UTRC/R89-957484-F ..... N90-12709 #

UVA/525425/MS89/104 ..... N90-12966 #

UWA/DME/TR-89/1 ..... N90-12735 #

VKI-TN-169 ..... N90-12890 #

VLSI-MEMO-89-524 ..... N90-13092 #
VLSI-MEMO-89-531 ..... N90-13093 #
VLSI-MEMO-89-544 ..... N90-12847 #

VPI-E-89-14 ..... N90-13065* #

WAES-TR-89-0010 ..... N90-12719 #

WIS-WRC-89-01 ..... N90-12814 #

WL-TR-89-14 ..... N90-12703 #

WRDC-TR-89-2038 ..... N90-12648 #
WRDC-TR-89-2044 ..... N90-12881 #
WRDC-TR-89-2047 ..... N90-12706 #
WRDC-TR-89-2077 ..... N90-12898 #
WRDC-TR-89-2096 ..... N90-13193 #
WRDC-TR-89-2120 ..... N90-12850 #
WRDC-TR-89-2122 ..... N90-12865 #
WRDC-TR-89-3076-VOL-1 ..... N90-12624 #
WRDC-TR-89-4081 ..... N90-12663 #

WSU-TR-88-001 ..... N90-12898 #

WYLE-60300-1 ..... N90-12645* #

YALEU/DCS/RR-700 ..... N90-13052 #
YALEU/DCS/RR-706 ..... N90-13054 #

Appendix—About STAR

Scientific and Technical Aerospace Reports (STAR) is a major component of a comprehensive National Aeronautics and Space Administration information system covering aeronautics, space, and supporting disciplines. *STAR* is issued on the 8th and 23rd of each month and announces current publications of the following types:

- NASA, NASA contractor, and NASA grantee reports
- Reports issued by other U.S. Government agencies, domestic and foreign institutions, universities, and private firms
- Translations in report form
- NASA-owned patents and patent applications
- Other U.S. Government agency and foreign patents and patent applications
- Domestic and foreign dissertations and theses

Journal, book, and conference literature, cover-to-cover journal translations, and certain foreign dissertations are announced in a companion journal, *International Aerospace Abstracts (IAA),* available on subscription from the American Institute of Aeronautics and Astronautics, Technical Information Service, 555 West 57th Street, 12th Floor, New York, NY 10019.

SUBJECT SCOPE

The subject scope of *STAR* and *IAA* includes all aspects of aeronautics and space research and development, supporting basic and applied research, and applications. Aerospace aspects of earth resources, energy development, conservation, oceanography, environmental protection, urban transportation, and other topics of high national priority are also covered.

OTHER NASA PUBLICATIONS

Other NASA publications and information services are described in the publication, *The NASA Scientific and Technical Information System ... and How to Use It,* available without charge from the NASA Scientific and Technical Information Facility, P.O. Box 8757, BWI Airport, MD 21240.

HOW TO USE *STAR* SUBJECT CATEGORIES

STAR is categorized by 10 major subject divisions broken down further into 76 specific subject categories and one general division/category. The major subject divisions are listed on page ii in the Table of Contents, together with a note for each that defines its scope and provides any cross-references. For example:

AERONAUTICS

Includes aeronautics (general); aerodynamics; air transportation and safety; aircraft communications and navigation; aircraft design, testing and performance; aircraft instrumentation; aircraft propulsion and power; aircraft stability and control; and research and support facilities (air).

For related information see also *Astronautics.*

Each major division is further divided into as many as nine specific categories, which are identified by category numbers.

Abstracts in *STAR* are grouped by subject category, the categories appearing in sequential order. Category breaks in the abstract section are identified by the category number and title, and a scope note. Cross-references to other categories are provided as appropriate. For example:

02 AERODYNAMICS

Includes aerodynamics of bodies, combinations, wings, rotors, and control surfaces; and internal flow in ducts and turbomachinery.

For related information see also *34 Fluid Mechanics and Heat Transfer.*

CROSS-REFERENCES

Individual *STAR* abstracts are not ordinarily cross-referenced, except for certain conference reports or book translations that have had separate abstracts written for their component papers or chapters. Citations and abstracts of the components follow immediately after those of the parent document. When the subject content of a component differs sufficiently from the general content of the parent, a cross-reference citation also is printed at the end of the category to which it normally would have been assigned if it were independent.

DOCUMENTS ON MICROFICHE

Documents on microfiche[1] are designated by a pound sign (#) following the accession number. The pound sign is used without regard to the source or quality of the microfiche.

LIMITED REPRODUCIBILITY

A Note of Limited Reproducibility appears in the citation, if one or a combination of the following factors affect the reproducibility of more than 20% of the document. These factors include: faint or broken type, color photographs, black and white photographs, foldouts, dot matrix print, charts/graphs with script notation, non-Roman alphabet, or some other factor that limits the reproducibility of that document. This notation also appears on the microfiche header, with the specific causing factor checked off on a list visible in the second frame.

AVAILABILITIES

One or more sources from which a document announced in *STAR* is available to the public is given in each citation. The most commonly indicated sources and their acronyms or abbreviations are listed below. If the publication is available from a source other than those listed, the publisher and his address will be displayed on the availability line or in combination with the corporate source line.

Avail: NTIS. Sold by the National Technical Information Service. Prices for hard copy (HC) and microfiche (MF) are indicated by a price code following the letters HC or MF in the *STAR* citation. Current values for the price codes are given in the tables on page A-7.

Initially distributed microfiche under the NTIS SRIM (Selected Research in Microfiche) is available at greatly reduced unit prices. For this service and for information concerning subscription to NASA printed reports, consult the NTIS Subscription Section, Springfield, VA 22161.

NOTE ON ORDERING DOCUMENTS: When ordering NASA publications (those followed by the * symbol), use the N accession number. NASA patent applications (only the specifications are offered) should be ordered by the US-Patent-Appl-SN number. Non-NASA publications (no asterisk) should be ordered by the AD, PB, or other *report number* shown on the last line of the citation, not by the N accession number. It is also advisable to cite the title and other bibliographic identification.

(1) A microfiche is a transparent sheet of film, 105 by 148 mm in size, containing as many as 60 to 98 pages of information reduced to micro images (not to exceed 26:1 reduction).

Avail: SOD (or GPO). Sold by the Superintendent of Documents, U.S. Government Printing Office, in hard copy. The current price and order number are given following the availability line. (NTIS will fill microfiche requests, as indicated above, for those documents identified by a # symbol.)

Avail: BLL (formerly NLL): British Library Lending Division, Boston Spa, Wetherby, Yorkshire, England. Photocopies available from this organization at the price shown. (If none is given, inquiry should be addressed to the BLL.)

Avail: DOE Depository Libraries. Organizations in U.S. cities and abroad that maintain collections of Department of Energy reports, usually in microfiche form, are listed in *Energy Research Abstracts*. Services available from the DOE and its depositories are described in a booklet, *DOE Technical Information Center - Its Functions and Services* (TID-4660), which may be obtained without charge from the DOE Technical Information Center.

Avail: ESDU. Pricing information on specific data, computer programs, and details on Engineering Sciences Data Unit (ESDU) topic categories can be obtained from ESDU International Ltd. Requesters in North America should use the Virginia address while all other requesters should use the London address, both of which are on page A-6.

Avail: Fachinformationszentrum, Karlsruhe. Sold by the Fachinformationszentrum Energie, Physik, Mathematik GMBH, Eggenstein Leopoldshafen, Federal Republic of Germany, at the price shown in deutschmarks (DM).

Avail: HMSO. Publications of Her Majesty's Stationery Office are sold in the U.S. by Pendragon House, Inc. (PHI), Redwood City, CA. The U.S. price (including a service and mailing charge) is given, or a conversion table may be obtained from PHI.

Avail: NASA Public Document Rooms. Documents so indicated may be examined at or purchased from the National Aeronautics and Space Administration, Public Documents Room (Room 126), 600 Independence Ave., S.W., Washington, DC 20546, or public document rooms located at NASA installations, and the NASA Pasadena Office at the Jet Propulsion Laboratory.

Avail: Univ. Microfilms. Documents so indicated are dissertations selected from *Dissertation Abstracts* and are sold by University Microfilms as xerographic copy (HC) and microfilm. All requests should cite the author and the Order Number as they appear in the citation.

Avail: US Patent and Trademark Office. Sold by Commissioner of Patents and Trademarks, U.S. Patent and Trademark Office, at the standard price of $1.50 each, postage free. (See discussion of NASA patents and patent applications below.)

Avail: (US Sales Only). These foreign documents are available to users within the United States from the National Technical Information Service (NTIS). They are available to users outside the United States through the International Nuclear Information Service (INIS) representative in their country, or by applying directly to the issuing organization.

Avail: USGS. Originals of many reports from the U.S. Geological Survey, which may contain color illustrations, or otherwise may not have the quality of illustrations preserved in the microfiche or facsimile reproduction may be examined by the public at the libraries of the USGS field offices whose addresses are listed in this Introduction. The libraries may be queried

concerning the availability of specific documents and the possible utilization of local copying services, such as color reproduction.

Avail: Issuing Activity, or Corporate Author, or no indication of availability. Inquiries as to the availability of these documents should be addressed to the organization shown in the citation as the corporate author of the document.

NASA PATENTS AND PATENT APPLICATIONS

Patents and patent applications owned by NASA are announced in *STAR* under appropriate subject categories and are referenced in the *STAR* indexes. In the Report/Accession Number Index, patents are indexed by the NASA Case Number (which appears in lieu of the report number in other indexes), the U.S. Patent Number, the U.S. Patent Application Serial Number, and the U.S. Patent Class. Patent applications for which patents have not yet been issued are indexed by the NASA Case Number and the U.S. Patent Application Serial Number.

NASA *patent application specifications* are sold in paper copy and microfiche by the National Technical Information Service (NTIS). The US-Patent-Appl-SN- number should be used in ordering either paper copy or microfiche from NTIS. Printed copies of *patents* (which are not microfiched) are available for purchase from:

Commissioner of Patents and Trademarks
U.S. Patent and Trademark Office
Washington, DC 20231

When ordering patents, the U.S. Patent Number should be used, and payment must be remitted in advance, by money order or check payable to the Commissioner of Patents and Trademarks. Prepaid purchase coupons for ordering are also available from the Patent and Trademark Office. The patents and patent applications announced in *STAR* are owned by NASA and are available for royalty-free licensing. Requests for licensing terms and further information should be addressed to:

Associate General Counsel for Intellectual Property/Code GP
National Aeronautics and Space Administration
Washington, DC 20546

ELIGIBILITY AND REGISTRATION FOR NASA INFORMATION PRODUCTS AND SERVICES

A variety of services is available to organizations of the following types that have registered with NASA to receive specific services or products:

1. NASA offices and installations, contractors, subcontractors, grantees, and consultants;
2. Other U.S. Government agencies and their contractors;
3. Libraries in the United States that have arrangements with NASA to maintain collections of NASA documents for public reference;
4. Other organizations in the United States having a need for NASA documents in work related to aeronautics and space research;
5. Organizations abroad that have established reciprocal document exchange arrangements with NASA.

Only the central service points or central points of document acquisition and control within qualified organizations are eligible to register for NASA products and services. Domestic organizations that may be eligible to receive various classes of NASA publications and services should address their requests for registration or for further information to:

NASA Scientific and Technical Information Facility
ATTN: Registration Services
P.O. Box 8757
BWI Airport, MD 21240
301-621-0153

Organizations abroad should direct requests to Manager, International STI Activities, NTT, NASA Headquarters, Washington, DC 20546.

AVAILABILITY OF *STAR* ABSTRACTS ON MICROFICHE

Microfiche of the abstract sections of this issue and other issues of *STAR* are available on annual subscription from NTIS as PB90-911300, Attn: Subscriptions, 5285 Port Royal Road, Springfield, VA 22161. Annual subscription rates are $75.50 North America; $151.00 foreign. Abstract sections for previous years retroactive to 1964 are available at the current rates. Microfiche for individual *STAR* issue abstract sections are not available.

PUBLIC COLLECTIONS OF NASA DOCUMENTS

DOMESTIC: NASA and NASA-sponsored documents and a large number of aerospace publications are available to the public for reference purposes at the library maintained by the American Institute of Aeronautics and Astronautics, Technical Information Service, 555 West 57th Street, 12th Floor, New York, NY 10019

EUROPEAN: An extensive collection of NASA and NASA-sponsored publications is maintained by the British Library Lending Division, Boston Spa, Wetherby, Yorkshire, England, for public access. The British Library Lending Division also has available many of the non-NASA publications cited in *STAR*. European requesters may purchase facsimile copy or microfiche of NASA and NASA-sponsored documents, those identified by both the symbols # and * from ESA - Information Retrieval Service, European Space Agency, 8-10 rue Mario-Nikis, 75738 Paris CEDEX 15, France.

FEDERAL DEPOSITORY LIBRARY PROGRAM

In order to provide the general public with greater access to U.S. Government publications, Congress established the Federal Depository Library Program under the Government Printing Office (GPO), with 51 regional depositories responsible for permanent retention of material, inter-library loan, and reference services. At least one copy of nearly every NASA and NASA-sponsored publication, either in printed or microfiche format, is received and retained by the 51 regional depositories. A list of the regional GPO libraries, arranged alphabetically by state, appears on the inside back cover. These libraries are *not* sales outlets. A local library can contact a Regional Depository to help locate specific reports, or direct contact may be made by an individual.

ADDRESSES OF ORGANIZATIONS

American Institute of Aeronautics and Astronautics
Technical Information Service
555 West 57th Street, 12th Floor
New York, New York 10019

British Library Lending Division,
Boston Spa, Wetherby, Yorkshire,
England

Commissioner of Patents and Trademarks
U.S. Patent and Trademark Office
Washington, DC 20231

Department of Energy
Technical Information Center
P.O. Box 62
Oak Ridge, Tennessee 37830

European Space Agency-Information Retrieval Service
ESRIN
Via Galileo Galilei
00044 Frascati (Rome) Italy

Engineering Sciences Data Unit International
P.O. Box 1633
Manassas, Virginia 22110

Engineering Sciences Data Unit International, Ltd.
251-259 Regent Street
London, W1R 7AD, England

Fachinformationszentrum Energie, Physik, Mathematik
GMBH
7514 Eggenstein Leopoldshafen
Federal Republic of Germany

Her Majesty's Stationery Office
P.O. Box 569, S.E. 1
London, England

NASA Scientific and Technical Information Facility
P.O. Box 8757
BWI Airport, Maryland 21240

National Aeronautics and Space Administration
Scientific and Technical Information Division (NTT)
Washington, DC 20546

National Technical Information Service
5285 Port Royal Road
Springfield, Virginia 22161

Pendragon House, Inc.
899 Broadway Avenue
Redwood City, California 94063

Superintendent of Documents
U.S. Government Printing Office
Washington, DC 20402

University Microfilms
A Xerox Company
300 North Zeeb Road
Ann Arbor, Michigan 48106

University Microfilms, Ltd.
Tylers Green
London, England

U.S. Geological Survey Library National Center
MS 950
12201 Sunrise Valley Drive
Reston, Virginia 22092

U.S. Geological Survey Library
2255 North Gemini Drive
Flagstaff, Arizona 86001

U.S. Geological Survey
345 Middlefield Road
Menlo Park, California 94025

U.S. Geological Survey Library
Box 25046
Denver Federal Center, MS914
Denver, Colorado 80225

NTIS PRICE SCHEDULES

(Effective January 1, 1990)

Schedule A
STANDARD PRICE DOCUMENTS AND MICROFICHE

PRICE CODE	NORTH AMERICAN PRICE	FOREIGN PRICE
A01	$ 8.00	$ 16.00
A02	11.00	22.00
A03	15.00	30.00
A04-A05	17.00	34.00
A06-A09	23.00	46.00
A10-A13	31.00	62.00
A14-A17	39.00	78.00
A18-A21	45.00	90.00
A22-A25	53.00	106.00
A99	*	*
N01	60.00	120.00
N02	59.00	118.00
N03	20.00	40.00

Schedule E
EXCEPTION PRICE DOCUMENTS AND MICROFICHE

PRICE CODE	NORTH AMERICAN PRICE	FOREIGN PRICE
E01	$10.00	$ 20.00
E02	12.00	24.00
E03	14.00	28.00
E04	16.50	33.00
E05	18.50	37.00
E06	21.50	43.00
E07	24.00	48.00
E08	27.00	54.00
E09	29.50	59.00
E10	32.50	65.00
E11	35.00	70.00
E12	38.50	77.00
E13	41.00	82.00
E14	45.00	90.00
E15	48.50	97.00
E16	53.00	106.00
E17	57.50	115.00
E18	62.00	124.00
E19	69.00	138.00
E20	80.00	160.00
E99	*	*

* Contact NTIS for price quote.

IMPORTANT NOTICE

NTIS Shipping and Handling Charges

U.S., Canada, Mexico — ADD $3.00 per TOTAL ORDER

All Other Countries — ADD $4.00 per TOTAL ORDER

Exceptions — Does NOT apply to:

ORDERS REQUESTING NTIS RUSH HANDLING

ORDERS FOR SUBSCRIPTION OR STANDING ORDER PRODUCTS *ONLY*

NOTE: Each additional delivery address on an order requires a separate shipping and handling charge.

FEDERAL REGIONAL DEPOSITORY LIBRARIES

ALABAMA

AUBURN UNIV. AT MONTGOMERY LIBRARY
Documents Department
Montgomery, AL 36193
(205) 279-9110 ext.253

UNIV. OF ALABAMA LIBRARY
Reference Department/Documents
Box S
Tuscaloosa, AL 35486
(205) 348-6046

ARIZONA

DEPT. OF LIBRARY, ARCHIVES, AND PUBLIC RECORDS
Third Floor State Capitol
1700 West Washington
Phoenix, AZ 85007
(602) 255-4121

ARKANSAS

ARKANSAS STATE LIBRARY
Documents Service Section
One Capitol Mall
Little Rock, AR 72201
(501) 371-2090

CALIFORNIA

CALIFORNIA STATE LIBRARY
Govt. Publications Section
914 Capitol Mall
Sacramento, CA 95814
(916) 322-4572

COLORADO

UNIV. OF COLORADO
Norlin Library
Government Publications Division
Campus Box 184
Boulder, CO 80309
(303) 492-8834

DENVER PUBLIC LIBRARY
Govt. Pub. Department
1357 Broadway
Denver, CO 80203
(303) 571-2346

CONNECTICUT

CONNECTICUT STATE LIBRARY
231 Capitol Avenue
Hartford, CT 06106
(203) 566-4971

FLORIDA

UNIV. OF FLORIDA LIBRARIES
Documents Department
Library West
Gainesville, FL 32611
(904) 392-0367

GEORGIA

UNIV. OF GEORGIA LIBRARIES
Government Documents Dept.
Athens, GA 30602
(404) 542-8949

HAWAII

UNIV. OF HAWAII
Hamilton Library
Government Documents Collection
2550 The Mall
Honolulu, HI 96822
(808) 948-8230

IDAHO

UNIV. OF IDAHO LIBRARY
Documents Section
Moscow, ID 83843
(208) 885-6344

ILLINOIS

ILLINOIS STATE LIBRARY
Federal Documents
Centennial Building
Springfield, IL 62756
(217) 782-5012

INDIANA

INDIANA STATE LIBRARY
Serials Section
140 North Senate Avenue
Indianapolis, IN 46204
(317) 232-3686

IOWA

UNIV. OF IOWA LIBRARIES
Government Publications Dept.
Iowa City, IA 52242
(319) 335-5926

KANSAS

UNIVERSITY OF KANSAS
Spencer Research Library
Government Documents
Lawrence, KS 66045
(913) 864-4662

KENTUCKY

UNIV. OF KENTUCKY LIBRARIES
Government Publications/Maps Dept.
Lexington, KY 40506
(606) 257-8400

LOUISIANA

LOUISIANA STATE UNIVERSITY
Middleton Library
Government Documents Dept.
Baton Rouge, LA 70803
(504) 388-2570

LOUISIANA TECHNICAL UNIV.
Prescott Memorial Library
Government Documents Dept.
Ruston, LA 71272
(318) 257-4962

MAINE

UNIVERSITY OF MAINE
Raymond H. Fogler Library
Govt. Documents & Microforms Dept.
Orono, ME 04469
(207) 581-1680

MARYLAND

UNIVERSITY OF MARYLAND
McKeldin Library
Documents/Maps Room
College Park, MD 20742
(301) 454-3034

MASSACHUSETTS

BOSTON PUBLIC LIBRARY
Government Documents Dept.
666 Boylston Street
Boston, MA 02117
(617) 536-5400 ext.226

MICHIGAN

DETROIT PUBLIC LIBRARY
5201 Woodward Avenue
Detroit, MI 48202
(313) 833-1409

LIBRARY OF MICHIGAN
Government Documents
P.O. Box 30007
735 E. Michigan Avenue
Lansing, MI 48909
(517) 373-1593

MINNESOTA

UNIVERSITY OF MINNESOTA
Wilson Library
Government Publications
309 Nineteenth Avenue South
Minneapolis, MN 55455
(612) 373-7813

MISSISSIPPI

UNIV. OF MISSISSIPPI LIB.
Government Documents Dept.
106 Old Gym Bldg.
University, MS 38677
(601) 232-5857

MISSOURI

University of Missouri at Columbia Library
Government Documents
Columbia, MO 65201
(314) 882-6733

MONTANA

UNIV. OF MONTANA
Mansfield Library
Documents Division
Missoula, MT 59812
(406) 243-6700

NEBRASKA

UNIVERSITY OF NEBRASKA - LINCOLN
Love Memorial Library
Documents Department
Lincoln, NE 68588
(402) 472-2562

NEVADA

UNIV. OF NEVADA-RENO LIB.
Govt. Pub. Department
Reno, NV 89557
(702) 784-6579

NEW JERSEY

NEWARK PUBLIC LIBRARY
U.S. Documents Division
5 Washington Street
P.O. Box 630
Newark, NJ 07101
(201) 733-7812

NEW MEXICO

UNIVERSITY OF NEW MEXICO
General Library
Government Publications/Maps Dept.
Albuquerque, NM 87131
(505) 277-5441

NEW MEXICO STATE LIBRARY
325 Don Gaspar Avenue
Santa Fe, NM 87501
(505) 827-3826

NEW YORK

NEW YORK STATE LIBRARY
Documents Sect. Cultural Educ. Ctr.
Empire State Plaza
Albany, NY 12230
(518) 474-5563

NORTH CAROLINA

UNIVERSITY OF NORTH CAROLINA AT CHAPEL HILL
Davis Library 080A
BA/SS Department Documents
Chapel Hill, NC 27514
(919) 962-1151

NORTH DAKOTA

NORTH DAKOTA STATE UNIVERSITY LIBRARY
Government Documents Dept.
Fargo, ND 58105
(701) 237-8352
In cooperation with Univ. of North Dakota, Chester Fritz Library Grand Forks

OHIO

STATE LIBRARY OF OHIO
Documents Section
65 South Front Street
Columbus, OH 43266
(614) 644-7051

OKLAHOMA

OKLAHOMA DEPT. OF LIBRARIES
Government Documents
200 NE 18th Street
Oklahoma City, OK 73105
(405) 521-2502, ext. 252

OKLAHOMA STATE UNIV. LIB.
Documents Department
Stillwater, OK 74078
(405) 624-0489

OREGON

PORTLAND STATE UNIV.
Millar Library
934 SW Harrison - P.O. Box 1151
Portland, OR 97207
(503) 229-3673

PENNSYLVANIA

STATE LIBRARY OF PENN.
Government Publications Section
Box 1601
Walnut St. & Commonwealth Ave.
Harrisburg, PA 17105
(717) 787-3752

SOUTH CAROLINA

CLEMSON UNIV. COOPER LIB.
Documents Department
Clemson, SC 29634
(803) 656-5174
In cooperation with Univ. of South Carolina, Thomas Cooper Library, Columbia

TEXAS

TEXAS STATE LIBRARY
Public Services Department
P.O. Box 12927 - 1201 Brazos
Austin, TX 78711
(512) 463-5455

TEXAS TECH. UNIV. LIBRARY
Documents Department
Lubbock, TX 79409
(806) 742-2268

UTAH

UTAH STATE UNIVERSITY
Merrill Library & Learning Resources Center, UMC-30
Documents Department
Logan, UT 84322
(801) 750-2682

VIRGINIA

UNIVERSITY OF VIRGINIA
Alderman Library
Government Documents
Charlottesville, VA 22903
(804) 924-3133

WASHINGTON

WASHINGTON STATE LIBRARY
Document Section
Olympia, WA 98504
(206) 753-4027

WEST VIRGINIA

WEST VIRGINIA UNIV. LIB.
Government Documents Section
P.O. Box 6069
Morgantown, WV 26506
(304) 293-3640

WISCONSIN

ST. HIST SOC. OF WISCONSIN LIB.
Government Pub. Section
816 State Street
Madison, WI 53706
(608) 262-2781
In cooperation with Univ. of Wisconsin-Madison, Memorial Library

MILWAUKEE PUBLIC LIBRARY
Documents Division
814 West Wisconsin Avenue
Milwaukee, WI 53233
(414) 278-3065

WYOMING

WYOMING STATE LIBRARY
Supreme Court & Library Bldg.
Cheyenne, WY 82002
(307) 777-5919

National Aeronautics and
Space Administration
Code NTT
Washington, D.C.
20546

Official Business

Penalty for Private Use, $300

SPECIAL FOURTH-CLASS RATE
POSTAGE & FEES PAID
NASA
PERMIT No. G27

POSTMASTER: If Undeliverable (Section 158 Postal Manual) Do Not Return